DEPARTMENT OF TERRESTRIAL MAGNETISM

M. A. TUVE, Director
J. A. FLEMING, Director
(Retired June 30, 1946)

The Geomagnetic Field, Its Description and Analysis

E. H. VESTINE
LUCILE LAPORTE
ISABELLE LANGE
W. E. SCOTT

CARNEGIE INSTITUTION OF WASHINGTON PUBLICATION 580
WASHINGTON, D. C.
1947

Lithoprinted from copy supplied by author
by
Edwards Brothers, Inc.
Ann Arbor, Michigan, U.S.A.

December, 1947

PREFACE

This book continues a descriptive study of geomagnetism begun with Carnegie Institution of Washington Publication 578, which was principally concerned with the description of the Earth's main magnetic field and its secular change. The present volume extends this work to the various known geomagnetic variations, with inclusion of some analyses.

To a considerable extent, the present book is actually a by-product of Publication 578, since extensive information on geomagnetic variations was required for the improving of estimates therein of geomagnetic secular change for the period 1905 to 1945. Because the latter required descriptive information respecting shorter-period time-variations on a world-wide scale and over these many years, the general scope of coverage is considerable. Moreover, the emphasis has been upon the description rather than upon the interpretation of results.

It is believed that the two volumes together comprise the first convenient detailed compendium of geomagnetic data especially suited to the needs of those engineering workers who are mainly concerned with the practical applications of geomagnetism. The wide use of illustrative diagrams (many initially drawn as a training exercise for the draftsmen who drew the maps of the first volume) enhances the effective description of geomagnetic phenomena of our environment. The books emerge therefore as a kind of picture supplement to the standard treatise Geomagnetism; the writer hopes that his teacher, Professor Chapman, senior author of that treatise, will not object to such suggestion, provided he be not held at fault for any mistakes that we may have made.

In the course of pursuing the major descriptive objectives of this war project, the writers could not resist the temptation to undertake some serious investigations of the extensive new data available. Hence attempts at explanation of certain phenomena will be found at intervals, between the stacks of figures and tables, along with some short discussions linking the present with previous work. The writers hope that in this way a more interesting and readable account has been provided.

The writers wish to thank our many coworkers whom we represent as authors of this volume. We wish to record especial indebtedness to Dr. J. A. Fleming for material assistance over a period of several years. We have benefited much also by the interest and encouragement of Dr. M. A. Tuve, Director, which facilitated the speedy production of a book including much troublesome detail. Among our many other coworkers, there were especially valuable contributions by E. Balsam, N. Davids, W. N. Dove, H. D. Harradon, D. T. Heck, W. C. Hendrix, H. F. Johnston, C. M. Martin, R. Mason, H. M. Myers, A. M. Palmer, W. E. Scott, J. W. Smith, M. B. Smith (administrative matters), E. J. Snyder, and O. W. Torreson (publication). We wish also to mention the skilled assistance of R. E. Tritt in the operation of punched-card computing equipment.

Finally, grateful acknowledgment is made to the Naval Ordnance Laboratory, United States Navy Department, for the financial help covering this work and report; it is a pleasure to record also our appreciation to the Naval technical representative, Dr. G. H. Shortley, now of Ohio State University, whose quick grasp of the problems of geomagnetism facilitated execution of this project.

This volume completes a final report on work done for the most part during the war period 1942 to 1946 under Contract NOrd-392.

E. H. Vestine,
Department of Terrestrial Magnetism

CONTENTS

CHAPTER I

CHAPTER II

CHAPTER III

CHAPTER IV

CHAPTER V

CHAPTER VI

CHAPTER VII

CONTENTS

CHAPTER VIII

CHAPTER IX

CHAPTER X

CHAPTER XI

CHAPTER I

INTRODUCTION

1. General scope of descriptive data of volume.--The present volume supplements the descriptions of geomagnetic phenomena given in a previous volume [1] which was devoted largely to the technique and results of mapping of the main magnetic field of the Earth and its secular change. The descriptions are here extended to include results of measurements of various geomagnetic variations, usually for all available well-distributed observatories. The new compilations are based in most cases on large samples of homogeneous data. Where averaged variations appear, these cover, in so far as possible, exactly the same time intervals at all observatories. Moreover, the time intervals used have been lengthened to include from one to three sunspot-cycles. Certain variations such as, for instance, the solar daily variation, are given in the form of 12-year averages by months rather than as an average by seasons and an individual year. Indication of the amplitude of the solar daily variation on every day for a period of approximately 40 years is likewise provided as being interesting because of its connection with ultraviolet radiation from the Sun. In the case of the disturbance daily variation, the average characteristics are shown for the first time on a world-wide scale (except in very high latitudes) for each month of the year throughout a sunspot-cycle. Included also are new data for the annual variation, post-perturbation, noncyclic change, and geomagnetic variation with sunspot-cycle, usually not previously deduced at more than a few stations. For many of these effects, data are given which are appropriate to almost all available observatories, throughout the period 1900 to 1942.

Hourly estimates of the storm-time and disturbance daily variation are made for a period of one year for low latitudes. Previous studies descriptive of the average storm-time variation in low and middle latitudes have also been extended, and the new data have been used to estimate storm-time variation in high latitudes. Hourly features of selected magnetic storms are considered on a world-wide scale. In addition, many new data are provided and summarized relating to various short-period geomagnetic fluctuations.

2. Analyses of geomagnetic fields.--A few geomagnetic fields have been subjected to potential analysis. In this way, the geomagnetic phenomena are perceived not only as measured at the Earth's surface, but also as they appear in adjacent regions, within the Earth, and within the atmosphere. Finally, causes, known or probable, of the various fields are discussed.

First on the list of great phenomena not yet understood is the Earth's main field and its secular change. There should, of course, be no such attribute of nature, so far as present day facts regarding the probable character of the Earth's interior are concerned. But its existence is verified by experiment, and its description in mapped form as given in a previous volume is subjected here to analysis. Chapters II and III include the results of such analysis, with calculated values of the field in the atmosphere and beyond, and of simple current functions at various depths within the Earth that could produce it. It is concluded that the site where it originates may be in the region from, say, 1000 km to 3000 km depth within the Earth.

The potential and space gradients of the main field and secular change are calculated and described for the Earth's surface.

The results of some analyses of average features of various geomagnetic variations are also discussed, with particular reference to the average current systems responsible for those features.

In later chapters of this volume, there are considered mainly some features of individual rather than averaged geomagnetic and allied phenomena. These studies relate chiefly to magnetic storms, bays, and accompanying ionospheric and cosmic-ray effects. Search is made for evidence of effects in magnetic disturbance of incoming particles of various energies.

Finally, the field patterns of short-period geomagnetic disturbances are derived, on the basis of data from various magnetic observatories, especially those of the Polar Year 1932-33. There are provided also extensive statistical compilations relating to the frequency of small disturbances of various amplitudes and durations. These are tentatively discussed in relation to possible characteristics of various incoming solar streams of particles.

In conclusion, a few remarks are appended concerning important outstanding problems of geomagnetism that challenge the attention and talents of future investigators in physical research.

CHAPTER II

THE EARTH'S MAIN FIELD AND ITS ANALYSIS

1. Scope and data.--A new and improved description of the Earth's main field (Figures A to G, presented at the end of this chapter) and its secular change, gleaned from the magnetic observations of the past four decades, was presented in a preceding volume [1]. The general aim was that of marshalling the information in a form suited to practical applications of geomagnetism, with a descriptive summary of new procedures used in attempting to obtain improved isomagnetic charts. The present treatment seeks to emphasize those features of purely scientific interest more adequately, the power of description being enhanced by analysis. For instance, the analyses permit the description of the main field in extensive regions adjacent to the Earth's surface and of attributes of this field not yet susceptible of measurement. These are of both practical and theoretical import.

From spherical harmonic coefficients there are computed on a world-wide scale the smoothed gradients of field in certain directions which are of interest in geophysical prospecting. Similar calculations are made of the potential of the main field, but disregarding a possible constant unlikely to be of consequence. Tentative positions of the geomagnetic poles for epoch 1945 are given. There are also included calculated spherical current sheets at various depths which could reproduce the residual part of the main field. These afford one of the simplest modes of representing the observed features of the field. Finally, these are discussed in relation to the probable depth at which we may seek the cause of the field.

The first spherical harmonic analysis of the main field was made by Gauss [2]. He proved that this field was almost entirely of internal origin. This was clearly a definite advance in the understanding of geomagnetism. Since the time of Gauss at least a dozen additional analyses have been made [3]. It seems that there has been consciousness of gradual improvement in the quality and quantity of magnetic observations. Consequently there has been, on the average, one such analysis per decade, though they seem to have appeared in groups. They have yielded coefficients of mathematical functions representing the main field, and the changing values of the coefficients have indicated how the main field, split into convenient component parts, has varied with time, part by part.

2. Method of analysis.--The procedures used here were similar to those used by Dyson and Furner [4] in their analysis of the British Admiralty charts of the magnetic field for 1922, and there were employed tabulations of the spherical harmonic functions of Schmidt [5].

A magnetic potential V over the Earth's surface can usually be expressed in terms of the series [3]

$$V = a \sum_{n=0}^{\infty} \sum_{m=0}^{n} P_n^m(\cos\theta)\Big[\Big\{c_n^m (r/a)^n + (1-c_n^m)(a/r)^{n+1}\Big\} \underline{A}_n^m \cos m\lambda + \Big\{s_n^m (r/a)^n + (1-s_n^m)(a/r)^{n+1}\Big\}\underline{B}_n^m \sin m\lambda\Big] \quad ..(1)$$

where a is the radius of the Earth, r the distance from the Earth's center, θ the colatitude, and λ the east longitude; c_n^m and s_n^m are numbers lying between zero and one, representing the parts of the harmonic term P_n^m cos $m\phi$ or P_n^m sin $m\phi$, in v, which at r = a, are due to matter outside the Earth. Also $\underline{A}_n^m$, $\underline{B}_n^m$ are coefficients usually sought in analysis. For the order m and degree n with $m \leq n \geq 0$, we have in the case $m > 0$

$$P_n^m(\cos\theta) = \Big\{2(n-m)!/(n+m)!\Big\}^{1/2} P_{n,m}(\cos\theta)$$

and when m = 0

$$P_n^m(\cos\theta) = P_{n,m}(\cos\theta)$$

The function

$$P_{n,m}(\cos\theta) = \sin^m\theta\, d^m P_n(\cos\theta)/d(\cos\theta)^m$$

may be written

$$P_{n,m}(\cos\theta) = \frac{(2n)!}{2^n n!(n-m)!}\sin^m\theta\Big\{\cos^{n-m}\theta - \frac{(n-m)(n-m-1)}{2(2n-1)}\cos^{n-m-2}\theta + \frac{(n-m)(n-m-1)(n-m-2)(n-m-3)}{2.4(2n-1)(2n-3)}\cos^{n-m-4}\theta - \ldots\Big\}$$

so that, for example, $P_{2,1}(\cos\theta) = 3/2 \sin 2\theta$.

It is convenient here to define the functions $X_n^m = dP_n^m(\cos\theta)/nd\theta$, and $Y_n^m = mP_n^m(\cos\theta)/n \sin\theta$, which together with $P_n^m = P_n^m(\cos\theta)$ have been extensively tabulated by Schmidt [5].

Noting that the north, east, and vertical intensities are $X = \partial V/r\partial\theta$, $Y = -\partial V/r \sin\theta\partial\lambda$, and $Z = \partial V/\partial r$, respectively, at r = a we obtain from (1), dropping summation signs, and putting $n\underline{A}_n^m = A_n^m$, $n\underline{B}_n^m = B_n^m$

$$\left.\begin{aligned} X &= X_n^m(A_n^m \cos m\lambda + B_n^m \sin m\lambda) \\ Y &= Y_n^m(A_n^m \sin m\lambda - B_n^m \cos m\lambda) \\ Z &= P_n^m\Big[\Big\{nc_n^m - (n+1)(1-c_n^m)\Big\}(A_n^m/n)\cos m\lambda \\ &\quad + \Big\{ns_n^m - (n+1)(1-s_n^m)\Big\}(B_n^m/n)\sin m\lambda\Big] \end{aligned}\right\} ..(2)$$

If c_n^m and s_n^m are zero, in which case the field is entirely of origin internal to the Earth,

$$Z = -P_n^m\Big[\frac{(n+1)}{n} A_n^m \cos m\lambda + \frac{n+1}{n} B_n^m \sin m\lambda\Big]$$

If c_n^m and s_n^m are not zero, we may analyze Z (at r = a) in the form

$$Z = P_n^m(\alpha_n^m \cos m\lambda + \beta_n^m \sin m\lambda)$$

whence knowing α_n^m and β_n^m we evaluate c_n^m and s_n^m from the relations

$$\left.\begin{aligned}\alpha_n^m &= \left\{ nc_n^m - (n+1)(1-c_n^m)\right\} A_n^m/n \\ \beta_n^m &= \left\{ ns_n^m - (n+1)(1-s_n^m)\right\} B_n^m/n\end{aligned}\right\} \quad \ldots\ldots\ldots (3)$$

The immediate problem here is that of finding the values of A_n^m and B_n^m from world charts of the main field separately for X and Y, and likewise the values of α_n^m and β_n^m from the corresponding chart in Z.

This is conveniently done by first analyzing the observed values of X, say, along parallels of colatitude into Fourier coefficients a_m, b_m of the series $a_m \cos m\lambda + b_m \sin m\lambda$. The coefficients a_m, b_m are functions of colatitude only. These are next fitted by the functions X_n^m, for corresponding values of m, where $m \leq n$, by solving sets of linear equations to obtain the values of A_n^m, B_n^m.

Tables 1, 2, and 3, presented at the end of this chapter, list in condensed form the data of the analyses. The actual data consist of new charted values of X, Y, and Z at 10°-intervals of latitude and longitude for epoch 1945.0. Values of a_m, b_m along each 10° parallel of colatitude $10° \leq \theta \leq 170°$ were found for $m \leq 6$, using 36-ordinate Fourier analyses and the more complete listing of values of the previous volume [1]. Weights w were assigned as follows:

for θ = 10° and 170°, w = 1; θ = 20° and 160°, w = 2;
θ = 30° and 150°, w = 3; θ = 40° and 140°, w = 5;
θ = 50° and 130°, w = 7; θ = 60° and 120°, w = 8;
θ = 70° and 110°, w = 9; θ = 80°, 90°, and 100°, w = 10.

and thus were nearly similar to weights used previously by Dyson and Furner [4]. Normal equations were formed, the coefficients A_n^m, B_n^m being, on solution, given in terms of a_m, b_m. In fact, since weights were assigned symmetrically about θ = 90°, the values A_n^m or B_n^m were in no instance calculated by a process more complicated than summing (using predetermined factors from matrix-elements) three products involving a_m or b_m. These same factors could again be used in later analyses of isoporic charts, where similar weights were assigned.

3. Results of analysis.--Table 4 lists the coefficients of equation (2) for values up to n = 6, as found from analyses of the values of X, Y, and Z for 1945.0. On the whole, the coefficients found independently from analyses of X and Y show rather good agreement. Tables 5 and 6 list observed minus computed values for X and Y.

4. Estimate of external part of field.--Values of c_n^m, s_n^m were computed by meaning values of the coefficients A_n^m, B_n^m derived from X and Y (except for zonal harmonic terms given by X alone). As was suggested by Dyson and Furner [4], the existence of an external part was not indicated with any great degree of certainty. In fact, though most values of c_n^m, s_n^m up to m = 3 and n = 3 indicated a few per cent of the field to be of external origin, the value of c_1^0 was 0.000. It seems likely that c_1^0 should be the largest fraction, yet our analysis for this component gives an external part less than 1 per cent. In fact, our analysis probably does not reveal the existence of any permanent external source of field.

Table 7 lists observed minus computed values of Z, based on adopted coefficients obtained from appropriate means of the coefficients for X and Y. The agreement is so good, considering the necessarily smoothed character of the computed distribution, that there seems little likelihood of an important contribution of external origin.

5. Test of Schrödinger's new field theory.--Schrödinger [6] has recently sketched a new unitary field theory for the gravitation, meson, and electromagnetic fields. One of the highly interesting consequences of the theory is that there should exist an external and nonpotential part of the main field of the Earth. Moreover, the vertical component of curl of field should not vanish but should vary with longitude. We have looked for this variation in longitude without success, using values of curl only for areas of chart without adjustments to give zero curl value. These results are apparent from Table 8.

We believe our charts to be more accurate than those of 1885 used by Schrödinger, and the estimated values of curl in the new charts are definitely of small average value.

This does not mean that Schrödinger's theory is necessarily incorrect, but rather that the constants he evaluates from the charts for 1885 are incorrect. We likewise find that the external field is probably very small, which on his theory presupposes a small value of the vertical component of curl.

6. Comparison of present with earlier analyses.--Since we cannot definitely ascribe a small part of our coefficients of Table 4 to an external field, we write

$$g_n^m = \underline{A}_n^m = A_n^m/n; \quad h_n^m = \underline{B}_n^m = B_n^m/n$$

and obtain the Gauss coefficients (external plus internal) for our analysis. In Table 9 these are compared with those of previous analyses. The significance of these coefficients as indicators of secular change will be discussed later, when our spherical harmonic analyses of isoporic charts at various epochs are presented.

7. The geomagnetic poles for epoch 1945.--The first-degree terms in V/a may be written [3]

$$V_1/a = g_1^0 P_1^0 + (g_1^1 \cos\lambda + h_1^1 \sin\lambda) P_1^1$$
$$= g_1^0 \cos\theta + (g_1^1 \cos\lambda + h_1^1 \sin\lambda)\sin\theta$$

Writing

$$H_0^2 = \left(g_1^0\right)^2 + \left(g_1^1\right)^2 + \left(h_1^1\right)^2, \quad \cos\theta_0 = g_1^0/H_0,$$
$$\tan\lambda_0 = h_1^1/g_1^1$$
$$\cos\Theta = \cos\theta\cos\theta_0 + \sin\theta\sin\theta_0\cos(\lambda-\lambda_0)$$

so that Θ is the angle between the direction (θ, λ) and the special direction (θ_0, λ_0). It then follows that

$$V_1 = H_0 \cos\Theta$$

which is the same as that of a sphere uniformly magnetized along the direction $(-\theta_0, -\lambda_0)$, with equatorial horizontal intensity H_0.

For 1945 we find for latitude and longitude of the north geomagnetic pole, ϕ = 78°.6 N, λ = 289°.9 E, and for the south magnetic pole, ϕ = 78°.6 S, λ = 109°.9 E. The magnetic moment of the Earth given by $M = H_0 a^3$ is found to be 8.06×10^{25} CGS.

The 1945 values of ϕ, λ differ from those for 1922 [3] (ϕ = 78°.5, λ = 291°.0) by -0°.1 in ϕ and -1°.1 in λ.

8. The main field within and beyond the Earth's atmosphere.--The components X, Y, and Z at any height $h = r - a$ above the Earth's surface can be computed from expressions obtained on differentiating equation (1). These have been computed with IBM (International Business Machines) automatic (punched-card) machines, using 48 coefficients derived from those for X and Y in Table 4, assuming c_n^m, s_n^m to be zero, and are given in Tables 10 to 24. The importance of c_n^m, s_n^m will increase with increasing height h, since, if they are not zero, the terms in $(r/a)^n$ by which they are multiplied in (1) will increase rapidly with increasing r when n is large. However, the approximation for the internal contribution of the main field at various heights should be almost as good as indicated in the comparisons of Tables 5 to 7. The accuracy of the computations is expected to decrease as h increases, since the process is fundamentally one of analytic continuation. However, at modest heights the synthesized values might well give a better fit with observed values, if the latter are available, than at the Earth's surface, since we cannot hope to represent the field accurately at the Earth's surface with the harmonics up to degree six. Harmonics of very high degree would be needed to represent magnetic anomalies. Thus the main field at the Earth's surface is more complex than the present isomagnetic charts indicate, but it simplifies rapidly, without sensible contribution from high-degree harmonics, at modest heights. The computed values of X, Y, and Z have application in electromagnetic problems of the ionosphere, and they may find practical application also in the guidance of air-borne vehicles and rockets.

In some applications it may be of interest to have computations of D, H, I, and F at various heights. These can be speedily computed with the usual simple formulas from the values of Tables 10 to 24, but we have not undertaken this. For instance, $\tan D = Y/X$, and $H = (X^2 + Y^2)^{1/2}$, at any height, where X and Y are the tabular values for that height.

Charts of the main field at great heights must necessarily be especially simple. The greater the height, the more closely will the charts resemble those for the centered dipole of the main field.

9. Effect of the electric currents causing geomagnetic variations and disturbances upon the computed values. --Within the upper atmosphere there flow varying electric currents in ionized regions. Except near the auroral zone, the electric conductivity varies slowly in any horizontal direction. Hence the electric currents are expected to have magnetic fields like those of thin, nearly uniform current sheets. Since their heights are usually small compared with the lateral dimensions of current flow, the field near these currents will not be very different in magnitude from that observed at the Earth's surface. Proceeding upwards along any radius r the values of Z will be continuous and those of X (or Y) discontinuous on crossing the current sheet.

Within two narrow belts of latitude, the northern and southern auroral zones, large and concentrated electric currents flow during strong and frequent magnetic disturbances [3]. At points near these currents, the field will vary nearly inversely as the distance to the current. However, very near the current, the field would scarcely be expected to exceed that of the main field itself, which presumably acts in some way as the guiding principle which brings it into being. Thus these currents, except under special circumstances and only within quite special regions, would seldom modify the computed values appreciably and then only by a few per cent.

The auroral-zone currents, on an average, are expected to be largest in the early morning and late afternoon, local time, and very small near noon and early evening.

10. Table of the Earth's surface potential of main field.--Table 25 shows the potential calculated from synthesis of the 48 spherical harmonic terms. So far as we are aware, this is the only tabulation of the potential published since that of Gauss, a century ago. As expected, its characteristics are simpler than those for its space gradients or for the components of field. Table 26 gives the potential of the residual field (terms in P_1^0 and P_1^1 removed).

11. Charts of vertical gradients of field components. --Tables 27 to 29 give computed values for the vertical gradients of X, Y, and Z.

Should the sources responsible for the main field be distributed within a layer of great thickness within the Earth, there arises an interesting point in connection with the charts of vertical gradients. Such charts reflect best the effects of sources quite near the Earth's surface. The distribution of potential at the Earth's surface, on the other hand, may include much greater proportionate contributions from distant internal sources than in the case of the gradients.

However, the dipole terms (those with $m = 0$ or 1, $n = 1$) dominate among the contributions of various harmonics of the main field. Hence the nondipole contributions in the derivatives of X, Y, Z with respect to r also have been synthesized. These results are shown in Tables 30 to 32; they apply to what is usually called the residual field of the Earth.

The complexities in pattern are now more evident, but it seems difficult definitely to relate them, say, to the surface distribution of continental areas, or to any other known geophysical phenomenon. The results seem compatible with a somewhat simple, broad distribution of sources with depth. However, they are also compatible with a distribution of sources within a thin layer.

12. Simple electric current functions at various depths reproducing main field at Earth's surface, or those for the residual part.--There is a possibility that the main field is due to electric currents flowing within the Earth. If so, these are likely to be maintained continuously by some mechanism not yet understood [7]. There is even a theoretical and somewhat academic possibility that they might consist of a freely decaying system, a survival of some old order of things, provided the electric conductivity within the Earth approaches superconductivity [8].

The studies of Chapman [3] and of Lahiri and Price [9] suggest very rapid increase in conductivity with depth near 700 km. Their estimates of conductivity were inferred from consequences of electromagnetic induction in relation to geomagnetic variations of aperiodic character lasting a few days.

Chapman and Whitehead [3] also inferred that the magnetic permeability of the Earth was about unity to depths of a few hundred km. Moreover, the percentage content of magnetic material in surface rocks probably averages less than 1 per cent. At a modest depth, a few tens of km, the Curie point will probably be reached, judging from the experiments on shift of Curie point with increasing pressure [10]. Under these conditions, the magnetic characteristics of the Earth's interior may closely resemble

those for free space, for a depth approaching that for the source of main field nearest the Earth's surface. Thus we may be able to calculate the main field at various depths within the Earth, from the spherical harmonic coefficients at the Earth's surface. The defects in the analytic continuation at the greater depths may be the only important factor limiting accuracy, rather than the small amount of magnetic matter known to exist in the Earth's crust.

We have not computed the field at various depths but have evaluated instead the current distribution over several thin spherical sheets, each concentric with the Earth. Any one of the computed distributions could reproduce the residual part of the main field at the surface of the ground.

Figures 1 to 8 give the current functions J for depths 0, 1000, 2000, and 3000 km for the main field and for the residual field. These become more complicated with increasing depth. They are found by summing the typical terms

$$J_n = (10/4\pi)[(2n+1)/n]\, V_n(a/r)^{n+1}$$

where J_n is the current function in amperes, a the radius of the Earth, r the radius of the spherical current sheet and V_n its potential at (r, θ).

It will be noted that the quantity $(a/r)^{n+1}$ becomes increasingly important as r diminishes, especially for larger values of n. Moreover, the series in V_n at $r = a$ does not converge rapidly. There are in fact neglected surface terms of degree greater than six needed to improve the fit of the potential at the Earth's surface. This means that the complex configuration for J shown for depth 3000 km is almost certain to be much too simple. Thus the current systems due to the thermoelectric forces recently discussed in a valuable and interesting series of papers by Elsasser [11] would be exceedingly complex. A highly complex current pattern is of course not impossible, yet we very much doubt from our work here that these currents arise from a depth as great as that postulated by Elsasser.

In drawing our isomagnetic charts over ocean areas, we believe we have noted indications of possible anomalies 1000 to 2000 km in linear cross-section. These anomalies may be only apparent rather than real, a consequence of defects in present survey data. However, it is our present opinion that they are very likely to be real, a point which could now be readily verified by means of measurements of total intensity by aeroplane [12]. Such anomalies could not arise from sources at 3000 km depth, except possibly through combinations of fantastic current patterns.

Smaller anomalies could and do arise in the Earth's crust. Anomalies of cross-section somewhat similar to the depth of the Earth's crust taken, say, to the Curie-point isotherm, are unlikely to arise from deeper sources. There is need for study of such anomalies, and an opportunity for important scientific contribution by those instituting magnetic surveys by aeroplane. It seems likely that some of these anomalies, because of their size, should be ascribed to sources within the mantle, and not to sources at depths as great as that of the central core.

We conclude that if the main field is due to electric currents the principal region of flow is likely to be below 1000 km but above 3000 km depth.

The current patterns calculated at various depths likewise give the strength of equivalent magnetic shells in electromagnetic units at those depths, on dividing the current shown in amperes by ten. With this model, the permissible ranges in depths of source will be from about 3000 km depth and upwards almost to the Earth's surface. However, the surface rocks do not show anything approaching the degree of magnetic polarization required, and the Curie point for magnetic materials is reached at a few tens of kilometers.

TABLES 1-32

Table 1. Scalings of values of north component (X) of magnetic field intensity for 1945 expressed in units of 10^{-4} CGS from U. S. Hydrographic Office charts

Geographic east longitude in degrees	Geographic colatitude in degrees								
	10	20	30	40	50	60	70	80	90
30	674	1063	1504	1968	2529	3040	3400	3429	3093
60	502	874	1413	1965	2599	3187	3620	3719	3423
90	270	688	1297	2044	2859	3500	3938	4057	3854
120	278	730	1448	2163	2885	3415	3770	3928	3876
150	363	1015	1722	2330	2759	3068	3310	3493	3636
180	331	1116	1838	2251	2469	2692	2917	3204	3461
210	174	818	1428	1908	2314	2587	2870	3152	3317
240	-17	266	904	1557	2201	2672	3016	3232	3237
270	-82	109	554	1160	1865	2464	2946	3176	3147
300	112	413	732	1217	1707	2156	2558	2838	2953
330	444	767	1148	1621	2086	2432	2684	2812	2700
360	692	1072	1414	1895	2384	2881	3163	3125	2762

Geographic east longitude in degrees	Geographic colatitude in degrees							
	100	110	120	130	140	150	160	170
30	2442	1789	1330	1235	1316	1307	1361	1045
60	2814	2187	1634	1381	1306	1249	1040	307
90	3333	2661	2007	1480	1139	850	389	-480
120	3585	3178	2550	1848	1183	610	94	-890
150	3592	3294	2755	2130	1420	670	-87	-940
180	3504	3267	2840	2337	1766	1035	250	-610
210	3305	3123	2839	2476	2049	1445	690	-140
240	3117	2969	2753	2533	2231	1769	1110	370
270	3063	2776	2574	2403	2339	2115	1600	1038
300	2803	2558	2360	2292	2354	2380	2070	1572
330	2436	2100	1863	1850	1989	2105	2155	1850
360	2265	1782	1483	1401	1529	1623	1622	1641

Table 2. Scalings of values of east component (Y) of magnetic field intensity for 1945 expressed in units of 10^{-4} CGS from U. S. Hydrographic Office charts

Geographic east longitude in degrees	Geographic colatitude in degrees								
	10	20	30	40	50	60	70	80	90
30	92	123	139	96	79	32	-30	-90	-205
60	291	371	368	315	241	128	32	-78	-221
90	267	272	243	161	55	-37	-117	-156	-222
120	113	-120	-255	-343	-293	-185	-26	117	176
150	70	-174	-310	-303	-251	-107	58	214	318
180	165	177	206	292	395	455	504	542	585
210	207	484	675	694	743	659	589	494	537
240	99	338	591	706	732	691	625	558	530
270	-160	-144	-133	6	130	285	377	469	521
300	-436	-650	-652	-692	-659	-606	-520	-424	-316
330	-432	-626	-671	-735	-759	-861	-988	-1074	-1058
360	-161	-247	-275	-307	-356.	-410	-484	-590	-704

Geographic east longitude in degrees	Geographic colatitude in degrees							
	100	110	120	130	140	150	160	170
30	-296	-384	-437	-549	-677	-922	-1361	-1640
60	-381	-570	-755	-939	-1119	-1377	-1652	-1741
90	-333	-566	-770	-1006	-1151	-1232	-1366	-1348
120	182	117	0	-207	-403	-463	-442	-771
150	365	416	441	414	341	269	50	30
180	630	694	719	768	779	783	706	727
210	607	698	803	887	977	1001	1011	1140
240	578	653	774	907	1059	1239	1381	1506
270	595	646	748	913	1066	1192	1347	1377
300	-201	-89	41	192	348	528	778	746
330	-964	-836	-700	-583	-452	-251	-105	-32
360	-793	-816	-789	-751	-743	-696	-825	-967

Table 3. Scalings of values of vertical component (Z) of magnetic field intensity for 1945 expressed in units of 10^{-4} CGS from U. S. Hydrographic Office charts

Geographic east longitude in degrees	Geographic colatitude in degrees								
	10	20	30	40	50	60	70	80	90
30	5360	5110	4810	4370	3710	2790	1470	- 20	-1390
60	5530	5460	5400	4940	4250	3260	1820	370	-1120
90	5730	5840	5840	5440	4650	3420	1840	160	-1530
120	5780	6110	5930	5420	4520	3280	1870	340	-1180
150	5780	5720	5330	4580	3580	2620	1540	460	- 870
180	5730	5510	5080	4180	3370	2550	1750	840	- 320
210	5760	5640	5320	4720	3940	3180	2270	1320	140
240	5790	5930	5920	5560	4870	3960	2850	1630	430
270	5690	5810	6080	5980	5480	4680	3610	2350	1120
300	5510	5590	5530	5380	5020	4410	3550	2580	1490
330	5260	5130	4930	4620	4070	3220	2330	1330	300
360	5190	5010	4690	4270	3610	2710	1470	80	-1130

Geographic east longitude in degrees	Geographic colatitude in degrees							
	100	110	120	130	140	150	160	170
30	-2380	-2850	-2980	-3080	-3300	-3800	-4730	-5450
60	-2330	-3050	-3260	-3530	-3760	-4480	-5320	-5800
90	-3000	-4040	-4670	-5020	-5150	-5530	-5980	-6170
120	-2710	-4060	-5130	-5850	-6420	-6510	-6630	-6530
150	-2280	-3670	-4860	-5760	-6420	-6850	-6970	-6630
180	-1680	-3030	-4170	-5070	-5830	-6540	-6670	-6560
210	-1120	-2270	-3360	-4280	-5140	-5970	-6290	-6370
240	- 670	-1710	-2670	-3580	-4430	-5350	-5630	-5910
270	- 40	-1070	-1870	-2580	-3330	-4120	-4770	-5470
300	440	- 430	-1070	-1660	-2360	-3310	-4240	-5180
330	- 570	-1180	-1560	-1880	-2400	-3110	-4120	-5110
360	-1890	-2290	-2470	-2630	-2950	-3370	-4270	-5200

Table 4. Values of spherical harmonic coefficients, main field, 1945 expressed in units of 10^{-4} CGS

m	n	A_n^m		α_n^m	B_n^m		β_n^m
		X	Y	Z	X	Y	Z
	1	-3057		6114			
	2	- 253		357			
	3	344		- 427			
	4	368		- 499			
	5	- 121		192			
	6	34		- 48			
1	1	- 190	- 230	455	577	584	-1158
1	2	594	590	- 882	- 329	- 334	514
1	3	- 510	- 527	703	- 154	- 157	187
1	4	309	313	- 375	70	43	- 58
1	5	163	116	- 219	- 12	42	- 5
1	6	38	87	- 29	1	- 85	32
2	2	331	322	- 495	124	90	- 142
2	3	364	362	- 481	61	50	- 82
2	4	244	217	- 296	- 103	- 119	146
2	5	82	115	- 82	47	24	- 52
2	6	10	- 41	- 35	73	103	- 88
3	3	243	282	- 369	17		- 1
3	4	- 153	- 151	203	- 41	- 25	52
3	5	- 35	- 25	27	- 8	- 14	- 1
3	6	- 159	- 150	170	- 18	0	13
4	4	123	120	- 146	- 51	- 51	61
4	5	- 71	- 74	78	- 63	- 72	77
4	6	- 13	- 19	19	2	0	4
5	5	- 30	- 38	59	26	51	- 55
5	6	14	22	- 27	0	- 9	4
6	6	- 60	- 69	66	- 35	- 17	

Table 5. Observed minus computed values of north component (X) of magnetic field intensity for 1945 expressed in units of 10^{-4} CGS

Geographic east longitude in degrees	Geographic colatitude in degrees								
	10	20	30	40	50	60	70	80	90
30	-115	-76	12	15	3	-48	-43	-9	35
60	-102	-83	10	7	5	-23	-19	-4	13
90	-105	-41	7	28	58	0	-24	-20	33
120	-20	-30	34	-1	17	-6	-7	-3	-2
150	-12	-32	-29	-15	-6	14	16	-20	-9
180	-69	-50	17	8	-2	34	-5	-40	-19
210	-58	-39	-8	-2	27	-26	-42	-6	20
240	-11	-99	39	69	54	-39	-60	10	29
270	-20	-41	2	10	18	-27	-1	15	-14
300	-47	30	6	32	10	-26	-16	13	48
330	-67	-40	0	43	39	-19	-20	42	34
360	-73	-23	-11	25	-23	-7	21	36	-5

Geographic east longitude in degrees	Geographic colatitude in degrees							
	100	110	120	130	140	150	160	170
30	-3	-36	-67	-8	5	-140	-113	-220
60	1	28	-34	-41	-35	-3	29	-276
90	54	45	6	-44	-22	36	3	-330
120	-24	45	43	21	14	57	150	-203
150	9	24	9	24	-5	-40	-34	-104
180	16	29	30	35	29	-29	-6	-7
210	14	-16	-27	-16	42	51	23	-41
240	3	-13	-47	4	75	78	-47	-205
270	40	-52	-56	-44	74	72	-129	-252
300	-15	-65	-57	-1	86	120	-71	-250
330	-1	-56	-57	29	**100**	58	23	-129
360	-35	-49	-3	54	98	-28	-205	-117

Table 6. Observed minus computed values of east component (Y) of magnetic field intensity for 1945 expressed in units of 10^{-4} CGS

Geographic east longitude in degrees	Geographic colatitude in degrees								
	10	20	30	40	50	60	70	80	90
30	-12	-24	6	-5	7	-8	-21	-3	-20
60	-39	-51	-57	-48	-24	-29	-16	-12	-24
90	-50	-50	-39	-41	-52	-58	-76	-60	-48
120	-40	-82	-57	-54	-8	5	11	1	-39
150	2	-15	51	41	10	-2	-6	14	27
180	10	24	13	28	50	38	30	21	15
210	-27	7	-4	-85	-18	-2	39	2	24
240	3	-13	30	19	11	6	8	-1	-10
270	70	28	-29	20	29	56	31	35	31
300	59	-41	24	4	10	-4	-13	-26	-27
330	63	-11	12	3	50	39	1	-31	-15
360	78	32	26	10	-7	5	32	42	28

Geographic east longitude in degrees	Geographic colatitude in degrees							
	100	110	120	130	140	150	160	170
30	-11	-8	31	34	62	9	-238	**-379**
60	-33	-50	-47	-37	-26	-110	-244	-242
90	-27	-67	-39	-48	-12	22	-56	-17
120	-42	-22	16	-3	-13	87	232	-17
150	17	28	26	-1	-25	4	-86	6
180	3	7	-17	2	6	18	-47	-18
210	12	2	20	33	48	-28	-140	-120
240	9	7	12	0	-11	5	2	24
270	58	41	32	46	35	19	77	59
300	-20	-20	-18	-19	-30	-13	103	-13
330	25	56	68	40	8	35	19	-22
360	-1	-12	-7	-2	-17	23	-100	-234

Table 7. Observed minus computed values of vertical component (Z) of magnetic field intensity for 1945 expressed in units of 10^{-4} CGS

Geographic east longitude in degrees	Geographic colatitude in degrees: 10	20	30	40	50	60	70	80	90
30	-24	55	69	11	-29	44	67	67	43
60	-28	40	188	93	38	48	-29	87	89
90	-26	-15	32	-12	-25	-33	-29	52	53
120	-89	105	33	13	9	-12	-1	-7	25
150	-88	-77	-31	-16	-61	-7	-40	26	-5
180	-95	-84	96	10	11	-72	-106	-53	7
210	-52	-42	37	30	-43	-15	-32	47	15
240	-13	31	45	-43	-117	-73	-6	10	-15
270	-35	-72	62	37	-27	3	64	69	76
300	-57	43	5	4	8	4	-31	-12	-34
330	-143	-23	17	49	49	-16	49	62	-3
360	-136	49	49	20	2	84	83	-17	-102

Geographic east longitude in degrees	Geographic colatitude in degrees: 100	110	120	130	140	150	160	170
30	12	28	75	34	3	-45	-278	-207
60	26	-20	123	81	192	-1	-226	-178
90	-18	-66	-77	-33	163	113	-51	-115
120	-7	-7	-27	5	-100	51	-28	-122
150	-8	-15	-48	-50	-80	-125	-140	-57
180	21	-3	-11	7	-6	-146	4	-33
210	-42	-29	-4	73	82	-70	-2	-69
240	-33	-62	-5	46	58	-161	53	27
270	26	-41	4	72	80	47	124	42
300	-49	-3	77	124	95	-44	-32	-30
330	-43	5	68	107	6	-71	-188	-141
360	-36	68	132	96	-39	-38	-207	-191

Table 8(A). Vertical air-earth currents computed from H- and D-charts of main field for 1945 expressed in milliamperes per kilometer squared

Latitude	Longitude east: 0°/30°	30°/60°	60°/90°	90°/120°	120°/150°	150°/180°	180°/210°	210°/240°	240°/270°	270°/300°	300°/330°	330°/360°
50°-40° N	+6	-39	+7	-60	-5	+64	+52	+42	-1	+27	+70	-14
40°-30° N	+17	-47	+42	+3	+6	+3	+10	-7	-52	+60	-53	-55
30°-20° N	-77	-37	+8	-15	+49	-55	-39	+80	-9	-6	-59	-48
20°-10° N	-24	+73	-62	+9	-9	-12	-12	+43	+52	-20	-27	-95
10°- 0° N	-49	+79	-37	-3	+7	-1	-12	-3	+19	-19	+18	-100
0°-10° S	-97	-6	+16	+4	-46	-9	+12	+33	-1	-33	+12	+25
10°-20° S	-21	-60	+53	-41	+17	-2	-43	+33	-47	+9	+62	+121
20°-30° S	+17	+77	+150	+57	0	+35	-59	+13	-90	+28	+31	+97
30°-40° S	-48	+27	+100	+66	0	-80	-70	-43	-67	+29	+10	+9

Table 8(B). Mean values of vertical air-earth currents

Epoch	America	"Zone"	Eurasia	1/2 Span	General mean
1885	+36.7	+26.7	-81.6	±59.2	-15.2
1922	+20.2	-30.1	-35.0	±27.6	-11.2
1945	-0.6	-6.5	+2.4	±0.9	-0.3

Table 9. The first eight Gauss coefficients of the Earth's magnetic potential (V) expressed in units of 10^{-4} CGS

Source	Epoch	g_1^0	g_1^1	h_1^1	g_2^0	g_2^1	h_2^1	g_2^2	h_2^2
Gauss	1835	-3235	-311	+625	+51	+292	+12	-2	+157
Erman-Petersen	1829	-3201	-284	+601	-8	+257	-4	-14	+146
Adams	1845	-3219	-278	+578	+9	+284	-10	+4	+135
Adams	1880	-3168	-243	+603	-49	+297	-75	+61	+149
Fritsche	1885	-3164	-241	+591	-35	+286	-75	+68	+142
Schmidt	1885	-3168	-222	+595	-50	+278	-71	+65	+149
Dyson and Furner	1922	-3095	-226	+592	-89	+299	-124	+144	+84
Afanasieva (8)	1945	-3032	-229	+590	-125	+288	-146	+150	+48
Vestine and Lange	1945	-3057	-211	+581	-127	+296	-166	+164	+54

Table 10. Computed values of north component (X) of magnetic field intensity for 1945 at height 100 km expressed in units of 10^{-4} CGS

Geographic east longitude in degrees	Geographic colatitude in degrees								
	10	20	30	40	50	60	70	80	90
30	748	1093	1441	1881	2417	2937	3264	3258	2909
60	584	927	1357	1885	2484	3057	3453	3529	3241
90	379	722	1254	1936	2671	3322	3753	3861	3626
120	309	751	1367	2069	2731	3253	3590	3736	3685
150	376	1009	1671	2232	2637	2918	3149	3352	3470
180	391	1110	1729	2136	2366	2553	2804	3098	3312
210	229	820	1370	1823	2187	2500	2783	3014	3143
240	3	364	841	1427	2046	2575	2922	3067	3060
270	- 52	162	548	1111	1763	2365	2796	3003	3010
300	152	377	709	1145	1628	2085	2455	2691	2768
330	480	774	1106	1516	1957	2337	2575	2641	2546
360	720	1049	1374	1798	2299	2745	2982	2934	2639

Geographic east longitude in degrees	Geographic colatitude in degrees							
	100	110	120	130	140	150	160	170
30	2344	1770	1368	1215	1264	1375	1385	1180
60	2690	2084	1620	1377	1282	1181	945	538
90	3125	2508	1928	1470	1115	774	361	- 148
120	3430	2980	2390	1747	1122	533	- 49	- 648
150	3405	3108	2613	2008	1359	678	- 47	- 784
180	3315	3080	2678	2195	1652	1009	245	- 561
210	3136	2991	2731	2373	1908	1325	638	- 82
240	2976	2848	2671	2411	2054	1613	1106	555
270	2887	2707	2519	2343	2164	1946	1643	1224
300	2690	2511	2321	2203	2169	2149	2025	1717
330	2335	2075	1856	1761	1816	1949	2013	1860
360	2207	1771	1448	1315	1385	1576	1725	1647

Table 11. Computed values of north component (X) of magnetic field intensity for 1945 at height 300 km expressed in units of 10^{-4} CGS

Geographic east longitude in degrees	Geographic colatitude in degrees								
	10	20	30	40	50	60	70	80	90
30	676	1009	1342	1745	2217	2665	2943	2937	2640
60	546	871	1270	1749	2280	2779	3118	3182	2935
90	380	702	1183	1788	2434	3004	3379	3476	3275
120	323	729	1277	1898	2483	2949	3252	3383	3336
150	373	938	1525	2029	2402	2669	2882	3060	3153
180	373	1010	1563	1942	2172	2357	2583	2833	3007
210	221	753	1249	1665	2003	2292	2548	2751	2864
240	19	357	792	1315	1861	2331	2645	2786	2792
270	- 35	180	536	1038	1611	2141	2524	2717	2736
300	138	362	673	1069	1501	1909	2237	2448	2519
330	425	713	1027	1400	1792	2129	2342	2405	2328
360	641	963	1276	1662	2102	2487	2693	2656	2405

Geographic east longitude in degrees	Geographic colatitude in degrees							
	100	110	120	130	140	150	160	170
30	2158	1663	1308	1158	1174	1243	1228	1030
60	2464	1940	1527	1291	1176	1057	829	460
90	2843	2306	1790	1369	1029	702	318	- 142
120	3105	2703	2176	1599	1033	494	- 37	- 577
150	3084	2815	2373	1829	1240	619	- 35	- 691
180	3003	2795	2438	1999	1499	911	227	- 485
210	2854	2723	2485	2155	1730	1202	588	- 52
240	2720	2604	2436	2195	1871	1471	1014	518
270	2638	2490	2316	2151	1980	1772	1489	1107
300	2457	2306	2144	2034	1988	1948	1818	1533
330	2147	1924	1734	1646	1679	1772	1803	1649
360	2035	1635	1374	1250	1295	1439	1541	1452

Table 12. Computed values of north component (X) of magnetic field intensity for 1945 at height 500 km expressed in units of 10^{-4} CGS

Geographic east longitude in degrees	Geographic colatitude in degrees								
	10	20	30	40	50	60	70	80	90
30	614	932	1249	1618	2037	2426	2664	2658	2404
60	511	819	1188	1623	2096	2533	2826	2880	2668
90	376	679	1115	1655	2225	2724	3055	3140	2968
120	330	703	1194	1745	2265	2682	2955	3073	3029
150	366	873	1396	1851	2195	2446	2643	2799	2873
180	354	922	1419	1772	1997	2178	2382	2597	2740
210	213	692	1142	1525	1839	2106	2338	2519	2616
240	30	348	744	1213	1699	2117	2403	2538	2553
270	- 22	190	519	968	1476	1944	2289	2467	2495
300	126	346	637	997	1386	1751	2045	2234	2300
330	378	657	954	1293	1645	1944	2137	2197	2133
360	574	885	1185	1537	1926	2262	2442	2413	2200

Geographic east longitude in degrees	Geographic colatitude in degrees							
	100	110	120	130	140	150	160	170
30	1990	1562	1246	1100	1093	1129	1095	905
60	2262	1806	1436	1209	1081	951	732	395
90	2594	2123	1663	1275	952	640	282	- 136
120	2821	2459	1988	1469	954	460	- 26	- 515
150	2803	2558	2161	1670	1134	568	- 23	- 610
180	2730	2544	2224	1825	1365	828	212	- 421
210	2606	2485	2268	1964	1574	1094	542	- 27
240	2493	2386	2229	2006	1709	1346	932	484
270	2416	2283	2132	1979	1816	1618	1354	1005
300	2250	2123	1982	1881	1827	1772	1639	1375
330	1979	1787	1621	1539	1554	1616	1621	1469
360	1880	1552	1301	1186	1211	1317	1384	1287

Table 13. Computed values of north component (X) of magnetic field intensity for 1945 at height 1000 km expressed in units of 10^{-4} CGS

Geographic east longitude in degrees	Geographic colatitude in degrees								
	10	20	30	40	50	60	70	80	90
30	490	770	1045	1344	1661	1942	2109	2105	1929
60	435	700	1006	1351	1711	2032	2242	2279	2130
90	354	613	959	1371	1797	2166	2409	2475	2355
120	324	630	1011	1428	1823	2143	2356	2448	2411
150	337	732	1135	1492	1774	1986	2147	2262	2304
180	308	744	1132	1426	1632	1797	1959	2109	2200
210	188	567	925	1237	1498	1718	1903	2040	2111
240	45	312	636	1000	1369	1690	1917	2036	2062
270	1	196	468	817	1199	1552	1818	1967	2004
300	100	305	552	840	1143	1425	1652	1799	1855
330	288	538	793	1067	1340	1570	1720	1774	1735
360	443	722	985	1269	1562	1807	1940	1926	1780

Geographic east longitude in degrees	Geographic colatitude in degrees								
	100	110	120	130	140	150	160	170	
30	1640	1332	1093	961	918	902	838	668	
60	1843	1513	1228	1027	887	746	550	277	
90	2087	1739	1387	1070	790	517	217	-118	
120	2247	1967	1604	1198	788	388	-5	-393	
150	2237	2040	1731	1345	918	465	-0	-454	
180	2181	2035	1788	1469	1095	663	183	-298	
210	2099	2001	1824	1577	1261	880	451	14	
240	2023	1937	1805	1621	1381	1091	763	411	
270	1959	1866	1749	1622	1479	1305	1082	801	
300	1827	1742	1640	1555	1491	1417	1287	1067	
330	1629	1493	1372	1301	1289	1299	1265	1123	
360	1555	1318	1132	1034	1027	1067	1076	971	

Table 14. Computed values of north component (X) of magnetic field intensity for 1945 at height 5000 km expressed in units of 10^{-4} CGS

Geographic east longitude in degrees	Geographic colatitude in degrees								
	10	20	30	40	50	60	70	80	90
30	129	220	306	384	451	502	531	536	517
60	144	229	315	396	470	528	563	571	553
90	147	230	317	404	484	549	591	605	589
120	143	230	321	410	490	554	597	615	605
150	129	227	321	407	452	538	578	599	597
180	103	205	300	384	453	508	549	574	580
210	64	161	254	340	414	475	522	552	564
240	26	113	201	289	370	441	497	533	550
270	9	87	169	253	335	408	468	509	531
300	21	101	180	257	331	395	448	485	505
330	57	144	226	302	368	423	461	483	488
360	99	191	276	353	418	466	497	505	493

Geographic east longitude in degrees	Geographic colatitude in degrees								
	100	110	120	130	140	150	160	170	
30	479	431	381	333	288	240	186	119	
60	512	456	393	328	262	193	118	38	
90	547	484	409	326	239	151	59	-32	
120	569	508	429	336	235	131	27	-72	
150	571	520	448	357	254	145	35	-69	
180	564	525	465	386	292	188	80	-24	
210	556	529	481	417	337	245	148	50	
240	548	529	493	443	380	305	223	136	
270	535	523	497	460	413	355	286	208	
300	510	501	481	453	417	372	316	247	
330	479	461	437	410	381	346	301	240	
360	466	431	394	360	328	293	251	193	

Table 15. Computed values of east component (Y) of magnetic field intensity for 1945 at height 100 km expressed in units of 10^{-4} CGS

Geographic east longitude in degrees	Geographic colatitude in degrees								
	10	20	30	40	50	60	70	80	90
30	82	124	115	87	59	27	-20	-93	-185
60	292	378	384	328	240	141	-39	-60	-191
90	285	288	252	181	96	18	-40	-92	-166
120	142	-32	-178	-260	-257	-170	-32	114	194
150	74	-133	-272	-303	-228	-86	67	174	279
180	157	156	192	257	330	397	450	495	542
210	230	452	637	729	715	627	529	478	498
240	99	333	526	643	676	645	586	535	519
270	-206	-153	-90	-6	98	216	324	405	460
300	-458	-565	-628	-648	-624	-563	-476	-376	-275
330	-466	-579	-646	-698	-766	-849	-930	-980	-980
360	-233	-270	-292	-309	-341	-403	-496	-611	-695

Geographic east longitude in degrees	Geographic colatitude in degrees							
	100	110	120	130	140	150	160	170
30	-280	-368	-456	-565	-711	-888	-1063	-1189
60	-333	-494	-670	-851	-1028	-1190	-1321	-1405
90	-289	-467	-681	-891	-1058	-1166	-1221	-1242
120	202	124	-18	-191	-362	-510	-624	-698
150	333	370	394	392	345	252	134	33
180	596	651	698	726	734	727	717	709
210	571	664	746	815	887	980	1092	1190
240	548	620	728	862	1013	1164	1298	1392
270	506	571	674	813	963	1094	1183	1229
300	-174	-69	51	192	347	498	622	700
330	-929	-840	-723	-588	-436	-274	-125	-21
360	-750	-763	-743	-714	-692	-686	-691	-698

Table 16. Computed values of east component (Y) of magnetic field intensity for 1945 at height 300 km expressed in units of 10^{-4} CGS

Geographic east longitude in degrees	Geographic colatitude in degrees								
	10	20	30	40	50	60	70	80	90
30	46	87	83	62	36	6	-38	-104	-185
60	228	304	313	269	197	113	24	-71	-180
90	231	233	204	146	77	13	-37	-85	-151
120	125	-22	-144	-212	-209	-138	-24	88	161
150	81	-92	-207	-233	-172	-56	73	182	257
180	160	159	189	242	304	361	407	449	491
210	221	407	562	642	634	567	490	450	466
240	104	301	463	565	596	575	530	491	480
270	-166	-122	-67	3	93	192	284	355	406
300	-395	-488	-544	-564	-546	-495	-423	-337	-250
330	-414	-515	-577	-629	-688	-759	-826	-867	-867
360	-222	-254	-275	-293	-324	-379	-468	-550	-628

Geographic east longitude in degrees	Geographic colatitude in degrees							
	100	110	120	130	140	150	160	170
30	-269	-349	-431	-530	-658	-808	-955	-1061
60	-305	-447	-601	-759	-914	-1055	-1168	-1241
90	-259	-413	-594	-773	-918	-1014	-1065	-1086
120	165	99	-21	-168	-314	-441	-538	-600
150	305	337	356	350	308	229	130	46
180	539	588	629	655	663	660	652	645
210	528	607	680	743	809	891	985	1065
240	507	571	665	781	910	1039	1152	1231
270	449	509	599	717	844	955	1033	1074
300	-162	-68	37	160	294	424	531	599
330	-823	-746	-645	-526	-393	-254	-128	-39
360	-676	-688	-673	-650	-631	-625	-628	-635

Table 17. Computed values of east component (Y) of magnetic field intensity for 1945 at height 500 km expressed in units of 10^{-4} CGS

Geographic east longitude in degrees	Geographic colatitude in degrees								
	10	20	30	40	50	60	70	80	90
30	18	57	57	40	18	- 10	- 52	- 111	- 182
60	177	245	255	222	161	89	11	- 73	- 170
90	188	190	165	118	62	8	- 35	- 78	- 139
120	111	- 14	- 116	- 173	- 170	- 111	- 18	75	134
150	86	- 58	- 156	- 179	- 129	- 32	77	170	236
180	160	160	185	229	280	329	371	408	447
210	212	368	499	568	566	514	453	422	436
240	106	273	411	499	529	515	480	451	445
270	- 135	- 97	- 49	11	87	172	251	313	360
300	- 343	- 424	- 475	- 492	- 479	- 438	- 376	- 303	- 227
330	- 370	- 460	- 519	- 567	- 620	- 681	- 737	- 771	- 770
360	- 211	- 239	- 259	- 277	- 306	- 356	- 426	- 503	- 570

Geographic east longitude in degrees	Geographic colatitude in degrees								
	100	110	120	130	140	150	160	170	
30	- 258	- 331	- 406	- 496	- 608	- 737	- 862	- 951	
60	- 281	- 406	- 541	- 680	- 816	- 939	-1037	-1100	
90	- 233	- 366	- 522	- 675	- 801	- 887	- 934	- 953	
120	136	79	- 23	- 148	- 273	- 382	- 466	- 518	
150	280	308	322	315	277	209	127	57	
180	489	533	569	593	602	600	594	589	
210	489	556	621	679	739	811	891	957	
240	470	526	608	709	820	931	1027	1094	
270	401	455	534	635	743	838	906	943	
300	- 149	- 66	27	135	251	362	455	515	
330	- 733	- 666	- 577	- 473	- 357	- 236	- 128	- 52	
360	- 611	- 623	- 612	- 593	- 577	- 572	- 574	- 579	

Table 18. Computed values of east component (Y) of magnetic field intensity for 1945 at height 1000 km expressed in units of 10^{-4} CGS

Geographic east longitude in degrees	Geographic colatitude in degrees								
	10	20	30	40	50	60	70	80	90
30	- 26	6	11	2	- 14	- 38	- 72	- 117	- 172
60	91	141	153	135	96	46	- 10	- 73	- 147
90	116	116	100	71	35	0	- 31	- 65	- 113
120	86	1	- 67	- 104	- 103	- 66	- 7	51	87
150	91	- 5	- 69	- 86	- 55	7	80	145	194
180	153	153	169	198	233	267	298	327	358
210	187	292	381	430	435	408	375	358	369
240	103	217	312	375	401	398	381	368	368
270	- 81	- 54	- 21	21	74	132	188	234	271
300	- 248	- 307	- 345	- 360	- 353	- 327	- 286	- 235	- 180
330	- 286	- 354	- 403	- 443	- 483	- 526	- 564	- 586	- 584
360	- 186	- 206	- 223	- 240	- 265	- 303	- 353	- 406	- 452

Geographic east longitude in degrees	Geographic colatitude in degrees								
	100	110	120	130	140	150	160	170	
30	- 230	- 288	- 348	- 418	- 500	- 590	- 675	- 736	
60	- 230	- 323	- 423	- 525	- 624	- 713	- 784	- 830	
90	- 182	- 276	- 386	- 493	- 583	- 647	- 685	- 702	
120	86	47	- 23	- 108	- 195	- 271	- 329	- 365	
150	226	246	254	246	218	171	117	72	
180	390	422	450	469	478	479	477	473	
210	405	452	501	547	594	646	701	744	
240	389	431	491	563	641	719	784	829	
270	306	350	407	478	552	618	666	694	
300	- 123	- 60	9	87	170	249	315	359	
330	- 557	- 509	- 445	- 368	- 285	- 199	- 124	- 71	
360	- 482	- 492	- 488	- 476	- 466	- 462	- 462	- 465	

Table 19. Computed values of east component (Y) of magnetic field intensity for 1945 at height 5000 km expressed in units of 10^{-4} CGS

Geographic east longitude in degrees	Geographic colatitude in degrees								
	10	20	30	40	50	60	70	80	90
30	-50	-45	-42	-42	-45	-49	-56	-65	-74
60	-23	-16	-13	-13	-16	-22	-30	-41	-53
90	1	1	0	-2	-6	-10	-15	-23	-31
120	24	15	8	4	3	4	7	9	10
150	47	38	32	30	31	35	42	48	54
180	66	66	68	71	75	79	84	90	96
210	69	79	89	96	101	104	106	108	112
240	46	58	70	79	86	91	95	98	102
270	2	6	10	16	23	30	38	46	54
300	-43	-51	-56	-59	-60	-58	-54	-48	-40
330	-70	-80	-90	-98	-105	-111	-115	-117	-116
360	-70	-73	-77	-82	-88	-94	-101	-107	-113

Geographic east longitude in degrees	Geographic colatitude in degrees							
	100	110	120	130	140	150	160	170
30	-85	-97	-109	-121	-133	-144	-154	-161
60	-67	-82	-98	-114	-128	-141	-152	-159
90	-42	-55	-68	-82	-94	-104	-111	-115
120	8	3	-4	-13	-22	-30	-36	-40
150	59	61	62	60	57	54	50	47
180	101	107	111	115	118	120	121	122
210	118	124	132	140	148	155	160	164
240	108	116	124	134	143	152	158	162
270	62	71	79	89	98	106	112	116
300	-31	-21	-10	0	11	22	31	37
330	-112	-106	-97	-87	-76	-66	-57	-50
360	-118	-121	-122	-122	-122	-122	-122	-122

Table 20. Computed values of vertical component (Z) of magnetic field intensity for 1945 at height 100 km expressed in units of 10^{-4} CGS

Geographic east longitude in degrees	Geographic colatitude in degrees								
	10	20	30	40	50	60	70	80	90
30	5170	4856	4546	4166	3564	2622	1360	-40	-1303
60	5327	5188	4977	4611	3986	3018	1721	243	-1141
90	5505	5581	5520	5169	4430	3278	1790	133	-1447
120	5606	5714	5593	5116	4260	3099	1745	297	-1154
150	5606	5526	5110	4389	3491	2531	1529	429	-806
180	5569	5346	4772	4002	3221	2496	1740	811	-346
210	5559	5431	5053	4491	3821	3070	2217	1233	123
240	5554	5633	5596	5324	4731	3821	2706	1534	402
270	5485	5622	5734	5651	5236	4458	3398	2207	1010
300	5341	5316	5282	5124	4762	4171	3377	2434	1409
330	5190	4952	4714	4380	3853	3111	2210	1248	314
360	5118	4771	4453	4059	3430	2488	1313	96	-964

Geographic east longitude in degrees	Geographic colatitude in degrees							
	100	110	120	130	140	150	160	170
30	-2236	-2739	-2924	-3006	-3199	-3628	-4277	-5011
60	-2240	-2903	-3243	-3481	-3816	-4311	-4880	-5365
90	-2802	-3762	-4374	-4767	-5084	-5395	-5658	-5768
120	-2581	-3837	-4844	-5560	-6009	-6242	-6282	-6096
150	-2159	-3464	-4581	-5438	-6038	-6400	-6493	-6248
180	-1635	-2882	-3955	-4833	-5548	-6085	-6344	-6203
210	-1021	-2152	-3205	-4155	-4977	-5613	-5977	-5989
240	-609	-1584	-2536	-3448	-4267	-4933	-5404	-5648
270	-37	-970	-1790	-2540	-3266	-3984	-4670	-5252
300	453	-399	-1104	-1926	-2377	-3150	-4036	-4917
330	-478	-1108	-1564	-1725	-2339	-2944	-3784	-4751
360	-1746	-2229	-2474	-2612	-2808	-3219	-3909	-4791

Table 21. Computed values of vertical component (Z) of magnetic field intensity for 1945 at height 300 km expressed in units of 10^{-4} CGS

Geographic east longitude in degrees	Geographic colatitude in degrees								
	10	20	30	40	50	60	70	80	90
30	4771	4485	4184	3805	3230	2366	1235	- 9	-1142
60	4899	4762	4549	4189	3597	2708	1538	220	-1031
90	5044	5083	4995	4653	3971	2931	1602	127	-1300
120	5126	5188	5049	4603	3828	2785	1565	258	-1069
150	5126	5033	4651	4004	3195	2316	1389	373	- 762
180	5098	4891	4382	3695	2981	2297	1578	714	- 336
210	5095	4972	4628	4118	3502	2806	2015	1112	111
240	5096	5149	5092	4829	4287	3473	2476	1422	406
270	5042	5146	5217	5115	4728	4028	3083	2019	961
300	4922	4890	4839	4674	4328	3781	3056	2201	1289
330	4794	4577	4344	4019	3527	2848	2031	1160	320
360	4730	4416	4106	3718	3127	2273	1223	137	- 818

Geographic east longitude in degrees	Geographic colatitude in degrees							
	100	110	120	130	140	150	160	170
30	-1981	-2464	-2675	-2791	-2993	-3384	-3953	-4588
60	-2013	-2641	-2991	-3244	-3562	-3998	-4487	-4899
90	-2503	-3386	-3968	-4353	-4658	-4938	-5163	-5250
120	-2341	-3472	-4383	-5038	-5452	-5667	-5702	-5534
150	-1973	-3146	-4155	-4935	-5482	-5807	-5885	-5664
180	-1494	-2617	-3595	-4400	-5050	-5527	-5749	-5620
210	- 937	-1964	-2922	-3784	-4524	-5091	-5413	-5428
240	- 540	-1439	-2308	-3135	-3874	-4475	-4901	-5127
270	- 10	- 868	-1627	-2324	-2993	-3647	-4264	-4782
300	407	- 373	-1032	-1621	-2231	-2934	-3720	-4494
330	- 414	-1000	-1439	-1799	-2202	-2760	-3507	-4353
360	-1536	-1996	-2251	-2411	-2619	-3006	-3622	-4392

Table 22. Computed values of vertical component (Z) of magnetic field intensity for 1945 at height 500 km expressed in units of 10^{-4} CGS

Geographic east longitude in degrees	Geographic colatitude in degrees								
	10	20	30	40	50	60	70	80	90
30	4408	4147	3855	3484	2938	2145	1126	16	- 999
60	4513	4378	4167	3816	3257	2439	1382	200	- 922
90	4632	4643	4536	4204	3574	2632	1439	120	-1158
120	4699	4726	4575	4158	3454	2512	1409	224	- 978
150	4699	4599	4246	3662	2929	2123	1265	326	- 710
180	4680	4487	4031	3415	2761	2118	1437	632	- 324
210	4682	4563	4249	3783	3216	2571	1839	1008	92
240	4686	4719	4649	4395	3899	3167	2272	1319	391
270	4644	4721	4762	4648	4286	3653	2807	1852	896
300	4543	4506	4443	4275	3946	3440	2775	1997	1170
330	4433	4235	4010	3698	3237	2614	1871	1079	314
360	4377	4092	3792	3415	2861	2084	1142	167	- 696

Geographic east longitude in degrees	Geographic colatitude in degrees							
	100	110	120	130	140	150	160	170
30	-1764	-2225	-2453	-2594	-2800	-3158	-3660	-4212
60	-1816	-2409	-2763	-3022	-3323	-3712	-4134	-4486
90	-2246	-3060	-3611	-3985	-4276	-4530	-4725	-4794
120	-2129	-3153	-3980	-4580	-4962	-5162	-5194	-5041
150	-1808	-2866	-3780	-4491	-4992	-5285	-5352	-5152
180	-1370	-2385	-3278	-4017	-4609	-5035	-5227	-5110
210	- 861	-1796	-2670	-3455	-4124	-4633	-4920	-4937
240	- 480	-1309	-2106	-2859	-3529	-4074	-4462	-4670
270	10	- 780	-1485	-2133	-2750	-3347	-3904	-4369
300	367	- 350	- 966	-1522	-2092	-2733	-3436	-4119
330	- 360	- 906	-1328	-1682	-2071	-2587	-3255	-4000
360	-1357	-1794	-2055	-2231	-2446	-2809	-3361	-4037

Table 23. Computed values of vertical component (Z) of magnetic field intensity for 1945 at height 1000 km expressed in units of 10^{-4} CGS

Geographic east longitude in degrees	Geographic colatitude in degrees								
	10	20	30	40	50	60	70	80	90
30	3639	3427	3166	2826	2352	1706	910	57	-729
60	3703	3577	3375	3057	2577	1909	1076	161	-711
90	3778	3744	3613	3310	2789	2043	1118	102	-887
120	3820	3793	3631	3275	2711	1967	1098	160	-790
150	3822	3713	3428	2960	2377	1721	1011	239	-597
180	3815	3653	3300	2819	2288	1740	1152	480	-289
210	3824	3718	3464	3088	2624	2088	1480	801	62
240	3834	3834	3747	3520	3118	2544	1847	1096	349
270	3810	3845	3837	3710	3403	2902	2246	1505	751
300	3744	3701	3622	3457	3170	2749	2211	1589	930
330	3666	3507	3306	3028	2639	2133	1538	906	291
360	3623	3397	3130	2790	2321	1700	966	209	-472

Geographic east longitude in degrees	Geographic colatitude in degrees							
	100	110	120	130	140	150	160	170
30	-1345	-1753	-1996	-2170	-2373	-2665	-2689	-3440
60	-1427	-1938	-2278	-2536	-2798	-3097	-3751	-3644
90	-1745	-2412	-2890	-3228	-3484	-3689	-4533	-3869
120	-1699	-2508	-3168	-3654	-3971	-4139	-4517	-4047
150	-1466	-2297	-3021	-3591	-3995	-4227	-3925	-4123
180	-1114	-1916	-2632	-3230	-3705	-4034	-3472	-4085
210	-703	-1453	-2154	-2781	-3309	-3705	-3577	-3950
240	-364	-1045	-1693	-2297	-2830	-3264	-3927	-3748
270	39	-609	-1196	-1737	-2247	-2729	-3870	-3528
300	287	-301	-822	-1300	-1781	-2296	-3188	-3351
330	-259	-720	-1096	-1426	-1774	-2200	-2365	-3271
360	-1014	-1399	-1655	-1850	-2067	-2377	-2103	-3305

Table 24. Computed values of vertical component (Z) of magnetic field intensity for 1945 at height 5000 km expressed in units of 10^{-4} CGS

Geographic east longitude in degrees	Geographic colatitude in degrees								
	10	20	30	40	50	60	70	80	90
30	1045	984	893	774	626	454	264	69	-118
60	1045	988	902	785	635	456	255	44	-161
90	1048	996	916	801	648	462	249	22	-202
120	1051	1001	918	799	644	456	244	18	-211
150	1056	1002	912	788	633	453	254	41	-177
180	1063	1012	924	803	657	489	305	108	-98
210	1072	1035	963	860	728	573	398	208	10
240	1080	1060	1010	929	816	672	503	317	123
270	1082	1069	1032	966	868	739	582	406	220
300	1075	1054	1009	938	840	716	570	407	235
330	1063	1023	956	864	746	607	451	287	120
360	1051	995	910	798	659	499	323	143	-29

Geographic east longitude in degrees	Geographic colatitude in degrees							
	100	110	120	130	140	150	160	170
30	-288	-433	-555	-660	-754	-840	-919	-985
60	-349	-513	-650	-763	-856	-932	-989	-1023
90	-412	-596	-749	-871	-962	-1024	-1057	-1059
120	-430	-629	-799	-933	-1028	-1084	-1102	-1083
150	-392	-594	-772	-918	-1024	-1089	-1110	-1088
180	-305	-504	-685	-839	-960	-1041	-1079	-1074
210	-190	-385	-566	-727	-860	-959	-1021	-1043
240	-71	-261	-440	-603	-744	-861	-949	-1005
270	32	-151	-325	-487	-636	-769	-881	-969
300	61	-108	-272	-427	-574	-712	-838	-946
330	-39	-190	-330	-462	-589	-713	-832	-941
360	-188	-327	-449	-559	-662	-764	-863	-955

Table 25. Computed values of magnetic potential (V), main field, for 1945 expressed in units of 10^5 CGS

Geographic east longitude in degrees	Geographic colatitude in degrees								
	10	20	30	40	50	60	70	80	90
30	-1844	-1736	-1590	-1400	-1152	- 839	- 473	- 87	277
60	-1857	-1771	-1641	-1455	-1202	- 879	- 496	- 83	317
90	-1877	-1818	-1707	-1525	-1257	- 905	- 487	- 37	404
120	-1891	-1834	-1715	-1516	-1235	- 884	- 482	- 52	384
150	-1897	-1818	-1663	-1434	-1148	- 823	- 470	- 91	307
180	-1903	-1815	-1647	-1419	-1156	- 871	- 562	- 219	156
210	-1914	-1854	-1726	-1539	-1305	-1032	- 725	- 386	- 26
240	-1925	-1906	-1839	-1709	-1507	-1235	- 912	- 559	- 201
270	-1922	-1918	-1881	-1788	-1622	-1379	-1075	- 733	- 380
300	-1900	-1871	-1810	-1705	-1544	-1328	-1063	- 761	- 441
330	-1870	-1796	-1689	-1538	-1336	-1085	- 797	- 491	- 187
360	-1848	-1743	-1604	-1422	-1185	- 889	- 551	- 201	125

Geographic east longitude in degrees	Geographic colatitude in degrees								
	100	110	120	130	140	150	160	170	
30	584	820	997	1141	1282	1436	1600	1755	
60	664	940	1151	1321	1473	1618	1746	1836	
90	801	1129	1385	1580	1728	1838	1906	1920	
120	802	1178	1493	1734	1900	1996	2024	1982	
150	711	1094	1430	1701	1897	2017	2054	2004	
180	545	922	1259	1544	1769	1926	2000	1981	
210	341	699	1034	1333	1584	1775	1890	1921	
240	150	489	812	1109	1370	1585	1744	1840	
270	- 35	290	593	875	1137	1377	1588	1757	
300	- 121	181	461	722	975	1227	1473	1695	
330	97	352	578	785	990	1208	1442	1673	
360	408	. 637	819	975	1128	1298	1493	1695	

Table 26. Computed values of magnetic potential (V), residual field, for 1945 expressed in units of 10^5 CGS

Geographic east longitude in degrees	Geographic colatitude in degrees								
	10	20	30	40	50	60	70	80	90
30	61	70	61	47	47	74	128	183	208
60	16	- 28	- 81	- 126	- 145	- 124	- 68	5	63
90	- 24	- 114	- 206	- 271	- 288	- 252	- 169	- 63	34
120	- 41	- 137	- 222	- 274	- 280	- 246	- 180	- 95	- 3
150	- 31	- 92	- 127	- 135	- 127	- 110	- 87	- 50	6
180	- 8	- 31	- 28	- 14	- 7	- 14	- 22	- 13	21
210	14	- 1	- 5	- 3	- 0	0	5	19	42
240	36	9	- 26	- 54	- 61	- 42	- 7	27	52
270	59	37	- 10	- 58	- 86	- 85	- 61	- 30	- 10
300	84	91	69	36	4	- 19	- 33	- 41	- 53
330	99	136	148	147	146	149	152	143	114
360	93	132	149	155	169	201	241	268	260

Geographic east longitude in degrees	Geographic colatitude in degrees								
	100	110	120	130	140	150	160	170	
30	178	90	- 35	- 162	- 254	- 285	- 253	- 174	
60	77	36	- 42	- 125	- 181	- 194	- 170	- 125	
90	98	115	91	44	- 1	- 32	- 49	- 61	
120	82	148	184	185	159	115	61	- 2	
150	76	145	196	218	212	179	120	34	
180	75	129	169	189	191	172	124	40	
210	70	98	120	134	137	123	84	15	
240	62	61	57	51	41	25	0	- 33	
270	- 9	- 28	- 59	- 92	- 116	- 123	- 114	- 95	
300	- 78	- 120	- 176	- 232	- 267	- 265	- 223	- 154	
330	56	- 30	- 134	- 236	- 308	- 327	- 284	- 191	
360	202	97	- 37	- 173	- 277	- 320	- 290	- 198	

Table 27. Computed values of the vertical gradient of north component of magnetic field intensity ($\partial X/\partial r$), main field, for 1945 expressed in units of 10^{-12} CGS

Geographic east longitude in degrees	Geographic colatitude in degrees								
	10	20	30	40	50	60	70	80	90
30	-420	-466	-525	-730	-1110	-1552	-1856	-1860	-1542
60	-205	-295	-462	-739	-1133	-1577	-1924	-2006	-1755
90	42	-64	-361	-815	-1342	-1832	-2160	-2231	-2018
120	126	-79	-478	-969	-1418	-1741	-1930	-2011	-1995
150	18	-386	-832	-1166	-1332	-1401	-1490	-1649	-1806
180	-85	-577	-960	-1108	-1080	-1067	-1214	-1495	-1741
210	-26	-379	-686	-894	-1030	-1160	-1319	-1481	-1587
240	109	-6	-250	-624	-1053	-1408	-1592	-1601	-1516
270	113	134	-31	-394	-864	-1295	-1567	-1641	-1561
300	-76	-60	-173	-408	-703	-992	-1230	-1383	-1418
330	-324	-334	-422	-637	-925	-1182	-1327	-1339	-1236
360	-465	-474	-516	-733	-1107	-1477	-1666	-1599	-1324

Geographic east longitude in degrees	Geographic colatitude in degrees							
	100	110	120	130	140	150	160	170
30	-1036	-555	-279	-277	-485	-758	-930	-891
60	-1268	-770	-475	-455	-604	-734	-698	-478
90	-1596	-1119	-743	-543	-476	-419	-264	17
120	-1858	-1584	-1212	-825	-492	-215	68	408
150	-1836	-1675	-1366	-1013	-680	-342	65	543
180	-1791	-1626	-1357	-1104	-874	-572	-116	442
210	-1598	-1522	-1395	-1237	-1024	-714	-294	186
240	-1430	-1378	-1329	-1227	-1049	-807	-523	-202
270	-1406	-1250	-1135	-1069	-1037	-996	-891	-678
300	-1324	-1145	-979	-927	-1013	-1154	-1209	-1080
330	-1049	-827	-649	-609	-751	-1012	-1232	-1242
360	-955	-608	-373	-321	-476	-778	-10·68	-1155

Table 28. Computed values of the vertical gradient of east component of magnetic field intensity ($\partial Y/\partial r$), main field, for 1945 expressed in units of 10^{-12} CGS

Geographic east longitude in degrees	Geographic colatitude in degrees								
	10	20	30	40	50	60	70	80	90
30	-232	-234	-191	-151	-135	-132	-117	-73	-10
60	-407	-465	-439	-359	-261	-171	-93	-21	58
90	-344	-353	-311	-223	-119	-32	18	43	82
120	-110	59	210	300	299	204	50	-109	-215
150	55	271	416	440	350	195	41	-66	-122
180	32	36	-3	-74	-151	-211	-247	-270	-294
210	-37	-261	-448	-527	-479	-347	-211	-141	-160
240	42	-186	-370	-469	-474	-411	-321	-245	-209
270	250	201	147	74	-25	-138	-238	-298	-319
300	385	464	504	506	470	403	314	223	140
330	308	377	392	401	444	521	606	661	665
360	58	90	93	81	82	120	198	298	384

Geographic east longitude in degrees	Geographic colatitude in degrees							
	100	110	120	130	140	150	160	170
30	49	90	123	179	287	446	618	745
60	154	268	395	530	666	794	901	970
90	172	325	518	704	841	911	930	928
120	-232	-160	-24	135	287	415	514	585
150	-151	-182	-219	-242	-219	-137	-17	94
180	-328	-367	-399	-410	-401	-383	-367	-363
210	-239	-325	-379	-405	-433	-501	-609	-721
240	-219	-270	-353	-461	-589	-724	-850	-943
270	-326	-355	-436	-564	-709	-831	-902	-927
300	69	-0	-84	-192	-321	-450	-553	-612
330	620	546	460	363	248	114	-19	-119
360	431	430	399	363	343	344	355	364

Table 29. Computed values of the vertical gradient of vertical component of magnetic field intensity ($\partial Z/\partial r$), main field, for 1945 expressed in units of 10^{-12} CGS

Geographic east longitude in degrees	Geographic colatitude in degrees								
	10	20	30	40	50	60	70	80	90
30	-2193	-2030	-2007	-2036	-1922	-1490	- 725	204	1024
60	-2374	-2372	-2398	-2388	-2231	-1806	-1068	- 132	748
90	-2584	-2824	-3003	-2981	-2664	-2018	-1092	- 22	991
120	-2709	-3009	-3141	-2971	-2493	-1809	-1034	- 234	574
150	-2707	-2805	-2611	-2172	-1653	-1193	- 794	- 337	281
180	-2645	-2560	-2173	-1677	-1297	-1096	- 930	- 584	27
210	-2600	-2584	-2384	-2089	-1785	-1489	-1148	- 699	- 141
240	-2561	-2735	-2871	-2841	-2543	-1982	-1280	- 599	- 42
270	-2467	-2679	-2943	-3075	-2929	-2473	-1794	-1046	- 364
300	-2316	-2367	-2487	-2548	-2470	-2230	-1844	-1344	- 787
330	-2176	-2057	-2049	-2017	-1840	-1482	-1001	- 481	0
360	-2123	-1933	-1918	-1924	-1731	-1227	- 491	277	887

Geographic east longitude in degrees	Geographic colatitude in degrees							
	100	110	120	130	140	150	160	170
30	1508	1595	1404	1163	1094	1312	1792	2394
60	1322	1491	1382	1258	1347	1701	2198	2651
90	1756	2180	2316	2330	2392	2573	2808	2962
120	1368	2083	2635	2988	3180	3281	3315	3225
150	1044	1810	2434	2866	3162	3379	3483	3358
180	795	1511	2050	2446	2808	3168	3408	3352
210	469	1061	1600	2100	2571	2979	3231	3226
240	404	825	1285	1780	2248	2625	2879	2990
270	183	599	923	1216	1530	1898	2306	2682
300	- 261	140	384	541	759	1162	1752	2399
330	387	626	702	680	713	970	1516	2243
360	1244	1351	1273	1112	1016	1143	1579	2248

Table 30. Computed values of the vertical gradient of north component of magnetic field intensity ($\partial X/\partial r$), residual field, for 1945 expressed in units of 10^{-12} CGS

Geographic east longitude in degrees	Geographic colatitude in degrees								
	10	20	30	40	50	60	70	80	90
30	- 120	74	238	234	24	- 280	- 485	- 433	- 102
60	228	373	419	329	90	- 237	- 507	- 555	- 315
90	561	685	595	320	- 64	- 448	- 714	- 765	- 578
120	659	682	490	175	- 131	- 351	- 478	- 544	- 555
150	488	315	81	- 70	- 86	- 43	- 61	- 192	- 366
180	262	8	- 154	- 106	86	228	172	- 60	- 301
210	173	65	- 10	- 7	39	60	16	- 72	- 147
240	174	309	307	157	- 71	- 254	- 303	- 216	- 77
270	93	370	451	321	62	- 185	- 307	- 271	- 121
300	- 108	162	298	297	215	111	24	- 15	21
330	- 294	- 51	105	117	34	- 46	- 50	39	203
360	- 313	- 75	117	115	- 68	- 279	- 446	- 198	115

Geographic east longitude in degrees	Geographic colatitude in degrees							
	100	110	120	130	140	150	160	170
30	486	780	942	793	400	- 82	- 485	- 691
60	230	518	677	527	177	- 176	- 382	- 412
90	- 112	140	366	383	239	63	- 29	- 1
120	- 376	- 329	- 108	93	213	256	291	376
150	- 344	- 398	- 230	- 53	74	185	348	573
180	- 277	- 307	- 160	- 65	- 24	61	282	594
210	- 58	- 152	- 123	- 101	- 59	49	245	486
240	133	38	11	- 4	20	74	145	232
270	172	196	248	209	98	- 39	- 141	- 159
300	256	305	410	359	131	- 186	- 447	- 548
330	520	601	708	636	344	- 99	- 530	- 773
360	593	778	922	845	525	27	- 483	- 807

Table 31. Computed values of the vertical gradient of east component of magnetic field intensity ($\partial Y/\partial r$), residual field, for 1945 expressed in units of 10^{-12} CGS

Geographic east longitude in degrees	Geographic colatitude in degrees								
	10	20	30	40	50	60	70	80	90
30	-519	-521	-241	-438	-422	-419	-404	-360	-297
60	-630	-688	-525	-582	-484	-394	-316	-244	-164
90	-443	-452	-411	-323	-218	-131	-81	-55	-16
120	-59	110	124	351	350	255	100	-58	-1.64
150	243	459	366	628	538	383	229	121	65
180	305	310	-3	199	122	62	26	3	-20
210	249	24	-398	-240	-192	-61	74	144	126
240	265	36	-284	-246	-251	-188	-98	-22	13
270	349	300	247	173	74	-39	-138	-199	-220
300	334	413	590	455	420	352	263	172	89
330	121	190	441	214	256	334	419	474	477
360	-215	-183	93	-191	-191	-153	-74	24	110

Geographic east longitude in degrees	Geographic colatitude in degrees							
	100	110	120	130	140	150	160	170
30	-237	-196	-163	-107	0	160	332	458
60	-68	45	172	308	443	571	678	747
90	73	225	418	605	742	812	831	829
120	-181	-109	26	186	338	465	565	636
150	35	5	-32	-55	-32	49	170	281
180	-54	-94	-125	-136	-128	-109	-94	-89
210	47	-38	-93	-118	-147	-214	-322	-434
240	3	-47	-130	-238	-366	-502	-627	-720
270	-226	-256	-336	-465	-610	-731	-803	-827
300	18	-51	-135	-243	-372	-501	-604	-663
330	433	359	273	176	61	-72	-206	-306
360	157	156	125	89	70	70	81	90

Table 32. Computed values of the vertical gradient of vertical component of magnetic field intensity ($\partial Z/\partial r$), residual field, for 1945 expressed in units of 10^{-12} CGS

Geographic east longitude in degrees	Geographic colatitude in degrees								
	10	20	30	40	50	60	70	80	90
30	624	641	436	103	-149	-139	164	604	922
60	396	205	-91	-423	-667	-690	-435	-1	373
90	156	-305	-782	-1127	-1232	-1052	-621	-61	443
120	26	-499	-934	-1133	-1081	-865	-588	-299	0
150	51	-251	-340	-253	-144	-139	-227	-276	-164
180	156	77	221	400	401	171	-131	-280	-170
210	253	156	160	182	143	38	-67	-99	-39
240	340	99	-190	-394	-405	-217	57	269	332
270	463	214	-175	-517	-659	-559	-295	-7	183
300	619	534	293	25	-179	-293	-320	-279	-213
330	737	801	667	474	352	343	402	457	446
360	747	840	674	408	271	384	680	973	1085

Geographic east longitude in degrees	Geographic colatitude in degrees							
	100	110	120	130	140	150	160	170
30	908	514	-123	-765	-1177	-1232	-948	-459
60	453	154	-382	-879	-1099	-979	-635	-250
90	717	680	402	59	-165	-194	-85	31
120	304	559	698	697	605	500	413	289
150	105	406	608	674	669	662	624	445
180	99	339	438	443	474	574	634	481
210	70	171	248	327	431	536	560	407
240	273	192	170	216	282	318	301	219
270	222	128	-42	-215	-323	-321	-212	-58
300	-196	-305	-559	-870	-1078	-1045	-757	-337
330	326	60	-351	-829	-1206	-1300	-1037	-515
360	939	553	5	-586	-1062	-1251	-1059	-552

FIGURES A-G and 1-8

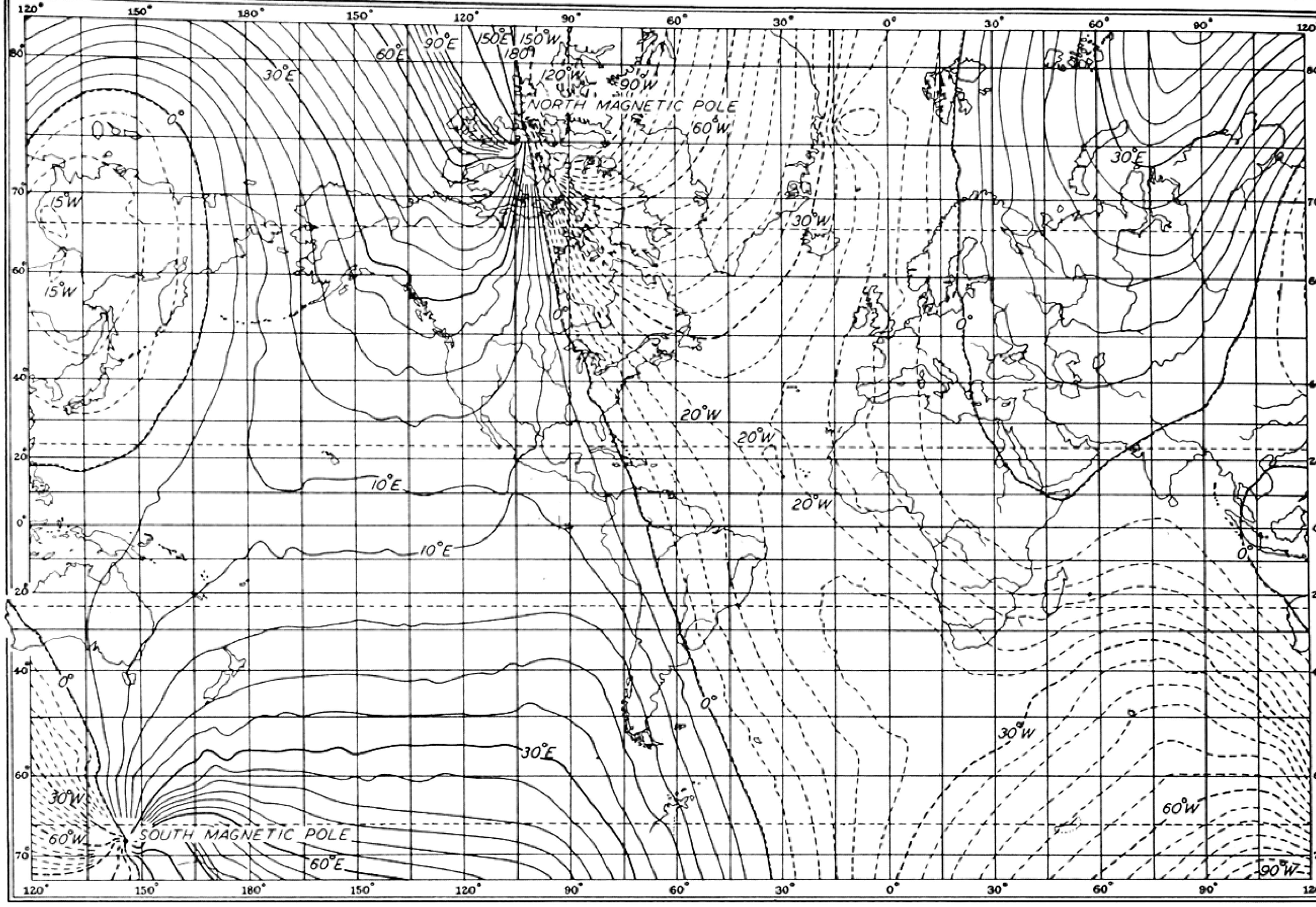

FIG. A —THE GEOMAGNETIC DECLINATION IN DEGREES OF ARC FOR 1945

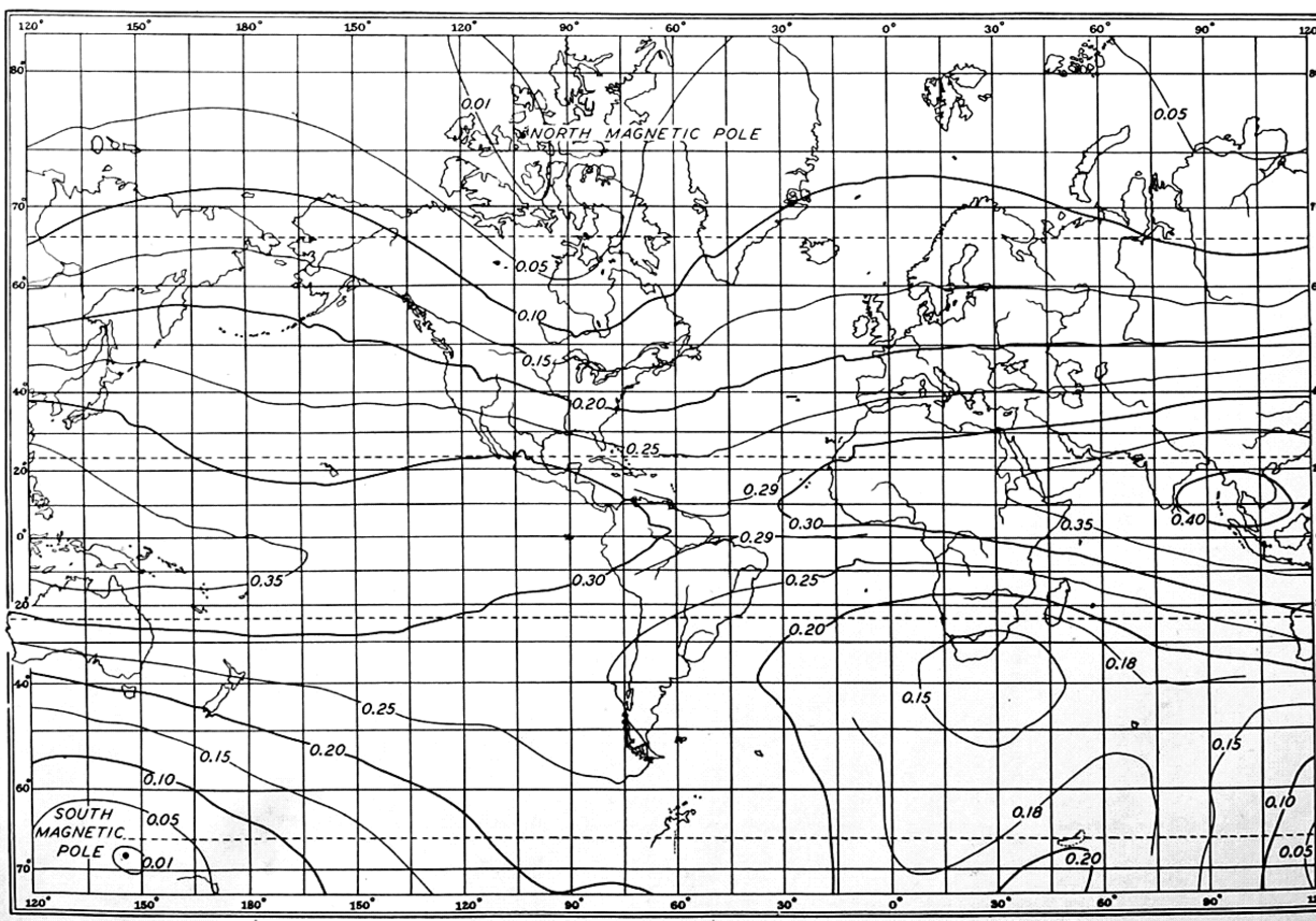

FIG. B —THE GEOMAGNETIC HORIZONTAL INTENSITY IN CGS-UNIT FOR 1945

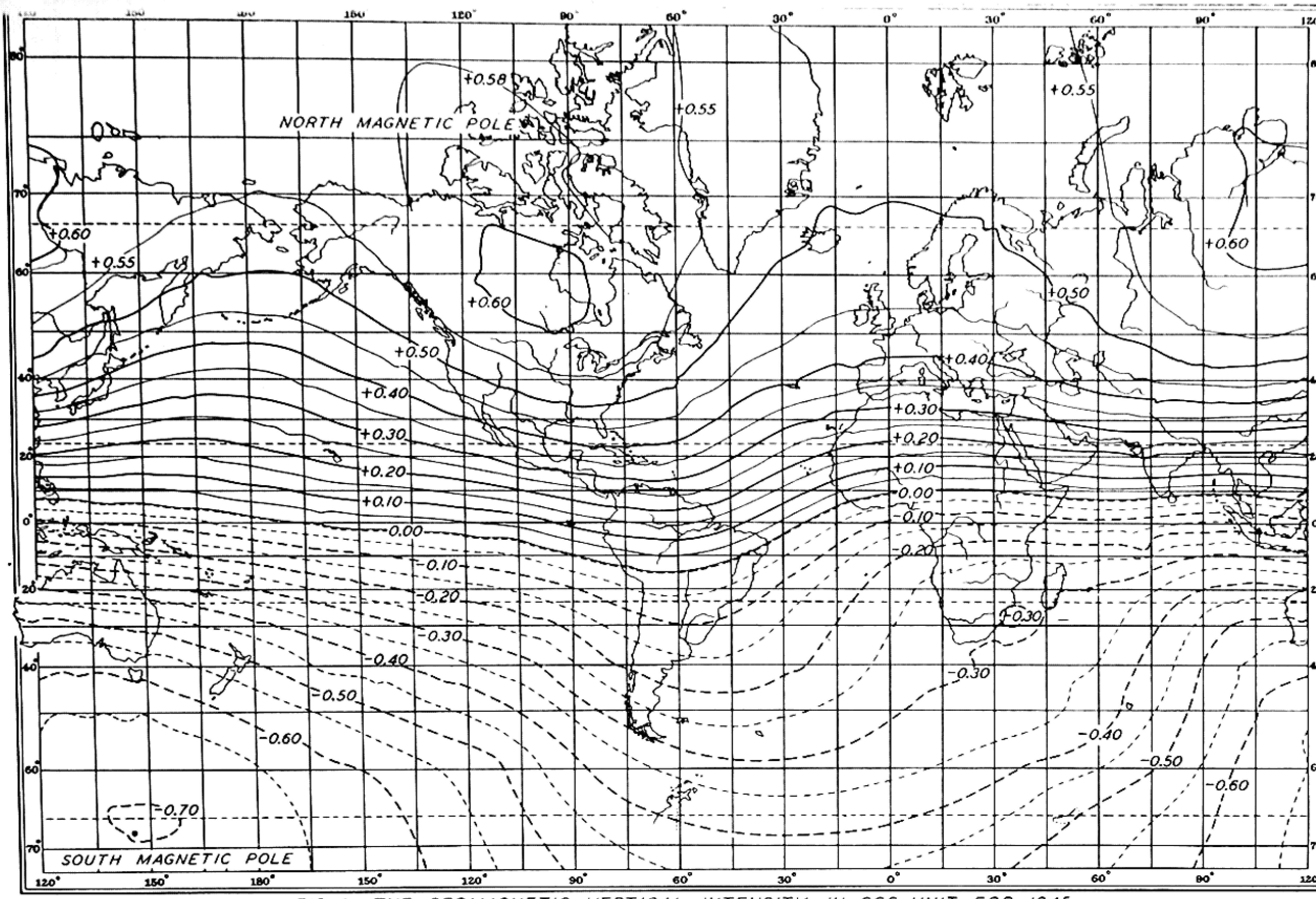

FIG. C —THE GEOMAGNETIC VERTICAL INTENSITY IN CGS-UNIT FOR 1945

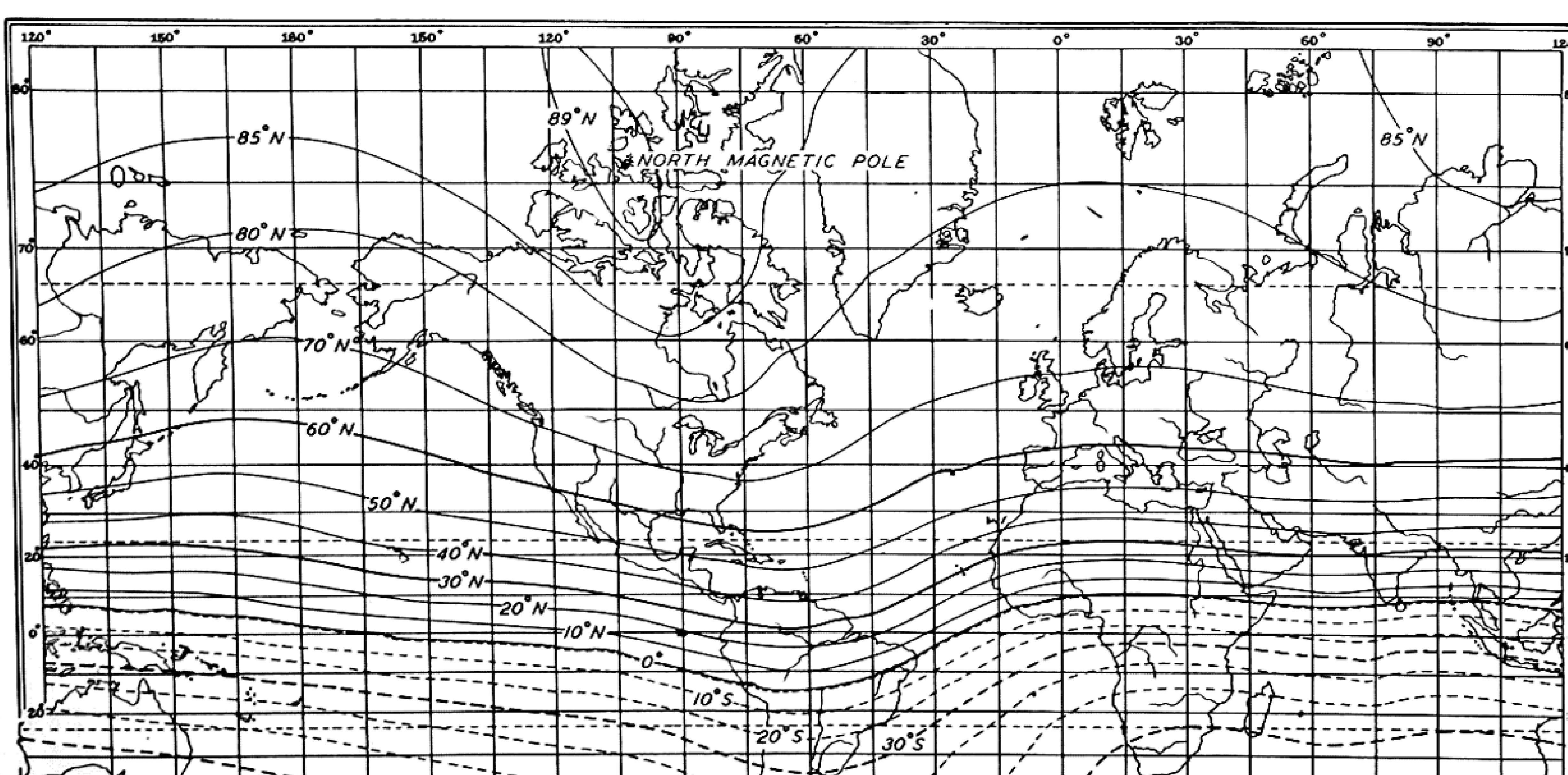

FIG. D —THE GEOMAGNETIC INCLINATION IN DEGREES OF ARC FOR 1945

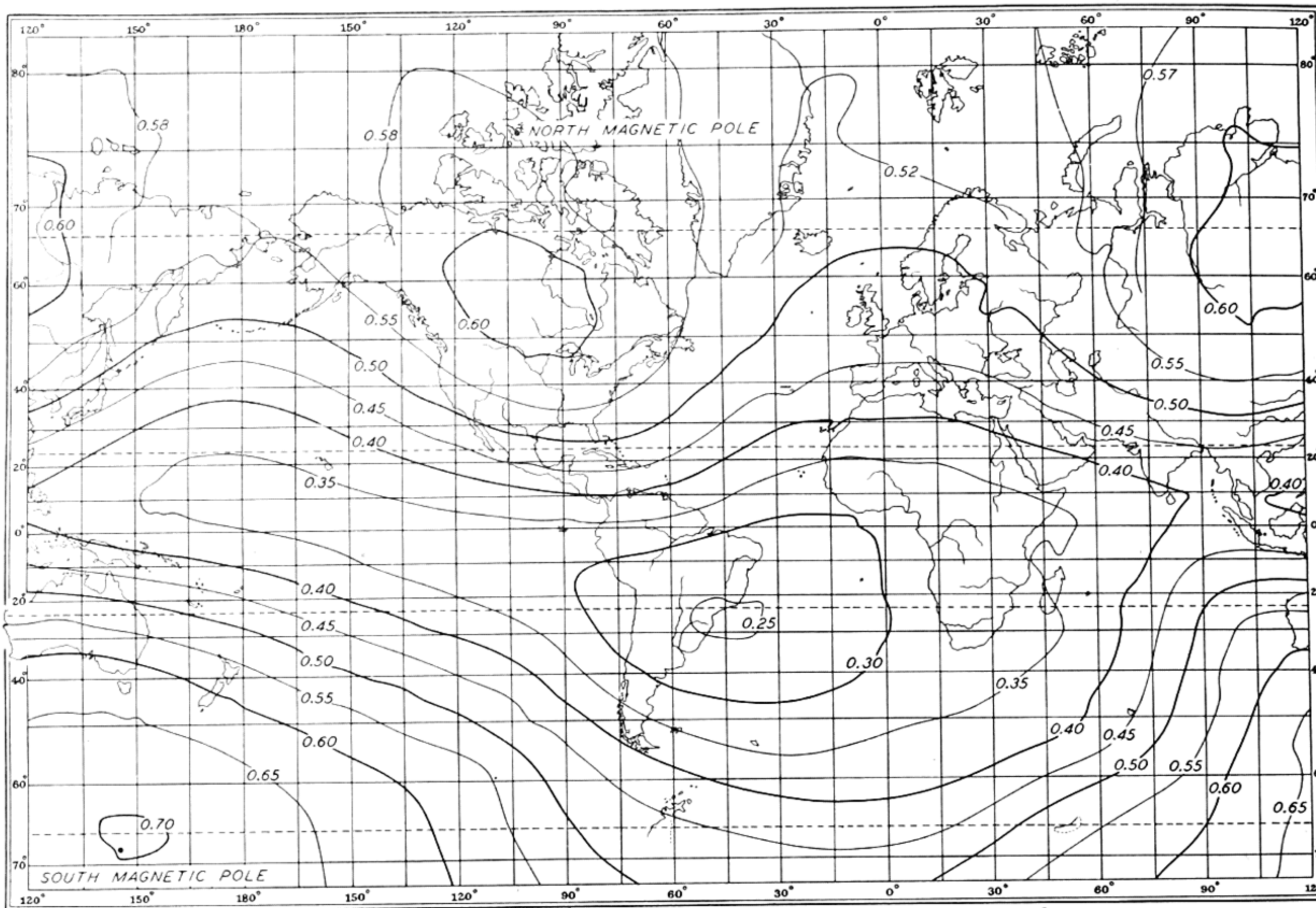

FIG. E —THE GEOMAGNETIC TOTAL INTENSITY IN CGS-UNIT FOR 1945

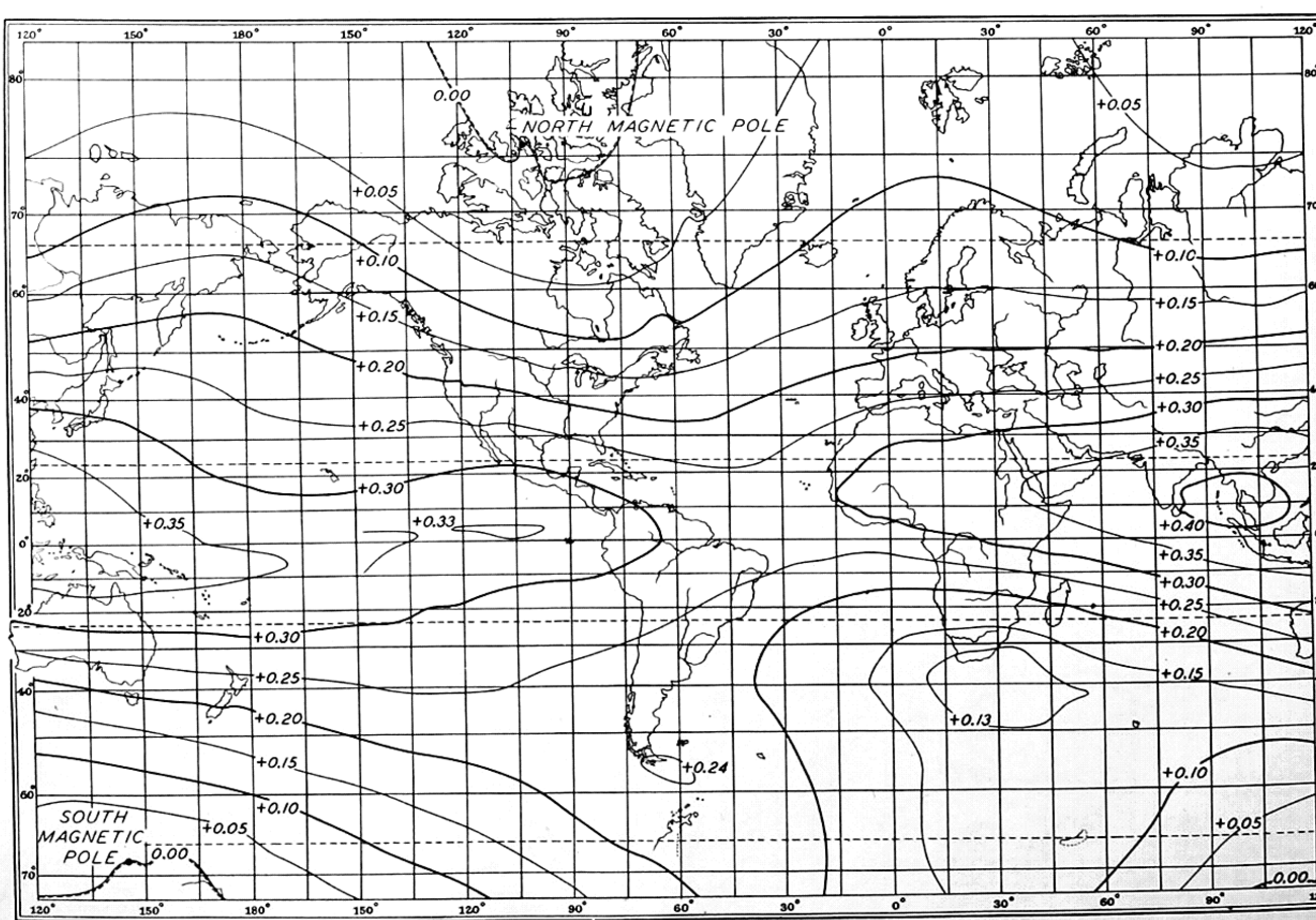

FIG. F —THE GEOMAGNETIC NORTH COMPONENT IN CGS-UNIT FOR 1945

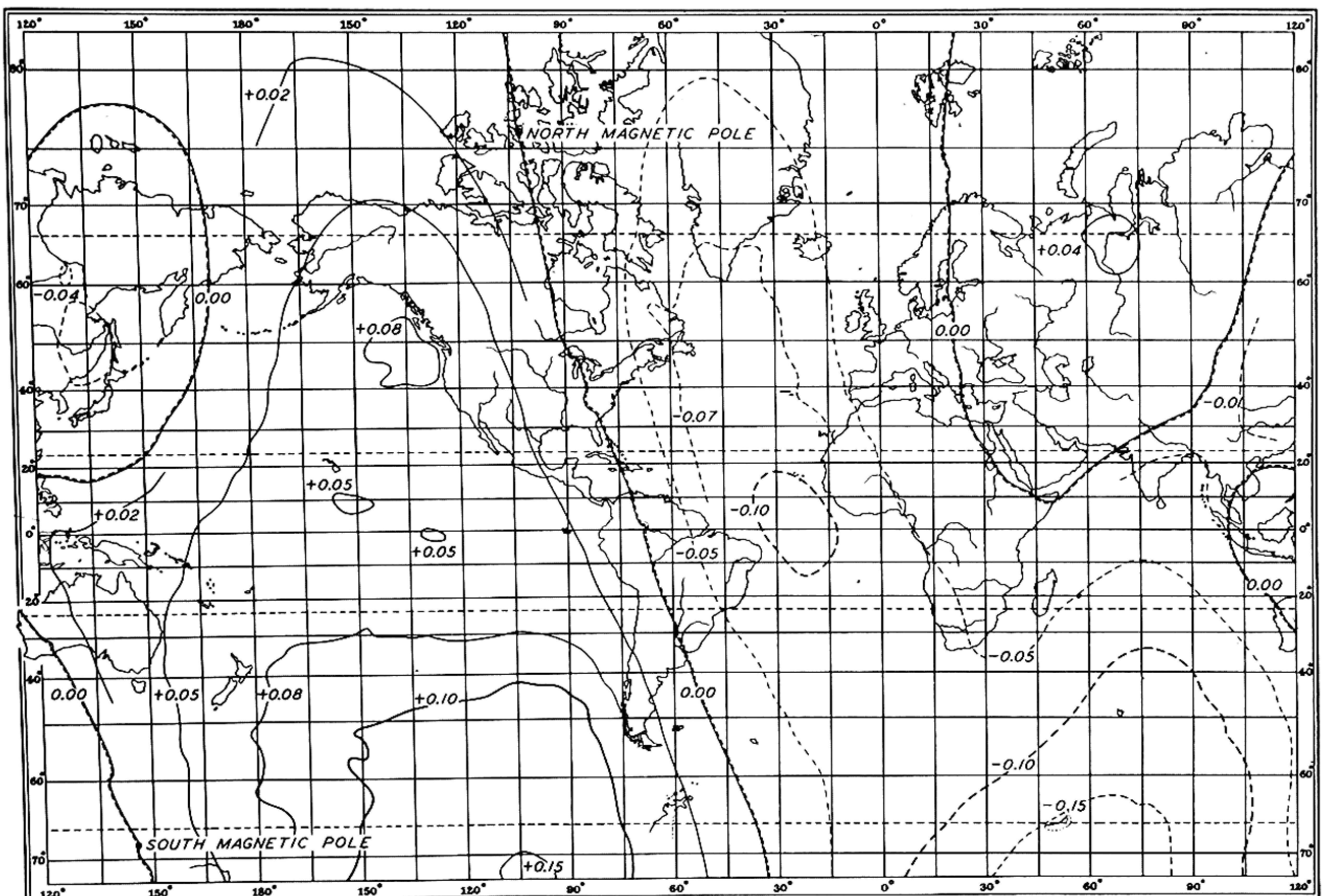

FIG. G —THE GEOMAGNETIC EAST COMPONENT IN CGS-UNIT FOR 1945

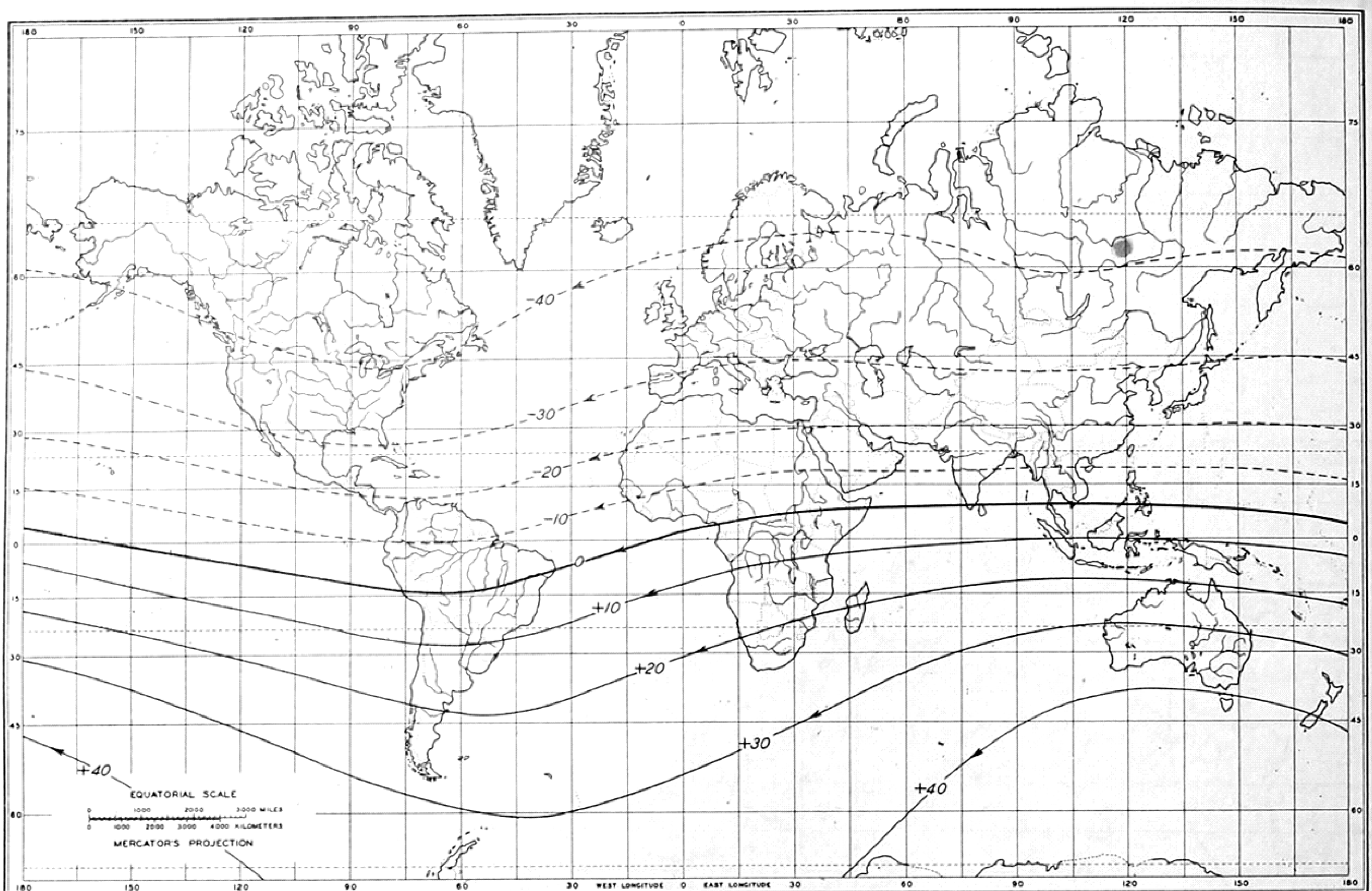

FIG. 1—CURRENT-FUNCTION IN 10^7 AMPERES FOR THIN SPHERICAL SHELL AT DEPTH ZERO WITHIN EARTH TO REPRODUCE SURFACE MAIN FIELD, EPOCH 1945

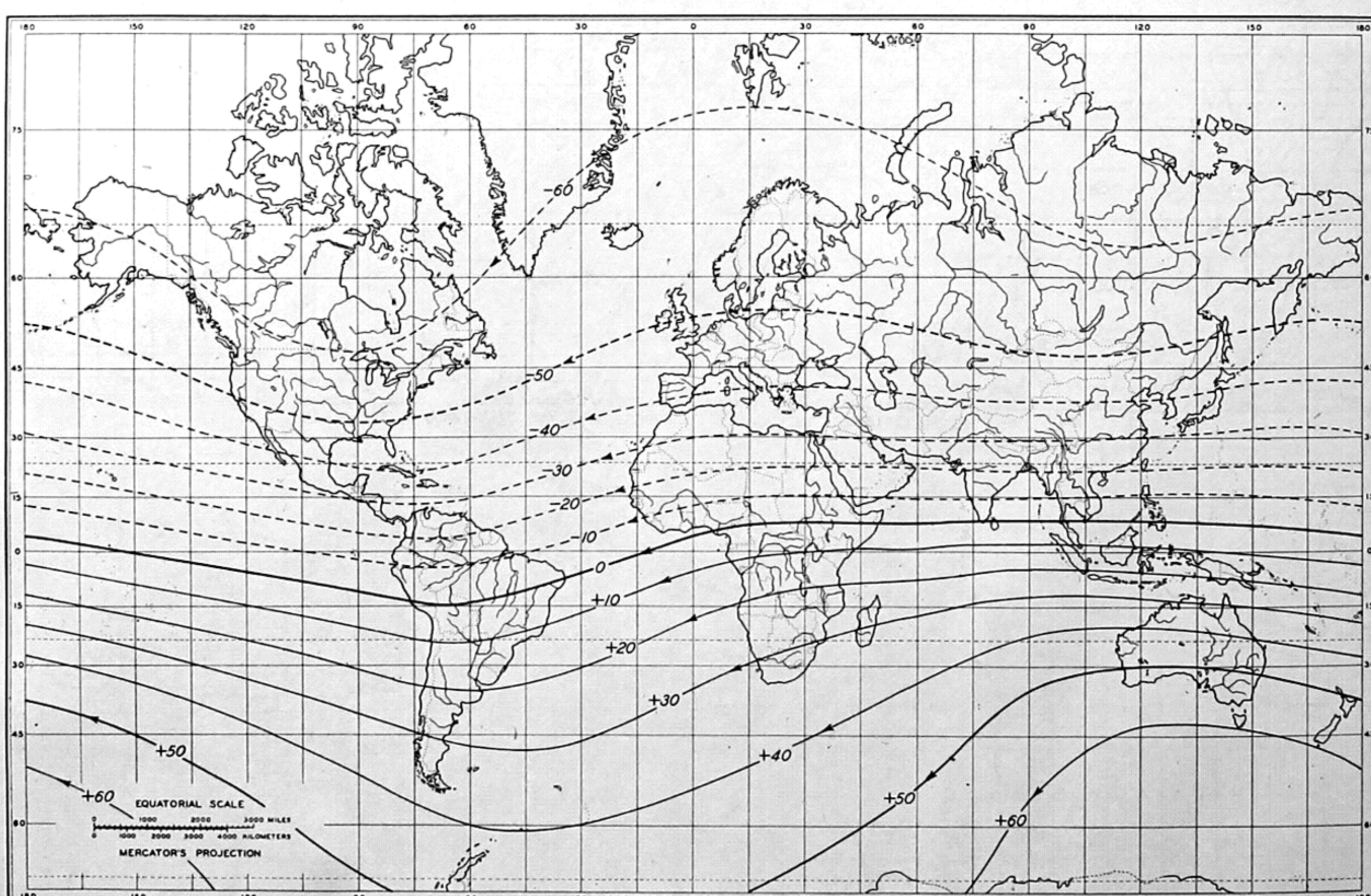

FIG. 2—CURRENT-FUNCTION IN 10^7 AMPERES FOR THIN SPHERICAL SHELL AT DEPTH 1000 KM WITHIN EARTH TO REPRODUCE SURFACE MAIN FIELD, EPOCH 1945

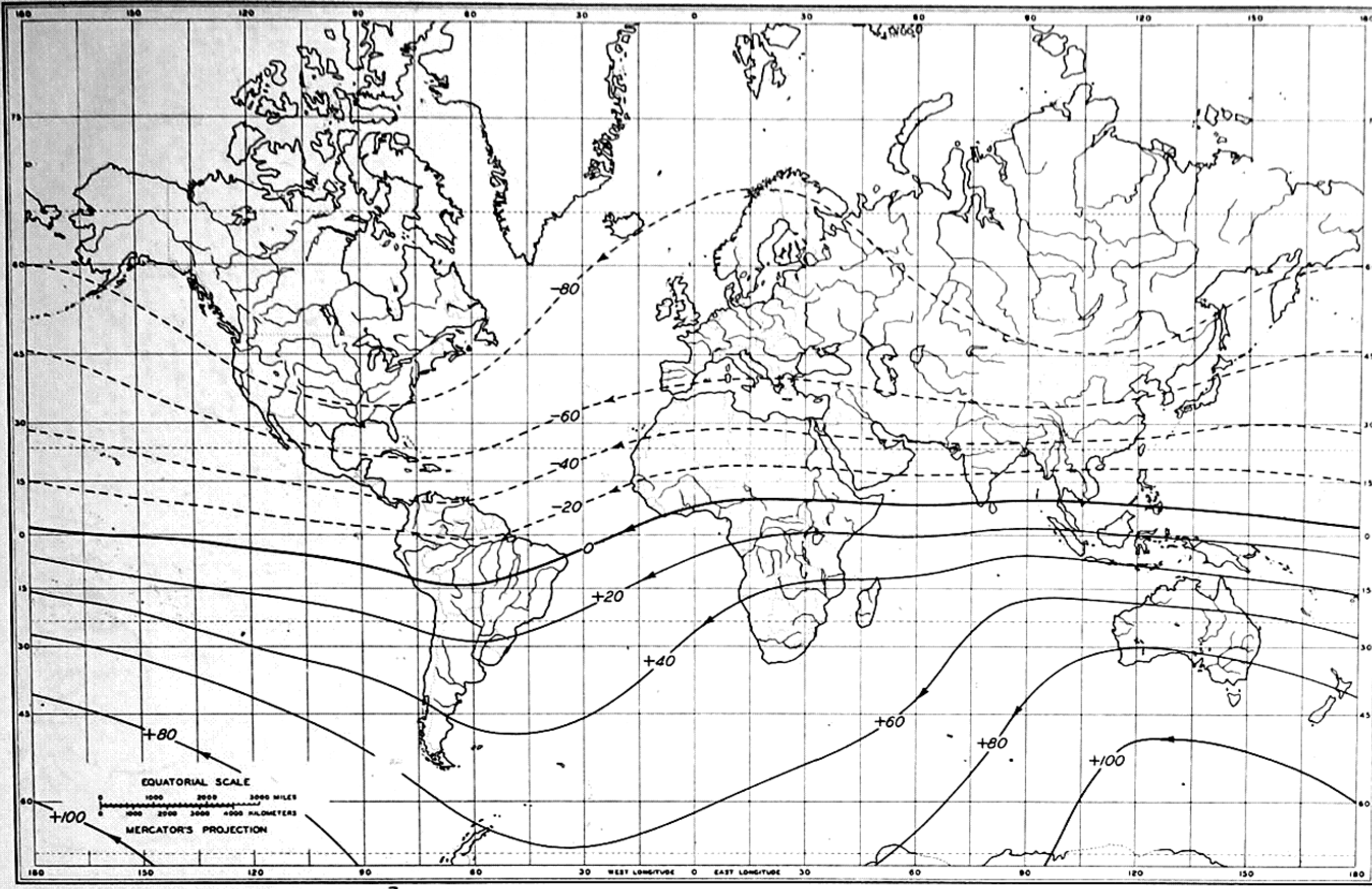

FIG. 3—CURRENT-FUNCTION IN 10^7 AMPERES FOR THIN SPHERICAL SHELL AT DEPTH 2000 KM WITHIN EARTH TO REPRODUCE SURFACE MAIN FIELD, EPOCH 1945

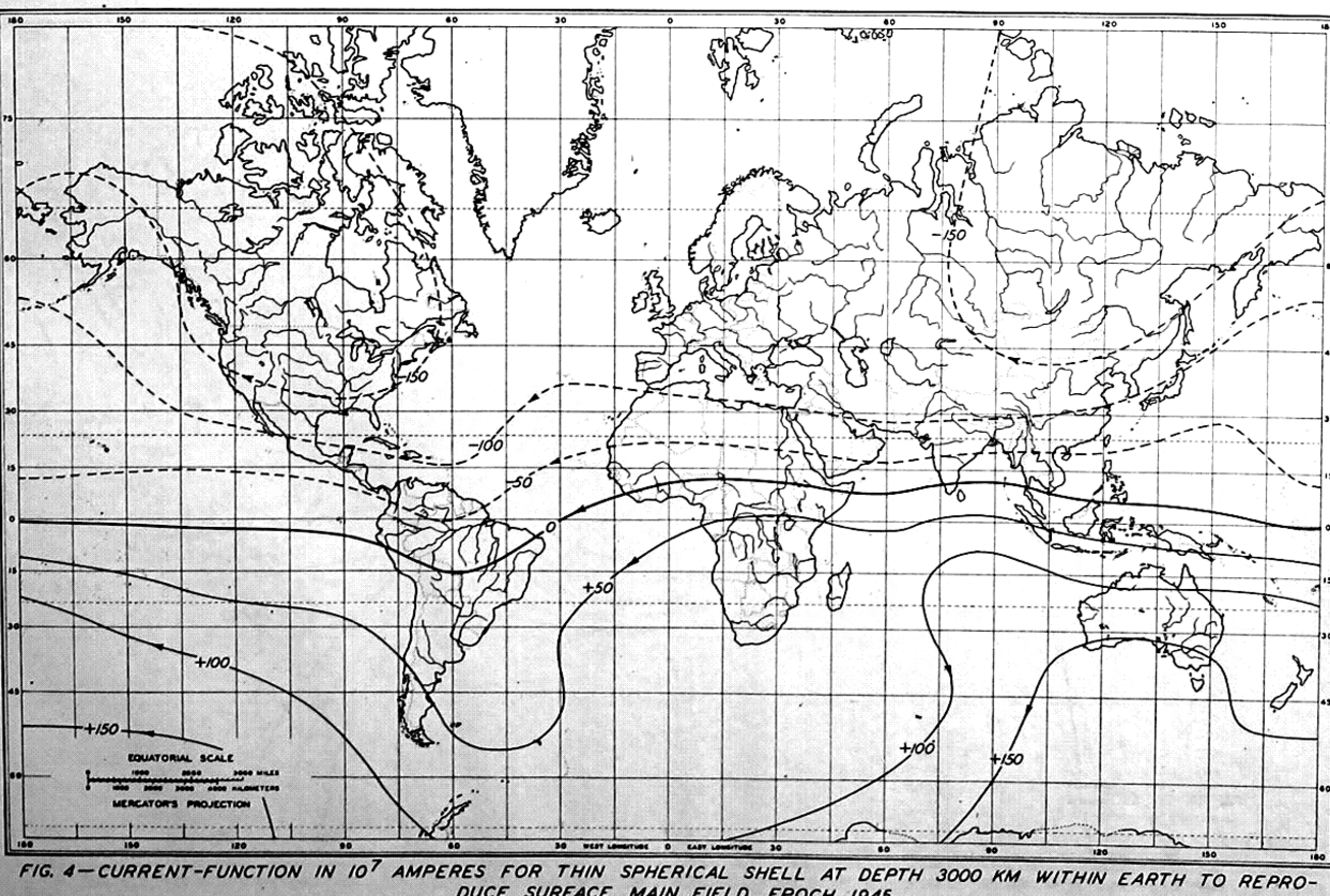

FIG. 4—CURRENT-FUNCTION IN 10^7 AMPERES FOR THIN SPHERICAL SHELL AT DEPTH 3000 KM WITHIN EARTH TO REPRODUCE SURFACE MAIN FIELD, EPOCH 1945

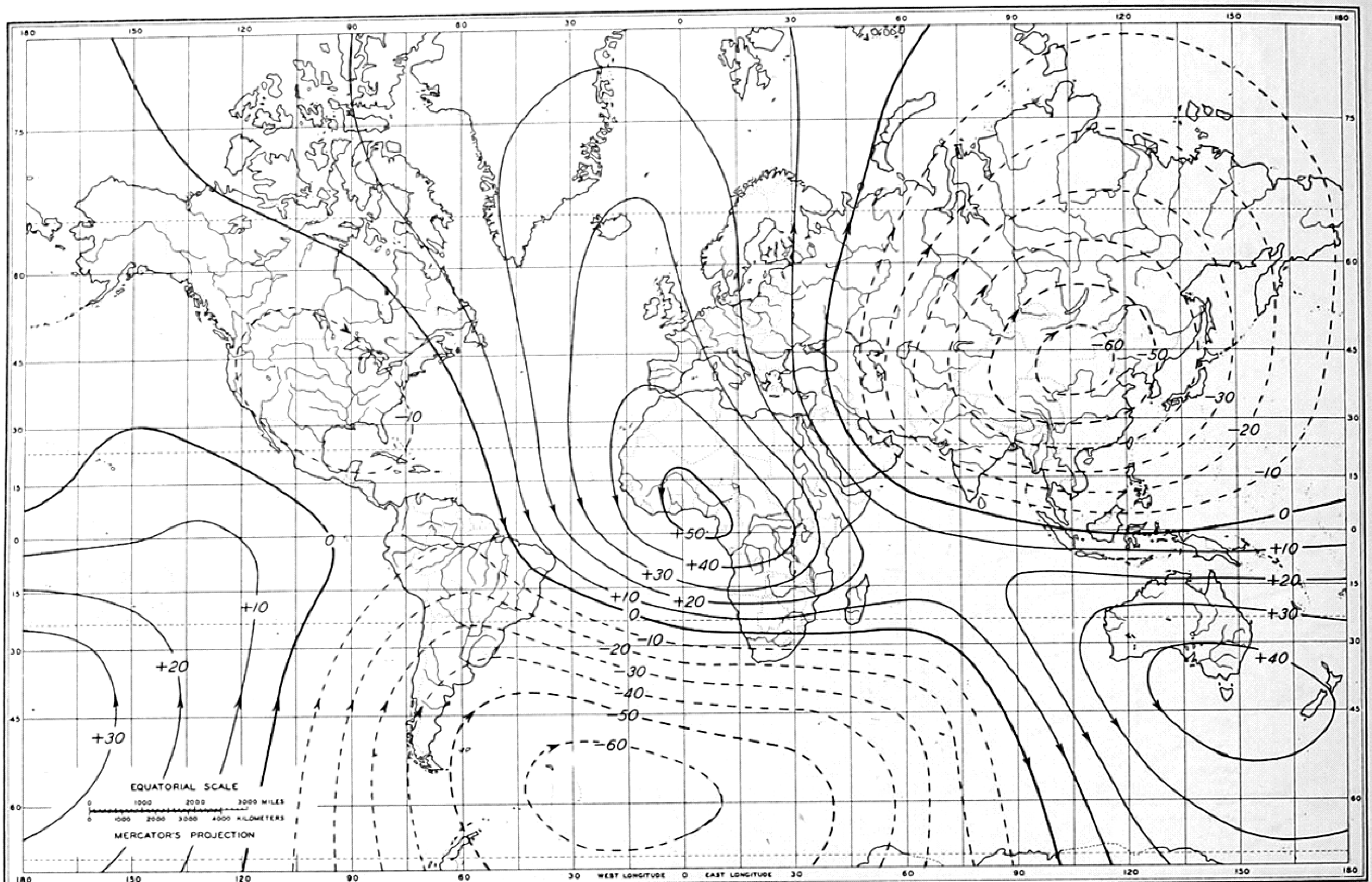

FIG. 5—CURRENT-FUNCTION IN 10^6 AMPERES FOR THIN SPHERICAL SHELL AT DEPTH ZERO WITHIN EARTH TO REPRODUCE RESIDUAL (NON-DIPOLE PART) OF MAIN FIELD, EPOCH 1945

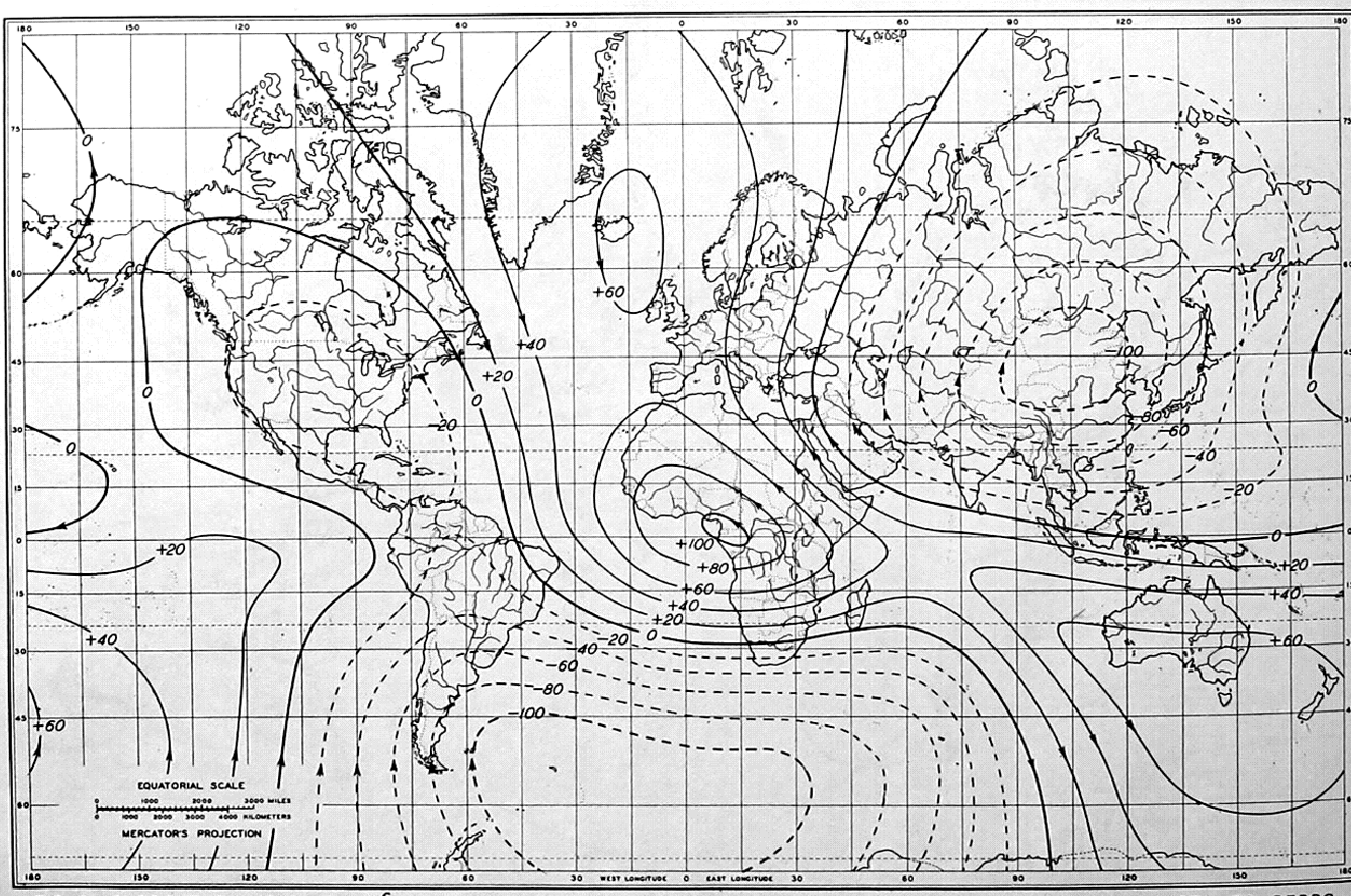

FIG. 6—CURRENT-FUNCTION IN 10^6 AMPERES FOR THIN SPHERICAL SHELL AT DEPTH 1000 KM WITHIN EARTH TO REPRODUCE RESIDUAL (NON-DIPOLE PART) OF MAIN FIELD, EPOCH 1945

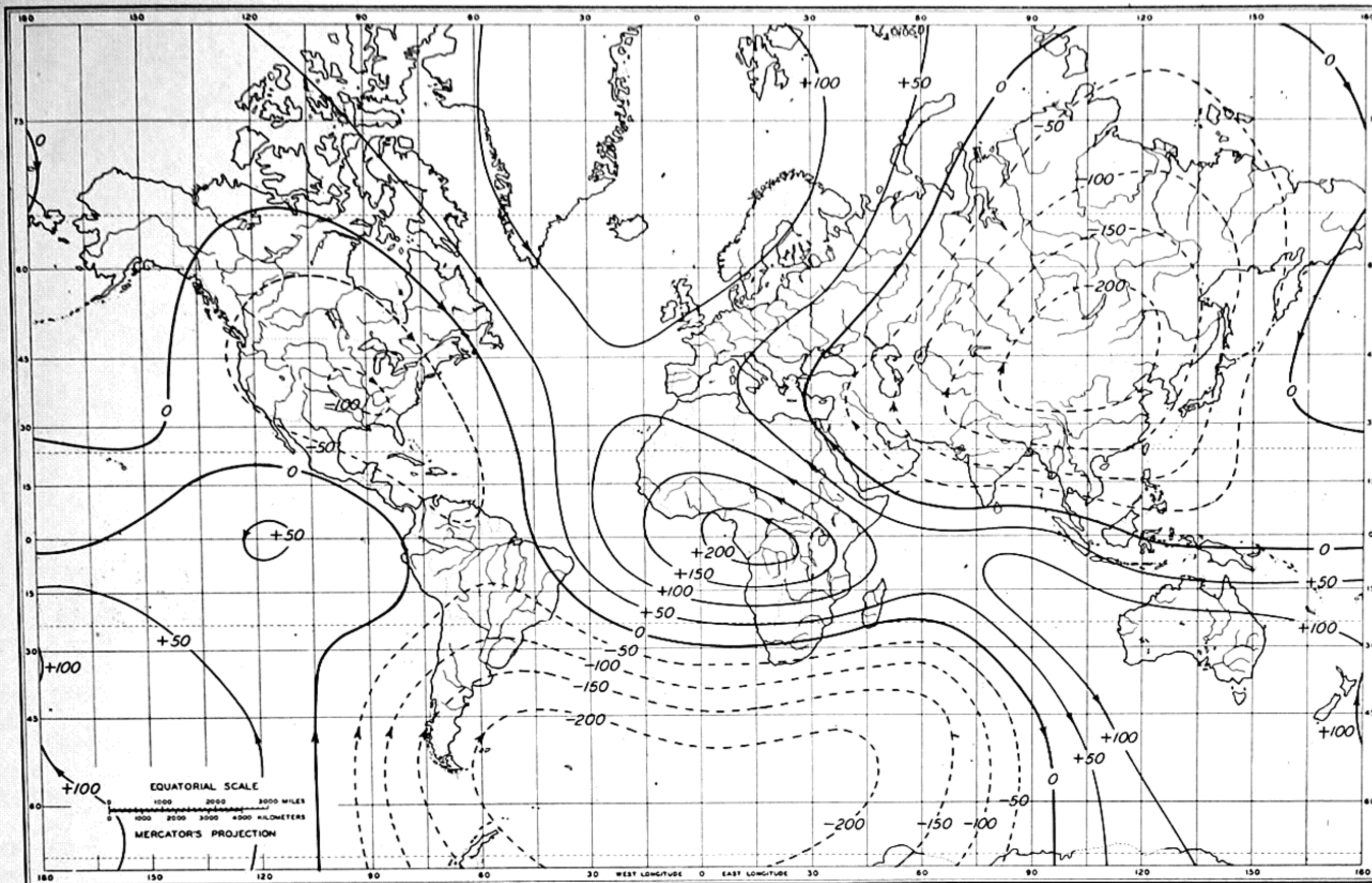

FIG. 7—CURRENT-FUNCTION IN 10^6 AMPERES FOR THIN SPHERICAL SHELL AT DEPTH 2000 KM WITHIN EARTH TO REPRODUCE RESIDUAL (NON-DIPOLE PART) OF MAIN FIELD, EPOCH 1945

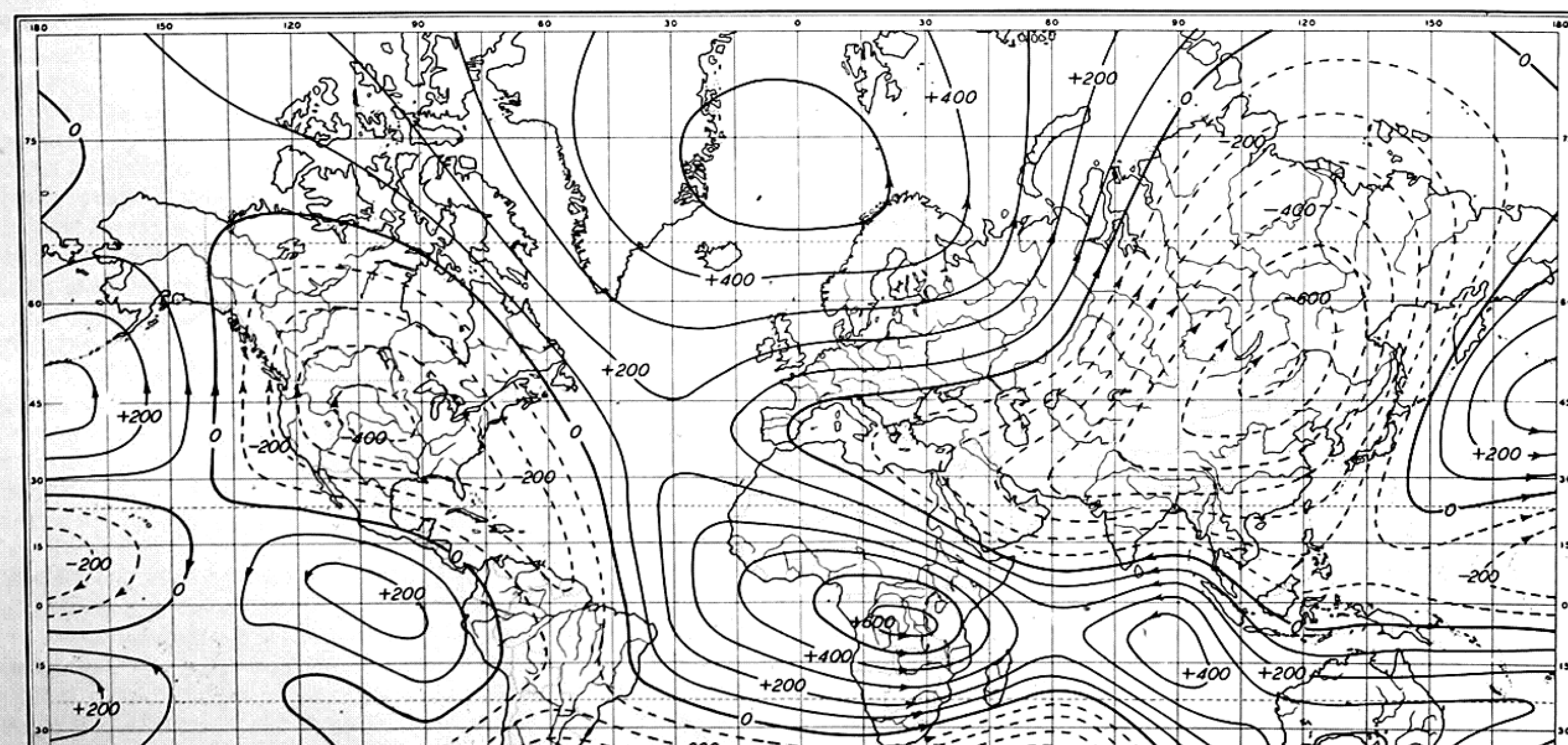

FIG. 8—CURRENT-FUNCTION IN 10^6 AMPERES FOR THIN SPHERICAL SHELL AT DEPTH 3000 KM WITHIN EARTH TO REPRODUCE RESIDUAL (NON-DIPOLE PART) OF MAIN FIELD, EPOCH 1945

CHAPTER III

GEOMAGNETIC SECULAR CHANGE AND ITS ANALYSIS

1. Introductory remarks.--Among previous analyses of secular change there are those of Carlheim-Gyllenskold and Bartels [3].

Carlheim-Gyllenskold expressed the potential at epochs 1787, 1700, and 1600, as sums of terms of the form

$$V_n^m/a = C_n^m \sin(m\lambda + \epsilon_n^m)P_n^m$$

where C_n^m was supposed approximately constant, and $\epsilon_n^m = \gamma_n^m + p_n^m t$, where t is the time in years. He supposed the period of revolution of field about the axis of rotation, T_n^m to be $2\pi/p_n^m$, and found $T_1^1 = 3{,}147$, $T_2^1 = 1{,}381$, and $T_2^2 = 454$ years.

Bartels analyzed the change in the main field at 14 observatories for the period 1902 to 1920, using harmonics up to and including the degree $n = 2$.

Chapman and Bartels [3] examined the coefficients from these two analyses, and some particulars of Table 9, Chapter II, and suggested

(a) The spherical harmonic series for the secular variation converges much more slowly than that of the main field. The predominance of the first-order term, so conspicuous in the main field, does not appear in the secular variation.

(b) Gyllenskold's phase formula is not valid, nor the isomagnetic charts drawn by Fritsche, for epochs extending back as far as A.D. 1000, based on extrapolations of similar formulas.

(c) The apparent decrease in the Earth's magnetic moment, by about 1/1000 of its whole value per annum, which is indicated by a comparison between the results of analyses of the main field at different epochs, appears also in Bartels' secular-variation analysis; he found the value of $+42\gamma$ for the annual change of g_1^0 (which in 1922 was about $-31{,}500\gamma$), or rather more than 0.1 per cent, and the percentage change in other harmonics much greater.

(d) While the main field may be regarded as a combination of a planetary field (the dipole field) and of weaker regional fields, the secular variation appears to have no outstanding part of planetary character; it consists largely of six regional changes which cannot easily be represented by a spherical harmonic series.

Elsasser [11] in his most recent paper on the origin of secular change finds a value T_1^1 of 3,000 years, using all available data except those of Table 9.

The validity of the estimates of such periods, using data over a relatively short period of time, is of course difficult to assess. Our colleague, E. A. Johnson, hopes to verify the possible existence of such periodicities from measurements on the remanent magnetizations of ancient varves, the yearly deposits preserved in nature and formed at the bottom of glacial lakes. In this way the periodicities shown over periods as long as 25,000 years may be forthcoming.

Our suggestions would be similar to those of Chapman and Bartels. In our preparation of isoporic charts of current epoch, we have experienced considerable difficulty in extrapolating secular change five years into the future, and we believe that extrapolation into the past is no less difficult and uncertain.

The results of spherical harmonic analyses of the charts for 1912.5, 1922.5, 1932.5, and 1942.5 are included here. Isoporic values for epochs 1932.5 and 1942.5 were computed, using automatic machines, to estimate values for various heights in the atmosphere. Computed values of $\dot{V}$ are provided for each of the four epochs, and for the vertical gradients of $\dot{X}$, $\dot{Y}$, and $\dot{Z}$. Finally, current functions, for each of the four epochs separately, are shown in mapped form for the same depths as used in similar calculations for the main field.

Finally, the probable depth at which secular change originates within the Earth is discussed. The rapid changes in current pattern in each ten-year interval is noted, and a few tentative comments are ventured respecting their bearing on the structure of the Earth's interior.

2. Data analyzed.--Tables 33 to 40 give values of $\dot{X}$ and $\dot{Y}$ at four epochs, which comprise the data for our analyses. Due to the use of machine techniques in analysis, the procedures were for convenience the same as those used for the main field. There were thus obtained 48 coefficients of spherical harmonic terms.

Table 41 lists the coefficients found for $\dot{X}$ and $\dot{Y}$ separately, epoch by epoch. It can scarcely be doubted that some of these are lacking in significance, especially the small terms of higher degree. However, the systematic changes with epoch seem fairly regular, and the fit of the original data, given in Tables 42 to 49, seems satisfactory.

Tabular values of $\dot{Z}$ at each epoch, computed from adopted coefficients of $\dot{X}$ and $\dot{Y}$, have been given in the preceding volume in Tables 12 to 15 [1] where they were successfully used in construction of isoporic charts in Z.

3. Secular-change values at various heights.--Tables 50 to 79 list computed values of $\dot{X}$, $\dot{Y}$, and $\dot{Z}$ at five elevations in and beyond the atmosphere, using the 48 coefficients as needed, for epochs 1932.5 and 1942.5. These permit adjustment of main field charts for 1945 to other epochs not too remote. As would be expected, higher order harmonics yielded insignificant contributions to the calculated change at greater heights. Table 80 gives an experimental calculation of $\dot{Z}$ at a depth of 1000 km.

4. Secular change in V.--Tables 81 to 84 list the computed values of $\dot{V}$ at four epochs, and Table 85 gives the value of $\dot{V}$ for the residual field at epoch 1942.5. These are interesting because they make possible qualitative inferences respecting the internal distribution of sources of secular change, in conjunction with values of $\dot{Z}$, and, say, of the vertical gradient of $\dot{Z}$.

5. The vertical derivatives of field components of secular change at various epochs.--Tables 86 to 97 give the space rate of change in a vertical direction of the field components $\dot{X}$, $\dot{Y}$, and $\dot{Z}$ of secular change at four epochs. These distributions were roughly mapped, in the hope that the gradients of secular change might reflect some shallow-seated effects related to crustal

features of the Earth. As Vening Meinesz [13] has pointed out, there seem to exist suggestive similarities in patterns of geomagnetic effects and those of crustal stresses which warrant further examination.

Tables 98 to 100 give values corresponding to those in Tables 86 to 97 but are for the changes in residual field for epoch 1942.5. We were not successful in deducing any important result from these tables. We give the values for the possible use of future investigators.

It might be mentioned in passing that the computed values appear small over the Pacific basin, where a granitic layer of the Earth's crust has not been found.

Table 101 lists the spherical harmonic coefficients found from our new charts as well as for previous analyses.

6. Current functions at various depths reproducing secular change at the surface of the ground.--Figures 9 to 24 show the current functions at depths 0, 1000, 2000, and 3000 km, for four epochs, estimated in a manner similar to that previously used for the main field. They give the yearly change in the current functions of the main field at various epochs.

Those for the residual field are shown in Figures 25 to 28, for 1942.5; these may be compared with Figures 5 to 8, presented in Chapter II, for the residual part of the main field.

As with the main field itself, the yearly changes in current rapidly increase in complexity with increasing depth. Again the current pattern given for depth 3000 km is likely to be much too simple. We may safely infer that a major part of secular change does not originate in a region of greater depth, and that a more modest depth of region is therefore probable, by virtue of greater simplicity in concepts. These results accord well with those of McNish [14] who found that the surface residual field and secular change could be represented rather well by a number of radial dipoles at depth (a/2).

The rapid changes in current pattern and intensity per decade call for special attention. They show that the Earth's interior is susceptible of rapid change with time in its attributes. The current density varies rapidly during the course of a decade. Thus, there occur considerable changes in electromotive driving forces in only ten years, if we regard secular change as due to electric currents. Alternatively, the electric conductivity at high pressures might be exceedingly high, even approaching superconductivity. In this way small changes in driving force could produce great change in current.

However, there is another aspect to trouble us. The pattern change in ten years is great. Are we then to suppose that weak electromotive forces, such as thermoelectric forces, can redistribute themselves with great rapidity? This does not appear reasonable in view of the now ancient status of the physical experiment which produces the magnetic field of the Earth. We have in our hypotheses adopted the ultimate favorable environment for the flow of huge electric currents as a consequence of feeble driving forces, but our first attempt to arrive at a check results in a need for a new hypothesis perhaps as revolutionary as the first.

We note that the changes with time in current pattern are highly systematic as well as rapid. They may arise therefore from gradually fluctuating processes, which began at some time during the past history of the Earth, and are still continuing. We know of no such processes, however, now going on with sufficient rapidity within the Earth's crust. Mountain building and continental changes take place at a slow rate compared with fluctuations which must account for secular change. The latter apparently occur, with some irregular tendencies, in cycles of a few hundred years' period, as judged by available observations and from measurements of varves [15].

There is real need for studies of the physical properties of earth materials at high pressures. These would permit discussion of some aspects of the origin of the main field and its secular change in terms of particulars within our experience. There is also need for further studies such as those on the magnetization of varves. These yield dated information over thousands of years where their results can be properly interpreted. It would also seem that varve investigations might well be supplemented by similar studies of such materials as suitable sedimentary rocks, in order that indications might be forthcoming, even though not so well dated, respecting long-term attributes of the variation of the main field. It would also seem of value to extend studies of possible stress-distributions within the Earth's interior.

TABLES 33-101

Table 33. Values of secular change in north component (X) of magnetic field intensity for 1912.5 expressed in units of 10^{-6} CGS per year

Geographic east longitude in degrees	Geographic colatitude in degrees								
	10	20	30	40	50	60	70	80	90
30	-170	-270	-400	-360	-170	20	160	100	-50
60	-260	-380	-600	-710	-610	-340	-110	-40	-100
90	-290	-390	-520	-590	-320	-30	310	370	220
120	-250	-340	-400	-310	-80	80	150	100	10
150	-170	-240	-250	-110	-90	60	110	10	-70
180	-40	-130	-100	-80	-110	-40	00	-20	-100
210	70	-10	10	-120	-220	-260	-270	-280	-310
240	150	90	90	-120	-340	-460	-400	-180	-160
270	220	220	190	-120	-570	-980	-850	-540	50
300	230	330	340	40	-470	-900	-1040	-600	00
330	130	170	220	270	290	120	00	-110	-230
360	-20	-30	-10	100	250	360	330	150	-70

Geographic east longitude in degrees	Geographic colatitude in degrees							
	100	110	120	130	140	150	160	170
30	-240	-460	-730	-600	-320	00	270	70
60	-160	-240	-300	-190	130	520	580	-40
90	50	-200	-630	-620	-170	310	230	-310
120	-130	-310	-480	-380	-130	80	-170	-570
150	-150	-270	-330	-220	-190	-290	-430	-520
180	-250	-440	-420	-240	-290	-400	-440	-220
210	-430	-550	-450	-270	-50	-70	-140	-20
240	-350	-550	-400	-210	-40	30	140	160
270	140	-60	-230	-340	-220	-130	80	370
300	260	10	-250	-540	-580	-370	-30	360
330	-300	-450	-630	-980	-1120	-730	-230	250
360	-240	-440	-710	-1150	-920	-550	-180	130

Table 34. Values of secular change in north component (X) of magnetic field intensity for 1922.5 expressed in units of 10^{-6} CGS per year

Geographic east longitude in degrees	Geographic colatitude in degrees								
	10	20	30	40	50	60	70	80	90
30	-230	-310	-390	-330	-160	30	80	90	-90
60	-340	-390	-600	-620	-440	-180	60	200	50
90	-320	-400	-560	-450	-250	-40	180	350	260
120	-240	-370	-390	-290	-140	10	120	130	60
150	-130	-300	-280	-190	-80	00	-10	-10	-110
180	20	-130	-150	-140	-160	-170	-200	-220	-200
210	180	40	-70	-190	-280	-340	-360	-360	-320
240	240	110	10	-180	-320	-450	-460	-420	-350
270	290	220	100	-150	-500	-680	-630	-510	-310
300	230	330	280	110	-290	-620	-680	-470	-160
330	70	200	230	240	250	160	90	-10	-210
360	-120	-70	20	90	210	330	300	110	-70

Geographic east longitude in degrees	Geographic colatitude in degrees							
	100	110	120	130	140	150	160	170
30	-330	-620	-870	-640	-320	50	140	80
60	-210	-480	-650	-470	-100	310	330	-50
90	110	-220	-610	-620	-300	20	30	-310
120	-40	-150	-340	-410	-210	-70	-280	-540
150	-160	-190	-250	-230	-180	-290	-430	-570
180	-200	-240	-330	-360	-300	-340	-420	-350
210	-300	-330	-410	-400	-240	-130	-190	-90
240	-360	-390	-390	-350	-260	-60	80	180
270	-240	-370	-490	-510	-370	-230	80	400
300	-120	-320	-500	-770	-850	-570	-130	350
330	-380	-530	-740	-980	-1180	-830	-290	240
360	-280	-520	-770	-1040	-820	-480	-230	130

Table 35. Values of secular change in north component (X) of magnetic field intensity for 1932.5 expressed in units of 10^{-6} CGS per year

Geographic east longitude in degrees	Geographic colatitude in degrees								
	10	20	30	40	50	60	70	80	90
30	-400	-470	-420	-280	-20	200	260	50	-200
60	-520	-580	-510	-330	-60	200	330	250	60
90	-430	-480	-360	-130	120	320	460	440	390
120	-300	-340	-210	-50	60	120	180	150	-100
150	-170	-200	-180	-80	10	80	140	60	-120
180	20	-40	-90	-50	10	60	40	-20	-120
210	160	60	20	-40	-80	-130	-160	-210	-270
240	260	170	90	-80	-200	-320	-400	-400	-390
270	350	280	130	-120	-520	-720	-640	-410	-280
300	280	320	280	30	-270	-480	-470	-310	-150
330	80	160	230	260	210	150	160	-10	-260
360	-200	-170	-40	60	250	430	310	30	-230

Geographic east longitude in degrees	Geographic colatitude in degrees							
	100	110	120	130	140	150	160	170
30	-470	-740	-830	-550	-250	70	230	280
60	-190	-540	-610	-420	-120	240	150	-140
90	90	-250	-600	-590	-270	-20	-150	-500
120	-10	-60	40	-50	20	-90	-290	-570
150	-240	-180	-120	-30	-110	-230	-370	-460
180	-330	-380	-340	-210	-260	-330	-310	-220
210	-370	-500	-530	-430	-290	-140	-90	50
240	-410	-510	-550	-580	-410	-190	190	410
270	-210	-250	-440	-650	-580	-390	90	670
300	-80	-190	-490	-740	-830	-610	-150	650
330	-470	-630	-750	-870	-870	-630	-230	400
360	-500	-690	-830	-790	-570	-350	-100	340

Table 36. Values of secular change in north component (X) of magnetic field intensity for 1942.5 expressed in units of 10^{-6} CGS per year

Geographic east longitude in degrees	Geographic colatitude in degrees								
	10	20	30	40	50	60	70	80	90
30	-170	-260	-240	-80	170	360	370	210	10
60	-290	-310	-170	-90	180	380	500	570	460
90	-310	-200	-90	110	350	530	560	520	460
120	-220	-100	40	220	210	250	220	180	160
150	-140	-50	90	50	50	70	60	40	20
180	-40	-20	120	70	20	-30	-40	-70	-140
210	80	40	110	60	-20	-100	-170	-230	-320
240	210	120	190	130	20	-100	-180	-280	-380
270	310	240	240	130	0	-130	-240	-340	-370
300	300	280	340	280	230	110	130	40	-60
330	120	140	320	440	530	390	180	40	-130
360	-20	-30	70	220	440	450	230	60	-110

Geographic east longitude in degrees	Geographic colatitude in degrees							
	100	110	120	130	140	150	160	170
30	-260	-590	-630	-270	-70	90	260	50
60	170	-170	-460	-500	-320	60	230	-270
90	320	30	-280	-500	-460	-90	80	-540
120	150	150	220	-190	-360	-220	-80	-720
150	-20	-60	-20	-30	-150	-250	-180	-480
180	-210	-250	-230	-190	-210	-130	-10	0
210	-390	-450	-390	-300	-210	-40	220	500
240	-470	-570	-620	-470	-200	40	310	860
270	-340	-400	-540	-670	-540	-240	260	980
300	-200	-420	-620	-890	-770	-510	20	870
330	-290	-460	-740	-830	-700	-450	-30	650
360	-250	-500	-640	-540	-400	-160	100	370

Table 37. Values of secular change in east component (Y) of magnetic field intensity for 1912.5 expressed in units of 10^{-6} CGS per year

Geographic east longitude in degrees	Geographic colatitude in degrees								
	10	20	30	40	50	60	70	80	90
30	173	161	310	420	580	700	770	850	890
60	40	-9	-10	-20	0	10	0	-30	-110
90	-40	-149	-310	-501	-620	-660	-691	-610	-460
120	-109	-170	-280	-289	-260	-230	-150	-60	20
150	-190	-170	-260	-240	-191	-120	-50	-120	-170
180	-253	-231	-190	-100	-30	40	70	100	110
210	-213	-120	-10	40	90	140	170	150	130
240	-92	-70	-70	-20	70	170	291	350	280
270	17	-70	-180	-180	-70	50	210	440	440
300	138	120	80	-20	-251	-570	-820	-970	-1010
330	253	339	370	289	110	-140	-450	-670	-660
360	259	319	460	531	550	560	591	580	500

Geographic east longitude in degrees	Geographic colatitude in degrees							
	100	110	120	130	140	150	160	170
30	961	971	1020	800	580	290	-129	-530
60	-200	-380	-320	-180	-170	-190	-380	-622
90	-440	-520	-560	-540	-571	-550	-450	-461
120	100	130	110	10	-190	-190	-91	-40
150	-170	-150	-110	-40	0	80	251	420
180	110	130	130	150	240	310	520	720
210	190	220	270	339	420	490	579	749
240	130	80	70	90	180	280	380	530
270	250	40	-130	-230	-190	-80	50	230
300	-920	-791	-710	-620	-520	-370	-269	-81
330	-480	-341	-249	-170	-190	-220	-289	-403
360	450	430	500	620	350	140	-120	-513

Table 38. Values of secular change in east component (Y) of magnetic field intensity for 1922.5 expressed in units of 10^{-6} CGS per year

Geographic east longitude in degrees	Geographic colatitude in degrees								
	10	20	30	40	50	60	70	80	90
30	161	251	380	481	590	650	660	740	820
60	-29	-29	-40	-70	-60	-50	-40	-120	-270
90	-179	-199	-250	-341	-440	-460	-470	-380	-200
120	-311	-330	-310	-280	-221	-191	-140	-70	20
150	-311	-310	-230	-160	-131	-110	-100	-90	-90
180	-190	-219	-160	-70	-10	30	40	70	90
210	-109	-111	-90	-40	0	50	120	160	220
240	-17	-79	-130	-170	-140	-50	50	180	230
270	81	-29	-130	-219	-150	-40	120	310	300
300	219	161	80	40	-101	-480	-720	-870	-920
330	340	389	380	310	191	30	-190	-350	-390
360	311	409	570	621	620	600	560	510	480

Geographic east longitude in degrees	Geographic colatitude in degrees							
	100	110	120	130	140	150	160	170
30	820	870	900	730	470	160	-231	-633
60	-431	-530	-570	-520	-481	-440	-421	-633
90	-210	-220	-230	-279	-370	-470	-430	-501
120	80	170	100	-50	-160	-220	-140	-17
150	-90	-40	-40	-50	79	130	231	380
180	160	180	210	240	310	440	579	760
210	280	300	330	350	429	520	649	829
240	220	230	249	260	280	380	480	628
270	140	-20	-170	-170	-120	-20	111	311
300	-840	-791	-700	-610	-571	-410	-231	-81
330	-301	-230	-130	-80	-79	-180	-371	-432
360	400	380	460	560	370	170	-301	-662

Table 39. Values of secular change in east component (Y) of magnetic field intensity for 1932.5 expressed in units of 10^{-6} CGS per year

Geographic east longitude in degrees	Geographic colatitude in degrees: 10	20	30	40	50	60	70	80	90
30	288	301	290	411	570	530	530	520	450
60	58	41	-60	-70	-90	-110	-120	-220	-390
90	-179	-219	-220	-280	-350	-350	-320	-231	-130
120	-311	-339	-280	-240	-110	-20	30	110	80
150	-380	-330	-270	-230	-191	-150	-110	-40	-60
180	-311	-269	-210	-149	-101	-40	30	100	140
210	-213	-181	-120	-79	-50	0	70	160	230
240	-109	-120	-170	-201	-110	20	90	110	160
270	40	-20	-180	-210	-90	-10	200	110	-20
300	242	199	120	40	-110	-339	-630	-880	-850
330	369	430	420	350	251	161	30	-100	-180
360	380	509	550	601	590	520	510	480	430

Geographic east longitude in degrees	Geographic colatitude in degrees: 100	110	120	130	140	150	160	170
30	380	370	420	339	210	100	-301	-720
60	-440	-560	-670	-590	-411	-380	-480	-714
90	-140	-190	-221	-290	-359	-370	-380	-432
120	120	230	330	300	70	-140	-79	17
150	-70	20	70	101	-20	80	260	443
180	90	80	100	200	350	510	681	812
210	270	320	370	429	531	620	681	841
240	150	160	120	90	140	340	541	691
270	-50	-80	-161	-260	-250	-180	161	409
300	-770	-691	-620	-550	-510	-390	-260	-17
330	-200	-130	-40	-20	-79	-190	-389	-449
360	420	441	480	440	350	130	-319	-720

Table 40. Values of secular change in east component (Y) of magnetic field intensity for 1942.5 expressed in units of 10^{-6} CGS per year

Geographic east longitude in degrees	Geographic colatitude in degrees: 10	20	30	40	50	60	70	80	90
30	190	269	240	320	390	370	370	320	250
60	52	120	10	-30	-80	-140	-220	-250	-400
90	-121	-79	-150	-260	-339	-339	-291	-200	-130
120	-271	-281	-250	-280	-210	-80	20	120	160
150	-340	-339	-270	-240	-210	-150	-120	-100	-60
180	-282	-240	-180	-120	-70	10	40	70	100
210	-179	-149	-70	-50	-10	50	130	210	260
240	-98	-120	-130	-131	-120	-80	-20	30	110
270	69	-50	-100	-120	-20	30	60	70	-10
300	219	120	80	-20	-150	-309	-541	-610	-620
330	340	310	340	271	140	50	-10	-110	-120
360	311	351	410	481	510	480	430	330	250

Geographic east longitude in degrees	Geographic colatitude in degrees: 100	110	120	130	140	150	160	170
30	200	220	230	90	-61	-210	-471	-783
60	-550	-630	-710	-770	-700	-590	-629	-703
90	-160	-210	-279	-350	-440	-490	-459	-328
120	210	291	320	110	-79	-70	9	322
150	-20	70	140	210	230	260	380	639
180	140	190	249	350	531	750	901	1019
210	301	370	430	510	601	700	860	910
240	170	160	140	170	219	250	389	489
270	-110	-170	-249	-339	-300	-220	-79	-98
300	-580	-530	-440	-420	-400	-360	-371	-570
330	-100	-20	80	80	-20	-120	-251	-680
360	210	280	360	290	170	0	-199	-674

Table 41. Values of spherical harmonic coefficients of secular change in north (X) and east (Y) components of magnetic field intensity expressed in units of 10^{-7} CGS per year

m	n	A_n^m 1912.5 X	1912.5 Y	1922.5 X	1922.5 Y	1932.5 X	1932.5 Y	1942.5 X	1942.5 Y
	1	2470		2839		2298		919	
	2	-1385		-2061		-2815		-3574	
	3	1695		1995		1258		533	
	4	1005		1054		1935		1825	
	5	-2384		-1946		-1031		-1146	
	6	684		763		400		1395	
1	1	92	103	575	160	67	202	502	-187
1	2	315	-832	309	-48	661	-132	-358	403
1	3	-1493	-1810	-2419	-2036	-2454	-1935	-2472	-1918
1	4	1684	1617	1441	1098	1361	630	752	472
1	5	-1794	-415	-601	-1276	-458	-1065	-11	560
1	6	665	1151	67	236	255	1373	-58	-140
2	2	5144	4371	3256	3347	2011	1918	-140	1119
2	3	-733	-83	-630	-546	382	44	1302	699
2	4	-746	-1394	-193	-1277	-1080	-1054	-168	-605
2	5	-2164	-1843	-1795	-1163	-1592	-1392	-669	-885
2	6	522	406	158	750	906	1385	773	827
3	3	3939	4117	1803	2647	769	1120	-376	424
3	4	-766	152	-787	263	701	647	1465	847
3	5	-1331	-1047	-516	-662	-231	-405	192	-383
3	6	-1017	-1211	-1266	-785	-769	-574	-575	-291
4	4	2291	1648	1293	1508	1632	1053	835	1270
4	5	-2174	-1328	-1077	-1013	-1302	-876	-109	-561
4	6	760	415	573	565	472	1043	712	445
5	5	-3103	-1999	-1164	-926	-765	-1109	-488	-895
5	6	36	-292	-341	-1043	-493	-566	-795	-837
6	6	-1498		-1063		-1078		-104	

m	n	B_n^m 1912.5 X	1912.5 Y	1922.5 X	1922.5 Y	1932.5 X	1932.5 Y	1942.5 X	1942.5 Y
1	1	-953	-424	-1102	-353	-879	-52	-248	515
1	2	-2149	-1567	-2837	-2783	-3562	-3483	-3967	-3919
1	3	-2136	-1480	-1569	-1376	-1537	-1576	432	-773
1	4	-269	-2810	-326	-1419	-2048	-1394	-1079	-1432
1	5	2945	4176	2400	4177	2509	3738	1304	3393
1	6	776	-629	-362	-1757	-535	-1585	-694	-1592
2	2	-3373	-3462	-3445	-3412	-2371	-3118	-2801	-2861
2	3	1208	641	1371	432	1471	635	1374	1108
2	4	-2074	-2530	-1998	-2440	-2866	-1688	-2324	-2392
2	5	532	353	928	246	1166	206	995	1014
2	6	1143	1680	442	1271	-271	128	349	481
3	3	-2897	-3735	-2921	-3738	-3712	-3957	-3043	-3225
3	4	170	621	1286	1415	1215	1302	1203	1172
3	5	519	234	-734	-49	-245	-253	-793	-79
3	6	433	338	426	203	293	159	302	30
4	4	-556	-1116	-658	-1380	-1517	-1231	-985	-798
4	5	-319	-80	-132	115	-153	77	402	-429
4	6	935	1522	852	590	573	676	-180	215
5	5	1189	1443	-320	1724	1448	1319	1851	1130
5	6	-1483	-894	-577	-1217	-959	-5	-458	-488
			472		1241		933		736

Table 42. Observed minus computed values of secular change in north component (X) of magnetic field intensity for 1912.5 expressed in units of 10^{-6} CGS per year

Geographic east longitude in degrees	Geographic colatitude in degrees								
	10	20	30	40	50	60	70	80	90
30	34	64	-26	-26	7	-2	8	-30	-9
60	4	83	25	-2	4	43	32	-22	-46
90	-20	7	82	1	59	20	64	-2	-47
120	-36	29	-11	-25	0	-26	-34	-38	4
150	-64	-46	-62	38	-29	32	32	-41	-19
180	-50	-186	-96	-53	-61	1	7	-20	-27
210	-27	-53	4	-34	-52	-54	-55	-36	17
240	-21	-13	98	101	60	-9	-28	82	76
270	-9	-104	44	84	79	-42	34	-20	142
300	22	32	37	31	5	-23	-114	-22	73
330	50	19	-78	-82	5	-4	43	35	-40
360	64	8	11	-20	-13	27	35	-21	-64

Geographic east longitude in degrees	Geographic colatitude in degrees							
	100	110	120	130	140	150	160	170
30	50	50	-115	-36	50	89	88	-277
60	29	63	-4	-51	20	180	141	-398
90	72	156	-70	-99	95	265	22	-439
120	24	-16	-114	-42	100	202	-61	-359
150	40	23	-26	12	-33	-118	-130	-74
180	-26	-70	-5	98	-66	-205	-140	226
210	0	-77	-55	-56	-19	-111	-102	189
240	-21	-90	96	153	68	-98	-71	62
270	21	-75	28	96	127	-78	-143	89
300	22	-146	-35	27	51	0	-47	74
330	-33	6	105	-14	-144	-32	1	37
360	-12	60	75	-168	42	123	28	-100

Table 43. Observed minus computed values of secular change in north component (X) of magnetic field intensity for 1922.5 expressed in units of 10^{-6} CGS per year

Geographic east longitude in degrees	Geographic colatitude in degrees								
	10	20	30	40	50	60	70	80	90
30	69	48	-28	130	-10	14	-51	-24	-21
60	43	61	-77	-74	6	35	9	9	-42
90	71	54	-59	23	76	34	-15	-5	-42
120	88	15	-8	-4	-12	-15	-1	-5	-12
150	65	-64	-46	-3	32	41	-10	3	-29
180	48	-73	-88	-56	-26	14	0	-38	-33
210	63	13	-13	-45	-45	-31	-12	-17	-8
240	1	9	88	76	74	16	13	16	42
270	-34	-39	2	12	-45	-23	46	14	16
300	-65	8	16	60	-17	-71	-62	-13	50
330	-47	48	5	-41	-15	-12	48	64	-32
360	0	74	91	17	-6	45	52	-14	-8

Geographic east longitude in degrees	Geographic colatitude in degrees							
	100	110	120	130	140	150	160	170
30	34	19	-122	-13	10	56	-61	-158
60	-2	44	-14	-12	-7	78	-3	-241
90	73	89	-60	-63	54	126	24	-234
120	6	32	-54	-88	90	205	18	-176
150	15	53	1	-18	11	-42	-55	-96
180	-9	12	-24	-46	-13	-65	-108	14
210	-6	-19	-64	-47	56	60	-90	1
240	17	14	47	60	13	-9	-67	-13
270	-4	-51	1	70	87	-77	-84	85
300	-29	-100	17	-5	-82	-73	-35	115
330	-61	14	86	66	-121	-29	58	125
360	18	49	52	-80	75	136	-9	-3

Table 44. Observed minus computed values of secular change in north component (X) of magnetic field intensity for 1932.5 expressed in units of 10^{-6} CGS per year

Geographic east longitude in degrees	Geographic colatitude in degrees								
	10	20	30	40	50	60	70	80	90
30	2	-43	-74	-112	-71	-25	-5	-74	-33
60	36	-32	-56	-45	7	47	29	-45	-38
90	123	22	12	45	61	28	0	-51	55
120	128	31	47	55	22	-5	47	73	-98
150	66	17	-14	2	-11	-29	14	17	-16
180	42	17	-31	-16	3	12	-13	-11	15
210	-19	-12	20	2	-6	-19	0	13	33
240	-91	-29	41	12	25	13	-9	-5	-11
270	-100	-38	7	18	-99	-93	15	86	-16
300	-128	-15	90	63	13	-22	2	14	-18
330	-117	-12	56	53	-27	-62	56	59	7
360	-84	-27	38	-16	-5	75	11	-55	-13

Geographic east longitude in degrees	Geographic colatitude in degrees								
	100	110	120	130	140	150	160	170	
30	27	-21	-106	-46	-87	-70	-54	33	
60	37	-19	5	23	-11	68	-77	-183	
90	66	69	-68	-66	83	167	29	-167	
120	50	8	76	-38	81	129	159	64	
150	-17	49	0	-29	-102	-32	112	211	
180	-53	-18	14	69	-44	-97	17	199	
210	22	-28	-24	26	28	3	-75	55	
240	-7	-18	43	14	5	-100	-31	65	
270	-73	-27	18	-8	5	-130	-76	210	
300	-20	12	12	33	-15	-56	-61	280	
330	-16	-4	36	27	4	14	-10	138	
360	13	36	-13	-12	44	-6	-75	85	

Table 45. Observed minus computed values of secular change in north component (X) of magnetic field intensity for 1942.5 expressed in units of 10^{-6} CGS per year

Geographic east longitude in degrees	Geographic colatitude in degrees								
	10	20	30	40	50	60	70	80	90
30	153	18	-80	-89	-22	26	-7	-63	-15
60	142	72	76	-24	49	50	4	15	30
90	90	101	0	-33	29	109	62	-12	-20
120	42	74	44	57	-34	25	54	44	10
150	-66	-13	59	-41	-55	-9	12	2	-19
180	-144	-108	29	-22	-45	-39	12	32	2
210	-144	-103	30	25	-10	-29	-25	-10	-31
240	-70	-64	55	19	-40	-51	10	32	15
270	31	25	40	-42	-66	-27	14	-34	-92
300	82	61	76	-16	-28	-46	76	41	-14
330	36.	-19	21	6	52	-6	-50	-9	-20
360	97	3	-49	-61	60	79	-29	-19	19

Geographic east longitude in degrees	Geographic colatitude in degrees								
	100	110	120	130	140	150	160	170	
30	26	-68	-73	97	-15	-108	7	-48	
60	48	74	21	-36	-80	64	188	-124	
90	36	61	59	-6	-1	253	.392	-109	
120	-9	33	199	-103	-179	57	327	-172	
150	-43	-46	33	43	-59	-100	95	-66	
180	-25	-22	16	18	-88	-93	8	82	
210	-38	-46	24	35	-62	-134	-61	196	
240	-9	-36	-38	45	69	-67	-137	290	
270	-63	-14	21	-31	-65	-156	-88	378	
300	-33	-7	88	-11	10	-100	-51	420	
330	-17	16	-47	-6	58	20	33	363	
360	87	11	-37	24	-13	-29	4	167	

Table 46. Observed minus computed values of secular change in east component (Y) of magnetic field intensity for 1912.5 expressed in units of 10^{-6} CGS per year

Geographic east longitude in degrees	Geographic colatitude in degrees								
	10	20	30	40	50	60	70	80	90
30	-14	-37	40	14	6	-25	-56	-26	-10
60	-18	-24	3	-1	8	8	10	29	25
90	22	-7	-30	-51	-25	3	-49	-44	34
120	44	26	-22	18	54	36	21	-6	-32
150	19	46	-45	-56	-61	-37	20	-22	-24
180	-33	-38	-33	13	33	50	26	6	-21
210	-24	10	21	-34	-59	-39	-3	-8	-24
240	34	56	24	9	8	4	36	50	-1
270	24	-9	-59	-40	1	-35	-67	28	24
300	-21	-38	-14	41	50	7	0	-1	-11
330	-28	-13	-13	-26	-14	11	-25	-64	-20
360	-23	-22	36	20	-24	-32	29	68	22

Geographic east longitude in degrees	Geographic colatitude in degrees								
	100	110	120	130	140	150	160	170	•
30	35	19	78	-42	-36	11	-28	-95	
60	10	-123	-59	61	62	77	-25	-154	
90	32	-15	-1	52	6	-28	2	-76	
120	-22	-5	20	6	-100	-32	76	66	
150	12	30	24	21	-21	-24	66	154	
180	-36	-11	-5	-6	56	-44	28	138	
210	21	20	25	29	13	-41	-72	40	
240	-78	-35	14	16	3	-52	-101	-34	
270	-24	-7	33	40	51	26	-13	20	
300	7	9	-41	-59	-42	25	19	74	
330	60	36	-12	8	16	60	57	-37	
360	-35	-95	-55	103	-22	13	42	-96	

Table 47. Observed minus computed values of secular change in east component (Y) of magnetic field intensity for 1922.5 expressed in units of 10^{-6} CGS per year

Geographic east longitude in degrees	Geographic colatitude in degrees								
	10	20	30	40	50	60	70	80	90
30	-52	4	65	62	50	0	-69	-32	25
60	-29	-10	-13	-45	-39	-17	43	61	42
90	10	30	43	35	7	10	-43	-41	53
120	-17	-35	-20	-2	35	27	19	10	14
150	-1	-37	-5	9	-14	-29	-31	-10	11
180	67	-24	-27	13	41	59	40	22	-16
210	62	19	-19	-31	-48	-46	-17	-13	18
240	50	39	42	34	47	59	34	32	-8
270	0	-14	-21	-69	-47	-60	-47	49	54
300	-37	-39	-20	91	152	1	-24	-16	6
330	-37	-14	-20	-31	-21	4	-20	-27	-1
360	-52	-18	63	33	-18	-28	4	53	94

Geographic east longitude in degrees	Geographic colatitude in degrees								
	100	110	120	130	140	150	160	170	
30	11	58	125	71	33	39	2	-85	
60	8	-11	-37	-26	-36	-6	61	-67	
90	3	19	85	125	96	17	39	-79	
120	2	62	17	-61	-83	-79	8	68	
150	28	82	65	13	72	25	10	51	
180	3	-4	17	25	26	28	13	86	
210	58	63	66	23	-10	-69	-83	25	
240	-42	-1	56	60	-1	-36	-74	-8	
270	15	27	22	75	70	37	10	68	
300	65	26	-2	-28	-89	-21	54	81	
330	60	43	52	61	92	75	-21	-25	
360	16	-66	-57	43	-14	49	-95	-165	

Table 48. Observed minus computed values of secular change in east component (Y) of magnetic field intensity for 1932.5 expressed in units of 10^{-6} CGS per year

Geographic east longitude in degrees	Geographic colatitude in degrees								
	10	20	30	40	50	60	70	80	90
30	-32	-42	83	-12	85	-4	-17	7	-4
60	-25	16	-24	14	19	13	37	14	-38
90	-32	-1	63	54	4	-13	-32	-5	44
120	-20	-39	-11	-37	16	40	37	66	-33
150	-42	-18	10	10	3	-2	-3	33	-13
180	-3	-22	-10	13	21	28	29	28	18
210	24	-6	-2	-3	-8	0	6	13	1
240	33	34	-5	-35	27	86	54	-26	-32
270	32	33	-82	-102	-13	0	137	5	-104
300	28	24	1	26	53	58	7	-69	22
330	-25	12	1	-27	-30	18	33	17	-10
360	-63	9	10	40	31	-13	21	36	10

Geographic east longitude in degrees	Geographic colatitude in degrees							
	100	110	120	130	140	150	160	170
30	-19	-2	59	15	-3	98	-20	-151
60	38	6	-83	-41	83	94	35	-119
90	12	-21	-2	1	8	60	82	12
120	-75	-33	53	85	-21	-100	34	104
150	-46	25	55	55	-116	-89	-3	89
180	-46	-43	-16	42	75	61	56	87
210	-17	2	26	29	22	-40	-117	-13
240	-34	29	35	-12	-67	-36	-4	42
270	-48	48	82	36	7	-48	118	187
300	49	7	-46	-59	-62	17	63	169
330	-41	-18	35	65	73	67	-31	-32
360	-12	-29	-19	-25	22	46	-99	-215

Table 49. Observed minus computed values of secular change in east component (Y) of magnetic field intensity for 1942.5 expressed in units of 10^{-6} CGS per year

Geographic east longitude in degrees	Geographic colatitude in degrees								
	10	20	30	40	50	60	70	80	90
30	-80	-22	-73	-22	20	-15	-6	-21	-40
60	-40	55	-10	-1	-5	-20	-39	22	-6
90	-19	65	49	-1	-37	-34	-26	-3	10
120	-23	-22	2	-57	-38	18	22	14	-49
150	-31	-46	-7	-13	-22	0	-8	-29	-31
180	4	-6	-9	-14	-22	10	-1	-10	-17
210	27	7	29	-11	-32	-36	-22	-6	-12
240	-1	-20	-17	-1	9	13	1	-35	-27
270	33	-50	-70	-82	-6	-1	-12	-5	-34
300	34	-17	12	10	16	17	-61	-19	9
330	29	6	52	17	-50	-47	-4	-21	0
360	-42	-39	-28	-6	-3	-13	4	-5	-13

Geographic east longitude in degrees	Geographic colatitude in degrees							
	100	110	120	130	140	150	160	170
30	-38	25	78	4	-30	-1	-41	-135
60	-23	7	-11	-64	-24	48	-16	-102
90	-29	-26	8	51	43	11	-11	10
120	-66	7	91	-22	-117	-64	-15	201
150	-31	19	44	49	-26	-120	-130	36
180	-14	-8	-16	-22	6	48	52	113
210	-15	13	18	12	-16	-48	9	29
240	1	-5	-12	6	-4	-73	-46	-38
270	-36	22	39	-6	14	14	32	-135
300	12	-21	-15	-44	-27	33	24	-223
330	-14	-10	22	13	-7	54	118	-146
360	-34	-1	28	-45	-60	-4	102	-68

Table 50. Computed values of secular change in north component (X) of magnetic field intensity for 1932.5 at height 100 km expressed in units of 10^{-6} CGS per year

Geographic east longitude in degrees	Geographic colatitude in degrees								
	10	20	30	40	50	60	70	80	90
30	-375	-396	-321	-157	43	202	236	106	-160
60	-521	-513	-424	-266	-63	139	274	266	84
90	-515	-471	-349	-165	53	267	420	446	302
120	-402	-348	-241	-100	33	114	124	73	0
150	-221	-202	-154	-77	18	97	111	35	-97
180	-19	-52	-54	-32	6	41	43	-15	-132
210	171	70	1	-40	-72	-107	-154	-215	-289
240	331	188	47	-88	-213	-314	-369	-375	-362
270	423	298	114	-130	-392	-580	-608	-466	-259
300	384	314	177	-29	-259	-421	-436	-307	-138
330	187	164	166	194	217	192	91	-70	-253
360	-106	-128	-67	73	235	323	269	71	-208

Geographic east longitude in degrees	Geographic colatitude in degrees							
	100	110	120	130	140	150	160	170
30	-461	-664	-669	-470	-160	118	251	222
60	-212	-480	-565	-410	-110	145	197	34
90	16	-295	-489	-485	-333	-184	-176	-310
120	-55	-66	-42	-25	-73	-217	-424	-586
150	-205	-212	-117	-15	-27	-200	-454	-620
180	-261	-340	-334	-269	-213	-228	-310	-390
210	-372	-446	-475	-428	-301	-140	-23	-12
240	-385	-465	-552	-549	-383	-88	194	308
270	-147	-223	-432	-593	-538	-243	144	412
300	-77	-208	-478	-720	-755	-515	-89	331
330	-429	-593	-742	-842	-817	-601	-208	235
360	-483	-681	-766	-731	-577	-326	-29	231

Table 51. Computed values of secular change in north component (X) of magnetic field intensity for 1932.5 at height 300 km expressed in units of 10^{-6} CGS per year

Geographic east longitude in degrees	Geographic colatitude in degrees								
	10	20	30	40	50	60	70	80	90
30	-327	-343	-277	-137	31	163	189	77	-148
60	-460	-451	-372	-233	-57	115	226	215	60
90	-460	-416	-308	-148	41	224	352	369	245
120	-356	-307	-213	-91	24	96	107	66	2
150	-195	-177	-134	-67	13	77	86	23	-86
180	-14	-43	-46	-27	3	30	27	-25	-125
210	155	67	3	-36	-67	-101	-144	-198	-264
240	296	170	42	-79	-191	-281	-331	-339	-332
270	375	262	97	-116	-340	-500	-526	-413	-248
300	341	277	155	-22	-218	-356	-375	-275	-146
330	169	150	150	170	183	157	69	-70	-230
360	-88	-103	-50	67	199	269	219	48	-192

Geographic east longitude in degrees	Geographic colatitude in degrees							
	100	110	120	130	140	150	160	170
30	-401	-570	-576	-411	-153	80	197	181
60	-188	-409	-480	-355	-110	100	147	21
90	5	-254	-417	-417	-296	-177	-167	-270
120	-48	-63	-52	-45	-91	-212	-379	-503
150	-175	-183	-112	-37	-54	-199	-404	-532
180	-234	-302	-300	-249	-205	-216	-280	-339
210	-336	-397	-420	-379	-271	-135	-35	-22
240	-353	-417	-483	-473	-330	-84	149	245
270	-159	-220	-385	-510	-458	-212	108	334
300	-103	-213	-434	-628	-651	-446	-89	268
330	-387	-532	-662	-744	-716	-525	-188	191
360	-430	-602	-677	-646	-511	-292	-36	189

Table 52. Computed values of secular change in north component (X) of magnetic field intensity for 1932.5 at height 500 km expressed in units of 10^{-6} CGS per year

Geographic east longitude in degrees	Geographic colatitude in degrees								
	10	20	30	40	50	60	70	80	90
30	-287	-298	-240	-121	21	131	151	54	-136
60	-406	-398	-327	-205	-52	95	187	175	42
90	-408	-369	-273	-133	31	188	295	307	200
120	-317	-273	-190	-83	17	81	92	58	4
150	-173	-156	-118	-59	8	60	67	13	-78
180	-11	-36	-39	-24	0	20	15	-32	-118
210	141	63	5	-33	-63	-95	-134	-183	-241
240	265	154	38	-71	-172	-252	-297	-307	-305
270	334	232	84	-103	-296	-434	-459	-369	-236
300	303	245	137	-17	-185	-304	-324	-249	-148
330	153	137	136	149	156	129	51	-70	-210
360	-74	-84	-37	62	170	225	179	30	-177

Geographic east longitude in degrees	Geographic colatitude in degrees							
	100	110	120	130	140	150	160	170
30	-350	-493	-498	-361	-145	52	155	149
60	-166	-352	-412	-309	-107	67	109	11
90	-3	-221	-357	-361	-265	-168	-158	-236
120	-42	-61	-58	-59	-103	-204	-339	-433
150	-151	-160	-107	-52	-72	-194	-361	-458
180	-211	-269	-270	-230	-196	-204	-253	-296
210	-304	-356	-374	-337	-244	-129	-43	-29
240	-323	-375	-425	-410	-287	-81	115	197
270	-165	-214	-345	-442	-394	-187	81	272
300	-119	-213	-395	-551	-565	-390	-86	218
330	-349	-479	-593	-660	-630	-461	-170	156
360	-383	-535	-601	-573	-454	-263	-40	156

Table 53. Computed values of secular change in north component (X) of magnetic field intensity for 1932.5 at height 1000 km expressed in units of 10^{-6} CGS per year

Geographic east longitude in degrees	Geographic colatitude in degrees								
	10	20	30	40	50	60	70	80	90
30	-211	-215	-173	-91	5	76	85	17	-113
60	-305	-296	-243	-153	-45	56	116	104	13
90	-309	-278	-207	-105	12	121	193	197	121
120	-240	-206	-145	-68	4	51	63	41	3
150	-130	-116	-86	-45	-0	32	34	-1	-61
180	-6	-24	-27	-18	-4	4	-4	-41	-102
210	110	53	7	-26	-53	-81	-113	-151	-195
240	203	119	30	-56	-134	-195	-231	-243	-247
270	253	173	60	-77	-215	-311	-333	-283	-205
300	230	183	103	-8	-126	-211	-233	-196	-144
330	120	110	107	109	106	80	21	-67	-171
360	-48	-51	-17	47	115	145	107	1	-146

Geographic east longitude in degrees	Geographic colatitude in degrees							
	100	110	120	130	140	150	160	170
30	-255	-351	-356	-267	-125	8	84	91
60	-125	-247	-286	-223	-96	15	48	-3
90	-14	-159	-251	-259	-203	-144	-134	-172
120	-32	-55	-63	-76	-111	-178	-258	-306
150	-109	-119	-95	-71	-94	-174	-274	-324
180	-166	-206	-211	-190	-169	-173	-198	-215
210	-240	-275	-285	-256	-192	-113	-53	-35
240	-261	-291	-315	-296	-208	-71	57	115
270	-163	-192	-267	-318	-278	-140	36	166
300	-135	-200	-315	-408	-407	-284	-77	132
330	-276	-374	-455	-497	-467	-341	-134	94
360	-294	-403	-452	-430	-343	-205	-44	97

Table 54. Computed values of secular change in north component (X) of magnetic field intensity for 1932.5 at height 5000 km expressed in units of 10^{-6} CGS per year

Geographic east longitude in degrees	Geographic colatitude in degrees								
	10	20	30	40	50	60	70	80	90
30	-33	-33	-28	-21	-13	-9	-11	-19	-32
60	-53	-52	-45	-33	-21	-10	-5	-7	-16
90	-57	-52	-43	-29	-14	-2	4	4	-3
120	-45	-40	-32	-21	-11	-4	-2	-3	-8
150	-25	-22	-18	-13	-9	-8	-9	-13	-19
180	-1	-3	-5	-7	-9	-12	-17	-25	-33
210	20	11	1	-8	-17	-25	-34	-42	-50
240	37	22	5	-12	-28	-41	-51	-58	-62
270	45	29	9	-12	-32	-48	-58	-61	-61
300	42	32	18	1	-16	-31	-42	-49	-54
330	25	23	19	14	7	-2	-15	-31	-49
360	-2	-2	0	3	5	2	-7	-23	-42

Geographic east longitude in degrees	Geographic colatitude in degrees							
	100	110	120	130	140	150	160	170
30	-46	-54	-55	-48	-35	-21	-8	1
60	-27	-37	-41	-37	-28	-19	-11	-7
90	-15	-28	-38	-41	-39	-35	-30	-24
120	-15	-22	-29	-36	-41	-45	-45	-39
150	-26	-31	-35	-39	-44	-48	-49	-42
180	-41	-47	-50	-50	-48	-45	-40	-32
210	-56	-59	-58	-54	-45	-34	-24	-15
240	-64	-64	-61	-53	-41	-25	-11	-1
270	-61	-61	-61	-57	-48	-31	-13	4
300	-60	-68	-74	-75	-68	-50	-25	1
330	-66	-81	-90	-90	-80	-59	-31	-0
360	-61	-75	-81	-77	-64	-44	-21	1

Table 55. Computed values of secular change in north component (X) of magnetic field intensity for 1942.5 at height 100 km expressed in units of 10^{-6} CGS per year

Geographic east longitude in degrees	Geographic colatitude in degrees								
	10	20	30	40	50	60	70	80	90
30	-299	-255	-145	11	179	309	347	249	22
60	-401	-353	-227	-59	125	309	460	511	393
90	-371	-278	-85	130	297	401	466	495	443
120	-243	-159	-3	149	225	212	161	134	143
150	-67	-32	31	85	98	74	47	36	35
180	98	84	86	85	59	8	-49	-96	-135
210	211	138	79	35	-10	-68	-139	-210	-274
240	266	178	130	103	51	-50	-180	-295	-373
270	267	209	190	160	62	-94	-233	-285	-266
300	211	213	252	278	241	147	51	-5	-53
330	85	157	283	405	444	369	215	46	-106
360	-105	-25	115	264	354	345	240	72	-122

Geographic east longitude in degrees	Geographic colatitude in degrees							
	100	110	120	130	140	150	160	170
30	-262	-477	-510	-340	-60	168	218	81
60	111	-223	-439	-427	-229	-19	22	-145
90	259	-30	-312	-456	-429	-330	-303	-407
120	148	105	14	-88	-179	-271	-389	-513
150	19	-15	-52	-73	-93	-151	-265	-386
180	-175	-215	-230	-196	-118	-42	-24	-79
210	-333	-380	-387	-311	-138	83	254	276
240	-435	-501	-540	-474	-246	97	406	519
270	-271	-371	-526	-591	-438	-81	313	547
300	-170	-396	-663	-816	-723	-384	56	407
330	-263	-453	-652	-770	-706	-441	-66	257
360	-316	-479	-564	-527	-365	-130	78	180

Table 56. Computed values of secular change in north component (X) of magnetic field intensity for 1942.5 at height 300 km expressed in units of 10^{-6} CGS per year

Geographic east longitude in degrees	Geographic colatitude in degrees								
	10	20	30	40	50	60	70	80	90
30	-256	-216	-121	13	156	265	294	210	17
60	-347	-304	-194	-47	113	272	398	435	330
90	-321	-240	-75	109	256	351	409	430	377
120	-209	-134	-3	126	193	188	150	128	131
150	-56	-23	29	74	85	66	43	32	28
180	88	77	77	73	50	6	-44	-87	-122
210	189	127	75	34	-9	-64	-127	-191	-248
240	240	165	119	89	38	-52	-164	-263	-333
270	245	194	173	140	52	-80	-198	-248	-243
300	197	200	230	247	212	130	46	-10	-62
330	85	149	255	354	385	320	189	41	-98
360	-84	-13	106	232	308	299	209	62	-108

Geographic east longitude in degrees	Geographic colatitude in degrees								
	100	110	120	130	140	150	160	170	
30	-220	-400	-431	-294	-67	119	162	53	
60	92	-186	-368	-364	-208	-41	-8	-141	
90	217	-28	-266	-391	-378	-304	-284	-364	
120	128	85	3	-89	-173	-257	-356	-451	
150	13	-17	-49	-72	-95	-150	-245	-339	
180	-158	-191	-204	-175	-110	-48	-32	-74	
210	-299	-337	-338	-270	-122	65	208	230	
240	-389	-442	-469	-404	-208	79	337	434	
270	-256	-341	-464	-508	-375	-76	253	455	
300	-171	-363	-584	-705	-623	-338	33	335	
330	-242	-410	-579	-675	-616	-389	-70	208	
360	-280	-421	-493	-463	-325	-127	50	141	

Table 57. Computed values of secular change in north component (X) of magnetic field intensity for 1942.5 at height 500 km expressed in units of 10^{-6} CGS per year

Geographic east longitude in degrees	Geographic colatitude in degrees								
	10	20	30	40	50	60	70	80	90
30	-221	-185	-101	14	136	228	251	177	13
60	-303	-263	-167	-37	103	240	345	372	279
90	-280	-208	-67	92	222	308	359	374	324
120	-181	-114	-2	107	167	167	139	121	119
150	-47	-17	28	65	74	59	39	28	22
180	79	71	69	64	42	3	-40	-78	-111
210	169	117	71	32	-9	-59	-116	-173	-225
240	217	153	109	77	28	-52	-149	-236	-299
270	223	181	157	123	44	-68	-170	-218	-222
300	183	187	210	220	187	115	40	-14	-68
330	83	141	231	312	335	279	166	35	-91
360	-68	-4	98	205	268	260	181	53	-98

Geographic east longitude in degrees	Geographic colatitude in degrees								
	100	110	120	130	140	150	160	170	
30	-187	-339	-366	-255	-71	81	118	32	
60	77	-157	-311	-312	-189	-56	-29	-135	
90	183	-26	-228	-338	-334	-279	-265	-325	
120	110	69	-5	-89	-166	-242	-324	-397	
150	8	-18	-47	-70	-96	-145	-225	-297	
180	-143	-171	-181	-156	-103	-52	-37	-67	
210	-269	-300	-297	-236	-108	50	172	193	
240	-349	-393	-409	-348	-178	64	281	366	
270	-240	-313	-411	-440	-323	-71	206	381	
300	-168	-333	-516	-614	-541	-298	16	277	
330	-223	-372	-516	-594	-540	-344	-72	169	
360	-248	-371	-434	-408	-291	-123	29	110	

Table 58. Computed values of secular change in north component (X) of magnetic field intensity for 1942.5 at height 1000 km expressed in units of 10^{-6} CGS per year

Geographic east longitude in degrees	Geographic colatitude in degrees								
	10	20	30	40	50	60	70	80	90
30	-156	-127	-66	15	99	160	172	119	7
60	-219	-187	-117	-22	80	177	246	257	189
90	-203	-149	-50	63	159	225	264	269	226
120	-131	-80	-2	74	119	127	114	101	94
150	-34	-8	23	48	55	45	31	21	13
180	59	56	52	45	28	-	-32	-62	-88
210	129	94	59	26	-8	-49	-94	-138	-176
240	169	124	88	55	12	-48	-119	-182	-231
270	179	148	125	91	32	-48	-121	-162	-179
300	150	156	167	167	140	86	28	-21	-73
330	76	120	180	231	243	202	121	23	-76
360	-39	8	80	152	194	187	130	36	-75

Geographic east longitude in degrees	Geographic colatitude in degrees								
	100	110	120	130	140	150	160	170	
30	-127	-229	-251	-185	-72	23	49	0	
60	50	-105	-210	-219	-150	-73	-57	-119	
90	123	-22	-160	-241	-250	-225	-218	-249	
120	78	40	-17	-84	-145	-202	-257	-294	
150	0	-19	-43	-65	-90	-129	-180	-218	
180	-112	-131	-137	-120	-86	-53	-40	-53	
210	-208	-227	-220	-172	-81	26	109	128	
240	-268	-295	-297	-245	-124	39	183	245	
270	-202	-252	-308	-316	-230	-60	127	251	
300	-153	-268	-387	-443	-389	-223	-7	177	
330	-181	-292	-391	-440	-397	-259	-70	102	
360	-187	-276	-321	-303	-224	-109	-3	59	

Table 59. Computed values of secular change in north component (X) of magnetic field intensity for 1942.5 at height 5000 km expressed in units of 10^{-6} CGS per year

Geographic east longitude in degrees	Geographic colatitude in degrees								
	10	20	30	40	50	60	70	80	90
30	-19	-14	-5	4	12	17	16	9	-2
60	-32	-26	-15	-1	11	23	28	27	18
90	-33	-23	-9	5	19	30	35	34	25
120	-23	-13	-2	7	16	20	21	19	14
150	-9	-2	2	5	7	6	4	1	-2
180	6	7	6	4	0	-4	-10	-16	-21
210	20	16	10	3	-5	-14	-23	-32	-38
240	31	25	16	6	-4	-16	-28	-39	-47
270	37	33	26	16	4	-8	-21	-33	-42
300	35	37	35	31	23	12	-0	-15	-30
330	23	29	35	38	35	27	13	-4	-23
360	1	9	17	24	27	23	14	-0	-17

Geographic east longitude in degrees	Geographic colatitude in degrees								
	100	110	120	130	140	150	160	170	
30	-15	-27	-32	-31	-27	-21	-18	-17	
60	3	-12	-25	-31	-33	-31	-31	-31	
90	10	-6	-23	-36	-44	-47	-47	-43	
120	6	-3	-15	-28	-38	-46	-48	-44	
150	-6	-11	-17	-23	-29	-33	-35	-30	
180	-25	-27	-27	-25	-22	-17	-12	-7	
210	-41	-42	-37	-28	-16	-3	8	14	
240	-52	-52	-47	-36	-20	-1	14	26	
270	-50	-55	-56	-50	-37	-17	4	23	
300	-46	-60	-70	-70	-60	-40	-14	11	
330	-43	-60	-71	-73	-65	-47	-23	0	
360	-33	-46	-53	-52	-45	-33	-19	-7	

Table 60. Computed values of secular change in east component (Y) of magnetic field intensity for 1932.5 at height 100 km expressed in units of 10^{-6} CGS per year

Geographic east longitude in degrees	Geographic colatitude in degrees								
	10	20	30	40	50	60	70	80	90
30	301	323	352	398	453	497	507	476	421
60	78	25	- 30	- 74	- 97	- 112	- 145	- 216	- 323
90	- 138	- 203	- 263	- 309	- 327	- 312	- 269	- 213	- 167
120	- 273	- 282	- 254	- 194	- 124	- 61	- 11	38	102
150	- 318	- 293	- 262	- 224	- 180	- 137	- 99	- 67	- 41
180	- 291	- 233	- 188	- 152	- 113	- 62	2	68	114
210	- 224	- 167	- 115	- 74	- 40	1	62	138	213
240	- 132	- 144	- 153	- 151	- 123	- 57	37	128	179
270	9	- 48	- 90	- 102	- 75	- 16	48	84	65
300	202	163	109	9	- 154	- 369	- 587	- 746	- 803
330	371	391	390	348	258	129	- 5	- 111	- 160
360	417	469	507	527	525	501	461	420	398

Geographic east longitude in degrees	Geographic colatitude in degrees								
	100	110	120	130	140	150	160	170	
30	371	344	330	294	190	- 1	- 257	- 517	
60	- 437	- 517	- 536	- 503	- 454	- 436	- 471	- 541	
90	- 148	- 162	- 207	- 271	- 340	- 396	- 422	- 403	
120	177	238	250	193	81	- 36	- 101	- 76	
150	- 19	0	20	49	95	162	245	326	
180	128	118	115	155	261	418	574	661	
210	268	298	322	373	471	605	728	776	
240	173	126	85	99	193	343	494	587	
270	- 13	- 126	- 228	- 274	- 238	- 125	34	198	
300	- 757	- 649	- 538	- 461	- 418	- 376	- 298	- 172	
330	- 150	- 109	- 75	- 82	- 141	- 234	- 325	- 379	
360	407	440	462	428	301	78	- 199	- 458	

Table 61. Computed values of secular change in east component (Y) of magnetic field intensity for 1932.5 at height 300 km expressed in units of 10^{-6} CGS per year

Geographic east longitude in degrees	Geographic colatitude in degrees								
	10	20	30	40	50	60	70	80	90
30	266	287	313	352	398	432	439	412	366
60	69	25	- 20	- 57	- 78	- 93	- 123	- 184	- 273
90	- 123	- 178	- 228	- 266	- 281	- 269	- 235	- 191	- 154
120	- 243	- 250	- 227	- 177	- 117	- 63	- 17	28	84
150	- 283	- 259	- 230	- 195	- 157	- 119	- 85	- 56	- 32
180	- 259	- 209	- 168	- 134	- 98	- 52	3	60	100
210	- 200	- 152	- 107	- 70	- 37	2	57	123	187
240	- 117	- 126	- 132	- 127	- 100	- 42	37	113	157
270	11	- 39	- 77	- 89	- 70	- 26	24	51	35
300	181	144	92	2	- 138	- 319	- 501	- 635	- 685
330	329	344	338	298	217	106	- 9	- 99	- 142
360	369	415	448	466	464	444	410	376	357

Geographic east longitude in degrees	Geographic colatitude in degrees								
	100	110	120	130	140	150	160	170	
30	322	295	279	243	153	- 6	- 218	- 430	
60	- 367	- 433	- 450	- 424	- 386	- 371	- 397	- 451	
90	- 138	- 150	- 187	- 238	- 292	- 335	- 353	- 334	
120	146	195	203	156	64	- 29	- 80	- 59	
150	- 11	7	26	52	91	147	213	277	
180	115	110	112	147	235	363	487	554	
210	234	261	283	326	405	512	609	645	
240	152	115	82	94	168	287	408	483	
270	- 29	- 120	- 202	- 237	- 206	- 111	21	158	
300	- 651	- 565	- 473	- 407	- 366	- 324	- 254	- 147	
330	- 136	- 102	- 73	- 77	- 123	- 197	- 271	- 315	
360	362	385	399	364	254	67	- 164	- 380	

Table 62. Computed values of secular change in east component (Y) of magnetic field intensity for 1932.5 at height 500 km expressed in units of 10^{-6} CGS per year

Geographic east longitude in degrees	Geographic colatitude in degrees								
	10	20	30	40	50	60	70	80	90
30	237	256	280	313	350	378	382	359	319
60	62	25	- 13	- 44	- 62	- 78	- 105	- 158	- 232
90	- 109	- 156	- 199	- 230	- 242	- 233	- 206	- 170	- 141
120	- 216	- 222	- 202	- 161	- 111	- 63	- 21	20	68
150	- 252	- 229	- 203	- 172	- 138	- 104	- 73	- 47	- 24
180	- 231	- 187	- 151	- 119	- 86	- 45	4	52	88
210	- 178	- 138	- 99	- 65	- 34	3	52	110	165
240	- 103	- 111	- 115	- 108	- 82	- 31	36	100	137
270	11	- 33	- 67	- 79	- 66	- 32	6	27	12
300	161	126	77	- 2	- 124	- 278	- 431	- 544	- 587
330	292	303	295	257	185	89	- 11	- 88	- 125
360	328	368	397	413	412	395	366	337	320

Geographic east longitude in degrees	Geographic colatitude in degrees								
	100	110	120	130	140	150	160	170	
30	281	256	237	203	124	- 10	- 184	- 360	
60	- 310	- 364	- 380	- 360	- 329	- 317	- 337	- 379	
90	- 129	- 138	- 168	- 209	- 253	- 286	- 298	- 279	
120	121	160	166	126	51	- 24	- 65	- 46	
150	- 5	11	30	53	87	133	187	237	
180	103	103	107	140	213	317	417	468	
210	205	230	250	286	351	437	513	540	
240	134	105	79	88	147	242	339	401	
270	- 40	- 113	- 179	- 207	- 179	- 100	11	127	
300	- 562	- 493	- 418	- 360	- 321	- 281	- 218	- 126	
330	- 122	- 95	- 70	- 72	- 108	- 167	- 227	- 265	
360	322	338	345	312	216	57	- 136	- 317	

Table 63. Computed values of secular change in east component (Y) of magnetic field intensity for 1932.5 at height 1000 km expressed in units of 10^{-6} CGS per year

Geographic east longitude in degrees	Geographic colatitude in degrees								
	10	20	30	40	50	60	70	80	90
30	180	196	214	236	260	276	276	259	232
60	48	24	- 0	- 21	- 36	- 50	- 72	- 108	- 158
90	- 81	- 114	- 143	- 163	- 172	- 167	- 151	- 130	- 113
120	- 163	- 167	- 155	- 127	- 93	- 58	- 26	6	41
150	- 191	- 173	- 152	- 127	- 101	- 76	- 52	- 31	- 13
180	- 177	- 144	- 115	- 89	- 62	- 31	5	39	66
210	- 137	- 109	- 80	- 53	- 26	4	42	84	123
240	- 77	- 83	- 82	- 74	- 52	- 15	31	74	99
270	10	- 22	- 48	- 60	- 55	- 38	- 18	- 8	- 18
300	122	92	52	- 9	- 96	- 200	- 302	- 378	- 411
330	219	223	213	181	127	58	- 11	- 65	- 93
360	247	277	298	309	309	297	278	258	245

Geographic east longitude in degrees	Geographic colatitude in degrees								
	100	110	120	130	140	150	160	170	
30	204	182	162	133	76	- 13	- 126	- 238	
60	- 208	- 243	- 254	- 244	- 226	- 218	- 229	- 250	
90	- 105	- 112	- 129	- 154	- 179	- 197	- 200	- 182	
120	75	100	102	76	30	- 15	- 38	- 24	
150	3	18	33	51	74	104	137	166	
180	80	85	93	118	166	230	289	316	
210	152	170	186	211	251	302	345	357	
240	99	82	67	72	107	163	221	258	
270	- 51	- 96	- 135	- 149	- 129	- 76	- 2	74	
300	- 399	- 358	- 310	- 269	- 237	- 202	- 154	- 90	
330	- 93	- 77	- 61	- 60	- 80	- 115	- 152	- 177	
360	243	248	244	215	146	38	- 89	- 209	

Table 64. Computed values of secular change in east component (Y) of magnetic field intensity for 1932.5 at height 5000 km expressed in units of 10^{-6} CGS per year

Geographic east longitude in degrees	Geographic colatitude in degrees								
	10	20	30	40	50	60	70	80	90
30	33	36	39	42	43	43	42	39	36
60	12	10	7	5	2	-1	-4	-9	-14
90	-10	-14	-18	-21	-22	-23	-23	-22	-22
120	-26	-27	-27	-24	-21	-17	-12	-7	-3
150	-32	-30	-26	-21	-16	-11	-7	-2	1
180	-31	-26	-20	-14	-8	-2	3	8	13
210	-25	-20	-15	-9	-3	3	9	15	21
240	-14	-14	-12	-10	-5	-1	3	8	11
270	0	-5	-9	-13	-15	-17	-17	-19	-20
300	18	11	3	-6	-17	-28	-39	-47	-52
330	35	33	29	23	16	7	-0	-7	-12
360	42	46	49	50	50	49	47	44	41

Geographic east longitude in degrees	Geographic colatitude in degrees							
	100	110	120	130	140	150	160	170
30	31	26	20	13	5	-3	-14	-23
60	-18	-21	-23	-24	-23	-23	-23	-23
90	-22	-22	-22	-23	-22	-21	-18	-14
120	0	2	3	2	0	-0	0	3
150	5	9	12	15	18	20	22	23
180	17	21	24	28	32	35	37	36
210	25	29	31	34	36	37	38	36
240	12	12	12	13	14	17	19	21
270	-22	-24	-25	-24	-20	-15	-7	0
300	-54	-52	-48	-43	-37	-30	-23	-15
330	-14	-15	-15	-15	-15	-17	-19	-21
360	38	34	29	22	12	1	-11	-22

Table 65. Computed values of secular change in east component (Y) of magnetic field intensity for 1942.5 at height 100 km expressed in units of 10^{-6} CGS per year

Geographic east longitude in degrees	Geographic colatitude in degrees								
	10	20	30	40	50	60	70	80	90
30	254	273	295	321	346	359	349	315	267
60	86	60	19	-26	-69	-112	-169	-252	-364
90	-97	-136	-187	-241	-280	-283	-246	-186	-136
120	-233	-244	-237	-211	-163	-94	-5	95	189
150	-290	-273	-246	-211	-175	-139	-102	-63	-23
180	-267	-219	-160	-99	-45	0	40	77	112
210	-193	-147	-93	-38	19	80	142	202	254
240	-92	-93	-104	-118	-115	-80	-14	64	129
270	33	-1	-30	-37	-17	22	57	59	13
300	174	128	63	-29	-154	-301	-442	-544	-580
330	293	286	270	236	175	88	-8	-84	-112
360	332	367	412	455	478	460	398	316	251

Geographic east longitude in degrees	Geographic colatitude in degrees							
	100	110	120	130	140	150	160	170
30	218	176	134	71	-37	-199	-399	-597
60	-485	-586	-644	-651	-625	-592	-569	-555
90	-129	-178	-271	-374	-448	-464	-415	-314
120	250	258	208	120	35	-5	21	109
150	15	53	96	156	244	355	471	552
180	147	190	253	353	492	651	783	831
210	296	336	388	466	574	692	783	808
240	159	156	145	156	209	299	401	485
270	-76	-180	-267	-306	-287	-214	-100	36
300	-548	-474	-398	-353	-348	-362	-361	-314
330	-82	-15	47	55	-16	-161	-337	-486
360	233	263	307	306	208	1	-277	-555

Table 66. Computed values of secular change in east component (Y) of magnetic field intensity for 1942.5 at height 300 km expressed in units of 10^{-6} CGS per year

Geographic east longitude in degrees	Geographic colatitude in degrees								
	10	20	30	40	50	60	70	80	90
30	224	243	262	284	304	312	301	270	227
60	74	51	17	-21	-58	-97	-147	-219	-313
90	-88	-123	-166	-211	-242	-244	-215	-167	-128
120	-207	-216	-211	-188	-147	-87	-9	76	156
150	-254	-239	-214	-184	-151	-118	-85	-50	-14
180	-234	-191	-140	-87	-39	2	38	71	103
210	-170	-130	-84	-34	16	69	124	178	224
240	-81	-82	-90	-97	-91	-59	-3	62	115
270	29	-2	-28	-36	-22	7	33	34	-4
300	153	111	54	-27	-134	-258	-377	-463	-495
330	259	252	237	205	150	73	-9	-74	-99
360	295	326	364	400	417	401	349	281	227

Geographic east longitude in degrees	Geographic colatitude in degrees							
	100	110	120	130	140	150	160	170
30	183	144	104	47	-45	-181	-346	-509
60	-414	-498	-548	-557	-537	-510	-491	-477
90	-124	-165	-242	-327	-387	-399	-358	-272
120	207	213	172	100	29	-4	17	88
150	21	56	94	147	220	312	403	467
180	136	175	231	317	433	563	669	704
210	263	299	344	410	499	594	667	685
240	140	139	131	141	184	258	342	413
270	-76	-161	-230	-260	-242	-179	-81	35
300	-472	-413	-351	-312	-303	-309	-302	-259
330	-76	-21	28	36	-22	-139	-283	-406
360	211	233	263	256	169	-4	-237	-469

Table 67. Computed values of secular change in east component (Y) of magnetic field intensity for 1942.5 at height 500 km expressed in units of 10^{-6} CGS per year

Geographic east longitude in degrees	Geographic colatitude in degrees								
	10	20	30	40	50	60	70	80	90
30	199	216	234	252	268	273	261	233	194
60	65	45	15	-17	-50	-85	-129	-191	-270
90	-80	-111	-148	-185	-210	-212	-188	-150	-120
120	-184	-193	-188	-169	-132	-80	-12	61	128
150	-225	-210	-188	-160	-131	-101	-71	-39	-6
180	-206	-168	-123	-77	-34	2	35	66	95
210	-150	-115	-75	-32	13	60	109	157	198
240	-72	-73	-77	-81	-73	-44	4	59	103
270	25	-3	-26	-35	-25	-2	16	15	-16
300	135	98	46	-25	-117	-223	-324	-397	-425
330	230	224	208	179	129	62	-9	-65	-87
360	262	291	323	352	365	350	307	251	206

Geographic east longitude in degrees	Geographic colatitude in degrees							
	100	110	120	130	140	150	160	170
30	154	118	81	30	-49	-164	-302	-438
60	-355	-427	-469	-478	-464	-443	-425	-412
90	-118	-153	-217	-286	-335	-345	-310	-237
120	172	177	143	83	25	-2	14	72
150	25	57	92	137	199	274	348	398
180	126	161	211	285	383	490	575	601
210	233	266	306	363	436	514	572	585
240	124	124	118	128	164	225	294	354
270	-75	-143	-199	-222	-205	-150	-66	34
300	-408	-361	-310	-276	-265	-265	-255	-216
330	-69	-25	15	21	-25	-122	-240	-343
360	191	206	226	215	139	-8	-204	-399

Table 68. Computed values of secular change in east component (Y) of magnetic field intensity for 1942.5 at height 1000 km expressed in units of 10^{-6} CGS per year

Geographic east longitude in degrees	Geographic colatitude in degrees								
	10	20	30	40	50	60	70	80	90
30	149	164	177	189	197	198	187	164	135
60	47	33	12	-11	-35	-61	-94	-138	-192
90	-62	-86	-111	-136	-151	-152	-138	-116	-100
120	-138	-146	-143	-129	-102	-64	-17	35	80
150	-167	-155	-138	-117	-94	-71	-46	-21	4
180	-153	-124	-91	-57	-24	4	30	55	78
210	-111	-86	-56	-24	9	45	82	117	149
240	-54	-54	-54	-52	-42	-20	13	50	79
270	18	-3	-22	-31	-27	-17	-7	-10	-31
300	101	71	32	-19	-85	-158	-227	-277	-299
330	173	168	154	129	91	42	-8	-48	-64
360	197	219	241	259	266	255	226	190	160

Geographic east longitude in degrees	Geographic colatitude in degrees							
	100	110	120	130	140	150	160	170
30	103	74	43	4	-52	-129	-220	-307
60	-248	-297	-326	-335	-329	-316	-304	-292
90	-101	-125	-166	-210	-241	-245	-220	-170
120	109	113	92	54	17	-	9	46
150	29	54	81	114	155	203	247	274
180	103	132	169	221	287	354	405	415
210	176	202	232	271	318	366	400	406
240	94	95	93	100	123	163	207	248
270	-68	-109	-142	-154	-140	-100	-41	30
300	-291	-263	-231	-206	-193	-186	-172	-142
330	-55	-28	-4	-	-29	-90	-164	-231
360	147	151	157	141	84	-16	-146	-275

Table 69. Computed values of secular change in east component (Y) of magnetic field intensity for 1942.5 at height 5000 km expressed in units of 10^{-6} CGS per year

Geographic east longitude in degrees	Geographic colatitude in degrees								
	10	20	30	40	50	60	70	80	90
30	24	26	28	29	29	27	24	20	15
60	7	5	2	0	-4	-9	-14	-20	-26
90	-10	-14	-18	-21	-22	-23	-23	-23	-24
120	-22	-24	-24	-22	-19	-14	-9	-3	1
150	-26	-24	-20	-16	-12	-7	-2	3	8
180	-23	-18	-12	-6	-1	4	10	15	21
210	-16	-12	-7	-1	4	11	17	23	28
240	-8	-7	-6	-3	0	2	6	10	13
270	2	-1	-5	-7	-10	-11	-12	-14	-15
300	15	10	3	-4	-13	-21	-29	-35	-39
330	27	25	22	17	11	5	-0	-6	-9
360	31	35	37	38	38	36	33	29	25

Geographic east longitude in degrees	Geographic colatitude in degrees							
	100	110	120	130	140	150	160	170
30	9	3	-3	-10	-18	-27	-35	-43
60	-32	-37	-41	-43	-44	-43	-42	-40
90	-25	-27	-30	-32	-33	-32	-29	-23
120	4	5	4	3	1	1	2	5
150	13	18	22	26	30	34	36	36
180	27	32	38	44	50	54	56	54
210	33	38	43	47	51	53	54	53
240	16	17	19	20	23	26	30	34
270	-17	-19	-19	-18	-14	-8	-1	7
300	-40	-39	-36	-33	-29	-25	-21	-15
330	-10	-11	-11	-12	-14	-19	-24	-29
360	22	18	13	7	-1	-13	-26	-38

Table 70. Computed values of secular change in vertical component (Z) of magnetic field intensity for 1932.5 at height 100 km expressed in units of 10^{-6} CGS per year

Geographic east longitude in degrees	Geographic colatitude in degrees								
	10	20	30	40	50	60	70	80	90
30	-174	71	336	525	554	403	144	-81	-134
60	-112	171	456	690	813	776	571	269	20
90	-115	123	317	430	439	321	62	-306	-674
120	-170	-6	117	182	186	129	21	-107	-197
150	-257	-172	-94	-17	33	11	-105	-261	-339
180	-353	-340	-324	-296	-263	-260	-318	-415	-475
210	-439	-469	-463	-431	-384	-328	-278	-232	-172
240	-506	-590	-621	-618	-578	-481	-323	-137	32
270	-540	-689	-797	-829	-715	-408	34	442	637
300	-513	-659	-780	-840	-785	-583	-280	-8	91
330	-419	-457	-484	-557	-718	-937	-1128	-1204	-1148
360	-289	-166	-26	33	-71	-329	-633	-839	-857

Geographic east longitude in degrees	Geographic colatitude in degrees							
	100	110	120	130	140	150	160	170
30	49	419	833	1134	1227	1119	905	709
60	-18	211	606	949	1049	884	618	486
90	-874	-789	-457	-65	175	201	151	252
120	-193	-89	35	73	-22	-163	-167	105
150	-249	-24	181	209	40	-162	-170	126
180	-416	-229	-1	148	169	125	150	326
210	-68	101	324	550	712	765	720	641
240	170	323	559	885	1207	1367	1262	946
270	579	423	413	685	1136	1484	1486	1123
300	-6	-167	-166	137	675	1181	1370	1136
330	-1003	-806	-536	-141	371	867	1135	1035
360	-695	-416	-84	269	614	886	993	887

Table 71. Computed values of secular change in vertical component (Z) of magnetic field intensity for 1932.5 at height 300 km expressed in units of 10^{-6} CGS per year

Geographic east longitude in degrees	Geographic colatitude in degrees								
	10	20	30	40	50	60	70	80	90
30	-154	58	284	442	467	340	126	-59	-100
60	-99	148	396	595	697	661	486	234	29
90	-102	107	277	377	383	279	55	-256	-561
120	-152	-9	99	157	159	107	10	-101	-180
150	-231	-156	-88	-25	14	-7	-103	-229	-289
180	-316	-306	-291	-267	-242	-242	-289	-366	-409
210	-393	-424	-421	-394	-353	-304	-258	-213	-154
240	-453	-532	-562	-557	-517	-425	-283	-117	34
270	-481	-615	-708	-731	-626	-362	11	356	528
300	-456	-587	-692	-744	-697	-526	-273	-45	45
330	-372	-410	-441	-510	-648	-831	-987	-1051	-1004
360	-257	-154	-41		-91	-310	-564	-735	-749

Geographic east longitude in degrees	Geographic colatitude in degrees							
	100	110	120	130	140	150	160	170
30	55	366	716	975	1062	982	812	655
60	0	193	522	808	899	776	570	469
90	-723	-648	-370	-42	165	202	178	274
120	-178	-92	13	53	-9	-104	-86	152
150	-213	-29	139	168	45	-100	-87	169
180	-353	-192	2	135	167	147	181	335
210	-56	96	292	489	632	685	655	595
240	162	303	510	786	1054	1187	1102	846
270	497	388	396	627	998	1282	1285	991
300	-20	-133	-112	153	604	1028	1190	1002
330	-877	-699	-452	-100	344	768	999	920
360	-608	-362	-65	251	555	792	886	801

Table 72. Computed values of secular change in vertical component (Z) of magnetic field intensity for 1932.5 at height 500 km expressed in units of 10^{-6} CGS per year

Geographic east longitude in degrees	Geographic colatitude in degrees								
	10	20	30	40	50	60	70	80	90
30	-138	47	240	374	394	289	110	-43	-75
60	-89	128	343	514	599	566	415	204	38
90	-92	92	242	330	335	243	49	-216	-470
120	-137	-11	84	134	136	89	3	-96	-164
150	-207	-143	-84	-31	0	-20	-101	-203	-249
180	-284	-277	-263	-242	-222	-224	-264	-324	-354
210	-354	-385	-384	-361	-325	-281	-238	-194	-137
240	-407	-481	-510	-505	-464	-378	-249	-102	34
270	-431	-551	-632	-648	-553	-323	-5	288	441
300	-407	-524	-618	-663	-622	-477	-263	-70	12
330	-332	-369	-403	-467	-586	-740	-870	-922	-881
360	-229	-143	-52	-23	-105	-291	-505	-648	-658

Geographic east longitude in degrees	Geographic colatitude in degrees							
	100	110	120	130	140	150	160	170
30	58	321	619	842	924	866	731	603
60	13	176	452	694	777	681	524	448
90	-601	-536	-301	-24	157	200	194	285
120	-163	-92	-1	39	1	-59	-27	183
150	-184	-32	108	138	49	-54	-26	198
180	-301	-162	5	125	163	161	200	335
210	-46	91	264	438	565	616	597	552
240	153	283	465	701	926	1037	969	760
270	430	356	376	574	881	1116	1119	880
300	-30	-106	-72	161	544	900	1039	889
330	-770	-608	-383	-69	319	684	883	823
360	-533	-315	-50	232	502	710	793	725

Table 73. Computed values of secular change in vertical component (Z) of magnetic field intensity for 1932.5 at height 1000 km expressed in units of 10^{-6} CGS per year

Geographic east longitude in degrees	Geographic colatitude in degrees								
	10	20	30	40	50	60	70	80	90
30	-109	24	157	248	262	193	78	-18	-35
60	-71	88	242	362	418	392	289	149	41
90	-74	63	174	239	242	174	38	-142	-308
120	-109	-15	55	92	92	55	-8	-80	-129
150	-163	-116	-73	-39	-22	-38	-91	-153	-177
180	-222	-219	-209	-194	-183	-186	-211	-244	-253
210	-276	-305	-308	-293	-266	-232	-195	-156	-104
240	-316	-378	-403	-396	-359	-287	-187	-74	33
270	-332	-425	-484	-489	-415	-251	-32	171	287
300	-313	-403	-473	-505	-476	-378	-235	-103	-36
330	-256	-290	-324	-377	-461	-563	-647	-679	-648
360	-178	-122	-68	-57	-119	-246	-387	-480	-483

Geographic east longitude in degrees	Geographic colatitude in degrees							
	100	110	120	130	140	150	160	170
30	57	236	440	599	667	645	569	492
60	32	182	325	489	555	513	428	391
90	-387	-338	-181	5	137	187	207	283
120	-130	-83	-18	21	19	10	60	216
150	-132	-34	58	89	54	17	63	226
180	-208	-107	12	105	150	171	216	316
210	-28	79	208	337	433	479	477	456
240	130	236	371	535	685	758	718	590
270	305	285	321	460	660	810	814	666
300	-41	-61	-10	163	424	662	761	673
330	-564	-436	-257	-18	264	521	663	632
360	-389	-226	-24	191	393	545	610	571

Table 74. Computed values of secular change in vertical component (Z) of magnetic field intensity for 1932.5 at height 5000 km expressed in units of 10^{-6} CGS per year

Geographic east longitude in degrees	Geographic colatitude in degrees 10	20	30	40	50	60	70	80	90
30	-38	-20	-4	6	10	8	3	0	4
60	-30	-5	17	34	42	41	34	26	22
90	-29	-6	12	24	27	21	8	-6	-17
120	-35	-19	-7	-0	0	-3	-10	-18	-22
150	-45	-37	-31	-27	-26	-27	-30	-31	-28
180	-56	-57	-56	-54	-52	-51	-49	-44	-36
210	-66	-74	-76	-74	-69	-60	-48	-34	-17
240	-73	-86	-91	-88	-78	-62	-40	-16	8
270	-76	-92	-101	-99	-87	-65	-36	-7	18
300	-72	-89	-101	-106	-103	-92	-75	-56	-37
330	-63	-73	-83	-94	-104	-113	-117	-115	-103
360	-50	-47	-45	-48	-56	-67	-76	-80	-72

Geographic east longitude in degrees	Geographic colatitude in degrees 100	110	120	130	140	150	160	170
30	-9	40	65	89	107	117	121	122
60	-2	39	58	77	92	101	107	113
90	-19	-10	7	29	51	70	87	104
120	8	-12	0	15	32	51	74	98
150	7	-8	6	21	36	54	75	99
180	-22	-4	16	37	57	74	91	108
210	-25	27	51	74	94	107	116	119
240	4	58	83	106	125	135	136	130
270	40	59	80	102	124	139	143	136
300	10	2	29	61	95	122	137	136
330	-54	-52	-14	28	71	107	129	133
360	-53	-24	11	49	84	110	125	128

Table 75. Computed values of secular change in vertical component (Z) of magnetic field intensity for 1942.5 at height 100 km expressed in units of 10^{-6} CGS per year

Geographic east longitude in degrees	Geographic colatitude in degrees 10	20	30	40	50	60	70	80	90
30	201	395	564	658	633	476	218	-46	-182
60	249	491	695	823	851	751	501	-137	-216
90	244	463	591	581	451	239	-45	-402	-780
120	186	344	414	352	199	39	-79	-164	-249
150	94	166	189	139	46	-40	-95	-131	-167
180	-1	-10	-37	-107	-203	-286	-325	-323	-296
210	-70	-113	-124	-135	-154	-163	-140	-86	-17
240	-101	-159	-192	-252	-335	-377	-320	-170	10
270	-94	-154	-217	-316	-395	-348	-140	137	328
300	-49	-90	-158	-288	-426	-482	-425	-329	-308
330	24	31	-28	-209	-485	-756	-922	-959	-911
360	115	212	255	193	18	-218	-446	-597	-627

Geographic east longitude in degrees	Geographic colatitude in degrees 100	110	120	130	140	150	160	170
30	-81	258	697	1020	1062	824	476	248
60	-380	-250	104	458	581	422	152	48
90	-1048	-1078	-850	-511	-263	-203	-227	-114
120	-334	-387	-388	-368	-375	-409	-378	-159
150	-198	-204	-184	-169	-192	-235	-214	-46
180	-249	-172	-53	84	194	233	214	201
210	63	179	363	604	820	986	768	501
240	173	341	585	926	1256	1382	1193	738
270	358	320	404	710	1127	1395	1282	827
300	-390	-459	-336	55	592	1002	1073	765
330	-826	-692	-448	-67	375	717	802	614
360	-513	-259	88	439	684	745	633	436

Table 76. Computed values of secular change in vertical component (Z) of magnetic field intensity for 1942.5 at height 300 km expressed in units of 10^{-6} CGS per year

Geographic east longitude in degrees	Geographic colatitude in degrees								
	10	20	30	40	50	60	70	80	90
30	187	351	494	569	544	408	189	-32	-145
60	229	436	610	717	735	642	423	111	-183
90	223	409	518	511	399	212	-39	-350	-670
120	172	302	358	306	177	37	-72	-155	-236
150	92	147	162	116	35	-40	-91	-125	-156
180	9	-4	-32	-94	-176	-246	-282	-281	-258
210	-51	-96	-114	-129	-146	-153	-132	-83	-19
240	-80	-139	-176	-230	-295	-324	-271	-140	16
270	-74	-138	-199	-285	-346	-304	-130	100	263
300	-36	-83	-152	-266	-383	-432	-388	-311	-289
330	29	24	-35	-195	-431	-661	-805	-843	-805
360	111	187	217	158	5	-199	-395	-524	-548

Geographic east longitude in degrees	Geographic colatitude in degrees								
	100	110	120	130	140	150	160	170	
30	-59	223	588	858	900	715	440	258	
60	-318	-211	81	374	483	366	161	88	
90	-893	-916	-727	-445	-231	-164	-162	-49	
120	-311	-357	-357	-336	-331	-340	-290	-88	
150	-182	-186	-169	-154	-165	-185	-150	5	
180	-215	-144	-39	81	178	219	213	213	
210	58	167	330	537	719	783	680	464	
240	163	318	533	820	1092	1197	1035	662	
270	301	290	376	638	982	1195	1109	737	
300	-344	-382	-261	74	525	874	935	686	
330	-728	-601	-379	-44	337	630	712	562	
360	-446	-223	78	383	597	659	574	416	

Table 77. Computed values of secular change in vertical component (Z) of magnetic field intensity for 1942.5 at height 500 km expressed in units of 10^{-6} CGS per year

Geographic east longitude in degrees	Geographic colatitude in degrees								
	10	20	30	40	50	60	70	80	90
30	173	313	433	495	470	351	164	-22	-115
60	211	388	537	627	637	551	358	92	-156
90	204	362	456	450	353	188	-34	-305	-578
120	159	266	312	267	153	34	-66	-147	-222
150	88	131	139	98	27	-39	-86	-118	-146
180	16	-1	-29	-83	-154	-214	-245	-246	-225
210	-37	-83	-104	-121	-138	-143	-123	-79	-19
240	-63	-123	-162	-209	-262	-281	-231	-117	21
270	-59	-123	-184	-257	-306	-267	-120	71	212
300	-26	-76	-144	-246	-346	-388	-354	-292	-270
330	32	19	-40	-181	-384	-581	-707	-743	-713
360	105	166	186	130	-4	-182	-352	-463	-481

Geographic east longitude in degrees	Geographic colatitude in degrees								
	100	110	120	130	140	150	160	170	
30	-43	193	499	727	768	624	404	259	
60	-268	-179	62	307	404	319	164	115	
90	-766	-784	-626	-389	-203	-133	-112	-2	
120	-290	-329	-329	-307	-292	-283	-221	-36	
150	-166	-169	-155	-140	-142	-146	-100	42	
180	-186	-121	-28	77	163	205	209	218	
210	53	155	301	479	634	688	605	429	
240	153	294	485	729	955	1040	904	595	
270	255	261	348	574	860	1037	965	659	
300	-304	-320	-204	87	469	763	819	617	
330	-643	-524	-322	-26	305	559	635	515	
360	-389	-194	69	334	523	584	521	393	

Table 78. Computed values of secular change in vertical component (Z) of magnetic field intensity for 1942.5 at height 1000 km expressed in units of 10^{-6} CGS per year

Geographic east longitude in degrees	Geographic colatitude in degrees								
	10	20	30	40	50	60	70	80	90
30	140	236	316	354	331	245	116	-8	-68
60	168	292	396	455	455	384	243	59	-107
90	162	271	336	332	263	139	-25	-220	-408
120	128	198	226	194	117	26	-54	-124	-187
150	76	99	98	65	13	-36	-75	-101	-122
180	23	3	-22	-63	-113	-155	-178	-179	-163
210	-17	-59	-84	-103	-117	-119	-102	-67	-17
240	-37	-92	-129	-166	-197	-201	-159	-76	26
270	-36	-96	-148	-200	-230	-199	-101	26	126
300	-12	-63	-124	-201	-271	-302	-284	-245	-224
330	32	10	-45	-150	-292	-430	-522	-553	-534
360	88	123	128	80	-18	-146	-265	-343	-353

Geographic east longitude in degrees	Geographic colatitude in degrees							
	100	110	120	130	140	150	160	170
30	-18	137	338	491	530	452	326	243
60	-180	-122	33	193	268	233	156	144
90	-533	-544	-440	-281	-148	-78	-34	62
120	-239	-267	-265	-242	-215	-181	-109	38
150	-136	-136	-124	-109	-98	-79	-23	91
180	-131	-80	-10	67	134	173	191	210
210	45	128	239	365	471	510	460	352
240	130	243	384	551	698	749	660	463
270	174	205	285	443	632	745	699	505
300	-228	-210	-109	99	359	558	603	479
330	-478	-378	-218	1	239	423	484	413
360	-283	-139	52	244	384	439	410	333

Table 79. Computed values of secular change in vertical component (Z) of magnetic field intensity for 1942.5 at height 5000 km expressed in units of 10^{-6} CGS per year

Geographic east longitude in degrees	Geographic colatitude in degrees								
	10	20	30	40	50	60	70	80	90
30	22	33	40	41	36	25	11	0	-3
60	28	44	55	60	56	43	25	5	-10
90	27	41	48	47	37	18	-4	-30	-51
120	22	29	30	25	14	-0	-17	-33	-45
150	13	13	10	3	-5	-14	-22	-29	-32
180	5	-0	-7	-14	-21	-26	-29	-28	-23
210	-1	-12	-20	-26	-28	-27	-22	-13	-0
240	-6	-19	-29	-35	-36	-32	-21	-6	13
270	-7	-22	-35	-44	-46	-41	-30	-14	4
300	-4	-19	-35	-49	-60	-65	-65	-59	-50
330	3	-7	-22	-39	-59	-76	-88	-92	-87
360	13	13	7	-2	-17	-34	-48	-55	-53

Geographic east longitude in degrees	Geographic colatitude in degrees							
	100	110	120	130	140	150	160	170
30	1	15	34	52	64	69	71	73
60	-17	-13	-1	15	29	40	49	61
90	-64	-65	-55	-36	-15	6	28	52
120	-54	-56	-52	-41	-25	-3	22	50
150	-33	-31	-25	-16	-3	13	34	56
180	-16	-4	8	23	37	50	61	70
210	15	34	53	71	85	92	91	85
240	34	57	80	100	114	119	112	96
270	22	42	64	87	107	117	115	100
300	-36	-16	10	42	73	96	105	98
330	-72	-48	-17	18	53	79	93	92
360	-40	-19	8	36	60	76	83	83

Table 80. Computed values of secular change in vertical component (Z) of magnetic field intensity for 1932.5 at depth 1000 km expressed in units of 10^{-6} CGS per year

Geographic east longitude in degrees	Geographic colatitude in degrees								
	10	20	30	40	50	60	70	80	90
30	-446	142	863	1428	1540	1087	271	-464	-666
60	-297	344	1041	1677	2102	2123	1619	721	-114
90	-271	269	691	919	956	749	160	-856	-2028
120	-361	29	299	423	439	366	188	-73	-277
150	-528	-326	-142	96	335	350	-22	-627	-1001
180	-713	-678	-684	-629	-480	-381	-517	-886	-1213
210	-872	-854	-795	-713	-600	-476	-387	-354	-329
240	-1016	-1067	-1057	-1094	-1147	-1079	-799	-388	-35
270	-1126	-1380	-1642	-1856	-1728	-972	317	1550	2023
300	-1117	-1394	-1643	-1811	-1697	-1122	-180	670	882
330	-949	-946	-838	-888	-1308	-2018	-2659	-2890	-2672
360	-689	-324	211	560	380	-348	-1262	-1875	-1931

Geographic east longitude in degrees	Geographic colatitude in degrees							
	100	110	120	130	140	150	160	170
30	-130	970	2173	2970	3073	2541	1714	1017
60	-322	365	1630	2701	2879	2075	918	305
90	-2780	-2623	-1601	-372	263	38	-501	-432
120	-225	120	500	486	-131	-1043	-1511	-903
150	-740	77	840	867	12	-1113	-1571	-841
180	-1162	-660	-18	298	86	-393	-601	-183
210	-200	122	625	1158	1507	1526	1243	878
240	166	380	905	1847	2895	3449	3073	1923
270	1517	598	238	1021	2592	3866	3871	2534
300	288	-637	-1036	-309	1343	2963	3496	2562
330	-2257	-1877	-1461	-704	529	1879	2609	2172
360	-1525	-933	-327	316	1047	1718	1993	1622

Table 81. Computed values of secular change in magnetic potential (V), main field, for 1912.5 expressed in units of 10^3 CGS per year

Geographic east longitude in degrees	Geographic colatitude in degrees								
	10	20	30	40	50	60	70	80	90
30	122	90	46	0	-30	-36	-21	0	6
60	116	76	16	-58	-132	-182	-200	-195	-190
90	116	79	29	-26	-73	-93	-82	-51	-20
120	122	97	69	48	39	41	49	54	50
150	132	121	112	105	100	95	90	85	75
180	144	147	152	156	152	141	129	119	109
210	155	165	171	167	149	122	92	63	34
240	163	180	184	167	129	80	35	3	-19
270	167	193	211	199	143	48	-57	-134	-163
300	162	190	218	228	196	119	19	-58	-84
330	150	160	178	205	235	258	267	264	253
360	135	120	106	105	126	166	211	246	257

Geographic east longitude in degrees	Geographic colatitude in degrees							
	100	110	120	130	140	150	160	170
30	-14	-63	-126	-184	-223	-236	-227	-205
60	-204	-239	-281	-305	-297	-261	-217	-186
90	-13	-42	-96	-151	-182	-182	-166	-160
120	33	3	-35	-71	-94	-103	-112	-136
150	54	21	-16	-47	-64	-72	-89	-128
180	89	53	5	-40	-71	-90	-109	-140
210	-2	-47	-95	-135	-160	-167	-167	-170
240	-46	-86	-139	-195	-234	-247	-232	-204
270	-150	-129	-134	-176	-232	-270	-267	-228
300	-61	-25	-22	-73	-157	-232	-260	-235
330	237	204	141	42	-74	-177	-233	-229
360	240	193	117	18	-86	-173	-219	-218

Table 82. Computed values of secular change in magnetic potential (V), main field, for 1922.5 expressed in units of 10^3 CGS per year

Geographic east longitude in degrees	Geographic colatitude in degrees								
	10	20	30	40	50	60	70	80	90
30	126	86	43	3	-23	-31	-19	-1	4
60	117	69	13	-48	-104	-141	-146	-126	-105
90	118	75	27	-21	-60	-80	-69	-34	6
120	129	97	65	37	20	15	19	28	34
150	145	129	109	90	74	64	59	59	55
180	163	161	154	143	128	111	96	81	66
210	178	185	179	161	135	105	75	44	13
240	189	206	204	183	148	104	56	7	-37
270	192	221	237	231	195	126	39	-42	-98
300	184	214	242	258	244	194	121	52	12
330	166	178	197	224	255	278	285	278	261
360	144	126	113	112	129	159	193	218	225

Geographic east longitude in degrees	Geographic colatitude in degrees							
	100	110	120	130	140	150	160	170
30	-20	-79	-156	-226	-270	-280	-267	-250
60	-109	-150	-214	-269	-290	-274	-243	-226
90	25	4	-52	-117	-164	-182	-184	-199
120	29	7	-27	-63	-92	-113	-137	-179
150	41	12	-24	-57	-80	-100	-130	-179
180	45	14	-25	-67	-103	-133	-163	-199
210	-19	-56	-97	-141	-182	-212	-229	-235
240	-80	-122	-169	-220	-268	-297	-296	-270
270	-125	-138	-164	-214	-277	-323	-328	-292
300	4	3	-25	-95	-192	-276	-313	-294
330	235	193	122	16	-107	-217	-280	-283
360	205	152	69	-34	-139	-222	-266	-267

Table 83. Computed values of secular change in magnetic potential (V), main field, for 1932.5 expressed in units of 10^3 CGS per year

Geographic east longitude in degrees	Geographic colatitude in degrees								
	10	20	30	40	50	60	70	80	90
30	67	21	-24	-57	-65	-48	-17	7	6
60	52	-6	-62	-106	-128	-124	-96	-57	-28
90	52	0	-42	-69	-74	-55	-14	38	86
120	65	28	0	-14	-17	-7	12	32	45
150	85	67	51	39	31	35	48	63	66
180	108	107	104	98	92	90	92	95	90
210	129	141	143	137	125	108	89	66	38
240	145	169	178	174	157	125	83	35	-12
270	151	186	207	207	179	120	42	-32	-83
300	144	178	205	216	206	172	122	72	38
330	123	139	154	174	202	233	255	258	239
360	94	77	62	59	79	117	158	181	174

Geographic east longitude in degrees	Geographic colatitude in degrees							
	100	110	120	130	140	150	160	170
30	-29	-92	-165	-223	-255	-258	-242	-224
60	-31	-70	-132	-190	-218	-215	-197	-192
90	106	86	31	-33	-83	-110	-127	-158
120	42	22	-5	-28	-40	-52	-80	-137
150	46	9	-28	-48	-52	-55	-81	-140
180	66	25	-22	-63	-90	-108	-132	-169
210	2	-43	-96	-147	-187	-210	-216	-214
240	-57	-104	-159	-219	-273	-301	-293	-256
270	-105	-116	-142	-196	-265	-317	-322	-280
300	23	11	-21	-91	-184	-267	-304	-281
330	200	143	69	-23	-127	-220	-272	-268
360	134	70	-8	-90	-168	-227	-256	-249

Table 84. Computed values of secular change in magnetic potential (V), main field, for 1942.5 expressed in units of 10^3 CGS per year

Geographic east longitude in degrees	Geographic colatitude in degrees								
	10	20	30	40	50	60	70	80	90
30	-46	-78	-103	-114	-105	-76	-35	4	22
60	-57	-100	-135	-153	-151	-126	-78	-17	35
90	-55	-93	-115	-114	-89	-45	12	78	140
120	-43	-67	-75	-63	-35	-2	29	56	80
150	-24	-31	-28	-15	3	22	37	48	55
180	-5	3	14	30	46	60	67	65	57
210	10	27	39	47	51	50	42	25	2
240	18	41	57	70	78	76	57	23	-17
270	19	45	66	86	95	84	49	4	-36
300	11	34	60	90	116	127	121	105	91
330	-5	7	31	71	121	167	198	207	196
360	-26	-35	-33	-13	21	64	104	127	128

Geographic east longitude in degrees	Geographic colatitude in degrees							
	100	110	120	130	140	150	160	170
30	5	-45	-111	-164	-183	-167	-136	-117
60	58	40	-9	-63	-93	-92	-79	-84
90	180	183	149	94	44	11	-15	-57
120	98	106	101	86	67	44	7	-49
150	59	56	47	35	22	5	-23	-68
180	43	21	-6	-38	-66	-85	-97	-108
210	-25	-60	-102	-148	-186	-201	-188	-155
240	-60	-105	-158	-216	-265	-282	-254	-192
270	-62	-84	-120	-178	-242	-279	-266	-206
300	82	63	18	-58	-148	-216	-234	-197
330	170	128	64	-16	-102	-168	-194	-175
360	100	48	-20	-90	-143	-169	-167	-148

Table 85. Computed values of secular change in magnetic potential (V), residual field, for 1942.5 expressed in units of 10^2 CGS per year

Geographic east longitude in degrees	Geographic colatitude in degrees								
	10	20	30	40	50	60	70	80	90
30	-1049	-1320	-1443	-1351	-1040	-560	7	559	968
60	-1147	-1504	-1698	-1659	-1375	-885	-258	393	921
90	-1137	-1487	-1681	-1656	-1402	-952	-364	267	804
120	-1022	-1273	-1399	-1349	-1124	-758	-298	194	627
150	-833	-920	-928	-820	-613	-352	-73	205	455
180	-621	-523	-394	-210	-5	160	255	300	332
210	-442	-189	59	316	534	638	592	443	285
240	-345	-5	313	622	867	960	855	607	332
270	-354	-21	299	624	902	1036	969	740	457
300	-469	-233	21	323	631	851	912	822	641
330	-658	-585	-448	-202	125	451	695	820	821
360	-870	-983	-984	-816	-488	-67	360	719	936

Geographic east longitude in degrees	Geographic colatitude in degrees							
	100	110	120	130	140	150	160	170
30	1107	915	461	-64	-449	-593	-568	-549
60	1171	1080	737	347	101	35	1	-206
90	1101	1095	866	602	461	437	352	-1
120	891	930	793	616	520	496	386	10
150	621	653	554	395	269	197	94	-175
180	359	336	213	1	-224	-377	-445	-508
210	168	55	-142	-465	-829	-1075	-1088	-899
240	106	-105	-414	-873	-1379	-1705	-1659	-1243
270	188	-103	-524	-1109	-1722	-2096	-2004	-1446
300	404	68	-441	-1111	-1770	-2145	-2032	-1456
330	679	346	-202	-891	-1518	-1845	-1739	-1270
360	932	652	123	-511	-1038	-1279	-1204	-938

Table 86. Computed values of secular change in the vertical gradient of north component of magnetic field intensity (∂X/ ∂r), main field, for 1912.5 expressed in units of 10^{-14} CGS per year

Geographic east longitude in degrees	Geographic colatitude in degrees								
	10	20	30	40	50	60	70	80	90
30	86	215	318	291	114	-137	-266	-230	-25
60	70	226	440	556	463	211	-83	-186	-61
90	75	206	344	368	225	-38	-281	-408	-292
120	83	147	146	63	-41	-114	-119	-36	38
150	58	61	40	21	17	26	19	-17	32
180	4	-50	-81	-38	43	79	16	-39	-32
210	-47	-83	-58	32	131	154	146	108	127
240	-100	-115	-21	141	263	274	142	25	12
270	-145	-234	-166	121	514	773	716	308	-160
300	-117	-243	-264	-37	389	744	753	383	-197
330	-9	-53	-160	-259	-265	-147	0	39	27
360	76	150	118	-44	-252	-379	-374	-223	-51

Geographic east longitude in degrees	Geographic colatitude in degrees							
	100	110	120	130	140	150	160	170
30	231	409	431	309	104	-91	-221	-242
60	182	347	292	33	-277	-454	-403	-164
90	6	326	477	363	66	-193	-210	38
120	126	203	217	127	-26	-119	-20	254
150	135	221	197	49	-113	-139	53	350
180	89	243	297	194	27	-51	57	269
210	202	271	258	142	-11	-115	-101	14
240	129	306	417	372	176	-86	-278	-295
270	-395	-250	140	462	459	126	-289	-492
300	-555	-436	64	564	694	379	-138	-499
330	30	169	456	738	795	529	46	-379
360	116	293	489	645	643	427	56	-275

Table 87. Computed values of secular change in the vertical gradient of north component of magnetic field intensity (∂X/ ∂r), main field, for 1922.5 expressed in units of 10^{-14} CGS per year

Geographic east longitude in degrees	Geographic colatitude in degrees								
	10	20	30	40	50	60	70	80	90
30	210	246	257	216	97	-65	-216	-218	-37
60	208	251	338	405	350	119	-158	-320	-212
90	180	219	269	286	208	18	-258	-439	-389
120	134	173	168	113	36	-45	-86	-100	-55
150	59	103	121	112	77	27	-52	-79	-22
180	-27	13	38	63	83	68	44	9	20
210	-91	-3	79	133	148	148	120	109	113
240	-142	-45	70	156	197	199	211	202	182
270	-174	-170	-106	58	306	545	599	433	130
300	-126	-198	-218	-81	210	492	583	363	-19
330	9	-48	-162	-259	-256	-136	-8	64	55
360	147	153	76	-63	-204	-293	-276	-197	-65

Geographic east longitude in degrees	Geographic colatitude in degrees							
	100	110	120	130	140	150	160	170
30	255	499	547	367	67	-249	-264	-183
60	120	447	522	275	-122	-456	-349	-59
90	-92	288	510	431	139	-175	-93	176
120	50	165	205	129	-3	-116	93	370
150	102	209	205	83	-51	-117	139	400
180	91	181	220	176	91	-11	123	251
210	132	169	209	223	182	21	-10	-37
240	171	206	287	347	289	9	-197	-348
270	-98	-78	174	445	479	128	-235	-517
300	-277	-192	197	610	727	375	-65	-475
330	57	187	463	746	823	514	115	-326
360	113	331	545	667	613	307	43	-225

Table 88. Computed values of secular change in the vertical gradient of north component of magnetic field intensity ($\partial X/\partial r$), main field, for 1932.5 expressed in units of 10^{-14} CGS per year

Geographic east longitude in degrees	Geographic colatitude in degrees								
	10	20	30	40	50	60	70	80	90
30	267	329	296	148	-71	-260	-310	-178	88
60	336	366	334	233	64	-144	-319	-354	-187
90	310	285	202	84	-57	-223	-387	-465	-363
120	224	189	123	45	-31	-102	-150	-142	-55
150	113	101	97	86	28	-81	-176	-155	8
180	7	17	27	42	32	-23	-92	-98	4
210	-76	-15	24	53	72	76	72	77	114
240	-156	-70	-15	29	92	174	238	245	207
270	-218	-163	-95	40	262	486	565	409	100
300	-199	-173	-123	-15	156	327	385	261	17
330	-75	-39	-56	-143	-241	-260	-162	4	150
360	110	170	135	-21	-230	-360	-322	-130	111

Geographic east longitude in degrees	Geographic colatitude in degrees							
	100	110	120	130	140	150	160	170
30	363	513	470	262	-8	-197	-254	-173
60	126	416	495	302	-44	-282	-262	1
90	-70	282	487	424	171	-34	10	289
120	77	167	132	-13	-133	-94	170	509
150	217	304	177	-74	-228	-136	193	524
180	172	288	265	123	-10	-13	130	307
210	186	264	302	263	142	12	-79	-71
240	188	246	362	428	319	47	-270	-424
270	-139	-111	175	488	544	245	-231	-569
300	-160	-101	204	563	709	473	-19	-490
330	234	303	425	589	675	517	125	-333
360	299	401	445	456	410	262	15	-237

Table 89. Computed values of secular change in the vertical gradient of north component of magnetic field intensity ($\partial X/\partial r$), main field, for 1942.5 expressed in units of 10^{-14} CGS per year

Geographic east longitude in degrees	Geographic colatitude in degrees								
	10	20	30	40	50	60	70	80	90
30	230	231	165	42	-114	-265	-339	-266	-32
60	296	284	206	94	-44	-217	-391	-467	-343
90	285	229	73	-95	-218	-308	-399	-467	-420
120	208	152	1	-149	-210	-181	-128	-108	-113
150	90	62	-23	-102	-122	-91	-55	-44	-43
180	-24	-20	-63	-110	-117	-76	-18	24	50
210	-94	-34	-14	-22	-21	8	54	88	103
240	-122	-52	-55	-93	-84	10	143	226	227
270	-117	-73	-107	-128	-34	162	327	319	149
300	-78	-68	-134	-186	-136	4	118	97	-26
330	-	-29	-154	-300	-358	-280	-119	22	95
360	114	90	-13	-155	-268	-299	-240	-112	56

Geographic east longitude in degrees	Geographic colatitude in degrees							
	100	110	120	130	140	150	160	170
30	280	508	504	247	-119	-375	-368	-123
60	-26	322	477	327	-17	-284	-251	75
90	-197	133	384	398	203	10	37	310
120	-92	-28	31	33	-8	3	158	418
150	-23	17	38	13	-28	-7	124	317
180	80	129	173	171	106	18	-21	31
210	128	193	277	305	201	-25	-257	-334
240	207	253	371	440	314	-29	-421	-609
270	-12	18	252	485	464	117	-362	-664
300	-98	28	334	616	637	325	-155	-527
330	141	238	403	542	523	291	-60	-348
360	237	390	458	395	208	-24	-195	-231

Table 90. Computed values of secular change in the vertical gradient of east component of magnetic field intensity ($\partial Y/\partial r$), main field, for 1912.5 expressed in units of 10^{-14} CGS per year

Geographic east longitude in degrees	Geographic colatitude in degrees								
	10	20	30	40	50	60	70	80	90
30	-2	5	-51	-169	-315	-442	-528	-581	-628
60	-2	2	-12	-44	-80	-101	-87	-28	65
90	-16	-0	80	219	368	470	499	473	437
120	4	33	93	150	169	133	46	-72	-191
150	49	102	150	155	119	77	71	119	195
180	78	110	133	138	121	82	25	-42	-105
210	80	69	13	-61	-119	-141	-132	-113	-108
240	66	107	132	120	63	-27	-114	-158	-134
270	6	59	133	166	98	-77	-301	-470	-499
300	-86	-140	-133	-28	170	414	630	752	756
330	-117	-236	-331	-324	-182	55	301	461	483
360	-60	-113	-209	-322	-412	-445	-413	-340	-270

Geographic east longitude in degrees	Geographic colatitude in degrees							
	100	110	120	130	140	150	160	170
30	-694	-771	-814	-769	-599	-316	13	311
60	161	228	244	219	192	209	287	410
90	432	465	513	542	534	499	461	430
120	-275	-294	-235	-106	58	204	281	262
150	257	272	235	169	106	57	14	-42
180	-146	-159	-150	-146	-171	-234	-315	-374
210	-127	-170	-226	-296	-381	-476	-559	-586
240	-53	40	79	24	-125	-319	-483	-556
270	-369	-143	70	177	142	1	-171	-310
300	665	536	422	347	299	238	137	-6
330	391	259	164	143	183	231	240	195
360	-243	-263	-302	-308	-245	-94	93	263

Table 91. Computed values of secular change in the vertical gradient of east component of magnetic field intensity ($\partial Y/\partial r$), main field, for 1922.5 expressed in units of 10^{-14} CGS per year

Geographic east longitude in degrees	Geographic colatitude in degrees								
	10	20	30	40	50	60	70	80	90
30	-72	-58	-90	-171	-278	-374	-431	-453	-467
60	18	29	22	-0	-29	-43	-19	54	167
90	83	75	103	175	259	308	294	227	154
120	137	121	118	123	127	117	84	19	-64
150	172	176	179	161	123	81	54	53	72
180	159	149	137	125	115	96	59	7	-45
210	110	84	27	-36	-83	-109	-118	-125	-135
240	47	98	147	176	169	120	42	-34	-83
270	-55	24	114	157	113	-18	-156	-248	-237
300	-180	-177	-131	-28	126	306	470	579	613
330	-239	-304	-344	-321	-216	-49	127	255	299
360	-183	-219	-283	-362	-426	-445	-407	-334	-275

Geographic east longitude in degrees	Geographic colatitude in degrees							
	100	110	120	130	140	150	160	170
30	-501	-551	-608	-592	-466	-226	80	370
60	291	385	422	409	373	358	386	451
90	126	172	274	390	471	494	464	401
120	-143	-183	-160	-74	45	150	193	153
150	95	106	95	63	15	-45	-116	-188
180	-78	-82	-75	-79	-142	-261	-400	-490
210	-151	-168	-196	-250	-342	-466	-582	-634
240	-90	-78	-87	-129	-233	-364	-476	-530
270	-131	30	154	195	141	26	-106	-225
300	581	506	446	398	361	311	224	97
330	264	195	126	110	146	206	259	274
360	-269	-326	-405	-440	-371	-185	72	318

Table 92. Computed values of secular change in the vertical gradient of east component of magnetic field intensity ($\partial Y/\partial r$), main field, for 1932.5 expressed in units of 10^{-14} CGS per year

Geographic east longitude in degrees	Geographic colatitude in degrees								
	10	20	30	40	50	60	70	80	90
30	-231	-226	-226	-249	-291	-336	-358	-350	-324
60	-75	-30	14	42	51	54	81	154	272
90	77	121	167	210	234	225	177	104	38
120	185	189	164	117	62	13	-31	-86	-165
150	235	221	204	178	149	131	132	152	176
180	229	189	164	148	127	87	24	-41	-86
210	193	148	103	72	50	27	-9	-56	-102
240	133	150	163	163	133	65	-26	-108	-145
270	16	61	87	74	14	-76	-163	-206	-178
300	-151	-144	-123	-56	79	270	463	594	619
330	-290	-328	-344	-311	-220	-86	48	137	154
360	-320	-353	-376	-389	-392	-376	-339	-293	-259

Geographic east longitude in degrees	Geographic colatitude in degrees								
	100	110	120	130	140	150	160	170	
30	-306	-315	-339	-339	-263	-85	176	456	
60	406	509	551	532	489	467	493	553	
90	10	44	138	268	397	490	519	476	
120	-254	-316	-309	-212	-50	109	194	163	
150	188	174	133	67	-12	-101	-188	-263	
180	-93	-71	-58	-101	-220	-393	-556	-630	
210	-134	-156	-193	-273	-409	-577	-717	-763	
240	-124	-68	-26	-48	-154	-318	-480	-582	
270	-82	50	171	235	218	120	-34	-208	
300	546	427	330	292	303	309	257	130	
330	105	29	-24	-21	44	146	243	302	
360	-262	-308	-372	-401	-341	-167	92	366	

Table 93. Computed values of secular change in the vertical gradient of east component of magnetic field intensity ($\partial Y/\partial r$), main field, for 1942.5 expressed in units of 10^{-14} CGS per year

Geographic east longitude in degrees	Geographic colatitude in degrees								
	10	20	30	40	50	60	70	80	90
30	-175	-191	-212	-243	-277	-298	-291	-254	-200
60	-56	-40	-1	44	78	97	120	173	270
90	80	99	140	196	242	247	195	100	2
120	191	188	160	111	50	-15	-85	-159	-232
150	239	235	214	183	154	135	127	123	115
180	208	176	131	84	42	10	-19	-51	-85
210	126	87	48	17	-1	-14	-25	-40	-58
240	33	34	62	104	131	118	64	-9	-66
270	-59	-38	-18	-15	-38	-75	-100	-86	-22
300	-145	-109	-63	4	102	222	340	422	446
330	-210	-193	-177	-158	-128	-85	-41	-14	-22
360	-230	-247	-283	-328	-356	-343	-283	-202	-146

Geographic east longitude in degrees	Geographic colatitude in degrees								
	100	110	120	130	140	150	160	170	
30	-153	-126	-116	-95	-31	93	271	459	
60	399	524	606	622	584	525	477	451	
90	-48	-22	76	208	322	376	355	269	
120	-288	-305	-269	-187	-90	-21	-14	-76	
150	96	61	8	-64	-157	-265	-370	-443	
180	-116	-146	-186	-255	-363	-501	-625	-678	
210	-80	-113	-171	-264	-390	-527	-632	-666	
240	-84	-68	-48	-61	-123	-221	-322	-396	
270	78	187	267	299	276	209	108	-15	
300	413	351	300	286	308	336	333	277	
330	-65	-122	-155	-132	-39	107	268	395	
360	-151	-220	-311	-356	-295	-111	154	422	

Table 94. Computed values of secular change in the vertical gradient of vertical component of magnetic field intensity ($\partial Z/\partial r$), main field, for 1912.5 expressed in units of 10^{-14} CGS per year

Geographic east longitude in degrees	Geographic colatitude in degrees								
	10	20	30	40	50	60	70	80	90
30	248	222	49	-204	-382	-359	-138	142	305
60	292	330	154	-239	-686	-964	-957	-751	-568
90	274	280	120	-158	-410	-479	-292	91	492
120	216	169	70	12	44	134	214	245	231
150	167	121	88	77	70	58	65	109	158
180	145	162	256	350	358	285	227	272	399
210	142	189	287	345	305	192	87	38	20
240	152	231	329	334	219	66	-2	58	182
270	164	315	577	737	581	79	-548	-952	-909
300	159	276	553	803	744	248	-494	-1050	-1062
330	150	113	162	348	619	844	927	888	845
360	181	72	-92	-177	-76	192	504	736	846

Geographic east longitude in degrees	Geographic colatitude in degrees							
	100	110	120	130	140	150	160	170
30	246	-12	-344	-613	-726	-661	-460	-208
60	-602	-869	-1197	-1350	-1195	-783	-317	-19
90	697	584	214	-187	-371	-247	35	184
120	177	79	-49	-136	-83	123	344	344
150	140	15	-153	-218	-71	228	458	392
180	481	410	209	37	38	201	351	292
210	-40	-180	-354	-456	-413	-241	-45	54
240	227	90	-217	-569	-801	-799	-572	-244
270	-497	-60	49	-262	-760	-1066	-945	-484
300	-540	118	418	145	-479	-983	-1012	-579
330	874	915	799	406	-177	-678	-815	-522
360	869	824	672	363	-63	-439	-567	-377

Table 95. Computed values of secular change in the vertical gradient of vertical component of magnetic field intensity ($\partial Z/\partial r$), main field, for 1922.5 expressed in units of 10^{-14} CGS per year

Geographic east longitude in degrees	Geographic colatitude in degrees								
	10	20	30	40	50	60	70	80	90
30	165	49	-92	-251	-372	-376	-226	15	193
60	196	135	9	-237	-559	-791	-772	-497	-168
90	220	162	54	-119	-319	-435	-340	-2	443
120	239	164	66	-4	-26	-9	30	89	148
150	270	221	143	60	-8	-40	-4	96	199
180	307	321	323	311	272	213	175	188	239
210	332	359	329	257	173	105	62	37	18
240	338	383	360	286	204	139	86	25	-35
270	321	424	558	653	599	324	-108	-504	-655
300	269	347	525	705	707	411	-87	-507	-575
330	199	146	189	366	618	816	873	818	767
360	157	12	-112	-138	-35	165	392	589	730

Geographic east longitude in degrees	Geographic colatitude in degrees							
	100	110	120	130	140	150	160	170
30	151	-149	-585	-938	-1033	-852	-534	-271
60	-64	-320	-796	-1169	-1169	-798	-321	-66
90	742	698	336	-91	-293	-174	73	132
120	163	95	-29	-109	-39	167	337	248
150	212	96	-77	-161	-55	180	337	221
180	265	213	93	-13	-29	44	110	47
210	-2	-39	-108	-212	-318	-371	-332	-233
240	-87	-148	-274	-502	-773	-936	-851	-529
270	-513	-256	-171	-416	-873	-1217	-1167	-725
300	-256	183	363	79	-517	-1034	-1128	-754
330	799	856	771	417	-145	-661	-857	-639
360	796	748	543	184	-233	-549	-628	-461

Table 96. Computed values of secular change in the vertical gradient of vertical component of magnetic field intensity ($\partial Z/\partial r$), main field, for 1932.5 expressed in units of 10^{-14} CGS per year

Geographic east longitude in degrees	Geographic colatitude in degrees								
	10	20	30	40	50	60	70	80	90
30	125	- 71	- 311	- 497	- 531	- 375	- 100	149	221
60	81	- 127	- 356	- 566	- 704	- 703	- 527	- 222	56
90	76	- 94	- 232	- 310	- 323	- 250	- 45	300	691
120	106	- 16	- 104	- 149	- 157	- 133	- 70	19	89
150	158	92	29	- 51	- 128	- 129	- 4	192	312
180	214	199	195	173	126	101	155	284	397
210	264	255	232	203	166	130	107	105	106
240	310	326	324	337	354	333	246	120	18
270	344	427	514	581	534	281	- 140	- 535	- 675
300	340	428	509	562	521	327	17	- 256	- 313
330	284	278	242	259	396	627	837	918	860
360	201	75	- 103	- 217	- 154	88	394	605	632

Geographic east longitude in degrees	Geographic colatitude in degrees							
	100	110	120	130	140	150	160	170
30	46	- 316	- 712	- 971	- 998	- 812	- 528	- 289
60	124	- 104	- 520	- 869	- 920	- 648	- 260	- 53
90	938	882	545	146	- 53	27	211	190
120	72	- 40	- 158	- 142	74	384	544	346
150	225	- 37	- 275	- 268	26	406	562	325
180	384	225	21	- 73	4	168	242	109
210	73	- 25	- 184	- 354	- 464	- 464	- 364	- 239
240	- 36	- 99	- 268	- 577	- 918	-1094	- 965	- 583
270	- 494	- 181	- 56	- 308	- 817	-1228	-1225	- 783
300	- 103	216	359	129	- 405	- 932	-1103	- 793
330	741	631	504	260	- 143	- 582	- 816	- 667
360	508	317	122	- 93	- 329	- 541	- 620	- 489

Table 97. Computed values of secular change in the vertical gradient of vertical component of magnetic field intensity ($\partial Z/\partial r$), main field, for 1942.5 expressed in units of 10^{-14} CGS per year

Geographic east longitude in degrees	Geographic colatitude in degrees								
	10	20	30	40	50	60	70	80	90
30	- 62	- 243	- 415	- 525	- 532	- 410	- 174	93	246
60	- 100	- 314	- 499	- 627	- 694	- 668	- 490	- 161	199
90	- 105	- 315	- 433	- 412	- 300	- 155	31	310	661
120	- 68	- 249	- 337	- 275	- 125	- 0	41	37	54
150	2	- 109	- 169	- 140	- 63	- 2	18	27	55
180	78	41	29	78	168	242	268	253	230
210	128	107	54	22	26	41	36	8	- 17
240	144	118	81	118	228	322	309	187	45
270	130	96	90	180	292	275	58	- 244	- 419
300	95	39	24	113	245	293	206	82	84
330	47	- 34	- 55	72	324	573	699	685	613
360	- 8	- 135	- 227	- 215	- 88	104	293	424	465

Geographic east longitude in degrees	Geographic colatitude in degrees							
	100	110	120	130	140	150	160	170
30	152	- 205	- 675	-1003	- 995	- 653	- 190	111
60	383	244	- 152	- 536	- 621	- 339	85	299
90	946	990	749	391	179	239	429	446
120	106	151	155	162	249	428	568	481
150	93	105	84	81	159	310	424	364
180	210	171	89	- 17	- 90	- 71	25	114
210	- 30	- 67	- 184	- 392	- 605	- 677	- 517	- 191
240	- 44	- 117	- 288	- 615	- 985	-1158	- 953	- 436
270	- 354	- 172	- 138	- 411	- 870	-1177	-1054	- 526
300	264	479	482	148	- 388	- 806	- 832	- 450
330	568	536	421	152	- 211	- 492	- 521	- 275
360	399	216	- 55	- 336	- 513	- 504	- 323	- 78

Table 98. Computed values of secular change in the vertical gradient of north component of magnetic field intensity ($\partial X/\partial r$), residual field, for 1942.5 expressed in units of 10^{-14} CGS per year

Geographic east longitude in degrees	Geographic colatitude in degrees								
	10	20	30	40	50	60	70	80	90
30	232	225	152	22	-141	-297	-376	-307	-75
60	298	278	192	73	-71	-250	-429	-508	-386
90	284	220	57	-118	-247	-342	-438	-509	-463
120	203	139	-19	-175	-242	-218	-168	-151	-156
150	79	45	-48	-132	-157	-130	-97	-87	-87
180	-39	-42	-91	-143	-155	-117	-61	-19	7
210	-111	-58	-44	-57	-60	-33	10	44	60
240	-139	-75	-85	-128	-123	-31	99	182	184
270	-131	-94	-134	-161	-72	121	284	276	106
300	-87	-85	-158	-215	-170	-34	77	54	-69
330	-4	-40	-173	-325	-389	-316	-159	-19	52
360	114	82	-28	-178	-296	-333	-279	-154	13

Geographic east longitude in degrees	Geographic colatitude in degrees								
	100	110	120	130	140	150	160	170	
30	235	464	462	208	-155	-405	-391	-139	
60	-71	278	435	288	-52	-314	-274	59	
90	-240	90	343	361	171	-17	17	296	
120	-135	-69	-6	-0	-38	-19	142	408	
150	-65	-22	3	-17	-53	-26	112	313	
180	39	91	139	143	84	2	-29	31	
210	87	156	245	278	181	-39	-263	-332	
240	166	216	338	413	293	-43	-427	-607	
270	-54	-20	218	456	441	101	-371	-665	
300	-140	-11	298	584	611	305	-169	-533	
330	97	196	364	507	492	266	-78	-359	
360	194	347	417	357	175	-52	-217	-245	

Table 99. Computed values of secular change in the vertical gradient of east component of magnetic field intensity ($\partial Y/\partial r$), residual field, for 1942.5 expressed in units of 10^{-14} CGS per year

Geographic east longitude in degrees	Geographic colatitude in degrees								
	10	20	30	40	50	60	70	80	90
30	-177	-193	-214	-245	-279	-300	-293	-255	-202
60	-53	-37	2	48	82	101	123	176	273
90	88	107	147	203	249	254	202	107	10
120	200	197	169	121	60	-5	-75	-150	-223
150	248	244	223	192	164	144	136	132	134
180	214	183	138	90	49	16	-13	-45	-79
210	127	88	49	19	0	-12	-24	-38	-56
240	29	30	58	100	127	115	60	-12	-69
270	-67	-45	-25	-22	-45	-82	-108	-94	-30
300	-154	-119	-72	-4	93	213	330	413	437
330	-219	-202	-186	-167	-137	-94	-50	-23	-32
360	-236	-254	-290	-334	-362	-349	-289	-209	-152

Geographic east longitude in degrees	Geographic colatitude in degrees								
	100	110	120	130	140	150	160	170	
30	-154	-128	-117	-97	-33	92	269	457	
60	403	528	609	625	587	528	480	455	
90	-40	-14	83	216	330	384	362	277	
120	-278	-295	-259	-177	-80	-11	-5	-66	
150	105	70	17	-55	-148	-256	-361	-434	
180	-110	-140	-180	-248	-357	-495	-619	-672	
210	-78	-111	-169	-262	-388	-525	-631	-664	
240	-87	-71	-51	-64	-126	-224	-326	-400	
270	71	179	260	291	269	201	100	-22	
300	404	342	291	277	299	326	323	267	
330	-75	-131	-165	-141	-48	98	258	386	
360	-157	-226	-317	-362	-301	-117	147	415	

Table 100. Computed values of secular change in the vertical gradient of vertical component of magnetic field intensity ($\partial Z/\partial r$), residual field, for 1942.5 expressed in units of 10^{-14} CGS per year

Geographic east longitude in degrees	Geographic colatitude in degrees								
	10	20	30	40	50	60	70	80	90
30	-151	-331	-500	-604	-603	-470	-221	59	225
60	-198	-401	-583	-705	-764	-727	-537	-194	178
90	-192	-401	-515	-487	-366	-209	-9	283	646
120	-154	-332	-414	-343	-183	-46	8	18	48
150	-82	-188	-240	-202	-113	-40	-4	19	37
180	-4	-35	-38	21	123	212	252	253	218
210	46	32	-10	-31	-14	15	25	12	-20
240	62	43	15	63	137	295	296	190	53
270	47	19	22	121	246	242	40	-247	-404
300	11	-40	-49	49	192	253	180	71	103
330	-38	-117	-134	2	263	524	663	663	631
360	-96	-221	-310	-291	-155	48	249	394	477

Geographic east longitude in degrees	Geographic colatitude in degrees							
	100	110	120	130	140	150	160	170
30	187	-104	-588	-1076	-1299	-1091	-535	54
60	368	281	-125	-686	-1076	-1039	-592	-33
90	890	961	720	220	-285	-513	-377	-49
120	27	72	90	29	-82	-156	-129	-21
150	17	4	11	37	65	70	43	11
180	160	84	41	54	97	117	86	29
210	-35	-109	-184	-208	-168	-89	-9	36
240	-0	-95	-228	-354	-398	-309	-113	66
270	-268	-85	-22	-128	-273	-274	-85	140
300	373	617	634	392	76	-71	28	223
330	674	695	580	307	14	-102	22	248
360	478	362	79	-297	-568	-544	-221	177

Table 101. Spherical harmonic coefficients for the average annual secular variation expressed in units of 10^{-5} CGS

Author	Epoch	g_1^0	g_1^1	h_1^1	g_2^0	g_2^1	h_2^1	g_2^2	h_2^2
Dyson-Schmidt	1922-1885	+20	- 1	- 1	-10	+ 6	-14	+21	-18
Bartels	1920-1902	+42	- 9	+12	- 7	+ 8	-25	+13	- 8
Carlheim-Gyllensköld	1920-1902	0	+13	+ 4	0	- 4	-12	+13	-17
Vestine-Lange	1912.5	+25	+ 1	- 7	- 7	- 1	- 9	+24	-17
	1922.5	+28	+ 4	- 7	-10	+ 1	-14	+17	-17
	1932.5	+23	+ 1	- 5	-14	+ 1	-18	+10	-14
	1942.5	+ 9	+ 2	+ 1	-18	0	-20	+ 2	-14

FIGURES 9-28

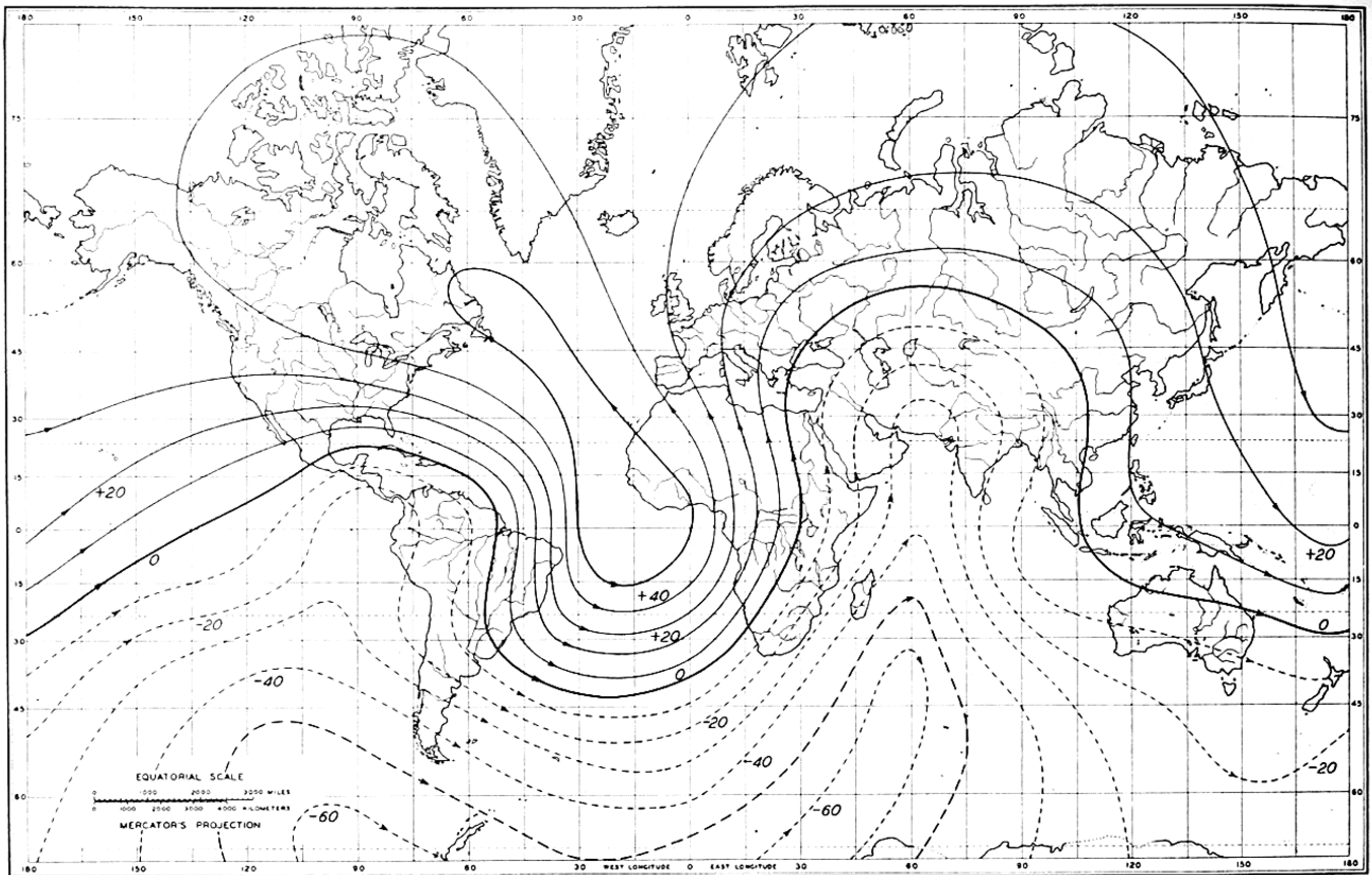

FIG. 9—CURRENT-FUNCTION IN 10^4 AMPERES FOR THIN SPHERICAL SHELL AT DEPTH ZERO WITHIN EARTH TO REPRODUCE GEOMAGNETIC SECULAR CHANGE, EPOCH 1912.5

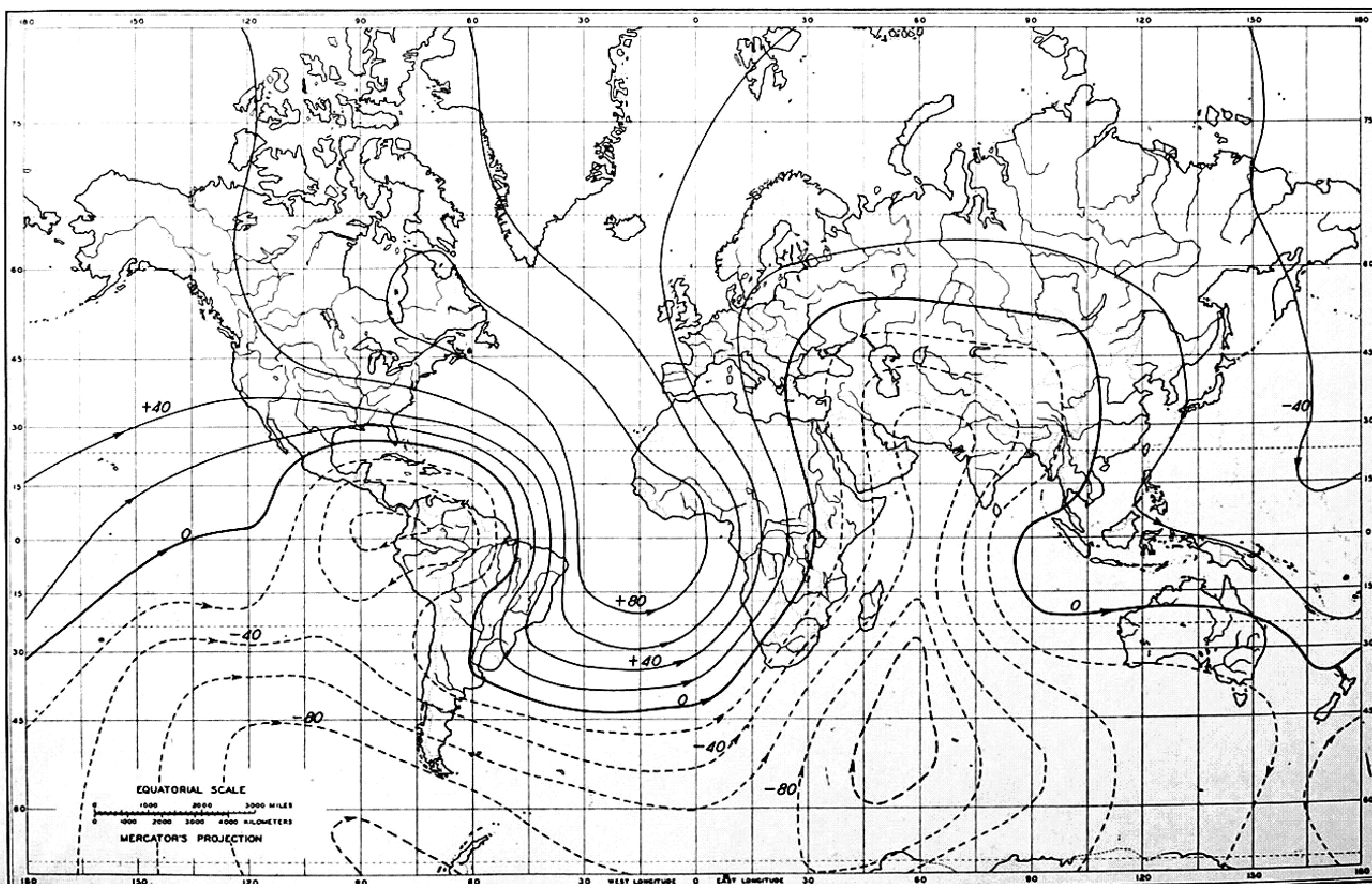

FIG. 10—CURRENT-FUNCTION IN 10^4 AMPERES FOR THIN SPHERICAL SHELL AT DEPTH 1000 KM WITHIN EARTH TO REPRODUCE GEOMAGNETIC SECULAR CHANGE, EPOCH 1912.5

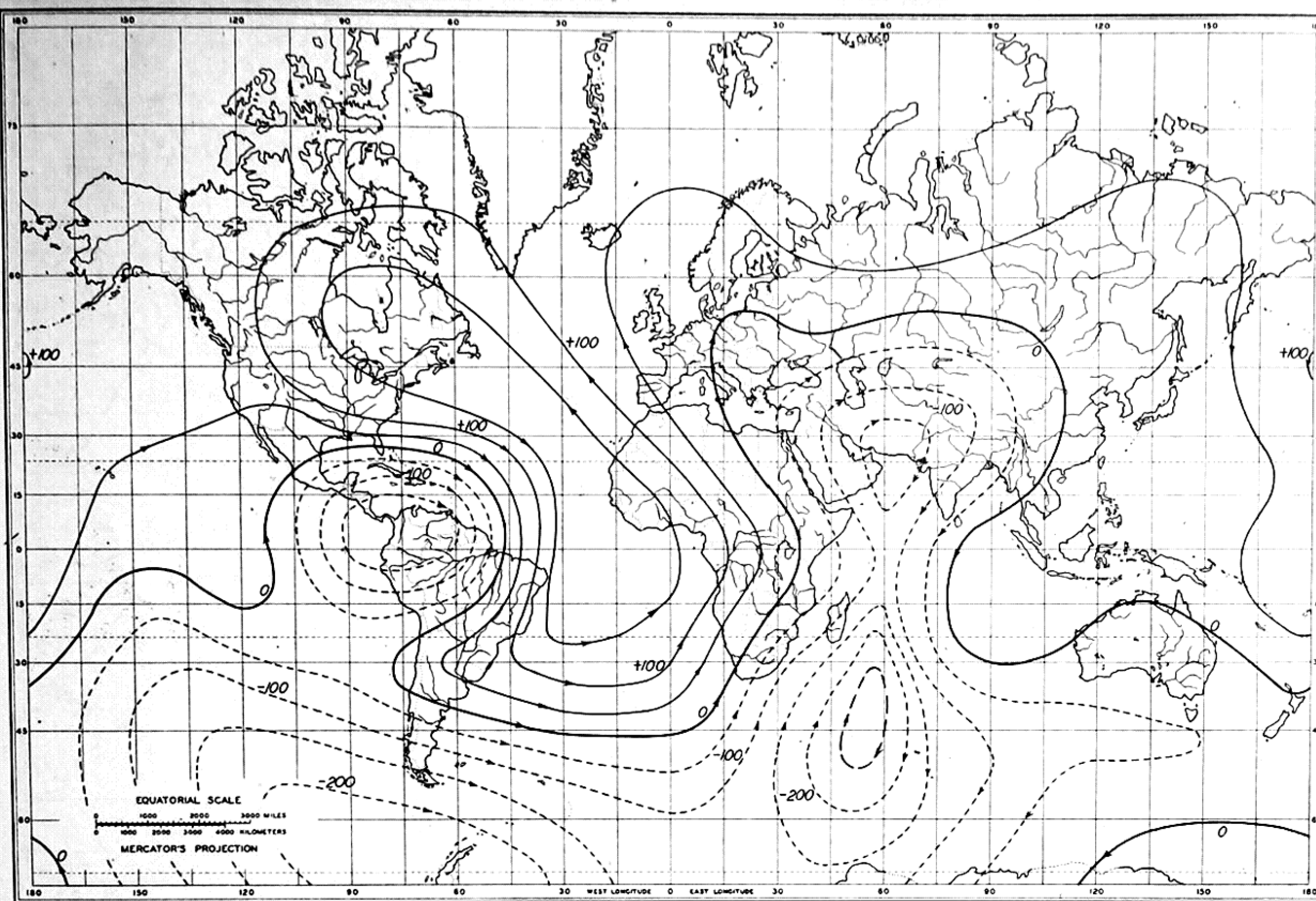

FIG. 11—CURRENT-FUNCTION IN 10^4 AMPERES FOR THIN SPHERICAL SHELL AT DEPTH 2000 KM WITHIN EARTH TO REPRODUCE GEOMAGNETIC SECULAR CHANGE, EPOCH 1912.5

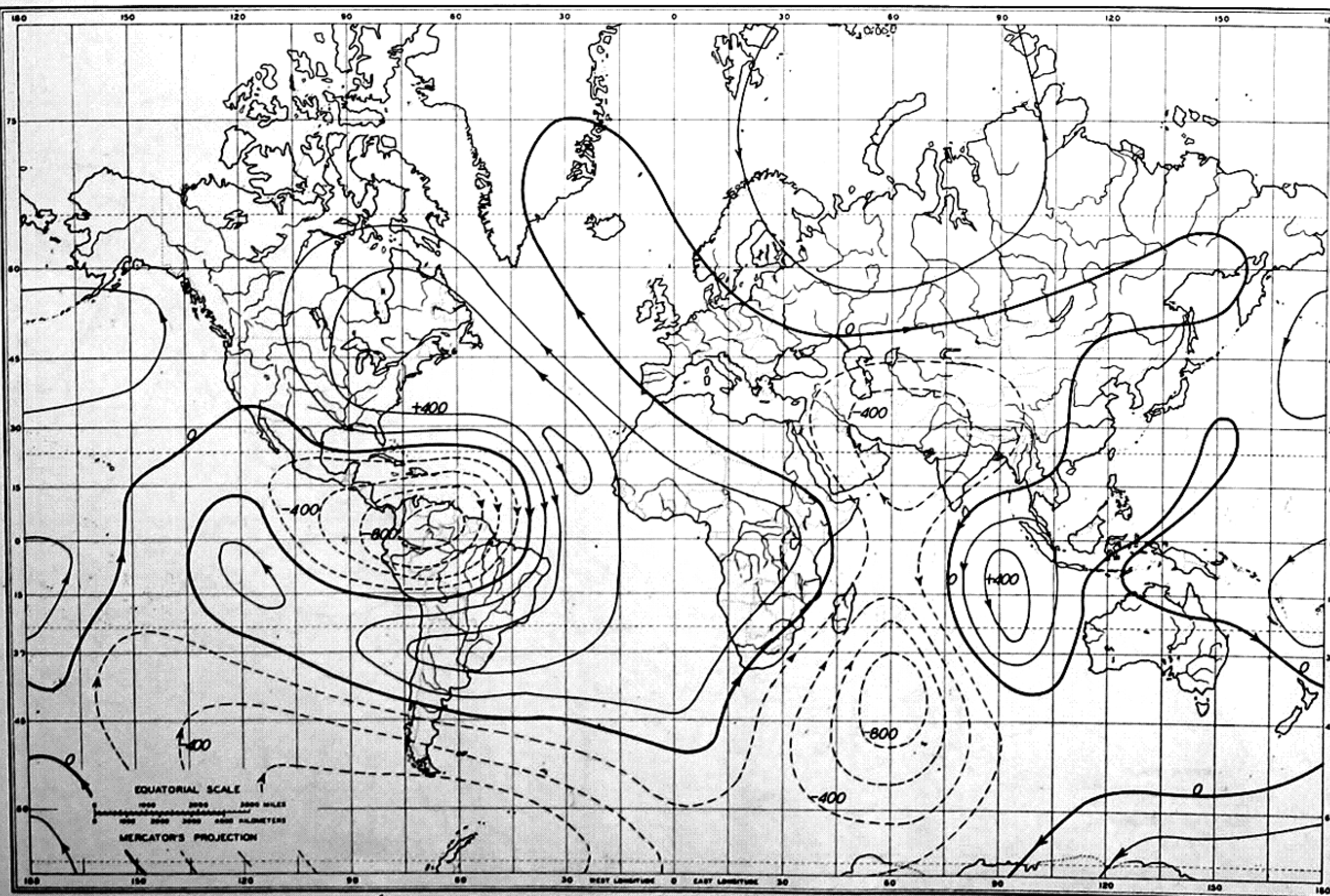

FIG. 12—CURRENT-FUNCTION IN 10^4 AMPERES FOR THIN SPHERICAL SHELL AT DEPTH 3000 KM WITHIN EARTH TO REPRODUCE GEOMAGNETIC SECULAR CHANGE, EPOCH 1912.5

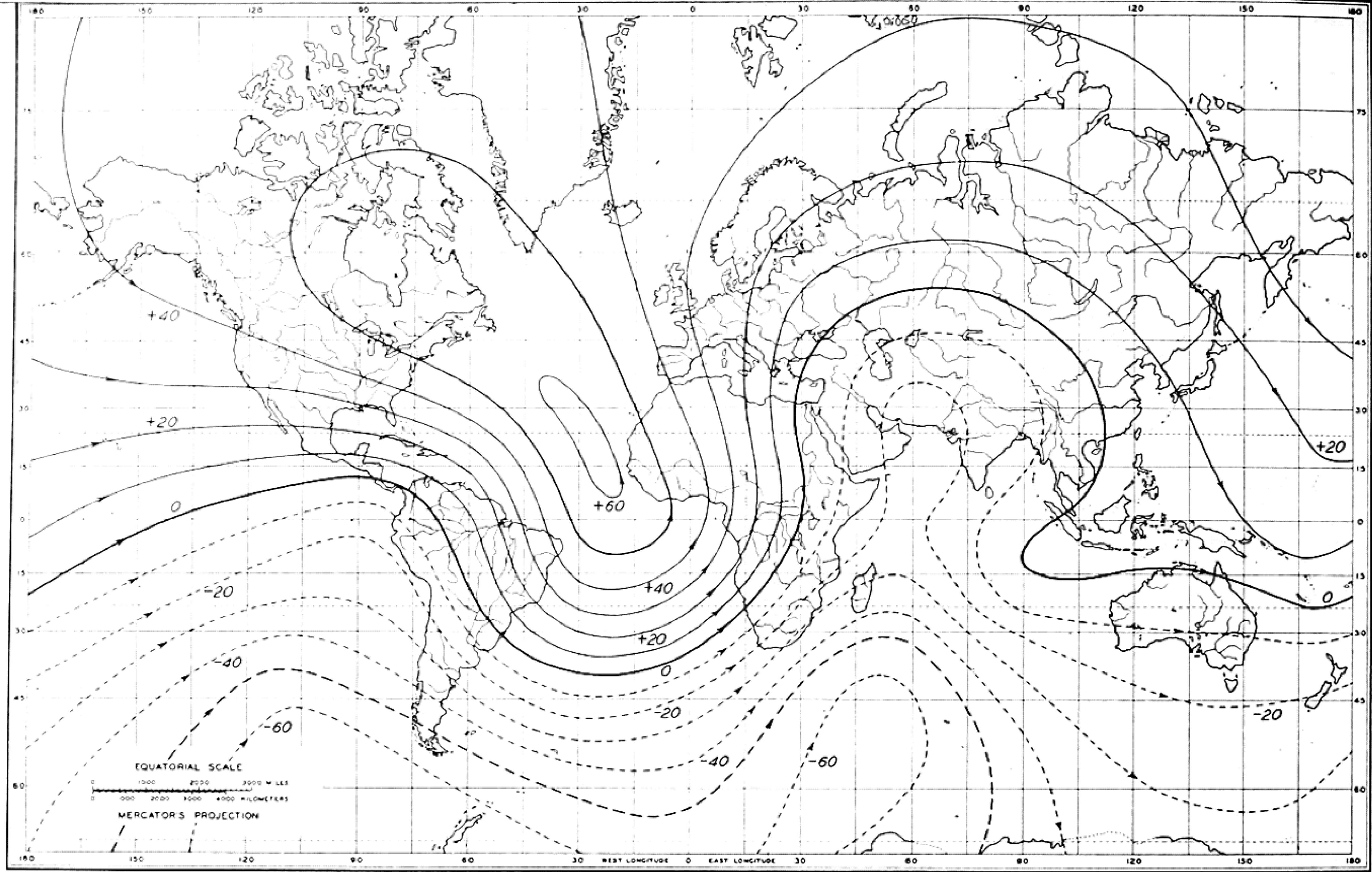

FIG. 13—CURRENT-FUNCTION IN 10^4 AMPERES FOR THIN SPHERICAL SHELL AT DEPTH ZERO WITHIN EARTH TO REPRODUCE GEOMAGNETIC SECULAR CHANGE, EPOCH 1922.5

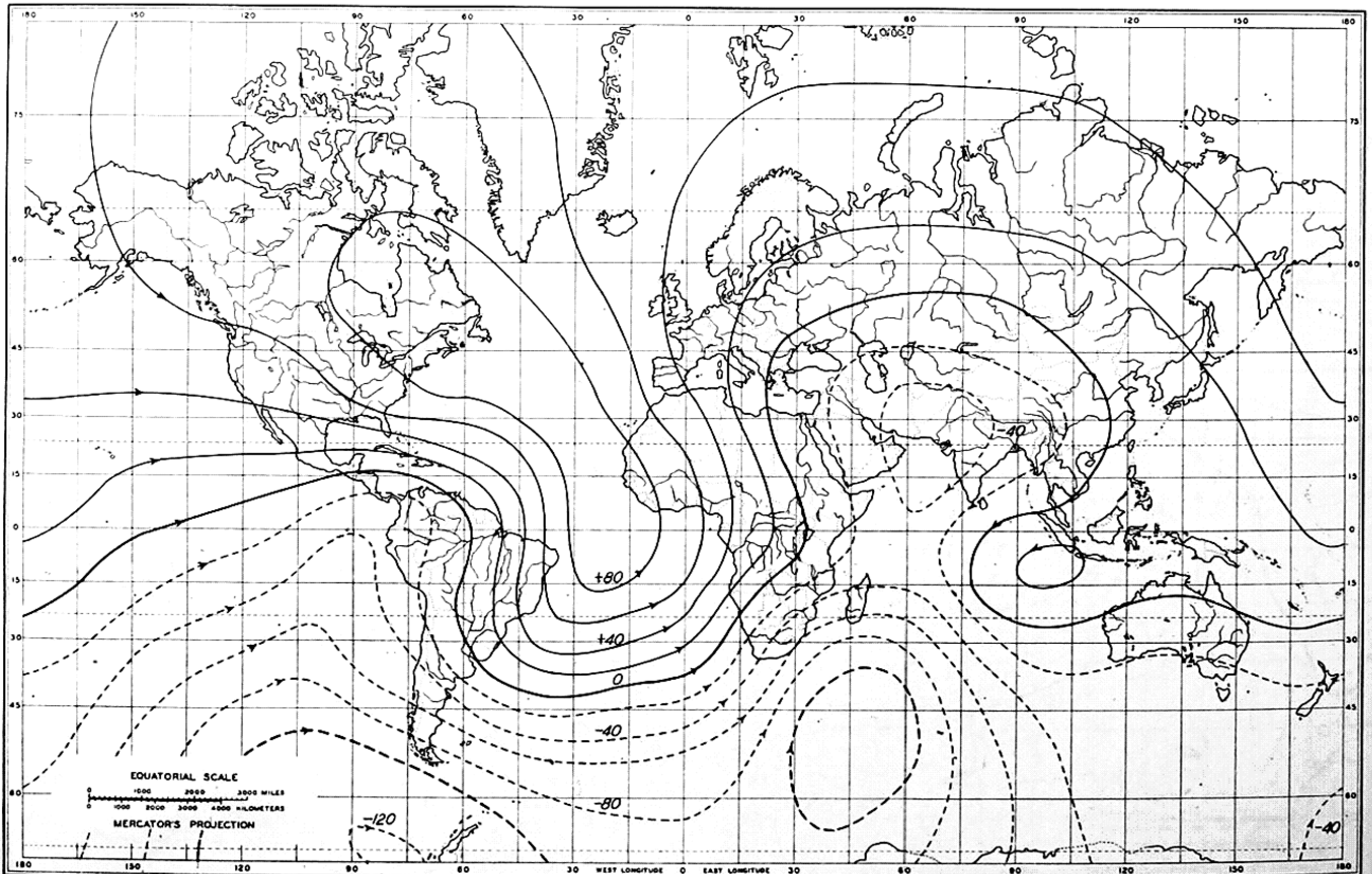

FIG. 14—CURRENT-FUNCTION IN 10^4 AMPERES FOR THIN SPHERICAL SHELL AT DEPTH 1000 KM WITHIN EARTH TO REPRODUCE GEOMAGNETIC SECULAR CHANGE, EPOCH 1922.5

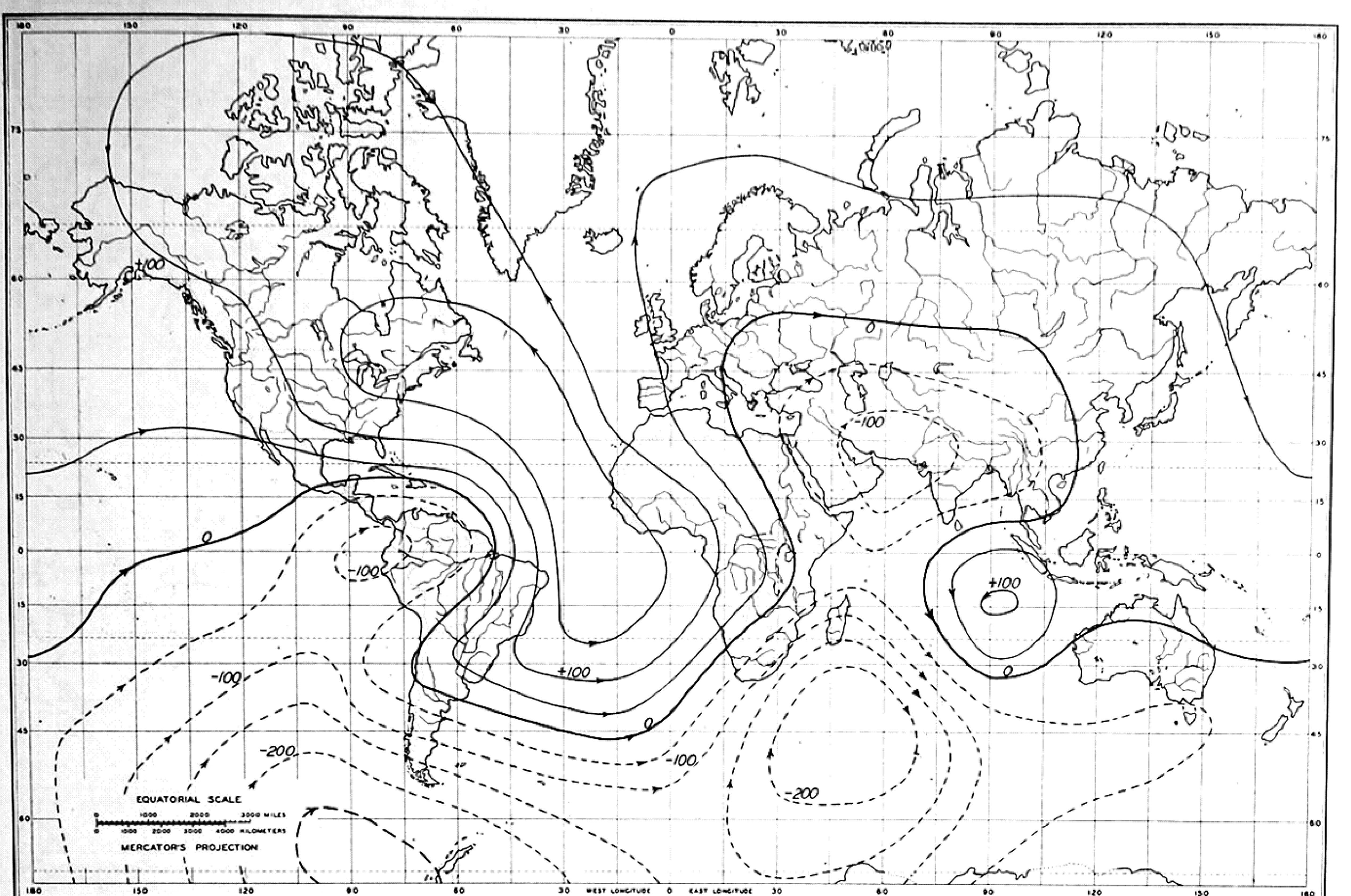

FIG. 15—CURRENT-FUNCTION IN 10^4 AMPERES FOR THIN SPHERICAL SHELL AT DEPTH 2000 KM WITHIN EARTH TO REPRODUCE GEOMAGNETIC SECULAR CHANGE, EPOCH 1922.5

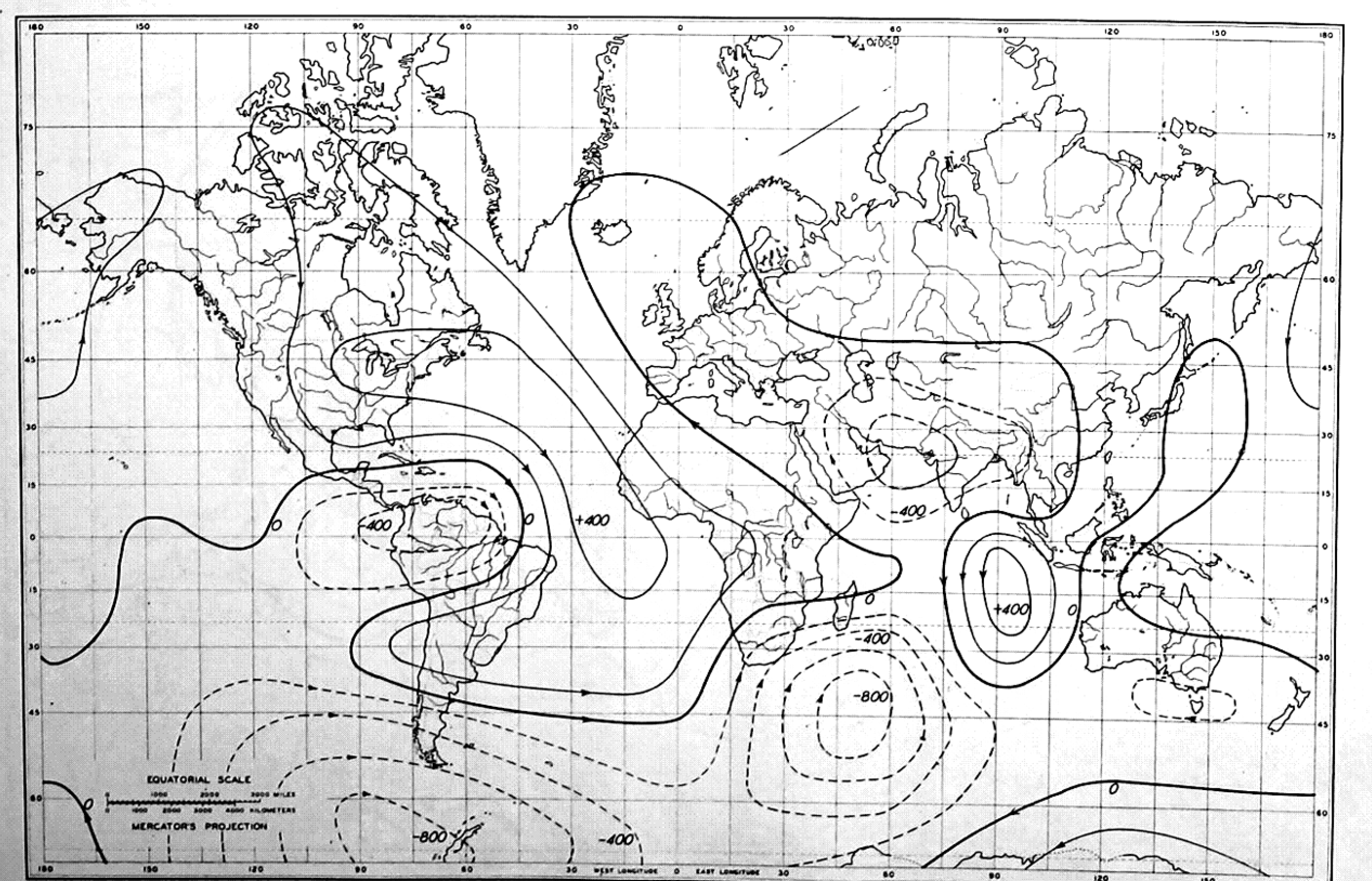

FIG. 16—CURRENT-FUNCTION IN 10^4 AMPERES FOR THIN SPHERICAL SHELL AT DEPTH 3000 KM WITHIN EARTH TO REPRODUCE GEOMAGNETIC SECULAR CHANGE, EPOCH 1922.5

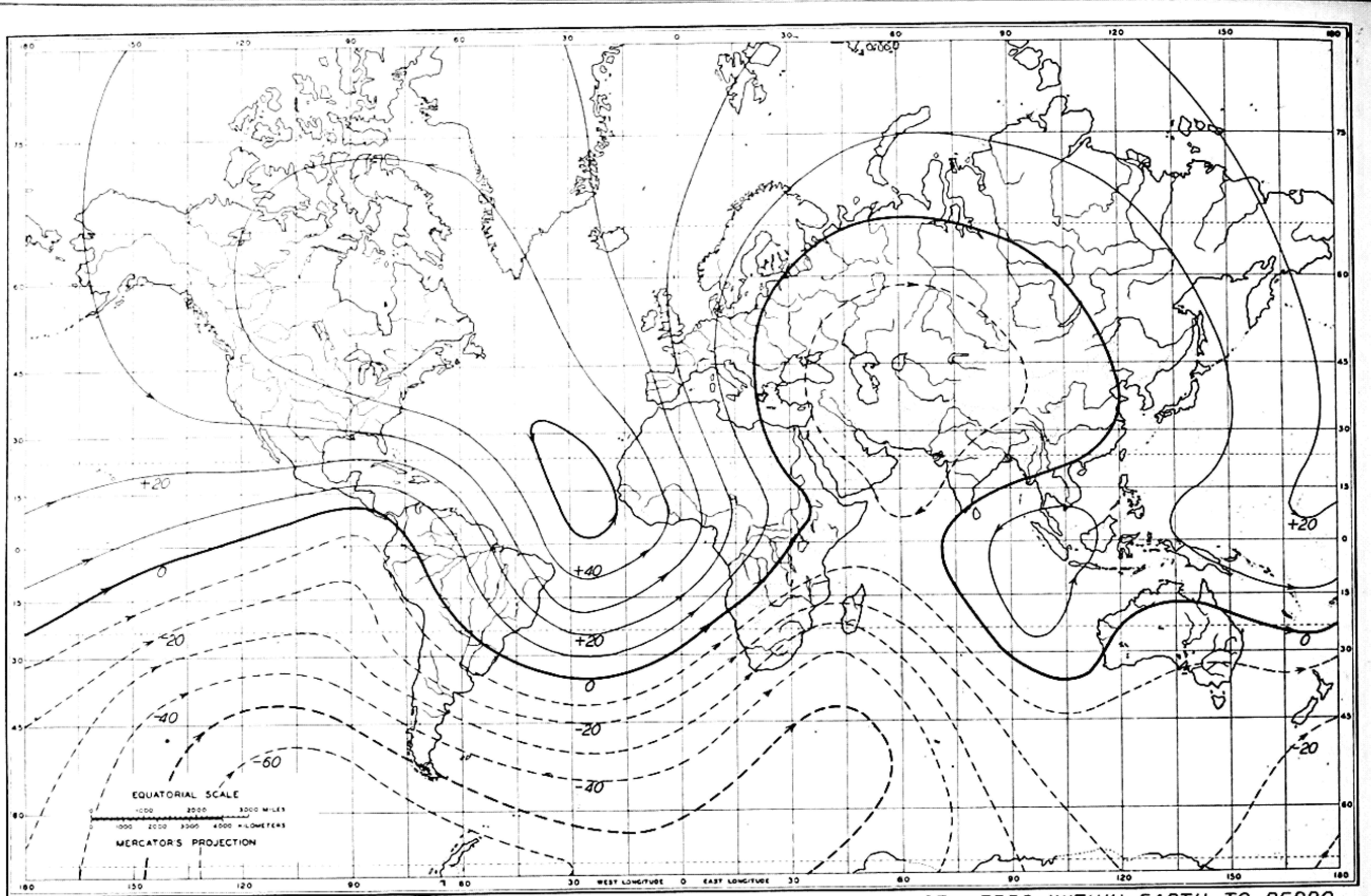

FIG. 17—CURRENT-FUNCTION IN 10^4 AMPERES FOR THIN SPHERICAL SHELL AT DEPTH ZERO WITHIN EARTH TO REPRODUCE GEOMAGNETIC SECULAR CHANGE, EPOCH 1932.5

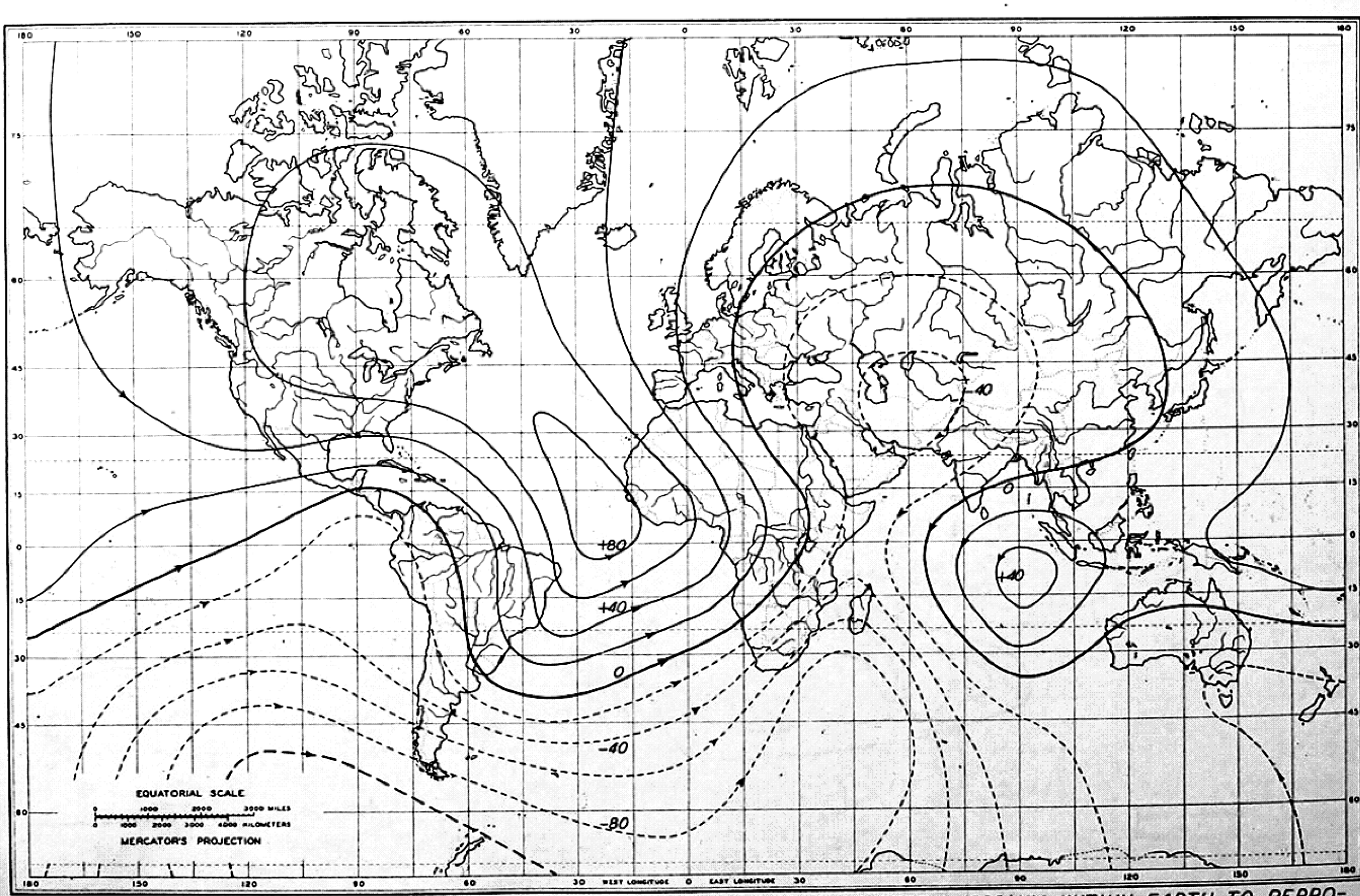

FIG. 18—CURRENT-FUNCTION IN 10^4 AMPERES FOR THIN SPHERICAL SHELL AT DEPTH 1000 KM WITHIN EARTH TO REPRODUCE GEOMAGNETIC SECULAR CHANGE, EPOCH 1932.5

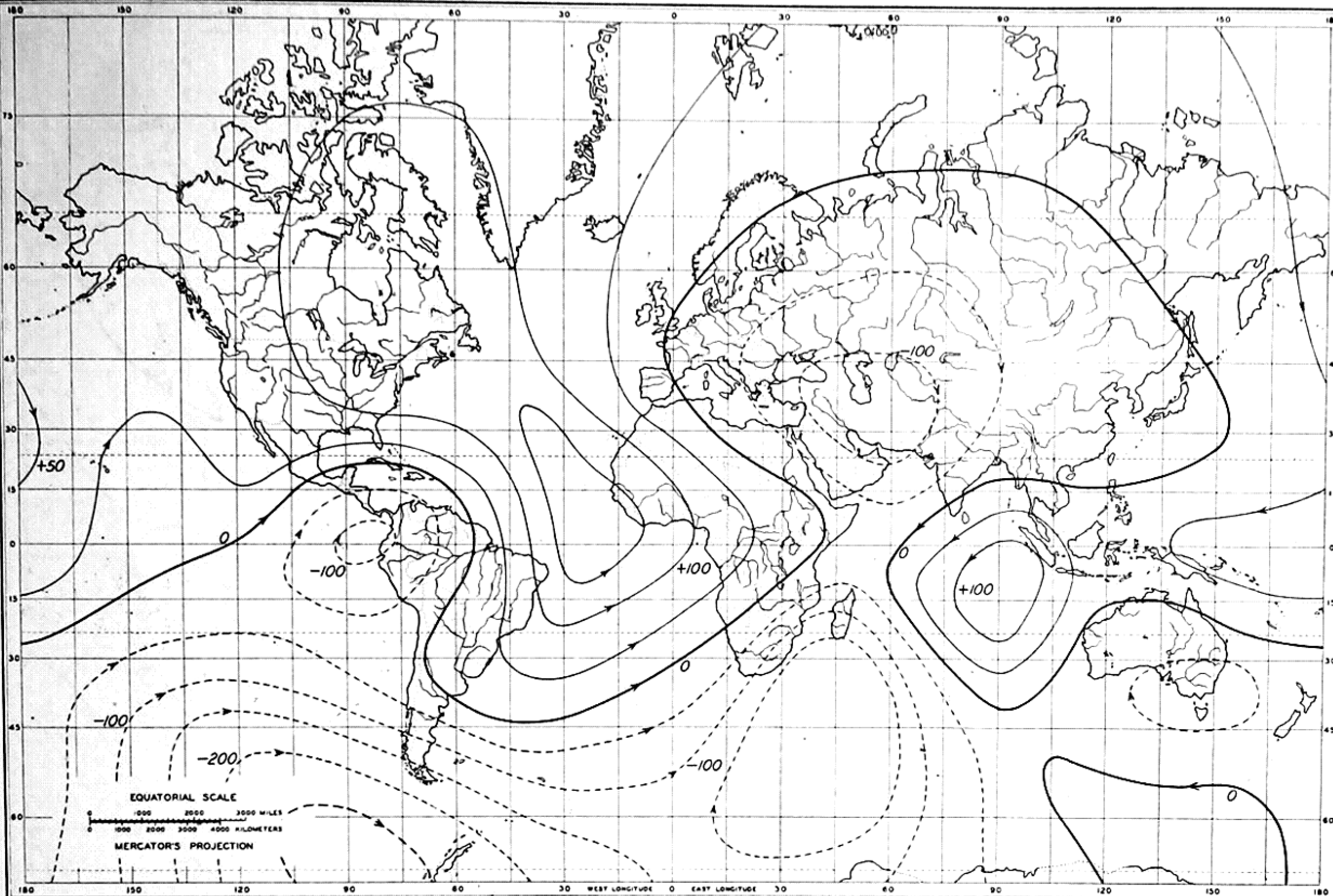

FIG. 19—CURRENT-FUNCTION IN 10^4 AMPERES FOR THIN SPHERICAL SHELL AT DEPTH 2000 KM WITHIN EARTH TO REPRODUCE GEOMAGNETIC SECULAR CHANGE, EPOCH 1932.5

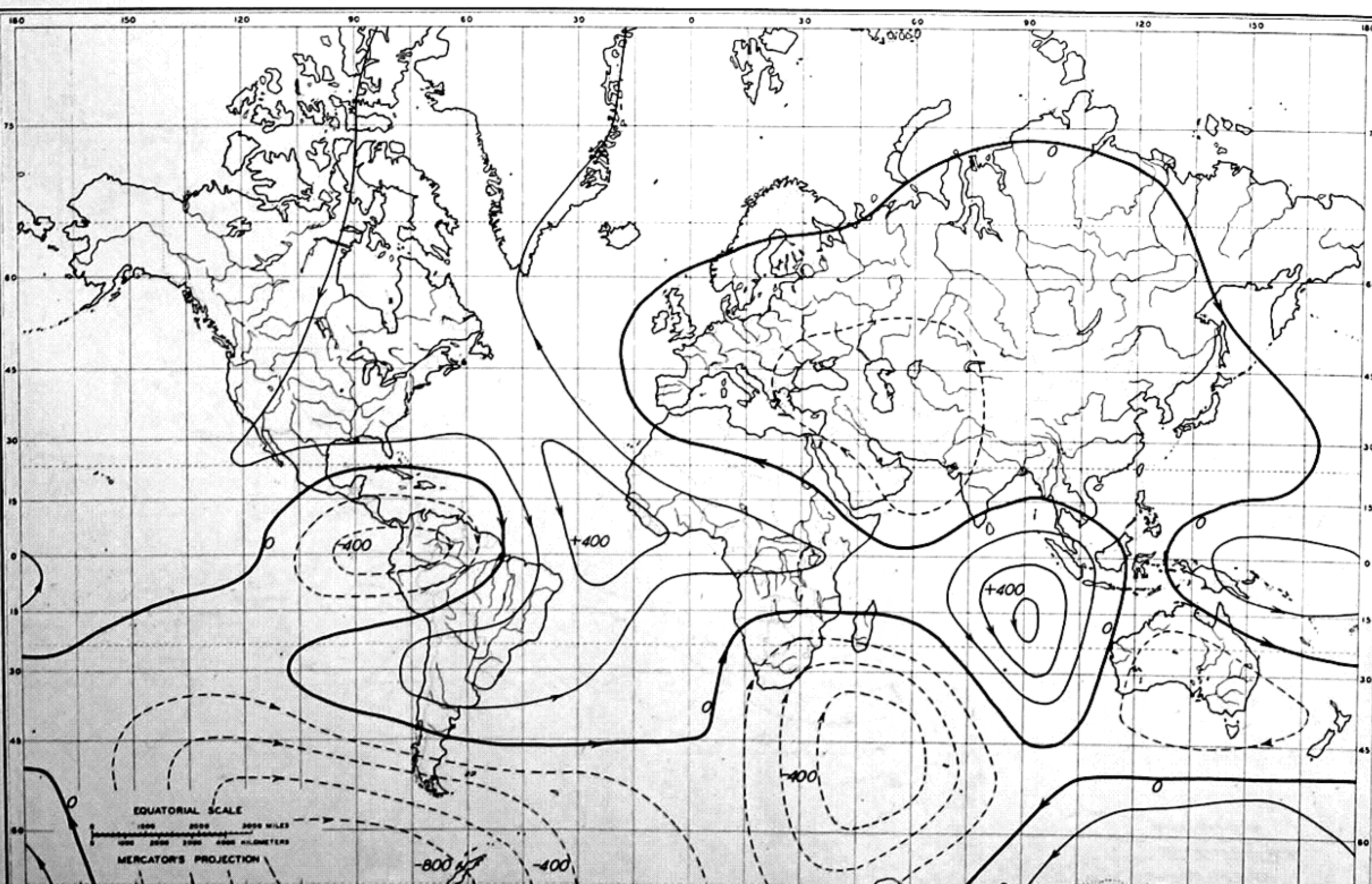

FIG. 20—CURRENT-FUNCTION IN 10^4 AMPERES FOR THIN SPHERICAL SHELL AT DEPTH 3000 KM WITHIN EARTH TO REPRODUCE GEOMAGNETIC SECULAR CHANGE, EPOCH 1932.5

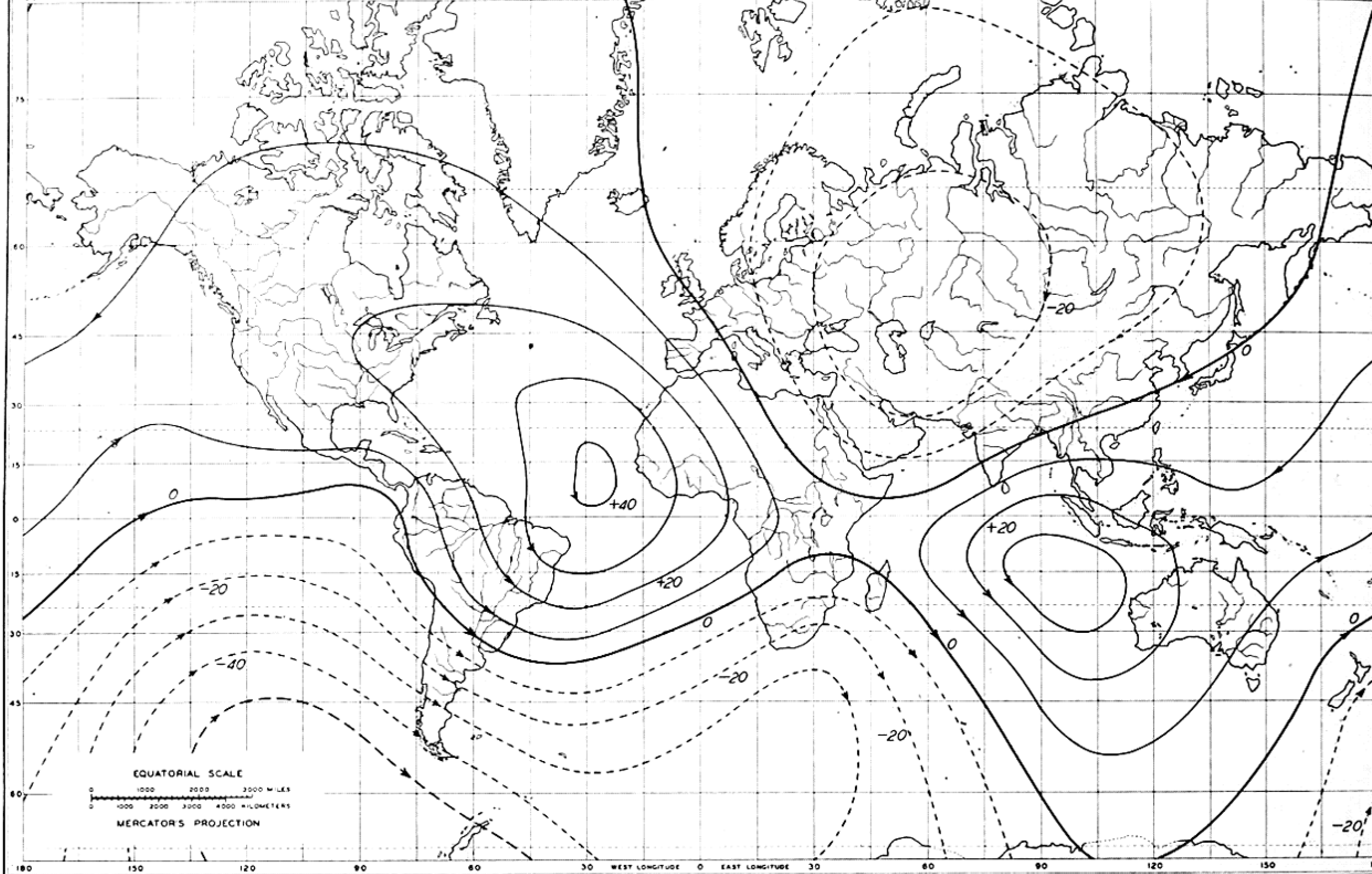

FIG. 21—CURRENT-FUNCTION IN 10^4 AMPERES FOR THIN SPHERICAL SHELL AT DEPTH ZERO WITHIN EARTH TO REPRODUCE GEOMAGNETIC SECULAR CHANGE, EPOCH 1942.5

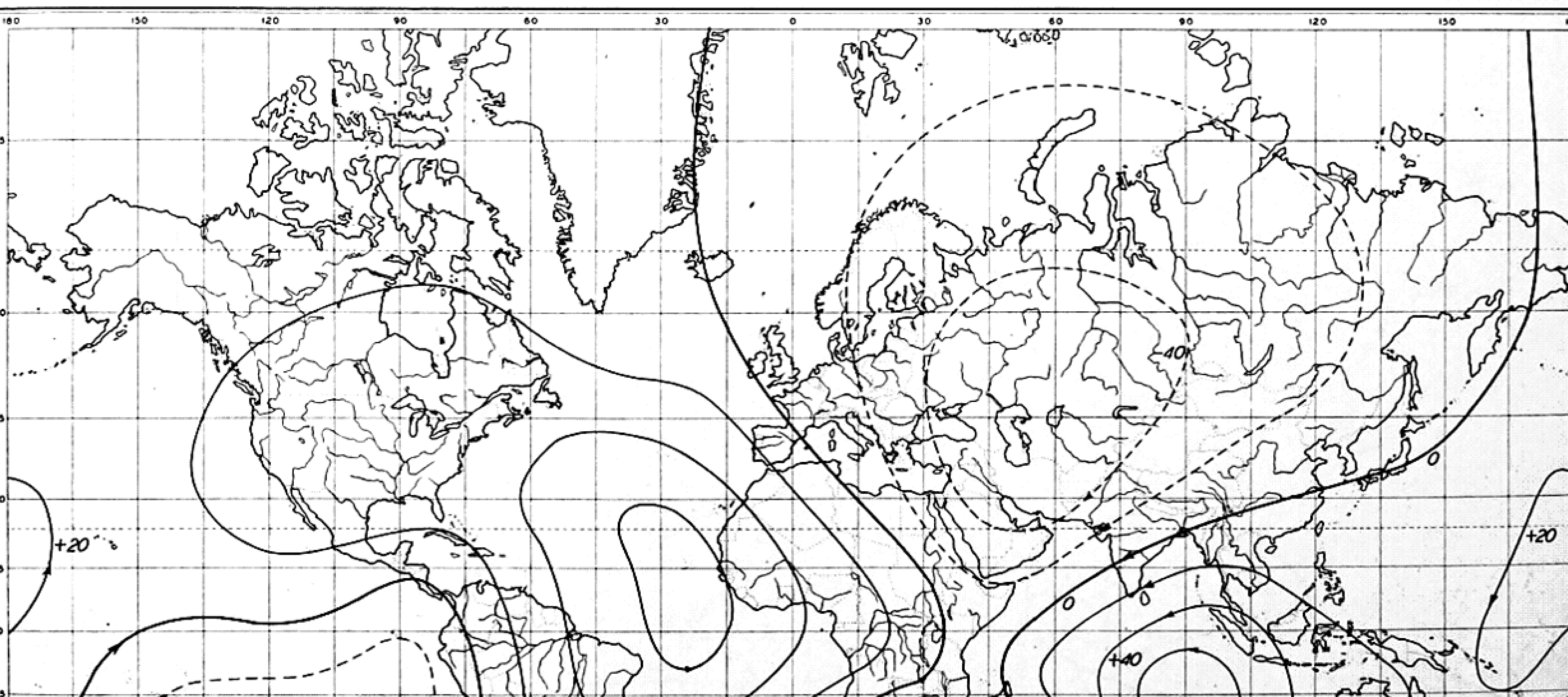

FIG. 22—CURRENT-FUNCTION IN 10^4 AMPERES FOR THIN SPHERICAL SHELL AT DEPTH 1000 KM WITHIN EARTH TO REPRODUCE GEOMAGNETIC SECULAR CHANGE, EPOCH 1942.5

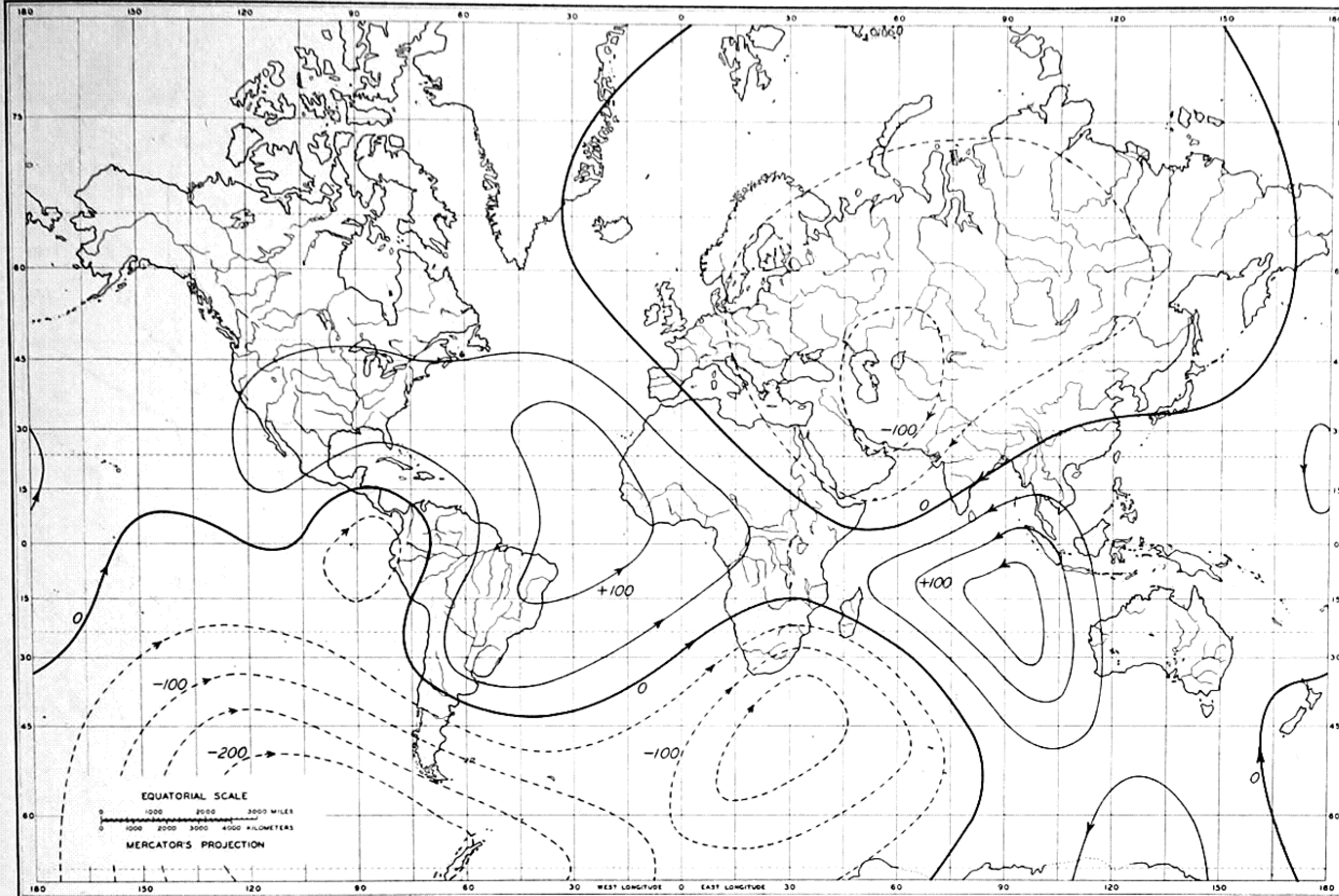

FIG. 23—CURRENT-FUNCTION IN 10^4 AMPERES FOR THIN SPHERICAL SHELL AT DEPTH 2000 KM WITHIN EARTH TO REPRODUCE GEOMAGNETIC SECULAR CHANGE, EPOCH 1942.5

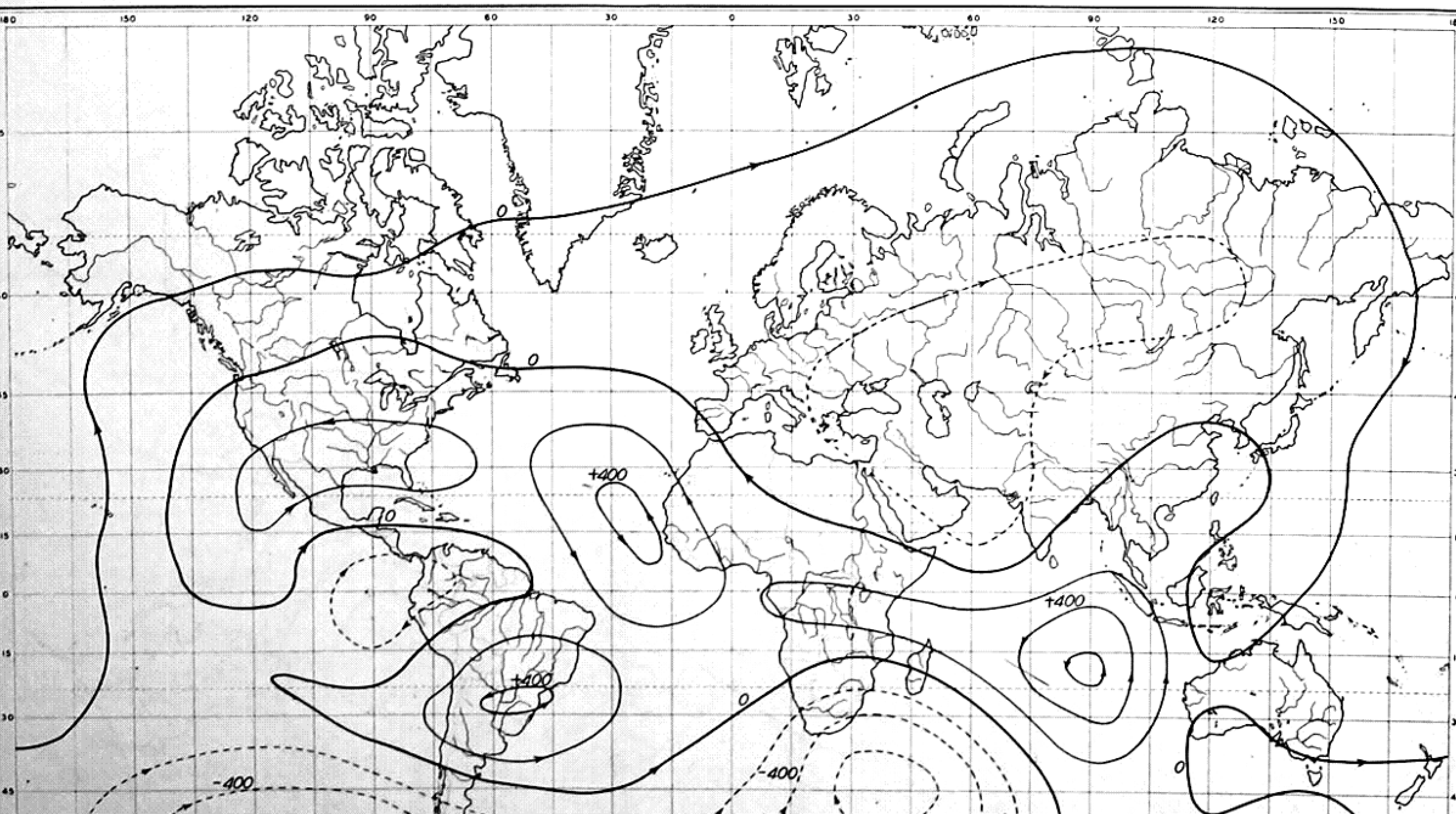

FIG. 24—CURRENT-FUNCTION IN 10^4 AMPERES FOR THIN SPHERICAL SHELL AT DEPTH 3000 KM WITHIN EARTH TO REPRODUCE GEOMAGNETIC SECULAR CHANGE, EPOCH 1942.5

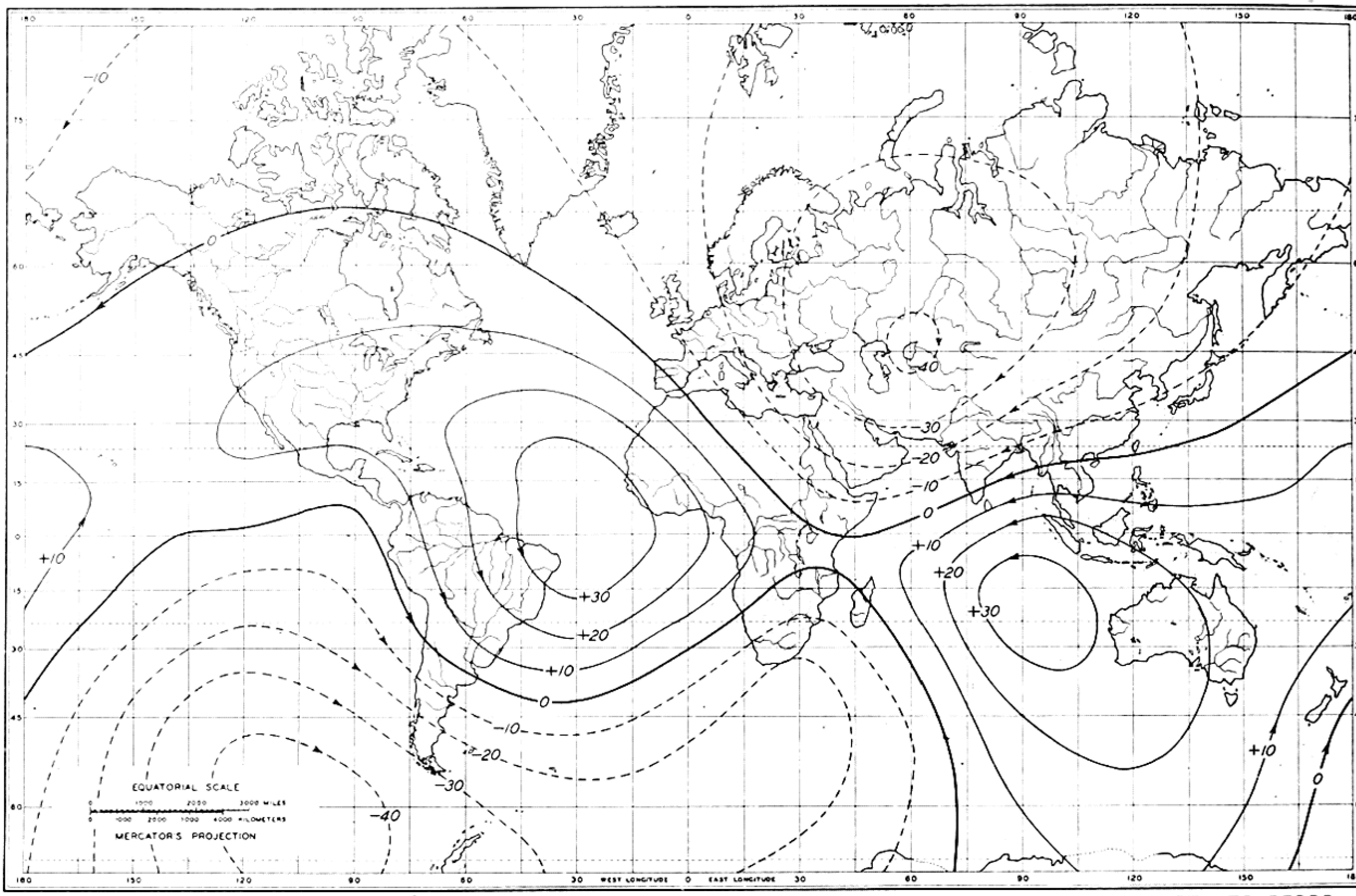

FIG. 25—CURRENT-FUNCTION IN 10^4 AMPERES FOR THIN SPHERICAL SHELL AT DEPTH ZERO WITHIN EARTH TO REPRODUCE RESIDUAL (NON-DIPOLE PART) OF GEOMAGNETIC CHANGE, EPOCH 1942.5

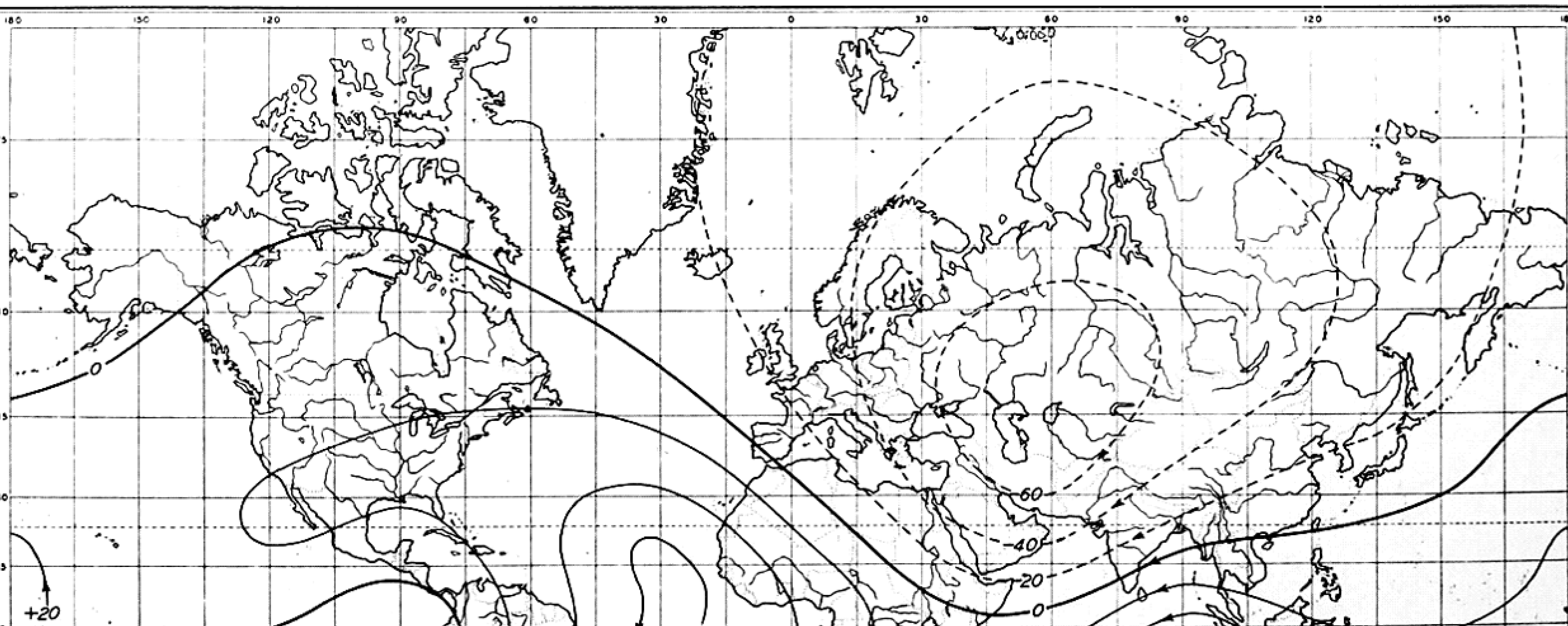

FIG. 26—CURRENT-FUNCTION IN 10^4 AMPERES FOR THIN SPHERICAL SHELL AT DEPTH 1000 KM WITHIN EARTH TO REPRODUCE RESIDUAL (NON-DIPOLE PART) OF GEOMAGNETIC CHANGE, EPOCH 1942.5

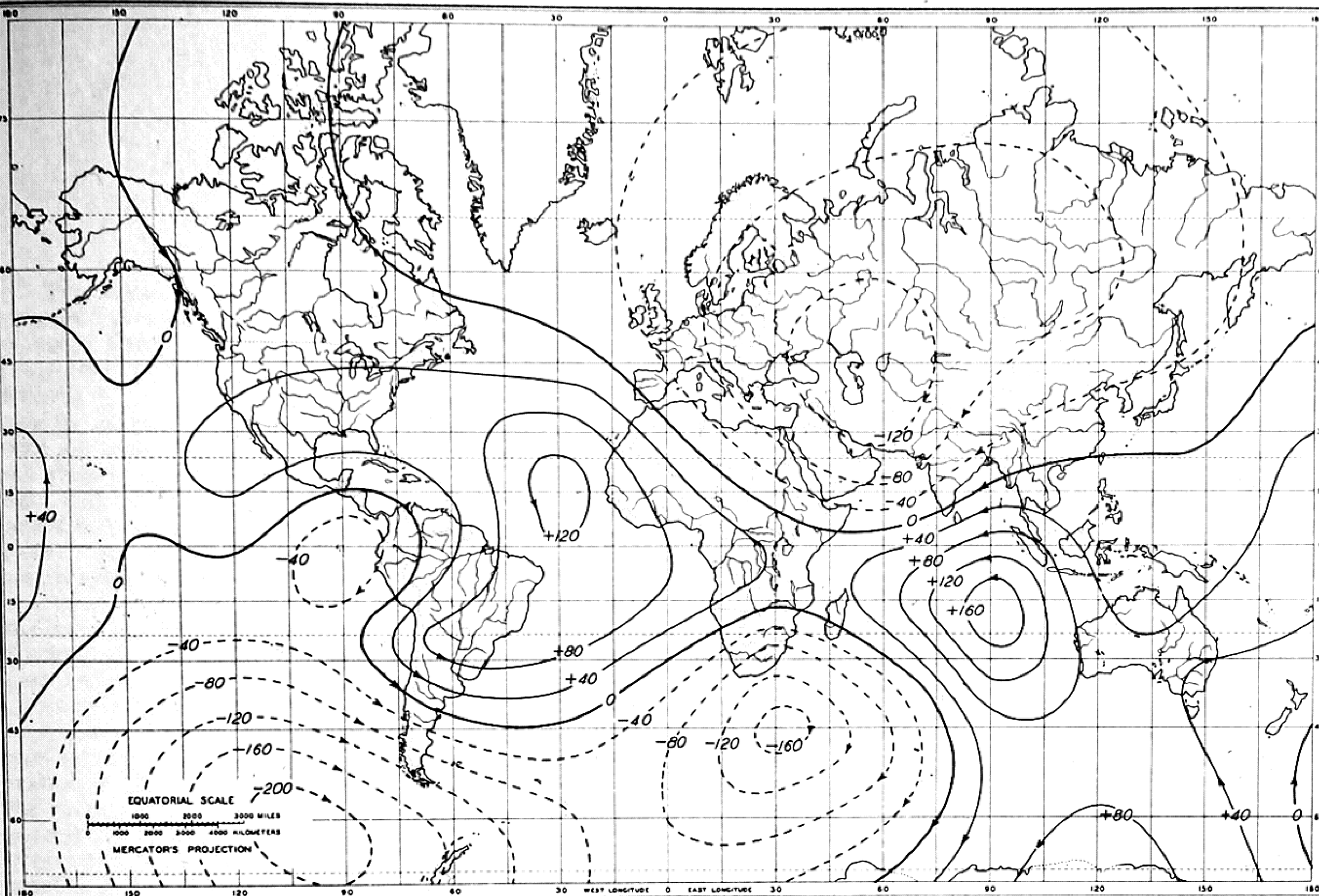

FIG. 27—CURRENT-FUNCTION IN 10^4 AMPERES FOR THIN SPHERICAL SHELL AT DEPTH 2000 KM WITHIN EARTH TO REPRODUCE RESIDUAL (NON-DIPOLE PART) OF GEOMAGNETIC CHANGE, EPOCH 1942.5

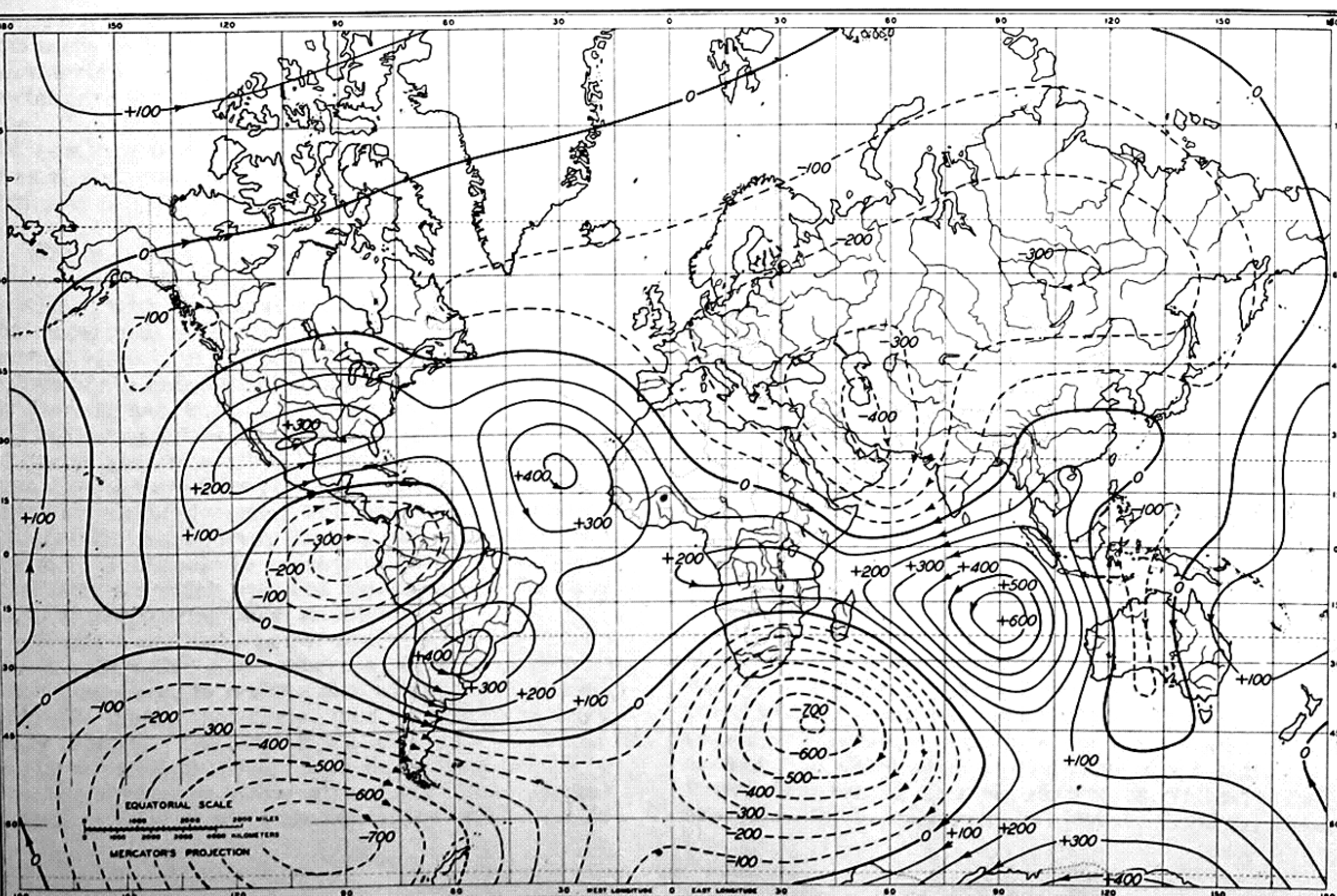

FIG. 28—CURRENT FUNCTION IN 10^4 AMPERES FOR THIN SPHERICAL SHELL AT DEPTH 3000 KM WITHIN EARTH TO REPRODUCE RESIDUAL (NON-DIPOLE PART) OF GEOMAGNETIC CHANGE, EPOCH 1942.5

CHAPTER IV

THE GEOMAGNETIC VARIATION WITH SUNSPOT-CYCLE, RV

The dependence of the annual mean values of the geomagnetic elements on solar activity has been demonstrated and examined by Moos [16], Schmidt [17], McNish [18], Scott [19], Wasserfall [20], and Chapman and Bartels [3]. It was noted that the annual mean in H are usually smaller in sunspot maximum years than in sunspot minimum years, and that this was a consequence of the greater incidence in the number of magnetic storms near sunspot maximum. The possibility that the effect might be due to a variation, with sunspot-cycle, of the secular variation arising from causes within the Earth was hence discounted by Fisk [21].

Schmidt [17] in his study used smoothed values of the annual means in three elements for Potsdam, and he derived normal values of field defined by annual means centered on individual months. He achieved considerable success in fitting the smoothed annual means at Potsdam by a quadratic expression involving the time, except for a part left over which varied with sunspot number. A derivation of RV is rendered difficult because the period of the variation is about 11 years, and thus is too long to permit very satisfactory derivation of its average characteristics from the short series of data available at most stations. Wasserfall [20] recently satisfactorily used nearly 100 years of data for Oslo, but few stations can be analyzed with confidence by a graphical method because the series of observations is too short.

The first attempt to derive RV on a world-wide scale was made by Fisk [21], for the H-component at ten observatories, and particular attention was given to the importance of the effect in his estimates of secular variation. He also considered the differences in the value of RV resulting from the use of days differing as to the degree of disturbance, and showed that the effect persisted with only slightly reduced amplitude even on selected quiet days.

The present work consists essentially of an extension of the work of Fisk, using more complete data since made available, with particular emphasis on the construction of tables permitting reduction of field-observations to their normal values, for the period 1905 to 1940. Annual mean values of the magnetic elements collected and compiled by Fleming and Scott [22], comprise the data analyzed.

Following Schmidt [17] smoothed biyearly means B of the geographic north (X), east (Y), and vertical (Z) components were first obtained. The values B were then fitted by various formulas at a few stations to observe whether the more slowly varying part of B afforded by the main field could be successfully fitted, yielding a part left over which would be approximately the same in form at neighboring observatories.

It was found that a power series in time t of the form $R = A + Bt + Ct^2 + Dt^3$, where A, B, C, and D are constants, appeared to remove also a part possibly associated with the sunspot-cycle. The term Dt^3 was accordingly dropped. The form $R = A + Bt + Ct^2$ was next fitted by the method of least squares to the values B, with considerably more encouraging results. Also, longer series of data for B were used and fitted by $R = A + Bt + b_1 \sin \alpha t + b_2 \sin 2\alpha t + b_3 \sin 3\alpha t$, where α was taken to be 13° 20′, so that the terms had periods of 54, 36, and 18 years, using a procedure somewhat similar to that employed by Fisk, who used periods of 48, 24, and 16 years. The justification for this procedure was that it appeared to work moderately well. The choice of period was such that periods of 11, 22, and 33 years, roughly indicated as present by successive differences of B for 1900 to 1940 at various stations, would be badly fitted. However, there is the obvious defect that the supposed values of RV in general would be partially fitted whatever the choice of period. Moreover, it is an obvious point that any smoothly varying function will not be fitted perfectly by an expression which is the sum of a constant, a linear term, and only three periodic terms. An alternative method was considered, based on the fitting of all periodic changes of RV when using a period of nearly 11 years, but this would be open to other objections and was accordingly discarded.

Figure 29 shows the results obtained using the expression with periodic terms in fitting the values B at many stations. In the geomagnetic north component the agreement, station by station, appears on the whole quite good, the results apparently being least consistent at Stonyhurst, for which annual means based on absolute observations only were available, and at Apia and Pilar in the Southern Hemisphere. It will be noted that the latter two stations also appear inconsistent with each other, with Pilar showing some resemblance to the results for the Northern Hemisphere.

In the case of the geomagnetic east and vertical components the results appear, on the whole, considerably less consistent station by station than in the case of the geomagnetic north component.

Certain defects arising from the mode of estimating RV should be reduced on averaging results for a number of stations.

Accordingly, the values for the first ten stations, excluding Stonyhurst, were meaned separately in the three components, and, using the known latitude distribution of disturbance given by D_{mi}, the equatorial value of RV in X′ was computed. The latitude distribution was then used to yield the computed values in the X′-component at each station, indicated by the smooth curves in Figure 29. The fit, station by station, appears to be about as good as might be expected in the north component, but the theoretical values for the east and vertical components which are to be compared with observed values are zero or practically zero (these are not shown because of difficulties of representation for the stations of Figure 29) and thus are in poor agreement with observation.

A different derivation of RV is afforded from the fit of the annual means by using the power series $R = A + Bt + Ct^2$. Figure 30 gives the results so obtained compared with the computed values of RV. The computed values were obtained, as before, for the X′-component at each station, using an equatorial value of RV estimated from means for the six stations, Sloutsk, Valencia, Rude Skov, De Bilt, Potsdam, and Val Joyeux. Good agreement

is on the whole again indicated for the geomagnetic north component, whereas the (small) east and vertical components (not shown) presumably remain unsatisfactorily defined on the basis of observation.

The comparison of Figure 30 is extended to include all additional stations for the geomagnetic north component in Figure 31, with similar satisfactory features in general evidence, except possibly for the stations noted for the Southern Hemisphere.

Figure 32 compares observed values of biyearly difference in B with those computed by the periodic formula whose constants were separately determined for each component, at each station, by fitting the values B from observation. The smoother characteristics of the biyearly differences given by the formula are clearly in evidence, in accordance with the assumption that the Earth's main field changes gradually and not discontinuously with time. This comparison shows that a fairly good fit of the observed data is obtained using such a formula, but this does not mean that the directly corresponding values in RV of Figure 29 are accurate; their accuracy is dictated by the quality of the observed data.

Figure 33 presents the means for the ten stations of the Northern Hemisphere in the geomagnetic north component of RV as found from the fit by formula with periodic terms, and for the mean of six stations referred to above as derived with the aid of the finite power series of three terms.

The results obtained using two imperfect methods give fair agreement in the estimated equatorial values of RV (we have not taken the trouble to compute the mean of the same ten stations for (B) as used for (A)). For (A), due to the formula used in fitting, estimates of RV are expected to be defective for early years of observation. Moreover, there is an undesirable arbitrary feature in fitting data by the so-called sinusoidal formula in that we have assigned the value $\alpha = 13^\circ\ 20'$; it was found that a change in α of only a few degrees changed the estimated RV by as much as 10 per cent. In the fit of data by the power series, the results in RV for the first and last few years may be bad because it seems unlikely that one could extrapolate so simple a formula for years prior to 1905 and following 1937 without gross errors. However, it seems considerably simpler to assume that the 40 years of data may be better fitted by a terminating power series, using a quadratic formula for, say, 25-year intervals overlapping in time. Our experience indicates that this assumption is at least fairly well substantiated. Hence, we regard the values of RV shown in Figure 30 as our better approximation over the years indicated.

The results seem in fair agreement with expectation of slow systematic change with latitude and with variation in the degree of magnetic disturbance with sunspot-cycle, in the X′-component. In Y′ we have been much concerned by the large and unexpected amplitude of RV. There is in evidence at De Bilt, Potsdam, and Val Joyeux, stations close together, considerable similarity in the Y′-component of RV. Values for Dehra Dun and Alibag, in another locality, likewise agree well with one another, though not with European stations. It seems likely that the similarities found locally are best explained as arising mainly from the inadequate representation of the generally much larger local phenomena of secular change by the simple power series. If this be true, all values shown for Y′ could well be fictitious, the true values being about zero, as expected from consideration of yearly means of Y′. In the case of the Z′-component, it is well known that measured results are of doubtful accuracy; the results of Figure 30 emphatically indicate the immediate need for drastic changes in the present instrumentation and practices for measuring Z, in order that magnetic observatories may obtain more accurate and useful values.

Shown in Figure 34 are the corresponding latitude distributions in the X′-component, as given by the values of RV meaned in yearly magnitude for each station, over the period 1905 to 1940. In the Northern Hemisphere especially, the latitude distributions found are clearly in good agreement with those also shown for D_{mi}, thus justifying the use of the latter in the earlier computations and comparisons for RV; it seems likely that the latitude distributions adopted are also applicable for the Southern Hemisphere.

Assuming then that the variation RV is a consequence of disturbance of form D_{mi}, approximate tables for the reduction of field-observations were constructed applicable in any latitude for the period 1905 to 1940 covered by the foregoing analysis. Tables 1-J and 1-K in the preceding volume [1] list the adopted values, for which it is apparent only a moderate degree of accuracy can be claimed.

The variation RV is of considerable theoretical interest due to its possible application in estimating the electric conductivity at greater depths within the Earth than has been possible from the use of daily and storm-time variations. However, there seems no possibility of making such estimates at the present time; they must await greatly improved control of recordings of vertical intensity. Therefore, the calculations can scarcely be made until some decades hence.

FIGURES 29-34

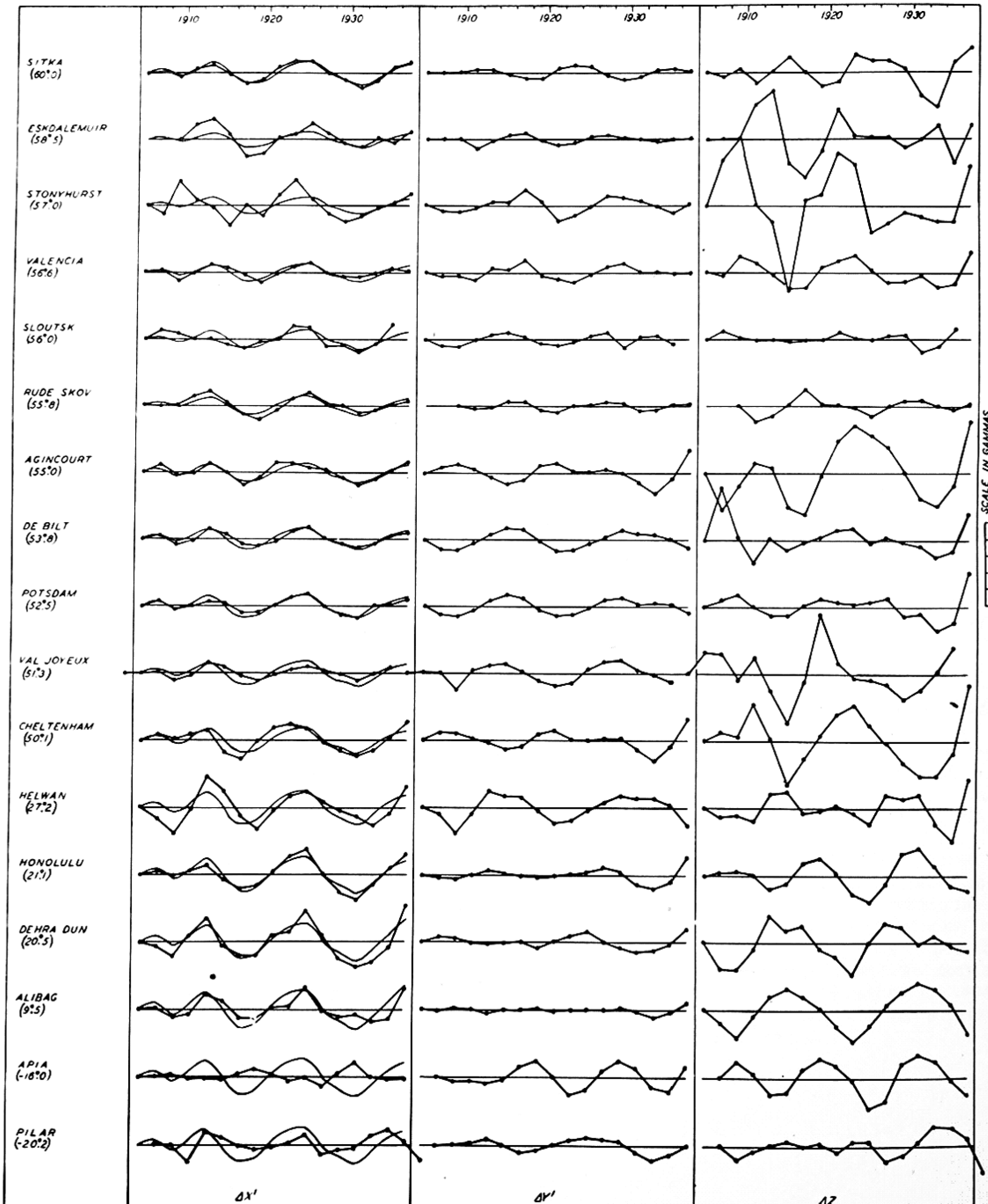

FIG. 29—ESTIMATED GEOMAGNETIC COMPONENTS OF VARIATION OF ANNUAL MEANS WITH SUNSPOT-CYCLE (RV) FROM SMOOTHED BI-YEARLY MEANS (B), MINUS VALUES OF (B) FITTED BASIS LEAST SQUARES BY $R = C + D(t - t_0) + b_1 \sin a t + b_2 \sin 2at + b_3 \sin 3at$, WHERE $a = 13°20'$ AND t THE TIME IN YEARS, COMPARED WITH MEAN VALUES (RV) FROM TEN STATIONS ASSUMING LATITUDE DISTRIBUTION THAT FOR DAILY MEANS OF DISTURBANCE (GEOMAGNETIC LATITUDES INDICATED IN PARENTHESES)

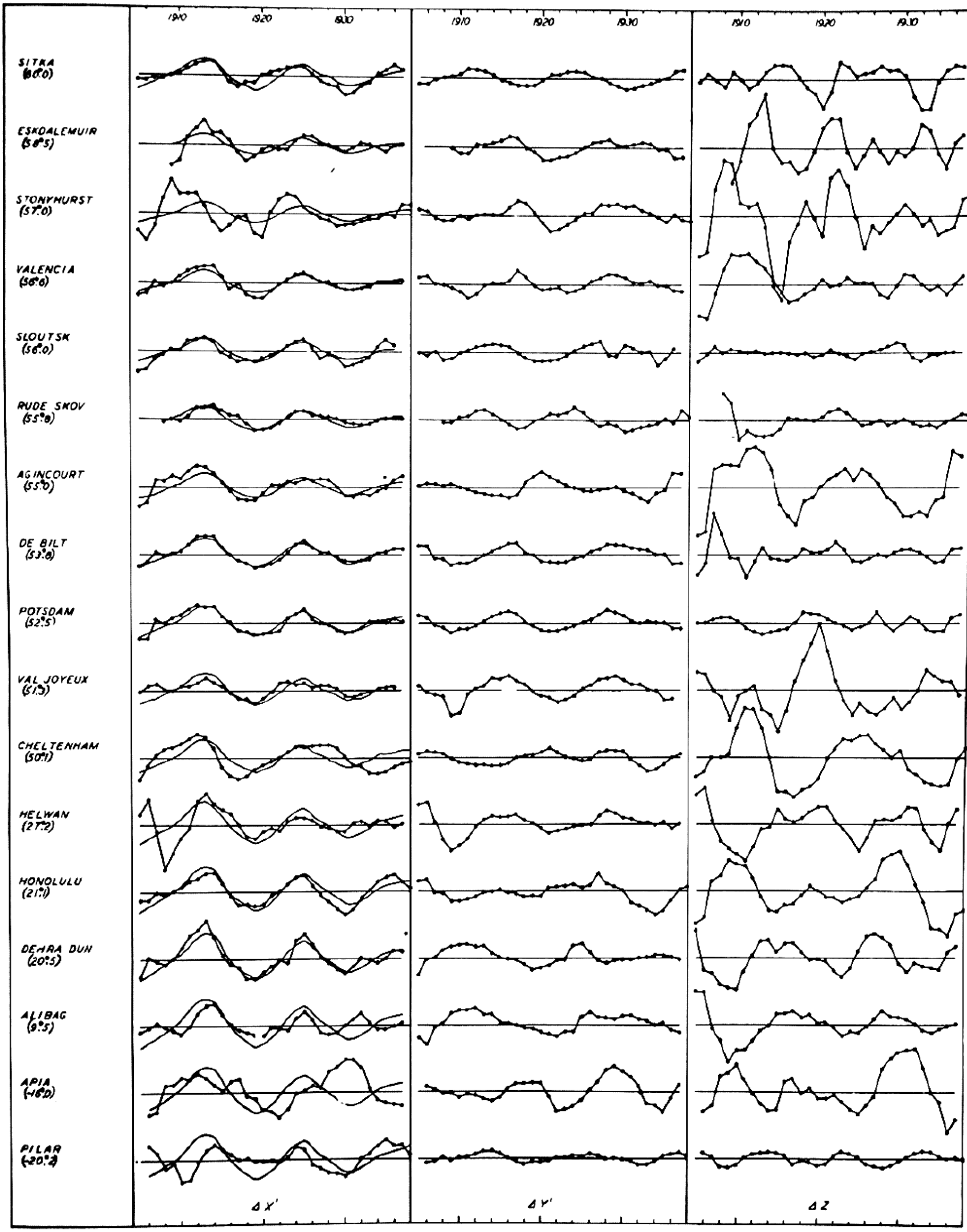

FIG. 30 — VALUES OF (RV) GIVEN BY SMOOTHED BI-YEARLY MEANS (B) MINUS VALUES $R = a + bt + ct^2$ FITTED TO (B) ON BASIS LEAST SQUARES COMPARED WITH ESTIMATED VALUES (RV)

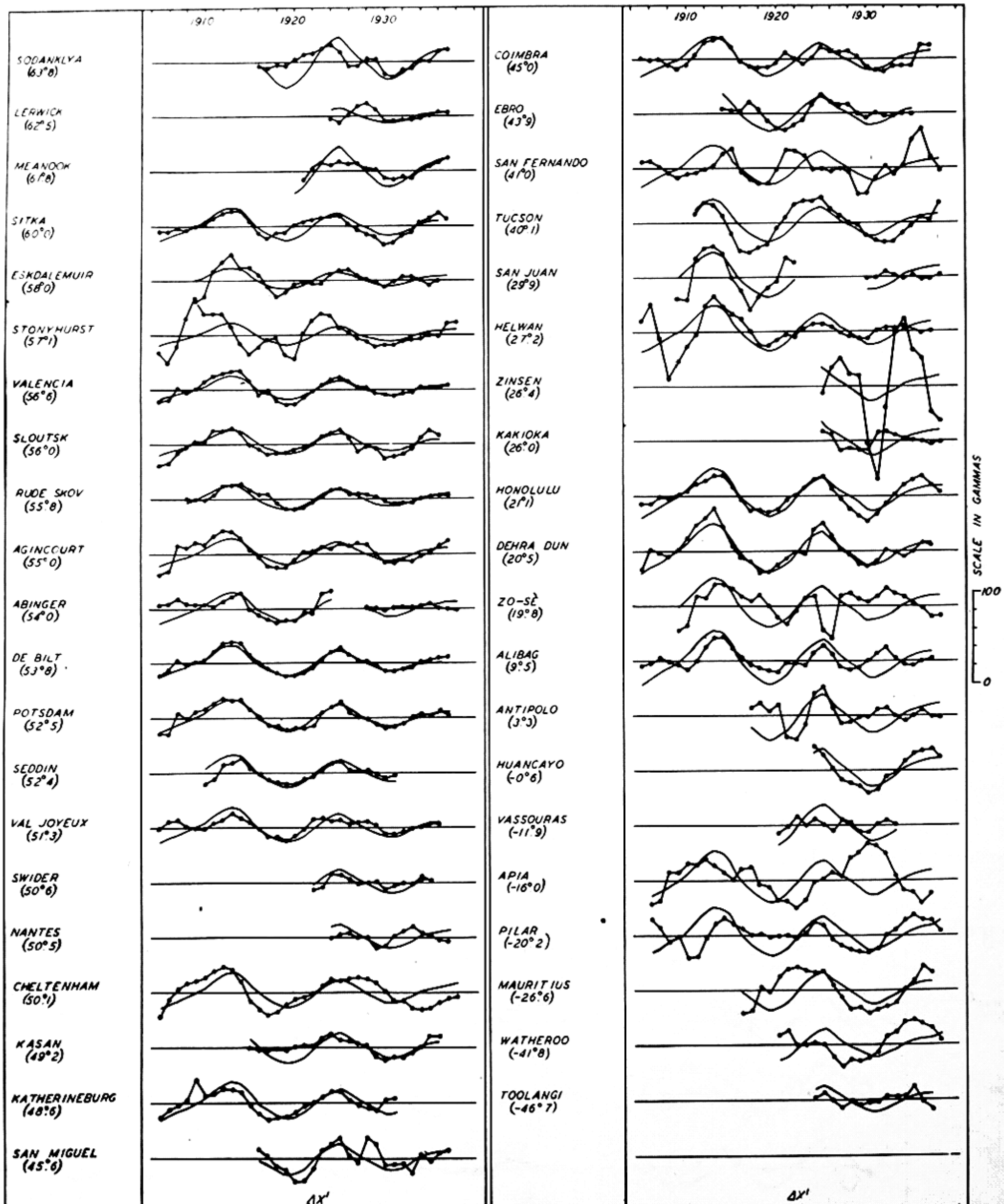

FIG. 31—YEARLY RESIDUES FOR SMOOTHED BI-YEARLY MEANS (B) MINUS VALUES OF (B) FITTED BY $R = a + bv + cv^2$, WITH v THE TIME IN YEARS AND a, b, AND c CONSTANTS COMPARED WITH ADOPTED VALUES OF GEOMAGNETIC VARIATION WITH SUNSPOT-CYCLE (RV), 1905-40

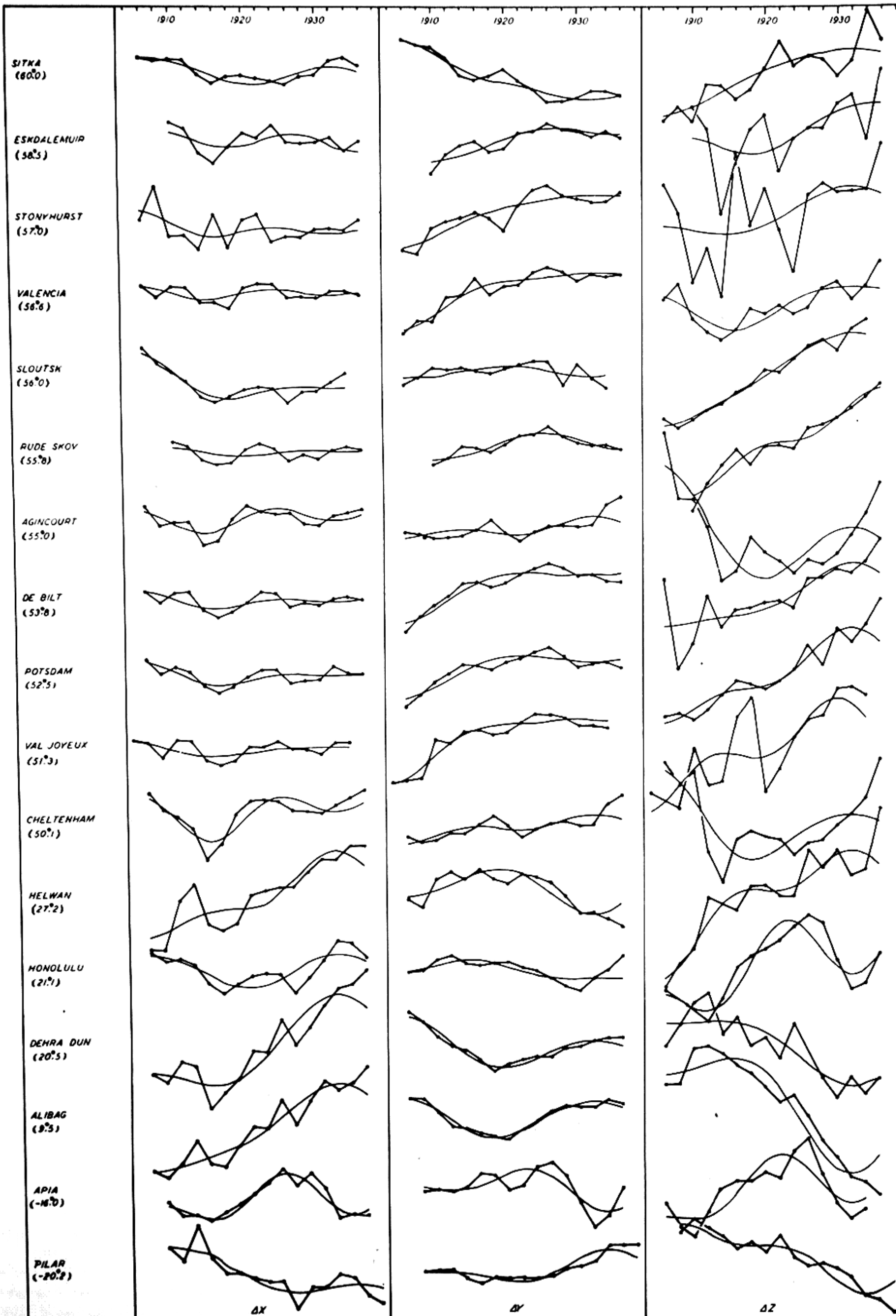

FIG. 32 — COMPARISON OF OBSERVED TWO-YEAR DIFFERENCES IN THE BI-YEARLY MEANS (B) OF COMPONENTS CORRECTED FOR SMOOTHING, GEOMAGNETIC VARIATION WITH SUNSPOT-CYCLE (RV), WITH VALUES COMPUTED FROM LATITUDE-DISTRIBUTION AND VALUE (RV), 1906-36 (GEOMAGNETIC LATITUDES INDICATED IN PARENTHESES)

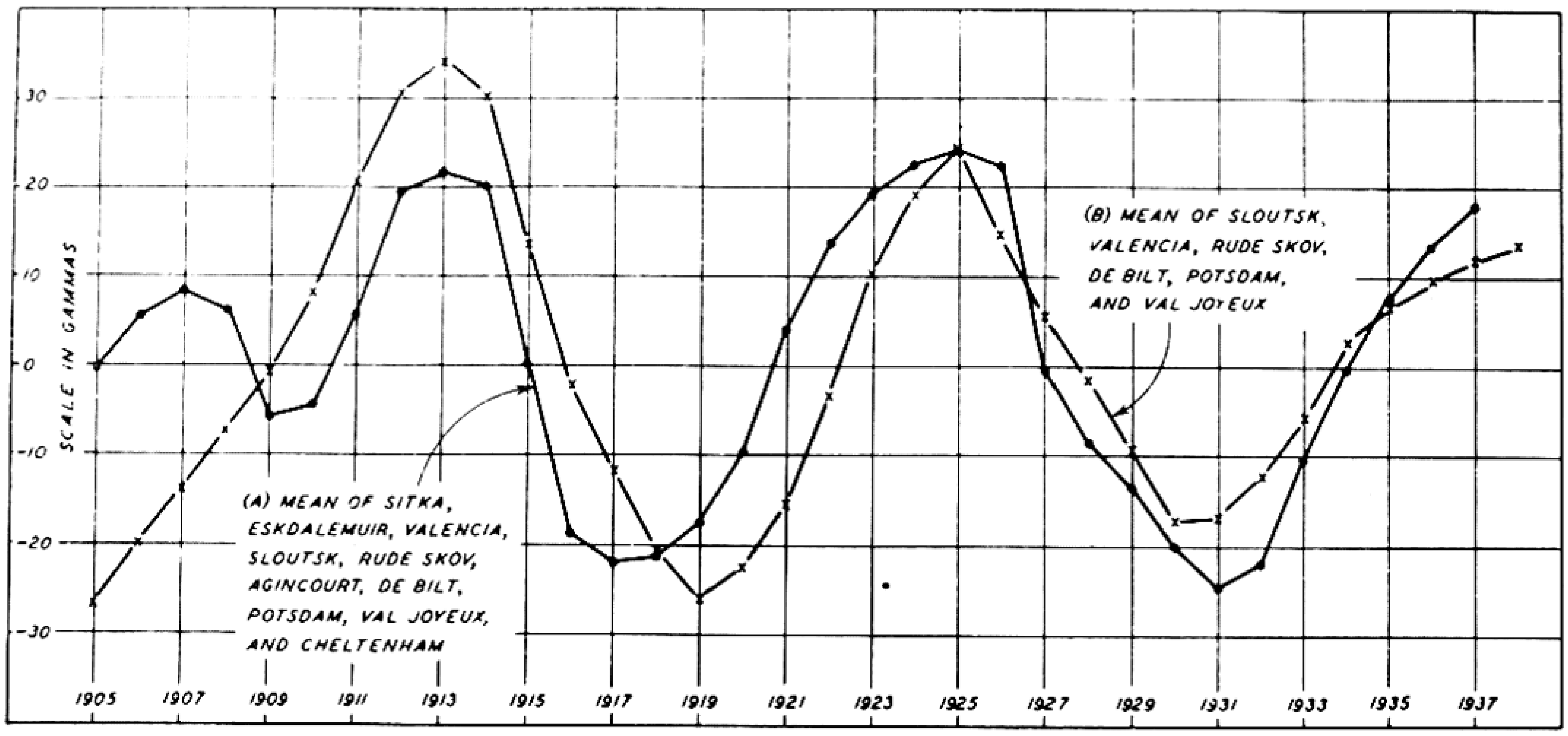

FIG. 33 — EQUATORIAL VALUES OF $\underline{RV}$ DERIVED USING LATITUDE DISTRIBUTION OF $\underline{D_{mi}}$ IN X′- COMPONENT AND (A) MEAN $\underline{RV}$ IN X′, SINUSOIDAL FORMULA, (B) MEAN $\underline{RV}$ IN X′, POWER SERIES FORMULA

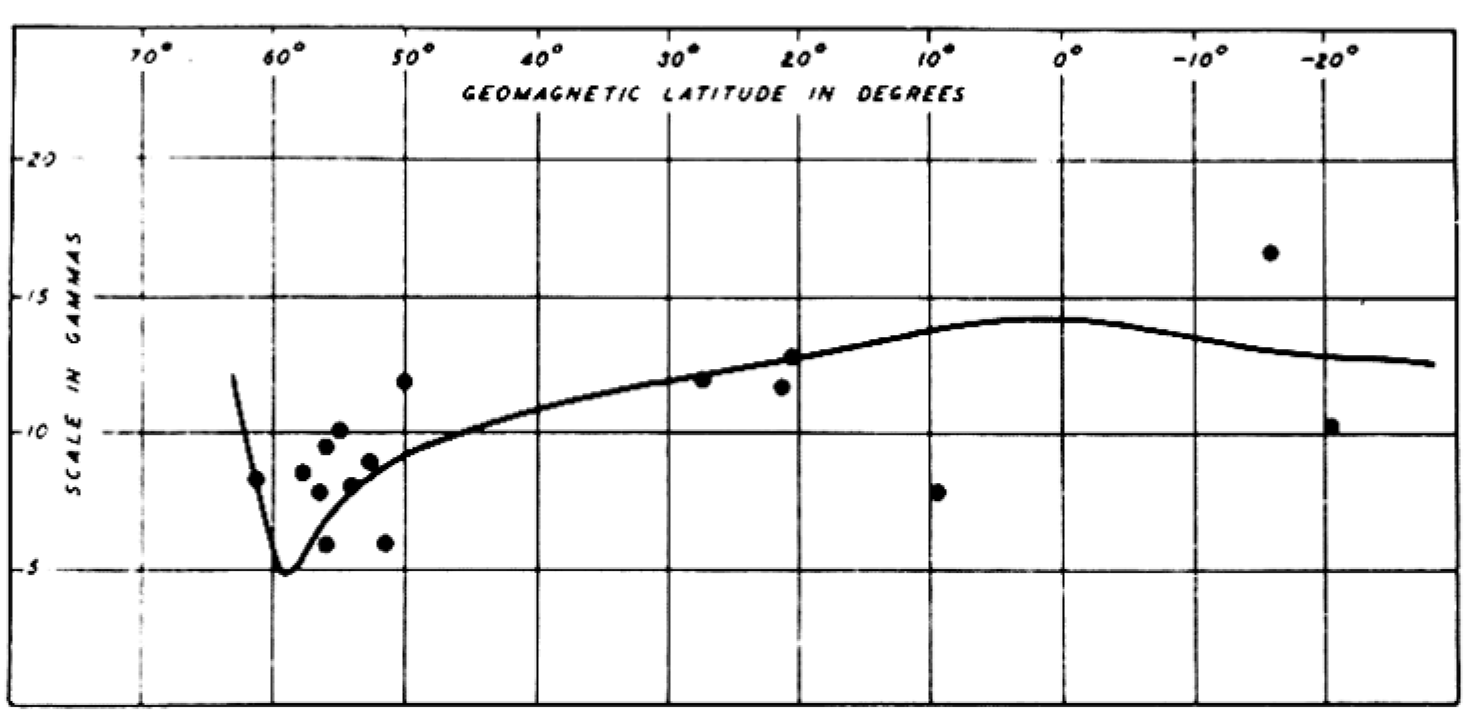

FIG 34 — COMPARISON OF LATITUDE DISTRIBUTION FOR AVERAGE YEARLY MAGNITUDE OF DEPARTURES OF GEOMAGNETIC VARIATION WITH SUNSPOT-CYCLE (RV) (POINT VALUES) WITH THAT OF DAILY MEANS OF DISTURBANCE (FULL LINE)

CHAPTER V

THE GEOMAGNETIC ANNUAL VARIATION, AV

1. General remarks.--The annual variation is scarcely a distinct and unique natural phenomenon since it arises from seasonal changes in the magnitudes of other geomagnetic variations. It is here conveniently regarded as the monthly mean departure from the annual mean value of a magnetic component, corrected for secular variation.

Derivations of the annual variation are affected in accuracy by uncertainties in base-line values of variometers. Thus the monthly mean departures for all days of a month from the annual mean of all days will be more accurately defined at the observatories obtaining more accurate absolute observations. It appears likely that at most observatories the absolute observations from which we derive vertical intensity do not permit sufficient control of variometers to indicate the annual variation at all in any individual year, except possibly in very high geomagnetic latitudes where the annual variation in Z is relatively large and susceptible of measurement with smaller percentage of error.

We first consider the general features found in the measured monthly departures from the annual means for various observatories of the Second International Polar Year, August, 1932, to August, 1933. Values averaged over different periods of years are next presented, and the general average latitude distribution of the annual variation AV is derived.

2. The annual variation for all days, Polar Year, 1932-33.--In order to obtain a general indication of the geographic distribution of AV with extensive coverage use was first made of the results for many observatories of the Polar Year, 1932-33. A and B of Figure 35 illustrate the measured results, corrected for secular change at the various observatories, in terms of the geomagnetic north (X'-), geomagnetic east (Y'-), and vertical (Z-) components.

A considerable degree of variability is shown, especially in the case of the Z-component. Differences of this kind can only be partially attributed to local geomagnetic conditions.

The agreement to within one or two gammas (one gamma = 10^{-5} CGS-unit) between such widely separated stations as Cheltenham in North America and Swider in Europe is truly remarkable. Good agreements of this kind for stations of nearly the same geomagnetic latitude can hardly be accidental when obtained for several months in succession. Such agreements are no doubt a consequence of the excellence of the absolute instruments and of the techniques of their use at the observatories. It will be noted that the results for a number of other observatories located in similar latitudes show almost identical results for the annual variation of the geomagnetic north component. The results for Z at these observatories do not agree at all well, and it may be concluded that they are open to suspicion. In the case of the geomagnetic east component (Y'), it would appear that it is small in all latitudes, although near the auroral zone (near geomagnetic latitudes 65° to 70° north) some variability from month to month is shown, presumably as the result of irregular disturbances there found predominating and because of the symmetry of the disturbance field about closed curves other than the parallels of geomagnetic latitude.

In regions near the auroral zone, it would in fact be expected that there should at times be evidence of change in amplitude of the annual variation with longitude. During magnetic storms the diurnally varying part, which depends mainly on local time in any region, would contribute unequally to the monthly means observed at stations in different longitudes. This effect would be most notable in the cases of great magnetic storms, where the influences of a single storm would tend strongly to affect the mean monthly value at an observatory.

It is of interest to see whether a selection of observatories can be made such that a systematic pattern is evinced in the latitude distribution of the annual variation. C of Figure 35 illustrates such a selection, using the data of A and B of Figure 35, the results for a few observatories being meaned.

An orderly, simple change with geomagnetic latitude in the character of the annual variation of the geomagnetic north component is at once apparent. The annual variation in the geomagnetic east component appears to be nearly zero in all latitudes. In the case of the vertical component, the results are disappointing except in very high latitudes where the variation is clearly of larger amplitude, and where the use of special equipment to determine the base lines of Z variometers resulted in superior determinations.

The values of the geomagnetic north component shown in Figure 35 can be analyzed into a part symmetrical about the equator and a sinusoidal part of one-year period, with six months' difference in phase between the Northern and Southern Hemispheres. Cynk [23] showed that the symmetrical part in any latitude varied in amplitude directly as the disturbed-day minus quiet-day means. Figure 36 shows the results of such an analysis based on the data of C of Figure 35. The observed values $\Delta X'$ of the annual variation are conveniently regarded as comprising two parts with simple latitude distributions, one part symmetrical about the equator, with minima near the equinoxes, varying with latitude proportionately to the daily means of disturbance, the other a sinusoidal part, showing in the Northern Hemisphere a maximum near the winter solstice and a minimum near the summer solstice, and in the Southern Hemisphere a maximum and minimum of opposite phase. Table 102 gives the sinusoidal part of C of Figure 35 in the form of the Fourier series $a_0 + a_1 \cos x + b_1 \sin x$, where x is an angular representation of the time at a rate of 30° per month beginning on September 1, 1932. Although there is evidence of systematic variation of the coefficients a_1 and b_1, the latitude distribution does not appear to be satisfactorily defined from data of a single year.

Since the symmetrical part depends upon the average value of disturbance, the comparatively large annual variation for disturbed days was next derived. The results of Figure 36 indicate quite clearly that an accurate description of the latitude distributions of the two parts of

the annual variation can be expected only from the averages of many years of data. Although years of data for this purpose have not been obtained for polar regions, a certain amount of useful information respecting the latitude distributions in high latitudes is available from the results for the single year of observation provided by the Polar Year, 1932-33.

A, B, and C of Figure 37 show the annual variations found for the Polar Year 1932-33, for international quiet days, international disturbed days, and for their differences, for many stations. It is evident from A of Figure 37 that the annual variation on quiet days closely resembles that found for all days, although somewhat smaller in amplitude than the latter. Thus the influences giving rise to at least the major part of the annual variation are likewise operative on magnetically quiet days. This is mainly a consequence of disturbance, since the quiet-day means in the geomagnetic north component are lower in months when there are stronger and more frequent disturbances. Of quite special interest are the comparatively large annual variations in Z in high latitudes as shown by Thule ($\Phi = 88^\circ.0$), Godhavn ($\Phi = 79^\circ.8$), and Juliannehaab ($\Phi = 70^\circ.8$).

In B of Figure 37 are shown the annual variations obtained for international disturbed days at polar stations. These afford an interesting comparison with the corresponding values of A of Figure 37. The most significant difference is the increase in amplitude shown in all latitudes in the case of the geomagnetic north component, unaccompanied by a corresponding increase in the amplitude of the vertical component in high latitudes. In fact, the latter is only slightly larger on disturbed days than on quiet days. Thus, if we seek to explain the sinusoidal part as due to electric currents above the Earth, flowing either from geomagnetic west to east or, preferably, geomagnetic east to west (since the annual variation in the geomagnetic east component is very small), there might be said to be such currents strongly in evidence on quiet days but not particularly strongly augmented on disturbed days.

A significant feature here is that the increase in magnitude of the symmetrical part with increased intensity of disturbance is not accompanied by a corresponding proportional increase in the amplitude of the sinusoidal part. Hence the annual variation comprises two parts free to vary somewhat independently of each other. This means further that in order to predict the annual variation in any latitude, from the observed annual variation at a particular latitude, the latitude distributions of the two parts of the annual variation must be independently derived, using corresponding latitude factors which, though related to the intensity of disturbance, will be in certain respects independent of each other.

C of Figure 37 illustrates for the same stations the differences between the annual variations on disturbed and quiet days. The annual variation for disturbed minus quiet days is of particular interest in that it is less susceptible to the influences of errors in base-line values and permits study also of the relationships of the two parts of the annual variation on days more disturbed than in the case of all days of a month or year. The general transition in the character of the variation from station to station is more clearly in evidence than in the case of disturbed and quiet days considered separately, but there are considerable discrepancies in Z, probably because of uncertainties in measurement.

3. The latitude distributions of the symmetrical and sinusoidal parts of the annual variation.--It is of interest to know whether the form of AV may change in some important respect with year, for instance with year of sunspot-cycle. A to H of Figure 38, giving averages of the annual variation for various sets of years of the period 1905 to 1940, show little evidence of important change with year in the annual variation for all days. It is evident that the results for the vertical component show large and erratic fluctuations which are of questionable significance, but the change with latitude in the geomagnetic north component is rather clearly defined. A to D of Figure 39 show the averages for groups of year near sunspot maximum and for groups near sunspot minimum. Figure 40 shows that the average amplitude is about twice as great for the sunspot maximum groups of years. Figure 41 illustrates year by year the close similarity of the annual variation at the high-latitude station Sitka ($\Phi = 60^\circ$) as compared with Cheltenham ($\Phi = 50^\circ.1$) for each year of the period 1905 to 1936.

In order to obtain a more accurate derivation of the latitude distributions of the symmetrical and sinusoidal parts of the annual variation than would be possible for the stations used in deriving the data of C of Figure 37 for the year 1932-33 (including our only important source of polar data), averages were derived for the 12 years of the period 1922 to 1933. Data for disturbed days minus quiet days are shown in A of Figure 42. The corresponding symmetrical and sinusoidal parts derived are illustrated in B and C of Figure 42. Results of the same type for a longer period of years are given in Figure 43. The sinusoidal part was derived by Fourier analysis and checked by subtracting (or adding in the case of Z) averages for Southern Hemisphere stations from those for Northern Hemisphere stations. The symmetrical part was then obtained by subtracting the sinusoidal part from the total annual variation and checked by adding results for Northern Hemisphere and Southern Hemisphere stations. Using the known latitude distribution of the daily means of disturbance for international disturbed days (D_{mi}) [1] the symmetrical part for each station was then reduced to give the equatorial value of the symmetrical part mostly closely in correspondence with the values at all stations. This equatorial value was then finally used in conjunction with the values of the latitude factor directly proportional to D_{mi} to obtain the illustrated symmetrical part for each station. The results showed good agreement with the symmetrical part at each station found originally from subtraction of the sinusoidal part from the observed annual variation at each station, except in the vertical component. In the case of the latter component, the symmetrical part was checked with that obtained from the geomagnetic north component by direct use of the known latitude distributions of both the geomagnetic north and vertical components of D_{mi} illustrated in Figure 44, as deduced for years 1922 to 1933.

Of special note is the presence of values notably different from zero in the geomagnetic east component in high latitudes. This seems to be a natural consequence of the choice of geomagnetic components instead of components normal to or parallel to the auroral zone.

Figure 44 gives the latitude distribution of the international-disturbed-day means minus quiet-day means, averaged for the years 1922 to 1933, except for high northern latitudes, for which data for only the Polar Year,

1932-33 were used. These were multiplied by the factor 1.21 (derived from lower latitude stations) in reducing them to the mean of 1922 to 1933. Values for stations in the range $\Phi = 60^\circ$ to 70° have been plotted and adjusted in position relative to a circular auroral zone located in geomagnetic latitude 67°.

The geomagnetic north component is negative in sign in all latitudes. It attains a minimum value of -61γ at the auroral zone, and has a secondary minimum of -25γ at the equator, about which the field in this component is symmetrical. The geomagnetic east component appears to be zero in low and middle latitudes. Near and inside the auroral zone the field, as before, does not show perfect symmetry relative to the geomagnetic axes. The vertical component of D_{mi} has a maximum value of 27γ just inside the auroral zone, and a minimum of -21γ just outside. The vertical component is zero near the equator and is opposite in sign on either side of it. We have noted previously that Figure 44 gives the latitude distribution of the symmetrical part of the annual variation, apart from a constant of proportionality, which is the same in all latitudes. The latitude distribution appears rather well determined, though the adopted values in polar regions are of course more uncertain than those for the region between the northern and southern auroral zones.

Figure 45 shows the latitude distributions and time-phases found for the geomagnetic north and vertical components of the sinusoidal part of the annual variation. On the upper left is shown the variation of the geomagnetic north component (X') with latitude as indicated by the amplitude ($C_1^{X'}$) and ($\alpha_1^{X'}$) of the expression $-C_1^{X'}\cos(t + \alpha_1) = a_1\cos t + b_1\sin t$ where t is the time reckoned at the angular rate of 30° per month commencing on January 1. The data for various years have been reduced to the mean of the years 1922 to 1933.

The values of $C_1^{X'}$, apart from proportional factors the same in value for all stations, in each particular mean of a group of years, appear to fit rather well a smoothed curve drawn by eye among the points. The values $C_1^{X'}$ are zero (by definition of the X'-component) at the geomagnetic north pole, and go to a maximum roughly half way between the pole and the auroral zone, after which they decrease rapidly at first then slowly to attain a zero-value at the equator, about which the component appears roughly symmetrical. The phase angle ($\alpha_1^{X'}$) in the Northern Hemisphere is the reverse of that in the Southern Hemisphere. On the lower left-hand side are shown the calculated points, from the Fourier analysis of the data, for the corresponding values $a_1^{X'}$ and $b_1^{X'}$, the curves drawn being those computed from the adopted curves for $C_1^{X'}$ and $\alpha_1^{X'}$, giving as should be expected, a reasonably good fit of the points for $a_1^{X'}$ and $b_1^{X'}$.

On the right are shown the corresponding values for the vertical component of the sinusoidal part of the annual variation. The values of C_1^Z decrease rapidly from the pole equatorwards, attaining a fairly constant value in middle and low latitudes. The phase angles α_1^Z are not well determined since there is some considerable scatter in the points obtained from the data. As drawn, there would seem to be indicated a slight but rather insignificant lead in phase in middle and low latitudes relative to the geomagnetic north component. However, the curve adopted for α_1^Z is naturally rough and somewhat tentative, although the values of a_1^Z and b_1^Z appear on this basis rather successfully fitted, and hence lend support to the authenticity of the curve adopted for α_1^Z.

Figure 46 indicates the grave difficulties attendant on estimating, in terms of the Fourier coefficients $-a_1$, b_1, the sinusoidal part of the annual variation in a particular latitude by individual years. In the case of the geomagnetic north component, the scatter of the yearly points about the mean (indicated by a vector) is not unduly great, and the vectors are determined with fair accuracy both in amplitude and phase. In the case of the vertical component, the results are clearly erratic both in amplitude and phase, and it is evident that the mean of 37 years is of an accuracy leaving much to be desired.

The foregoing results were used in deriving Tables 1-C to 1-F of the previous volume [1].

A zonal harmonic analysis was attempted of the Fourier components of the sinusoidal part of the annual variation. However, the computed fractions for external origin for harmonics of different degrees did not agree well with one another. This would suggest that our latitude distributions for the Fourier coefficients were not sufficiently accurate for the purpose.

The electric current system which could reproduce the symmetrical part of AV seems to resemble closely that proposed by Chapman [3] for the storm-time variation. Due to the sinusoidal part of the annual variation, its general form will undergo a considerable seasonal variation.

Table 102. Values of Fourier coefficients of series for sinusoidal part [Figure 35(C)], annual variation, Polar Year, 1932-33

Station		A_0	A_1	b_1
Thule	88.0	+1.73	+ 3.98	-8.34
Godhavn	79.8	- .33	+14.52	-8.76
Juliannehaab	70.8	+ .58	+ .87	+ .80
Tromsö, Fort Rae, College, Fairbanks	66.9	.00	+ .53	-3.14
Sodankyla	63.8	.00	+ 1.70	-2.96
Lerwick, Sitka	61.2	+ .17	+ 2.47	-3.18
Eskdalemuir, Lovo, Sloutsk	57.5	- .17	+ 1.88	-3.19
Rude Skov	55.8	- .33	+ 1.61	-2.92
Agincourt, Abinger	54.5	- .58	+ 2.23	-3.70
Val Joyeux, Cheltenham	50.7	+ .83	+ .49	-4.17
Tucson	40.4	.00	+ .81	-3.81
Helwan	27.2	.00	- 1.97	-7.68
Honolulu	21.1	+ .17	+ .93	-0.39
Lukiapang	20.0	+ .50	- .33	- .07
Alibag	9.5	.00	- 3.46	-1.18
Huancayo	- 0.6	- .08	+ 1.61	+2.08
Pilar	-20.2	- .75	- 4.06	+5.50
Cape Town	-32.7	- .17	- 3.39	+5.75
Watheroo	-41.8	+ .25	- 3.68	+2.32
Toolangi	-46.7	+ .17	- 2.48	+2.16
Amberley	-47.7	.00	- 1.31	+4.55
South Orkneys	-50.0	- .08	+ .19	+5.01

FIGURES 35-46

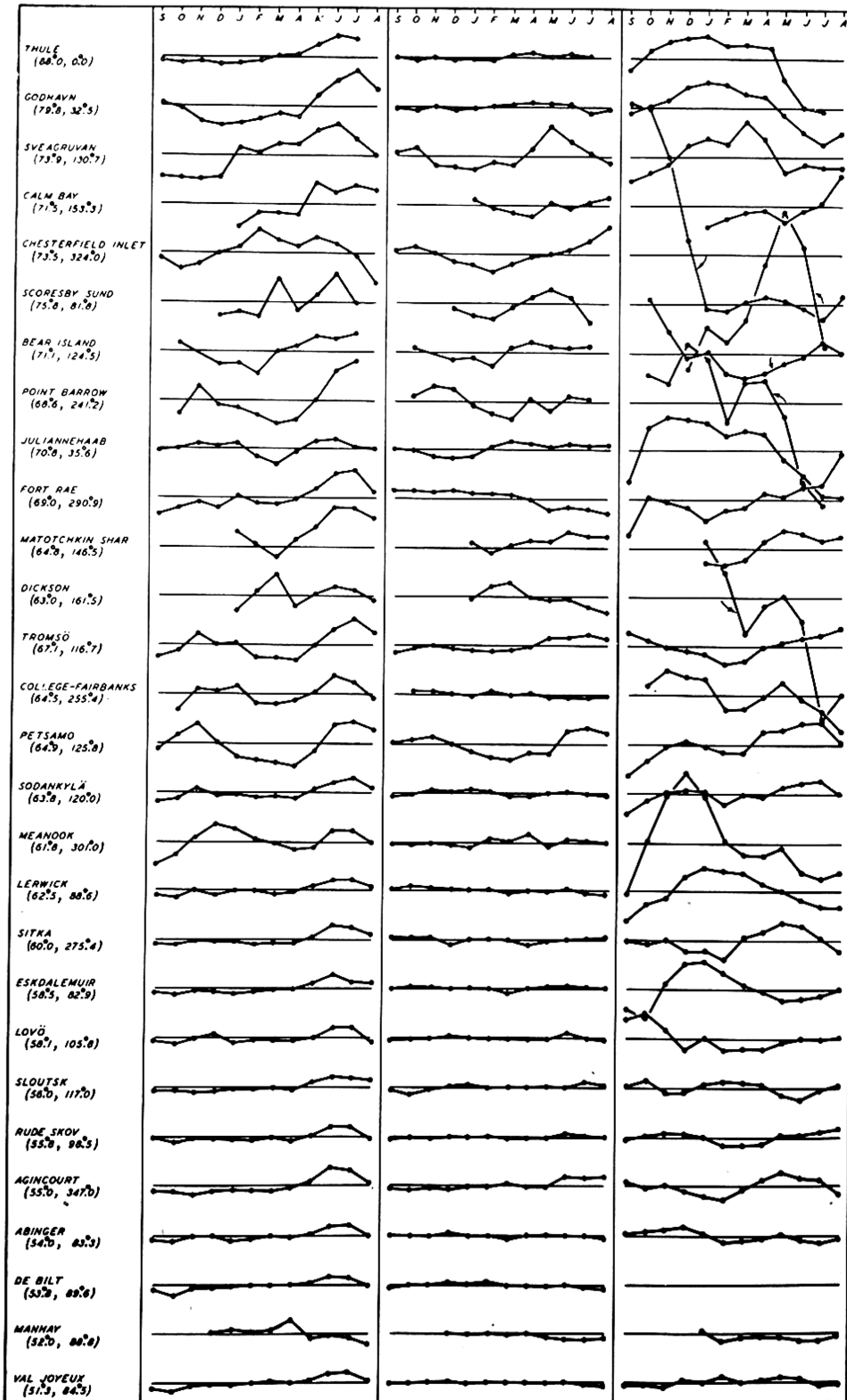

FIG. 35(A)–MONTHLY MEAN DEPARTURES FROM ANNUAL MEANS OF MAGNETIC INTENSITY FOR GEOMAGNETIC NORTH (ΔX'), EAST (ΔY'), AND VERTICAL (ΔZ) COMPONENTS AT VARIOUS OBSERVATORIES, SEPTEMBER 1932 TO AUGUST 1933 (GEOMAGNETIC LATITUDES AND LONGITUDES INDICATED RESPECTIVELY IN PARENTHESES)

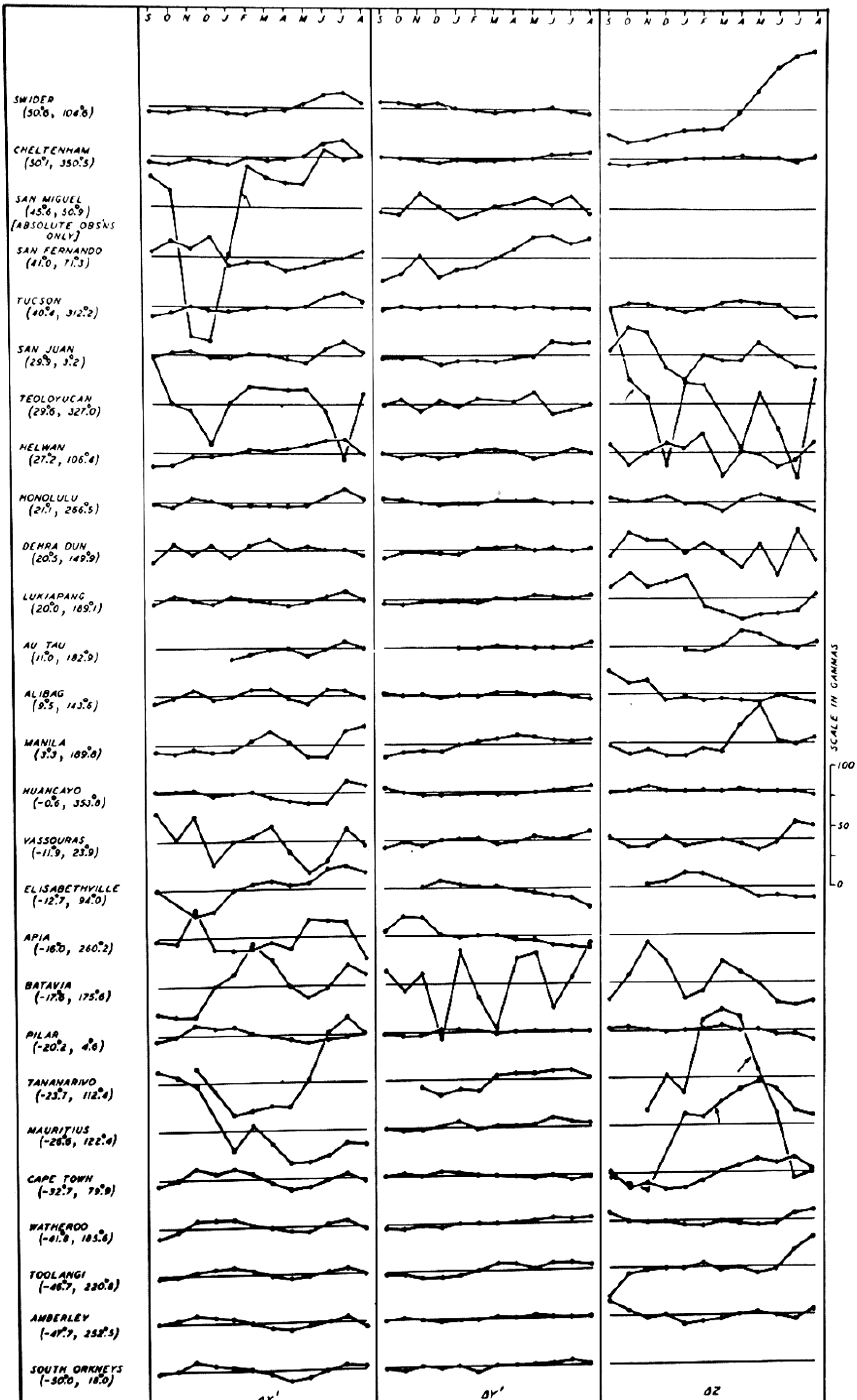

FIG. 35(B)—MONTHLY MEAN DEPARTURES FROM ANNUAL MEANS OF MAGNETIC INTENSITY FOR GEOMAGNETIC NORTH (ΔX'), EAST (ΔY'), AND VERTICAL (ΔZ) COMPONENTS AT VARIOUS OBSERVATORIES, SEPTEMBER 1932 TO AUGUST 1933 (GEOMAGNETIC LATITUDES AND LONGITUDES INDICATED RESPECTIVELY IN PARENTH[illegible]ES)

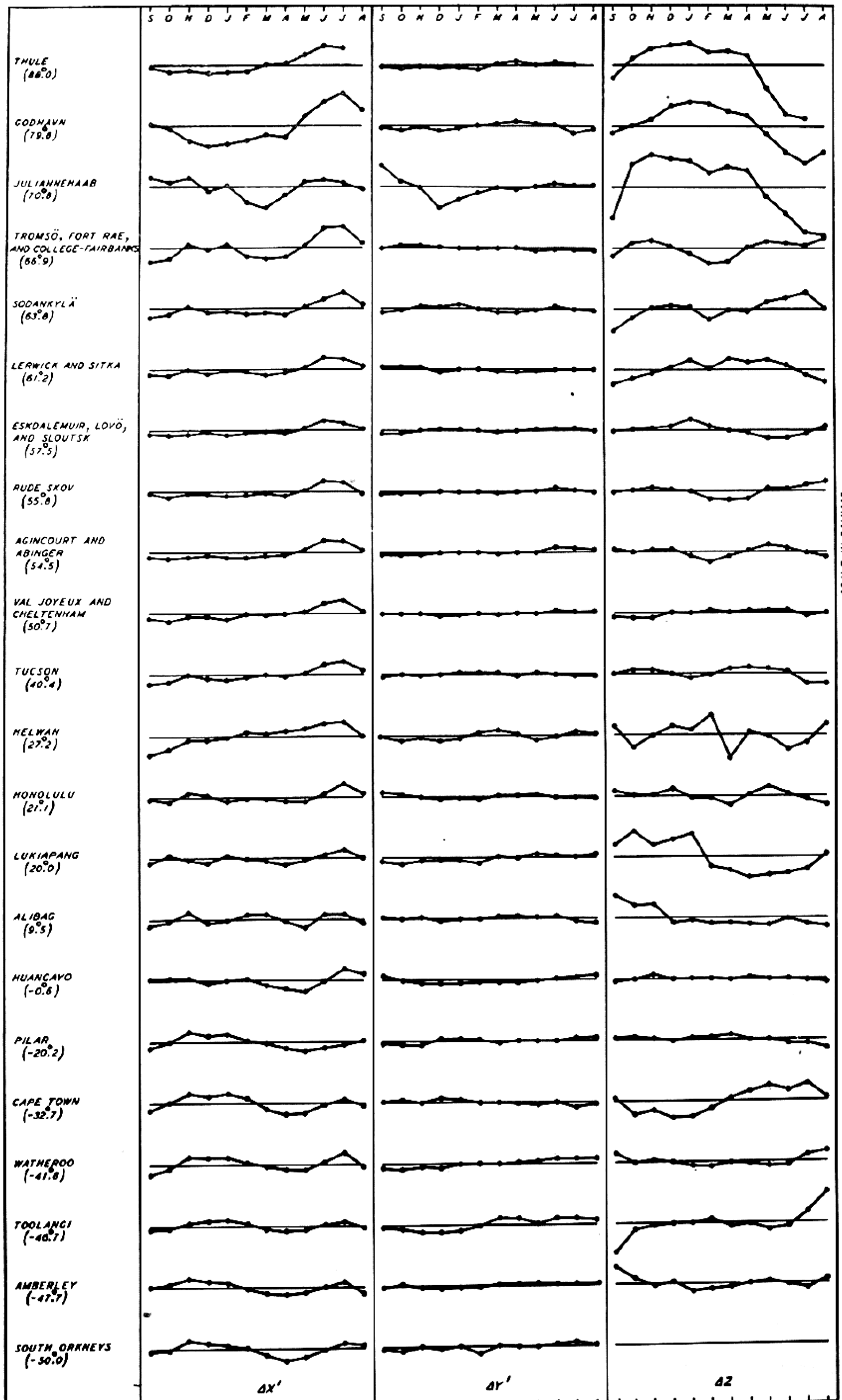

FIG. 35(C)-VARIATION WITH GEOMAGNETIC LATITUDE OF MONTHLY MEAN DEPARTURES FROM ANNUAL MEANS OF GEOMAGNETIC COMPONENTS OF INTENSITY, SEPTEMBER 1932 TO AUGUST 1933 (GEOMAGNETIC LATITUDES INDICATED IN PARENTHESES)

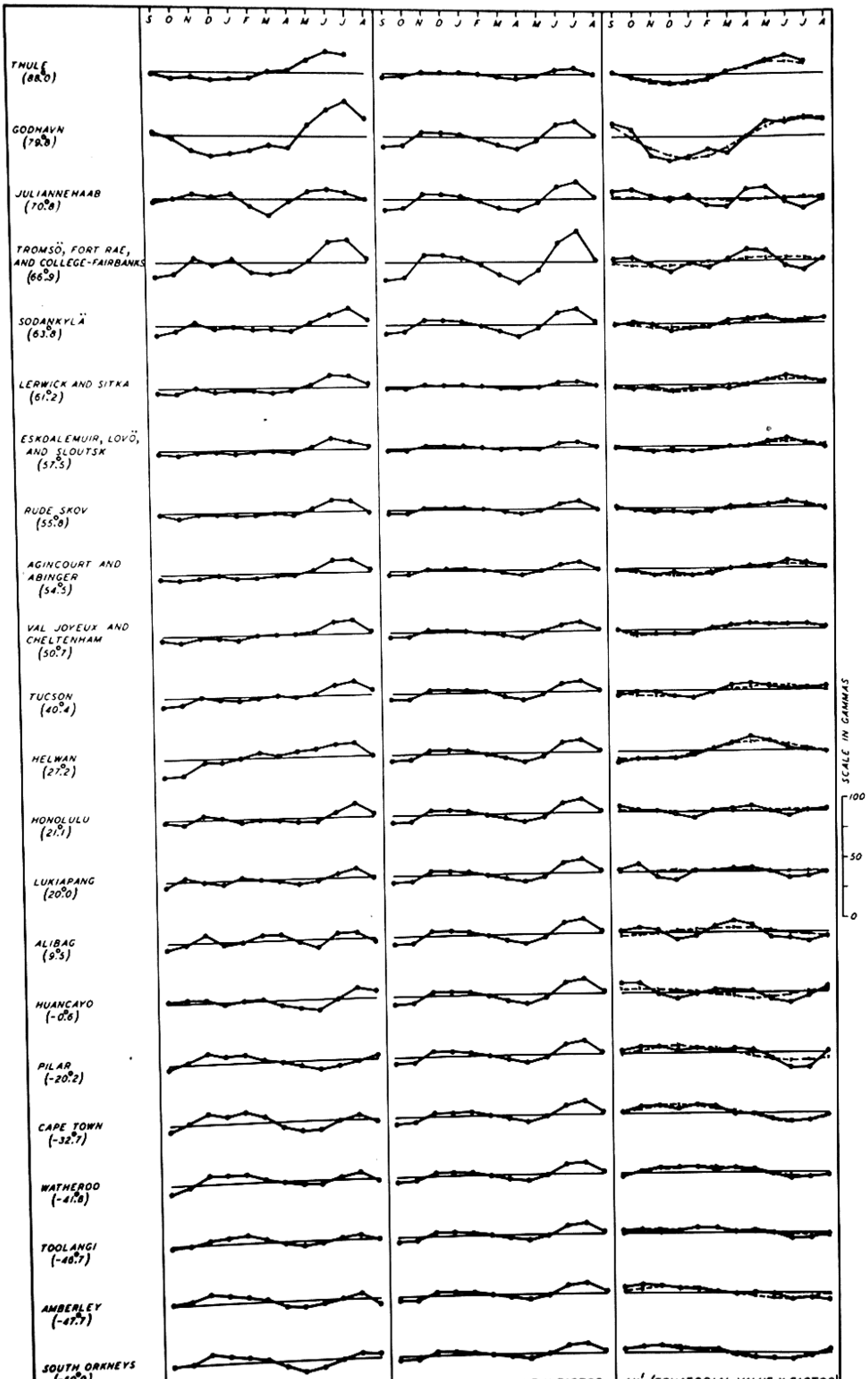

FIG.36—MONTHLY MEANS MINUS ANNUAL MEANS, 1932-33, OF GEOMAGNETIC NORTH COMPONENT (X') WITH ESTIMATED PART SYMMETRICAL ABOUT GEOMAGNETIC EQUATOR, AND SEASONAL PART FITTED WITH FOURIER TERM ($a_0 + a_1 \sin x + b_1 \cos x$) SHOWN DOTTED, WHERE x IS AN ANGULAR REPRESENTATION OF TIME AT THE RATE OF 30° PER MONTH BEGINNING SEPTEMBER 1, 1932 (GEOMAGNETIC LATITUDES INDICATED IN PARENTHESES)

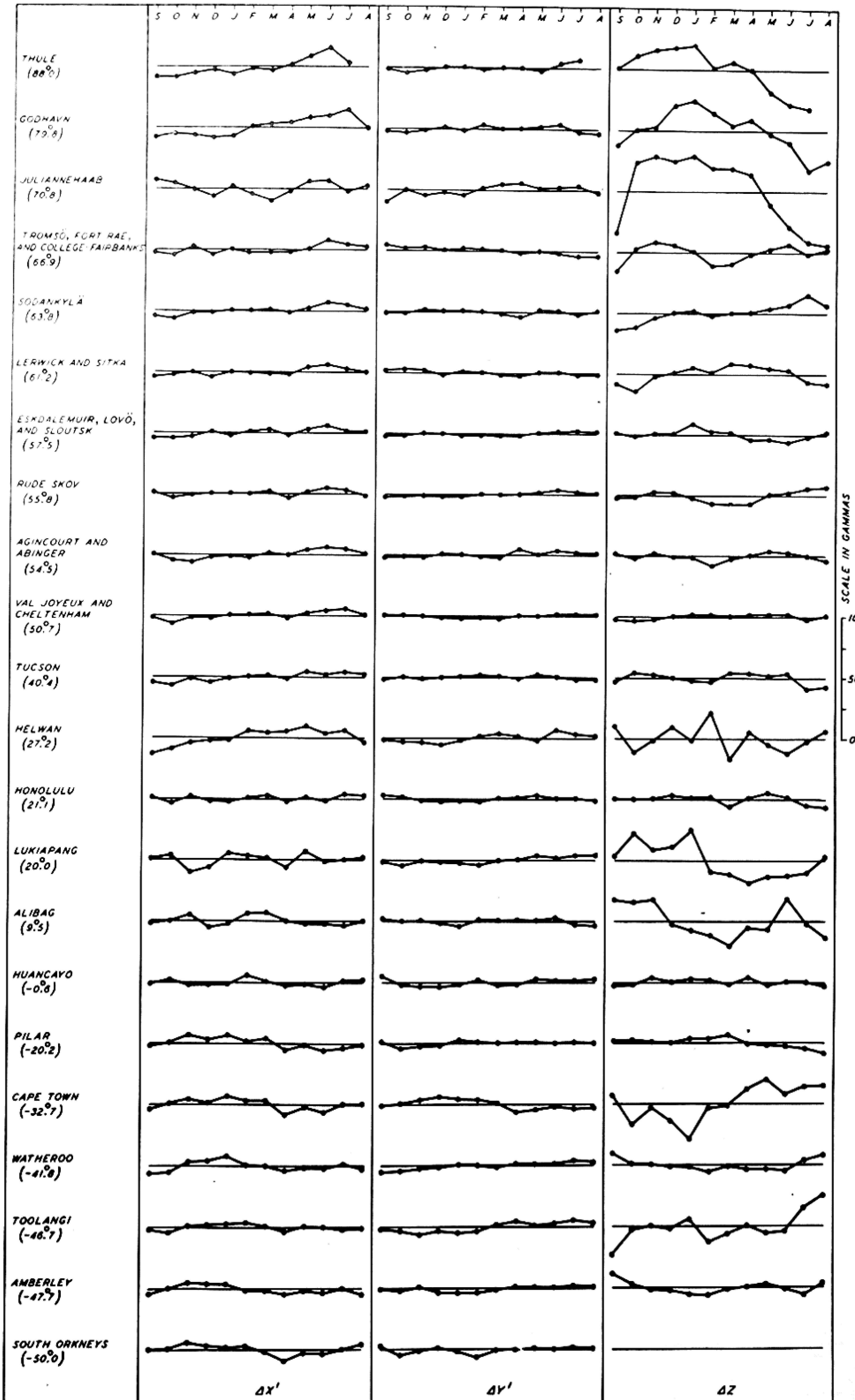

FIG.37(A)-MONTHLY MEAN DEPARTURES FROM ANNUAL MEANS, GEOMAGNETIC COMPONENTS X', Y', AND Z, QUIET DAYS, POLAR YEAR, 1932-33 (GEOMAGNETIC LATITUDES INDICATED IN PARENTHESES)

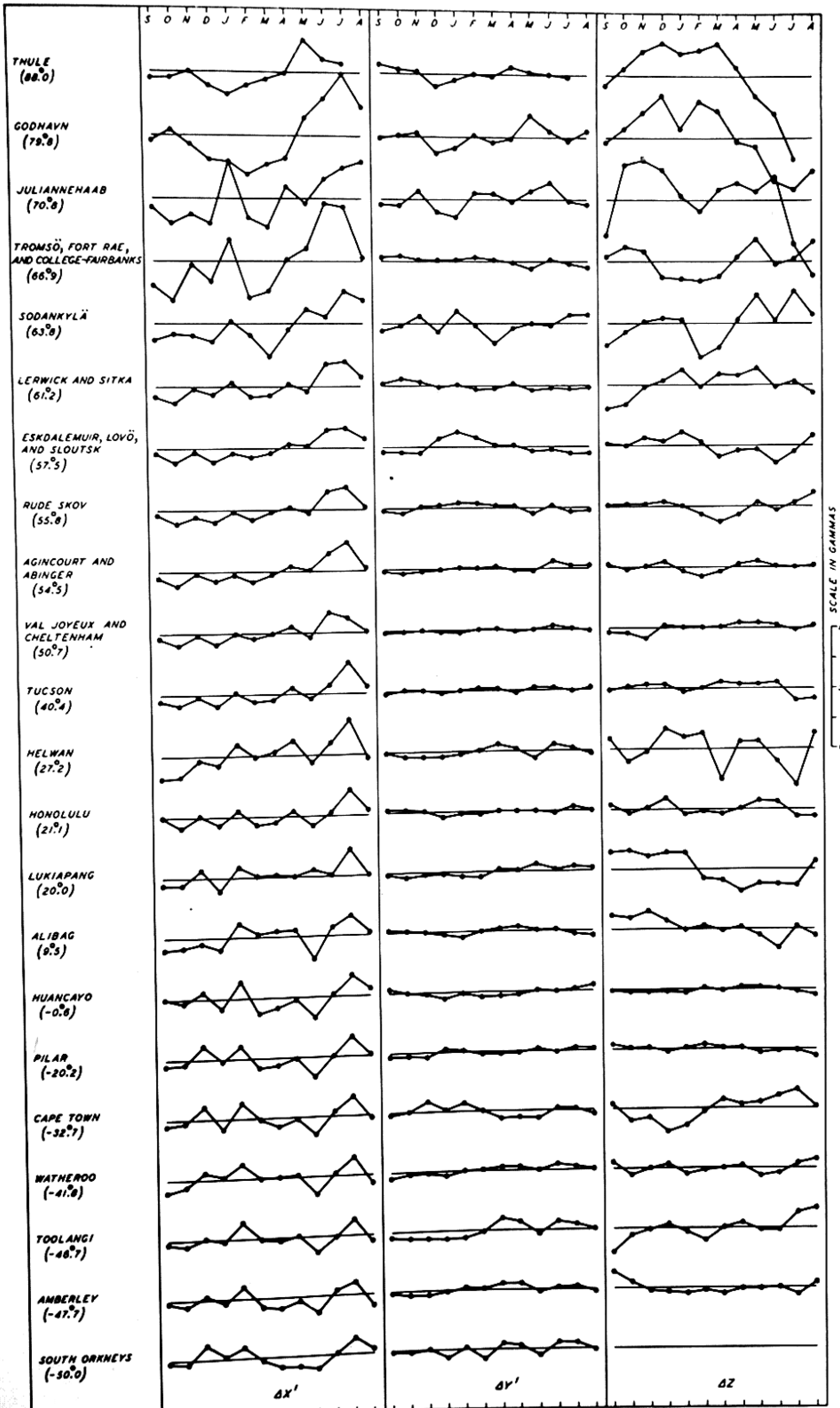

FIG. 37(B)—MONTHLY MEAN DEPARTURES FROM ANNUAL MEANS, GEOMAGNETIC COMPONENTS X', Y', AND Z, DISTURBED DAYS, POLAR YEAR, 1932-33 (GEOMAGNETIC LATITUDES INDICATED IN PARENTHESES)

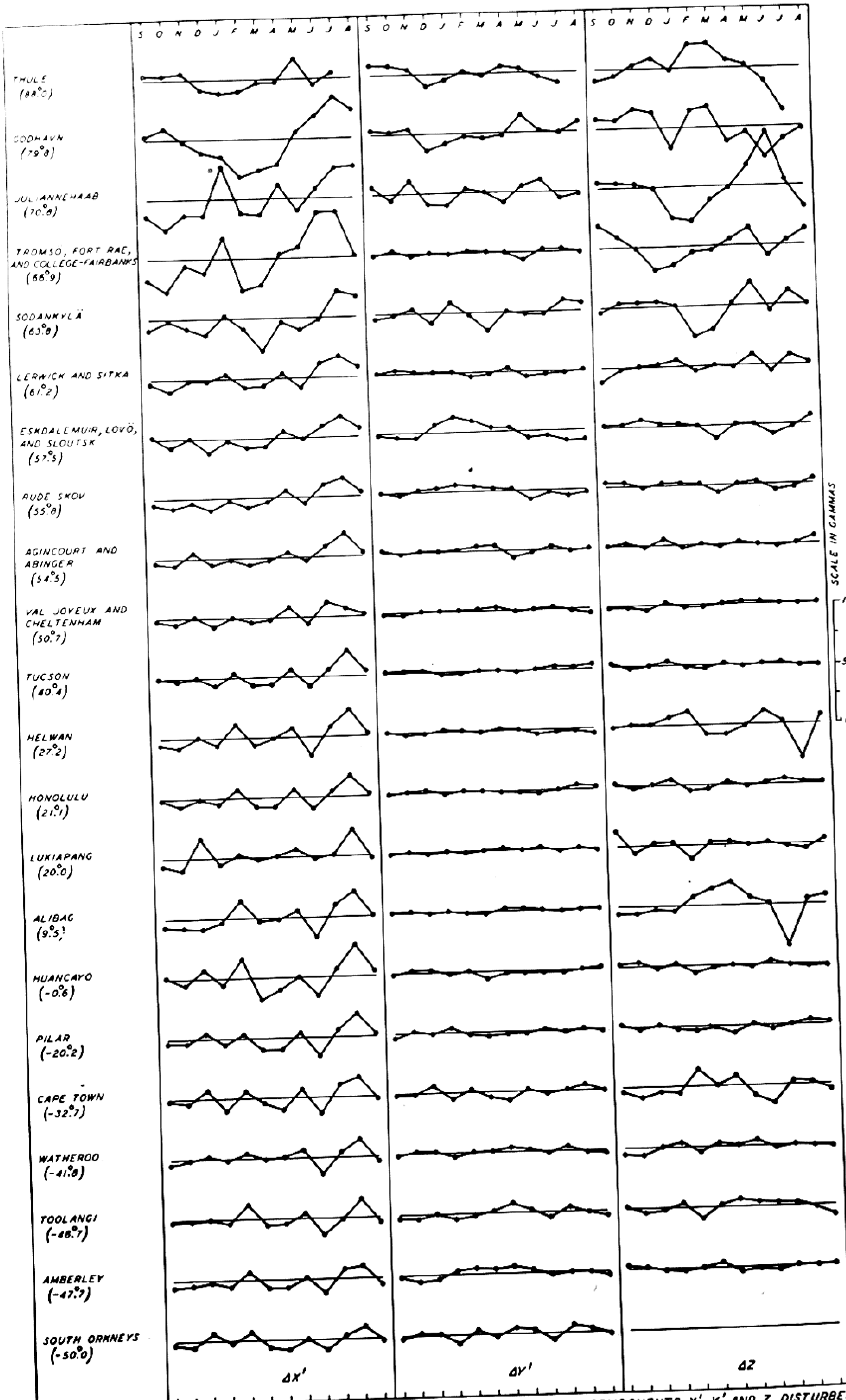

FIG.37(C)-MONTHLY MEAN DEPARTURES FROM ANNUAL MEANS, GEOMAGNETIC COMPONENTS X', Y', AND Z, DISTURBED MINUS QUIET DAYS, POLAR YEAR, 1932-33 (GEOMAGNETIC LATITUDES INDICATED IN PARENTHESES)

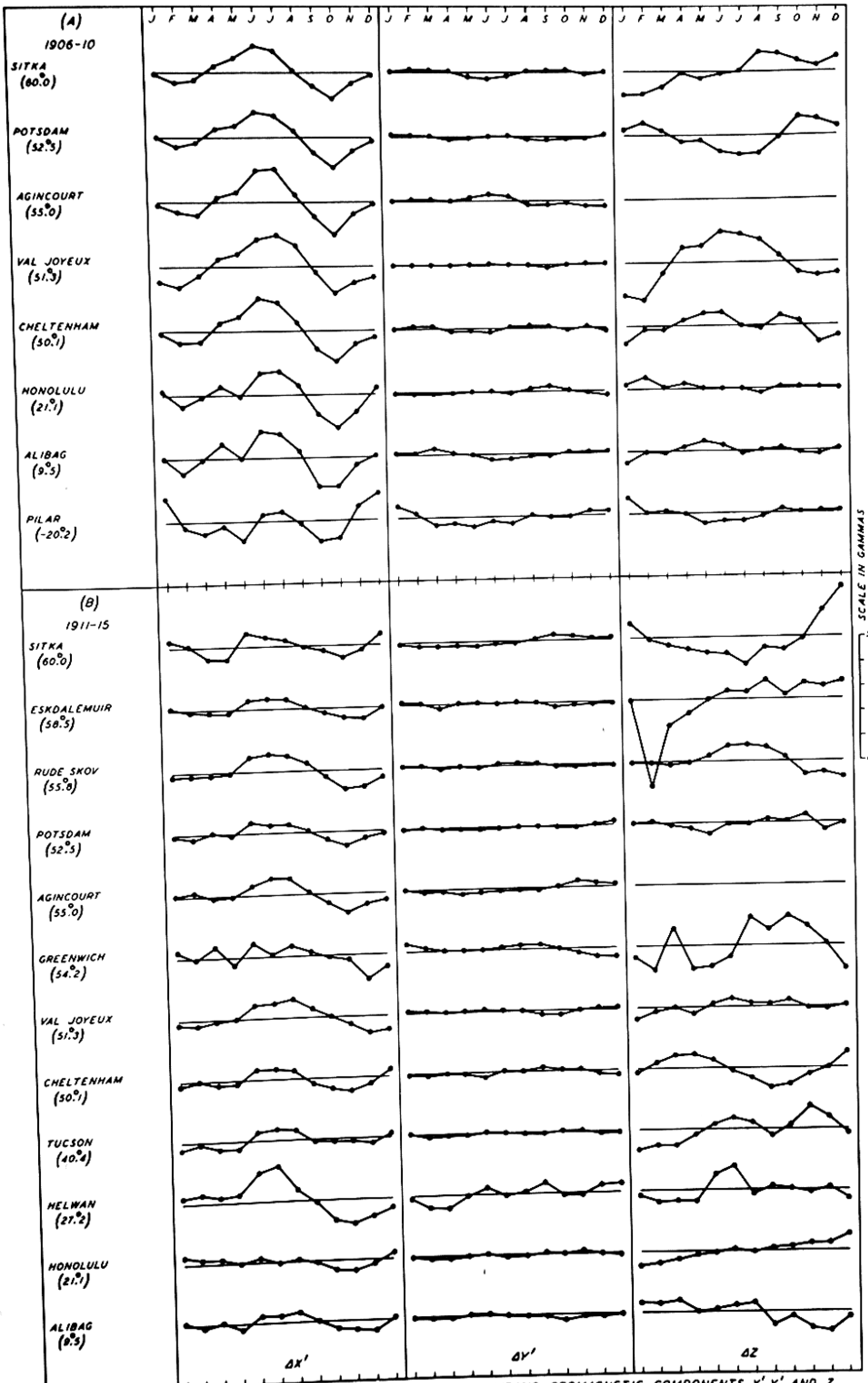

FIG. 38(A) AND (B)—MONTHLY MEAN DEPARTURES FROM ANNUAL MEANS, GEOMAGNETIC COMPONENTS X', Y', AND Z, VARIOUS GROUPS OF YEARS (GEOMAGNETIC LATITUDES INDICATED IN PARENTHESES)

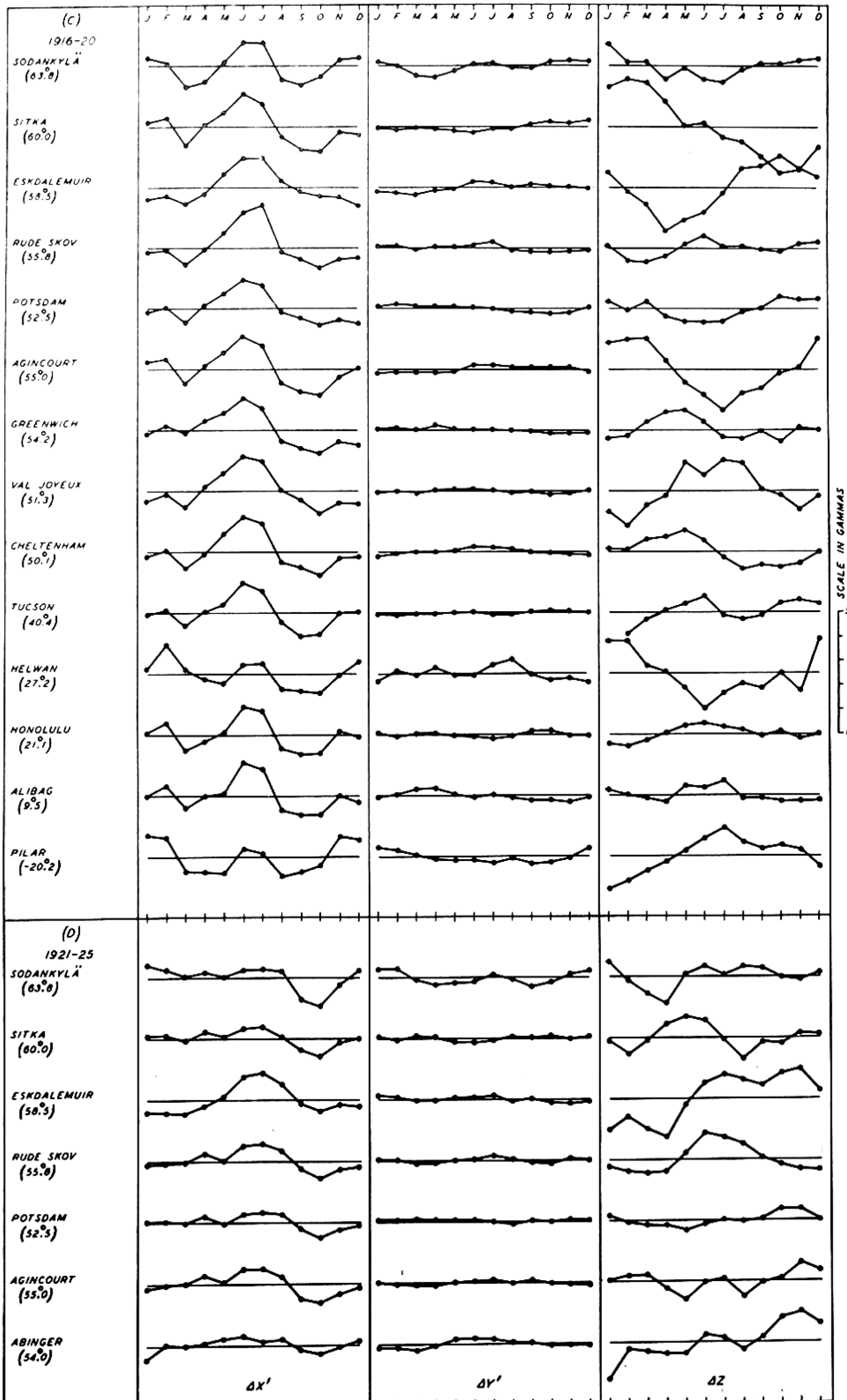

FIG. 38(C) AND (D)—MONTHLY MEAN DEPARTURES FROM ANNUAL MEANS, GEOMAGNETIC COMPONENTS X', Y', AND Z, VARIOUS GROUPS OF YEARS (GEOMAGNETIC LATITUDES INDICATED IN PARENTHESES)

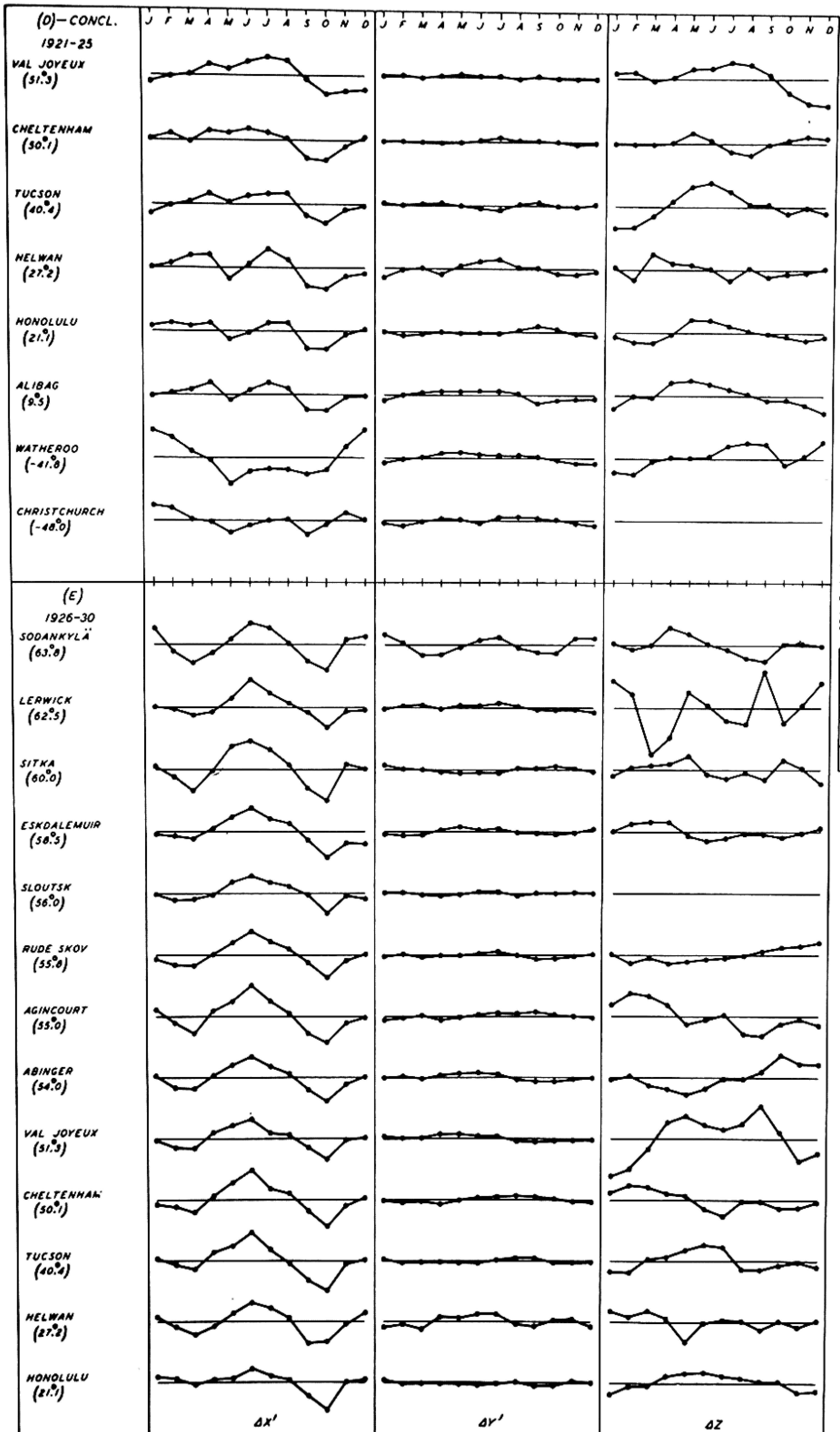

FIG. 38(D) AND (E)—MONTHLY MEAN DEPARTURES FROM ANNUAL MEANS, GEOMAGNETIC COMPONENTS X', Y', AND Z, VARIOUS GROUPS OF YEARS (GEOMAGNETIC LATITUDES INDICATED IN PARENTHESES)

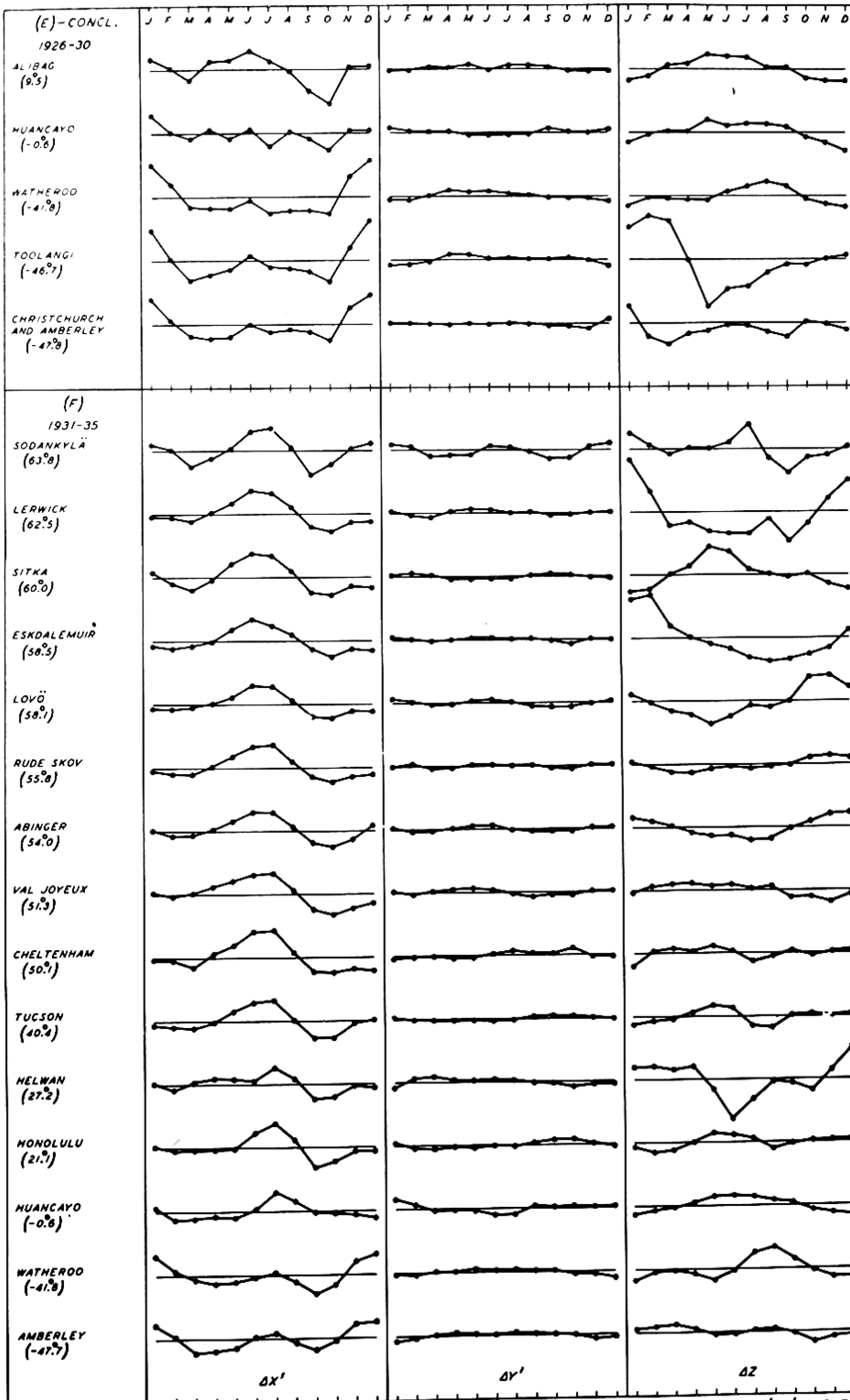

FIG.38(E)AND(F)—MONTHLY MEAN DEPARTURES FROM ANNUAL MEANS, GEOMAGNETIC COMPONENTS X', Y', AND Z, VARIOUS GROUPS OF YEARS (GEOMAGNETIC LATITUDES INDICATED IN PARENTHESES)

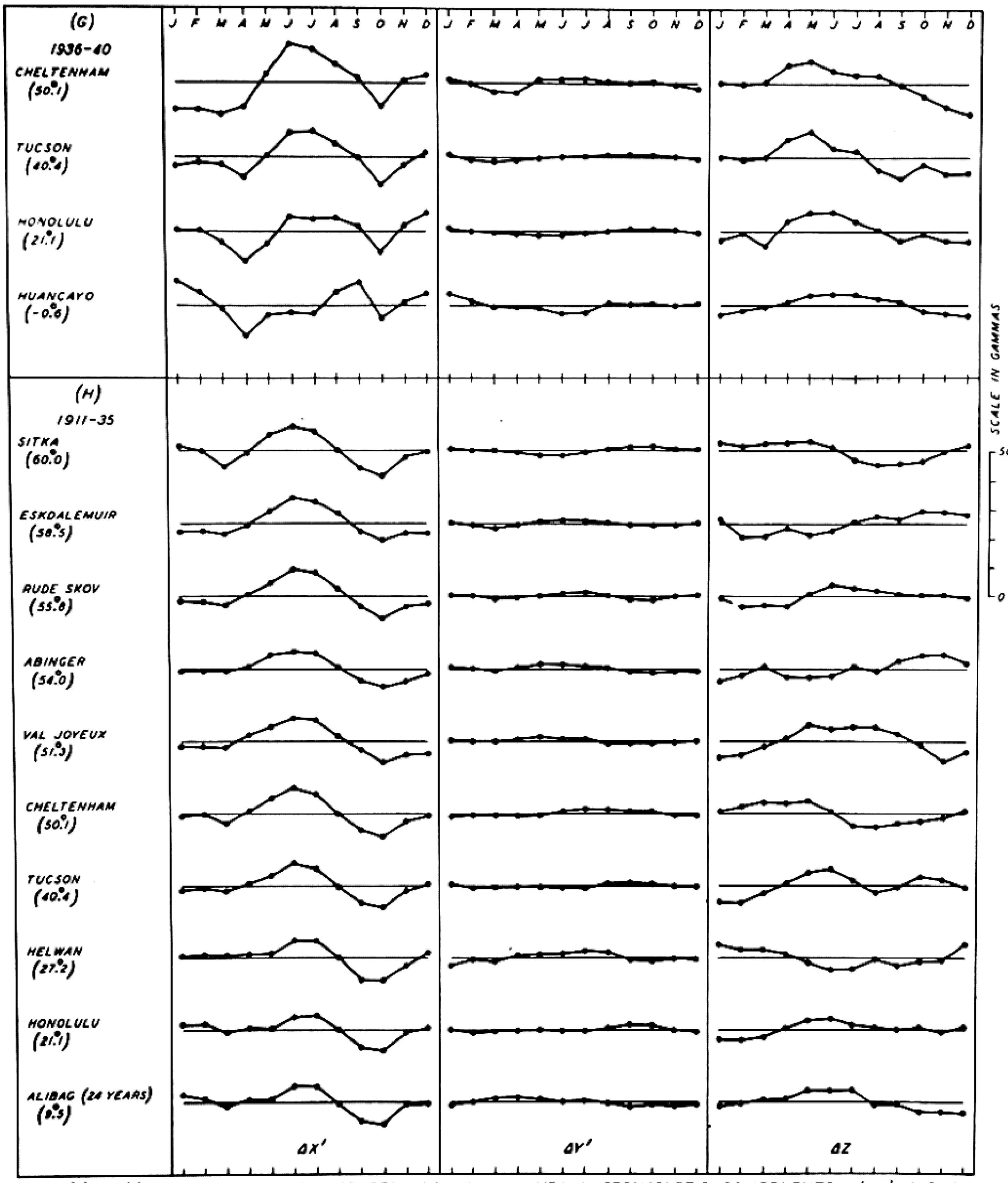

FIG.38(G) AND (H)—MONTHLY MEAN DEPARTURES FROM ANNUAL MEANS, GEOMAGNETIC COMPONENTS X′, Y′, AND Z, VARIOUS GROUPS OF YEARS (GEOMAGNETIC LATITUDES INDICATED IN PARENTHESES)

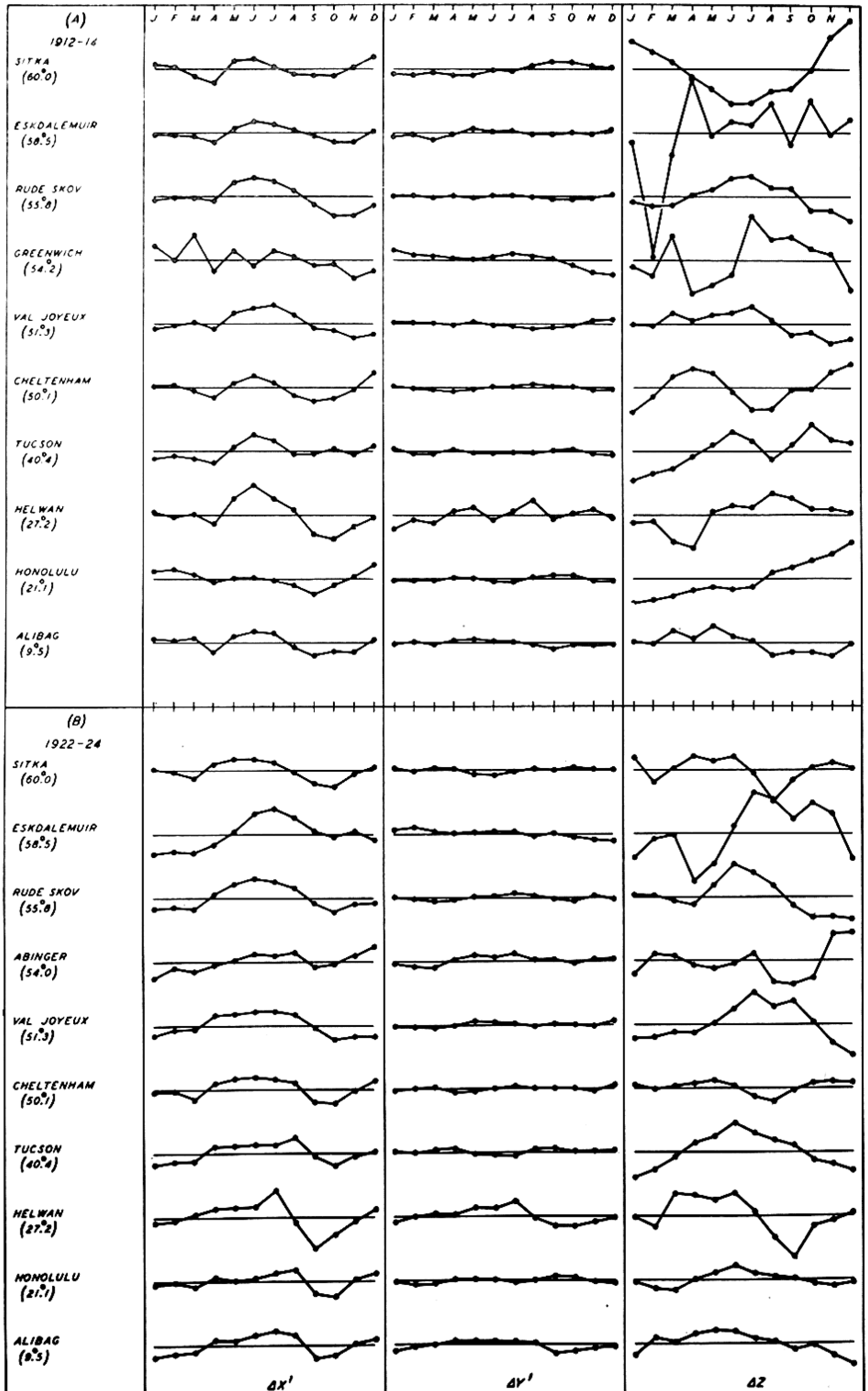

FIG. 39(A) AND (B)—MONTHLY MEAN DEPARTURES FROM ANNUAL MEANS, GEOMAGNETIC COMPONENTS X', Y', AND Z; SUNSPOT MINIMUM YEARS: (A) 1912-14, (B) 1922-24 (GEOMAGNETIC LATITUDES INDICATED IN PARENTHESES)

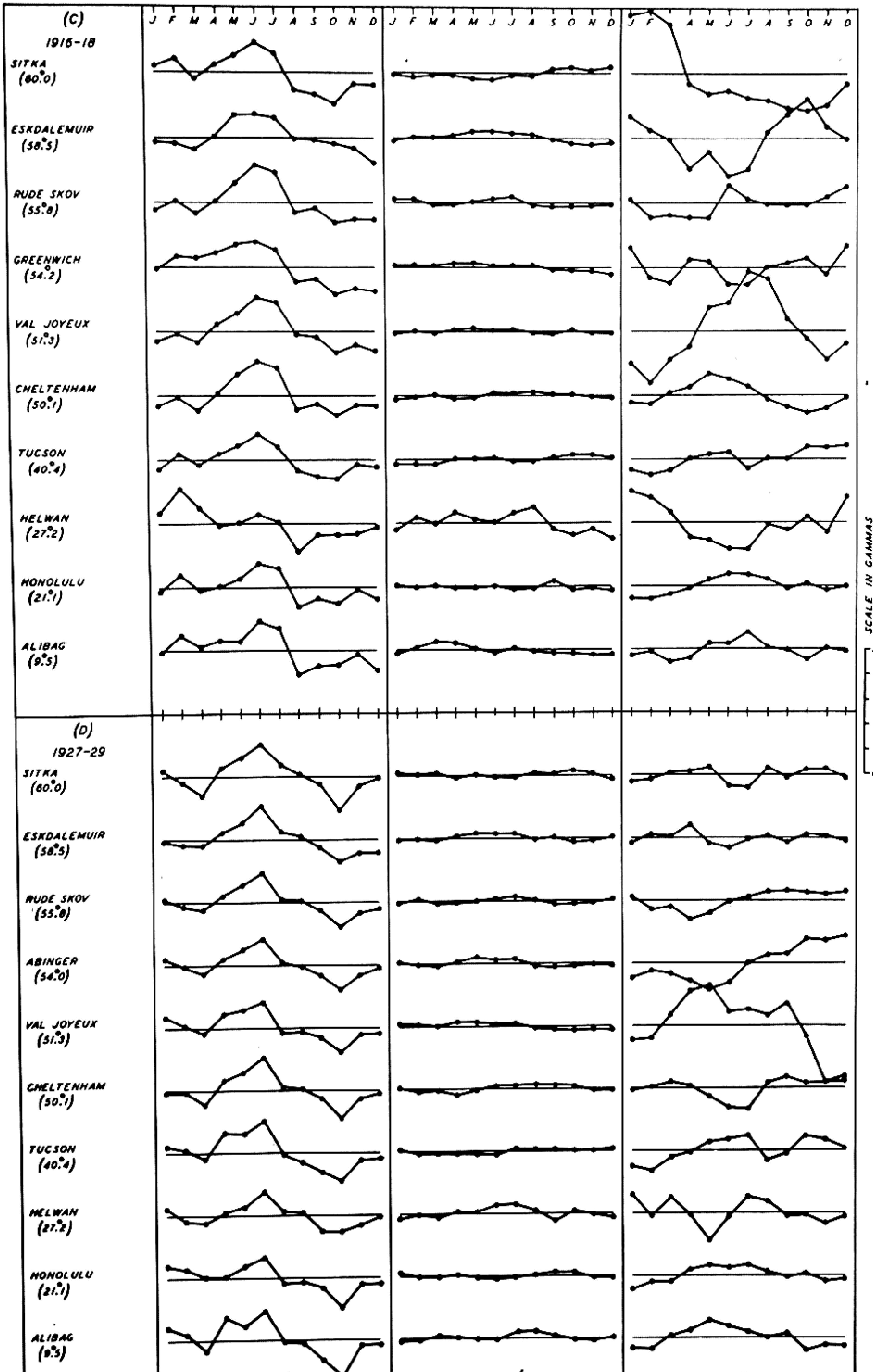

FIG. 39(C) AND (D) — MONTHLY MEAN DEPARTURES FROM ANNUAL MEANS, GEOMAGNETIC COMPONENTS X', Y', AND Z; SUNSPOT MAXIMUM YEARS: (C) 1916-18, (D) 1927-29 (GEOMAGNETIC LATITUDES INDICATED IN PARENTHESES)

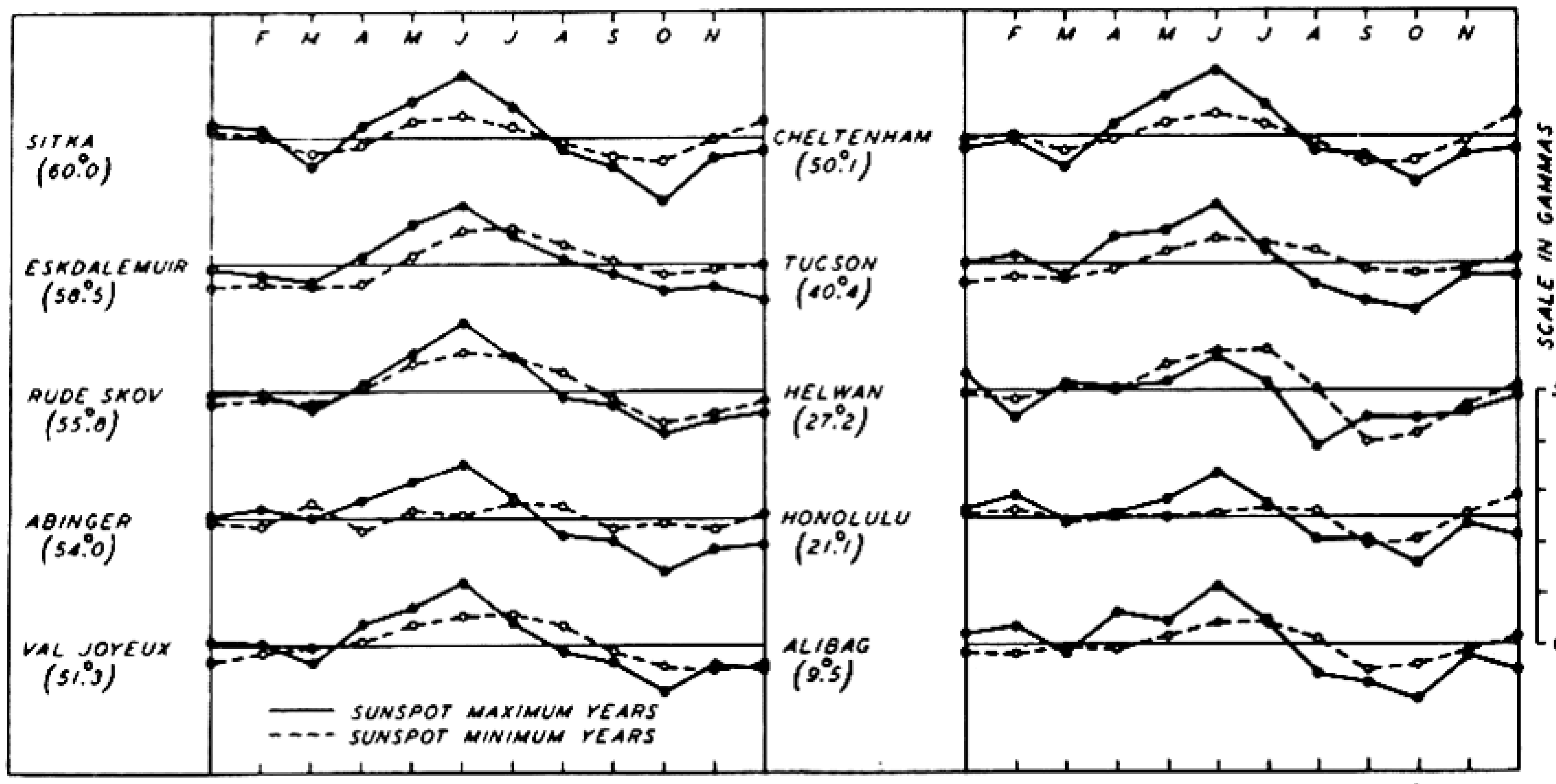

FIG. 40-MONTHLY MEAN DEPARTURES FROM ANNUAL MEANS, GEOMAGNETIC COMPOMPONENT ΔX', SUNSPOT MINIMUM (1912-14, 1922-24) AND MAXIMUM (1916-18, 1927-29) YEARS (GEOMAGNETIC LATITUDES INDICATED IN PARENTHESES)

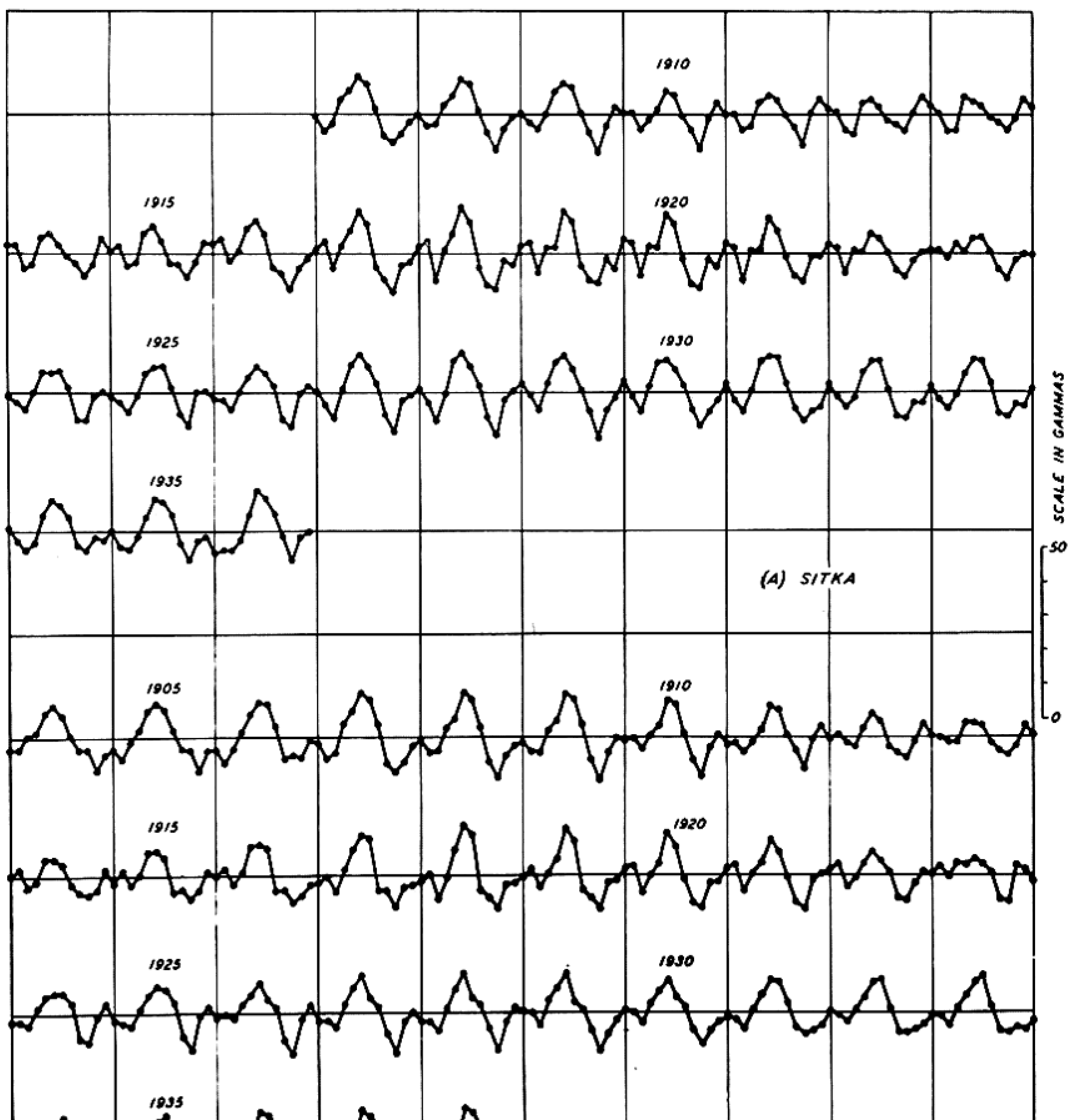

FIG. 41-SUCCESSIVE OVERLAPPING FIVE-YEAR AVERAGES OF MONTHLY MEAN DEPARTURES FROM ANNUAL MEANS, (A) SITKA, 1907-37, AND (B) CHELTENHAM, 1902-40

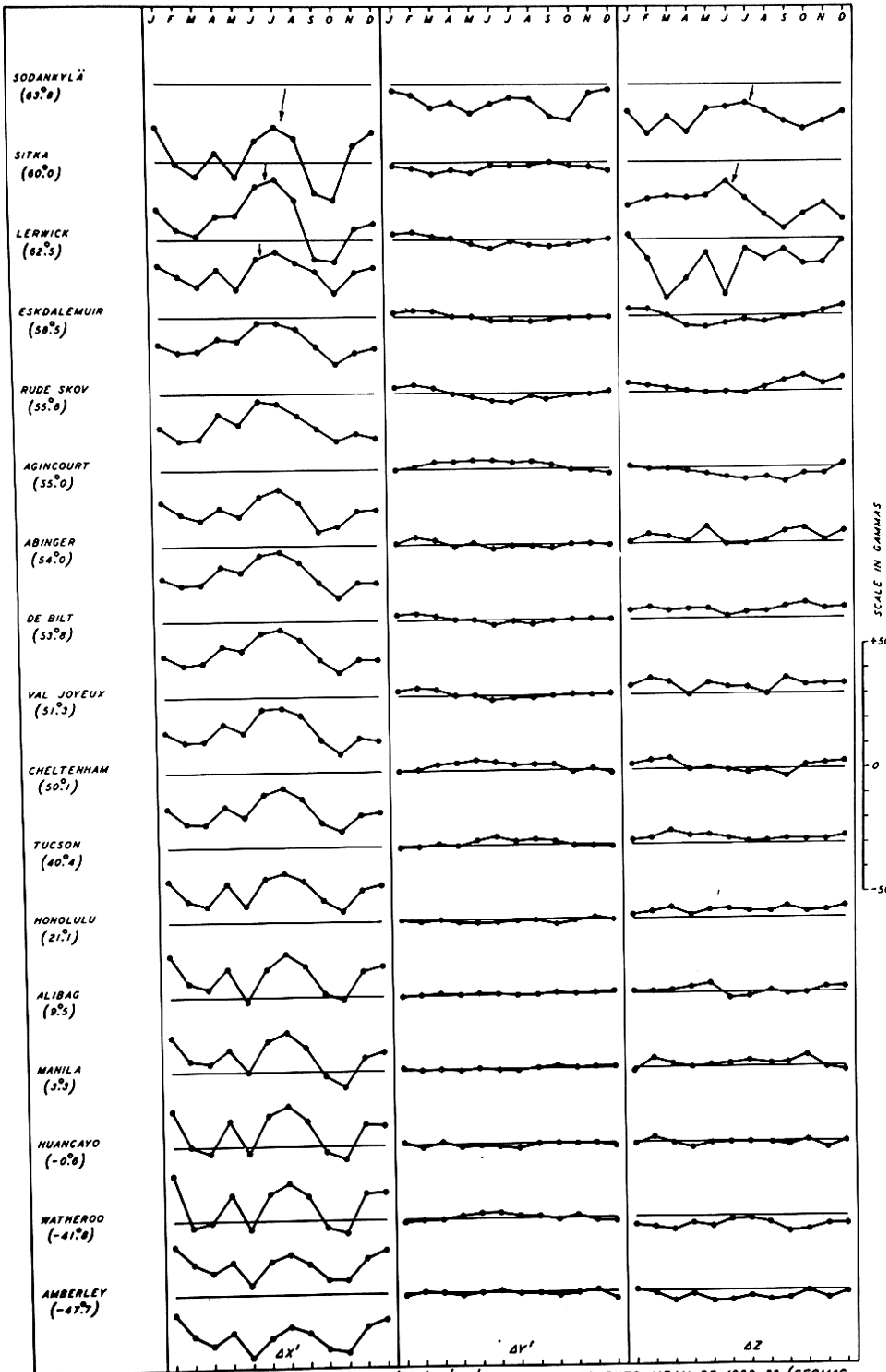

FIG. 42(A)—DISTURBED MINUS QUIET DAY MEANS (D_{mi}), X'-, Y'-, AND Z-COMPONENTS, MEAN OF 1922-33 (GEOMAGNETIC LATITUDES INDICATED IN PARENTHESES)

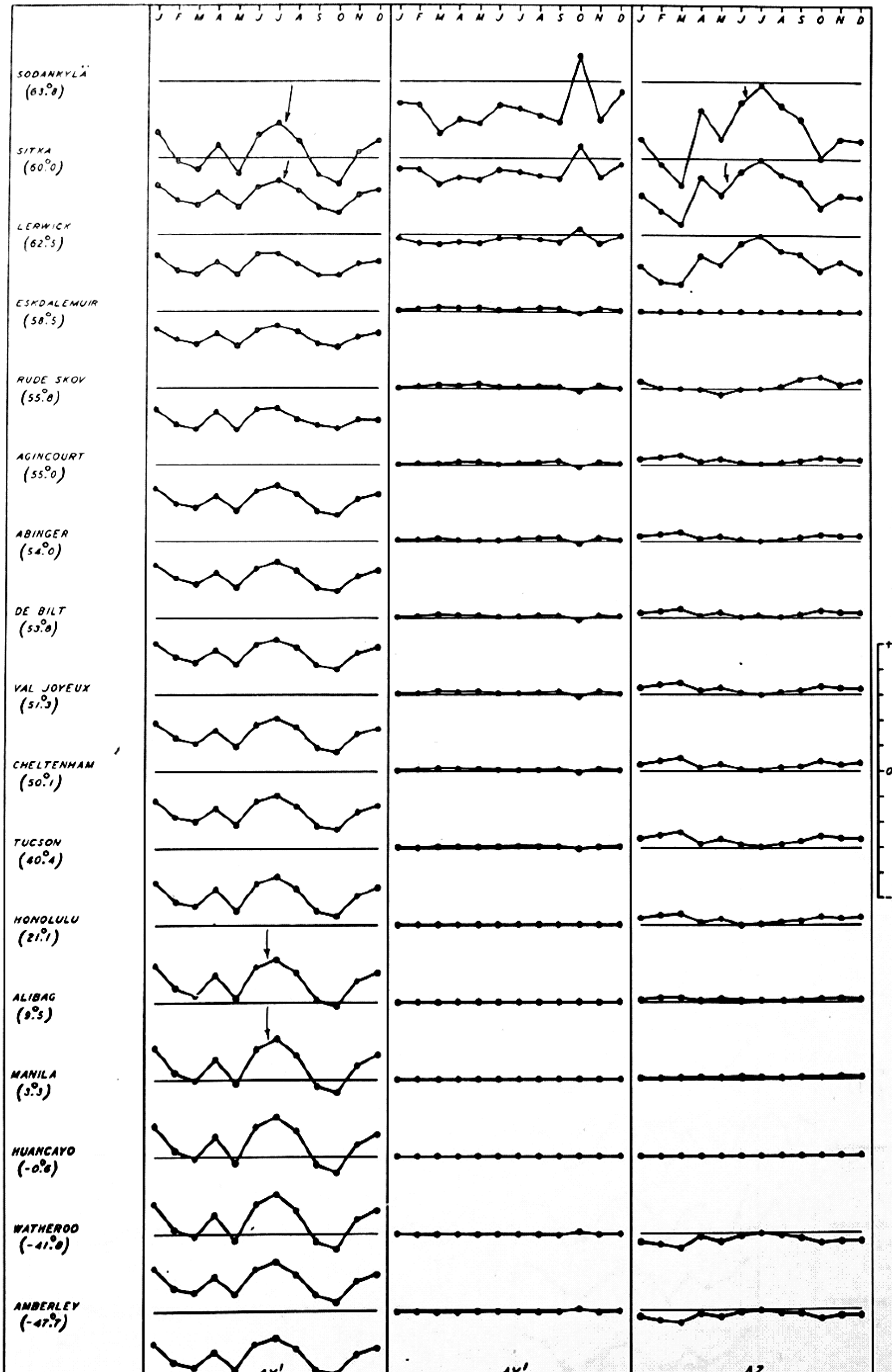

FIG. 42(B)—PART OF D_{mi} SYMMETRICAL ABOUT EQUATOR, X'-, Y'-, AND Z-COMPONENTS, MEAN OF 1922-33 (GEOMAGNETIC LATITUDES INDICATED IN PARENTHESES)

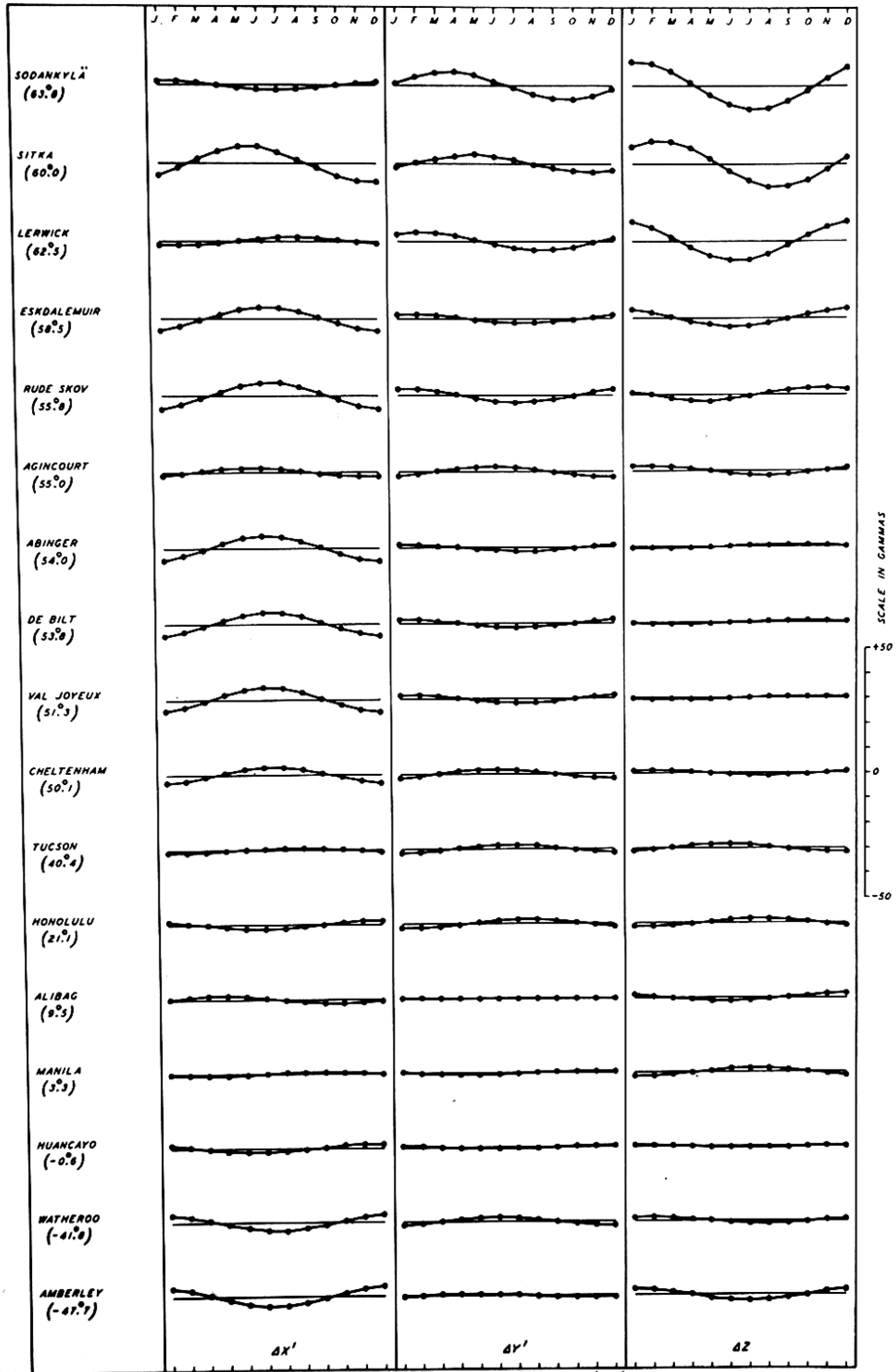

FIG. 42(C)—SINUSOIDAL PART OF D_{mi} ANTI-SYMMETRICAL ABOUT EQUATOR, X^1-, Y^1-, AND Z-COMPONENTS, MEAN OF 1922-33 (GEOMAGNETIC LATITUDES INDICATED IN PARENTHESES)

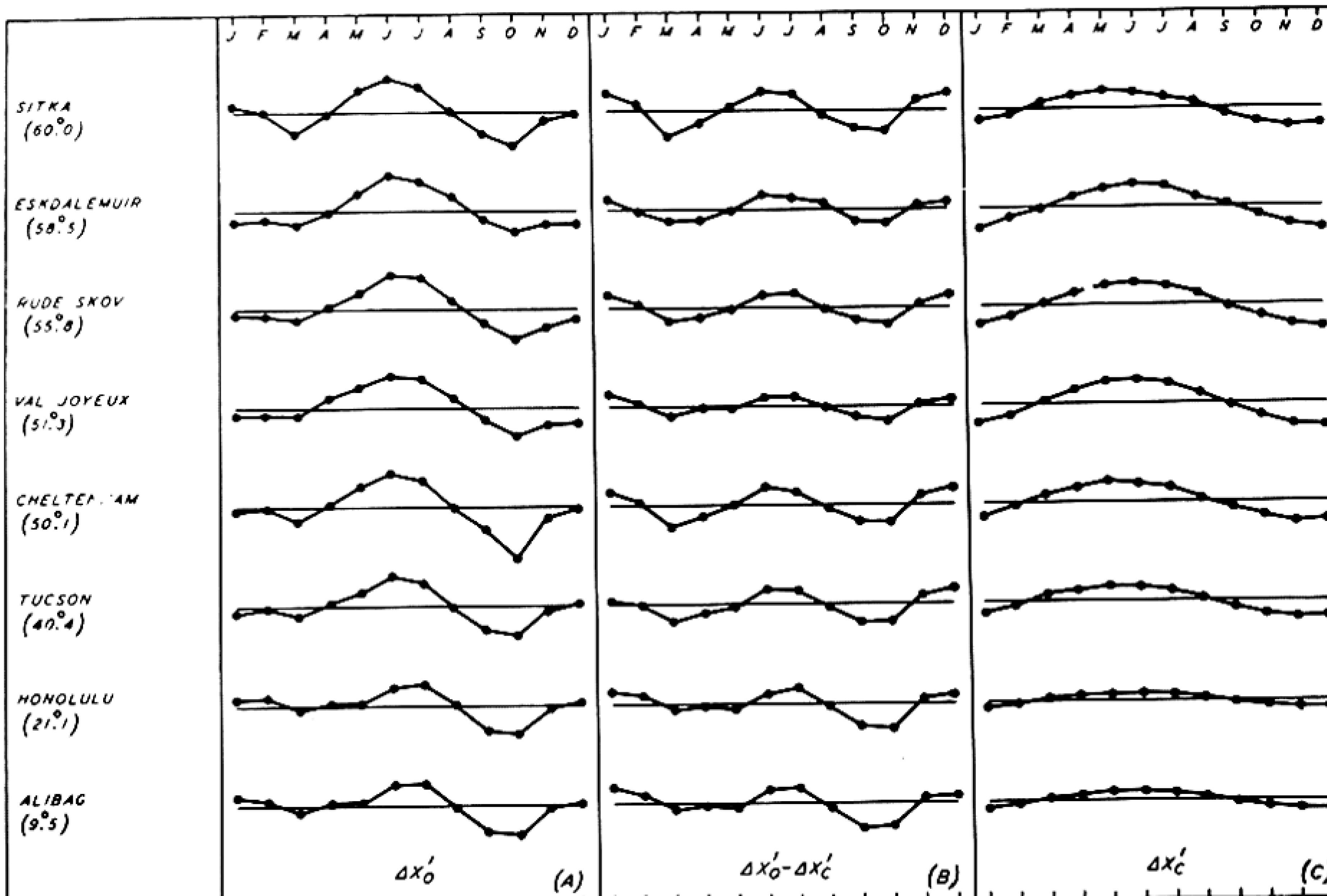

FIG. 43—(A) MONTHLY MEAN DEPARTURES FROM ANNUAL MEANS IN GEOMAGNETIC X'-COMPONENT, (B) PART SYMMETRICAL ABOUT EQUATOR, AND (C) SINUSOIDAL PART, 1911-35 (GEOMAGNETIC LATITUDES INDICATED IN PARENTHESES)

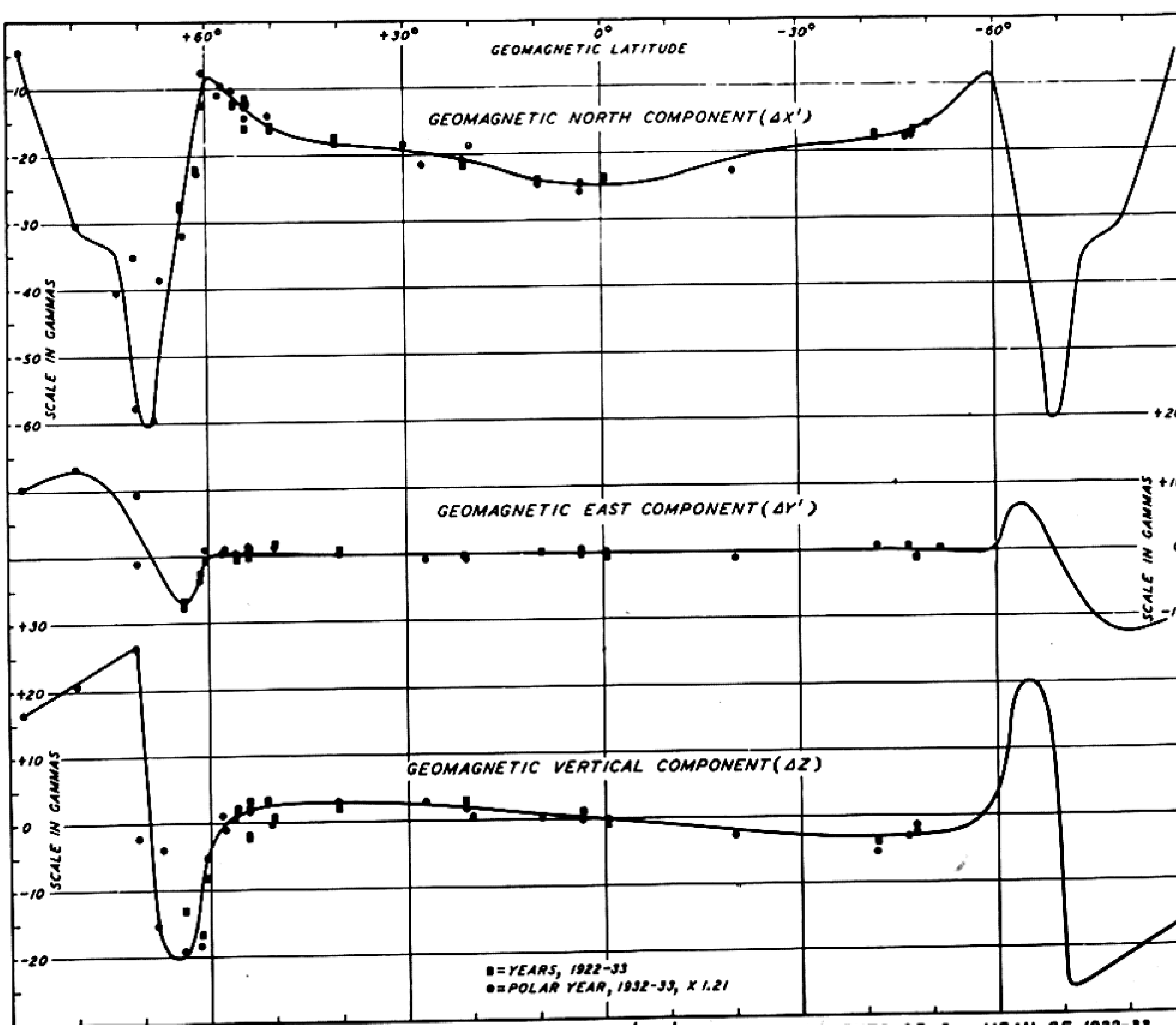

FIG. 44-VARIATION WITH GEOMAGNETIC LATITUDE OF X', Y', AND Z-COMPONENTS OF D_{m1}, MEAN OF 1922-33

FIG. 45—VARIATION WITH LATITUDE OF SINUSOIDAL PART $-c_1 \cos(t+\alpha_1) = a_1 \cos t + b_1 \sin t$ OF ANNUAL VARIATION, ALL DAYS, IN GEOMAGNETIC NORTH (X') AND VERTICAL (Z) COMPONENTS, VARIOUS GROUPS OF YEARS 1905-41, REDUCED TO MEAN OF 1922-33

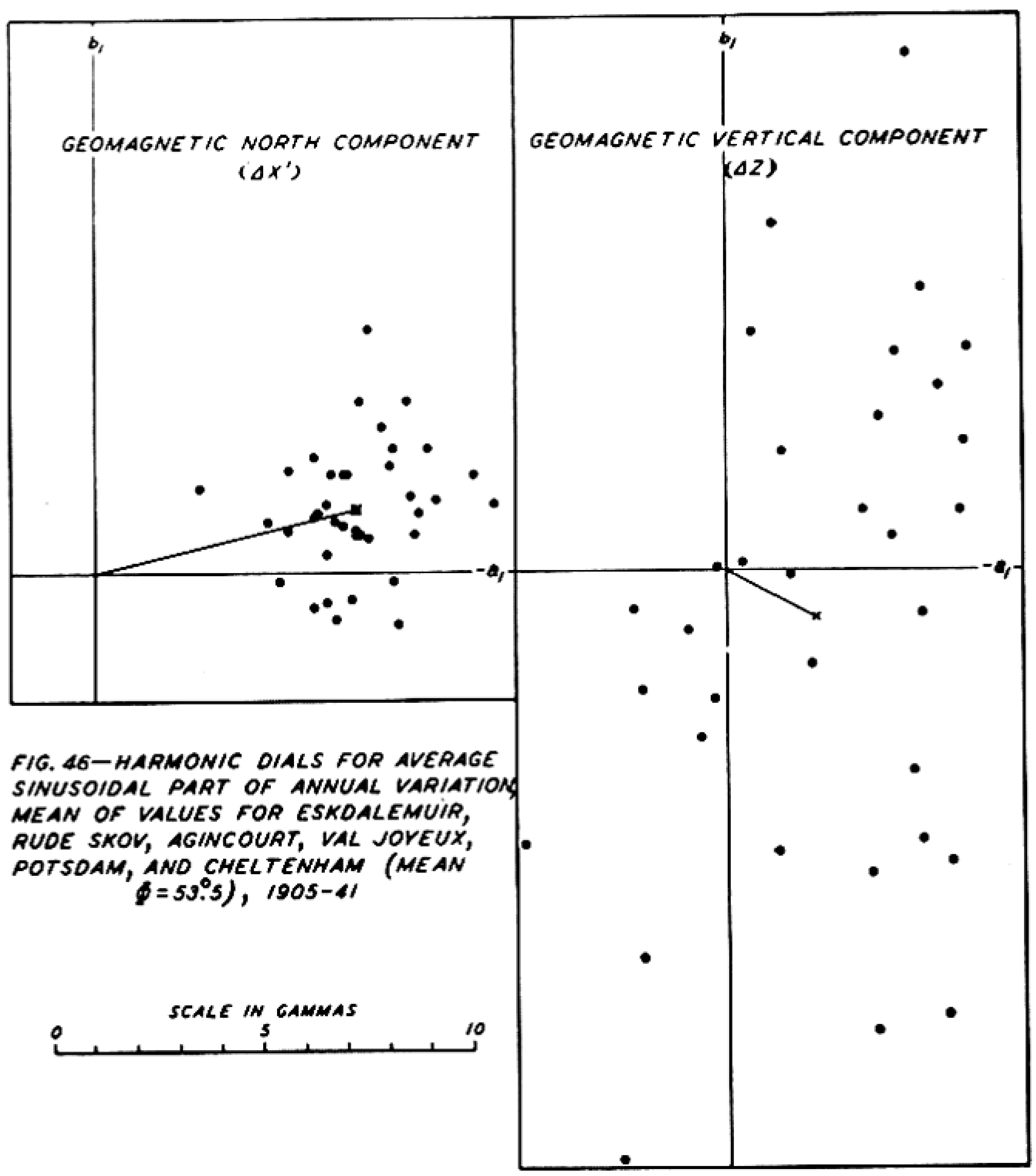

FIG. 46—HARMONIC DIALS FOR AVERAGE SINUSOIDAL PART OF ANNUAL VARIATION, MEAN OF VALUES FOR ESKDALEMUIR, RUDE SKOV, AGINCOURT, VAL JOYEUX, POTSDAM, AND CHELTENHAM (MEAN $\Phi = 53^\circ.5$), 1905–41

SCALE IN GAMMAS
0 5 10

CHAPTER VI

THE GEOMAGNETIC POST-PERTURBATION, P

1. General remarks.--It has been noted that the monthly mean values of the geomagnetic field undergo changes due to the variation of average geomagnetic disturbance with season. In the same way, the daily means are affected by disturbance on individual days. This effect in most latitudes is pronounced decrease in H at times of disturbance.

The value of H increases above the monthly average on quiet days. A and B of Figure 47 give the effect of post-perturbation as shown by the daily mean departures from the monthly mean during a period of disturbance and of recovery, May 1 and 2, 1933, for the X'-, Y'-, and Z-components of intensity. The X'-component is reduced below the monthly mean during the disturbed period and later rises during the period of recovery, throughout the region from pole to equator. The departures in X' are large inside the auroral zone, are largest and most irregular near this zone, and then decrease with decreasing latitude. In Y' the changes are relatively smaller in all latitudes. In Z the departures near the center of the northern auroral zone are large and become smaller in lower latitudes, with reversal of sign in the Southern Hemisphere.

The consistency in values from observatory to observatory is marked, and the post-perturbation is evidently fairly well determined by only two or three observatories if the latitude distribution is known.

2. The latitude distribution of the post-perturbation, P.--Figure 48 shows the latitude distribution of P, the daily means minus the monthly means for a number of days of the Polar Year, 1932-33. On September 17, 1932, the value of H was about 25 gammas above the monthly mean in low latitudes. On December 17, 1932, it was about 25 gammas below. Evidently field-observations, if made on two such days about five years apart, would give a total apparent and fictitious change in the Earth's permanent field of 50 gammas, seriously affecting the estimate of secular change in H. It is particularly to be noted in Figure 48 that the stations, although differing widely in their longitudes, exhibit on the whole rather good agreement with each other, except possibly near the auroral zone, where considerable irregularity appears. In general, it appears that any longitude effect in P can be neglected in most applications. In fact, the mean departures derived for two or three stations suffice approximately to estimate these departures at all other stations, when the latitude distribution appropriate to each month of the year is also known.

The average latitude distribution of the daily means minus monthly means can be obtained by averaging such values for a sufficient number of years by months. As a good approximation, we may take the values D_{mi}, the values for disturbed days minus quiet days by months, since the all-day minus quiet-day means are small.

A of Figure 49 gives the latitude distribution of D_{mi} by months as derived for the average of the years 1922 to 1933. Values for the Polar Year, 1932-33, reduced tc 1922 to 1933, are included to give a rough indication of the latitude distribution in polar regions.

The change from month to month is largest in high latitudes due to the presence of a sinusoidal annual term of considerable magnitude in the X'- and Z-components. The Y'-component is very small and nearly zero in all months.

From the latitude distributions of A and B of Figure 49, average monthly proportionality factors for various latitudes can be derived which, when multiplied by the known daily mean departure from the monthly mean in a particular latitude, yield an estimate of the corresponding value in any other latitude. With this purpose in mind, the daily mean departures (on 75th meridian time) from the monthly mean of the H-component for Cheltenham ($\Phi = 50°.1$) and San Juan ($\Phi = 29°.9$) were meaned for each day of the period 1905 to 1942 and tabulated for presentation as Table 1-G of the preceding volume [1]. The corresponding proportionality factors, by months, for each two degrees of geomagnetic latitude were given in Tables 1-H and 1-I of the same volume. A correction for secular change in H was neglected.

In a number of cases, data for either Cheltenham, San Juan, or both were missing. In such cases, values for other low-latitude stations were substituted, also on a 75th meridian time basis, reduced by the known average latitude distribution of D_{mi} to a mean assumed appropriate to that of Cheltenham and San Juan. Such substitutions are indicated by appropriate footnotes.

It was also found on occasion that the values for Cheltenham and San Juan sometimes differed by more than ten gammas. In this event, a value was taken from a third station, on 75th meridian time, reduced to the mean of Cheltenham and San Juan. The three values were then compared and a mean was taken either of all three values, or of two of the three depending upon the values. If two values agreed well but the third showed marked disagreement (in excess of ten gammas difference from either value for the other two), it was assumed that the third value was defective. On a few occasions, there were several successive days for which values for Cheltenham and San Juan disagreed by more than ten gammas, as if there might have been changes in base-line values during the month. A third station, it was thought, permitted a more accurate choice of value in such cases. The third station usually used was Tucson, 1905 to 1910, Manila, 1931 to 1938, or Watheroo, 1939 to 1941.

The daily mean departures from the monthly means at various stations were, where necessary, multiplied by appropriate factors given from the latitude distribution for D_{mi}, in estimating values for the mean of Cheltenham and San Juan. The following multiplicative factors were adopted: Cheltenham, 1.1; Tucson, 1.0; San Juan, 0.9; Honolulu, 0.8; Manila, 0.7; Alibag, 0.7; Huancayo, 0.7; and Watheroo, 1.0.

Even in low and middle latitudes, where disturbances are less marked than in polar regions, it was sometimes found that the values at three stations differed greatly from one another, and the discrepancies in P on such days would then be found erratic at many stations. Values given by the mean of P at San Juan, Cheltenham, and

a third station, were in any case entered in Table 1-G [1], with a suffix s indicating considerable magnetic disturbance or storm. As unusual and erratic examples of the results for San Juan, Cheltenham, and a third station, respectively, the following values of P in gammas were noted: July 8, 1928, -66, -55, and -131; January 25, 1938, -77, +6, and -70; April 24, 1939, -43, +2, -43; July 5, 1941, -130, -227, and -213.

FIGURES 47-49

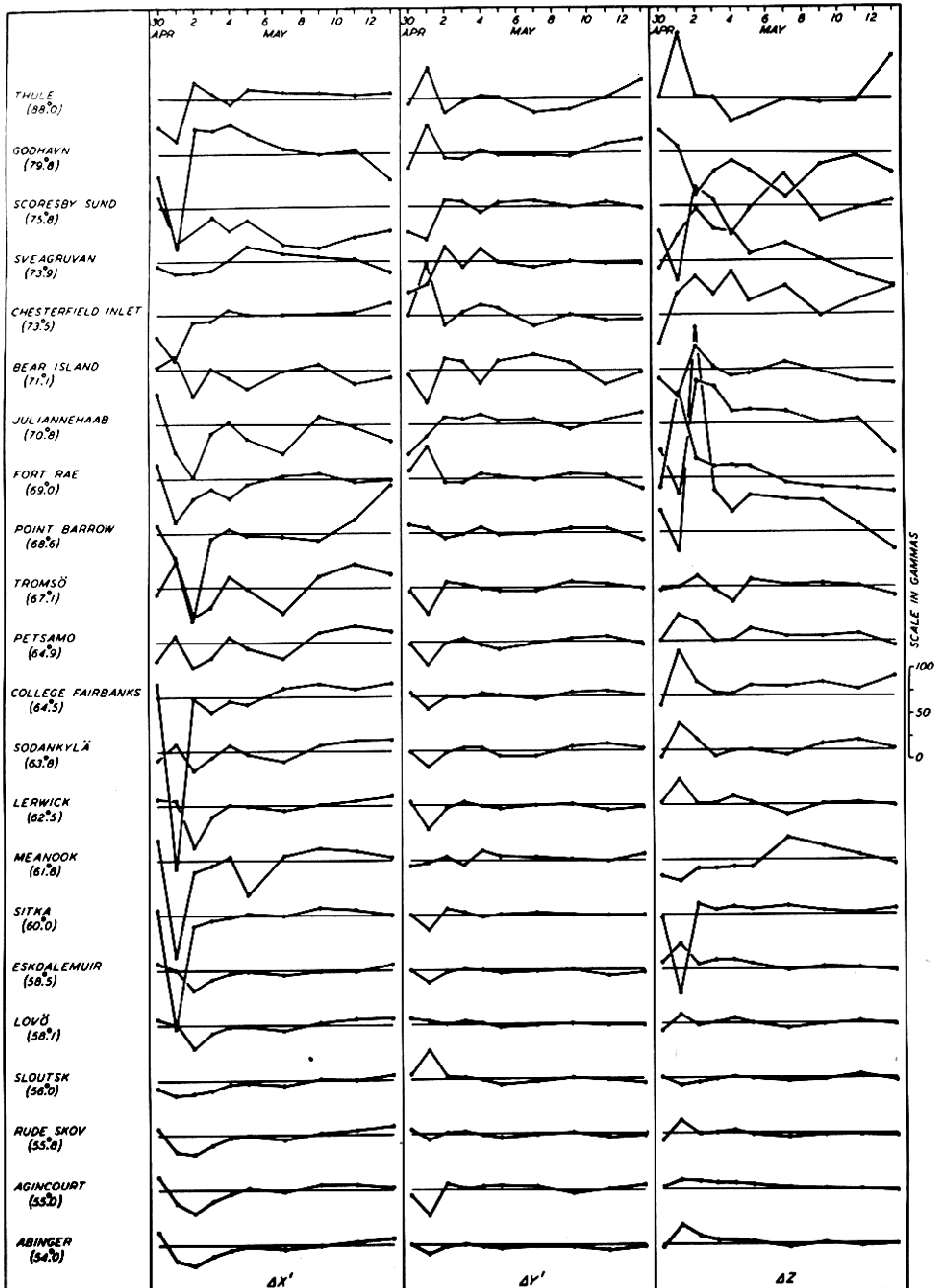

FIG. 47(A)—DAILY MEANS MINUS MONTHLY MEAN OF MAY 1933 FOR GEOMAGNETIC NORTH (ΔX'), EAST (ΔY'), AND VERTICAL (ΔZ) COMPONENTS, MAGNETIC STORM OF MAY 1, 1933, AND DAYS FOLLOWING, AT VARIOUS OBSERVATORIES, APRIL 30 TO MAY 13, 1933 (GEOMAGNETIC LATITUDES INDICATED IN PARENTHESES)

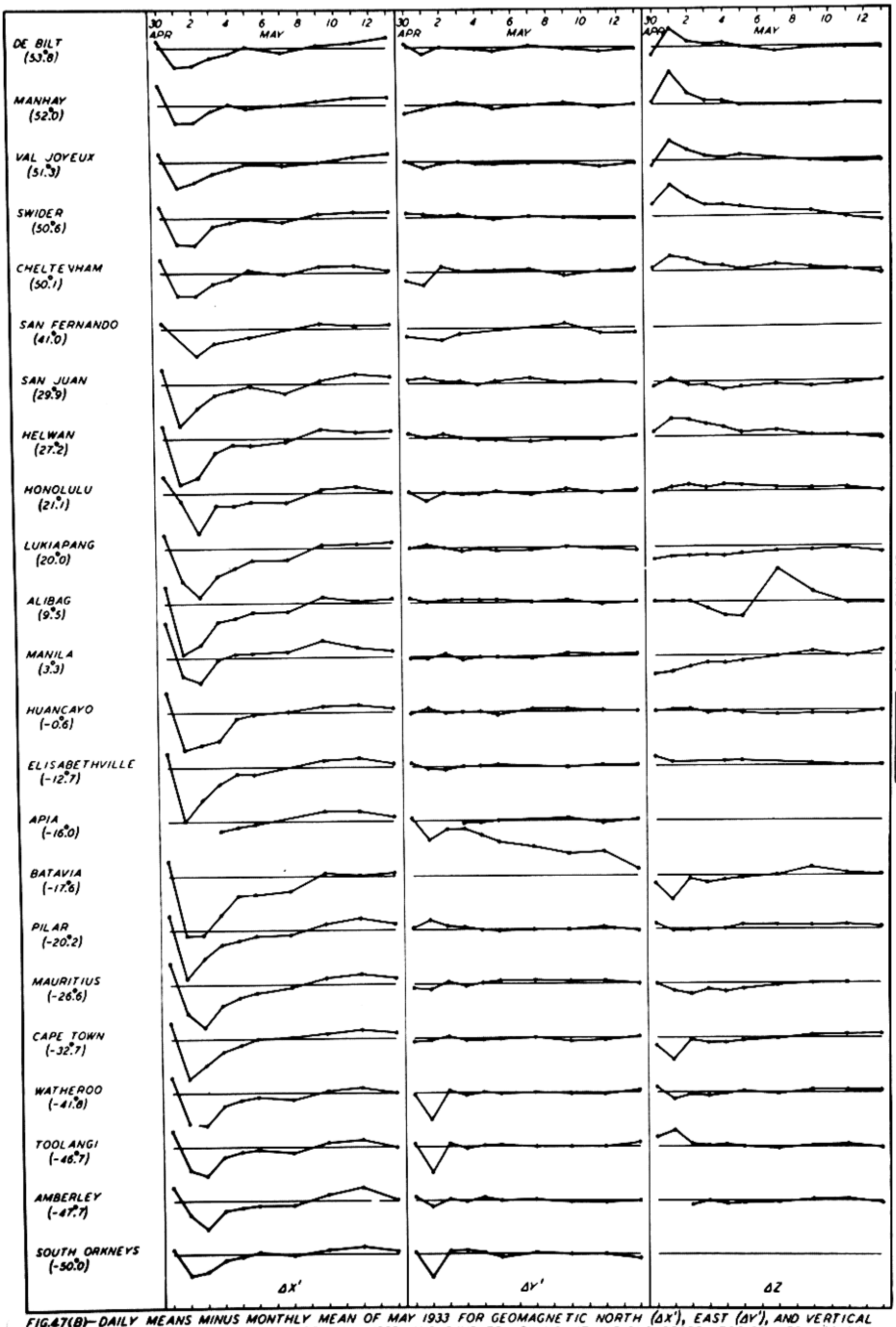

FIG. 47(B)—DAILY MEANS MINUS MONTHLY MEAN OF MAY 1933 FOR GEOMAGNETIC NORTH (ΔX'), EAST (ΔY'), AND VERTICAL (ΔZ) COMPONENTS, MAGNETIC STORM OF MAY 1, 1933, AND DAYS FOLLOWING, AT VARIOUS OBSERVATORIES, APRIL 30 TO MAY 13, 1933 (GEOMAGNETIC LATITUDES INDICATED IN PARENTHESES)

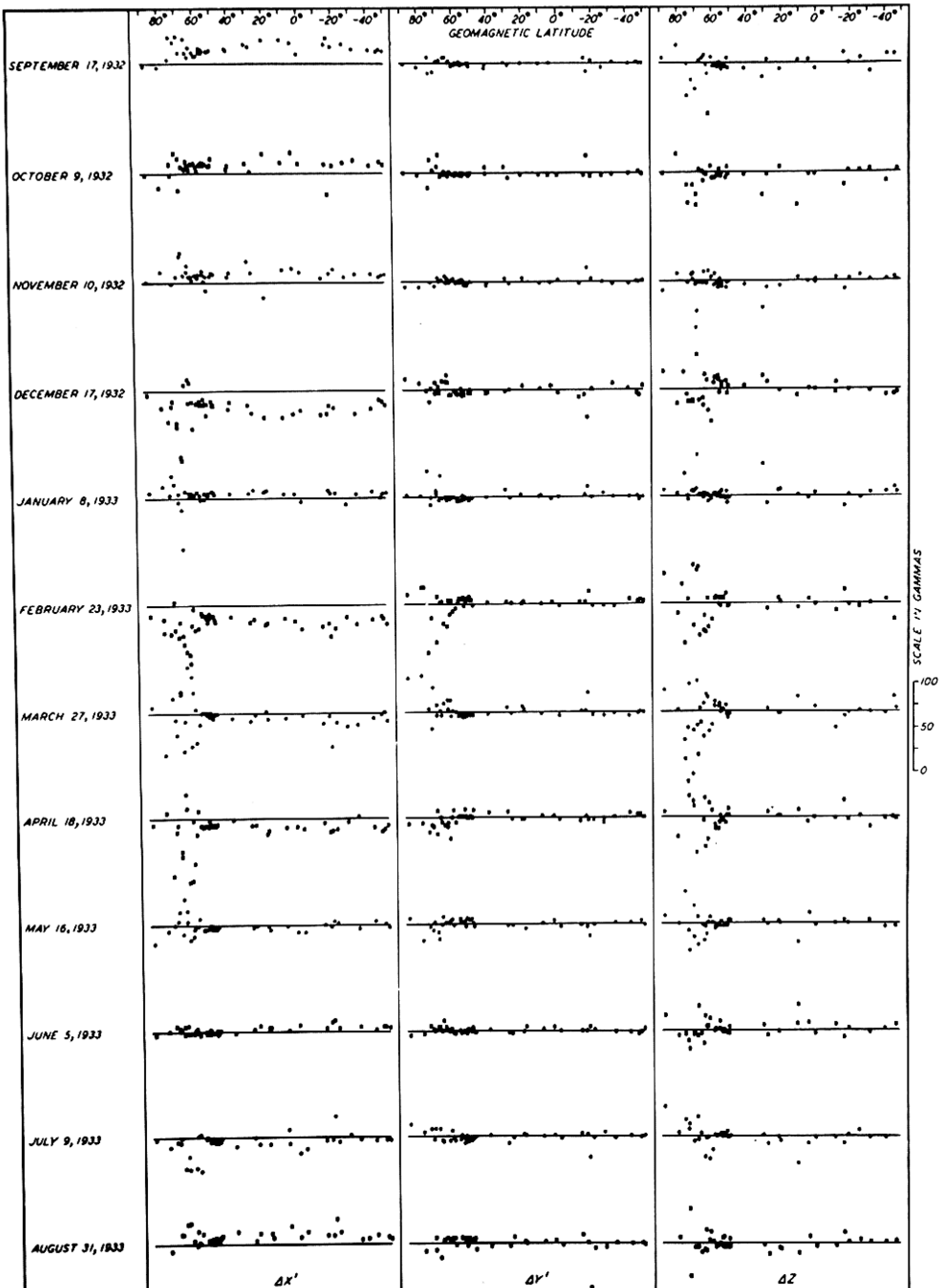

FIG. 48—CHANGE WITH GEOMAGNETIC LATITUDE OF DEPARTURES OF DAILY MEANS FROM MONTHLY MEANS AT MAGNETIC OBSERVATORIES (TO AVOID CONFUSION, POINTS ON DATES ARE INDICATED ALTERNATELY BY SQUARES AND CIRCLES)

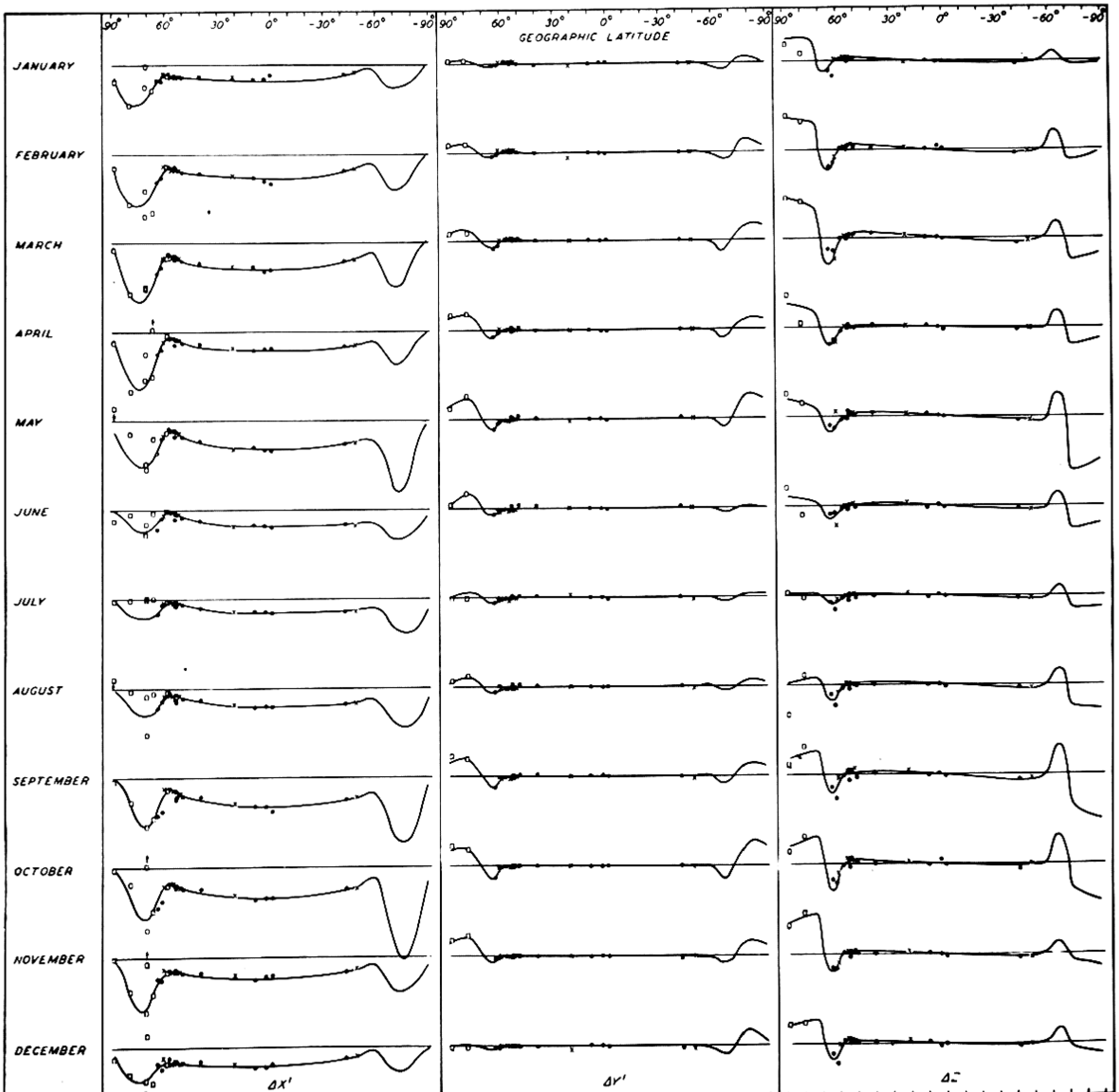

FIG. 49(A)—LATITUDE-DISTRIBUTION OF AVERAGE MONTHLY DISTURBANCE, DISTURBED MINUS QUIET DAYS, 1922-33, VALUES FOR POLAR YEAR, 1932-33, REDUCED TO 1922-33

LEGEND: •=STATIONS, 1922-33; ○=STATIONS, 1932-33; x=LERWICK, 1926-33, RUDE SKOV, 1927-33, VAL JOYEUX, HONOLULU, AND AMBERLEY, 1923-33

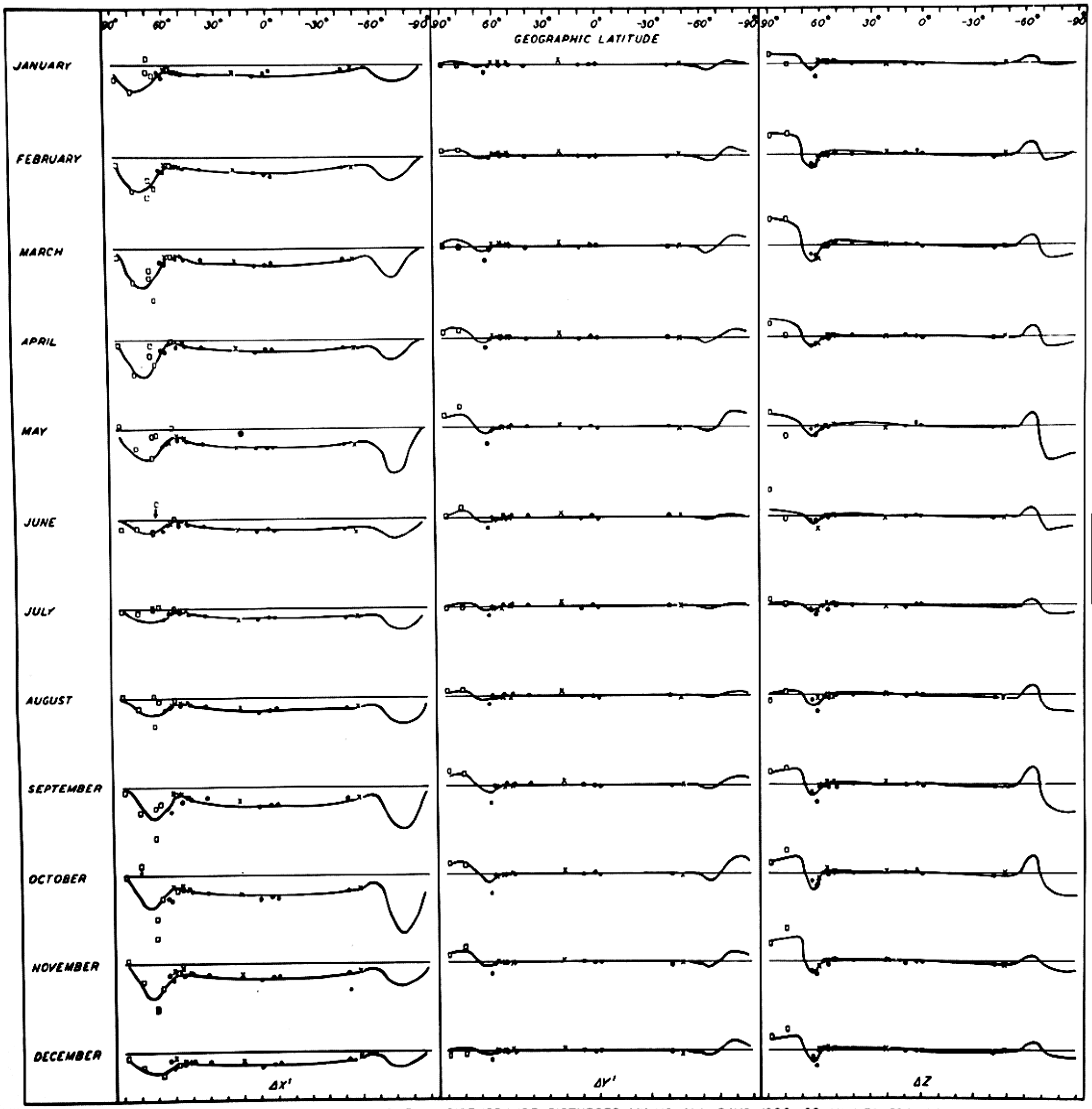

FIG. 49(B) — LATITUDE-DISTRIBUTION OF AVERAGE MONTHLY DISTURBANCE, DISTURBED MINUS ALL DAYS, 1922-33, VALUES FOR POLAR YEAR, 1932-33, REDUCED TO 1922-33

LEGEND: • = STATIONS, 1922-33; ▫ = STATIONS, 1932-33; × = LERWICK, 1926-33, RUDE SKOV, 1927-33, VAL JOYEUX, HONOLULU, AND AMBERLEY, 1923-33

CHAPTER VII

THE SOLAR DAILY VARIATION ON QUIET DAYS, S_q

1. Previous studies of S_q, and scope of present work. --The solar daily variation has been studied extensively by many writers. Schuster [24] established its origin as external to the Earth, by the application of the method of spherical harmonic analysis. His studies were later elaborated on and greatly extended by Chapman [3, 25] who derived S_q by seasons and year for the sunspot minimum year, 1902, and the sunspot maximum year, 1905, using many stations. The latitude distribution of S_q was established with considerable completeness. A more careful spherical harmonic analysis was made and a dynamo-theory of its origin was developed, based on air motions of the upper atmosphere and solar ultraviolet radiation. McNish [26] derived and discussed results showing a variation in S_q with longitude, using in his analysis the anomalously large values of S_q at Huancayo and from data on solar-flare disturbances, he established the close dependence of S_q on the intensity of solar ultraviolet radiation. A further description of the variation of S_q with longitude recently has been given in more detail by Benkova [27], based on data for the summer season of the Polar Year, 1932-33, the variation of S_q with longitude being expressed analytically in terms of spherical harmonics.

It is the purpose here to obtain a description of S_q from a considerably greater volume of data, permitting estimates of S_q on a world-wide scale for all days of the period 1905 to 1942. Account is taken of the considerable change in amplitude of S_q with sunspot cycle [3], with month of year, and with day of year. Estimates useful for most days of magnetic storm are also provided. The change in S_q with longitude is taken into account, although the data available for this purpose are in several respects inadequate in many ocean areas.

2. The solar daily variation on international quiet days, by seasons and year, Polar Year, 1932-33.--During the Polar Year, 1932-33, a comparatively large number of observatories operated, especially in polar regions, and there were additional stations operating also in low and middle latitudes. That year was near sunspot minimum and hence less influenced by disturbances which always appear to some degree even on the five most magnetically quiet days in each month. The data of this particular year hence afford especially valuable material for the delineation of the latitude and longitude distribution of S_q.

In high latitudes there is considerable disturbance present even on international quiet days. A certain proportion of this disturbance is present also in low latitudes. However, the irregular features of disturbance, because of their smaller magnitudes in low as compared with high latitudes, tend to cancel out in the average of many days. In order that S_q may be determined in high latitudes, a sufficient number of days of very low magnetic activity (low character-figure) are necessary though in a few instances successful use has been made of quiet hours rather than days. In the present treatment, a choice of data on this basis has not been made, although the material for this purpose is partially available. Some of the results indicate, in so far as international quiet days are concerned, the importance of disturbance in high latitudes even on quiet days. Data were used for all stations for which they were available among those listed in Table 103.

Figures 50 to 53 show the observed average daily variations found for many stations, in the geomagnetic north (X'-), east (Y'-), and vertical (Z-) components, first by seasons separately, and finally, averaged for the entire year; Figure 53(C) gives inhomogeneous data for the year at high latitude stations. It will be noted that the sign of the variation in X' is the same north and south of the equator, with reversal near latitudes 30° north and south. The variations in Y' and Z are opposite in sign on either side of the equator.

Although there is notable similarity in the form of the curves for stations in similar latitudes, there is evidence of a variation of the amplitude of S_q with longitude. At Huancayo, as has been noted by McNish [18], the amplitude in the north component is considerably greater than at other stations. On close examination it appears that this is also the case at Manila, a station likewise in a region where the geomagnetic and geographic equators diverge widely from each other. With these two exceptions, which are of course accompanied by transitional changes in the intervening regions of the equatorial belt, the asymmetry in longitude appears slight and secondary in importance to the more notable close dependence on geographic (or geomagnetic) latitude and local time.

The world-wide distribution of S_q, as previously noted by Chapman for the years 1902 and 1905, shows appreciable change with season in amplitude and to some extent also in form, especially in regions of transition where changes in sign of the components appear. Figures 50 and 52 show that in general the amplitude is greater in local summer than in winter. Figures 51 and 53 indicate that S_q at the equinoxes closely resembles its yearly average, both in amplitude and phase.

3. The solar daily variation on international quiet days, by months, seasons, and year, 1922 to 1933.--Figures 50 to 53 indicated considerable change in S_q with season, and it is evident that averaging the quiet days into three divisions or intervals representing the seasons does not provide either accurate or convenient basis for interpolation to give values of S_q typical of each month. Furthermore, it has been mentioned that S_q shows considerable daily variability [28], and hence the mean of the five quiet days per month available from the observatories of the Polar Year does not permit adequate description of the monthly mean of S_q. Accordingly, means by months for the 12-year period 1922 to 1933 were derived, for stations between the northern and southern auroral zones. The means were taken so as to include homogeneous data intercomparable at all stations, using the same days and hours so far as possible. These means, corrected for noncyclic change, are illustrated in Figures 54 to 69.

It will be noted that the results agree well with those of Figures 50 to 53. The monthly means are each based

on 60 days of the 12-year period, and delineate the average amplitude and form of S_q at each station, and the transitional characteristics from month to month. In a previous volume, tables were given of mean monthly estimates of S_q for each 10°-parallel of geographic latitude. These were derived by reading from smoothed graphs of the Fourier coefficients a_n, b_n up to $n = 4$, the values of a_n, b_n for each 10°-parallel of latitude. The results so found were next synthesized to give the results of Tables 1-L, 1-M, and 1-N in that volume. These tables, used in conjunction with later tables that provide factors which take into account the daily variability of S_q, permitted the approximate correction of field-observations for the influence of S_q [1].

It should of course be remarked that S_q depends about as closely on geographic as on geomagnetic latitude, the differences being negligible in low latitudes and very slight in middle latitudes. In high latitudes, however, S_q is itself presumably small, and the effects of disturbance may dominate even on international quiet days. In the work of the previous volume [1], it was convenient to use geomagnetic components for S_q, since these were also used for AV, P, and RV. The small differences in middle latitudes involved for the east component, resulting from the asymmetry of the S_q-field relative to the geomagnetic axis, were not neglected, since the variation of S_q with longitude was taken approximately into account at a later stage.

Figures 70 to 85 give the values of S_q by 10°-parallels of latitude, as derived from interpolated and synthesized values.

4. The dependence of S_q on longitude.--The variations with longitude apparent from inspection of Figures 40 to 49, presented in Chapter VI, and Figures 50 to 69 in the present chapter would be expected on the basis of the dynamo-theory which is generally accepted as explaining the main contribution of S_q. Apart from seasonal influences, the air motions yielding the causative electric currents in the atmosphere by dynamo-action seem likely to be most nearly symmetrical about the Earth's axis of rotation, but the lines of force of the vertical component of the Earth's main field, cut by the moving conducting air layers, are to the best first approximation symmetrical about the geomagnetic axis. Hence in low latitudes where the geographic and geomagnetic equators diverge most widely from one another, there must appear effects observable in S_q depending on the divergence of the two equators. The results for Huancayo, interpreted from this standpoint by McNish [26], seem cogent, and similar arguments can be brought to bear in the case of Manila. The data of Figures 50 to 69 show the amplitude of the geomagnetic north component at Manila to be augmented above its expected value, though on a smaller scale than at Huancayo.

In mapping the dependence of S_q on longitude in this equatorial belt of about 20° width in latitude, and covering much of the Earth's surface, a great handicap is experienced as a result of the paucity of data. It would seem highly desirable to locate an observatory near the junction of the geomagnetic and geographic equators, at an island near Baker Island in the Pacific, and at one or two additional equatorial sites in other longitudes.

The world-wide features of S_q are well defined, although the oceans present extensive areas where no observations of S_q have been made. As may be expected, there are small variations in the otherwise regular features of S_q which depend on highly localized conditions, such as those occasioned by the proximity of stations to induced electric currents flowing in the oceans.

In order to obtain the approximate variation of S_q with longitude, the values of Figures 70 to 85 were subtracted from the observed values at all available observatories. Results by hours were mapped on world charts, for each geomagnetic component. This was done in seeking the simplest possible distribution giving contours fully closed. In many regions the results so found are at best only a considered guess. Due to the highly tentative character of the results for many regions, tables of the variation of S_q with longitude given in the preceding volume [1] included only values of field greater than three gammas. Values for X′ were given in Table 1-O, a sample of which appears in the preceding volume. The values in Table 1-P for the Y′-component were considerably smaller in general than were those for the X′-component. In the case of the Z-component, the variation with longitude was particularly small, and it was not thought worth while to include a table for these small values (in general less than about five gammas).

5. The variation in the amplitude of S_q with sunspot-cycle.--Chapman [3] has studied the variation in form and amplitude of S_q with sunspot-cycle, for data on a world-wide scale for the years 1902 and 1905, and also for the station Greenwich for the long series of years 1889 to 1914. The results indicated at most only a slight variation in form with sunspot-cycle. The amplitude of S_q was found to be about 30 per cent greater in sunspot maximum years than in minimum years. These findings were supported by extensive studies of Ellis [3] and Moos [16].

The results derived here for the years 1922 to 1933 are also in good agreement. Examination revealed that the average phase and form of S_q differed little from year to year (except in special locations such as Huancayo), with the amplitude greatest near sunspot maximum.

The dependence of amplitude of S_q on sunspot-cycle is conveniently examined by deriving the mean annual ranges in the H-component of S_q for international quiet days. Figure 86 shows the yearly averages of the daily amplitude of S_q for the period 1922 to 1933 for various stations. The results from station to station agree well, and changes in the averages from year to year correspond closely with the changes in yearly sunspot number. These data show that the regions of the Sun emitting the ultraviolet radiation which is responsible indirectly for S_q, attain their maximum effectiveness as radiators at the time of maximum sunspots. They show further that the change in amplitude of S_q from year to year is gradual.

6. The daily variability of S_q.--Figure 87 shows S_q on several selected international quiet days. Chapman and Stagg [28] examined the day to day changes in S_q for Eskdalemuir and Greenwich for quiet days of the period 1913 to 1923. They found the differences in field from average for these observatories closely correlated (correlation coefficient 0.77 in X and 0.84 in Y), and found less correlation for stations farther apart. They also found that the phase of S_q is independent of the amplitude.

Hasegawa [3] considered in detail the changes in the S_q current systems on successive days showing marked differences in the amplitude of S_q. The changes in S_q revealed considerable shifts in the current system responsible, both to the north and south of the average position; this feature appeared also in a statistical study of

the amplitudes of S_q carried out for the transitional station of Watheroo by Bartels [3].

In order to examine this question further, the day to day movement of the transition region in middle latitudes was estimated from changes in the H-component of force at the time of the noon maximum. Use was made of the shift in the monthly mean latitude distributions at noon for the stations Tucson, Lukiapang, and Watheroo. The average daily shift or oscillation about the average position of transition was several degrees of latitude. Therefore, in all regions except those in and near the zones of transition, where the value of S_q is in any case small in the component most affected and varies only slowly with latitude in other components, there will in general be but a few abnormal days which will not be adequately described by averaged values.

Although the phase of S_q is somewhat variable from day to day, and there are some daily variations in form, the value of S_q throughout low and middle latitudes can be estimated to a certain degree of accuracy on the basis of suitable multiplicative factors to be applied to the average monthly mean in a component. The studies of Chapman and Stagg [3] indicate that the proportional increases or decreases in S_q relative to the normal or mean value are highly correlated from station to station. This finding was independently confirmed here by actual comparisons on individual days for many stations. It was therefore concluded that a suitable multiplicative factor, derived as a mean for several stations in low latitudes for which the usual S_q on each day is large in amplitude in H and only slightly affected by disturbance, would be useful. The procedure of relating the daily amplitude and phase of S_q to its average monthly value also afforded the additional attractive feature of correcting for the variation in amplitude of S_q with sunspot-cycle.

After some experimentation, it was found that a quantity derived by taking the mean hourly departure in H near noon from the daily mean in H, at an equatorial station, and dividing by the appropriate monthly average value obtained from 12 years of data, showed fairly good agreement from station for station. Such quantities derived from data of the period 1922 to 1933 therefore provide valuable multiplicative factors applicable to the averages of S_q at stations in all latitudes. Comparisons revealed that on slightly disturbed days the discrepancies among stations were rather marked, but on such days the influence of disturbance in the higher latitudes is sufficient to mask results of the comparisons.

The factors derived on the basis of individual low-latitude stations have been listed in Table 1-P, a sample of which appears in the preceding volume [1]. These afford useful estimates of S_q even on many days of storm, in view of the predominently large amplitude of S_q in H near noon near the equator as compared with the disturbance daily variation (S_D) there, which is ordinarily small in H. However, for Huancayo, it must be noted that the factors include a periodic effect as great as 20 per cent due to the lunar daily variation.

Table 103. List of magnetic observatories

Station	ϕ	λ	Φ	Λ	Ψ	D
	°	°	°	°	°	°
Thule	76.5	291.0	88.0	0.0	0.0	-81.3
Godhavn	69.2	306.5	79.8	32.5	-17.5	-57.9
Scoresby Sund	70.5	338.0	75.8	81.8	-36.2	-34.6
Sveagruvan	77.9	16.8	73.9	130.7	-46.2	- 4.9
Chesterfield Inlet	63.3	269.3	73.5	324.0	14.9	-12.6
Calm Bay	80.3	52.8	71.5	153.3	-32.2	21.2
Bear Island	74.5	19.2	71.1	124.5	-37.9	- 1.9
Juliannehaab	60.7	314.0	70.8	35.6	-13.8	-43.4
Fort Rae	62.8	243.9	69.0	290.9	24.1	37.5
Point Barrow	71.3	203.3	68.6	241.2	33.0	28.7
Tromsö	69.7	18.9	67.1	116.7	-30.8	- 3.7
Petsamo	69.5	31.2	64.9	125.8	-27.6	5.8
Matotchkin Shar	73.3	56.4	64.8	146.5	-22.4	21.7
College, Fairbanks	64.9	212.2	64.5	255.4	27.0	30.5
Sodankylä	67.4	26.6	63.8	120.0	-26.7	3.0
Dickson	73.5	80.4	63.0	161.5	-12.8	28.5
Lerwick	60.1	358.8	62.5	88.6	-23.6	-13.6
Meanook	54.6	246.7	61.8	301.0	17.2	26.4
Sitka	57.0	224.7	60.0	275.4	21.4	30.2
Eskdalemuir	55.3	356.8	58.5	82.9	-20.4	-14.3
Lovö	59.4	17.8	58.1	105.8	-22.1	- 2.6
Sloutsk	59.7	30.5	56.0	117.0	-20.6	4.4
Rude Skov	55.8	12.4	55.8	98.5	-20.6	- 5.6
Agincourt	43.8	280.7	55.0	347.0	3.6	- 7.6
Abinger	51.2	359.6	54.0	83.3	-18.4	-11.9
De Bilt	52.1	5.2	53.8	89.6	-18.9	- 8.9
Manhay	50.3	5.7	52.0	88.8	-18.2	- 8.6
Val Joyeux	48.8	2.0	51.3	84.5	-17.5	-10.5
Swider	52.1	21.2	50.6	104.6	-18.3	- 1.6
Cheltenham	38.7	283.2	50.1	350.5	2.4	- 7.1
San Miguel	37.8	334.4	45.6	50.9	-11.3	-18.2
San Fernando	36.5	353.8	41.0	71.3	-13.6	-12.2
Tucson	32.2	249.2	40.4	312.2	10.1	13.9
San Juan	18.4	293.9	29.9	3.2	- 0.7	- 5.2
Teoloyucan	19.8	260.8	29.6	327.0	6.6	9.5
Helwan	29.9	31.3	27.2	106.4	-12.7	0.0
Honolulu	21.3	201.9	21.1	266.5	12.3	10.1
Dehra Dun	30.3	78.0	20.5	149.9	- 6.6	1.1
Lukiapang	31.3	121.0	20.0	189.1	2.1	- 3.6
Au Tau	22.4	114.0	11.0	182.9	0.6	- 0.7
Alibag	18.6	72.9	9.5	143.6	- 7.2	- 0.2
Manila	14.6	121.2	3.3	189.8	2.0	0.5
Huancayo	-12.0	284.7	- 0.6	353.8	1.3	7.4
Vassouras	-22.4	316.4	-11.9	23.9	- 5.0	-13.0
Elisabethville	-11.7	27.5	-12.7	94.0	-11.7	- 9.5
Apia	-13.8	188.2	-16.0	260.2	11.7	10.7
Batavia	- 6.2	106.8	-17.6	175.6	- 0.9	1.1
Pilar	-31.7	296.1	-20.2	4.6	- 1.1	6.1
Tananarivo	-18.9	47.5	-23.7	112.4	-11.2	- 8.3
Mauritius	-20.1	57.6	-26.6	122.4	-10.3	-12.6
Cape Town	-33.9	18.5	-32.7	79.9	-13.7	-24.7
Watheroo	-30.3	115.9	-41.8	185.6	1.3	- 3.9
Toolangi	-37.5	145.5	-46.7	220.8	9.5	8.5
Amberley	-43.5	172.7	-47.7	252.5	15.1	18.0
South Orkneys	-60.8	315.0	-50.0	18.0	- 7.2	+ 3.1

FIGURES 50-87

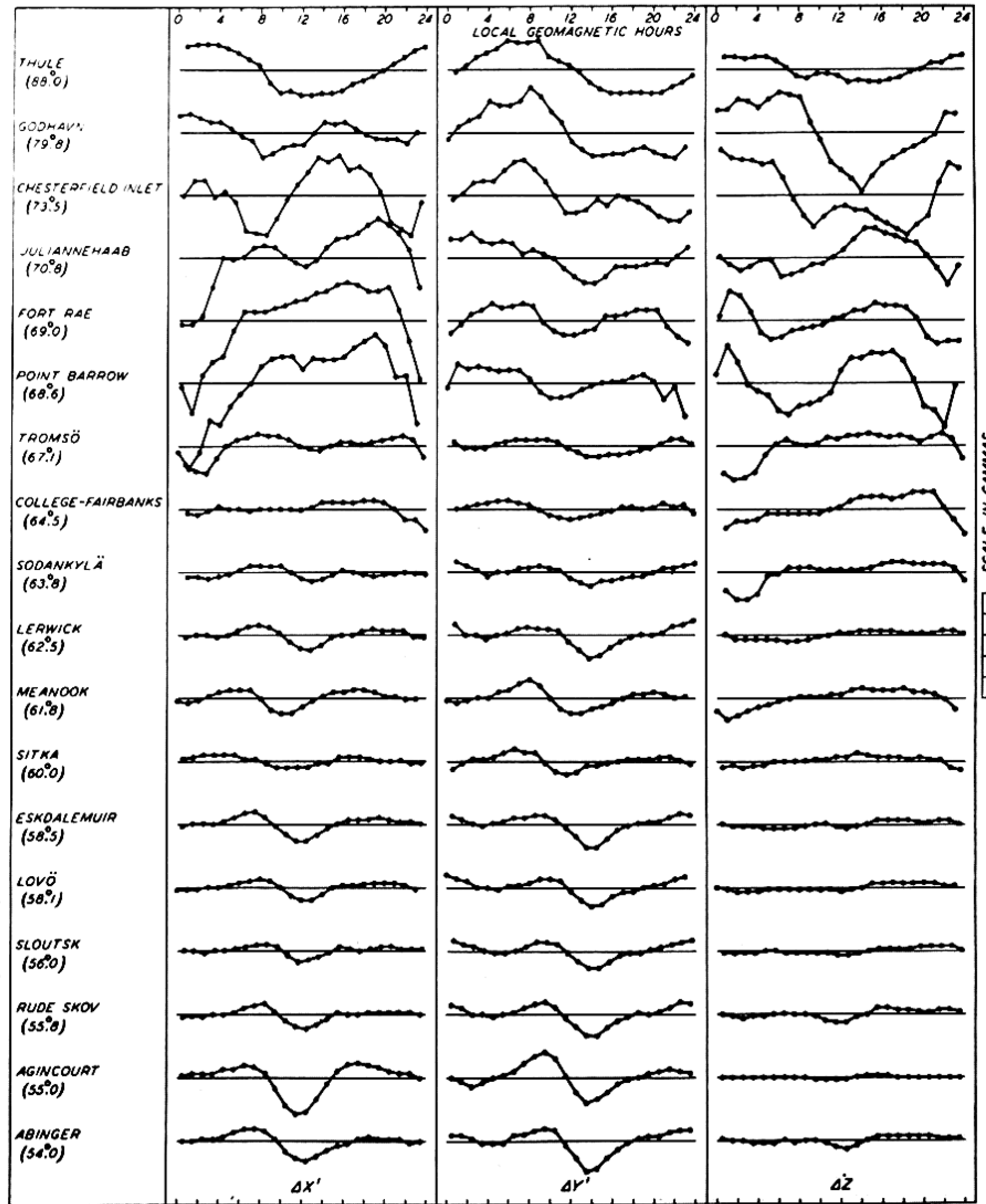

FIG. 50(A)—AVERAGE DAILY VARIATION, QUIET DAYS, GEOMAGNETIC COMPONENTS, WINTER, POLAR YEAR, 1932-33 (GEOMAGNETIC LATITUDES INDICATED IN PARENTHESES)

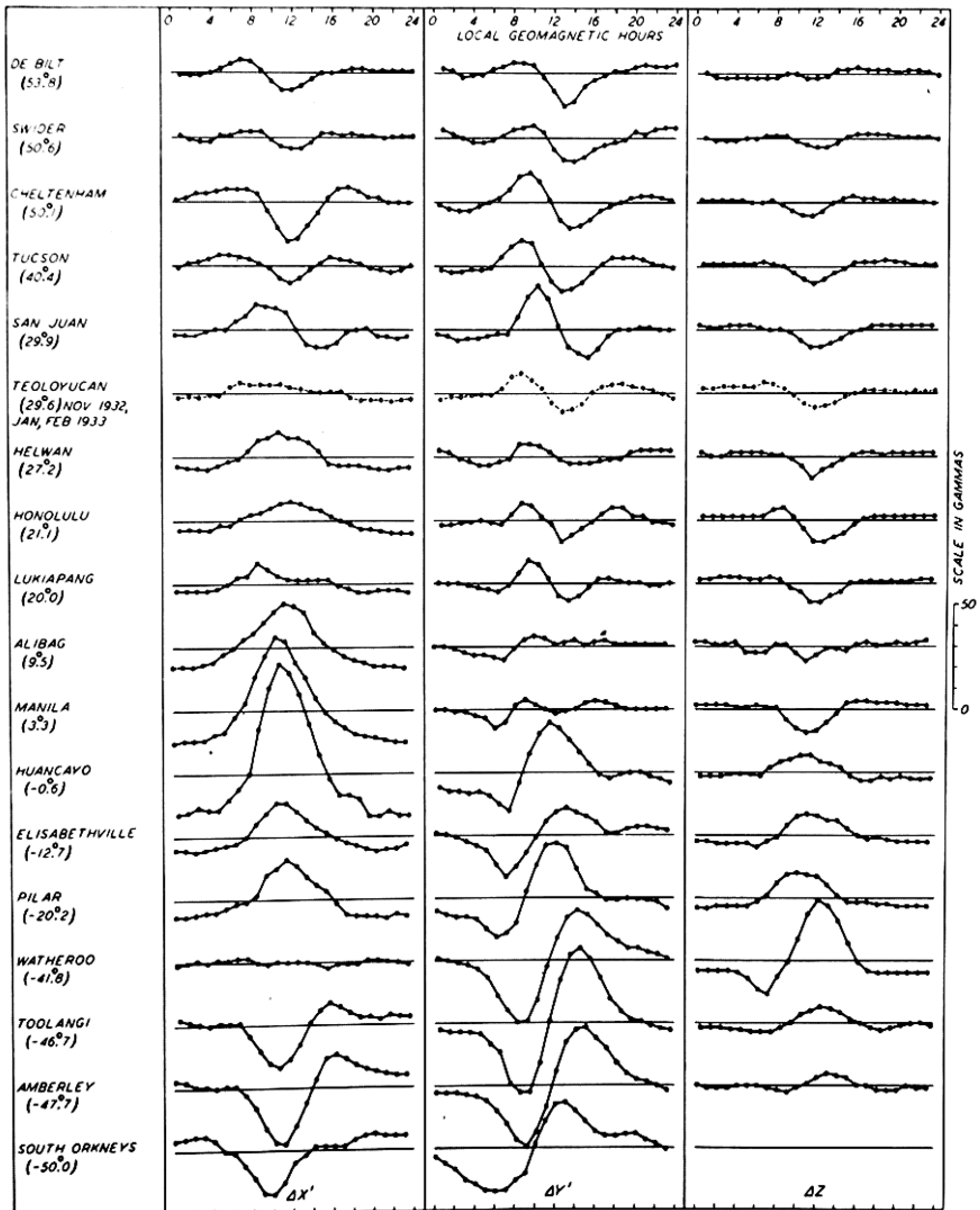

FIG. 50(B)— AVERAGE DAILY VARIATION, QUIET DAYS, GEOMAGNETIC COMPONENTS, WINTER, POLAR YEAR, 1932-33 (GEOMAGNETIC LATITUDES INDICATED IN PARENTHESES)

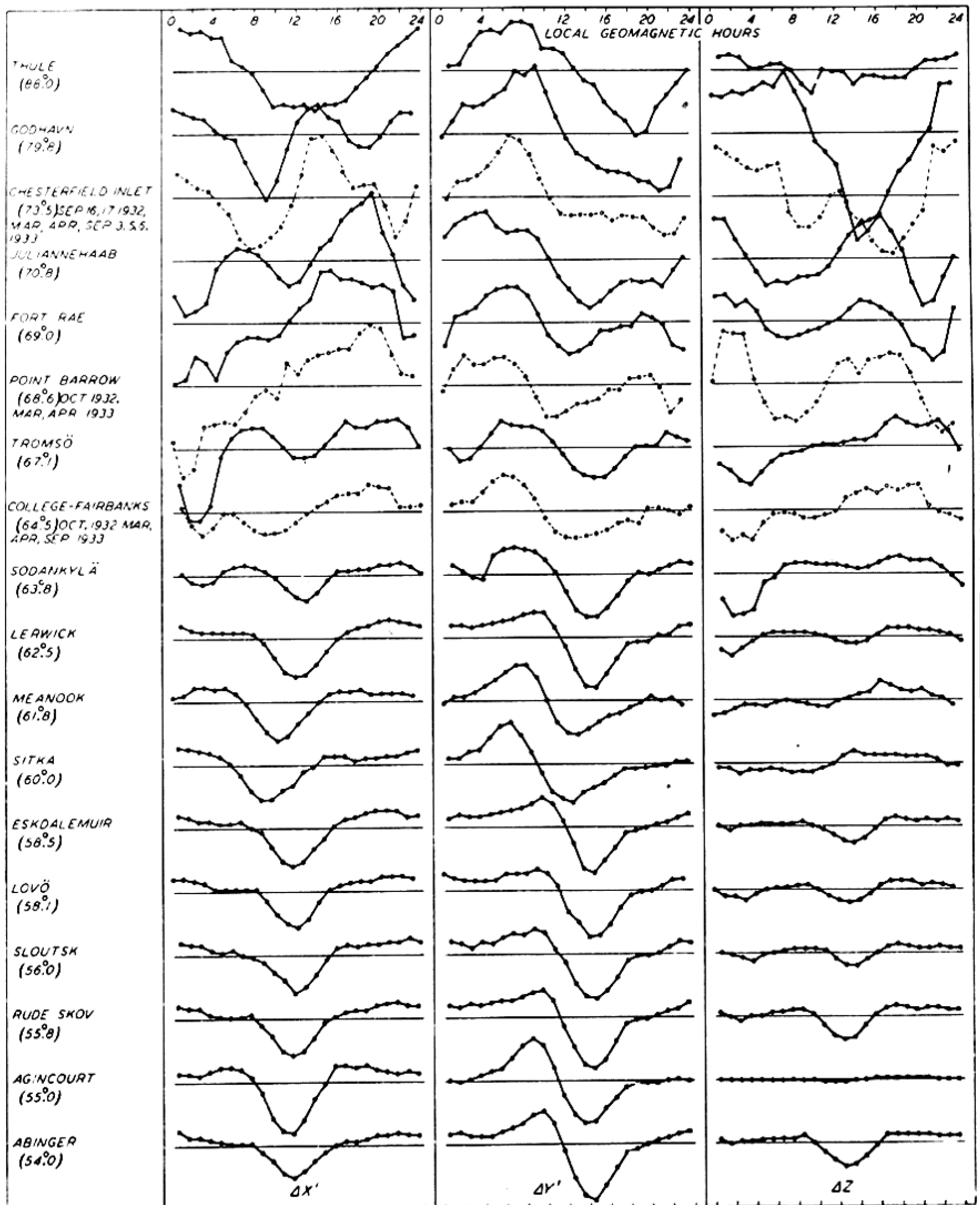

FIG. 51(A)-AVERAGE DAILY VARIATION, QUIET DAYS, GEOMAGNETIC COMPONENTS, EQUINOX, POLAR YEAR, 1932-33 (GEOMAGNETIC LATITUDES INDICATED IN PARENTHESES)

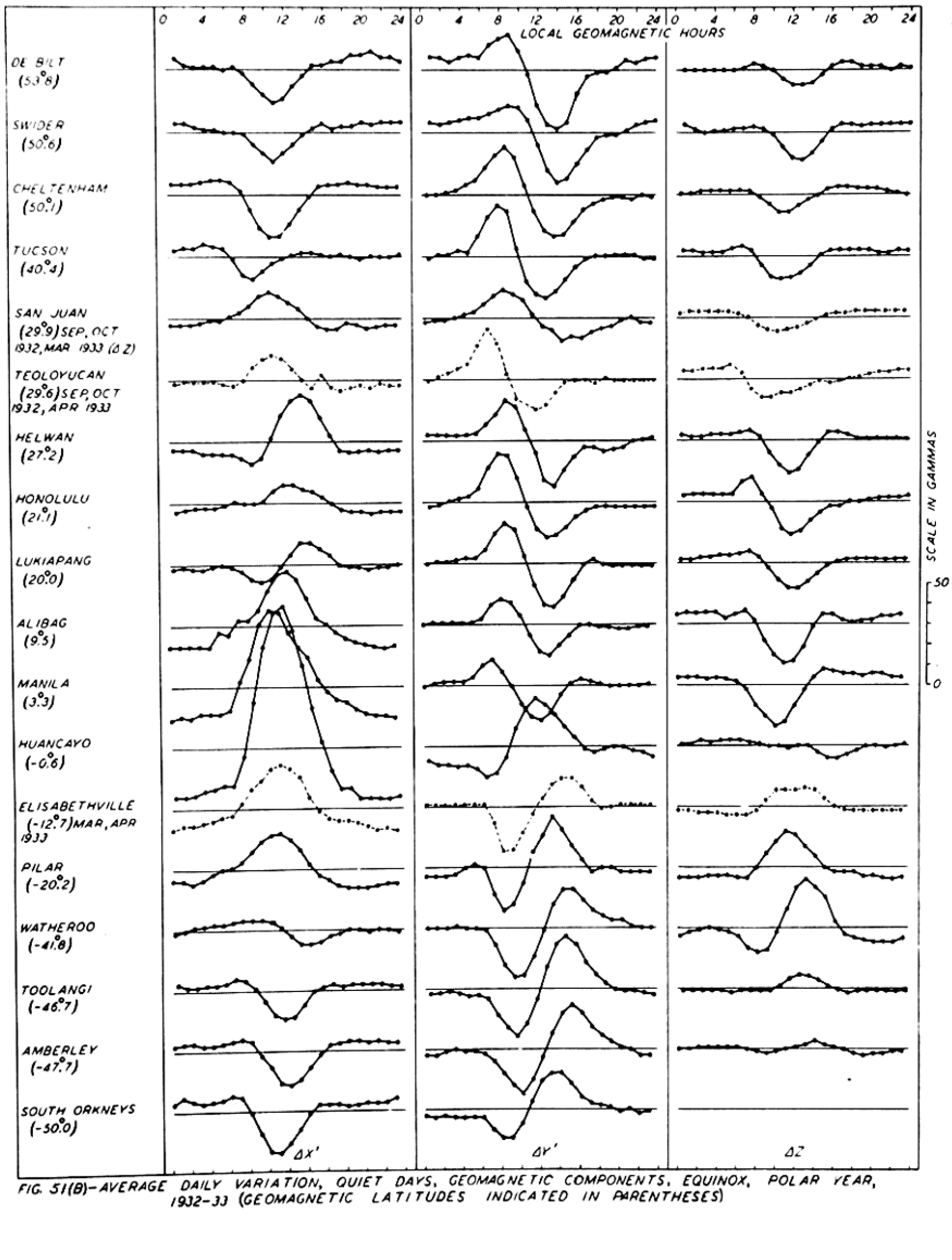

FIG. 51(B)—AVERAGE DAILY VARIATION, QUIET DAYS, GEOMAGNETIC COMPONENTS, EQUINOX, POLAR YEAR, 1932-33 (GEOMAGNETIC LATITUDES INDICATED IN PARENTHESES)

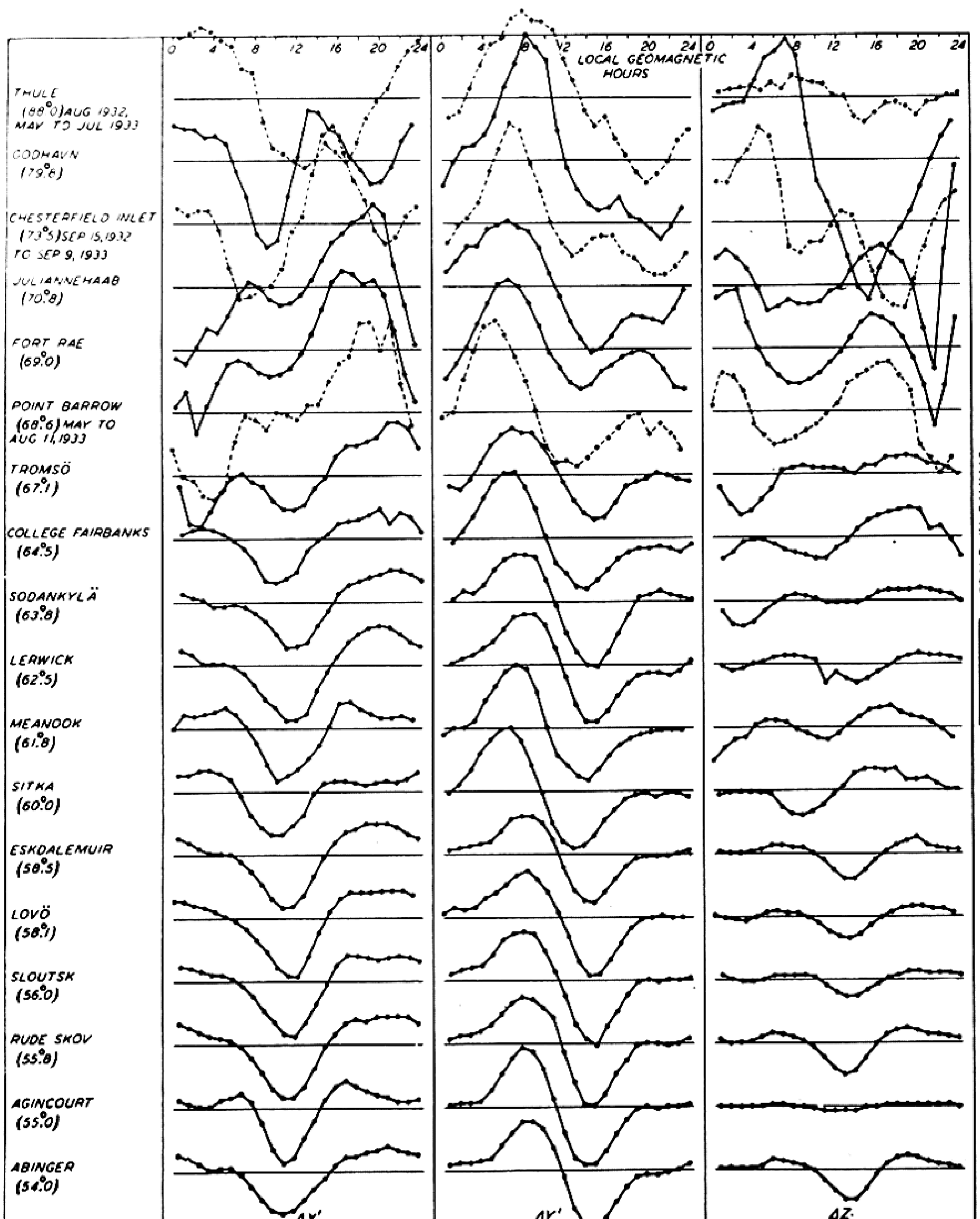

FIG. 52(A)—AVERAGE DAILY VARIATION, QUIET DAYS, GEOMAGNETIC COMPONENTS, SUMMER, POLAR YEAR, 1932-33 (GEOMAGNETIC LATITUDES INDICATED IN PARENTHESES)

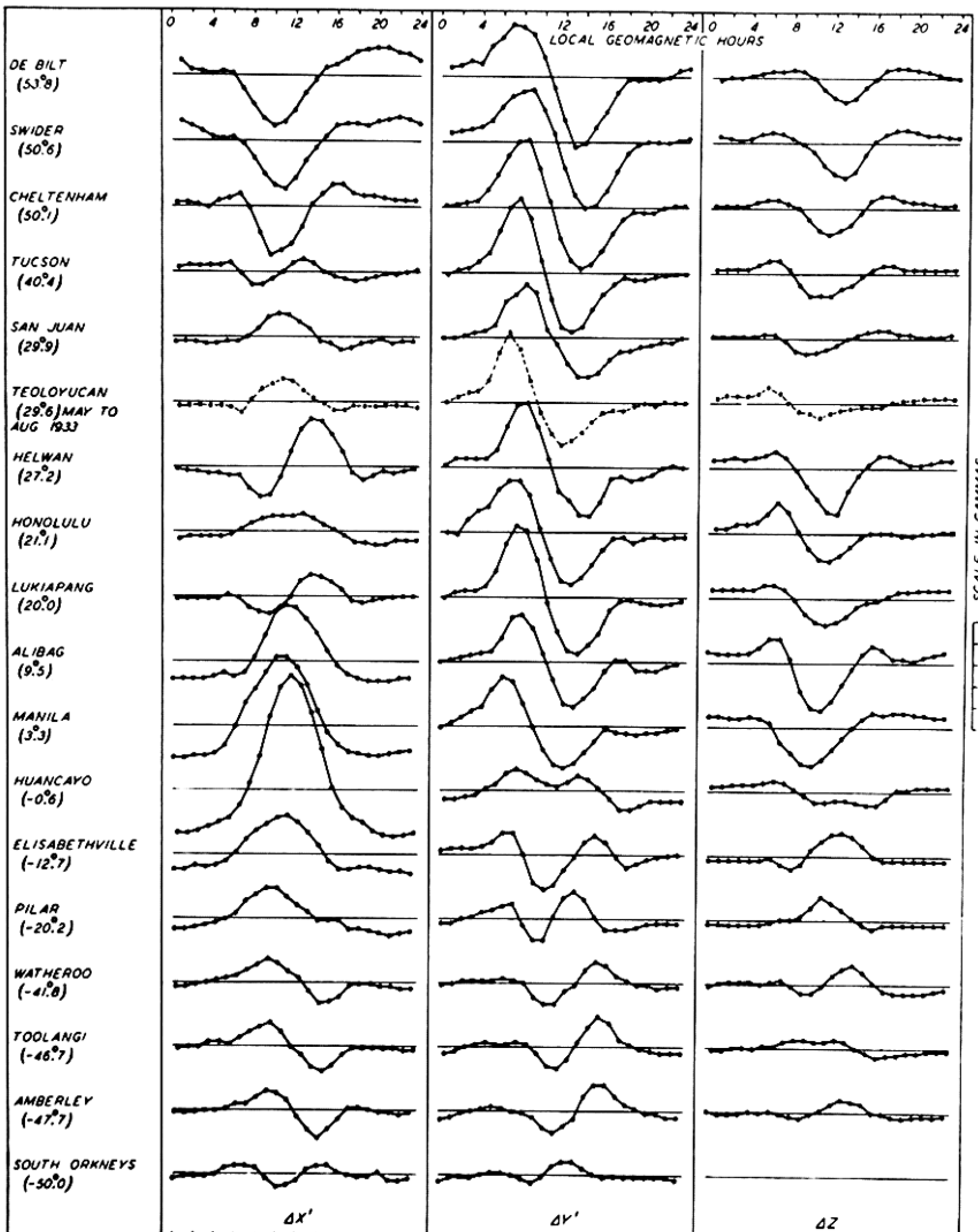

FIG. 52(B)—AVERAGE DAILY VARIATION, QUIET DAYS, GEOMAGNETIC COMPONENTS, SUMMER, POLAR YEAR, 1932-33 (GEOMAGNETIC LATITUDES INDICATED IN PARENTHESES)

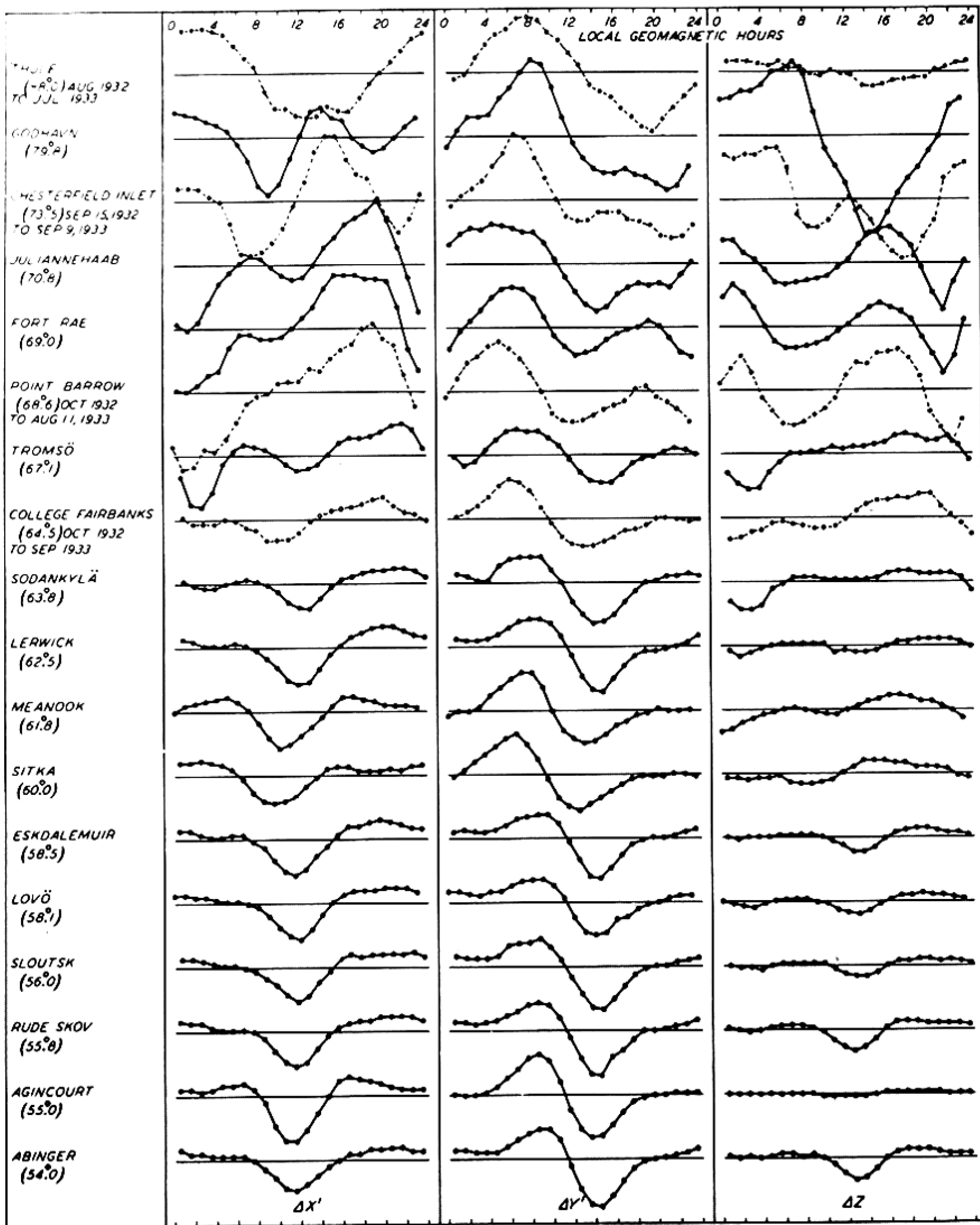

FIG. 53(A)—AVERAGE DAILY VARIATION, QUIET DAYS, GEOMAGNETIC COMPONENTS, MEAN OF 12 MONTHS, POLAR YEAR, 1932-33 (GEOMAGNETIC LATITUDES INDICATED IN PARENTHESES)

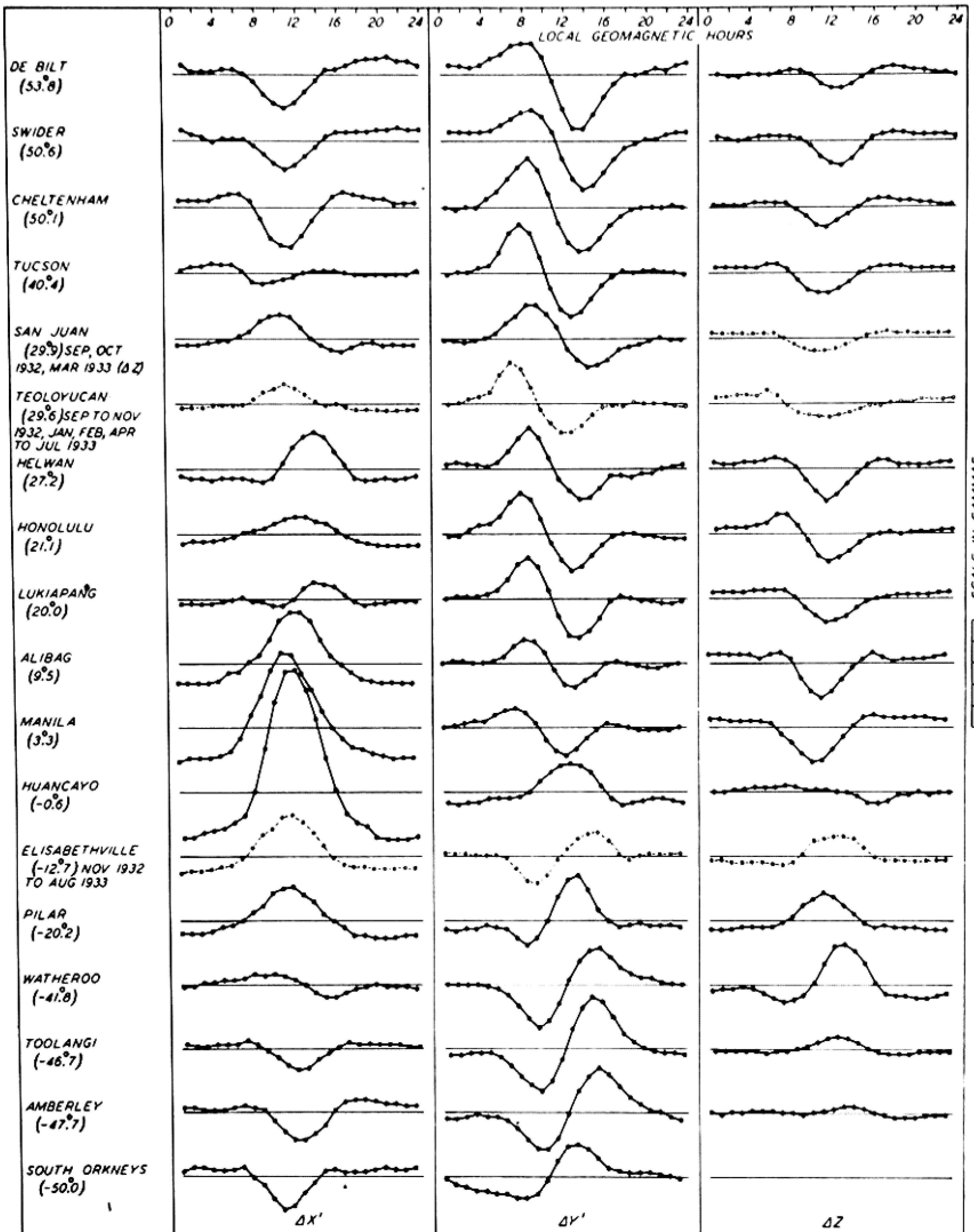

FIG. 53(B)—AVERAGE DAILY VARIATION, QUIET DAYS, GEOMAGNETIC COMPONENTS, MEAN OF 12 MONTHS, POLAR YEAR, 1932-33 (GEOMAGNETIC LATITUDES INDICATED IN PARENTHESES)

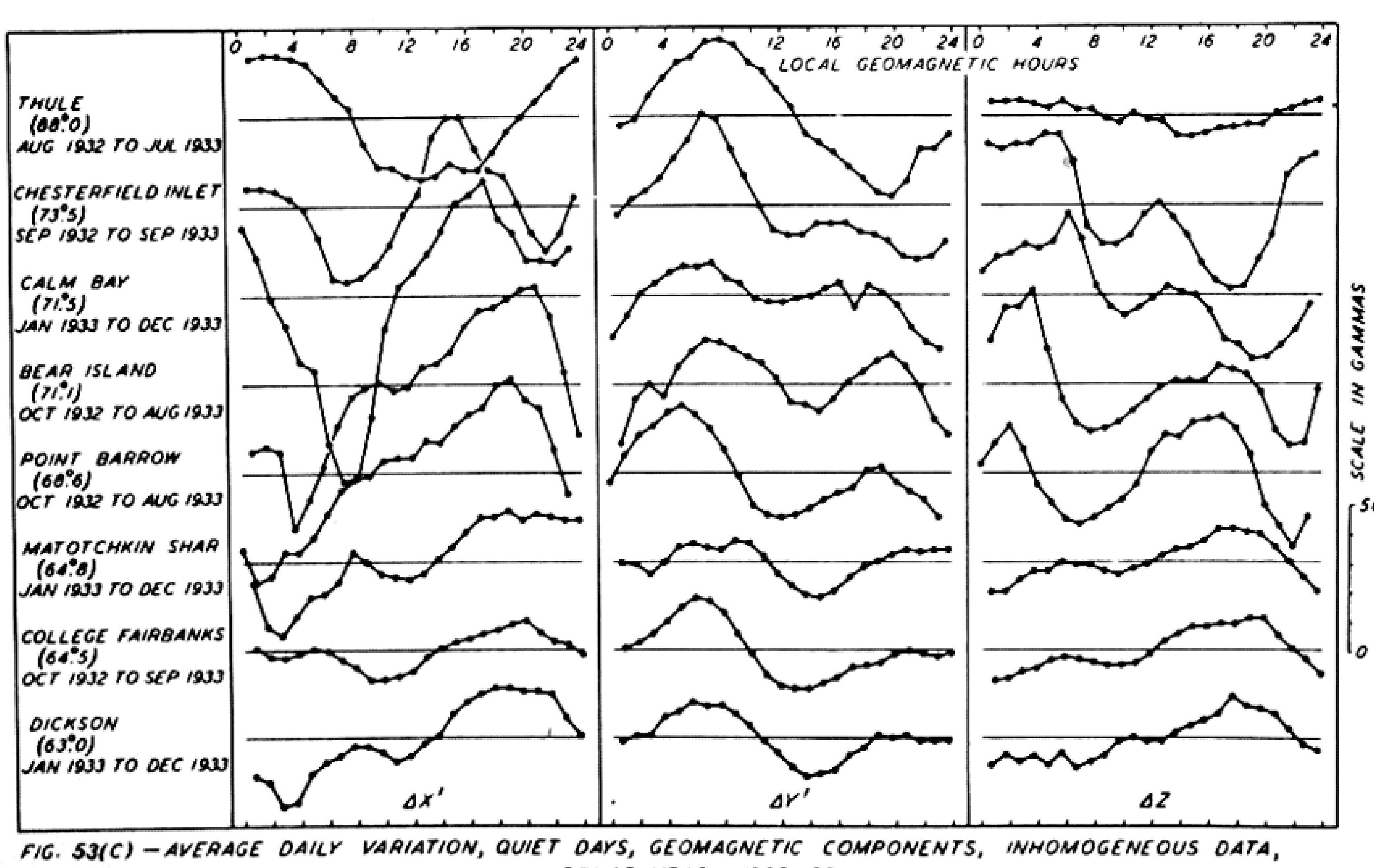

FIG. 53(C) —AVERAGE DAILY VARIATION, QUIET DAYS, GEOMAGNETIC COMPONENTS, INHOMOGENEOUS DATA, POLAR YEAR, 1932-33

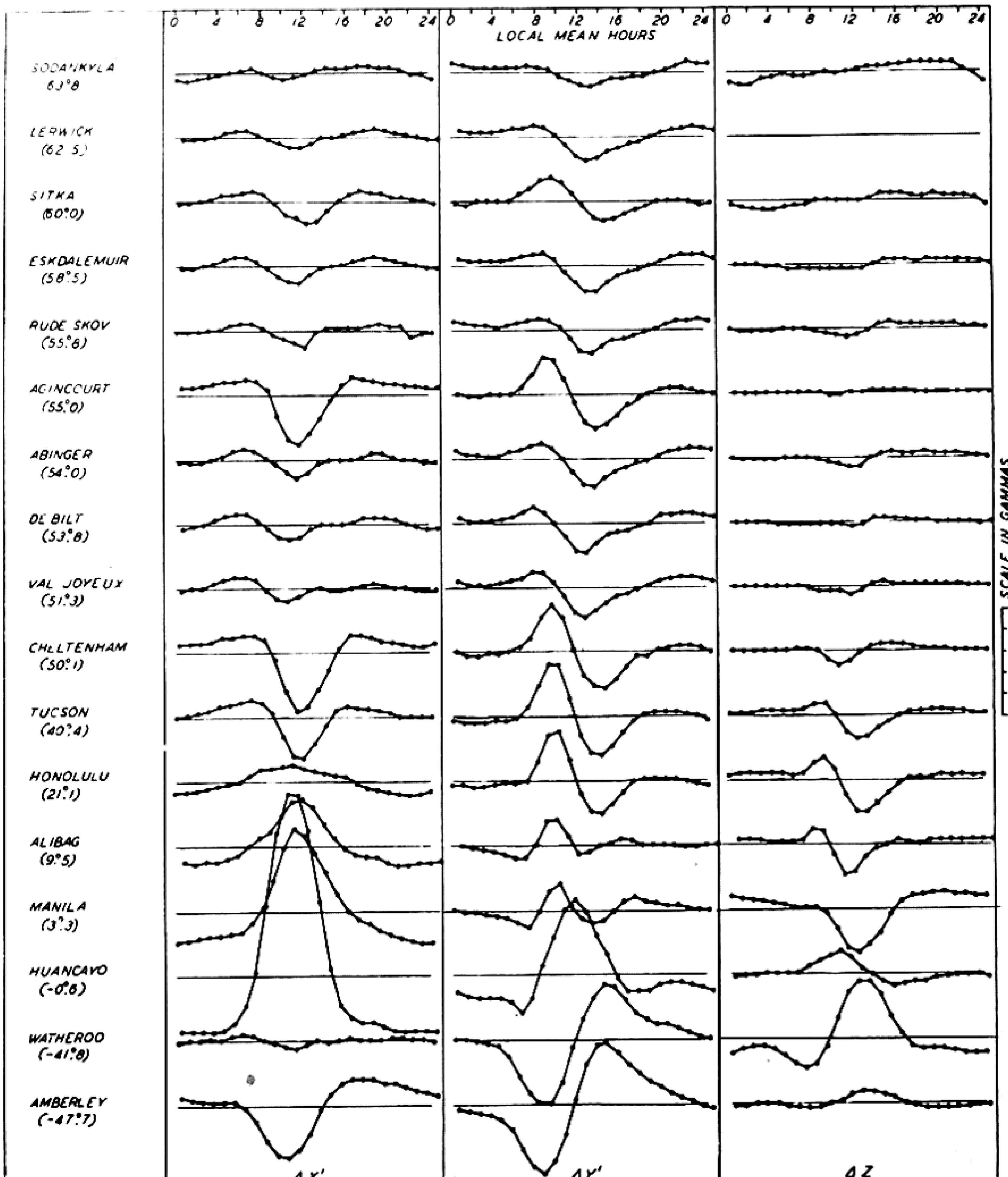

FIG. 54—SOLAR DAILY VARIATION ON QUIET DAYS (Sq), VARIOUS STATIONS, GEOMAGNETIC COMPONENTS, JANUARY, 1922-33 (GEOMAGNETIC LATITUDES INDICATED IN PARENTHESES)

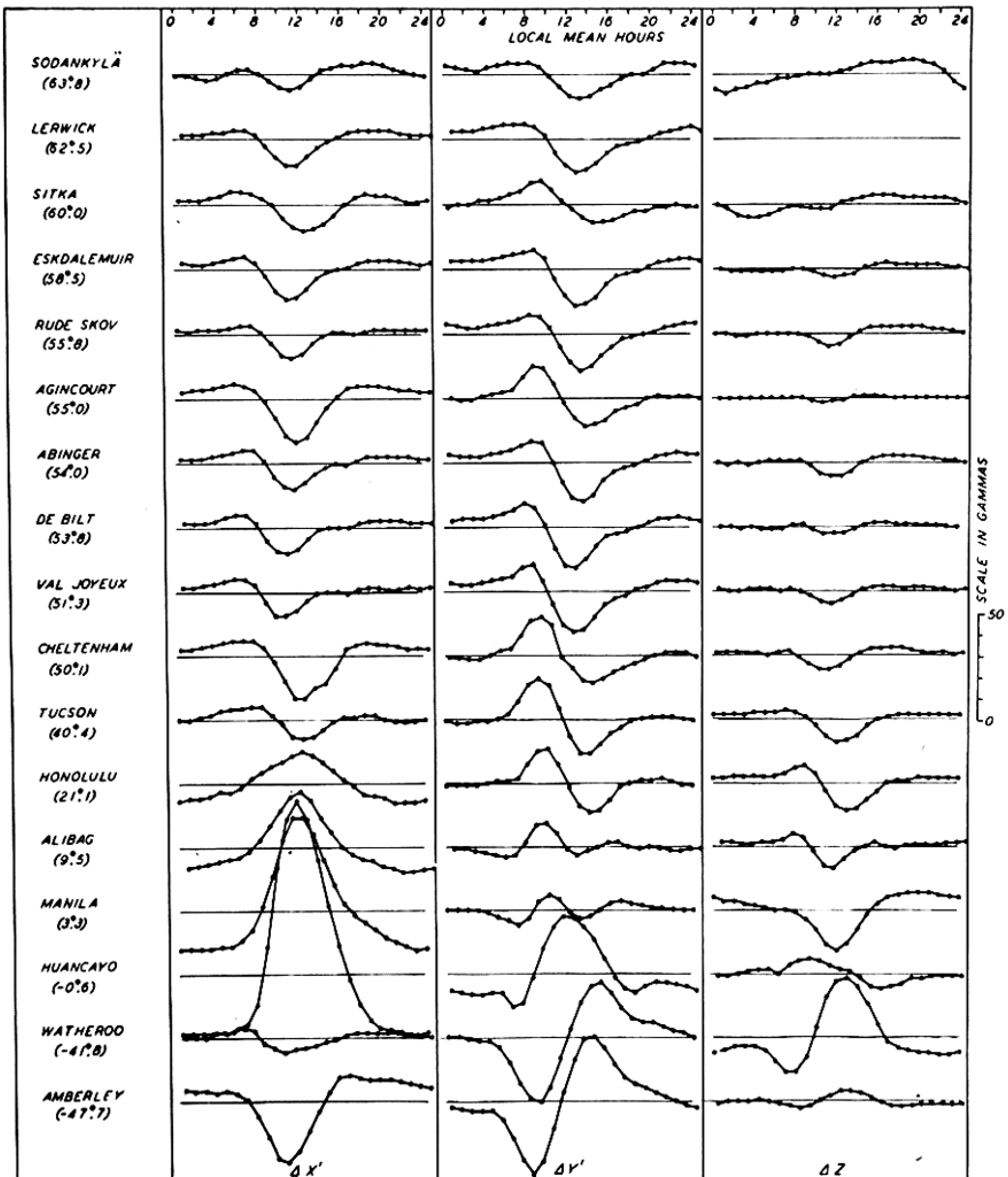

FIG. 55—SOLAR DAILY VARIATION ON QUIET DAYS (S_q), VARIOUS STATIONS, GEOMAGNETIC COMPONENTS, FEBRUARY, 1922-33 (GEOMAGNETIC LATITUDES INDICATED IN PARENTHESES)

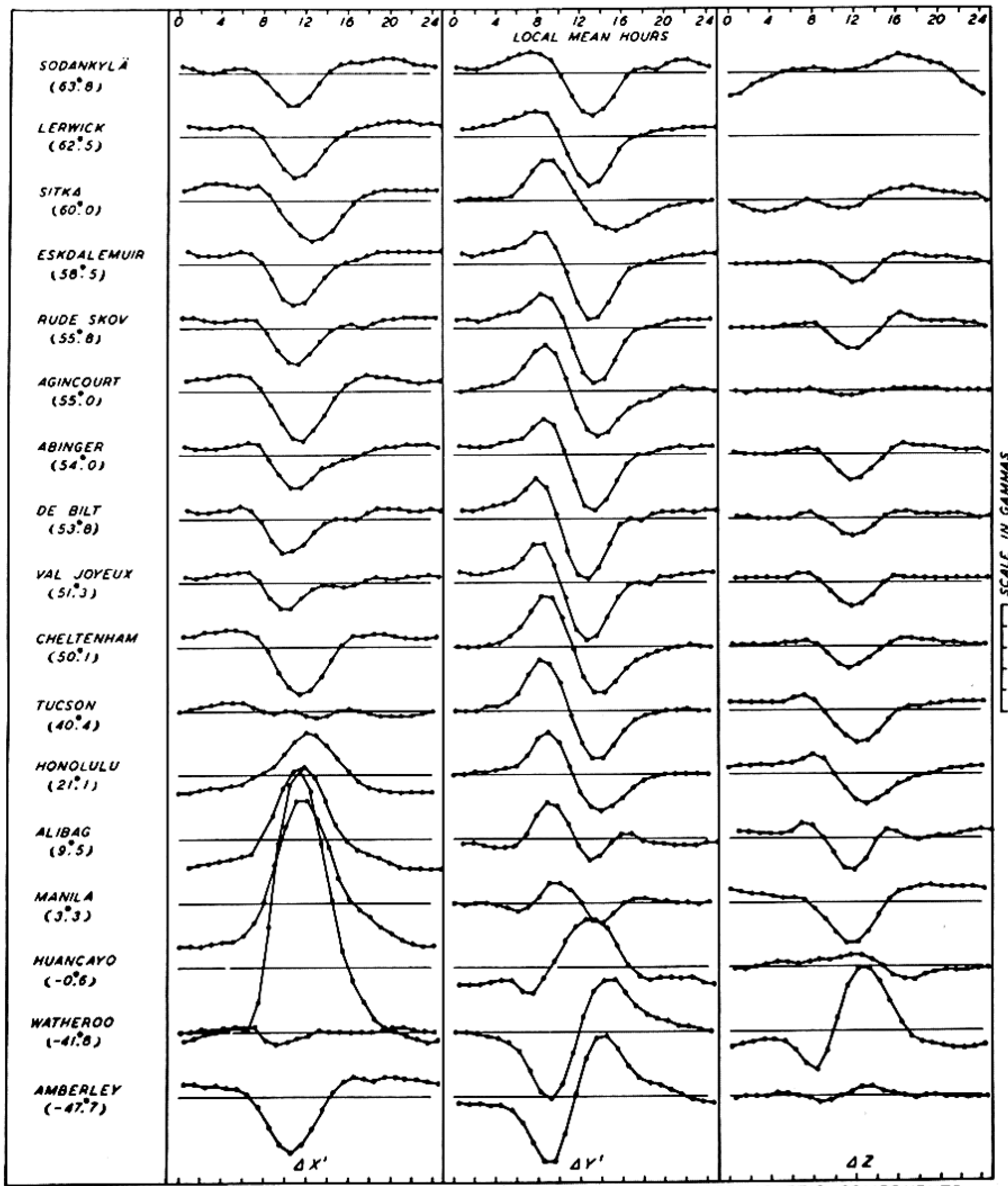

FIG. 56—SOLAR DAILY VARIATION ON QUIET DAYS (S_q), VARIOUS STATIONS, GEOMAGNETIC COMPONENTS, MARCH, 1922-33 (GEOMAGNETIC LATITUDES INDICATED IN PARENTHESES)

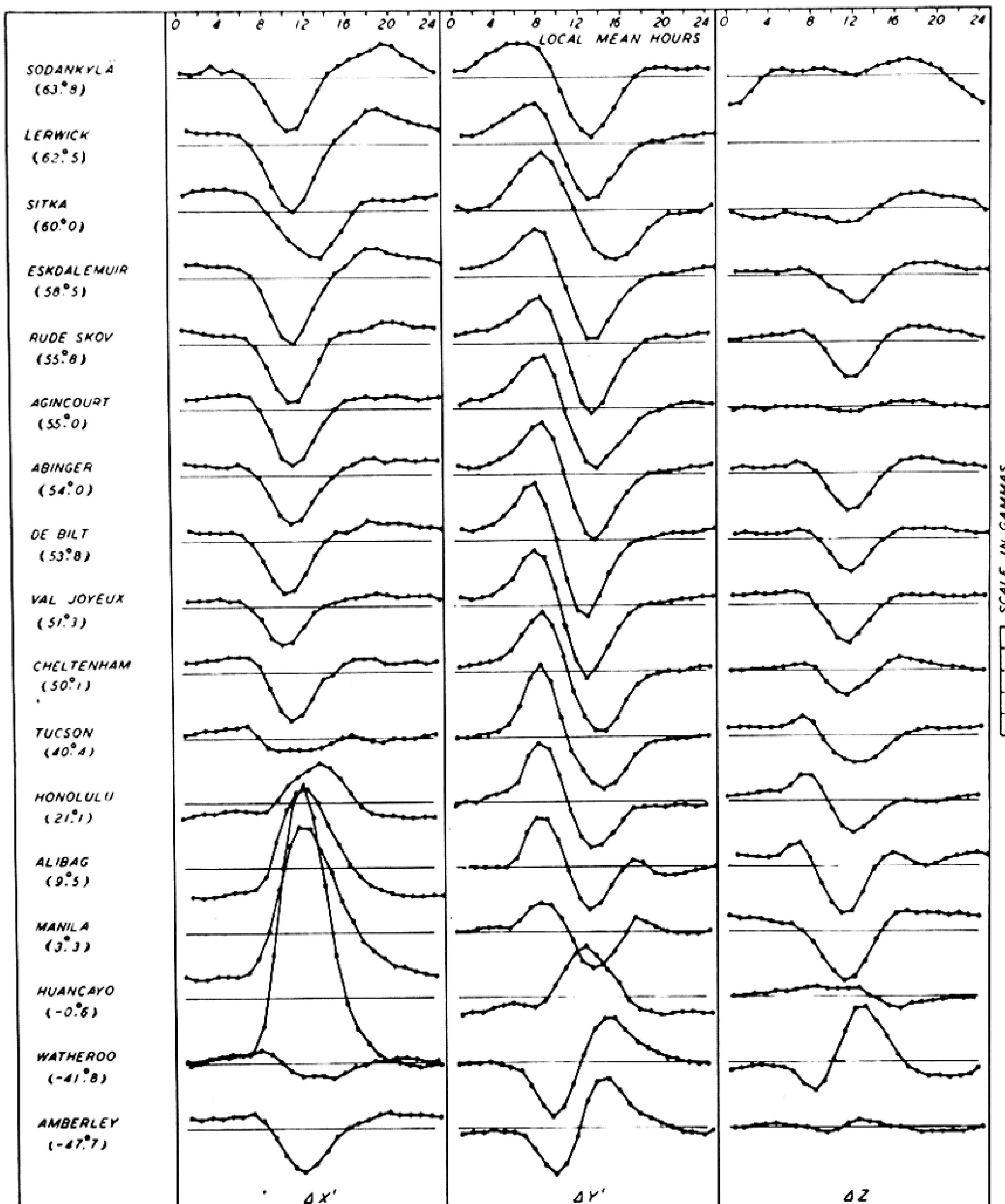

FIG. 57—SOLAR DAILY VARIATION ON QUIET DAYS (Sq), VARIOUS STATIONS, GEOMAGNETIC COMPONENTS, APRIL, 1922-33 (GEOMAGNETIC LATITUDES INDICATED IN PARENTHESES)

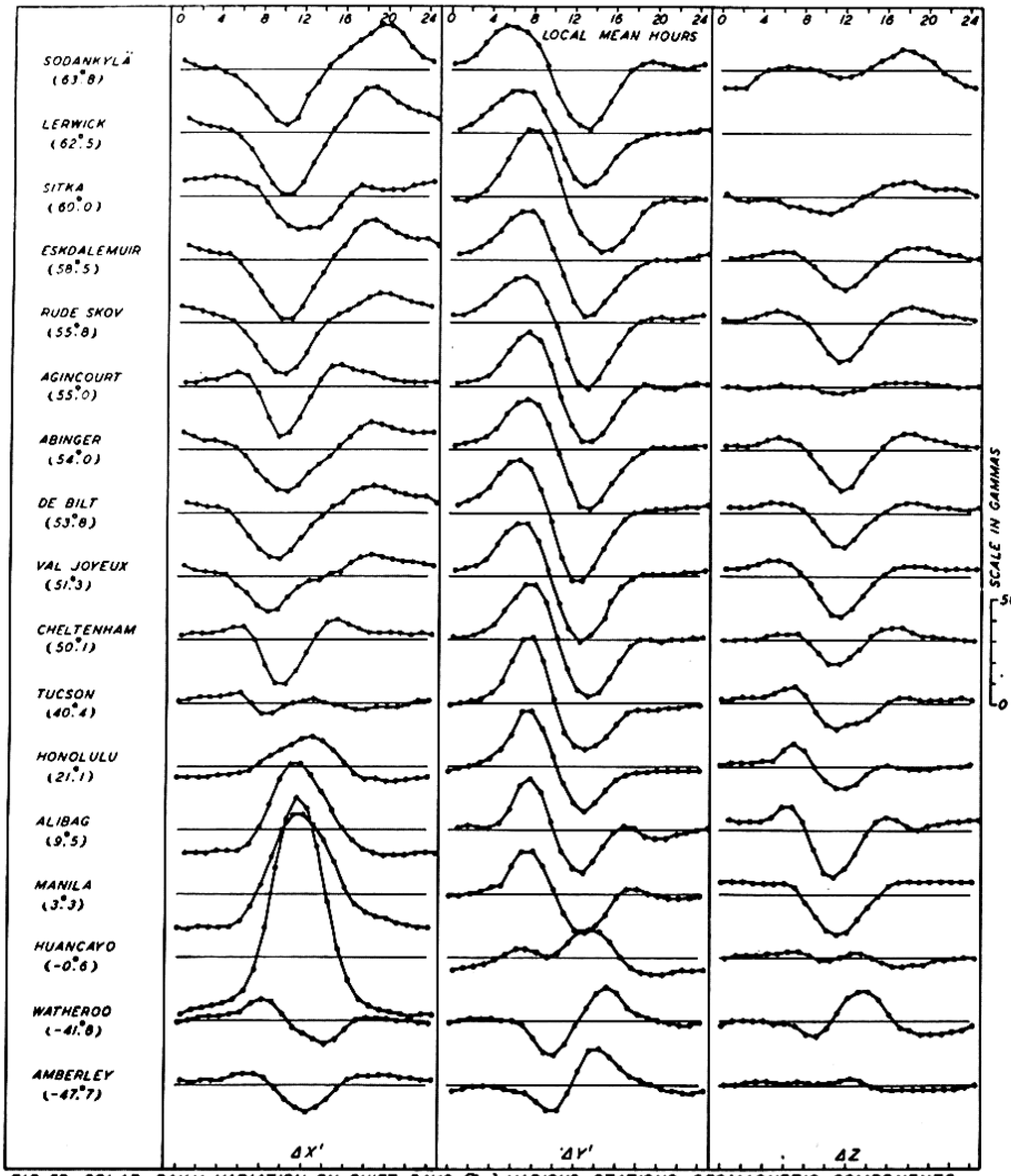

FIG. 58—SOLAR DAILY VARIATION ON QUIET DAYS (Sq), VARIOUS STATIONS, GEOMAGNETIC COMPONENTS, MAY, 1922-33 (GEOMAGNETIC LATITUDES INDICATED IN PARENTHESES)

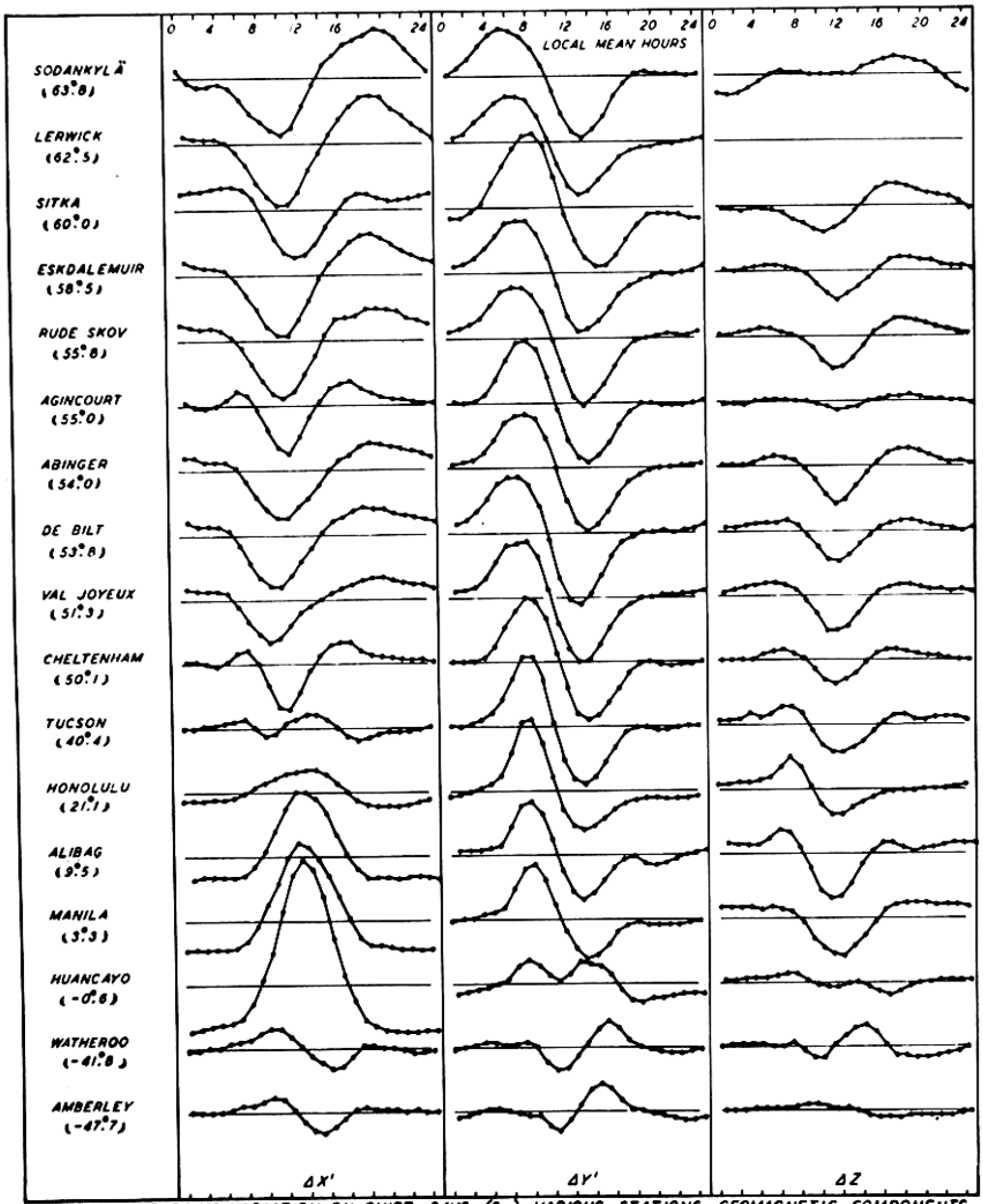

FIG. 59—SOLAR DAILY VARIATION ON QUIET DAYS (Sq), VARIOUS STATIONS, GEOMAGNETIC COMPONENTS, JUNE, 1922-33 (GEOMAGNETIC LATITUDES INDICATED IN PARENTHESES)

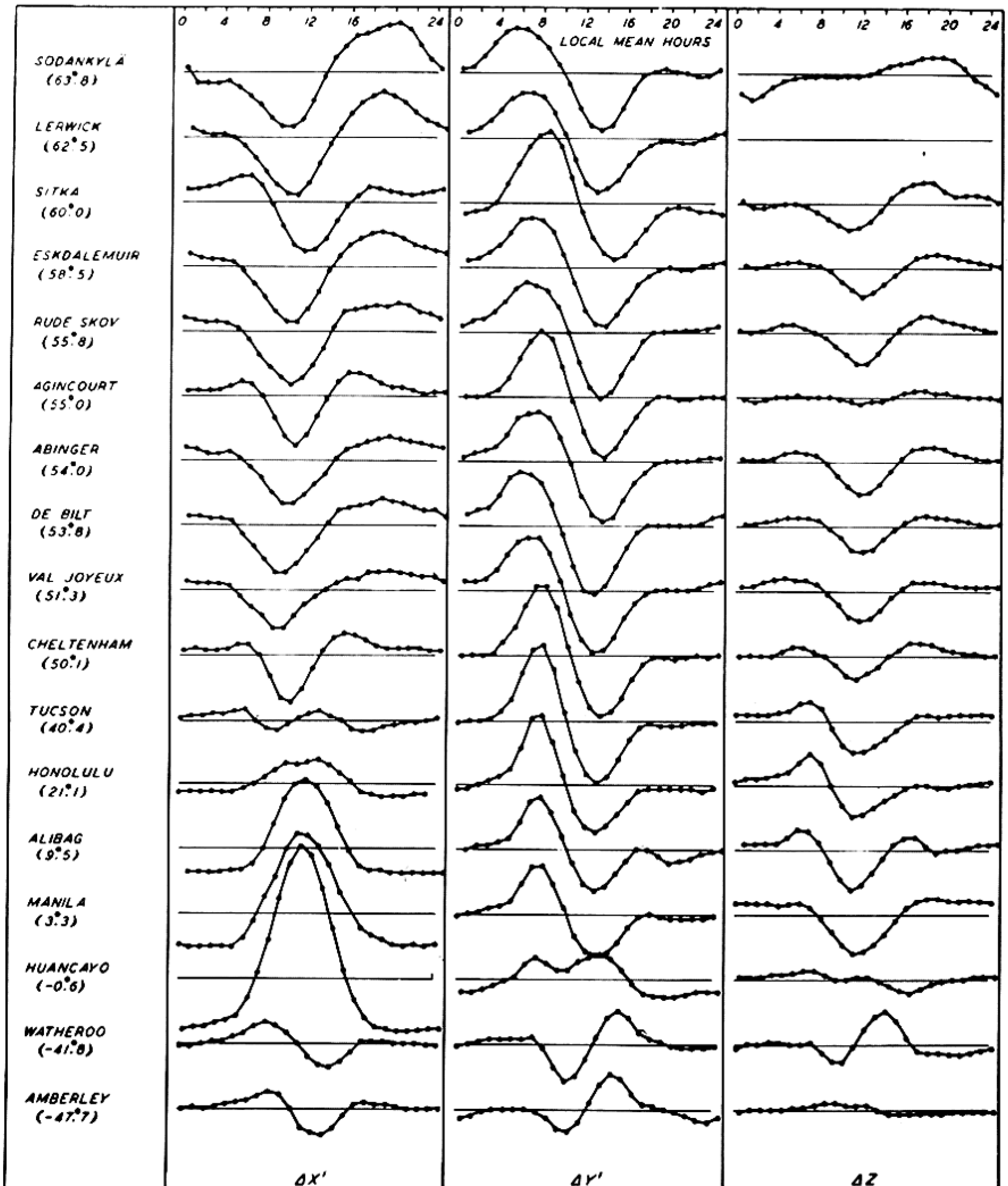

FIG. 60—SOLAR DAILY VARIATION ON QUIET DAYS (Sq), VARIOUS STATIONS, GEOMAGNETIC COMPONENTS, JULY, 1922-33 (GEOMAGNETIC LATITUDES INDICATED IN PARENTHESES)

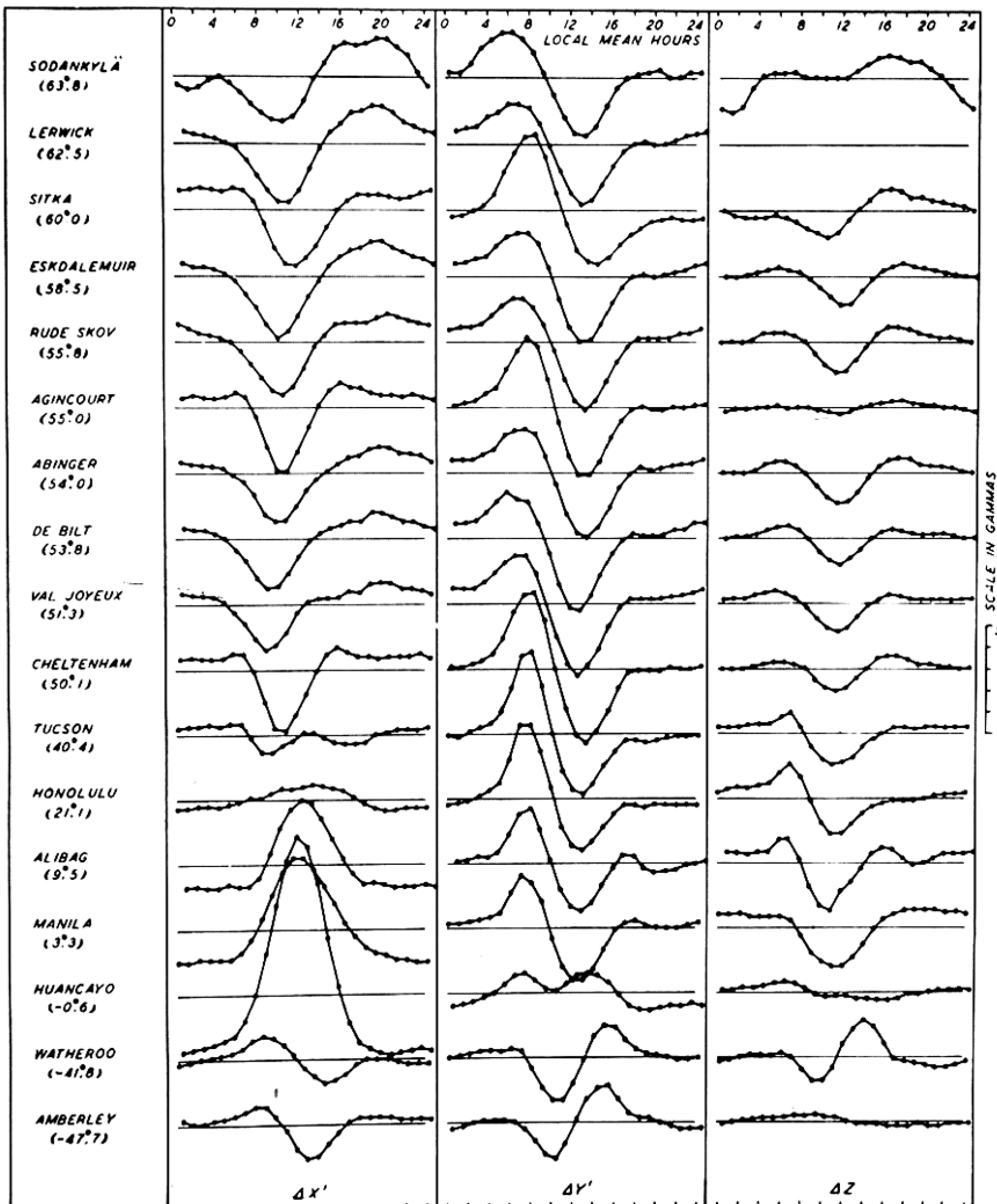

FIG.61—SOLAR DAILY VARIATION ON QUIET DAYS (S_q). VARIOUS STATIONS, GEOMAGNETIC COMPONENTS, AUGUST, 1922-33 (GEOMAGNETIC LATITUDES INDICATED IN PARENTHESES)

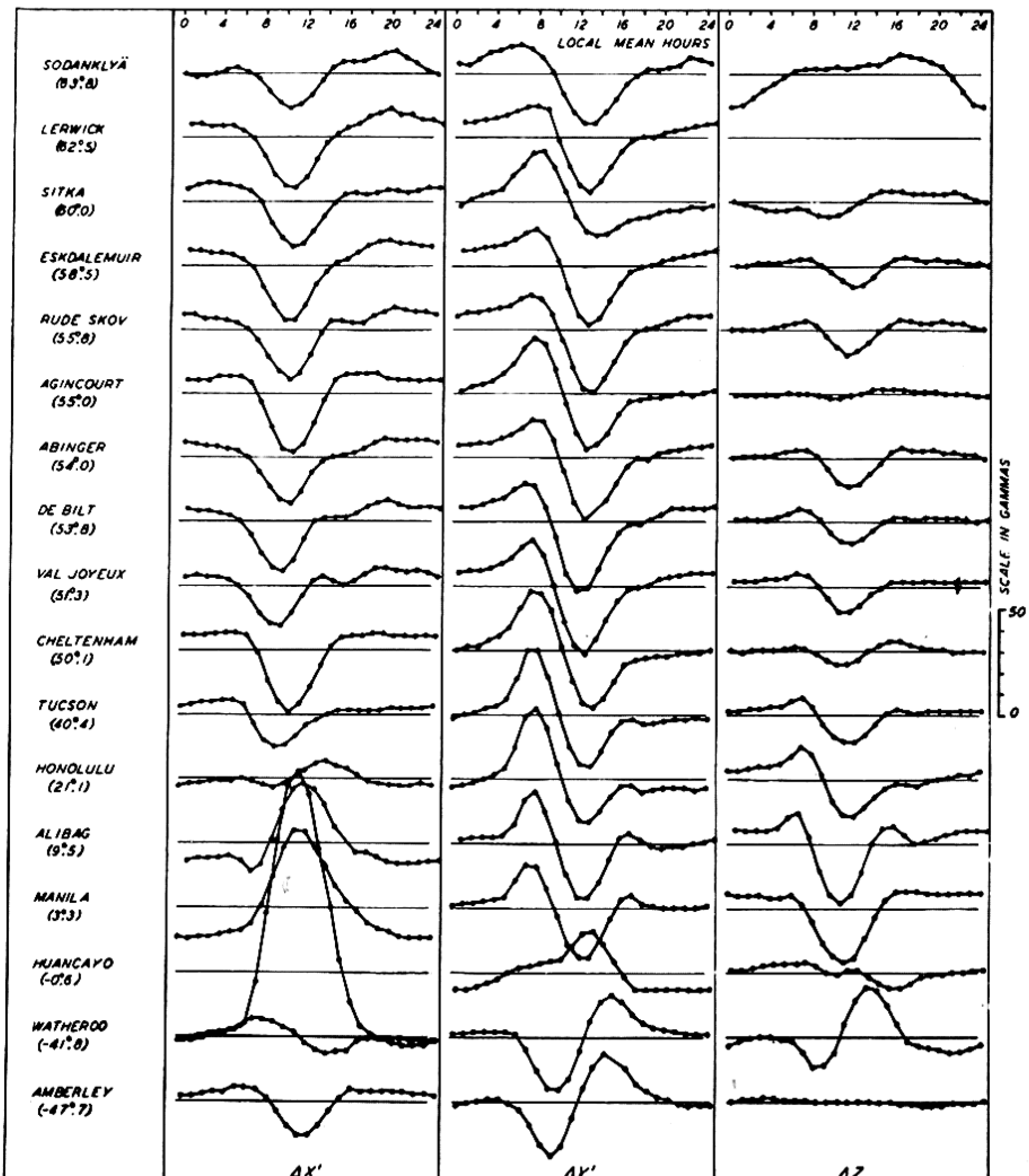

FIG. 62—SOLAR DAILY VARIATION ON QUIET DAYS (Sq), VARIOUS STATIONS, GEOMAGNETIC COMPONENTS, SEPTEMBER, 1922-33 (GEOMAGNETIC LATITUDES INDICATED IN PARENTHESES)

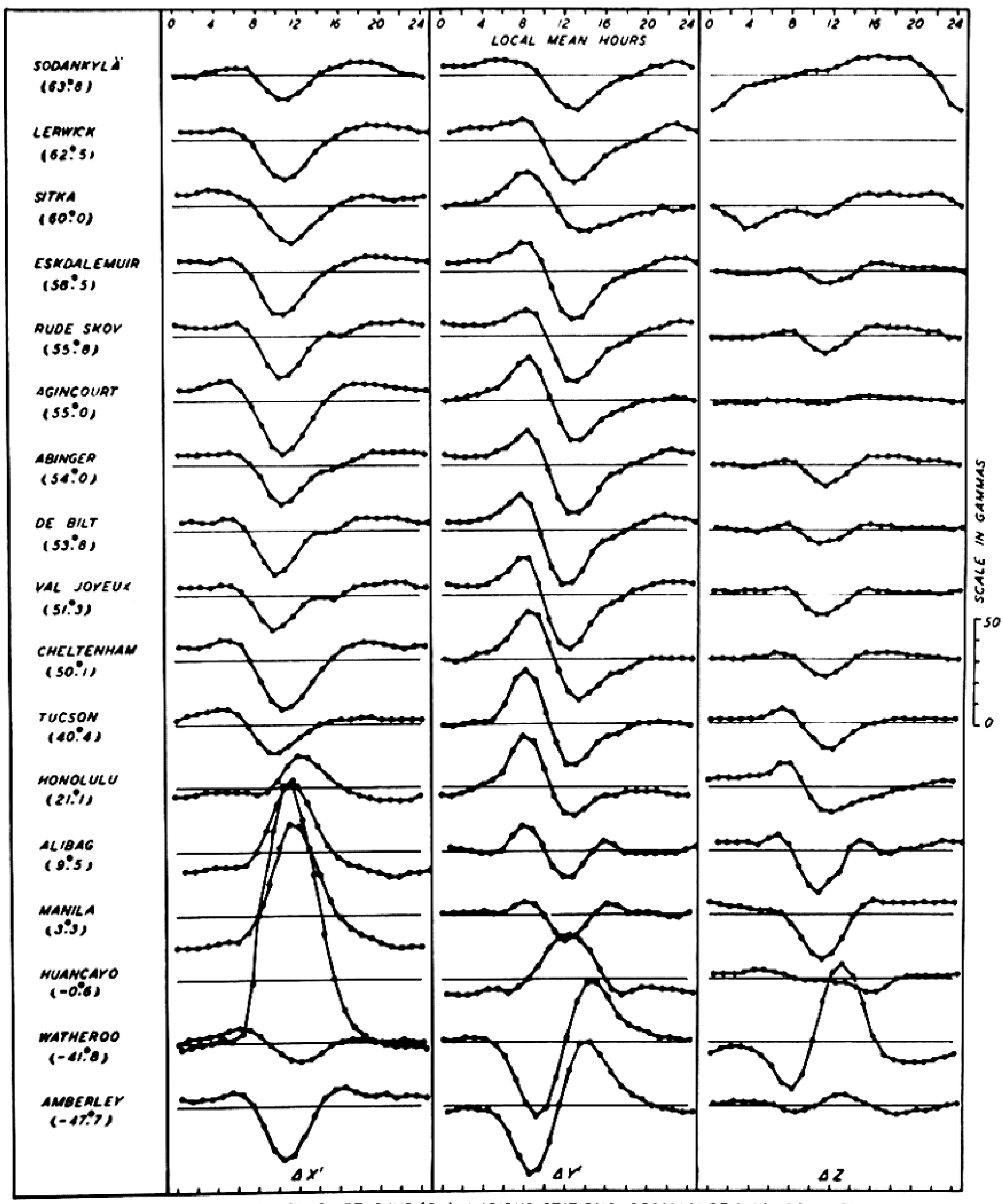

FIG. 63—SOLAR DAILY VARIATION ON QUIET DAYS (S_q), VARIOUS STATIONS, GEOMAGNETIC COMPONENTS, OCTOBER, 1922-33 (GEOMAGNETIC LATITUDES INDICATED IN PARENTHESES)

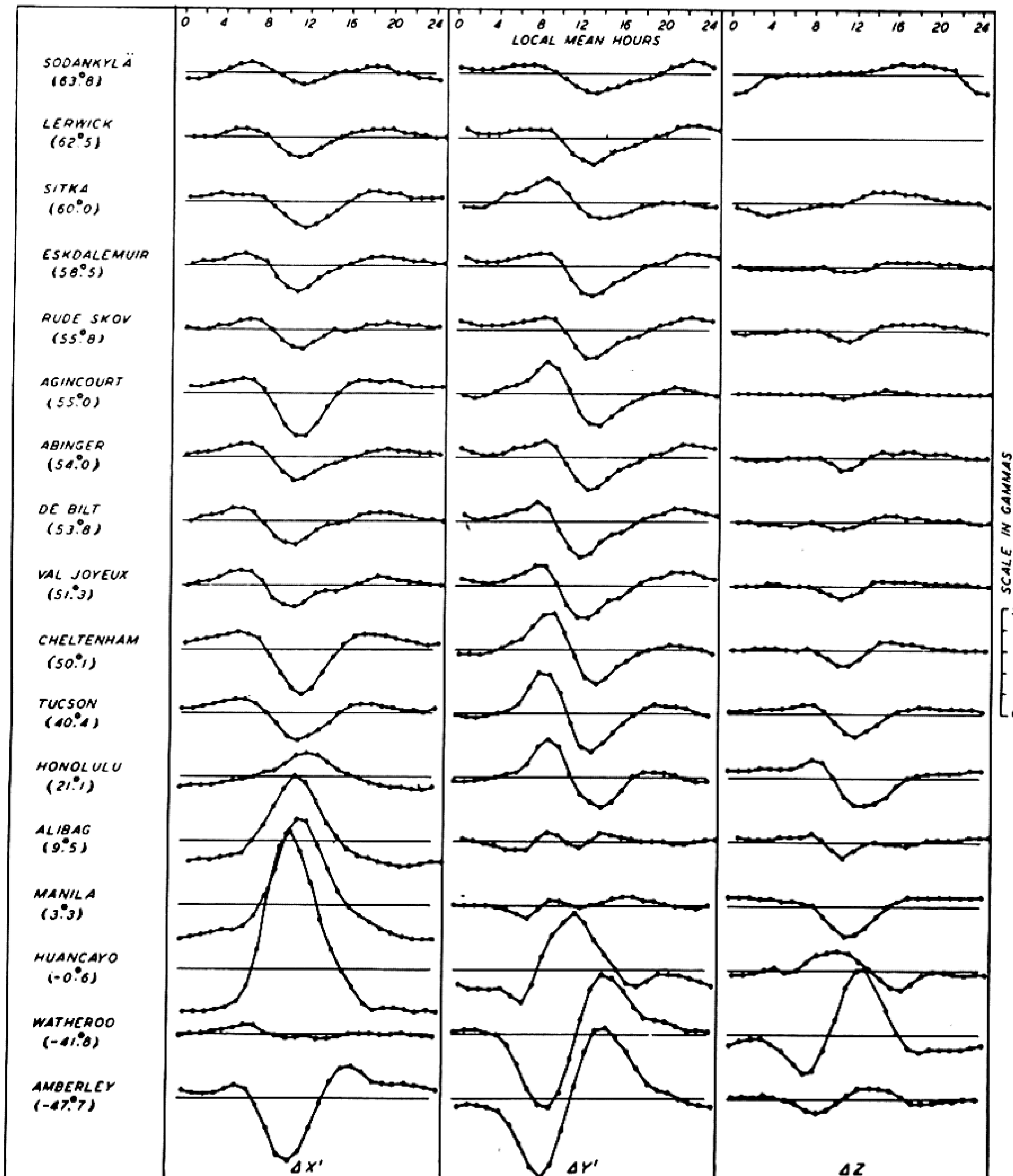

FIG. 64—SOLAR DAILY VARIATION ON QUIET DAYS (Sq), VARIOUS STATIONS, GEOMAGNETIC COMPONENTS, NOVEMBER, 1922-33 (GEOMAGNETIC LATITUDES INDICATED IN PARENTHESES)

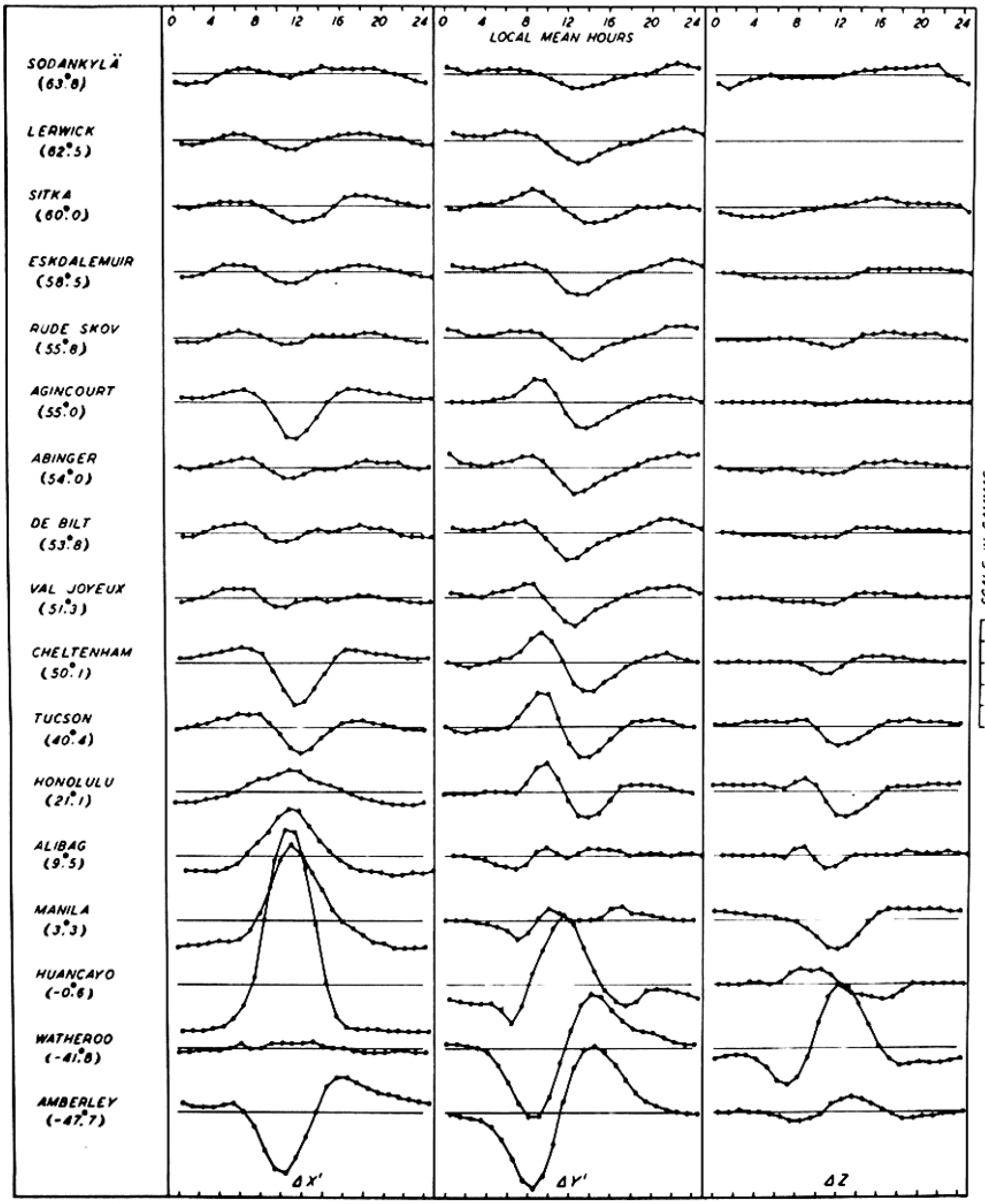

FIG. 65—SOLAR DAILY VARIATION ON QUIET DAYS (Sq), VARIOUS STATIONS, GEOMAGNETIC COMPONENTS, DECEMBER, 1922–33 (GEOMAGNETIC LATITUDES INDICATED IN PARENTHESES)

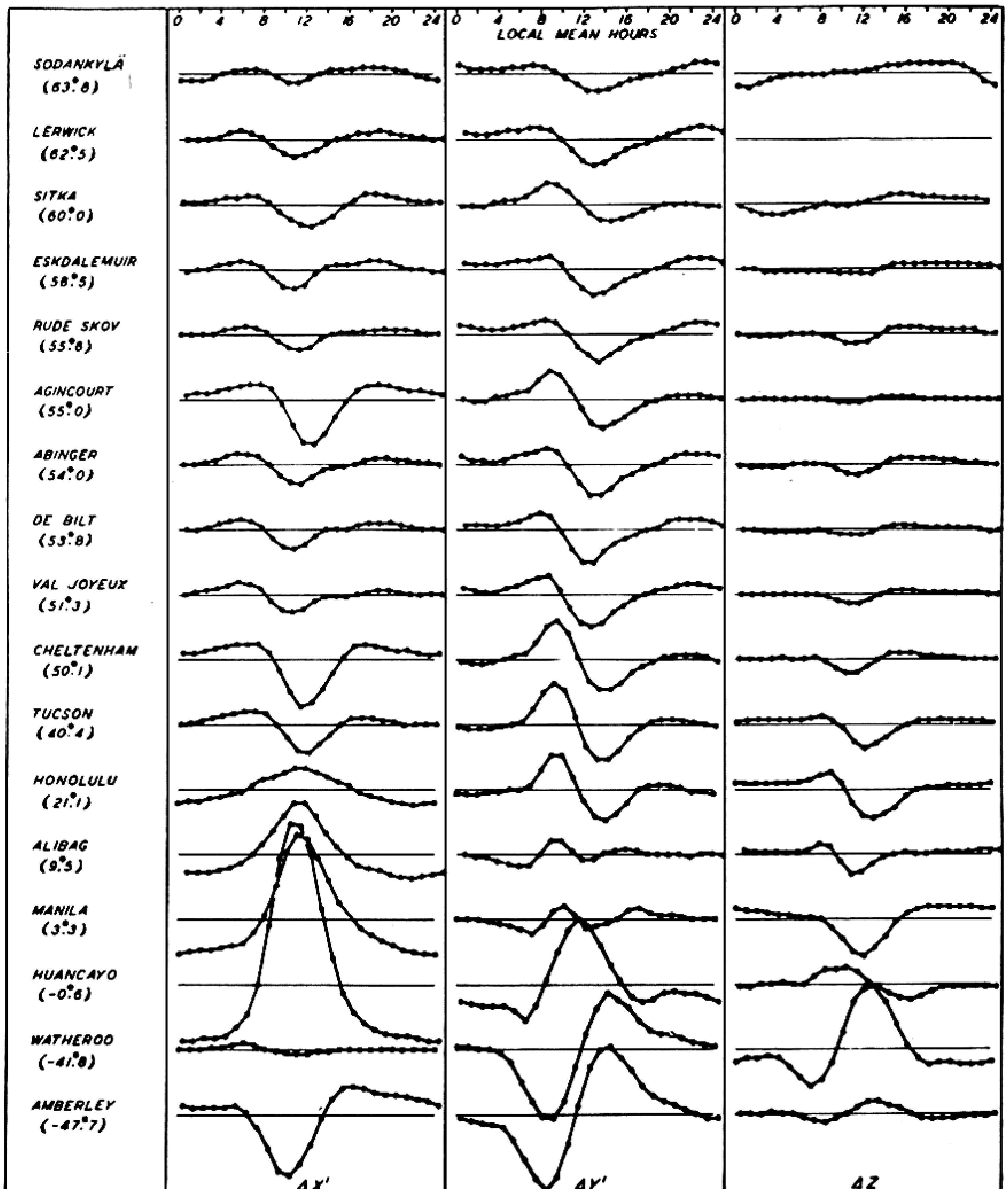

FIG. 66—SOLAR DAILY VARIATION ON QUIET DAYS (Sq), VARIOUS STATIONS, GEOMAGNETIC COMPONENTS, WINTER, 1922–33 (GEOMAGNETIC LATITUDES INDICATED IN PARENTHESES)

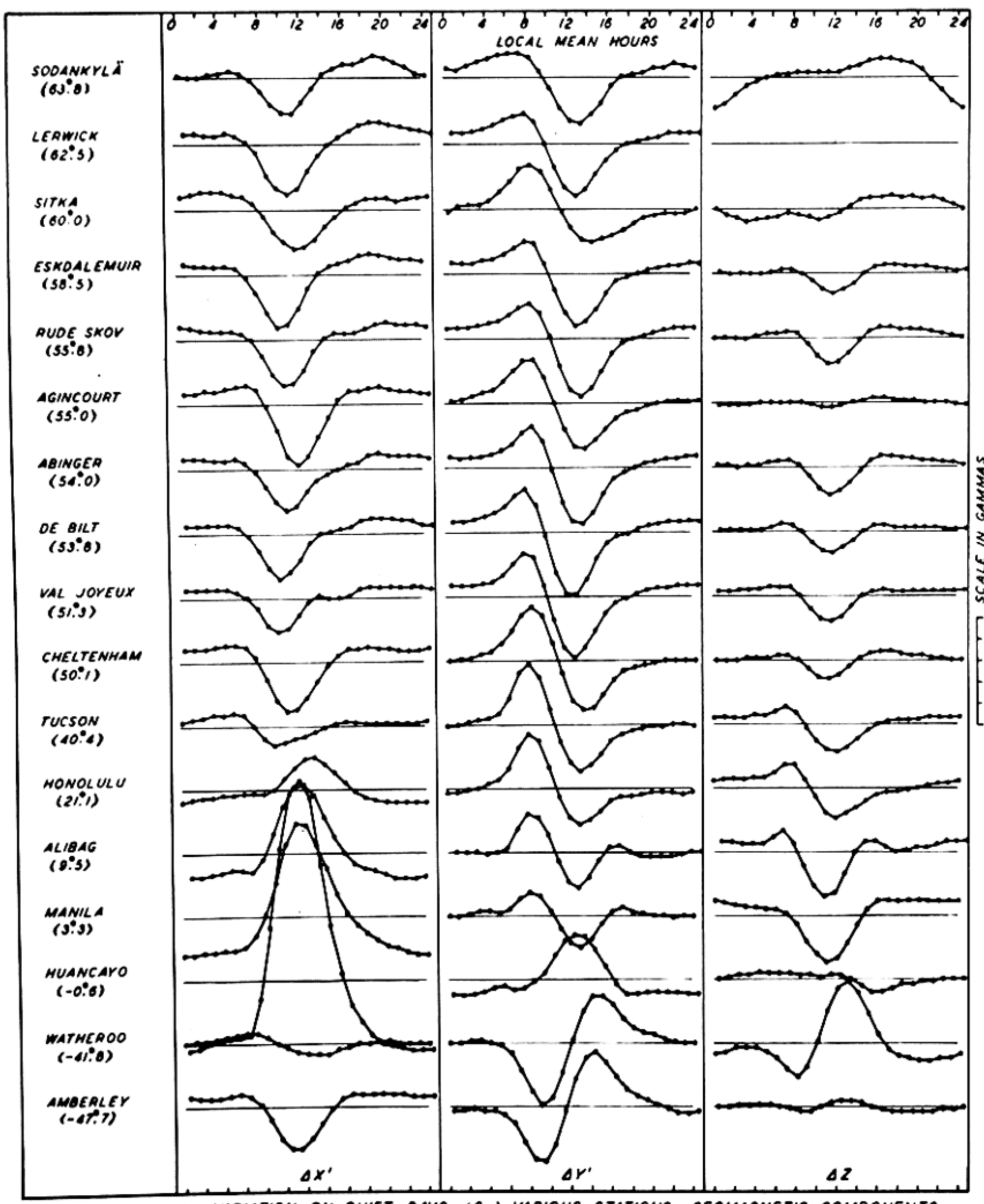

FIG.67—SOLAR DAILY VARIATION ON QUIET DAYS (Sq), VARIOUS STATIONS, GEOMAGNETIC COMPONENTS, EQUINOX, 1922-33 (GEOMAGNETIC LATITUDES INDICATED IN PARENTHESES)

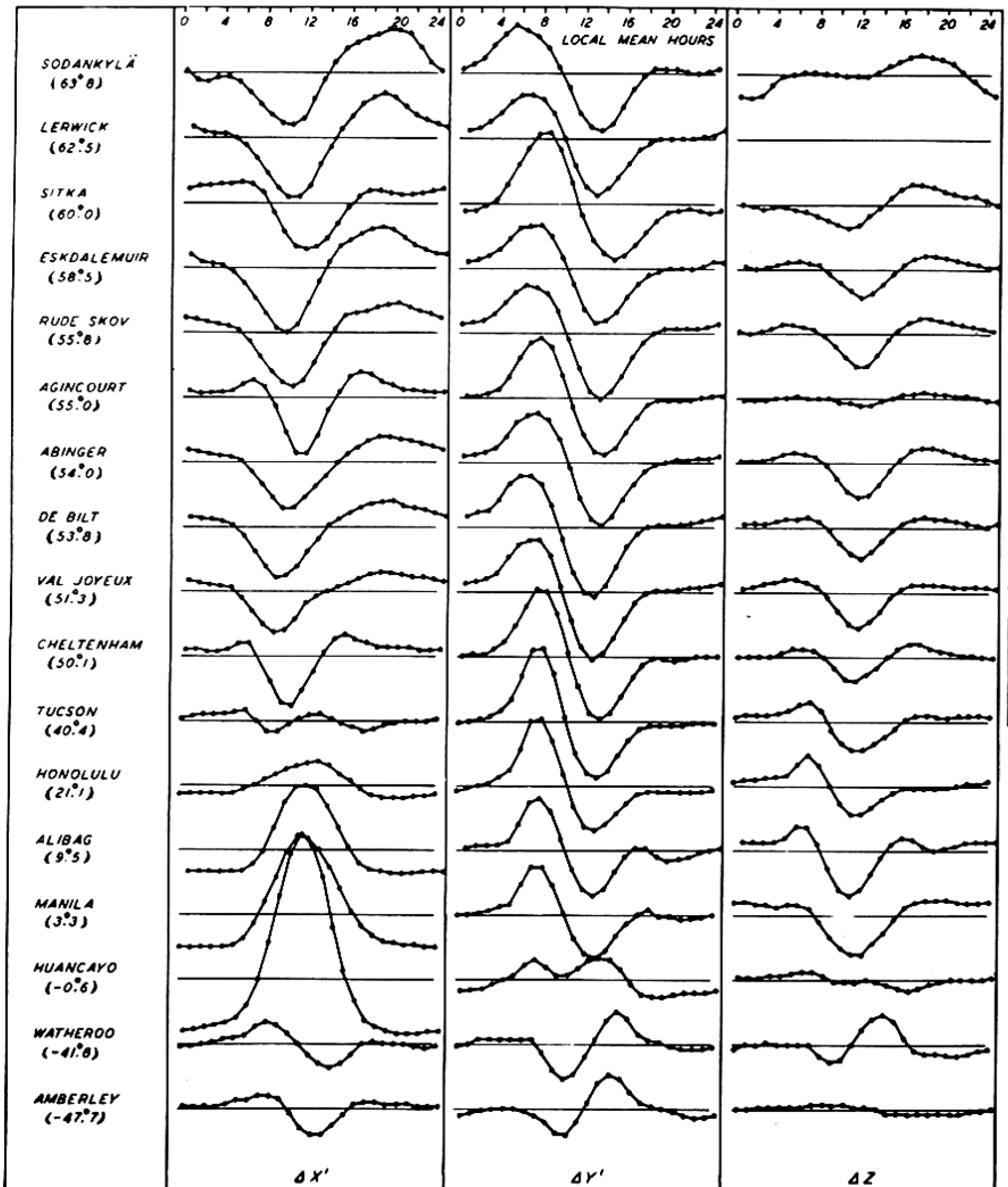

FIG. 68—SOLAR DAILY VARIATION ON QUIET DAYS (Sq), VARIOUS STATIONS, GEOMAGNETIC COMPONENTS, SUMMER, 1922-33 (GEOMAGNETIC LATITUDES INDICATED IN PARENTHESES)

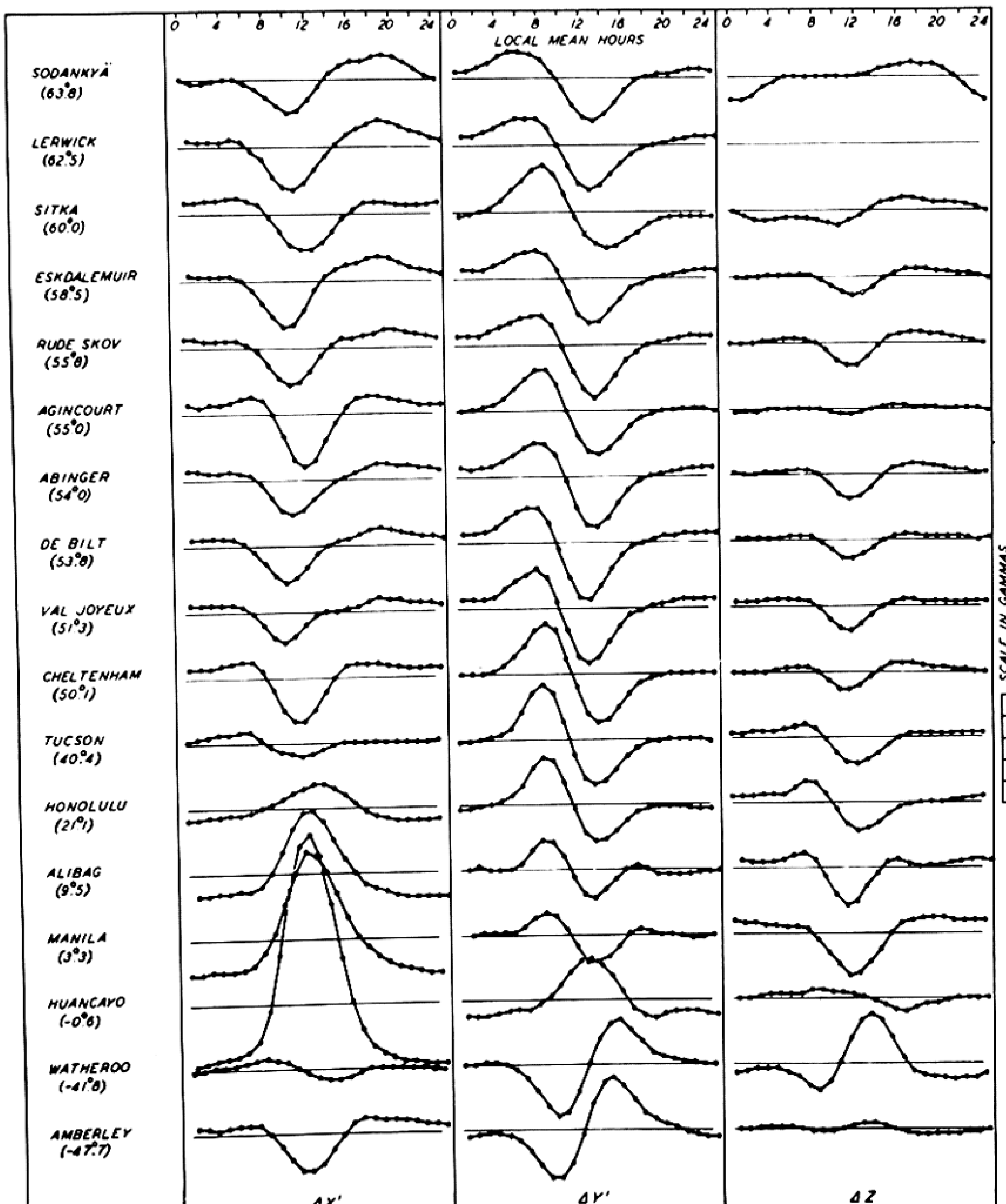

FIG. 69—SOLAR DAILY VARIATION ON QUIET DAYS (Sq), VARIOUS STATIONS, GEOMAGNETIC COMPONENTS, YEAR, 1922-33 (GEOMAGNETIC LATITUDES INDICATED IN PARENTHESES)

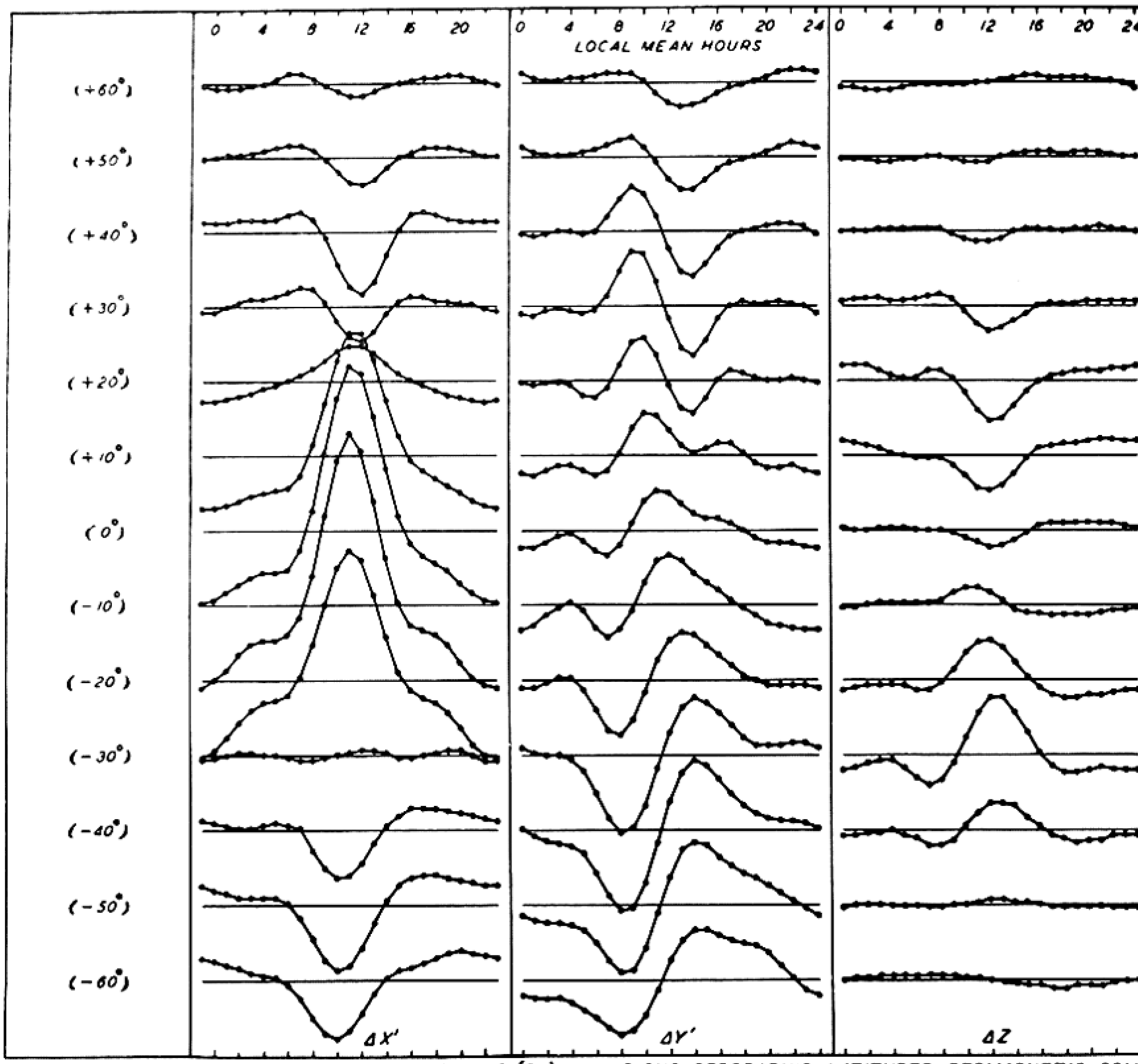

FIG. 70—SOLAR DAILY VARIATION ON QUIET DAYS (Sq), IN VARIOUS GEOGRAPHIC LATITUDES, GEOMAGNETIC COMPONENTS, JANUARY, 1922-33

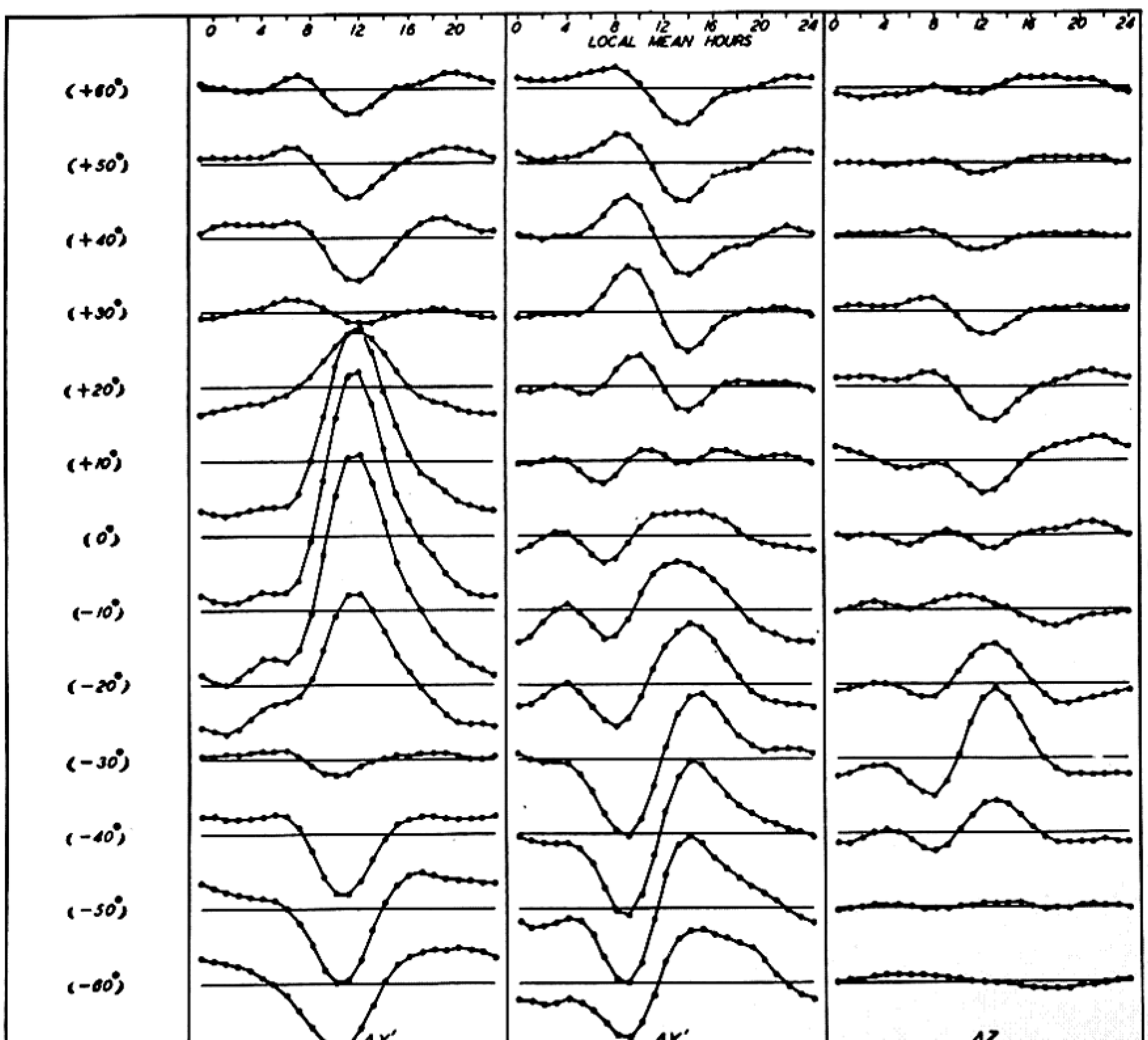

FIG. 71—SOLAR DAILY VARIATION ON QUIET DAYS (Sq), IN VARIOUS GEOGRAPHIC LATITUDES, GEOMAGNETIC COMPONENTS, FEBRUARY, 1922-33

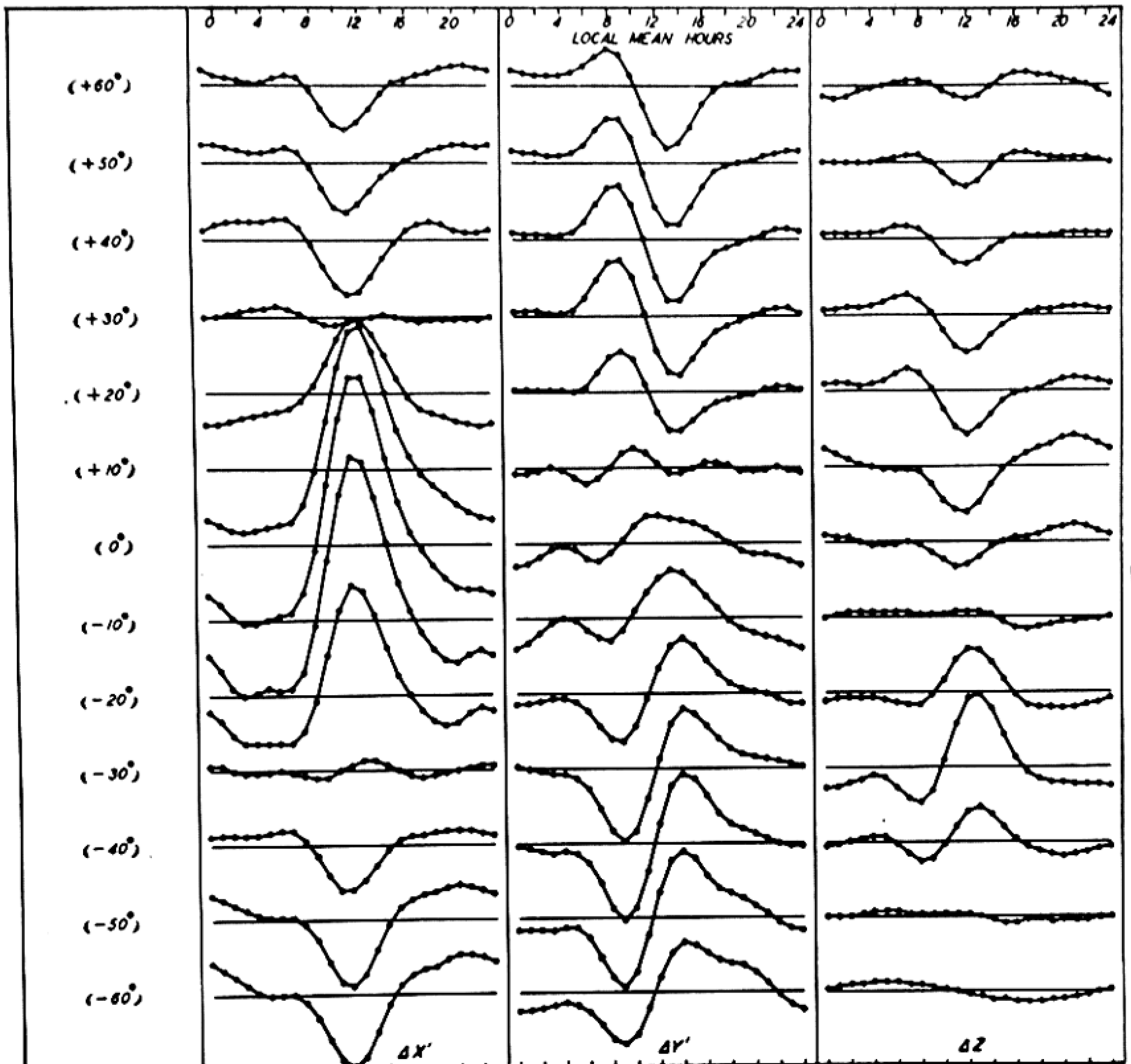

FIG. 72—SOLAR DAILY VARIATION ON QUIET DAYS (Sq), IN VARIOUS GEOGRAPHIC LATITUDES, GEOMAGNETIC COMPONENTS, MARCH, 1922-33

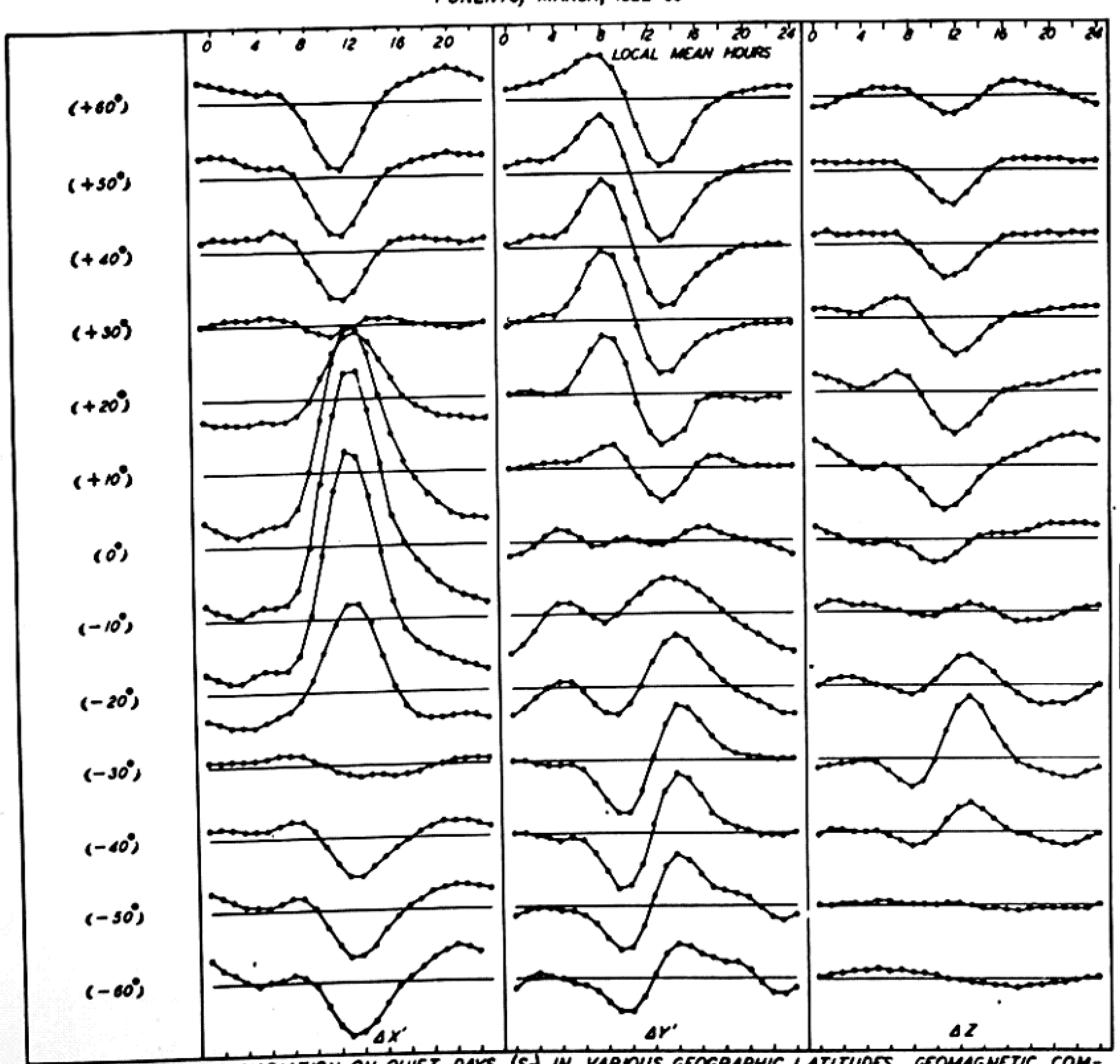

FIG 73—SOLAR DAILY VARIATION ON QUIET DAYS (Sq), IN VARIOUS GEOGRAPHIC LATITUDES, GEOMAGNETIC COMPONENTS, APRIL, 1922-33

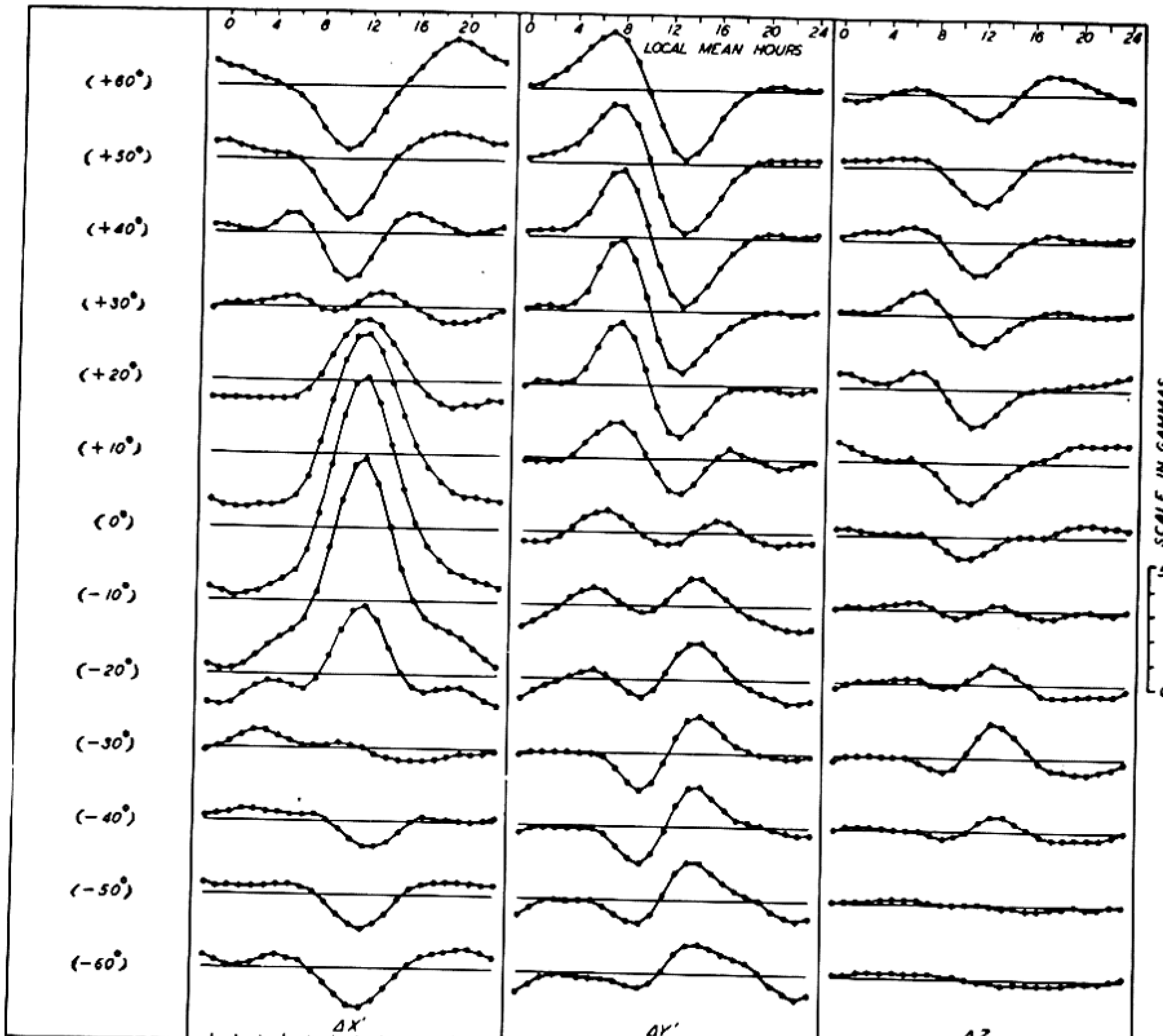

FIG. 74—SOLAR DAILY VARIATION ON QUIET DAYS (S_q), IN VARIOUS GEOGRAPHIC LATITUDES, GEOMAGNETIC COMPONENTS, MAY, 1922-33

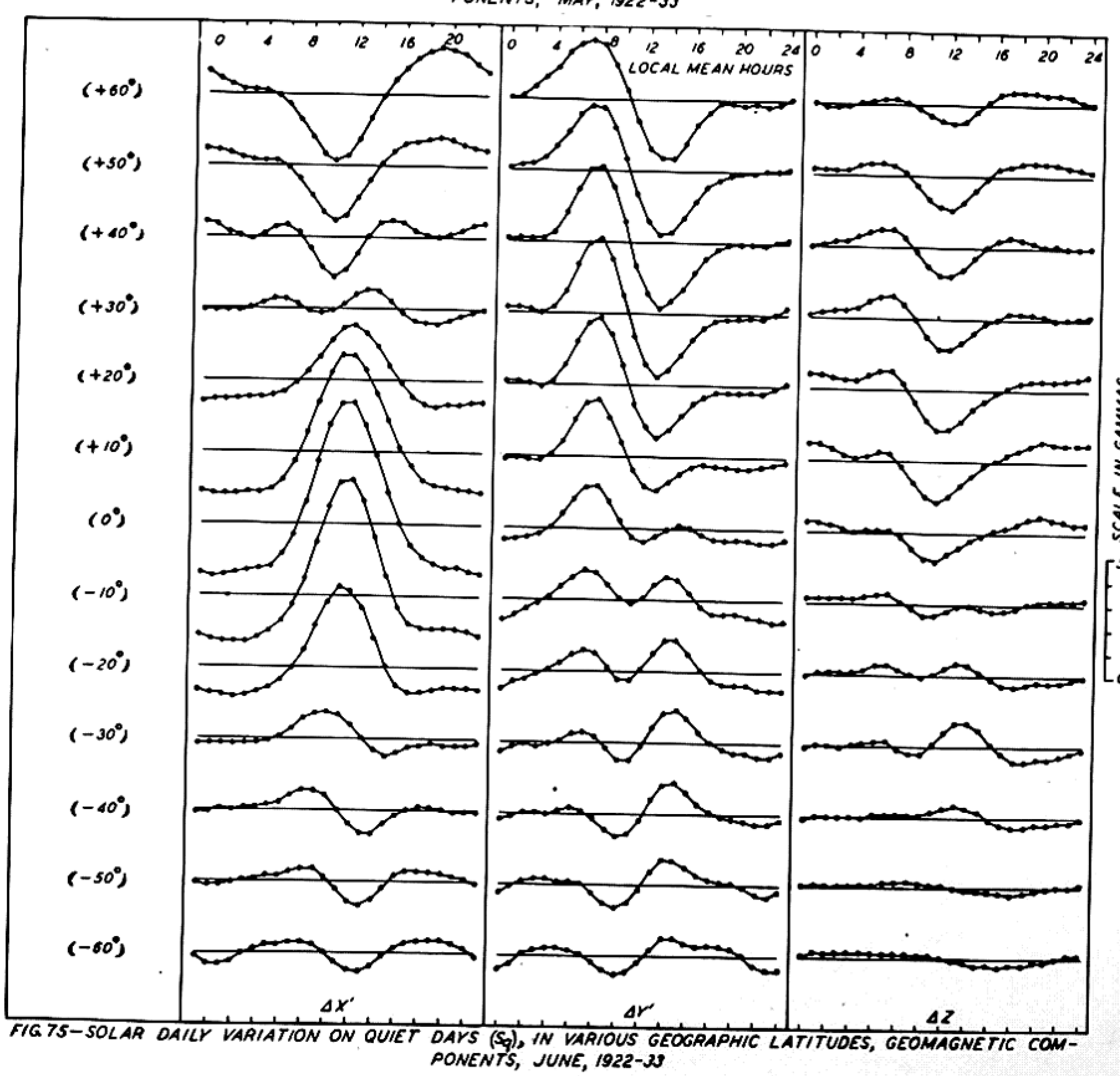

FIG. 75—SOLAR DAILY VARIATION ON QUIET DAYS (S_q), IN VARIOUS GEOGRAPHIC LATITUDES, GEOMAGNETIC COMPONENTS, JUNE, 1922-33

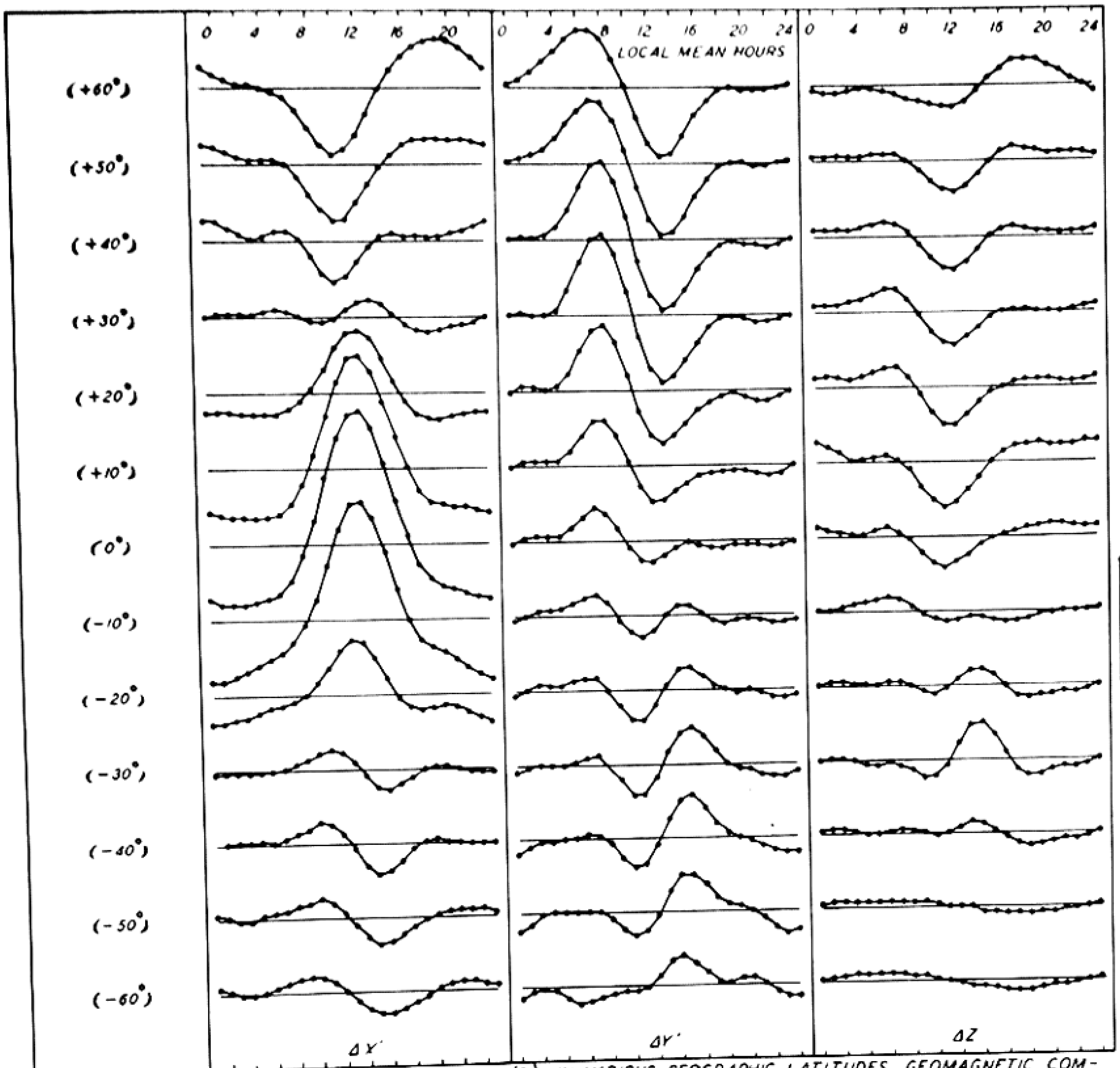

FIG 76—SOLAR DAILY VARIATION ON QUIET DAYS (S_q), IN VARIOUS GEOGRAPHIC LATITUDES, GEOMAGNETIC COMPONENTS, JULY, 1922-33

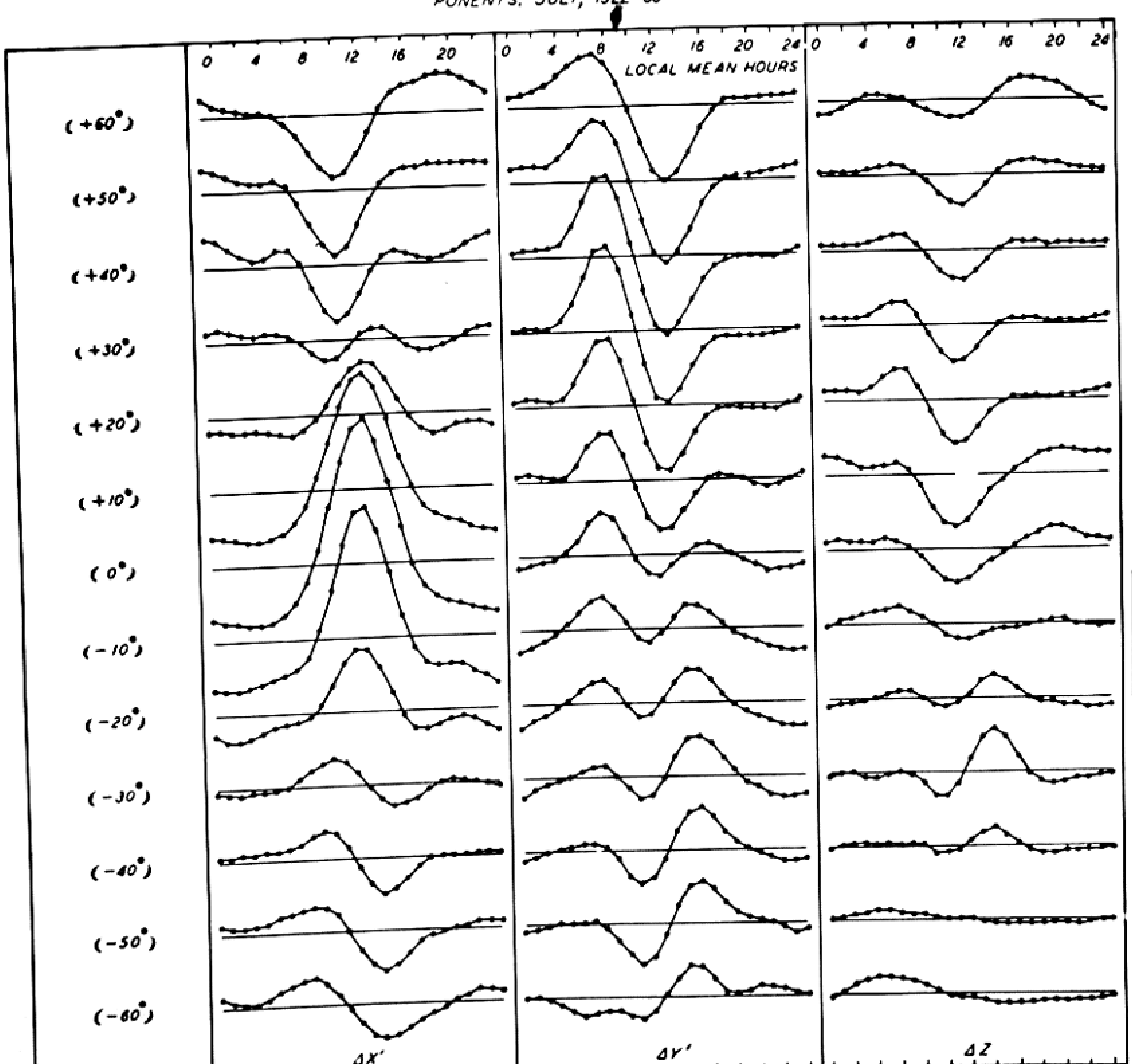

FIG. 77—SOLAR DAILY VARIATION ON QUIET DAYS (S_q), IN VARIOUS GEOGRAPHIC LATITUDES, GEOMAGNETIC COMPONENTS, AUGUST, 1922-33

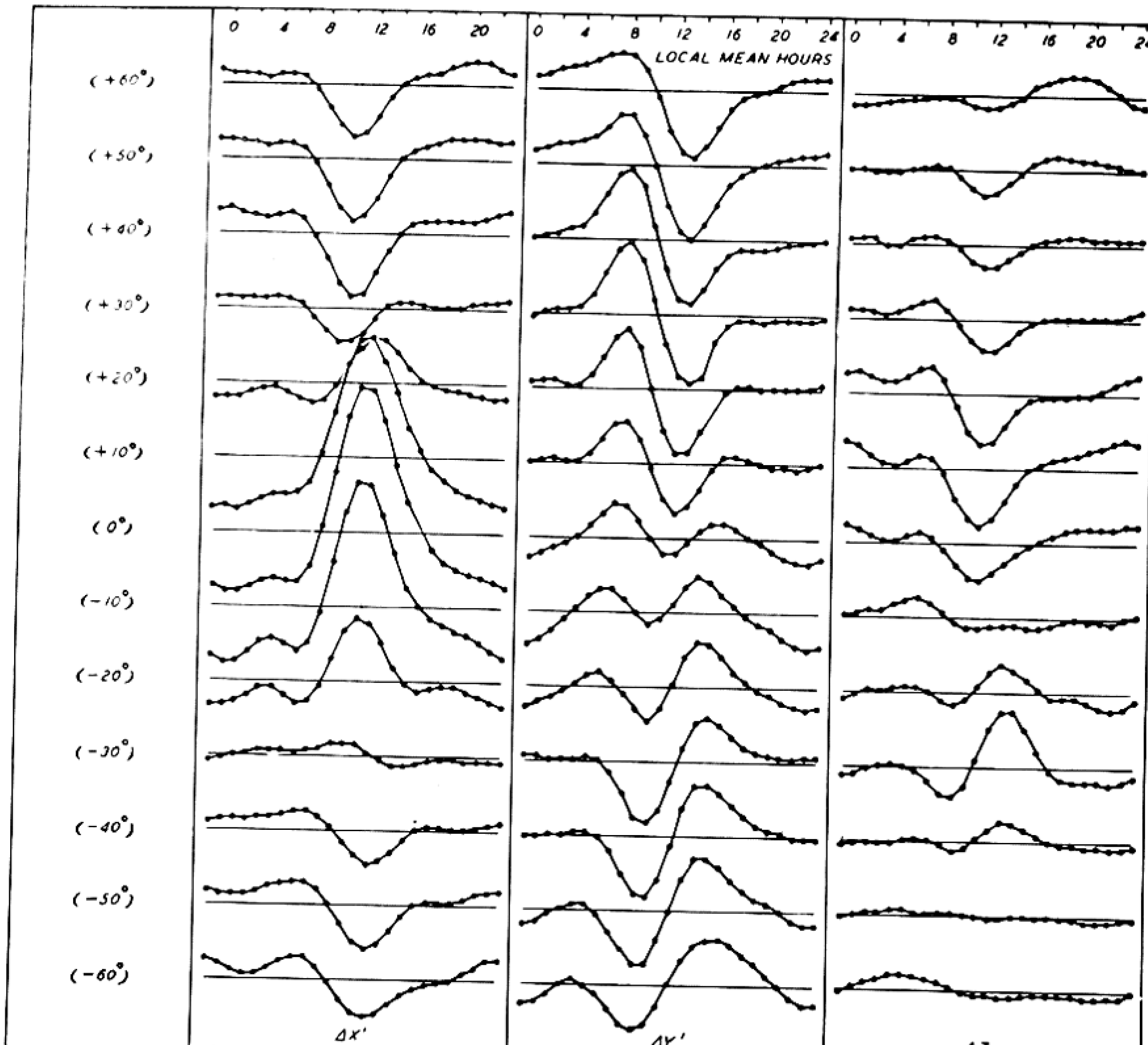

FIG. 78—SOLAR DAILY VARIATION ON QUIET DAYS (S_q), IN VARIOUS GEOGRAPHIC LATITUDES, GEOMAGNETIC COMPONENTS, SEPTEMBER, 1922-33

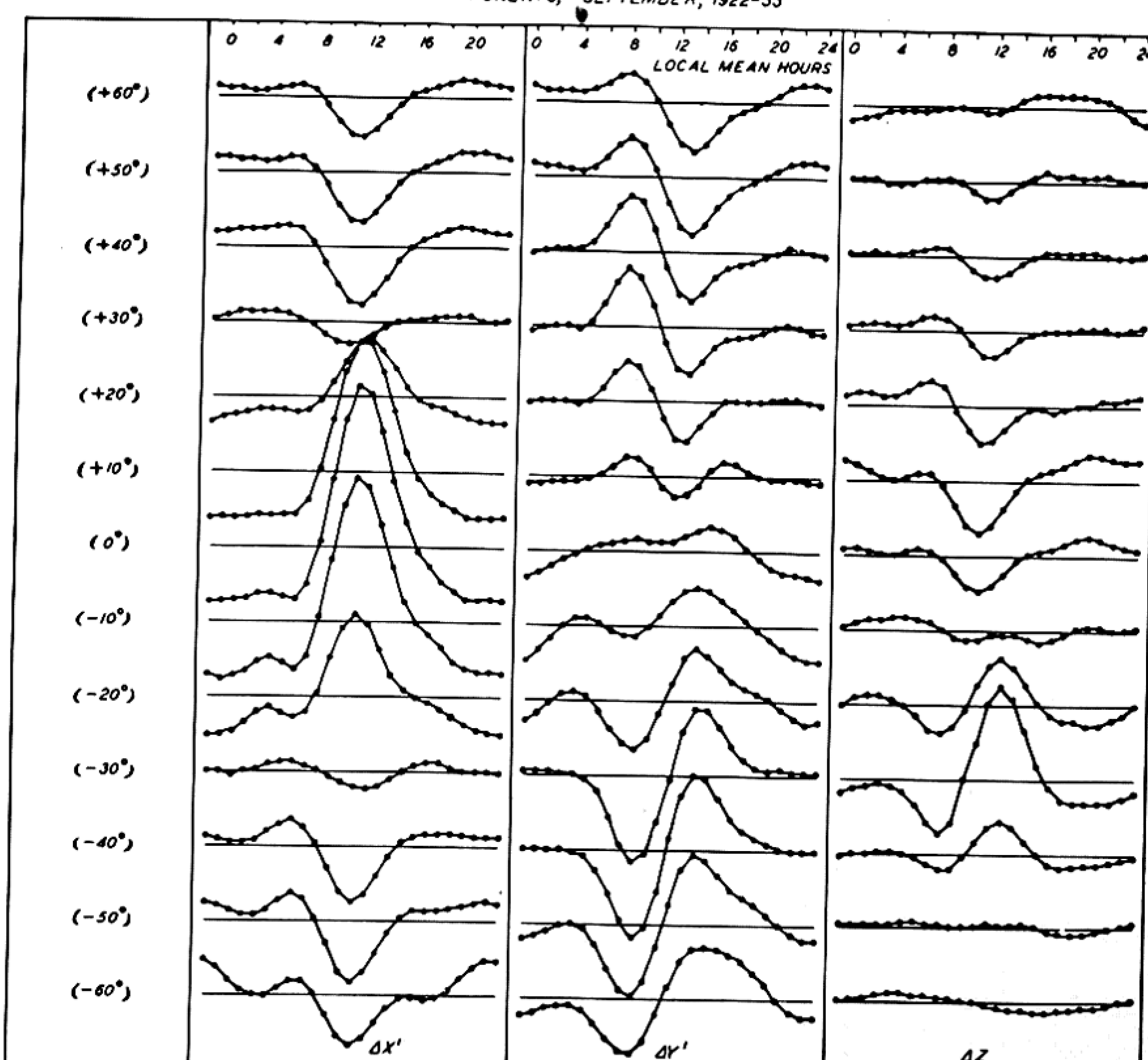

FIG. 79—SOLAR DAILY VARIATION ON QUIET DAYS (S_q), IN VARIOUS GEOGRAPHIC LATITUDES, GEOMAGNETIC COMPONENTS, OCTOBER, 1922-33

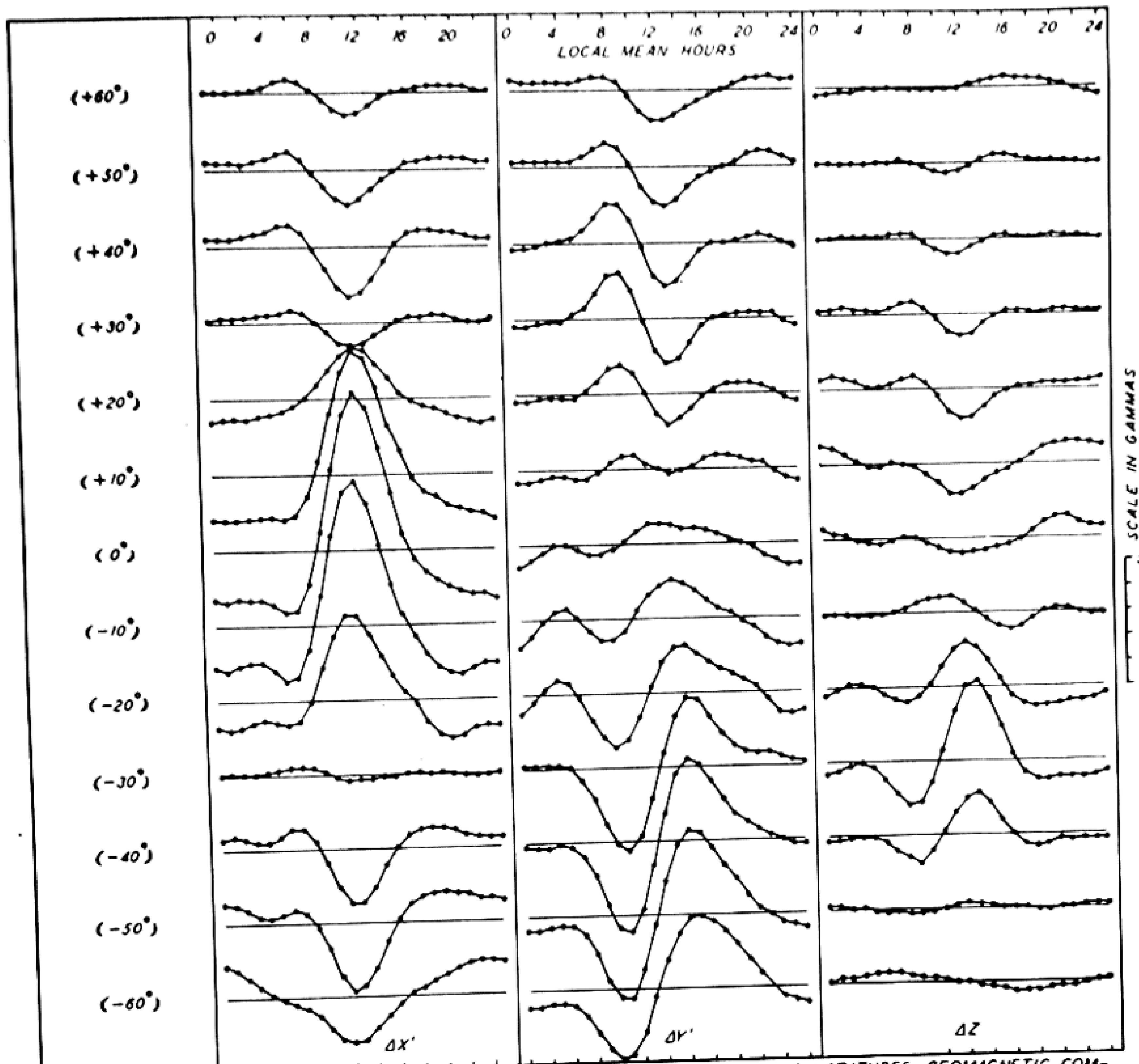

FIG. 80—SOLAR DAILY VARIATION ON QUIET DAYS (S_q), IN VARIOUS GEOGRAPHIC LATITUDES, GEOMAGNETIC COMPONENTS, NOVEMBER, 1922-33

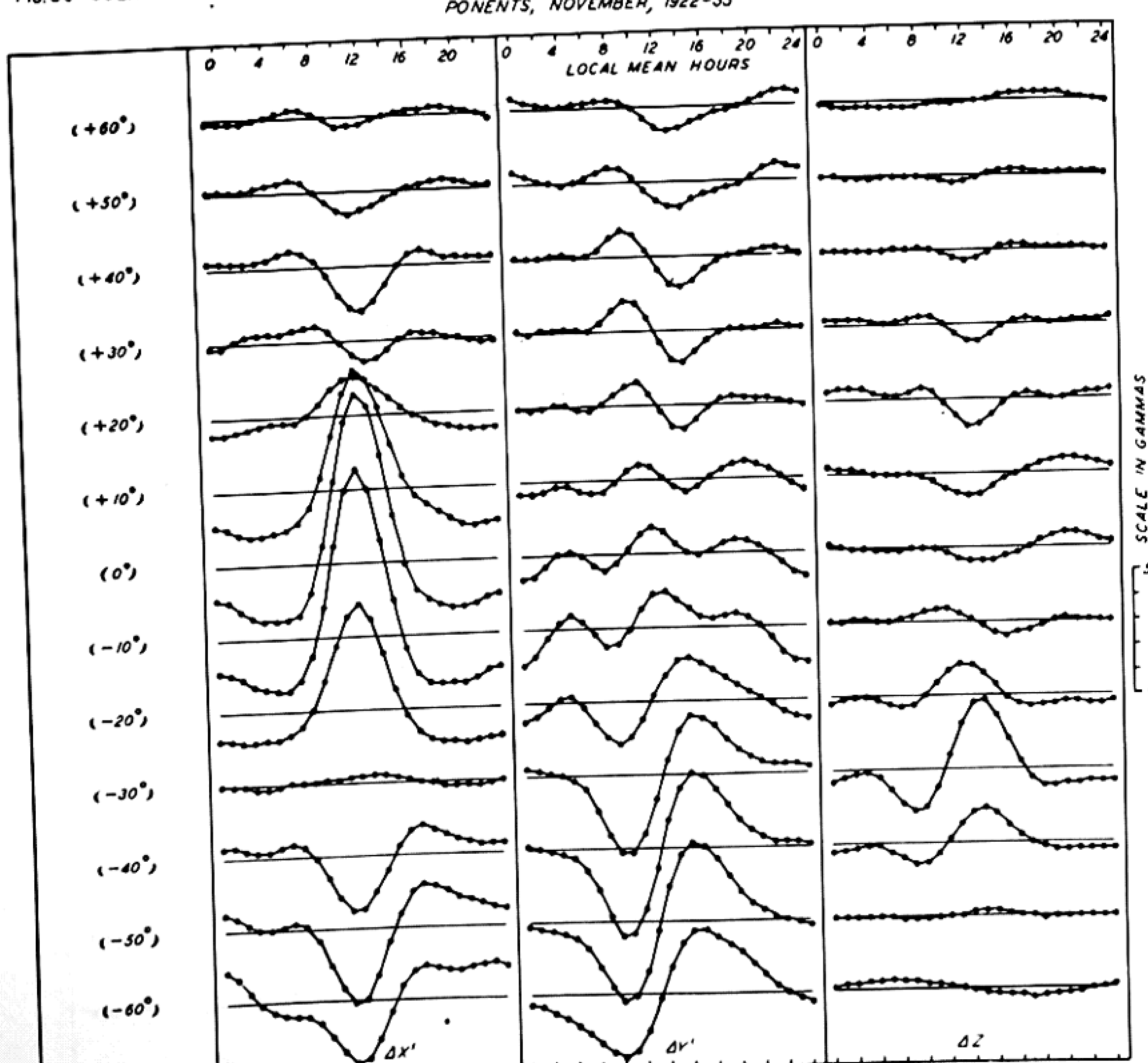

FIG. 81—SOLAR DAILY VARIATION ON QUIET DAYS (S_q), IN VARIOUS GEOGRAPHIC LATITUDES, GEOMAGNETIC COMPONENTS, DECEMBER, 1922-33

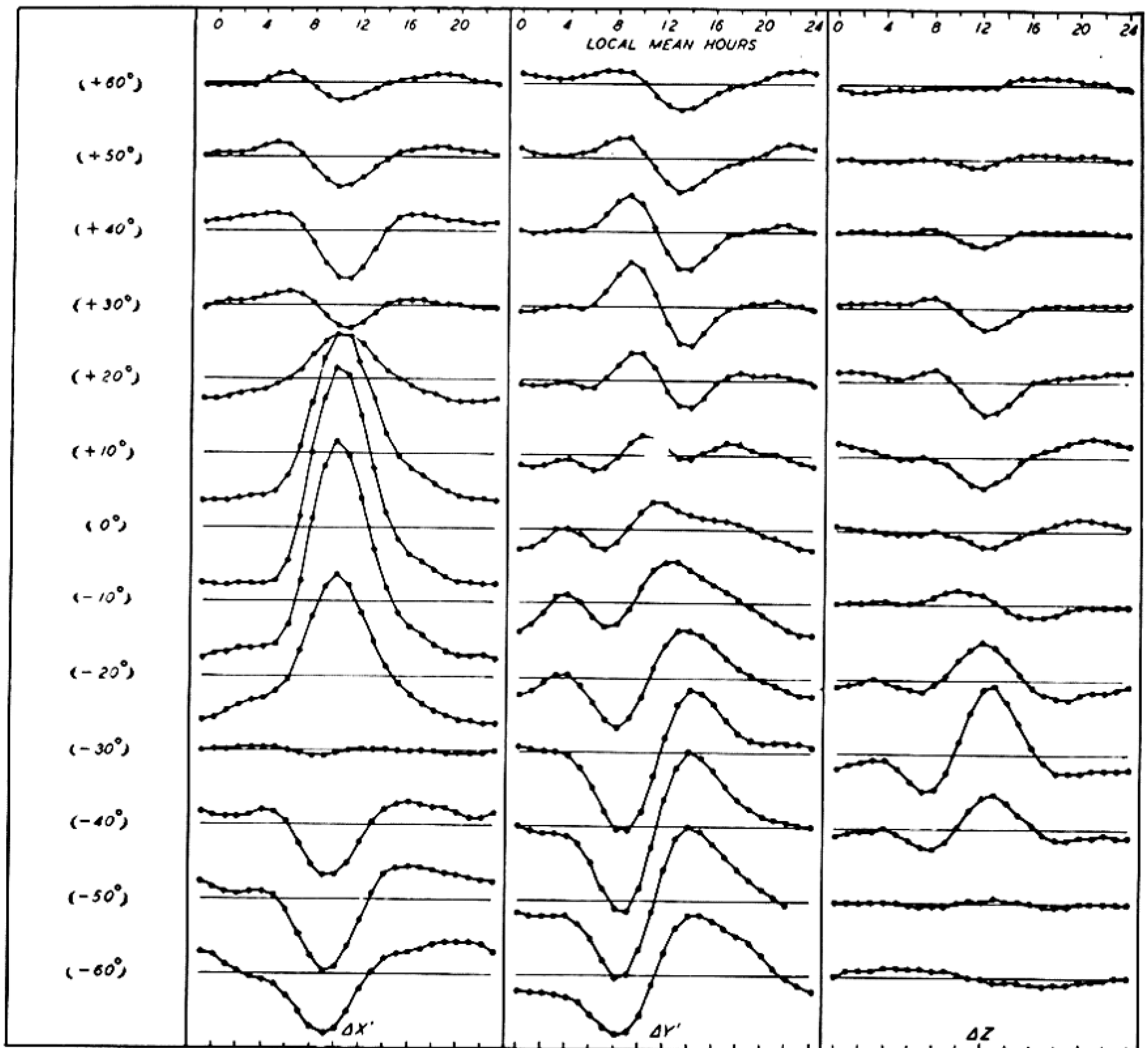

FIG. 82—SOLAR DAILY VARIATION ON QUIET DAYS (S_q) IN VARIOUS GEOGRAPHIC LATITUDES, GEOMAGNETIC COMPONENTS, WINTER, 1922-33

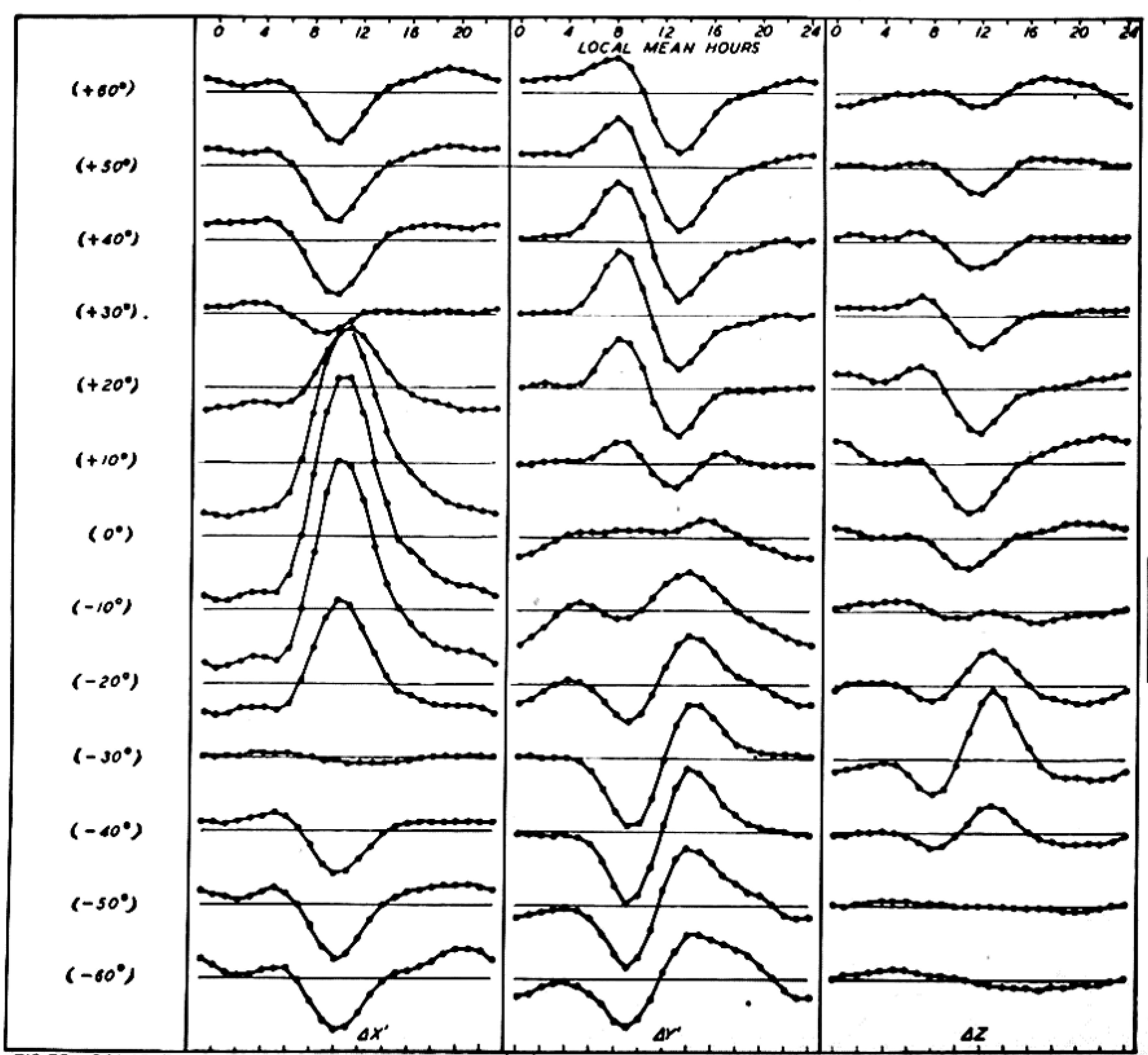

FIG. 83—SOLAR DAILY VARIATION ON QUIET DAYS (S_q), IN VARIOUS GEOGRAPHIC LATITUDES, GEOMAGNETIC COMPONENTS, EQUINOX, 1922-33

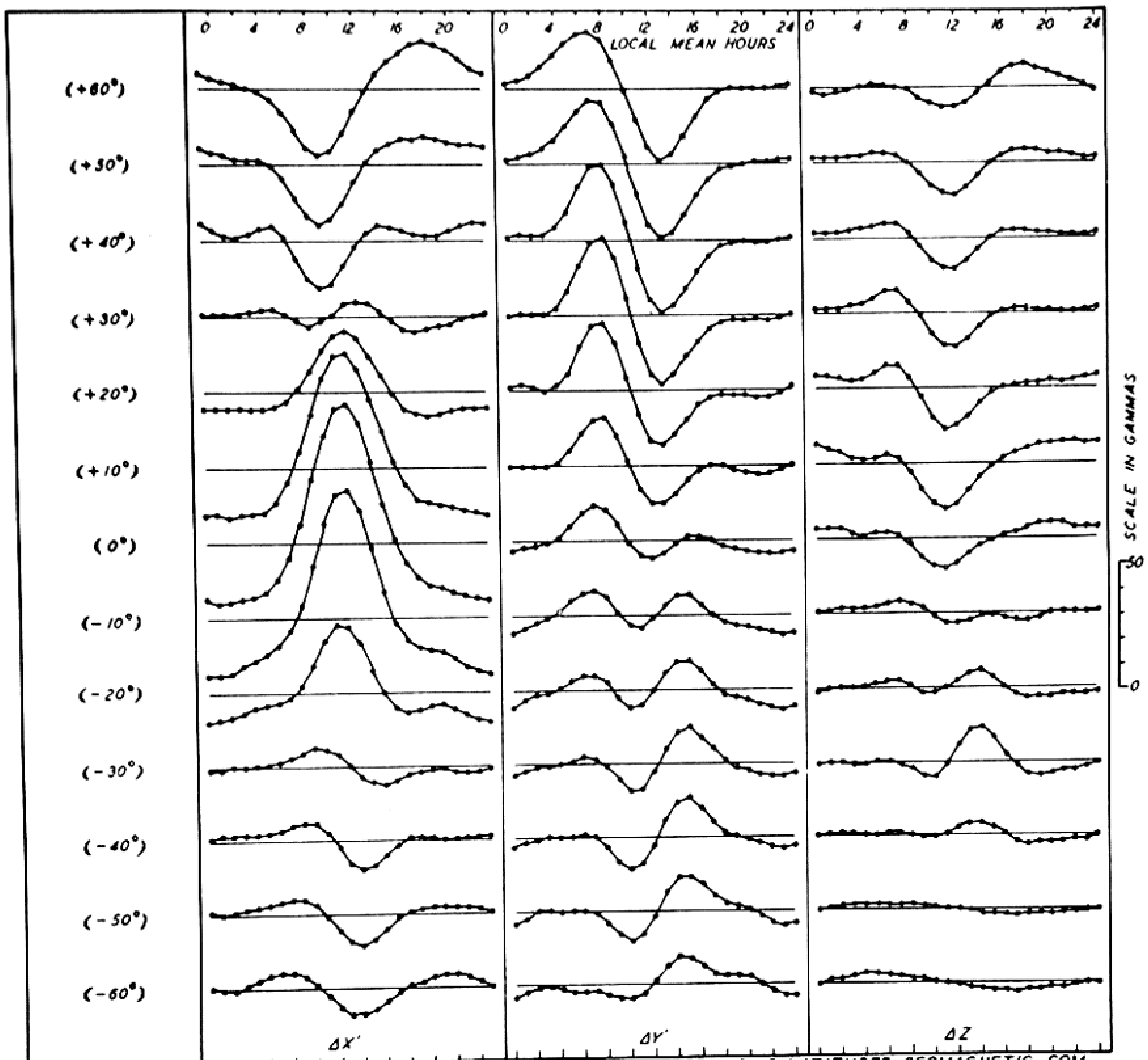

FIG. 84—SOLAR DAILY VARIATION ON QUIET DAYS (S_q), IN VARIOUS GEOGRAPHIC LATITUDES, GEOMAGNETIC COMPONENTS, SUMMER, 1922-33

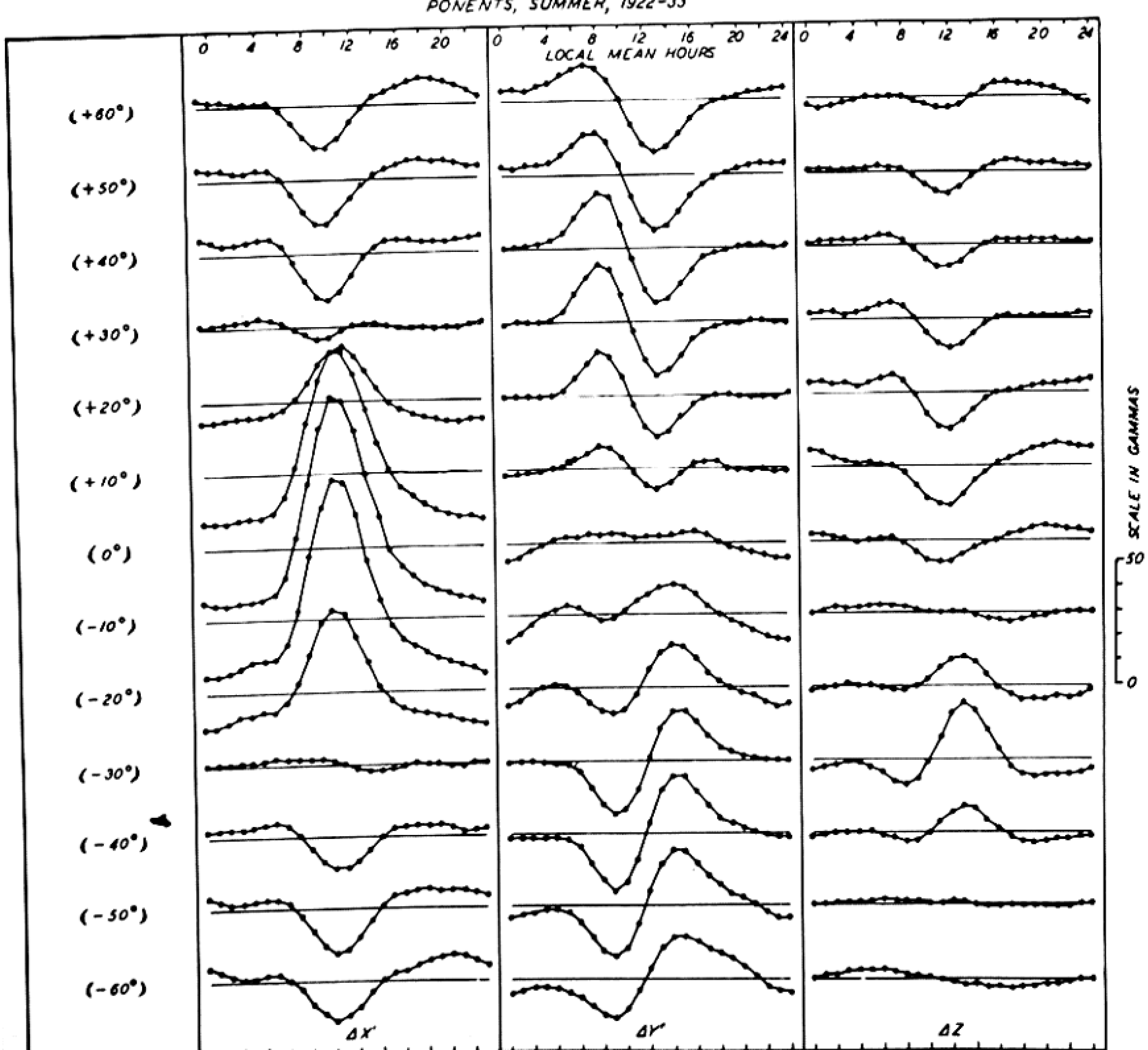

FIG. 85—SOLAR DAILY VARIATION ON QUIET DAYS (S_q), IN VARIOUS GEOGRAPHIC LATITUDES, GEOMAGNETIC COMPONENTS, YEAR, 1922-33

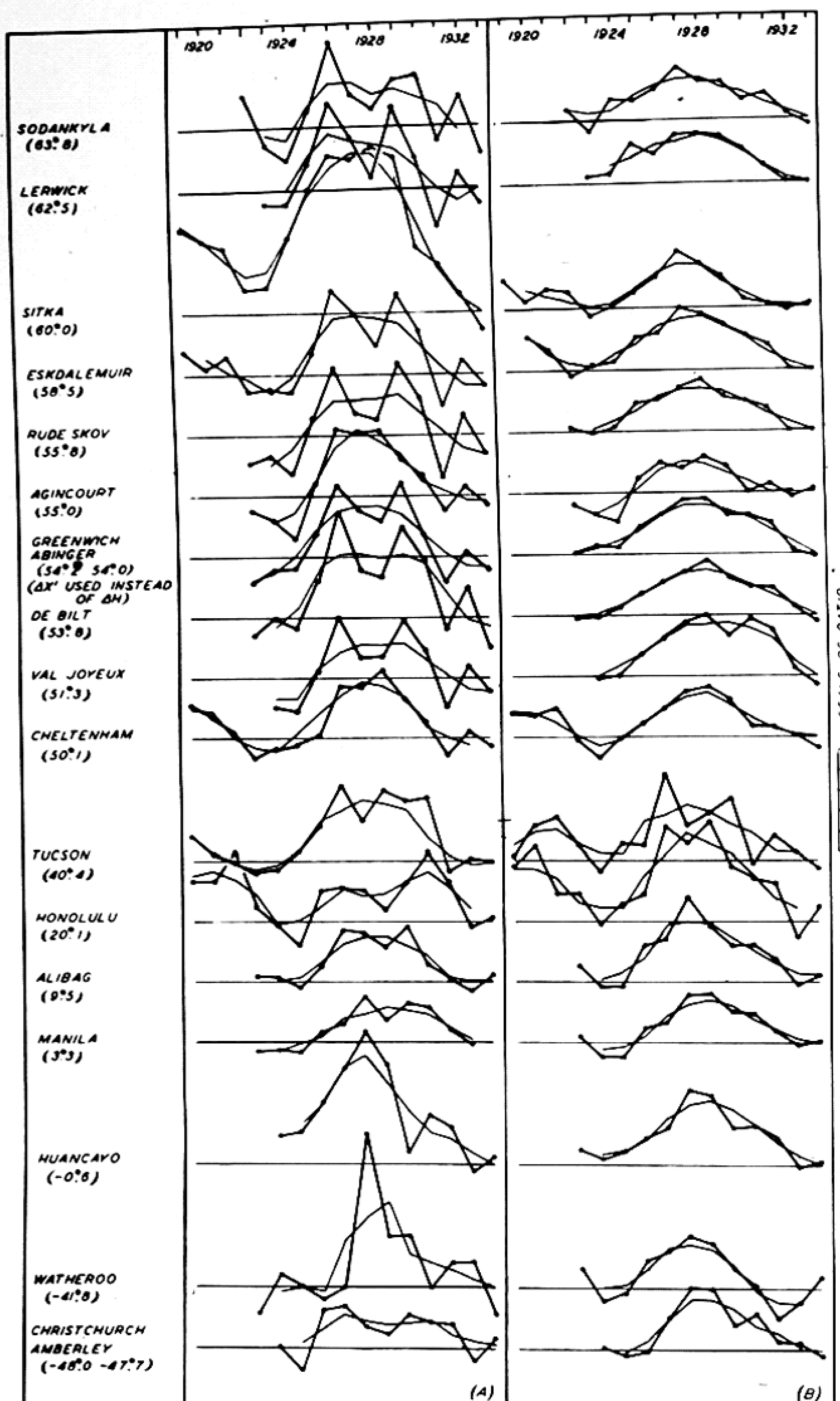

FIG. 86 (A) AND (B)—YEARLY MEANS OF DAILY RANGE OF HORIZONTAL INTENSITY (H), INTERNATIONAL QUIET DAYS, EXPRESSED AS RATIO TO CORRESPONDING MEAN RANGE AT STATION FOR PERIOD 1932-33; (A) WINTER, (B) EQUINOX

LEGEND: ——— 3-YEAR MEANS —•—•— ANNUAL VALUES

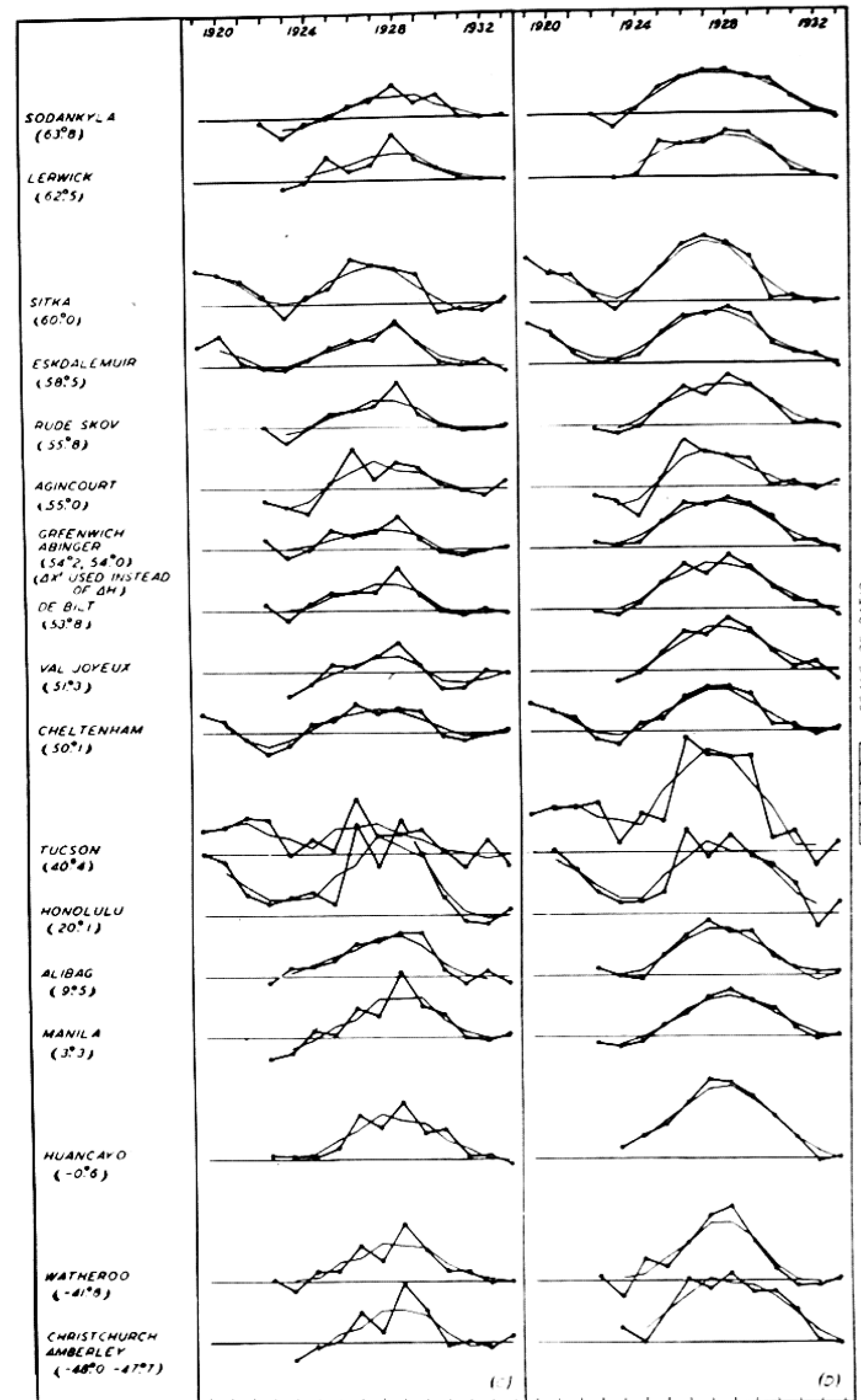

FIG. 86 (C) AND (D)—YEARLY MEANS OF DAILY RANGE OF HORIZONTAL INTENSITY (H), INTERNATIONAL QUIET DAYS, EXPRESSED AS RATIO TO CORRESPONDING MEAN RANGE AT STATION FOR PERIOD 1932-33; (C) SUMMER, (D) YEAR

LEGEND: ——— 3-YEAR MEANS —•—•— ANNUAL VALUES

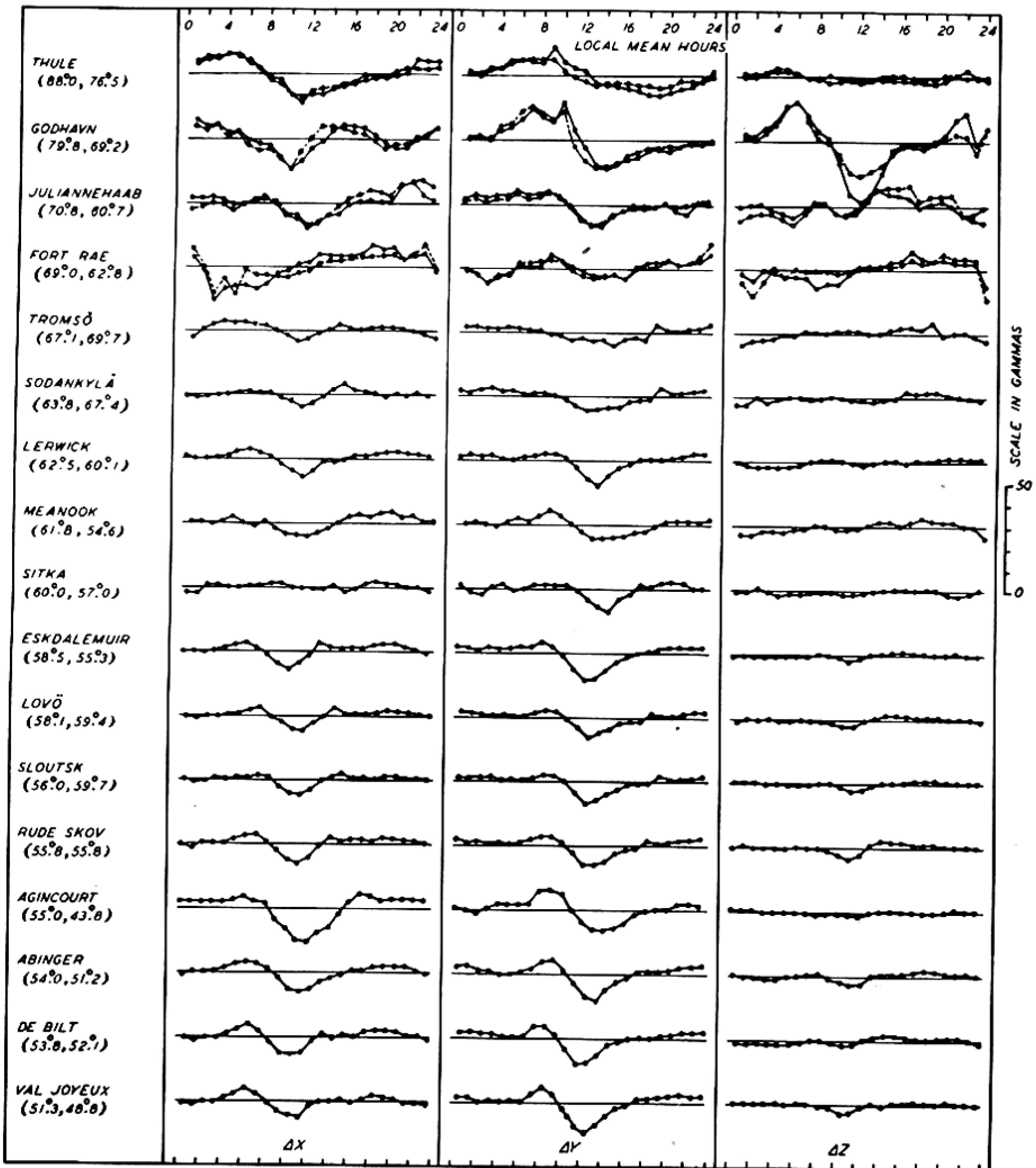

FIG. 87(A)—SOLAR DAILY VARIATION (Sq), IN GEOGRAPHIC COMPONENTS, X, Y, AND Z, VERY QUIET DAYS (C = 0.0) JANUARY 4, 5, AND FEBRUARY 17, 1933 (GEOMAGNETIC AND GEOGRAPHIC LATITUDES INDICATED RESPECTIVELY IN PARENTHESES)
LEGEND: MEAN OF JANUARY 4, 5, AND FEBRUARY 17, 1933; MEAN OF JANUARY 5 AND FEBRUARY 17, 1933

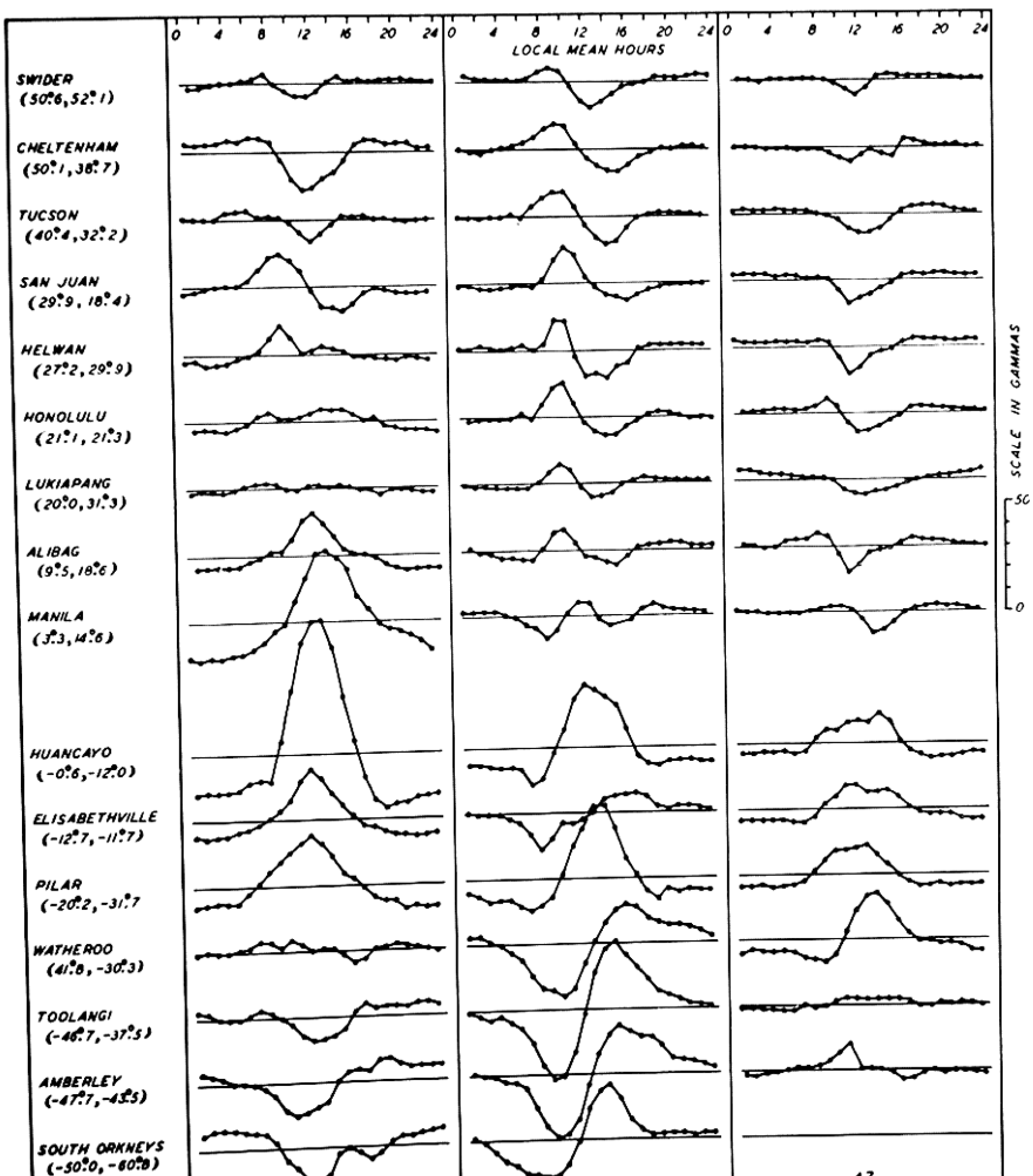

FIG. 87(B)—SOLAR DAILY VARIATION (Sq), IN GEOGRAPHIC COMPONENTS, X, Y, AND Z, VERY QUIET DAYS (C=0.0) JANUARY 4, 5, AND FEBRUARY 17, 1933 (GEOMAGNETIC AND GEOGRAPHIC LATITUDES INDICATED RESPECTIVELY IN PARENTHESES)

CHAPTER VIII

THE DISTURBANCE DAILY VARIATION, S_D, AND STORM-TIME VARIATION, D_{st}

1. Introduction.--The geomagnetic disturbance fields of our environment introduce effects of some practical importance in human affairs. When at times they become intense, they are associated with serious disruptions in world-wide radio communications. The rapid changes in field also induce currents in telegraph cables, and interfere with transformer-operation in power-transmission circuits, thus disrupting services of commercial organizations. The disturbance fields can, in certain highly restricted regions, slightly affect navigation by compass, and near the auroral zones, they can temporarily limit the accuracy of navigation by other components of the main field. They likewise are accompanied by brilliant auroral displays in the higher latitudes.

At any station recording geomagnetic changes, those due to disturbance appear highly variegated and complex. It was thought interesting and instructive to consider to what extent one might, from knowledge of the disturbance field at one station, estimate the manifestations of disturbance elsewhere. A simple case in which such information would be of practical value is that of improving homogeneity of measurements of the main magnetic field at survey stations. However, as mentioned in the preceding volume [1], we were unsuccessful in achieving a practical scheme, applicable anywhere, for obtaining such improvement.

Since the average aspects of disburbance seem rather orderly and simple, as compared with transient aspects over short intervals of time, an extensive summary is given here of average characteristics of disturbance. These may be found useful in various practical applications, and also provide a useful store of information for scientific study. In describing how the average characteristics of disturbance were derived, the discussion here will be confined mainly to those aspects of analysis dealing with our approach to removing the effect of disturbance from survey measurements of the main field.

In the problem of adjusting magnetic observations for disturbance effects, in so far as the reduction from mean of hour to mean of day is concerned, the disturbance daily variation S_D (that part of disturbance which varies mainly with local time), and storm-time variation D_{st} (the part of disturbance which depends on time of onset of disturbance) are of great importance in high latitudes. In low and middle latitudes, where by far the largest number of field-observations have been made, the values of S_D and D_{st} are in general relatively small in comparison with S_q, even on the average international disturbed day. However, on a few highly disturbed days in each year, S_D and D_{st} assume a dominant role in all latitudes. Although the large fluctuations appearing in the geomagnetic field on such days are of considerable scientific interest, for the present problem they are usually of slight practical import, since observers at field-stations have from experience found measurements on such days unreliable, and have postponed them until more quiet conditions have been restored. Usually, therefore, reductions from mean of hour to mean of day are made for data obtained under the more quiet conditions, and large corrections for S_D and D_{st}, for regions between the northern and southern auroral zones, are rarely involved.

For the polar regions, where S_D is in general large even on international quiet days, a correction would be useful, if it could be made. Because the number of field-observations there are comparatively few, uncorrected observations are likely to leave estimates of secular change completely undetermined.

Unfortunately, the corrections in high latitudes, although large, are for several special reasons not readily derivable. The S_D-field is there highly complicated in pattern and this pattern, furthermore, oscillates irregularly to the north and south about the position of the average auroral zone. The field also undergoes highly erratic changes during short intervals of time. Hence, the number of observatories necessary to determine S_D with fairly high precision at intervening points would need to be so large as to become, in all probability, impractical.

The problem immediately in hand is that of determining whether or not something can be done at present with the small number of field-observations already made in high latitudes. Since the number is small, the possibility that each field-observation should be treated individually must be considered. Such treatment might meet with some success in certain years, such as the Polar Year, 1932-33, when there were about 30 magnetic observatories in operation in north polar regions. However, in other years there were few or no polar observatories. Hence, the only alternative is that of attempting to predict, from values of S_D and D_{st} in lower latitudes, the corresponding probable values at a field-station in high latitudes. This is a problem of great difficulty, and its solution in convenient and satisfactory form has not been found.

The disturbance daily variation has been studied by a number of writers. One of the more important of early studies was that of Moos [16] who seems first to have separated the observed average storm-field into parts varying according to local time and storm-time, S_D and D_{st}, respectively. This was effected by averaging a number of storms at Bombay. Chapman [3] in a series of papers has considered data for 40 storms of moderate intensity at many stations, using a procedure similar to that of Moos. In this work he derived the approximate latitude distributions of S_D and D_{st}, for S_D from the pole to the equator, and for D_{st} in all except for the polar regions. He also derived possible atmospheric-electric current systems to account for both S_D and D_{st}. In a somewhat earlier and highly important work, Birkeland [29] made extensive studies of magnetic storms and bays on individual days, indicating by numerous examples the world-wide distribution of the storm-field. Other studies, notably by Broun [30], van Bemmelen [31], Ad. Schmidt [32], Lüdeling [33], together with the more recent studies of Stagg [34], Slaucitajs and McNish [35], Forbush [36], and Vestine [10], have served further to clarify the geographical distribution and description of the field of storms. Vestine and Chapman [37] made preliminary derivations of S_D and D_{st} from the extensive

data afforded by the Polar Year observations, 1932-33, with particular reference to determinations of S_D and D_{st} (as shown by daily means) in high latitudes. A later study indicated the dependence of S_D on longitude and extended the results for high latitudes southward to the equator [38].

2. Disturbance daily variation S_D on disturbed days, by seasons and year, Polar Year, 1932-33.--Following procedures similar to those previously adopted for determining S_q, the disturbance daily variation on disturbed days was derived for stations of the Polar Year, 1932-33. Care was taken to maintain strict homogeneity in the choice of data for all stations. Due to the fact that records were missing on a few international disturbed days at some stations, days next in order of intensity of disturbance were substituted at all stations. Such days, used in obtaining the averages according to season and year, were as follows: May 2, 1933, was substituted for the international day May 29, 1933, and July 8, 10, 11, 17 18, 1933, for the international days July 9, 23, 24, 27, 1933. Included also in the data are the results for stations falling into a nonhomogeneous category for intervals of time indicated in the figures discussed in succeeding paragraphs.

A and B of Figures 88 to 91 show the seasonal and annual means of the geomagnetic components of S_D, for the Polar Year taken from September 1, 1932, to August 31, 1933. The observations are given in terms of local geomagnetic time, reckoned relative to the geomagnetic north pole as reference.

It will be noted that the components of S_D vary mainly with geomagnetic latitude. The north component reverses in sign near geomagnetic north latitude $\Phi = 72°$, attains its maximum range at the auroral zone, again reverses in sign near $\Phi = +55°$, and is small and nearly uniform in magnitude throughout low and middle latitudes. In general, its magnitude is largest in the early morning and early evening. The geomagnetic east component is largest within the interior of the auroral zone, reverses in sign at the auroral zone, and then remains small and fairly uniform in low and middle latitudes. The vertical component shows a large and pronounced morning maximum just inside, and a small minimum just outside the auroral zone, both of which appear also in the evening but reversed in sign. This component reverses in sign near the equator and is relatively small in low and middle latitudes.

The changes with season are most marked in high latitudes where S_D is smallest in winter and largest in summer.

The seasonal averages of S_D based on the single year of observation reveal certain irregularities. These are no doubt due to the fact that only 20 days were available per season. Moreover, since the quiet-day data of Figures 50 to 53, shown in Chapter VII, include also some part of S_D, this small part of S_D actually has been removed from the disturbed day values.

We have previously noted from Figures 50 to 53 that S_D is appreciable even in the average of international quiet days in high latitudes. Hence S_D is present practically every day of the year, and the data for all days minus quiet days usefully supplement those for international disturbed days. Figures C and D of 88 to 91 give the results for all days minus quiet days of the Polar Year, 1932-33, thus providing data respecting S_D from about 120 days per season. Figures 91(E) and 91(F) give annual means from the inhomogeneous data, for disturbed days minus quiet days and all days minus quiet days, respectively, in high latitudes. It will be noted that the results in general fully confirm those obtained from the data consisting mainly of international disturbed days, except for a reduction in amplitude resulting from a necessarily different choice of days.

3. Disturbance daily variation S_D by months, seasons, and year, 1922 to 1933.--Figures 92 to 107 give the values of S_D derived mainly from international disturbed days minus quiet days averaged by month, season, and year for the period 1922 to 1933, arranged by stations. Unfortunately there are no data for high latitudes, but the average characteristics of S_D between the northern and southern auroral zones are fairly well defined. The transitions in character of field are more definitely delineated than in Figures 88 to 90, with which good agreement is shown.

4. Disturbance daily variation S_D by month, season, and year, for various parallels of latitude.--Figures 108 to 123 give the values of S_D from geomagnetic latitude 62°.5 N to 62°.5 S as found from Fourier syntheses of the data. The data of the Polar Year, 1932-33, have been reduced to the means of 1922 to 1933 to obtain approximate correction for the difference in the average intensity of disturbance.

5. Variation of S_D with longitude.--The data of Figures 108 and 123 give the values of S_D averaged around parallels of geomagnetic latitude, approximately adjusted to a circular auroral zone in latitude $\Phi = +67°$. These data could in turn be subtracted from the observed values at each station for one or more positions of the Sun relative to the geomagnetic meridian $\Lambda = 180°$ to obtain the additional part of S_D dependent on geomagnetic longitude. This was done in the case of the geomagnetic north component for the Sun in a position in the plane of $\Lambda = 0$. No important change in amplitude with longitude was found.

6. The storm-time variation D_{st}.--The storm-time variation D_{st} forms a characteristic feature of magnetic storms, and its course depends on the time reckoned from the commencement of disturbance. In the case of Chapman's derivation of D_{st}, the force components for 40 storms in low and middle latitudes, arranged according to storm-time, were meaned, the values of S_D tending to cancel by virtue of their dependence on local time.

In the present study, in order to obtain possible indications of the character of the storm-time variation in high latitudes, a similar derivation was made for 11 storms of the Polar Year, 1932-33. Since the number of storms available was small and there was considerable variation in their intensities, the data for each storm were multiplied by a weighting factor which was the same for all latitudes, and was given by the value of the maximum range in D_{st} near the equator. The equatorial value of D_{st} was obtained by meaning, according to Greenwich time, the values in H at Alibag, Honolulu, and San Juan, stations spaced roughly 120° apart in longitude so that the values of S_D might cancel because of their dependence on local time (Figure 124A). B and C of Figure 124 show the results found for D_{st} in the geomagnetic north, east, and vertical components of the polar-year storms. Although there is evidence of the presence of a 24-hour periodic component, suggesting incomplete removal of S_D, the general latitude distribution of D_{st} is clearly shown for each of several groups of stations, the stations being arranged in order in each group according to decreasing geomagnetic latitude.

In B of Figure 124, which illustrates the results found for high latitude stations, it is clear that the D_{st}

in X′ begins with a zero or negative initial value (except possibly for the mean of Thule and Godhavn, where the detailed course of D_{st} appears to be masked somewhat by S_D) which decreases to a minimum in 20 to 24 hours, followed by a fairly gradual recovery to a value near the initial value in about 70 hours. In the case of the most southerly group, consisting of Sodankylä, Meanook and Sitka, the initial value appears slightly positive. In Y′ the value of D_{st} appears to be comparatively small, and must actually be nearly zero, since it is likely that some of the systematic regularities shown are due to incomplete removal of S_D. The Z-component of D_{st} appears small near the pole. Proceeding southwards, it becomes large and positive, its magnitude being similar that of the X′-component but opposite in sign. The large increase in amplitude in the Z-component shown for the two groups of stations near $\Phi = 70°$, as compared with values for the adjacent groups to the north and south, is particularly interesting. On the basis of Chapman's current system [3] it suggests that the two opposed halves of the polar current system of storms vary in size with the course of storm-time, the part accompanied by westward currents along the auroral zone being the larger when D_{st} is larger [37]. At the auroral zone, as shown by the results for Tromsö and College, the characteristic changes in the Z-component of D_{st} already resemble those in lower latitudes, which are in general negative in sign. At Sodankylä, Meanook, and Sitka, the transition in Z is complete.

C of Figure 124 shows, on a scale two times as open as that of B, the geomagnetic components of D_{st} found for the region between the northern and southern auroral zones. The results given here, corrected from D_{st} at the equator to the level of intensity of the storm of May 1, 1933, are in good agreement with those found by Chapman [3] for the mean of 40 moderate magnetic storms for this region. In X′ the value of D_{st} attains a maximum near the equator, about which field-changes appear to be approximately symmetrical. In Y′ the time-changes are small in all latitudes. In Z the values are small and in general positive throughout low and middle latitudes of the Northern Hemisphere and are of similar magnitude but opposite in sign in the Southern Hemisphere.

7. The values of S_D and D_{st} on individual days of storm.--In two important memoirs, Birkeland [29] examined in detail the vector changes of disturbance. He plotted vector field-changes for various instants of time on maps of the world in the case of many disturbances and bays. These maps, while providing important data for the study of individual magnetic storms, do not give separately the component parts S_D and D_{st}. Later Vestine and Chapman [37] made a derivation of the current systems for single hours of the storms of October 15, 1932, and May 1, 1933, which permitted a separation of the current system into the component parts S_D and Dst.

Figure 125 shows estimated values of S_D and D_{st} for the storm of May 1, 1933, obtained after removal of S_q by first meaning every alternate hour in H according to Greenwich mean time for the stations Alibag, Honolulu, and San Juan to get the value of D_{st}, and then, after subtraction of D_{st}, taking means according to local time in order to obtain S_D.

After the average value of D_{st} was obtained for the three stations, it was reduced to its equatorial value; then, on the assumption that the latitude distribution in this case was the same as that for the X′-component of D_{mi}, values of D_{st} were computed for various stations. The value of D_{st} obtained in this manner for each station was then subtracted from the observed value, the latter first being corrected for S_q, to give a computed value of S_D. It appears from Figure 125(C) that S_D varies in amplitude with D_{st}, but the time-phase remains near its average value.

It was thought possible that a law could be found from which S_D could be calculated when D_{st} is known. It was noted first that the computed values of S_D were not directly proportional to D_{st}. A search was next made, but without success, for a function of storm-time which would be effective at all stations; the relationship appeared to be a complicated function of position of the station, and its general nature remained undetermined. This result suggested that S_D and D_{st} should each show considerable variability in values for individual days from the average value of many days, in general form and phase. However, the removal of values of S_q before determining S_D and D_{st} might be subject to some error, thus adding further complication to the apparent storm-field. A to I of Figure 126 show for many stations the hourly mean departures from the mean of day in the geomagnetic north, east, and vertical components for the storm of April 30, 1933. These reveal the general world-wide characteristics of disturbance, but they show no evidence of a simple relationship between S_D and D_{st}. It should, however, be borne in mind that the irregular features of disturbance, D_i (discussed in a later section) are not fully removed in taking hourly means of magnetic data. It would seem necessary to remove in some way D_i (as well as S_q) from these data. An important consideration which suggests the necessity for this procedure is that bays, although evincing mainly an S_D-field with little D_{st} in evidence, except near the auroral zone, nevertheless frequently appear during storms. Their appearance disturbs and masks any relationship sought between S_D and D_{st} which might possibly have a systematic pattern.

Figure 127 illustrates actual hourly mean departures from mean of day (without removal of S_q), at many stations. These are shown for several days, on Greenwich mean time, with international character-figures, C, of different values, as follows: October 9 (C = 0.9), December 17 (C = 1.3), 1932; February 23 (C = 1.5), April 18 (C = 1.1), June 5 (C = 0.0), and August 31 (C = 0.1), 1933. The reader will find it interesting to compare the departures for February 23, where storm conditions prevail, with those of the very quiet day of June 5. These figures are helpful in a descriptive sense, although the original purpose for which they were derived was that of training computers and draftsmen for later work.

One point emerging from the present study is that there seems little hope of predicting accurately the changes in the polar disturbance-field from the field-changes observed in low latitudes in the reduction of magnetic observations. It appears, however, that useful corrections in low and middle latitudes might be effected, and further study might well result in a practical method of making such corrections.

8. The irregular geomagnetic disturbance D_i.--The irregular features of disturbance seem first to have been extensively studied by Birkeland [29]. From maps showing the world-wide field-distributions in terms of vectors, he concluded that there were world-wide diminutions in horizontal intensity, of some minutes' duration, among the oscillatory changes appearing on magnetograms, and also others for which the sign and magnitude depended on the local time of occurrence at a station. He also

made extensive studies of bays which may also be regarded as a manifestation of D_i [3].

Studies of the data on bays for the Polar Year, 1932-33, have shown that the pattern of the field of bays very closely resembles that for S_D. However, there is also present in the field of bays a part which, when averaged along parallels of geomagnetic latitude, is not zero, and shows an especially large negative value just inside the auroral zone. The latter is clearly due to the component D_{st} of bays. Thus there is a qualitative but not a detailed correspondence between the field of bays and S_D as derived here.

The pattern of field evinced during bays appears, without great change in general form, on any day of the year, although there are systematic changes with season. Thus, from a station located near the center of the auroral zone, where the field-changes are large and nearly independent, in magnitude, of the local time of appearance of a bay, one can hope roughly to estimate the magnitude and time-variation of the bay at any point elsewhere on the Earth's surface.

The average geographical distribution of bays has been roughly estimated by Silsbee and Vestine [39]. These results should, however, be further amplified by taking into account the considerable seasonal changes in high latitudes, thus permitting the preparation of tables likely to give useful estimates of the intensity and time-variation of bays in all latitudes. The estimates may not be entirely successful, however, near the auroral zone, due to the expansions and contractions of this zone during a bay.

9. The latitude distributions of noncyclic change, NC.--Figure 128 shows the latitude distributions of the noncyclic change for international quiet days, all days minus quiet days, and disturbed minus quiet days of the Polar Year, 1932-33, in the geomagnetic north, east, and vertical components.

FIGURES 88-128

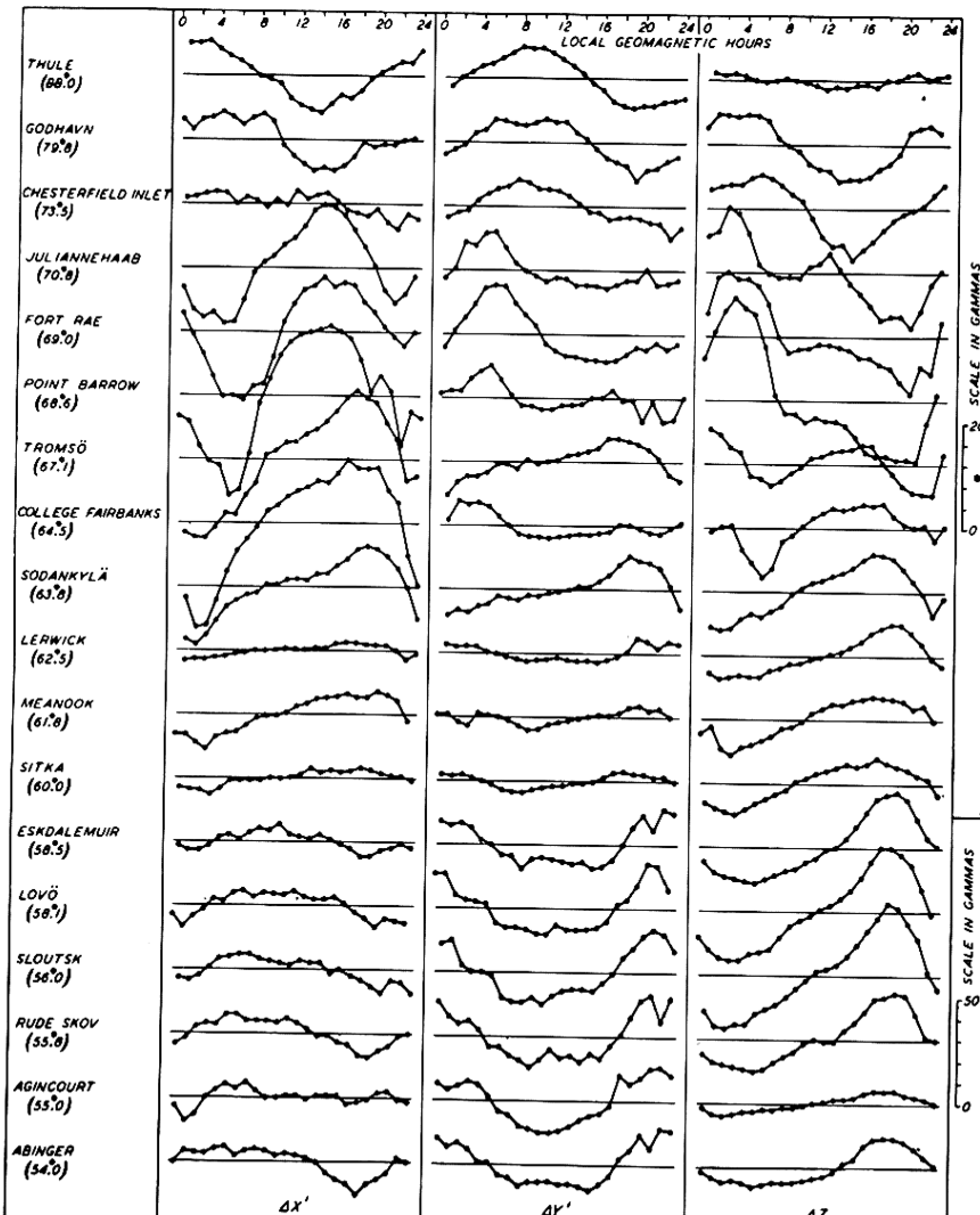

FIG. 88(A)—AVERAGE DAILY VARIATION, DISTURBED MINUS QUIET DAYS, (SD), GEOMAGNETIC COMPONENTS, WINTER, POLAR YEAR, 1932–33 (GEOMAGNETIC LATITUDES INDICATED IN PARENTHESES)

* NOTE PARTICULARLY THAT SCALES FOR GRAPHS IN AURORAL REGIONS ARE DIFFERENT THAN FOR OTHERS

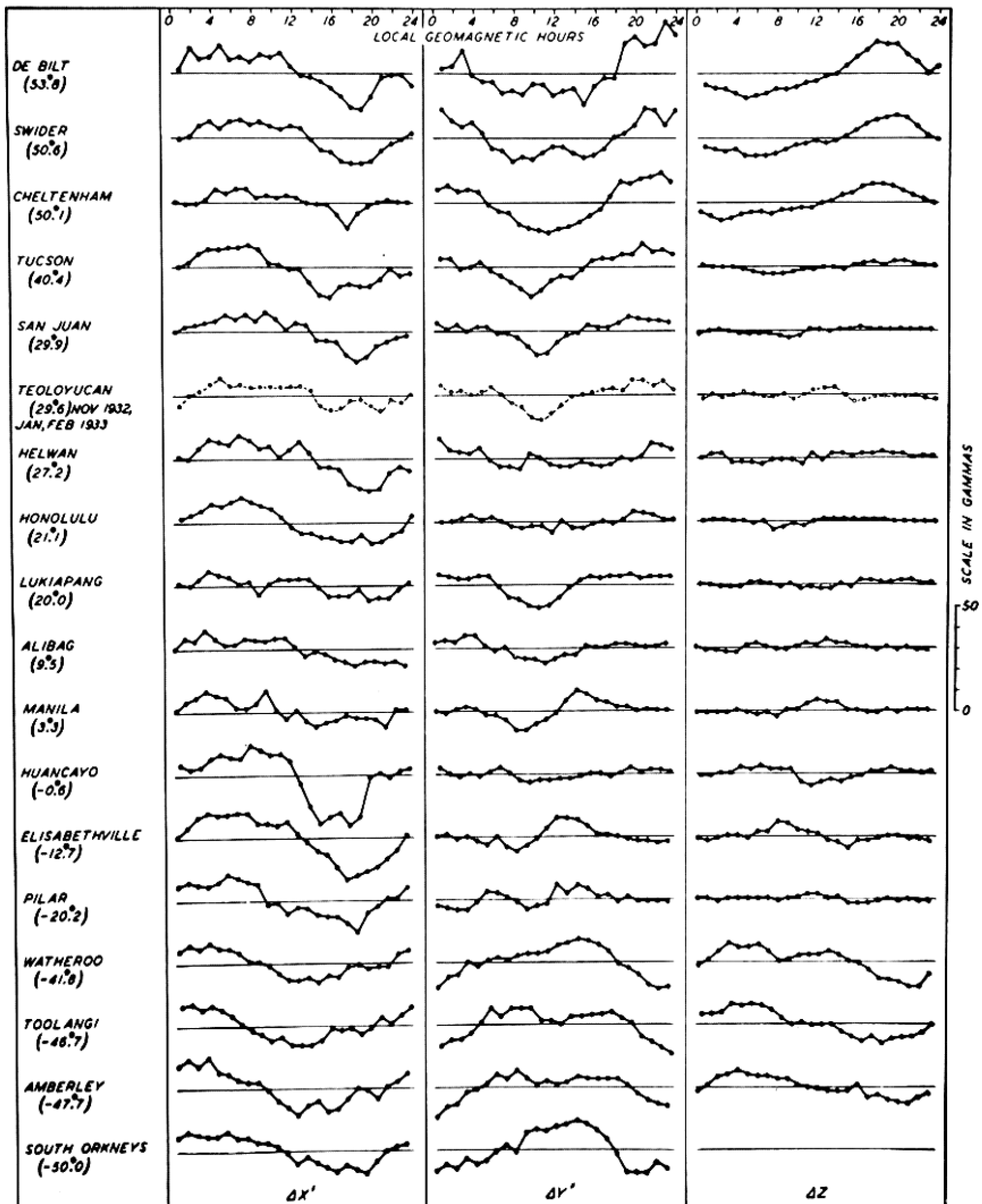

FIG. 88 (B)—AVERAGE DAILY VARIATION, DISTURBED MINUS QUIET DAYS, (S_D), GEOMAGNETIC COMPONENTS, WINTER, POLAR YEAR, 1932-33 (GEOMAGNETIC LATITUDES INDICATED IN PARENTHESES)

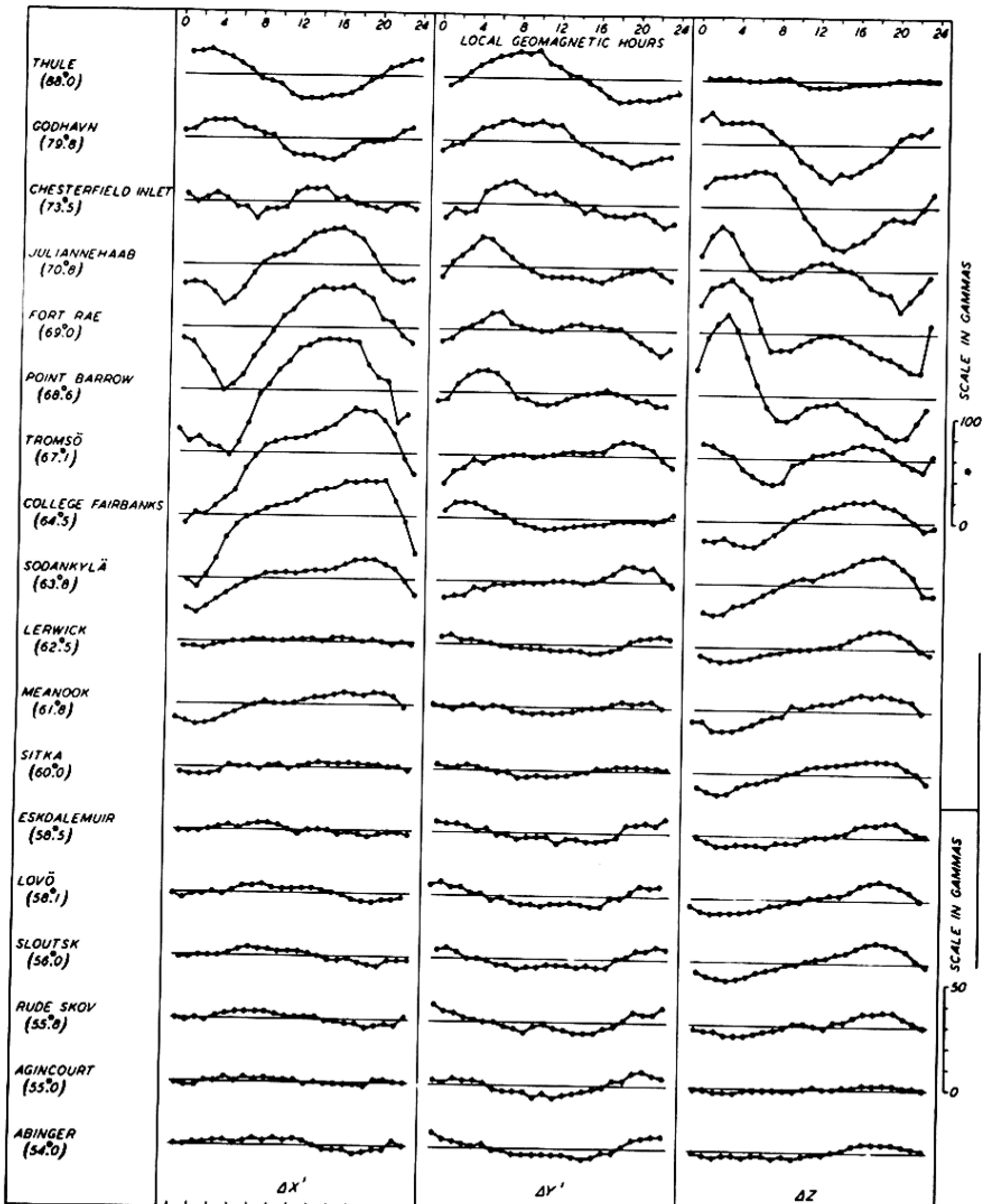

FIG. 88(C)— AVERAGE DAILY VARIATION, ALL MINUS QUIET DAYS, GEOMAGNETIC COMPONENTS, WINTER, POLAR YEAR, 1932-33 (GEOMAGNETIC LATITUDES INDICATED IN PARENTHESES)

* NOTE PARTICULARLY THAT SCALES FOR GRAPHS IN AURORAL REGIONS ARE DIFFERENT THAN FOR OTHERS

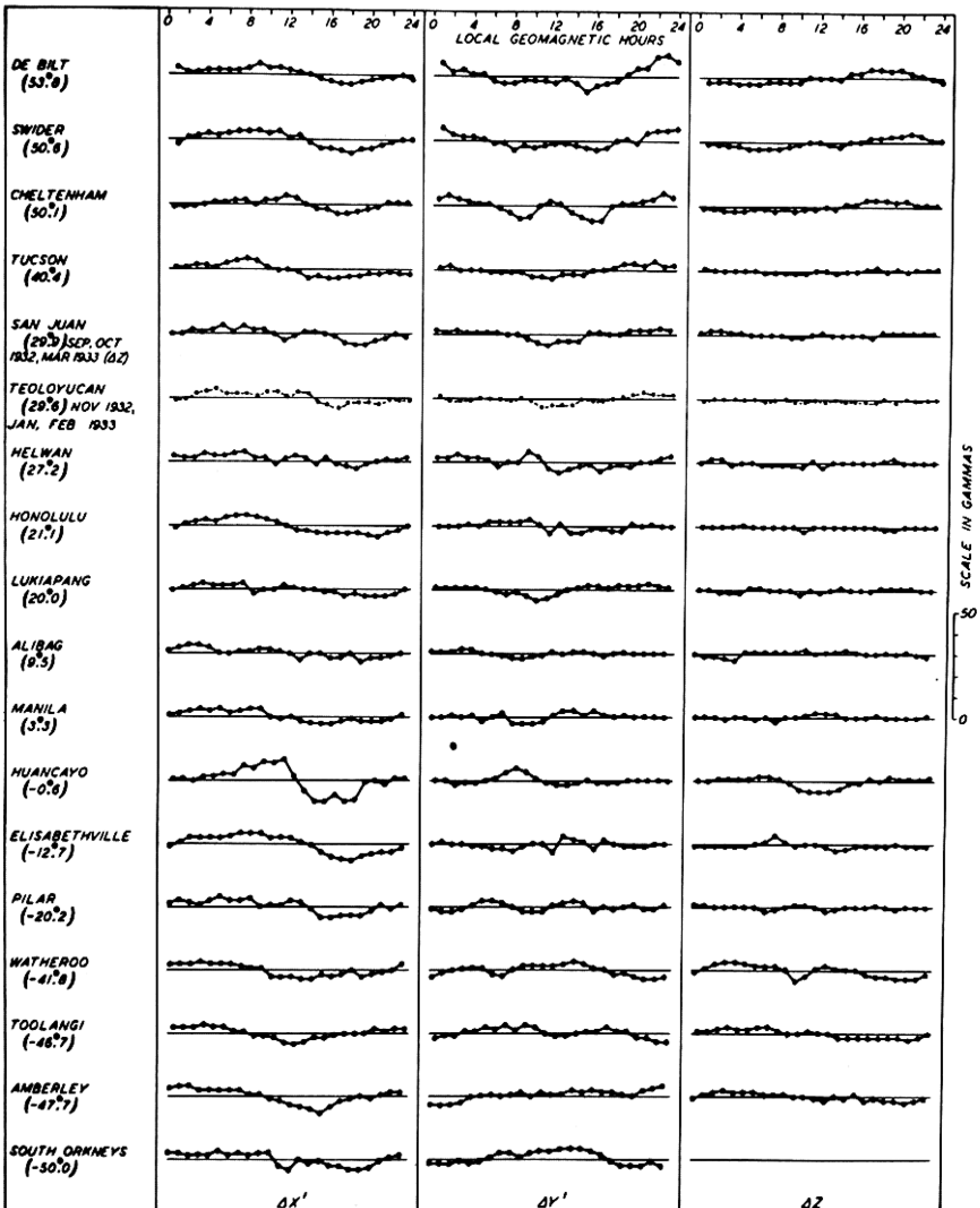

FIG. 88(D)— AVERAGE DAILY VARIATION, ALL MINUS QUIET DAYS, GEOMAGNETIC COMPONENTS, WINTER, POLAR YEAR, 1932-33 (GEOMAGNETIC LATITUDES INDICATED IN PARENTHESES)

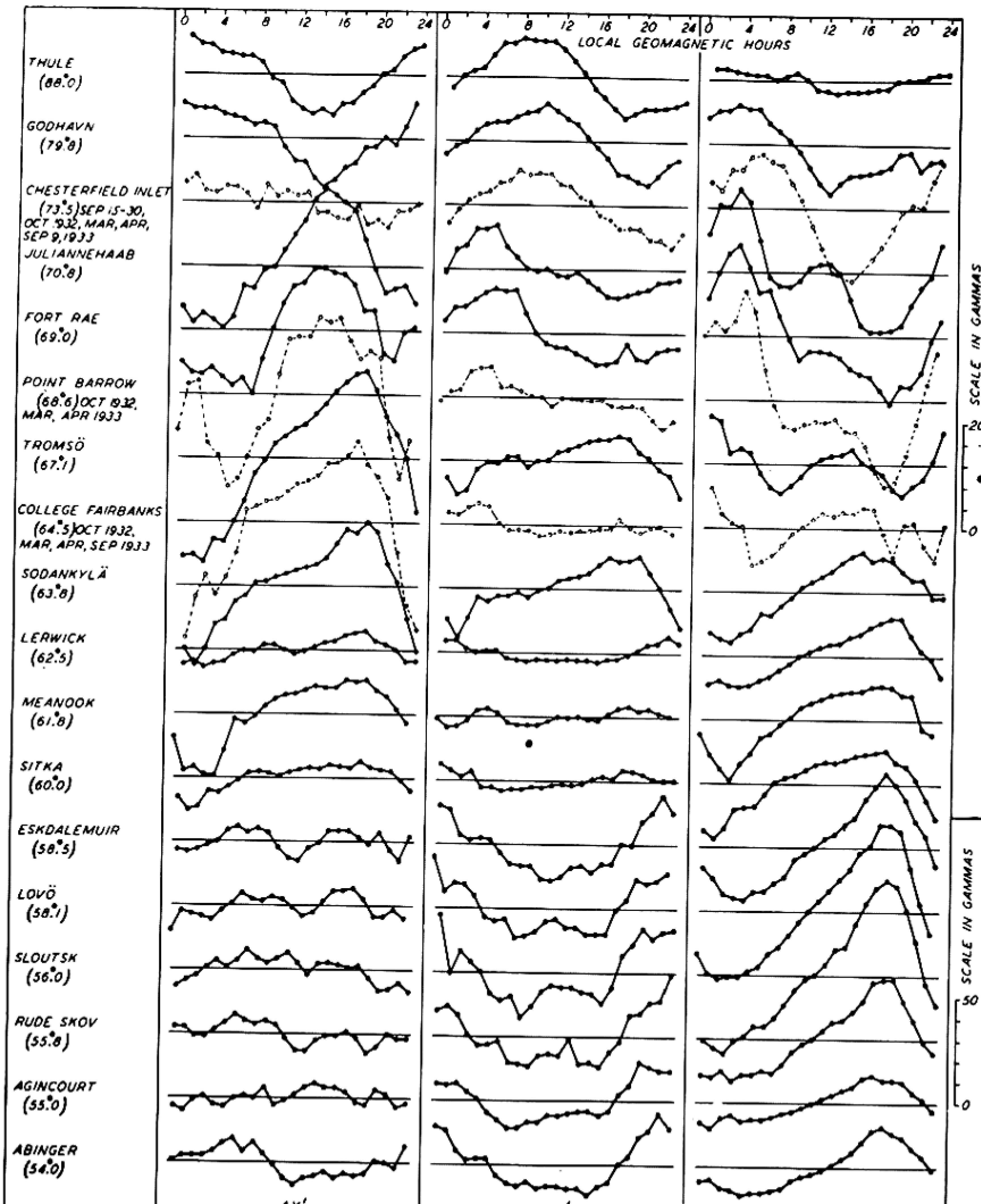

FIG. 89(A)—AVERAGE DAILY VARIATION, DISTURBED MINUS QUIET DAYS, (S_D), GEOMAGNETIC COMPONENTS, EQUINOX, POLAR YEAR, 1932-33 (GEOMAGNETIC LATITUDES INDICATED IN PARENTHESES)

• NOTE PARTICULARLY THAT SCALES FOR GRAPHS IN AURORAL REGIONS ARE DIFFERENT THAN FOR OTHERS

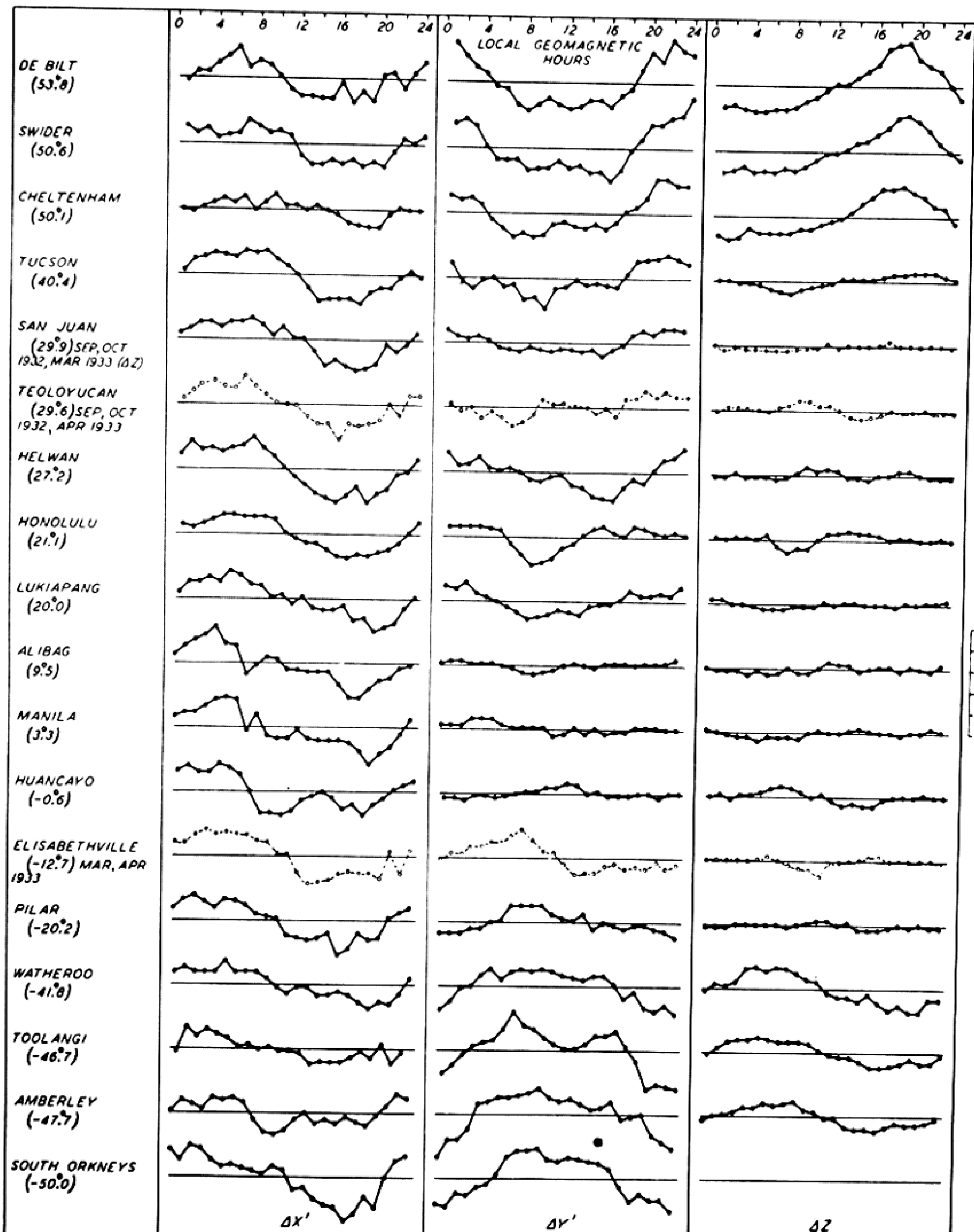

FIG. 89(B)—AVERAGE DAILY VARIATION, DISTURBED MINUS QUIET DAYS, (SD), GEOMAGNETIC COMPONENTS, EQUINOX, POLAR YEAR, 1932-33 (GEOMAGNETIC LATITUDES INDICATED IN PARENTHESES)

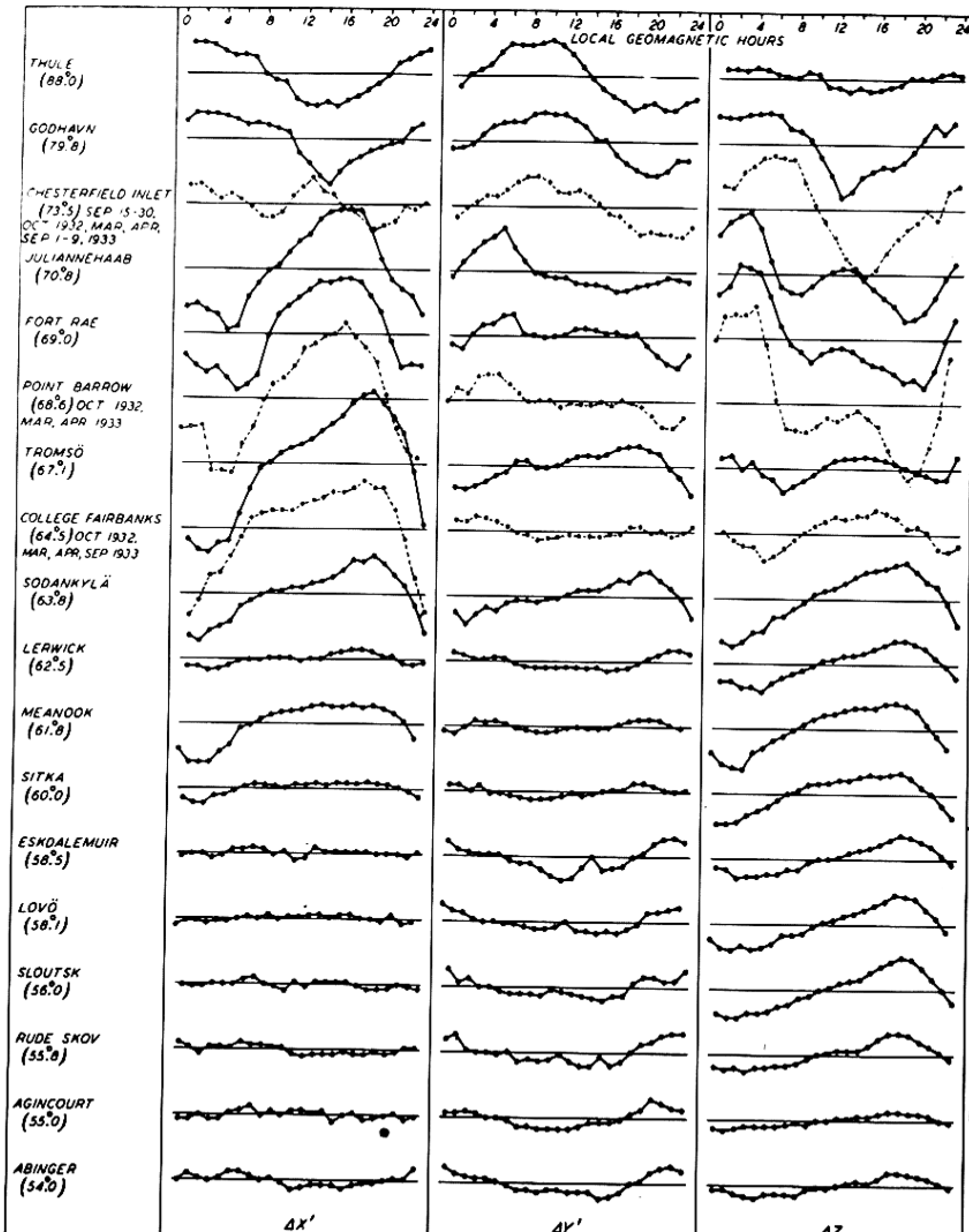

FIG. 89(C)— AVERAGE DAILY VARIATION, ALL MINUS QUIET DAYS, GEOMAGNETIC COMPONENTS, EQUINOX, POLAR YEAR, 1932-33 (GEOMAGNETIC LATITUDES INDICATED IN PARENTHESES)

• NOTE PARTICULARLY THAT SCALES FOR GRAPHS IN AURORAL REGIONS ARE DIFFERENT THAN FOR OTHERS

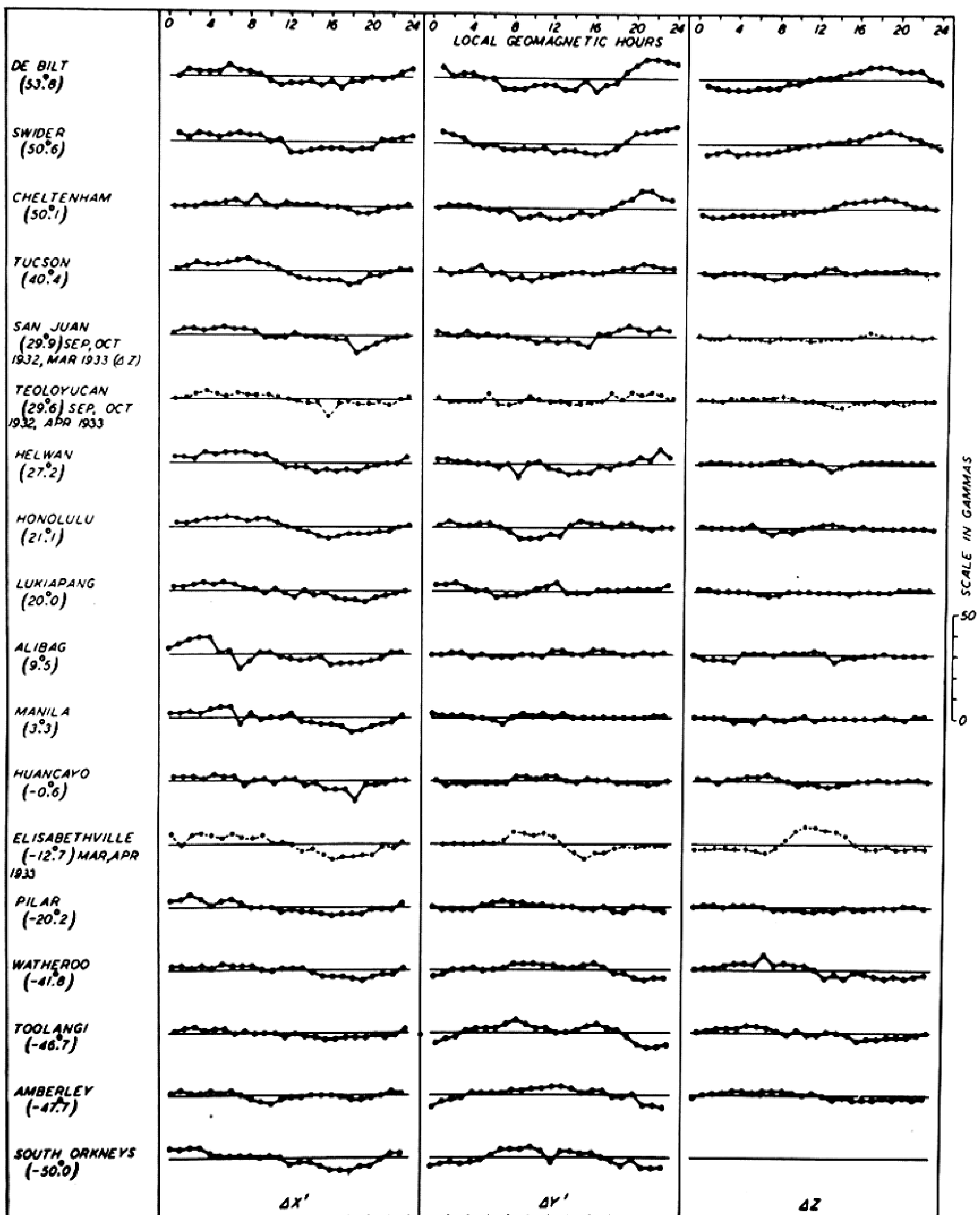

FIG. 89(2)— AVERAGE DAILY VARIATION, ALL MINUS QUIET DAYS, GEOMAGNETIC COMPONENTS, EQUINOX, POLAR YEAR, 1932-33 (GEOMAGNETIC LATITUDES INDICATED IN PARENTHESES)

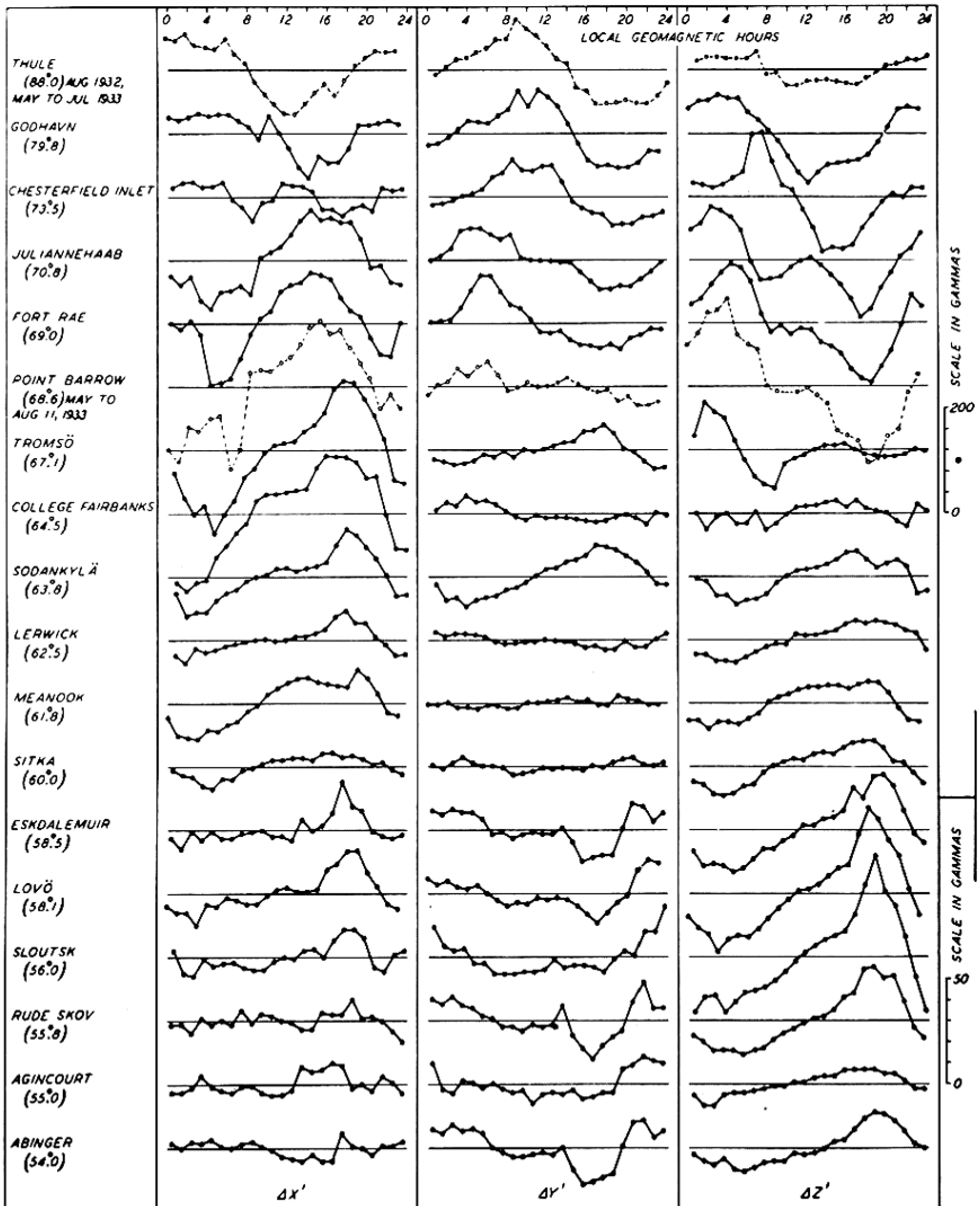

FIG. 90(A)—AVERAGE DAILY VARIATION, DISTURBED MINUS QUIET DAYS, (S_D) GEOMAGNETIC COMPONENTS, SUMMER, POLAR YEAR, 1932-33 (GEOMAGNETIC LATITUDES INDICATED IN PARENTHESES)

* NOTE PARTICULARLY THAT SCALES FOR GRAPHS IN AURORAL REGIONS ARE DIFFERENT THAN FOR OTHERS

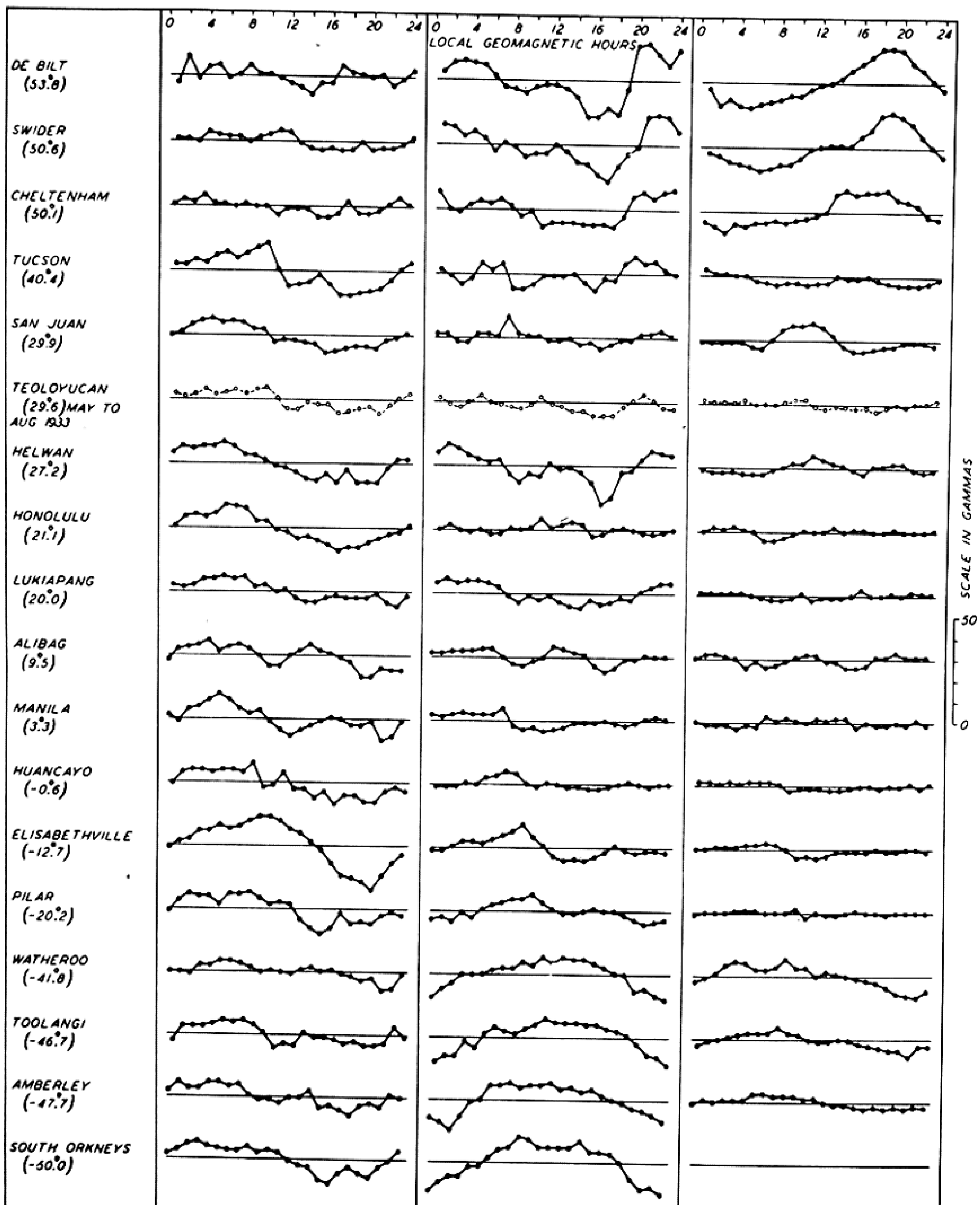

FIG. 90(B)-AVERAGE DAILY VARIATION, DISTURBED MINUS QUIET DAYS, (S_D), GEOMAGNETIC COMPONENTS, SUMMER, POLAR YEAR, 1932-33 (GEOMAGNETIC LATITUDES INDICATED IN PARENTHESES)

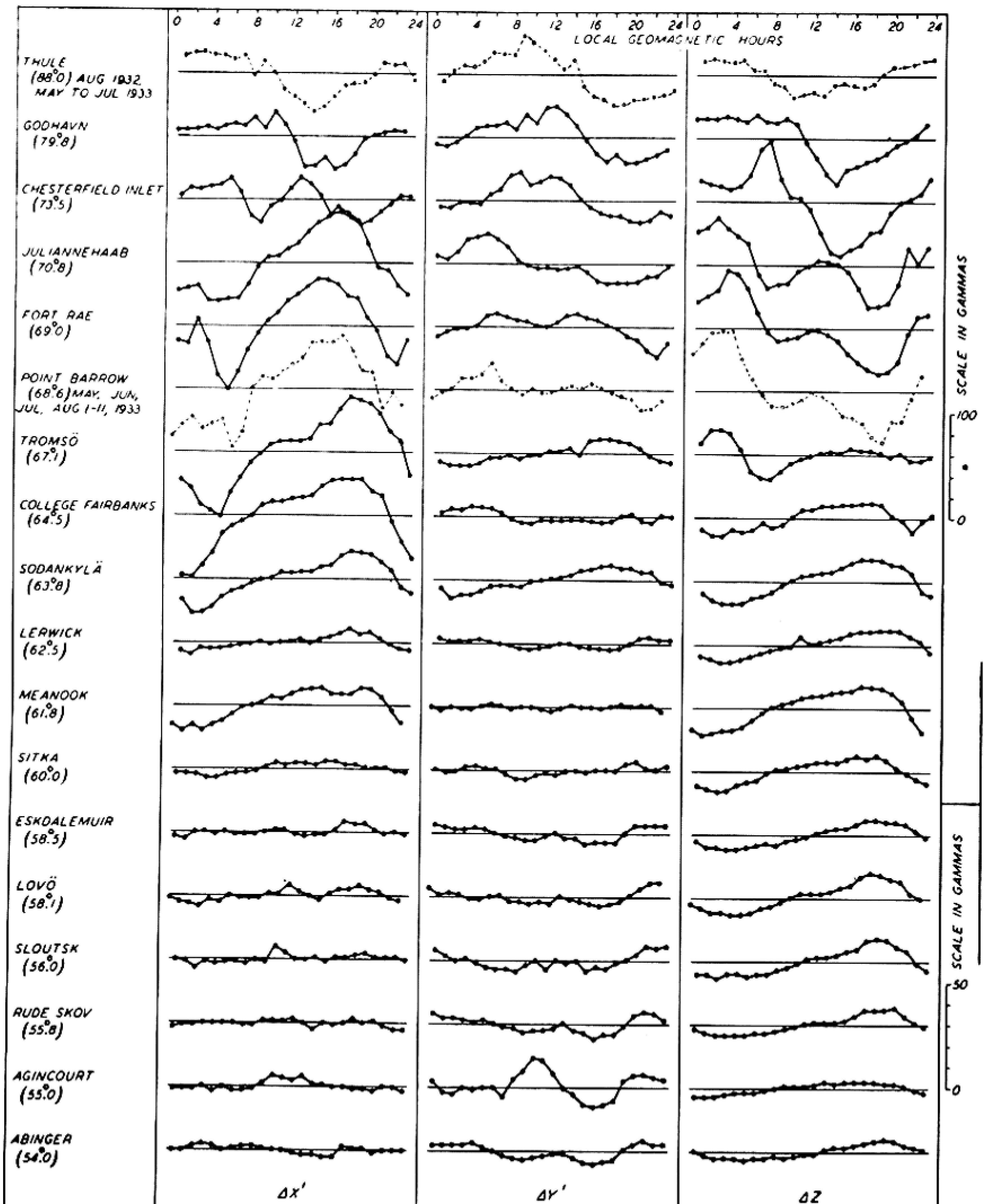

FIG. 90(C)—AVERAGE DAILY VARIATION, ALL MINUS QUIET DAYS, GEOMAGNETIC COMPONENTS, SUMMER, POLAR YEAR, 1932-33 (GEOMAGNETIC LATITUDES INDICATED IN PARENTHESES)

* NOTE PARTICULARLY THAT SCALES FOR GRAPHS IN AURORAL REGIONS ARE DIFFERENT THAN FOR OTHERS

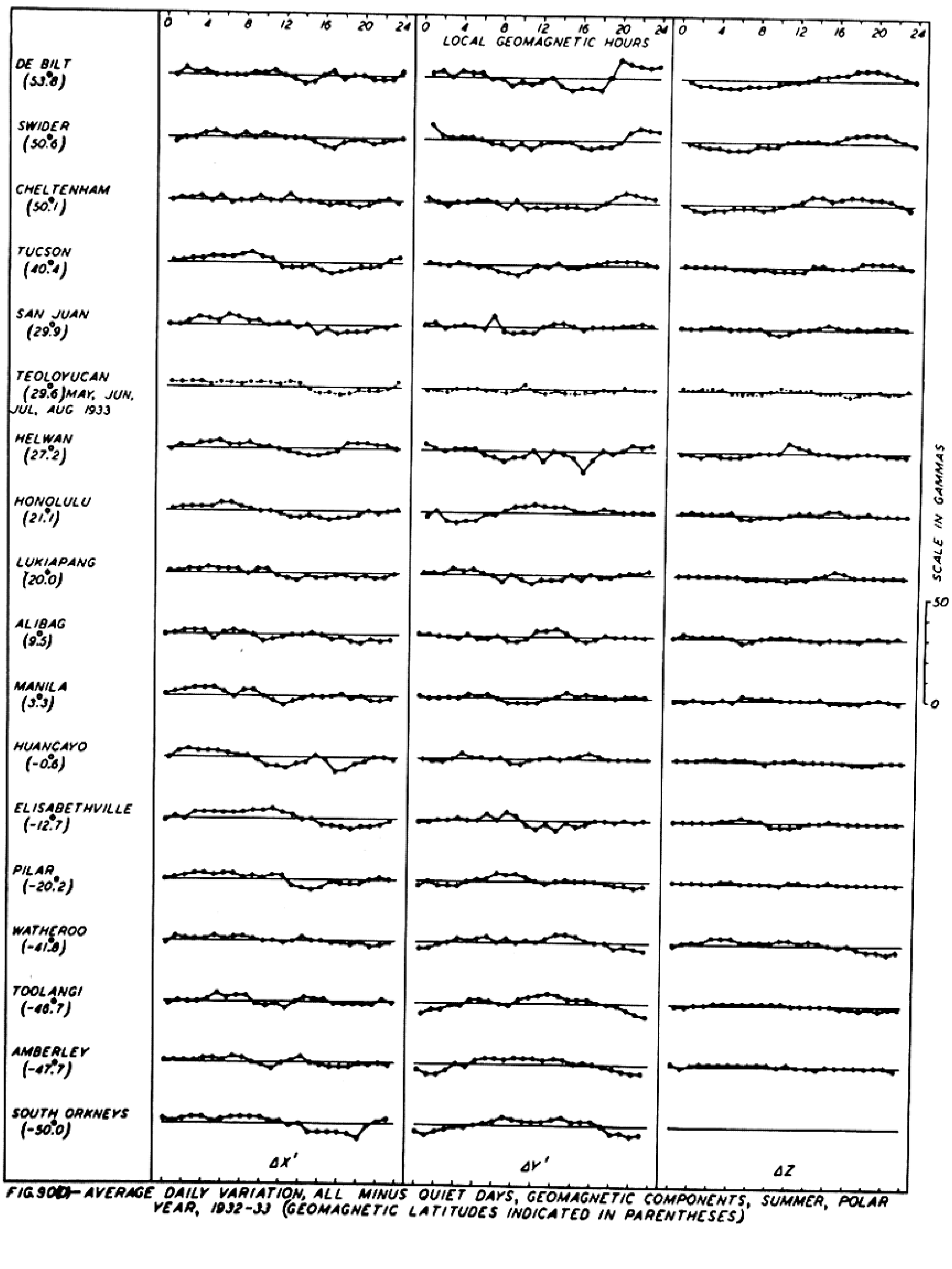

FIG. 90[illegible]—AVERAGE DAILY VARIATION, ALL MINUS QUIET DAYS, GEOMAGNETIC COMPONENTS, SUMMER, POLAR YEAR, 1932-33 (GEOMAGNETIC LATITUDES INDICATED IN PARENTHESES)

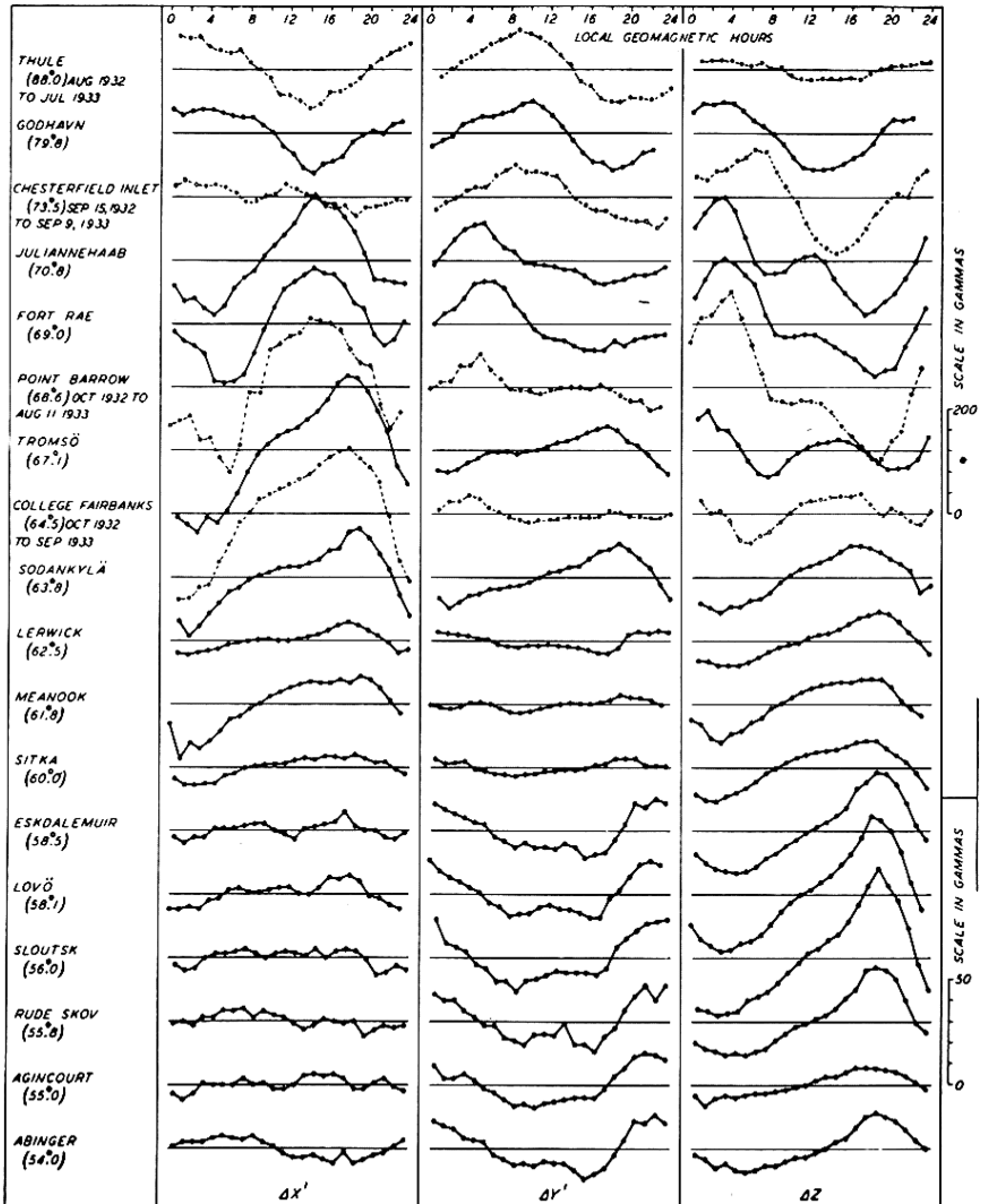

FIG. 91 (A)—AVERAGE DAILY VARIATION, DISTURBED MINUS QUIET DAYS, (SD), GEOMAGNETIC COMPONENTS, MEAN OF 12 MONTHS, POLAR YEAR, 1932-33 (GEOMAGNETIC LATITUDES INDICATED IN PARENTHESES)

* NOTE PARTICULARLY THAT SCALES FOR GRAPHS IN AURORAL REGIONS ARE DIFFERENT THAN FOR OTHERS

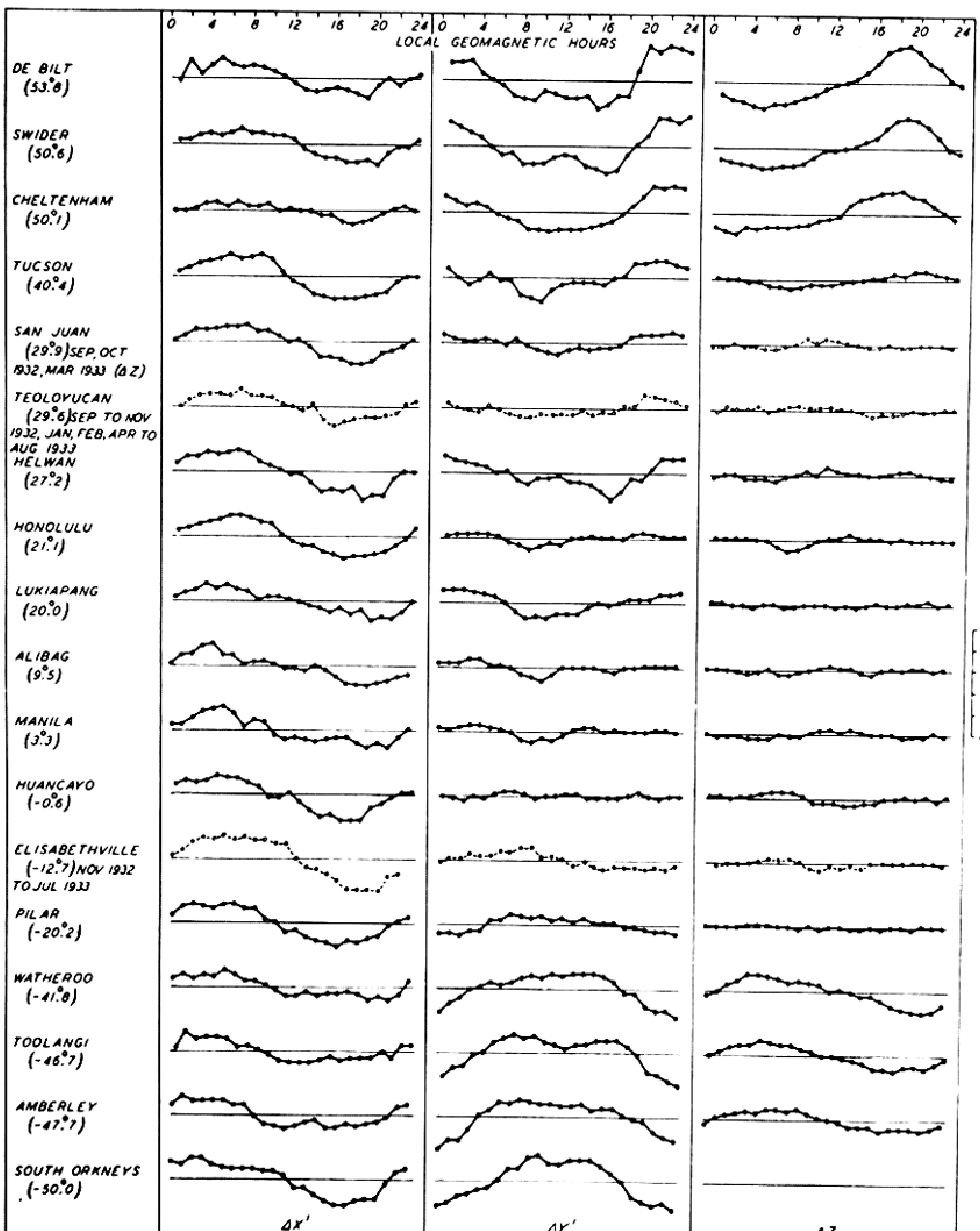

FIG. 91(B)—AVERAGE DAILY VARIATION, DISTURBED MINUS QUIET DAYS, (SD), GEOMAGNETIC COMPONENTS, MEAN OF 12 MONTHS, POLAR YEAR, 1932-33 (GEOMAGNETIC LATITUDES INDICATED IN PARENTHESES)

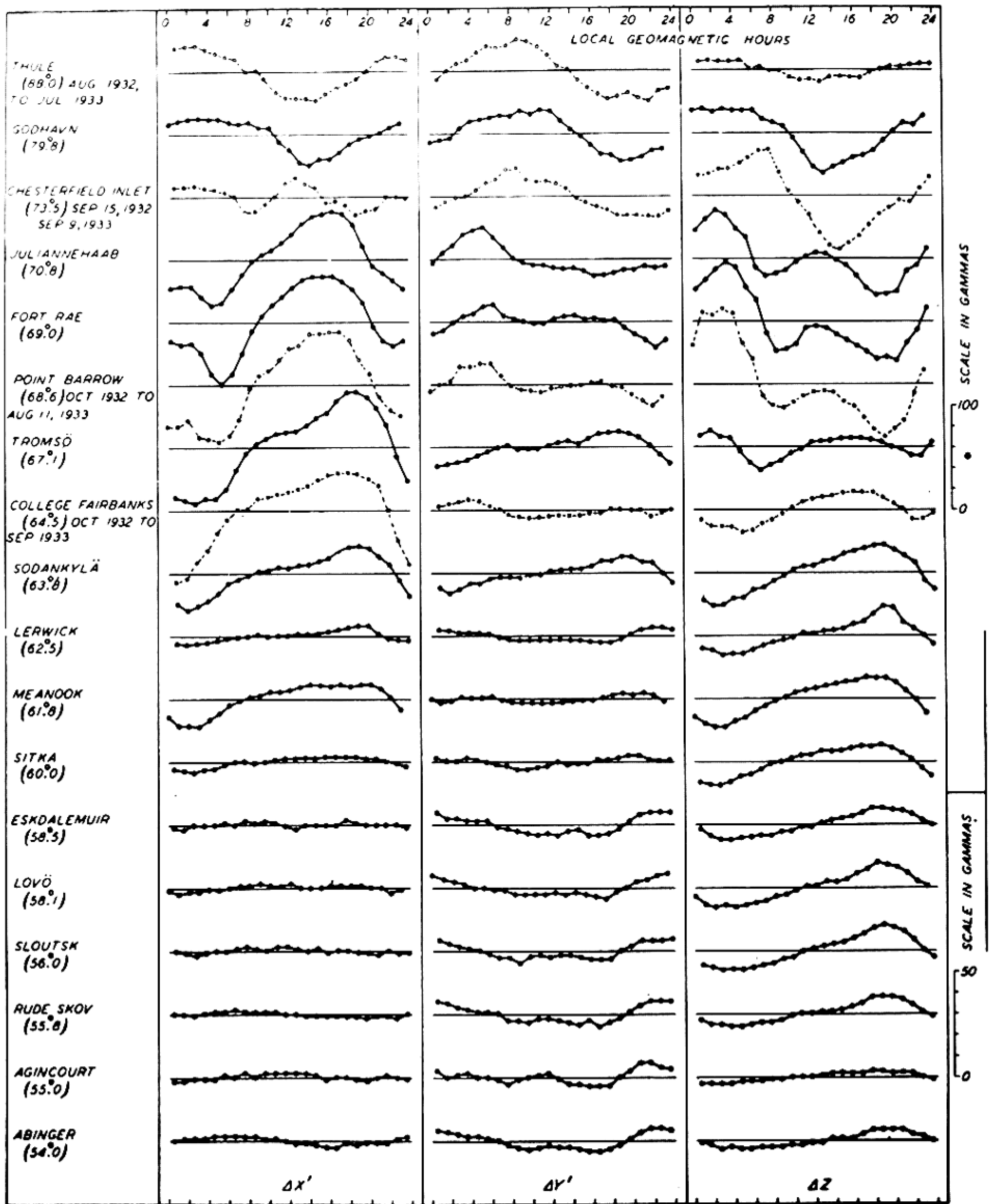

FIG. 91(C) — AVERAGE DAILY VARIATION, ALL MINUS QUIET DAYS, GEOMAGNETIC COMPONENTS, MEAN OF 12 MONTHS, POLAR YEAR, 1932-33 (GEOMAGNETIC LATITUDES INDICATED IN PARENTHESES)

* NOTE PARTICULARLY THAT SCALES FOR GRAPHS IN AURORAL REGIONS ARE DIFFERENT THAN FOR OTHERS

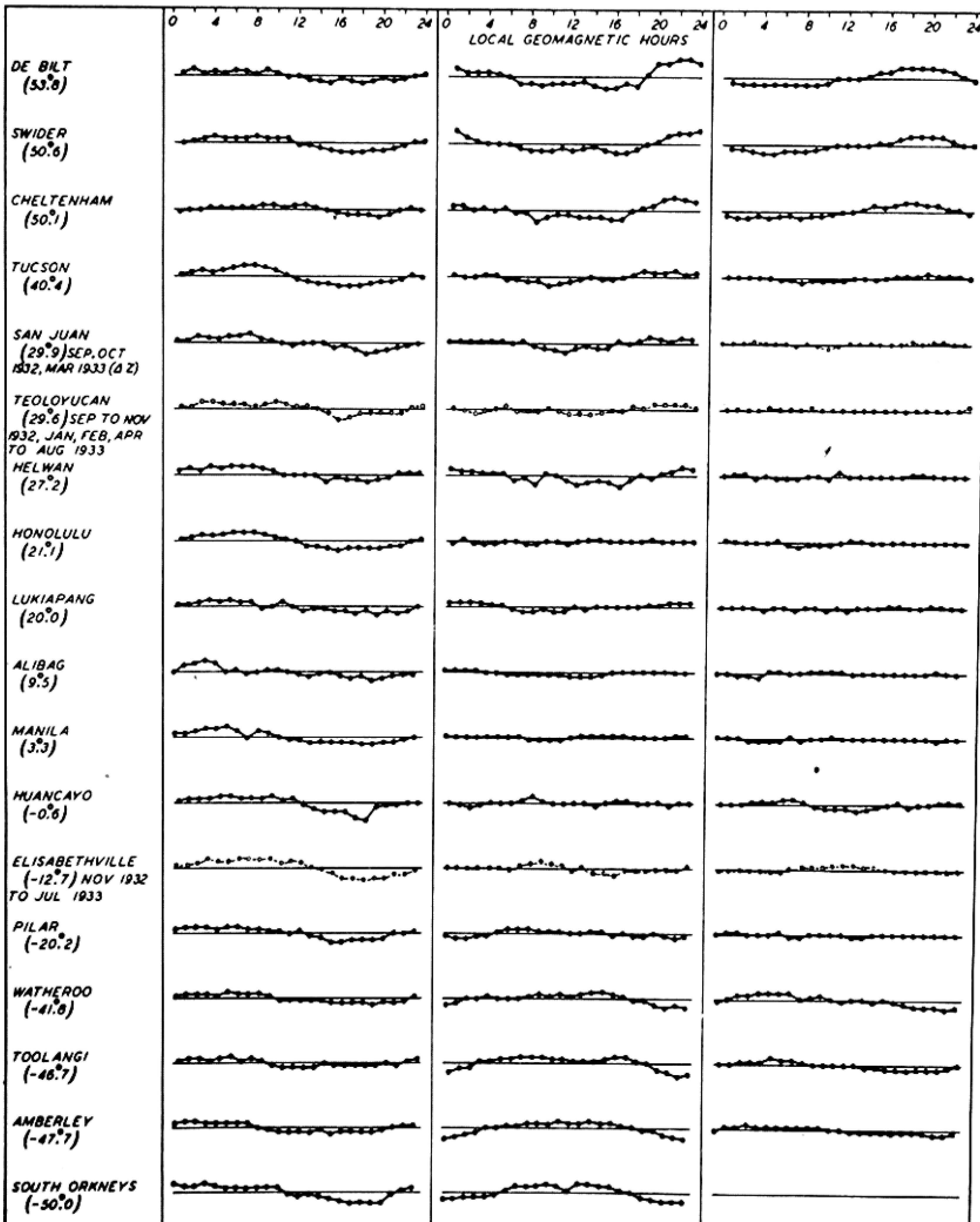

FIG. 91(D)— AVERAGE DAILY VARIATION, ALL MINUS QUIET DAYS, GEOMAGNETIC COMPONENTS, MEAN OF 12 MONTHS, POLAR YEAR, 1932-33 (GEOMAGNETIC LATITUDES INDICATED IN PARENTHESES)

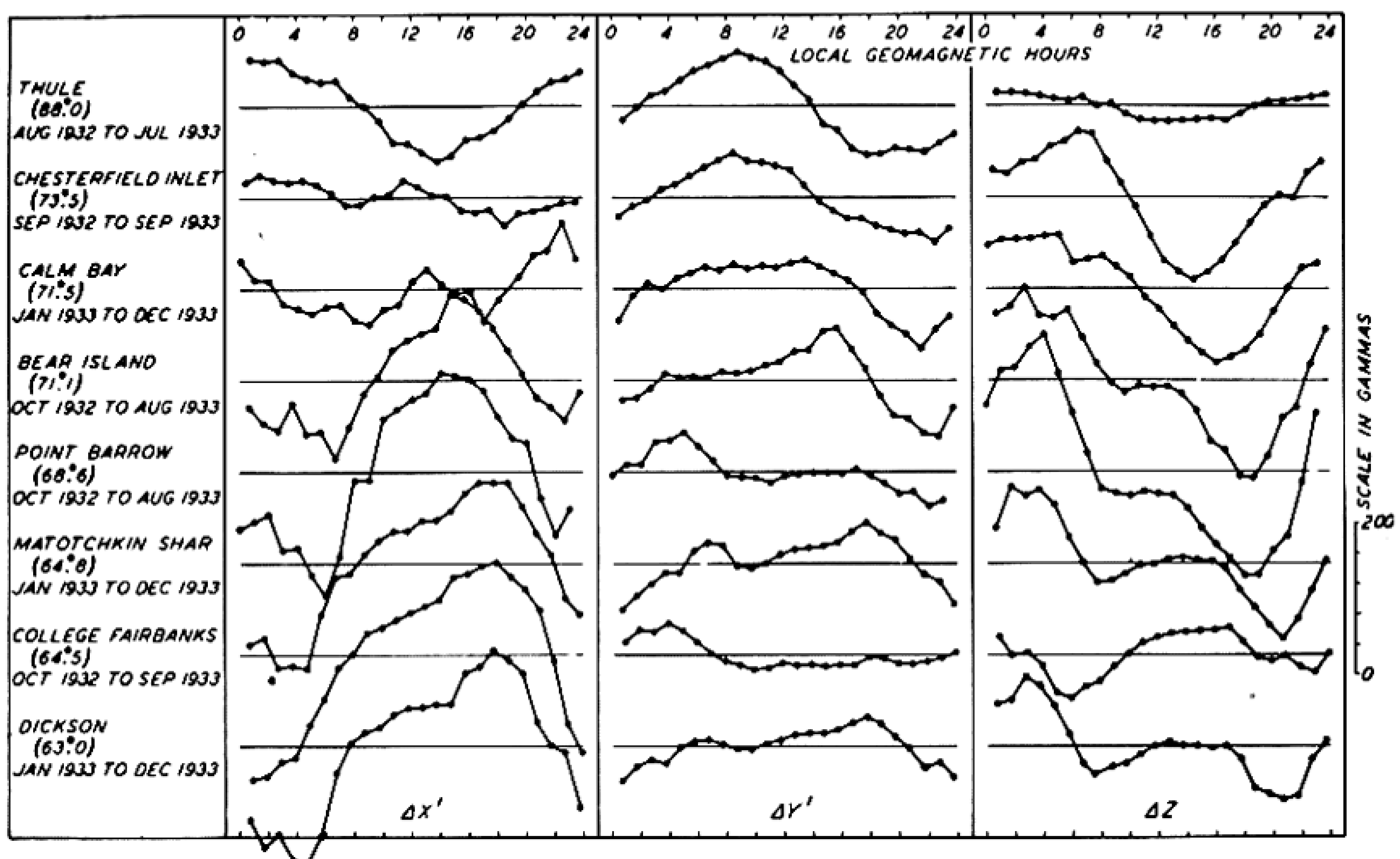

FIG. 91 (E) – AVERAGE DAILY VARIATION, DISTURBED MINUS QUIET DAYS, (S_D) GEOMAGNETIC COMPONENTS, INHOMOGENEOUS DATA, POLAR YEAR, 1932–33

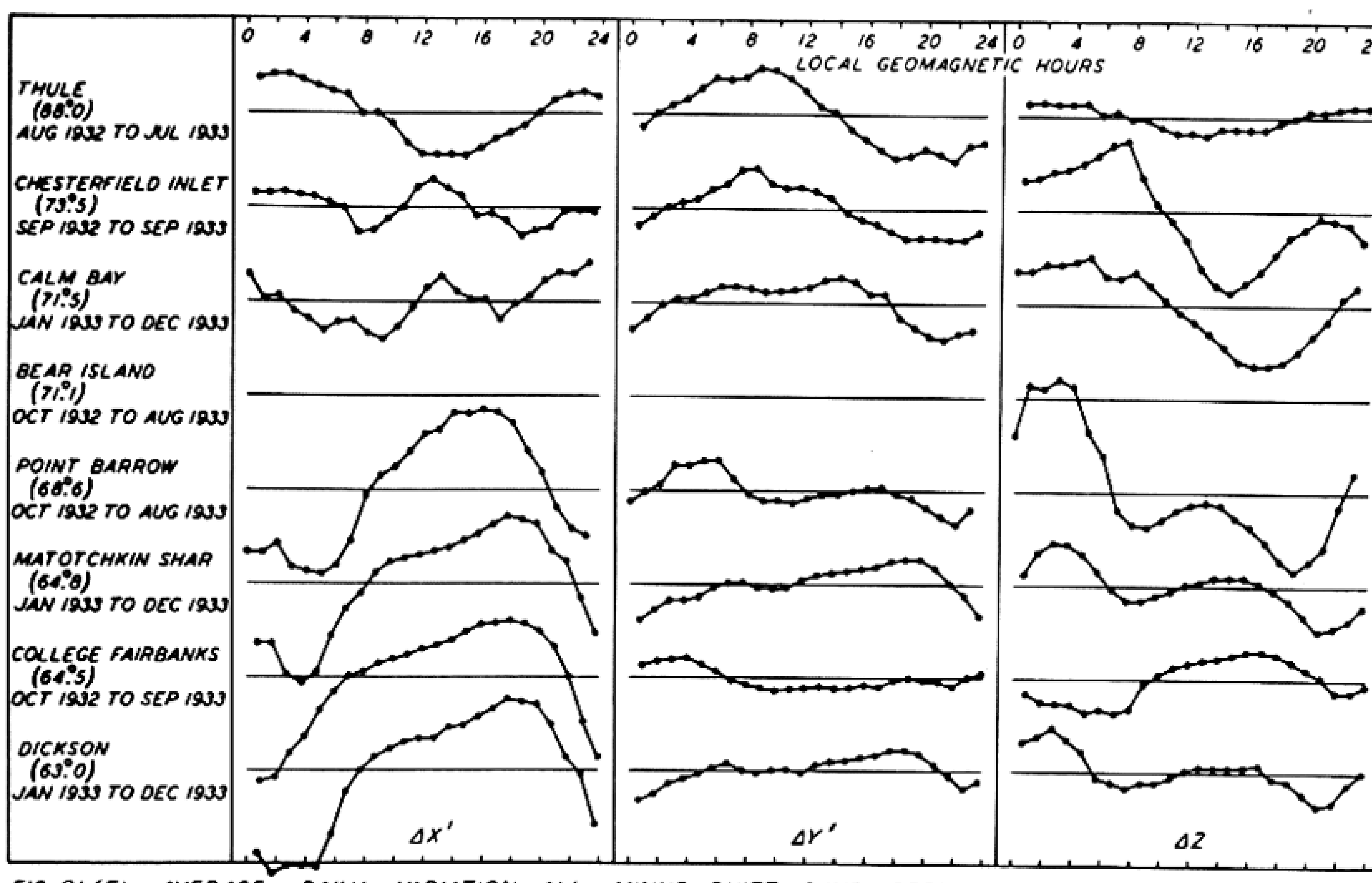

FIG. 91 (F)—AVERAGE DAILY VARIATION, ALL MINUS QUIET DAYS, GEOMAGNETIC COMPONENTS, INHOMOGENEOUS DATA, POLAR YEAR, 1932-33

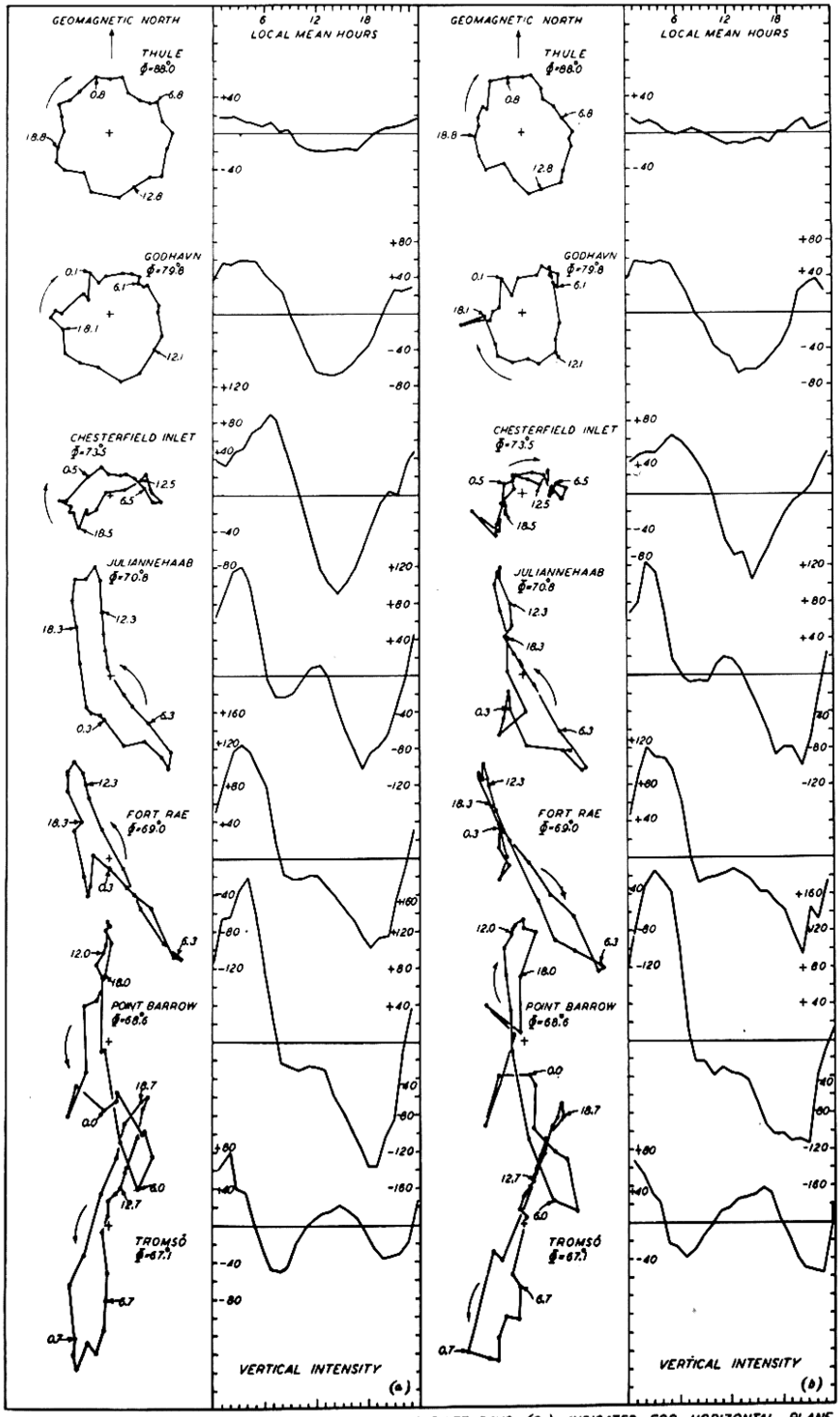

FIG. 91 (G) — AVERAGE DAILY VARIATION, DISTURBED MINUS QUIET DAYS, (S_D), INDICATED FOR HORIZONTAL PLANE, BY VECTOR-DIAGRAMS LOCAL GEOMAGNETIC TIME, AND FOR VERTICAL INTENSITY, (a) YEAR AND (b) WINTER, POLAR YEAR, 1932-33

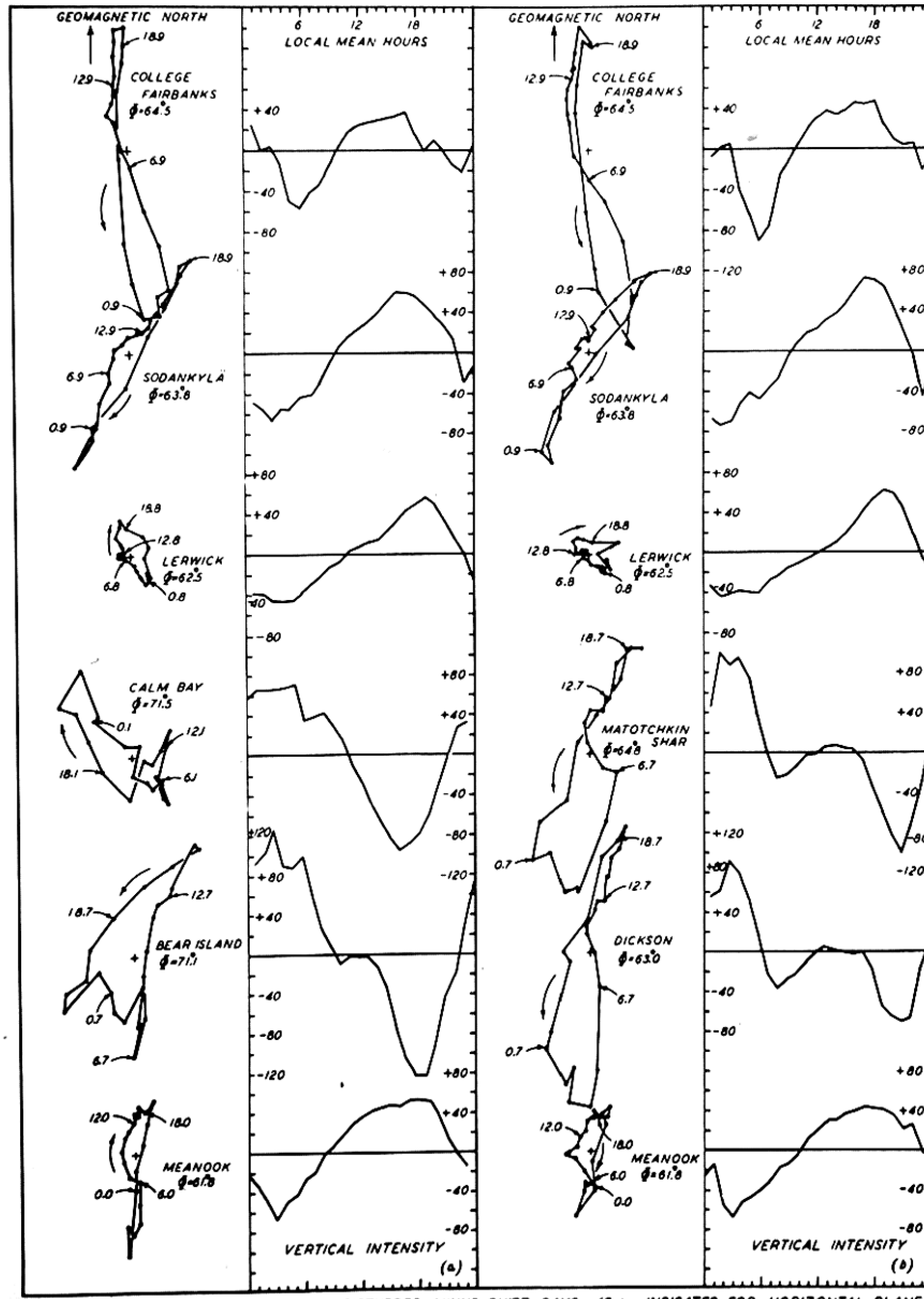

FIG. 91 (H)—AVERAGE DAILY VARIATION, DISTURBED MINUS QUIET DAYS, (S_D), INDICATED FOR HORIZONTAL PLANE, BY VECTOR-DIAGRAMS LOCAL GEOMAGNETIC TIME, AND FOR VERTICAL INTENSITY, (a) YEAR AND (b) WINTER, POLAR YEAR, 1932-33

(NOTE:—MATOTCHKIN SHAR, DICKSON AND CALM BAY ARE FOR THE YEAR 1933, BEAR ISLAND IS FOR OCTOBER 1932 THROUGH AUGUST, 1933)

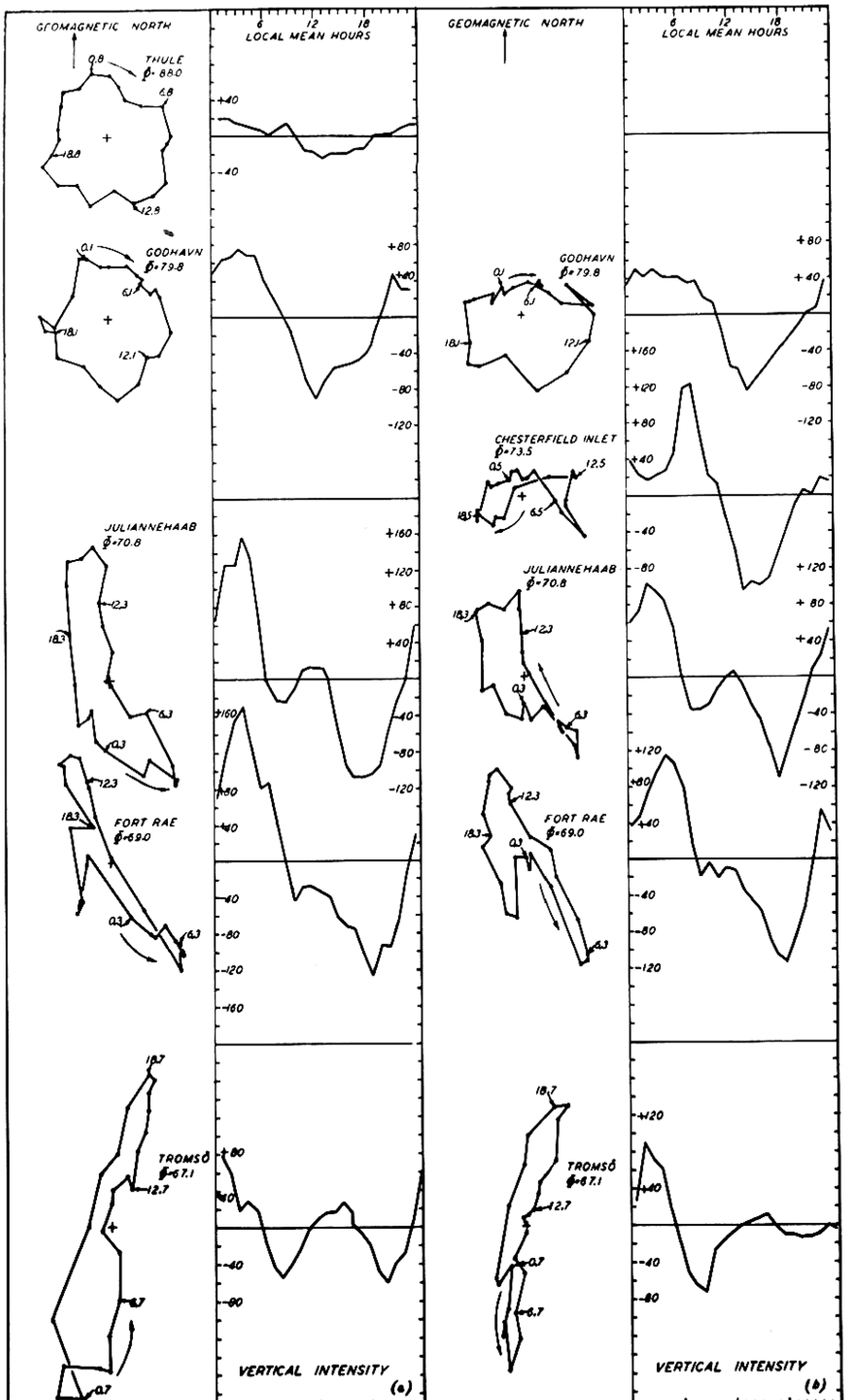

FIG. 91 (I)—AVERAGE DAILY VARIATION, DISTURBED MINUS QUIET DAYS, (S_D) INDICATED FOR HORIZONTAL PLANE, BY VECTOR-DIAGRAMS LOCAL GEOMAGNETIC TIME, AND FOR VERTICAL INTENSITY, (a) EQUINOX AND (b) SUMMER, POLAR YEAR, 1932-33

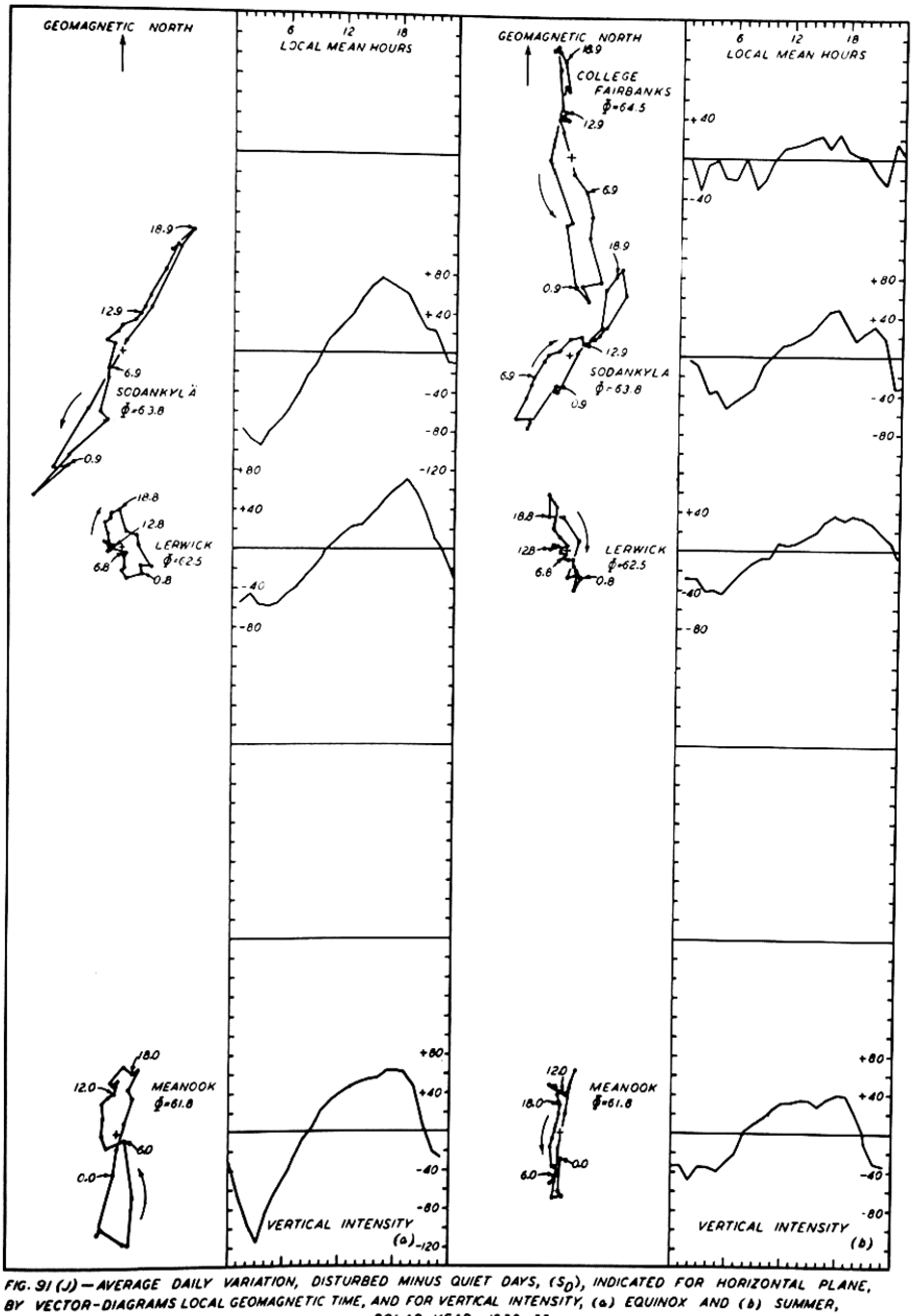

FIG. 91 (J) — AVERAGE DAILY VARIATION, DISTURBED MINUS QUIET DAYS, (S_D), INDICATED FOR HORIZONTAL PLANE, BY VECTOR-DIAGRAMS LOCAL GEOMAGNETIC TIME, AND FOR VERTICAL INTENSITY, (a) EQUINOX AND (b) SUMMER, POLAR YEAR, 1932-33

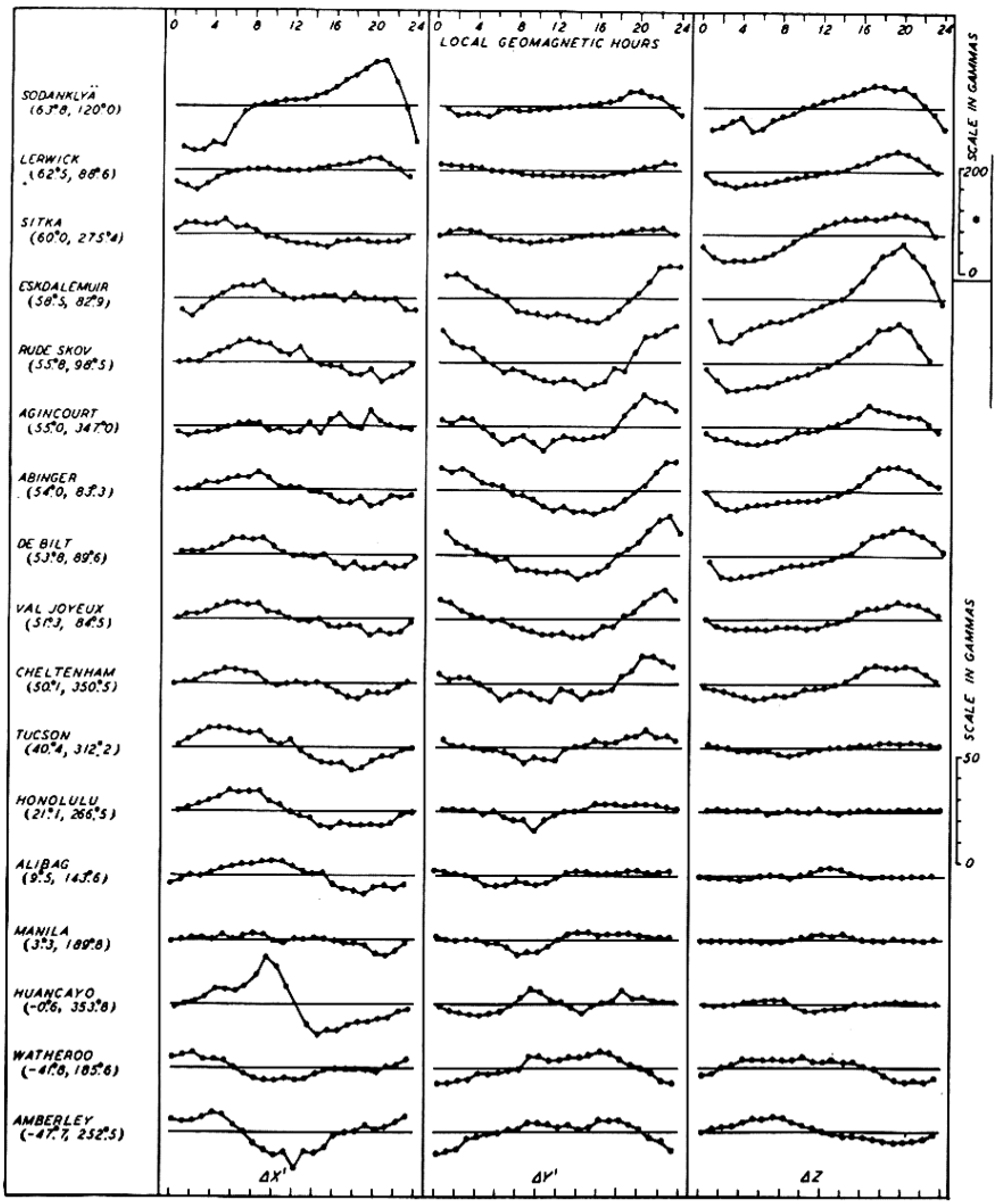

FIG. 92—DISTURBANCE DAILY VARIATION (S_D), DISTURBED DAYS, JANUARY, 1922-33 (GEOMAGNETIC LATITUDES AND LONGITUDES INDICATED RESPECTIVELY IN PARENTHESES)

* NOTE PARTICULARLY THAT SCALES FOR GRAPHS IN AURORAL REGIONS ARE DIFFERENT THAN FOR OTHERS

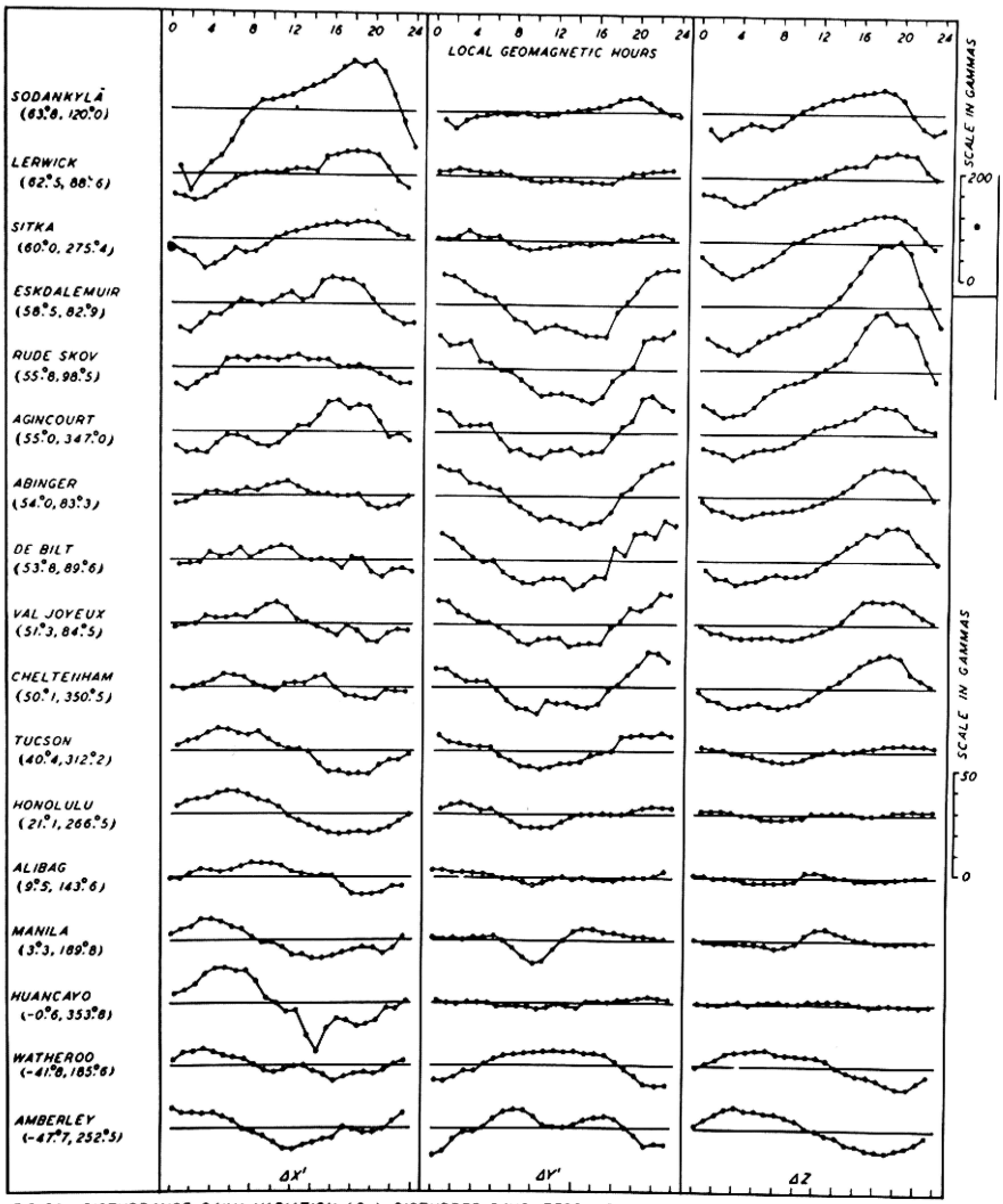

FIG. 93 — DISTURBANCE DAILY VARIATION (S_D), DISTURBED DAYS, FEBRUARY, 1922–33 (GEOMAGNETIC LATITUDES AND LONGITUDES INDICATED RESPECTIVELY IN PARENTHESES)

* NOTE PARTICULARLY THAT SCALES FOR GRAPHS IN AURORAL REGIONS ARE DIFFERENT THAN FOR OTHERS

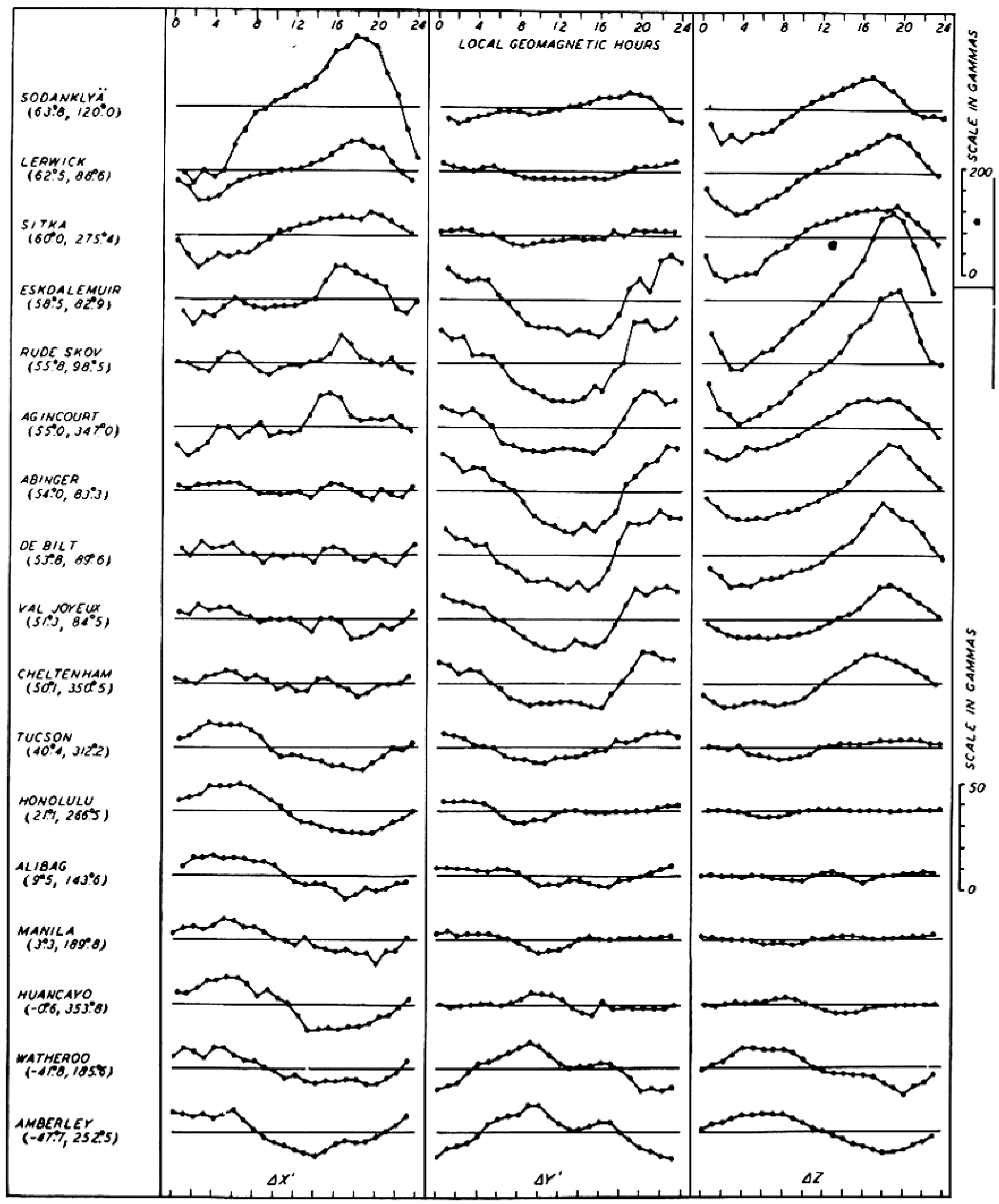

FIG. 94 — DISTURBANCE DAILY VARIATION (S_D), DISTURBED DAYS, MARCH, 1922–33 (GEOMAGNETIC LATITUDES AND LONGITUDES INDICATED RESPECTIVELY IN PARENTHESES)

* NOTE PARTICULARLY THAT SCALES FOR GRAPHS IN AURORAL REGIONS ARE DIFFERENT THAN FOR OTHERS

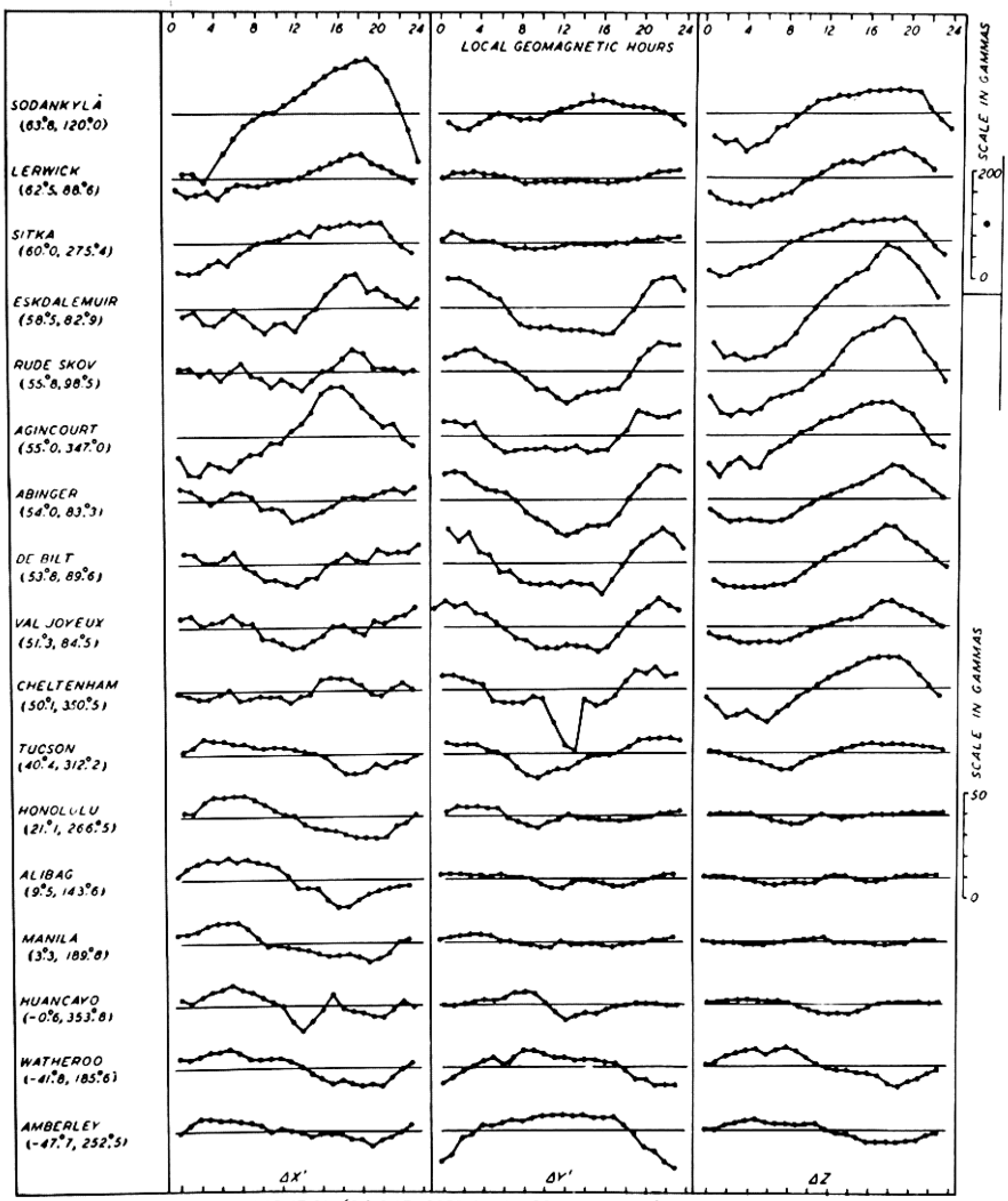

FIG. 95—DISTURBANCE DAILY VARIATION (S_D) DISTURBED DAYS, APRIL, 1922-33 (GEOMAGNETIC LATITUDES AND LONGITUDES INDICATED RESPECTIVELY IN PARENTHESES)

* NOTE PARTICULARLY THAT SCALES FOR GRAPHS IN AURORAL REGIONS ARE DIFFERENT THAN FOR OTHERS

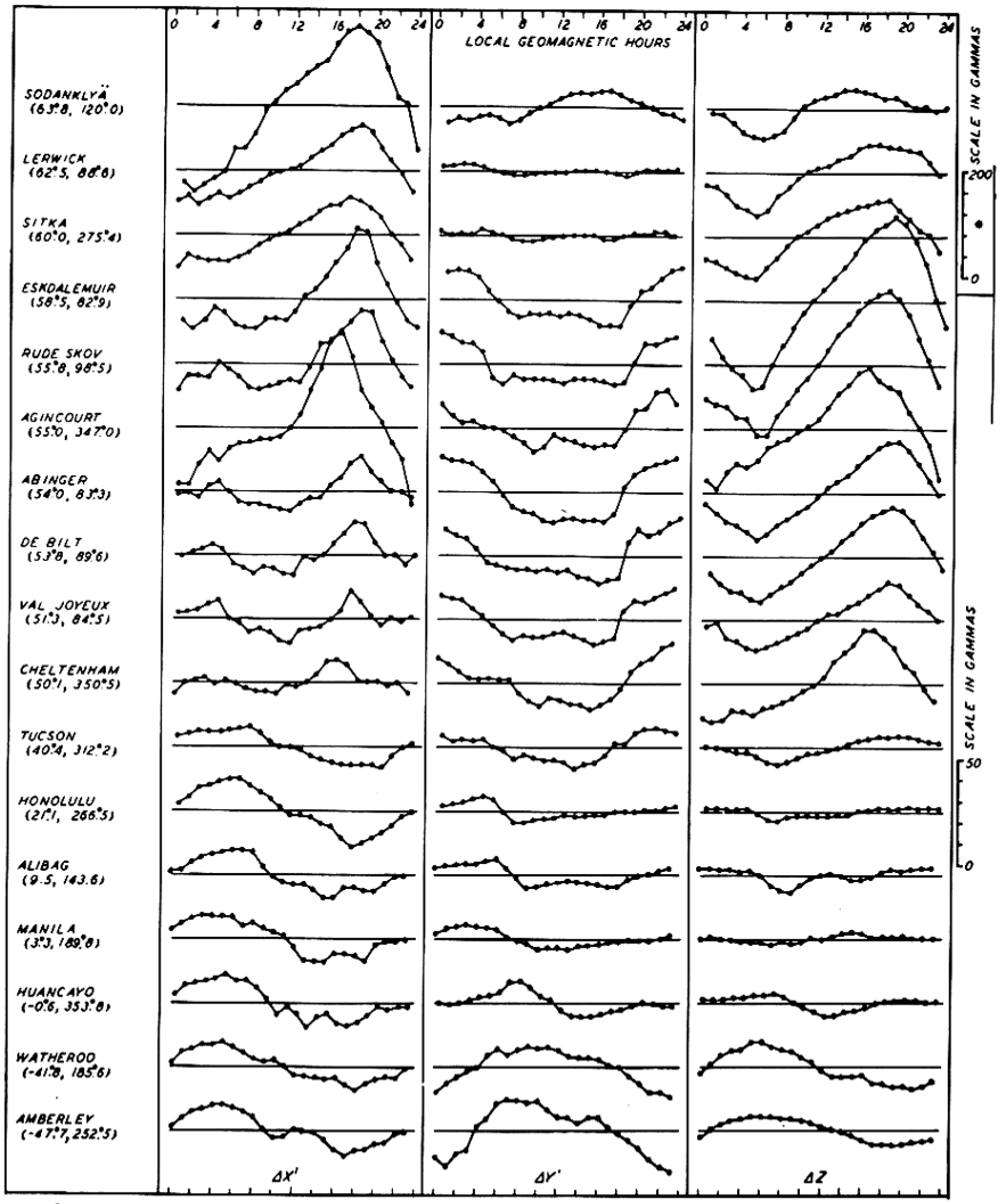

FIG. 96 - DISTURBANCE DAILY VARIATION (S_D), DISTURBED DAYS, MAY, 1922-33 (GEOMAGNETIC LATITUDES AND LONGITUDES INDICATED RESPECTIVELY IN PARENTHESES)

* NOTE PARTICULARLY THAT SCALES FOR GRAPHS IN AURORAL REGIONS ARE DIFFERENT THAN FOR OTHERS

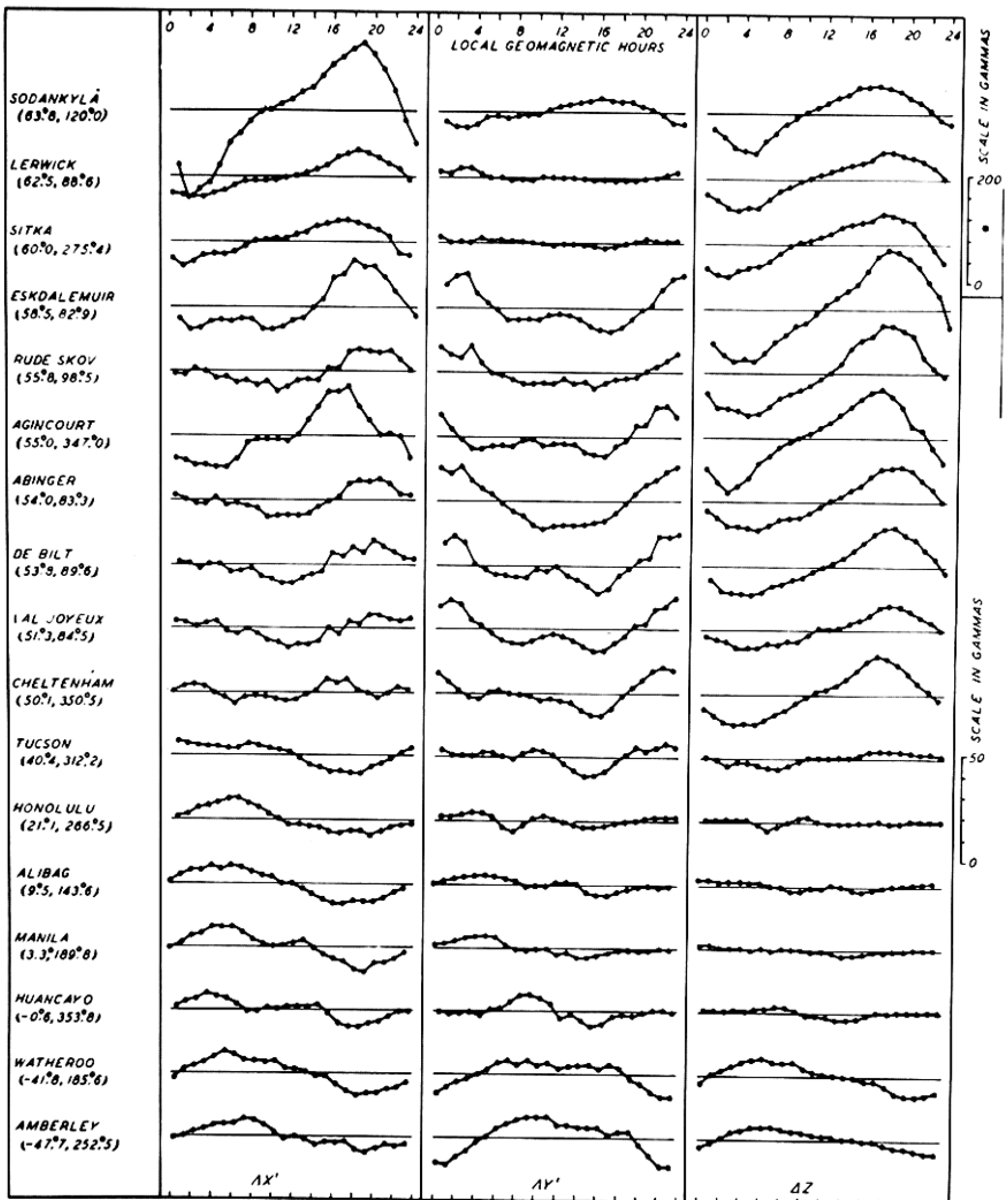

FIG. 97 – DISTURBANCE DAILY VARIATION (S_D), DISTURBED DAYS, JUNE, 1922 – 33 (GEOMAGNETIC LATITUDES AND LONGITUDES INDICATED RESPECTIVELY IN PARENTHESES)

* NOTE PARTICULARLY THAT SCALES FOR GRAPHS IN AURORAL REGIONS ARE DIFFERENT THAN FOR OTHERS

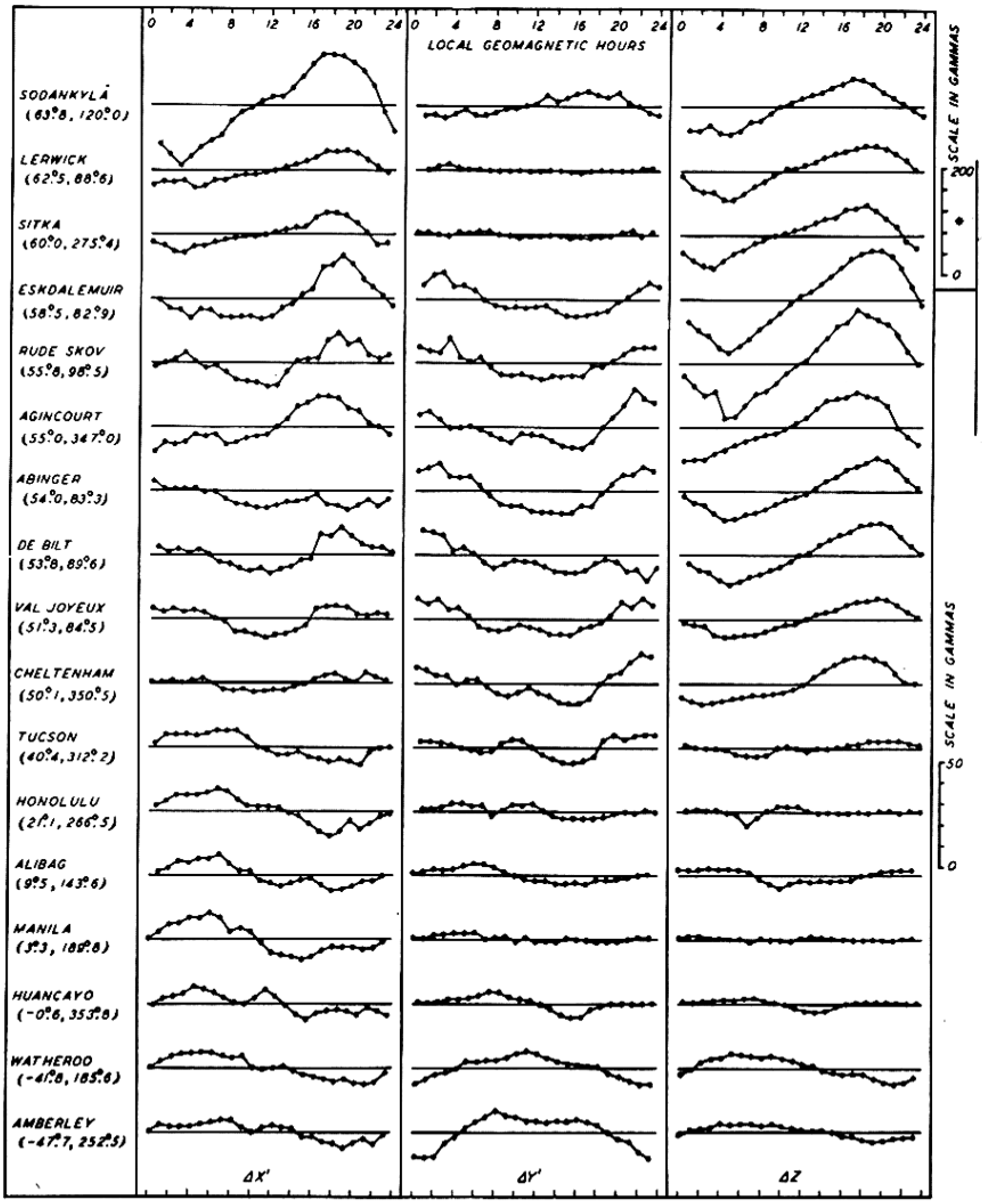

FIG. 98— DISTURBANCE DAILY VARIATION (S_D), DISTURBED DAYS, JULY, 1922-33 (GEOMAGNETIC LATITUDES AND LONGITUDES INDICATED RESPECTIVELY IN PARENTHESES)

* NOTE PARTICULARLY THAT SCALES FOR GRAPHS IN AURORAL REGIONS ARE DIFFERENT THAN FOR OTHERS

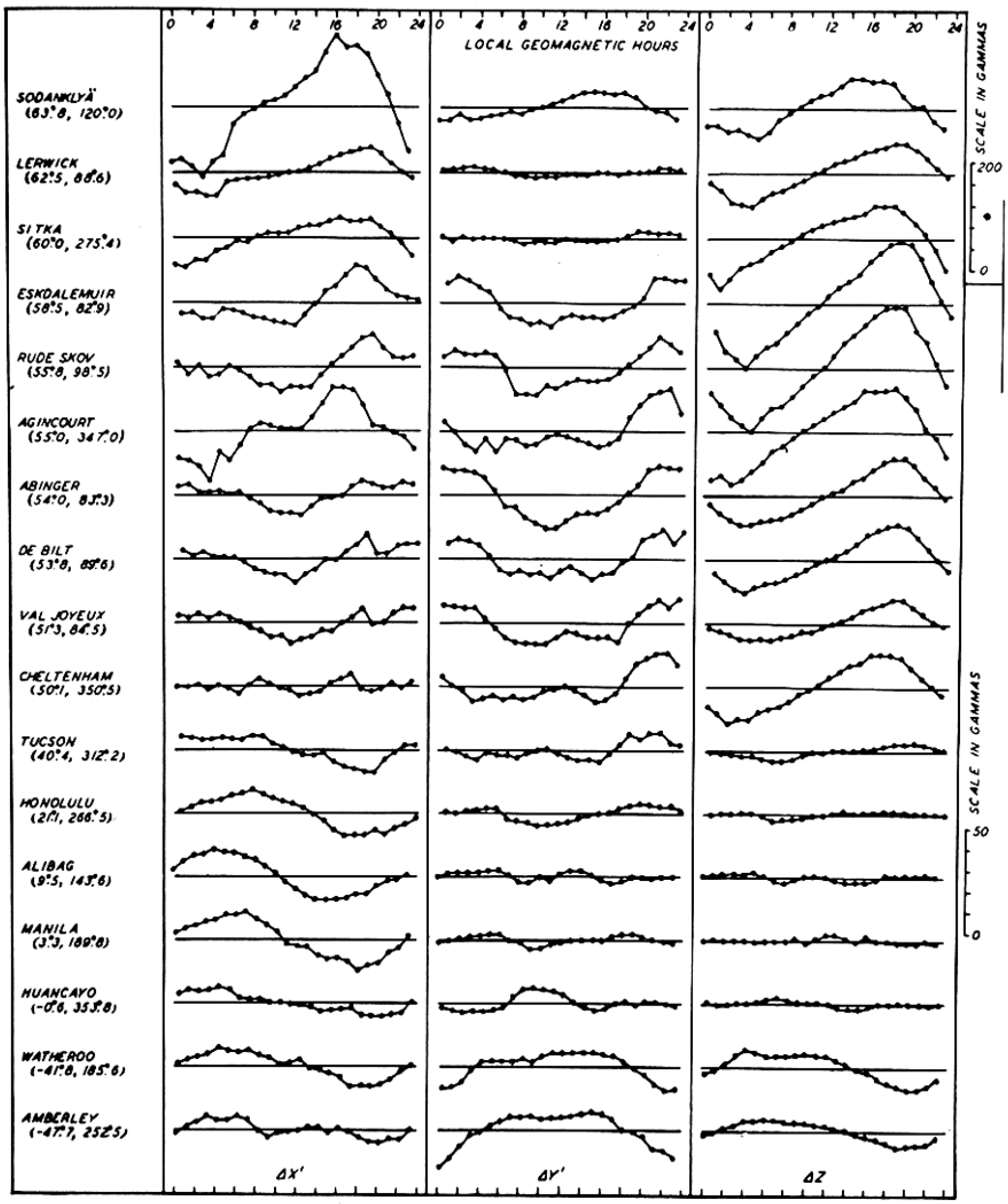

FIG. 99 — DISTURBANCE DAILY VARIATION (S_D), DISTURBED DAYS, AUGUST, 1922-33 (GEOMAGNETIC LATITUDES AND LONGITUDES INDICATED RESPECTIVELY IN PARENTHESES)

* NOTE PARTICULARLY THAT SCALES FOR GRAPHS IN AURORAL REGIONS ARE DIFFERENT THAN FOR OTHERS

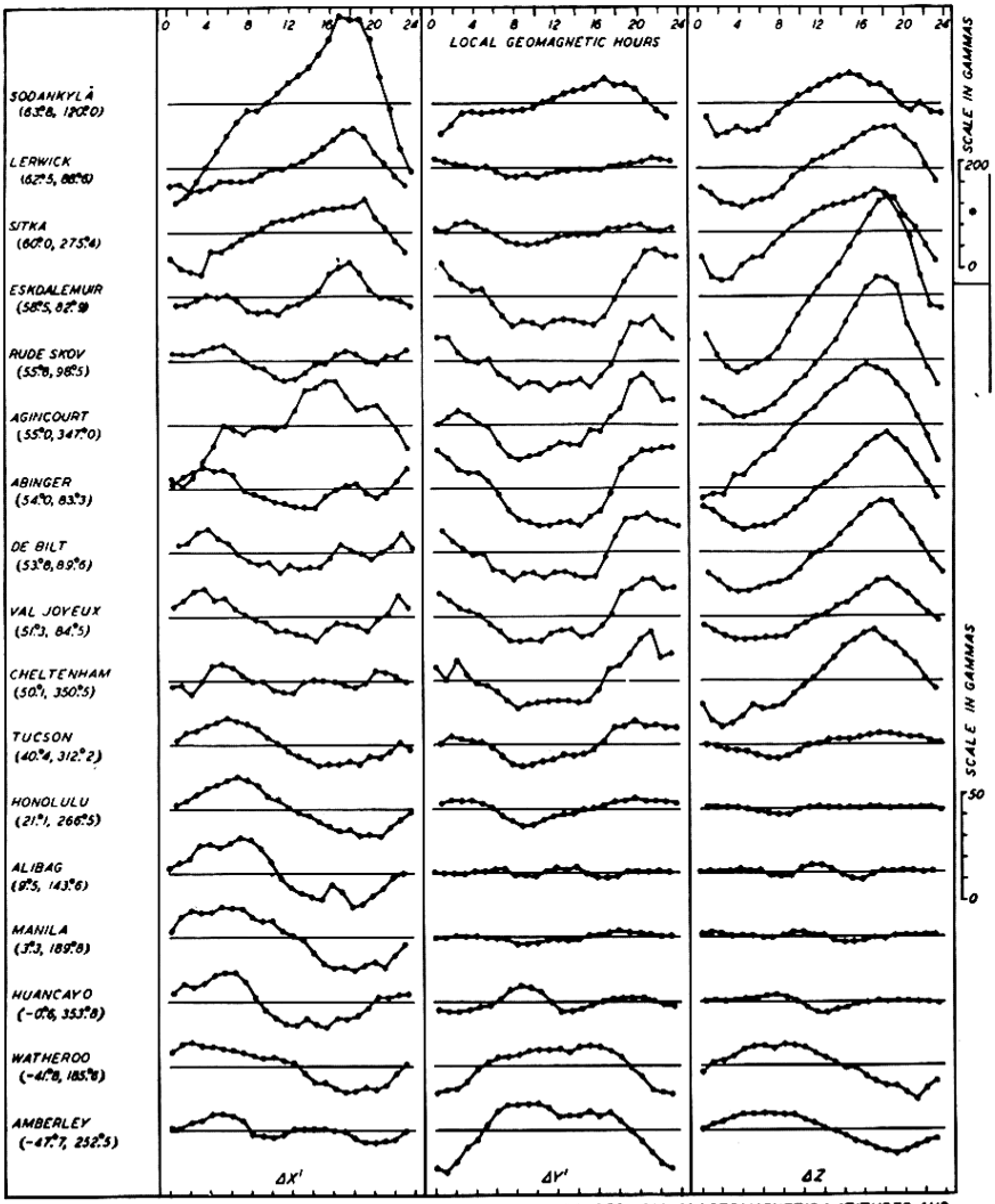

FIG. 100-DISTURBANCE DAILY VARIATION (S_D), DISTURBED DAYS, SEPTEMBER, 1922-33 (GEOMAGNETIC LATITUDES AND LONGITUDES INDICATED RESPECTIVELY IN PARENTHESES)

* NOTE PARTICULARLY THAT SCALES FOR GRAPHS IN AURORAL REGIONS ARE DIFFERENT THAN FOR OTHERS

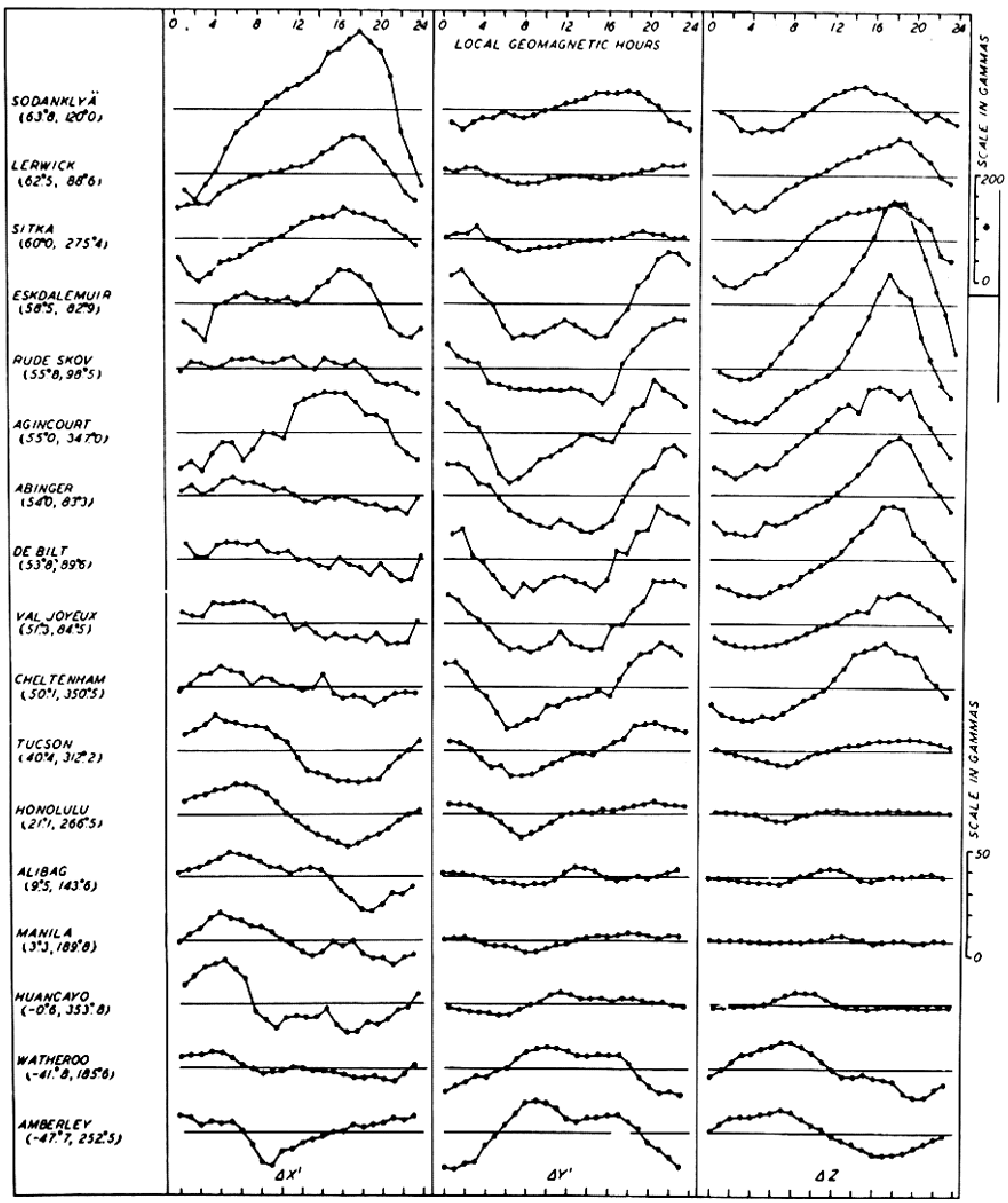

FIG. 101—DISTURBANCE DAILY VARIATION (S_D), DISTURBED DAYS, OCTOBER, 1922–33 (GEOMAGNETIC LATITUDES AND LONGITUDES INDICATED RESPECTIVELY IN PARENTHESES)

* NOTE PARTICULARLY THAT SCALES FOR GRAPHS IN AURORAL REGIONS ARE DIFFERENT THAN FOR OTHERS

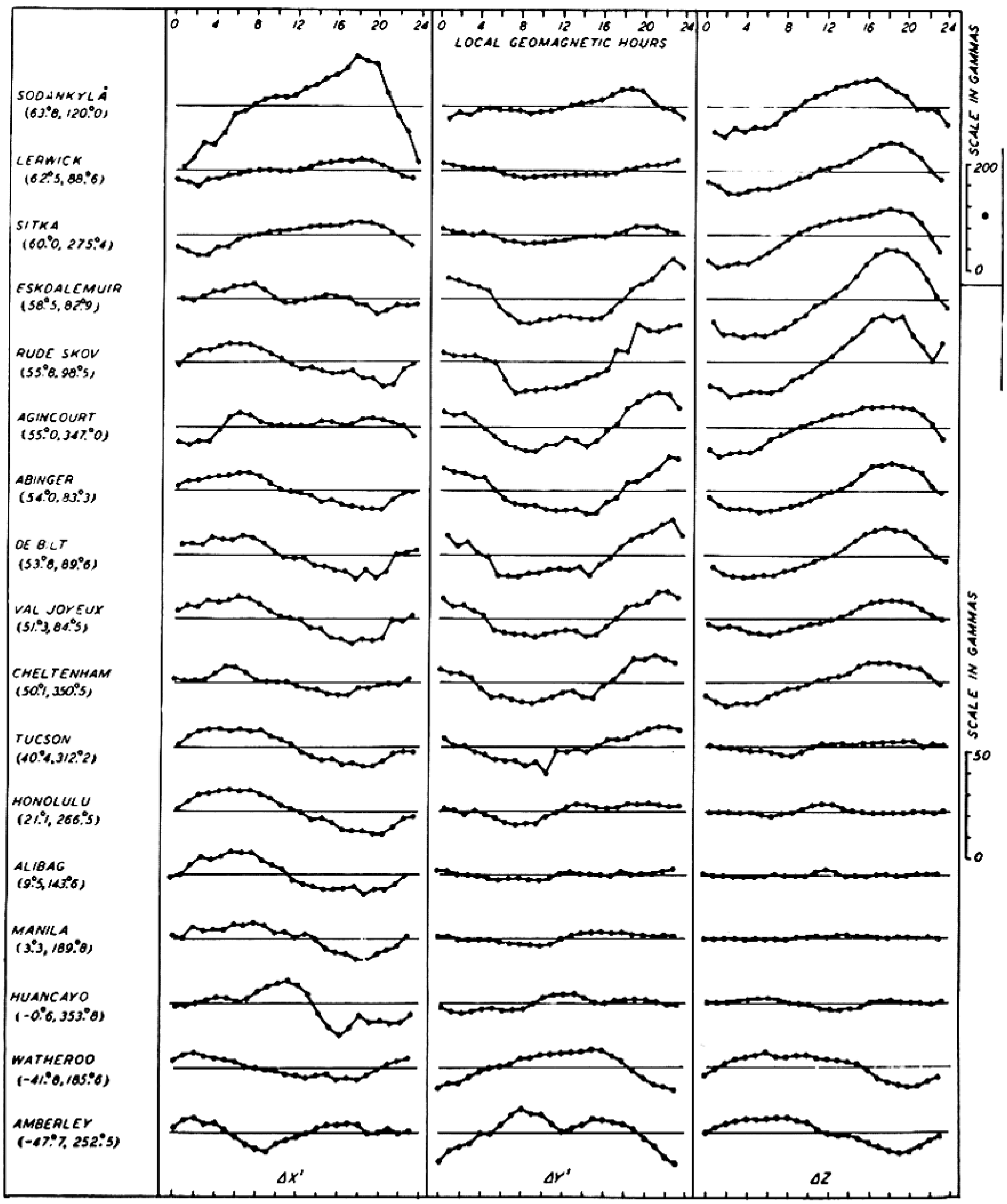

FIG. 102 – DISTURBANCE DAILY VARIATION (S_D), DISTURBED DAYS, NOVEMBER, 1922-33 (GEOMAGNETIC LATITUDES AND LONGITUDES INDICATED RESPECTIVELY IN PARENTHESES)

* NOTE PARTICULARLY THAT SCALES FOR GRAPHS IN AURORAL REGIONS ARE DIFFERENT THAN FOR OTHERS

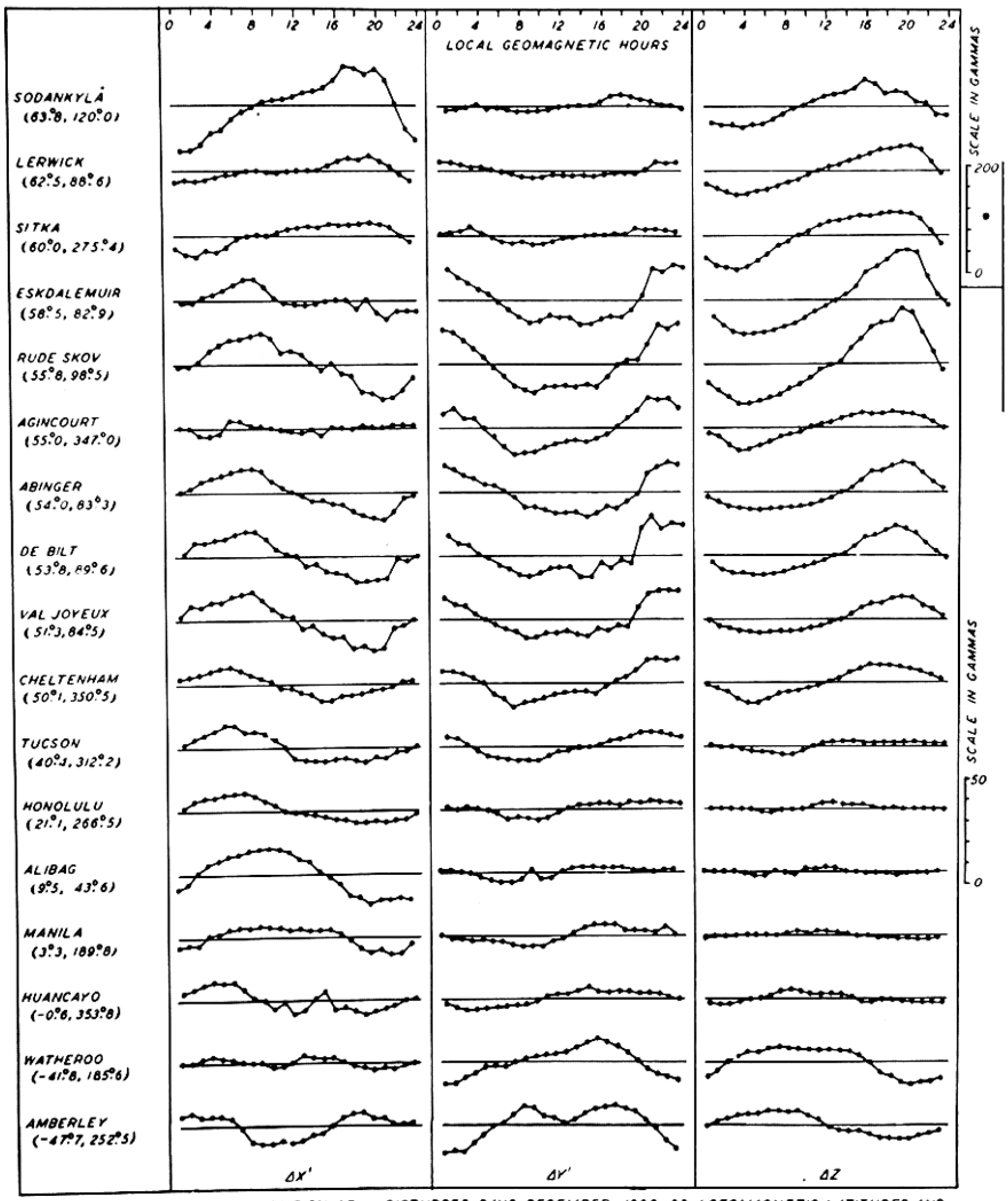

FIG. 103—DISTURBANCE DAILY VARIATION (S_D), DISTURBED DAYS, DECEMBER, 1922-33 (GEOMAGNETIC LATITUDES AND LONGITUDES INDICATED RESPECTIVELY IN PARENTHESES)

* NOTE PARTICULARLY THAT SCALES FOR GRAPHS IN AURORAL REGIONS ARE DIFFERENT THAN FOR OTHERS

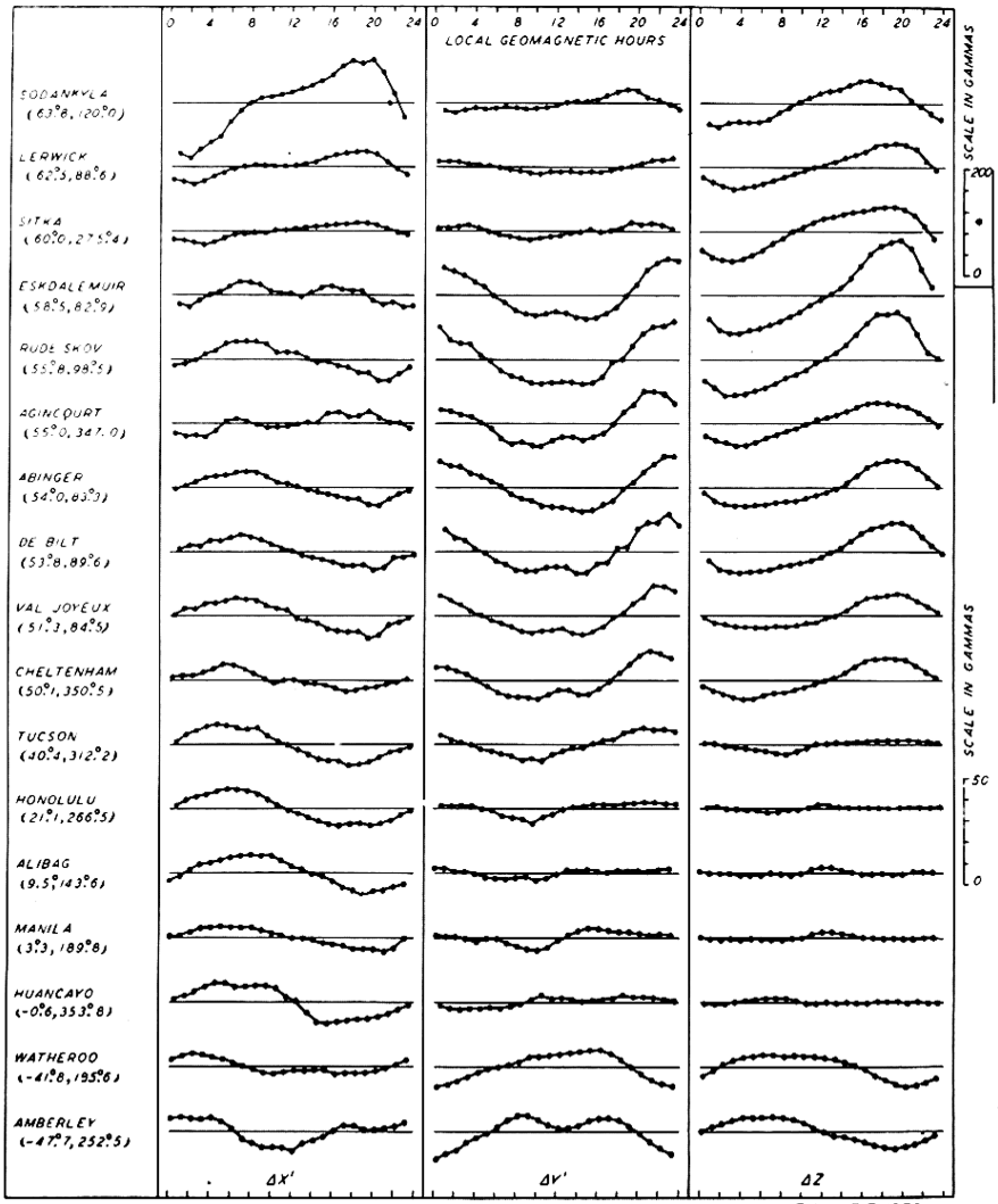

FIG. 104 - DISTURBANCE DAILY VARIATION (S_D), DISTURBED DAYS, WINTER, 1922-33 (GEOMAGNETIC LATITUDES AND LONGITUDES INDICATED RESPECTIVELY IN PARENTHESES)

* NOTE PARTICULARLY THAT SCALES FOR GRAPHS IN AURORAL REGIONS ARE DIFFERENT THAN FOR OTHERS

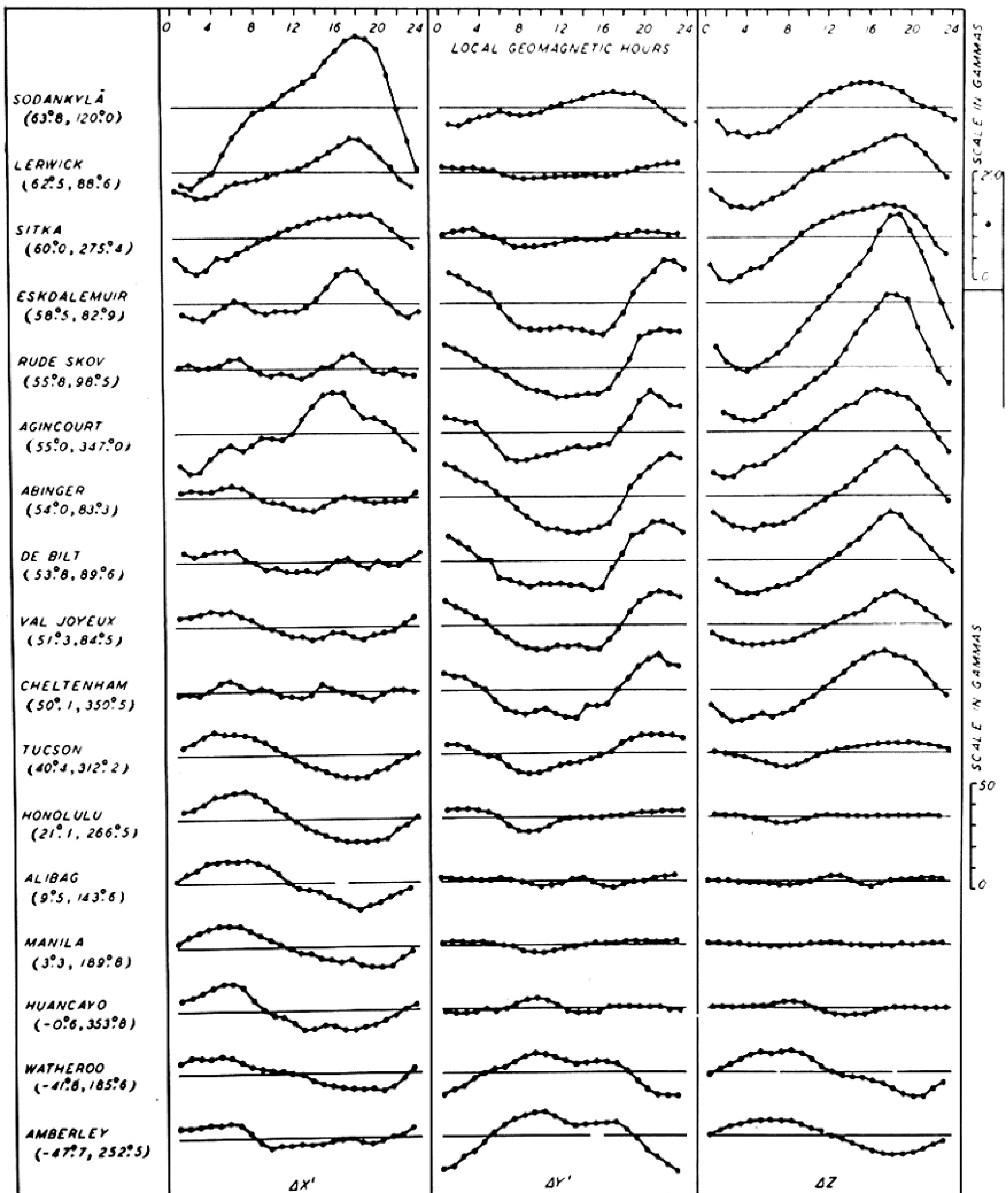

FIG. 105—DISTURBANCE DAILY VARIATION (S_D), DISTURBED DAYS, EQUINOX, 1922-33 (GEOMAGNETIC LATITUDES AND LONGITUDES INDICATED RESPECTIVELY IN PARENTHESES)

• NOTE PARTICULARLY THAT SCALES FOR GRAPHS IN AURORAL REGIONS ARE DIFFERENT THAN FOR OTHERS

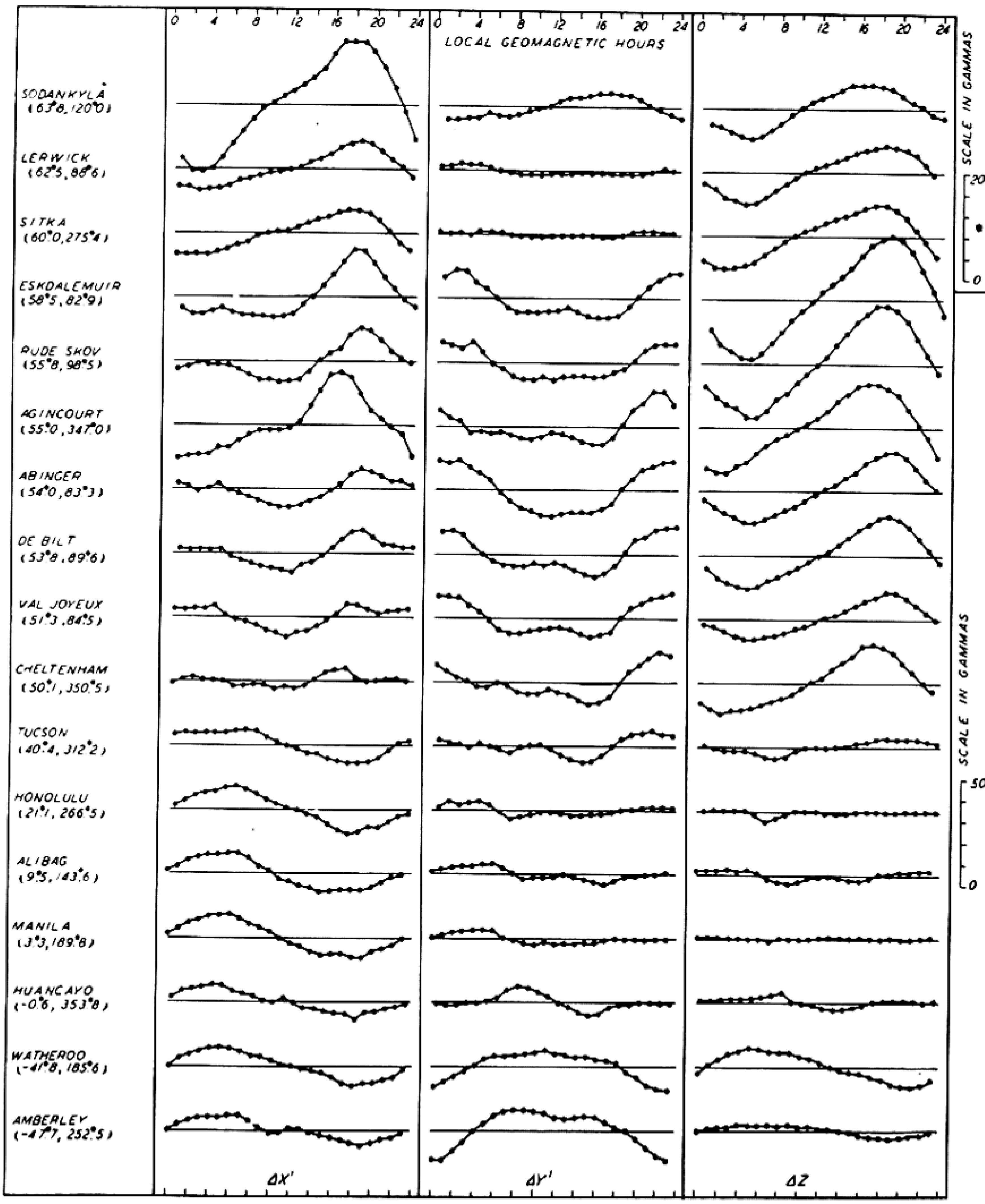

FIG. 106–DISTURBANCE DAILY VARIATION (S_D), DISTURBED DAYS, SUMMER, 1922-33 (GEOMAGNETIC LATITUDES AND LONGITUDES INDICATED RESPECTIVELY IN PARENTHESES)

* NOTE PARTICULARLY THAT SCALES FOR GRAPHS IN AURORAL REGIONS ARE DIFFERENT THAN FOR OTHERS

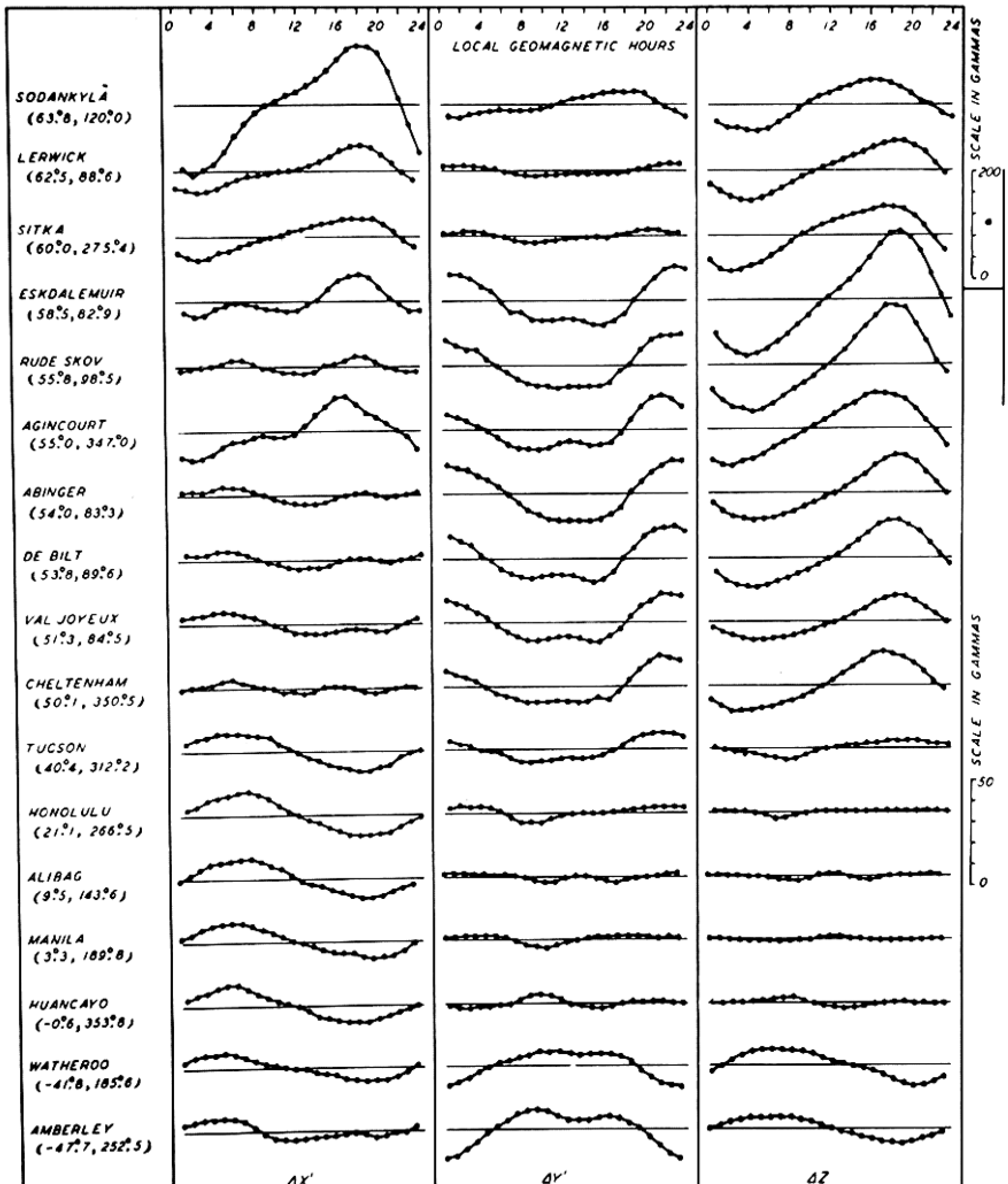

FIG. 107–DISTURBANCE DAILY VARIATION (S_D), DISTURBED DAYS, YEAR, 1922-33 (GEOMAGNETIC LATITUDES AND LONGITUDES INDICATED RESPECTIVELY IN PARENTHESES)

* NOTE PARTICULARLY THAT SCALES FOR GRAPHS IN AURORAL REGIONS ARE DIFFERENT THAN FOR OTHERS

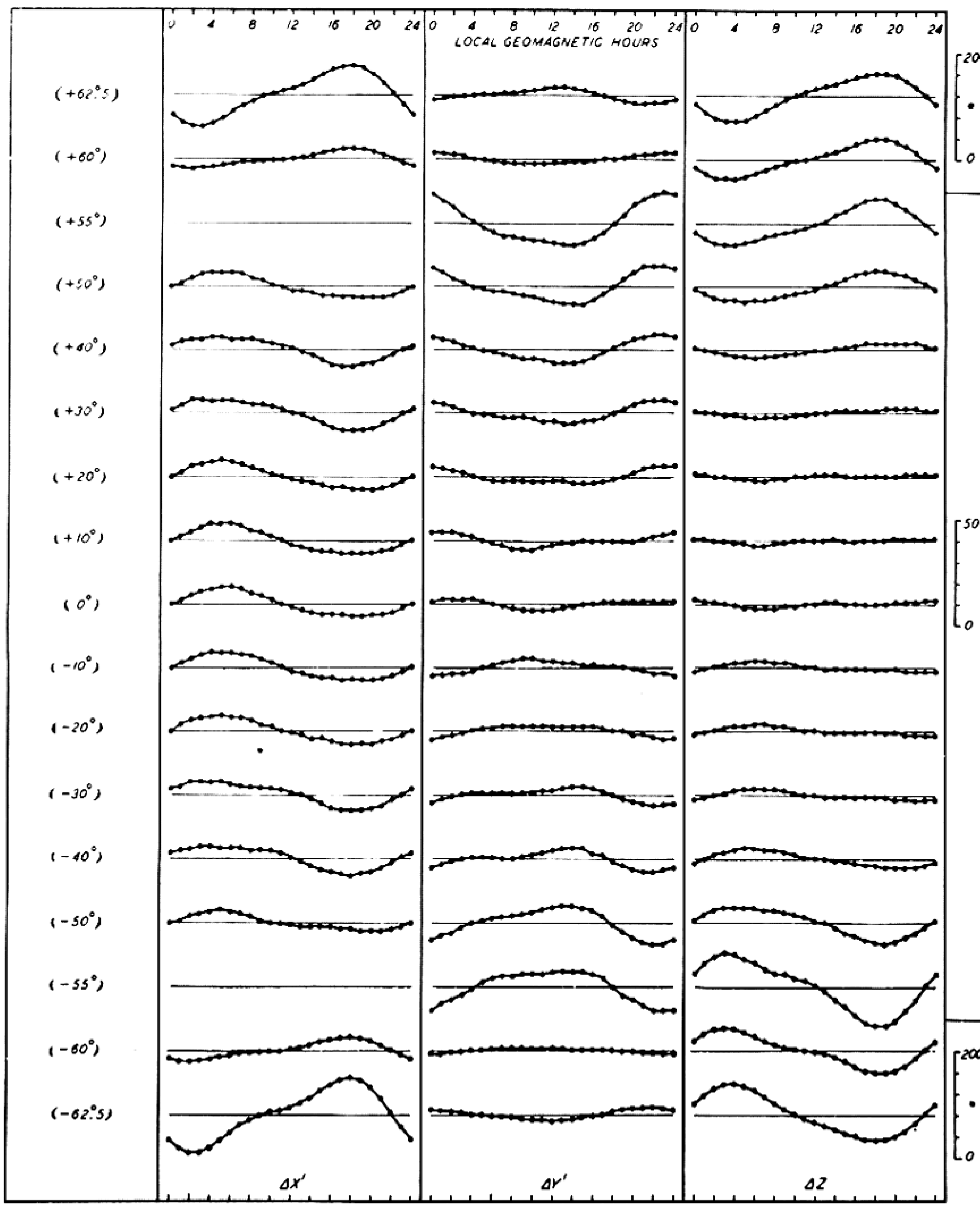

FIG. 108—DISTURBANCE DAILY VARIATION ON DISTURBED DAYS (S_D), IN VARIOUS GEOMAGNETIC LATITUDES, GEOMAGNETIC COMPONENTS, JANUARY, 1922 – 33

* NOTE PARTICULARLY THAT SCALES FOR GRAPHS IN AURORAL REGIONS ARE DIFFERENT THAN FOR OTHERS

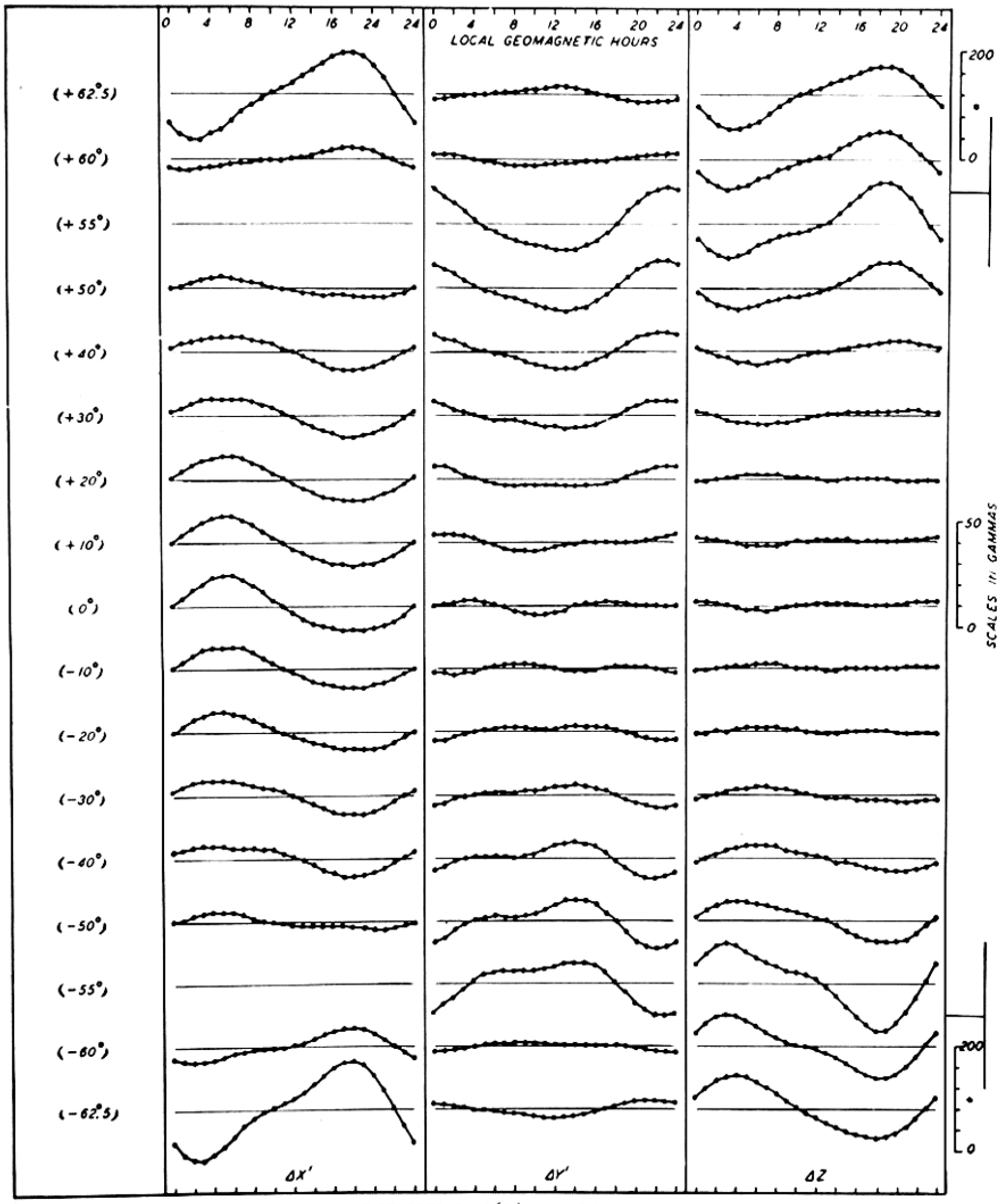

FIG. 109–DISTURBANCE DAILY VARIATION ON DISTURBED DAYS (S_D), IN VARIOUS GEOMAGNETIC LATITUDES, GEOMAGNETIC COMPONENTS, FEBRUARY, 1922–33

* NOTE PARTICULARLY THAT SCALES FOR GRAPHS IN AURORAL REGIONS ARE DIFFERENT THAN FOR OTHERS

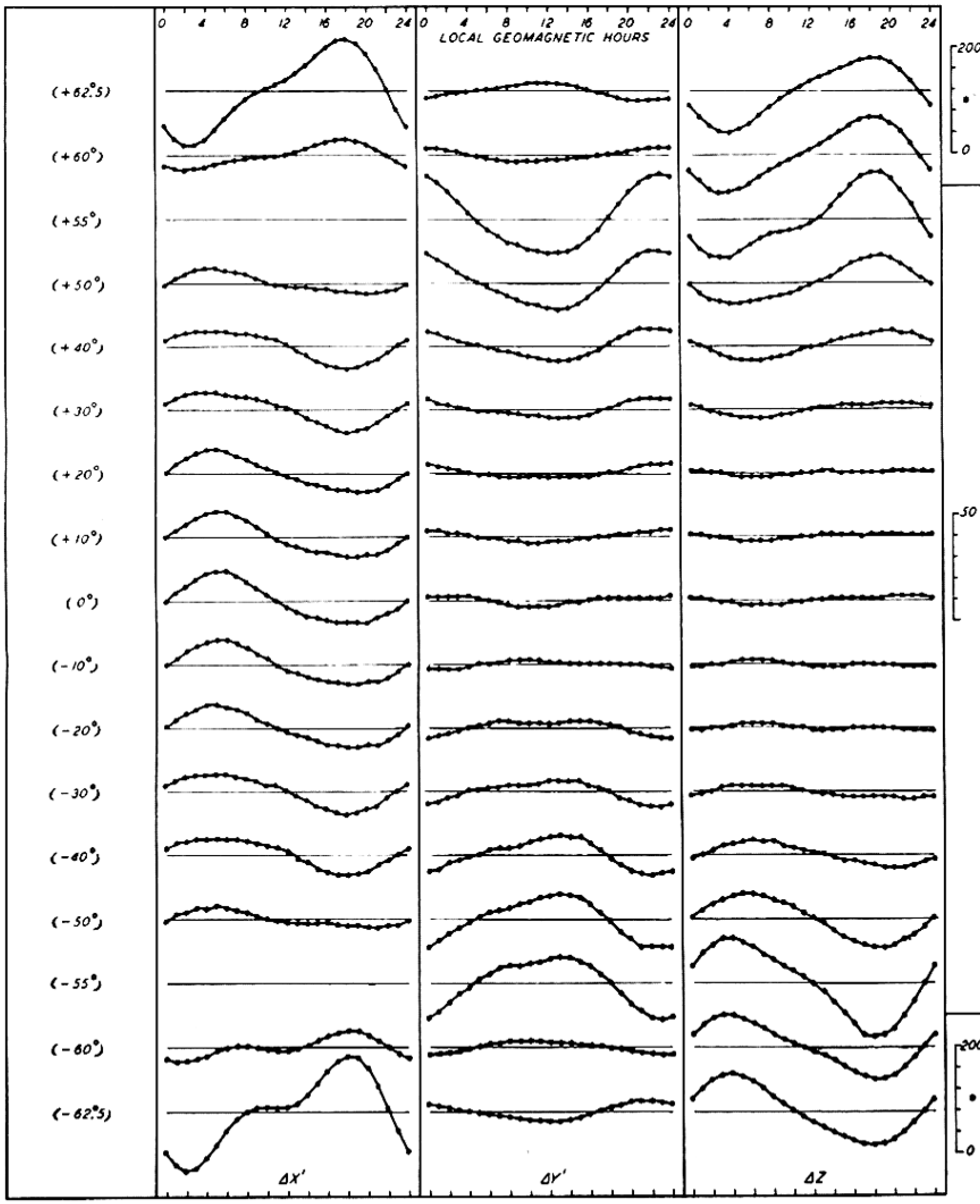

FIG. 110 — DISTURBANCE DAILY VARIATION ON DISTURBED DAYS (S_D), IN VARIOUS GEOMAGNETIC LATITUDES, GEOMAGNETIC COMPONENTS, MARCH, 1922-33

* NOTE PARTICULARLY THAT SCALES FOR GRAPHS IN AURORAL REGIONS ARE DIFFERENT THAN FOR OTHERS

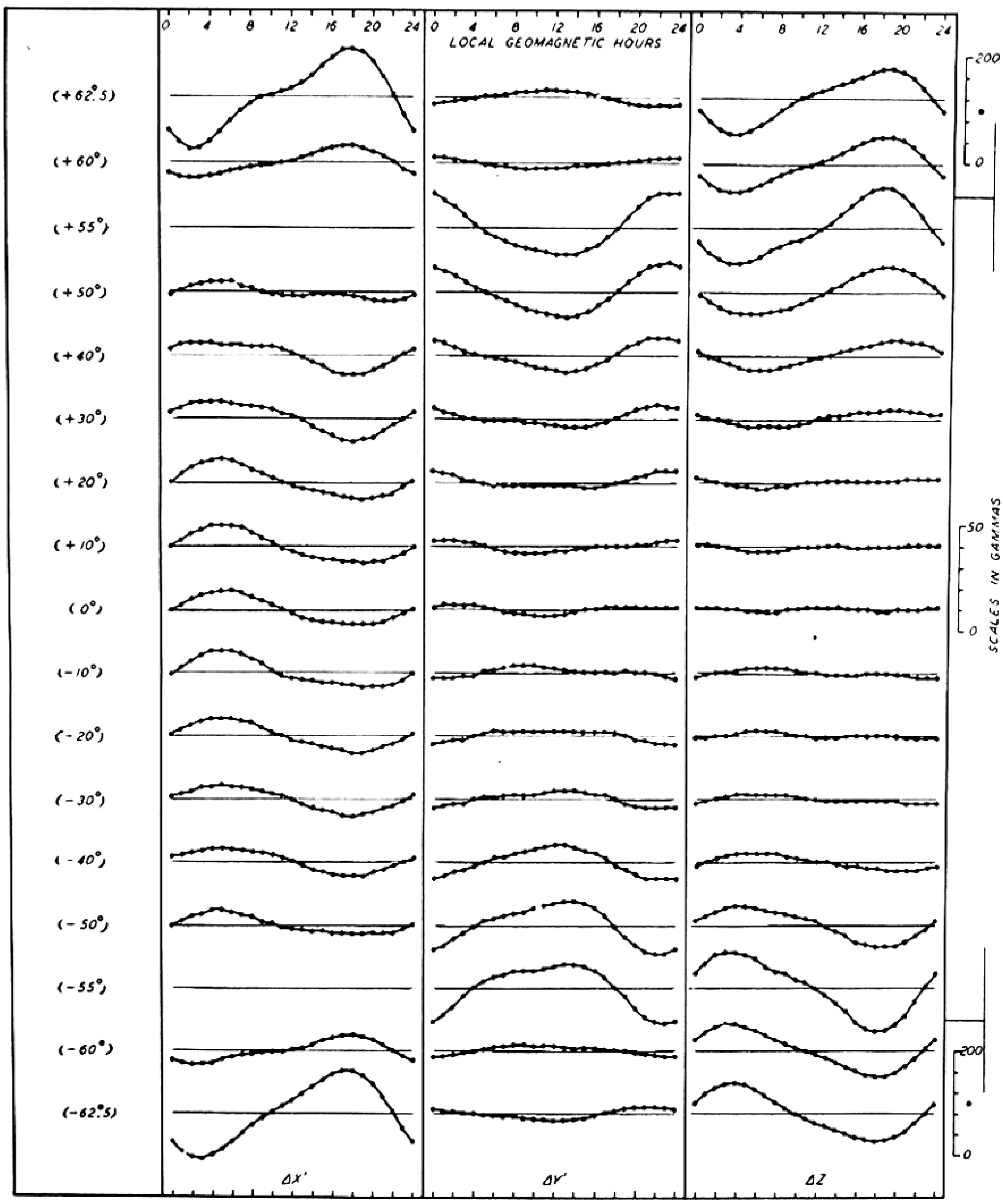

FIG. 111 — DISTURBANCE DAILY VARIATION ON DISTURBED DAYS (S_D), IN VARIOUS GEOMAGNETIC LATITUDES, GEOMAGNETIC COMPONENTS, APRIL, 1922 – 33

* NOTE PARTICULARLY THAT SCALES FOR GRAPHS IN AURORAL REGIONS ARE DIFFERENT THAN FOR OTHERS

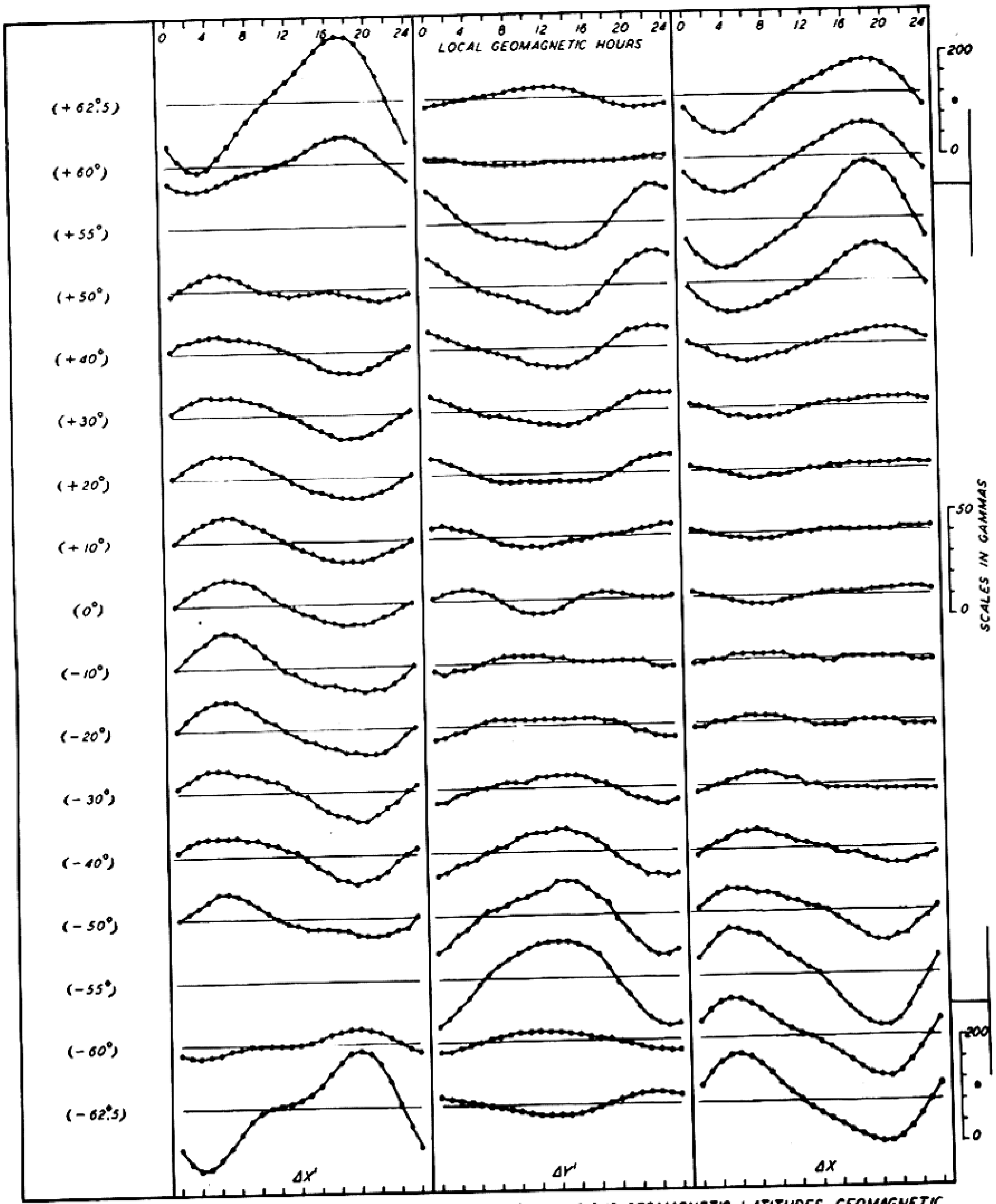

FIG. 112—DISTURBANCE DAILY VARIATION ON DISTURBED DAYS (S_D), IN VARIOUS GEOMAGNETIC LATITUDES, GEOMAGNETIC COMPONENTS, MAY, 1922–33

• NOTE PARTICULARLY THAT SCALES FOR GRAPHS IN AURORAL REGIONS ARE DIFFERENT THAN FOR OTHERS

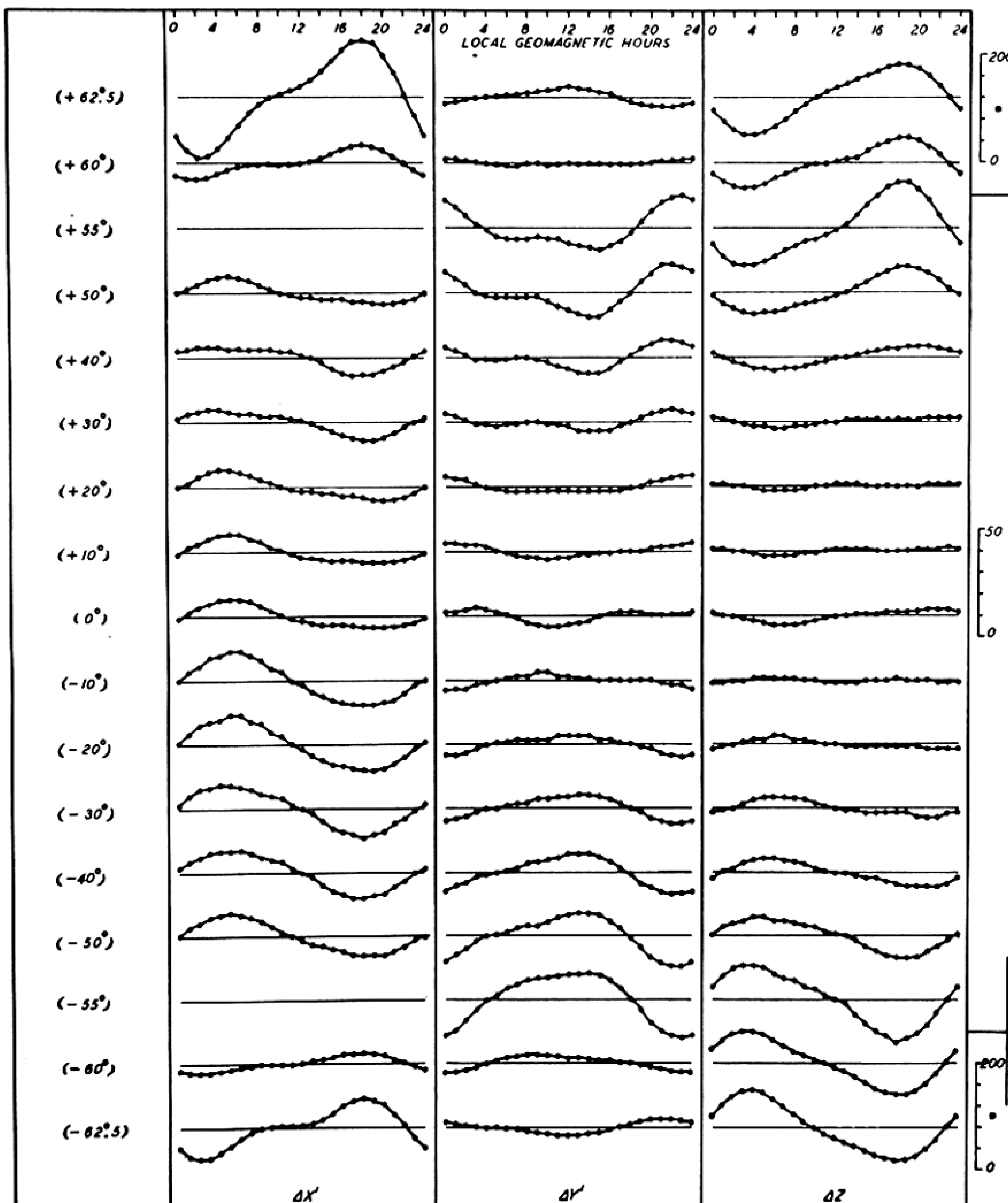

FIG. 113 – DISTURBANCE DAILY VARIATION ON DISTURBED DAYS (S_D), IN VARIOUS GEOMAGNETIC LATITUDES, GEOMAGNETIC COMPONENTS, JUNE, 1922 – 33

• NOTE PARTICULARLY THAT SCALES FOR GRAPHS IN AURORAL REGIONS ARE DIFFERENT THAN FOR OTHERS

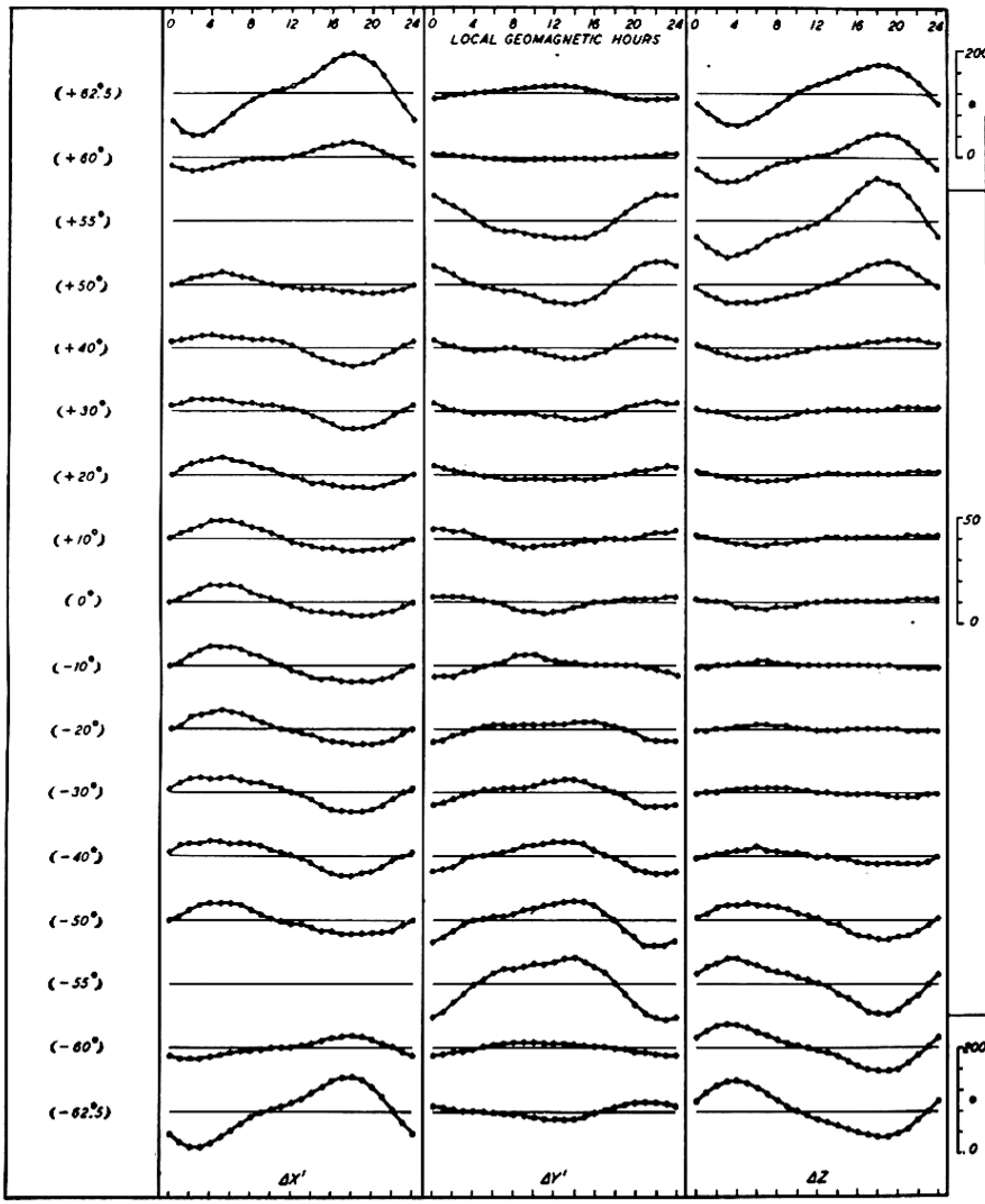

FIG. 114—DISTURBANCE DAILY VARIATION ON DISTURBED DAYS (S_D), IN VARIOUS GEOMAGNETIC LATITUDES, GEOMAGNETIC COMPONENTS, JULY, 1922-33

* NOTE PARTICULARLY THAT SCALES FOR GRAPHS IN AURORAL REGIONS ARE DIFFERENT THAN FOR OTHERS

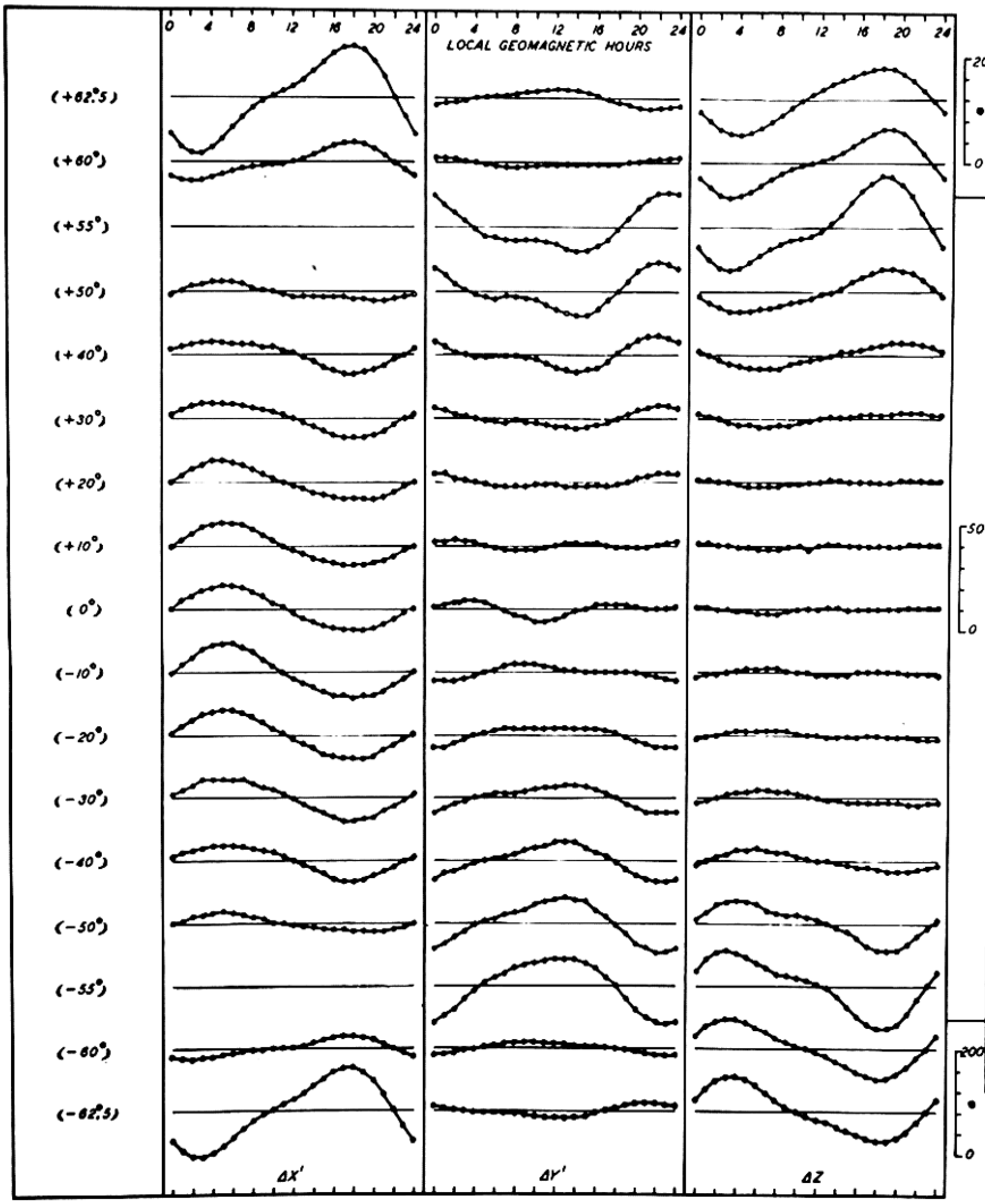

FIG. 115 – DISTURBANCE DAILY VARIATION ON DISTURBED DAYS (S_D), IN VARIOUS GEOMAGNETIC LATITUDES, GEOMAGNETIC COMPONENTS, AUGUST, 1922 – 33

* NOTE PARTICULARLY THAT SCALES FOR GRAPHS IN AURORAL REGIONS ARE DIFFERENT THAN FOR OTHERS

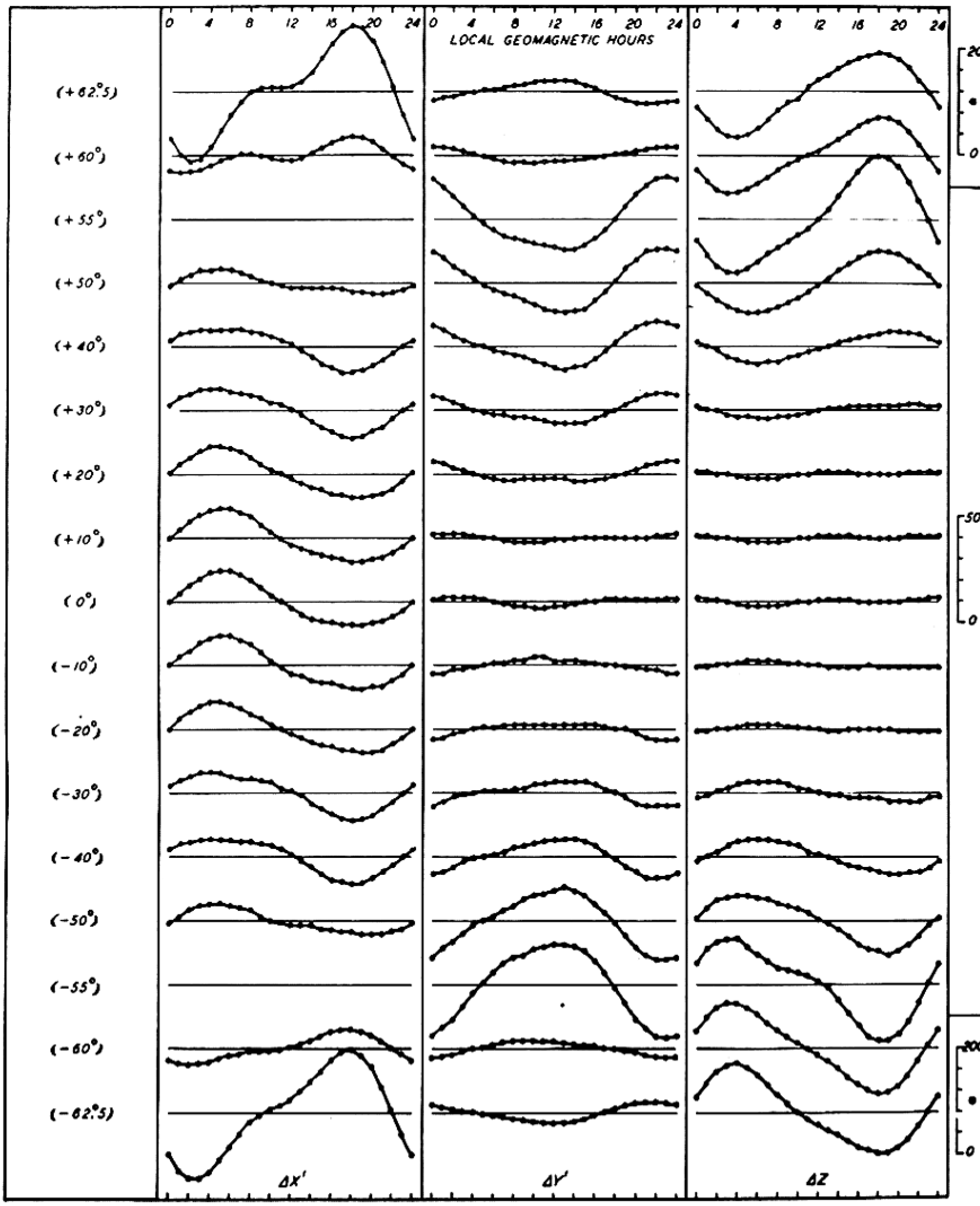

FIG. 116—DISTURBANCE DAILY VARIATION ON DISTURBED DAYS (S_D), IN VARIOUS GEOMAGNETIC LATITUDES, GEOMAGNETIC COMPONENTS, SEPTEMBER, 1922–33

* NOTE PARTICULARLY THAT SCALES FOR GRAPHS IN AURORAL REGIONS ARE DIFFERENT THAN FOR OTHERS

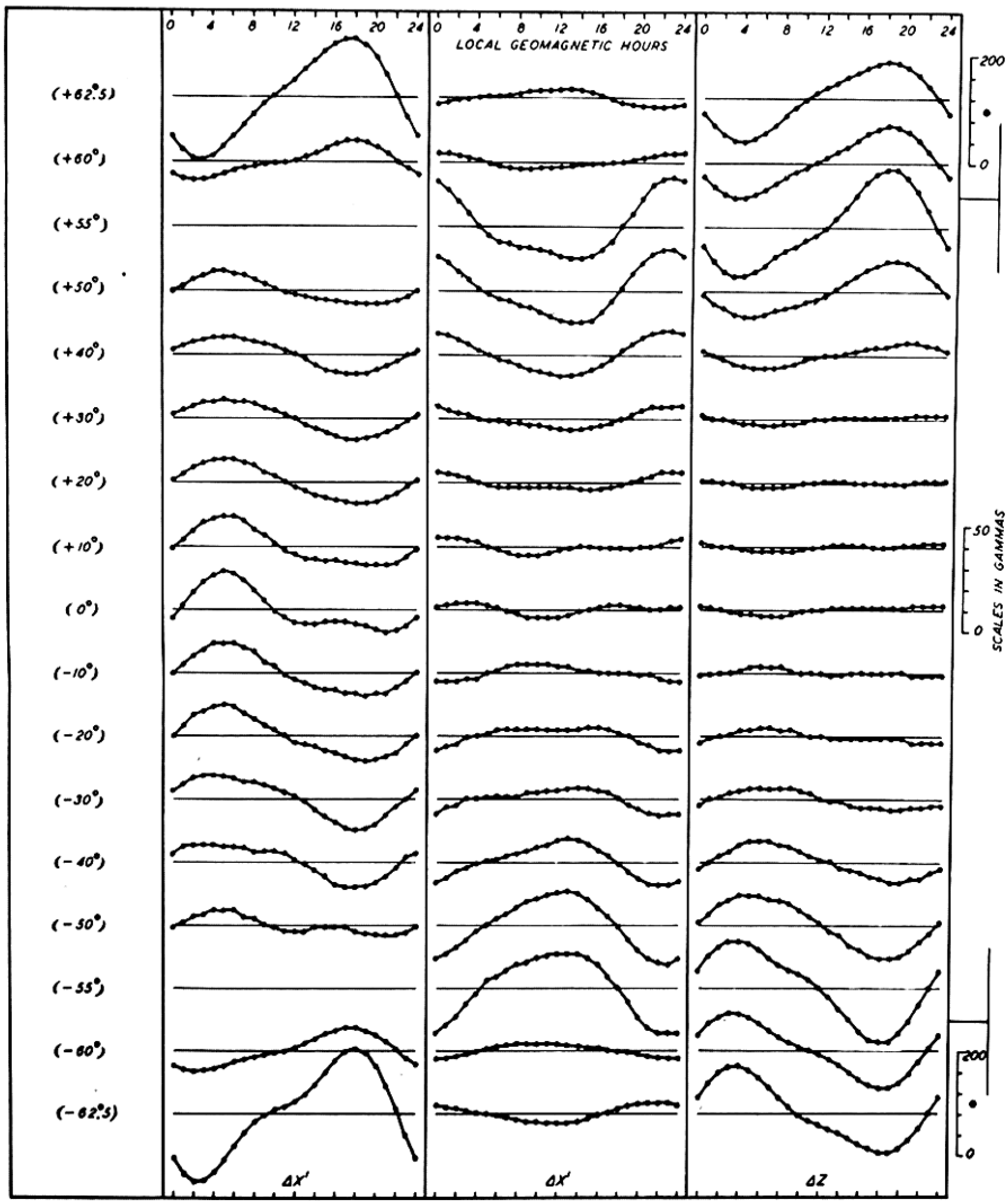

FIG. 117 - DISTURBANCE DAILY VARIATION ON DISTURBED DAYS (S_D), IN VARIOUS GEOMAGNETIC LATITUDES, GEOMAGNETIC COMPONENTS, OCTOBER, 1922-33

• NOTE PARTICULARLY THAT SCALES FOR GRAPHS IN AURORAL REGIONS ARE DIFFERENT THAN FOR OTHERS

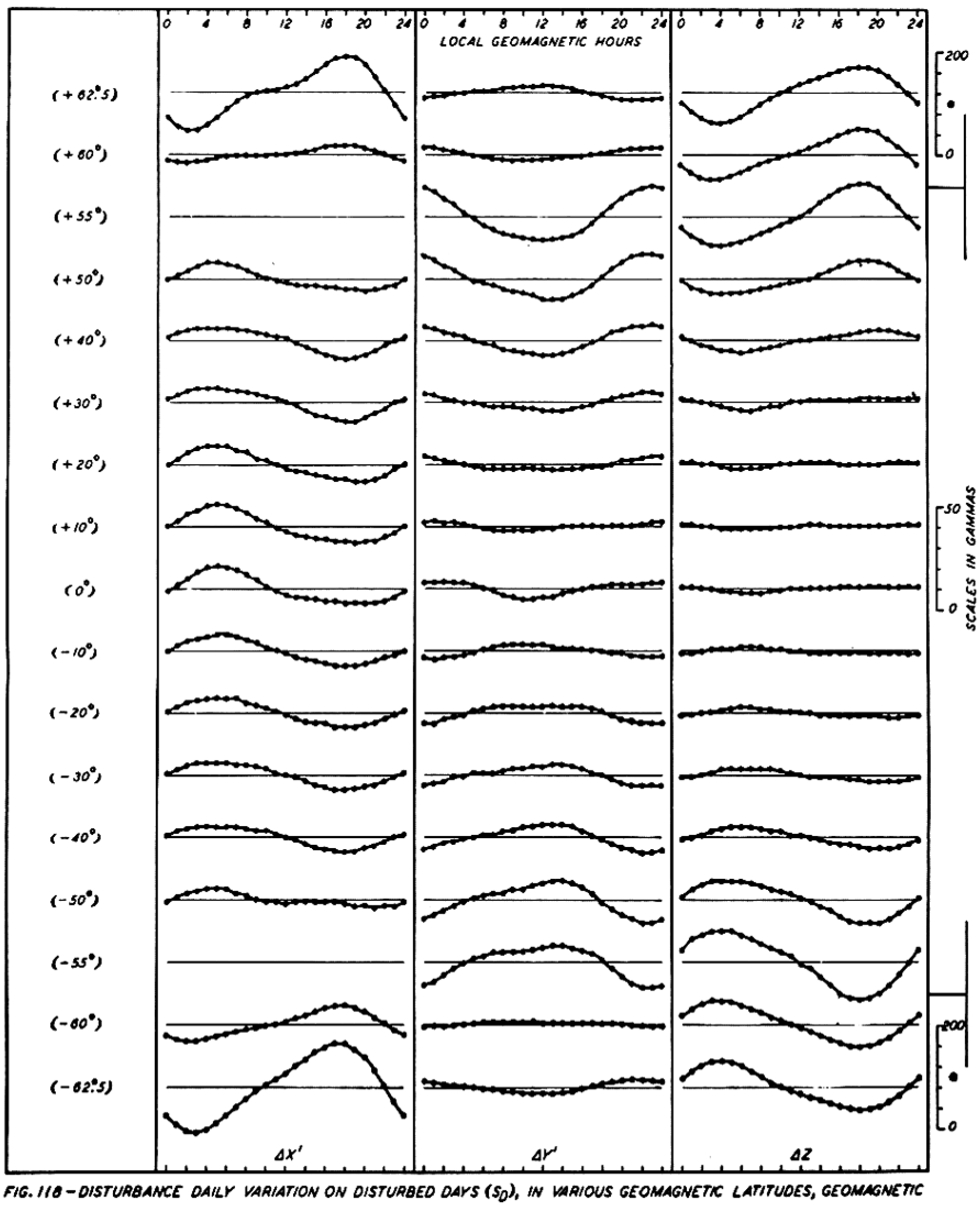

FIG. 118 — DISTURBANCE DAILY VARIATION ON DISTURBED DAYS (S_D), IN VARIOUS GEOMAGNETIC LATITUDES, GEOMAGNETIC COMPONENTS, NOVEMBER, 1922–33

* NOTE PARTICULARLY THAT SCALES FOR GRAPHS IN AURORAL REGIONS ARE DIFFERENT THAN FOR OTHERS

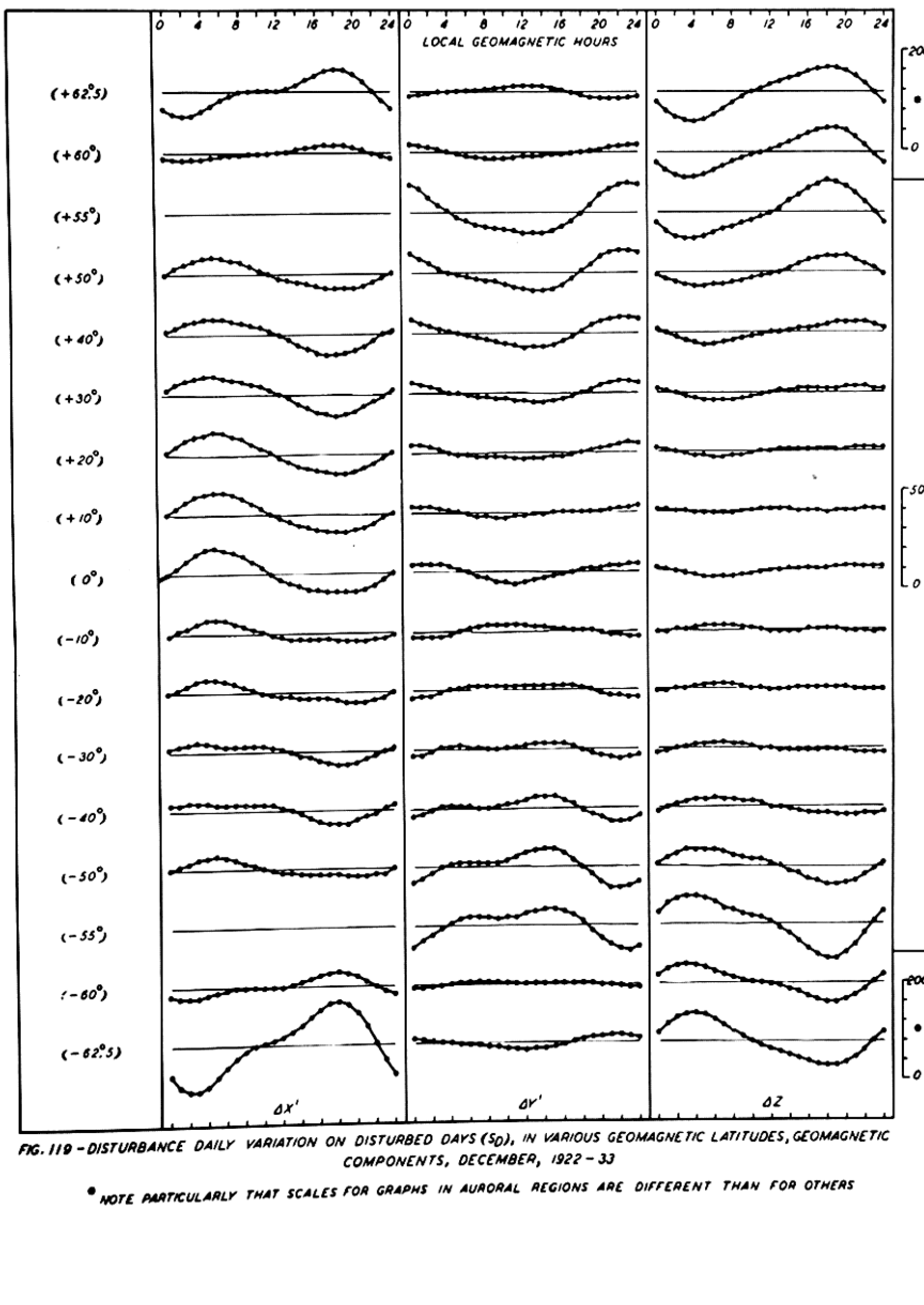

FIG. 119 - DISTURBANCE DAILY VARIATION ON DISTURBED DAYS (S_D), IN VARIOUS GEOMAGNETIC LATITUDES, GEOMAGNETIC COMPONENTS, DECEMBER, 1922 - 33

* NOTE PARTICULARLY THAT SCALES FOR GRAPHS IN AURORAL REGIONS ARE DIFFERENT THAN FOR OTHERS

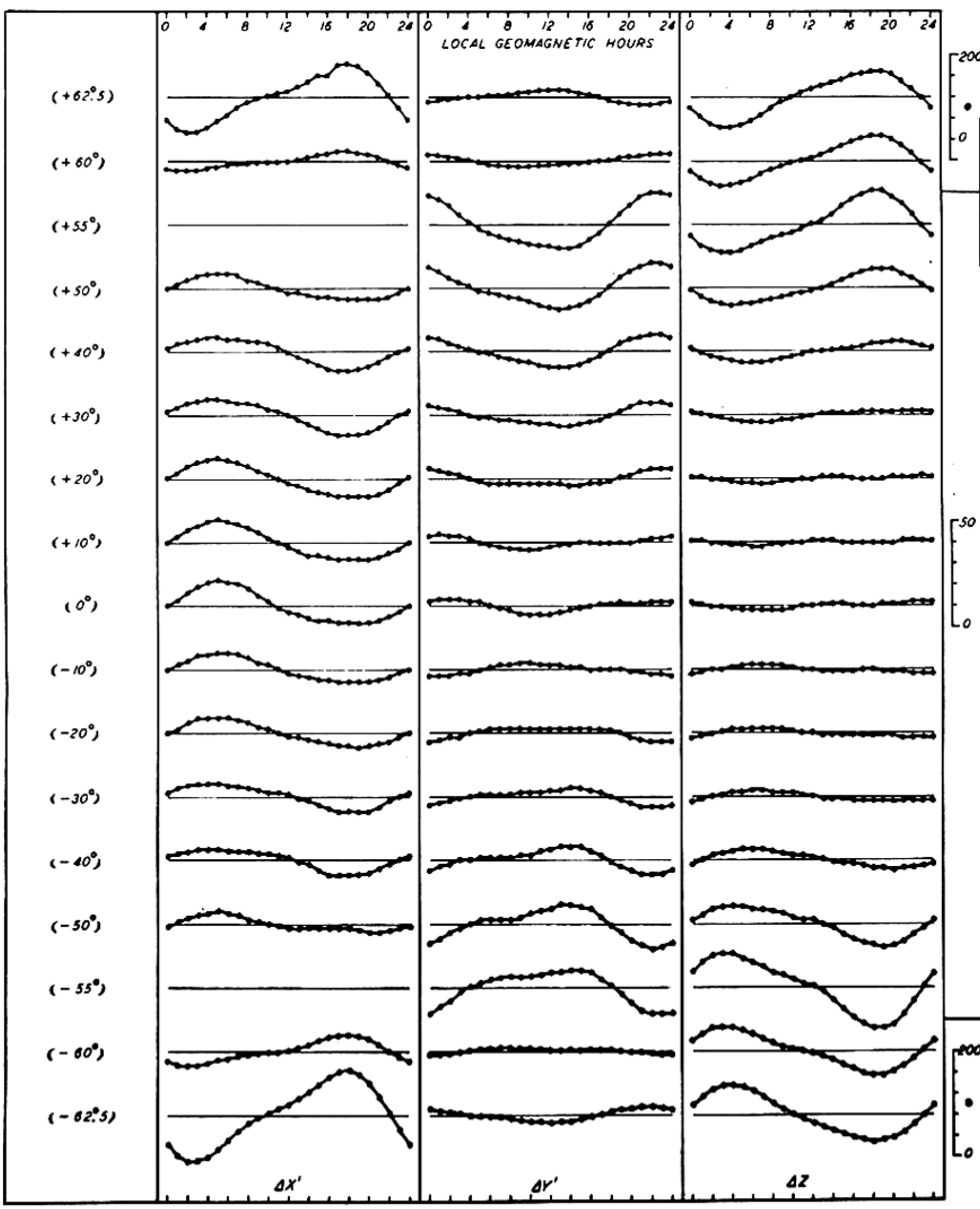

FIG. 120—DISTURBANCE DAILY VARIATION ON DISTURBED DAYS (S_D), IN VARIOUS GEOMAGNETIC LATITUDES, GEOMAGNETIC COMPONENTS, WINTER, 1922–33

• NOTE PARTICULARLY THAT SCALES FOR GRAPHS IN AURORAL REGIONS ARE DIFFERENT THAN FOR OTHERS

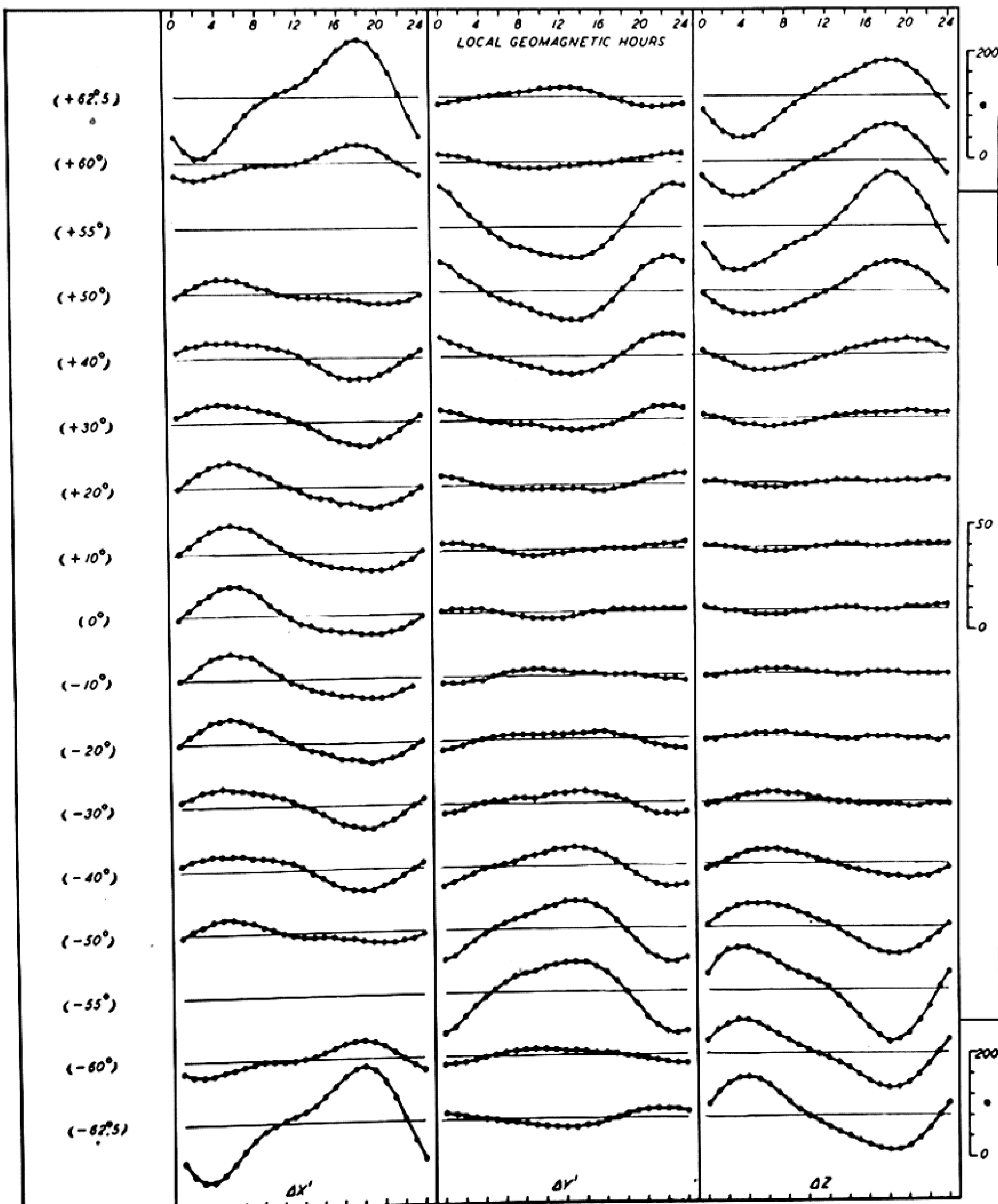

FIG. 121—DISTURBANCE DAILY VARIATION ON DISTURBED DAYS (S_D), IN VARIOUS GEOMAGNETIC LATITUDES, GEOMAGNETIC COMPONENTS, EQUINOX, 1922–33

* NOTE PARTICULARLY THAT SCALES FOR GRAPHS IN AURORAL REGIONS ARE DIFFERENT THAN FOR OTHERS

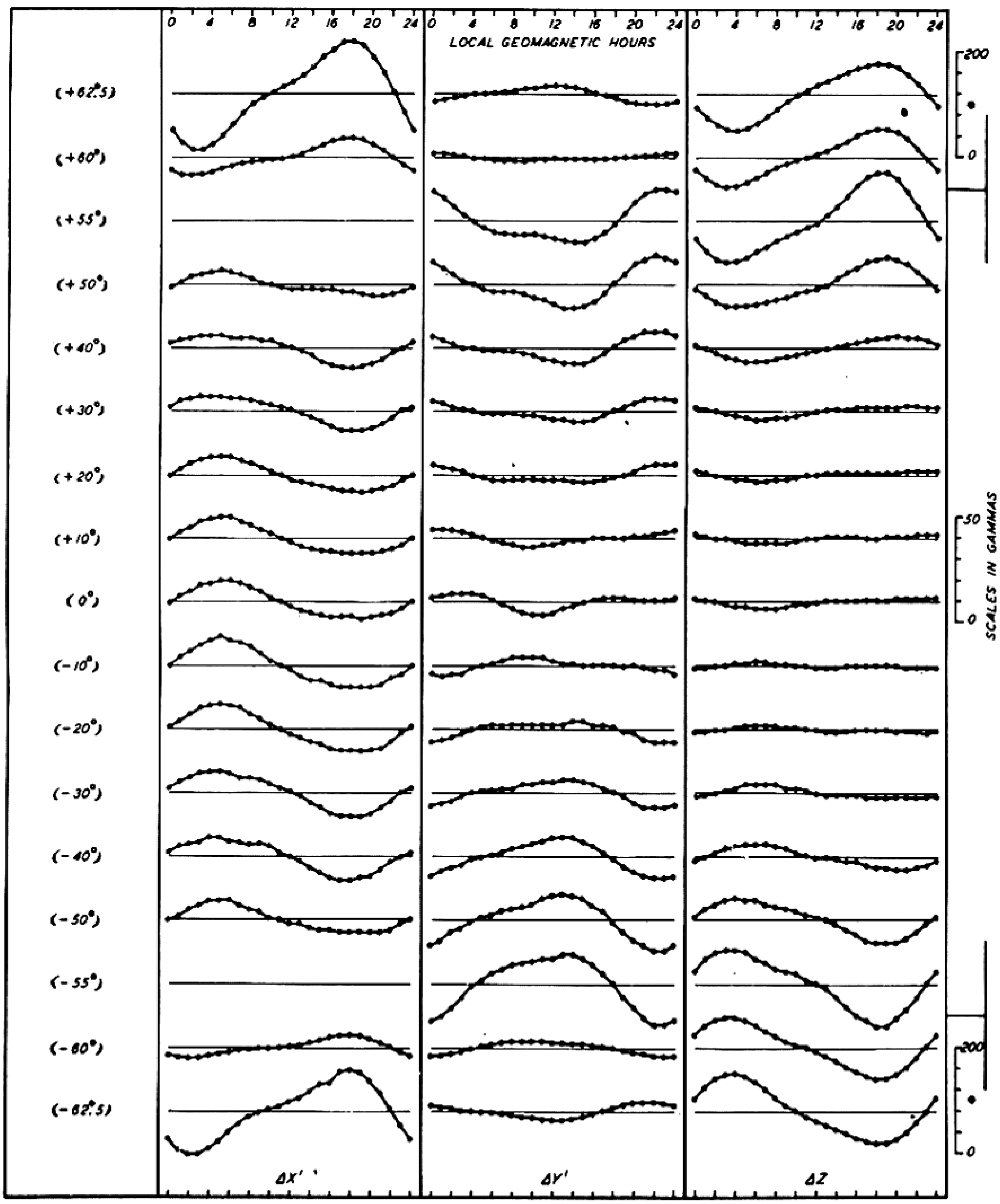

FIG. 122—DISTURBANCE DAILY VARIATION ON DISTURBED DAYS (S_D), IN VARIOUS GEOMAGNETIC LATITUDES, GEOMAGNETIC COMPONENTS, SUMMER, 1922–33

* NOTE PARTICULARLY THAT SCALES FOR GRAPHS IN AURORAL REGIONS ARE DIFFERENT THAN FOR OTHERS

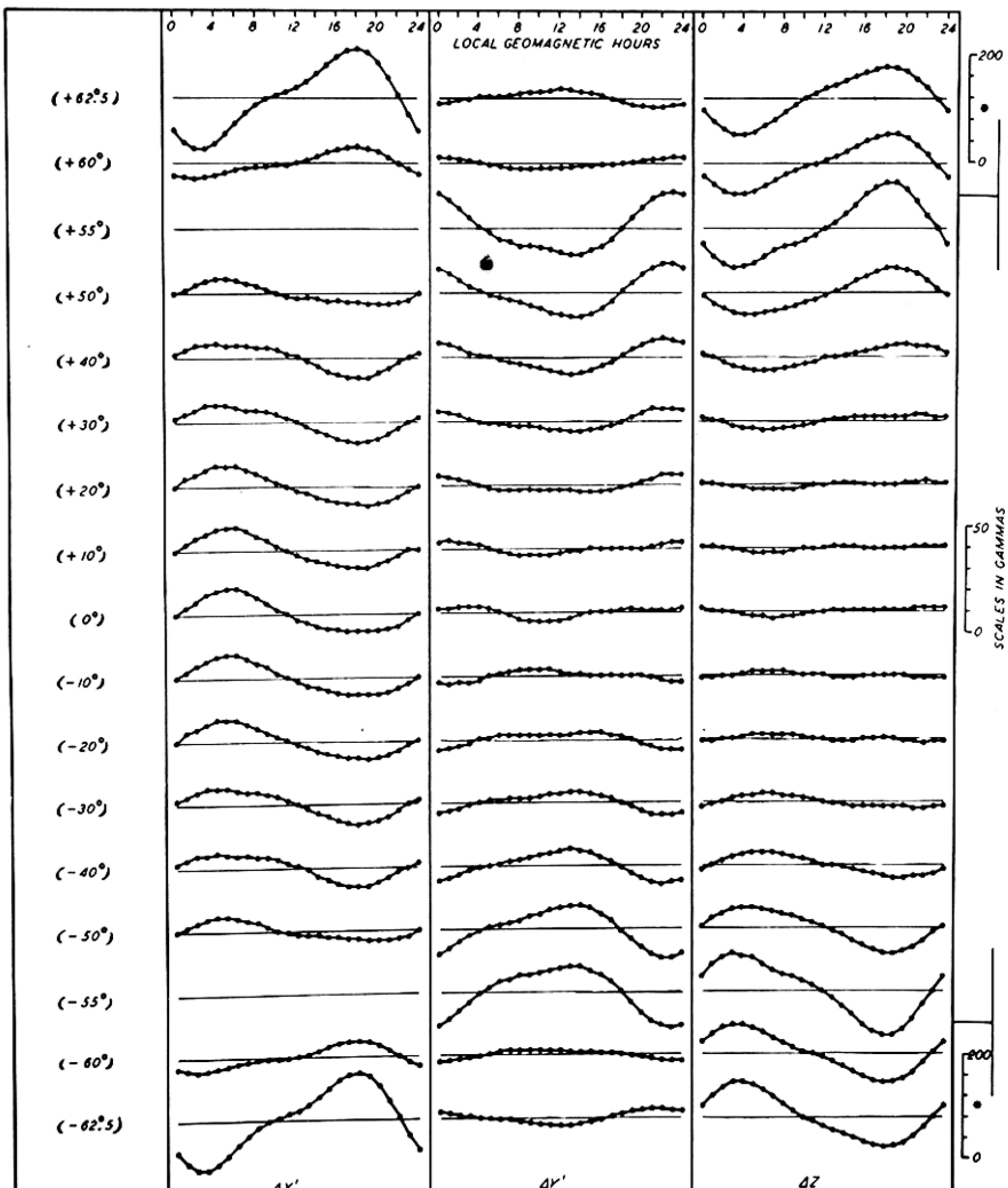

FIG. 123—DISTURBANCE DAILY VARIATION ON DISTURBED DAYS (S_D), IN VARIOUS GEOMAGNETIC LATITUDES, GEOMAGNETIC COMPONENTS, YEAR, 1922-33

* NOTE PARTICULARLY THAT SCALES FOR GRAPHS IN AURORAL REGIONS ARE DIFFERENT THAN FOR OTHERS

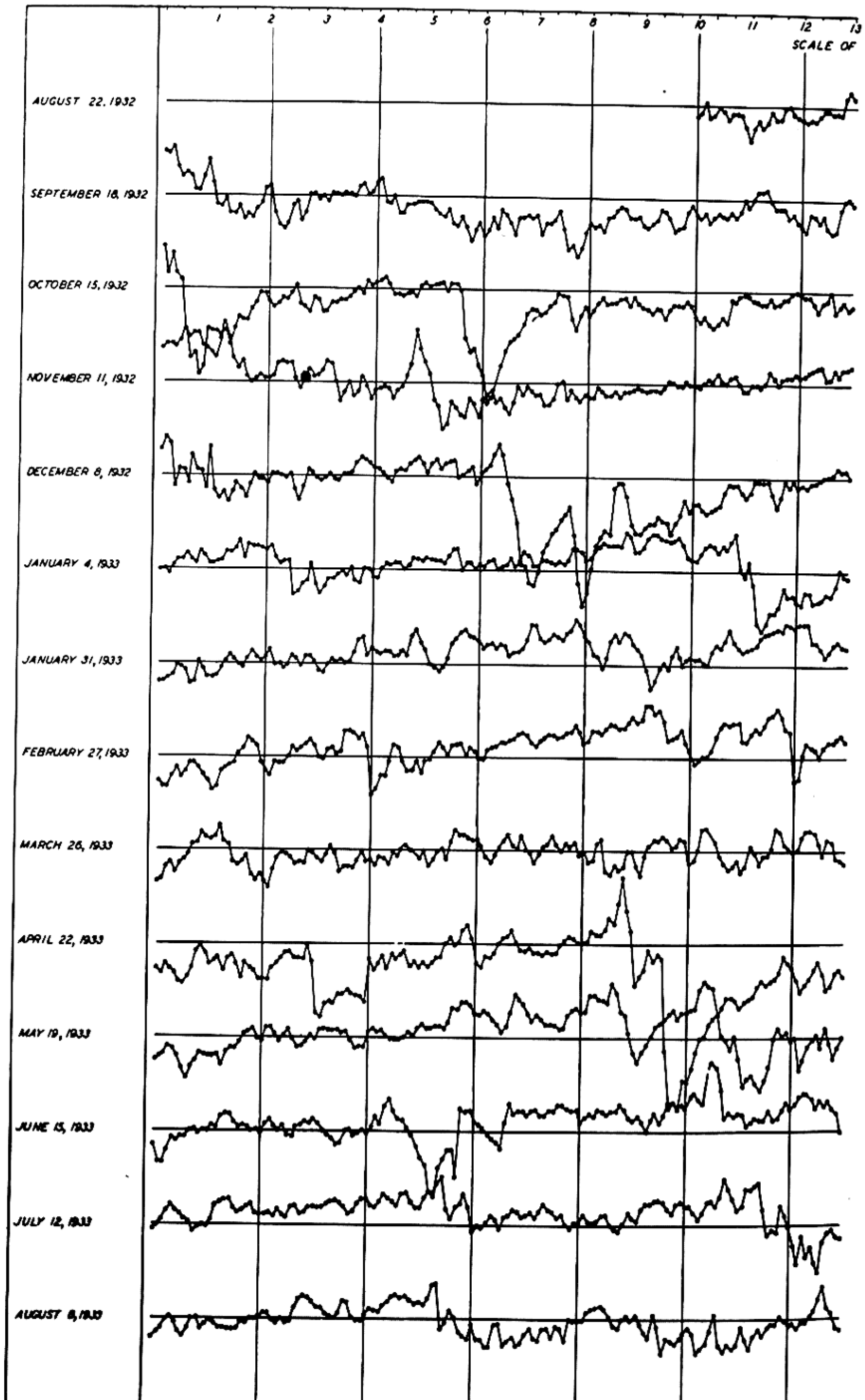

FIG. 124(A)—STORM-TIME VARIATION (D_{st}) IN EQUATORIAL REGIONS AS GIVEN BY SAN JUAN, ALIBAG, AND HONOLULU

AS DEPARTURES FROM ANNUAL MEAN, BY SUNSPOT-ROTATIONS, SEPTEMBER 1, 1932 TO AUGUST 31, 1933

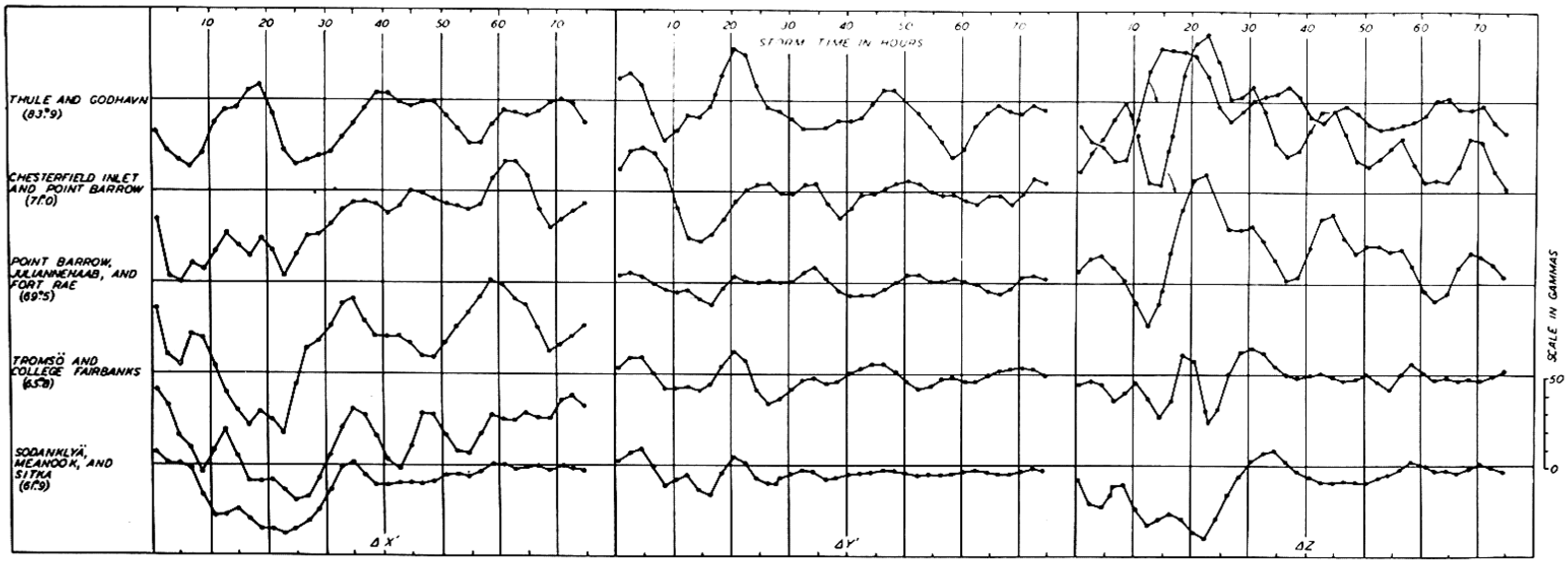

FIG. 124(B) —AVERAGE STORM-TIME (D_{st}), WEIGHTED AVERAGE OF 11 STORMS, 1932–33

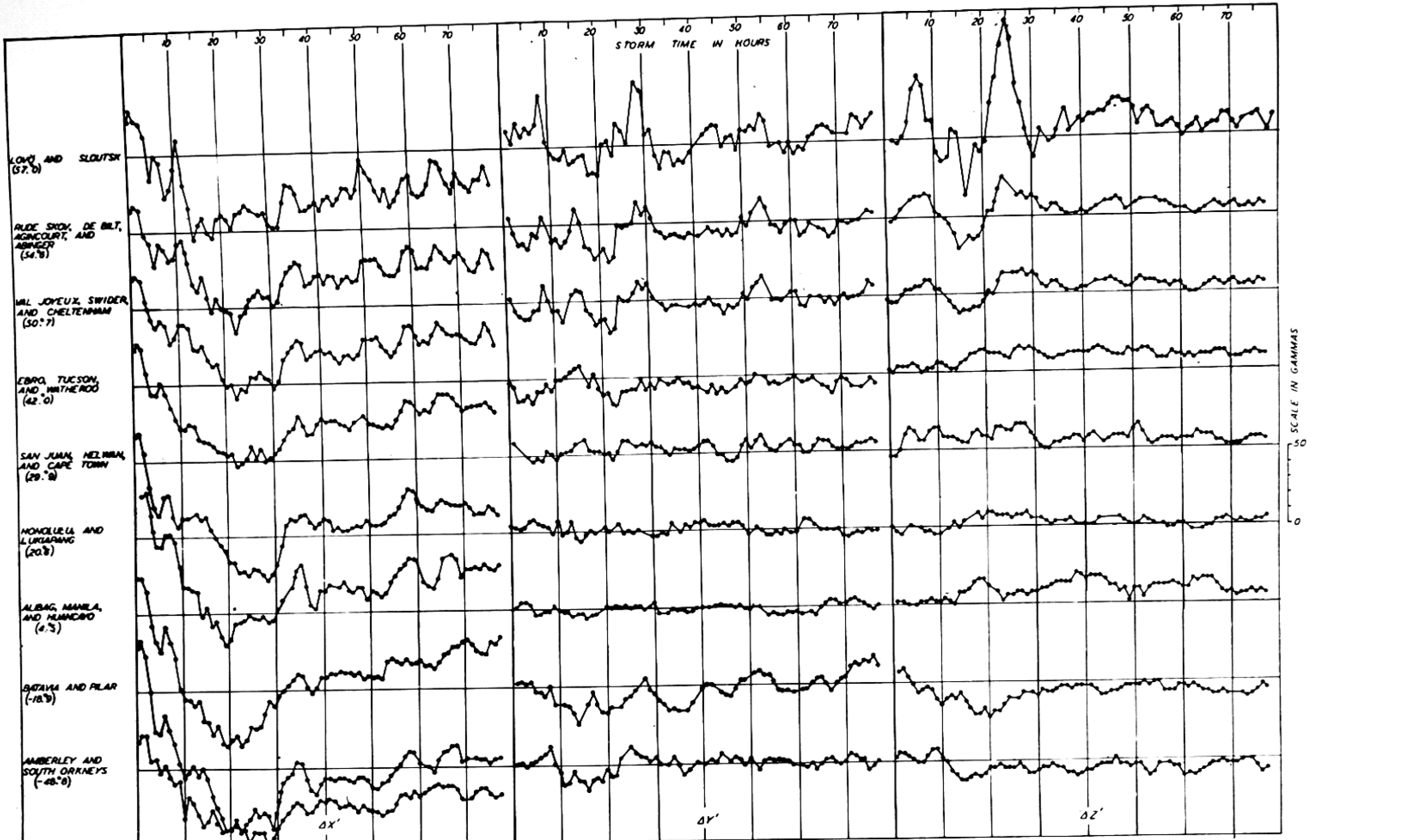

FIG. 124 (C)—AVERAGE STORM-TIME (D_{st}), WEIGHTED AVERAGE OF 11 STORMS, 1932–33

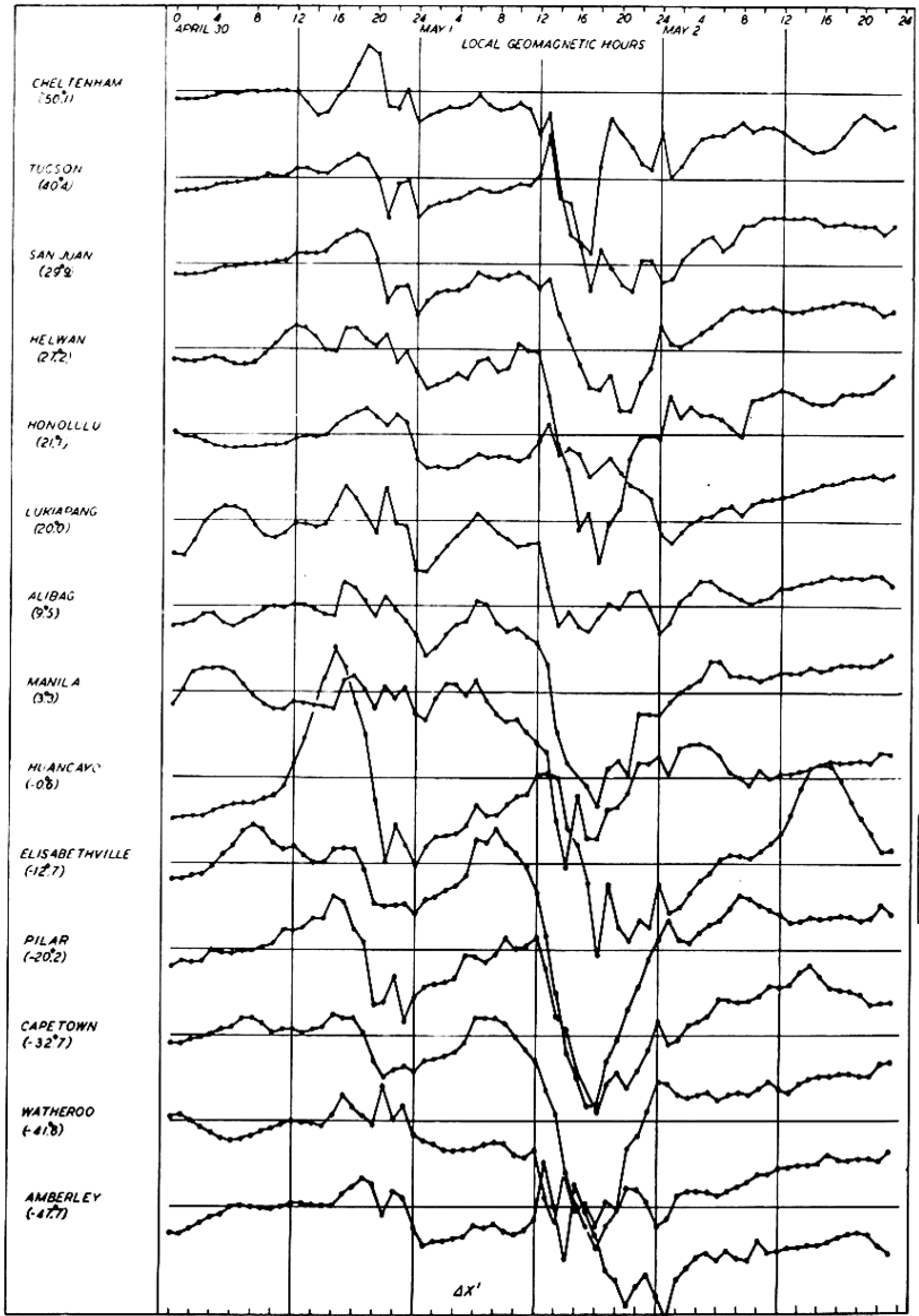

FIG. 125(A)—HOURLY MEAN DEPARTURES OF GEOMAGNETIC NORTH COMPONENT FROM MEAN OF APRIL 30, 1933 (GEOMAGNETIC LATITUDES INDICATED IN PARENTHESES)

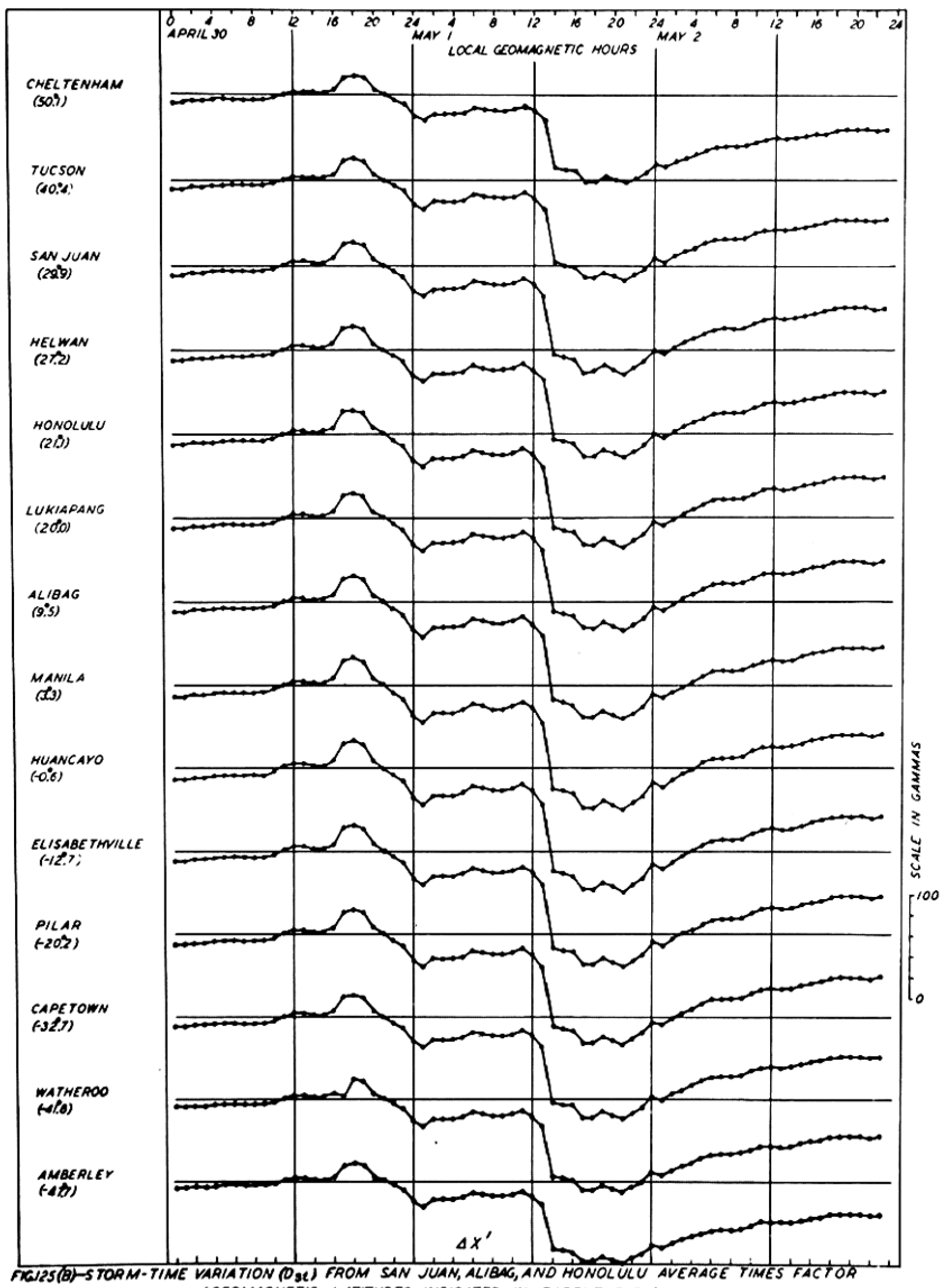

FIG.125(B)—STORM-TIME VARIATION (D_{st}) FROM SAN JUAN, ALIBAG, AND HONOLULU AVERAGE TIMES FACTOR (GEOMAGNETIC LATITUDES INDICATED IN PARENTHESES)

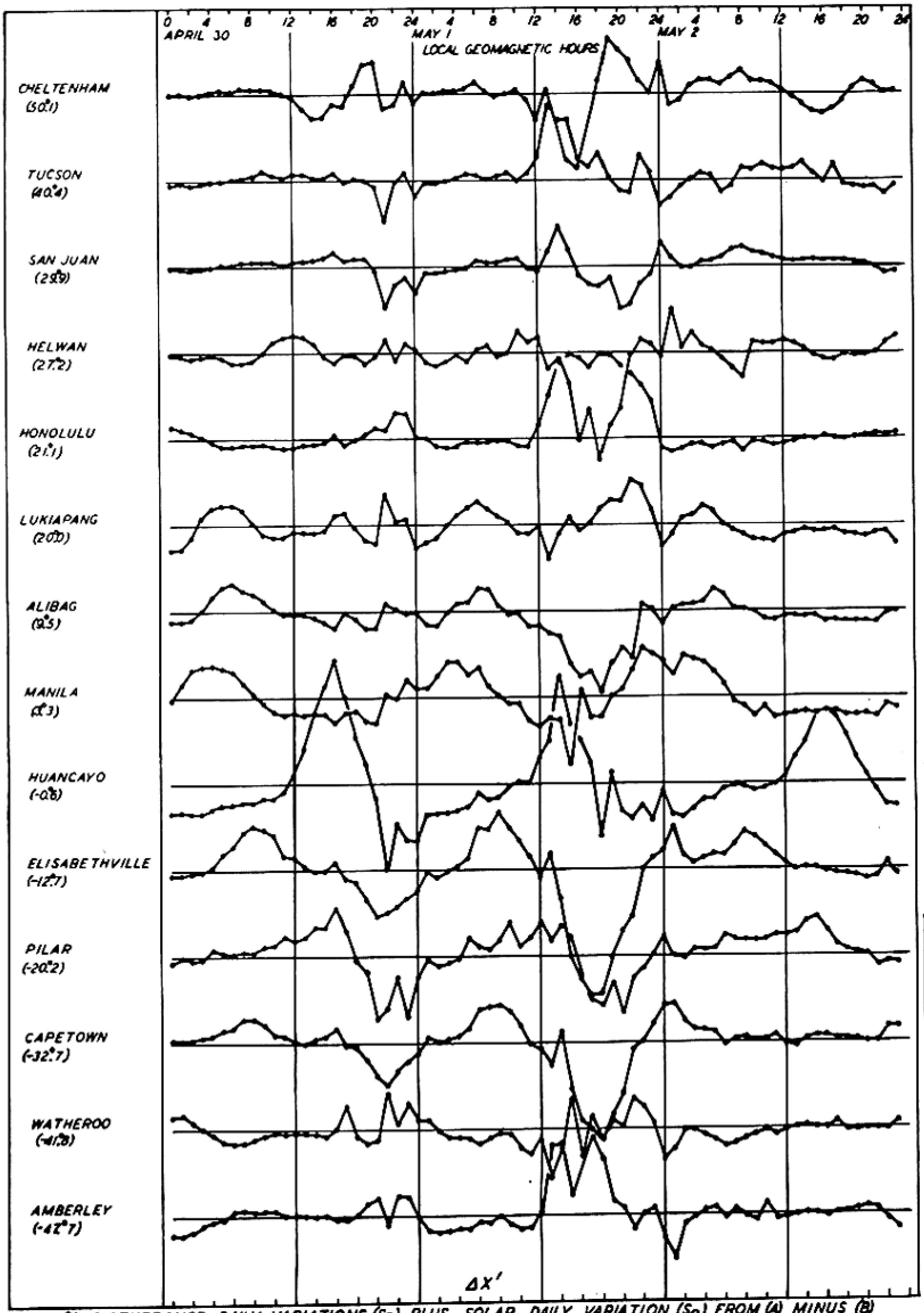

FIG. 125(C) - DISTURBANCE DAILY VARIATIONS (S_D) PLUS SOLAR DAILY VARIATION (S_q) FROM (A) MINUS (B)
(GEOMAGNETIC LATITUDES INDICATED IN PARENTHESES)

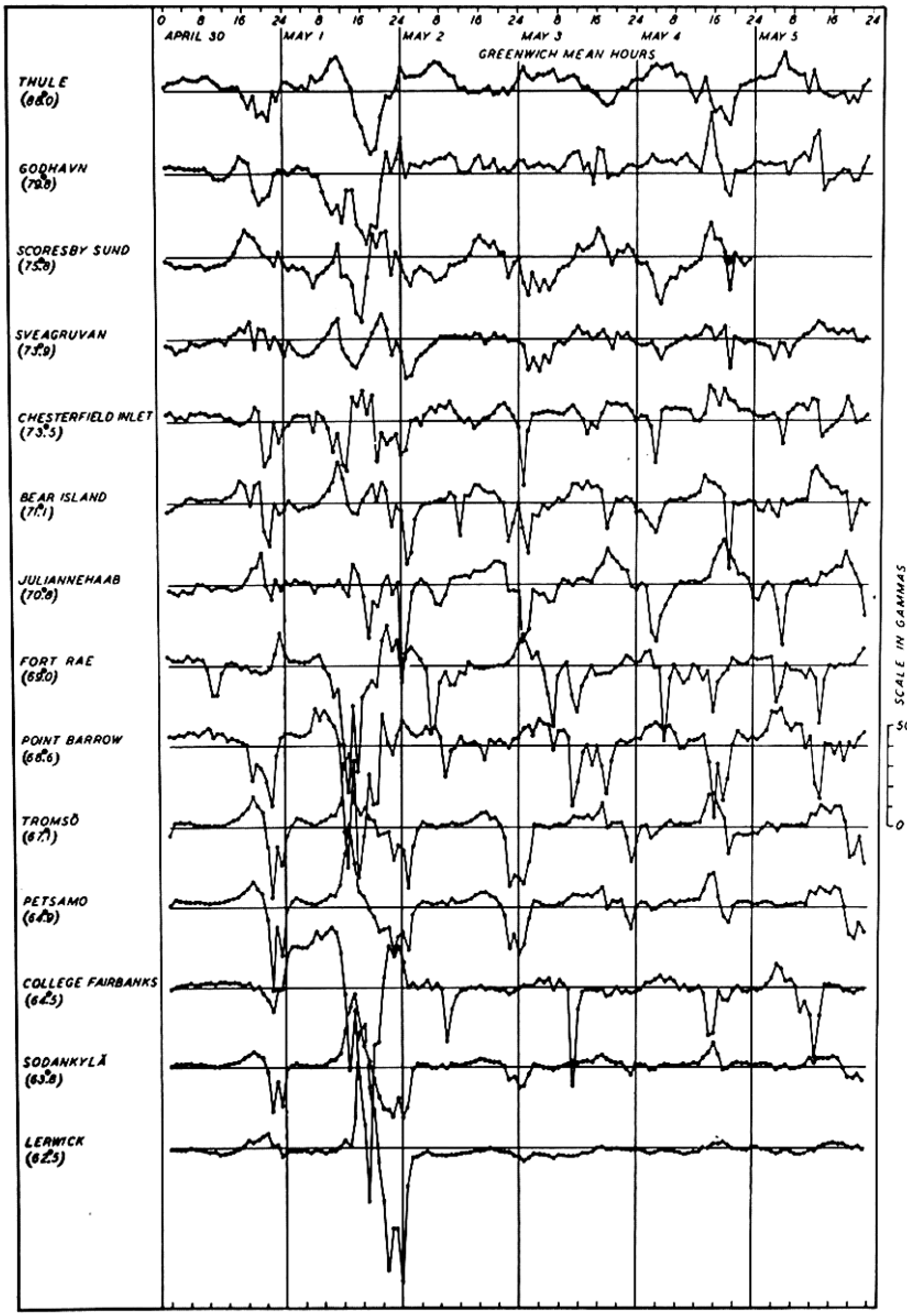

FIG. 126(A)– HOURLY MEAN DEPARTURES IN GEOMAGNETIC NORTH COMPONENT (X') FROM MEAN OF APRIL 30, 1933, STORM OF MAY 1, 1933 (GEOMAGNETIC LATITUDES INDICATED IN PARENTHESES)

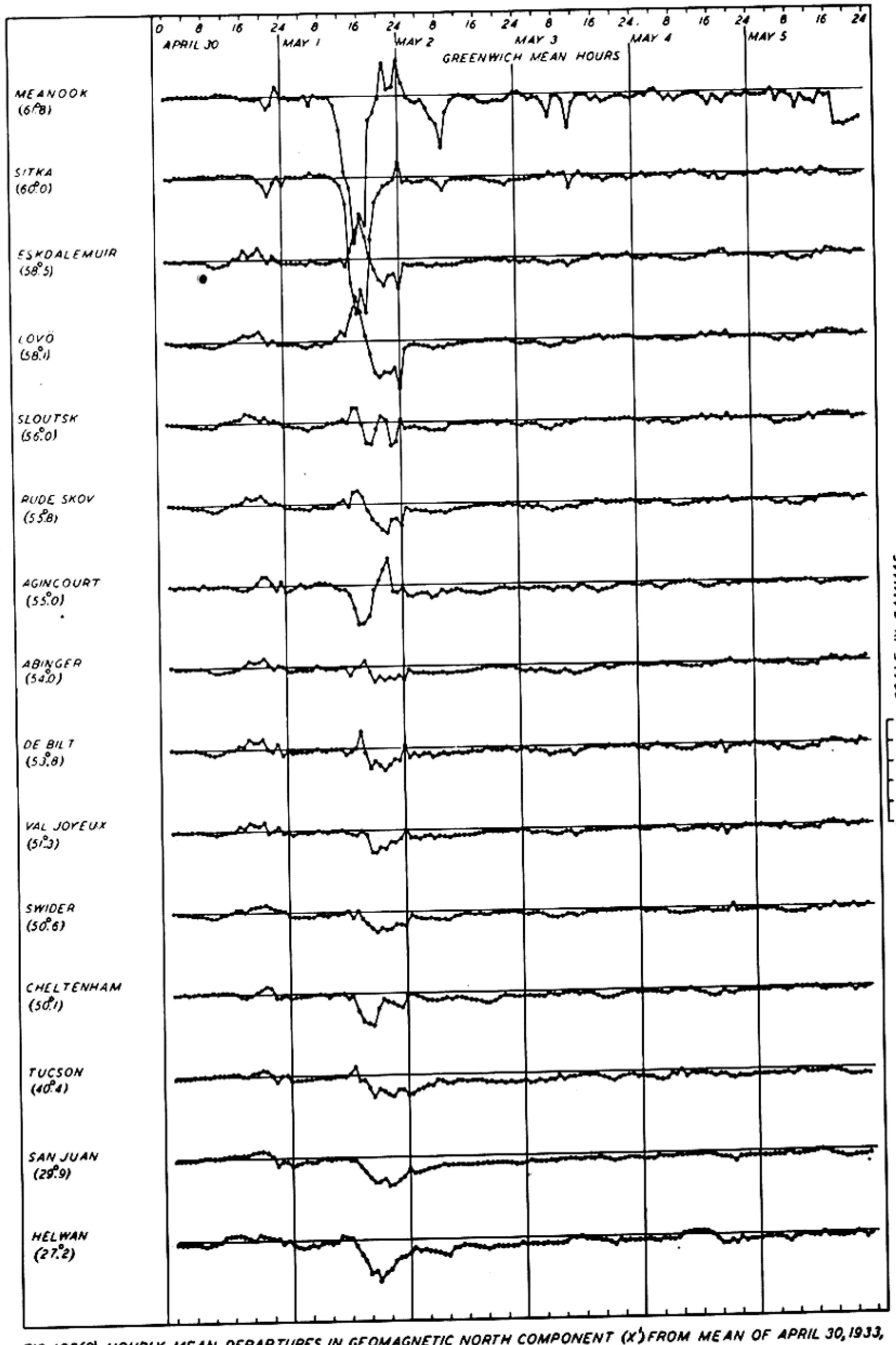

FIG. 126(B)—HOURLY MEAN DEPARTURES IN GEOMAGNETIC NORTH COMPONENT (X') FROM MEAN OF APRIL 30, 1933, STORM OF MAY 1, 1933. (GEOMAGNETIC LATITUDES INDICATED IN PARENTHESES)

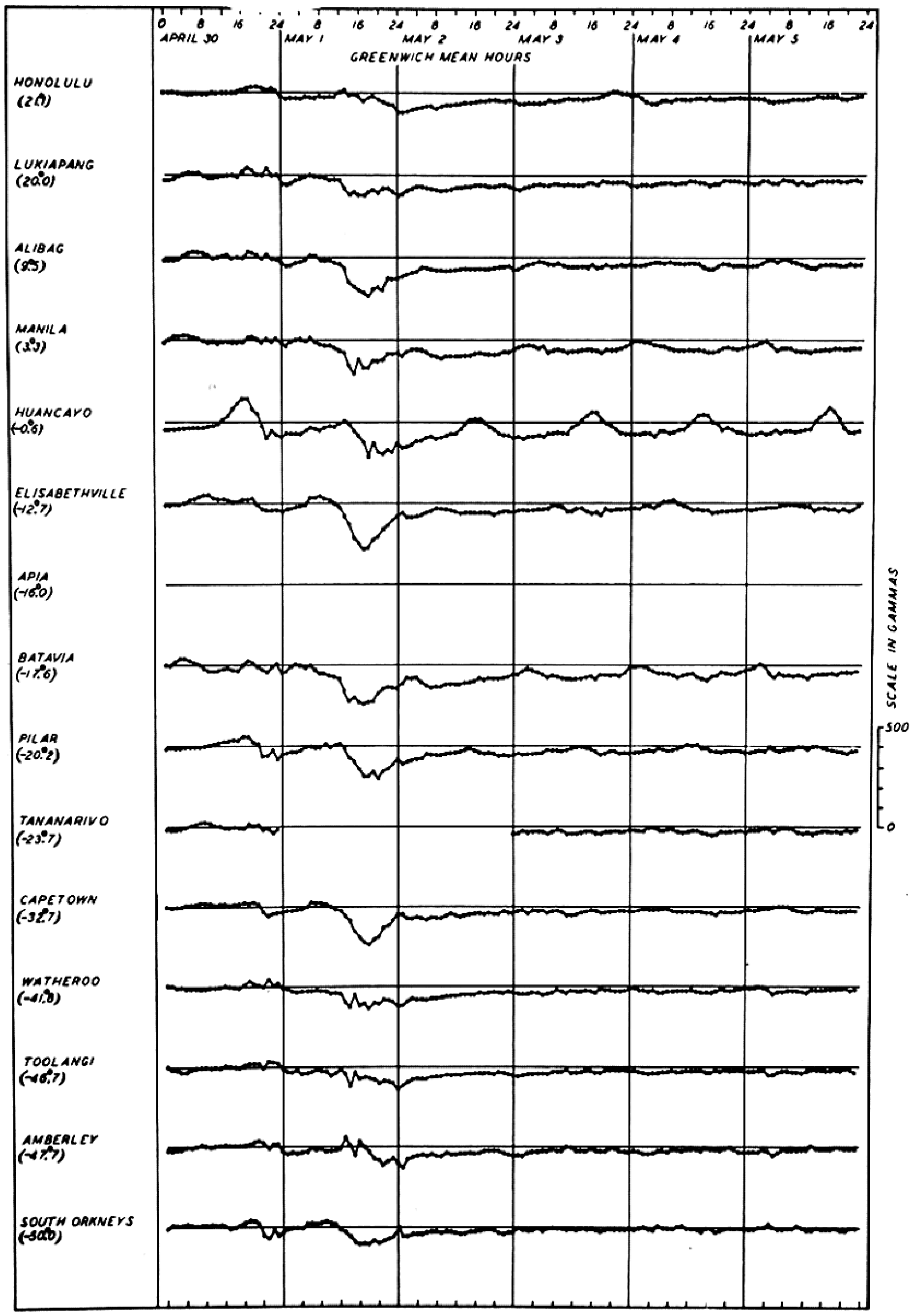

FIG. 126(C)- HOURLY MEAN DEPARTURES IN GEOMAGNETIC NORTH COMPONENT (X') FROM MEAN OF APRIL 30, 1933, STORM OF MAY 1, 1933 (GEOMAGNETIC LATITUDES INDICATED IN PARENTHESES)

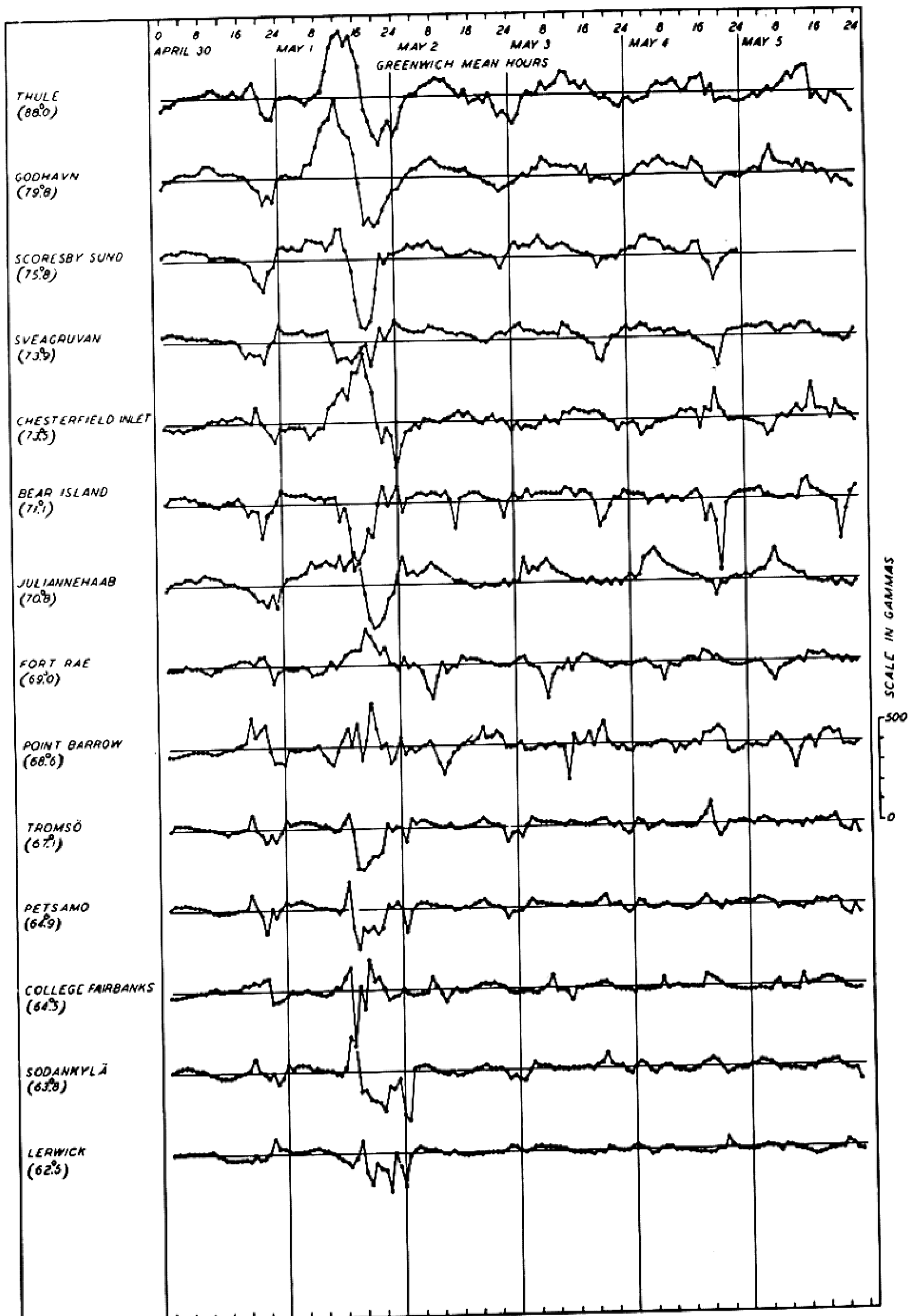

FIG. 126(D)—HOURLY MEAN DEPARTURES IN GEOMAGNETIC EAST COMPONENT (Y') FROM MEAN OF APRIL 30, 1933, STORM OF MAY, 1, 1933. (GEOMAGNETIC LATITUDES INDICATED IN PARENTHESES)

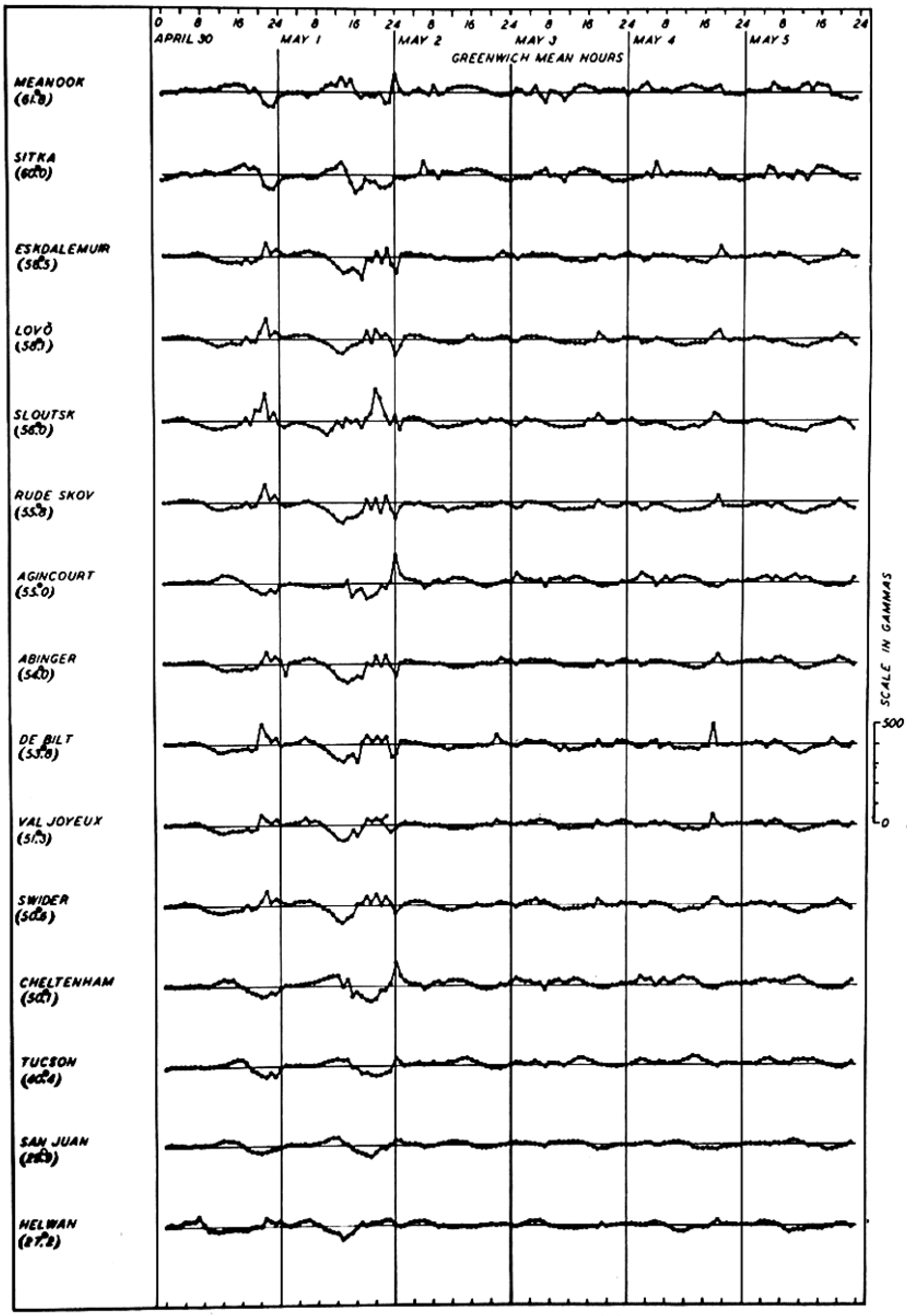

FIG. 126(E)—HOURLY MEAN DEPARTURES IN GEOMAGNETIC EAST COMPONENT (Y') FROM MEAN OF APRIL 30, 1933, STORM OF MAY 1, 1933 (GEOMAGNETIC LATITUDES INDICATED IN PARENTHESES)

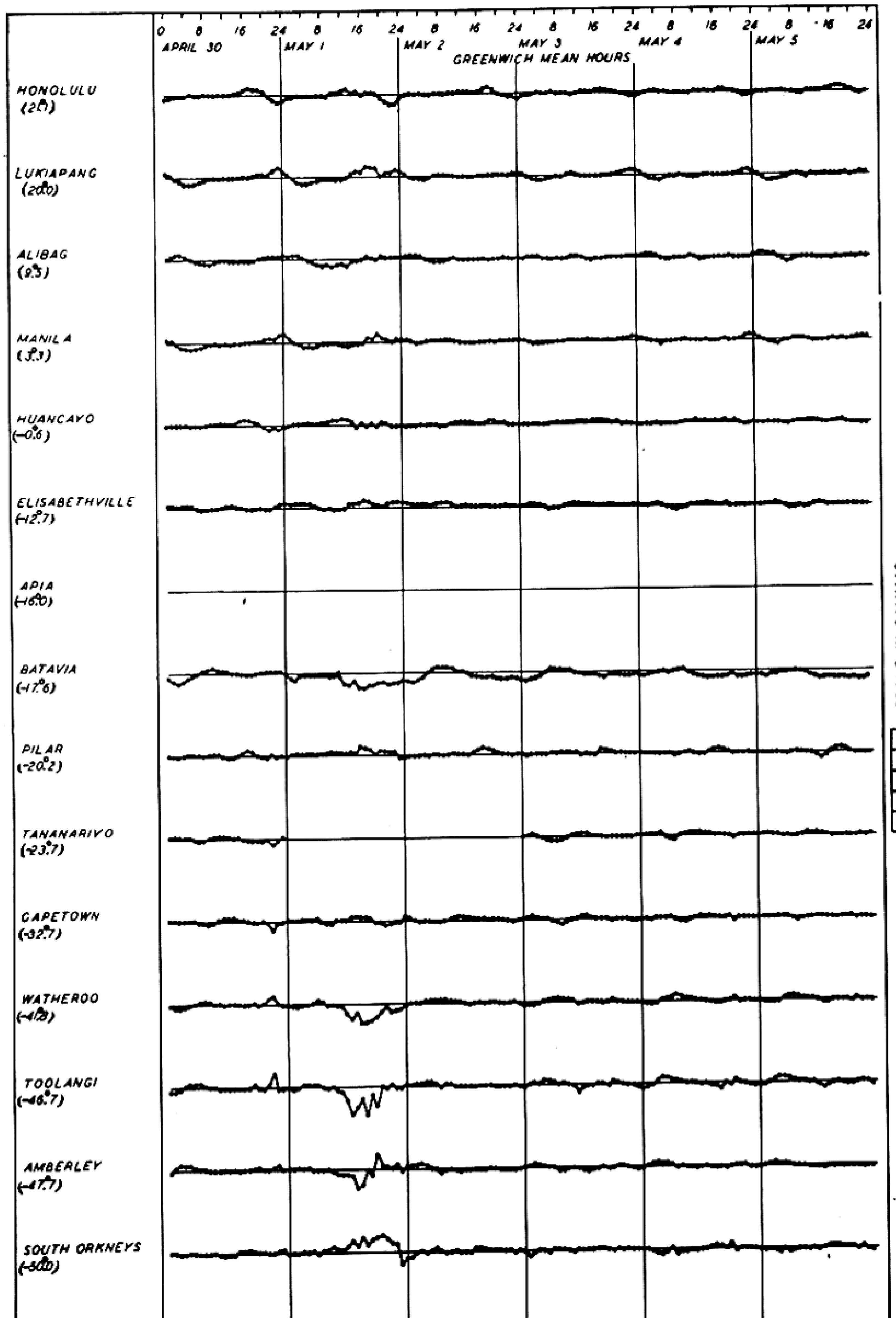

FIG. 126(F)—HOURLY MEAN DEPARTURES IN GEOMAGNETIC EAST COMPONENT (Y') FROM MEAN OF APRIL 30, 1933, STORM OF MAY 1, 1933. (GEOMAGNETIC LATITUDES INDICATED IN PARENTHESES)

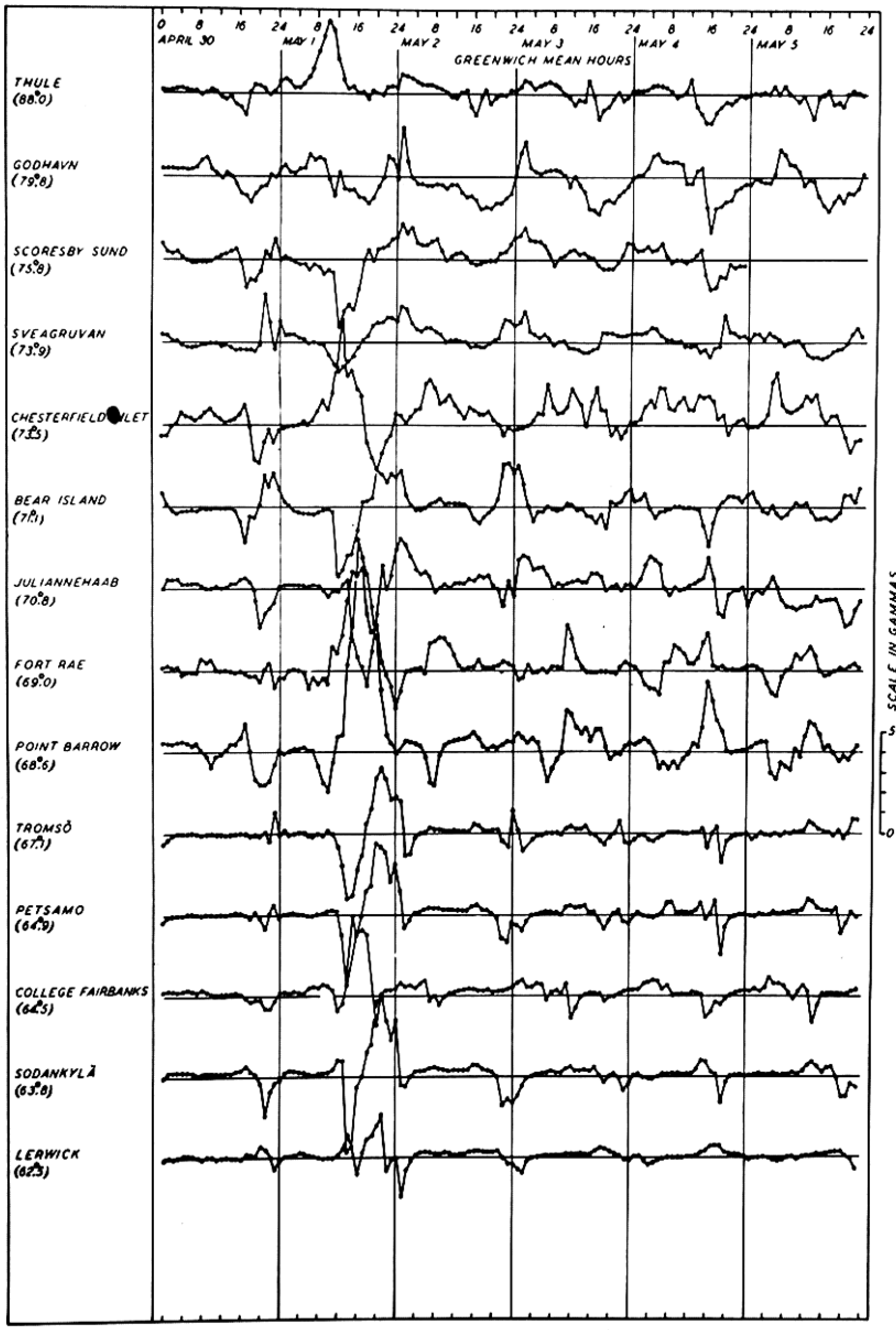

FIG. 126(G)—HOURLY MEAN DEPARTURES IN GEOMAGNETIC VERTICAL COMPONENT (Z) FROM MEAN OF APRIL 30, 1933, STORM OF MAY 1, 1933. (GEOMAGNETIC LATITUDES INDICATED IN PARENTHESES)

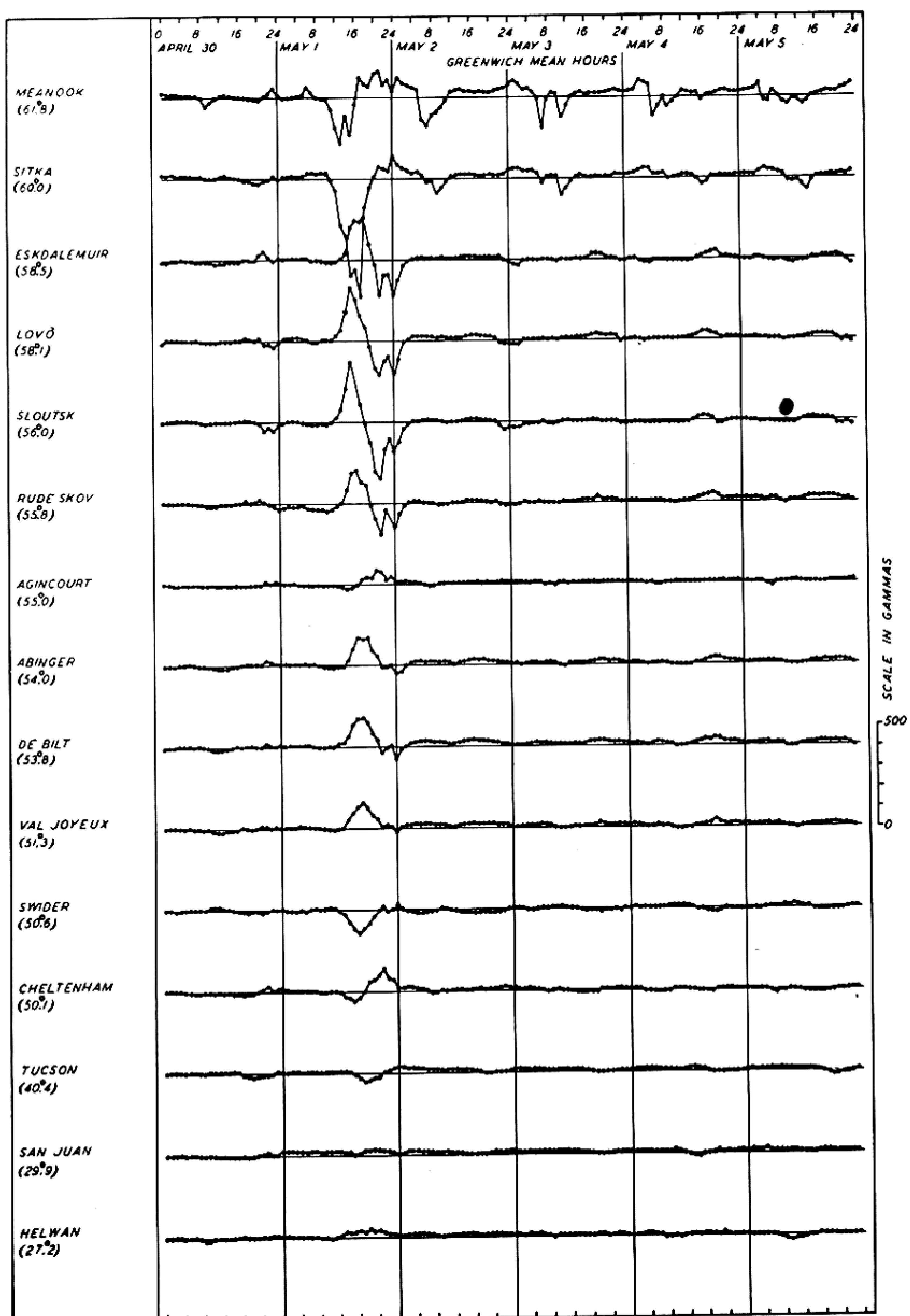

FIG. 126(H)—HOURLY MEAN DEPARTURES IN GEOMAGNETIC VERTICAL COMPONENT (Z) FROM MEAN OF APRIL 30, 1933, STORM OF MAY 1, 1933. (GEOMAGNETIC LATITUDES INDICATED IN PARENTHESES)

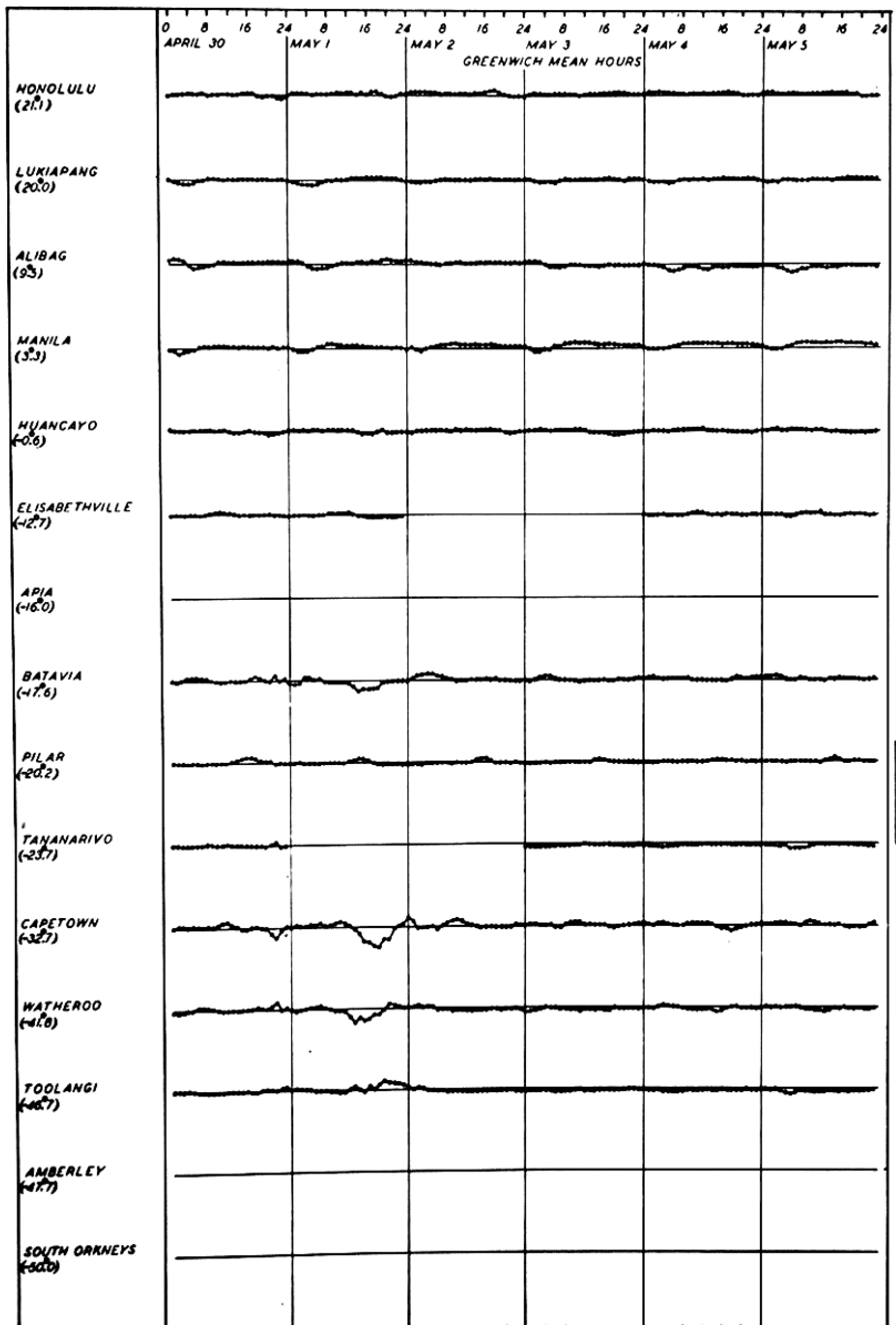

FIG. 126(I)—HOURLY MEAN DEPARTURES IN GEOMAGNETIC VERTICAL COMPONENT (Z) FROM MEAN OF APRIL 30, 1933, STORM OF MAY 1, 1933. (GEOMAGNETIC LATITUDES INDICATED IN PARENTHESES)

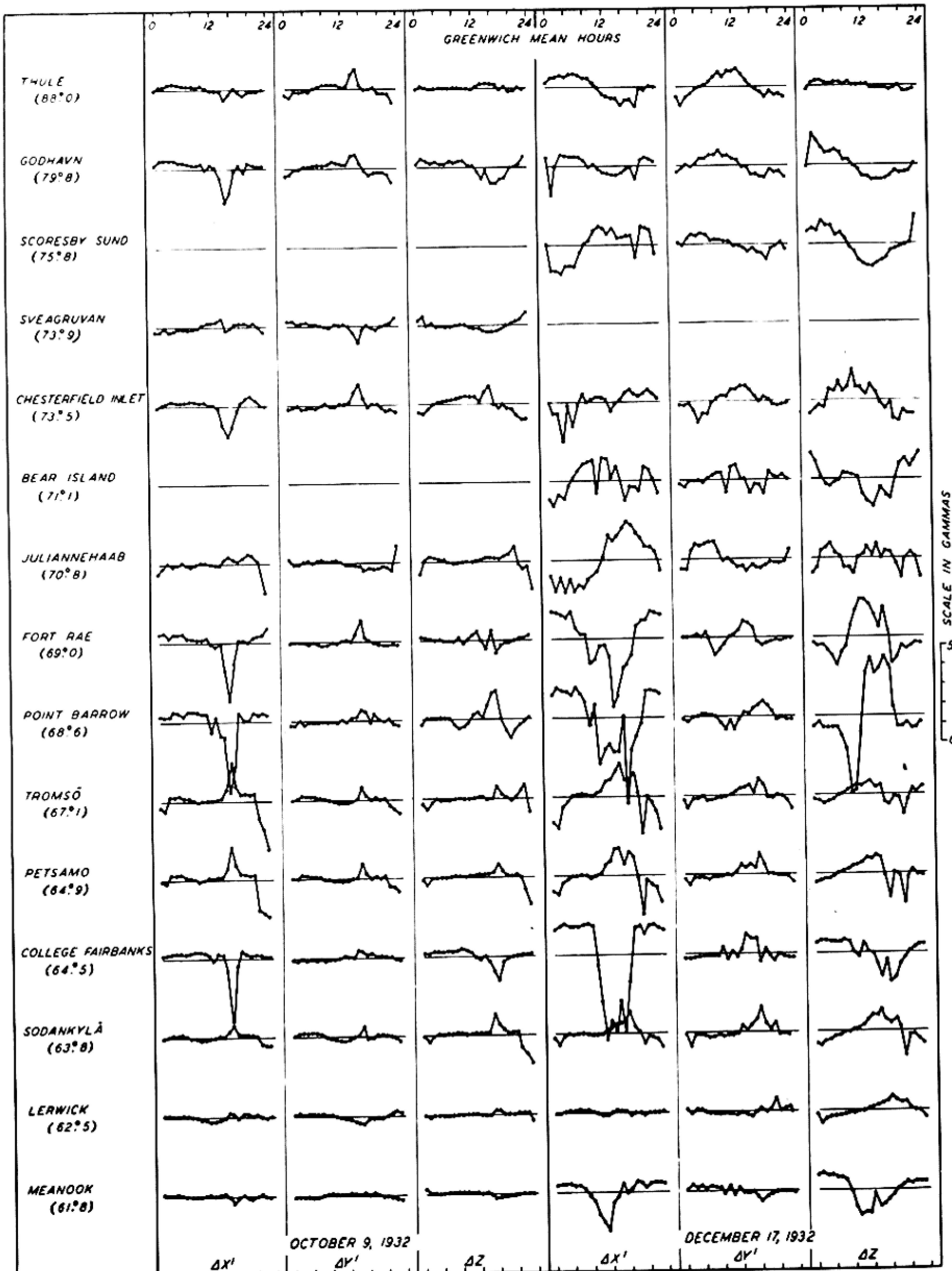

FIG. 127(A)—HOURLY DEPARTURES FROM MEAN OF DAY, GEOMAGNETIC COMPONENTS ΔX', ΔY', AND ΔZ (GEOMAGNETIC LATITUDES INDICATED IN PARENTHESES)

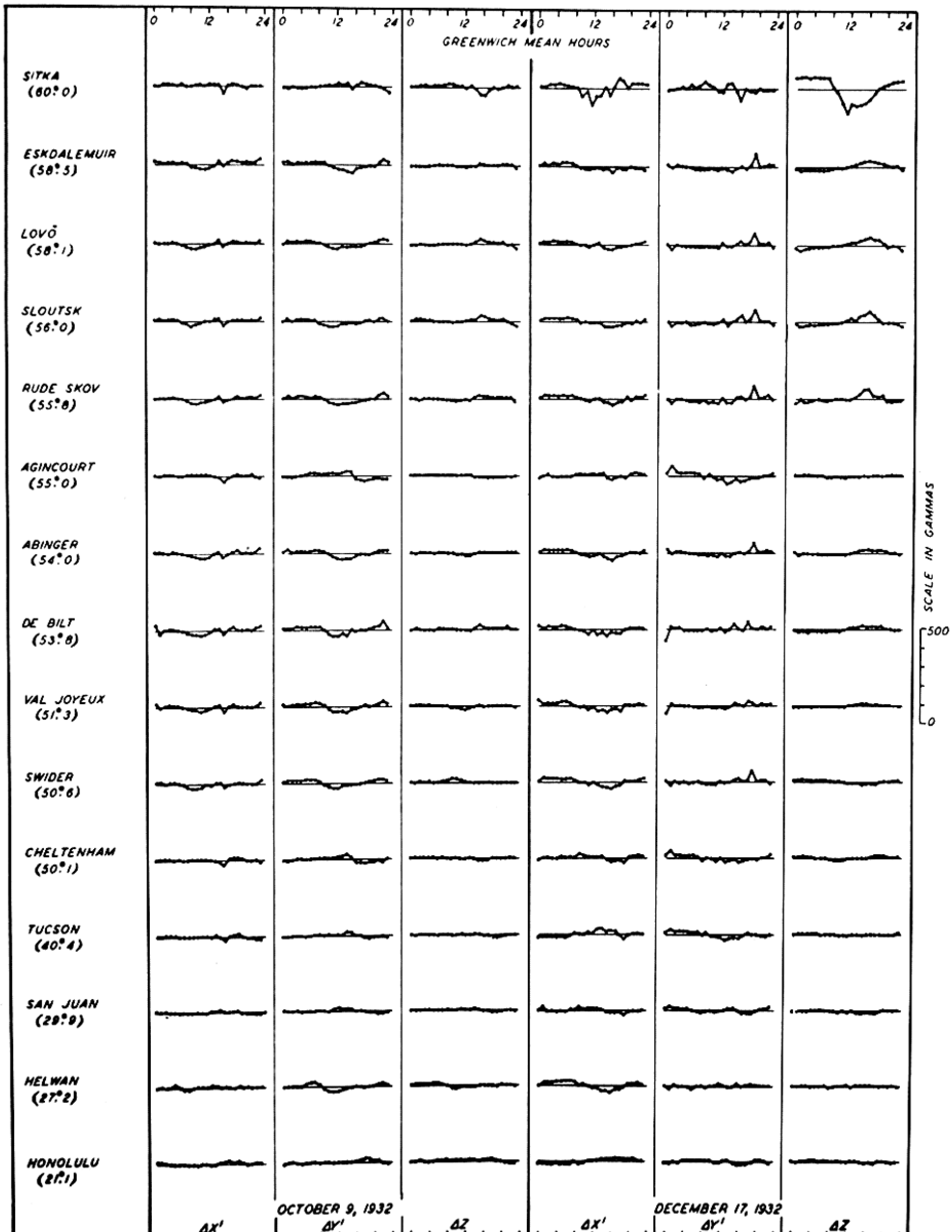

FIG. 127B—HOURLY DEPARTURES FROM MEAN OF DAY, GEOMAGNETIC COMPONENTS ΔX', ΔY', AND ΔZ (GEOMAGNETIC LATITUDES INDICATED IN PARENTHESES)

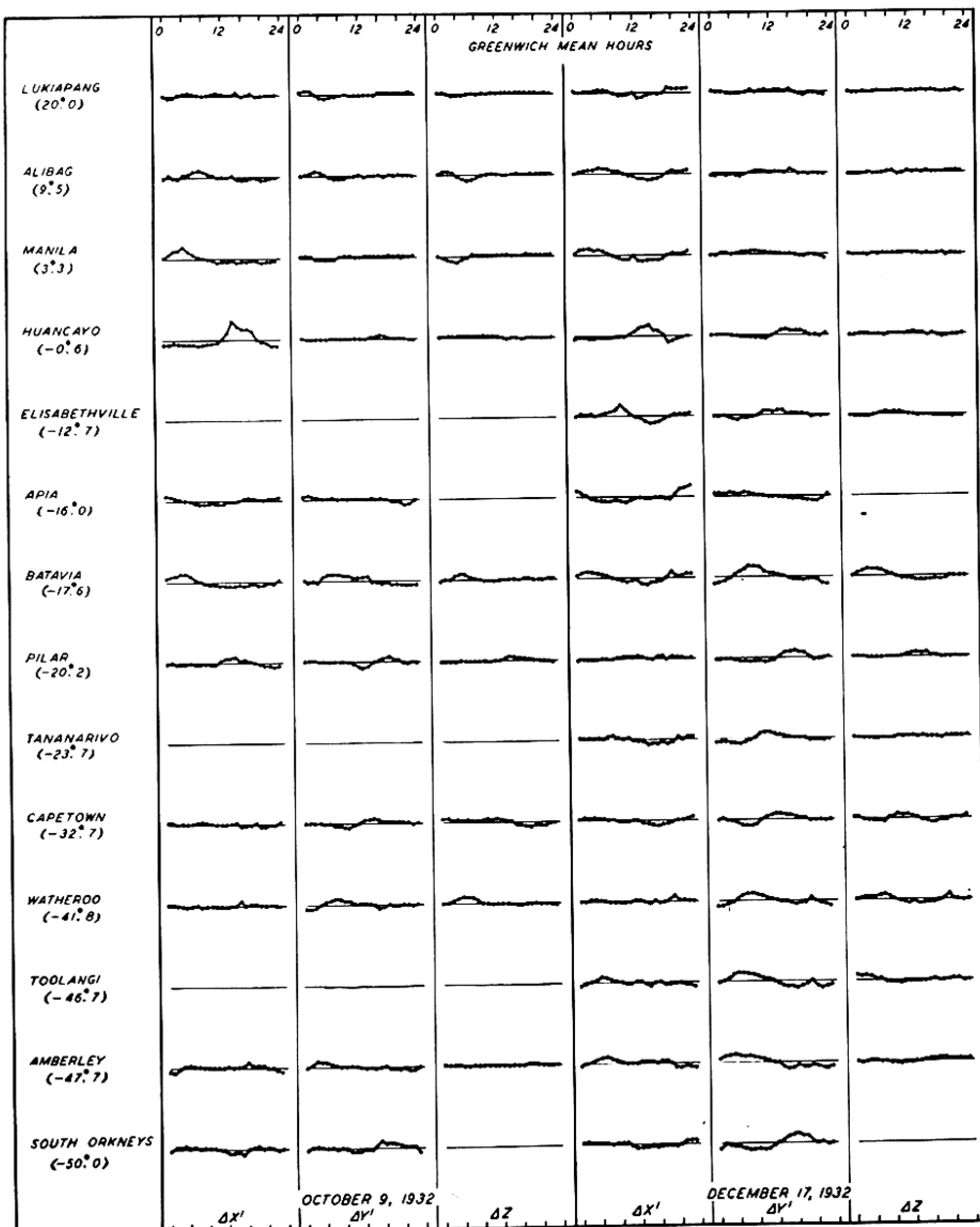

FIG. 127 (C)—HOURLY DEPARTURES FROM MEAN OF DAY, GEOMAGNETIC COMPONENTS ΔX', ΔY', AND ΔZ (GEOMAGNETIC LATITUDES INDICATED IN PARENTHESES)

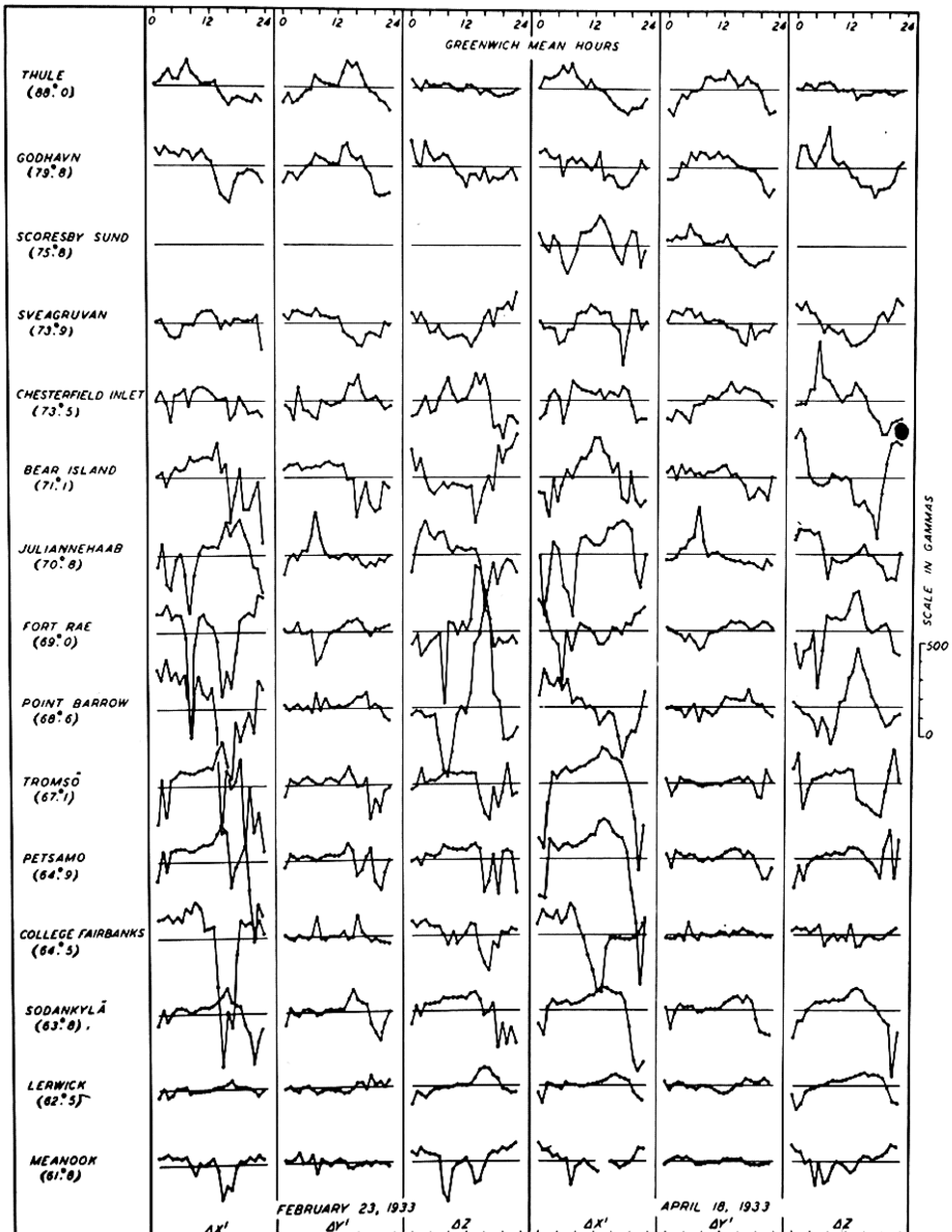

FIG. 127(D)—HOURLY DEPARTURES FROM MEAN OF DAY, GEOMAGNETIC COMPONENTS ΔX', ΔY', AND ΔZ (GEOMAGNETIC LATITUDES INDICATED IN PARENTHESES)

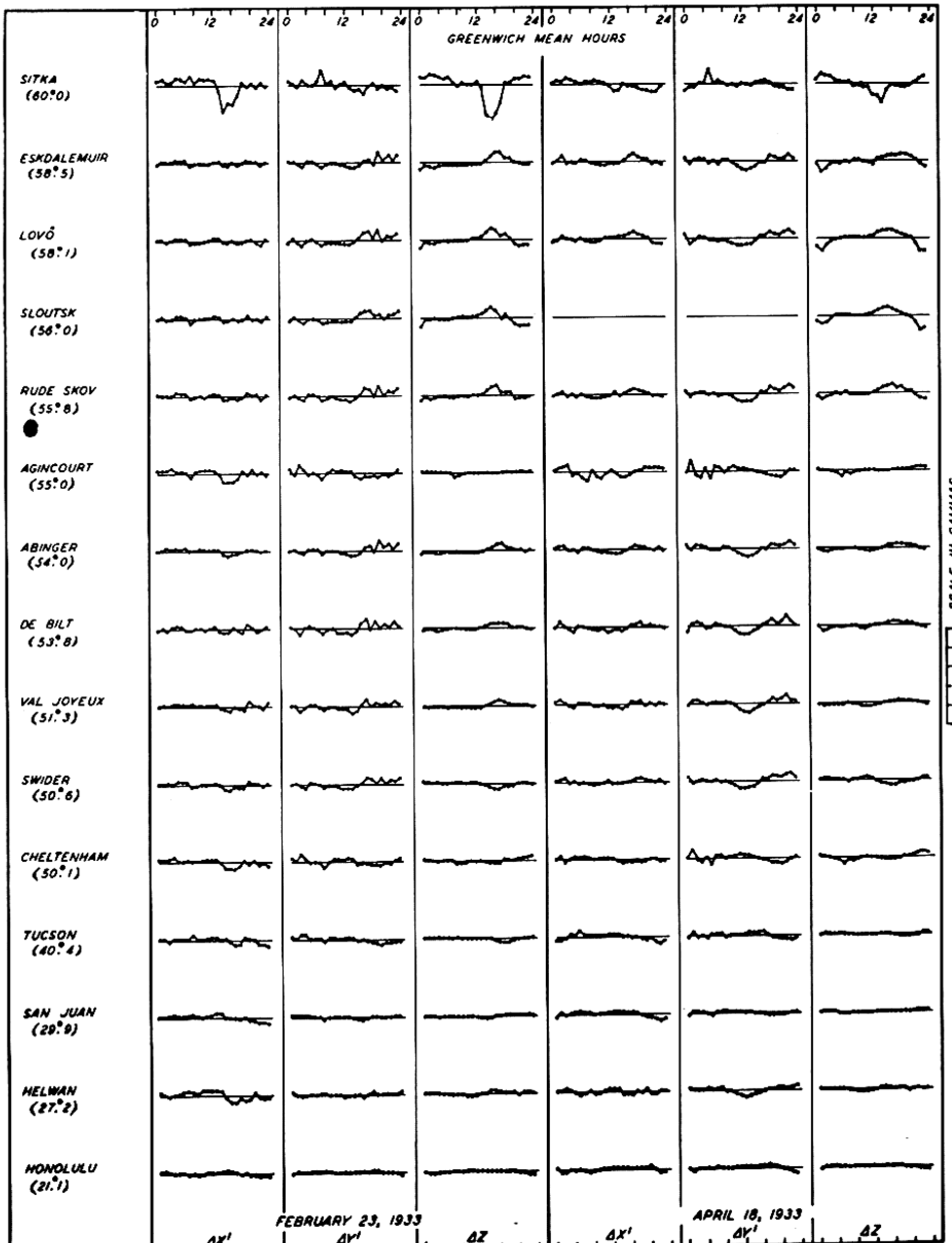

FIG. 127(E)—HOURLY DEPARTURES FROM MEAN OF DAY, GEOMAGNETIC COMPONENTS ΔX', ΔY', AND ΔZ (GEOMAGNETIC LATITUDES INDICATED IN PARENTHESES)

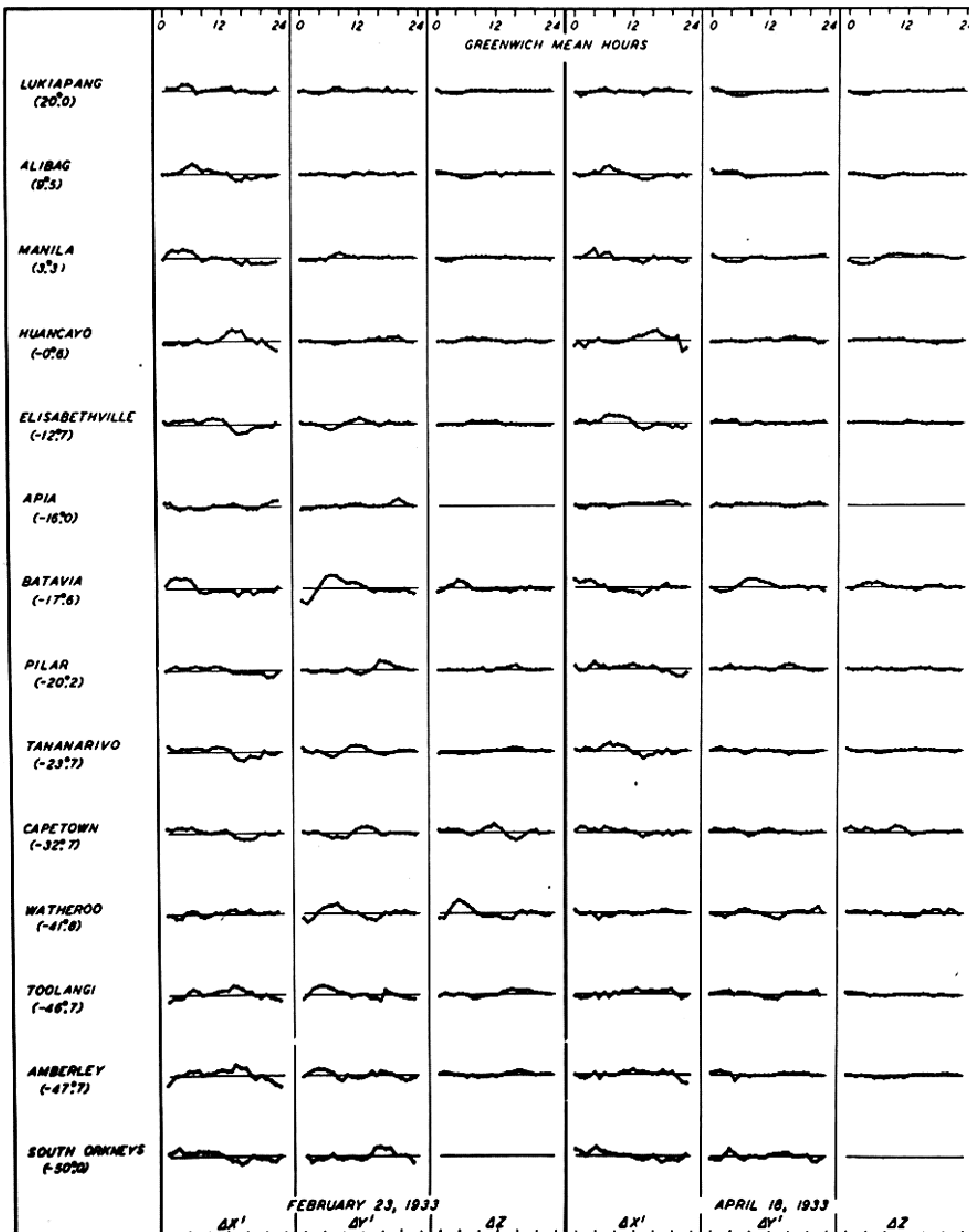

FIG. 127(F)—HOURLY DEPARTURES FROM MEAN OF DAY, GEOMAGNETIC COMPONENTS ΔX', ΔY', AND ΔZ (GEOMAGNETIC LATITUDES INDICATED IN PARENTHESES)

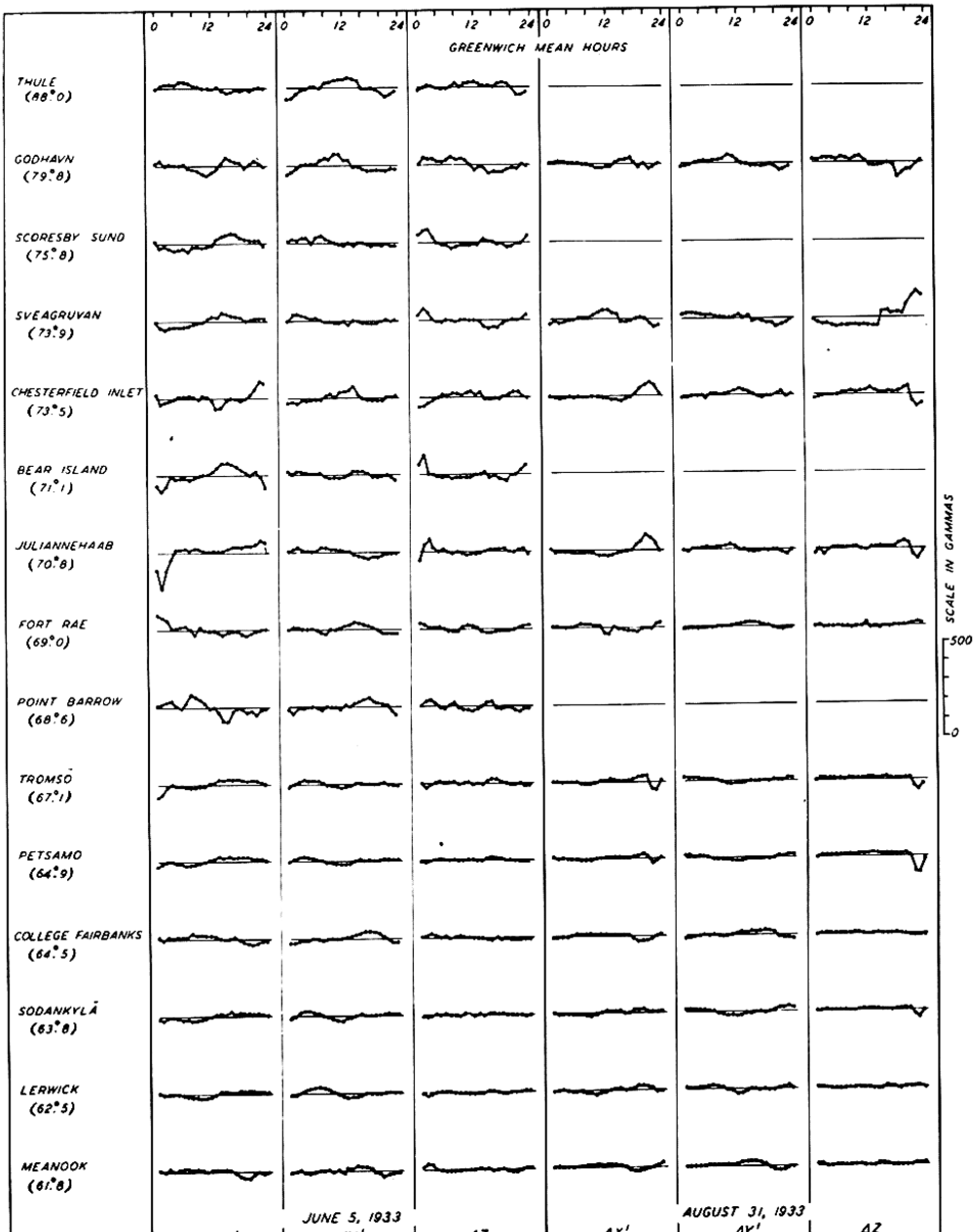

FIG. 127(G) —HOURLY DEPARTURES FROM MEAN OF DAY, GEOMAGNETIC COMPONENTS ΔX', ΔY', AND ΔZ (GEOMAGNETIC LATITUDES INDICATED IN PARENTHESES)

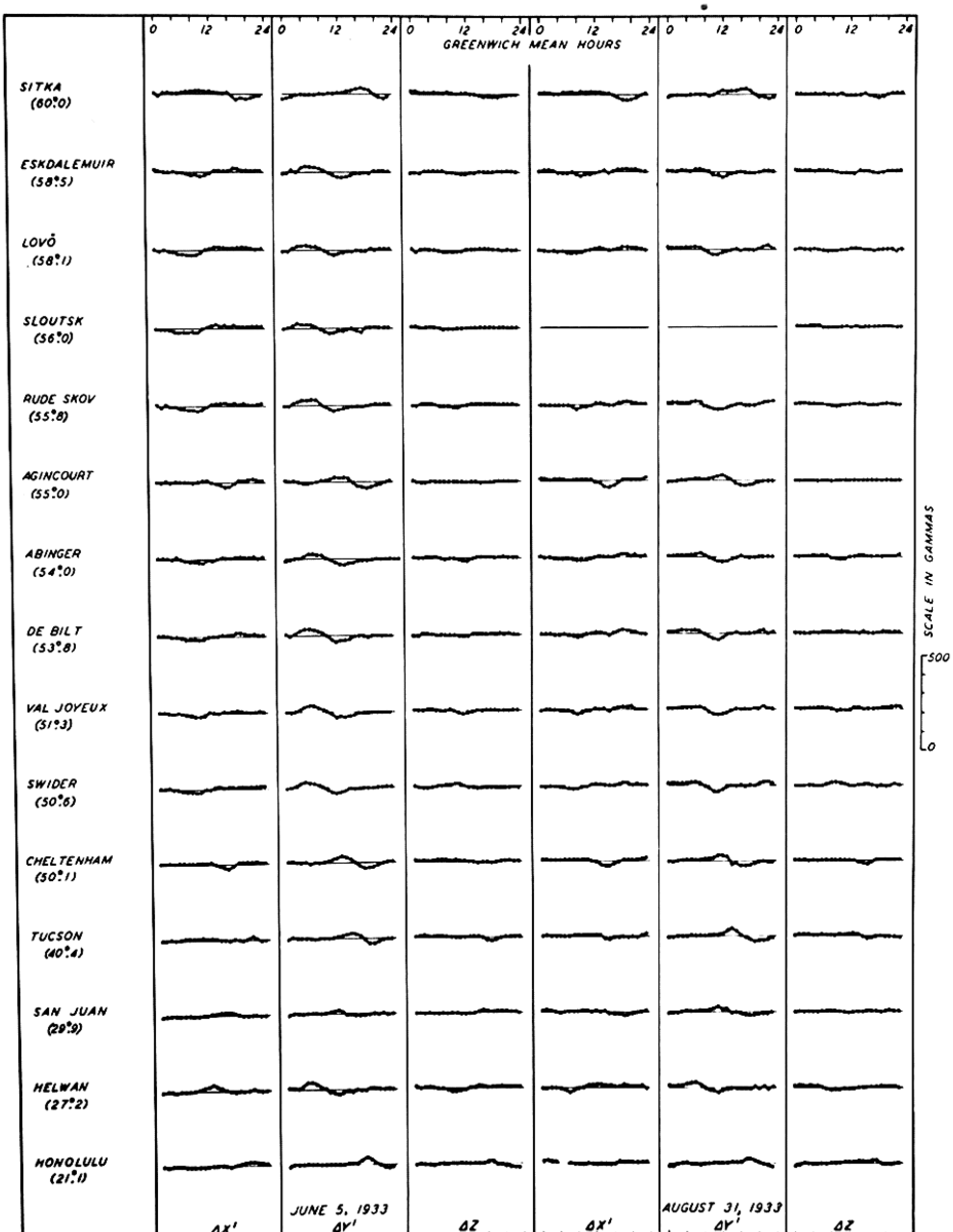

FIG. 127(0)—HOURLY DEPARTURES FROM MEAN OF DAY, GEOMAGNETIC COMPONENTS ΔX', ΔY', AND ΔZ (GEOMAGNETIC LATITUDES INDICATED IN PARENTHESES)

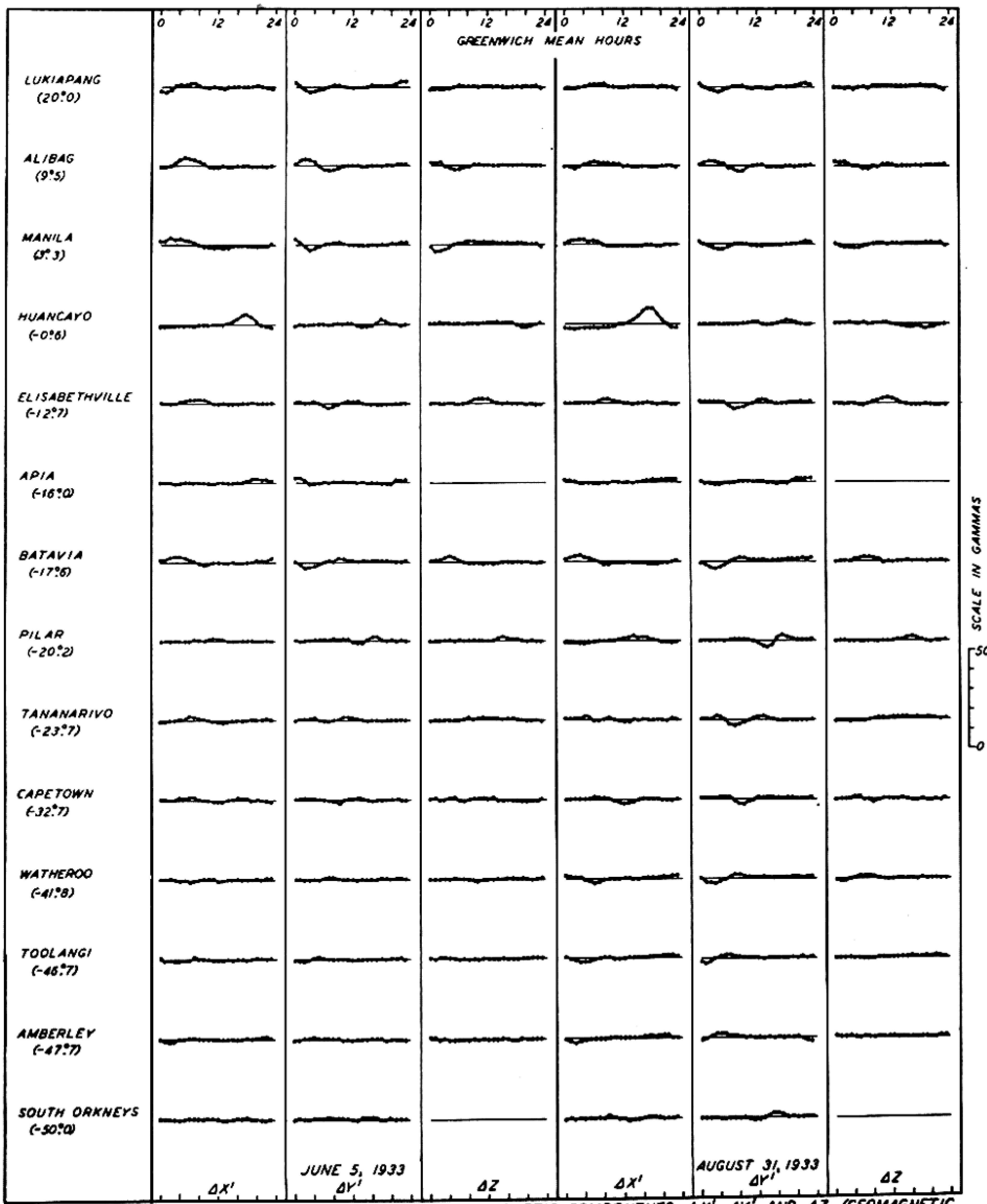

FIG. 127(I)—HOURLY DEPARTURES FROM MEAN OF DAY, GEOMAGNETIC COMPONENTS ΔX', ΔY', AND ΔZ (GEOMAGNETIC LATITUDES INDICATED IN PARENTHESES)

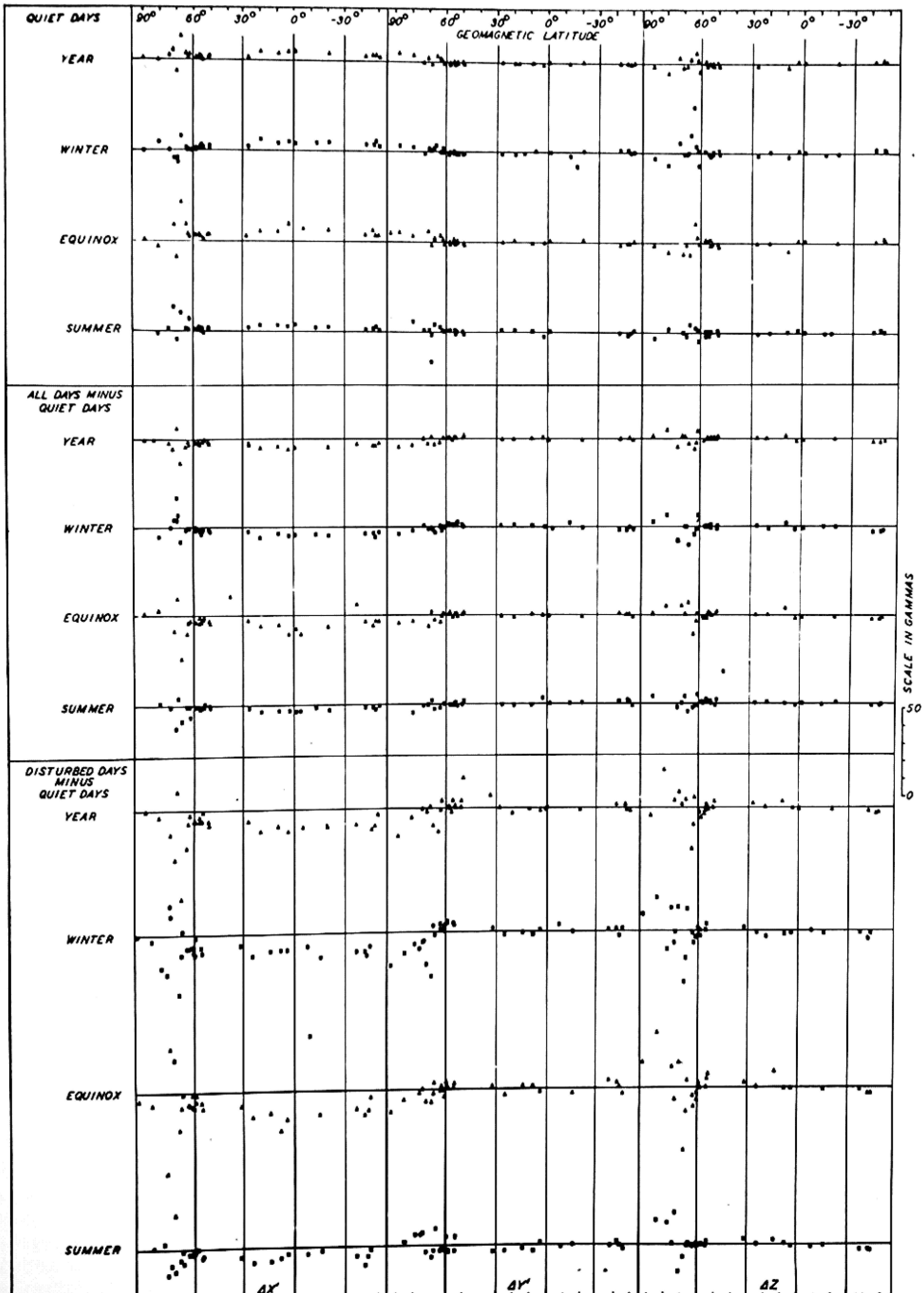

FIG. 128—VARIATION WITH GEOMAGNETIC LATITUDE IN NON-CYCLIC CHANGE FOR QUIET DAYS, ALL DAYS MINUS QUIET DAYS, AND DISTURBED DAYS MINUS QUIET DAYS GEOMAGNETIC COMPONENTS X' Y' AND Z BY YEAR AND BY SEASONS 1932-33 (TO AVOID CONFUSION POINTS ON SEASONS ARE INDICATED ALTERNATELY BY TRIANGLES AND SQUARES)

CHAPTER IX

FREQUENCIES OF GEOMAGNETIC FLUCTUATIONS OF VARIOUS INTENSITIES AND DURATIONS

1. General remarks.--The present chapter is concerned mainly with descriptive statistical aspects of geomagnetic fluctuations. These are considered with respect to their magnitudes and durations in various geographic localities.

The fidelity of response of the types of magnetic variometers customarily used at observatories is first considered. Data on long-period changes of durations of one day to about one year, as indicated by range in field-values, are next described. A short discussion is then given of three-hourly ranges, followed by extensive treatment of short-period fluctuations having durations of a few minutes to less than one second. There is finally appended a short discourse on the influence of electromagnetic induction on the observed character of the changes in the geomagnetic field.

2. Magnetic variometers.--Various types of magnetic variometers are in use at magnetic observatories, but their general principles of operation and construction are similar. The types in most prevalent use at present are those known as la Cour variometers. These record variations in D, H, and Z. Since the la Cour variometers are typical of most others, a short discussion of them is included here, summarizing general features which are given in more detail in standard treatises and their references [3].

Though the discussion is confined to la Cour variometers, the general principles are applicable also to many other types of instruments, such as compasses on moving conveyances and galvanometers and meters using magnet-systems in detecting and measuring magnetic fields.

Included in the presentation of the theory of the variometers are the differential equations satisfied by their responses. The solutions of these equations when the impressed fields are arbitrary continuous functions of time are next derived. The results permit the discussion for the first time of the magnitude of certain observed micropulsations in the Earth's field detected but very inadequately measured. On the basis of some experimental determinations of the responses of H-, D-, and Z-variometers to sinusoidal fields, a few sample computations are made to check the agreement between theory and observation.

It is shown that the apparent large rates of change and amplitudes (over 100γ, $1\gamma = 0.00001$ CGS unit) of rapid micropulsations recorded are the result of the amplification, through resonance, of what are considerably smaller fluctuations, though accompanied for short intervals of time by high rates of change. It is also found that the inaccuracies of responses of la Cour variometers to fluctuations down to the smallest durations measured, namely ten seconds, are small.

The H-variometer shown in Figure 129 uses a small magnet hung on a short suspension of much greater torsion than in the case of the D-variometer. In this instrument, which has a somewhat larger housing than that of the D-variometer, a prism is attached with brass supports to a bimetallic strip, for temperature compensation. The brass supports are located less than a centimeter away from the magnet but do not surround it; hence, little damping of the motion of the magnet would be expected. The free periods of oscillation of the H- and D-magnets vary with H, and for the instruments at the stations considered here will be of the order of about two seconds.

Figure 130 shows a view of the la Cour D-variometer and its magnet-system. A small magnet of magnetic moment about one CGS is attached at its center on an axle mounted at the base of a small vertical mirror. The mirror is affixed at its top to a fine quartz fiber freely suspended from a torsion-head. The housing of copper is at no point closer to the magnet than two cm so that little damping is to be expected.

Figure 131 shows the la Cour Z-variometer and its magnet-system. The magnet, the mirror, and the supporting knife-edges are one piece of steel. The magnetic moment of the magnet is of the order 100 CGS. The knife-edges rest on agate supports, the magnetic axis of the magnet being accurately aligned horizontally. The motion of the magnet is slightly damped as it passes between small vertical slots in the base carrying the agate supports. The characteristics of the instrument with respect to damping have not been thoroughly investigated; the magnet when set in motion by an artificial field will continue to oscillate for several minutes, the free period of oscillation varying with Z but being of the order ten seconds in the case of the stations considered in this study. The moment of inertia of the magnet-system is much greater than in the case of the H- and D-magnets; the response of this instrument hence will be somewhat more sluggish to small and rapid fluctuations.

A of Figure 132 shows a typical record for the day May 17, 1933, at Petsamo in northern Finland very near the auroral zone. The record was obtained with a la Cour recorder having a suitable mechanism for restricting the record to successive narrow strips of the photographic paper. This record shows the variations in the magnetic elements H, D, and Z at a time-rate of about 180 mm per hour. Shown also in the magnetogram are time-marks indicated by short vertical lines recorded at five-minute intervals, and three successive vertical lines at one-minute intervals indicating the hour. With the use of records of this type, it is possible to measure durations of fluctuations as short as ten seconds when the record is sufficiently distinct. At most stations (Table 104) the scale values used are somewhat less than for the data of A of Figure 132, being of the order of five gammas per mm.

B of Figure 132 shows a magnetogram of another type for the same day at Petsamo recorded at the rate of 15 mm per hour.

In addition to data obtained from magnetograms of the foregoing kind, use has also been made of recordings of (dZ/dt), where t is the time, as measured by the induction produced in a coil of many turns in series with a galvanometer. This Mitchell-loop apparatus was operated at College, Alaska, during 1932-33 and gave results in good agreement with findings based on magnetograms.

Records of geomagnetic fluctuations have also been obtained with new types of equipment such as recording fluxmeters and the magnetic air-borne detector [12], but these will be little considered here. These new devices permit extension of measurements to include geomagnetic fluctuations of higher frequencies.

3. General theory of magnetic variometers.--In discussing the fidelity of response of the la Cour variometers yielding the major portion of the data used in the present study, consideration is first given to the theory of variometers used in the measurement of variations of the geomagnetic field.

Consider a magnet of axis A, magnetic moment M, and free to turn about a fixed axis B perpendicular to A. We suppose the magnet in stable equilibrium under the influence of the mechanical couple MS_0 due to a steady component S_0 of the Earth's field acting perpendicular to the plane including A and B; also a couple G due either to gravity, an orthogonal component of field, the torsion of a suspending fiber, or to a combination of these. For equilibrium we obtain the equation $G = MS_0$. We then regard the magnet as being in a position of zero deflection, corresponding to the variometer's base value.

If the field changes from S_0 to $(S_0 + s)$, where s is a function of the time small in magnitude compared with S_0, we have

$$G = M(S_0 + s) \quad \ldots\ldots\ldots\ldots\ldots \quad (1)$$

which is the approximate basic formula used in general magnetic observatory practice. This formula permits the determination of s when the motion of the magnet associated with the change in G is known, when s varies sufficiently slowly with time.

If s varies rapidly with time, the motion is initially retarded by the effect of the moment of inertia K of the magnet-system. There are also retardations of motion due to damping caused by air friction and induced currents in surrounding electric conductors; these retardations are both usually directly proportional to the angular velocity of the magnet-system about its axis of rota tion. The general equation of motion of a variometer magnet then becomes

$$K\ddot{\theta} + 2kK\dot{\theta} + G(\theta) = M(S_0 + s)\cos\theta \quad \ldots\ldots \quad (2)$$

where θ is the angular displacement of the magnet in radians from its position of zero deflection corresponding to S_0. The damping factor $(k\pi/p)$ is the logarithmic decrement per half-period. The period $(2\pi/p)$ of the damped oscillation is defined as the interval between successive instants at which θ is a maximum, following the sudden application of a magnetic impulse.

In the case of a D-variometer, the couple $G(\theta) = MH \sin\theta$, $S_0 = 0$, and putting $s = T$, where T is a magnetic force transverse to the magnetic meridian acting in the direction of increasing θ, (2) becomes, when θ is small

$$K\ddot{\theta} + 2kK\dot{\theta} + MH\theta = MT \quad \ldots\ldots\ldots \quad (3)$$

For an H-variometer, we have $G(\theta) = C(\delta + \theta)$ where δ is the initial angular twist in the vertical supporting fiber required to align the magnet perpendicular to the magnetic meridian in the presence of the constant field $S_0 = H_0$. In this case (2) becomes

$$K\ddot{\theta} + 2kK\dot{\theta} + C\theta = Mh \quad \ldots\ldots\ldots\ldots \quad (4)$$

where θ is small, $C\delta = MH_0$, and $s = h$

In the Z-variometer, the magnet is balanced with its magnetic axis horizontal against the couple MZ_0 of the standard field or base value Z_0. When Z_0 changes to $(Z_0 + z)$, the balance is achieved through opposing couples $M(H_0 + h)\sin\theta\cos p$, where p is the azimuth of the north-seeking end of the magnet measured from the magnetic north around by east, and the couple mga cos $(\alpha - \theta)$; here m is the mass of the magnet, g the acceleration of gravity, a the perpendicular distance from the center of gravity P of the magnet-system to a point O on the axis of rotation, and α the acute angle between the magnetic axis A and OP. Thus

$$G(\theta) = MH\sin\theta\cos p + mga\cos(\alpha - \theta)$$

so that (2) becomes

$$K\ddot{\theta} + 2kK\dot{\theta} + MH\cos p\sin\theta + mga\cos(\alpha - \theta)$$

$$= M(Z_0 + z)\cos\theta$$

When θ is small

$$K\ddot{\theta} + 2kK\dot{\theta} + [mga\sin\alpha + MH\cos p]\theta = Mz \ldots \quad (5)$$

noting that $MZ_0 = mga\cos\alpha$.

We may rewrite (3), (4), and (5)

$$\ddot{\theta} + 2k\dot{\theta} + n^2\theta = Ms/K \quad \ldots\ldots\ldots\ldots \quad (6)$$

appropriate to a D-, H-, or Z-variometer if, respectively we have $s = T$, h, or z and $n^2 = (MH/K)$, (C/K), or $[mga\sin\alpha + MH\cos p]/K$.

We note (6) is the familiar equation of forced vibrations applicable to a system free to oscillate in one dimension when retarded by a restraining force proportional to the velocity. If $k = 0$ and $s = 0$, the magnet is then imagined to oscillate about its equilibrium position without damping and has a frequency n and period $(2\pi/n)$. If $n > k$, $k \neq 0$, the frequency p is given by $p^2 = (n^2 - k^2)$ so that the introduction of damping lengthens the period of free oscillation.

If s varies slowly with time so that $2k\dot{\theta}$ and $\ddot{\theta}$ are small compared with $n^2\theta$, (6) becomes

$$(Kn^2/M)\theta = s \quad \ldots\ldots\ldots\ldots \quad (7)$$

where (Kn^2/M) is the scale value of the variometer (for D, H, or Z, respectively, the values being H, C/M, or $[mga\sin\alpha + MH\cos p]/M$) in CGS units per radian of deflection when θ is not too large. The scale value in gammas per minute of arc is thus

$$e_b = [\pi/(180 \times 60)]\, 10^5\, Kn^2/M = 29.09\, Kn^2/M \ldots \quad (8)$$

If a mirror properly aligned and rigidly attached to the magnet reflects a light beam from a fixed source on to a screen, (8) becomes

$$\epsilon_b = 10^5\, Kn^2/2dM \quad \ldots\ldots\ldots\ldots \quad (9)$$

in gammas per millimeter deflection at the scale, d being the optical distance in millimeters from the magnet mirror to the scale or recording drum. This value ϵ_b may be called the base scale value of the variometer, since it is the scale value at the position of zero deflection corresponding to the base value of the variometer.

The variation in scale value with ordinate ℓ in millimeters is found less directly by differentiation of the variables entering in the unsimplified expressions for the couples for each variometer, where sin θ is not replaced by θ and cos θ not replaced by unity. We thus obtain

$$\epsilon_D = \epsilon_{bD} \sec^2 \theta \doteqdot \epsilon_{bD} [1 + \ell^2/8d^2]$$

$$\epsilon_H = \epsilon_{bH} \sec \theta + 10^5 H_0 \tan \theta/2d$$

$$\doteqdot \epsilon_{bH} + 10^5 \ell H_0/4d^2$$

$$\epsilon_Z = \epsilon_{bZ} + 10^5 z \tan \theta/2d = \epsilon_{bZ} + 10^5 \ell z/4d^2$$

in gammas per millimeter. In practice, the base scale value suffices for calculating deflections to the nearest gamma, except for rare large deflections in (H) (most frequently experienced in auroral regions). The derivation of scale values and the theory of H-variometers has been carefully and extensively considered by George Hartnell [40].

Using (7) and (9), we get $(S_0 + s) = (S_0 + \epsilon_b \ell)$. If the temperature varies, the magnetic moment changes, and

$$M = M_0(1 - \beta \underline{T}) \quad \ldots\ldots\ldots\ldots\ldots \quad (10)$$

where M_0 is the moment at a standard temperature $\underline{T}_0$, $\underline{T}$ the temperature, and β the temperature coefficient in gammas per degree of temperature. We then get

$$(S_0 + s) = [B + \beta(\underline{T} - \underline{T}_0) + \epsilon_b \ell] \quad \ldots\ldots \quad (11)$$

where $B = (S_0 + \epsilon_b \ell')$, say, the known base-line value at the recorder (in general provided by a light beam from a fixed mirror and but slightly removed from the light spot for zero deflection), and ℓ' the departure in millimeters with proper sign from the position of zero deflection.

The effect of change in temperature upon the values of n^2 and ϵ_b is small (when s is small) and is usually neglected; its effect is that of producing an apparent change in the base values $S_0 = (H_0, Z_0)$ due to changes in the balancing couples dependent on M. We had actually $H_0 = C\delta/[M_0\{1 = \beta\underline{T}\}] = C\delta\{1 + \beta\underline{T}\}/M_0$, $Z_0 \doteqdot mgd \cos \alpha\{1 + \beta\underline{T}\}/M_0$, so that a correction linear with temperature is indicated. For a D-variometer, the temperature coefficient is usually negligible.

In (11) the impressed field s and the response are equivalent, since s varies slowly with time. When s varies rapidly with time, the remaining terms of (6), depending on the acceleration and velocity of the moving magnet-system, require evaluation. For this purpose, the constants k, n, and (M/K) may be obtained experimentally.

The factor k is most readily found from the amplitudes of successive deflections during free oscillations of the magnet-system or less simply by fitting a function $Ae^{-kt} \sin(pt + \nu)$ to a photographic record of these deflections. The timing of oscillations yields the constant p, whence $n^2 = (p^2 + k^2)$ can be calculated, and further permits the calculation of (K/M) using (9) when the scale value ϵ_b has been obtained with the aid of a Helmholtz coil and milliammeter.

Since (K/M) from (9) is known to four figures, the calculation of H to the same accuracy is possible, noting that for the D-variometer $n^2 = (MH/K)$, whence $H = (Kn^2/M)$. The value of H can also be obtained by a method used by la Cour, by arranging a Helmholtz coil on a D-variometer to give a horizontal field T transverse to the magnetic meridian deflecting the magnet through an observed angle θ (determined from the deflected beam on a screen); then since $MH \sin \theta = MT \cos \theta$ we have $H = T \cot \theta$. In using the latter method, a correction of the deflection for torsion of the suspension-fiber is desirable and θ should be as large as possible.

The values of K and M for either a D- or H-variometer can also be obtained apart from their ratio (K/M), since the magnet-systems are interchangeable. When the magnet-system is mounted as in an H-variometer, we may by an oscillation experiment find p, whence also finding k we get $n^2 = (p^2 + k^2) = (C/K)$, having a value different from that for the magnet in the meridian. By a torsion experiment we next obtain C, whence K becomes known, since n^2 is known. Having K, we obtain M from the value (K/M).

The accuracy of determination of constants is largely dependent on the accuracy of the milliammeter used. However, when H is known to about five figures, we can obtain (K/M) to about five figures from the relation $n^2 = (MH/K)$, (most readily when k is small) for either the H or D magnet-systems mounted as in a D-variometer.

In the case of a Z-variometer, after finding k, and the moment M of the magnet from deflections of the magnet system of the D-variometer (account being taken of the distribution coefficient), we may then obtain α, K, and a by the timing of oscillations. We have $p^2 = (n^2 - k^2)$ when $n > k$, and from (6), with $n^2 = (mga \sin \alpha + MH_0 \cos p)/K$, $MH_0 = mga \cos \alpha \cot I$, where I is the magnetic dip, and $MZ_0 \tan \alpha = mga \sin \alpha$, there results

$$(n_S^2/n_N^2) = (mga \sin \alpha + MH_0)/(mga \sin \alpha - MH_0)$$

$$= (1 + \cot \alpha \cot I)/(1 - \cot \alpha \cot I) \quad \ldots\ldots \quad (12)$$

whence

$$\left.\begin{aligned} \cot \alpha &= (n_S^2 - n_N^2) \tan I/(n_S^2 + n_N^2), \\ K &= M(Z_0 \tan \alpha + H_0 \cos p)/n^2, \\ a &= MZ_0 \sec \alpha/mg \end{aligned}\right\} \ldots \quad (13)$$

As before, using (9) we get

$$(K/M) = (2 \times 10^{-5}\, d\, \epsilon_b/n^2) \quad \ldots\ldots\ldots \quad (14)$$

in terms of the scale value in gammas per mm when the distance d is also in mm. We can evidently also find ϵ_b from (13) and (14) by timing oscillations when H_0 and Z_0 are known.

4. Solution of the response equation.--In (6) we had for any unifilar variometer and standard vertical intensity balance

$$(\ddot{\theta} + 2k\dot{\theta} + n^2\theta) = (Ms/K)$$

where θ is the angular deflection of the magnet in radians for the impressed field s. On writing $f(t) = (MS/K)$ this becomes the equation of forced vibrations for a mechanical system free to oscillate in one dimension. Its solution may be obtained directly from the differential equation using the integrating factors $e^{kt} \sin pt$ and $e^{kt} \cos pt$ [41] in the form

$$p\theta = \int_0^t e^{-k(t-\tau)} \sin p(t-\tau)\, f(\tau)\, d\tau \;\ldots\ldots (15)$$

if $\theta = 0$, $\dot{\theta} = 0$ when $t = 0$. If the impressed field $[(K/M)\, f(t)]$ is arbitrary and expressible in terms of a Fourier series, we have

$$f(t) = \sum_0^{\infty} C_m \sin(mt + \epsilon_m)$$

whence, putting $u = (t - \tau)$

$$\theta = \sum_0^{\infty} \frac{C_m}{p} \int_0^t e^{-\omega u} \sin[m(u+t) + \epsilon_m]\, du \;\ldots (16)$$

where $\omega = (k - ip)$ so that θ is the imaginary part of (16). However, it is likely to be found in practice more convenient to calculate θ by numerical methods from (15).

With the aid of Fourier integrals, a solution may also be obtained in the form of a contóur-integral. Writing (6) in the form

$$(\ddot{\theta} + 2k\dot{\theta} + n^2\theta) = \phi(t),\ t > 0 \;\ldots\ldots (17)$$

putting $\omega = (u + iv)$, we get the Fourier transform

$$\sqrt{2\pi}\,\theta\ (\omega) = \int_0^{\infty} \theta(t)\, e^{i\omega t}\, dt$$

$$= -(1/i\omega)\ \theta(0) - (1/i\omega)\int_0^{\infty} \dot{\theta}(t)\, e^{-i\omega t}\, dt$$

$$= -(1/i\omega)\ \theta(0) - (1/\omega^2)\ \dot{\theta}(0) - (1/\omega^2)\int_0^{\infty} \ddot{\theta}(t)\, e^{i\omega t}\, dt$$

after integrating by parts. Also

$$2\pi\,\Phi(\omega) = \int_0^{\infty} \phi(t)\, e^{i\omega t}\, dt = \int_0^{\infty} (\ddot{\theta} + 2k\dot{\theta} + n^2\theta)\, e^{i\omega t}\, dt$$

$$= -(\omega/i)\ \theta(0) - \dot{\theta}(0) - 2k\,\theta(0) - \sqrt{2\pi}\,(\omega^2 + 2ki\omega - n^2)\,\theta\ (\omega)$$

Hence

$$\theta(t) = (1/2\pi)\int_{ia-\infty}^{ia+\infty} [e^{-i\omega t}/(\omega^2 + 2ki\omega - n^2)]$$

$$[(2k - i\omega)\ \theta(0) - \dot{\theta}(0) + \Phi\ (\omega)]\, d\omega \;\ldots\ldots (18)$$

when a is sufficiently large. This integral is evaluated by the method of residues, when $\Phi(\omega)$ obtained from $\phi(t)$ is known.

In illustration of the application of (15) suppose $f(t) = A(1 - e^{-vt})$. Then

$$\theta = (A/p)\int_0^t e^{-\omega u}\,[1 - e^{-v(t-u)}]\, du$$

$$= (A/p)\,[\{p - g(t)\}/n^2 - \{pe^{-vt} - g(t) + ve^{-kt}\sin pt\}$$

$$/(n^2 - 2kv + v^2)] \;\ldots\ldots\ldots\ldots\ldots (19)$$

where $g(t) = e^{-kt}(k \sin pt + p \cos pt)$. The first term is that due to a field (KA/pM) at $t = 0$ and subsequently maintained constant.

When $n^2 = k^2$, as in a dead-beat galvanometer, the free motion is

$$x = (A + Bt)\, e^{-kt}$$

where A and B are arbitrary constants. If $k^2 > n^2$ the free motion becomes

$$x = Ae^{-ut} + Be^{-vt}$$

where u and v are roots of the equation

$$(z^2 - 2kz + n^2) = 0$$

so that the free motion includes two exponential terms decaying at different rates.

When the response θ is measured, $f(t)$ is found by obtaining $\dot{\theta}$ and $\ddot{\theta}$ graphically or otherwise from θ, to obtain the terms on the left of (6). Suppose $\theta = c(1 - \cos mt)$, so that $\dot{\theta} = cm \sin mt$, $\ddot{\theta} = cm \cos mt$. Then from (6)

$$f(t) = (cK/M)$$

$$[n^2 + \{(m^2 - n^2)^2 + 4k^2m^2\}^{1/2} \cos(mt + \nu)] \,.. (20)$$

where $\tan \nu = [2km/(m^2 - n^2)]$. Here the impressed field yielding the prescribed response θ is made up of a suddenly impressed constant part proportional to n^2 and a sinusoidal part of amplitude proportional to $\{(m^2 - n^2)^2 + 4k^2m^2\}^{1/2}$ as compared with n^2 of the periodic response. The proportional increase in amplitude over that for a perfect response is thus $n^2/\{(m^2-n^2)^2 + 4k^2m^2\}^{1/2}$ for the periodic part. The following table gives this amplitude ratio for various values of m^2 and periods in seconds, using constants approximating those of the la Cour variometers. For a fluctuation of this type, of period ten seconds or more, it is evident that the error is less than 4 per cent (1 per cent for period 20 seconds). The lag in phase of the response is very slight, only a fraction of a degree. As resonance $(m^2 = n^2)$ is approached, the amplitude ratio increases to 100 and the lag in phase of the response increases to 90°; at resonance the amplitude ratio is $(n^2/2km) = (m^2/2km) = (m/2k)$. Thus the smaller the value of k, the greater the magnification achieved. Below resonance, the response rapidly deteriorates and lags behind the impressed field in phase, this lag approaching 180° as the period of the impressed field becomes very small.

Variation of amplitude-ratio, actual response $c(1 - \cos mt)$ to true response, with frequency m of impressed field, $n^2 = 10$, $k = 0.0165$ CGS units

m^2	Period	$(m^2-n^2)^2$	$4k^2m^2$	Amplitude ratio	ν
					°
0.01	62.8	100.00	0.00	1.00	0.02
0.1	19.8	98.01	0.00	1.01	0.07
0.4	9.9	92.16	0.00	1.04	0.1
1.0	6.3	81.00	0.00	1.11	0.2
4.0	3.1	36.00	0.00	1.67	0.6
10.0	2.0	0	0.01	100	90.0
40.0	1.0	900.00	0.04	0.33	179.6
100.0	0.63	8100.00	0.10	0.11	179.8

The amplification through resonance suggests the use of H-, D, and Z-variometer magnet-systems in evacuated, nearly nonconducting containers, with the damping, and hence the value of k and of the period ($2\pi/n$), being controlled by varying the air-content within and adjusting magnets outside. An apparatus of this type could then be used accurately to measure tuned responses to periodic changes in the Earth's field with amplitudes of very small fractions of a gamma--phenomena as yet hardly investigated.

5. Experimental determinations of responses of la Cour variometers to various impressed fields.--Introduction. The following sections are concerned mainly with a few illustrative examples of responses to periodic and suddenly impressed magnetic fields, measured by R. G. Fitzsimmons and W. F. Wallis of the Department of Terrestrial Magnetism. The experimental constants needed for the theory were also obtained, and the results of theory were compared with observation. These experiments were carried out under the difficulties inherent to the making of accurate magnetic measurements in an urban area. Although the effects of stray magnetic fields are at times all too evident, these effects are nevertheless thought to be generally small compared with the magnitudes of measured responses.

Apparatus. The apparatus used consisted of a la Cour D-variometer which was employed also as an H-variometer, and a la Cour Z-variometer [42]. These variometers were mounted in the sub-basement of the Department of Terrestrial Magnetism.

In the D-variometer, the magnet was suspended on a fine quartz fiber and was free to move about a vertical axis in response to magnetic changes transverse to the magnetic meridian.

When used as an H-variometer, the D-variometer was equipped with a heavy quartz fiber and the magnet was held in an east-west position by the torsion of the fiber. In this position it responded to changes in the horizontal component of the Earth's field.

The magnet of the Z-variometer, balanced horizontally on knife-edges, was free to rotate about a horizontal axis in response to changes in the vertical intensity.

The impressed magnetic fields to which these variometers were allowed to respond were produced by a cylindrical magnet (moment 337 CGS units for the D- and H-variometers and moment 677 CGS units for the Z-variometer) mounted in a hole drilled through a cylindrical shaft at right-angles to the axis. The shaft was rotated by a synchronous motor. It was possible to regulate the speed of rotation of the shaft, by means of a friction-clutch, to within 0.05 second.

In all cases, the deflecting magnet, as mounted on the rotating shaft, turned within a plane perpendicular to the normal position of the magnetic axes of the variometer magnets and was located at the same height as the latter. The deflecting distances were so varied as to yield suitable deflections.

An optical system was arranged so that a beam of light reflected from mirrors rigidly attached to the variometer magnets produced light spots upon photographic paper on a rotating drum. This drum was rotated so as to give a record with a time-scale of 10.6 mm per second.

Procedure.--The damping-curves for the determination of the damping-factors k of (6) were obtained by allowing the variometer magnets to come to rest after being set in free oscillation. Responses to impressed fields initially zero were obtained with the turning (deflecting) magnet starting from rest from a position of zero deflection. In the case of the Z-variometer, the recording light, recording drum, and turning magnet were started simultaneously; for the D- and H-variometers, the turning magnet was started a second or two after starting the drum and recording light.

The micropulsations sometimes found on la Cour rapid recorders were simulated by subjecting the variometers to a sinusoidal field of period near that of resonance of the magnet-systems, applied intermittently at successive intervals of one-half minute.

The initial response to a "square-wave" of long duration was obtained by having the variometers record for a few seconds when deflected by the field of a Helmholtz-coil, this field being subsequently suddenly reduced to zero.

A commutator consisting of 12 equally spaced sections served to break the recorder-lamp circuit several times per second so that identification of the position of the turning magnet could be made at all times.

Results. The following table lists the constants of the variometers obtained by methods previously described.

Constants of magnet systems Nos. D31 and ZTC of variometers in CGS units

Constant	H	D	Z
M	3	3	55.5
K	0.038	0.038	2.39
(K/M) adopted	0.013	0.013	0.043
e_b	$5.5\gamma/1'$	$3.0\gamma/1'$	$16.1\gamma/1'$
m	0.701	0.701	2.17
p	3.105	3.58	3.83
k	0.0213	0.0148	0.0275
n^2	12.82	9.64	14.67
a	....	....	0.013
α	....	....	-157°.4
a sin α	....	....	0.005

Figure 133 shows damping-curves obtained for the D-, H-, and Z-variometers. Also shown are the corresponding values of the damping-factor k of e^{-kt}, the exponential law of decrease in amplitude with time. The value is least for the D-variometer and greatest for the Z-variometer. The values of frequency found are of the same order of magnitude for each variometer.

Figures 134(A), 134(B), and 134(C) show for the D-, H-, and Z-variometers, respectively, the initial (a) and steady (b) responses to the field of a cylindrical magnet, rotated about an axis through its center and perpendicular to its magnetic axis. The responses are shown for periods of rotation one, two, three, and four seconds, and "beats" are shown near $\lambda = 2$. Curves (b) measured about ten minutes after those of (a) show a steady sinusoidal response, following the exponential decay of the initial wave having the frequency p of the magnet-systems.

Figures 135, 136, and 137 show more clearly than does Figure 134 the transitions in the character of the response to impressed fields at 0.05-second intervals with period below that of resonance. The amplitude at resonance is much greater than that of the impressed field shown at the left in each figure.

Figure 138(A) shows the initial (a) and steady (b) responses (after ten minutes) to impressed fields of period four seconds. The uneven character of the initial responses is probably due to a certain initial jerkiness in the torque obtained from the motor and drive shaft attached to the

rotating magnet. The steady responses in D, H, and Z show amplitudes about 30, 25, and 20 per cent greater, respectively, than those of the corresponding measured impressed fields. In Figure 138(B) for period nine seconds, the corresponding amplitudes of response are only about 2, 8(?), and 3 per cent greater than the measured impressed fields, so that the response has now become fairly good and will improve rapidly as the period increases. For purposes of the present investigation, it is concluded that the statistics on short-period geomagnetic fluctuations are insignificantly affected by the quality of response for durations greater than 10 to 20 seconds.

Figure 139 gives the responses for suddenly impressed constant fields.

6. Estimates of magnitudes of micropulsations in the Earth's field.--Near and just outside the auroral zone, there frequently appear micropulsations of the Earth's field. At Sodankylä, Finland (ϕ = 67°.4 N, λ = 26°.6 E), about one hour out of every 30 shows evidence of their presence. They have periods of the order of two to five seconds. A of Figure 140 shows an example of micropulsations in horizontal intensity observed at Lycksele, Sweden, over an interval of about one hour. Their period was evidently near that for resonance of the H-variometer, so that their amplitude is greatly magnified; their absence from the corresponding records of the D- and Z- variometers suggests that their period in this instance may have been maintained near that of resonance for only the H-variometer. B of Figure 140 shows a similar record at Lycksele in which the pulsations are indicated appreciably only by the Z-variometer. If it is assumed that the results given in the table in section four above (page 260) apply for these instruments and that resonance was attained, the amplitudes of the pulsations may be estimated as about one-hundredth the recorded values or about 0.04 gamma. C of Figure 140 shows pulsations with period of a minute or more.

Figures 141 and 142 (note the change in time-scale) give responses near resonance frequencies for both intermittent and steadily impressed sinusoidal fields. The amplitudes of the impressed fields were too small to be indicated to scale conveniently on the diagram; they are estimated to be of the order one to two gammas.

Figure 143 gives a record of artificial disturbances affecting, at times, the results of the foregoing experiments.

7. Comparison of calculated responses of magnetic variometers with observation.--The equation satisfied by the response θ to an impressed field s was previously shown in (6) to be

$$(\ddot{\theta} + 2k\dot{\theta} + n^2\theta) = (Ms/K)$$

For the impressed field s = K(1 - cos mt)/M, with $\theta = \dot{\theta} = 0$ at t = 0, Miss C. M. Martin found the solution to be

$$\theta = Ae^{-kt} \sin (pt + \mu) + B \cos (mt + \nu) + 1/n^2 \quad .. (21)$$

where $A = (m^2r/np)$, $B = r$, $\sin \mu = -(pqr/n)$, $\cos \nu = qr$, $q = (m^2 - n^2)$, $r = [1/(q^2 + 4k^2m^2)^{1/2}]$, and $p^2 = (n^2 - k^2)$.

The response X in gammas due to the impressed field s (in CGS units) then becomes

$$X = 10^5 (K/M) n^2\theta \quad .... (22)$$

where K, M, and n are the constants appropriate to the variometer used.

Figure 144 shows for D, H, and Z, respectively, the computed responses near resonance (λ = 1.9, 2.0, and 1.6), for impressed fields s = cK(1 - cos mt)/M. The values of the constant c were adjusted to give responses with amplitudes the same as those of the corresponding experimental responses of the instruments used for Figures 133, 134, 135, and 136. The impressed fields s are illustrated only for the first complete cycle, and show good agreement with observed steady deflections produced by the disturbing magnet at rest.

Figure 145 gives results of calculations made like those for Figure 144 but for periods (λ) of four and nine seconds. For λ = four seconds, the computed responses are about 30 per cent greater in amplitude than that of perfect response. This is mainly due to the period being near that of resonance. The calculated defect in response is only a few per cent for λ = nine seconds; the deficiency in the response thus decreases rapidly with increasing period, in good agreement with the results of the table given in section four above (page 260).

8. Stability of magnet-system.--In the theory, it is noteworthy that, intimately associated with n^2, there is the ratio K/M involving two quantities somewhat difficult of measurement individually. Evidently the ratio K/M yields an important stability factor in variometer performance. It thus appears desirable that a magnet-system should be constructed of material susceptible to as little change as possible in K with time; the effects of chemical action, chipping, or other changes in contour should be minimized. Of equal importance is the maintenance of slow and regular change in M. It seems that here considerable improvement might still be effected. For instance, some new alloys for permanent magnets do not appear yet to have been used in geomagnetic instruments, although use has been made of Alnico. The high coercive force of Alnico as well as its high energy value promises improved stability in M. An alloy apparently not yet tried which might provide results quite superior in stability even to some types of Alnico is one of platinum-cobalt, with a coercive force about ten times that of Alnico and of somewhat smaller remanence [43]. A hard material of this type would wear slowly, thus ensuring more stable values of K.

Magnets having a highly constant value of K/M might also be of use in simple field-instruments for measurements of the Earth's field from oscillation experiments alone, or from deflection experiments alone.

The value K/M of a variometer magnet can be obtained from (14). It is suggested that estimates of the variation of K/M with time can usefully serve in checking the performance of suspended magnet-systems, when k is not too large so that n^2 can be readily obtained.

9. Effect of change in damping on the response of variometer.--The variometers studied experimentally here were found to have values of n^2 of the order of ten. A of Figure 146 shows the responses for a suddenly impressed field of unit strength for various values of damping-factor k.

When k = 0.0165, which is roughly the magnitude found for the variometers tested, the response consists of a damped oscillation, decaying slowly with time, about the value 0.01 CGS unit. As k increases, the response improves, becoming best for a value slightly less than that for the dead-beat condition (k = 3.162).

B of Figure 146 shows the ratio of amplitude of the observed to impressed fields, when the observed field is

of the form c (1 - cos mt), for various values of the frequency m. The computed effect of resonance is most marked for k = 0.0165 for which the amplitude ratio rises to 72.8. As in A of Figure 132, the response is best for k = 2.236.

C of Figure 146 shows the angular lag in phase for the same fields as mentioned in connection with B of this figure, as a function of frequency m. For fields of period greater than about four seconds, the lag in phase is very slight when k = 0.0165, but as much as 30° for k = 2.236. This lag in phase, however, is less than one-half second for periods greater than four seconds and therefore seldom would be significant in practice. A value of k greater than one but less than n would thus result in improved performance of the la Cour variometers. Although a small value of k such as that ordinarily used may yield a trace more highly serrated, a few of these small periodic fluctuations appear magnified in amplitude and the base scale value does not apply. A value of k in excess of unity would hence appear desirable.

In the next section, discussion will relate to data on geomagnetic fluctuations measured with variometers the same as or similar to those just described and will begin with consideration of fluctuations of relatively long duration or period.

10. Survey of world-wide distribution of ranges with time in magnetic elements, horizontal intensity (H), declination (D), and vertical intensity (Z).--In this section there are considered results relating to the world-wide distribution of daily ranges of magnetic intensity.

The daily range in the magnetic elements varies in a marked way with geographical position. In two narrow zones near geomagnetic latitudes roughly 67° north and south, large daily ranges in H, D, and Z occur most frequently and with highest intensity. These are the so-called auroral zones, and the magnetic conditions therein tend to dominate those observed elsewhere, even to some extent those in the equatorial regions. There is also a tendency toward symmetry in geomagnetic disturbance fields relative to the geomagnetic axis and equator, and to the auroral zones. The geographical distribution of magnetic disturbances is thus conveniently studied by selecting stations in various geomagnetic latitudes, neglecting small differences due to longitude except in regions near the auroral zones.

The asymmetries of disturbance in longitude are most marked in auroral regions where the differences between geomagnetic local mean time and geographic local mean time are greater. The major asymmetries arise because the auroral zone is not a circle of geomagnetic latitude but actually an oval. Other very slight asymmetries in longitude appear, due to noncoincidence of the Earth's geomagnetic and geographical axes.

Table 105 lists selected stations of the Second International Polar Year, August, 1932, to August, 1933, providing data for high latitudes as well as for middle and low latitudes. It gives the positions of the selected stations in terms of both geographic and geomagnetic co-ordinates. Geomagnetic co-ordinates of position are measured from the point (latitude ϕ = 78°.5 N, longitude λ = 69°.0 W) as pole (serving also as the pole of reference for geomagnetic time), and is the point where the axis of uniform magnetization intersects the Earth's surface. At any point on the Earth, the angle Ψ is the angular difference in direction between the geographic and geomagnetic meridians, positive when measured from north around by east. Also given in Table 105 is the approximate magnetic declination, D, at each station. The positions of the selected stations are included among others in Figure 147.

Figure 148(A) gives frequencies of daily ranges in H for the 12-month period of the Polar Year, 1932-33. The corresponding distributions for D and Z are given in Figures 148(B) and 148(C).

The largest ranges tend to occur more frequently in high latitudes, especially in the region near the auroral zone, as shown by the stations Tromsö, Petsamo, Fort Rae, and Sodankylä (Fort Rae is usually slightly inside the zone of maximum auroral frequency and Sodankyla a few hundred kilometers outside). Near the center of the auroral zone, as shown by results at Thule, the ranges in H and D are of nearly equal intensity and their frequency distributions are somewhat similar, while the daily ranges in Z are of somewhat lesser intensity.

The frequency distribution at Thule could probably be fairly readily fitted by one of the Poisson type. This type of frequency distribution applies in the case of large numbers of trials for which the probability of the occurrence of a single event is small.

The largest fluctuations of the Earth's field are due to intense electric currents in the atmosphere flowing along the auroral zone, the circuit probably being completed by a current-sheet flowing towards the Sun and across the polar cap. The measured values of gross magnetic fluctuations at Thule thus tend to respond to average conditions near the auroral zone. Fleeting and patchy areas of varying ionization near the auroral zone, due to incoming groups of charged solar corpuscles, may be the cause of many of the rapid small pulsations in current. The main flow of current may hence be diverted due to changed electric conductivity or electromotive forces in the air in ionized regions. It seems likely that the return flow then takes place mainly in the form of broadly distributed current-sheets inside and outside the auroral zone. The magnitudes of the ranges attain a maximum in H and D near the auroral zone. The daily ranges in Z, although large near the auroral zone, are probably greatest on an average just inside and outside the zone. Just outside the auroral zone, the ranges decrease very rapidly with decreasing latitude and then remain relatively small throughout low and middle latitudes.

Figure 149 shows lines of equal auroral frequencies as derived by Vestine for the Northern Hemisphere. It will be noted that the auroral zone expands equatorwards from time to time. Large magnetic disturbances or storms are closely associated with such expansions of the auroral zone.

The preceding results, derived mainly from data of the Polar Year, 1932-33, were obtained in a year near the sunspot minimum and hence for a period less disturbed magnetically than the average of the sunspot-cycle. Frequency distributions of daily ranges in magnetic intensity will now be taken over much longer intervals of time and compared with those obtained for the Polar Year. Figure 150 shows the frequency distribution of daily ranges in H and Z at Sitka for the 22 years from 1905 to 1926. Shown also are the corresponding values for the Polar Year multiplied by 22. It will be noted that the frequency distribution obtained for the 12-month period of 1932-33 corresponds well with that found for the much longer interval of time. Figure 151 shows a similar comparison made in the case of Cheltenham with similar good correspondence in values. However, it would appear that the correspondence is best for small ranges and that a

single year of observation forms too small a statistical sample to permit discussion of very large daily ranges at times of severe magnetic storm.

Figure 152 gives the frequency distribution of ranges in H, D, and Z at Sloutzk (near Leningrad) for the 62-year period 1878 to 1939. At Sloutzk magnetic storms have been selected by Benkova according to a definition that at that station a magnetic disturbance becomes a magnetic storm if the daily range in D is greater than 60γ. Included also in Figure 152 is the frequency distribution of ranges at Bombay during 1882 to 1905 derived by Moos from a catalog of magnetic storms. These data provide information respecting the probability of occurrences of magnetic storms in other regions, since such storms are world-wide in their incidence. Hence their frequencies and probabilities of occurrence can be conveniently examined using data for only one or two suitably selected magnetic stations.

The monthly variations in frequency distributions of daily ranges in horizontal and vertical intensities, as derived for Cheltenham during 1905 to 1930, are illustrated in Figure 153. It will be noted that the variation in disturbance with season is not marked, although larger ranges appear with greater frequency near the equinoxes.

Table 106 gives the probabilities for daily ranges in excess of various assigned magnitudes estimated from the data of Figures 148(A), 148(B), and 148(C) for the year 1932-33. The reciprocals of these values are given in Table 107 and provide estimates of the expectations, in days, of daily ranges in H, D, and Z in excess of various assigned magnitudes.

Table 108 shows the observed cumulative frequencies and the computed expected frequencies per year, and probabilities and expectations, in days, for ranges in magnetic intensity in excess of various magnitudes. Since the ranges in the magnetic elements vary with geomagnetic latitude, the probabilities for ranges in excess of given magnitudes vary with different stations. As is also shown by the data for Figures 150, 151, and 152, the expected frequencies for storms of given range vary from station to station.

The results of Table 108 were included with those derived from Tables 106 and 107 in constructing Figures 154 and 155. From Figure 154 it appears that ranges as great as, or greater than 50γ occur daily, or at least every few days, at all stations from pole to pole. While ranges in excess of 300γ are unlikely to appear in low and middle-latitude regions between the northern and southern auroral zones, such ranges do appear in the latter regions at times of great magnetic storm of which there was no example during the year 1932-33. Near the auroral zone, as shown particularly by the stations Tromsö and Petsamo, there is considerable probability of daily ranges greater than 1200γ in H and Z. The same is true for a considerable region inside the auroral zone.

Figure 155 shows the variation with geomagnetic latitude of the expection, in days, of ranges in H, D, and Z in excess of 50γ, 100γ, 150γ, 200γ, 500γ, and 1000γ. These results are derived from Tables 106 to 108, and as it is assumed that there is symmetry relative to the Earth's geomagnetic axis and equator, the results for the Northern and Southern Hemispheres, based on data for both hemispheres, give, in the case of each component and assigned range, curves reflected in latitude relative to the position of the geomagnetic equator. Since large values of expectations, in days, result from probability calculated on the basis of very small numbers of the total cases, they are in general highly uncertain; for this reason, expectations in excess of 250 days are not shown. However, it will be noted that the expectations derived from the longer series of data for magnetic storms give results which are in very rough general agreement with those found for the year 1932-33.

Using the results of Figure 155 (in which no attempt was made to adjust the data for the variations in the position in the auroral zone with longitude), a rough and tentative estimate has been made, and presented in the form of isochronic lines in Figures 156 to 161, for ranges in excess of 200γ and 1000γ for H, D, and Z. Useful in constructing such figures are the maps of Figures 147, 162, and 163. These data, roughly adjusted to the auroral zones, afford expectations, in days, strictly applicable only to daily ranges. For longer intervals of time they afford, therefore, an estimate of average upper limit of expectation. It may be remarked that, except for large ranges, the statistics for daily ranges afford practically the same result as do those for longer intervals of time.

The daily ranges in H, D, and Z are in general smaller than those for longer periods of time, such as those for several days, week, month, and year. It not infrequently happens, however, that the maximum weekly, monthly, or annual ranges in an element may be those obtained for single days of magnetic storm.

It should be carefully noted that the maximum ranges for shorter intervals of time vary to a much lesser degree than do the mean annual ranges. It is then reasonably certain that the frequency distribution for daily ranges differs from those for longer intervals of time. The nature of these frequency distributions will be discussed in sections 11 to 13.

Figures 164, 165, and 166 for Sitka, Alaska, illustrate for the Polar Year, 1932-33, the variation from day to day in the maximum and minimum values of H, D, and Z, respectively, relative to arbitrary values used as zero. It will be noted that the successive daily ranges, as indicated by the differences between corresponding maximum and minimum values, are evidently correlated with each other. Small values of daily ranges are likely to be followed by small values, and large values by large values. Thus, as in the case of most geophysical data, the time series of the quantities which interest us show positive conservation. Hence the statistical probabilities and expectations derived in the present report relate to events averaged over considerable intervals of time.

11. Survey of weekly, monthly, and yearly ranges in magnetic fluctuations.--The survey of the world-wide distribution of ranges with time in geomagnetic elements, continues with discussion of weekly, monthly, and yearly ranges. Statistics respecting the frequency of various magnitudes of range in the magnetic elements for intervals longer than a few days are necessarily based on somewhat scanty data. Considerable difficulty consequently has been experienced in preparing the present survey because the number of years of operation of most magnetic observatories is too short. A statistical treatment of ranges in the magnetic elements is also greatly complicated by the lack of random character of the data. The data are classed statistically as conservative in character, meaning that large ranges tend to be followed in succession by additional large ranges and small ranges by successive small ranges. These two factors have contributed greatly to the difficulty of the preparation of the

isochronic charts presented later and complicate their interpretation in practical applications. It has been necessary to draw some of these isochronics in accordance with general considerations and personal judgment, especially in the region inside the auroral zone where no magnetic observatory has ever operated over a considerable length of time.

12. Tables of probabilities and expectations of ranges in magnetic elements.--The published data on maxima and minima in the geomagnetic elements at the stations listed in Table 105 were used to obtain the weekly, monthly, two-, three-, four-, six-, and twelve-monthly ranges in H, D, and Z. The data were considered in two sets. The first set comprised the data for the Polar Year, 1932-33, permitting fairly satisfactory statistics for ranges during intervals as long as a week. The remaining set consisted mainly of data for the stations Tromsö ($\Phi = 67°$), Sitka ($\Phi = 60°$), Cheltenham ($\Phi = 50°$), and Honolulu ($\Phi = 21°$); the results for these stations were supplemented by those for a 62-year interval for Sloutzk ($\Phi = 56°$) and for a 34-year interval for Bombay ($\Phi = 10°$). There are, of course, additional data available for other stations for many years but unfortunately it would be necessary to have access to the actual magnetograms, since values of the daily maxima and minima in magnetic elements have not been published for most stations except in recent years. Wherever possible, use has been made, however, of data for recent years when they appeared likely to be helpful.

Table 109 lists the probabilities of weekly ranges in excess of various assigned magnitudes in gammas. These data supplement those of Table 106 in which corresponding probabilities are presented for daily ranges in the magnetic elements.

Table 110 gives the average probabilities of ranges over various intervals as long as a year for the four stations Tromsö, Sitka, Cheltenham, and Honolulu. It is noted that the probabilities of large ranges are greatest near the auroral zone. It further appears that the probabilities of ranges in excess of a given magnitude tend to diminish slightly as the interval of time for which the range is derived increases. This curious finding is a result of the tendency for large ranges during short intervals of time being followed by other similar large ranges; in other words, it is due to the fact that the ranges show a considerable degree of serial correlation.

Tables 111 and 112 give the average expectations for various intervals of time for ranges in excess of various magnitudes in H, D, and Z. These expectations are calculated as the reciprocals of the probabilities in Tables 109 and 110. The features previously noted in the tables of probabilities again appear. The calculated interval of time elapsing before a range is exceeded or attained during a prescribed time interval becomes longer with longer time interval. In the case of random data, the longer the interval of time elapsing, the greater would be the expected frequencies per interval for large ranges. For instance, from Tables 111 and 112, a weekly range in H of 1000γ or more is expected, on an average, in one out of every 18 weeks, whereas the three-monthly range of this magnitude or greater is expected in one out of every two three-month intervals. The point is that one can sometimes find in a three-month interval more than one range in H greater than 1000γ, although only a single (total) three-monthly range is taken.

The probabilities of daily and weekly ranges in H, D, and Z in excess of various magnitudes are shown in Figure 167. The probabilities for ranges during longer intervals of time are illustrated in Figure 168(A), (B), (C), and (D).

13. Isochronic charts showing expectations of ranges in H, D, and Z.--In order to make the foregoing data more readily applicable for practical purposes, an attempt has been made to estimate the positions of isochronic lines drawn on world charts to show the expected times elapsing before ranges of various magnitudes are exceeded or attained. Figure 169 shows the isochronic lines giving the expected number of three-month periods elapsing before the three-monthly range in H exceeds 500γ (five milligauss). Throughout a belt nearly 2000 miles wide on either side of the auroral zone, it is expected on an average that there will be experienced during every three-month period a range in H greater than or equal to 500γ. From the center of Greenland and northwards to the geomagnetic north pole, only one out of three three-month intervals is expected on an average to experience a range in H exceeding 500γ. The isochronic line for four three-month periods passes through northern England; this means that in one out of four three-month intervals the prescribed range will be exceeded. It is found that in low latitudes only one out of every 20 or 30 three-month intervals is expected to have a range in H greater than 500γ. Figures 170 and 171 present the corresponding isochronic lines for D and Z.

Figures 172, 173, and 174 give the isochronic lines showing the expected number of weeks elapsing before the weekly ranges in H, D, and Z exceed 1000γ (ten milligauss). Figures 175 to 186, inclusive, give the isochronic lines for various intervals of time in excess of a week for ranges in H, D, and Z in excess of 1000γ. These charts are based on less satisfactory data than are those for ranges in excess of 500γ because the frequency of occurrence of ranges of 1000γ is much less than that for ranges of 500γ in most latitudes. In fact, for D and Z, no example has ever been found of the occurrence of a range as great as 1000γ in low and equatorial latitudes. In immediately adjacent regions, magnetic data for about 25 years reveal only one case of ranges in D and Z of this magnitude so that reliable statistics respecting frequencies are not available. In view of the limitations of the data, it is important to know that the isochronic charts for ranges in excess of 1000γ are in some respects rather tentative, but should on the whole have a fair degree of reliability.

Figures 187 and 188 give the isochronic lines in terms of three-month periods for three-monthly ranges in H and D in excess of 1500γ, as estimated from somewhat scanty data; in the case of Z, a range as great as 1500γ was not found in any latitude.

Figures 189, 190, and 191 give the regions (indicated by hatched lines) in which the probability is at least one-tenth that the total range during any average three-month period will exceed 1000γ. There are no regions in which the probability is 0.1 that the total range in H, D, or Z during an average three-month period will exceed 1500γ.

14. Survey of short-period magnetic fluctuations.--The present study, dealing with geomagnetic fluctuations of durations from ten seconds to ten hours, continues the discussion of fluctuations persisting for various periods of time.

Early results on the study of short-period magnetic fluctuations include Balfour Stewart's observation [44] that magnetic records show numerous trains of more or less regular waves or pulsations of period about 30 seconds.

Kohlrausch [45] noted a fluctuation of period 12 seconds by eye readings of a magnetometer. Arendt [46] studied fluctuations of a period of several minutes in connection with studies of thunderstorms. Eschenhagen [47] noted a maximum near noon in the frequency of fluctuations of 30 seconds' duration. Birkeland [48] found frequent groups of waves of periods of about 10 and 30 seconds. Using records for three observatories, van Bemmelen [49] found that trains of waves or magnetic pulses appeared more frequently near midnight at Batavia and Zi-ka-wei, and in the daytime at Kew. Terada [50] made an extensive study of magnetic fluctuations observed during a four-year period at the station Misaki. He hoped to correlate the fluctuations with earthquakes. The sensitivity of the variometers used was about 0.2 gamma per mm in the north, east, and vertical components. The magnets were from two to four cm long, approximately, and about two mm thick, so that the response to fluctuations of periods less than 10 to 20 seconds would not be good. He noted that pulsations varied in period from about 20 seconds to nearly one hour. During the daytime, he found that fluctuations of 30 to 60 seconds predominated, whereas those of 90 to 150 seconds appeared more frequently at night. He also noted a reduction and phase-retardation of about one-quarter period in Z as compared with H, and that the disturbing field usually yields a vector rotating with time. He suggested that the fluctuations probably were due to the more or less vertical oscillation of limited portions of layers of the upper atmosphere, where incoming aggregations of particles from the Sun affect the electric conductivity.

In the present study, these earlier findings, which were based usually on single stations, are extended, using more homogeneous data of the Polar Year, 1932-33. During the average day, a marked maximum in frequency is found for a duration of about 50 seconds, although the largest amplitudes appear for fluctuations enduring from one to several hours in all latitudes. The latitude distribution of the fluctuations has been roughly estimated. It is found that there is a marked maximum in the amplitude of these small fluctuations near and just inside the auroral zones. In these regions the fluctuations are of larger magnitude in the horizontal component and least in Z. In low and middle latitudes the number of fluctuations of appreciable intensity is sharply reduced, and they seldom appear in Z. At times of magnetic storm (defined as days for which magnetic character-figures K exceed five--a few days per year), marked fluctuations, both local and world-wide, may appear in all components in lower latitudes.

Rates of change up to about ten gammas per second in the horizontal component have been observed at such rare intervals as once in several years during severe magnetic storms in almost all latitudes. In equatorial regions rates of change in Z as great as ten gammas per second have never been observed and probably seldom if ever occur. In auroral regions, there appear some thousands of examples per year of rates of change of the order of one gamma per second, enduring usually for intervals of less than one or two minutes. In low and middle latitudes, the number is very sharply reduced, especially in Z; only a few examples per year of rates as great as one gamma per second appear even in the comparatively high geomagnetic latitude of Copenhagen. The short-period fluctuations near the equinoxes appear to be about twice as numerous as near the solstices. Their frequency appears to be more closely correlated with sunspot number than with certain measures now in use for magnetic activity.

At times of storm, the numbers of small fluctuations do not show a marked variation with time of day. On ordinary days, fluctuations of duration less than one minute are, on the average, most numerous near local noon; those of longer duration tend to be more numerous in the early morning and late afternoon or evening.

Pulsations or fluctuations of durations greater than ten seconds frequently appear simultaneously in both the Northern and Southern Hemispheres. Ordinarily they appear in series or groups, sometimes in superposed form. In their usual complex form they are difficult to trace from station to station. In the case of seven isolated examples of about ten-minute duration, appearing on days in other respects magnetically quiet, their incidence appeared world-wide, though of very small amplitude in low latitudes. The disturbance caused by such fluctuation is most marked in the region near and inside the auroral zone, where regularities and patterns of field can be fairly readily traced from station to station.

Studies of vector diagrams of fluctuations in polar regions strongly suggest that the relatively small amplitude of fluctuations in Z in low and middle latitudes is due to earth currents opposing the external field of the high-latitude electric currents causing the fluctuations, and almost nullifying the external field in Z. These earth currents augment the field at the Earth's surface in the case of H, so that small fluctuations in this component are more readily recorded in low latitudes than are those of greatly reduced amplitude in Z; the number of fluctuations in H and Z is of course the same.

The current sytems of small fluctuations sometimes resemble those for the polar part of the electric current system of magnetic storms, though greatly diminished in intensity. They no doubt contribute a principal part of the fluctuating earth currents by induction, especially in surface layers of the highly conducting oceanic areas.

Although the oceans are somewhat ill-connected, they comprise most of the surface area of the Earth. It is likely that the induced electric currents due to short-period magnetic fluctuations could readily be calculated, with but slight modification of the existing theory used in estimating the Earth's internal electric conductivity from longer-period magnetic variations.

Fluctuations in the region between those of "atmospherics" which show electromagnetic waves with periods up to 10^{-4} second and those of pulsations of the order of one second have never been investigated. The development of new methods of measurement by H. Aschenbrenner and G. Goubau [51] may yield a useful experimental approach. F. Schindelhauer [52] has discussed various features of atmospherics.

Studies by van Bemmelen, Eschenhagen, Rolf, Sucksdorff, Harang, Lubiger, la Cour, and others reveal that in addition to the fluctuations just discussed, there appear others of distinctly local character. In auroral regions very rapid fluctuations of duration less than one or two seconds are noted [53]. Very regular sinusoidal pulsations of local character having periods of some seconds to several minutes [54, 55] also occur in auroral regions, and sometimes in low and middle latitudes.

Large fluctuations known as bays, most marked in polar regions, with durations about one to five hours, appear a few hundred times per year. They are world-wide in incidence. In low and middle latitudes their amplitudes are in general small, sometimes smaller than fluctuations

of shorter duration. They appear to result from a marked intensification of the current system responsible for the disturbance daily variation, and hence show morning and evening maxima in frequency at nearly all stations [3, 56].

New data on magnetic fluctuations of short duration were obtained for the present volume from data of the Polar Year, 1932-33. Nearly all data were measured from microfilm reproductions of magnetograms. These were studied with the aid of microfilm projectors yielding enlargements on a screen at three times natural size. Table 104 gave the stations used and their particulars. Their locations were given in Figure 147.

A fluctuation of the geomagnetic field was regarded as a departure of the field from a normal undisturbed value, followed by a subsequent recovery. In general, no distinctions were made respecting the sign of a fluctuation, as represented by an increase or decrease in field with time. It frequently happened that several fluctuations appeared together in superposed form. In this event attempts were made to separate the component fluctuations, their durations and amplitudes being entered separately in records of the various classes of fluctuations. The duration of a fluctuation was taken as the time from the beginning of the departure of field from normal up to the time of recovery. The amplitude is the maximum departure from the normal value.

In the accompanying tables or graphs, showing rates of change and durations of fluctuations at various stations, the rate of change recorded is the maximum appearing between the time of beginning and maximum of the fluctuations and also between the maximum departure and the end of fluctuation, irrespective of the sign of the fluctuation. In all cases an attempt was made to measure a maximum rate of change consistent with the general smoothed trend of the fluctuation. Some difficulties were experienced in a number of special cases due to the incidence of small superposed departures with greater rates of change, but in general these were readily separated from the fluctuation under consideration. The duration in the case of fluctuations studied with respect to maximum rate of change was defined slightly differently from that used in discussing the amplitude of fluctuations. For rates of change of fluctuations, the semiduration was used as measured by the interval between beginning of the fluctuation and its maximum departure in amplitude, or from the time of maximum amplitude to the time of ending of the fluctuation.

Figure 192 shows the frequency of fluctuations of various amplitudes at Petsamo for the period August 1, 1932, to October 31, 1932. The observed frequencies of fluctuations of amplitudes 10γ, 20γ, ... 70γ are totaled for durations in seconds, 0-20, 21-40, ..., in H, D, and Z, and plotted for the center of each interval. During the 92-day period, marked fluctuations of amplitude 0γ to 10γ appear most frequently. A maximum in frequency is shown by durations of about 40 to 50 seconds in H, D, and Z. Fluctuations of larger amplitude were measured most frequently in the case of H and least frequently in the case of Z. In the case of very small fluctuations of 0γ to 10γ, the number found is to some extent affected by the sensitivity of the variometer. In the case of D, this sensitivity was 4 γ/mm as compared with 13 γ/mm for H and 20 γ/mm for Z. If greater sensitivities had been available for H and Z, it is likely that distributions more nearly similar to those for D would have been obtained. It will be noted that the three-month period provided insufficient data for defining clearly the frequency distribution for amplitudes of 50γ to 80γ. These results agree well with those of Terada for Misaki although his frequency distribution shows a smaller relative number of fluctuations for intervals 0 to 30 seconds than does Figure 192. This is possibly due in part to the longer periods of oscillation of the magnets used by Terada.

Figure 193 gives the frequency distributions of fluctuations with various rates of change and durations at Petsamo for the period September 1, 1932, to August 31, 1933. A pronounced maximum in frequency occurs in all elements for semidurations of 20 to 30 seconds, and thus in good agreement with results of Figure 192. These measurements extend over a longer period than was used in deriving Figure 192 and show greatest frequencies for H and least for Z.

The results for Petsamo, near the auroral zone, may be compared with those for Copenhagen, a station in middle latitudes, shown in Figure 194, for the same interval of time (note the change in frequency scale and also in the scale for rate of change). In the case of Copenhagen, a very extensive compilation was made in order that greater certainty might be ascribed to measures of semidurations less than 20 seconds. It also appeared desirable to obtain the relative frequency of the rate of one gamma per second, on a significant basis, for comparison with Petsamo. A marked decrease with latitude is shown in the magnitude of the rate of change (Tables 113 and 114) by the data from the two stations.

At both Petsamo and Copenhagen, the largest number of fluctuations in H, D, and Z appear with semidurations of about 20 seconds. The following table gives a comparison of the total number of fluctuations per year for various rates of change, irrespective of duration, noted at Petsamo and Copenhagen. No example of a rate of change as great as ten gammas per second was noted at either station. For slower rates of change, the effect of change of latitude is marked; for instance, for one gamma per second, there were in H 3,786 cases at Petsamo as compared with only 58 at Copenhagen. An additional noteworthy feature is the marked decrease in the rate of change of Z from Petsamo to Copenhagen.

Fluctuations for various rates of change for H, D, and Z
Petsamo and Copenhagen, September 1, 1932,
to August 31, 1933

Rate of change γ/sec	Observation					
	Petsamo			Copenhagen		
	D	H	Z	D	H	Z
0.1	....	....	....	47,596	19,233	242
0.2	....	....	....	21,884	16,188	58
0.4	....	....	....	2,875	2,490	7
0.6	....	....	....	319	282	0
0.8	....	....	....	162	89	0
1	3,786	3,769	1,442	58	13	0
2	1,180	471	595	3	3	0
4	221	58	143	0	1	0
6	39	14	28	1	0	0
8	19	15	10	1	0	0
10	0	0	0	0	0	0

A very rough survey of the fluctuations at stations in other latitudes suggests that the results for Copenhagen will not differ notably in magnitude from those of other

middle- and low-latitude stations. The results for Petsamo, on the other hand, are probably representative, in rough order of magnitude, of other stations within a belt of latitude about 10° wide, centered near, or slightly inside, the average auroral zone.

The data of 1932-33 do not include a case of a great magnetic storm. The storms of the Polar Year were of only moderate intensity, such as those of October 14 and December 15, 1932, and May 1 and August 4, 1933. At times of magnetic storm, the auroral zones expand equatorwards to different distances at different times, and to a degree depending somewhat on the intensity of storm. Rates of change at times of great magnetic storm as large as about ten gammas per second in H and Z in middle latitudes and in H near the equator have been noted.

Figures 195 and 196 show, respectively, the monthly variations in frequency of fluctuations of various rates of change and durations at Petsamo and Copenhagen. At both stations there is considerable evidence of a seasonal variation in frequency. The observed frequencies are greatest near the equinoxes and least at the solstices.

The correspondence between the number of fluctuations per day and sunspot number is not close, but it is much greater for large sunspot numbers and large rates of change than for small sunspot numbers and small rates of change. There is an averaged and not a detailed correspondence between the frequency of small fluctuations and sunspot number.

15. Latitude distribution of fluctuations.--Figure 197 shows evidence of a marked variation with latitude in the frequencies of small fluctuations with durations 10 to 500 seconds in H, D, and Z and amplitudes greater than five gammas. It appears that in all latitudes fluctuations of this type occur most frequently for durations of about 50 seconds. Very few fluctuations in Z appear with amplitudes greater than five gammas, even though two days of storm, March 24 and May 1, 1933, were included.

Figure 198 shows the corresponding magnitudes per day of totaled magnetic impulses ($1/2\,\Sigma\Delta f\,\Delta t$, where Δf is the amplitude of the fluctuation and Δt the duration in seconds) for the same data as were used in deriving Figure 197 for days having various magnetic character-figures C. In general, marked increase in totaled impulses accompanies the increase in C, although it is noted that the totaled impulses on March 24 (C = 1.5) is considerably greater than on May 1 (C = 1.9). These results are shown in a somewhat different way in Figure 199 where the corresponding total numbers of fluctuations per day are given for various latitudes.

The variation with local geomagnetic time in the numbers of fluctuations is shown in Figure 200. At times of storm, there appears little variation in the bihourly frequencies. On less disturbed days in polar regions, the fluctuations are most numerous in the morning and evening near times when the maximum departures in the average disturbance daily variation appear. At Huancayo special conditions prevail and fluctuations are more numerous near noon. This tendency is possibly in evidence at other low- and middle-latitude stations also.

Figure 201 shows that positive and negative departures in each magnetic component appear with about equal frequency at all hours of day. The differences shown are unlikely to be real but rather indicate a psychological preference for positive fluctuations on the part of the measurer. Figure 202 shows roughly the variation with latitude of totaled impulses averaged according to local geomagnetic time.

16. Frequency distribution of fluctuations of duration five minutes to ten hours.--The foregoing sections were concerned chiefly with fluctuations of durations from ten seconds to five minutes. It was noted that very large numbers of fluctuations appeared with durations of about 50 seconds, if duration of the fluctuation be defined as the time elapsing from its beginning to its ending. In view of the possibility of maxima in frequency for somewhat longer durations, a cursory examination of the frequency of fluctuations of greater than five-minute duration was undertaken. For this purpose use was made of records for one month only, December, 1932, for the stations Petsamo and Copenhagen.

Tables 115 and 116 show the frequencies of fluctuations found in H at Petsamo and Copenhagen. It will be noted that the frequencies diminish rapidly with increasing amplitude at both stations. These results are given separately for positive fluctuations (defined as those yielding a departure in the direction of the increasing horizontal intensity) and negative fluctuations (defined as those yielding a departure in the direction of decreasing horizontal intensity). Although there may be a possibility of some secondary maximum in frequency for durations between five minutes and ten hours, it is seen that this maximum must at any rate be small. It may also be noted that negative fluctuations appear more frequently than positive fluctuations at Petsamo, whereas at Copenhagen the situation is reversed.

17. Geographical distribution of large short-period magnetic fluctuations.--A considered estimate is now presented, though based on scanty data, of the probability of occurrence of large amplitudes in short-period fluctuations, for different geographical positions. The class of fluctuations dealt with includes all those with durations of 150 seconds or less as measured from beginning to ending of the fluctuation, whether a part of a larger and longer fluctuation or otherwise. In all cases, it is understood that the fluctuation has an obvious initial departure and a complete subsequent recovery.

The process used in arriving at a distribution of amplitudes is rather unsatisfactory. In the first place, the frequency of fluctuations per three-month interval cannot be statistically assessed with much pretense at accuracy without, say, 20 to 30 years of data. Such extensive data on short-period fluctuations have never been obtained. In high latitudes, the longest series of short-period data measured has been obtained for about one year, giving a statistical sample for four three-month intervals. In low and middle latitudes, the time-scales used ordinarily have not had sufficient resolution for any except the longer periods of fluctuation of one to two minutes. Moreover, in earlier years larger magnets were used in variometers so that the fidelity of response to fluctuations of duration less than one-half minute was probably frequently at fault. However, to obtain a rough approximation to the variation in amplitude with latitude, the 10, 20, and 30 largest fluctuations observed on six days in March to July, 1933, were tabulated for several stations. In all components, the largest amplitudes appear near the auroral zone in the three sets of fluctuations as shown in the table at the top of the next page.

It is now assumed that the latitude distribution above indicated applies also to the larger fluctuations--those so large that they appear on an average only in one three-month interval out of ten. (In a certain sense we may suppose this rate of appearance to be equivalent to the average incidence of one fluctuation per interval of 30

months or somewhat longer, say once every three years.) Hence, a fluctuation of the large amplitude sought is only infrequently found on the records of magnetic observatories. A rapid inspection of magnetograms for one year

Observatory	Φ[a]	Maximum amplitudes for 10, 20, and 30 fluctuations in								
		H			D			Z		
		10	20	30	10	20	30	10	20	30
	°	γ	γ	γ	γ	γ	γ	γ	γ	γ
Thule	88.0	20	16	14	17	14	12	14	12	11
Godhavn	79.8	41	34	30	25	22	20	32	26	24
Reykjavik	70.2	74	62	54	52	44	38	36	28	25
Petsamo	64.9	56	51	48	44	36	31	77	60	50
Rude Skov	55.8	19	16	14	14	12	10	6[b]	0	0
Ebro	43.9	6	0	0	6	0	0	5[b]	0	0
Huancayo	- 0.6	11	10	9	7[b]	0	0	0	0	0
Watheroo	-41.8	6	0	0	9	8	8	5[b]	0	0

[a]Geomagnetic latitude. [b]Less than ten cases measured.

showed that there were two or three fluctuations of duration about two to three minutes with an amplitude in horizontal intensity (H) between 250γ and 300γ at Petsamo. Thus, the probability of such amplitudes in H near the auroral zone appears greater than 0.1 per three-month interval. If we suppose then that the amplitude is about 600γ at the auroral zone, for an average probability of 0.1 per three-month interval, and we extrapolate from this and from corresponding amplitudes of fluctuations of probability 1.0, 0.5, and 0.25 per three-month interval, we arrive at a rough approximation such as that of Figure 203. In a similar manner we obtain Figures 204 and 205.

As a rough and general check, the isomagnetic lines show a latitude distribution in amplitude somewhat similar to the known latitude distribution of the disturbance daily variation. Among the cases observed over a long period of time, there will be included a few of the sudden commencements of occasional large magnetic storms.

Near the equator there are two regions where the solar daily variation on quiet days is anomalously large and sometimes accompanied by sharp fluctuations near noon. Accordingly, the records for one year at Huancayo were used to arrive at a possible amplitude for the fluctuations.

It may be remarked that our study of short-period fluctuations has revealed that fluctuations of notably large amplitude usually have the longer durations. On the other hand, the duration of fluctuations in H, D, and Z which appear most frequently in all latitudes is about 50 seconds.

18. The nature of magnetic fluctuations and their possible current systems.--In view of the importance of an understanding of the variation in frequency of fluctuation with geomagnetic latitude, a short study was made of the geographical distribution of the disturbance vectors of small fluctuations. Figures 206 to 209 show to scale the maximum disturbances of several separate fluctuations of about ten-minute duration. The measurements are rough due to incomplete data respecting exact time. The horizontal disturbance at the time of maximum departure of the fluctuation is shown by an arrow drawn from the station as origin and of a length proportional to the magnitude of the horizontal disturbance. The disturbance in vertical intensity (regarded as positive when in direction of the Earth's center) is indicated by a line drawn from the station as origin and positive when in the direction of the geomagnetic north pole.

It appears from the figures that the larger part of disturbance is confined to the region near and within the auroral zone (shown by a dotted curve). The persistence of very small fluctuations throughout this extensive area is truly remarkable. In fact, each fluctuation appears to occur according to a systematic pattern, though distorted in the region just inside the auroral zone where its incidence and magnitude are less susceptible of accurate measurement because of additional small local irregularities in field.

Outside the auroral zone, the fluctuations, though small in amplitude, are usually clearly evident. There is usually very small disturbance in vertical intensity.

It will be noted that the fluctuations selected have field-characteristics somewhat similar in form. However, it cannot be concluded that these are typical in field-distribution of all other small fluctuations. In particular, it has been suggested by Chapman's students that in the case of highly regular sinusoidal pulsations, the disturbance felt at the Earth's surface more nearly resembles that due to a small oscillating magnet or dipole in the upper atmosphere or that of a wave-line dipole parallel to the Earth's surface. The field of fluctuations is further complicated by uncertainties as to the amount of the contribution due to induced earth currents produced by variations in the external inducing field.

It is impossible in principle to infer uniquely from magnetic measurements at the Earth's surface alone the location and form of the electric current system responsible. The problem has not one but an infinity of solutions. A possible current system seems to resemble that of the diurnally varying part of the electric current system of geomagnetic disturbances as shown in the case of magnetic storms, the resemblance in low and middle latitudes being least clearly defined. It appears that the current system tends to remain more or less fixed relative to the position of the Sun. This finding is in harmony with a dependence of fluctuations in number and intensity upon local time.

The observed daily variations in frequency are in accord with the supposition that the fluctuations are larger at times of day when the current intensity is greater overhead in the current systems responsible for the large systematic variations of geomagnetism. The fluctuations may then be regarded as due to statistical fluctuations in the distribution and magnitude of the electrical conductivity in ionized regions of the atmosphere. Irregularities of patchy and transient form in the ionosphere are in fact known to occur from radio echoes, as shown by sporadic E-region reflections and others. It is more or less established that the currents responsible for the solar daily variation flow near the 100-km level of the atmosphere; since transient changes appear in ionization at this level, especially in higher latitudes, they must be accompanied by current-fluctuations. This conclusion is strengthened somewhat by the fact that the abnormally large solar daily variation at Huancayo is accompanied by abnormally large short-period fluctuations near noon.

In the same way, the morning and evening maxima in magnitude of fluctuations of slightly longer period appear at times when the disturbance daily variation, most marked near the auroral zone, is greatest in amplitude [37]. It may be possible to account for a large number of the smaller irregular fluctuations on this basis.

The trains of fluctuations appearing successively at times seem, on the other hand, to imply regular fluctuating current on such occasions. As Terada suggests, these may be due to regional vertical oscillations of the atmosphere; evidence of such oscillations may in fact be indicated by the oscillations in electron-density detected by Harang above Tromsö. These had the same period as an accompanying sinusoidal magnetic fluctuation [55].

The fluctuations of about ten-minute duration shown in Figures 206 to 209 are of different type than those just mentioned in that they are world-wide rather than local in character. The electromotive forces driving the current originate possibly in auroral regions, and there is a return circuit of current symmetrical about the equator in low and middle latitudes. The simultaneous incidence of the small fluctuations in both the Northern and Southern Hemispheres is remarkable.

The observed rapid decay of field suggests that the electric currents responsible flow near or below the E-region of the ionosphere where the collisional frequency of ions and electrons is greater, so that rapid decay is possible.

A suggestion was made several years ago by Johnson that it was possible that emanations emitted by the Sun would show certain qualities characteristic of thermionic emitters in general. According to the theory of magnetic disturbances of Chapman and Ferraro, neutral streams or beams of charged particles proceed from equatorial regions of the Sun. These streams, propelled from the rotating Sun, overtake the Earth as it moves along its orbit. If these streams comprise individual clouds of particles suitably distributed statistically, the preferred frequency of fluctuations for durations of the order of 50 seconds might be explained on the basis of the size of cloud, its velocity and cross-section area. Because of energy considerations, the direct field of moving charges would be less likely to be responsible than would the indirect effect of changed conductivity of impinging particles in the atmosphere. In other words, a study of the spectrum of geomagnetic fluctuations may throw light on the statistical distribution of the numbers of component particles of the stream.

Studies of magnetic fluctuations in conjunction with high-speed ionospheric recordings are of considerable interest. Those conducted by Japanese scientists in 1942 showed numerous rapid changes in electron-density of the F2-region during disturbances. These findings were independently verified by Wells, Watts, and George [57].

19. Dependency of frequency and magnitude of small fluctuations of magnetic activity.--Using the data of Figure 197 for Copenhagen, an examination was made of the dependence of frequency of fluctuations per day upon the magnetic character-figure C of the day. The correlation, carried out for the H-component only, was quite small and nearly negligible. The correlation-coefficient increased to +0.3 in the case of fluctuations with time-rate of change greater than 0.6γ per second. It was concluded that the frequency of small fluctuations does not depend much on magnetic activity in the latitude of Copenhagen but that larger fluctuations appear with greater frequency when the magnetic activity is greater.

20. Short-period magnetic fluctuations on land compared with those over or within ocean areas.--Short-period geomagnetic fluctuations induce electric currents in the oceans which give a field additive to that of the inducing field. A colleague, Dr. Norman Davids, calculated the magnitude of the induction effects for the case of an electrically conducting ocean confined between two parallel planes. The ocean conductivity was taken as 10^{-11} CGS, ten thousand times that of surface rocks.

The results indicate that the short-period geomagnetic fluctuations measured over the ocean will have an amplitude in horizontal intensity not in excess of twice that noted on land, and in the vertical component, an amplitude less that that on land. The value of the horizontal component falls off rapidly with depth of ocean, when the linear cross-section of the inducing field is 100 times or more that of the depth of ocean, and the period of this field is of the order one minute. Under these conditions, both the horizontal and vertical components are almost zero at a depth of 100 meters.

The slower the period of the inducing field, the deeper do the induced currents penetrate. For short-period fluctuations of some minutes' duration, the induced currents flow mainly near the surface of the ocean. With increasing depth, the shielding effect on the vertical component increases; in the case of horizontal intensity, there is no shielding but rather augmentation of field. The maximum difference between values observed on land and at the ocean's bottom is 100 per cent.

A brief mathematical analysis showed that lightning occurring vertically above the ocean's surface can yield fields of several gauss in horizontal intensity enduring about 0.001 second, in a neighborhood within the ocean some tens of meters away from the point of discharge. Within the water, the field falls off rapidly with increasing horizontal distance and depth.

Magnetograms for the Huancayo Magnetic Observatory, where the incidence of thunderstorms is high, do not reveal deflections in excess of 30 gammas per three-month interval due to lightning (see Figure 210); it is to be noted that the period of free oscillation of the magnet-system of the variometer is of the order of a few seconds. Because the area of influence is small and the discharges infrequent, the effects of lightning discharges are rarely recorded at observatories.

21. Measurements of fluctuations of very short period with instruments of improved response and increased time resolution.--As mentioned previously, few data are available respecting geomagnetic fluctuations of frequencies from 10^4 to about three cycles per second. It has already been noted that la Cour magnetographs use magnet-systems which do not respond well to fluctuations of a few seconds' duration and less. However, the indications from the latter have been that geomagnetic fluctuations of higher frequency exist, but little reliable information as to their true magnitude has been obtained.

Accordingly, the Naval Ordnance Laboratory arranged to provide photoelectric recording fluxmeters and search coils, with good response to fluctuations from about one to ten cycles per second. These are described in as yet unpublished reports of W. G. Marburger, S. Gilford, and E. A. Campbell of that laboratory. The response at lower frequencies was intentionally repressed, so that the record would show mainly those fluctuations of higher frequency. However, as shown in the preceding analysis, most short-period fluctuations of large amplitude endure for about 50 seconds, and these were recorded with fair response, but those of periods of some minutes were rather successfully repressed, except on rare occasions when they were large in amplitude and hence accompanied by large rates of change of field. The search coils used were so designed that scale values of a few gammas per millimeter were

achieved on the pen-and-ink record, with time resolution of about 0.2 seconds.

Installations of equipment were made at College, Alaska, and Cheltenham, Maryland.

22. Fluxmeter apparatus.--The fluxmeters used both at College and Cheltenham are described in General Electric Instructions GEI-14903 [58].

The installation at Cheltenham, Maryland, has also been described by others [59], as well as the adjustment and calibration of the instruments [60].

The fluxmeter installations were designed to measure short-period magnetic changes in horizontal intensity (H) and vertical intensity (Z) at a sensitivity of about 3γ. During August, 1942, the instruments were operated continuously at a chart speed of six inches per minute--permitting time resolution to better than 0.2 second.

The response characteristics of the fluxmeters used in obtaining the data here discussed will not be considered in detail. For convenience in recording, it was necessary to maintain an appreciable restoring torque in these instruments. Their response approximated that of a true fluxmeter for short-period fluctuations. The results consequently are unsuitable for the study of geomagnetic fluctuations having durations of some minutes.

Figures 211 and 212 show the calculated responses of fluxmeters of the type here considered, for two different values of return-time-constants, namely, 80 seconds and 51 seconds, as used at College, Alaska, during most of August, 1942. It is supposed that the impressed field is of the form $c(1 - \cos mt)$, where c is a constant, m the frequency, and t the time in seconds; the calculations were made in the usual way, assuming that the response to a suddenly impressed unit magnetic field is initially perfect and that there then follows an exponential decay of the deflection in accordance with the return-time-constant. The return-time-constant is the time in seconds required to give an ordinate of trace equal to $1/e$ (where $e = 2.718$) of its initial deflection.

It appears that the results are in good agreement with expectation. The response for the initial half-period of the periodic impressed field is good for half-periods (durations) of one to about ten seconds. For longer durations, the response deteriorates more rapidly as the period of the impressed field lengthens, when the return-time-constant is small.

The calculations from theory agree well with those obtained experimentally. The response of the search-coil for horizontal intensity measurements with the fluxmeter [61] shows that the quality of response is good for simple continuous fluctuations of field of durations one-half second to five seconds. It also appears that under certain conditions, for instance when isolated rather than successive waves of geomagnetic fluctuations occur, the response may remain fair for fluctuations of duration of about a minute. This is shown by Figure 213, supplied by the Naval Ordnance Laboratory; the fidelity of response in amplitude apart from phase is indicated for various single-cycle fields, as measured at the Naval Ordnance Laboratory. A permalloy core in a coil was used for this experiment, however, so that the results indicated are in some respects approximate. For the particular fluxmeter tested, the response is rather good for a single-cycle field of two to ten seconds' duration for amplitudes as great as one milligauss (100γ). For a single-cycle field of about 100 seconds' duration, the recorded error in amplitude is about 40 per cent. Moreover, since a restoring torque is used yielding return-time-constants of the order of 30 to 50 seconds, when several fluctuations of duration of about a minute or so appear in quick succession the record is very difficult to interpret without special detailed mathematical analyses. Without data of the type shown in Figure 213 for the actual fluxmeters in use at Cheltenham or College, it was of course practically useless to make any attempt at an elaborate analysis which would require data on the response to a suddenly impressed unit field. Some data for fluctuations of duration longer than ten seconds were presented earlier for stations in different latitudes, obtained with instruments showing relatively high fidelity of response for durations greater than ten seconds.

23. Fluxmeter installation at Cheltenham, Maryland.--A of Figure 215 shows a view of the coil-installations at Cheltenham and of their underground locations as indicated by the disturbed soil in the foreground. The small building on the right in the foreground houses the fluxmeters. B of Figure 215 shows the H- and Z-fluxmeters as installed at Cheltenham by Curtiss, Marburger, and others of the Naval Ordnance Laboratory. Each unit consists essentially of a large search-coil (about 18 feet in diameter with 1010 turns in five sections) of low resistance, connected directly to the fluxmeter element of a General Electric photoelectric recording fluxmeter. The coil for the H-fluxmeter was placed with its axis approximately along the magnetic meridian. For the Z-fluxmeter the search-coil was placed with its axis vertical.

Each coil consisted of five turns of 101-pair lead-covered telephone cable, with each turn separately spliced so that all conductors were in series. Each loop of the cable then consisted of 202 turns, five sections having a total of 1010 turns per coil.

In the initial exploratory installation, the fluxmeters at Cheltenham were operated to give a record at six inches per hour. A control (shown at the left of Figure 215) was provided for increasing the rate of travel of recording paper to six inches per minute at times of more marked magnetic disturbance. Later records were obtained using a rate of 24 inches per hour. The installation at Cheltenham was maintained by the Naval Ordnance Laboratory, in co-operation with the United States Coast and Geodetic Survey.

From the initial calibrations in June, 1942 [60], the sensitivities found were about 3.6γ/mm for H and 3.9γ/mm for Z. The sensitivities of the H- and Z-coils were 1881.5 and 1853.0 maxwell-turns per gamma, respectively, and the fluxmeter sensitivities were 13.1 and 13.8 kilomaxwell-turns, respectively. The return-time-constants were 58 seconds and 52 seconds, respectively, for positive and negative deflections in H, and 35 seconds and 32 seconds for corresponding deflections in Z.

Several changes of instruments were made during the work, and there was some interruption of record during the testing of other types of equipment. A Z-fluxmeter installed March 13, 1943, had a scale value of 3.9γ/mm with return-time-constants of 71 seconds and 45 seconds for deflections to the left and to the right, respectively. On April 8, 1943, the Naval Ordnance Laboratory advised that the H-fluxmeter needed replacement. The new fluxmeter then installed had a sensitivity of 4.1γ/mm with return-time-constants of 33 seconds and 20 seconds.

24. Fluxmeter installation at College, Alaska.--At College, an installation similar to that at Cheltenham was made by the Department of Terrestrial Magnetism of the Carnegie Institution of Washington in accordance with specifications and instructions furnished by the Naval

Ordnance Laboratory. During August, 1942, the fluxmeters at College were operated to yield records at six inches per minute, and later at 24 inches per hour.

Figure 214 gives an aerial view of the College site taken in July, 1941. The location selected for the fluxmeter coils is indicated. Details of construction of the H- and Z-coils are included in Figure 216, and the general plan of installation in Figure 217. As at Cheltenham, rigid underground construction eliminated spurious effects due to mechanical vibration such as might be produced by wind if the coils were placed aboveground.

The average diameters of the H- and Z-coils were 15 feet 2 inches and 15 feet 3 inches, respectively, with corresponding areas of 16.78 and 16.97 square meters, with 1010 turns in five sections as at Cheltenham.

A schematic wiring diagram of the electrical circuits of the fluxmeter installation, showing means for the calibration and control of the instruments, is included in Figure 218.

A standard mutual inductance with its secondary in series with the fluxmeter and search-coil was used to obtain the sensitivity of the meters. The breaking of a known primary current corresponded to a change of a given number of flux-turns, the meter deflection then giving directly the sensitivity in maxwell-turns per division.

Table 117 lists the sensitivities and return-time-constants of the fluxmeters. The sensitivity of the system is the ratio of the meter-sensitivity to the coil-sensitivity.

Table 118 shows the variation in coil resistances as measured from time to time during the year. This variation--due mainly to changes in ground temperature--is interesting in that the lowest resistance obtained corresponds to a temperature only slightly below freezing, this in spite of air temperatures falling at times to -50° C

Table 119 gives sample determinations of fluxmeter sensitivities.

General operation was for the most part without serious incident. In August, 1942, when continuous records at six inches per minute were taken, considerable difficulty was experienced at first with the stopping of the driving mechanisms. This difficulty was largely overcome by the introduction of a variac voltage control. It was necessary to maintain a continuous watch of the apparatus during this month in order to ensure proper operation. At the later regular speed of trace of 24 inches per hour, little attention was required except for daily change of trace.

25. Results of fluxmeter measurements, Cheltenham and College.--The chief finding from the fluxmeter measurements is that the short-period fluctuations of durations of one to ten seconds are small in amplitude (usually only a few gammas) both near the auroral zone and in middle latitudes. This is in good agreement with the results of sections 14 to 16, where interpolated values on graphs such as Figure 195 suggested that few fluctuations of large amplitude and short duration would be found. As previously, for purposes of the foregoing conclusions, a fluctuation is regarded as a departure of the geomagnetic field from normal, either representing a gradual diminution or an intensification to a minimum or maximum value, followed by a subsequent recovery to a normal value; the duration of a fluctuation is the time occupied in the complete process of appreciable change from and return to the normal value. A few of the short-period, low-amplitude fluctuations recorded by the fluxmeters could be attributed to sharp variations in the 110-volt, 60-cycle power supply.

So far as the results for Cheltenham are concerned, only one fluctuation in October, 1942, attained an amplitude in H of 30γ. There was none of comparable size in either H or Z during August. The October fluctuation had a duration of 30 seconds measured at half its (total) maximum amplitude (30γ); the initial rate of change at half-amplitude was 2γ per second and the rate of recovery was similar.

Since the times of beginning and ending of a fluctuation are as a rule rather indefinite, it is difficult to specify exactly the duration. At the suggestion of the Naval Ordnance Laboratory, the duration was defined as the length in seconds on the time-scale measured at half-amplitude.

Positive and negative fluctuations were taken to be in the directions of the respective increase or decrease in a field-component. The rates of change with time were measured at the position of the trace at half-amplitude, both for ascending and descending trace.

Table 120 lists the frequencies of positive and negative fluctuations of different amplitudes in H for various durations of fluctuations as defined above. Shown also in parentheses are the frequencies tentatively corrected using the results of Figures 211 and 212; these corrections are of course uncertain as it is very difficult to maintain consistent values of return-time-constant. The maximum frequencies are shown for durations of about 60 seconds, in good agreement with results already discussed; five cases were found with corrected amplitudes between 200γ and 250γ.

Table 121 gives the corresponding results for Z. The number of fluctuations is less than one-tenth as great, the largest amplitude 110γ, and the frequency distribution appears similar to that in H.

Tables 122 and 123 list the same fluctuations in terms of initial and recovery rates of change in gammas per second for various durations in seconds. The largest observed initial rate of change in H was 12γ/sec (corrected value 16γ/sec) with duration 60 seconds; the largest recovery rate in H was 10γ/sec (corrected value 12γ/sec) with duration 30 seconds. For Z the corresponding values were 6γ/sec (corrected value 8γ/sec) with duration 50 seconds, and 2γ/sec (corrected value 2γ/sec) with duration 50 seconds.

Table 124 lists the incidence of the fluctuations with time of day. They are most numerous in H near 10h and 11h GMT (near or just after local midnight at College).

The H-fluxmeter system at College was calibrated once each month and was operated at a sensitivity of about 8γ per scale-division. Table 125 gives the four fluctuations of largest amplitude per month from October 1, 1943, to January 31, 1944, uncorrected for return-time-constant of about 80 seconds. During the four-month period, the largest positive and negative fluctuations had amplitudes of +307γ and -306γ, respectively; the largest positive rate of change was +7.6γ per second and the largest negative change -9.6γ per second, for the class of fluctuations with complete duration less than 150 seconds.

Figures 219 to 221 are examples of simultaneous records obtained at Cheltenham and College for quiet and disturbed days. It is noted that only rarely do the Cheltenham records depart appreciably from straight lines.

Additional sample records for College are given in Figure 222, showing how they may be characterized in one case by a series of regular damped oscillations, and in another case by high-frequency oscillations of fairly large amplitude--with periods of the order of 12 seconds--superposed on long-period variations.

Fluxmeters afford at any location a useful visual gage of current magnetic conditions. Disturbance ratings can in fact be assigned on an appropriate scale which will compare almost exactly with similar ratings derived from the usual magnetograms. It has been found--particularly in subpolar regions--that all radio-communication disturbances may be assessed for degree of disturbance by examination of the records of a suitable magnetic recorder so that where ease of operation and maintenance is a significant factor, a fluxmeter installation may to some extent supplant the more complex ionospheric apparatus.

As supplementing the usual records available at an observatory, fluxmeters may be of use in that they permit the study of rapid magnetic changes associated with intense sporadic E-region ionization and auroral activity.

26. Unusually large short-period geomagnetic fluctuations measured at Ivigtut, Greenland.--In the summer of 1942, a magnetograph was installed by K. Thiesen at Ivigtut, Greenland. It was operated intermittently during that summer while a magnetic survey was in progress. In May, 1943, S. O. Corp, manager of the Ivigtut Cryolite Mines, generously offered to operate the observatory continuously. Dr. Thiesen returned to Ivigtut for a short time in 1943 to put the magnetograph in operation. The opportunity was taken also to have Dr. Thiesen install specially made short-period measuring elements in another set of la Cour variometers already mounted.

Of particular interest at Ivigtut were a number of fluctuations of very short duration but of large amplitude (see Figure 223); such fluctuations were not observed in the fluxmeter records for College nor on the records of the la Cour magnetographs at other stations during the Polar Year, 1932-33. The most marked of the Ivigtut fluctuations were: A fluctuation of 60γ in H of semiduration five seconds; 65γ in D of semiduration five seconds; and 50γ in Z of semiduration ten seconds. The records were not appreciably affected by the operations at the cryolite mines so that these changes indicate short-period fluctuations of considerable magnitude at points just inside the auroral zone.

27. Background, very small short-period fluctuations, at Turtle Mound, Florida, with portable magnetograph.--A portable magnetograph, designed and constructed at the Department of Terrestrial Magnetism of the Carnegie Institution of Washington, with flat response from zero to about three cycles per second, was operated at Turtle Mound, Florida, from December 1 to 15, 1943. A view of the portable magnetograph is given in Figure 225. The detecting element is shown in Figure 226; it consists of a small Alnico magnet attached to a quartz fiber, one side being polished to give a mirror-surface. The same element, of double-suspension type, can be used in the measurement of either H, D, or Z, and three elements are used. Auxiliary magnets are used for temperature-compensation and to adjust scale values. The motions of the magnet-systems are recorded optically on 35-mm microfilm. One loading of film will serve for 24 hours at high-speed operation with a time-resolution of about 0.3 second, or for about 140 days at slow speed. At Turtle Mound the sensitivity was somewhat less than one gamma per millimeter, the deflection of light spots being photographed as they appeared on a milk-glass in front of the elements.

The possible presence in low and middle latitudes of small geomagnetic fluctuations of amplitude greater than 0.2γ and period one second or less had been conjectured. The results at Turtle Mound (see typical five-minute record in Figure 224) revealed no evidence of fluctuations greater than 0.2γ and duration less than one second. The magnetograph and the results at Turtle Mound will be described in greater detail later in this volume.

TABLES 104-125

Table 104. List of magnetic observatories

Station	φ	λ	Φ	Λ	Ψ	D
	°	°	°	°	°	°
Thule	+76.5	291.0	+88.0	0.0	+ 0.0	-81.3
Godhavn	+69.2	306.5	+79.8	32.5	-17.5	-57.9
Scoresby Sund	+70.5	338.0	+75.8	81.8	-36.2	-34.6
Sveagruvan	+77.9	16.8	+73.9	130.7	-46.2	- 4.9
Jan Mayen	+71.0	351.5	+73.4	96.3	-37.5	-22.7
Calm Bay	+80.3	52.8	+71.5	153.3	-32.2	+21.2
Bear Island	+74.5	19.2	+71.1	124.5	-37.9	- 1.9
Julianehaab	+60.7	314.0	+70.8	35.6	-13.8	-43.4
Reykjavik	+64.1	338.2	+70.2	70.8	-25.6	-30.8
Fort Rae	+62.8	243.9	+69.0	290.9	+24.1	+37.5
Point Barrow	+71.3	203.3	+68.6	241.2	+33.0	+28.7
Lycksele	+64.6	18.7	+67.1	116.4	-30.8	- 1.9
Tromsö	+69.7	18.9	+67.1	116.7	-30.8	- 3.7
Petsamo	+69.5	31.2	+64.9	125.8	-27.6	+ 5.8
Matotchkin Shar	+73.3	56.4	+64.8	146.5	-22.4	+21.7
College	+64.9	212.2	+64.5	255.4	+27.0	+30.5
Sodankylä	+67.4	26.6	+63.8	120.0	-26.7	+ 3.0
Dickson	+73.5	80.4	+63.0	161.5	-12.8	+28.5
Kandalakscha	+67.1	32.4	+62.5	124.2	-25.0	+ 1.8
Lerwick	+60.1	358.8	+62.5	88.6	-23.6	-13.6
Dombaas	+62.1	9.1	+62.3	100.0	-23.6	- 8.5
Meanook	+54.6	246.7	+61.8	301.0	+17.2	+26.4
Kajaani	+64.2	27.8	+60.7	118.0	-23.9	+ 3.1
Sitka	+57.0	224.7	+60.0	275.4	+21.4	+30.2
Eskdalemuir	+55.3	356.8	+58.5	82.9	-20.4	-14.3
Lovö	+59.4	17.8	+58.1	105.8	-22.1	- 2.6
Sloutsk	+59.7	30.5	+56.0	117.0	-20.6	+ 4.4
Copenhagen (Rude Skov)	+55.8	12.4	+55.8	98.5	-20.6	- 5.6
Agincourt	+43.8	280.7	+55.0	347.0	+ 3.6	- 7.6
Abinger	+51.2	359.6	+54.0	83.3	-18.4	-11.9
Val Joyeux	+48.8	2.0	+51.3	84.5	-17.5	-10.5
San Miguel	+37.8	334.4	+45.6	50.9	-11.3	-18.2
Ebro	+40.8	0.5	+43.9	79.7	-15.0	- 9.9
Fernando Poo	+ 3.4	8.7	+ 5.7	78.6	-11.3	- 1.4
Huancayo	-12.0	284.7	- 0.6	353.8	+ 1.3	+ 7.4
Mogadiscio	+ 2.0	45.4	- 2.7	114.3	-10.5	- .9
Elisabethville	-11.7	27.5	-12.7	94.0	-11.7	- 9.5
Apia	-13.8	188.2	-16.0	260.2	+11.7	+10.7
Cape Town	-33.9	18.5	-32.7	79.9	-13.7	-24.7
Watheroo	-30.3	115.9	-41.8	185.6	+ 1.3	- 3.9
Toolangi	-37.5	145.5	-46.7	220.8	+ 9.5	+ 8.5
South Orkneys	-60.8	315.0	-50.0	18.0	- 7.2	+ 3.1

Table 105. List of selected magnetic observatories

Observatory (a) and abbreviation (b)		Geomagnetic*		Angle	Geographic*		Geomagnetic elements, 1932-33		
(a)	(b)	Latitude Φ	Longitude Λ	Ψ **	Latitude φ	Longitude λ	Declination* D	Horizontal intensity H	Vertical intensity V
		°	°	°	°	°	°	cgs	cgs
Thule	Th	+88.0	0.0	0.0	+76.5	291.1	-81.3	.046	+.558
Godhavn	Go	+79.8	32.5	-17.5	+69.2	306.5	-57.9	.082	+.554
Bear Island	BI	+71.1	124.5	-37.9	+74.5	19.2	- 1.9	.095	+.516
Julianehaab	Ju	+70.8	35.6	-13.8	+60.7	314.0	-43.4	.116	+.529
Reykjavik	Re	+70.2	70.8	-25.6	+64.1	338.2	-30.8	.127	+.500
Fort Rae	FR	+69.0	290.9	+24.1	+62.8	243.9	+37.5	.077	+.600
Tromsö	Tr	+67.1	116.7	-30.8	+69.7	18.9	- 3.7	.115	+.502
Petsamo	Pe	+64.9	125.8	-27.6	+69.5	31.2	+ 5.8	.113	+.508
Sodankylä	So	+63.8	120.0	-26.7	+67.4	26.6	+ 3.0	.121	+.493
Sitka	Si	+60.0	275.4	+21.4	+57.0	224.7	+30.2	.154	+.551
Sloutzk	Sl	+56.0	117.0	-20.6	+59.7	30.5	+ 4.4	.154	+.473
Rude Skov	RS	+55.8	98.5	-20.6	+55.8	12.4	- 5.6	.168	+.448
Cheltenham	Ch	+50.1	350.5	+ 2.4	+38.7	283.2	- 7.1	.185	+.542
Tucson	Tu	+40.4	312.2	+10.1	+32.2	249.2	+13.9	.263	+.450
Honolulu	Ho	+21.1	266.5	+12.3	+21.3	201.9	+10.1	.285	+.234
Bombay	Bo	+ 9.5	143.6	- 7.2	+18.9	72.8	- 0.2	.374	+.178
Huancayo	Hu	- 0.6	353.8	+ 1.3	-12.0	284.7	+ 7.4	.296	+.010
Pilar	Pi	-20.2	4.6	- 1.1	-31.7	296.1	+ 6.1	.246	-.119
Watheroo	Wa	-41.8	185.6	+ 1.3	-30.3	115.9	- 3.9	.247	-.513
South Orkneys	SO	-50.0	18.0	- 7.2	-60.8	315.0	+ 3.1	.239	(-.33)

*North latitudes considered positive, south latitudes negative; all longitudes are east; east declination positive west declination negative, horizontal intensity positive, vertical intensity positive in north and negative in south geomagnetic latitude.

**Ψ = angular difference in direction at observatory between geographic and geomagnetic meridians, positive when measured from north around by east.

Table 106. Probability that daily ranges of horizontal intensity (H), magnetic declination (D), and vertical intensity (Z) will exceed various magnitudes in different geomagnetic latitudes (Φ), 12 months, 1932-33

Element	Observatory	Φ*	Probability that daily ranges will exceed magnitude in γ of															
			0	50	100	150	200	300	400	500	600	700	800	900	1000	1100	1200	1300
		°																
H	Thule	+88.0	1.000	.943	.730	.490	.298	.098	.035	.012	.003							
	Godhavn	+79.8	1.000	.990	.935	.775	.578	.239	.174	.100	.056	.036	.024	.013	.006	.001		
	Bear Island	+71.1	1.000	.990	.962	.909	.840	.671	.498	.341	.221	.137	.086	.056	.035	.020	.009	.002
	Julianehaab	+70.8	1.000	.990	.971	.926	.862	.699	.529	.373	.256	.174	.120	.085	.058	.038	.021	
	Fort Rae	+69.0	1.000	.990	.971	.926	.870	.719	.565	.426	.310	.226	.168	.126	.095	.074	.058	
	Tromsö	+67.1	1.000	.943	.855	.746	.641	.478	.365	.278	.211	.159	.118	.087	.062	.043	.029	
	Petsamo	+64.9	1.000	.909	.735	.633	.549	.427	.331	.252	.189	.139	.098	.067	.044	.027	.015	
	Sodankylä	+63.8	1.000	.862	.592	.478	.402	.299	.231	.181	.144	.115	.090	.070	.053	.037	.025	
	Sitka	+60.0	1.000	.654	.309	.205	.152	.098	.063	.037	.016	.003						
	Rude Skov	+55.8	1.000	.602	.123	.026	.006											
	Cheltenham	+50.1	1.000	.463	.060	.012	.003											
	Tucson	+40.4	1.000	.372	.030	.005												
	Honolulu	+21.1	1.000	.186	.022	.005												
	Huancayo	- 0.6	1.000	.980	.685	.212	.045											
	Pilar	-20.2	1.000	.375	.047	.008	.000											
	Watheroo	-41.8	1.000	.272	.013													
	South Orkneys	-50.0	1.000	.348	.028	.005												
D	Thule	+88.0	1.000	.901	.654	.389	.208	.043	.007	.002								
	Godhavn	+79.8	1.000	.980	.870	.667	.412	.204	.113	.069	.044	.027	.015	.007	.002			
	Bear Island	+71.1	1.000	.971	.885	.741	.585	.353	.198	.096	.037	.012	.003					
	Julianehaab	+70.8	1.000	.962	.826	.690	.568	.385	.251	.158	.096	.057	.030	.012	.003			
	Fort Rae	+69.0	1.000	.971	.847	.714	.599	.413	.275	.174	.103	.055	.027	.012	.003			
	Tromsö	+67.1	1.000	.885	.602	.467	.362	.217	.132	.086	.055	.031	.014	.003				
	Petsamo	+64.9	1.000	.826	.538	.407	.310	.178	.099	.052	.023	.006						
	Sodankylä	+63.8	1.000	.794	.408	.232	.153	.087	.051	.027	.009	.001						
	Sitka	+60.0	1.000	.855	.418	.222	.128	.056	.031	.015	.004							
	Rude Skov	+55.8	1.000	.725	.176	.061	.022											
	Cheltenham	+50.1	1.000	.746	.173	.043	.012											
	Tucson	+40.4	1.000	.680	.041	.005												
	Honolulu	+21.1	1.000	.403	.008													
	Huancayo	- 0.6	1.000	.176	.008													
	Pilar	-20.2	1.000	.380	.010													
	Watheroo	-41.8	1.000	.595	.056	.016	.007											
	South Orkneys	-50.0	1.000	.488	.064	.013	.005											
Z	Thule	+88.0	1.000	.709	.373	.179	.075	.013	.001									
	Godhavn	+79.8	1.000	.990	.962	.877	.756	.505	.299	.156	.080	.041	.020	.009	.003			
	Bear Island	+71.1	1.000	.990	.935	.855	.756	.599	.375	.244	.164	.113	.078	.049	.028	.012	.003	
	Julianehaab	+70.8	1.000	.990	.971	.917	.840	.629	.424	.287	.203	.150	.114	.088	.068	.052	.039	
	Fort Rae	+69.0	1.000	.990	.943	.862	.775	.588	.429	.304	.209	.139	.089	.055	.033	.016	.005	
	Tromsö	+67.1	1.000	.917	.741	.565	.446	.306	.205	.139	.091	.058	.035	.020	.009	.004	.001	
	Petsamo	+64.9	1.000	.917	.769	.617	.490	.324	.224	.155	.108	.075	.050	.034	.022	.014	.008	
	Sodankylä	+63.8	1.000	.847	.645	.508	.405	.255	.148	.081	.044	.026	.016	.009	.005	.003	.001	
	Sitka	+60.0	1.000	.637	.424	.284	.193	.104	.063	.044	.028	.016	.008	.002				
	Rude Skov	+55.8	1.000	.364	.126	.059	.039	.025	.011	.003								
	Cheltenham	+50.1	1.000	.137	.024	.007												
	Tucson	+40.4	1.000	.053	.009	.004												
	Honolulu	+21.1	1.000	.483														
	Huancayo	- 0.6	1.000	.011														
	Pilar	-20.2	1.000	.015														
	Watheroo	-41.8	1.000	.408	.125													
	South Orkneys	-50.0																

*Geomagnetic latitude

Table 107. Expectation of average number of days elapsing before daily ranges in horizontal intensity (H), magnetic declination (D), and vertical intensity (Z) will exceed various magnitudes in different geomagnetic latitudes (Φ), 12 months, 1932-33

Element	Observatory	Φ*	Expected average number of days elapsing before daily ranges exceed magnitude in γ of															
			0	50	100	150	200	300	400	500	600	700	800	900	1000	1100	1200	1300
		°																
H	Thule	+88.0	1	1	1	2	3	10	28	85	380							
	Godhavn	+79.8	1	1	1	1	2	4	6	10	18	28	41	74	185	740		
	Bear Island	+71.1	1	1	1	1	1	1	2	3	5	7	12	18	29	50	110	445
	Julianehaab	+70.8	1	1	1	1	1	1	2	3	4	6	8	12	17	27	48	
	Fort Rae	+69.0	1	1	1	1	1	1	2	2	3	4	6	8	10	14	17	
	Tromsö	+67.1	1	1	1	1	2	2	3	4	5	6	8	12	16	23	35	
	Petsamo	+64.9	1	1	1	2	2	2	3	4	5	7	10	15	23	36	65	
	Sodankylä	+63.8	1	1	2	2	2	3	4	6	7	9	11	14	19	27	40	
	Sitka	+60.0	1	2	3	5	7	10	16	27	61	325						
	Rude Skov	+55.8	1	2	8	39	155											
	Cheltenham	+50.1	1	2	17	80	400											
	Tucson	+40.4	1	3	33	200												
	Honolulu	+21.1	1	5	46	215												
	Huancayo	- 0.6	1	1	1	5	22											
	Pilar	- 20.2	1	3	21	125	2400											
	Watheroo	- 41.8	1	4	75													
	South Orkneys	- 50.0	1	3	36	220												
D	Thule	+88.0	1	1	2	3	5	23	150	630								
	Godhavn	+79.8	1	1	1	2	2	5	9	14	23	38	65	140	490			
	Bear Island	+71.1	1	1	1	1	2	3	5	10	27	86	380					
	Julianehaab	+70.8	1	1	1	1	2	3	4	6	10	17	33	81	300			
	Fort Rae	+69.0	1	1	1	1	2	2	4	6	10	18	37	80	320			
	Tromsö	+67.1	1	1	2	2	3	5	8	12	18	32	72	315				
	Petsamo	+64.9	1	1	2	2	3	6	10	19	43	160						
	Sodankylä	+63.8	1	1	2	4	7	12	20	37	110	1900						
	Sitka	+60.0	1	1	2	4	8	18	32	68	240							
	Rude Skov	+55.8	1	1	6	16	46											
	Cheltenham	+50.1	1	1	6	24	82											
	Tucson	+40.4	1	1	24	180												
	Honolulu	+21.1	1	3	125													
	Huancayo	- 0.6	1	6	125													
	Pilar	- 20.2	1	3	104													
	Watheroo	- 41.8	1	2	18	64	140											
	South Orkneys	- 50.0	1	2	16	75	190											
Z	Thule	+88.0	1	1	3	6	13	80	720									
	Godhavn	+79.8	1	1	1	1	1	2	3	6	12	25	51	110	380			
	Bear Island	+71.1	1	1	1	1	1	2	3	4	6	9	13	20	36	83	330	
	Julianehaab	+70.8	1	1	1	1	1	2	2	3	5	7	9	11	15	19	25	
	Fort Rae	+69.0	1	1	1	1	1	2	2	3	5	7	11	18	30	61	180	
	Tromsö	+67.1	1	1	1	2	2	3	5	7	11	17	29	51	106	275	1400	
	Petsamo	+64.9	1	1	1	2	2	3	4	6	9	13	20	30	44	71	130	
	Sodankylä	+63.8	1	1	2	2	2	4	7	12	23	38	64	110	190	380	1500	
	Sitka	+60.0	1	2	2	4	5	10	16	23	35	61	130	460				
	Rude Skov	+55.8	1	3	8	17	26	40	90	360								
	Cheltenham	+50.1	1	7	42	150												
	Tucson	+40.4	1	19	110	230												
	Honolulu	+21.1	1	21														
	Huancayo	- 0.6	1	94														
	Pilar	- 20.2	1	69														
	Watheroo	- 41.8	1	2	8													
	South Orkneys	- 50.0																

*Geomagnetic latitude

Table 108. Observed cumulative frequencies (f_c), and computed probabilities (P), expected frequencies per year (f_e), and expected number of days elapsing (E) for various daily ranges (R) at different stations

R	f_c	P	f_e	E	f_c	P	f_e	E	f_c	P	f_e	E	f_c	P	f_e	E
γ	days		days	days	days		days	days	days		days	days	days		days	days
	Sitka, 1905-26								Sitka, 1932-33							
	Horizontal intensity (H)				Vertical intensity (Z)				Horizontal intensity (H)				Vertical intensity (Z)			
0	7874	1.0000	365	1	7865	1.0000	365	1	362	1.0000	365	1	362	1.0000	365	1
100	2106	0.2675	98	4	2516	0.3199	117	3	95	0.2624	96	4	139	0.3840	140	3
200	973	0.1236	45	8	1163	0.1479	54	7	34	0.0939	34	11	61	0.1685	62	6
300	596	0.0757	28	14	622	0.0791	29	13	15	0.0414	15	24	26	0.0718	26	14
400	396	0.0503	18	20	356	0.0453	17	22	8	0.0221	8	45	12	0.0331	12	30
500	281	0.0357	13	28	189	0.0240	9	42	3	0.0083	3	120	6	0.0166	6	60
600	191	0.0243	9	41	105	0.0134	5	75	1	0.0028	1	360	4	0.0110	4	91
700	148	0.0188	7	53	51	0.0065	2	154	1	0.0028	1	360	1	0.0028	1	360
800	106	0.0135	5	74	23	0.0029	1	345	0	0.0000	0		1	0.0028	1	360
900	72	0.0091	3	110	10	0.0013	0	769					1	0.0028	1	360
1000	44	0.0056	2	178	8	0.0010	0	1000					1	0.0028	1	360
1100	30	0.0038	1	263	5	0.0006	0	1700					0	0.0000	0	
1200	22	0.0028	1	357	3	0.0004	0	2500								
1300	15	0.0019	1	526	0	0.0000	0									
1400	5	0.0006	0	1700												
	Sloutzk, 1878-1939												Bombay, 1882-1905			
	Horizontal intensity (H)				Declination (D)				Vertical intensity (Z)				Horizontal intensity (H)			
20?									1072	0.04737	17	21				
60?	1029	0.04547	17	22												
60					1062	0.0469	17	21								
70													346	0.0395	14	25
100	963	0.04255	16	24	1022	0.0416	15	22	913	0.04034	15	25	294	0.0336	12	30
200	355	0.01568	6	64	384	0.0170	6	59	435	0.01922	7	52	63	0.0072	3	139
300	138	0.00609	2	164	116	0.0051	2	195	206	0.00910	3	110	19	0.0022	1	454
400	72	0.00318	1	314	50	0.0018	1	568	98	0.00433	2	231	8	0.0009	0	1100
500	38	0.00167	1	600	27	0.0012	0	840	53	0.00234	1	427	4	0.0005	0	2000
600.	22	0.00097	0	1030	12	0.0005	0	2000	27	0.00119	0	840	3	0.0003	0	3300
700	13	0.00057	0	1750	6	0.0003	0	3300	12	0.00053	0	1890	1	0.0001	0	10000
800	9	0.00040	0	2500	4	0.0002	0	5000	6	0.00026	0	3800	1	0.0001	0	10000
900	7	0.00031	0	3200	2	0.0001	0	10000	3	0.00013	0	7700	0	0.0000	0	
1000	2	0.00009	0	11000	1	0.00004	0	25000	1	0.00004	0	25000				
1100	2	0.00009	0	11000	0	0.00000	0		1	0.00004	0	25000				
1200	2	0.00009	0	11000					0	0.00000	0					
1300	1	0.00004	0	25000												
1400	1	0.00004	0	25000												
3200	1	0.00004	0	25000												
	Cheltenham, 1905-30								Cheltenham, 1932-33							
	Horizontal intensity (H)				Vertical intensity (Z)				Horizontal intensity (H)				Vertical intensity (Z)			
0	9485	1.0000	365	1	9487	1.0000	365	1	365	1.0000	365	1	365	1.0000	365	1
25									357	0.9781	357	1	143	0.3918	143	3
50									181	0.4959	181	2	36	0.0986	36	10
75									45	0.1233	45	8	7	0.0192	7	52
100	836	0.0881	32	12	299	0.0315	11	32	15	0.0411	15	24	3	0.0082	3	120
125									3	0.0082	3	120	1	0.0027	1	370
150									1	0.0027	1	370	1	0.0027	1	370
175									1	0.0027	1	370	1	0.0027	1	370
200	77	0.0081	3	123	81	0.0085	3	117	0	0.0000	0		0	0.0000	0	
300	27	0.0028	1	357	32	0.0034	1	294								
400	12	0.0013	0	769	16	0.0017	1	588								
500	9	0.0009	0	1100	11	0.0012	0	833								
600	6	0.0006	0	1700	6	0.0006	0	1700								
700	5	0.0005	0	2000	3	0.0003	0	3300								
800	2	0.0002	0	5000	1	0.0001	0	10000								
900	1	0.0001	0	10000	0	0.0000	0									
1000	0	0.0000	0													

Table 109. Probability that weekly ranges of horizontal intensity (H), magnetic declination (D), and vertical intensity (Z) will exceed various magnitudes in different geomagnetic latitudes (Φ)

(Probabilities based on data for 12 months during Polar Year of 1932-33)

Element	Observatory and Φ[a]	Probability that weekly ranges will exceed magnitude of γ in																			
		0	50	100	150	200	300	400	500	600	700	800	900	1000	1100	1200	1300	1400	1500	1600	1700
H	Th +88.0	1.000	1.000	.980	.901	.787	.481	.115	.038												
	Go +79.8	1.000	1.000	1.000	1.000	.980	.826	.578	.424	.308	.154	.135	.115	.077							
	BI +71.1	1.000	1.000	1.000	1.000	1.000	1.000	.952	.877	.714	.617	.476	.405	.310	.214	.071	.024				
	Ju +70.8	1.000	1.000	1.000	1.000	1.000	1.000	.980	.943	.826	.694	.559	.424	.288	.192	.115	.096	.058	.019		
	FR +69.0	1.000	1.000	1.000	1.000	1.000	1.000	1.000	.962	.901	.826	.633	.442	.403	.250	.192	.096	.058			
	Tr[b] +67.1	1.000	1.000	1.000	1.000	1.000	.943	.885	.617	.481	.365	.270	.058								
	Pe +64.9	1.000	1.000	.980	.980	.980	.980	.926	.885	.787	.617	.518	.424	.308	.231	.173	.096	.038	.019		
	So +63.8	1.000	1.000	1.000	.943	.926	.926	.826	.654	.500	.500	.442	.365	.308	.115	.096	.038	.019	.019		
	Si +60.0	1.000	1.000	.787	.654	.481	.308	.173	.077	.058	.038	.038	.019	.019	.019	.019	.019	.019	.019		
	RS +55.8	1.000	.980	.500	.135	.038	.019														
	Ch +50.1	1.000	.943	.403	.038	.019															
	Tu +40.4	1.000	.885	.250	.019	.019															
	Ho +21.1	1.000	.769	.154	.019																
	Hu - 0.6	1.000	1.000	.980	.730	.308	.019	.019													
	Pi - 20.2	1.000	.980	.288	.058	.019															
	Wa - 41.8	1.000	.885	.154	.019																
	SO - 50.0	1.000	.926	.211																	
D	Th +88.0	1.000	1.000	.980	.901	.769	.365	.058	.019												
	Go +79.8	1.000	1.000	1.000	1.000	.926	.806	.538	.365	.173	.135	.058	.019								
	BI +71.1	1.000	1.000	1.000	1.000	1.000	.909	.645	.422	.156	.067	.022									
	Ju +70.8	1.000	1.000	1.000	1.000	1.000	.943	.847	.654	.538	.403	.192	.077	.058	.038						
	FR +69.0	1.000	1.000	1.000	1.000	1.000	.962	.806	.633	.424	.288	.173	.115	.019							
	Tr[b] +67.1	1.000	1.000	.901	.654	.442	.115	.019													
	Pe +64.9	1.000	1.000	1.000	.943	.901	.667	.450	.255	.098	.078										
	So +63.8	1.000	1.000	.962	.769	.518	.385	.192	.135	.077	.038										
	Si +60.0	1.000	1.000	.943	.709	.518	.231	.058	.019												
	RS +55.8	1.000	1.000	.694	.308	.173															
	Ch +50.1	1.000	.980	.617	.154	.115															
	Tu +40.4	1.000	.943	.308																	
	Ho +21.1	1.000	.752	.019																	
	Hu - 0.6	1.000	.578																		
	Pi - 20.2	1.000	.752	.019																	
	Wa - 41.8	1.000	.943	.231	.038	.019															
	SO - 50.0	1.000	.980	.365	.019	.019															
Z	Th +88.0	1.000	.926	.709	.450	.308	.135	.019													
	Go +79.8	1.000	1.000	1.000	1.000	1.000	1.000	.901	.595	.442	.211	.135	.019								
	BI +71.1	1.000	1.000	1.000	1.000	1.000	1.000	.952	.820	.645	.422	.222	.156	.111	.044	.022					
	Ju +70.8	1.000	1.000	1.000	1.000	1.000	1.000	.980	.826	.654	.559	.481	.327	.211	.173	.135	.077	.038	.019	.019	.019
	FR +69.0	1.000	1.000	1.000	1.000	1.000	1.000	.980	.962	.826	.694	.500	.403	.308	.250	.135	.077	.058	.038	.038	.019
	Tr[b] +67.1	1.000	1.000	1.000	.962	.787	.538	.308	.173	.058											
	Pe +64.9	1.000	1.000	1.000	1.000	1.000	.806	.633	.500	.461	.365	.270	.173	.096	.077	.058	.019	.019			
	So +63.8	1.000	1.000	1.000	1.000	1.000	.885	.578	.365	.231	.154	.077	.038	.038	.038						
	Si +60.0	1.000	.980	.926	.787	.694	.442	.288	.154	.096	.019	.019	.019	.019							
	RS +55.8	1.000	.847	.442	.192	.038	.019	.019													
	Ch +50.1	1.000	.481	.077	.038																
	Tu +40.4	1.000	.058																		
	Ho +21.1	1.000	.173																		
	Hu - 0.6	1.000	.154																		
	Pi - 20.2	1.000	.019																		
	Wa - 41.8	1.000	.885	.115																	
	SO - 50.0	No available data																			

[a]Geomagnetic latitude; see Table 105 for abbreviations to designate observatories. [b]Ranges determined from mean hourly values at extremes.

Table 110. Probability that weekly, 1-, 2-, 3-, 4-, and 6-monthly ranges in horizontal intensity (H), magnetic declination (D), and vertical intensity (Z) will exceed various magnitudes at Tromsö, Sitka, Cheltenham, and Honolulu

(Probabilities based on 8 years of data from Tromsö Observatory and 26 years of data at each from Sitka, Cheltenham, and Honolulu Observatories)

Ele-ment	Time-period	Probability that time-period ranges will exceed magnitude in γ of																		
		0	50	100	150	200	300	400	500	600	700	800	900	1000	1100	1200	1300	1400	1500	1600
							TROMSÖ (Φ = +67°.1), based on data for 8 years, 1930-37													
H	Weekly	1.000	1.000	1.000	.983	.966	.898	.794	.637	.462	.310	.179	.099	.051	.017	.005	.002			
	Monthly	1.000	1.000	1.000	1.000	1.000	1.000	1.000	.990	.896	.771	.594	.437	.292	.083	.031	.010			
	2-monthly	1.000	1.000	1.000	1.000	1.000	1.000	1.000	1.000	.989	.979	.832	.674	.474	.253	.081	.021			
	3-monthly	1.000	1.000	1.000	1.000	1.000	1.000	1.000	1.000	1.000	1.000	.926	.833	.633	.442	.168	.032			
	4-monthly	1.000	1.000	1.000	1.000	1.000	1.000	1.000	1.000	1.000	1.000	.990	.943	.709	.559	.258	.054			
	6-monthly	1.000	1.000	1.000	1.000	1.000	1.000	1.000	1.000	1.000	1.000	1.000	.990	.893	.735	.450	.121			
D	Weekly	1.000	1.000	.868	.670	.489	.164	.046	.012											
	Monthly	1.000	1.000	1.000	1.000	.885	.635	.229	.073	.021										
	2-monthly	1.000	1.000	1.000	1.000	1.000	.874	.442	.189	.053										
	3-monthly	1.000	1.000	1.000	1.000	1.000	.980	.671	.319	.085										
	4-monthly	1.000	1.000	1.000	1.000	1.000	1.000	.826	.420	.140										
	6-monthly	1.000	1.000	1.000	1.000	1.000	1.000	.943	.617	.242										
Z	Weekly	1.000	1.000	.989	.882	.747	.523	.339	.168	.074	.022	.003	.003	.003						
	Monthly	1.000	1.000	1.000	1.000	1.000	.964	.845	.595	.333	.167	.036	.012	.012						
	2-monthly	1.000	1.000	1.000	1.000	1.000	1.000	.976	.881	.607	.298	.107	.024	.024						
	3-monthly	1.000	1.000	1.000	1.000	1.000	1.000	.990	.990	.746	.433	.157	.036	.036						
	4-monthly	1.000	1.000	1.000	1.000	1.000	1.000	1.000	1.000	.855	.556	.222	.049	.049						
	6-monthly	1.000	1.000	1.000	1.000	1.000	1.000	1.000	1.000	.990	.800	.304	.076	.076						
							SITKA (Φ = +60°.0), based on data for 26 years, 1905-30													
H	Weekly	1.000	.971	.741	.585	.490	.370	.294	.234	.175	.140	.108	.079	.056	.045	.030	.020	.005		
	Monthly	1.000	1.000	.990	.943	.870	.781	.704	.613	.515	.437	.372	.308	.253	.176	.131	.093	.026		
	2-monthly	1.000	1.000	1.000	.990	.952	.909	.870	.800	.709	.613	.532	.461	.389	.318	.251	.190	.058		
	3-monthly	1.000	1.000	1.000	.990	.980	.971	.943	.893	.813	.725	.617	.552	.500	.417	.336	.258	.090	.003	
	4-monthly	1.000	1.000	1.000	1.000	.990	.990	.971	.926	.870	.787	.685	.613	.578	.493	.424	.333	.123	.006	
	6-monthly	1.000	1.000	1.000	1.000	1.000	1.000	1.000	.952	.926	.855	.781	.714	.658	.565	.503	.441	.192	.016	
D	Weekly	1.000	.990	.855	.633	.439	.224	.128	.079	.049	.032	.023	.015	.009	.006	.004	.003	.002	.001	
	Monthly	1.000	1.000	1.000	.980	.877	.613	.413	.282	.215	.135	.090	.964	.032	.022	.016	.010	.006	.003	.003
	2-monthly	1.000	1.000	1.000	1.000	.980	.800	.585	.441	.330	.235	.172	.118	.067	.048	.029	.019	.013	.006	.006
	3-monthly	1.000	1.000	1.000	1.000	.990	.885	.685	.546	.413	.307	.235	.171	.103	.077	.048	.029	.019	.010	.010
	4-monthly	1.000	1.000	1.000	1.000	1.000	.926	.758	.629	.472	.366	.294	.214	.133	.100	.071	.042	.026	.013	.013
	6-monthly	1.000	1.000	1.000	1.000	1.000	.952	.820	.714	.562	.446	.382	.280	.176	.156	.120	.068	.039	.020	.020
Z	Weekly	1.000	.962	.826	.690	.585	.417	.303	.207	.123	.064	.029	.016	.007	.003	.002				
	Monthly	1.000	1.000	.990	.980	.935	.820	.685	.575	.388	.237	.128	.071	.026	.010	.006				
	2-monthly	1.000	1.000	1.000	.990	.980	.935	.847	.725	.578	.370	.244	.138	.058	.026	.019				
	3-monthly	1.000	1.000	1.000	1.000	.990	.990	.909	.806	.676	.488	.319	.203	.097	.042	.029				
	4-monthly	1.000	1.000	1.000	1.000	1.000	.990	.943	.877	.752	.595	.405	.256	.139	.065	.045	.003			
	6-monthly	1.000	1.000	1.000	1.000	1.000	1.000	.971	.917	.840	.741	.498	.355	.189	.085	.062	.020	.007	.003	

Table 110. Probability that weekly, 1-, 2-, 3-, 4-, and 6-monthly ranges in horizontal intensity (H), magnetic declination (D), and vertical intensity (Z) will exceed various magnitudes at Tromsö, Sitka, Cheltenham, and Honolulu--concluded

(Probabilities based on 8 years of data from Tromsö Observatory and 26 years of data at each from Sitka, Cheltenham, and Honolulu Observatories)

Element	Time-period	Probability that time-period ranges will exceed magnitude in γ of																		
		0	50	100	150	200	300	400	500	600	700	800	900	1000	1100	1200	1300	1400	1500	1600
		CHELTENHAM (Φ = +50°.1), based on data for 26 years, 1905-30																		
H	Weekly	1.000	.962	.442	.151	.062	.018	.011	.007	.005	.004	.002	.001							
	Monthly	1.000	1.000	.885	.538	.247	.074	.048	.032	.022	.019	.006	.006	.003	.003	.003				
	2-monthly	1.000	1.000	.935	.741	.446	.154	.093	.064	.045	.039	.013	.013	.006	.006	.006				
	3-monthly	1.000	1.000	.962	.826	.552	.223	.132	.094	.068	.058	.019	.019	.010	.010	.010				
	4-monthly	1.000	1.000	.980	.885	.709	.285	.181	.126	.094	.078	.026	.026	.013	.013	.013				
	6-monthly	1.000	1.000	1.000	.935	.820	.382	.251	.186	.147	.117	.042	.039	.020	.020	.020				
D	Weekly	1.000	.962	.544	.229	.096	.024	.009	.004	.004	.004	.002	.002	.002	.002	.002	.001	.001	.001	.001
	Monthly	1.000	1.000	.926	.637	.350	.102	.035	.016	.013	.013	.006	.006	.006	.006	.006	.006	.006	.003	.003
	2-monthly	1.000	1.000	.990	.840	.599	.196	.077	.032	.026	.026	.013	.013	.013	.013	.013	.013	.013	.006	.006
	3-monthly	1.000	1.000	1.000	.935	.735	.291	.123	.055	.039	.039	.019	.019	.019	.019	.019	.019	.019	.010	.010
	4-monthly	1.000	1.000	1.000	.952	.800	.333	.149	.074	.062	.062	.039	.036	.036	.026	.026	.026	.026	.013	.013
	6-monthly	1.000	1.000	1.000	.990	.870	.478	.231	.114	.078	.078	.049	.039	.039	.039	.039	.039	.039	.020	.020
Z	Weekly	1.000	.485	.186	.096	.061	.026	.014	.009	.005	.003	.001								
	Monthly	1.000	.892	.562	.340	.247	.122	.067	.038	.022	.013	.003								
	2-monthly	1.000	.971	.763	.559	.424	.238	.141	.090	.045	.029	.006								
	3-monthly	1.000	.980	.862	.676	.541	.342	.210	.139	.065	.042	.016	.003	.003	.003					
	4-monthly	1.000	1.000	.926	.769	.633	.433	.275	.185	.084	.055	.026	.007	.007	.007					
	6-monthly	1.000	1.000	.990	.909	.752	.588	.417	.297	.127	.078	.036	.016	.016	.016					
		HONOLULU (Φ = +21°.1), based on data for 26 years, 1905-30																		
H	Weekly	1.000	.847	.291	.085	.035	.007	.004	.004	.002	.001									
	Monthly	1.000	1.000	.741	.358	.151	.032	.016	.013	.006	.003									
	2-monthly	1.000	1.000	.901	.610	.301	.074	.032	.026	.013	.009									
	3-monthly	1.000	1.000	.952	.725	.417	.110	.048	.039	.019	.010									
	4-monthly	1.000	1.000	.980	.883	.508	.162	.065	.052	.026	.013									
	6-monthly	1.000	1.000	1.000	.901	.641	.253	.097	.078	.039	.019									
D	Weekly	1.000	.847	.075	.005	.001	.001													
	Monthly	1.000	.962	.290	.029	.009	.009													
	2-monthly	1.000	.990	.441	.055	.006	.006													
	3-monthly	1.000	.990	.592	.087	.010	.010													
	4-monthly	1.000	1.000	.662	.119	.013	.013													
	6-monthly	1.000	1.000	.763	.181	.019	.019													
Z	Weekly	1.000	.241	.004	.002	.001														
	Monthly	1.000	.662	.019	.010	.003														
	2-monthly	1.000	.877	.042	.019	.006														
	3-monthly	1.000	.943	.077	.029	.010														
	4-monthly	1.000	.980	.110	.039	.013														
	6-monthly	1.000	1.000	.221	.058	.019														

Table 111. Expectation of average number of weeks elapsing before weekly ranges in horizontal intensity (H), magnetic declination (D), and vertical intensity (Z) will exceed various magnitudes in different geomagnetic latitudes (Φ)

(Expectations based on data for 12 months during Polar Year 1932-33)

Element	Observatory and Φ[a]		Expected average number of weeks elapsing before daily ranges exceed magnitude in γ of																		
		°	0	50	100	150	200	300	400	500	600	700	800	900	1000	1100	1200	1300	1400	1500	1600	1700
H	Th	+88.0	1.0	1.0	1.0	1.1	1.3	2.1	8.7	26.0												
	Go	+79.8	1.0	1.0	1.0	1.0	1.0	1.2	1.7	2.4	3.2	6.5	7.4	8.7	13.0							
	BI	+71.1	1.0	1.0	1.0	1.0	1.0	1.0	1.0	1.1	1.4	1.6	2.1	2.5	3.2	4.7	14.0	42.0				
	Ju	+70.8	1.0	1.0	1.0	1.0	1.0	1.0	1.0	1.1	1.2	1.4	1.8	2.4	3.5	5.2	8.7	10.4	17.3	52.0		
	FR	+69.0	1.0	1.0	1.0	1.0	1.0	1.0	1.0	1.0	1.1	1.2	1.6	2.3	2.5	4.0	5.2	10.4	17.3	52.0		
	Tr[b]	+67.1	1.0	1.0	1.0	1.0	1.0	1.1	1.1	1.6	2.1	2.7	3.7	17.3								
	Pe	+64.9	1.0	1.0	1.0	1.0	1.0	1.0	1.1	1.1	1.3	1.6	1.9	2.4	3.2	4.3	5.8	10.4	26.0	52.0		
	So	+63.8	1.0	1.0	1.0	1.1	1.1	1.1	1.2	1.5	2.0	2.0	2.3	2.7	3.2	8.7	10.4	26.0	52.0	52.0		
	Si	+60.0	1.0	1.0	1.3	1.5	2.1	3.2	5.8	13.0	17.3	26.0	26.0	52.0	52.0	52.0	52.0	52.0	52.0	52.0		
	RS	+55.8	1.0	1.0	2.0	7.4	26.0	52.0														
	Ch	+50.1	1.0	1.1	2.5	26.0	52.0															
	Tu	+40.4	1.0	1.1	4.0	52.0	52.0															
	Ho	+21.1	1.0	1.3	6.5	52.0																
	Hu	- 0.6	1.0	1.0	1.0	1.4	3.2	52.0	52.0													
	Pi	-20.2	1.0	1.0	3.5	17.3	52.0															
	Wa	-41.8	1.0	1.1	6.5	52.0																
	SO	-50.0	1.0	1.1	4.7																	
D	Th	+88.0	1.0	1.0	1.0	1.1	1.3	2.7	17.3	52.0												
	Go	+79.8	1.0	1.0	1.0	1.0	1.1	1.2	1.9	2.7	5.8	7.4	17.3	52.0								
	BI	+71.1	1.0	1.0	1.0	1.0	1.0	1.1	1.6	2.4	6.4	15.0	45.0									
	Ju	+70.8	1.0	1.0	1.0	1.0	1.0	1.1	1.2	1.5	1.9	2.5	5.2	13.0	17.3	26.0						
	FR	+69.0	1.0	1.0	1.0	1.0	1.0	1.0	1.2	1.6	2.4	3.5	5.8	8.7	52.0							
	Tr[b]	+67.1	1.0	1.0	1.1	1.5	2.3	8.7	52.0													
	Pe	+64.9	1.0	1.0	1.0	1.1	1.1	1.5	2.2	3.9	10.2	12.8										
	So	+63.8	1.0	1.0	1.0	1.3	1.9	2.6	5.2	7.4	13.0	26.0										
	Si	+60.0	1.0	1.0	1.1	1.4	1.9	4.3	17.3	52.0												
	RS	+55.8	1.0	1.0	1.4	3.2	5.8															
	Ch	+50.1	1.0	1.0	1.6	6.5	8.7															
	Tu	+40.4	1.0	1.1	3.2																	
	Ho	+21.1	1.0	1.3	52.0																	
	Hu	- 0.6	1.0	1.7																		
	Pi	-20.2	1.0	1.3	52.0																	
	Wa	-41.8	1.0	1.1	4.3	26.0	52.0															
	SO	-50.0	1.0	1.0	2.7	52.0	52.0															
Z	Th	+88.0	1.0	1.1	1.4	2.2	3.2	7.4	52.0													
	Go	+79.8	1.0	1.0	1.0	1.0	1.0	1.0	1.1	1.7	2.3	4.7	7.4	52.0								
	BI	+71.1	1.0	1.0	1.0	1.0	1.0	1.0	1.0	1.2	1.6	2.4	4.5	6.4	9.0	22.5	45.0					
	Ju	+70.8	1.0	1.0	1.0	1.0	1.0	1.0	1.0	1.2	1.5	1.8	2.1	3.1	4.7	5.8	7.4	13.0	26.0	52.0	52.0	52.0
	FR	+69.0	1.0	1.0	1.0	1.0	1.0	1.0	1.0	1.0	1.2	1.4	2.0	2.5	3.2	4.0	7.4	13.0	17.3	26.0	26.0	52.0
	Tr[b]	+67.1	1.0	1.0	1.0	1.0	1.3	1.9	3.2	5.8	17.3											
	Pe	+64.9	1.0	1.0	1.0	1.0	1.0	1.2	1.6	2.0	2.2	2.7	3.7	5.8	10.4	13.0	17.3	52.0	52.0			
	So	+63.8	1.0	1.0	1.0	1.0	1.0	1.1	1.7	2.7	4.3	6.5	13.0	26.0	26.0	26.0						
	Si	+60.0	1.0	1.0	1.1	1.3	1.4	2.3	3.5	6.5	10.4	52.0	52.0	52.0	52.0							
	RS	+55.8	1.0	1.2	2.3	5.2	26.0	52.0	52.0													
	Ch	+50.1	1.0	2.1	13.0	26.0																
	Tu	+40.4	1.0	17.3																		
	Ho	+21.1	1.0	5.8																		
	Hu	- 0.6	1.0	6.5																		
	Pi	-20.2	1.0	52.0																		
	Wa	-41.8	1.0	1.1	8.7																	
	SO	-50.0	No available data																			

[a]Geomagnetic latitude; see Table 105 for abbreviations to designate observatories. [b]Ranges determined from mean hourly values at extremes.

Table 112. Expectation of average number of time-periods elapsing before weekly, 1-, 2-, 3-, 4-, and 6-monthly ranges in horizontal intensity (H), magnetic declination (D), and vertical intensity (Z) will exceed various magnitudes at Tromsö, Sitka, Cheltenham, and Honolulu

(Expectancies based on 8 years of data from Tromsö Observatory and 26 years of data at each from Sitka, Cheltenham, and Honolulu Observatories)

Element	Time-period	Expected average number of time-periods elapsing before ranges exceed magnitude in γ of																		
		0	50	100	150	200	300	400	500	600	700	800	900	1000	1100	1200	1300	1400	1500	1600
		TROMSÖ (Φ = +67°.1), based on data for 8 years, 1930-37																		
H	Weekly	1.00	1.00	1.00	1.02	1.04	1.11	1.26	1.57	2.16	3.23	5.58	10.1	19.7	59.0	206	413			
	Monthly	1.00	1.00	1.00	1.00	1.00	1.00	1.00	1.01	1.12	1.30	1.68	2.29	3.43	12.0	32.0	96.0			
	2-monthly	1.00	1.00	1.00	1.00	1.00	1.00	1.00	1.00	1.01	1.02	1.20	1.48	2.11	3.96	11.9	47.5			
	3-monthly	1.00	1.00	1.00	1.00	1.00	1.00	1.00	1.00	1.00	1.00	1.08	1.20	1.58	2.26	5.94	31.7			
	4-monthly	1.00	1.00	1.00	1.00	1.00	1.00	1.00	1.00	1.00	1.00	1.01	1.06	1.41	1.79	3.88	18.6			
	6-monthly	1.00	1.00	1.00	1.00	1.00	1.00	1.00	1.00	1.00	1.00	1.00	1.01	1.12	1.36	2.22	8.27			
D	Weekly	1.00	1.00	1.15	1.49	2.04	6.10	21.5	81.8											
	Monthly	1.00	1.00	1.00	1.00	1.13	1.57	4.36	13.7	48.0										
	2-monthly	1.00	1.00	1.00	1.00	1.00	1.14	2.26	5.28	19.0										
	3-monthly	1.00	1.00	1.00	1.00	1.00	1.02	1.49	3.13	11.8										
	4-monthly	1.00	1.00	1.00	1.00	1.00	1.00	1.21	2.38	7.15										
	6-monthly	1.00	1.00	1.00	1.00	1.00	1.00	1.06	1.62	4.14										
Z	Weekly	1.00	1.00	1.01	1.13	1.34	1.91	2.95	5.95	13.4	45.4	363	363	363						
	Monthly	1.00	1.00	1.00	1.00	1.00	1.04	1.18	1.68	3.00	6.00	28.0	84.0	84.0						
	2-monthly	1.00	1.00	1.00	1.00	1.00	1.00	1.02	1.14	1.65	3.36	9.33	42.0	42.0						
	3-monthly	1.00	1.00	1.00	1.00	1.00	1.00	1.01	1.01	1.34	2.31	6.38	27.7	27.7						
	4-monthly	1.00	1.00	1.00	1.00	1.00	1.00	1.00	1.00	1.17	1.80	4.50	20.3	20.3						
	6-monthly	1.00	1.00	1.00	1.00	1.00	1.00	1.00	1.00	1.01	1.25	3.29	13.2	13.2						
		SITKA (Φ = +60°.0), based on data for 26 years, 1905-30																		
H	Weekly	1.00	1.03	1.35	1.71	2.04	2.70	3.40	4.28	5.73	7.13	9.23	12.7	17.7	22.4	33.7	49.9	192		
	Monthly	1.00	1.00	1.01	1.06	1.15	1.28	1.42	1.63	1.94	2.29	2.69	3.25	3.95	5.67	7.61	10.8	39.0		
	2-monthly	1.00	1.00	1.00	1.01	1.05	1.10	1.15	1.25	1.41	1.63	1.88	2.17	2.57	3.14	3.99	5.27	17.3		
	3-monthly	1.00	1.00	1.00	1.01	1.02	1.03	1.06	1.12	1.23	1.38	1.62	1.81	2.00	2.40	2.98	3.88	11.1	310	
	4-monthly	1.00	1.00	1.00	1.00	1.01	1.01	1.03	1.08	1.15	1.27	1.46	1.63	1.73	2.03	2.36	3.00	8.13	155	
	6-monthly	1.00	1.00	1.00	1.00	1.00	1.00	1.00	1.05	1.08	1.17	1.28	1.40	1.52	1.77	1.99	2.27	5.20	61.4	
D	Weekly	1.00	1.01	1.17	1.58	2.28	4.47	7.79	12.7	20.2	30.8	43.7	67.8	113	169	226	338	452	1355	
	Monthly	1.00	1.00	1.00	1.02	1.14	1.63	2.42	3.55	4.66	7.43	11.1	15.6	31.2	44.6	62.4	104	156.0	312	312
	2-monthly	1.00	1.00	1.00	1.00	1.02	1.25	1.71	2.27	3.03	4.26	5.83	8.51	15.0	21.0	35.0	52.5	78.8	158	158
	3-monthly	1.00	1.00	1.00	1.00	1.01	1.13	1.46	1.83	2.42	3.26	4.25	5.85	9.69	12.9	20.7	34.4	51.7	103	103
	4-monthly	1.00	1.00	1.00	1.00	1.00	1.08	1.32	1.59	2.12	2.73	3.40	4.68	7.54	9.97	14.0	23.8	38.6	77.2	77.2
	6-monthly	1.00	1.00	1.00	1.00	1.00	1.05	1.22	1.40	1.78	2.24	2.62	3.57	5.69	6.40	8.30	14.6	25.6	51.2	51.2
Z	Weekly	1.00	1.04	1.21	1.45	1.71	2.40	3.30	4.84	8.11	15.7	34.7	64.5	150	338	451				
	Monthly	1.00	1.00	1.01	1.02	1.07	1.22	1.46	1.74	2.58	4.22	7.80	14.2	39.0	104	156				
	2-monthly	1.00	1.00	1.00	1.01	1.02	1.07	1.18	1.38	1.73	2.70	4.09	7.23	17.3	38.9	51.8				
	3-monthly	1.00	1.00	1.00	1.00	1.01	1.01	1.10	1.24	1.48	2.05	3.13	4.92	10.0	23.8	34.4				
	4-monthly	1.00	1.00	1.00	1.00	1.00	1.01	1.06	1.14	1.33	1.68	2.47	3.91	7.19	15.4	22.1	309			
	6-monthly	1.00	1.00	1.00	1.00	1.00	1.00	1.03	1.09	1.19	1.35	2.01	2.82	5.29	11.8	16.2	51.2	154		

Table 112. Expectation of average number of time-periods elapsing before weekly, 1-, 2-, 3-, 4-, and 6-monthly ranges in horizontal intensity (H), magnetic declination (D), and vertical intensity (Z) will exceed various magnitudes at Tromsö, Sitka, Cheltenham, and Honolulu--concluded

(Expectancies based on 8 years of data from Tromsö Observatory and 26 years of data at each from Sitka, Cheltenham, and Honolulu Observatories)

Element	Time-period	Expected average number of time-periods elapsing before ranges exceed magnitude in γ of																		
		0	50	100	150	200	300	400	500	600	700	800	900	1000	1100	1200	1300	1400	1500	1600
		CHELTENHAM (Φ = 50°.1), based on data for 26 years, 1905-30																		
H	Weekly	1.00	1.04	2.26	6.62	16.2	54.3	90.5	136	194	271	678	1357							
	Monthly	1.00	1.00	1.13	1.86	4.05	13.6	20.8	31.2	44.6	52.0	156	156	312	312	312				
	2-monthly	1.00	1.00	1.07	1.35	2.24	6.48	10.7	15.6	22.1	25.9	77.8	77.8	156	156	156				
	3-monthly	1.00	1.00	1.04	1.21	1.81	4.49	7.56	10.7	14.8	17.2	51.7	51.7	103	103	103				
	4-monthly	1.00	1.00	1.02	1.13	1.41	3.51	5.52	7.92	10.7	12.9	38.6	38.6	77.2	77.2	77.2				
	6-monthly	1.00	1.00	1.00	1.07	1.22	2.62	3.99	5.39	6.82	8.53	23.6	25.6	51.2	51.2	51.2				
D	Weekly	1.00	1.04	1.84	4.36	10.36	42.4	113	226	271	271	452	678	678	678	1357	1357	1357	1357	1357
	Monthly	1.00	1.00	1.08	1.57	2.86	9.75	28.4	62.4	78.0	78.0	156	156	156	156	156	156	156	312	312
	2-monthly	1.00	1.00	1.01	1.19	1.67	5.11	13.0	31.2	39.0	39.0	78.0	78.0	78.0	78.0	78.0	78.0	78.0	156	156
	3-monthly	1.00	1.00	1.00	1.07	1.36	3.44	8.16	18.2	25.8	25.8	51.7	51.7	51.7	51.7	51.7	51.7	51.7	103	103
	4-monthly	1.00	1.00	1.00	1.05	1.25	3.00	6.72	13.4	16.3	16.3	25.8	28.1	28.1	38.6	38.6	38.6	38.6	77.2	77.2
	6-monthly	1.00	1.00	1.00	1.01	1.15	2.09	4.32	8.77	12.8	12.8	20.5	25.6	25.6	25.6	25.6	25.6	25.6	51.2	51.2
Z	Weekly	1.00	2.06	5.36	10.4	16.4	37.7	71.4	113	194	339	1357								
	Monthly	1.00	1.12	1.78	2.94	4.05	8.21	14.9	26.0	44.6	78.0	312								
	2-monthly	1.00	1.03	1.31	1.79	2.36	4.20	7.07	11.1	22.2	34.6	156								
	3-monthly	1.00	1.02	1.16	1.48	1.85	2.92	4.77	7.21	15.5	23.8	62.0	310	310	310					
	4-monthly	1.00	1.00	1.08	1.30	1.58	2.31	3.64	5.42	11.9	18.2	38.6	154	154	154					
	6-monthly	1.00	1.00	1.01	1.10	1.33	1.70	2.40	3.37	7.87	12.8	27.9	61.4	61.4	61.4					
		HONOLULU (Φ = 21°.1), based on data for 26 years, 1905-30																		
H	Weekly	1.00	1.18	3.44	11.8	28.3	136	271	271	452	1357									
	Monthly	1.00	1.00	1.35	2.79	6.64	31.2	62.4	78.0	156	312									
	2-monthly	1.00	1.00	1.11	1.64	3.32	13.6	31.2	39.0	78.0	106									
	3-monthly	1.00	1.00	1.05	1.38	2.40	9.12	20.7	25.8	51.7	103									
	4-monthly	1.00	1.00	1.02	1.20	1.97	6.18	15.4	19.3	38.6	77.2									
	6-monthly	1.00	1.00	1.00	1.11	1.56	3.95	10.2	12.8	25.7	51.3									
D	Weekly	1.00	1.18	13.3	194	1358	1358													
	Monthly	1.00	1.04	3.45	34.7	106	106													
	2-monthly	1.00	1.01	2.27	18.3	156	156													
	3-monthly	1.00	1.01	1.69	11.5	103	103													
	4-monthly	1.00	1.00	1.57	8.35	77.2	77.2													
	6-monthly	1.00	1.00	1.31	5.50	51.3	51.3													
Z	Weekly	1.00	4.15	226	452	1356														
	Monthly	1.00	1.51	52.0	104	312														
	2-monthly	1.00	1.14	24.0	51.8	156														
	3-monthly	1.00	1.06	12.9	34.4	103														
	4-monthly	1.00	1.02	9.09	25.8	77.2														
	6-monthly	1.00	1.00	4.53	17.1	51.3														

Table 113. Total number of fluctuations of various rates of change and semidurations for H, D, and Z, Petsamo September 1, 1932, to August 31, 1933

Semi-duration, sec	Number of fluctuations for rate of change in γ/sec																	
	Horizontal intensity						Declination						Vertical intensity					
	1	2	4	6	8	Total	1	2	4	6	8	Total	1	2	4	6	8	Total
10	421	141	33	13	13	621	985	135	28	9	11	1,168	67	35	11	7	3	123
20	848	296	49	6	3	1,202	970	105	8	2	3	1,088	294	120	27	8	3	452
30	812	231	47	1	0	1,091	597	75	7	0	0	679	309	112	27	2	0	450
40	493	139	20	8	0	660	342	52	2	1	0	397	196	85	16	1	0	298
50	353	109	22	1	2	487	243	33	4	2	0	282	151	59	23	3	2	238
60	196	54	12	1	0	263	136	20	3	0	0	159	102	33	4	2	1	142
70	177	38	3	3	0	221	116	13	2	0	0	131	50	36	6	0	0	92
80	102	32	8	1	1	144	80	12	1	0	0	93	41	16	6	3	0	66
90	88	16	3	0	0	107	52	2	1	0	0	55	29	17	4	0	0	50
100	79	36	11	0	0	126	49	8	0	0	0	57	57	16	2	0	0	75
110	46	14	2	2	0	64	34	2	2	0	0	38	26	6	5	1	0	38
120	33	11	4	2	0	50	37	1	0	0	0	38	23	6	3	0	1	33
130	21	11	2	1	0	35	27	2	0	0	0	29	15	6	1	1	0	23
140	21	4	1	0	0	26	17	3	0	0	0	20	16	5	3	0	0	24
150	22	16	1	0	0	39	16	0	0	0	0	16	15	8	1	0	0	24
160	10	2	0	0	0	12	7	0	0	0	0	7	3	5	0	0	0	8
170	9	3	0	0	0	12	15	1	0	0	1	17	4	6	0	0	0	10
180	8	4	0	0	0	12	6	2	0	0	0	8	2	4	0	0	0	6
190	4	2	1	0	0	7	2	1	0	0	0	3	9	5	0	0	0	14
200	12	4	0	0	0	16	10	1	0	0	0	11	11	2	0	0	0	13
210	3	1	0	0	0	4	4	1	0	0	0	5	4	0	0	0	0	4
220	4	5	1	0	0	10	3	0	0	0	0	3	8	1	0	0	0	9
230	4	2	0	0	0	6	3	1	0	0	0	4	2	2	1	0	0	5
240	6	3	0	0	0	9	4	1	0	0	0	5	2	2	1	0	0	5
250	4	1	1	0	0	6	7	0	0	0	0	7	4	1	1	0	0	6
260	4	2	0	0	0	6	3	0	0	0	0	3	1	1	0	0	0	2
270	3	1	0	0	0	4	3	0	0	0	0	3	1	4	1	0	0	6
280	3	2	0	0	0	5	1	0	0	0	0	1	0	2	0	0	0	2
Total	3,786	1,180	221	39	19	5,245	3,769	471	58	14	15	4,327	1,442	595	143	28	10	2,218

Table 114. Total number of fluctuations of various rates of change and semidurations for H, D, and Z, Copenhagen, September 1, 1932, to August 31, 1933

Semi-duration sec	Number of fluctuations for rate of change in γ/sec																							
	Horizontal intensity											Declination[a]									Vertical intensity[a]			
	0.1	0.2	0.4	0.6	0.8	1	2	4	6	8	Total	0.1	0.2	0.4	0.6	0.8	1	2	4	Total	0.1	0.2	0.4	Total
10	9,011	6,555	997	130	98	24	2	0	0	1	16,818	3,958	5,670	1,169	113	51	4	2	1	10,968	8	9	0	17
20	20,208	9,620	1,073	110	29	20	0	0	1	0	31,061	7,395	6,396	892	128	24	4	1	0	14,840	40	8	0	48
30	10,651	3,634	505	41	21	6	1	0	0	0	14,859	4,044	2,958	284	22	5	3	0	0	7,316	46	6	0	52
40	3,663	1,132	160	13	6	3	0	0	0	0	4,977	1,700	685	72	13	4	1	0	0	2,475	23	7	0	30
50	1,729	414	64	13	4	1	0	0	0	0	2,225	875	235	24	3	1	0	0	0	1,138	23	0	0	23
60	797	200	26	3	1	0	0	0	0	0	1,027	393	100	16	0	1	0	0	0	510	7	4	0	11
70	418	96	11	2	0	2	0	0	0	0	529	281	50	10	0	0	0	0	0	341	12	1	0	13
80	259	50	12	1	0	0	0	0	0	0	322	148	24	4	2	0	1	0	0	179	8	1	0	9
90	154	38	4	1	1	0	0	0	0	0	198	91	13	3	1	0	0	0	0	108	5	0	0	5
100	184	40	5	0	0	0	0	0	0	0	229	91	8	2	0	0	0	0	0	101	7	1	0	8
110	85	13	3	2	0	2	0	0	0	0	105	30	9	1	0	1	0	0	0	41	4	1	1	6
120	88	17	2	1	0	0	0	0	0	0	108	46	10	4	0	0	0	0	0	60	8	2	0	10
130	64	13	3	0	1	0	0	0	0	0	81	22	2	3	0	1	0	0	0	28	5	1	0	6
140	57	10	2	1	0	0	0	0	0	0	70	29	3	1	0	0	0	0	0	33	2	1	0	3
150	58	12	1	0	0	0	0	0	0	0	71	36	4	1	0	1	0	0	0	42	6	2	1	9
160	16	8	0	0	0	0	0	0	0	0	24	14	0	0	0	0	0	0	0	14	4	0	0	4
170	29	7	1	0	0	0	0	0	0	0	37	10	1	0	0	0	0	0	0	11	0	1	0	1
180	18	7	1	0	0	0	0	0	0	0	26	16	1	0	0	0	0	0	0	17	4	2	0	6
190	15	4	3	1	0	0	0	0	0	0	23	8	1	0	0	0	0	0	0	9	2	2	1	5
200	22	4	0	0	0	0	0	0	0	0	26	14	3	1	0	0	0	0	0	18	6	2	1	9
210	12	4	2	0	0	0	0	0	0	0	18	6	1	1	0	0	0	0	0	8	1	1	0	2
220	12	1	0	0	0	0	0	0	0	0	13	5	2	0	0	0	0	0	0	7	2	2	1	5
230	11	3	0	0	0	0	0	0	0	0	14	6	2	1	0	0	0	0	0	9	4	1	1	6
240	5	0	0	0	0	0	0	0	0	0	5	5	1	1	0	0	0	0	0	7	4	0	1	5
250	17	2	0	0	0	0	0	0	0	0	19	5	5	0	0	0	0	0	0	10	8	2	0	10
260	7	0	0	0	0	0	0	0	0	0	7	1	2	0	0	0	0	0	0	3	1	1	0	2
270	6	0	0	0	1	0	0	0	0	0	7	4	2	0	0	0	0	0	0	6	2	0	0	2
Total	47,596	21,884	2,875	319	162	58	3	0	1	1	72,899	19,233	16,188	2,490	282	89	13	3	1	38,299	242	58	7	307

[a]There were no fluctuations in D for 6 and 8 γ/sec and in Z for 0.6, 0.8, 1, 2, 4, 6, and 8 γ/sec.

Table 115. Frequency distribution of fluctuations in horizontal intensity of various amplitudes and durations of five minutes or more, Petsamo, December, 1932

Duration, minutes	Number of fluctuations of amplitude in γ from													
	0-10	11-20	21-30	31-40	41-50	51-60	61-70	71-80	81-90	91-100	101-150	151-200	> 200	Total
						Number of positive fluctuations								
5 - 7.5	20	16	3	4	3	3	1	0	0	0	0	0	0	50
7.5- 12.5	14	14	7	5	3	3	1	1	2	2	4	0	0	56
12.5- 17.5	6	7	7	4	2	2	2	0	0	0	0	0	0	30
17.5- 22.5	2	6	0	3	1	2	0	0	0	0	2	0	1	17
22.5- 27.5	1	1	5	1	3	0	1	2	0	0	2	0	0	16
27.5- 32.5	1	3	2	1	1	1	1	0	0	1	0	0	0	11
32.5- 37.5	1	2	0	1	0	0	0	0	0	1	0	0	0	5
37.5- 42.5	0	0	1	0	1	1	0	0	0	1	0	1	0	5
42.5- 47.5	1	0	1	3	0	0	0	0	0	0	2	0	0	7
47.5- 52.5	0	1	2	0	1	0	0	0	0	0	0	1	0	5
52.5- 62.5	0	1	0	0	1	0	1	0	0	1	0	1	0	5
62.5- 72.5	0	0	0	0	0	0	0	0	1	0	0	0	0	1
72.5- 82.5	0	0	0	0	1	0	0	0	0	0	0	1	1	3
82.5- 92.5	0	0	0	0	0	1	0	0	0	0	0	0	0	1
92.5-102.5	0	0	0	0	1	0	0	0	0	0	1	0	0	2
102.5-122.5	0	0	0	0	0	0	0	1	0	0	0	0	1	2
122.5-142.5	0	0	0	0	0	0	0	0	0	1	0	0	0	1
142.5-162.5	0	0	0	0	0	0	0	0	0	0	0	0	1	1
162.5-182.5	0	0	1	0	0	0	0	0	0	0	1	0	0	2
182.5-202.5	0	0	0	0	0	0	0	0	0	0	1	1	2	4
>202.5	0	0	0	0	0	0	0	0	0	0	0	0	0	0
Total positive	46	51	28	23	18	13	7	4	3	7	13	5	6	224
						Number of negative fluctuations								
5 - 7.5	139	81	30	16	5	7	5	1	11	1	4	2	1	293
7.5- 12.5	52	58	25	8	7	7	4	4	0	4	6	3	2	180
12.5- 17.5	25	39	11	8	5	5	2	2	3	1	12	7	6	126
17.5- 22.5	13	19	12	9	4	2	1	0	0	2	3	0	1	66
22.5- 27.5	2	10	6	5	1	2	1	1	0	1	2	1	2	34
27.5- 32.5	4	6	5	0	0	1	0	2	0	1	3	1	0	23
32.5- 37.5	0	2	0	0	0	0	0	1	0	1	0	2	0	6
37.5- 42.5	1	0	3	2	0	1	0	0	0	1	0	1	1	10
42.5- 47.5	0	3	2	1	0	0	0	1	0	0	0	0	1	8
47.5- 52.5	3	0	1	0	3	0	0	0	0	1	2	0	1	11
52.5- 62.5	3	2	1	1	1	0	0	0	0	0	0	1	1	10
62.5- 72.5	0	2	2	2	1	0	1	0	0	0	0	0	0	8
72.5- 82.5	0	0	0	0	0	0	0	0	0	0	0	0	1	1
82.5- 92.5	0	0	2	0	1	0	1	0	0	0	0	0	4	8
92.5-102.5	0	0	0	0	0	0	0	0	0	0	0	1	0	1
102.5-122.5	0	0	1	0	0	0	0	0	0	0	1	0	1	3
122.5-142.5	0	0	0	0	0	0	0	0	0	0	0	1	1	2
142.5-162.5	0	0	0	0	1	0	0	0	1	0	0	0	0	2
162.5-182.5	0	0	1	0	0	0	0	0	0	0	0	0	1	2
182.5-202.5	0	0	0	0	0	0	0	0	0	0	0	0	2	2
>202.5	0	0	0	0	0	1	0	0	0	0	2	1	7	11
Total negative	242	222	102	53	28	26	15	13	4	13	35	21	33	807

Table 116. Frequency distribution of number of fluctuations in horizontal intensity of various amplitudes and durations of five minutes or more. Copenhagen, December, 1932

Duration, minutes	Number of fluctuations of amplitude in γ from															
	0-10	11-20	21-30	31-40	41-50	51-60	61-70	Total	0-10	11-20	21-30	31-40	41-50	51-60	61-70	Total
	Positive fluctuations								Negative fluctuations							
5 - 7.5	52	4	2	0	0	0	0	58	9	1	0	1	0	0	0	11
7.5- 12.5	30	12	3	0	1	0	0	46	4	1	0	0	0	0	0	5
12.5- 17.5	18	7	4	0	1	0	0	30	5	2	0	0	0	0	0	7
17.5- 22.5	8	1	5	0	1	0	0	15	3	3	0	0	0	1	0	7
22.5- 27.5	14	3	2	1	2	0	0	22	7	3	0	0	1	0	0	11
27.5- 32.5	9	6	7	0	2	0	0	24	2	0	0	0	1	0	0	3
32.5- 37.5	1	5	1	1	1	1	0	10	1	0	0	0	0	0	0	1
37.5- 42.5	3	4	0	1	0	0	0	8	0	2	1	0	0	0	0	3
42.5- 47.5	0	5	4	1	0	0	0	10	0	1	1	0	0	0	0	2
47.5- 52.5	2	5	0	1	1	0	0	9	0	1	1	0	0	0	0	2
52.5- 62.5	2	3	1	3	0	1	0	10	0	0	1	1	1	0	0	3
62.5- 72.5	1	2	2	0	0	0	0	5	1	1	2	0	0	1	0	5
72.5- 82.5	0	1	2	0	2	1	1	7	0	3	1	1	0	0	0	5
82.5- 92.5	0	1	0	0	0	0	0	1	0	0	0	0	1	0	0	1
92.5-102.5	0	2	0	0	0	0	0	2	0	0	0	0	0	0	0	0
102.5-122.5	0	0	1	2	0	0	0	3	0	0	0	0	1	0	0	1
122.5-142.5	0	0	0	0	0	0	0	0	0	1	0	0	0	0	0	1
142.5-162.5	0	0	0	0	0	0	0	0	0	0	0	1	0	0	0	1
>162.5	0	0	0	0	1	0	0	1	0	0	0	0	0	0	0	0
Total	140	61	34	10	12	3	1	261	32	19	7	4	5	2	0	69

Table 117. Sensitivities and return-time-constants of fluxmeters, College, Alaska

Date	H-fluxmeter			Z-fluxmeter		
	Scale value	Return-time-constant		Scale value	Return-time-constant	
		+	-		+	-
	γ/mm	sec	sec	γ/mm	sec	sec
Jul 28, 1942[a]	3.54	35	32	4.42	22	25
Aug 31, 1942	3.52	80	104	3.85	51	70
Nov 22, 1942[b]	3.52	24	22	3.85	32	30
Dec 22, 1942	3.39	28	20	3.97	22	27
Jan 26, 1943	3.39	25	22	3.97	30	23
Jan 28, 1943	3.39	40	38	3.97	38	37
Apr 23, 1943	3.49	29	28	3.69	20	21

[a]Basic element of Z-fluxmeter replaced August 3, 1942
[b]Basic elements adjusted to reduce return-time-constant

Table 118. Resistances in ohms of H- and Z-coils, fluxmeter installation, College, Alaska

Date	1	2	3	4	5	1-5
			H-coil			
Jul 29, 1942	78.29	78.43	78.33	78.43	78.99	
Nov 17, 1942	75.00	75.15	75.07	75.84	76.41	374.0(?)
Dec 4, 1942	74.82	74.94	74.87	74.97	74.90	374.3
Dec 21, 1942	74.62	74.73	74.66	74.74	74.71	371.9
Jan 26, 1943	74.27	74.39	74.33	74.44	74.76	370.3
Feb 25, 1943	74.16	74.27	74.20	74.30	74.85	369.7
Mar 30, 1943	74.07	74.19	74.12	74.20	74.76	369.2
Apr 14, 1943	74.12	74.23	74.16	74.32	74.34	372.4
Apr 23, 1943	74.19	74.26	74.17	74.31	74.35	369.4
			Z-coil			
Jul 29, 1942	79.29	79.04	78.86	79.08	79.08	390.82
Nov 17, 1942	75.32	75.00	74.61	74.80	74.77	373.0
Dec 4, 1942	75.12	74.75	74.47	74.65	74.48	372.1
Dec 21, 1942	74.97	74.60	74.18	74.48	74.42	371.2
Jan 26, 1943	74.65	74.31	73.74	74.18	74.09	369.6
Feb 25, 1943	74.57	74.25	73.39	74.11	74.06	369.2
Mar 30, 1943	74.64	74.31	73.33	74.20	74.16	369.4
Apr 14, 1943	74.61	74.28	73.10	74.17	74.12	369.3
Apr 23, 1943	74.59	74.27	73.00	74.16	74.13	369.4

Table 119. Determination with standard mutual inductor of sensitivities of H- and Z-fluxmeters, College, Alaska; I = primary current in milliamperes

Element	I	Deflection (scale divisions)			Maxwell-turns per division
		Positive	Negative	Mean	
H	50	4.4	4.45	4.42	11.32
	100	8.75	8.8	8.78	11.40
	150	13.1	13.4	13.25	11.32
	200	17.2	17.7	17.45	11.47
				Mean	11.38
Z	50	4.1	4.1	4.10	12.21
	100	7.9	8.0	7.95	12.59
	150	11.7	12.0	11.85	12.65
	200	15.4	15.8	15.6	12.82
				Mean	12.57

Table 120. Frequency distribution of fluctuations in horizontal intensity of various amplitudes and durations measured at half-amplitude and also corresponding frequencies (in parentheses) roughly corrected for response defects of fluxmeter, College, Alaska, August, 1942

Duration, seconds	Number of fluctuations of amplitude in γ from 25-34	35-44	45-54	55-64	65-74	75-84	85-94	95-104	105-114	115-124	125-134	135-144	145-194	195-254	Total
							Positive fluctuations								
15-24 (16-26)	8 (8)	3 (0)	1 (3)	0 (1)	0 (0)	0 (0)	0 (0)	0 (0)	0 (0)	0 (0)	0 (0)	0 (0)	0 (0)	0 (0)	12 (12)
25-34 (27-38)	10 (0)	7 (10)	4 (7)	3 (4)	0 (3)	0 (0)	0 (0)	1 (0)	0 (0)	0 (1)	0 (0)	0 (0)	0 (0)	0 (0)	25 (25)
35-44 (39-50)	9 (0)	16 (9)	9 (16)	2 (0)	1 (9)	2 (2)	0 (1)	0 (2)	0 (0)	1 (0)	0 (0)	0 (0)	0 (1)	0 (0)	40 (40)
45-54 (51-63)	15 (0)	7 (15)	4 (0)	3 (7)	2 (4)	2 (0)	0 (3)	0 (2)	0 (2)	1 (0)	0 (0)	0 (0)	0 (1)	0 (0)	34 (34)
55-64 (64-76)	20 (0)	10 (0)	5 (20)	6 (10)	3 (0)	2 (5)	0 (0)	0 (0)	0 (3)	0 (2)	0 (0)	0 (0)	0 (0)	0 (0)	46 (46)
65-74 (77-89)	12 (0)	13 (0)	4 (12)	3 (0)	0 (13)	3 (4)	1 (0)	2 (3)	0 (0)	0 (0)	1 (0)	0 (3)	0 (3)	0 (1)	39 (39)
75-84 (90-103)	5 (0)	4 (0)	4 (0)	3 (5)	1 (4)	2 (0)	1 (4)	0 (0)	0 (3)	0 (0)	0 (1)	0 (0)	0 (3)	0 (0)	20 (20)
85-94 (104-117)	0 (0)	0 (0)	0 (0)	0 (0)	0 (0)	0 (0)	0 (0)	1 (0)	0 (0)	0 (0)	0 (0)	0 (0)	0 (0)	0 (1)	1 (1)
Total	79 (8)	60 (34)	31 (58)	20 (27)	7 (33)	11 (11)	2 (14)	4 (7)	0 (8)	2 (3)	1 (1)	0 (3)	0 (8)	0 (2)	217 (217)
							Negative fluctuations								
15-24 (16-26)	3 (3)	4 (0)	1 (4)	1 (1)	0 (1)	0 (0)	0 (0)	0 (0)	0 (0)	0 (0)	0 (0)	0 (0)	0 (0)	0 (0)	9 (9)
25-34 (27-38)	10 (0)	8 (10)	1 (8)	2 (1)	0 (2)	0 (0)	1 (0)	0 (0)	0 (1)	0 (0)	0 (0)	0 (0)	0 (0)	0 (0)	22 (22)
35-44 (39-50)	6 (0)	12 (6)	2 (12)	4 (0)	0 (2)	1 (4)	0 (0)	0 (1)	0 (0)	0 (0)	0 (0)	0 (0)	0 (0)	1 (1)	26 (26)
45-54 (51-63)	4 (0)	10 (4)	0 (0)	2 (10)	0 (0)	1 (0)	0 (2)	0 (0)	0 (1)	0 (0)	0 (0)	0 (0)	0 (0)	0 (0)	17 (17)
55-64 (64-76)	7 (0)	10 (0)	2 (7)	5 (10)	2 (0)	3 (2)	0 (5)	0 (0)	1 (2)	2 (3)	0 (0)	0 (0)	0 (3)	1 (1)	33 (33)
65-74 (77-89)	4 (0)	9 (0)	2 (4)	2 (0)	1 (9)	2 (2)	0 (0)	1 (2)	0 (0)	0 (1)	0 (0)	1 (2)	0 (1)	0 (1)	22 (22)
75-84 (90-103)	0 (0)	4 (0)	1 (0)	1 (0)	0 (4)	1 (0)	0 (1)	1 (0)	0 (1)	0 (0)	0 (0)	0 (0)	0 (2)	0 (0)	8 (8)
85-94 (104-117)	0 (0)	1 (0)	0 (0)	1 (0)	0 (0)	0 (1)	0 (0)	0 (0)	0 (0)	0 (1)	0 (0)	0 (0)	0 (0)	0 (0)	2 (2)
Total	34 (3)	58 (20)	9 (35)	18 (22)	3 (18)	8 (9)	1 (8)	2 (3)	1 (5)	2 (5)	0 (0)	1 (2)	0 (6)	2 (3)	139 (139)

Table 121. Frequency distribution of fluctuations in vertical intensity of various amplitudes and durations measured at half-amplitude and also corresponding frequencies (in parentheses) roughly corrected for response defects of fluxmeter, College, Alaska, August, 1942

Duration, seconds	Number of fluctuations of amplitude in γ from									
	25-34	35-44	45-54	55-64	65-74	75-84	85-94	95-104	105-114	Total
Positive fluctuations										
15-24 (16-27)	0 (0)	0 (0)	0 (0)	0 (0)	0 (0)	0 (0)	0 (0)	0 (0)	0 (0)	0 (0)
25-34 (28-40)	2 (0)	0 (2)	0 (0)	0 (0)	0 (0)	0 (0)	0 (0)	0 (0)	0 (0)	2 (2)
35-44 (41-53)	2 (0)	1 (0)	0 (2)	0 (1)	0 (0)	0 (0)	0 (0)	0 (0)	0 (0)	3 (3)
45-54 (54-67)	0 (0)	1 (0)	0 (0)	0 (0)	0 (1)	0 (0)	0 (0)	0 (0)	0 (0)	1 (1)
55-64 (68-81)	1 (0)	1 (0)	1 (0)	0 (1)	0 (0)	0 (1)	0 (0)	0 (1)	0 (0)	3 (3)
65-74 (82-94)	1 (0)	0 (0)	0 (0)	0 (1)	0 (0)	0 (0)	0 (0)	0 (0)	0 (0)	1 (1)
75-84 (95-108)	1 (0)	0 (0)	0 (0)	0 (0)	0 (1)	0 (0)	0 (0)	0 (0)	0 (0)	1 (1)
85-94 (109-122)	1 (0)	0 (0)	0 (0)	0 (0)	0 (0)	0 (1)	0 (0)	0 (0)	0 (0)	1 (1)
Total	8 (0)	3 (2)	1 (2)	0 (3)	0 (2)	0 (2)	0 (0)	0 (1)	0 (0)	12 (12)
Negative fluctuations										
15-24 (16-27)	0 (0)	0 (0)	0 (0)	0 (0)	0 (0)	0 (0)	0 (0)	0 (0)	0 (0)	0 (0)
25-34 (28-40)	0 (0)	0 (0)	0 (0)	0 (0)	0 (0)	0 (0)	0 (0)	0 (0)	0 (0)	0 (0)
35-44 (41-53)	1 (0)	0 (0)	0 (1)	0 (0)	0 (0)	0 (0)	0 (0)	0 (0)	0 (0)	1 (1)
45-54 (54-67)	3 (0)	0 (0)	1 (3)	0 (0)	0 (0)	0 (0)	0 (1)	0 (0)	0 (0)	4 (4)
55-64 (68-81)	3 (0)	0 (0)	0 (0)	0 (3)	0 (0)	0 (0)	0 (0)	0 (0)	0 (0)	3 (3)
65-74 (82-94)	1 (0)	0 (0)	0 (0)	0 (1)	0 (0)	0 (0)	0 (0)	0 (0)	0 (0)	1 (1)
75-84 (95-108)	0 (0)	0 (0)	0 (0)	0 (0)	0 (0)	0 (0)	0 (0)	0 (0)	0 (0)	0 (0)
85-94 (109-122)	1 (0)	1 (0)	0 (0)	0 (0)	0 (0)	0 (1)	0 (0)	0 (0)	0 (1)	2 (2)
Total	9 (0)	1 (0)	1 (4)	0 (4)	0 (0)	0 (1)	0 (1)	0 (0)	0 (1)	11 (11)

Table 122. Total number of fluctuations in horizontal intensity of various rates of change and durations measured at half-amplitude and also corresponding frequencies (in parentheses) corrected for response defects of fluxmeter, College, Alaska, August, 1942

Duration, seconds	Number of fluctuations with rates of change in γ/sec											
	0.4	0.6	0.8	1.0	2.0	4.0	6.0	8.0	10.0	12.0	16.0	Total
	Fluctuations, initial rate											
15-24 (16-26)	0 (0)	2 (2)	1 (1)	2 (2)	12 (12)	3 (3)	1 (1)	0 (0)	0 (0)	0 (0)	0 (0)	21 (21)
25-34 (27-38)	1 (1)	0 (0)	0 (0)	11 (11)	28 (28)	5 (5)	2 (2)	0 (0)	0 (0)	0 (0)	0 (0)	47 (47)
35-44 (39-50)	3 (3)	4 (0)	5 (4)	18 (23)	26 (26)	9 (9)	0 (0)	0 (0)	1 (0)	0 (1)	0 (0)	66 (66)
45-54 (51-63)	3 (0)	4 (3)	5 (4)	22 (27)	14 (14)	1 (0)	2 (1)	0 (2)	0 (0)	0 (0)	0 (0)	51 (51)
55-64 (64-76)	9 (0)	7 (9)	13 (7)	19 (32)	27 (27)	3 (0)	0 (3)	0 (0)	0 (0)	1 (0)	0 (1)	79 (79)
65-74 (77-89)	6 (0)	10 (6)	11 (10)	15 (26)	13 (13)	6 (0)	0 (6)	0 (0)	0 (0)	0 (0)	0 (0)	61 (61)
75-84 (90-103)	0 (0)	4 (0)	5 (0)	11 (9)	8 (11)	0 (8)	0 (0)	0 (0)	0 (0)	0 (0)	0 (0)	28 (28)
85-94 (104-117)	0 (0)	0 (0)	0 (0)	1 (0)	1 (1)	1 (1)	0 (1)	0 (0)	0 (0)	0 (0)	0 (0)	3 (3)
Total	22 (4)	31 (20)	40 (26)	99 (130)	129 (132)	28 (26)	5 (14)	0 (2)	1 (0)	1 (1)	0 (1)	356 (356)
	Fluctuations, recovery rate											
15-24 (16-26)	0 (0)	1 (1)	0 (0)	1 (1)	17 (17)	1 (1)	1 (1)	0 (0)	0 (0)	0 (0)	0 (0)	21 (21)
25-34 (27-38)	1 (1)	1 (1)	4 (4)	13 (13)	20 (20)	8 (8)	0 (0)	0 (0)	0 (0)	0 (0)	0 (0)	47 (47)
35-44 (39-50)	5 (5)	2 (2)	3 (3)	16 (16)	32 (32)	2 (2)	3 (3)	1 (1)	1 (1)	0 (0)	0 (0)	65 (65)
45-54 (51-63)	1 (1)	4 (4)	7 (7)	17 (17)	20 (20)	1 (1)	1 (1)	0 (0)	0 (0)	0 (0)	0 (0)	51 (51)
55-64 (64-76)	6 (6)	8 (8)	17 (17)	21 (21)	21 (21)	4 (4)	2 (2)	0 (0)	0 (0)	0 (0)	0 (0)	79 (79)
65-74 (77-89)	11 (11)	7 (7)	10 (10)	21 (21)	11 (11)	1 (1)	0 (0)	0 (0)	0 (0)	0 (0)	0 (0)	61 (61)
75-84 (90-103)	4 (4)	2 (0)	6 (2)	12 (18)	3 (3)	1 (1)	0 (0)	0 (0)	0 (0)	0 (0)	0 (0)	28 (28)
85-94 (104-117)	0 (0)	1 (0)	0 (1)	0 (0)	1 (1)	1 (0)	0 (1)	0 (0)	0 (0)	0 (0)	0 (0)	3 (3)
Total	28 (28)	26 (23)	47 (44)	101 (107)	125 (125)	19 (18)	7 (8)	1 (1)	1 (1)	0 (0)	0 (0)	355 (355)

Table 123. Total number of fluctuations in vertical intensity of various rates of change and durations measured at half-amplitude and also corresponding frequencies (in parentheses) corrected for response defects of fluxmeter, College, Alaska, August, 1942

Duration, seconds	Number of fluctuations with rates of change in γ/sec											
	0.4	0.6	0.8	1.0	2.0	4.0	6.0	8.0	10.0	12.0	16.0	Total
	Fluctuations, initial rate											
15-24 (16-27)	0 (0)	0 (0)	0 (0)	0 (0)	0 (0)	0 (0)	0 (0)	0 (0)	0 (0)	0 (0)	0 (0)	0 (0)
25-34 (28-40)	0 (0)	0 (0)	0 (0)	0 (0)	0 (0)	0 (0)	0 (0)	0 (0)	0 (0)	0 (0)	0 (0)	0 (0)
35-44 (41-53)	0 (0)	0 (0)	0 (0)	1 (1)	2 (2)	0 (0)	0 (0)	0 (0)	0 (0)	0 (0)	0 (0)	3 (3)
45-54 (54-67)	0 (0)	1 (0)	1 (1)	4 (5)	1 (1)	0 (0)	1 (0)	0 (1)	0 (0)	0 (0)	0 (0)	8 (8)
55-64 (68-81)	0 (0)	1 (0)	1 (0)	3 (2)	1 (3)	0 (1)	0 (0)	0 (0)	0 (0)	0 (0)	0 (0)	6 (6)
65-74 (82-94)	0 (0)	0 (0)	0 (0)	2 (0)	0 (2)	0 (0)	0 (0)	0 (0)	0 (0)	0 (0)	0 (0)	2 (2)
75-84 (95-108)	0 (0)	1 (0)	0 (0)	0 (1)	0 (0)	0 (0)	0 (0)	0 (0)	0 (0)	0 (0)	0 (0)	1 (1)
85-94 (109-122)	0 (0)	0 (0)	1 (0)	1 (0)	1 (2)	0 (1)	0 (0)	0 (0)	0 (0)	0 (0)	0 (0)	3 (3)
Total	0 (0)	3 (0)	3 (1)	11 (9)	5 (10)	0 (2)	1 (0)	0 (1)	0 (0)	0 (0)	0 (0)	23 (23)
	Fluctuations, recovery rate											
15-24 (16-27)	0 (0)	0 (0)	0 (0)	0 (0)	0 (0)	0 (0)	0 (0)	0 (0)	0 (0)	0 (0)	0 (0)	0 (0)
25-34 (28-40)	0 (0)	0 (0)	0 (0)	0 (0)	0 (0)	0 (0)	0 (0)	0 (0)	0 (0)	0 (0)	0 (0)	0 (0)
35-44 (41-53)	0 (0)	0 (0)	0 (0)	1 (1)	2 (2)	0 (0)	0 (0)	0 (0)	0 (0)	0 (0)	0 (0)	3 (3)
45-54 (54-67)	0 (0)	2 (0)	1 (2)	3 (4)	2 (2)	0 (0)	0 (0)	0 (0)	0 (0)	0 (0)	0 (0)	8 (8)
55-64 (68-81)	1 (1)	1 (0)	1 (1)	2 (3)	1 (1)	0 (0)	0 (0)	0 (0)	0 (0)	0 (0)	0 (0)	6 (6)
65-74 (82-94)	0 (0)	1 (0)	1 (1)	0 (1)	0 (0)	0 (0)	0 (0)	0 (0)	0 (0)	0 (0)	0 (0)	2 (2)
75-84 (95-108)	0 (0)	1 (0)	0 (1)	0 (0)	0 (0)	0 (0)	0 (0)	0 (0)	0 (0)	0 (0)	0 (0)	1 (1)
85-94 (109-122)	1 (0)	0 (1)	2 (0)	0 (2)	0 (0)	0 (0)	0 (0)	0 (0)	0 (0)	0 (0)	0 (0)	3 (3)
Total	2 (1)	5 (1)	5 (5)	6 (11)	5 (5)	0 (0)	0 (0)	0 (0)	0 (0)	0 (0)	0 (0)	23 (23)

Table 124. Number of fluctuations for each GMT hour, College, Alaska, August, 1942

Hour, GMT	Number of fluctuations of amplitude in γ from 25-34	35-44	45-54	55-64	65-74	75-84	85-94	95-104	105-114	115-124	125-134	135-144	145-194	195-254	Total
	Horizontal intensity														
h h															
00-01	1	0	0	0	0	0	0	0	0	0	0	0	0	0	1
01-02	3	1	0	2	0	0	0	0	0	0	0	0	0	0	6
02-03	1	3	1	0	0	0	0	0	0	0	0	0	0	0	5
03-04	3	8	2	0	0	0	0	0	0	0	0	0	0	0	13
04-05	5	1	2	3	1	1	0	0	0	0	0	0	0	0	13
05-06	3	1	0	0	0	0	0	0	0	0	0	0	0	0	4
06-07	4	4	1	1	0	1	0	0	0	0	0	0	0	0	11
07-08	9	4	2	4	0	0	0	0	0	0	0	0	0	1	20
08-09	12	15	3	4	0	0	1	0	0	1	0	0	0	0	36
09-10	4	5	5	1	0	2	2	2	1	1	0	0	0	0	23
10-11	8	15	5	3	2	3	0	1	0	2	0	0	0	1	40
11-12	10	18	4	7	0	2	0	1	0	0	0	0	0	0	42
12-13	10	12	2	2	1	1	0	0	0	0	0	1	0	0	29
13-14	10	7	3	0	0	1	0	0	0	0	0	0	0	0	21
14-15	3	1	0	0	0	0	0	0	0	0	0	0	0	0	4
15-16	3	9	5	2	1	2	0	0	0	0	1	0	0	0	23
16-17	6	4	1	5	1	2	0	1	0	0	0	0	0	0	20
17-18	5	1	1	1	3	2	0	0	0	0	0	0	0	0	13
18-19	3	0	0	0	0	0	0	0	0	0	0	0	0	0	3
19-20	0	1	2	2	0	2	0	1	0	0	0	0	0	0	8
20-21	0	3	0	0	0	0	0	0	0	0	0	0	0	0	3
21-22	4	1	0	1	0	0	0	0	0	0	0	0	0	0	6
22-23	5	2	1	0	0	0	0	0	0	0	0	0	0	0	8
23-24	1	2	0	0	1	0	0	0	0	0	0	0	0	0	4
Total	113	118	40	38	10	19	3	6	1	4	1	1	0	2	356
	Vertical intensity														
00-01	0	0	0	0	0	0	0	0	0	0	0	0	0	0	0
01-02	0	1	0	0	0	0	0	0	0	0	0	0	0	0	1
02-03	0	0	0	0	0	0	0	0	0	0	0	0	0	0	0
03-04	0	0	0	0	0	0	0	0	0	0	0	0	0	0	0
04-05	0	0	0	0	0	0	0	0	0	0	0	0	0	0	0
05-06	0	0	0	0	0	0	0	0	0	0	0	0	0	0	0
06-07	0	0	0	0	0	0	0	0	0	0	0	0	0	0	0
07-08	2	1	1	0	0	0	0	0	0	0	0	0	0	0	4
08-09	0	0	0	0	0	0	0	0	0	0	0	0	0	0	0
09-10	3	0	0	0	0	0	0	0	0	0	0	0	0	0	3
10-11	2	0	0	0	0	0	0	0	0	0	0	0	0	0	2
11-12	2	0	0	0	0	0	0	0	0	0	0	0	0	0	2
12-13	2	0	0	0	0	0	0	0	0	0	0	0	0	0	2
13-14	1	1	0	0	0	0	0	0	0	0	0	0	0	0	2
14-15	0	0	0	0	0	0	0	0	0	0	0	0	0	0	0
15-16	3	1	1	0	0	0	0	0	0	0	0	0	0	0	5
16-17	2	0	0	0	0	0	0	0	0	0	0	0	0	0	2
17-18	0	0	0	0	0	0	0	0	0	0	0	0	0	0	0
18-19	0	0	0	0	0	0	0	0	0	0	0	0	0	0	0
19-20	.0	0	0	0	0	0	0	0	0	0	0	0	0	0	0
20-21	0	0	0	0	0	0	0	0	0	0	0	0	0	0	0
21-22	0	0	0	0	0	0	0	0	0	0	0	0	0	0	0
22-23	0	0	0	0	0	0	0	0	0	0	0	0	0	0	0
23-24	0	0	0	0	0	0	0	0	0	0	0	0	0	0	0
Total	17	4	2	0	0	0	0	0	0	0	0	0	0	0	23

Table 125. Summary of largest positive and negative fluctuations, durations less than 150 seconds, horizontal intensity, H-fluxmeter, College Alaska, November 1, 1943, to January 31, 1944*

Date	Amplitude	Rate of change	Date	Amplitude	Rate of change
1943	γ	γ/sec	1943	γ	γ/sec
Oct 8	+139	+6.9	Dec 17	+182	+5.9
	-268	-6.9		-254	-4.8
Oct 11	+187	+6.6	Dec 21	+307	+7.6
	-303	-4.8		-166	-5.3
Oct 25	> +210	+3.7	Dec 22	+203	+5.5
	-299	-5.5		-294	-5.4
Oct 27	?	?	Dec 28	+187	+3.0
	< -288	-9.6		-244	-3.1
Nov 20	+230	+6.7	1944		
	-306	-5.2	Jan 10	+268	+5.9
Nov 23	+204	+5.4		-214	-5.9
	-147	-3.8	Jan 12	+ 84	+2.4
Nov 25	?	?		-168	-2.8
	-200	-5.5	Jan 14	+162	+3.4
Nov 26	+119	+6.7		-142	-2.8
	-220	-4.3	Jan 17	-183	+4.1
				+ 66	-2.4

*Prepared by C. W. Malich, College Magnetic Observatory

FIGURES 126-226 --Concluded

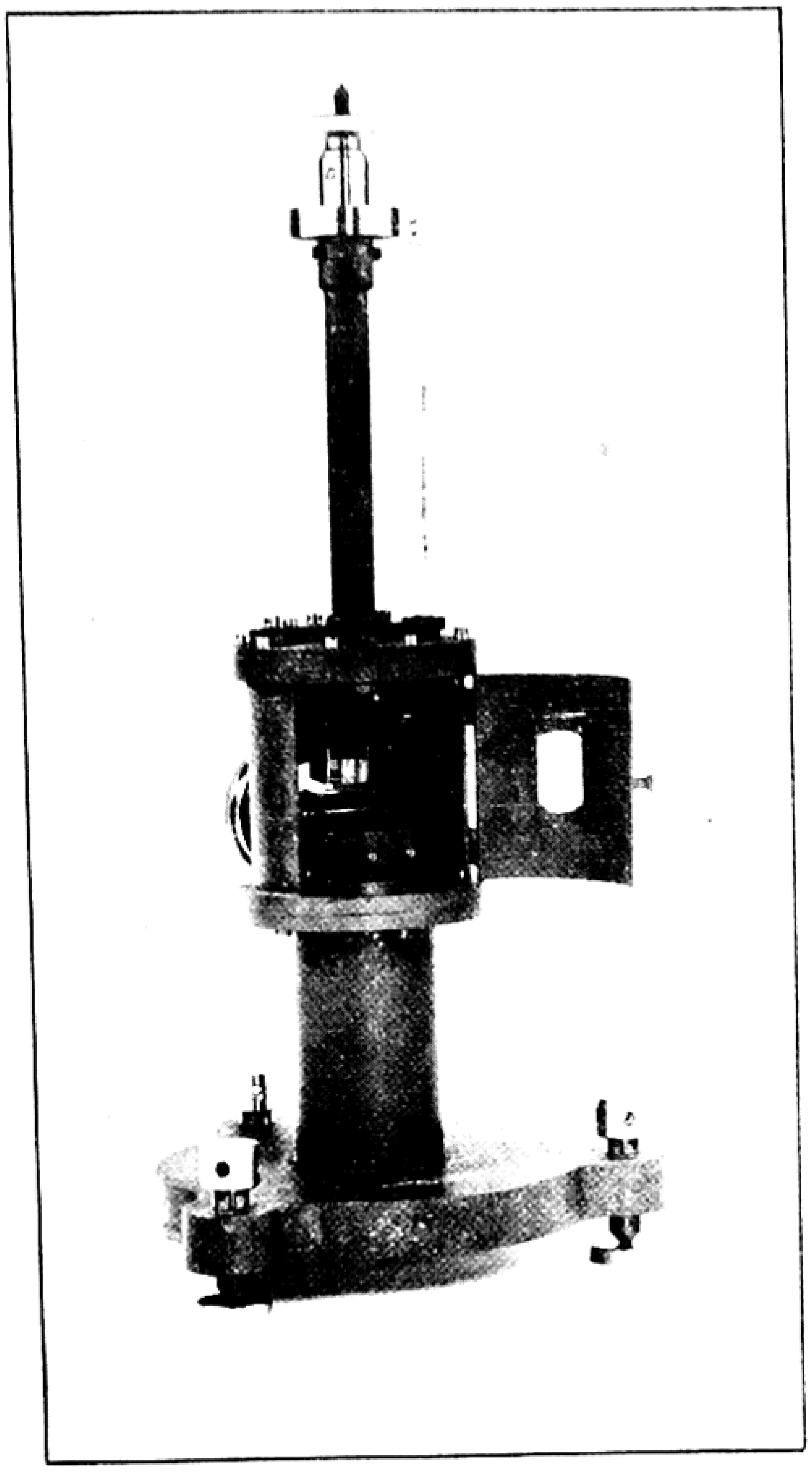

Fig. 129. La Cour horizontal-intensity variometer

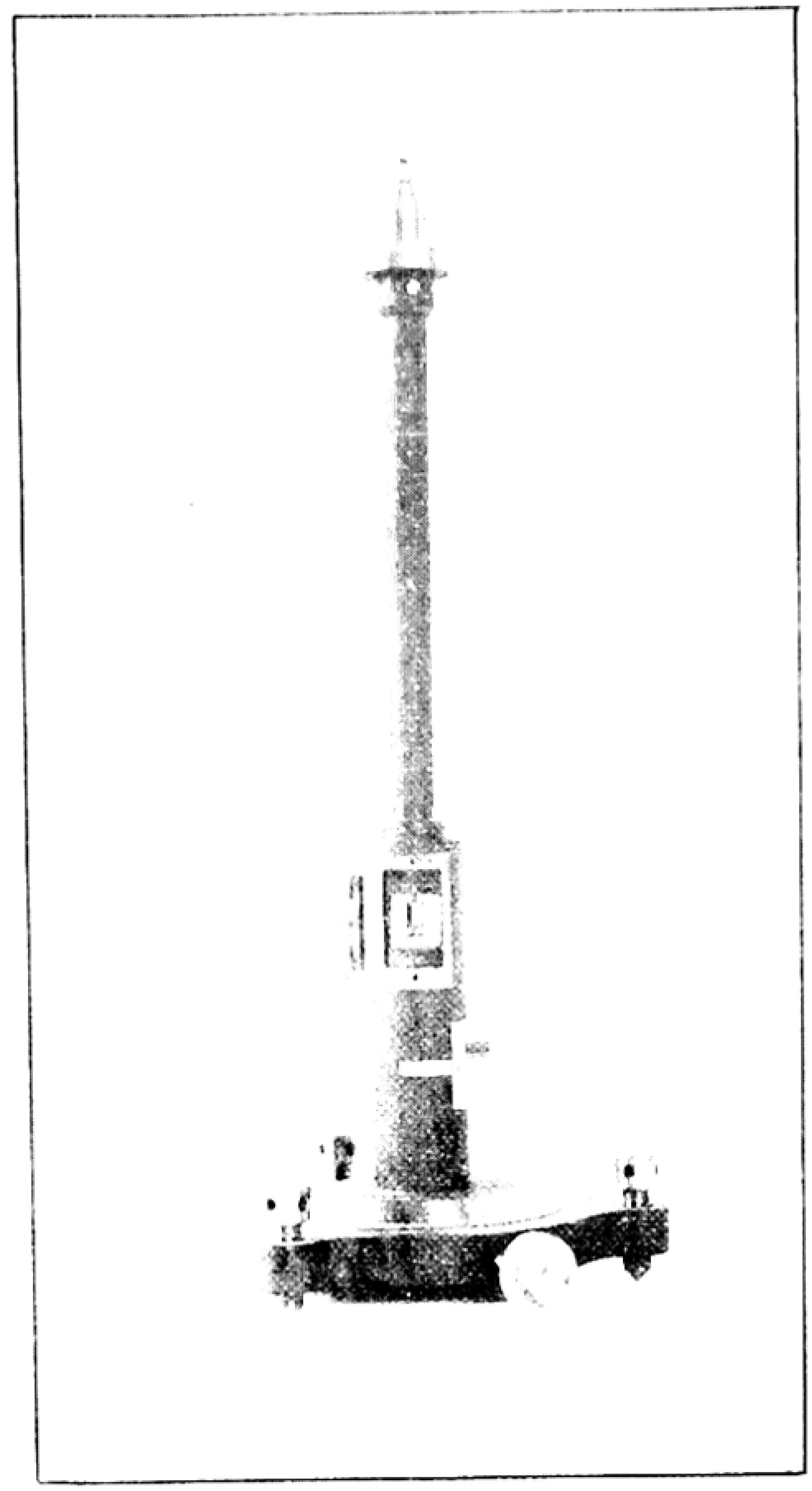

Fig. 130. La Cour declination variometer

Fig. 131. La Cour vertical-intensity variometer

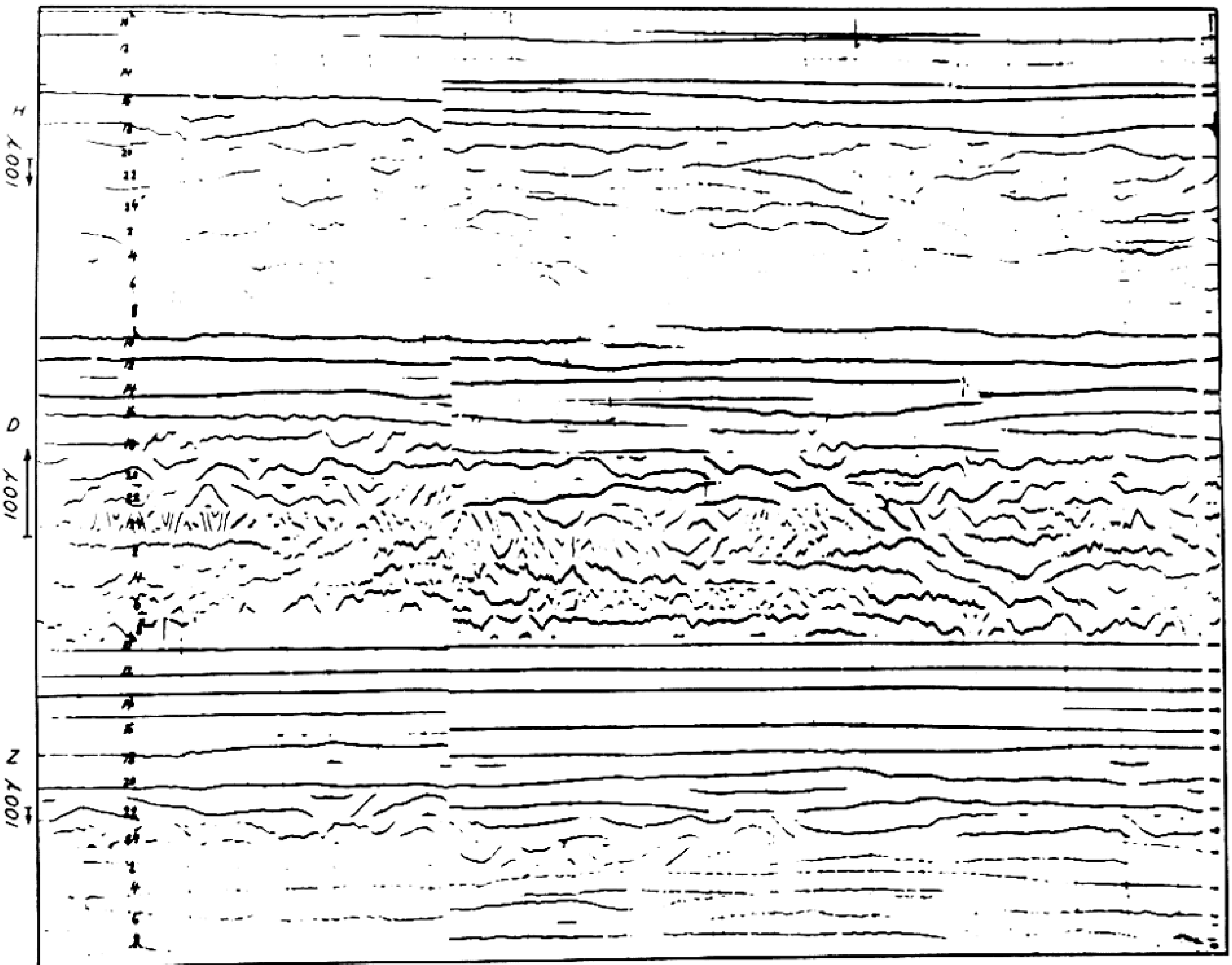

FIG. 132 (A) — QUICK-RUN MAGNETOGRAM, PETSAMO, FINLAND, MAY 17–18, 1933 (ORIGINAL TIME-SCALE 180 MM/HOUR)

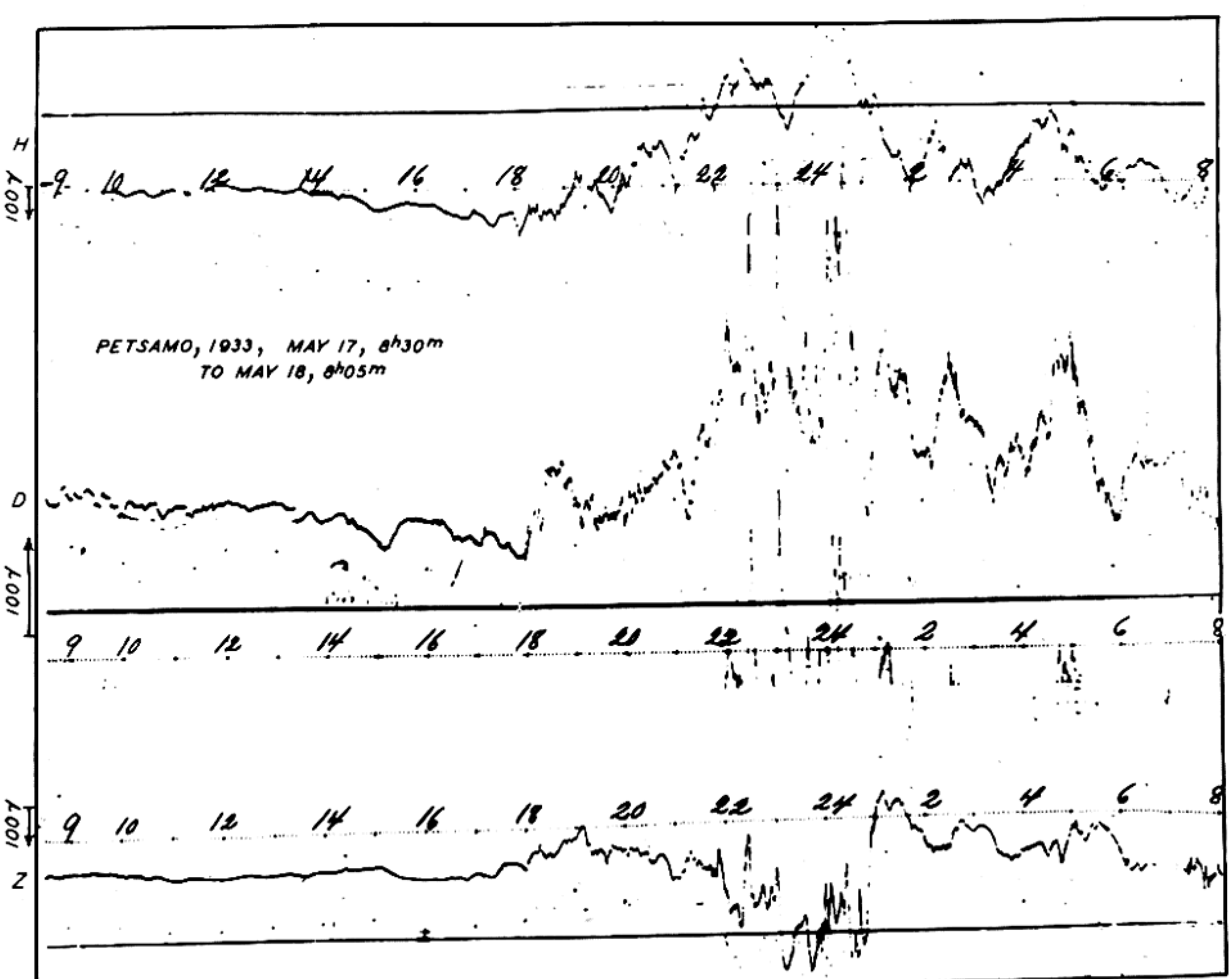

FIG. 132 (B) — MAGNETOGRAM, PETSAMO, FINLAND, MAY 17–18, 1933 (ORIGINAL TIME-SCALE 15 MM/HOUR)

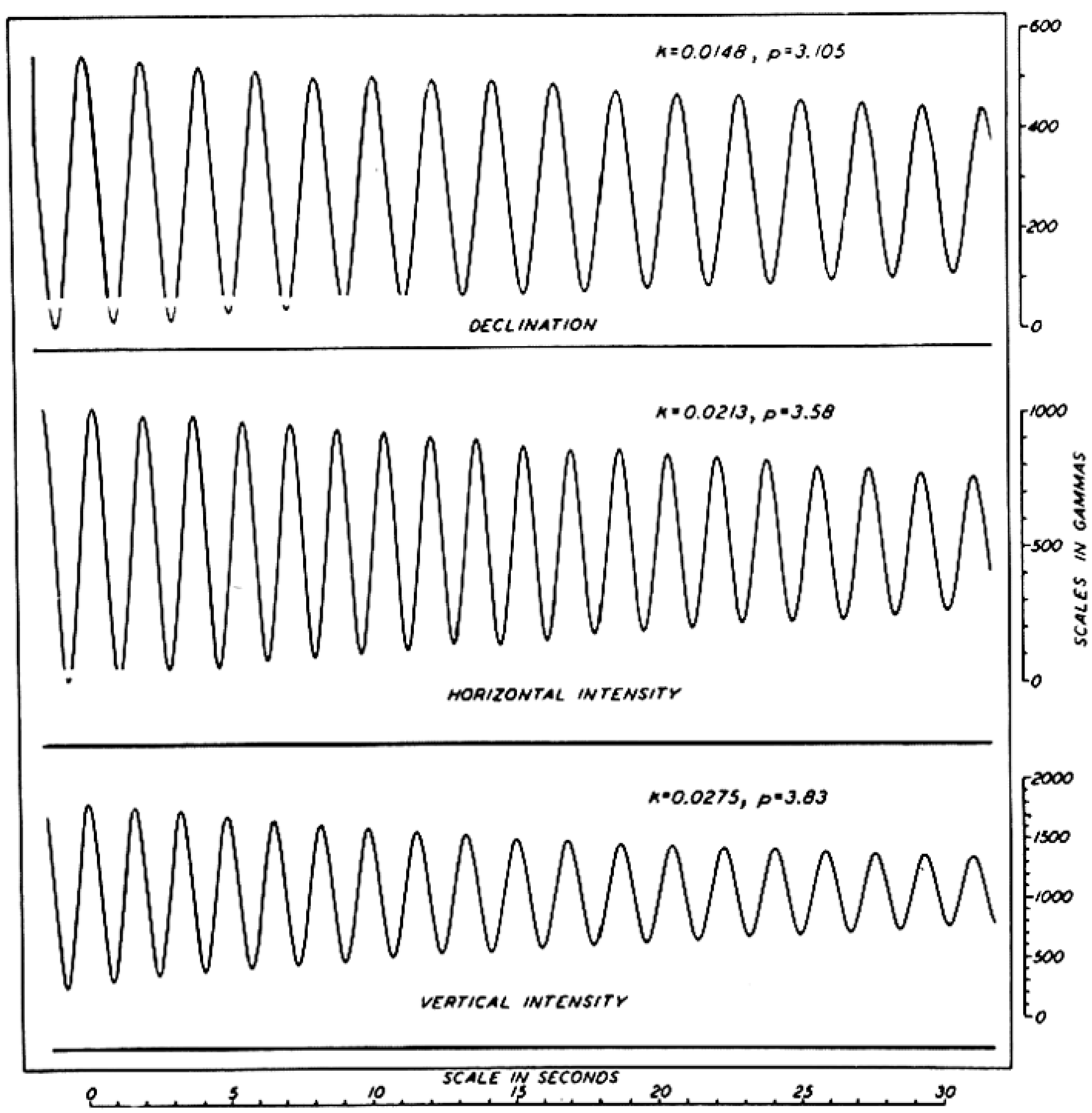

FIG. 133—RESPONSE OF LA COUR D-, H-, AND Z-VARIOMETERS AFTER SUDDEN IMPULSE

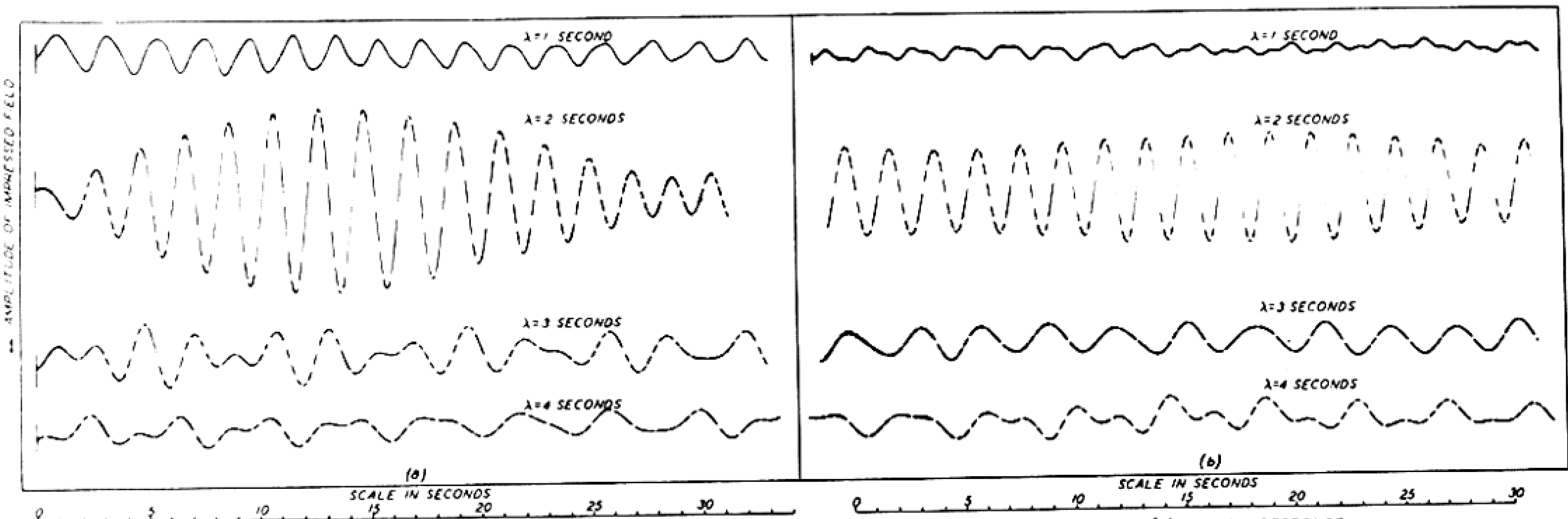

FIG. 134 (A)—RESPONSE OF LA COUR D-VARIOMETER TO SINUSOIDAL MAGNETIC FIELDS; (a) INITIAL RESPONSE, AND (b) STEADY RESPONSE

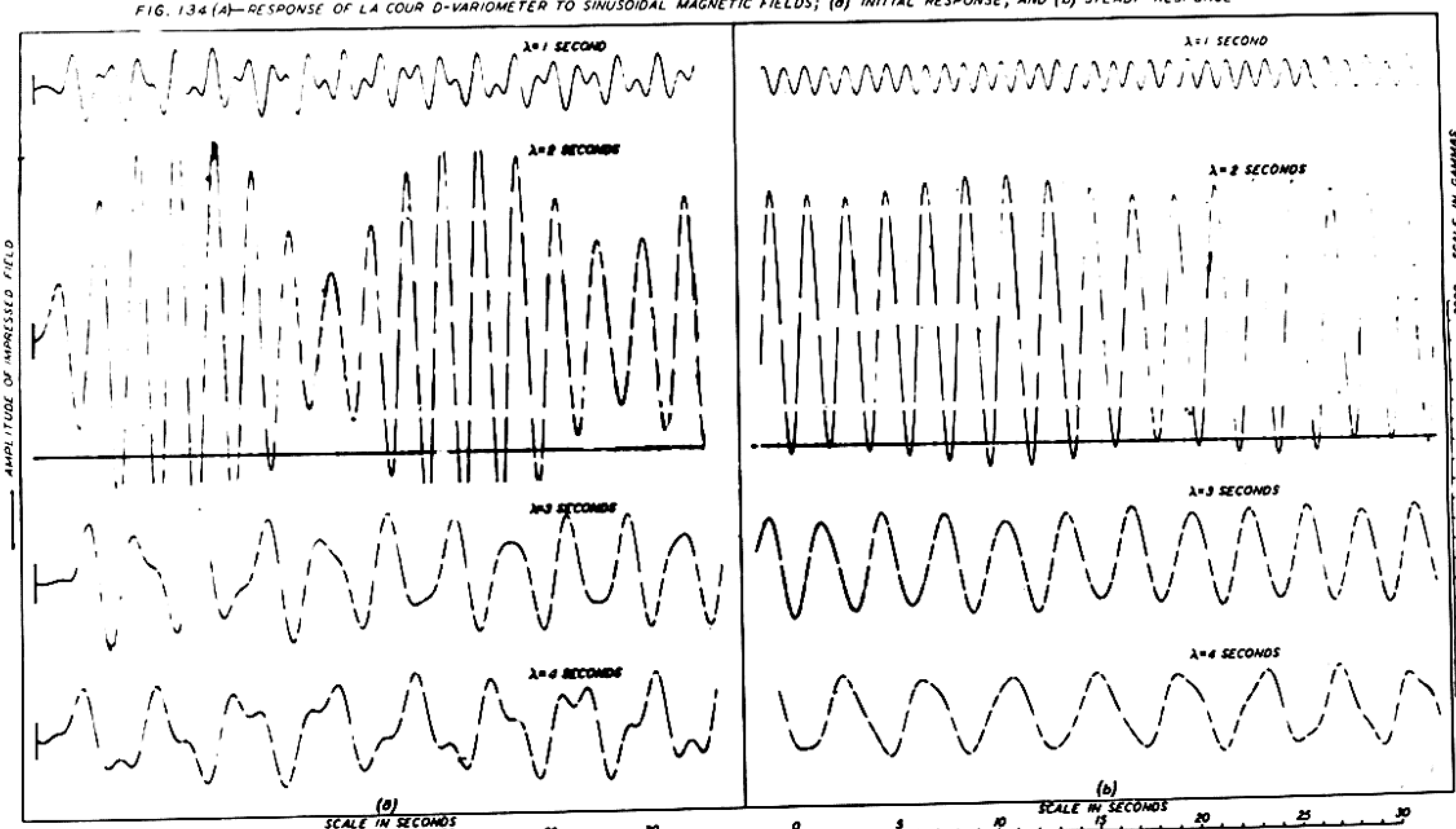

FIG 134 (B)—RESPONSE OF LA COUR H-VARIOMETER TO SINUSOIDAL MAGNETIC FIELDS; (a) INITIAL RESPONSE, AND (b) STEADY RESPONSE

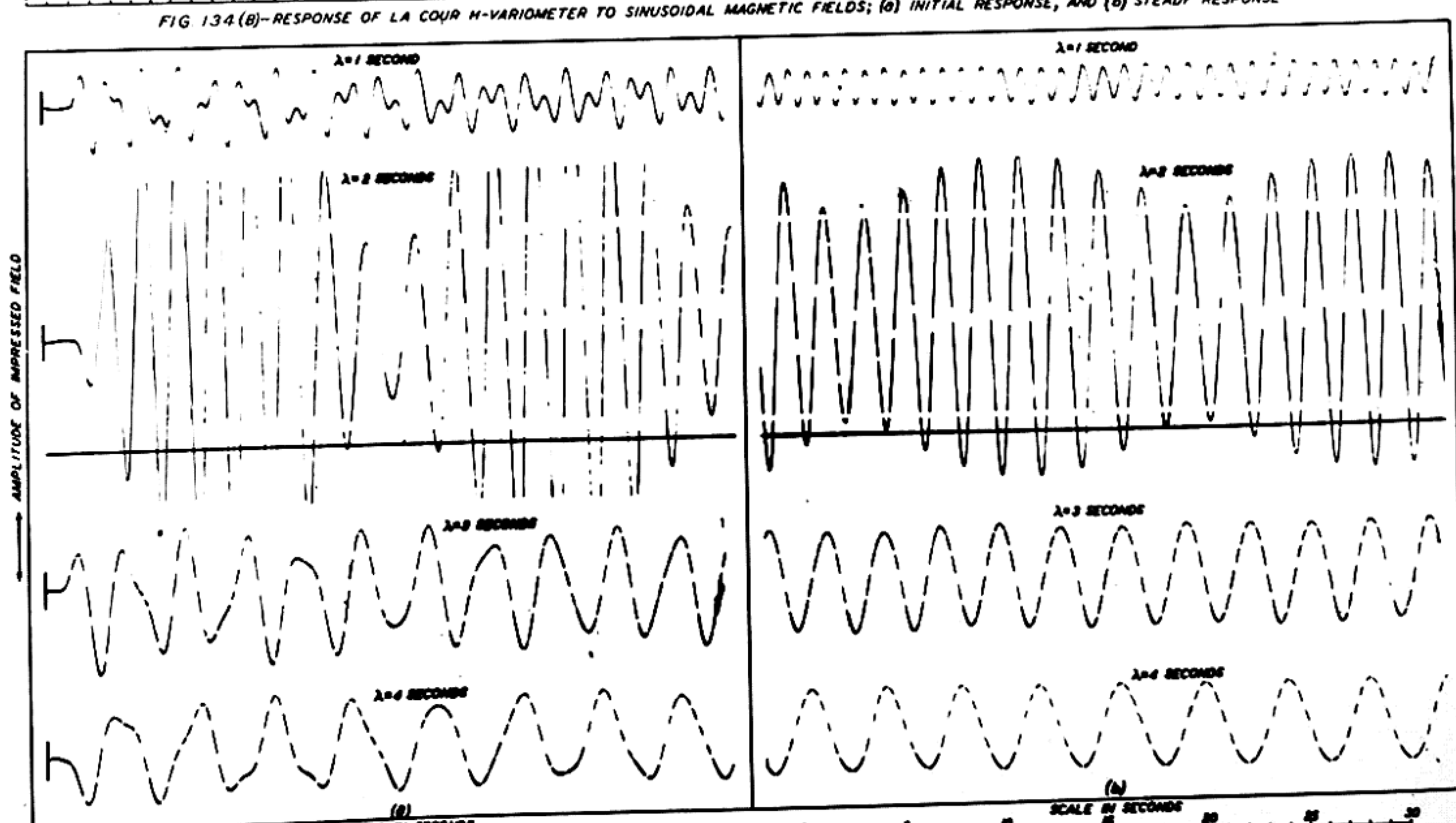

FIG. 134 (C)—RESPONSE OF LA COUR Z-VARIOMETER TO SINUSOIDAL MAGNETIC FIELDS; (a) INITIAL RESPONSE, AND (b) STEADY RESPONSE

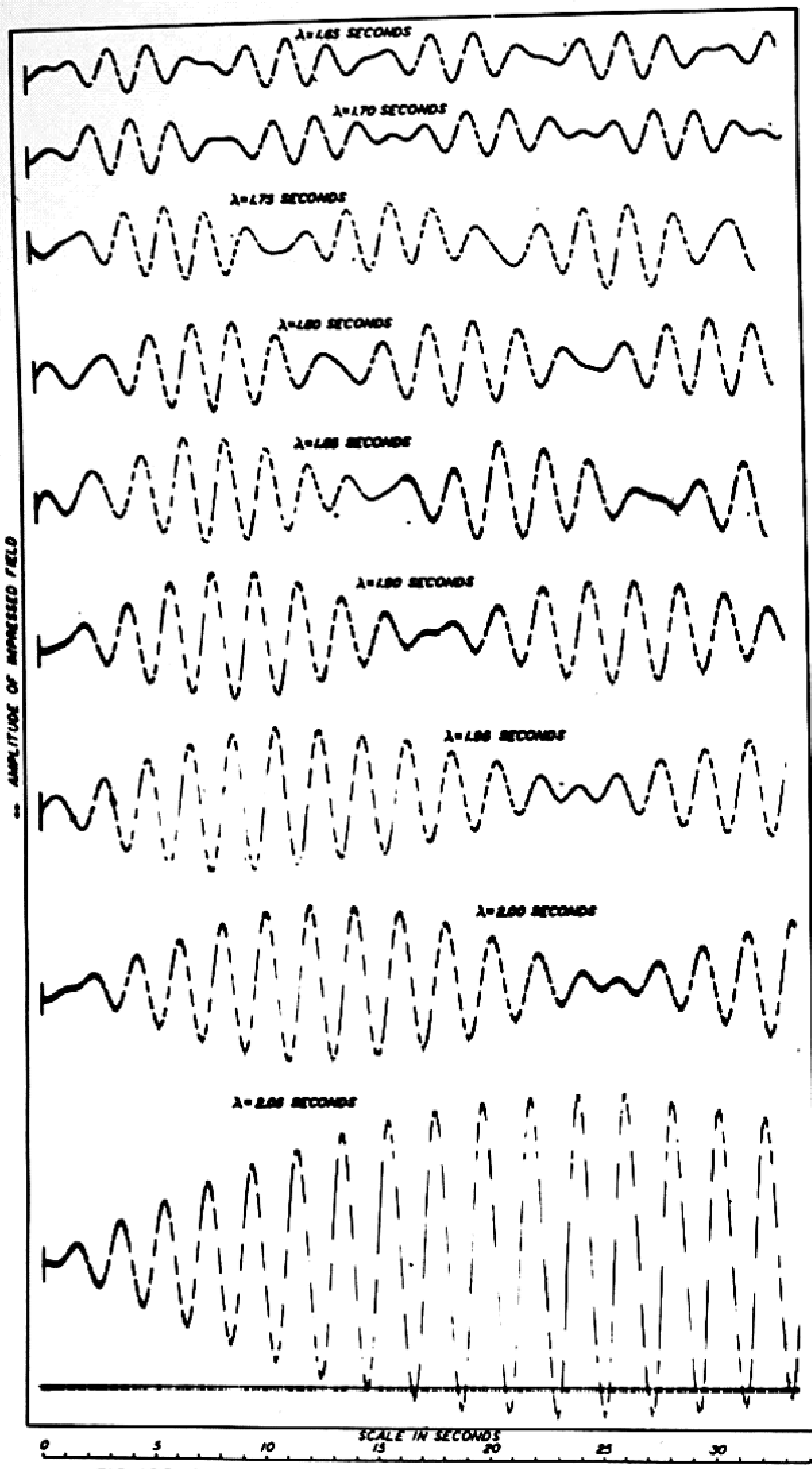

FIG. 135—BEATS NEAR RESONANCE-FREQUENCY, D-VARIOMETER

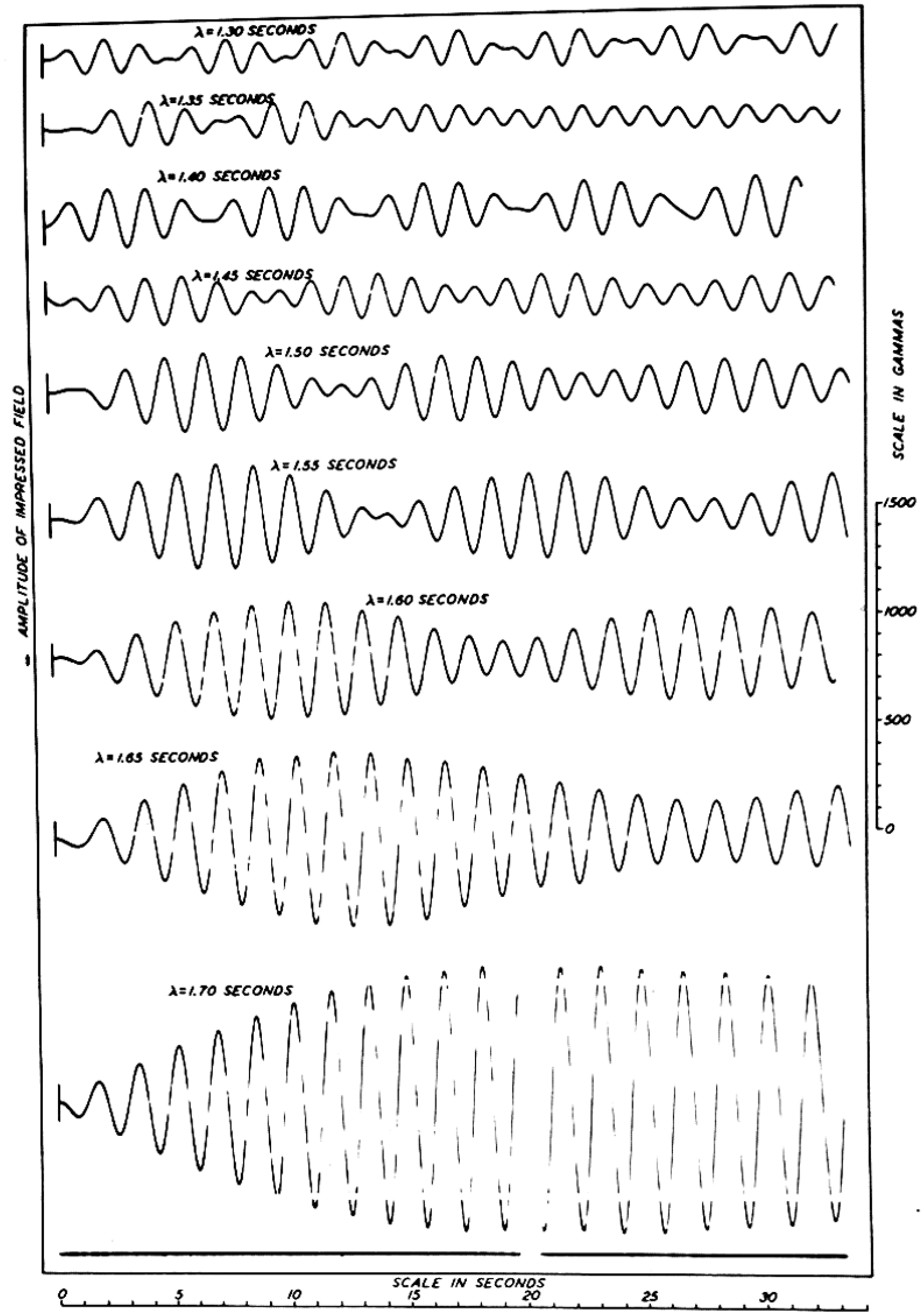

FIG. 136—BEATS NEAR RESONANCE-FREQUENCY, H-VARIOMETER

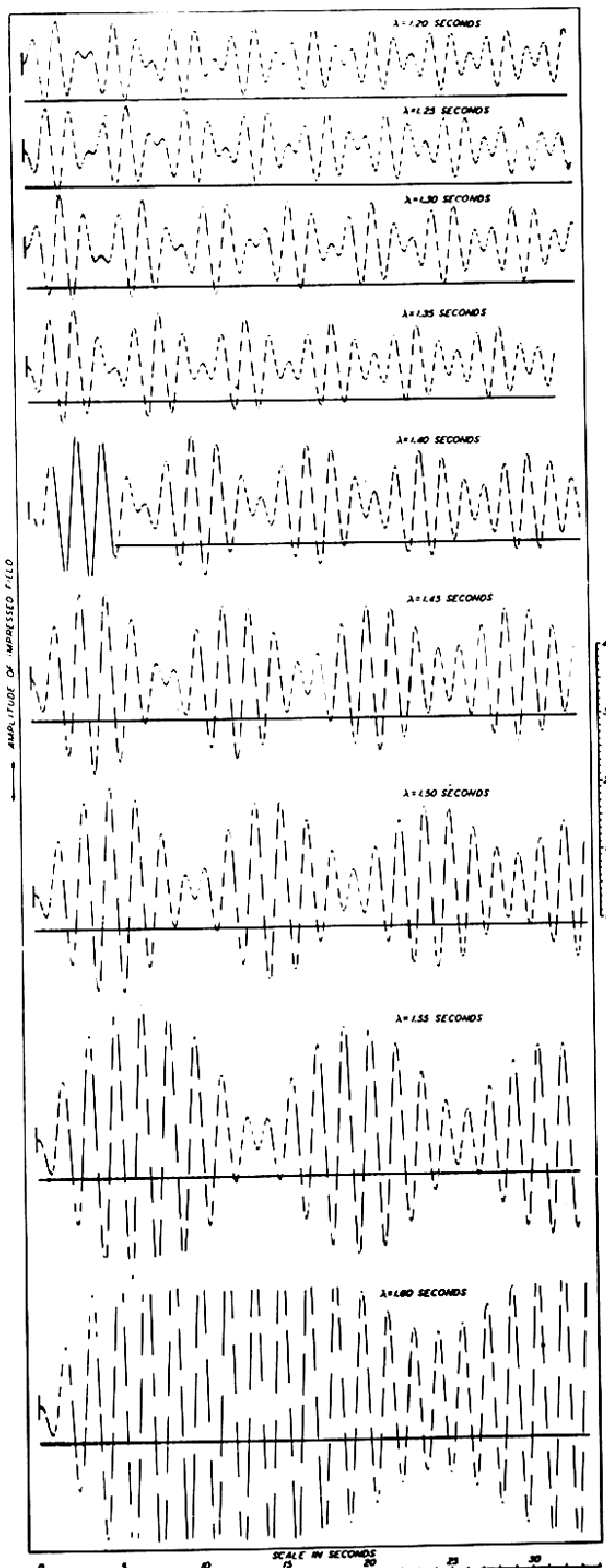

FIG. 137—BEATS NEAR RESONANCE-FREQUENCY, Z-VARIOMETER

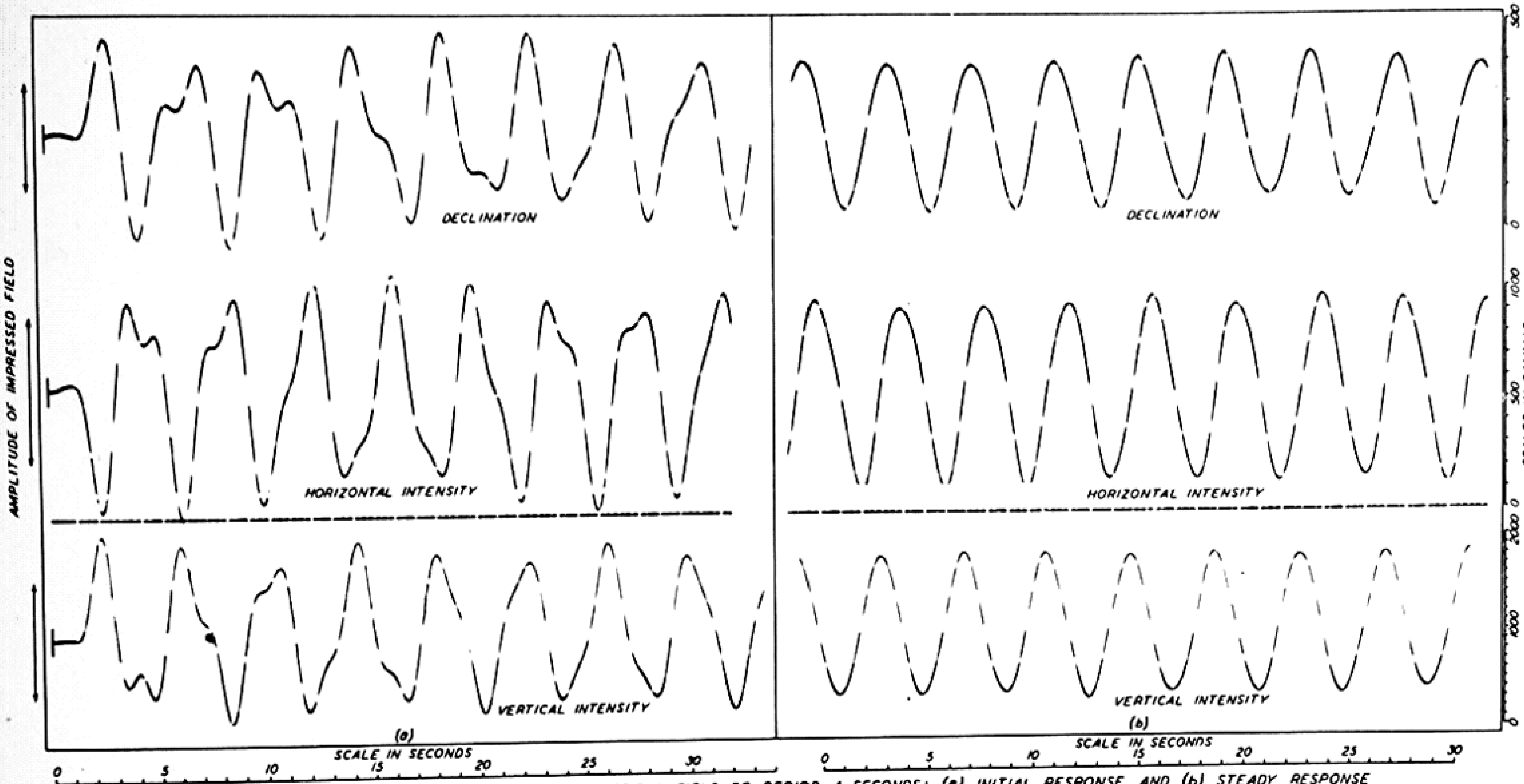

FIG. 138(A)—RESPONSE OF D, H, AND Z LA COUR VARIOMETERS TO SINUSOIDAL FIELD OF PERIOD 4 SECONDS; (a) INITIAL RESPONSE, AND (b) STEADY RESPONSE

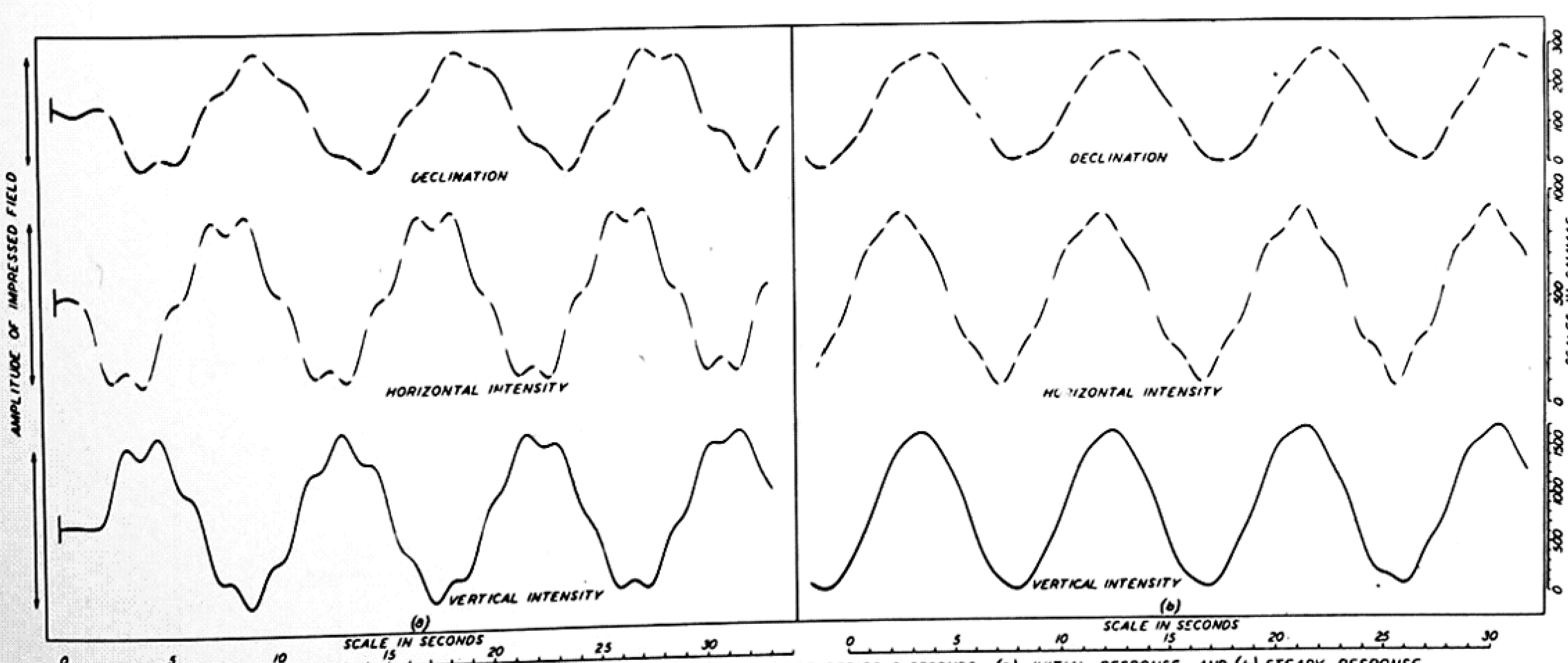

FIG. 138(B)—RESPONSE OF D, H, AND Z LA COUR VARIOMETERS TO SINUSOIDAL FIELD OF PERIOD 9 SECONDS; (a) INITIAL RESPONSE, AND (b) STEADY RESPONSE

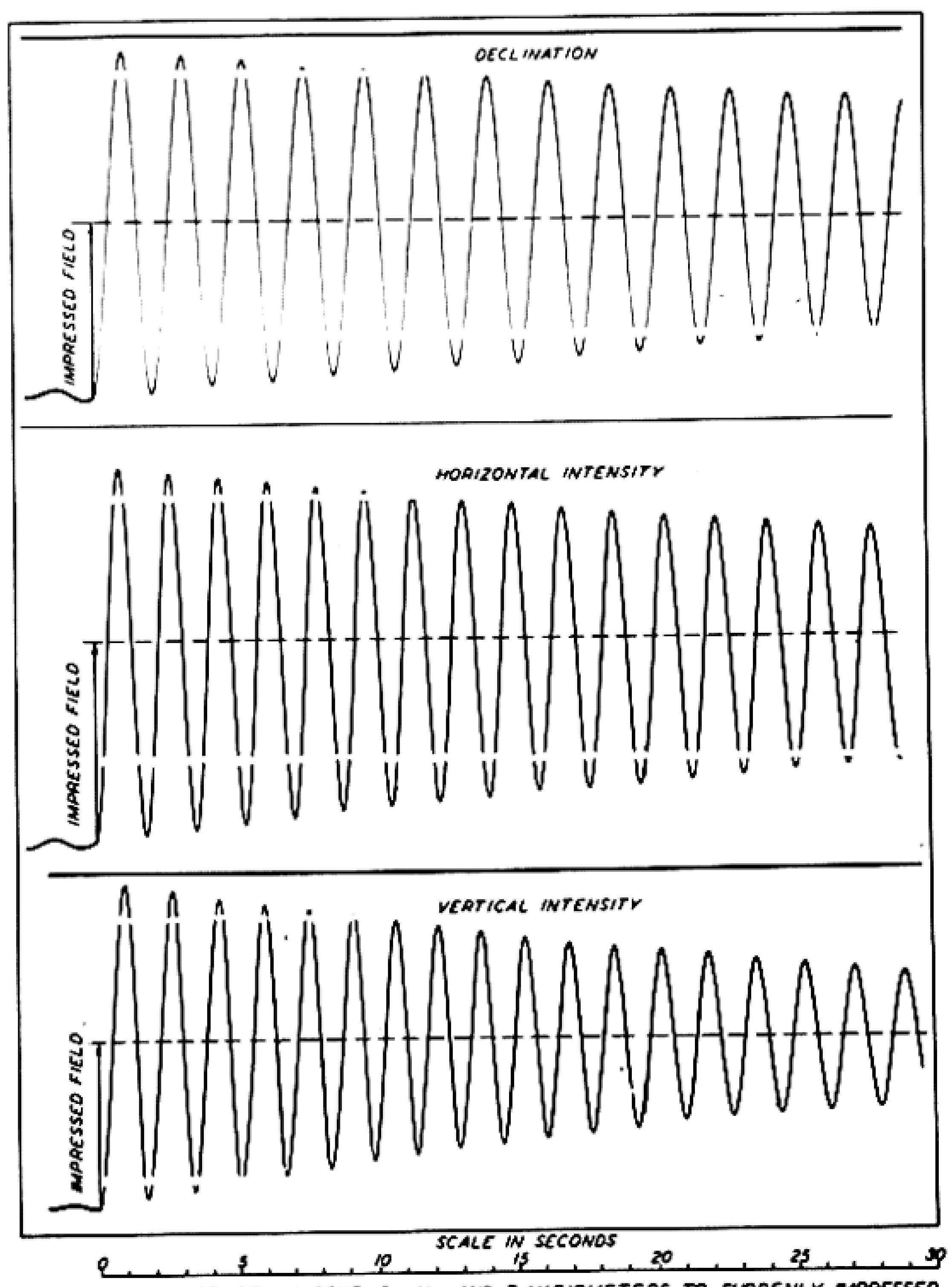

FIG. 139—RESPONSE OF LA COUR D-, H-, AND Z-VARIOMETERS TO SUDDENLY IMPRESSED FIELD OF CONSTANT VALUE

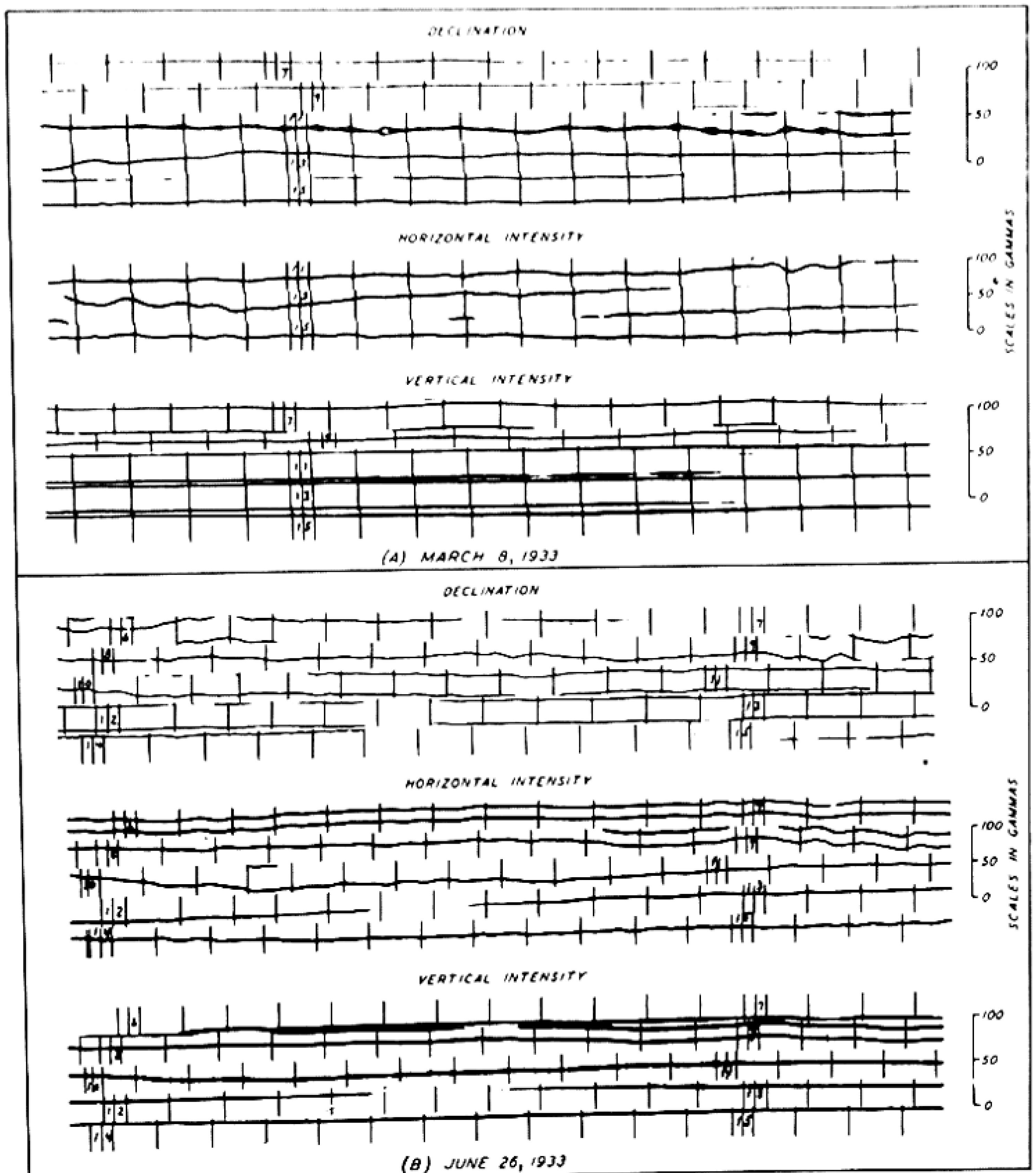

FIG. 140(A) AND (B)– MICROPULSATIONS AT LYCKSELE, SWEDEN (LAT. 64° 36.'0 N, LONG. 18° 40.'7 E); TIME INDICATED IN HOURS, GMT

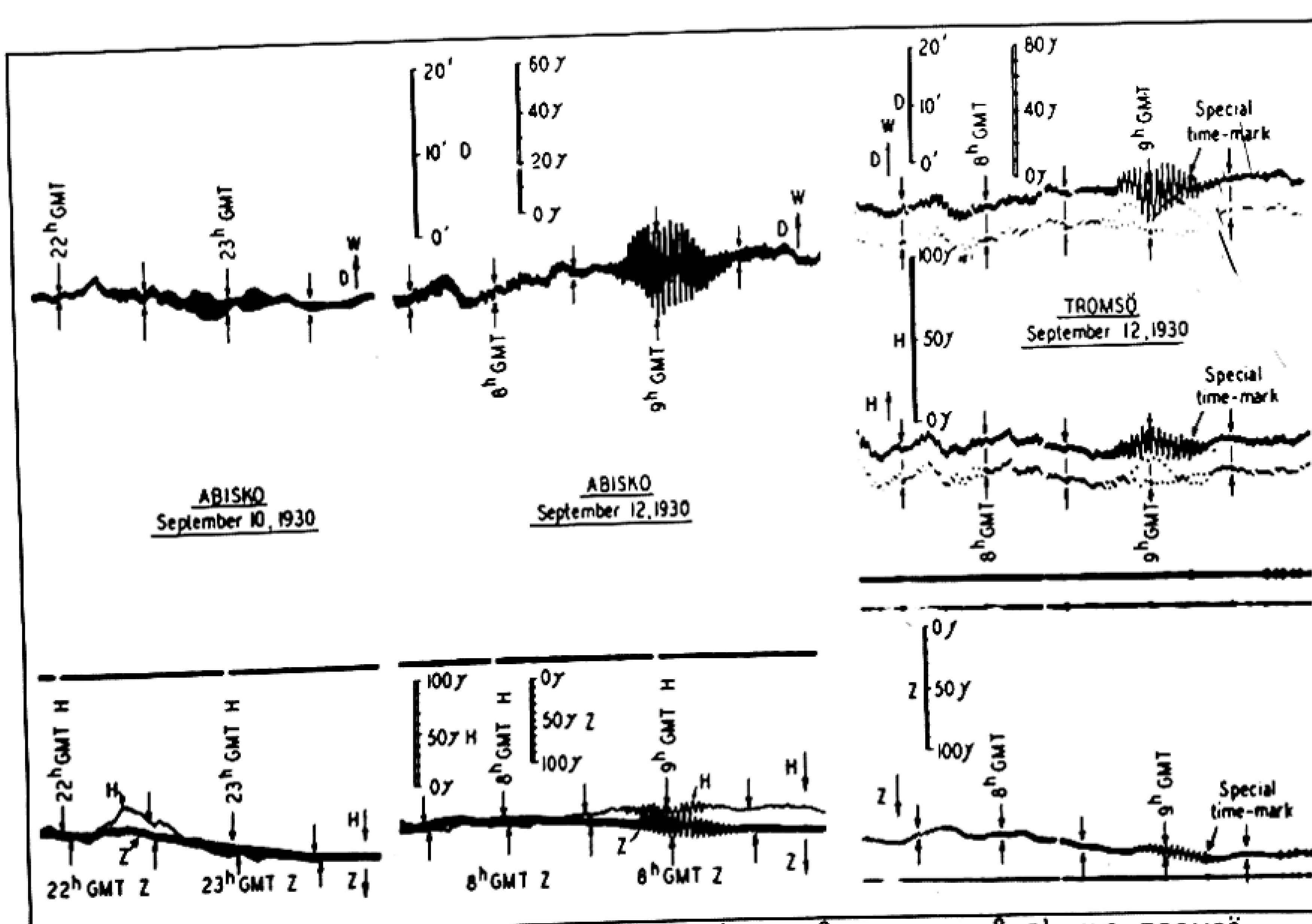

FIG. 140(C)–GIANT PULSATIONS AT ABISKO, SWEDEN (LAT. 68.°4 N, LONG. 18.°8 E), AND TROMSÖ, NORWAY (LAT. 69.°7 N, LONG. 18.°9 E)

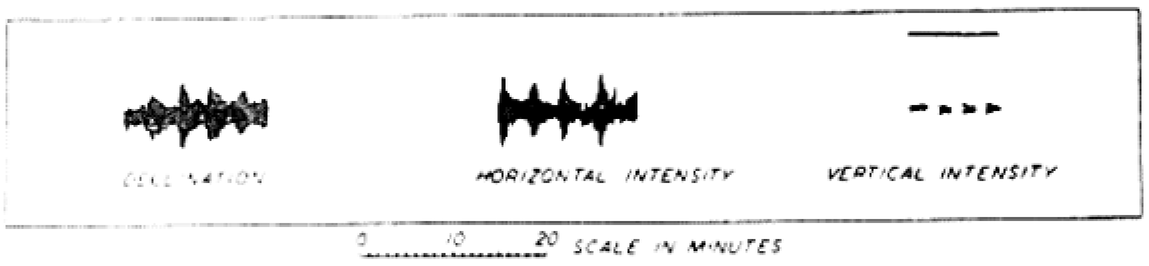

FIG.141—BEAT-RESPONSES OF VARIOMETERS FOR INTERMITTENT SINUSOIDAL FIELDS OF ONE-HALF MINUTE DURATION APPEARING AT SUCCESSIVE THREE-MINUTE INTERVALS, D, H, AND Z

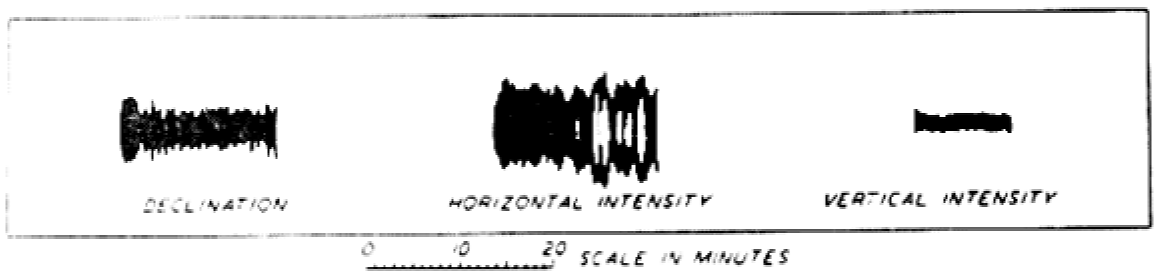

FIG.142—RESPONSES NEAR RESONANCE-FREQUENCY, D, H, AND Z

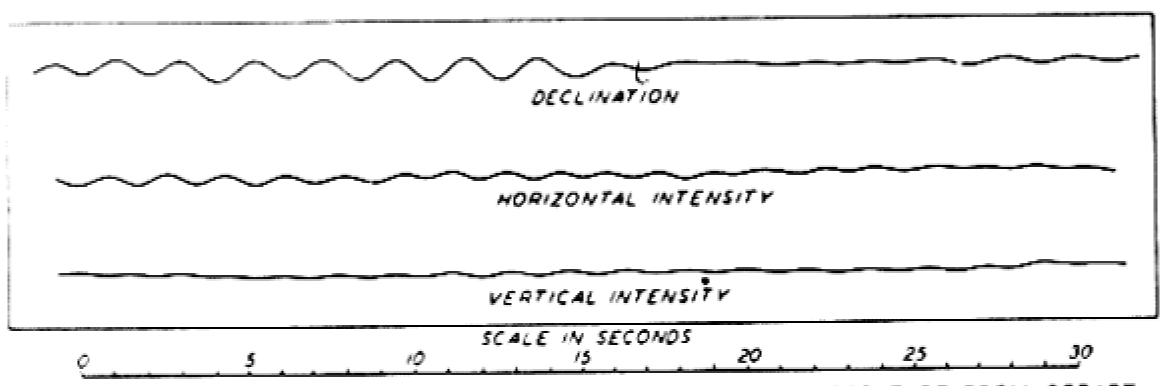

FIG.143—ARTIFICIAL DISTURBANCES, D, H, AND Z, CONSTANT-TEMPERATURE ROOM, DEPARTMENT OF TERRESTRIAL MAGNETISM

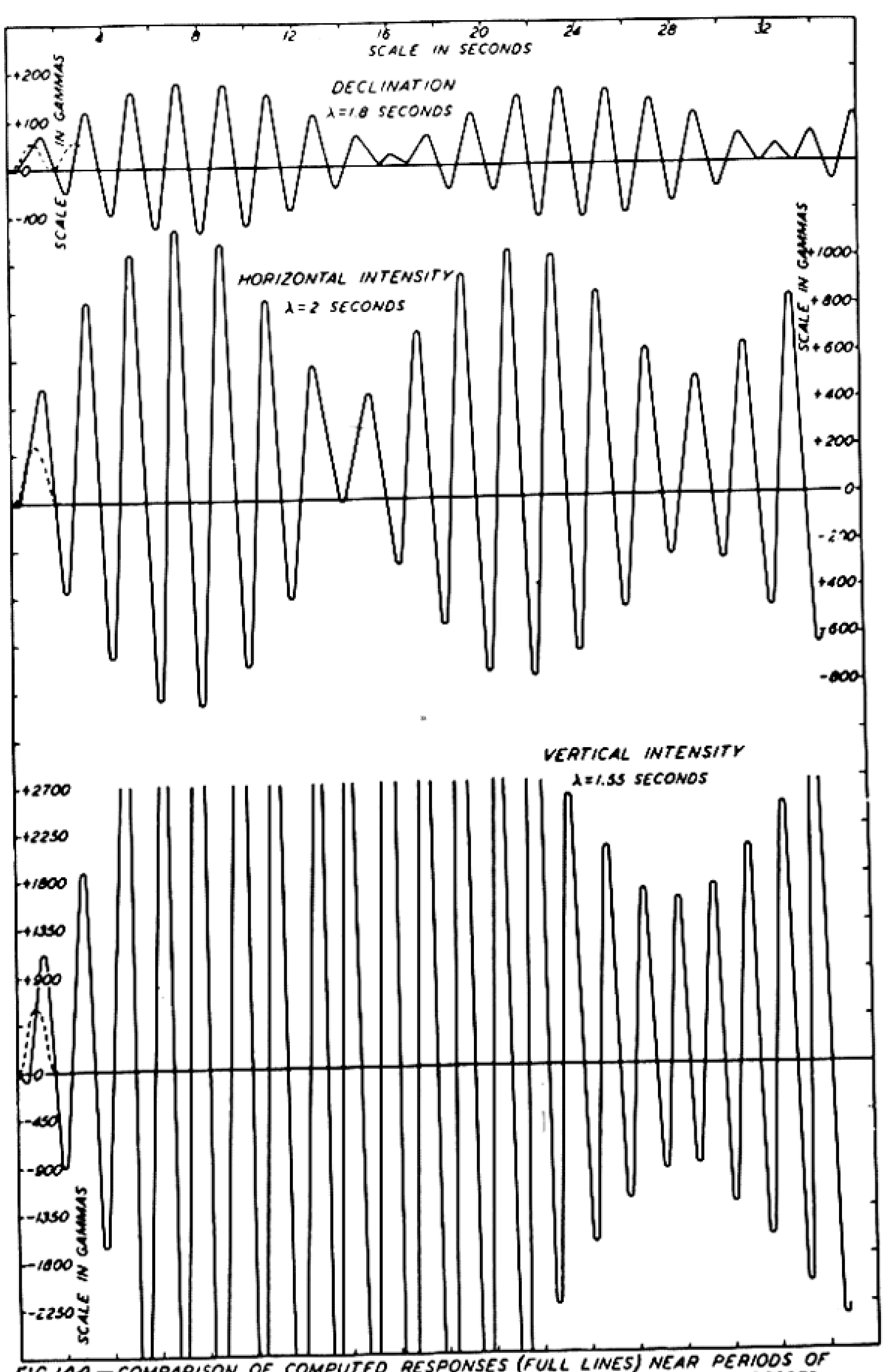

FIG.144—COMPARISON OF COMPUTED RESPONSES (FULL LINES) NEAR PERIODS OF RESONANCE OF D-, H-, AND Z-VARIOMETERS WITH CORRESPONDING IMPRESSED FIELDS s = CK (1-cos mt) / M (BROKEN LINES)

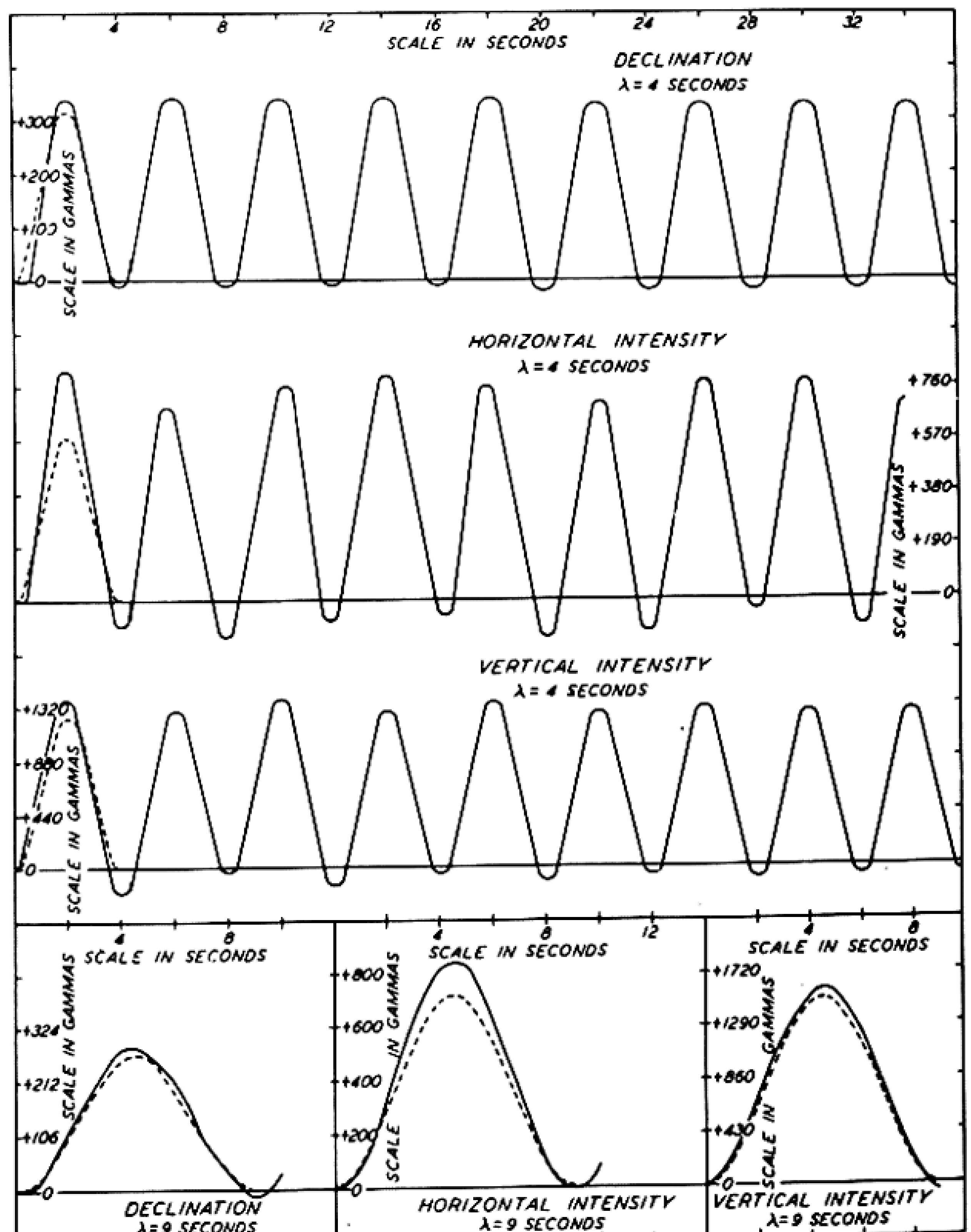

FIG.145—COMPARISON OF COMPUTED RESPONSES (FULL LINES) OF D-, H-, AND Z-VARIOMETERS WITH CORRESPONDING IMPRESSED FIELDS s=CK(1-cos mt)/M (BROKEN LINES) OF PERIODS 4 AND 9 SECONDS

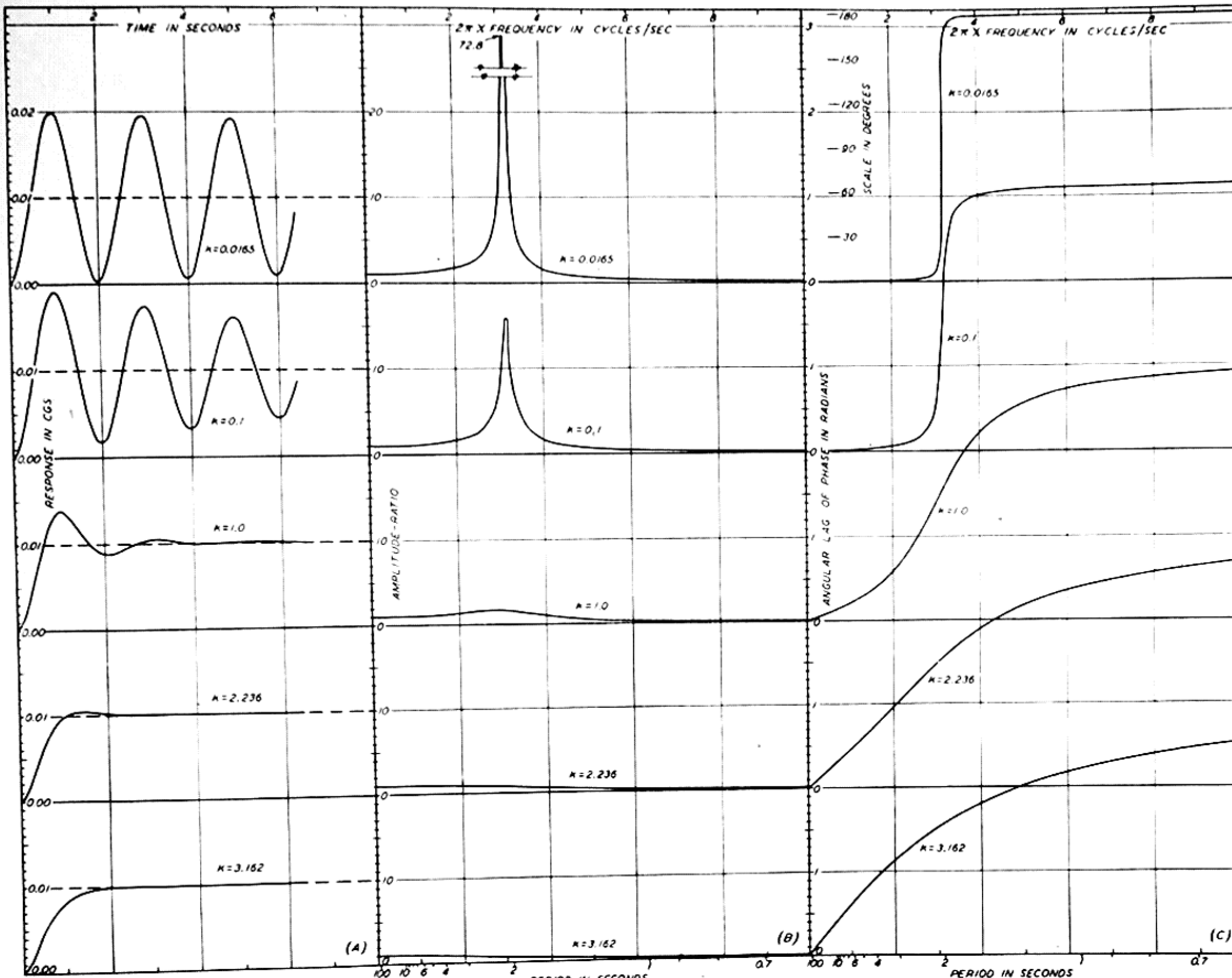

FIG. 146—VARIATION IN RESPONSE-CHARACTERISTICS OF VARIOMETERS WITH VARIOUS DAMPING FACTORS κ FOR $n^2=10$: (A) RESPONSE TO SUDDENLY IMPRESSED FIELD YIELDING 0.01 RADIAN TRUE DEFLECTION; (B) VARIATION WITH κ OF AMPLITUDE-RATIO, OBSERVED TO TRUE RESPONSE, FOR SINUSOIDAL IMPRESSED FIELDS OF CONSTANT AMPLITUDE AND PERIOD; AND (C) CORRESPONDING LAGS IN PHASE OF RESPONSE RELATIVE TO IMPRESSED FIELDS OF (A)

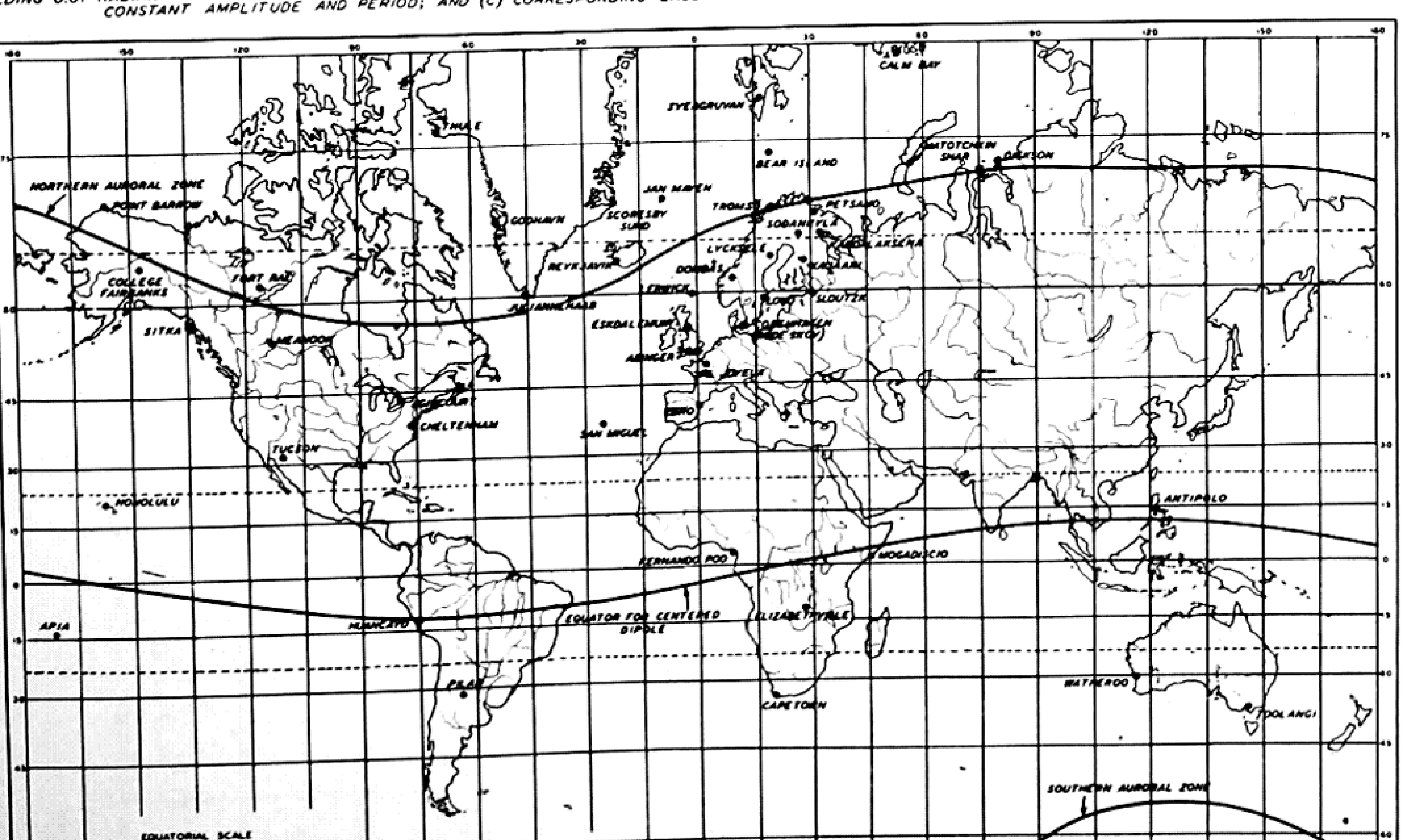

FIG. 147—NORTHERN AND SOUTHERN ZONES OF MAXIMUM AURORAL FREQUENCY, EQUATOR FOR CENTERED DIPOLE, AND MAGNETIC STATIONS SELECTED FOR DISCUSSION OF GEOGRAPHICAL DISTRIBUTION OF RANGES IN H, D, AND Z

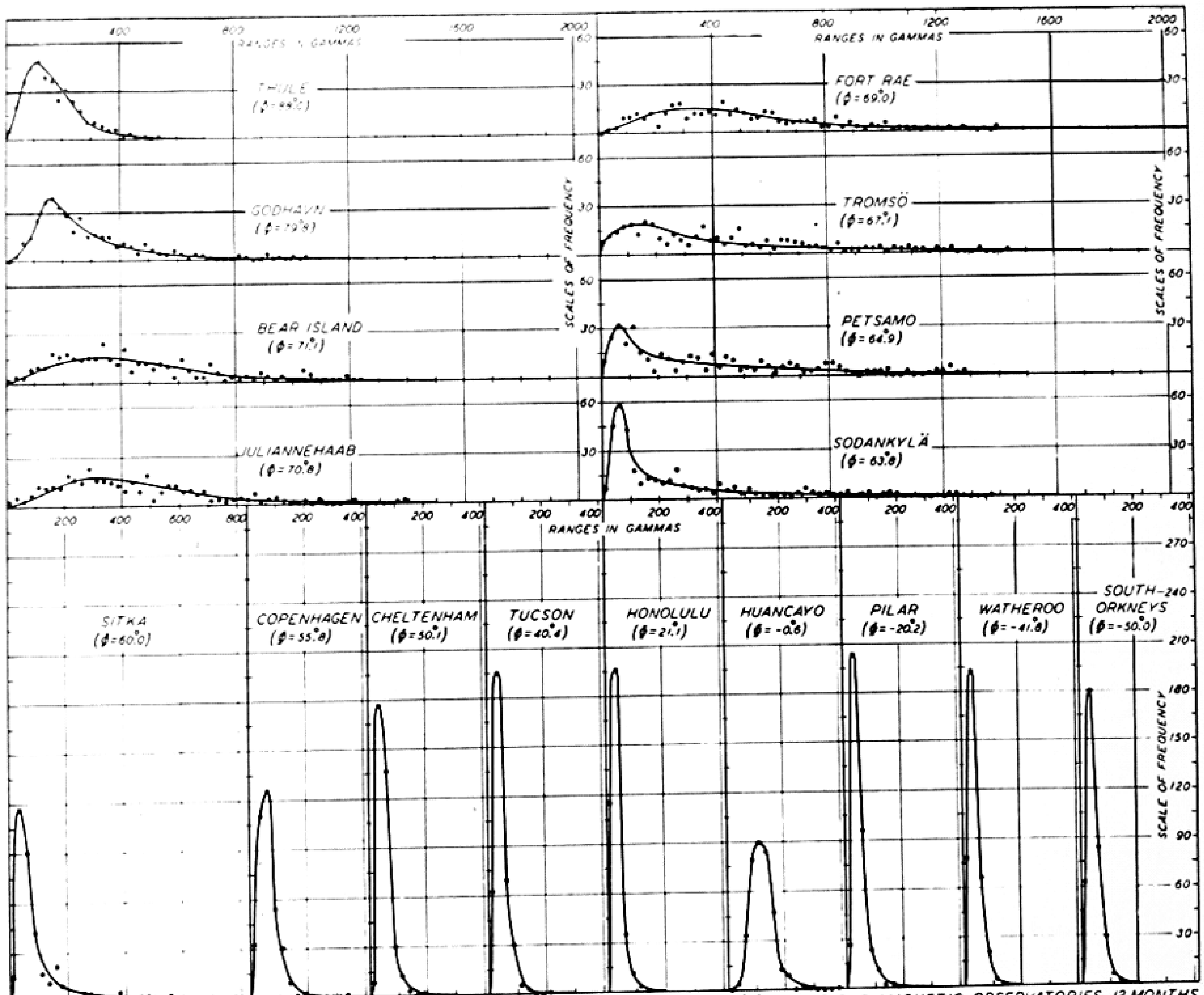

FIG. 148 (A)—FREQUENCY-DISTRIBUTIONS OF DAILY RANGES IN HORIZONTAL INTENSITY (H) AT VARIOUS MAGNETIC OBSERVATORIES, 12 MONTHS OF POLAR YEAR (AUGUST 1932 TO AUGUST 1933)

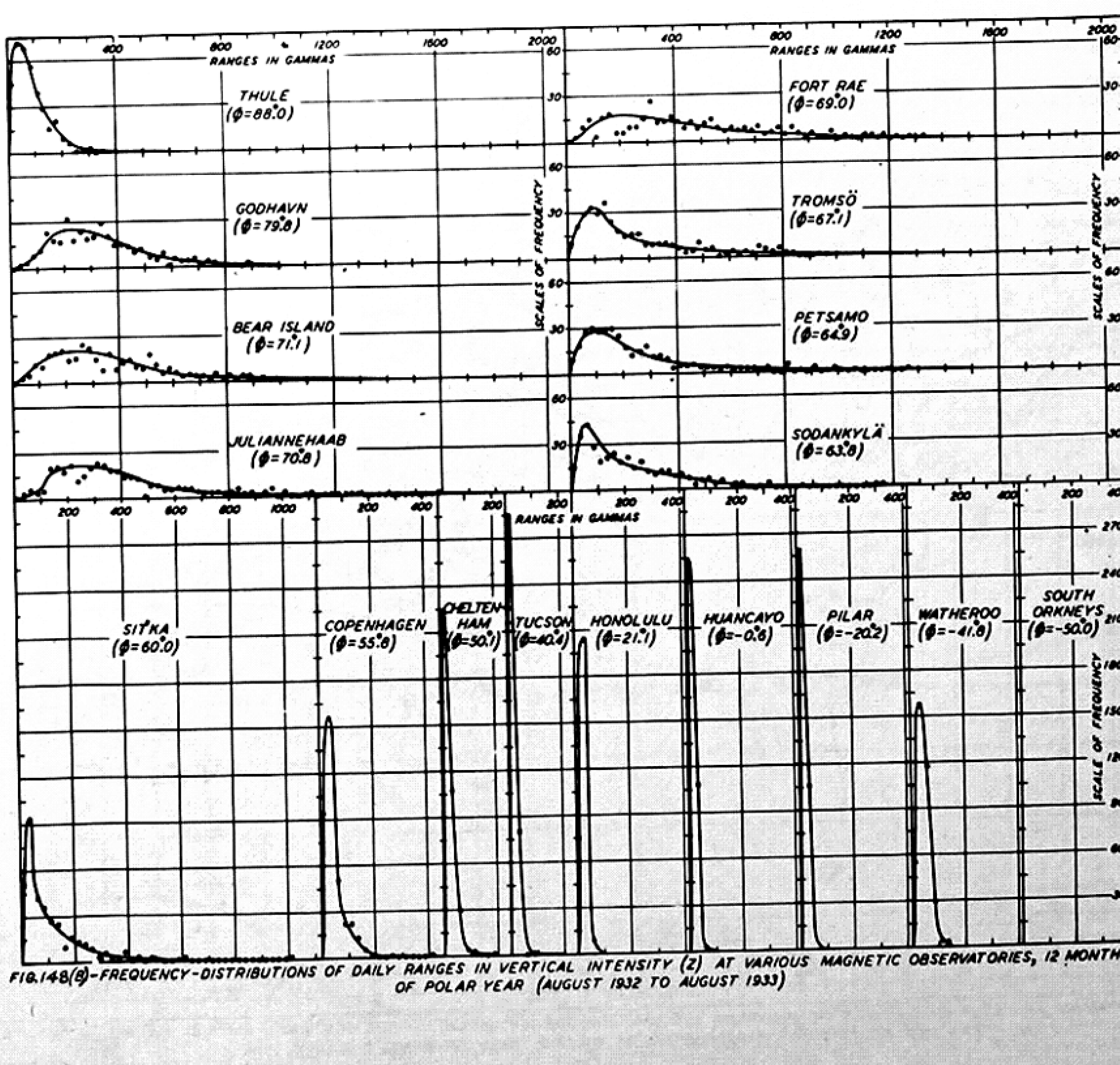

FIG. 148 (B)—FREQUENCY-DISTRIBUTIONS OF DAILY RANGES IN VERTICAL INTENSITY (Z) AT VARIOUS MAGNETIC OBSERVATORIES, 12 MONTHS OF POLAR YEAR (AUGUST 1932 TO AUGUST 1933)

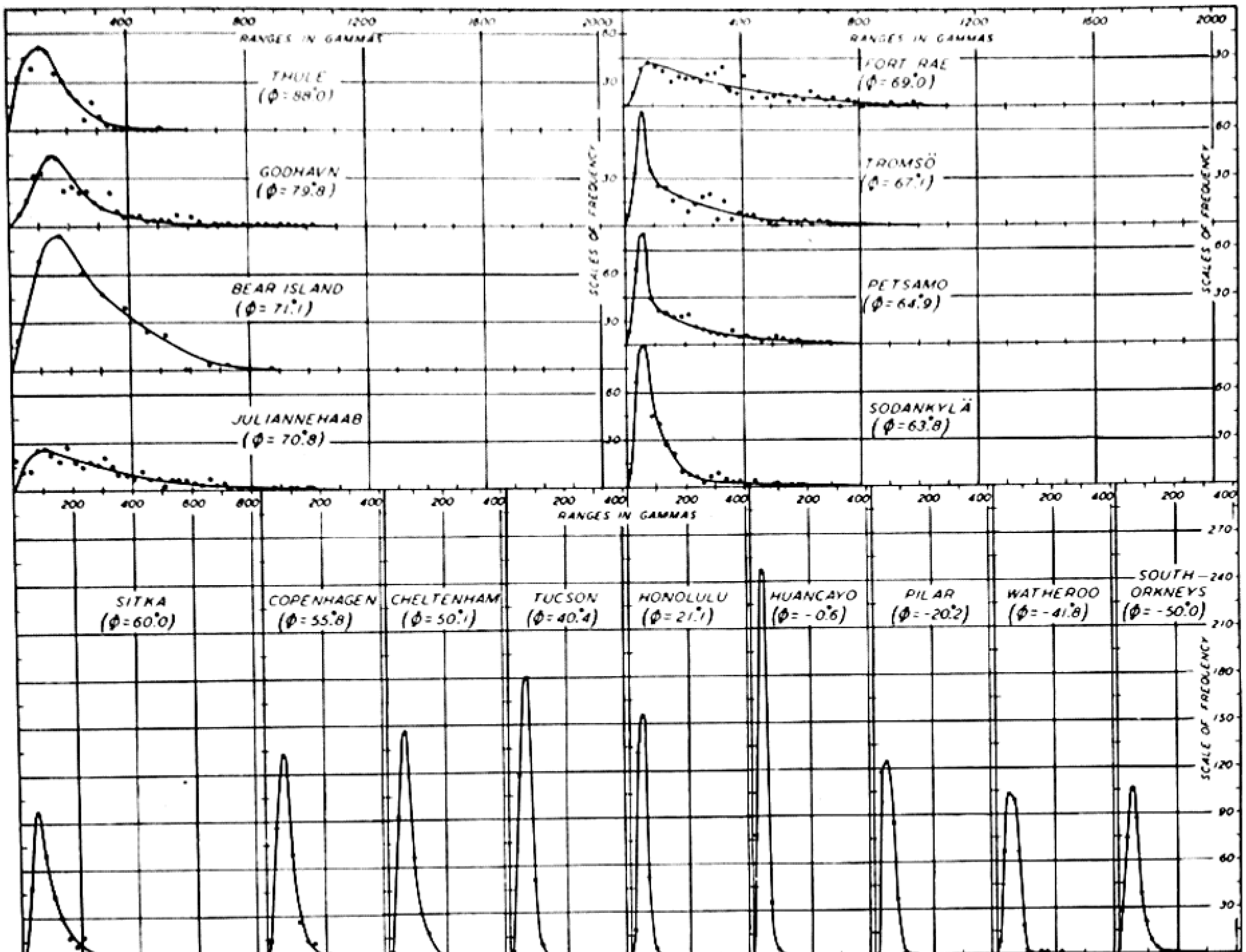

FIG. 148(C)—FREQUENCY-DISTRIBUTIONS OF DAILY RANGES IN MAGNETIC DECLINATION (D) AT VARIOUS MAGNETIC OBSERVATORIES, 12 MONTHS OF POLAR YEAR (AUGUST 1932 TO AUGUST 1933)

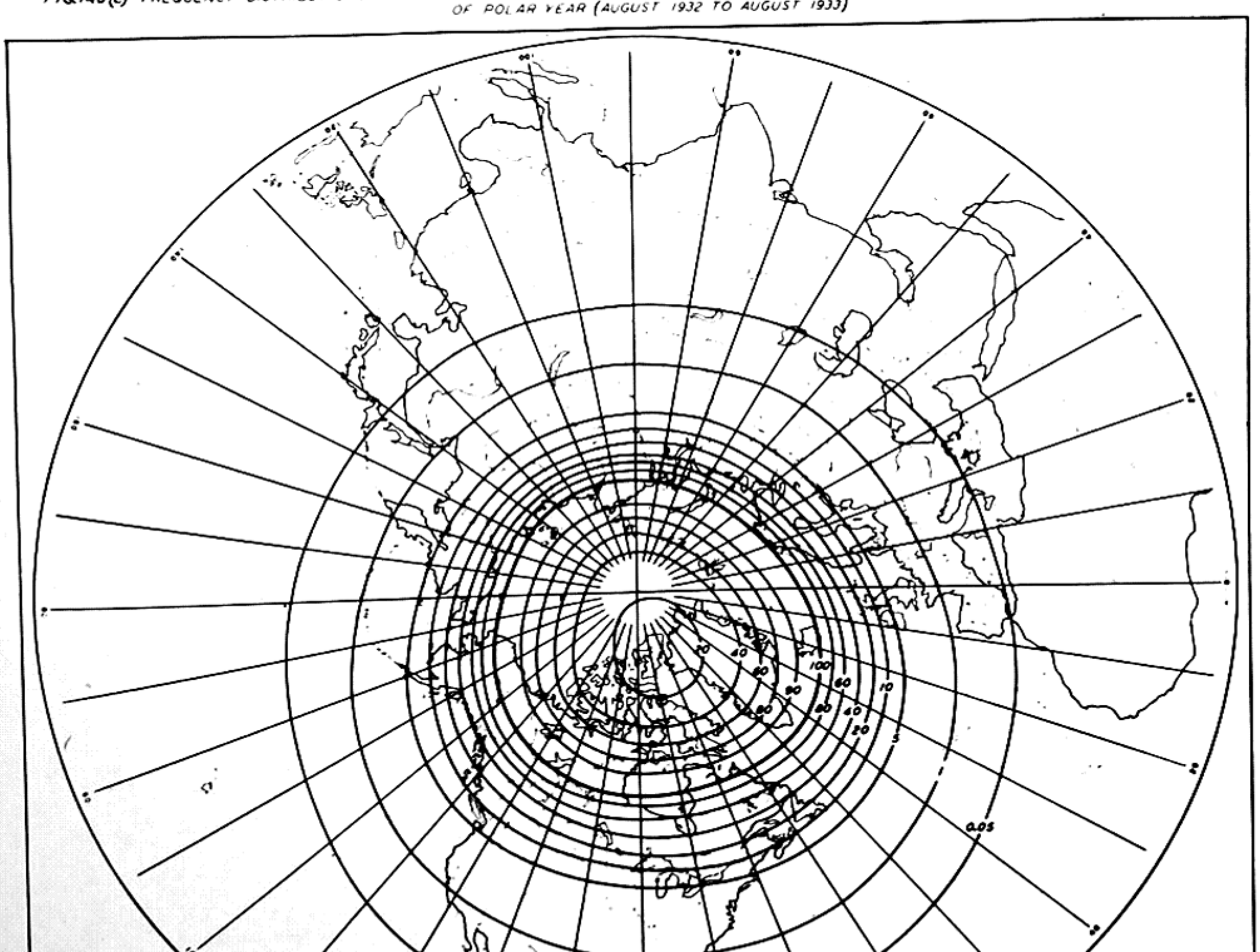

FIG. 149—ESTIMATED PERCENTAGE-FREQUENCY OF DAYS WITH OCCURRENCE OF AURORA, CLEAR NIGHTS, NORTHERN HEMISPHERE

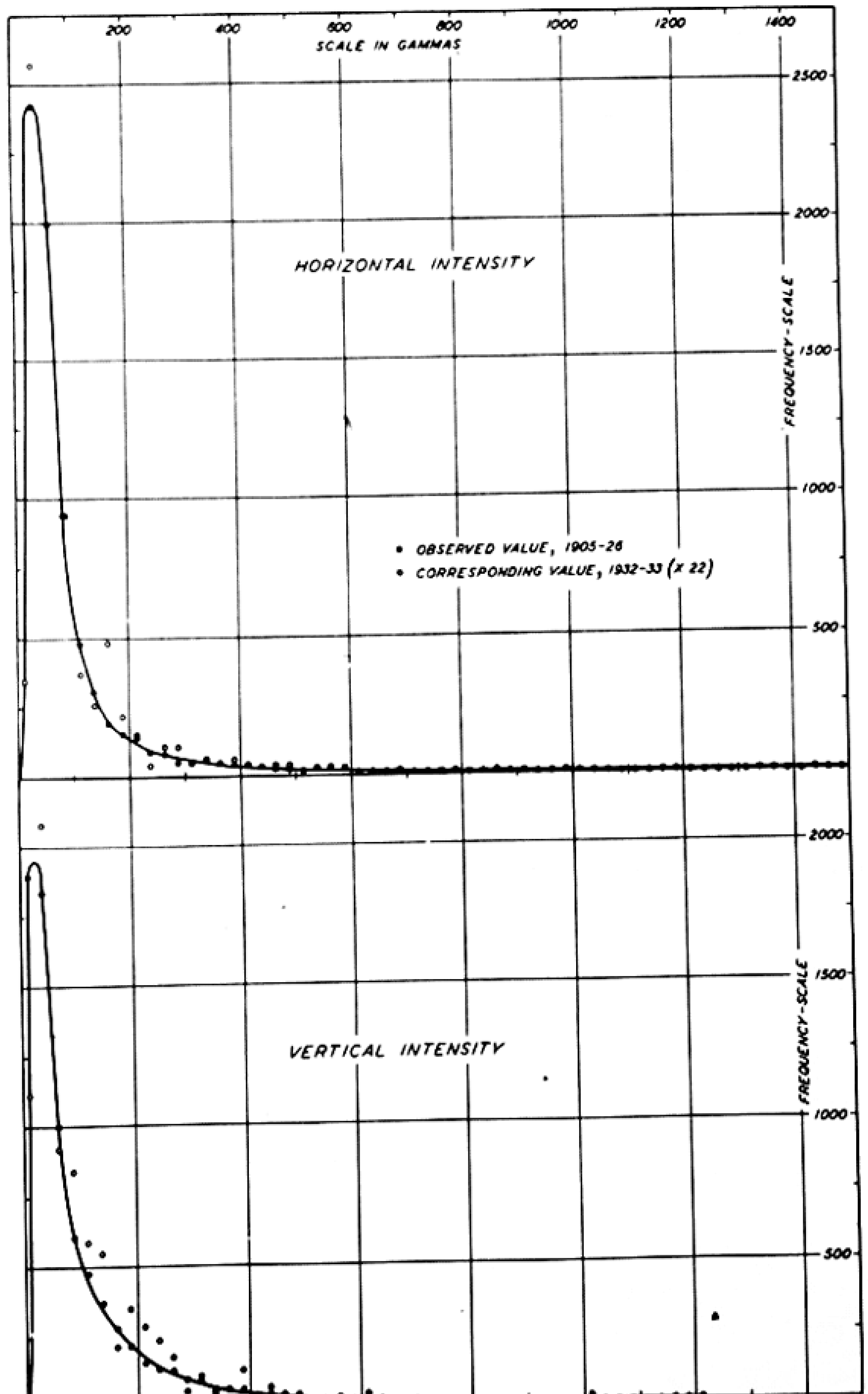

FIG. 150 - FREQUENCY-DISTRIBUTIONS OF DAILY RANGES IN H AND Z, SITKA, 1905-26, AND CORRESPONDING VALUES (X 22), SEPTEMBER, 1932, TO AUGUST, 1933

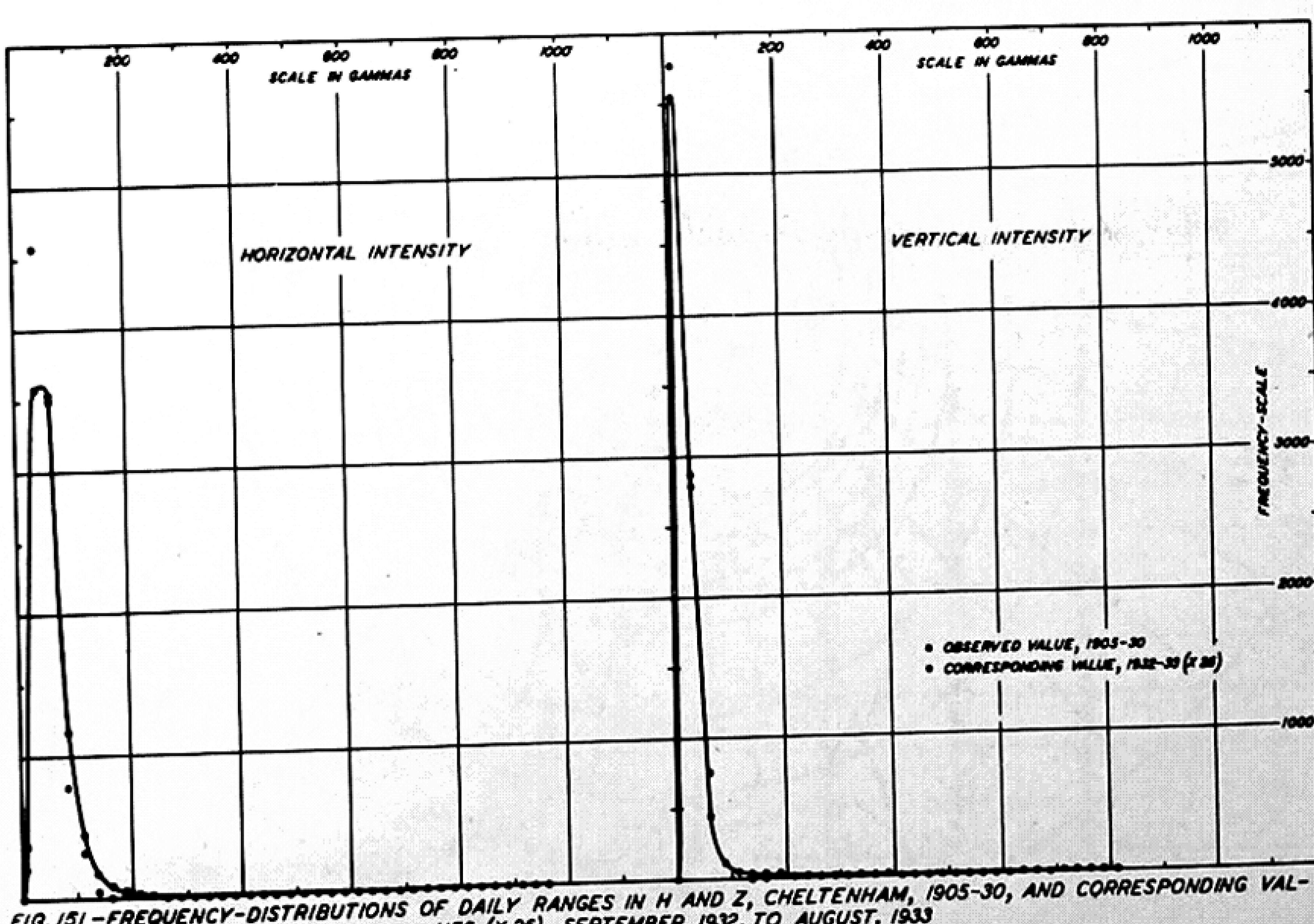

FIG. 151 - FREQUENCY-DISTRIBUTIONS OF DAILY RANGES IN H AND Z, CHELTENHAM, 1905-30, AND CORRESPONDING VALUES (X 26), SEPTEMBER, 1932, TO AUGUST, 1933

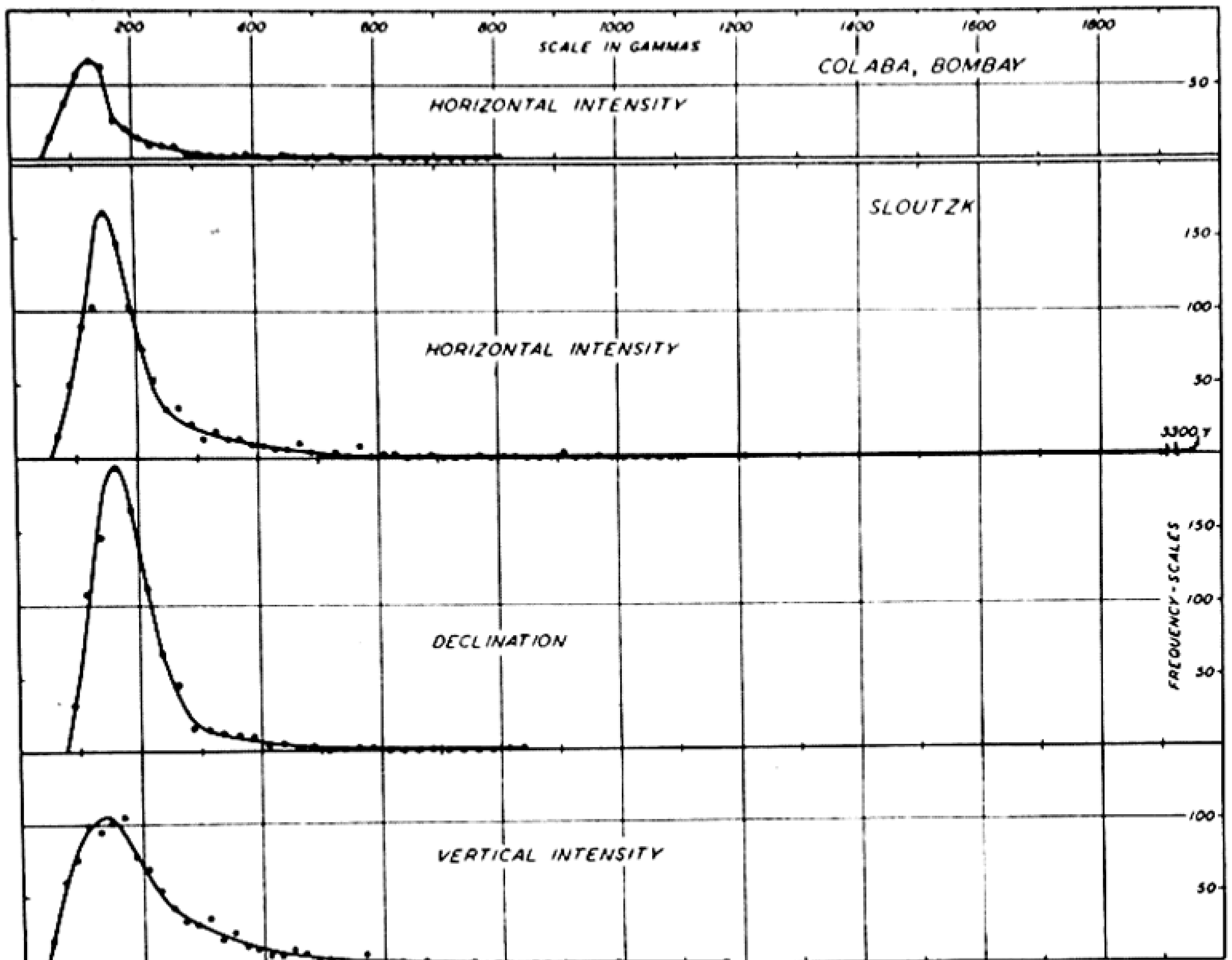

FIG. 152 — FREQUENCY-DISTRIBUTIONS OF RANGES FOR MAGNETIC STORMS GREATER THAN 70γ IN H, 24- TO 77-HOUR INTERVALS, BOMBAY, 1882-1905, AND OF DAILY RANGES FOR STORMS GREATER THAN 50γ IN D, SLOUTZK, 1878-1940

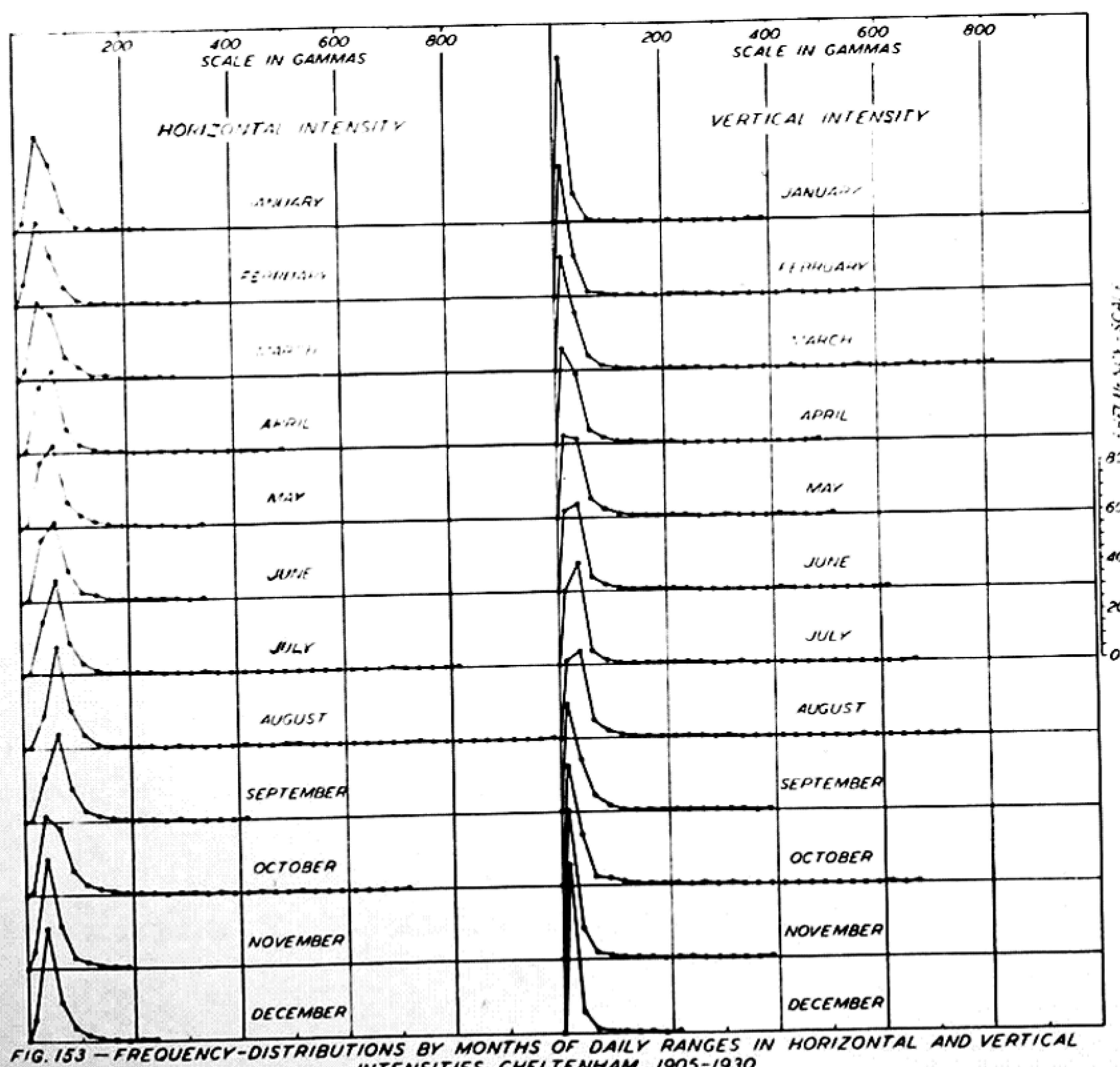

FIG. 153 — FREQUENCY-DISTRIBUTIONS BY MONTHS OF DAILY RANGES IN HORIZONTAL AND VERTICAL INTENSITIES, CHELTENHAM, 1905-1930

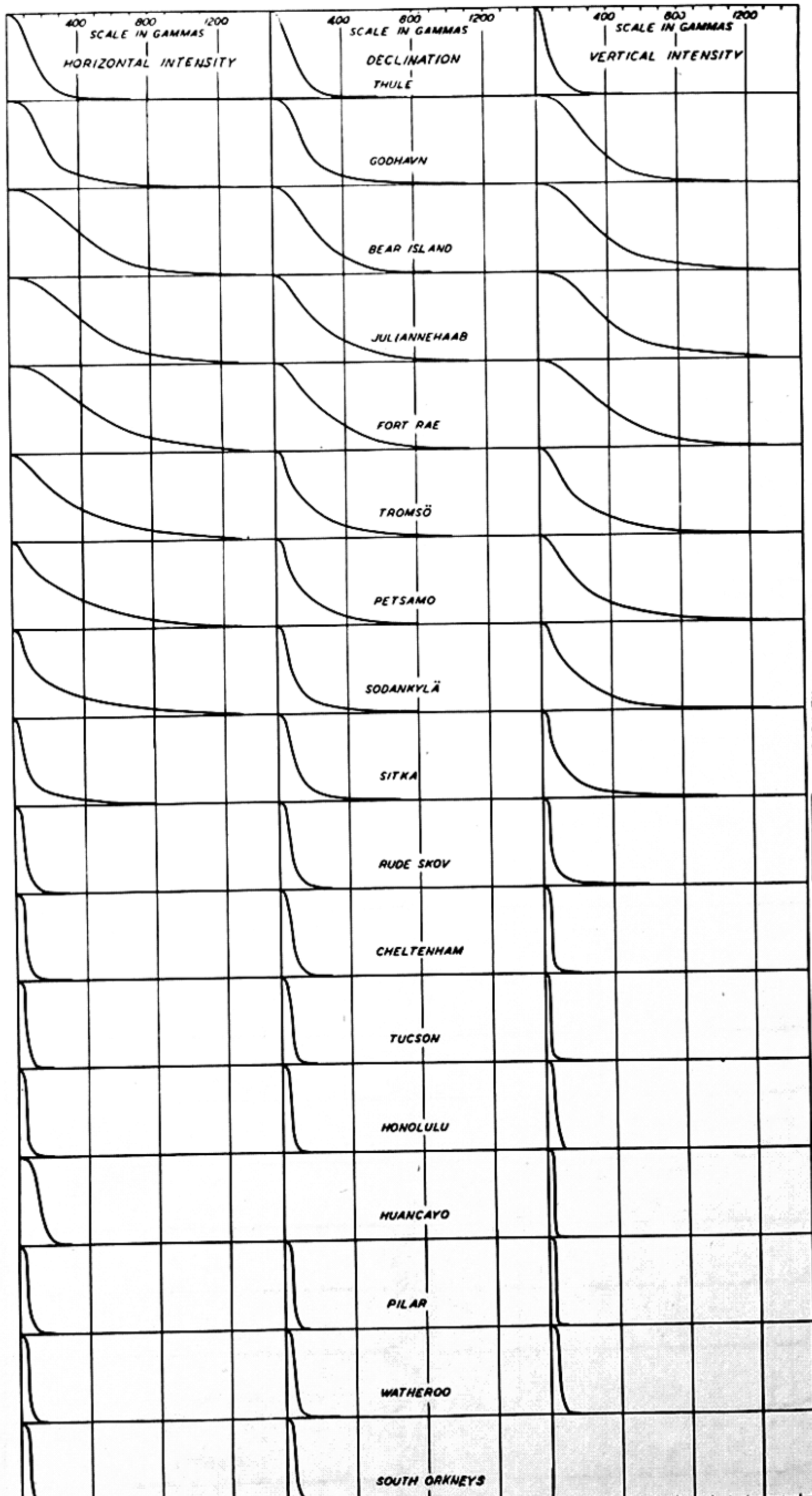

FIG. 154—PROBABILITY THAT DAILY RANGES OF H, D, AND Z EXCEED VARIOUS MAGNITUDES, 12 MONTHS, 1932-33

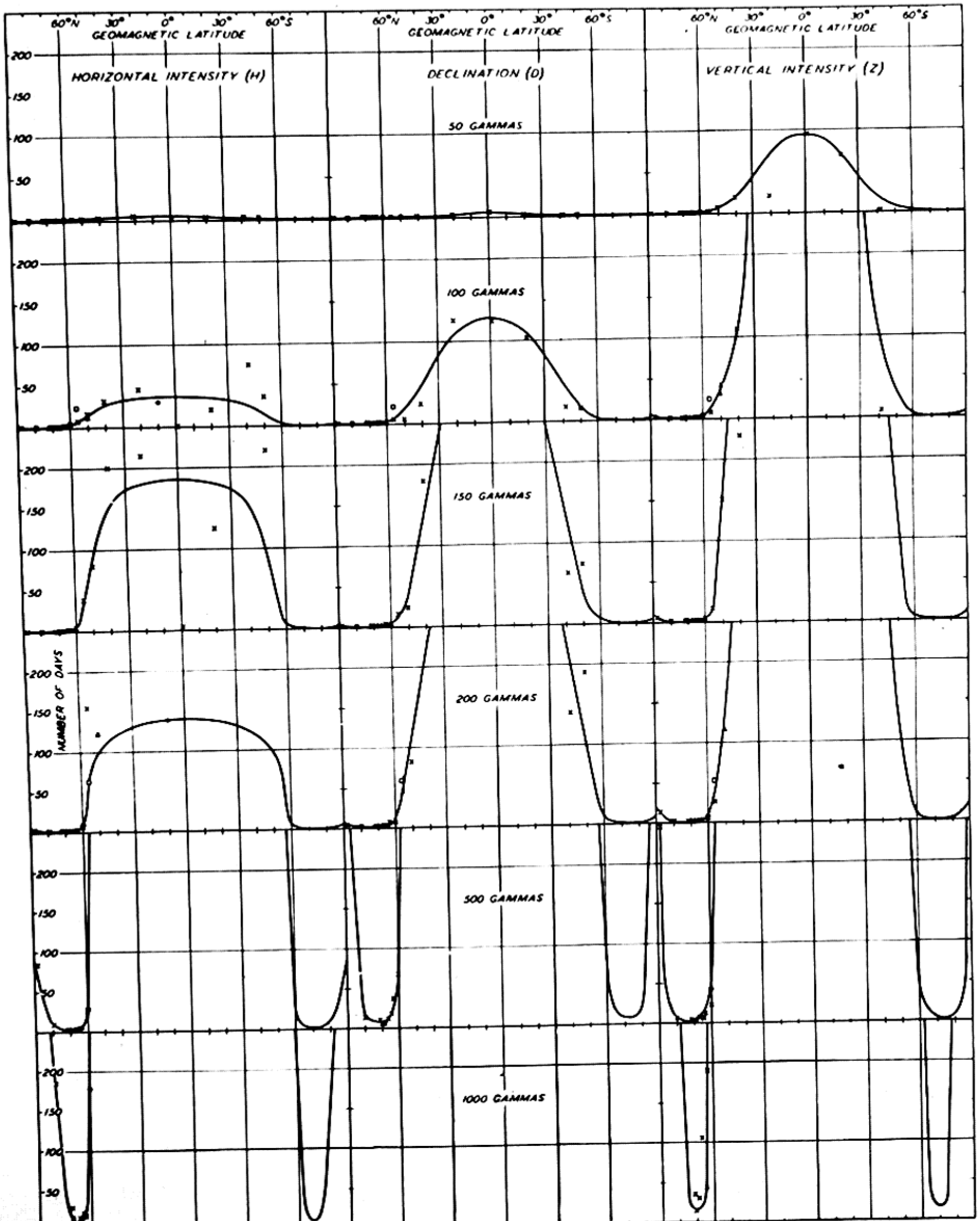

FIG.155—VARIATION WITH LATITUDE OF EXPECTATIONS IN DAYS FOR RANGES IN EXCESS OF VARIOUS MAGNITUDES, IN H, D, AND Z
LEGEND: × = POLAR YEAR, 12 MONTHS, 1932-33; • = SITKA, 1905-26; o = SLOUTZK, 1878-1939; ▵ = CHELTENHAM, 1905-30; • = BOMBAY, 1882-1905

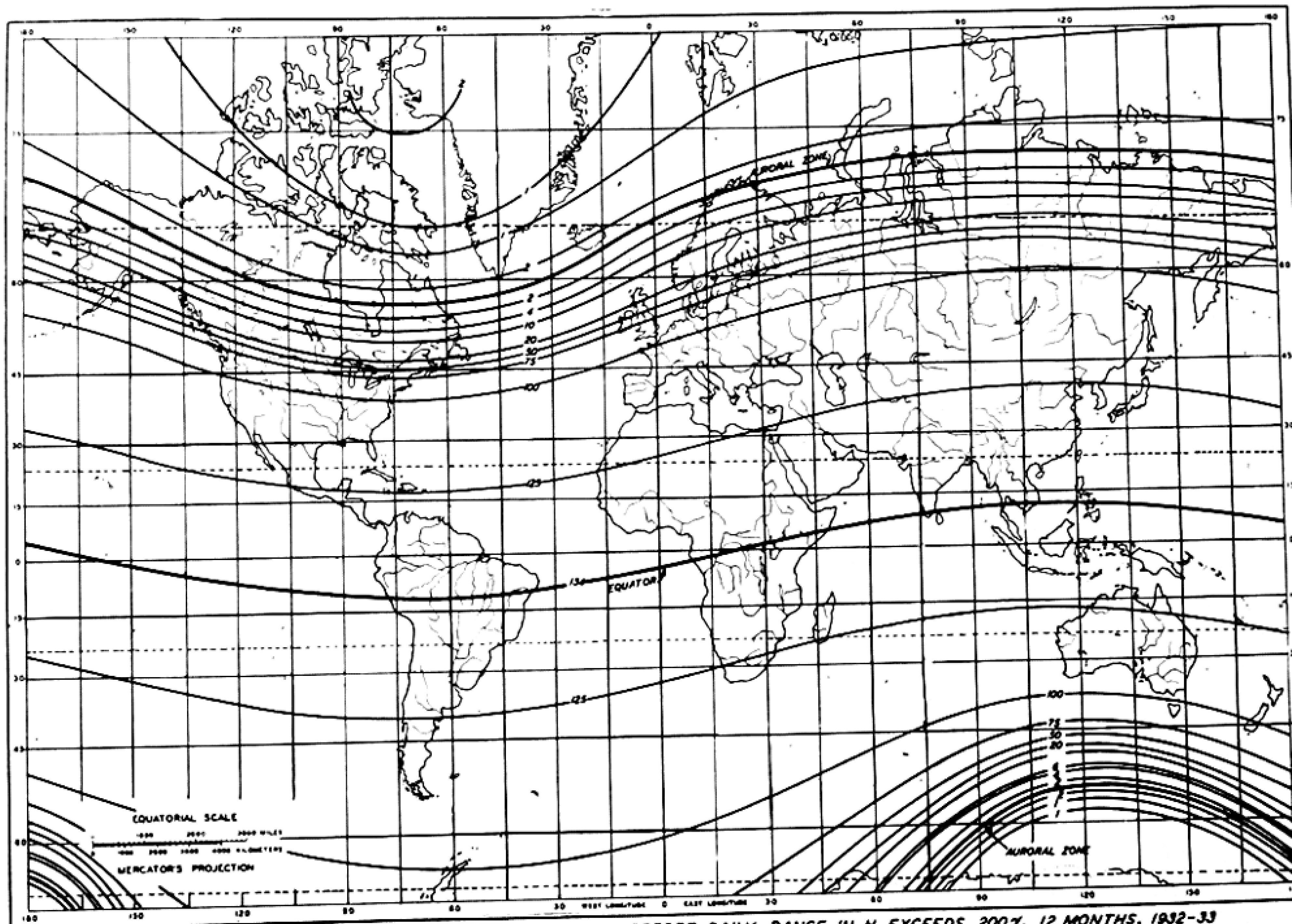

FIG.156—ISOCHRONIC LINES FOR EXPECTATION IN DAYS BEFORE DAILY RANGE IN H EXCEEDS 200γ, 12 MONTHS, 1932-33

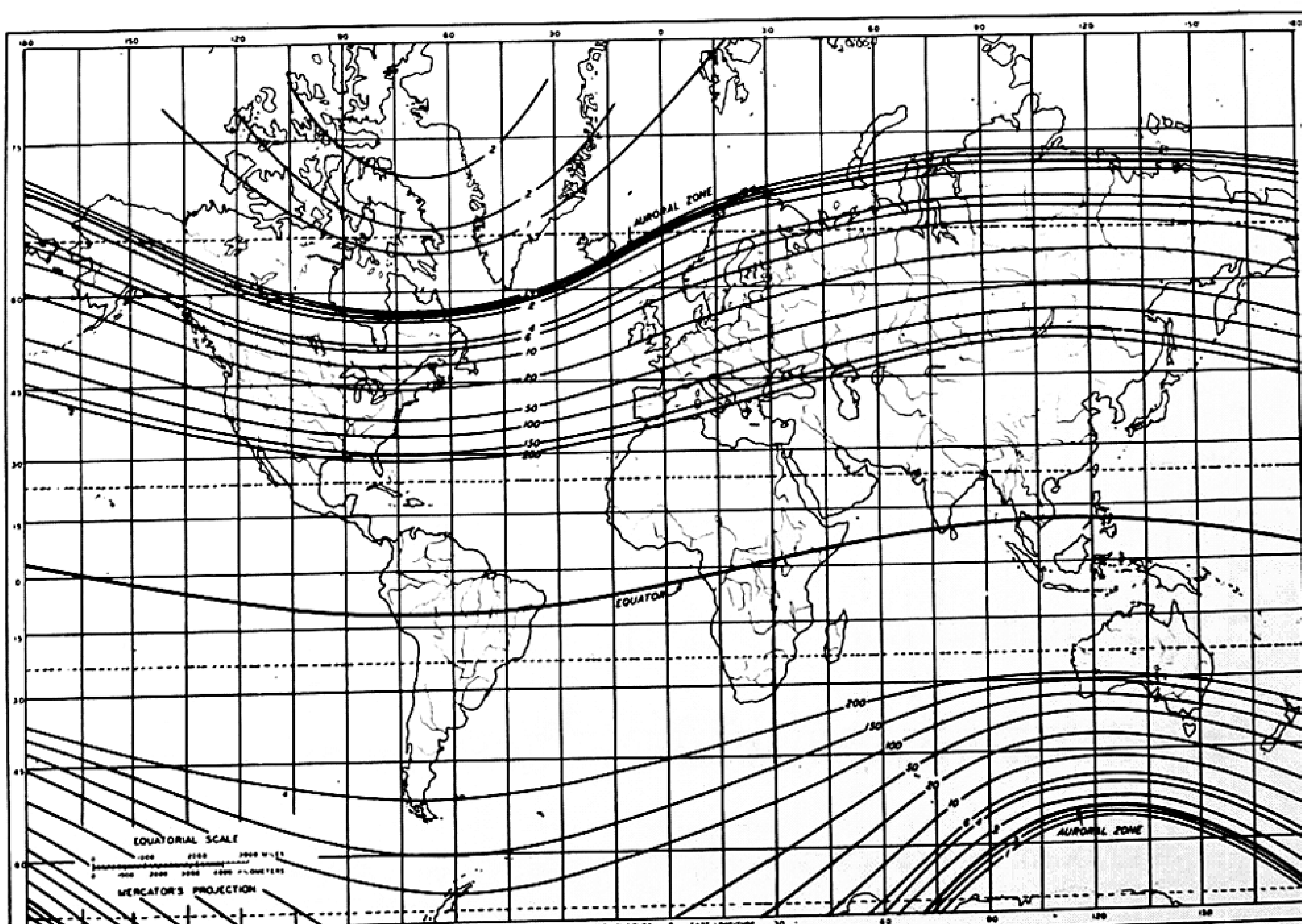

FIG.157—ISOCHRONIC LINES FOR EXPECTATION IN DAYS BEFORE DAILY RANGE IN D EXCEEDS 200γ, 12 MONTHS, 1932-33

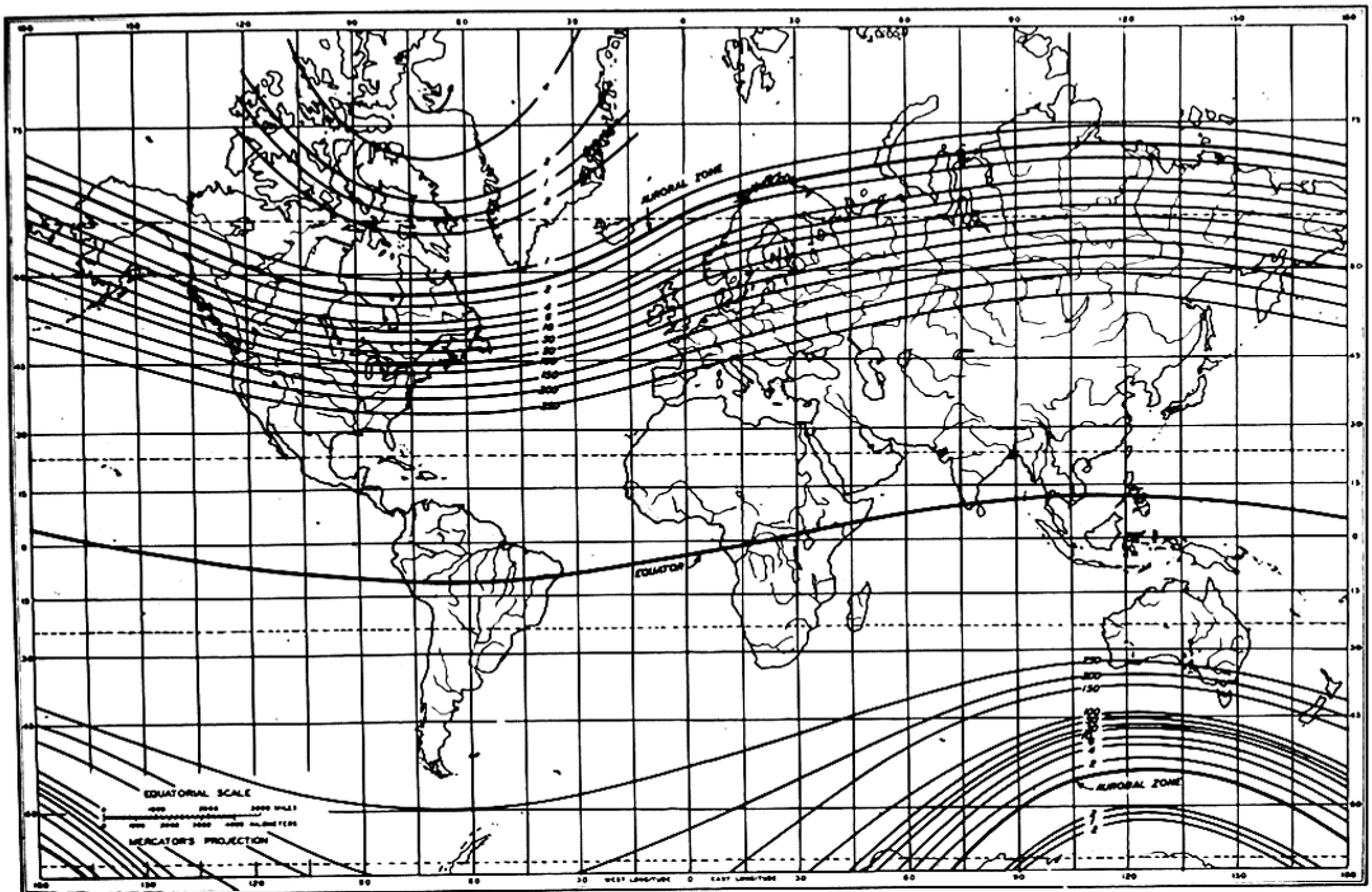

FIG. 158—ISOCHRONIC LINES FOR EXPECTATION IN DAYS BEFORE DAILY RANGE IN Z EXCEEDS 200γ, 12 MONTHS, 1932-33

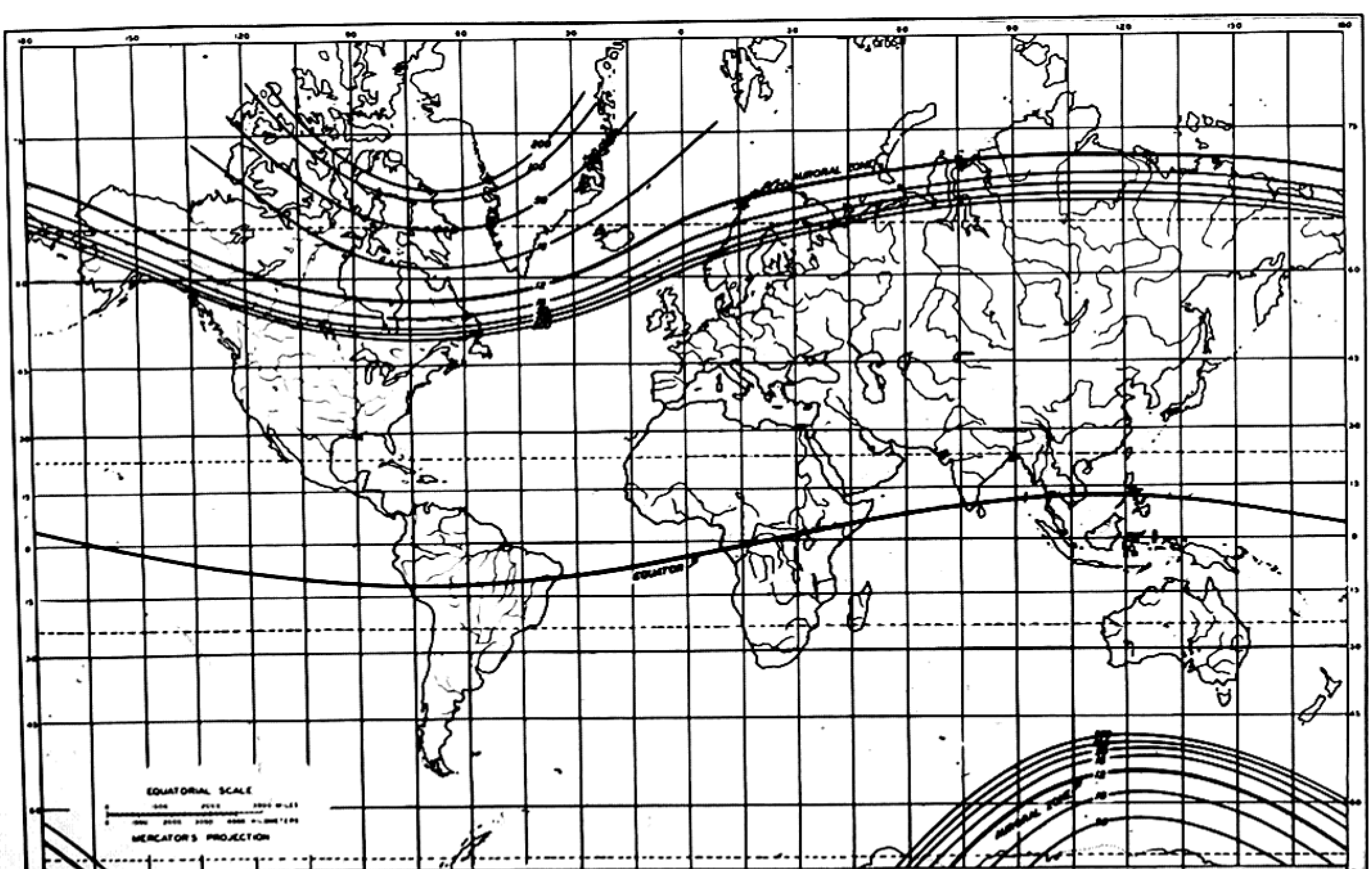

FIG. 159—ISOCHRONIC LINES FOR EXPECTATION IN DAYS BEFORE DAILY RANGE IN H EXCEEDS 1000γ, 12 MONTHS, 1932-33

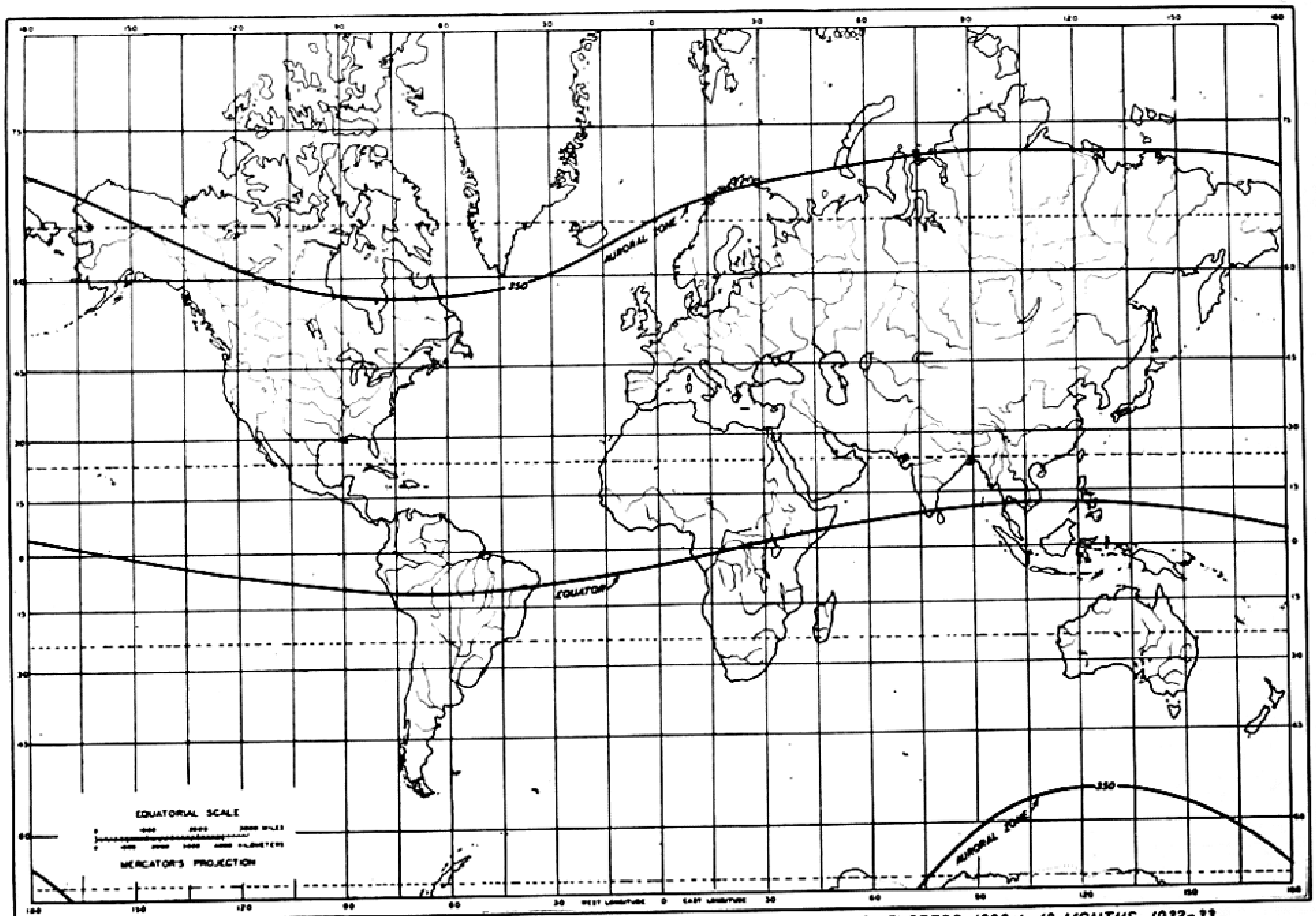

FIG. 160—ISOCHRONIC LINES FOR EXPECTATION IN DAYS BEFORE DAILY RANGE IN D EXCEEDS 1000γ, 12 MONTHS, 1932-33

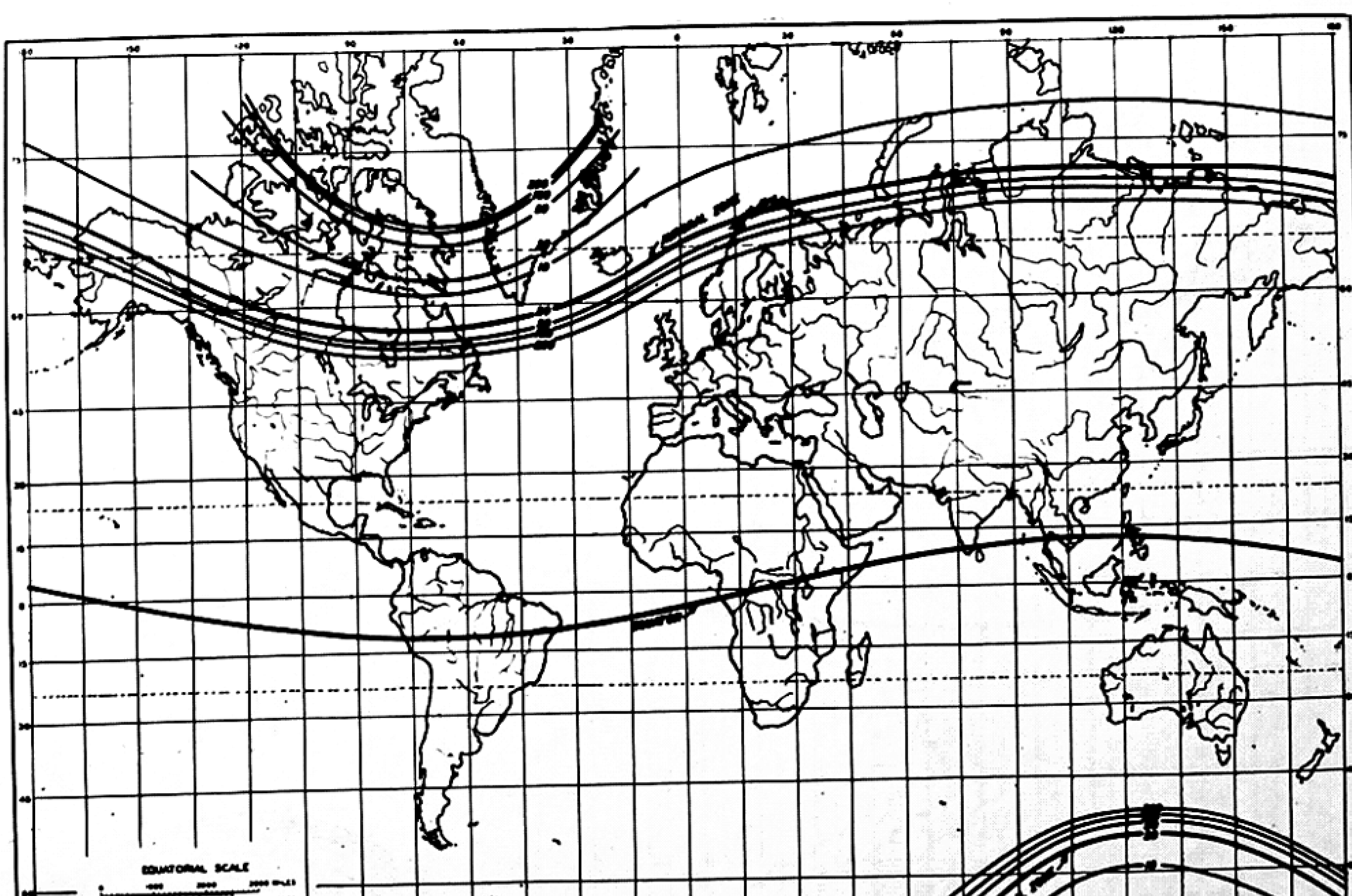

FIG. 161—ISOCHRONIC LINES FOR EXPECTATION IN DAYS BEFORE DAILY RANGE IN Z EXCEEDS 1000γ, 12 MONTHS, 1932-33

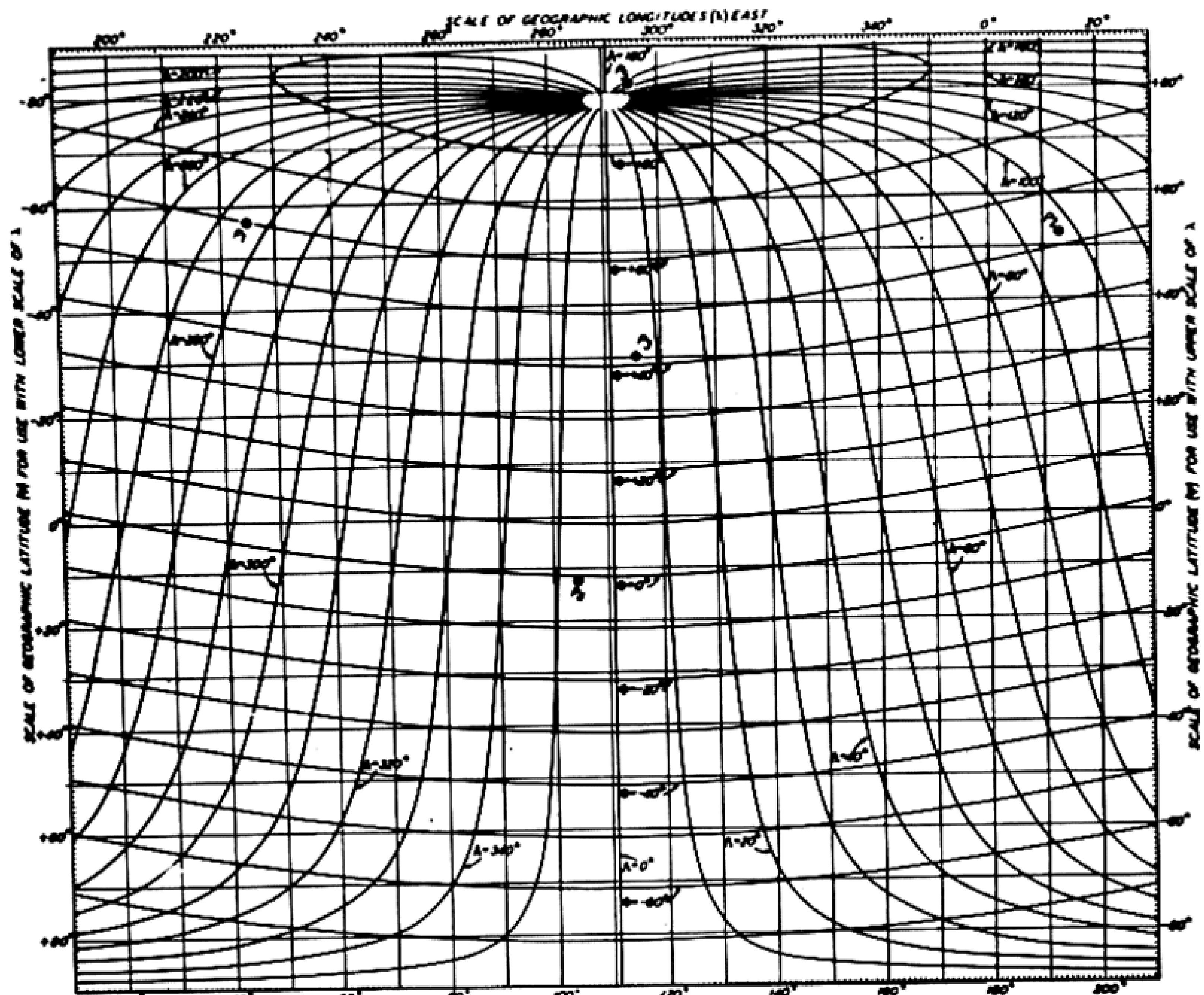

FIG. 182 — GEOGRAPHIC AND GEOMAGNETIC COORDINATE-SYSTEMS FOR ENTIRE EARTH
(FOR BOTTOM SCALE OF LONGITUDE, CHART-READINGS OF GEOMAGNETIC LATITUDE (Φ) AND LONGITUDE (Λ) ARE SOUTH AND EAST FROM 180°, RESPECTIVELY)

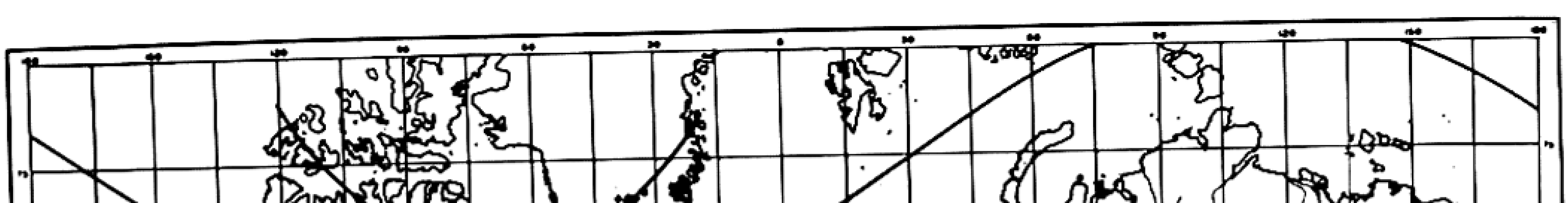

FIG. 163 — LINES OF EQUAL GEOMAGNETIC LATITUDE

FIG. 184—DAILY MAXIMA AND MINIMA HORIZONTAL INTENSITY, SITKA, ALASKA, SEPTEMBER 1, 1932, TO AUGUST 31, 1933

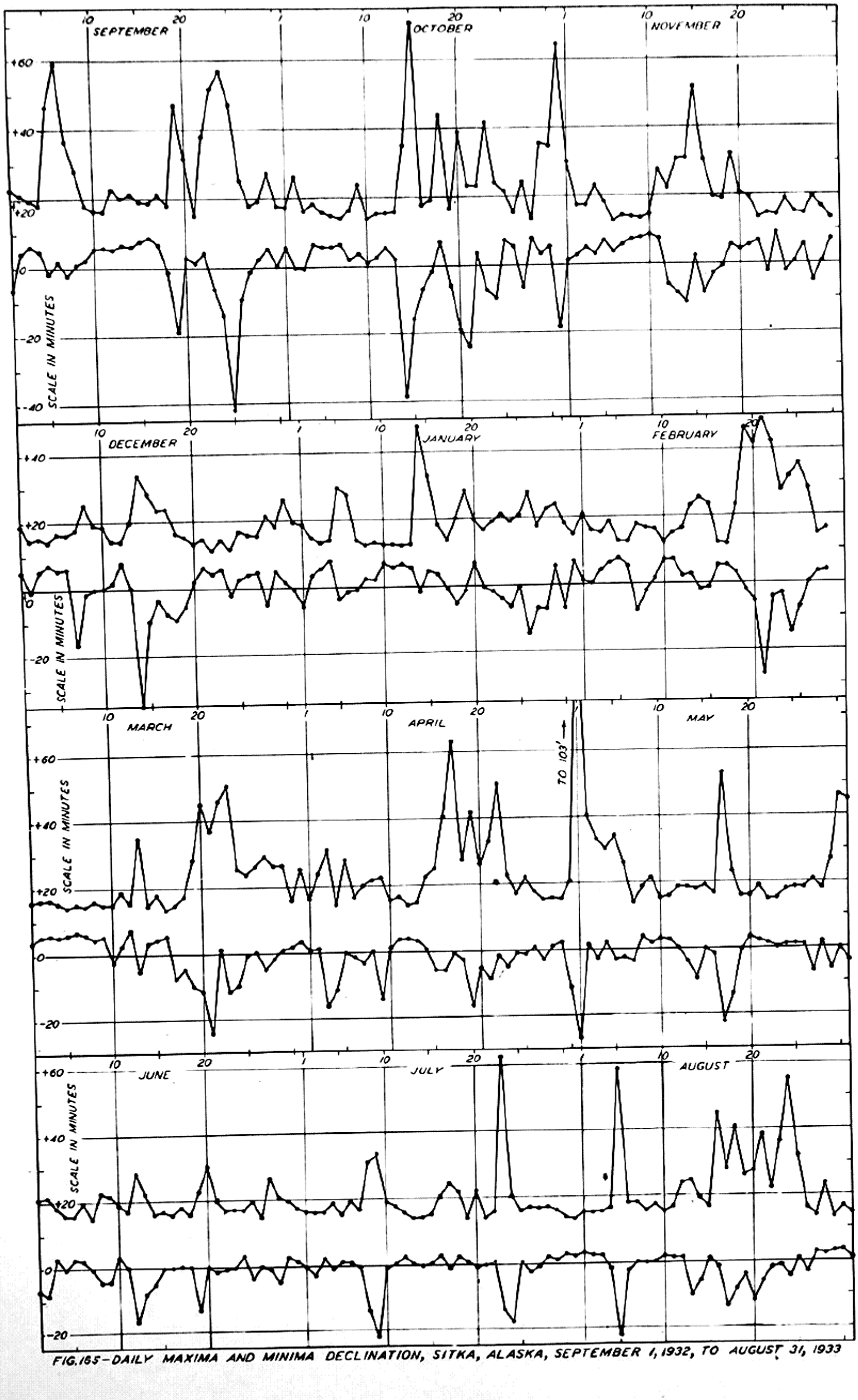

FIG. 165—DAILY MAXIMA AND MINIMA DECLINATION, SITKA, ALASKA, SEPTEMBER 1, 1932, TO AUGUST 31, 1933

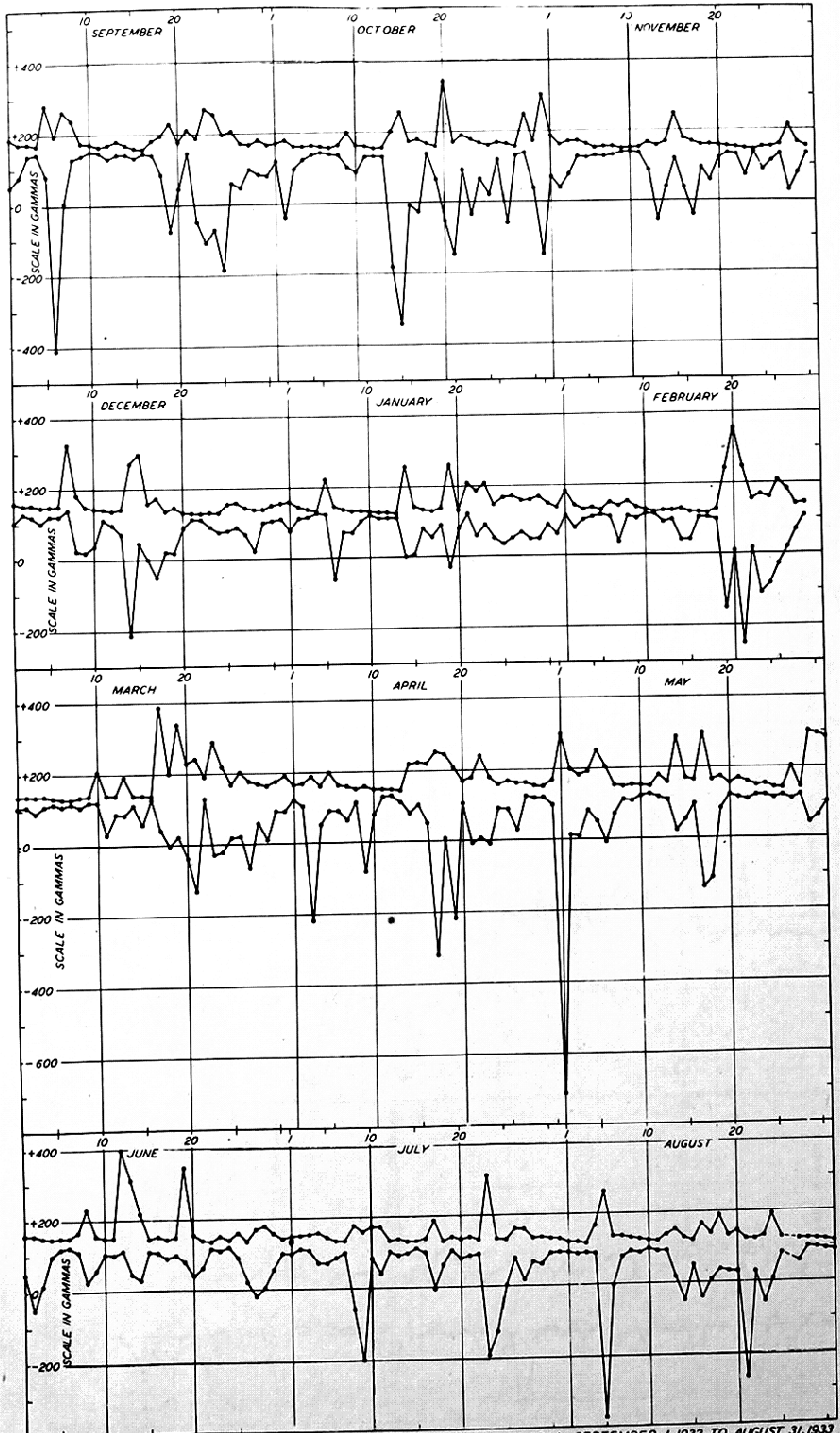

FIG. 186—DAILY MAXIMA AND MINIMA VERTICAL INTENSITY, SITKA, ALASKA, SEPTEMBER 1, 1932, TO AUGUST 31, 1933

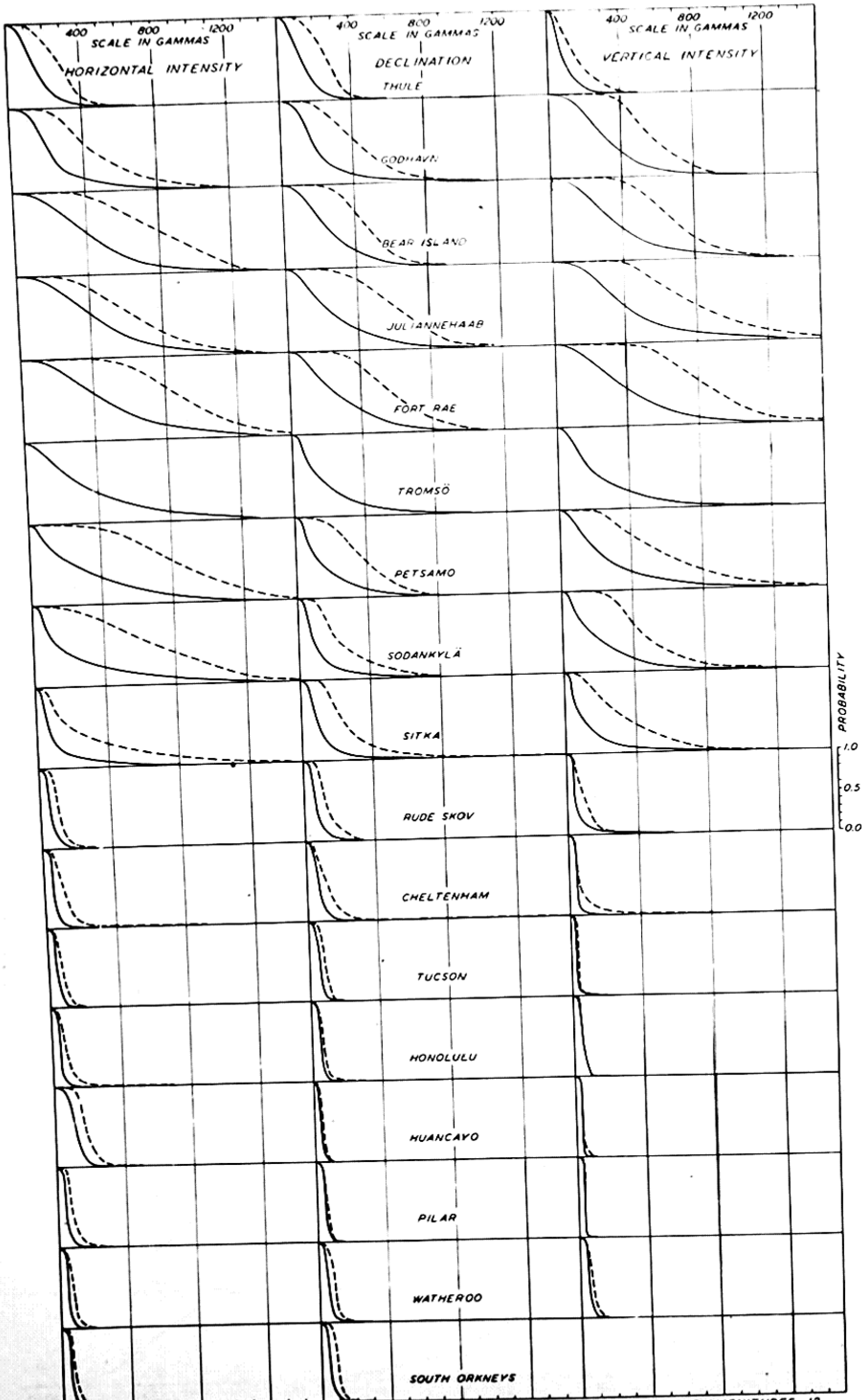

FIG. 167—PROBABILITY THAT DAILY AND WEEKLY RANGES OF H, D, AND Z EXCEED VARIOUS MAGNITUDES, 12 MONTHS, 1932-33

—— DAILY RANGES ---- WEEKLY RANGES

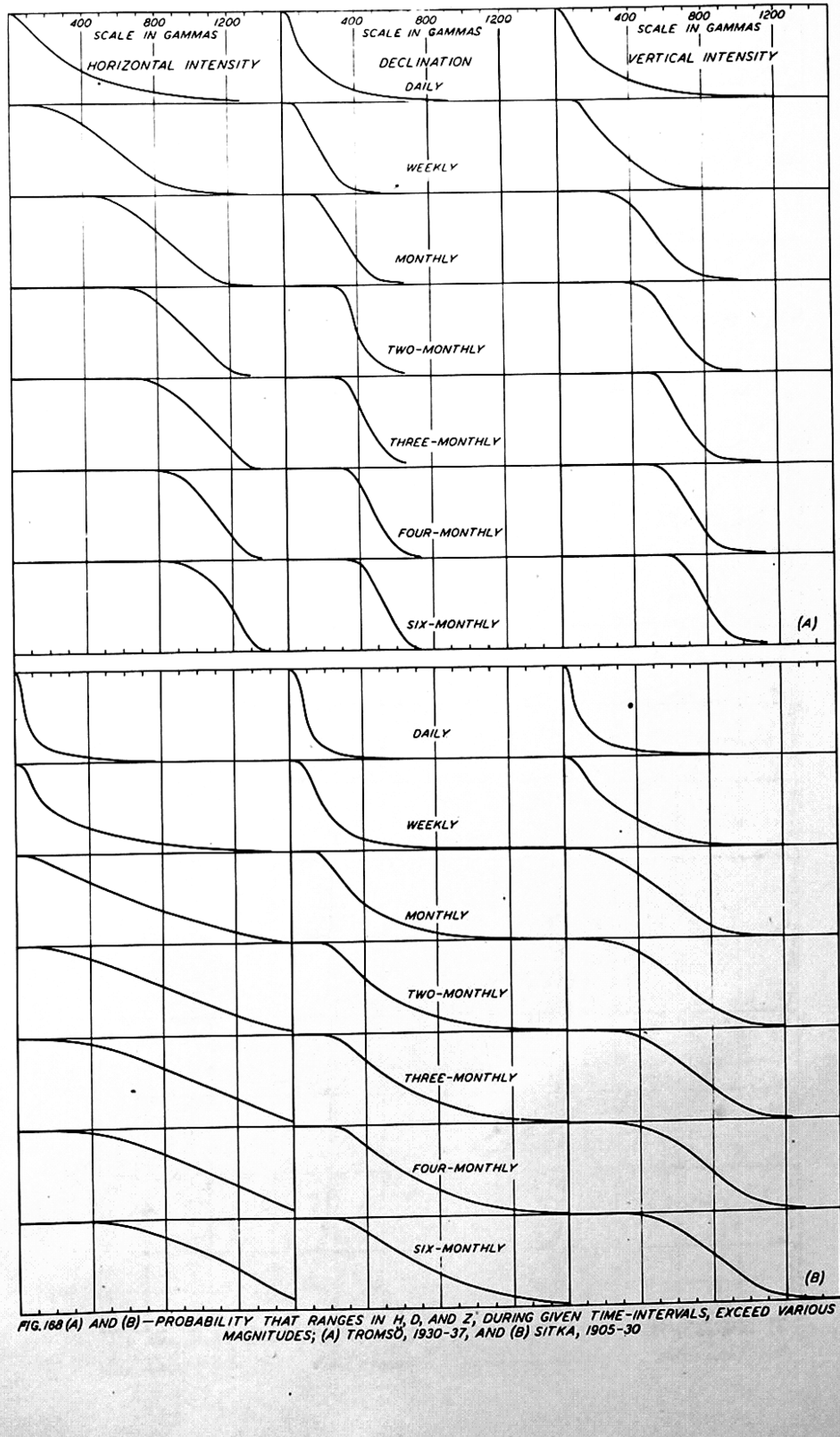

FIG. 168 (A) AND (B)—PROBABILITY THAT RANGES IN H, D, AND Z, DURING GIVEN TIME-INTERVALS, EXCEED VARIOUS MAGNITUDES; (A) TROMSÖ, 1930-37, AND (B) SITKA, 1905-30

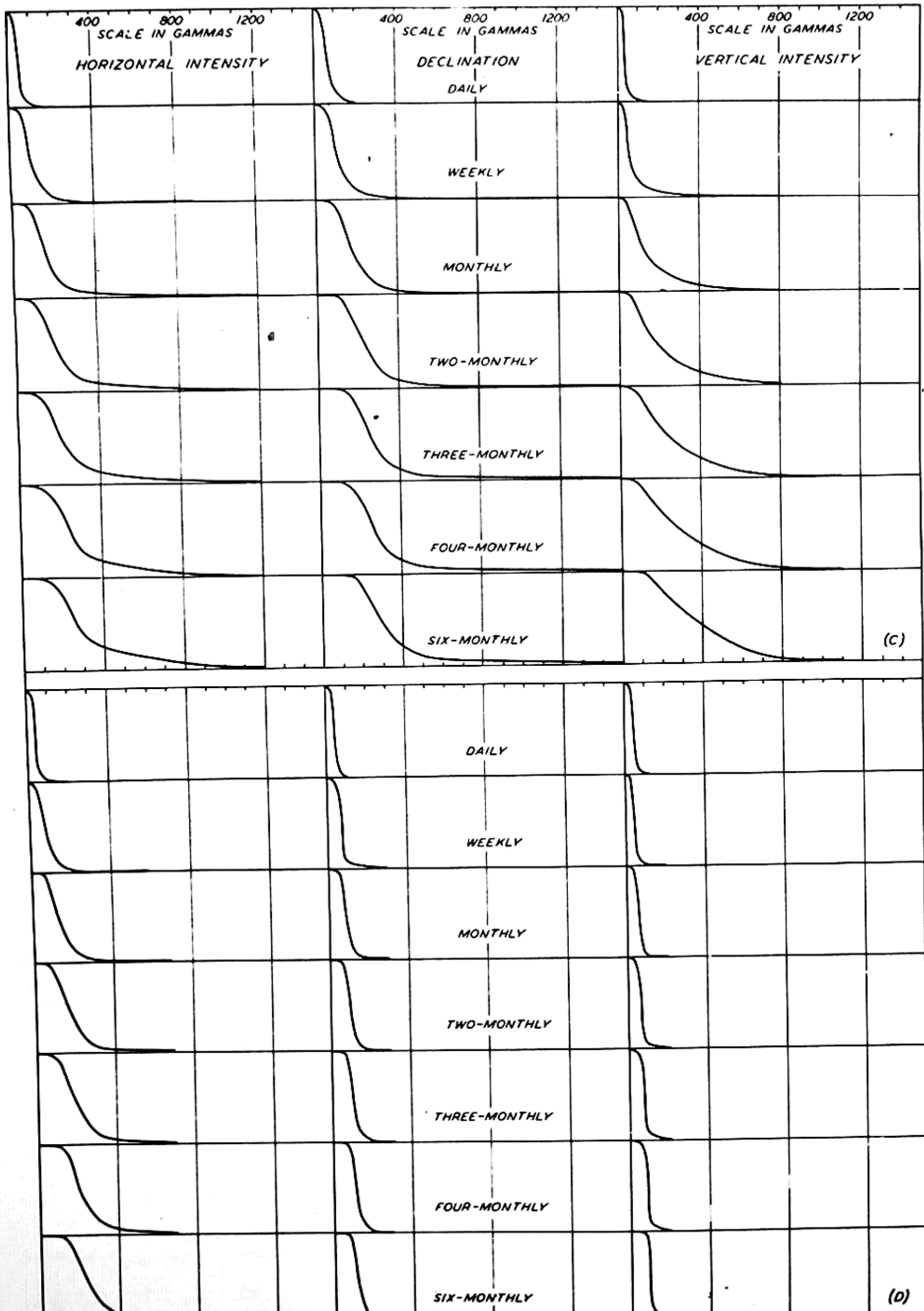

FIG. 188(C) AND (D)—PROBABILITY THAT RANGES IN H, D, AND Z, DURING GIVEN TIME-INTERVALS, EXCEED VARIOUS MAGNITUDES; (C) CHELTENHAM, 1905-30, AND (D) HONOLULU, 1905-30

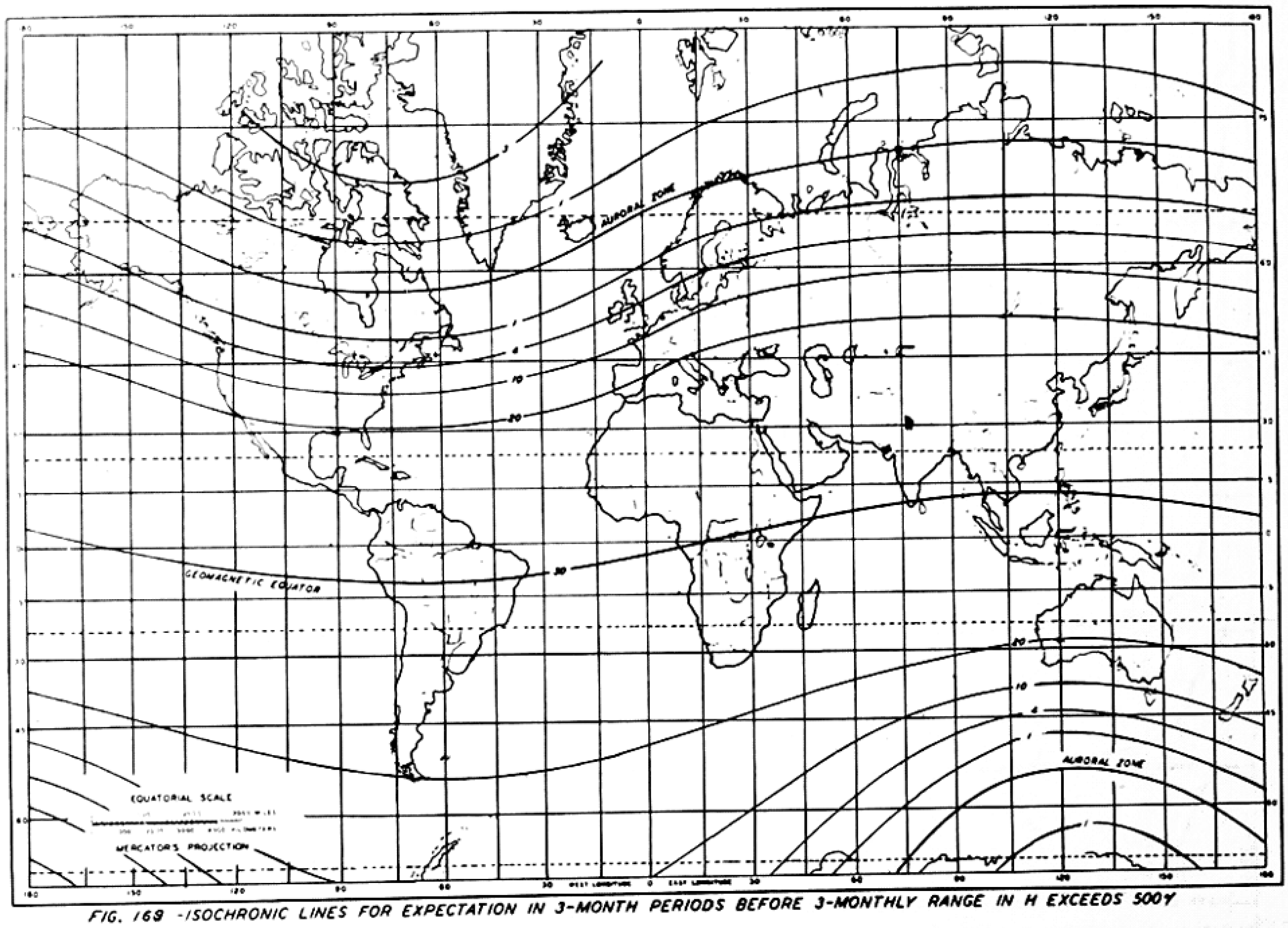

FIG. 169 -ISOCHRONIC LINES FOR EXPECTATION IN 3-MONTH PERIODS BEFORE 3-MONTHLY RANGE IN H EXCEEDS 500γ

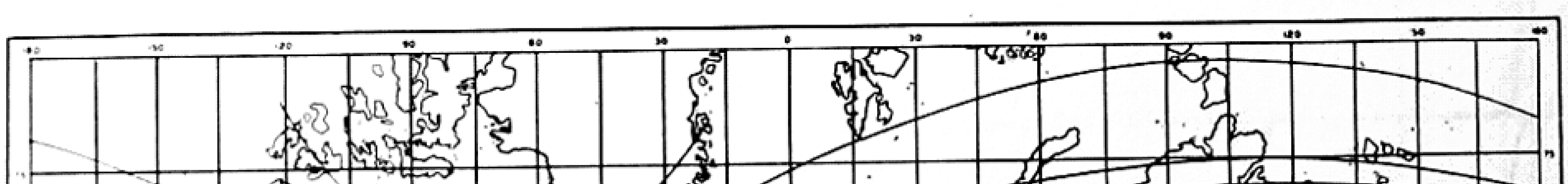

FIG. 170—ISOCHRONIC LINES FOR EXPECTATION IN 3-MONTH PERIODS BEFORE 3-MONTHLY RANGE IN D EXCEEDS 500γ

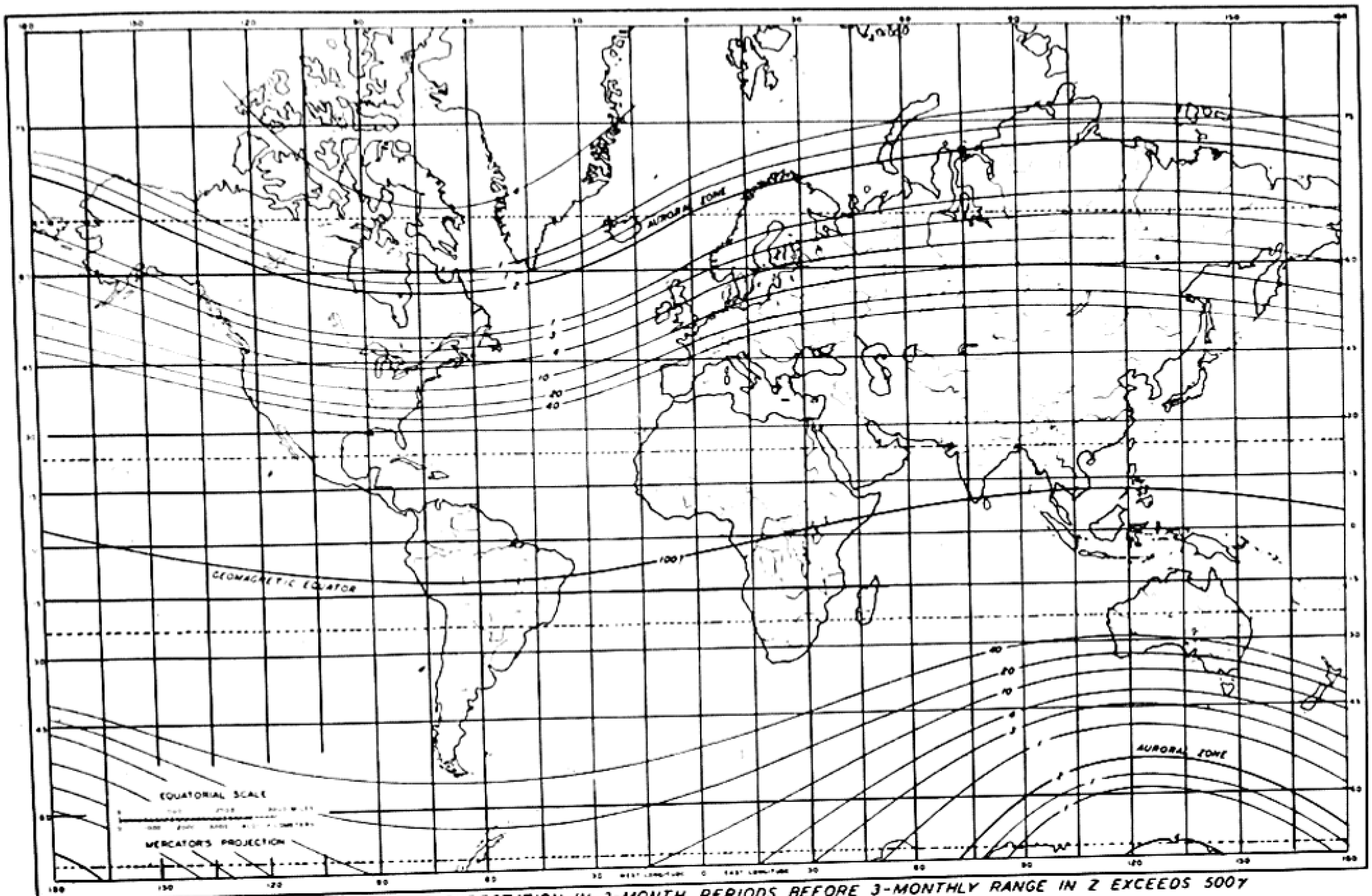

FIG. 171 —ISOCHRONIC LINES FOR EXPECTATION IN 3-MONTH PERIODS BEFORE 3-MONTHLY RANGE IN Z EXCEEDS 500γ

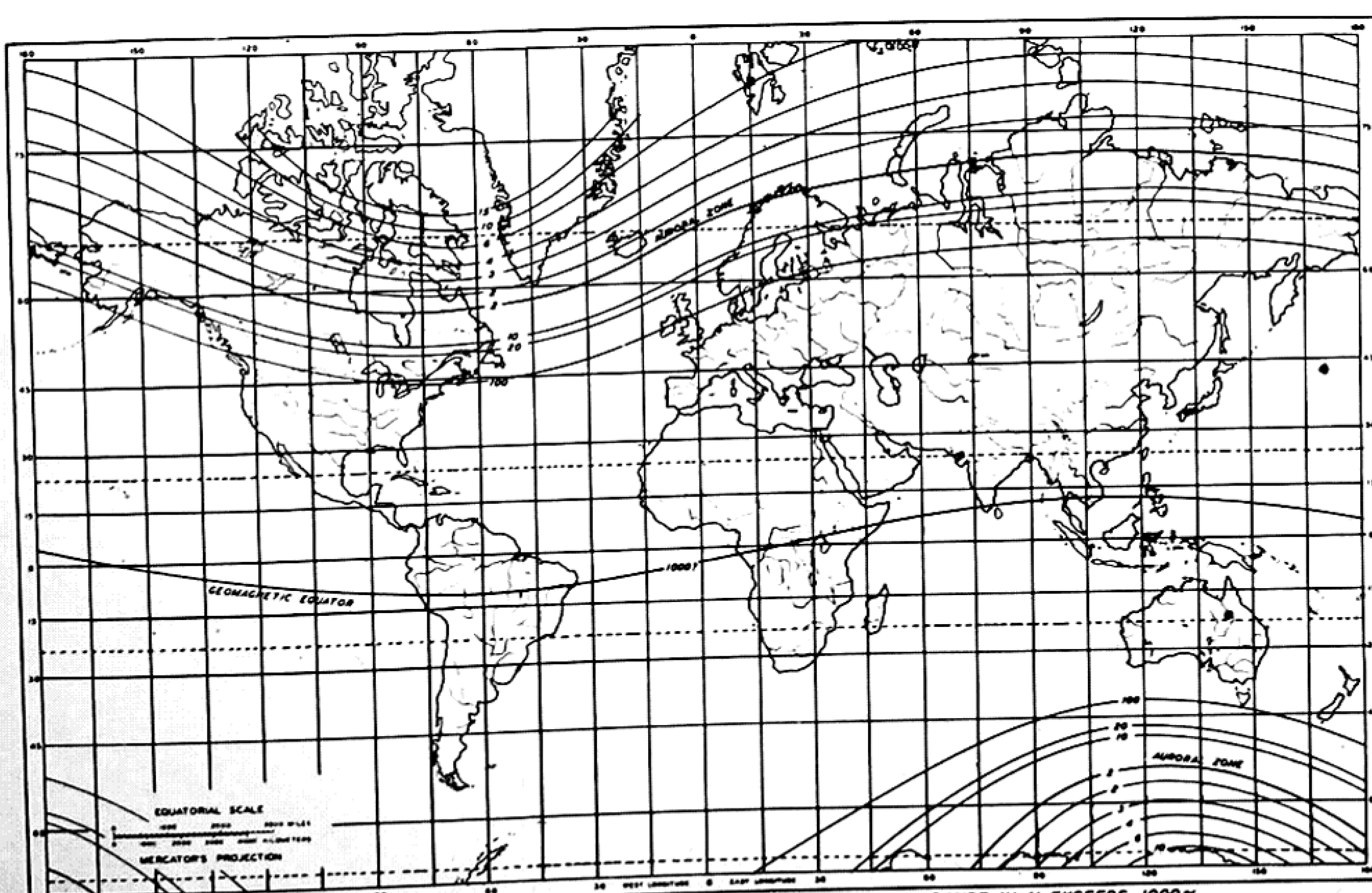

FIG. 172—ISOCHRONIC LINES FOR EXPECTATION IN WEEKS BEFORE WEEKLY RANGE IN H EXCEEDS 1000γ

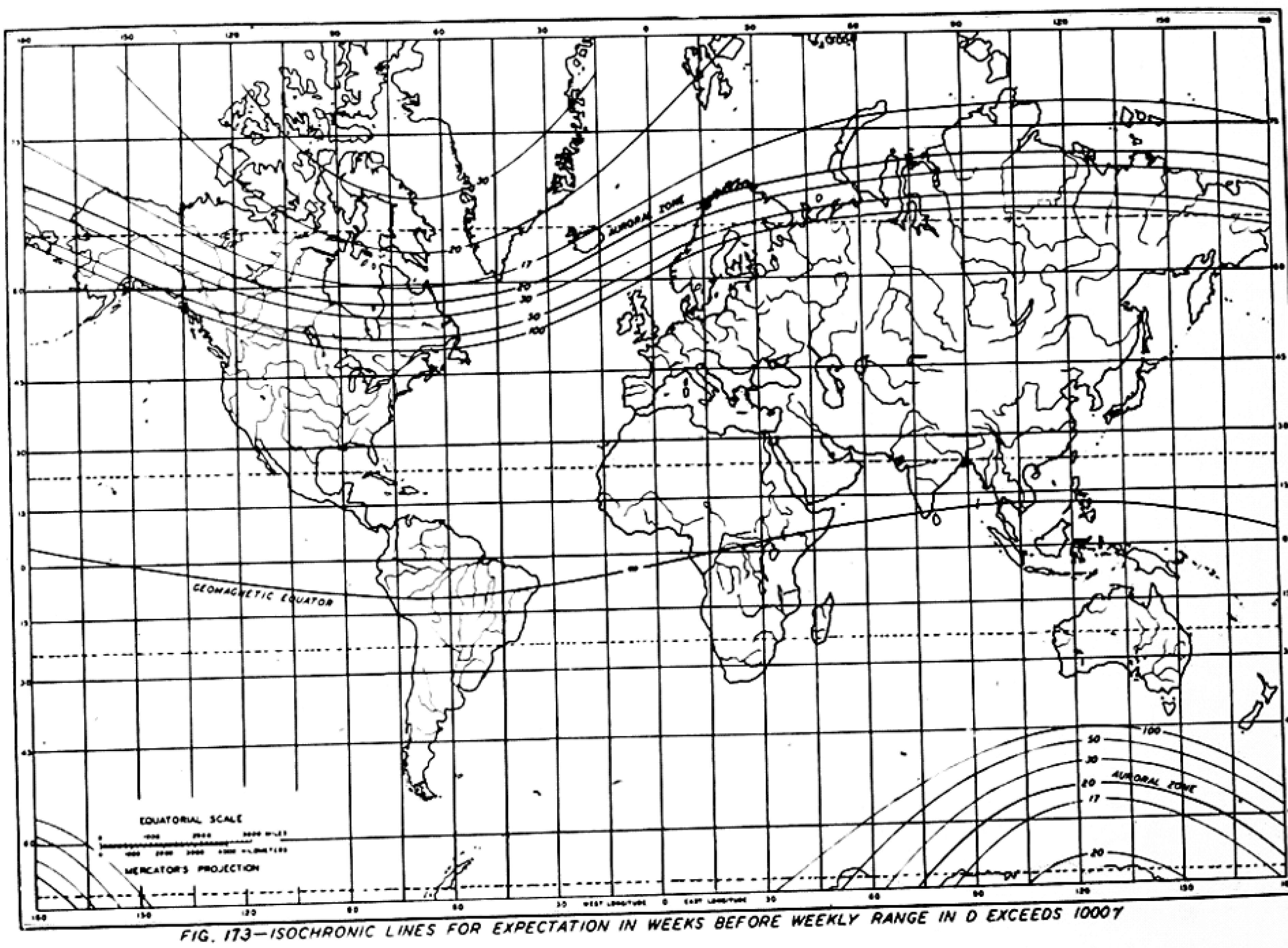

FIG. 173—ISOCHRONIC LINES FOR EXPECTATION IN WEEKS BEFORE WEEKLY RANGE IN D EXCEEDS 1000γ

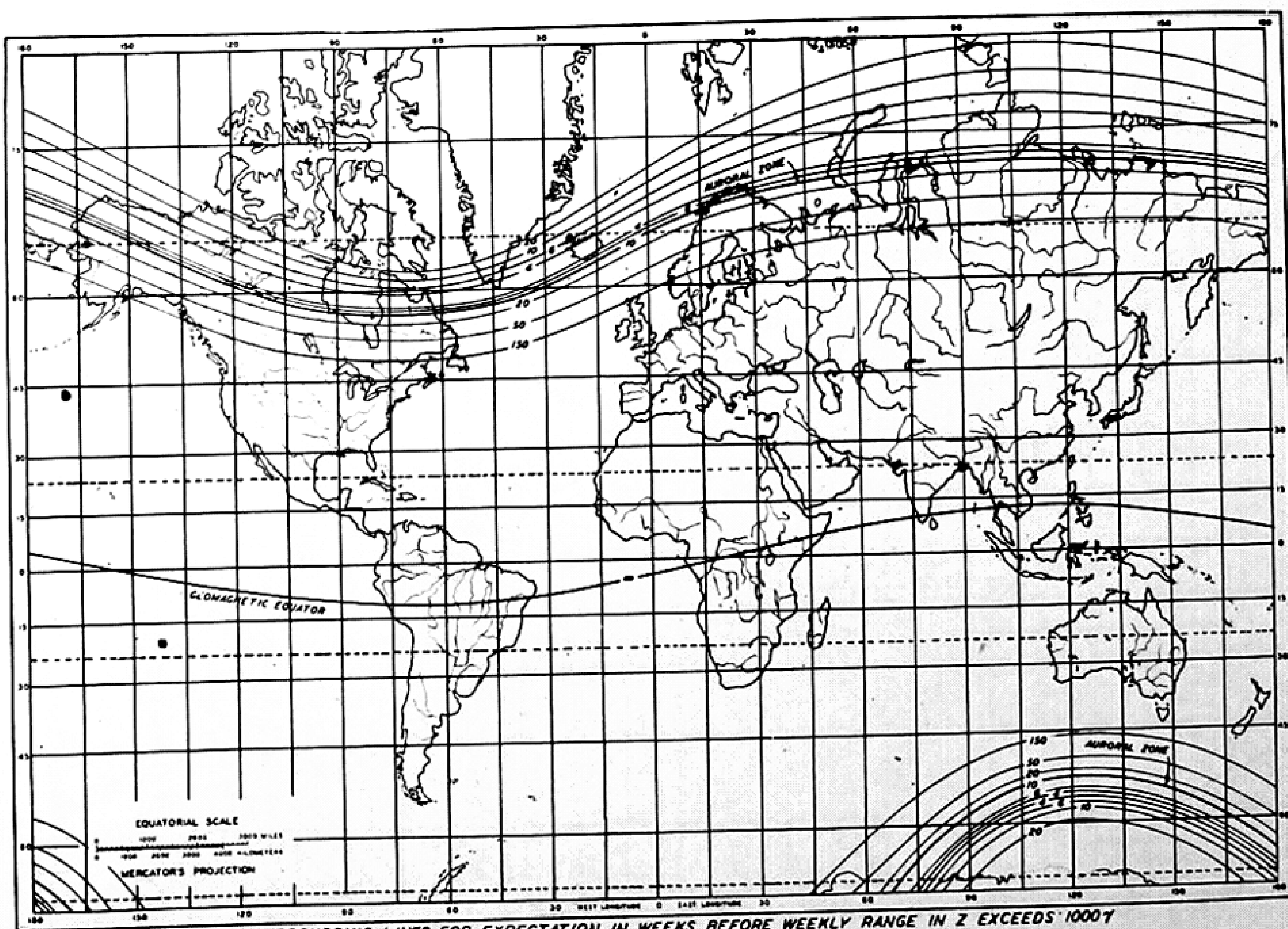

FIG. 174—ISOCHRONIC LINES FOR EXPECTATION IN WEEKS BEFORE WEEKLY RANGE IN Z EXCEEDS 1000γ

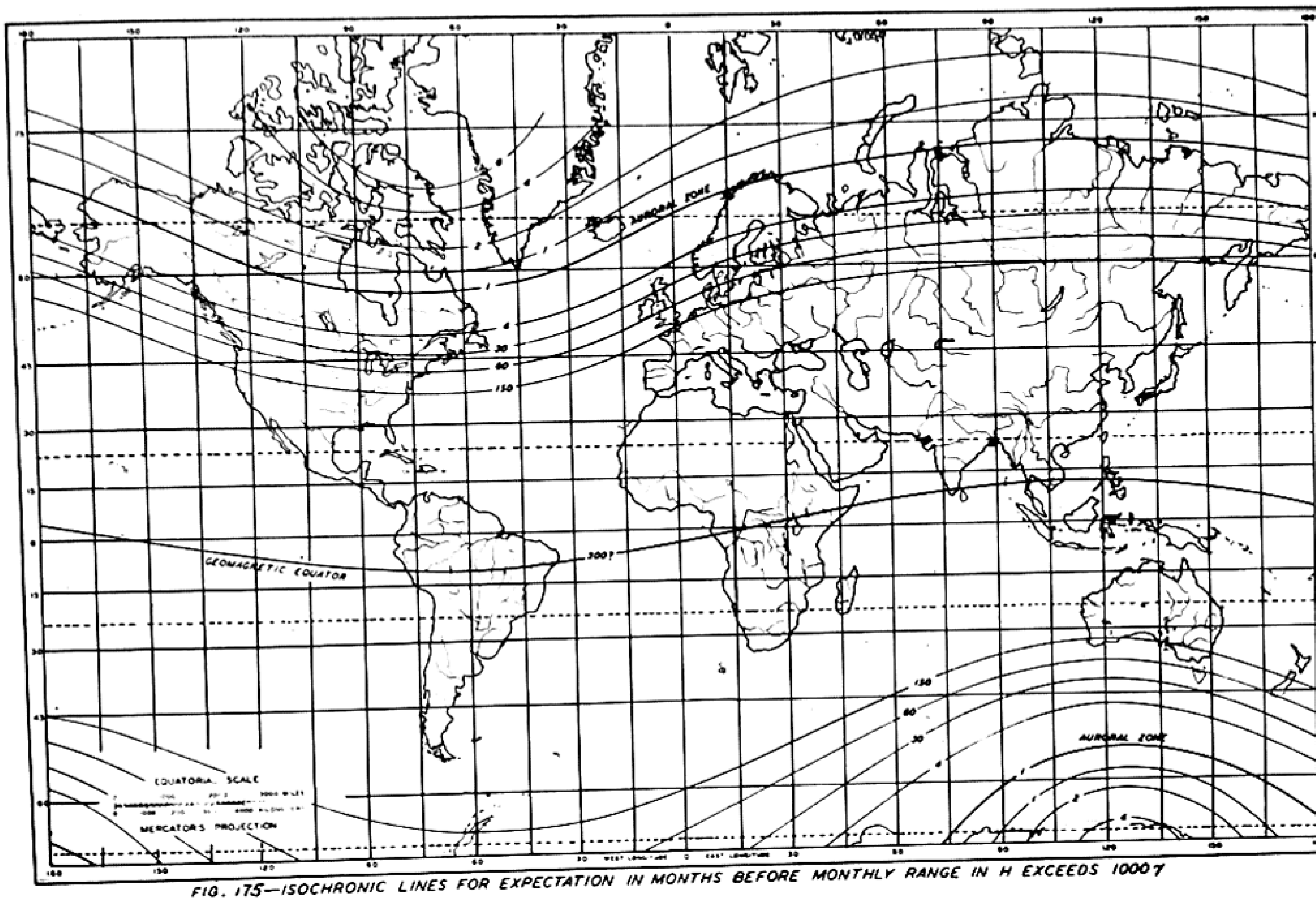

FIG. 175—ISOCHRONIC LINES FOR EXPECTATION IN MONTHS BEFORE MONTHLY RANGE IN H EXCEEDS 1000γ

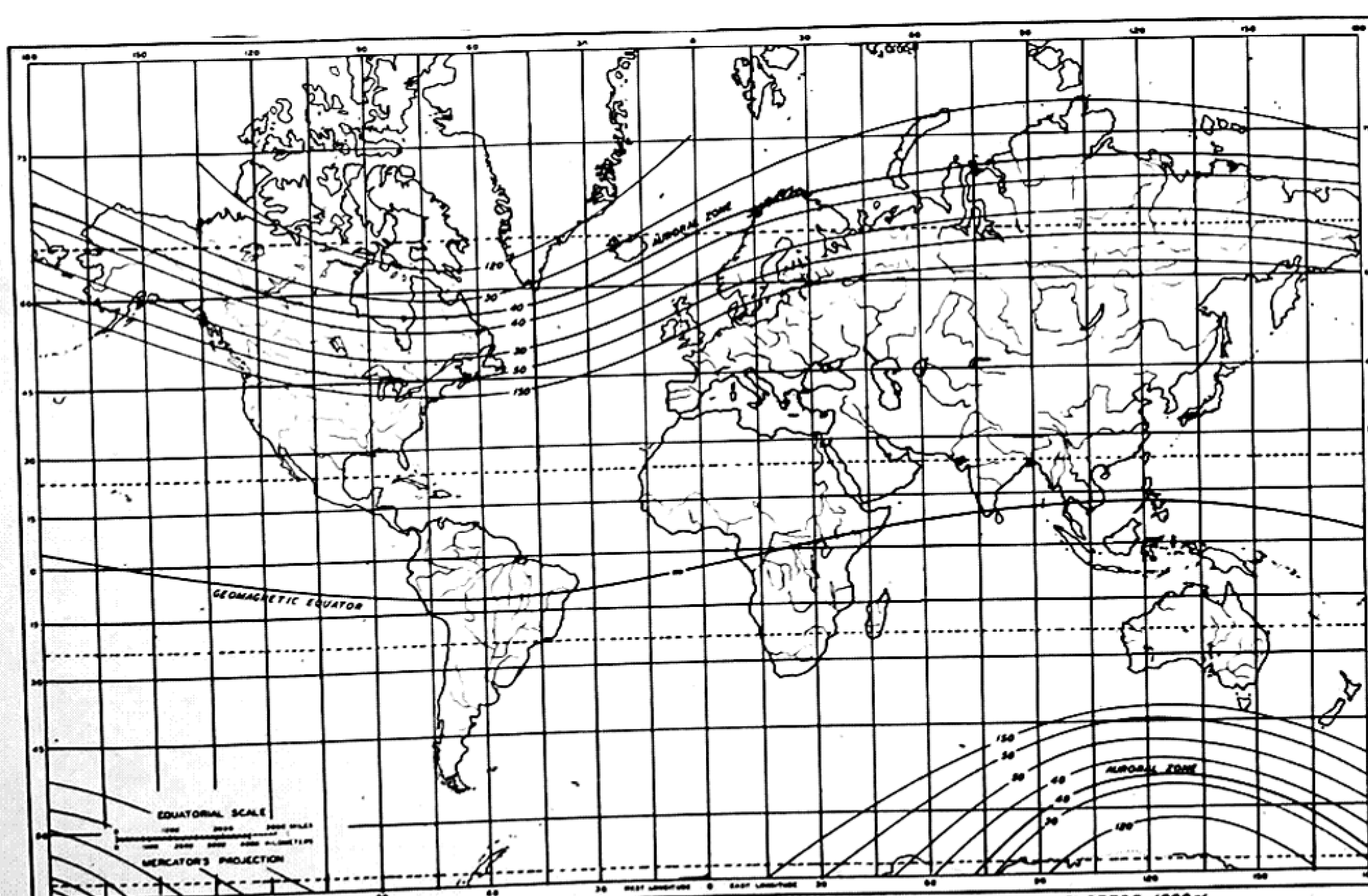

FIG. 178 —ISOCHRONIC LINES FOR EXPECTATION IN MONTHS BEFORE MONTHLY RANGE IN D EXCEEDS 1000γ

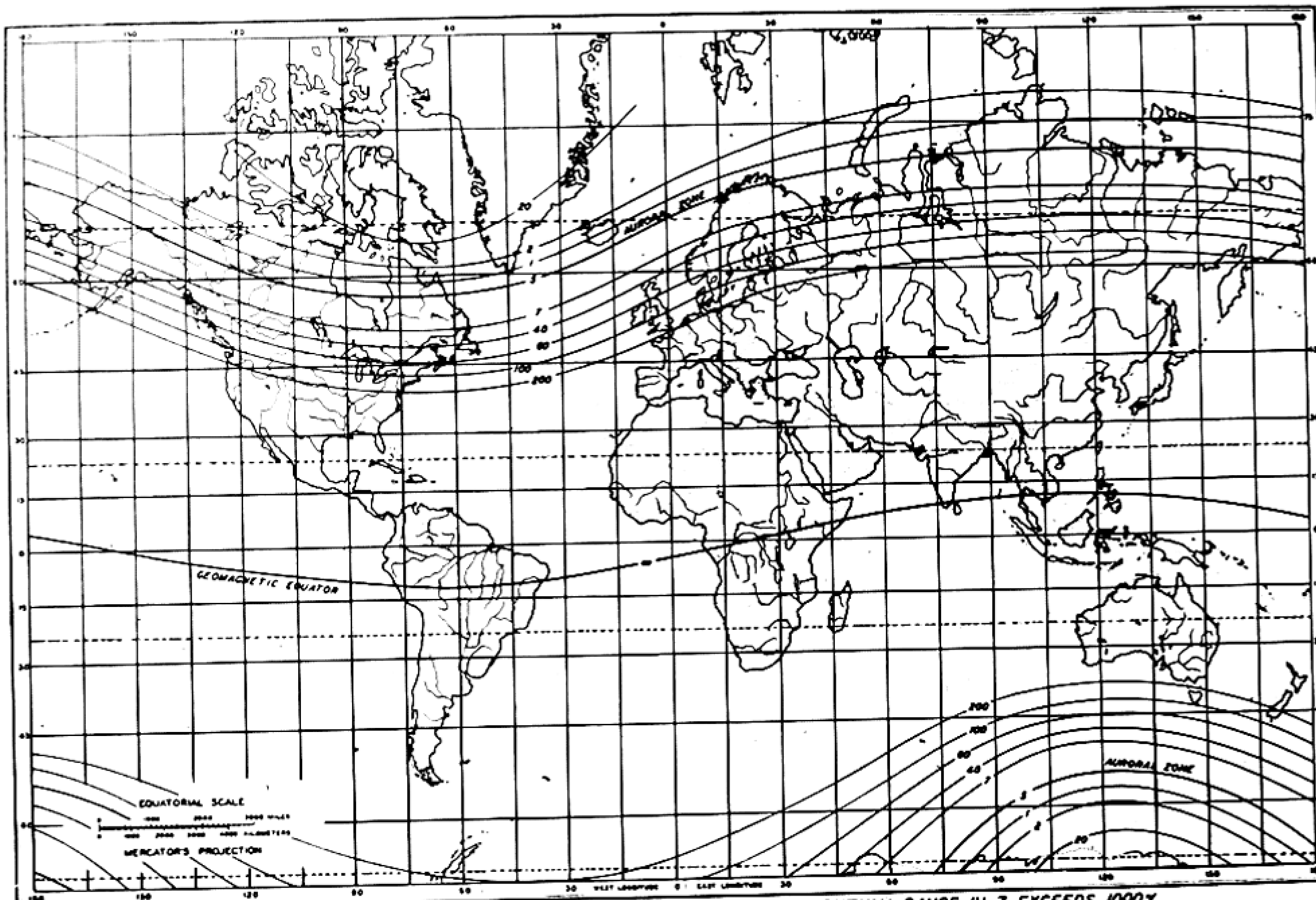

FIG. 177—ISOCHRONIC LINES FOR EXPECTATION IN MONTHS BEFORE MONTHLY RANGE IN Z EXCEEDS 1000γ

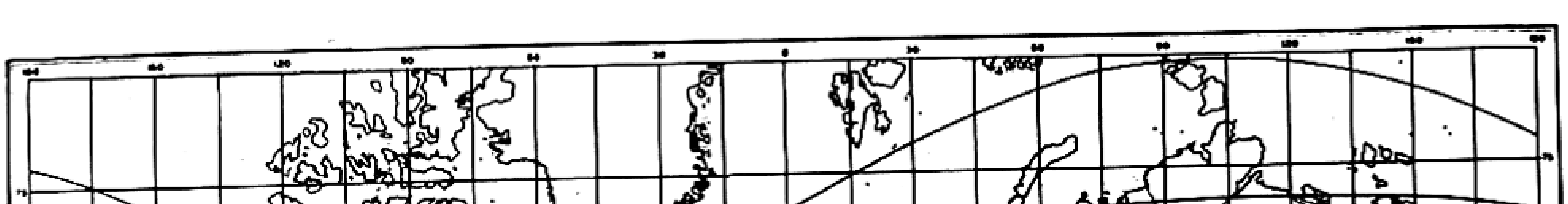

FIG. 178—ISOCHRONIC LINES FOR EXPECTATION IN 3-MONTH PERIODS BEFORE 3-MONTHLY RANGE IN H EXCEEDS 1000γ

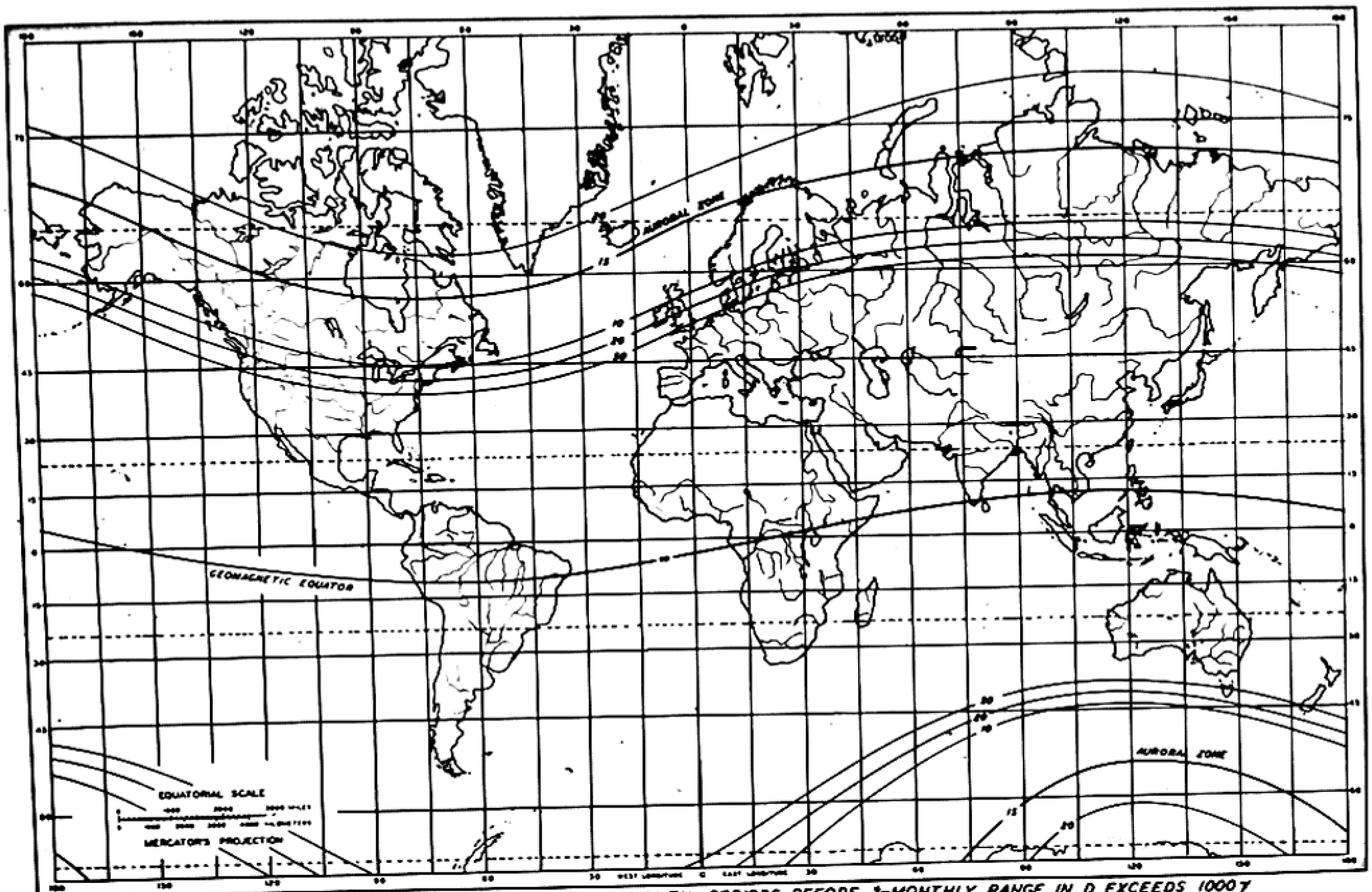

FIG. 179—ISOCHRONIC LINES FOR EXPECTATION IN 3-MONTH PERIODS BEFORE 3-MONTHLY RANGE IN D EXCEEDS 1000γ

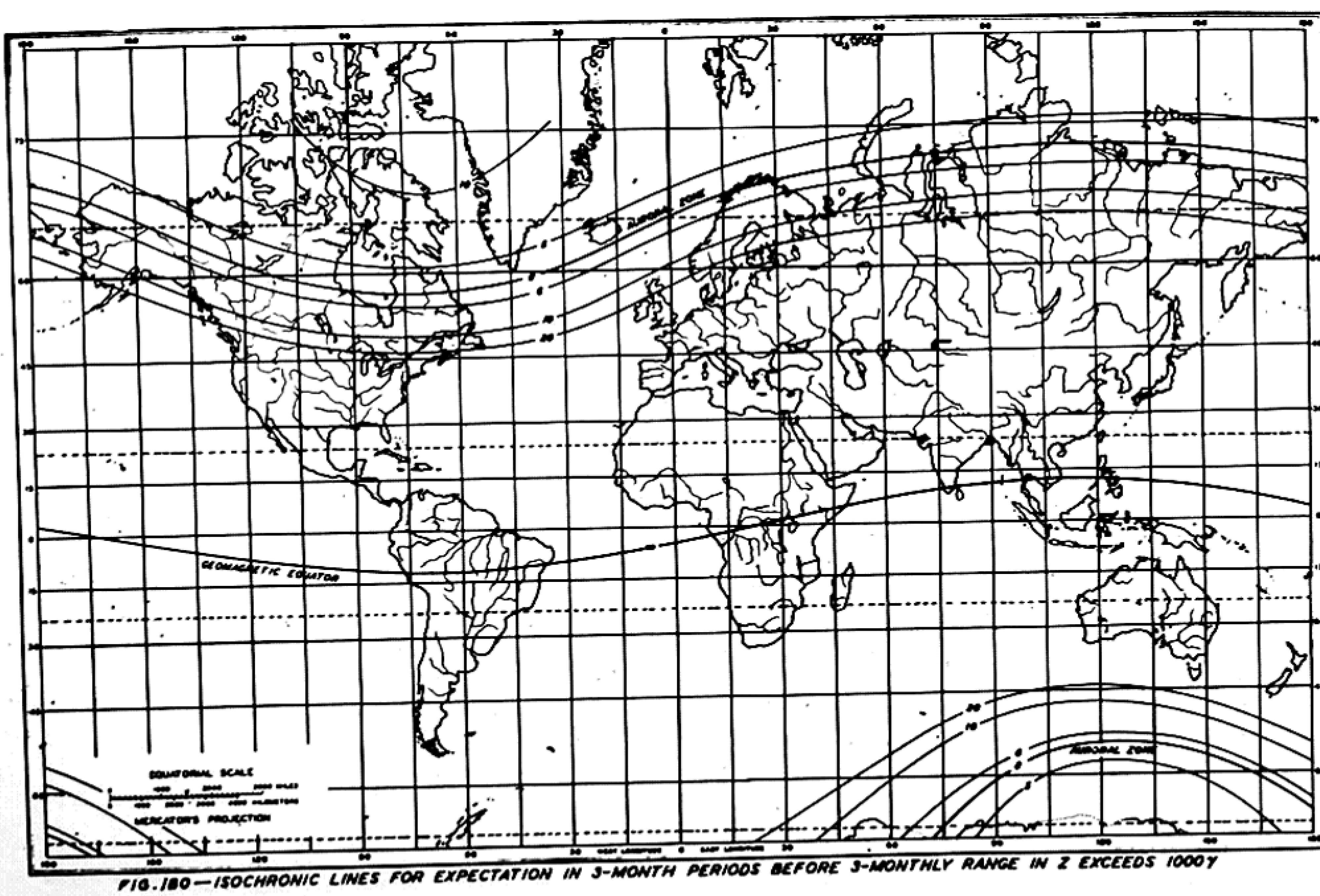

FIG. 180—ISOCHRONIC LINES FOR EXPECTATION IN 3-MONTH PERIODS BEFORE 3-MONTHLY RANGE IN Z EXCEEDS 1000γ

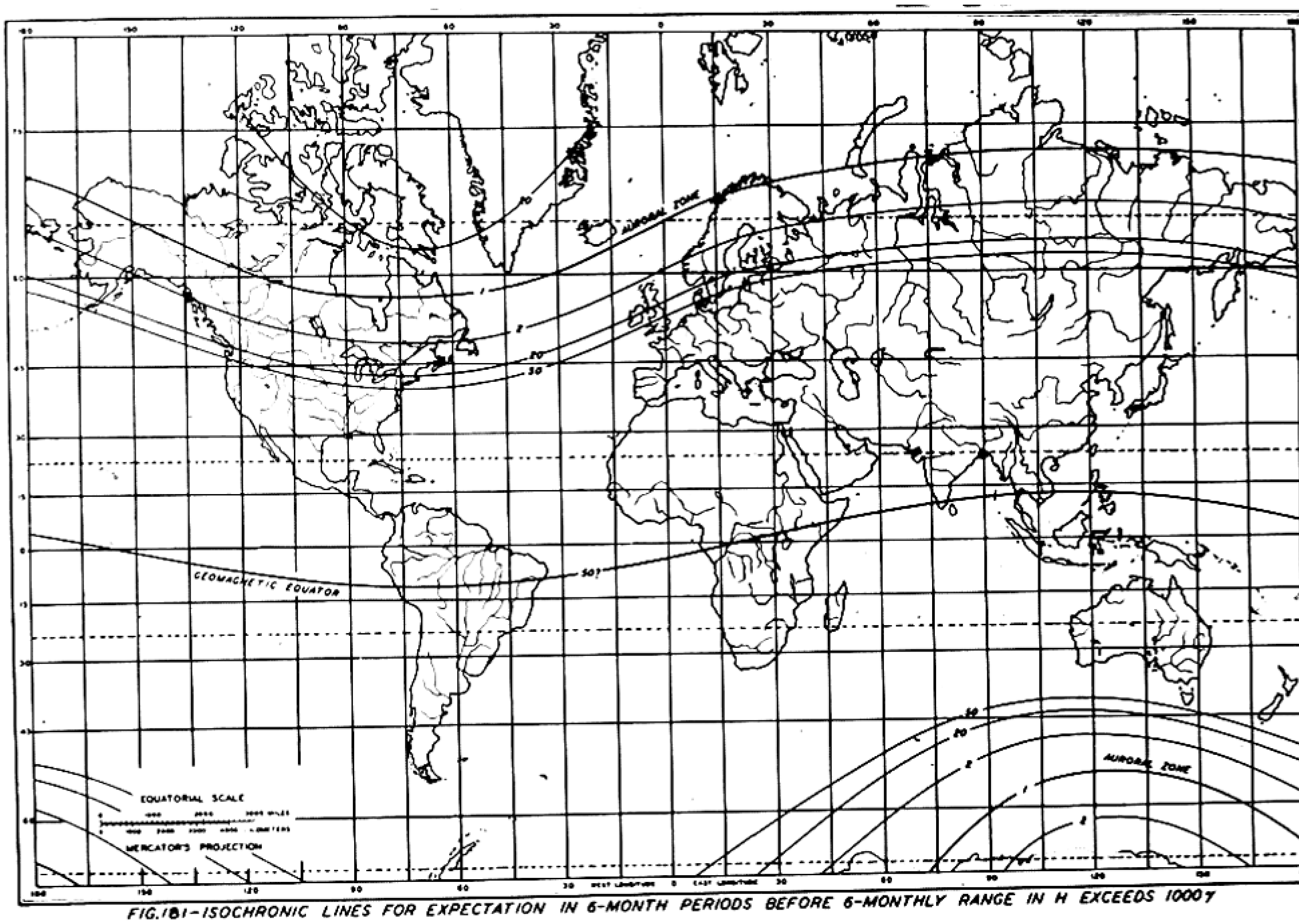

FIG. 181—ISOCHRONIC LINES FOR EXPECTATION IN 6-MONTH PERIODS BEFORE 6-MONTHLY RANGE IN H EXCEEDS 1000γ

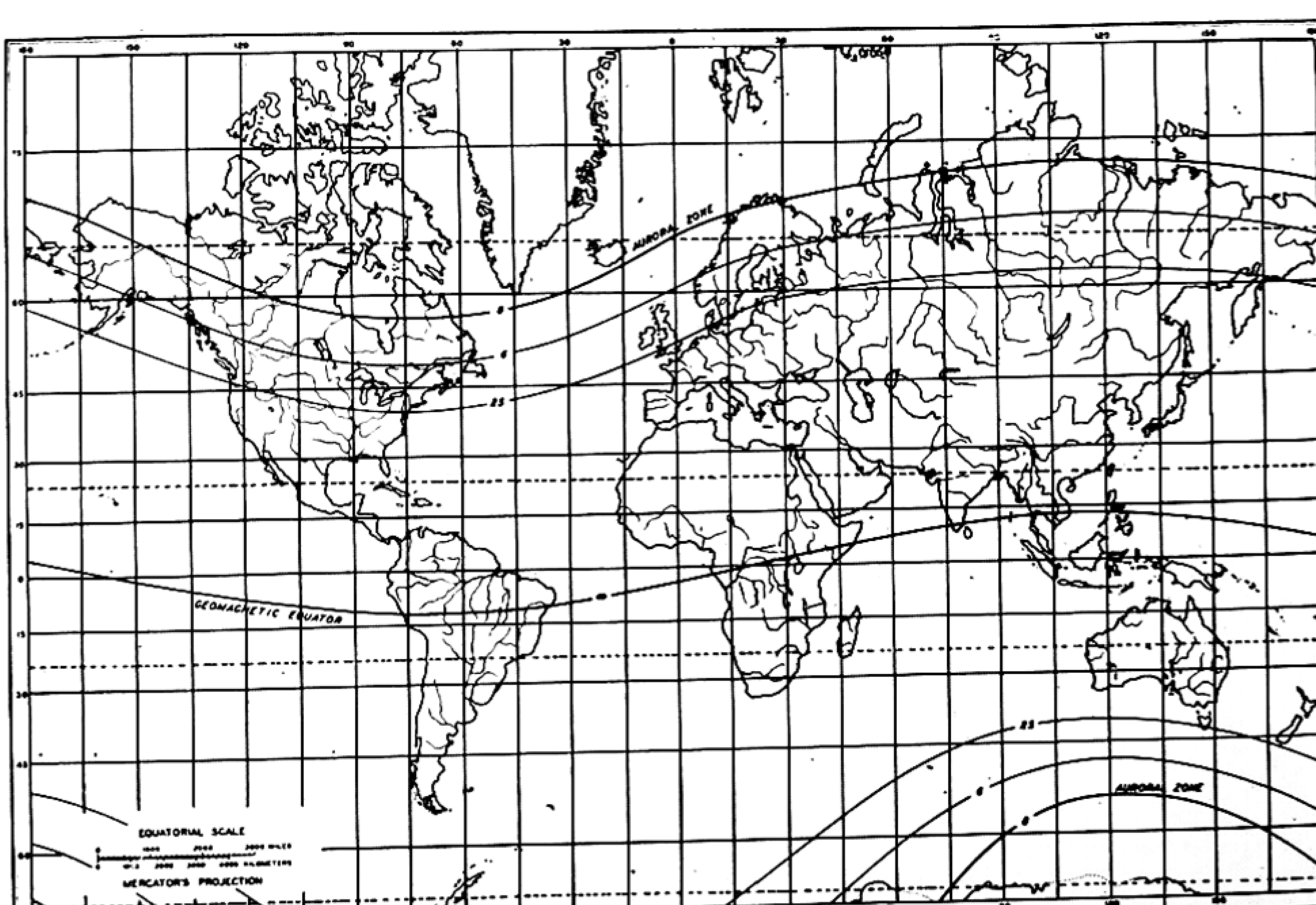

FIG. 182—ISOCHRONIC LINES FOR EXPECTATION IN 6-MONTH PERIODS BEFORE 6-MONTHLY RANGE IN D EXCEEDS 1000γ

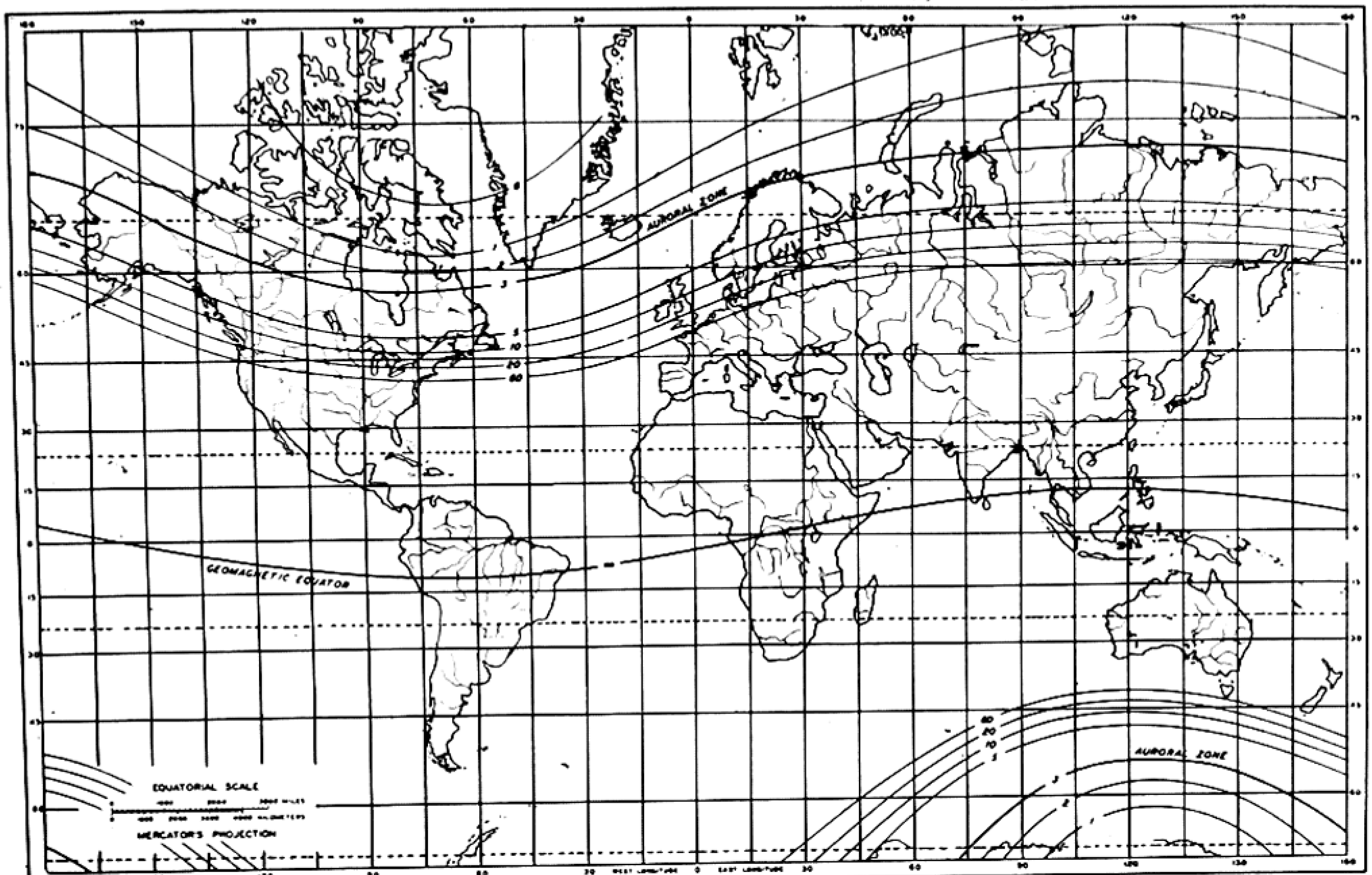

FIG. 183—ISOCHRONIC LINES FOR EXPECTATION IN 6-MONTH PERIODS BEFORE 6-MONTHLY RANGE IN Z EXCEEDS 1000γ

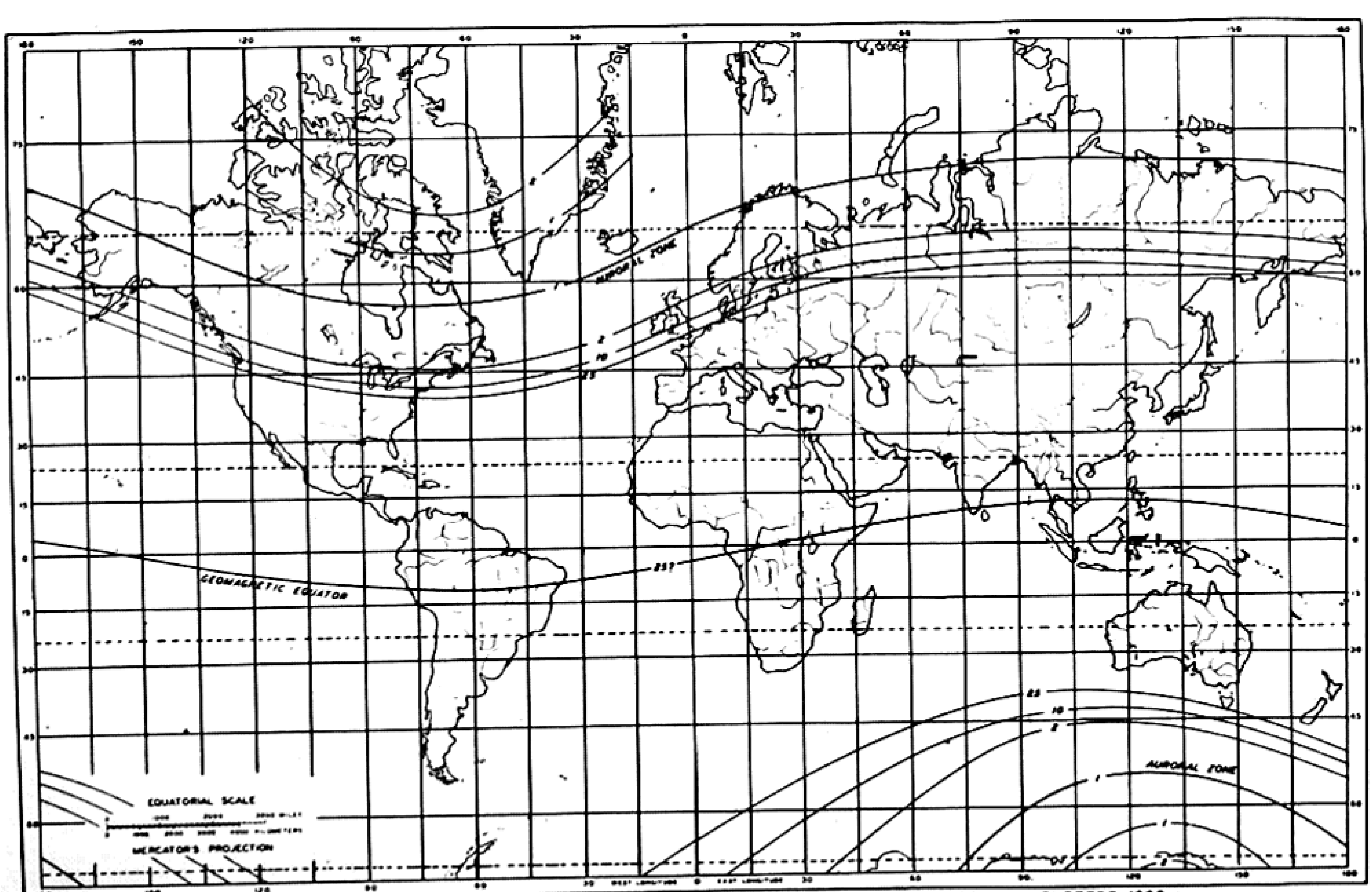

FIG. 184—ISOCHRONIC LINES FOR EXPECTATION IN YEARS BEFORE YEARLY RANGE IN H EXCEEDS 1000γ

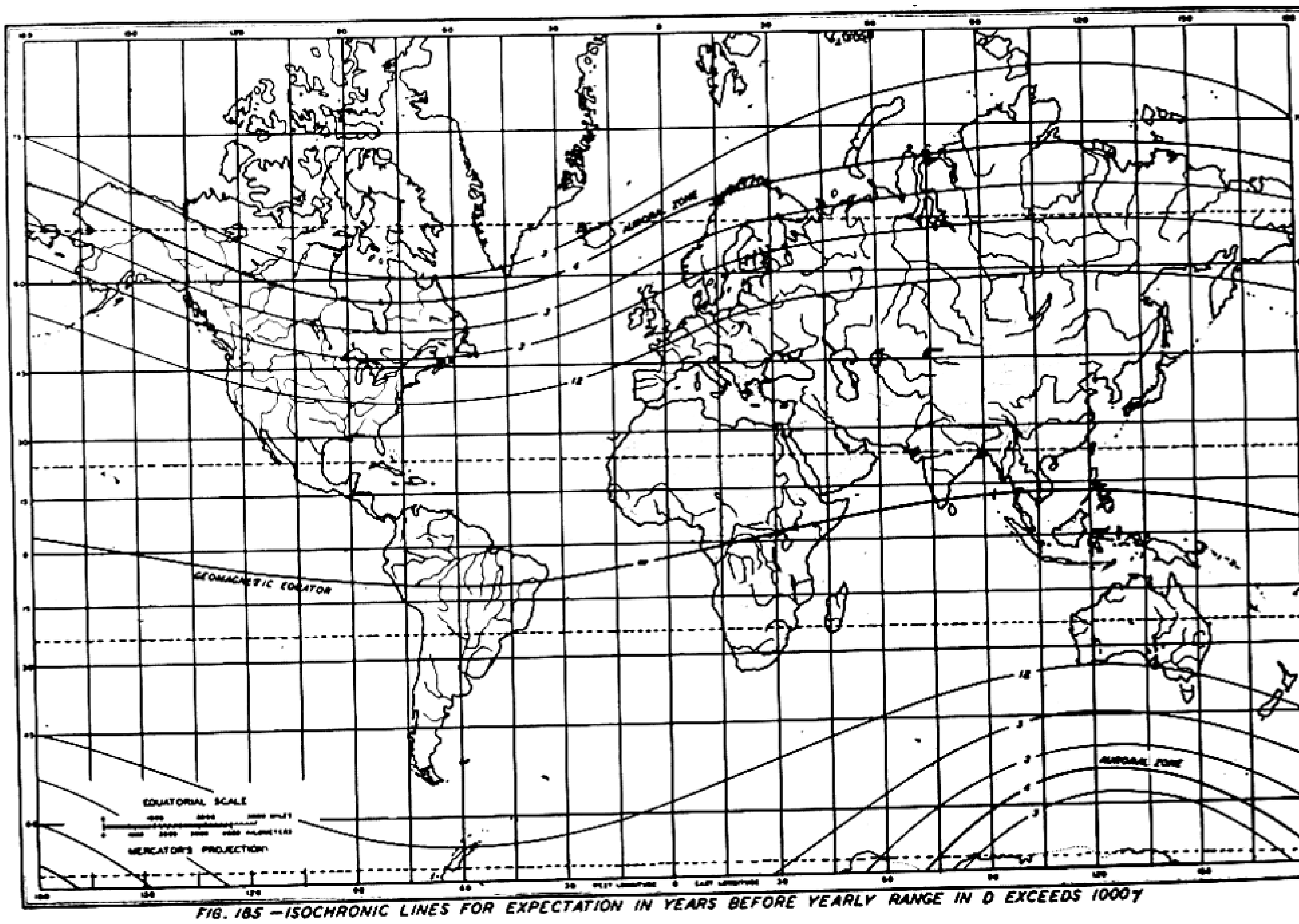

FIG. 185 —ISOCHRONIC LINES FOR EXPECTATION IN YEARS BEFORE YEARLY RANGE IN D EXCEEDS 1000γ

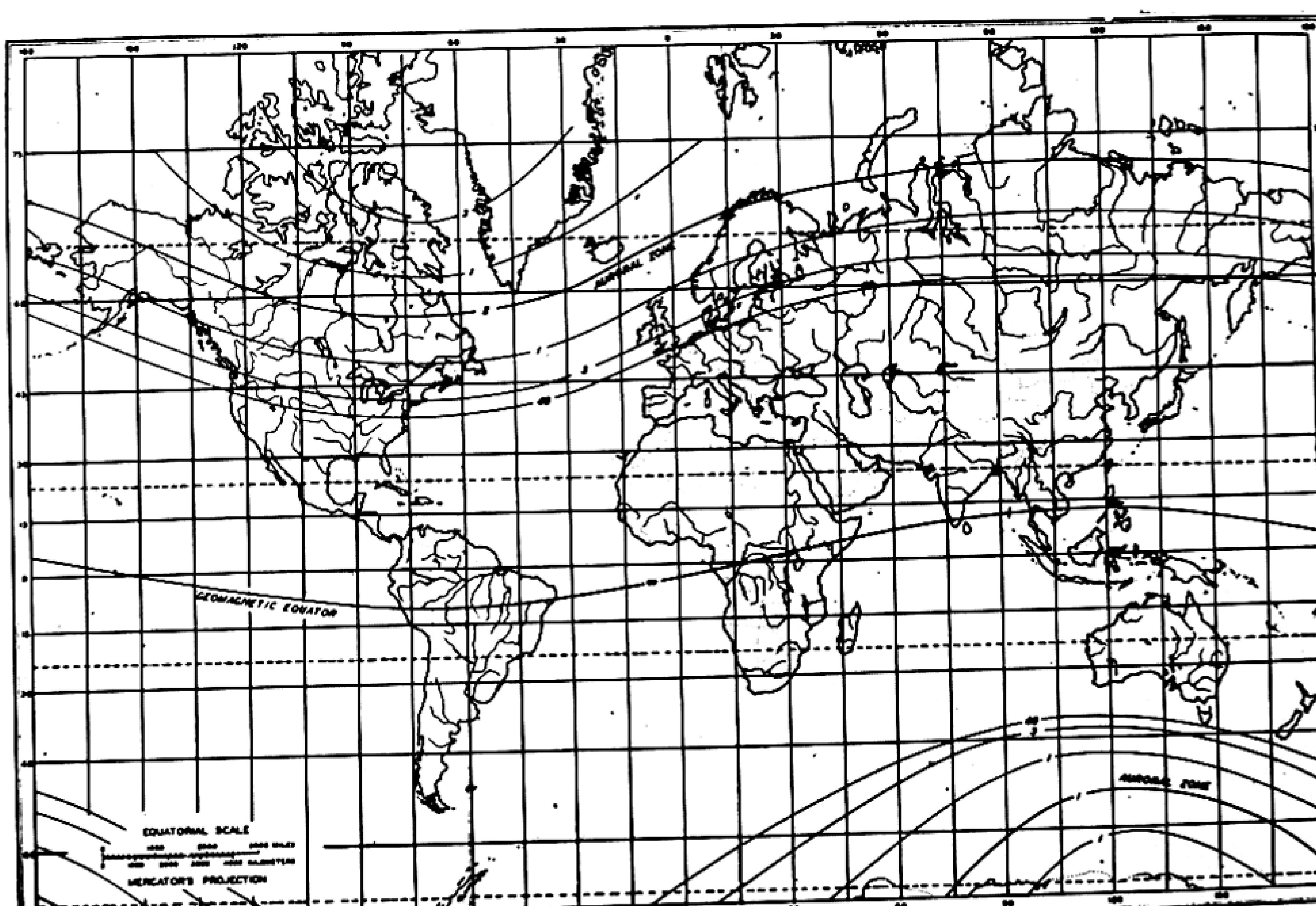

FIG. 186 —ISOCHRONIC LINES FOR EXPECTATION IN YEARS BEFORE YEARLY RANGE IN Z EXCEEDS 1000γ

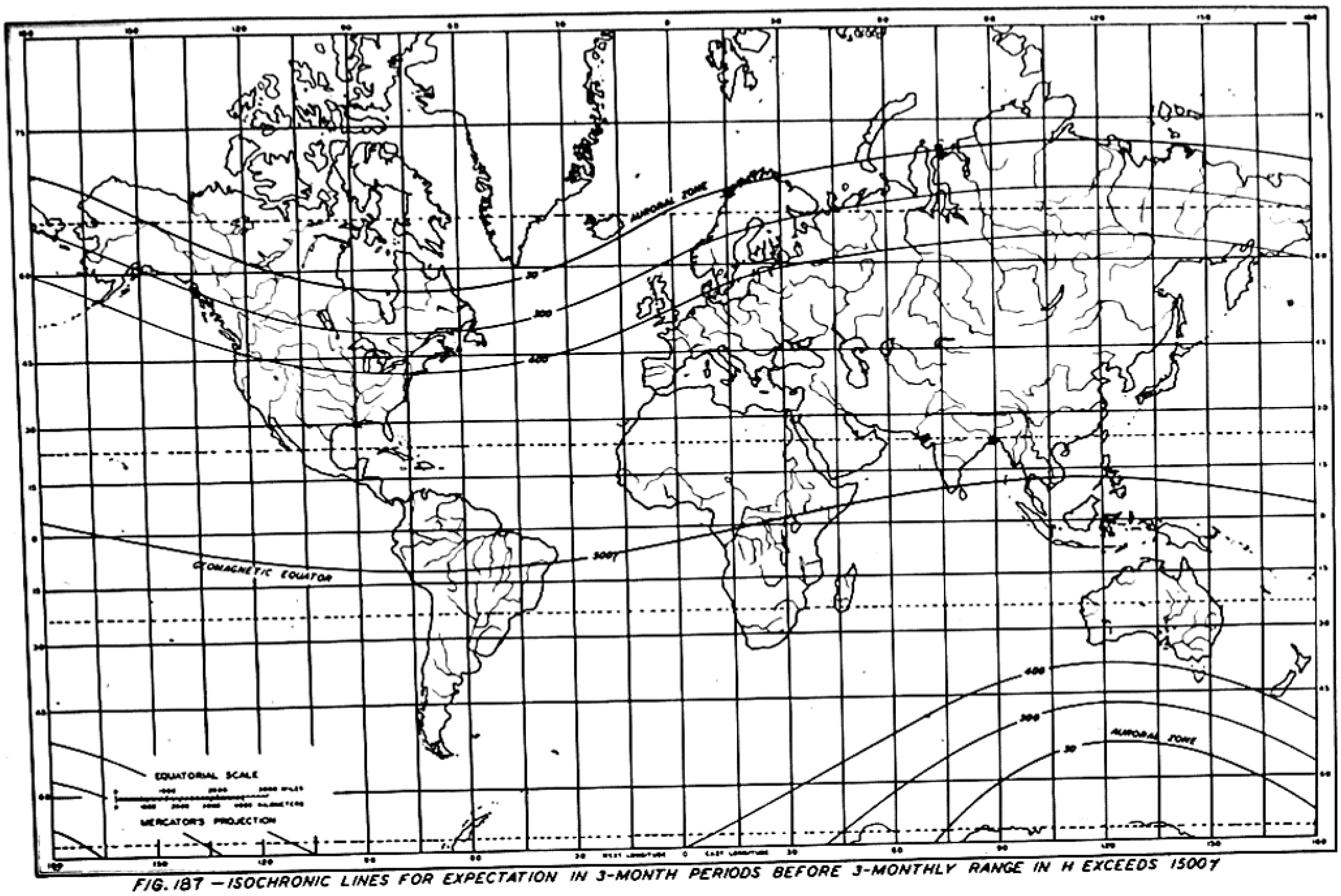

FIG. 187 — ISOCHRONIC LINES FOR EXPECTATION IN 3-MONTH PERIODS BEFORE 3-MONTHLY RANGE IN H EXCEEDS 1500γ

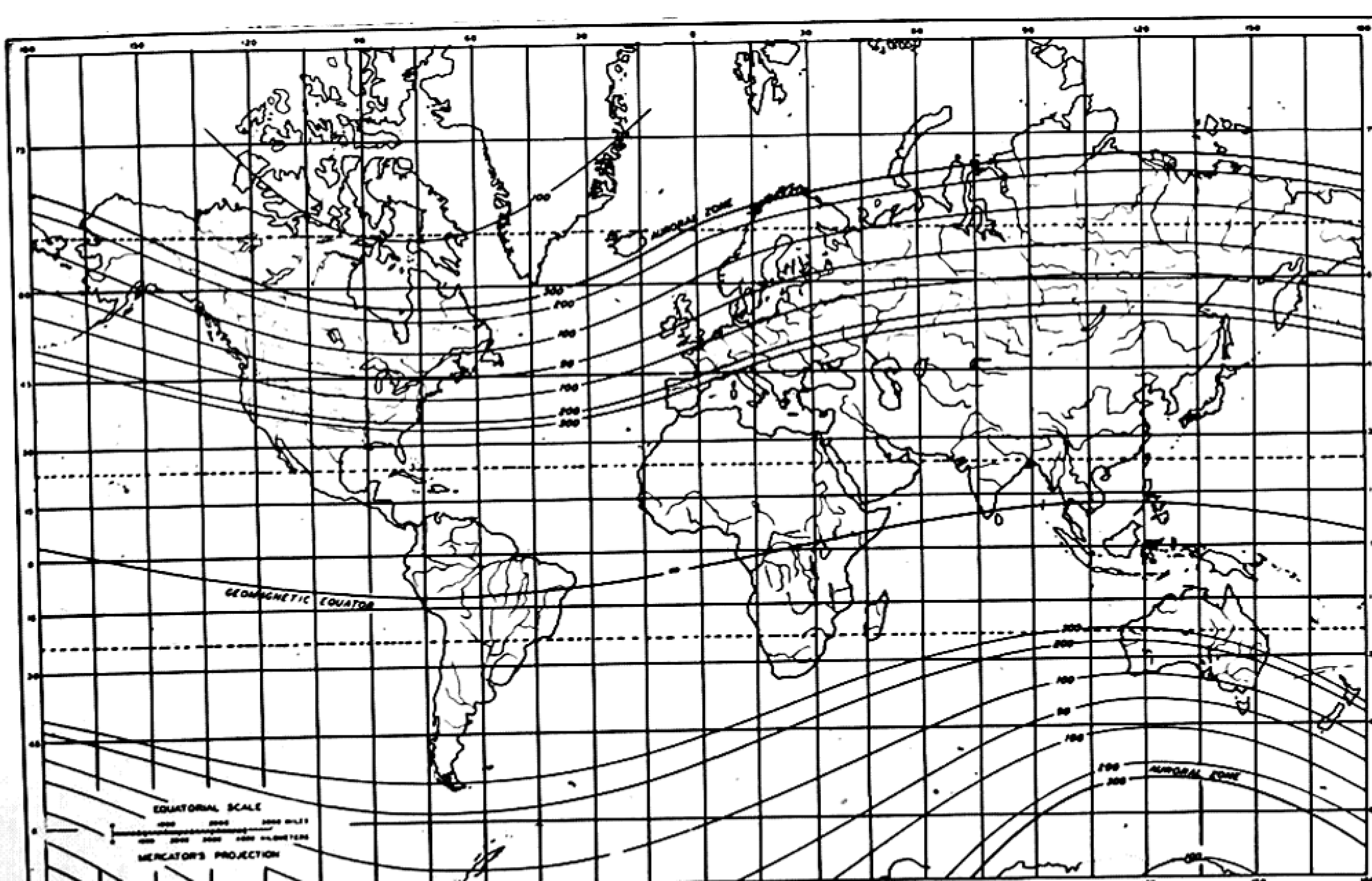

FIG. 188 — ISOCHRONIC LINES FOR EXPECTATION IN 3-MONTH PERIODS BEFORE 3-MONTHLY RANGE IN D EXCEEDS 1500γ

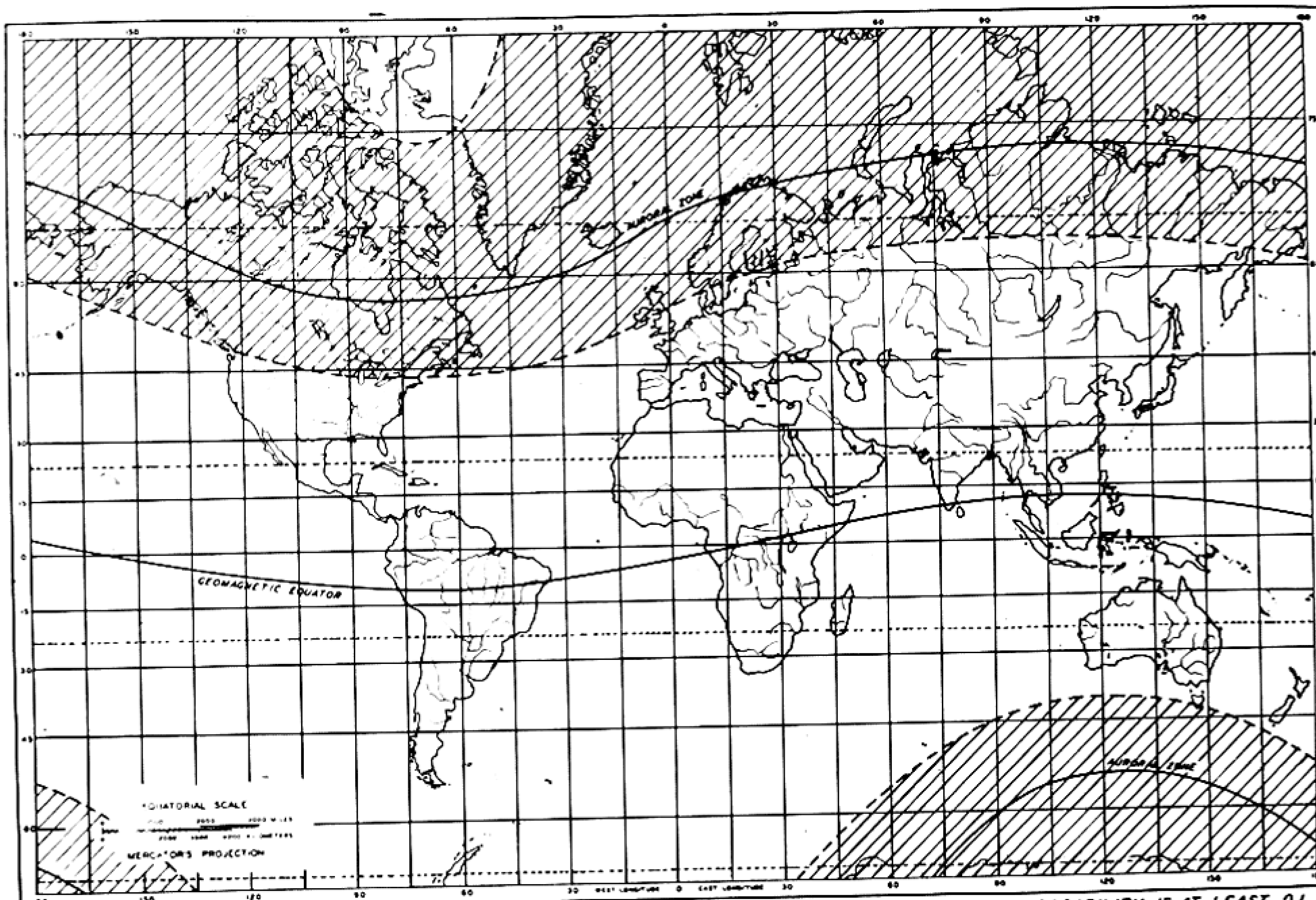

FIG. 189 —BELTS (BOUNDARIES SHOWN BY BROKEN LINES) NEAR EACH AURORAL ZONE IN WHICH AVERAGE PROBABILITY IS AT LEAST 0.1 THAT TOTAL 3-MONTHLY RANGE IN H EQUALS OR EXCEEDS 1000γ

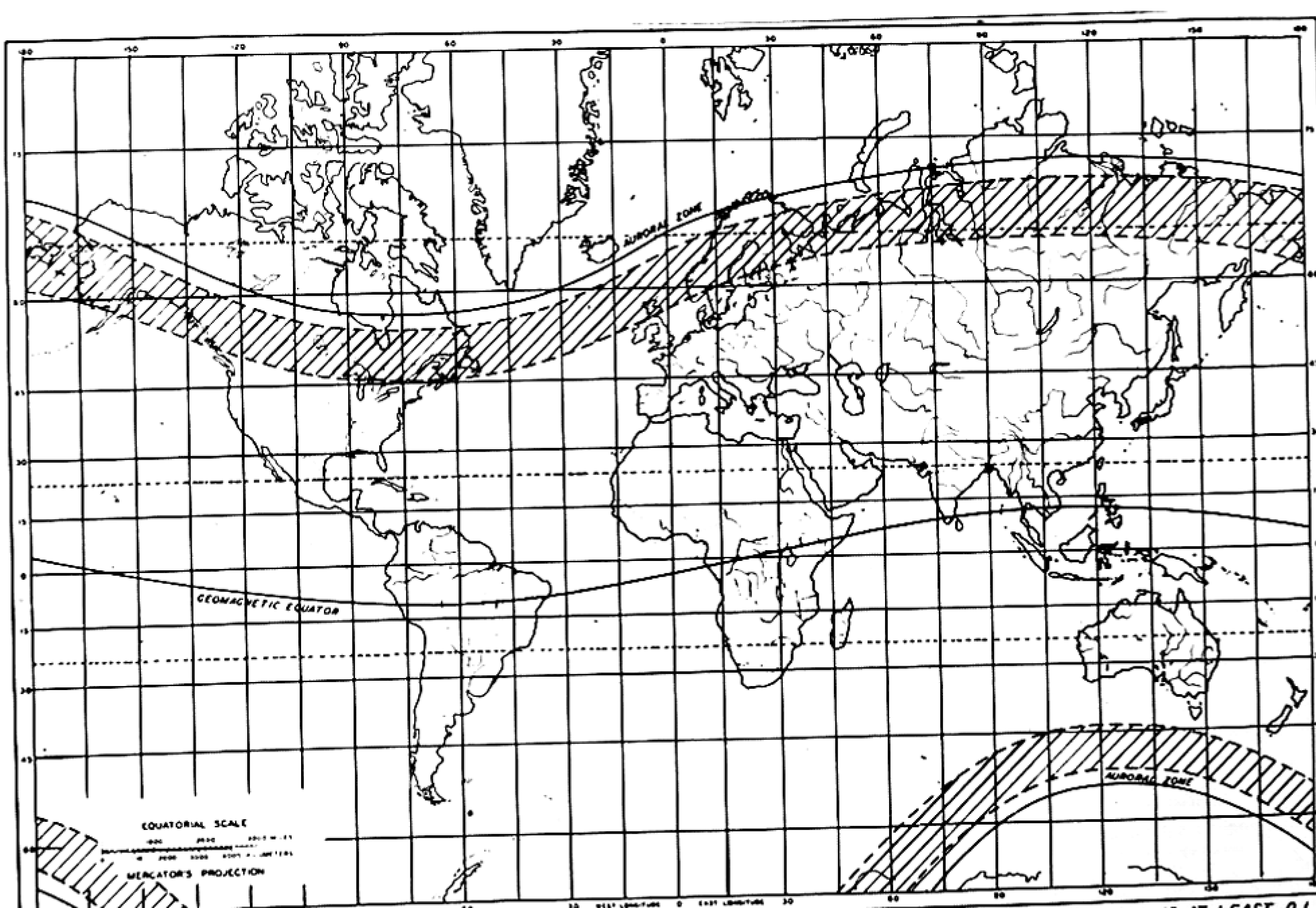

FIG. 190 —BELTS (BOUNDARIES SHOWN BY BROKEN LINES) NEAR EACH AURORAL ZONE IN WHICH AVERAGE PROBABILITY IS AT LEAST 0.1 THAT TOTAL 3-MONTHLY RANGE IN D EQUALS OR EXCEEDS 1000γ

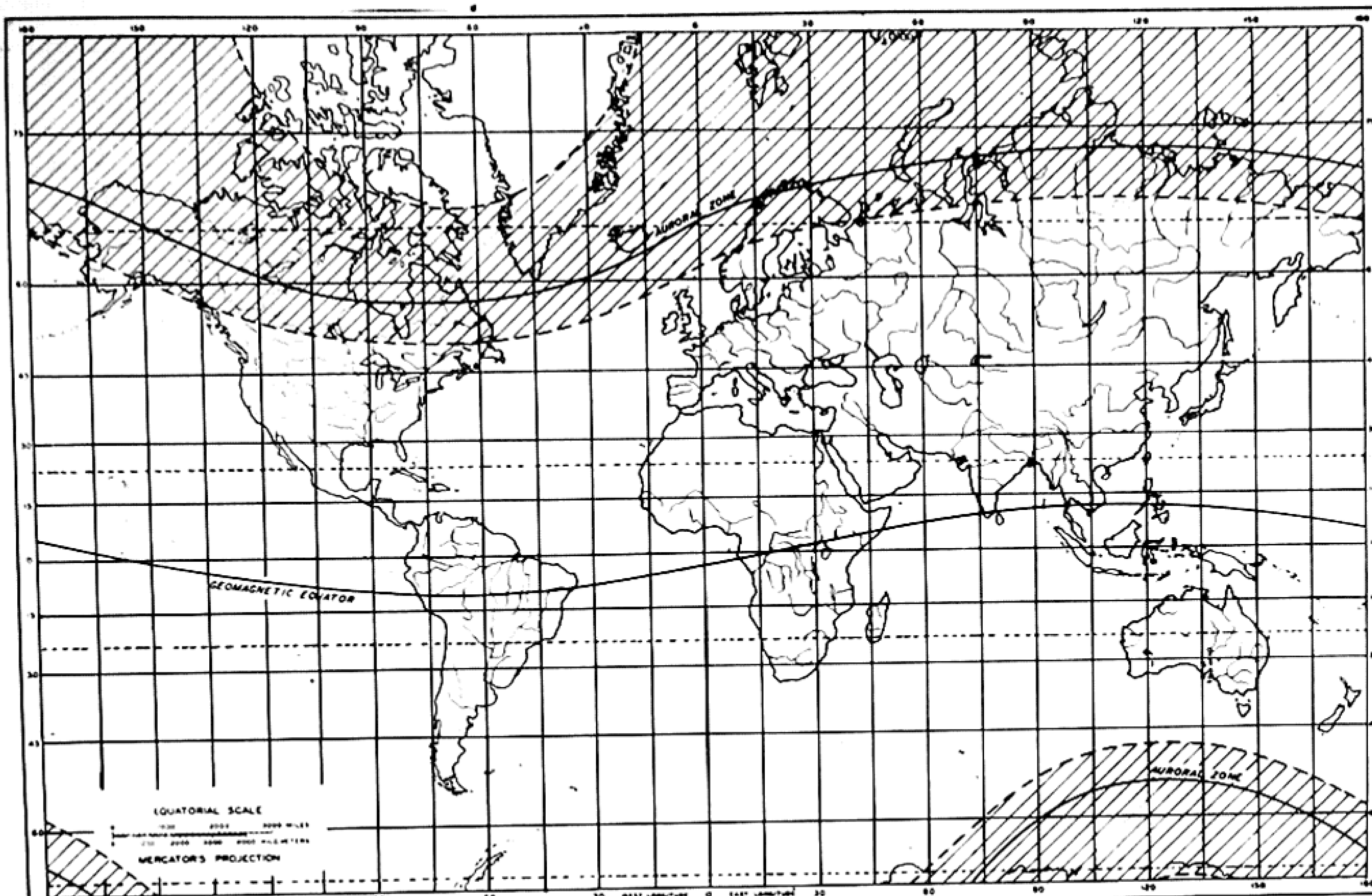

FIG. 191—BELTS (BOUNDARIES SHOWN BY BROKEN LINES) NEAR EACH AURORAL ZONE IN WHICH AVERAGE PROBABILITY IS AT LEAST 0.1 THAT TOTAL 3-MONTHLY RANGE IN Z EQUALS OR EXCEEDS 1000γ

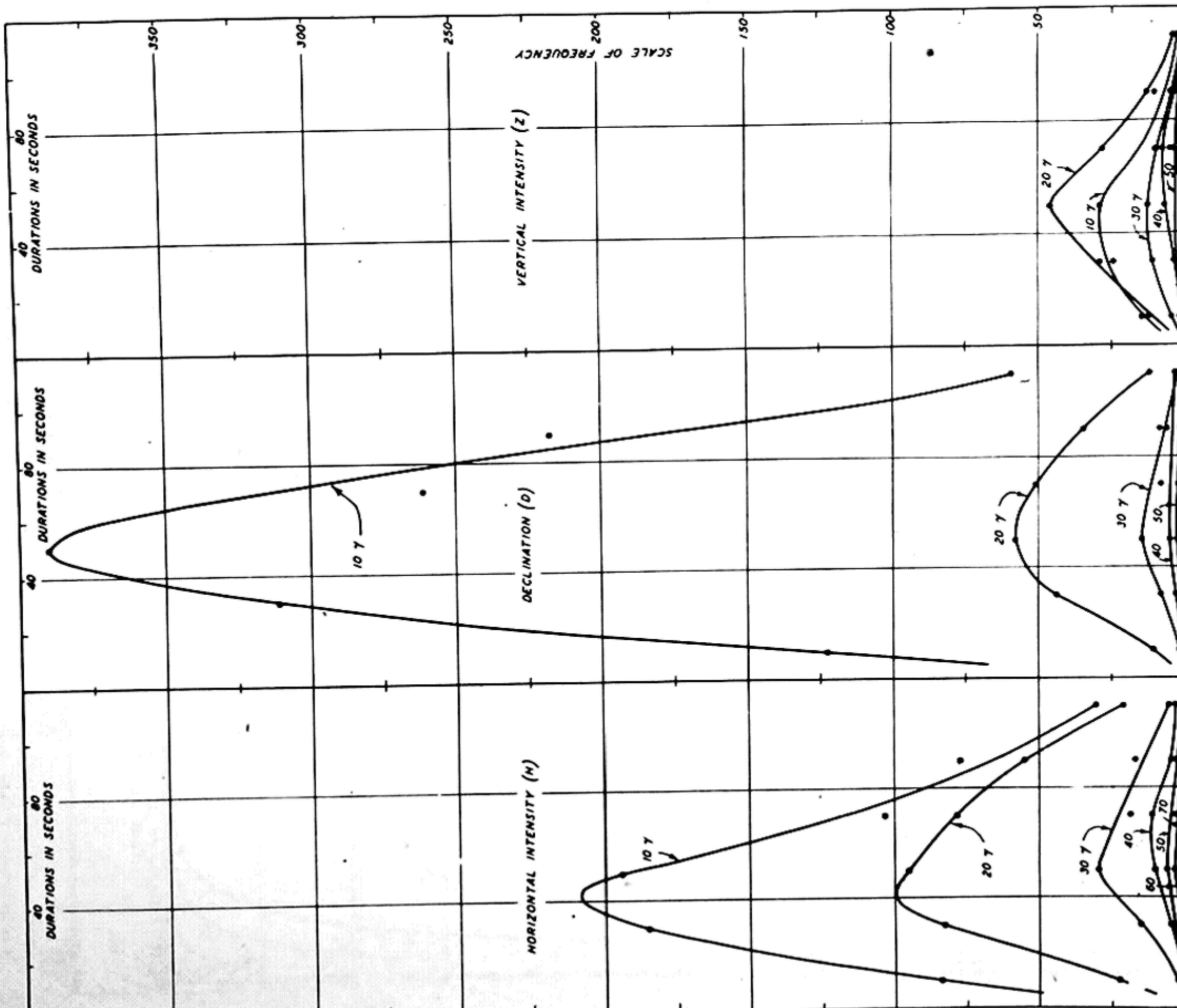

FIG. 192—FREQUENCIES OF FLUCTUATIONS OF VARIOUS AMPLITUDES IN GAMMAS AND DURATIONS IN SECONDS, H, D, AND Z, PETSAMO, AUGUST 1 TO OCTOBER 31, 1932

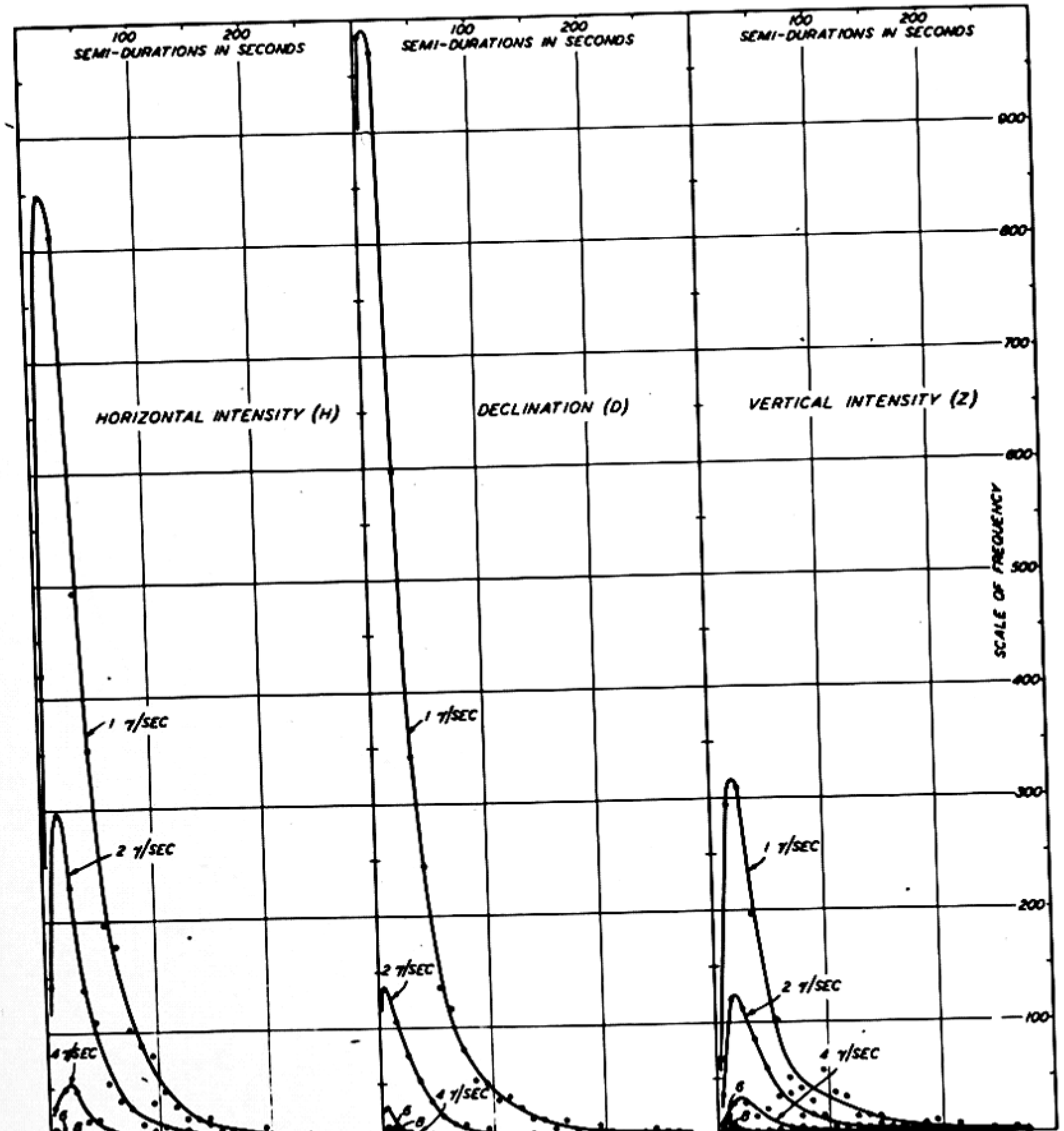

FIG. 193—FREQUENCIES OF FLUCTUATIONS IN H, D, AND Z, HAVING VARIOUS RATES OF CHANGE IN GAMMAS PER SECOND AND SEMI-DURATIONS, PETSAMO, SEPTEMBER 1, 1932, TO AUGUST 31, 1933

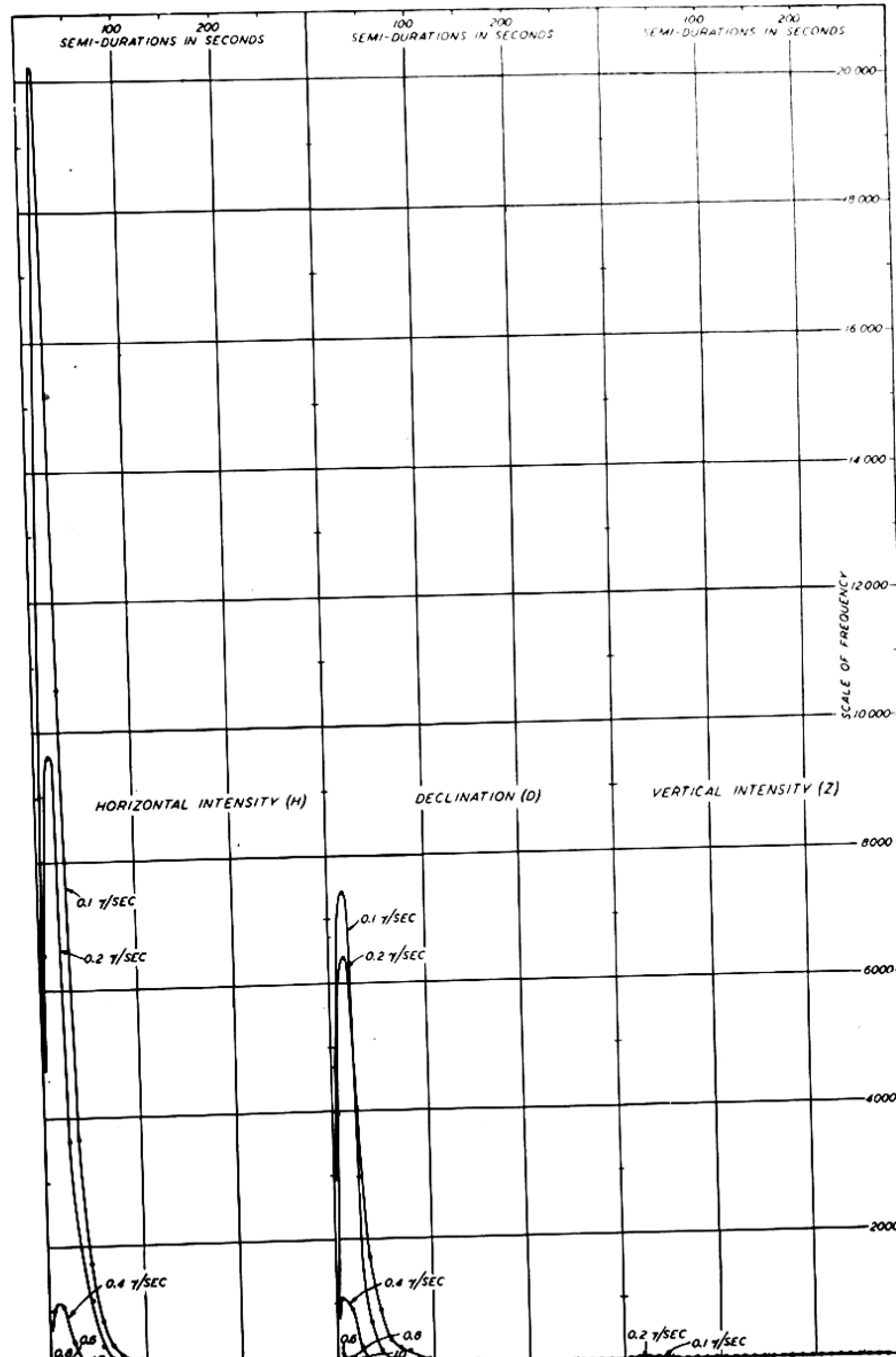

FIG. 194—FREQUENCIES OF FLUCTUATIONS IN H, D, AND Z, HAVING VARIOUS RATES OF CHANGE IN GAMMAS PER SECOND AND SEMI-DURATIONS, COPENHAGEN, SEPTEMBER 1, 1932, TO AUGUST 31, 1933

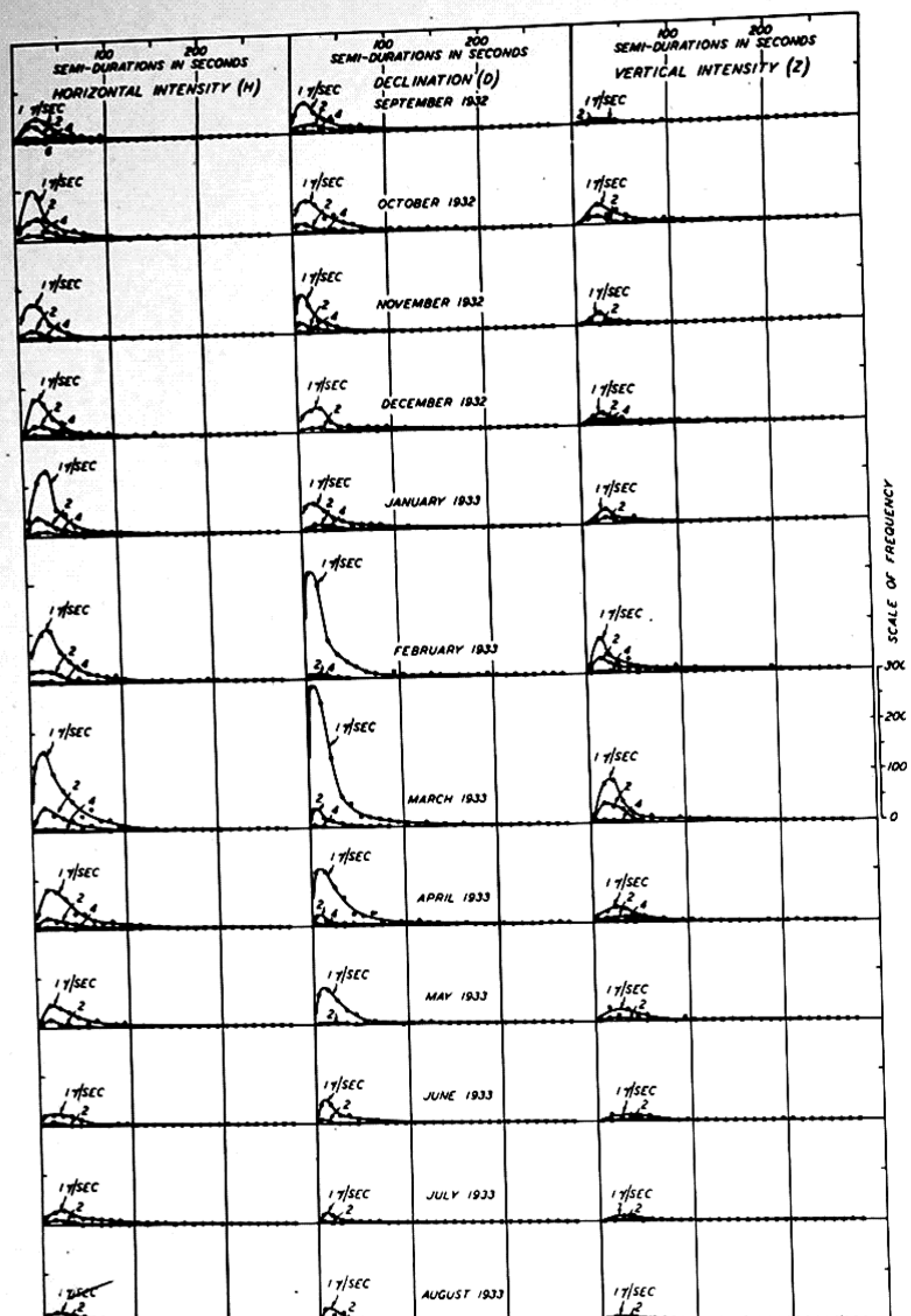

FIG. 195—MONTHLY FREQUENCIES OF FLUCTUATIONS IN H, D, AND Z, HAVING VARIOUS RATES OF CHANGE IN GAMMAS PER SECOND AND SEMI-DURATIONS, PETSAMO, SEPTEMBER, 1932 TO AUGUST, 1933

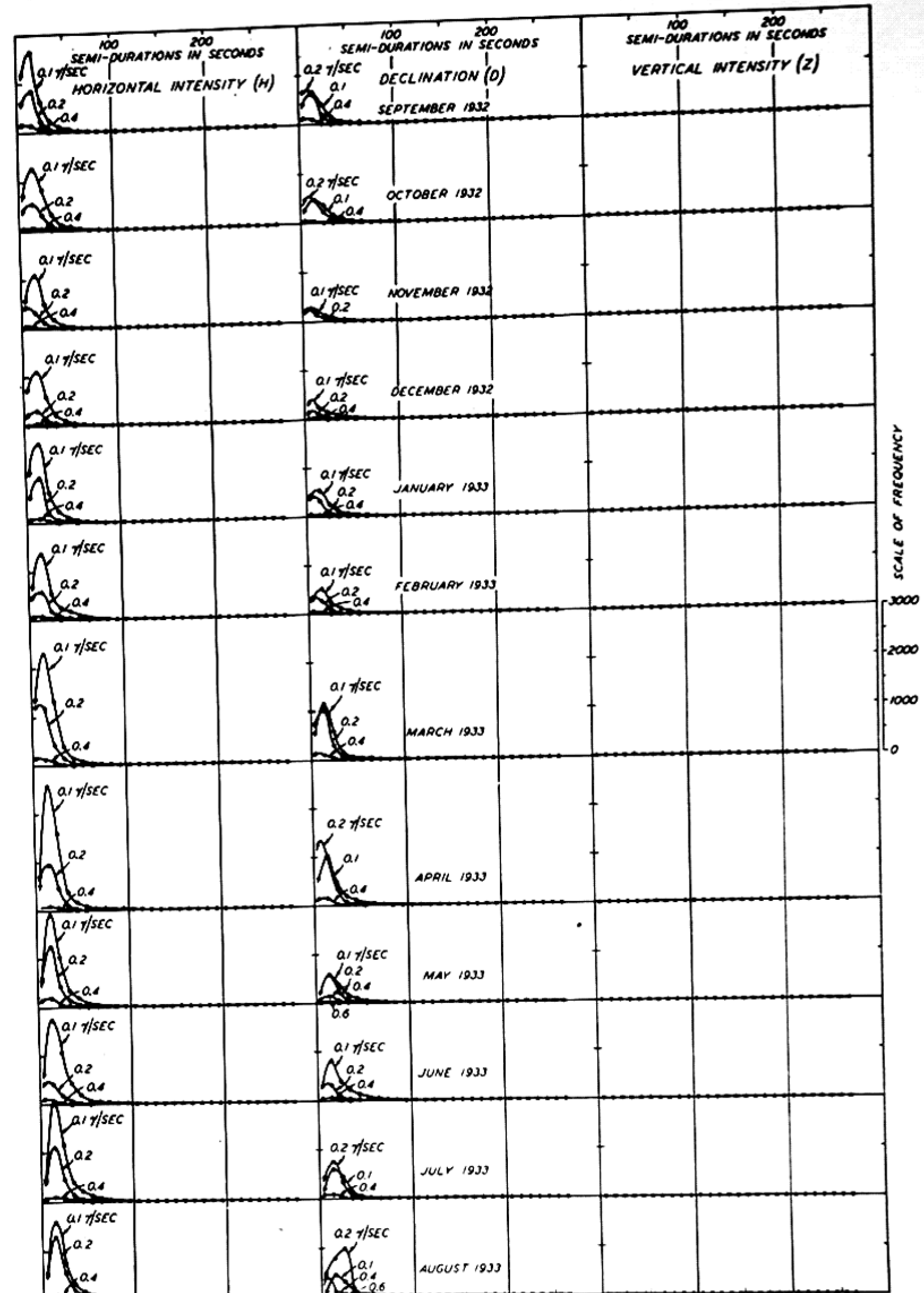

FIG. 196—MONTHLY FREQUENCIES OF FLUCTUATIONS IN H, D, AND Z, HAVING VARIOUS RATES OF CHANGE IN GAMMAS PER SECOND AND SEMI-DURATIONS, COPENHAGEN, SEPTEMBER, 1932 TO AUGUST, 1933

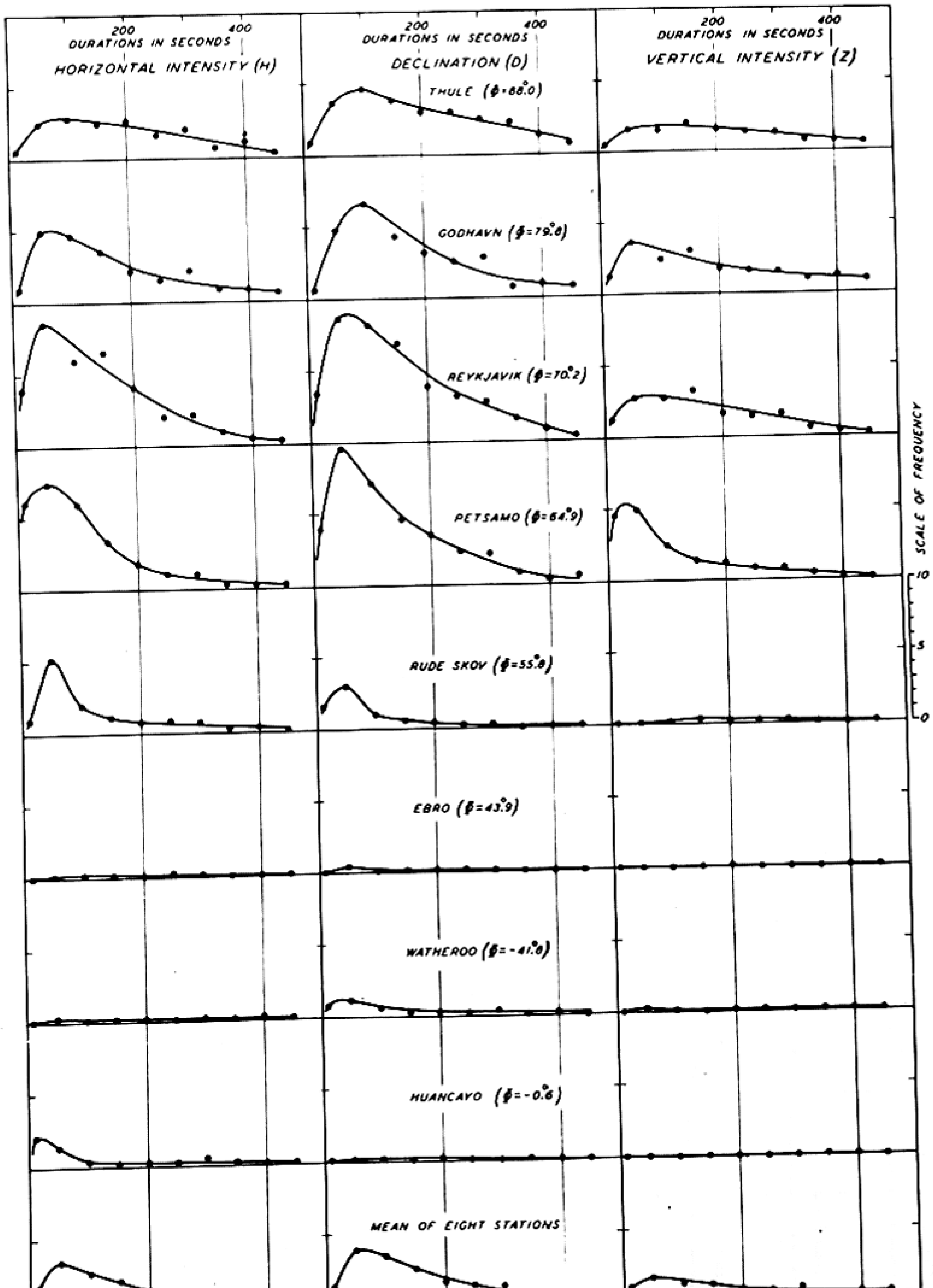

FIG. 197 —VARIATION WITH LATITUDE OF FREQUENCIES OF FLUCTUATIONS OF VARIOUS DURATIONS, 10 TO 500 SECONDS, H, D, AND Z, MEAN OF SIX DAYS, MAY 9 (C=0.0), JULY 4 (C=0.4), MAY 5 (C=0.8), MAY 31 (C=1.2), MARCH 24 (C=1.5), AND MAY 1 (C=1.9), 1933

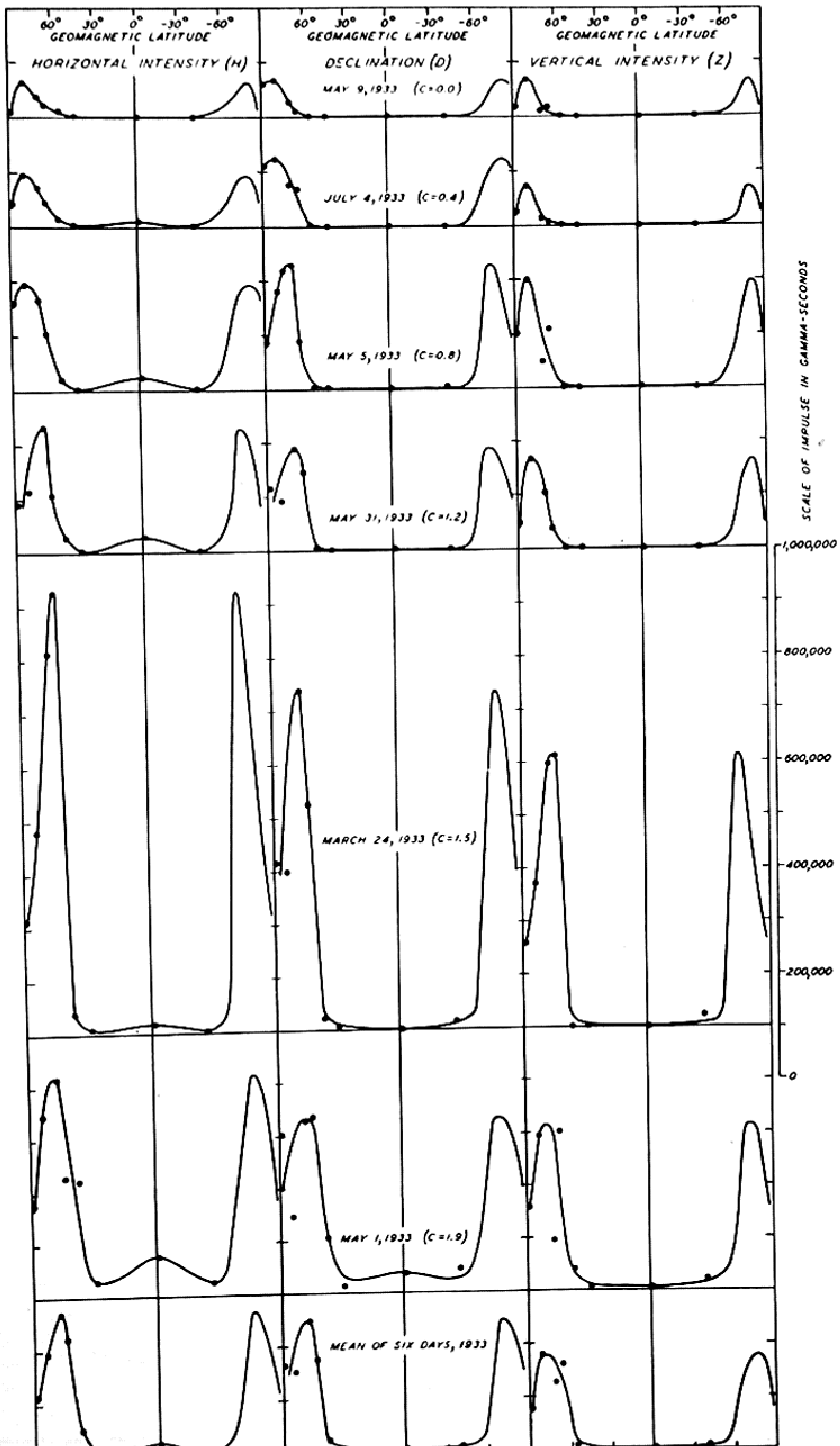

FIG. 198—VARIATION WITH GEOMAGNETIC LATITUDE OF MAGNITUDE OF TOTAL IMPULSE, AS MEASURED BY 1/2 $\Sigma\, \Delta r \Delta t$, WITH Δr THE AMPLITUDE AND Δt THE DURATION, FOR FLUCTUATIONS OF DURATION 10 TO 500 SECONDS FOR DAYS OF VARIOUS MAGNETIC CHARACTER-FIGURES C

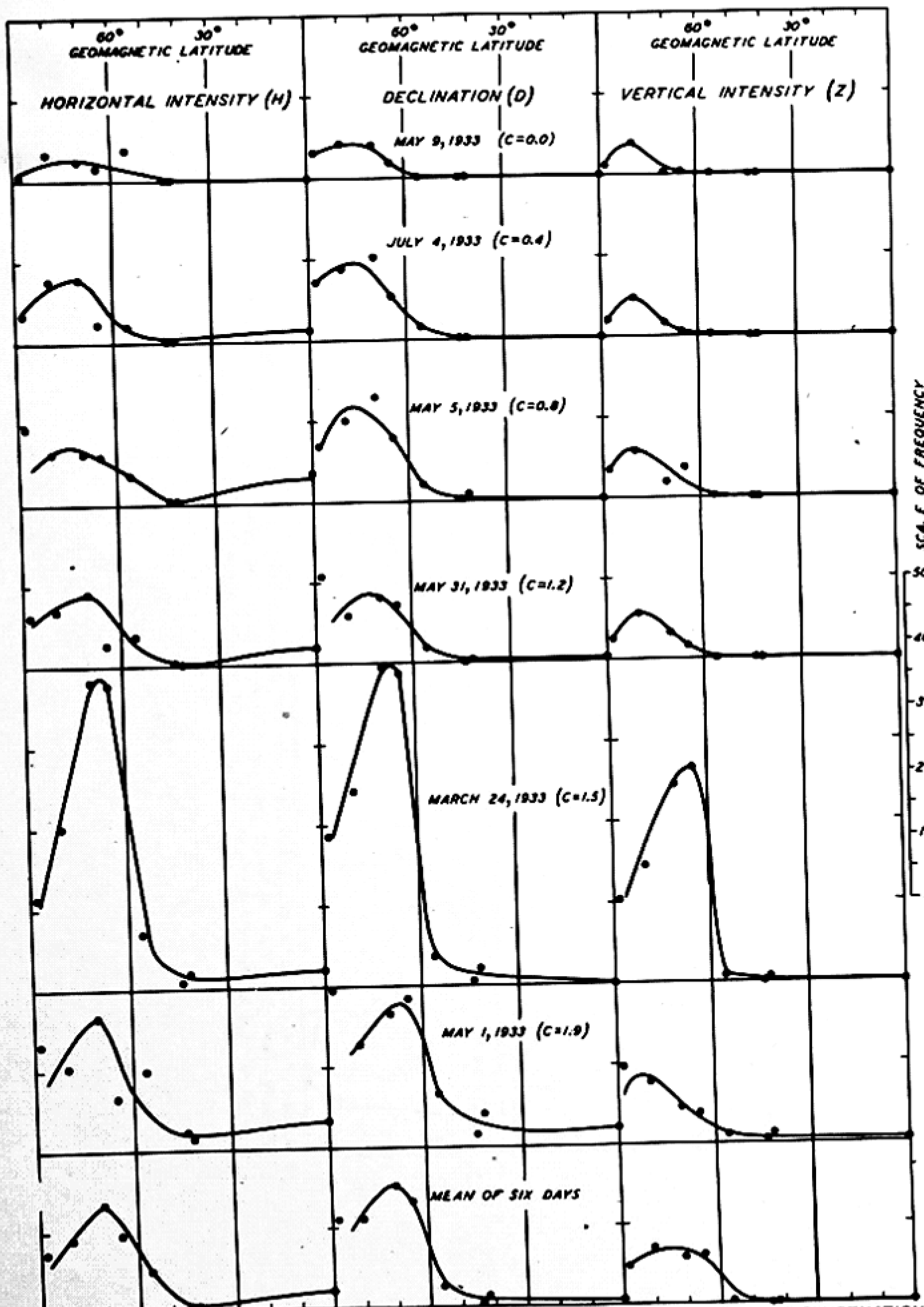

FIG. 199—VARIATION WITH GEOMAGNETIC LATITUDE OF DAILY FREQUENCY OF FLUCTUATIONS, DURATIONS 10 TO 500 SECONDS, H, D, AND Z, FOR VARIOUS VALUES OF MAGNETIC CHARACTER-FIGURE C

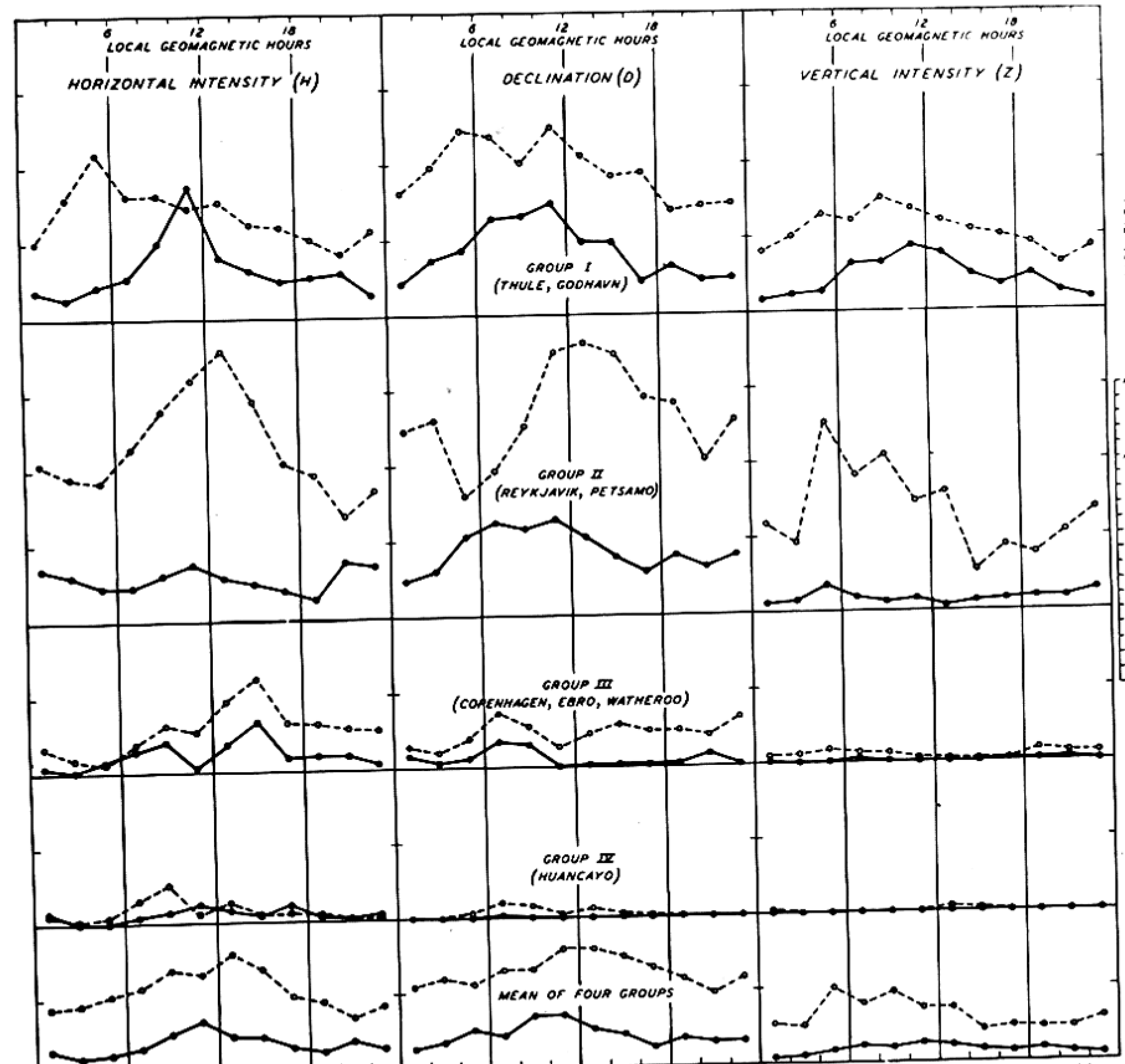

FIG. 200—HOURLY VARIATION WITH GEOMAGNETIC LATITUDE OF FREQUENCY OF FLUCTUATIONS, DURATIONS 10 TO 500 SECONDS, H, D, AND Z; ——MEAN OF DAYS MAY 9 (C=0.0), JULY 4 (C=0.4), MAY 5 (C=0.8), ----MEAN OF DAYS MAY 31 (C=1.2), MARCH 24 (C=1.5), AND MAY 1 (C=1.9), 1933

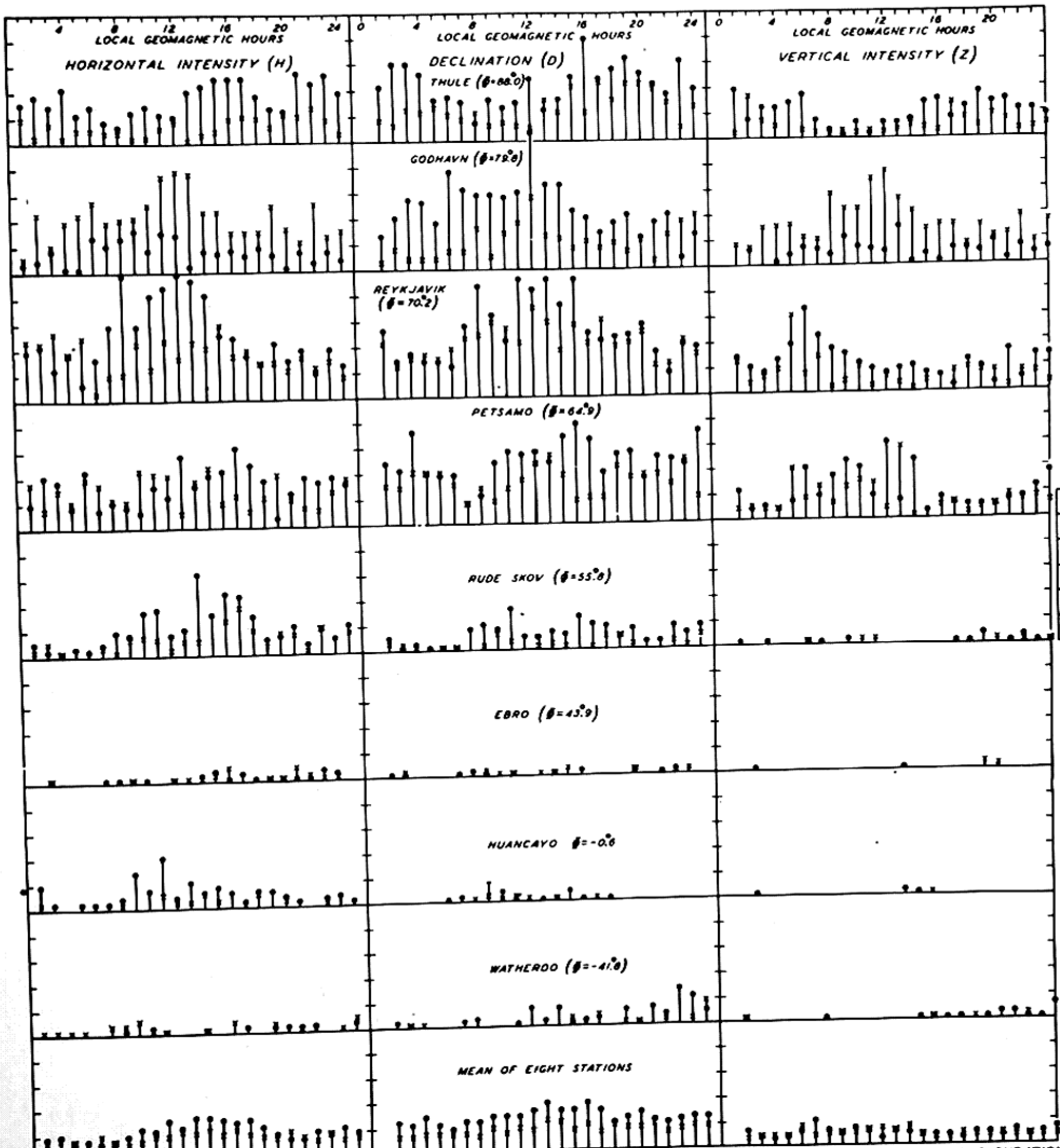

FIG. 201—VARIATION WITH GEOMAGNETIC LATITUDE IN HOURLY FREQUENCY OF POSITIVE AND NEGATIVE FLUCTUATIONS, DURATIONS 10 TO 500 SECONDS, H, D, AND Z, MEAN OF SIX DAYS, MAY 9 (C=0.0), JULY 4 (C=0.4), MAY 5 (C=0.8), MAY 31 (C=1.2), MARCH 24 (C=1.5), MAY 1 (C=1.9), 1933; • = POSITIVE FLUCTUATION, × = NEGATIVE FLUCTUATION

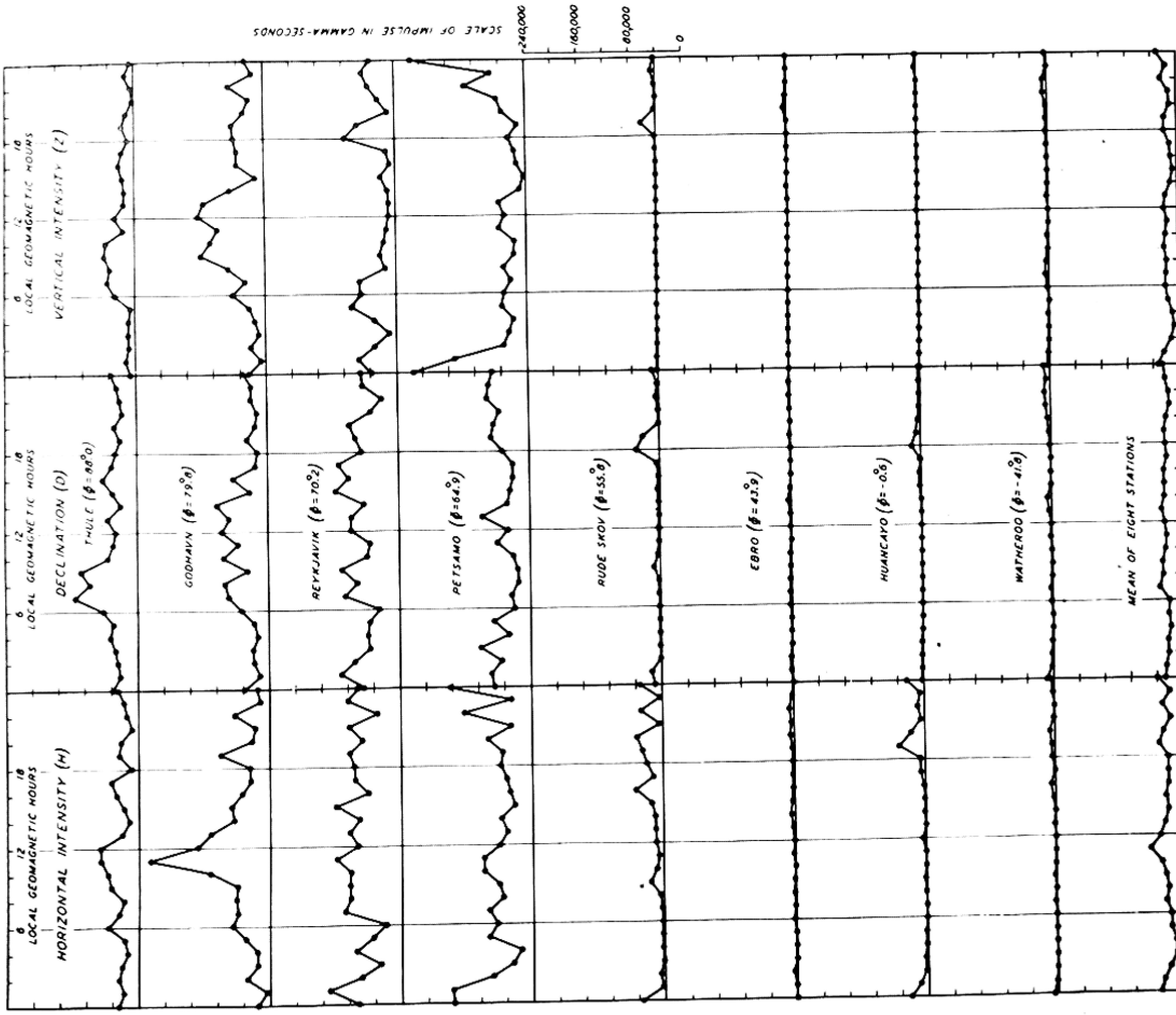

FIG. 202—VARIATION WITH GEOMAGNETIC LATITUDE OF MAGNITUDE OF TOTAL IMPULSE, AS MEASURED BY $1/2\ \Sigma \Delta\Gamma \Delta t$, WITH $\Delta\Gamma$ THE AMPLITUDE AND Δt THE DURATION, FOR FLUCTUATIONS OF DURATION 10 TO 500 SECONDS, MEAN OF SIX DAYS, MAY 9 (C=0.0), JULY 4 (C=0.4), MAY 5 (C=0.8), MAY 31 (C=1.2), MARCH 24 (C=1.5), MAY 1 (C=1.9), 1933

FIG. 203—ISOMAGNETIC LINES FOR AMPLITUDE OF FLUCTUATIONS IN H, 0 TO 150 SECONDS DURATION, WITH AVERAGE PROBABILITY OF 0.1 FOR 3-MONTH INTERVALS

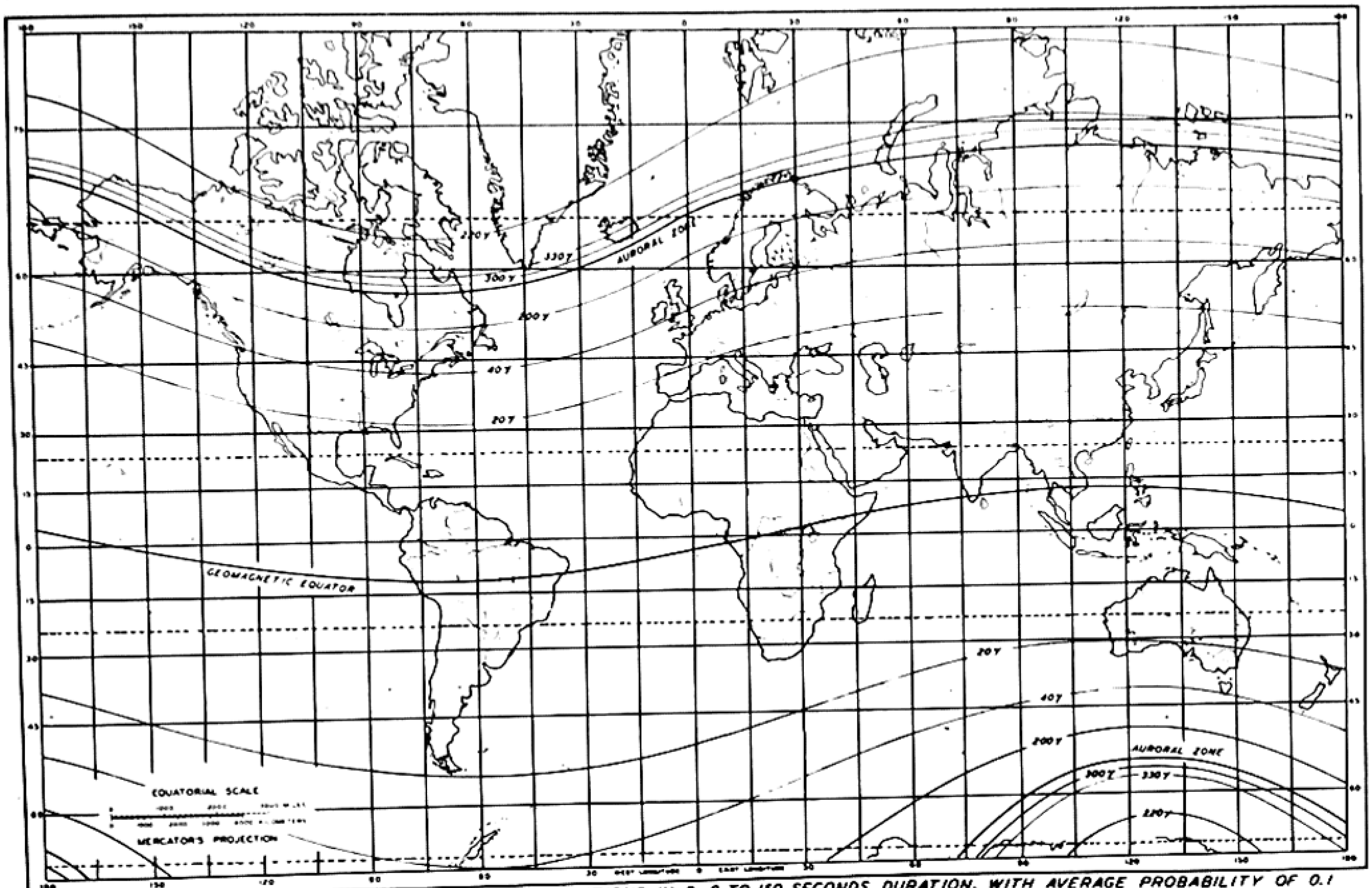

FIG. 204—ISOMAGNETIC LINES FOR AMPLITUDE OF FLUCTUATIONS IN D, 0 TO 150 SECONDS DURATION, WITH AVERAGE PROBABILITY OF 0.1 FOR 3-MONTH INTERVALS

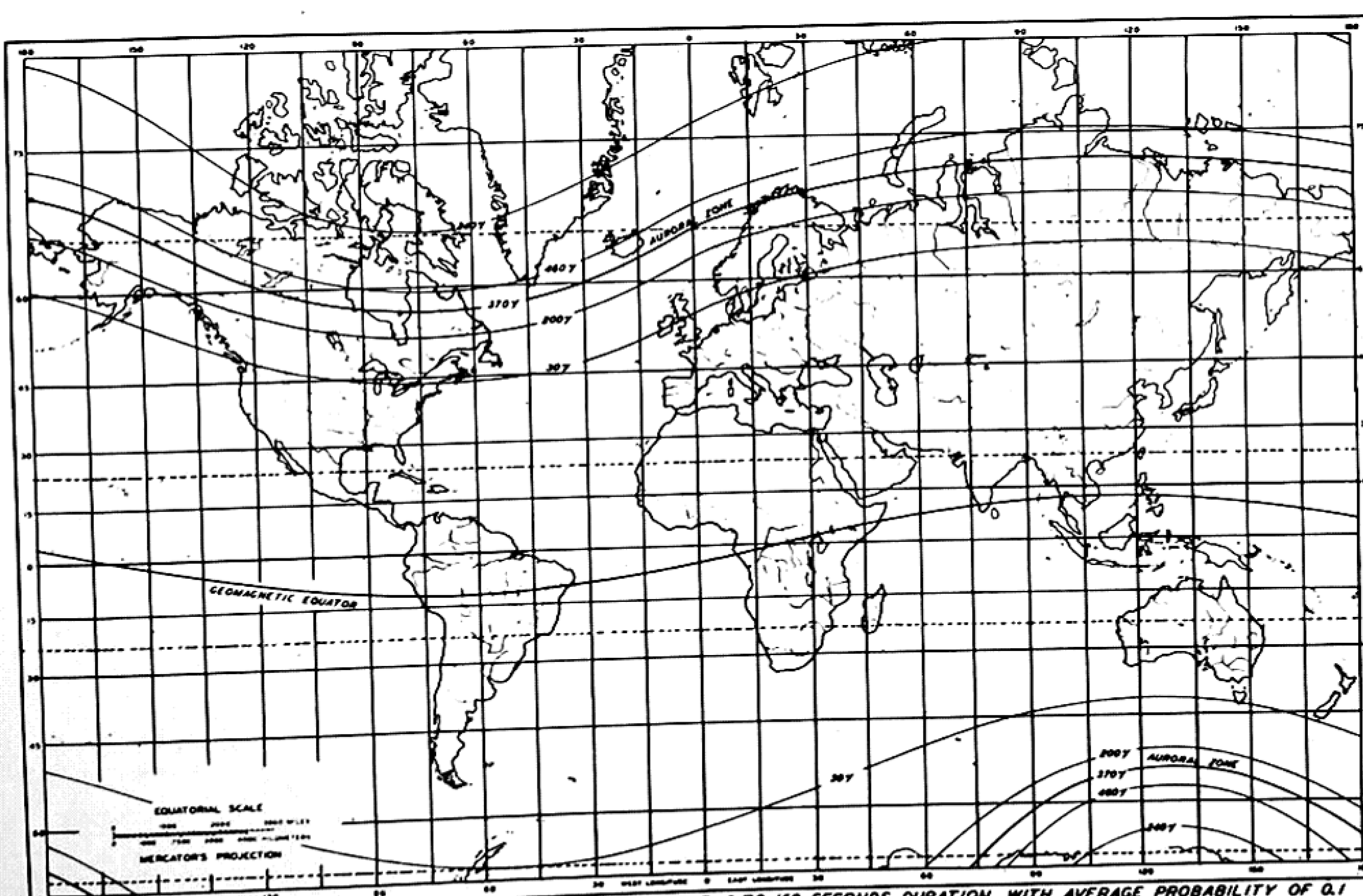

FIG. 205—ISOMAGNETIC LINES FOR AMPLITUDE OF FLUCTUATIONS IN Z, 0 TO 150 SECONDS DURATION, WITH AVERAGE PROBABILITY OF 0.1 FOR 3-MONTH INTERVALS

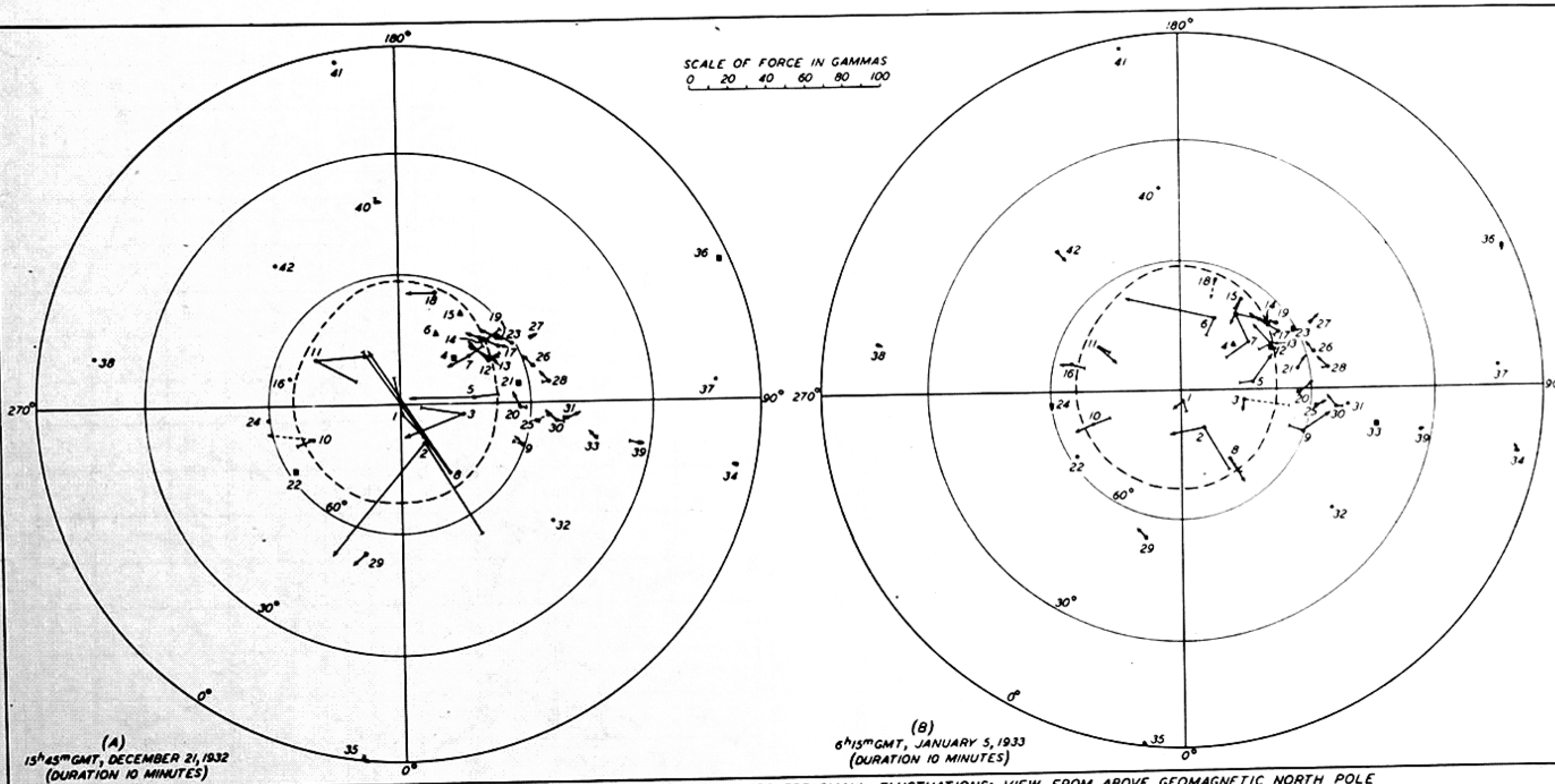

FIG. 206—LATITUDE-DISTRIBUTIONS OF MAXIMUM DISTURBANCE-VECTORS FOR SMALL FLUCTUATIONS; VIEW FROM ABOVE GEOMAGNETIC NORTH POLE (SOUTHERN-LATITUDE STATIONS SHOWN IN CORRESPONDING NORTHERN LATITUDES WITH EAST AND VERTICAL COMPONENTS REVERSED IN SIGN)

LEGEND

HORIZONTAL FORCE — VERTICAL FORCE (VERTICAL COMPONENT POSITIVE WHEN DRAWN TOWARD GEOMAGNETIC NORTH POLE) ----- ESTIMATED — — — AVERAGE AURORAL ZONE

■ = STATIONS DATA MISSING ▲ = STATIONS TOO DISTURBED

STATIONS

1 THULE
2 GODHAVN
3 SCORESBY SUND
4 SVEAGRUVAN
5 JAN MAYEN
6 CALM BAY
7 BEAR ISLAND
8 JULIANNEHAAB
9 REYKJAVIK
10 FORT RAE
11 POINT BARROW
12 LYCKSELE
13 TROMSÖ
14 PETSAMO
15 METOTCHKIN SHAR
16 COLLEGE FAIRBANKS
17 SODANKYLÄ
18 DICKSON
19 KANDALAKSCHA
20 LERWICK
21 DOMBÅS
22 MEANOOK
23 KAJANNI
24 SITKA
25 ESKDALEMUIR
26 LOVÖ
27 SLOUTZK
28 RUDE SKOV
29 AGINCOURT
30 ABINGER
31 VAL JOYEUX
32 SAN MIGUEL
33 EBRO
34 FERNANDO POO
35 HUANCAYO
36 MOGADISCIO
37 ELIZABETHVILLE
38 APIA
39 CAPETOWN
40 WATHEROO
41 ANTIPOLO
42 TOOLANGI

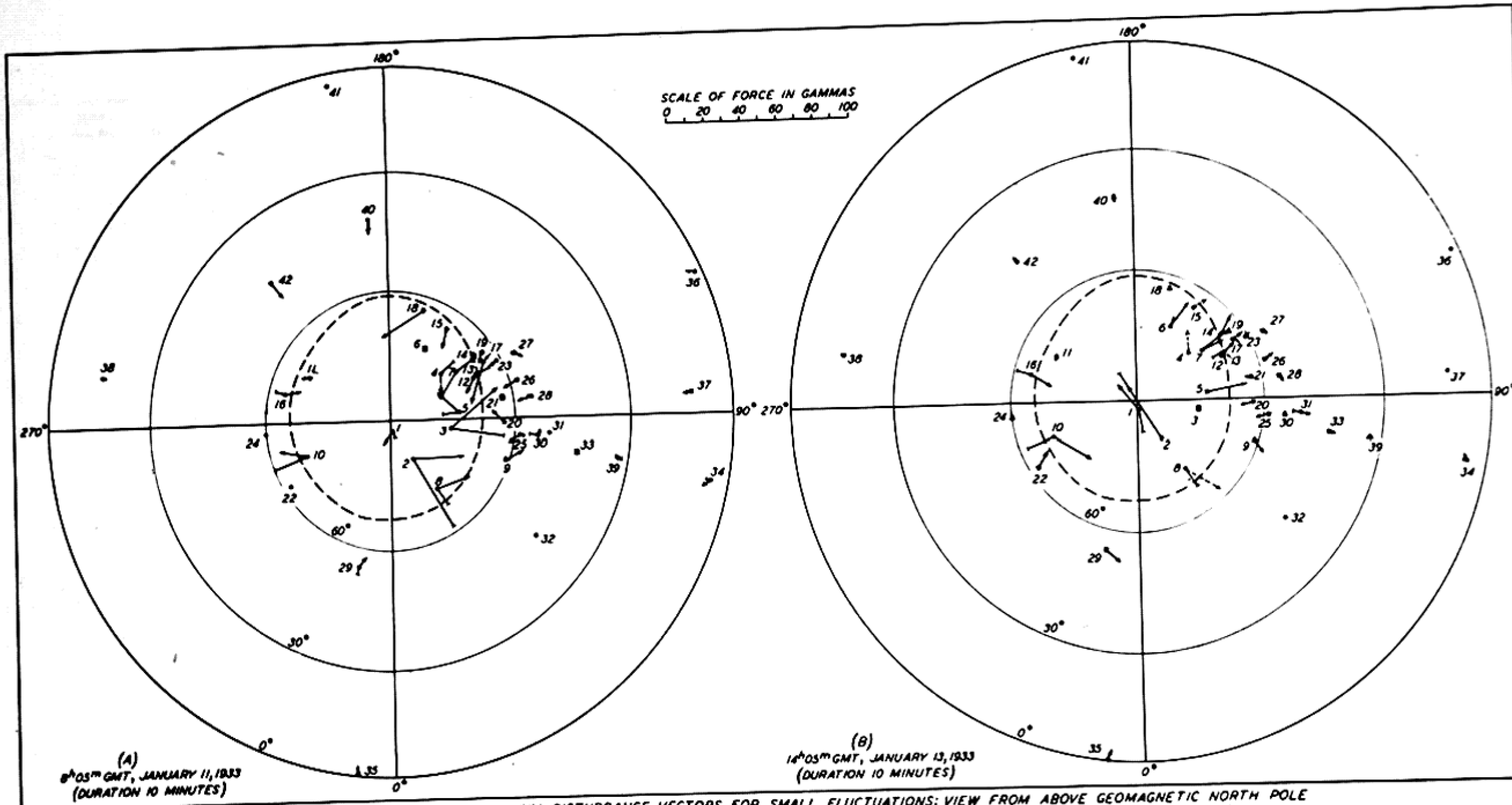

FIG. 207–LATITUDE-DISTRIBUTIONS OF MAXIMUM DISTURBANCE-VECTORS FOR SMALL FLUCTUATIONS; VIEW FROM ABOVE GEOMAGNETIC NORTH POLE
(SOUTHERN-LATITUDE STATIONS SHOWN IN CORRESPONDING NORTHERN LATITUDES WITH EAST AND VERTICAL COMPONENTS REVERSED IN SIGN)
LEGEND AS IN FIGURE 206

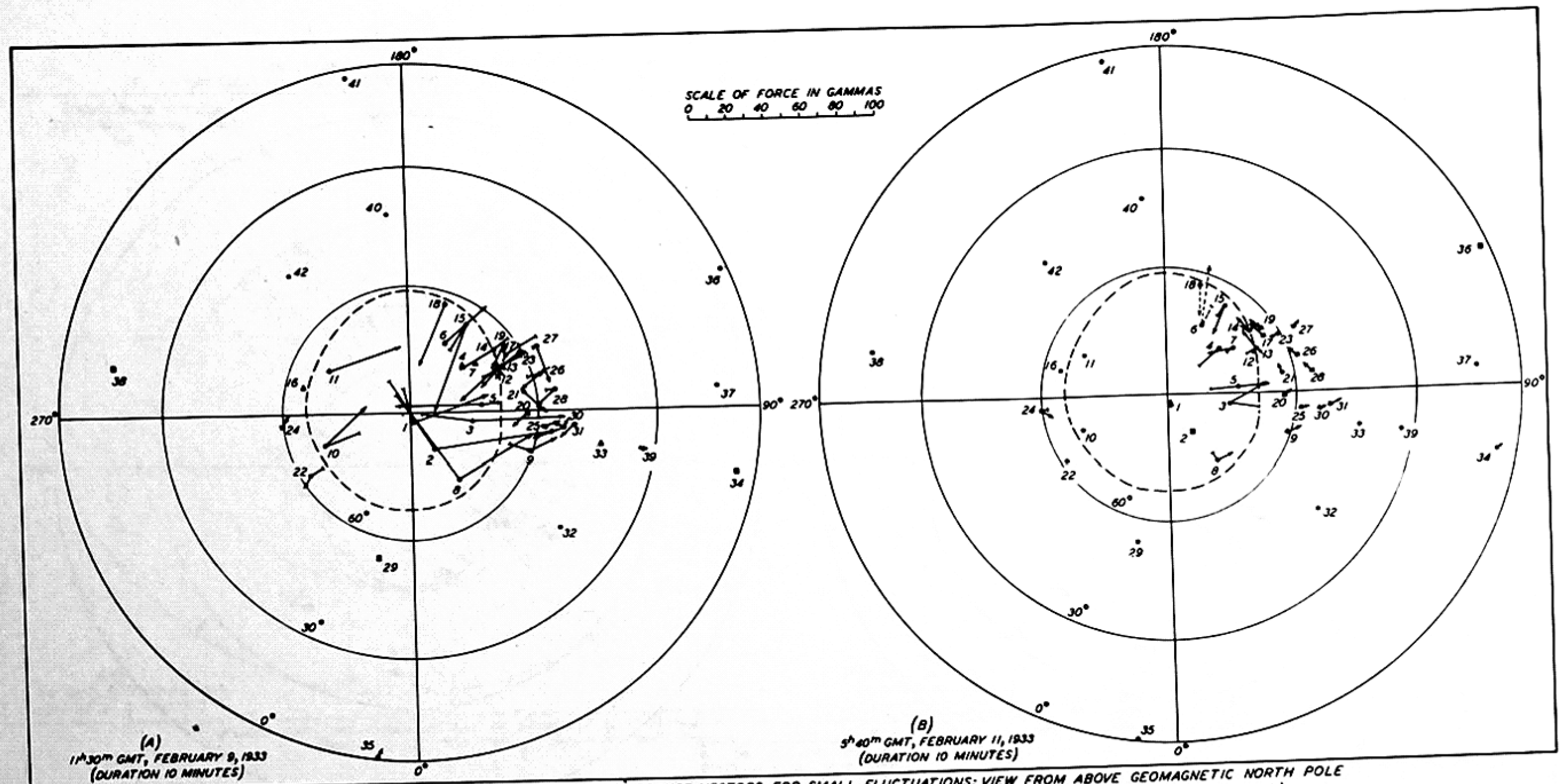

FIG. 208—LATITUDE-DISTRIBUTIONS OF MAXIMUM DISTURBANCE-VECTORS FOR SMALL FLUCTUATIONS; VIEW FROM ABOVE GEOMAGNETIC NORTH POLE
(SOUTHERN-LATITUDE STATIONS SHOWN IN CORRESPONDING NORTHERN LATITUDES WITH EAST AND VERTICAL COMPONENTS REVERSED IN SIGN)
LEGEND AS IN FIGURE 206

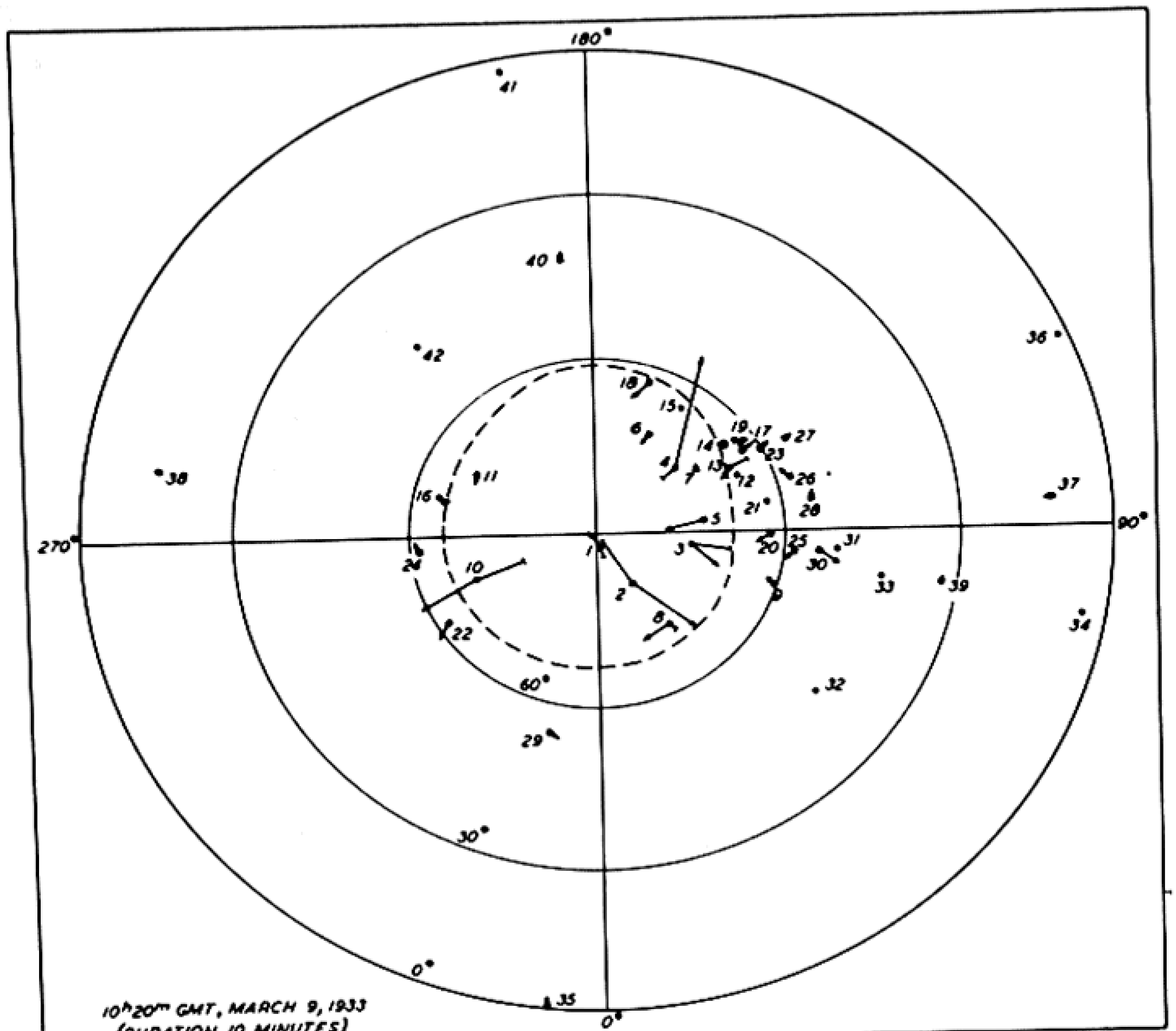

FIG. 209 – LATITUDE-DISTRIBUTIONS OF MAXIMUM DISTURBANCE-VECTORS FOR SMALL FLUCTUATIONS; VIEW FROM ABOVE GEOMAGNETIC NORTH POLE
(SOUTHERN-LATITUDE STATIONS SHOWN IN CORRESPONDING NORTHERN LATITUDES WITH EAST AND VERTICAL COMPONENTS REVERSED IN SIGN)
LEGEND AS IN FIGURE 206

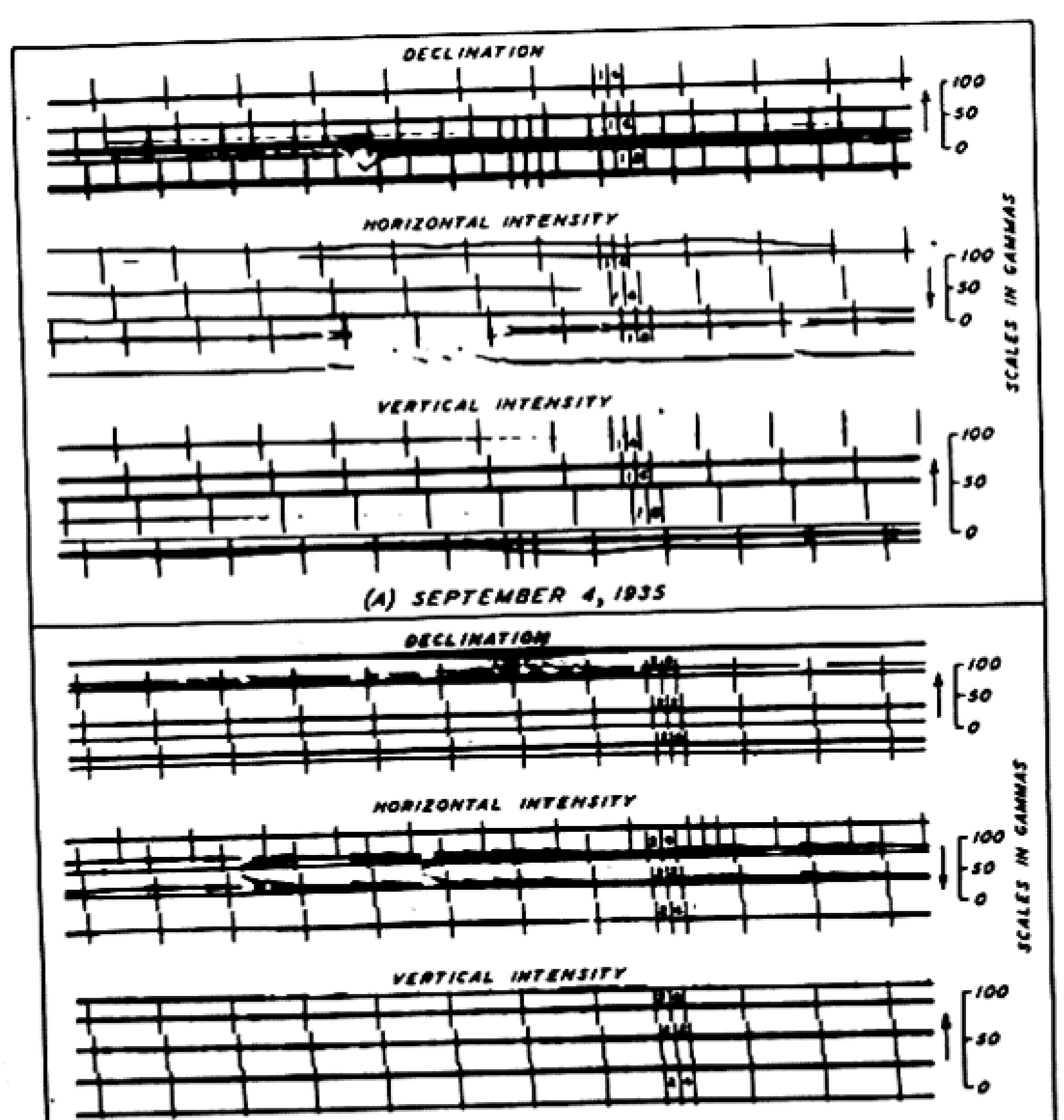

FIG. 210 – GEOMAGNETIC EFFECTS LIGHTNING-DISCHARGES, HUANCAYO, PERU
(VERTICAL TIME-MARKS AT FIVE-MINUTE INTERVALS WITH ONE-MINUTE INTERVALS AT HOUR)

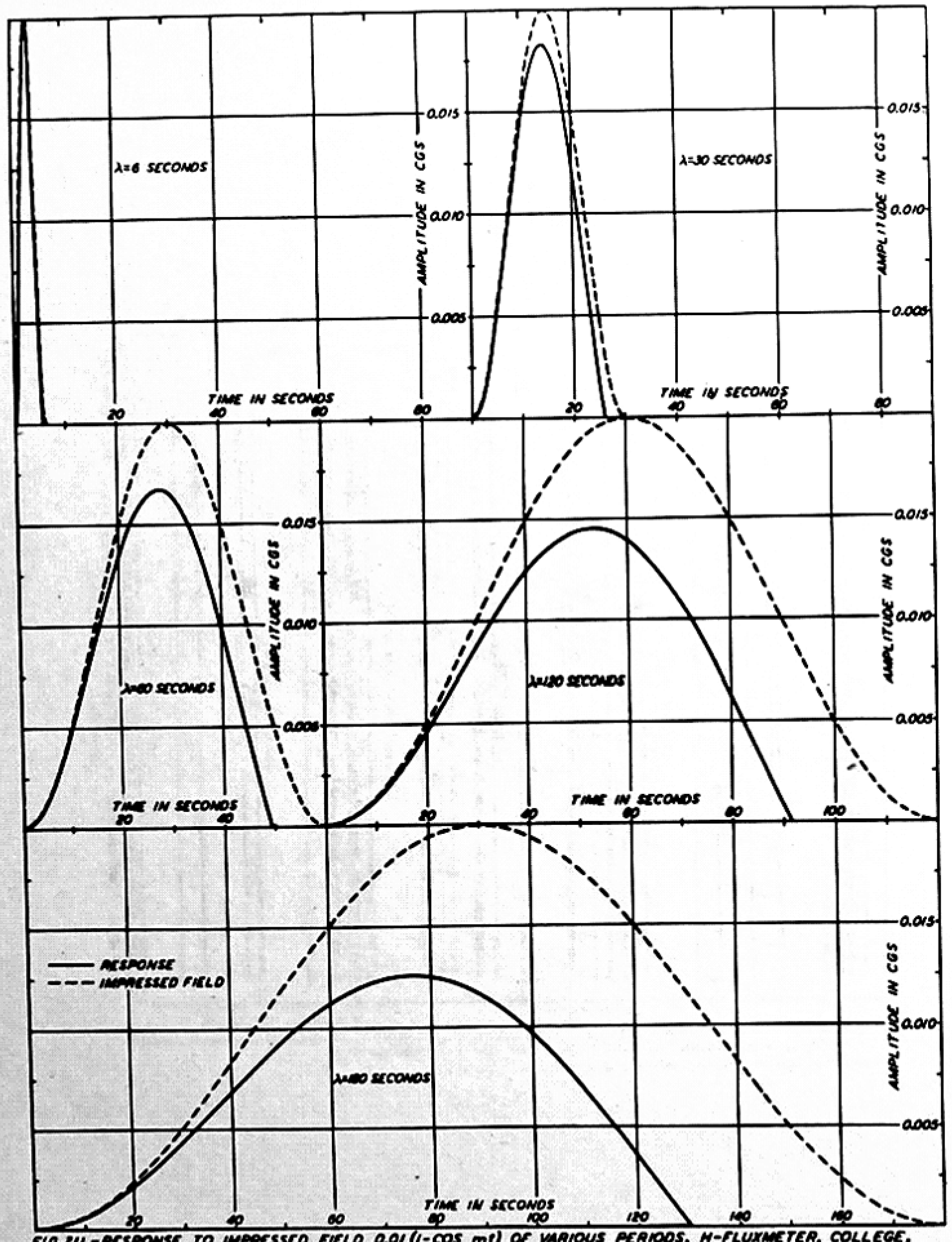

FIG. 211—RESPONSE TO IMPRESSED FIELD 0.01 (1-COS mt) OF VARIOUS PERIODS, H-FLUXMETER, COLLEGE, ALASKA, AUGUST, 1942 (RETURN-TIME CONSTANT 80 SECONDS)

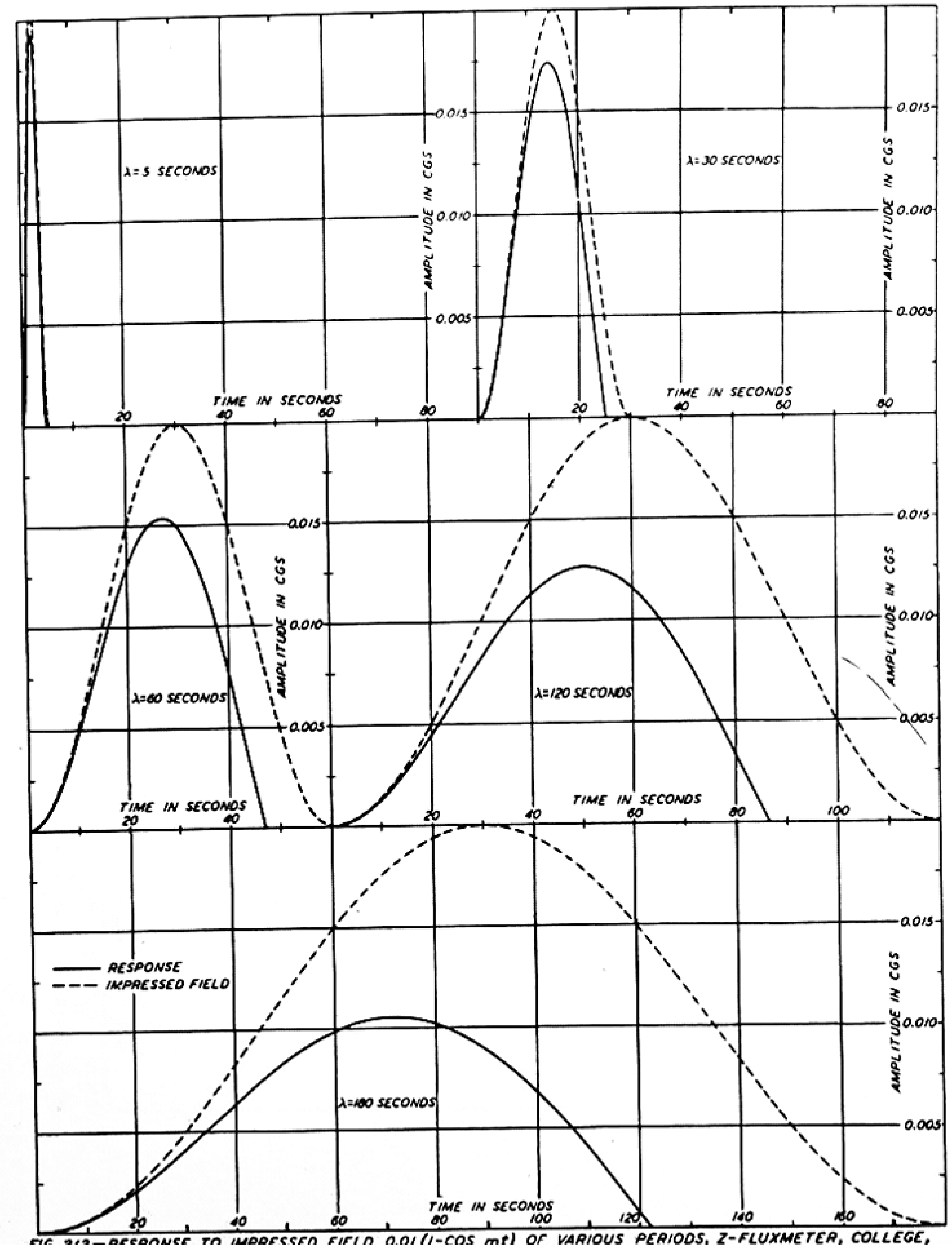

FIG. 212—RESPONSE TO IMPRESSED FIELD 0.01 (1-COS mt) OF VARIOUS PERIODS, Z-FLUXMETER, COLLEGE, ALASKA, AUGUST, 1942 (RETURN-TIME CONSTANT 51 SECONDS)

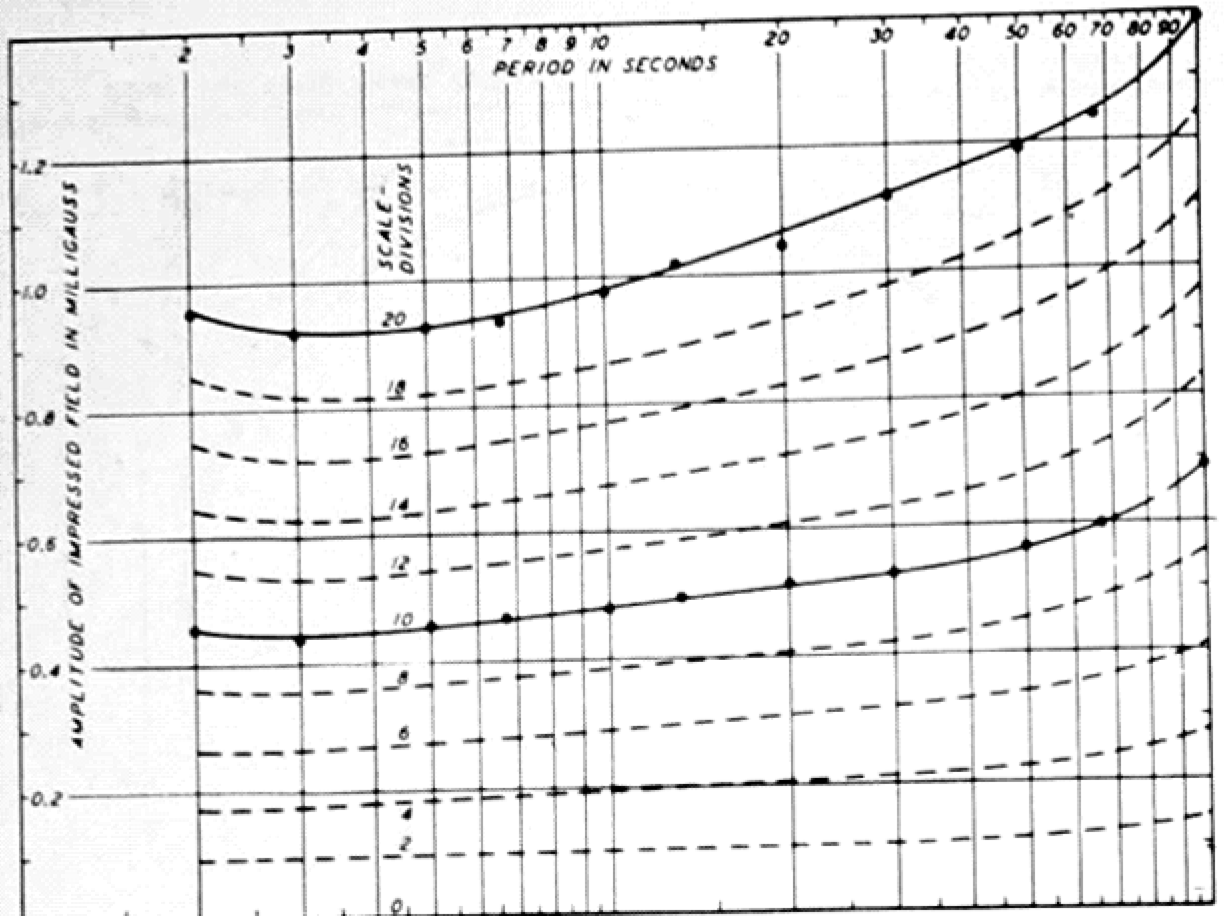

FIG.213—RESPONSE IN SCALE-DIVISIONS OF G.E. FLUXMETER NO. 725024 TO SINGLE-CYCLE FIELDS OF VARIOUS AMPLITUDES AND PERIODS, USING PULSE-COUNTER C.R. LAB. NO. 50

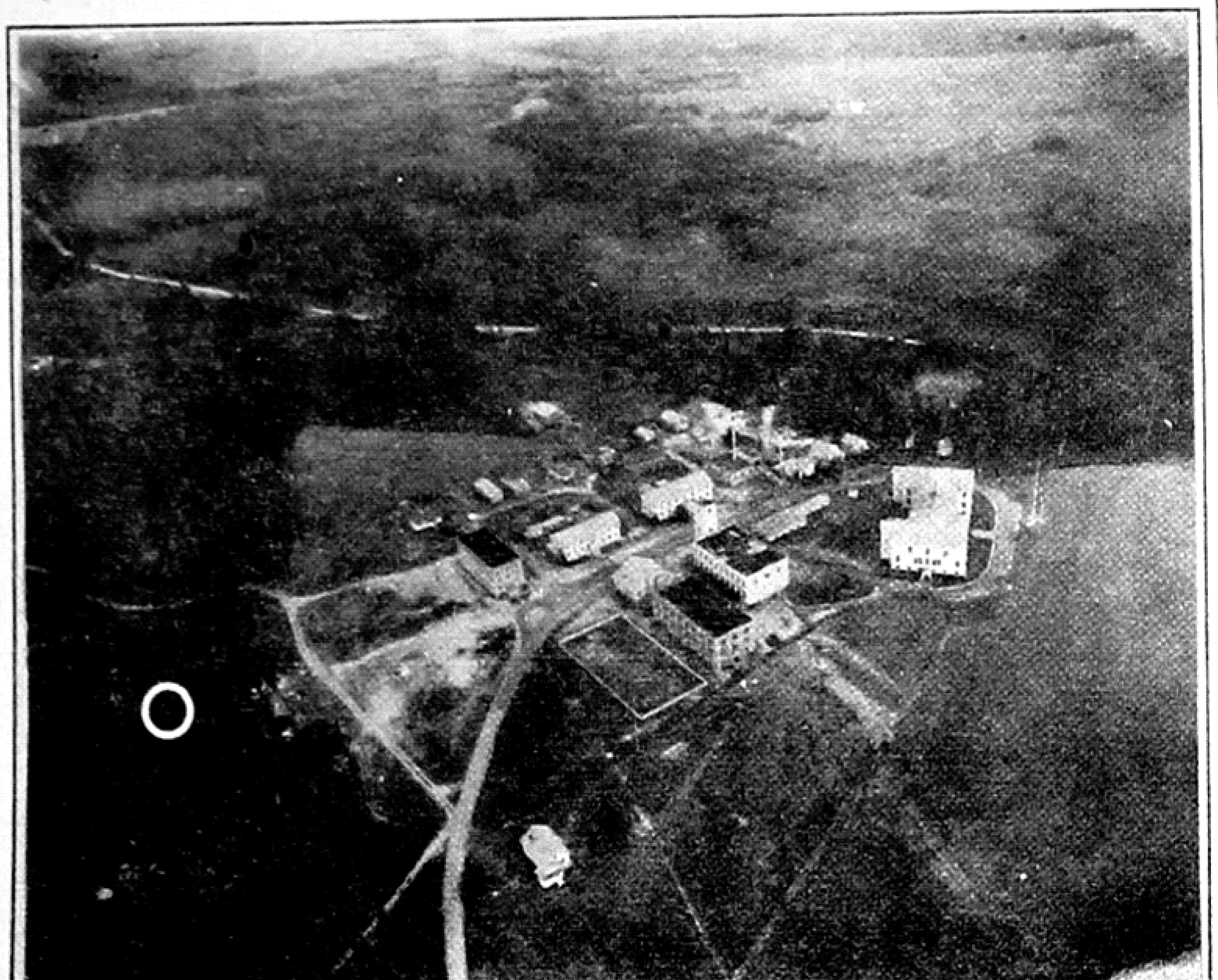

Fig. 214. General view, University of Alaska, showing approximate location of fluxmeter installation (white circle at left)

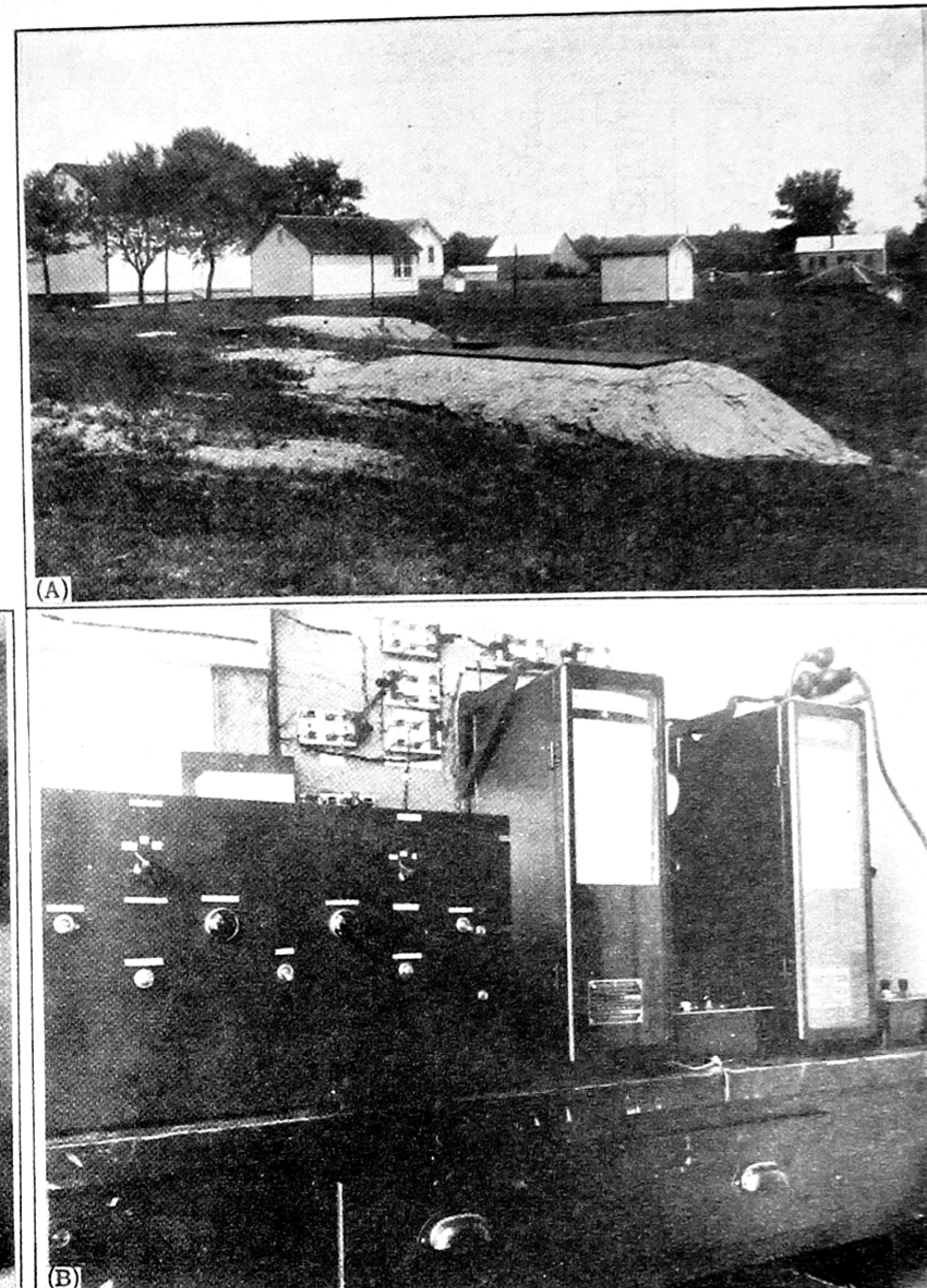

Fig. 215. Cheltenham Magnetic Observatory. (A) Location of buried fluxmeter coils indicated under mounds in foreground. (B) Fluxmeters and control apparatus

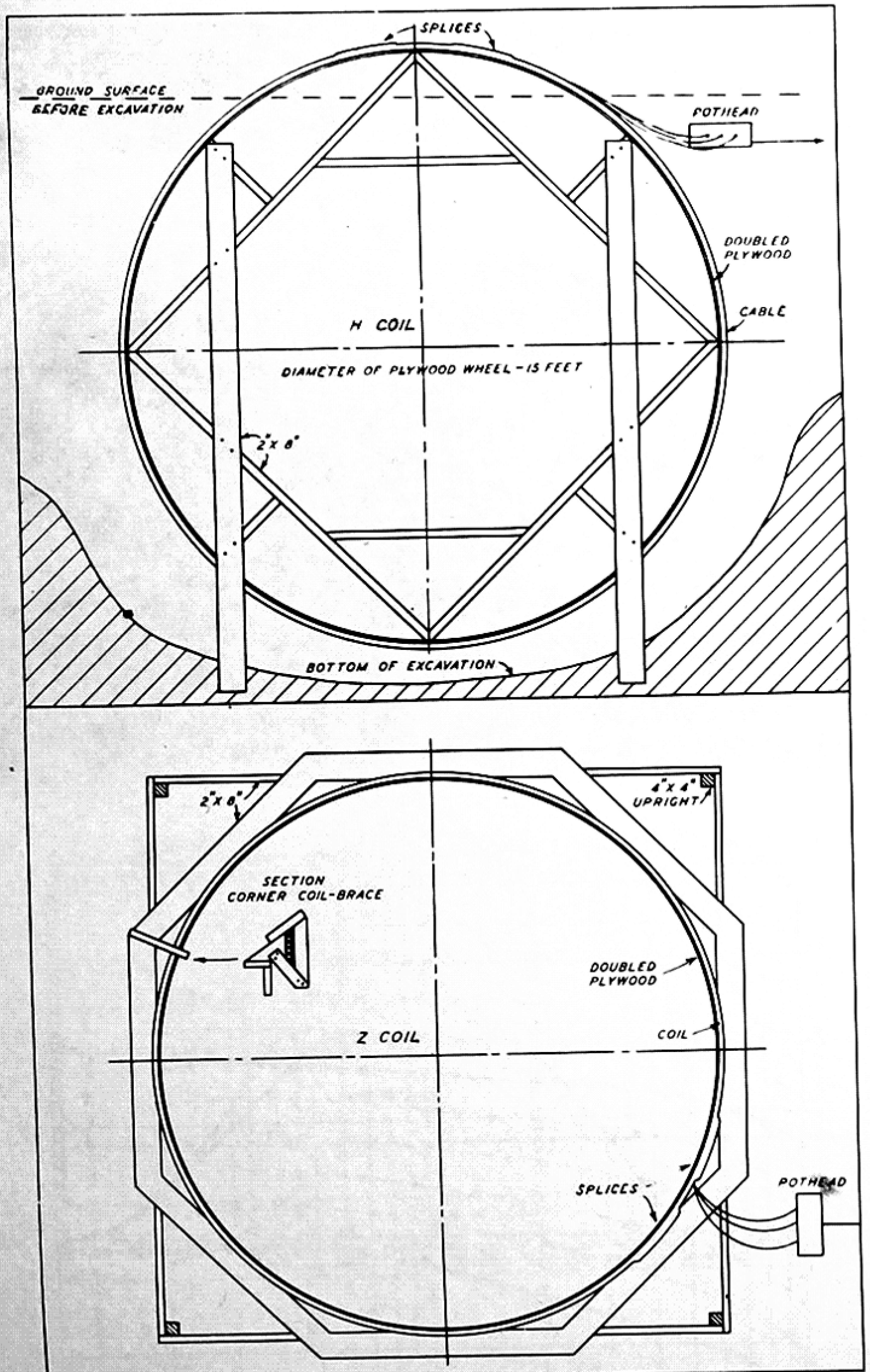

FIG.216 CONSTRUCTIONAL DETAILS OF H- AND Z-COILS, COLLEGE, ALASKA

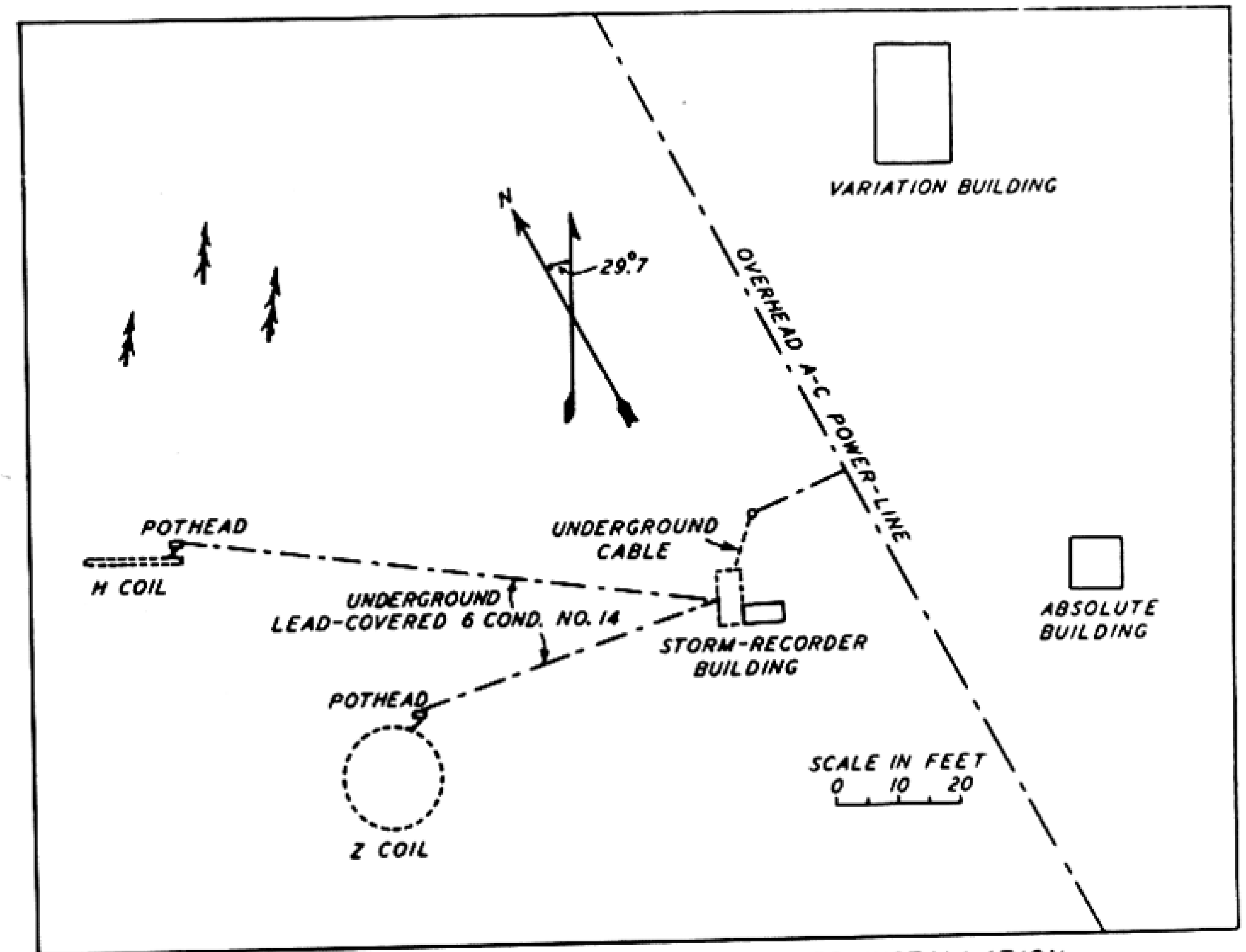

FIG.217—GENERAL PLAN, STORM-RECORDER INSTALLATION

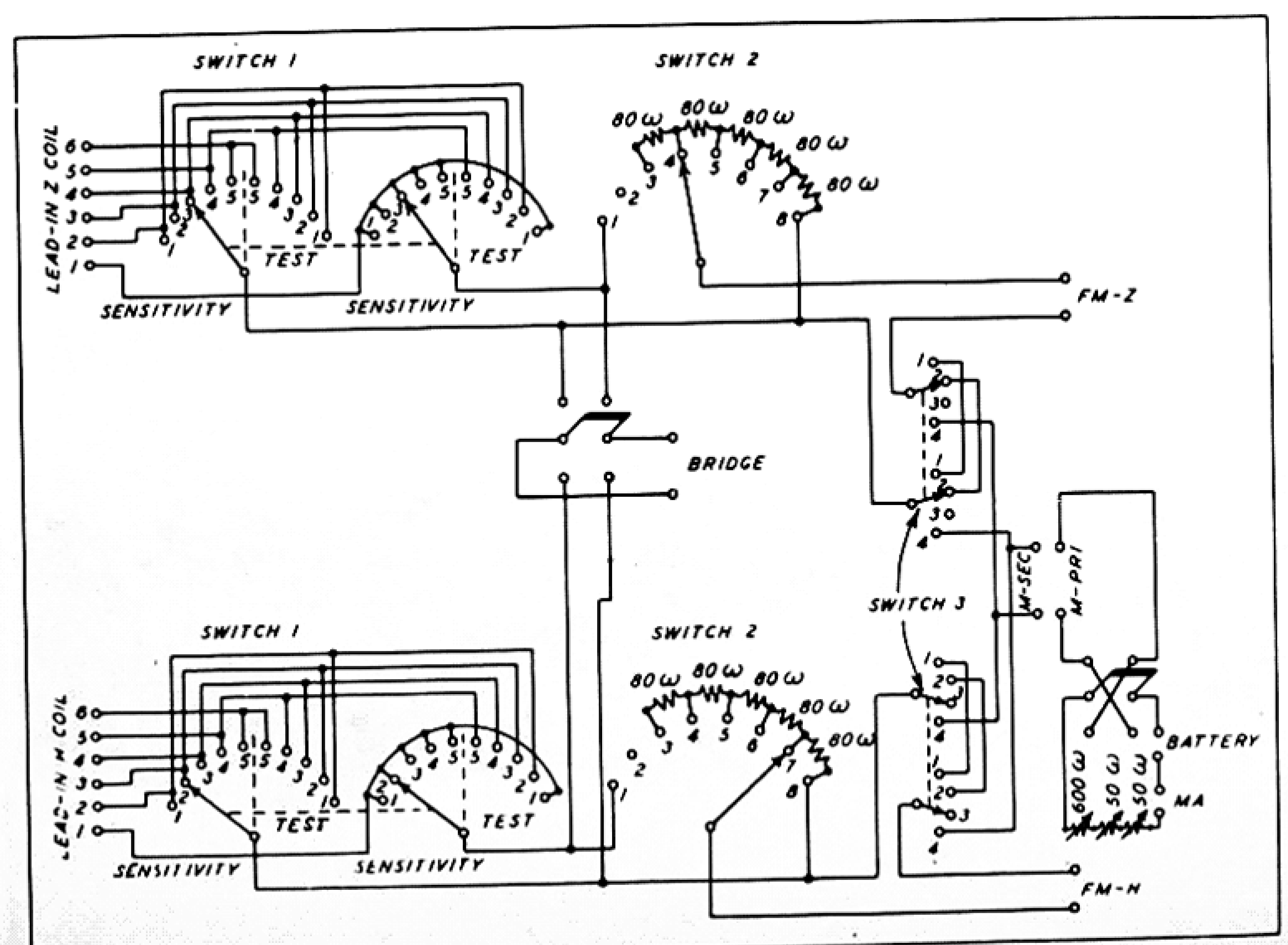

FIG.218—SCHEMATIC DIAGRAM OF ELECTRICAL CIRCUIT, FLUXMETER-INSTALLATION, SHOWING MEANS OF CALIBRATION AND CONTROL

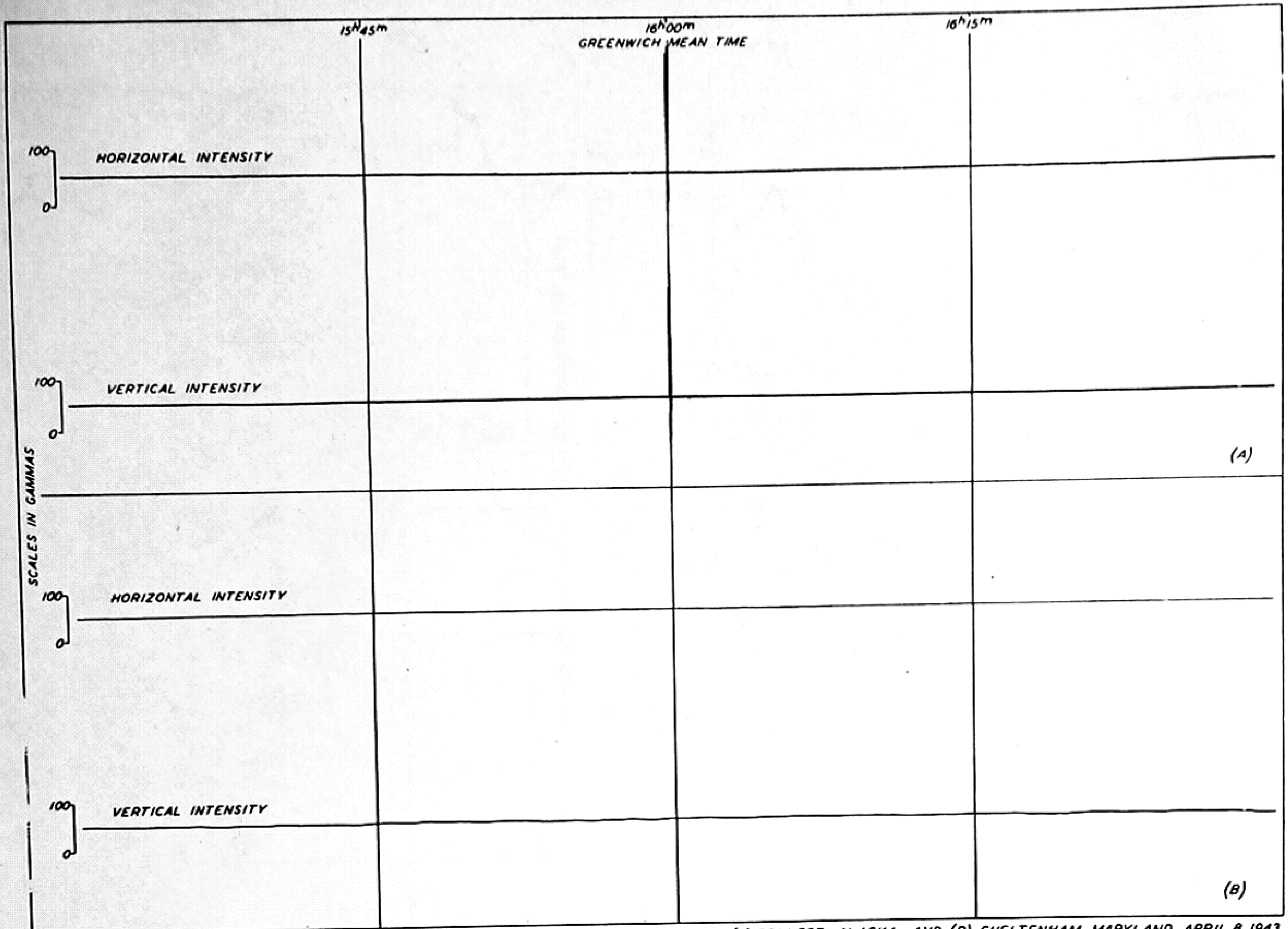

FIG. 219—SIMULTANEOUS FLUXMETER RECORDS ON MAGNETICALLY QUIET DAY; (A) COLLEGE, ALASKA, AND (B) CHELTENHAM, MARYLAND, APRIL 8, 1943

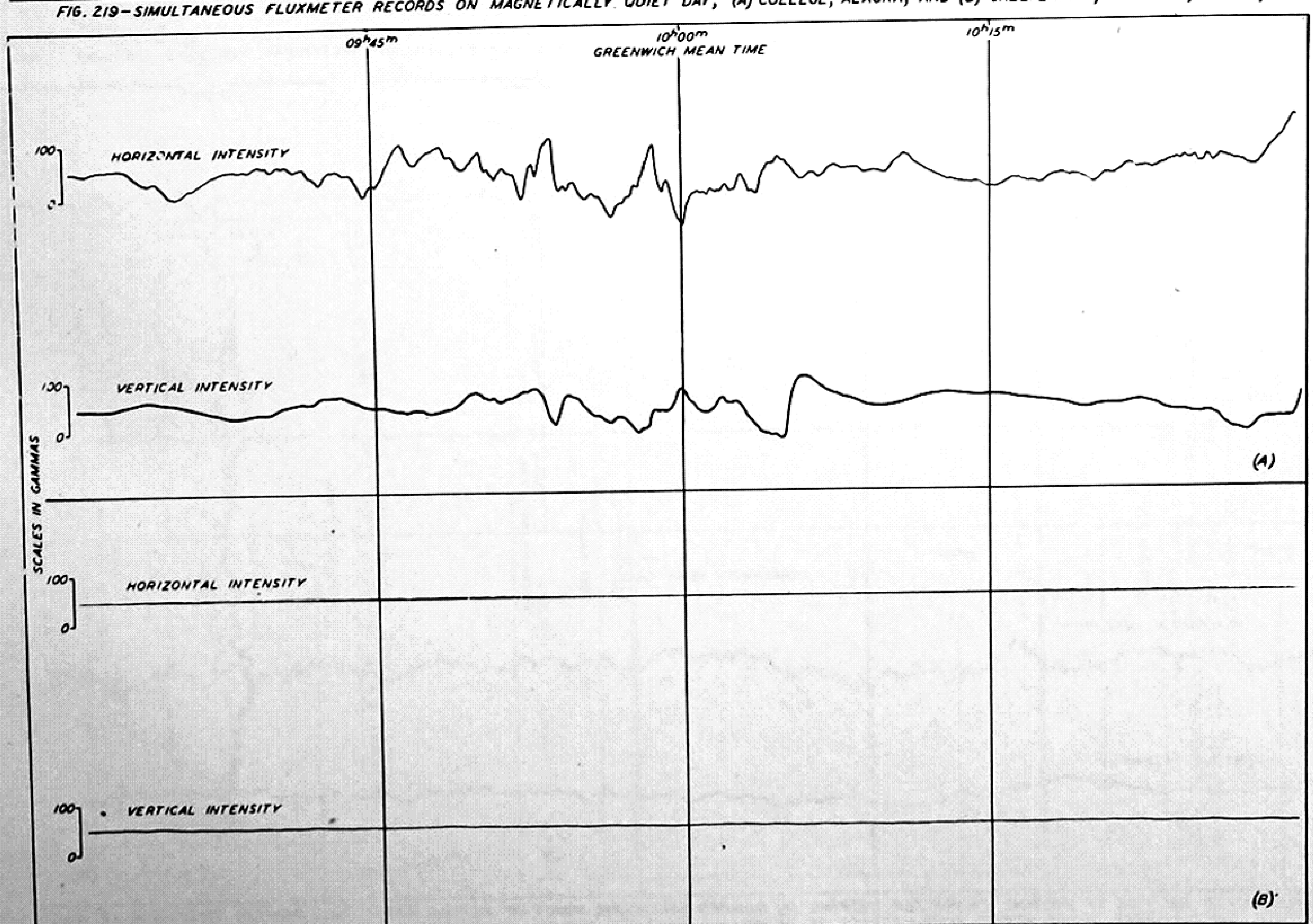

FIG. 220—SIMULTANEOUS FLUXMETER RECORDS ON MODERATELY DISTURBED DAY; (A) COLLEGE, ALASKA, AND (B) CHELTENHAM, MARYLAND, APRIL 10, 1943

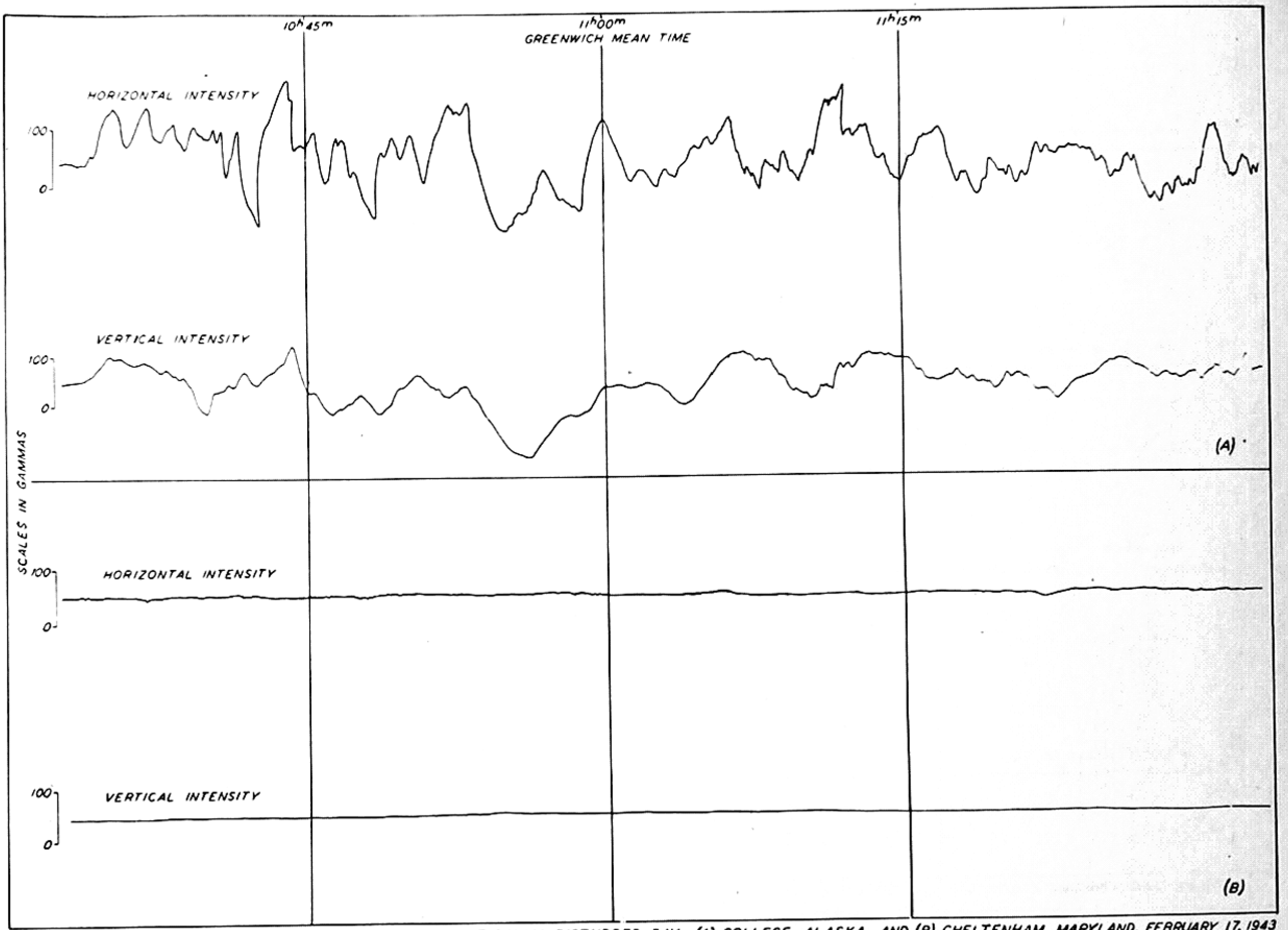

FIG. 221—SIMULTANEOUS FLUXMETER RECORDS ON MAGNETICALLY DISTURBED DAY; (A) COLLEGE, ALASKA, AND (B) CHELTENHAM, MARYLAND, FEBRUARY 17, 1943

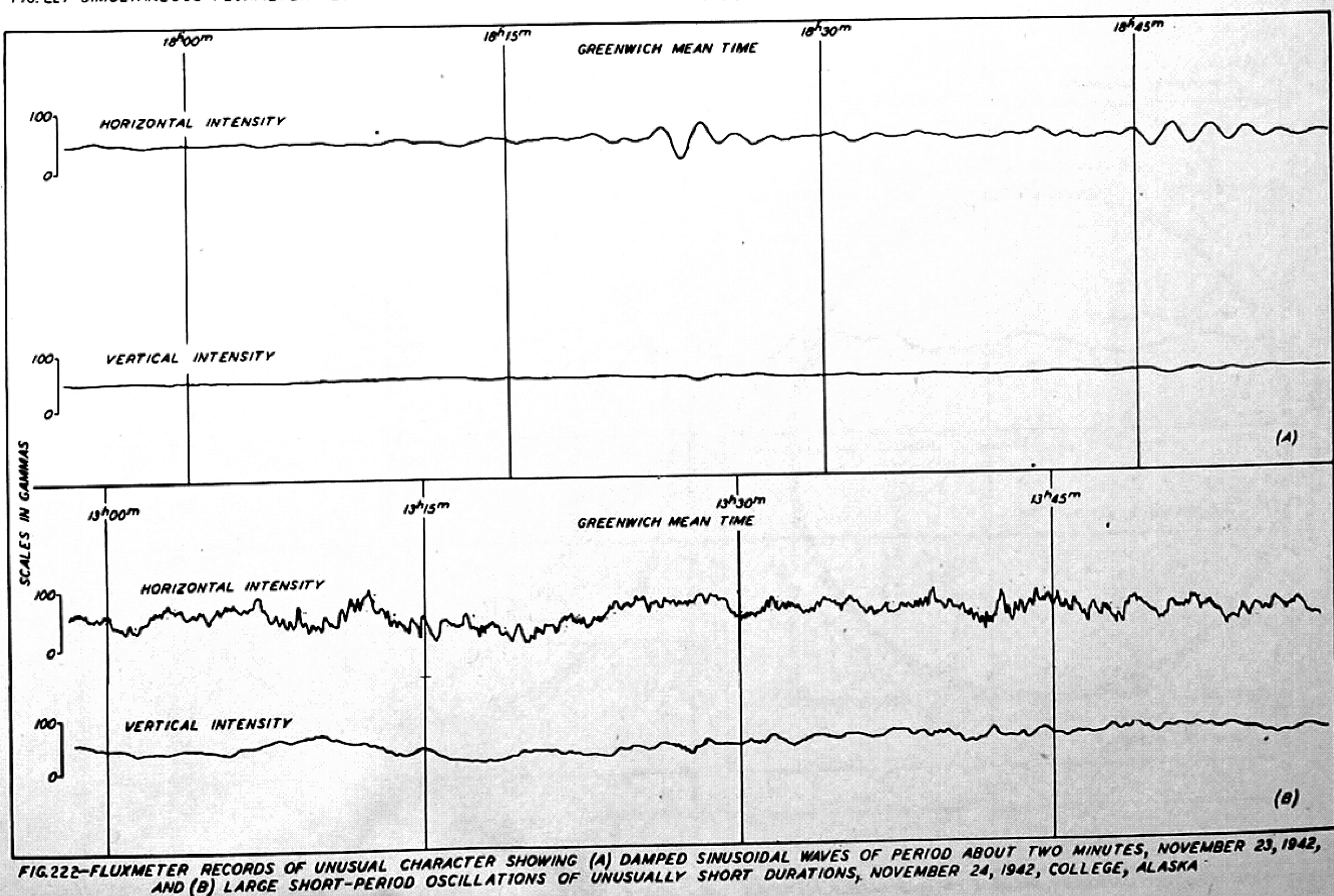

FIG. 222—FLUXMETER RECORDS OF UNUSUAL CHARACTER SHOWING (A) DAMPED SINUSOIDAL WAVES OF PERIOD ABOUT TWO MINUTES, NOVEMBER 23, 1942, AND (B) LARGE SHORT-PERIOD OSCILLATIONS OF UNUSUALLY SHORT DURATIONS, NOVEMBER 24, 1942, COLLEGE, ALASKA

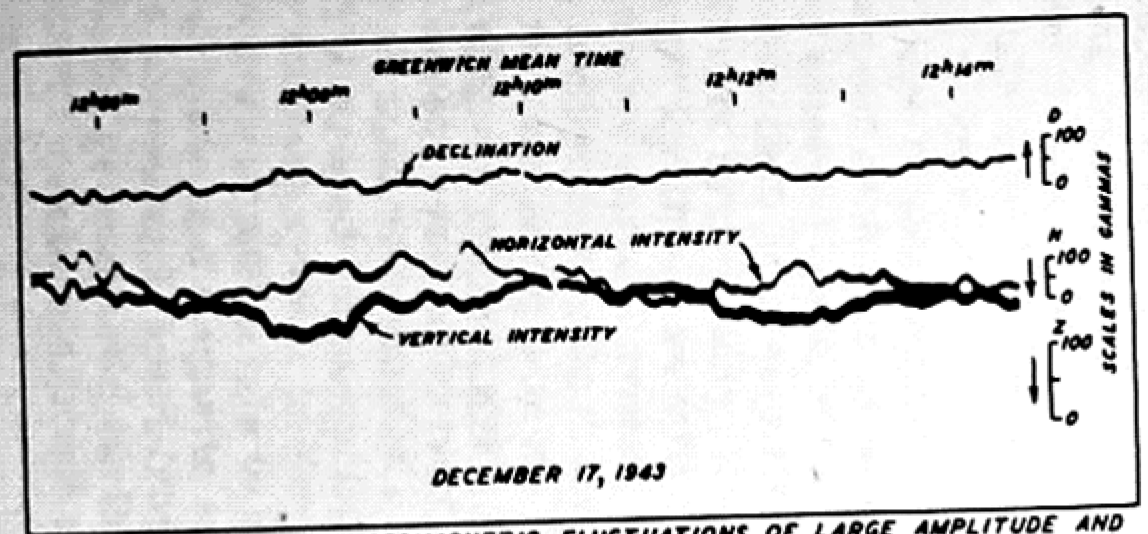

FIG.223—SHORT-PERIOD GEOMAGNETIC FLUCTUATIONS OF LARGE AMPLITUDE AND SHORT DURATION, IVIGTUT, GREENLAND

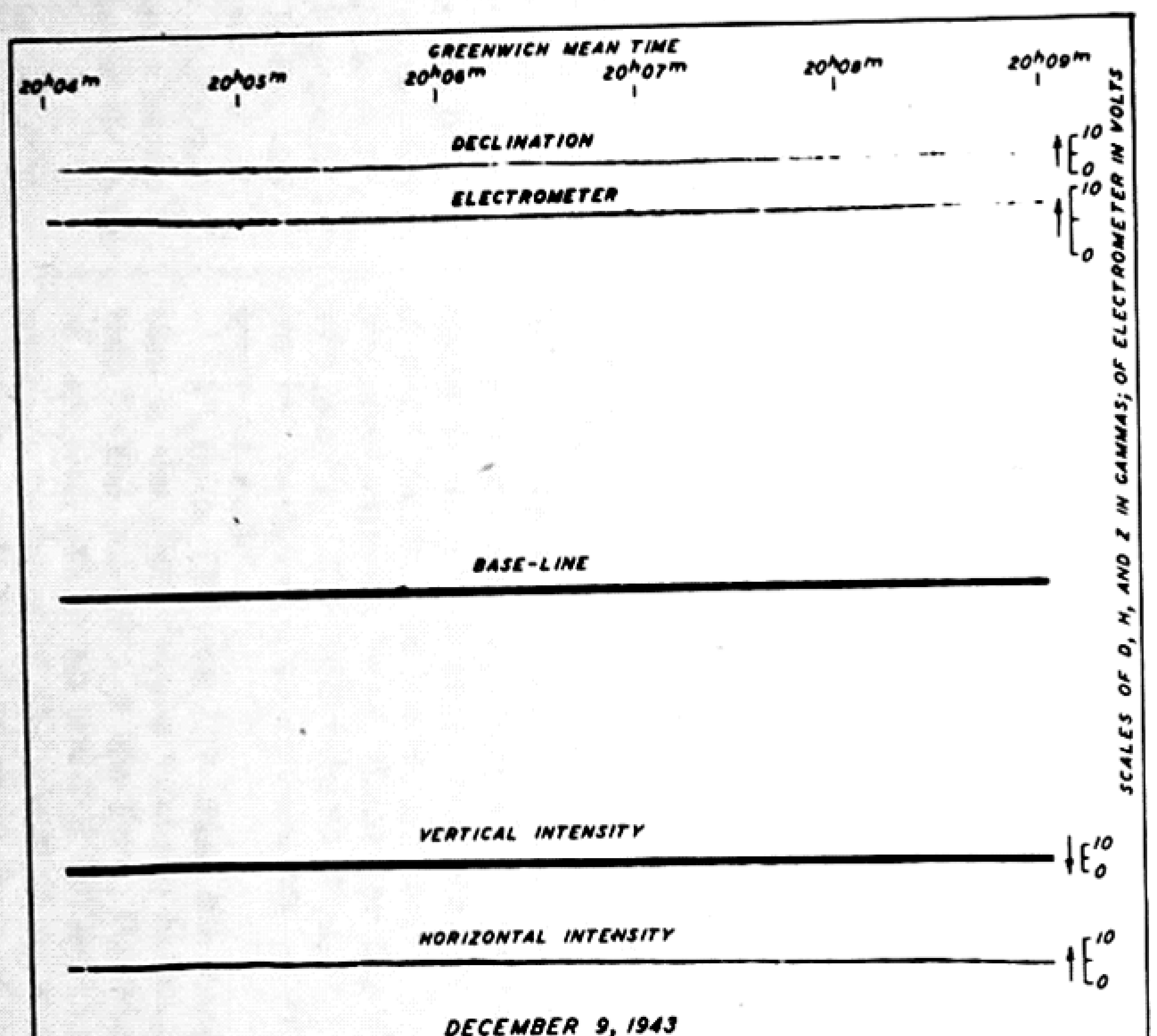

FIG.224—TYPICAL RECORD PORTABLE MAGNETOGRAPH OPERATED AT HIGH SENSITIVITY, TURTLE MOUND, FLORIDA (NOTE ABSENCE SHORT-PERIOD FLUCTUATIONS ONE-SECOND OR LESS DURATION; SIMPLE ELECTROMETER WAS INSERTED TO RECORD LIGHTNING-DISCHARGES)

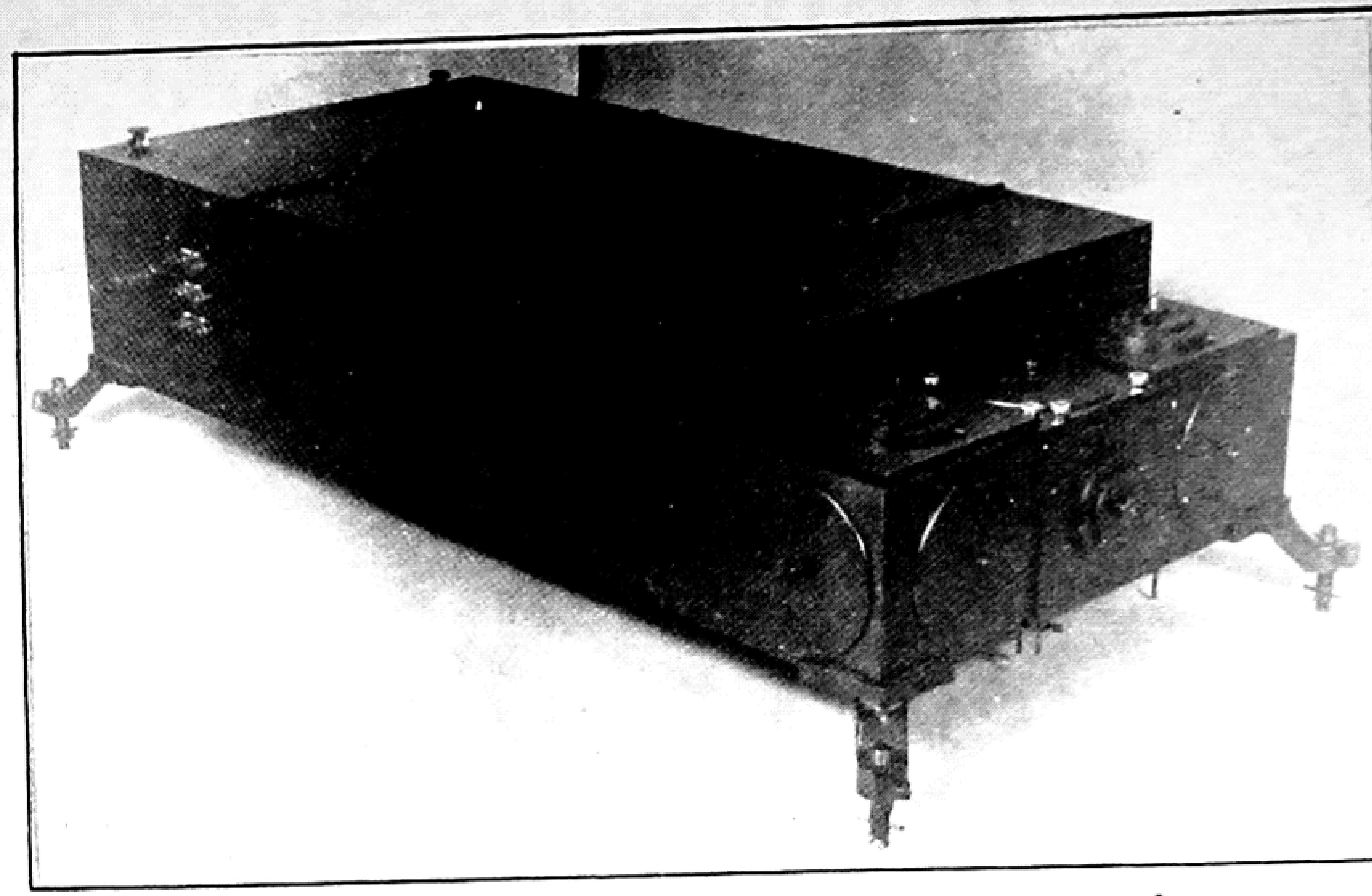

Fig. 225. General view of CIW portable magnetograph

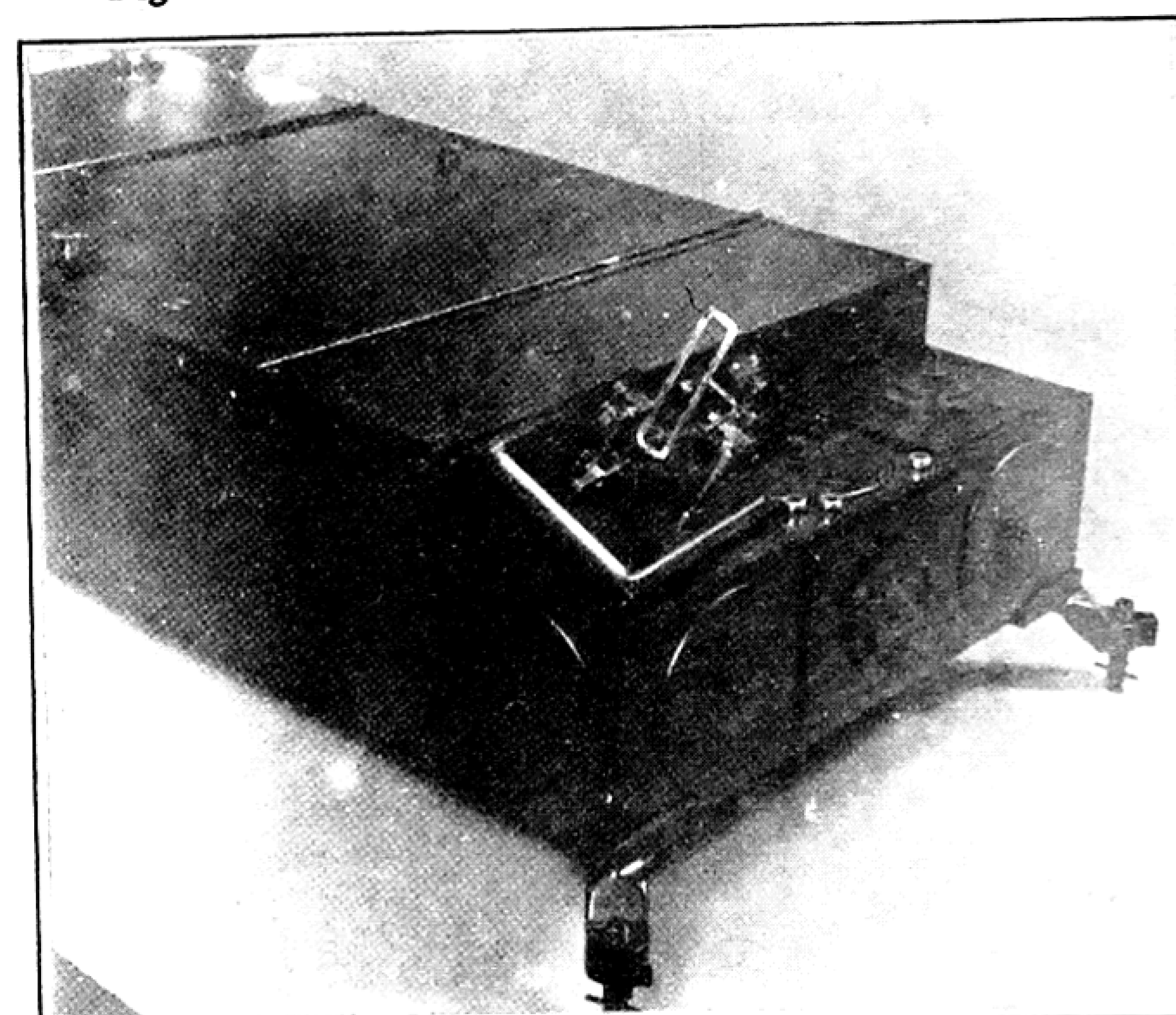

Fig. 226. CIW portable magnetograph showing quartz-fiber double-suspension universal detecting element and mount

CHAPTER X

MAGNETIC STORMS AND ASSOCIATED PHENOMENA

1. Introduction.--Birkeland [29] has studied world-wide features of geomagnetic disturbance for individual magnetic storms. In a number of memoirs Chapman [62, 63, 64] made important extensions of these investigations, using more extensive data involving field-characteristics averaged for many storms. As a result of these studies, he proposed an electric current system of storms in which the polar parts at least flowed in the atmosphere. In a subsequent paper, Vestine and Chapman [37] showed that this current system was in good general agreement with the average characteristics derived from data for the Polar Year, 1932-33. It was concluded that the magnetic data were compatible with the simple form of current system, in which at least the circuits of the intense polar current circulation were closed in the atmosphere. It was estimated that these currents flowed at a height 100 to 150 km above the Earth, for the region near the auroral zone, in good agreement with other estimates by McNish [65]. It was further concluded that the polar current system suggested by Birkeland, in which the current circuits were not closed in the atmosphere, was inconsistent with observation in several important respects.

In the present investigation, the current system proposed by Chapman is examined to check its agreement with observation for individual hours of magnetic storm; the present study thus supplements the previous discussion based on the average characteristics of storms. The possibility that a part of the current may flow in the form of an equatorial ring [66] at a distance of a few earth-radii is not considered. The comparisons are effected through independent derivations of the currents required in the atmosphere for selected hours of four magnetic storms, using rough tentative corrections for induced earth currents. The derivations are made for the case of the real rather than an ideal Earth previously considered by Chapman.

A knowledge of the storm-field alone at the Earth's surface does not enable us to determine the form and position of the external electric current system responsible. The space distribution of electrical conductivity suggests that this current system may flow in the atmosphere. Added support for this view will result if it is found that this atmospheric current system appears simpler than other possible systems calculated from the storm-field alone, for regions in space more distant from the Earth.

2. The electric current system.--Let us first consider the current system derived by Chapman for the average of 40 moderate magnetic storms and other supplementary averaged characteristics of the observed field. The current system is shown in A of Figure 227 where it is drawn appropriate to a spherical Earth having its geographic and magnetic axes coincident. It is intended to correspond, apart from irregular disturbances, with the geomagnetic variations (or disturbance D) of the Earth's field additional to those present on magnetically quiet days.

On the left-hand side is shown a view from the Sun for a time of magnetic storm (main phase). On the right a view from above the north pole is represented. The current system is thus supposed fixed in orientation relative to the Sun, and the Earth revolves within it. A total of 10,000 amperes flows between successive current lines. The currents are most concentrated along the zones of maximum auroral frequency.

The current system may be analyzed into two partial systems shown in B and C of Figure 227. B of Figure 227 represents that responsible for the storm-time component (D_{st}) of disturbance (it is the nonpolar part of this system that is not definitely assigned to the Earth's atmosphere); C of Figure 227 shows the part responsible for the disturbance daily variation (S_D) depending mainly on local magnetic time.

The current system is given an idealized pattern and alters markedly in intensity, and to some extent also in form and sign, with the time. This then is the current system (and its parts) derived from consideration of the average fields of storms, and which we seek to compare with corresponding systems appropriate to individual hours of storm. We will first consider the characteristics of the mean hourly disturbance field of polar regions for various selected hours of disturbance.

3. The polar field of magnetic storms.--The storms of October 14 and December 14, 1932, and of April 30 and August 5, 1933, were selected for study, being four of the most intense storms of the Polar Year, 1932-33--a year near the sunspot minimum. These do not include an example of a very great magnetic storm.

Mean hourly disturbance vectors were derived for about 30 hours of each storm, for about 25 stations in magnetic latitudes north of 65°. At a few stations, data for the whole or part of the storm were sometimes missing for various reasons, one important reason being the use of instruments not sufficiently insensitive. The disturbance was measured as the departure from the mean of an international quiet day near the day of storm. The quiet days used were (where possible) those of October 14 and December 12, 1932, and May 12 and August 1, 1933, the same for all stations. The disturbance vectors were derived from published or other tables of mean hourly values of magnetic force or, in a few cases, from microfilm reproductions of magnetograms. It is thought that inaccuracies of measurement seldom exceeded 25γ for the polar stations of the Union of Soviet Socialist Republics and Jan Mayen for which the microfilms were used.

The disturbance vectors so derived were plotted on maps of the north polar regions, for each of the 30 hours of each storm. Of these, a number have been selected for reproduction here; those for the storm of April 30 and May 1, 1933, and others thought to be fairly typical for the remaining three storms (or of special interest) were selected.

Figures 228 and 229 show the geographical distribution of the disturbance vectors at polar stations in relation to the position of the Sun. Geomagnetic co-ordinates of position are used and the dotted curve represents the average position of the auroral zone as estimated from magnetic data for disturbed days of the Polar Year [38]. A and B of Figure 228 are for the hour of maximum of

the initial phase of the storms of October 14, 1932, and April 30, 1933, respectively. For these two special cases, only the disturbance vectors at each station are measured as the departures from the mean hourly values of the force found for the hours ending at 16h and 17h GMT, respectively, just before the commencements of the storms.

The data of A of Figure 228 suggest the presence of D_{st} in the form of electric currents external to the Earth flowing from west to east and nearly symmetrical about the Earth's magnetic axis. There is also a suggestion that there may be a current circulation, anticlockwise as seen from above the Earth, centered somewhat south of the auroral zone and near a magnetic longitude of 270° E. It is noteworthy that the disturbance vectors are relatively small and in general very little larger in magnitude in polar than in low latitudes.

B of Figure 228, drawn for the maximum of the initial phase of the storm of April 30, 1933, shows markedly different characteristics from those of A, in high latitudes. A possible explanation may be that a considerable amount of irregular disturbance has appeared in polar regions in the case of B (note the change in the scale of force). In lower latitudes, as in the case of A, there is some evidence of a symmetrical storm-time part consisting of a current flowing from west to east.

C to F of Figure 228 and A to F of Figure 229 relate to the main phase of magnetic storms. The appropriate scale of force is given at the bottom of the page, except in certain cases where it is shown on the particular map to which it refers.

For the main phase of each storm, the changes with time in the polar disturbance field depend in a marked way upon the position of the Sun. This is very clearly in evidence near the center of the auroral zone where the horizontal component of disturbance is relatively large and persistent and in a direction tending to be nearly perpendicular to the meridian plane including the Sun. Near the auroral zone, the disturbance is most intense and highly differentiated locally. The polar disturbance field inside the auroral zone usually, and perhaps always, consists of two areas in which the vertical components are opposite in sense. This is in good agreement with the previous findings of Birkeland, but the intense horizontal disturbance near the center of the auroral zone is different from the characteristics ascribed by him to this region on the basis of his more scanty data.

Progressing southwards from the center of the auroral zone, the north component tends to reverse in sign near the center of the region between the pole and the auroral zone, attains a marked maximum change near the auroral zone, and again reverses sign just outside the auroral zone.

The eastward component of the horizontal force inside the auroral zone tends to be large and positive near local noon, large and negative in the evening, and reverses near the auroral zone, becoming relatively small in lower latitudes.

The vertical component tends to be relatively small near the center of the auroral zone. With decreasing latitude, it attains a considerable magnitude just inside the auroral zone and reverses sign near the zone. It again becomes large and opposite in sense just outside the auroral zone, after which it rapidly decreases in magnitude. The disturbance in the vertical component is largest for times near local dawn and evening, and smallest near noon and midnight.

The polar disturbance field for individual hours of storm shows distinct evidence of important systematic changes with time. In general, these closely resemble those found from the average characteristics of the field, although there may be considerable variability from hour to hour during an individual storm.

There is also evidence to suggest the presence of important seasonal change in the character of the polar disturbance field. For the storm of December 15, 1932, there is very little indication of eastward-flowing electric currents along and above the auroral zone, although those flowing westward apparently attain considerable intensities. It appears probable that near the times of equinox and summer the eastward currents are more nearly comparable in magnitude with the westward currents, though perhaps always weaker in magnitude.

E of Figure 228 shows that the storm-field may appear relatively simple when the disturbance shows its maximum general development in intensity.

The disturbances recorded at stations near the auroral zone are particularly complicated because of the rotation and lateral displacement with time of a highly differentiated disturbance field. It may also be mentioned that rapid, oscillatory changes in the force are most marked in this region, perhaps especially during the early morning hours.

4. The electric current systems for individual hours of storm.--Whatever the form of the disturbance field at the Earth's surface, this field could be reproduced by electric currents flowing as a thin, nearly spherical current sheet within the atmosphere. Even if this current system does not closely resemble the actual one, it affords a simple means of representation of the observed features of storms. It can also be used to derive the real current system, if this should be of a different type, with the aid of sufficient additional information concerning other nonmagnetic considerations.

The atmospheric-electric current systems flowing in a spherical shell at a given height can be derived from the observed surface field of disturbance, using the methods of general potential theory. These methods require a knowledge of the magnetic potential (or field) of the currents for points everywhere on the Earth, but may give satisfactory results provided sufficient accuracy is attainable by interpolation of values between points at which the field is measured. It would obviously be difficult to effect a formal interpolation of the data of Figures 228 and 229. It therefore appears useful to estimate the form and intensity of the current systems approximately at first, using speedy but simple methods similar to those used previously by Chapman and Vestine [37]. These methods involve a knowledge of the fields due to simple model current systems, and the assumption that the current circuits are closed in the atmosphere. Before making such estimates, it is desirable to obtain a rough indication of the magnitude of that part of the observed surface field which is of external origin, and we will now consider correction of the data for induced earth currents.

The corrections here applied are rough and only tentative. We have seen that the main systematic features of the polar disturbance field of storms just discussed show considerable resemblance to those deduced from average characteristics. It thus appears likely that corrections for induced currents estimated for the average field may afford a rough but useful approximation to those required in the case of mean hourly disturbance during storms. The effects of induced currents are

likely, in general, to augment the horizontal components and decrease the vertical components of origin external to the Earth. A study of this kind gave a rough approximation for the required correction, in the case of the average polar characteristics of storms, using considerations of general potential theory. In this analysis, the polar cap of the Earth was supposed plane. This study suggested that the observed horizontal components should be multiplied by factors estimated to be roughly 0.9 near the center of the auroral zone, 0.7 near the boundary of the zone, and decreasing to about 0.6 outside the zone, in obtaining the contribution of external origin. Corresponding ratios were adopted for the vertical components, the corrections in these cases resulting in increasing the observed magnitudes. These values were then interpolated linearly with distance, measured from the center of the auroral zone, and applied to the mean hourly disturbance vectors of storms. The number of stations used for Figures 228 and 229 was increased to 45 by the addition of data for low latitudes.

Figures 230 to 235 show to scale the disturbance vectors and their geomagnetic distribution after applying the foregoing rough corrections for induced currents. The representation is for the Northern Hemisphere as viewed from directly above the geomagnetic north pole. The disturbance vectors for stations in low latitudes of the Southern Hemisphere have been assumed approximately the same as for stations in the same geomagnetic latitude and longitude in the Northern Hemisphere, except for reversal of direction in the eastward and vertical geomagnetic components of force. Except in A of Figure 230, the scale of force is five times as open in lower latitudes (stations south of a magnetic latitude Φ = 60°) as in polar regions. The average position of the auroral zone estimated from magnetic data for international disturbed days of the Polar Year, 1932-33, is shown by a broken line [38]. The approximate direction to the Sun is indicated by an arrow drawn outwards (vertically downwards in the diagrams) from the geomagnetic north pole. The disturbance vectors at stations south of Φ = 55° have been corrected for the quiet-day daily variation given by the mean of the five international quiet days of the month.

Also shown in the figures are the corresponding electric current systems estimated from the data. The estimates of current above the neighborhood of a station were made by approximate methods. For instance, near station 38 of A of Figure 230, the field is nearly uniform and could be caused by electric currents flowing approximately from west to east above the Earth. The field in this region will be less affected by currents flowing at greater distances from the station than by currents immediately above the station. The field near the station resembles fairly closely that of a complete spherical current sheet, in which the current varies only as the cosine of the latitude. Using simple graphs giving the distance between successive current lines for a flow of 10,000 amperes, in terms of the observed horizontal component of force, we obtain approximate estimates of the current near an individual station.

In regions where the current flow extends over shorter distances without abrupt change in direction, estimates were obtained using the known fields of infinite uniform plane current sheets or uniform ribbon currents. In general, there was good qualitative agreement between the currents derived from the horizontal components and the observed signs and magnitudes of the vertical components.

The spacings between successive current lines and directions of flow were estimated for a restricted region above each station in turn. The current lines were then connected and shifted slightly, where necessary, so that the current circuits were closed. In regions where data were not available, the spacing of the current lines is of course uncertain and some liberties have been taken in drawing such lines; in certain cases it was supposed that some degree of symmetry was required relative to current lines more accurately determined for adjacent regions, subject to the condition of continuity of current flow.

In the foregoing manner there was estimated to be a total of 130,000 amperes in the large circuit involving anticlockwise flow of current, and about 15,000 amperes in the small opposed equatorial current circulation. So far as the writer is aware, this procedure, though simple, has not previously been applied in the study of the initial and main phase of individual magnetic storms.

A of Figure 230 shows the current system estimated for the maximum of the initial phase of the storm with sudden commencement at 17h 47m, October 14, 1932. A total of 10,000 amperes flows between the successive current lines. The disturbance in polar regions is of the same order of magnitude as in lower latitudes. The currents from the equator and northwards circulate from west to east about a center slightly south of Fort Rae. Except in the region north of Fort Rae, there has been an initial increase in the northward component of force--a well-known characteristic of the initial phase of magnetic storms.

There are striking differences between the current system in A of Figure 230 for the initial phase and the current system in A of Figure 227 for the main phase of storms. If A of Figure 230 be analyzed into its symmetrical (D_{st}) and antisymmetrical (S_D) parts, the storm-time currents in low latitudes would flow from west to east instead of from east to west as in the main phase. The S_D-part would resemble that of C of Figure 227 in general type, but the polar circuits would be much weaker relative to the lower-latitude circuits than for the case of the main phase. In the present case, there is also some possibility that the S_D- and D_{st}-parts in lower latitudes are somewhat distorted due to incomplete removal of the effect of the quiet-day daily variation, since the magnitude of the disturbance is relatively small.

B of Figure 230 shows the current system derived for the maximum of the initial phase for the storm with sudden commencement at 16h 27m, April 30, 1933. In low latitudes the characteristics show considerable resemblance in general type with A of Figure 230, though of greater intensity. In polar regions, for which the disturbance vectors are here drawn to a scale one-fifth as open as for lower latitudes, there is marked disturbance in the region near and within the auroral zone. However, there appears to be some possibility that a considerable part of the polar disturbance, as well as that in lower latitudes, was occasioned by the superposition of the field of a magnetic bay upon the general storm-field. The intensity of the polar current circulation was estimated on the basis of approximate methods used previously by Vestine and Chapman [37], on the assumption that the current circuits are completed in the atmosphere.

A of Figure 231, for the main phase of storms, has been included because of the rather special features shown. In this case, the disturbance near the center of

the auroral zone is more marked than elsewhere. During the 17-hour interval following the commencement time for B of Figure 230, there was but little magnetic disturbance in polar regions. The disturbance at stations one and two gradually increased for several hours to attain a maximum value (for station one) at 11h, May 1, as shown in A of Figure 231. This characteristic was not found in the other three storms studied, and the marked disturbance in the vertical component appears a matter of particular interest. In the storm of May 1, it was first clearly present at 7h, increased to maximum intensity near 11h, after which a transition to conditions at 14h (B of Figure 231) gradually took place. There appears to be evidence for a relatively intense current circulation near the center of the auroral zone, but there are insufficient data to trace out the form of current flow with much degree of certainty.

In lower latitudes, it would appear that the variation D_{st} is produced by current circulations weaker than those for S_D (A of Figure 231), and the situation thus is different from the case of A of Figure 227, where the opposite tendency is shown. We shall later discuss the fact that A of Figure 227 appears to correspond more closely with conditions operative near the maximum of the main phase of storms; in the present storm the maximum appears about six hours later.

In B of Figure 231, the field-changes appear more intense than in the case of A. The current sheet flowing across the polar cap tending in a direction towards the Sun, if nearly uniform, is estimated to have an intensity of 1,900,000 amperes. This estimate was found to agree fairly well also with independent estimates of the intense currents returning along the auroral zone, on the basis of the approximation of an infinite linear auroral zone current for stations some distance outside the zone, or on the assumption of an infinite plane ribbon current for stations very near or at the zone.

In low latitudes, the currents are somewhat symmetrically arranged relative to the Sun, and the current density is less on the morning than on the evening side of the Earth.

In the sequence B of Figure 231 to A of Figure 234, the main phase of the storm is well developed, attaining its maximum intensity near 16h, May 1, when a total of 2,000,000 amperes flows in the interzonal sheet current across the polar cap of the Earth. The estimates of the width in latitude of the auroral zone currents, made on a ribbon current hypothesis, are very rough and only tentative.

A of Figure 234 shows the storm-field considerably reduced in intensity and the eastward flow of current appears relatively much weaker than the westward flow along the zone. In this storm it would thus appear that D_{st} is relatively greater in intensity with respect to S_D during the phase of recovery than during the maximum of the main phase.

B of Figure 234, and A and B of Figure 235, for the main phase of other storms, show characteristics similar in general type to those for the storm of May 1, 1933. In the case of the storm of December 15, 1932, the only hour of the storm in which evidence was found of eastward flowing currents along the auroral zone was on December 15, shown in A of Figure 235. This may result from a seasonal effect and suggests that D_{st} is relatively more intense with respect to S_D in winter than it is in summer.

The current systems derived for the main phase of storms show good general agreement in type with A of Figure 227, proposed by Chapman, apart from differences in intensity. There are a few minor differences apparent in the current systems here derived for the case of the real Earth. In most cases, the polar current system as seen from above shows a greater amount of clockwise rotation relative to the position of the Sun than in the case of A of Figure 227. In their expansion with increasing intensity of storm, the auroral zone currents seem also to show considerable symmetry relative to the average position of the auroral zone, which in the case of the real Earth is of course not circular.

A and B of Figure 236 show the results of analyzing A of Figure 232 into its symmetrical (D_{st}) and antisymmetrical (S_D) parts. This separation was effected by averaging the current in A of Figure 232 along parallels of latitude; in the case of the polar part the intensity of the current was averaged along the path of the auroral zone current. The magnitude of the symmetrical part within the auroral zone could not be estimated with accuracy, due to the scanty magnetic data, but the indications clearly suggest that the storm-time currents in this region are relatively much smaller than in B of Figure 227.

The following table gives a comparison of the results of Figure 236 with those found by Chapman for the average of 40 storms, given in Figure 227. Thus, by multiplying the estimates given by Chapman by about four, we obtain rather good agreement with the corresponding current estimates found here for the currents during an individual hour of storm. This suggests that the magnetic storm of May 1, 1933, was about four times as intense as the average of the 40 magnetic storms considered by Chapman. Chapman also estimates that the great magnetic storm of May 15, 1921, was about 15 times as intense as the average for the 40 magnetic storms [64]; this great magnetic storm was therefore probably associated with electric currents (if flowing in the same region above the Earth) about four times as intense as those for the magnetic storm of May 1, 1933.

Comparison of current-intensities in amperes for 16h, May 1, 1933 (A), with corresponding values averaged for 40 storms (B)

Region	D_{st}	
	(A)	(B)
Lower latitudes	700,000	200,000
High latitudes (auroral zone)	300,000	75,000

Region	S_D			
	(A)		(B)	
	Morning	Evening	Morning	Evening
Lower latitudes	250,000	200,000	50,000	50,000
High latitudes (auroral zone)	1,000,000	1,000,000	275,000	275,000

Figure 237 shows the result of an analysis for the initial phase of the storm of October 14, 1932. In the

case of both D_{st} and S_D, the electric currents estimated are much weaker than those for the main phase, as can be seen from an inspection of B of Figure 235 for the same storm. The most interesting feature is that the polar part of the S_D current system, as it appears in the main phase, seems to be missing, the parts ordinarily flowing in lower latitudes apparently extending directly over the polar cap. The symmetrical part also flows in the opposite direction to that for the main phase.

5. Electric current system of magnetic bays.--With the use of three-hour disturbance vectors from data of the Polar Year, 1932-33 [29], an estimate of the average electric current system of bays was attempted. This current system is shown plotted for 00h GMT in Figure 238, as derived using the method due to Chapman [64]. The average horizontal disturbance at each station is indicated by an arrow drawn from the station as origin; the vertical component is indicated by a line with bar--positive when in the direction of the geomagnetic north pole. It was assumed tentatively that a correction given by 0.6 times the observed horizontal disturbance removed the influence of induced earth currents. A correction was also applied to obtain the corresponding increase in the vertical component. The vectors preceding and following the average vector for 00h GMT by intervals of three hours were also plotted by rotating position of the station through a roughly approximate angular displacement about the geomagnetic axis. With the use of small current-system models and with the current assumed to flow on the surface of a spherical shell 150 km above the Earth, the approximate current system of Figure 238 was obtained. A total of 50,000 amperes flows between successive current lines in the figure.

The interzonal current sheet flowing across the polar cap has an intensity of 600,000 amperes which divides so that 100,000 amperes flows eastward along the auroral zone and 500,000 amperes westward in this closed polar current circuit. The currents flowing along the auroral zone are augmented by additional contributions from the two low-latitude current circulations so that in the most concentrated portions about 150,000 amperes flow eastward and about 600,000 amperes westward.

The current system resembles that of the diurnally varying part of the S_D current system of magnetic storms. The storm-time part of the current system of storms is in evidence, as indicated by the greater intensity of westward than eastward flowing electric currents along the auroral zone. The current system remains fixed in average position relative to the Sun, the Earth rotating inside. Consequently, a point on the Earth's surface will experience a varying magnetic field corresponding somewhat to its proximity to the more concentrated portions of the current circulation. In view of the fact that the current system here represented for the time of maximum of bays does not usually endure for more than one to five hours, the effect of the Earth's rotation may be a secondary factor determining the course of a bay.

The greater number of negative bays as compared with positive bays selected in auroral regions can be attributed to the greater current intensity of the westward current as compared with the eastward currents flowing along the auroral zone; the number of positive and negative bays should be the same but because of the selection rules adopted, which reject bays below a certain amplitude, the observed disparity results. In low and middle latitudes, a total of 250,000 amperes flows in the more intense circulation and 200,000 amperes in the less intense circulation. Hence in these latitudes, since the eastward currents are stronger than are the westward currents, the selected positive bays are more numerous than are the negative bays. In the region near the center of the auroral zone, as shown by Thule, it is clear that little dependence in frequency on local time would appear. These findings are in good general agreement with observation. In another study of the current systems of several individual bays, the results showed good general agreement with the average current system derived here, though there was marked seasonal distortion in polar regions.

6. Association of magnetic disturbance with ionospheric phenomena and cosmic rays.--A rather direct association of magnetic bays with marked ionospheric absorption in auroral regions has been found by Wells [67] for College, Alaska, an association suggested by previous observations at Tromsö in 1932-33, studied by Appleton [68]. It was found by Wells that during each of 69 significant bays, there occurred high absorption which produced partial to complete radio blackouts (Figure 239), limited in time to the duration of the bay. However, it was noted that radio blackouts could appear also in the absence of a bay.

The absorption effect is explained as due to intense ionization below the E-layer, caused by corpuscular radiation from the Sun.

Another pronounced effect is the rapid increase in height of the maximum electron concentration of the F-layer during the main (intense) phase of great magnetic storms [69]. After an hour or so, the F-layer, which may have attained heights as much as 1000 km, returns to its more customary level of about 300 km. It is not yet clear how this effect should be interpreted. There is certainly migration and redistribution of electrons within the outer atmosphere, when there are present strong electric currents which produce the main phase of storms.

In Chapter V we noted a purely sinusoidal part of the annual variation which arises as a disturbance feature. This sinusoidal variation has its counterpart in F2-region ionization [70] and in average cosmic-ray intensity [71]. The amplitude of the sinusoidal variation appears symmetrical about the geomagnetic equator and approximately in phase for the geomagnetic, ionospheric, and cosmic-ray changes, though the phase reverses on either side of the equator. These effects are not understood, but in view of a recent finding by Forbush [72] of an increase in cosmic-ray intensity preceding storms, it would be interesting to attempt an explanation on the basis of seasonal variation in high-energy radiation accompanied by ionization of the atmosphere.

Figure 240 shows three marked increases in cosmic rays during February and March, 1942, and July, 1946. These Forbush found beginning nearly simultaneously with solar flares or radio fade-outs. The effect was noted in high and middle latitudes, but not at the equator where the cosmic rays may have had insufficient energy to penetrate to ground level in the presence of the geomagnetic field. This important observation has been interpreted as suggesting that charged particles of very high energy may have been emitted from the Sun to produce increases in cosmic-ray intensity, with simultaneous emission of ultraviolet radiation yielding an augmentation of the solar magnetic daily variation. During the main phase of great magnetic storms, there are sometimes

noted less marked decreases in cosmic-ray intensity [36,71,72], an effect likewise not yet understood, though it has been suggested that an equatorial ring current at a distance of a few earth-radii might cause cosmic rays to deviate from their customary statistical distribution in latitude. It is of interest to note that the charged particles of energies suitable for exciting auroral lines appear in lower latitudes at times of great magnetic storms as shown by the well-known expansion equatorwards of the auroral zone [3].

7. Solar radiation responsible for magnetic disturbance and allied phenomena.--The nature of the charged particles from the Sun which cause magnetic disturbances has not yet been established, but it has been shown by Chapman and Ferraro that emission from the Sun in any suitable quantity requires streams or clouds of particles to be nearly neutral electrostatically to a high degree of approximation [3]. Although an outburst of matter from the Sun initially must comprise many kinds of particles, charged and uncharged, the mutual repulsions between particles of like sign will ensure a nearly neutral stream aggregation after traversal over the great distance to the Earth. It is likewise natural to expect that these emitted particles will vary in energy, so that it may even be possible that the components of a neutral stream may be different in early phases of a storm as compared with later phases. Thus an initial part of a stream reaching the neighborhood of the Earth might sometimes consist of protons and electrons, and a later part mainly of ions, electrons, and neutral particles. However, initial increase of cosmic-ray intensity, in the special cases noted by Forbush, need not be attributed to neutral aggregations, since the energy of such particles is exceedingly high, and they might hence proceed in too narrow a beam to account for the effects observed.

It may be that the ring configuration near the geomagnetic pole at 11h, May 1, 1933, shown in A of Figure 231, is evidence for neutral stream constituents of protons and electrons, since the radius of the area in which currents appear is only a few degrees of latitude. This is unfortunately the only instance found throughout the Polar Year, 1932-33, in the records for Thule near the geomagnetic pole. Since the auroral zone is usually about 20°-23° in radius, this may indicate that electrons and ions are the preponderant constituents of the solar streams that cause disturbance.

8. Statistical fluctuations in stream density.--A feature to which it seems that insufficient attention has yet been drawn is that of the probable linear extent in space of clouds of particles comprising a solar stream. Although the average variations of magnetic field taken for many storms yields a function varying rather smoothly with time, the most predominant features are the large and numerous statistical departures from this average, especially in higher latitudes.

It was previously noted (Chapter IX) that the great majority of short-period fluctuations endure for about 50 seconds. If we then assume approximately one day to be the travel time from Sun to Earth, as suggested by studies of sunspots and storms, the velocity of the particles will be about 10^8 centimeter per second. A particular cloud hence may have a linear extent, measured along the average stream lines, of 5×10^9 cm (50,000 km), or about four earth-diameters. The cross-section of such a cloud, at some considerable distance from the Earth, cannot be inferred from existing data. Figures 206 to 209 of Chapter IX suggest the arrival of particles in patches in auroral regions under the guiding influence of the geomagnetic field [29,48]. They may introduce ionization and hence increased electric conductivity within these areas of penetration, which, in the presense of electromotive driving forces, yields intensification of current flow locally, with completion of the circuit on a world-wide scale.

The rather strong preference for durations of about 50 seconds is truly remarkable. A preferred linear extent of about 50,000 km for an incoming cloud requires explanation. It would be interesting to search for solar phenomena predominantly of 50 seconds' duration, near active energetic sunspot groups, and likewise in terrestrial aurora.

Gartlein [73] has recorded fluctuations of about 50 seconds' duration in photoelectric recordings of auroral intensity, which might be explained by cloud distributions. However, the particles causing auroral fluctuations need not necessarily penetrate the atmosphere to levels in which the magnetic fluctuations are generated, and this explains the lack of detailed correspondence between magnetic and auroral fluctuations.

Wells, Watts, and George [57] have recently detected effects of incoming aggregations of particles or clouds having ionization-densities of 2 to 4×10^5 electrons per cc with the aid of high-speed multifrequency ionospheric recorders. These observations were made during the magnetic storm of March 25-27, 1946, near Washington, D.C., and hence in middle latitudes. (See A and B of Figure 241.) The principal effects of influx of clouds were: (1) sudden changes in F-layer ionization; (2) rapid changes in F-layer heights, indicating turbulence which is often progressive from great to low heights and from high to low frequencies; (3) rapid fluctuations of echoes at the lower frequencies with occasional temporary disappearance indicating high absorption.

Paralleling the case of aurora, where greatest brightness is apt to be found at the lower limit of visible auroral rays, there seems to be most intense ionization formed by incoming cloud particles at the lowest level of penetration. The particles seem to penetrate to F2- and F1-layers during strong disturbance, but there was little evidence found for penetration to the E-layer or below.

On the basis of Störmer's calculations for aurora, the colatitude α of particles arriving singly is given by $\sin \alpha = (2a/\ell)^{1/2}$, where a is the distance to the Earth's center, and $\ell^2 = eM/mv$; here e is the electronic charge of either sign, M the magnetic moment of the Earth, m the mass of the particle, and v its velocity.

For the present observations, $\alpha = 40°$, roughly, so that ℓ becomes about 3×10^9 CGS. Since e/m for electrons, protons, and calcium atoms is, respectively, 1.8×10^7, 9.6×10^3, and 2.4×10^2, the value 3×10^9 for ℓ would presuppose very high velocities for these incoming particles, well in excess of 10^8 cm/sec required to give a travel time of about one day from Sun to Earth. Hence, these particles with shallow penetration, which seem to be charged, since they may arrive either by night or by day, are likely to arrive near the Earth in neutral streams. Their apparent terminus of path after traversing only a small air-equivalent of path [3], if they arrive at vertical incidence, is compatible with velocities more nearly of the order of 10^8 cm/sec or less. If we interpret the increase in ionization near the terminus of path as an indication of size of particles, the particles contributing most effectly to the observed effects are more likely to be ions or protons rather than electrons.

9. Rocket experiments.--Many of the outstanding uncertainties with respect to magnetic storms and their associated phenomena seem likely to be removed in future years by means of direct measurements within the upper atmosphere. Thus we might expect cloud-chamber and other experiments on rocket flights to give indication of the nature of corpuscular and wave-radiation from the Sun. There will no doubt also be radio-pulse observations at great heights yielding information on structure of the ionized regions within and beyond the atmosphere. Since the current sheets of the electric current systems of the atmosphere have fields discontinuous in the horizontal component or passing vertically through these current sheets, direct magnetic measurements may be expected to establish their true heights.

FIGURES 227-241

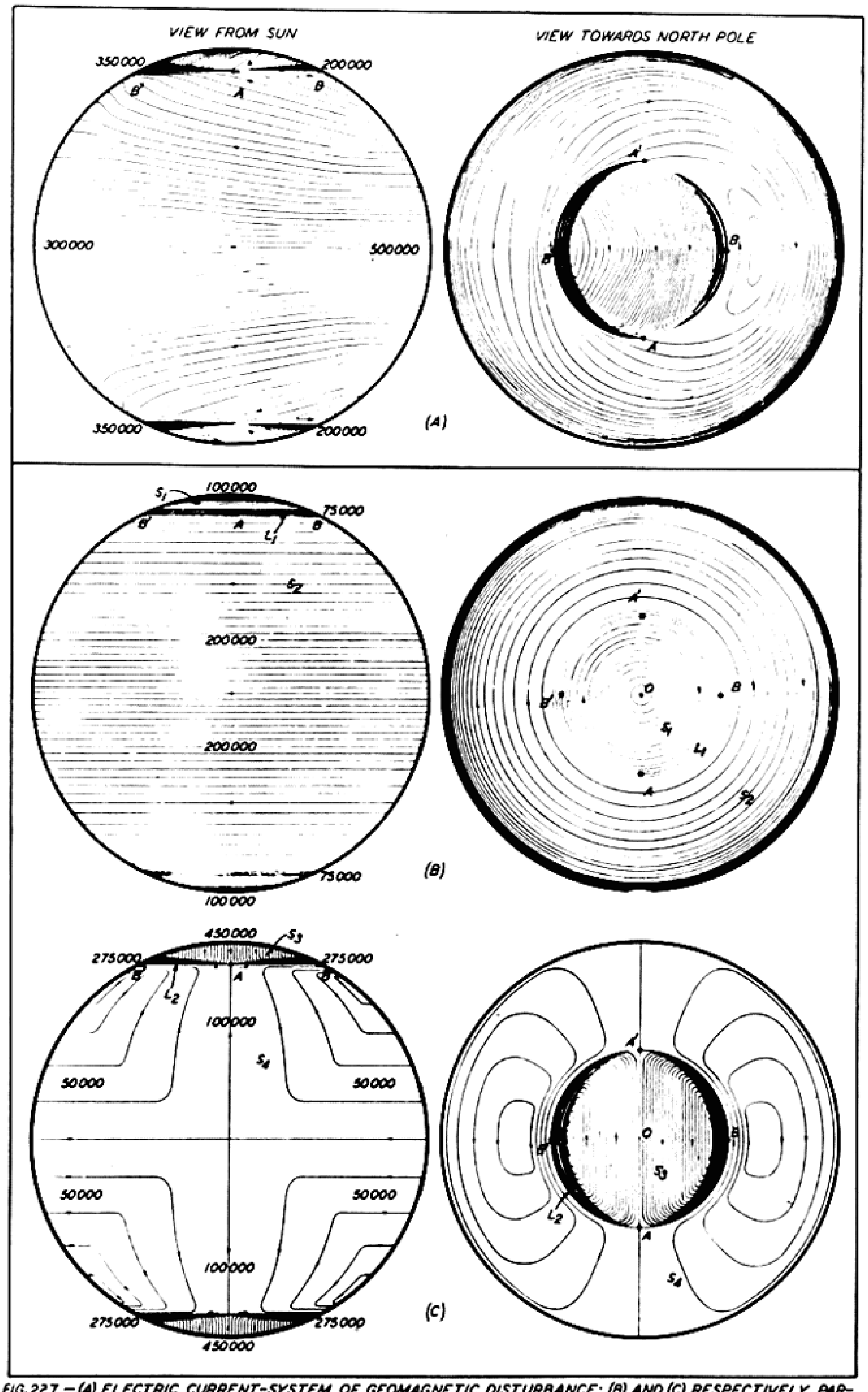

FIG. 227 — (A) ELECTRIC CURRENT-SYSTEM OF GEOMAGNETIC DISTURBANCE; (B) AND (C) RESPECTIVELY, PARTIAL CURRENT-SYSTEMS D_{st} AND S_D COMPRISING (A)

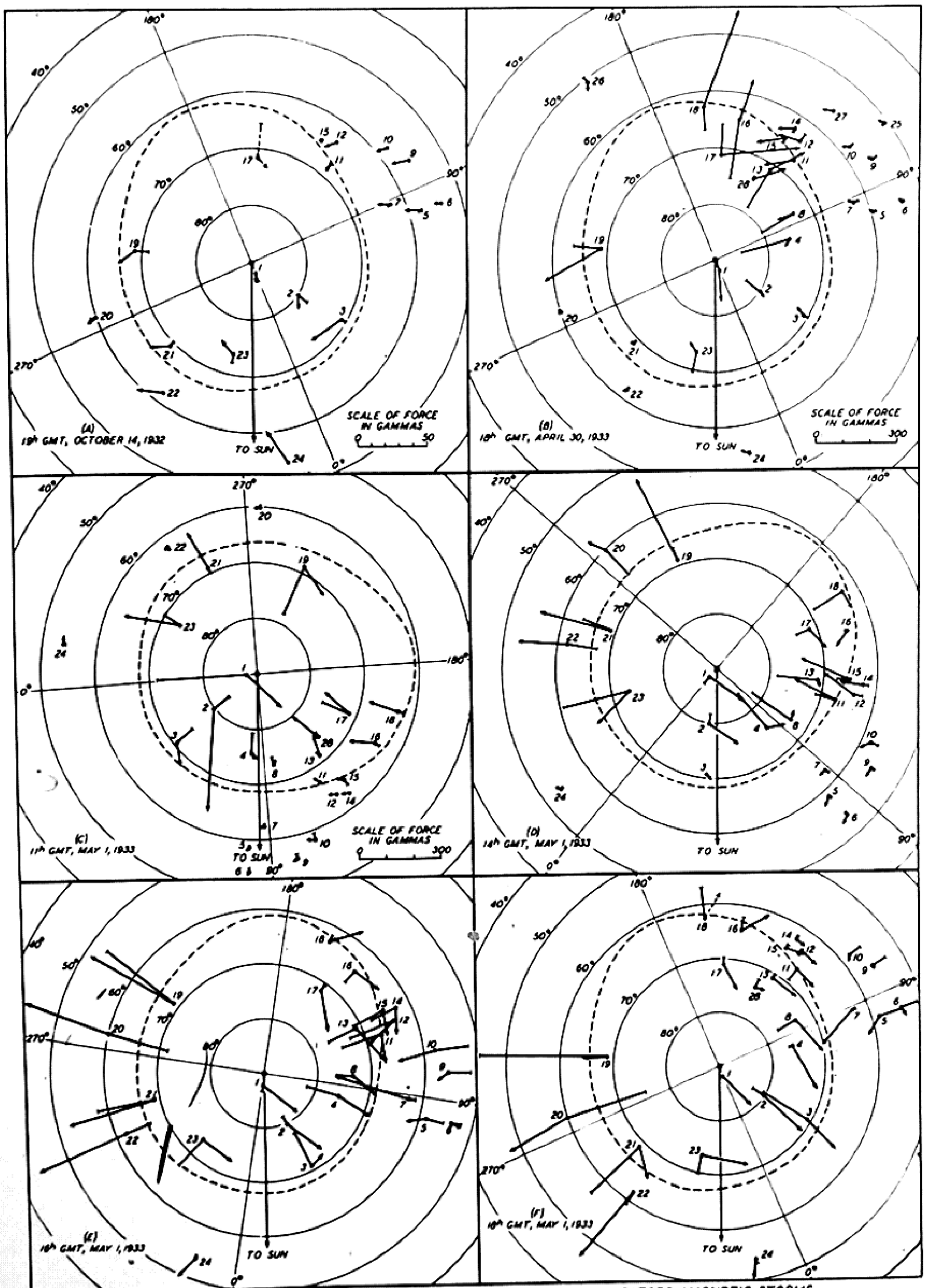

FIG. 228—GEOGRAPHICAL DISTRIBUTIONS OF MEAN HOURLY MAGNETIC VECTORS, MAGNETIC STORMS

LEGEND

HORIZONTAL FORCE ⟶ VERTICAL FORCE —— (VERTICAL COMPONENT POSITIVE WHEN DRAWN OUTWARDS FROM GEOMAGNETIC NORTH POLE)

- - - - - AURORAL-ZONE CURVE

STATIONS

1. THULE
2. GODHAVN
3. JULIANNEHAAB
4. SCORESBY SUND
5. ESKDALEMUIR
6. GREENWICH
7. LERWICK
8. JAN MAYEN
9. RUDE SKOV
10. LOVÖ
11. TROMSÖ
12. SODANKYLÄ
13. BEAR ISLAND
14. KANDALAKSCHA
15. PETSAMO
16. MATOTCHKIN SHAR
17. FRANZ JOSEF LAND
18. DICKSON
19. POINT BARROW
20. SITKA
21. FORT RAE
22. MEANOOK
23. CHESTERFIELD INLET
24. AGINCOURT
25. SWIDER
26. YAKOUTSK
27. SLOUTZK
28. SVEAGRUVAN

SCALE OF FORCE IN GAMMAS FOR 14h, 16h, AND 18h, MAY 1

0 500 1000

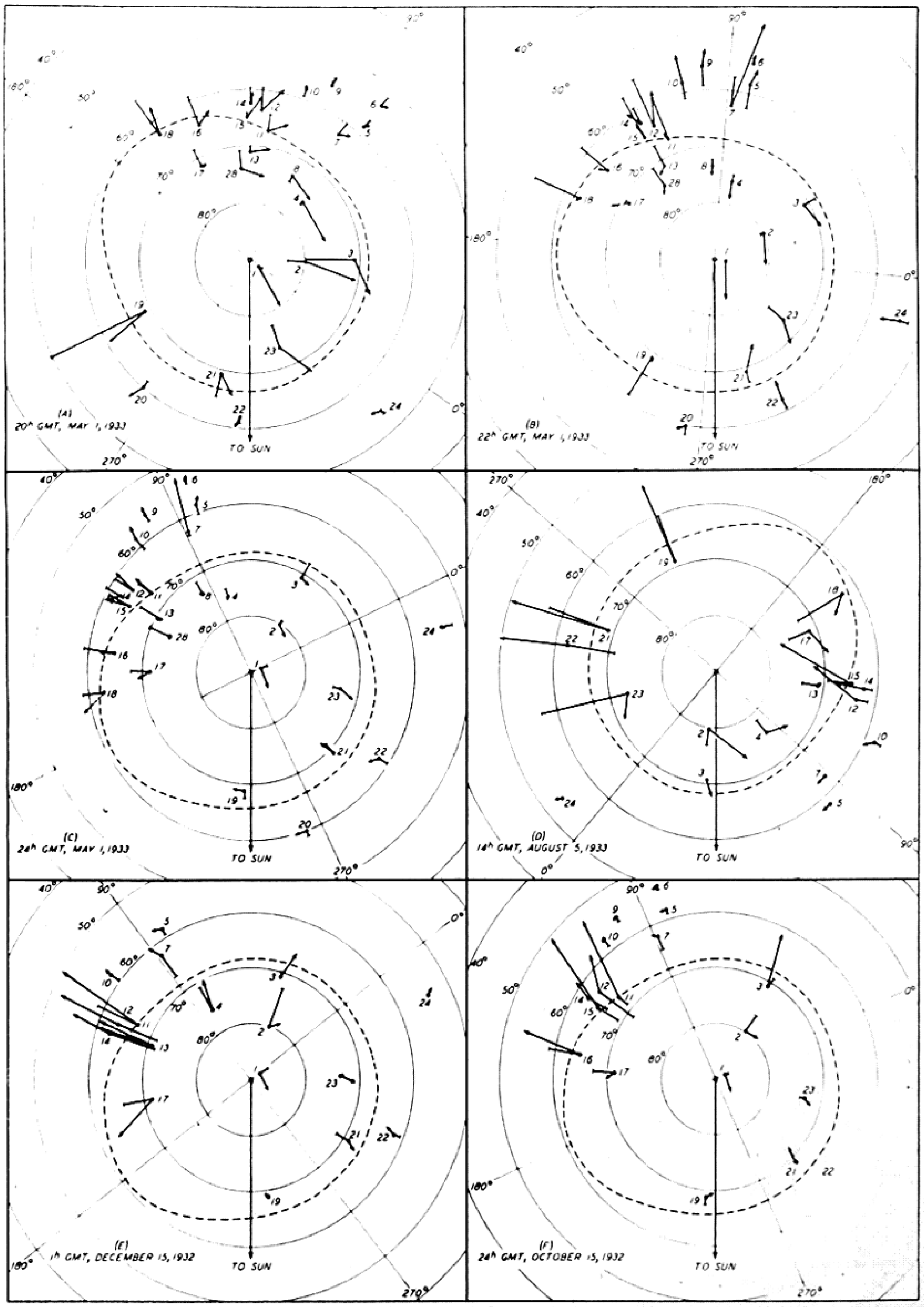

FIG. 229—GEOGRAPHICAL DISTRIBUTIONS OF MEAN HOURLY MAGNETIC VECTORS, MAGNETIC STORMS

LEGEND

HORIZONTAL FORCE ⟶ VERTICAL FORCE —— (VERTICAL COMPONENT POSITIVE WHEN DRAWN OUTWARDS FROM GEOMAGNETIC NORTH POLE)

- - - - - AURORAL-ZONE CURVE

STATIONS

1. THULE
2. GODHAVN
3. JULIANNEHAAB
4. SCORESBY SUND
5. ESKDALEMUIR
6. GREENWICH
7. LERWICK
8. JAN MAYEN
9. RUDE SKOV
10. LOVÖ
11. TROMSÖ
12. SODANKYLÄ
13. BEAR ISLAND
14. KANDALAKSCHA
15. PETSAMO
16. MATOTCHKIN SHAR
17. FRANZ JOSEF LAND
18. DICKSON
19. POINT BARROW
20. SITKA
21. FORT RAE
22. MEANOOK
23. CHESTERFIELD INLET
24. AGINCOURT
25. SWIDER
26. YAKOUTSK
27. SLOUTZK
28. SVEAGRUVAN

SCALE OF FORCE IN GAMMAS

0 500 1000

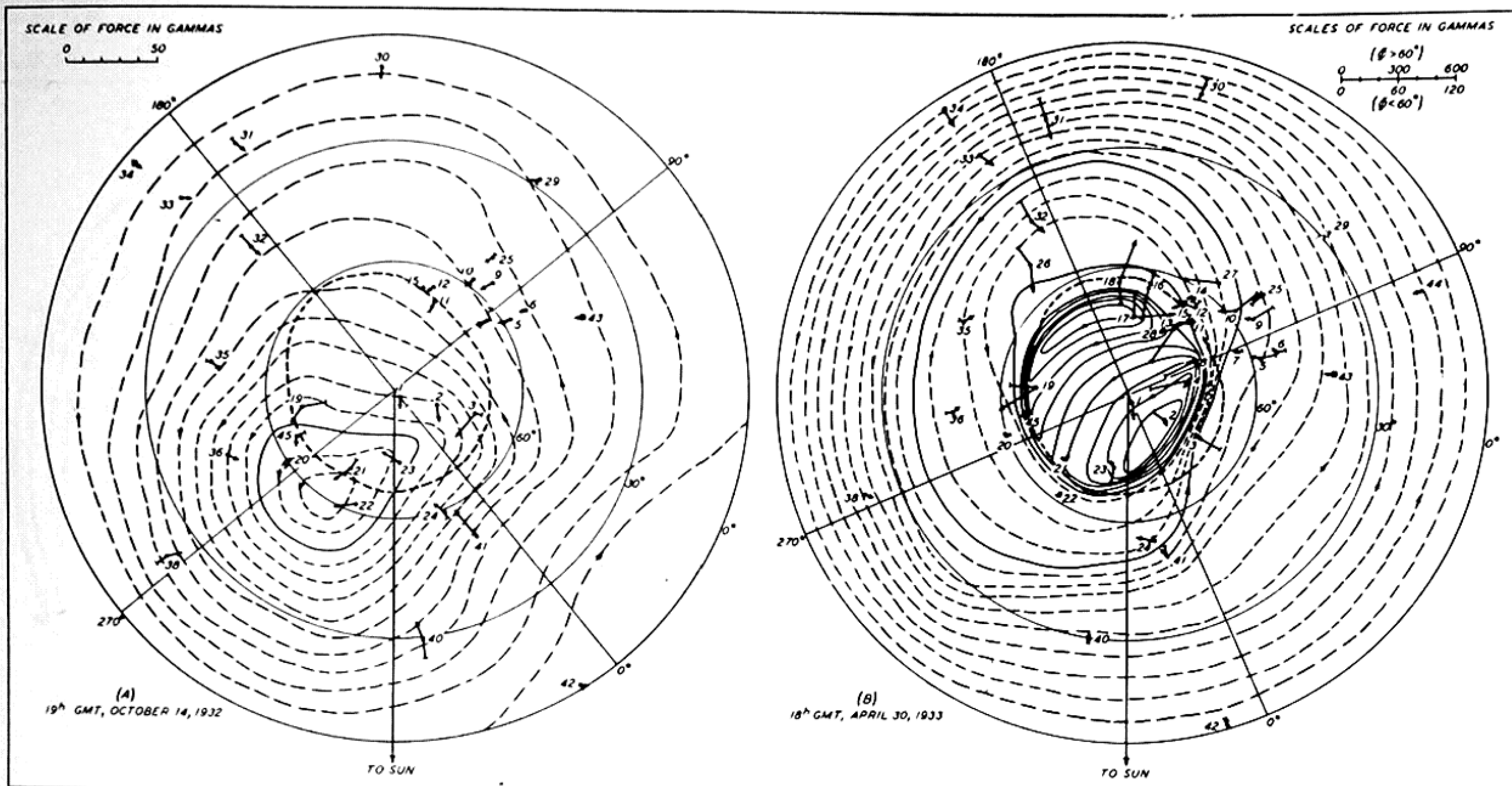

FIG. 230—MEAN HOURLY DISTURBANCE-VECTORS AND CORRESPONDING ELECTRIC CURRENT-SYSTEMS FOR HEIGHT 150 KM FOR MAXIMUM OF INITIAL PHASE OF MAGNETIC STORMS; VIEW FROM ABOVE GEOMAGNETIC NORTH POLE

LEGEND

HORIZONTAL FORCE ——→ VERTICAL FORCE ——— (VERTICAL COMPONENT POSITIVE WHEN DRAWN OUTWARDS FROM GEOMAGNETIC NORTH POLE) AVERAGE AURORAL ZONE — — — STATIONS MISSING DATA •

(100 000 AMPERES FLOWS BETWEEN SUCCESSIVE FULL-DRAWN CURRENT-LINES)

STATIONS

1 THULE
2 GODHAVN
3 JULIANNEHAAB
4 SCORESBY SUND
5 ESKDALEMUIR
6 GREENWICH
7 LERWICK
8 JAN MAYEN
9 RUDE SKOV
10 LOVÖ
11 TROMSÖ
12 SODANKYLÄ
13 BEAR ISLAND
14 KANDALAKSCHA
15 PETSAMO
16 MATOTCHKIN SHAR
17 FRANZ JOSEF LAND
18 DICKSON
19 POINT BARROW
20 SITKA
21 FORT RAE
22 MEANOOK
23 CHESTERFIELD INLET
24 AGINCOURT
25 SWIDER
26 YAKHOUTSK
27 SLOUTZK
28 SVEAGRUVAN
29 HELWAN
30 ALIBAG
31 KUYPER
32 WATHEROO
33 LUKIAPANG
34 ANTIPOLO
35 TOOLANGI
36 CHRISTCHURCH
37 APIA
38 HONOLULU
39 TUCSON
40 TEOLOYUCAN
41 CHELTENHAM
42 HUANCAYO
43 SAN FERNANDO
44 ELIZABETHVILLE
45 COLLEGE FAIRBANKS

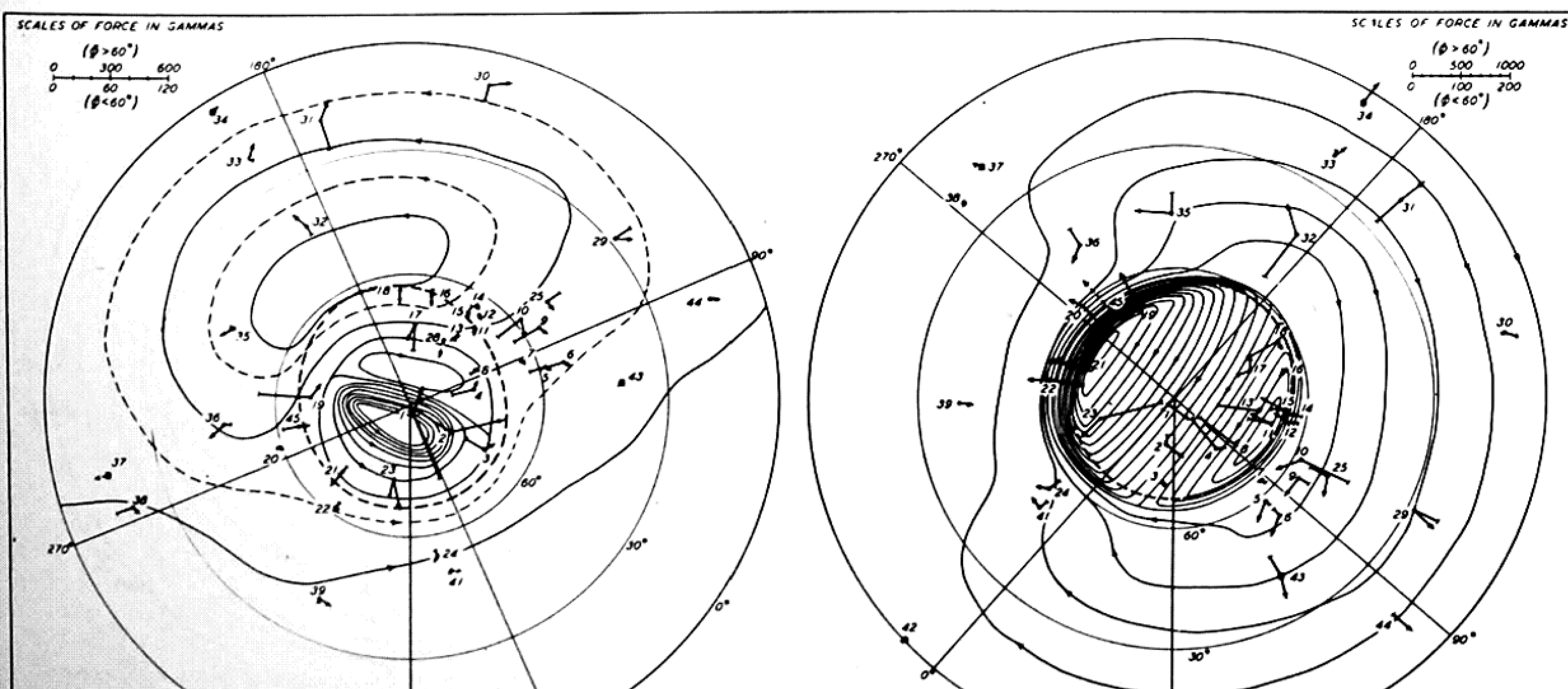

FIG. 231—MEAN HOURLY DISTURBANCE-VECTORS AND CORRESPONDING ELECTRIC CURRENT-SYSTEMS FOR HEIGHT 150 KM FOR MAIN PHASE OF MAGNETIC STORMS; VIEW FROM ABOVE GEOMAGNETIC NORTH POLE (LEGEND AS IN FIGURE 230)

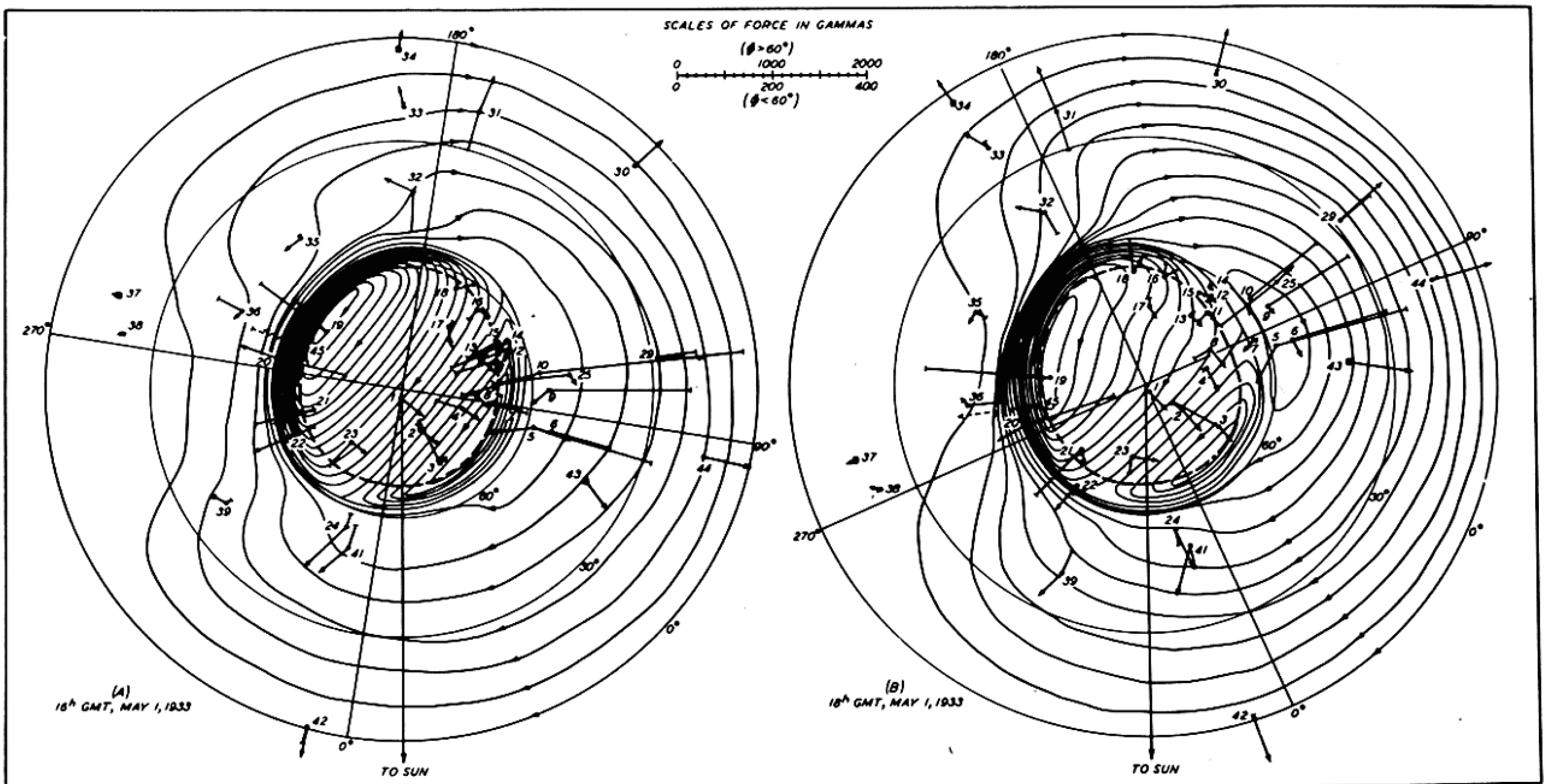

FIG. 232—MEAN HOURLY DISTURBANCE-VECTORS AND CORRESPONDING ELECTRIC CURRENT-SYSTEMS FOR HEIGHT 150 KM FOR MAIN PHASE OF MAGNETIC STORMS; VIEW FROM ABOVE GEOMAGNETIC NORTH POLE (LEGEND AS IN FIGURE 230)

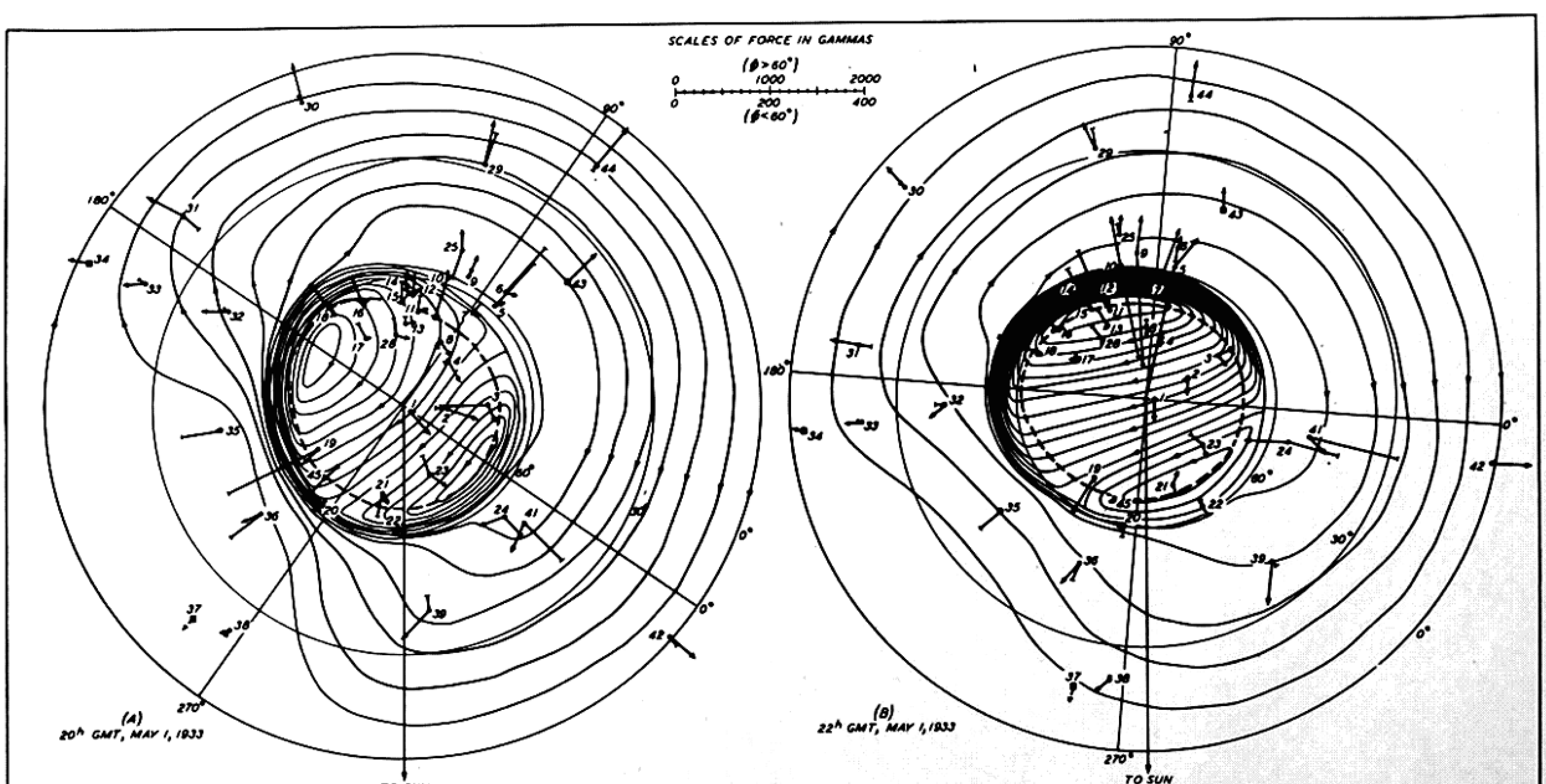

FIG. 233—MEAN HOURLY DISTURBANCE-VECTORS AND CORRESPONDING ELECTRIC CURRENT-SYSTEMS FOR HEIGHT 150 KM FOR MAIN PHASE OF MAGNETIC STORMS; VIEW FROM ABOVE GEOMAGNETIC NORTH POLE (LEGEND AS IN FIGURE 230)

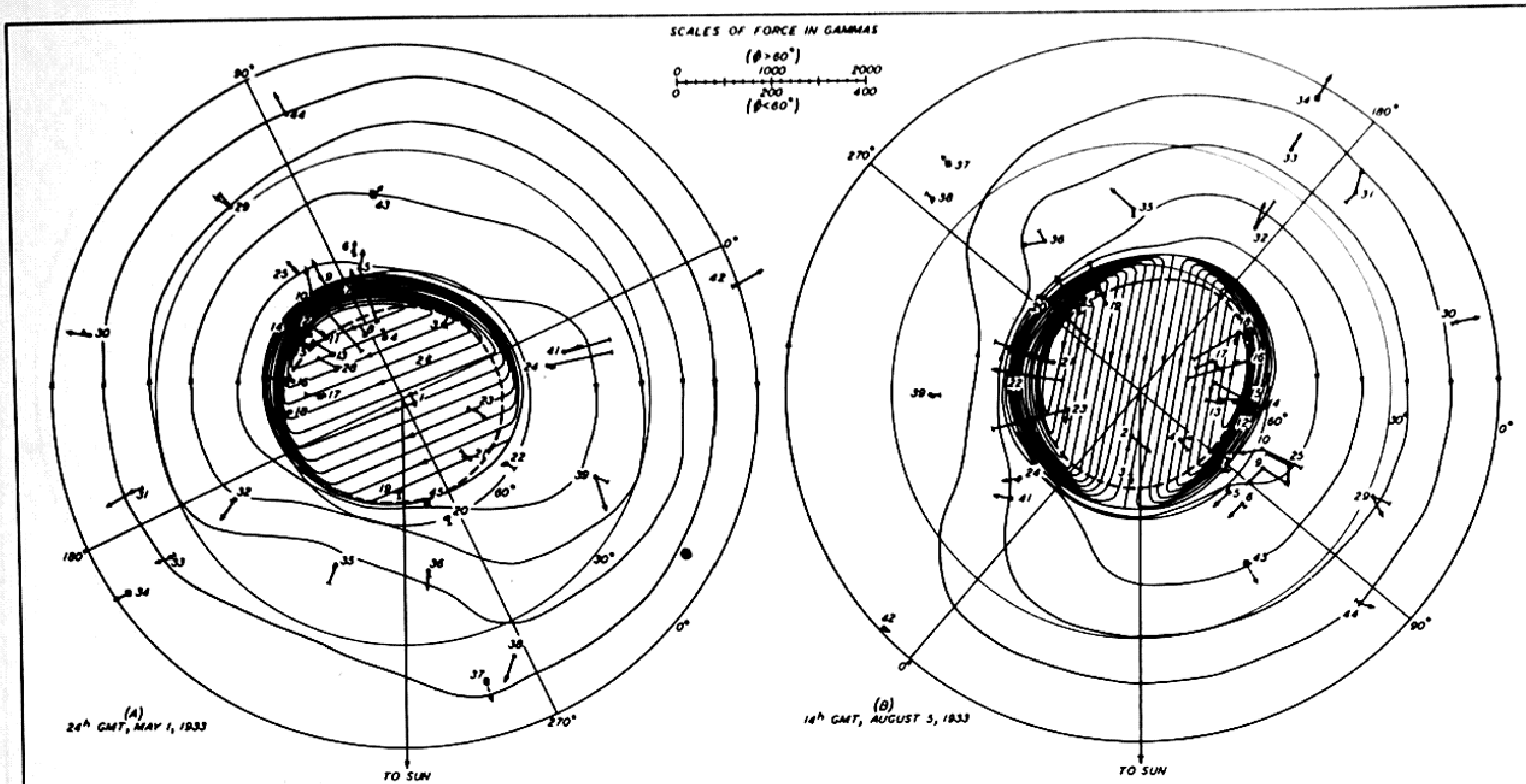

FIG.234—MEAN HOURLY DISTURBANCE-VECTORS AND CORRESPONDING ELECTRIC CURRENT-SYSTEMS FOR HEIGHT 150 KM FOR MAIN PHASE OF MAGNETIC STORMS; VIEW FROM ABOVE GEOMAGNETIC NORTH POLE (LEGEND AS IN FIGURE 230)

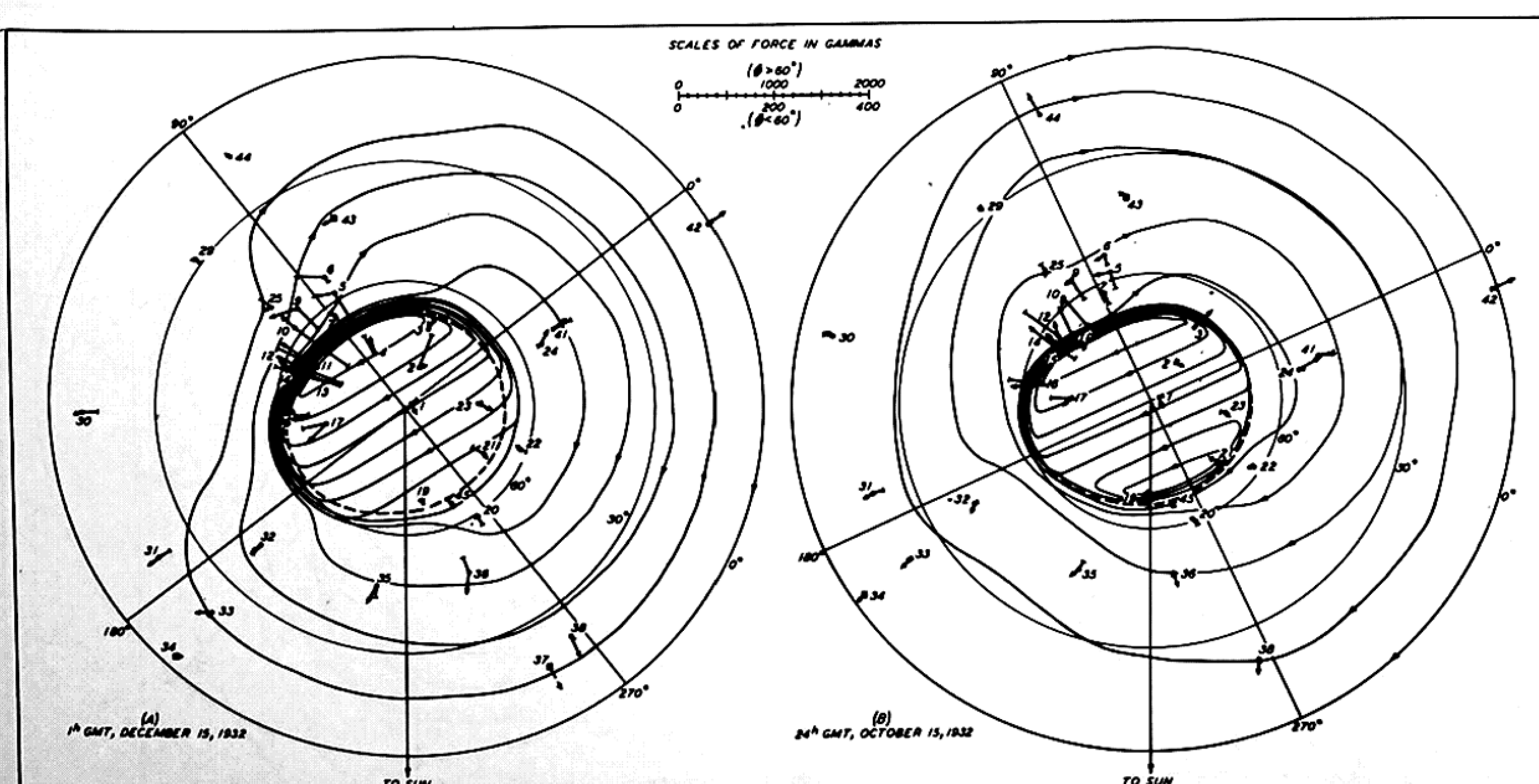

FIG.235—MEAN HOURLY DISTURBANCE-VECTORS AND CORRESPONDING ELECTRIC CURRENT-SYSTEMS FOR HEIGHT 150 KM FOR MAIN PHASE OF MAGNETIC STORMS; VIEW FROM ABOVE GEOMAGNETIC NORTH POLE (LEGEND AS IN FIGURE 230)

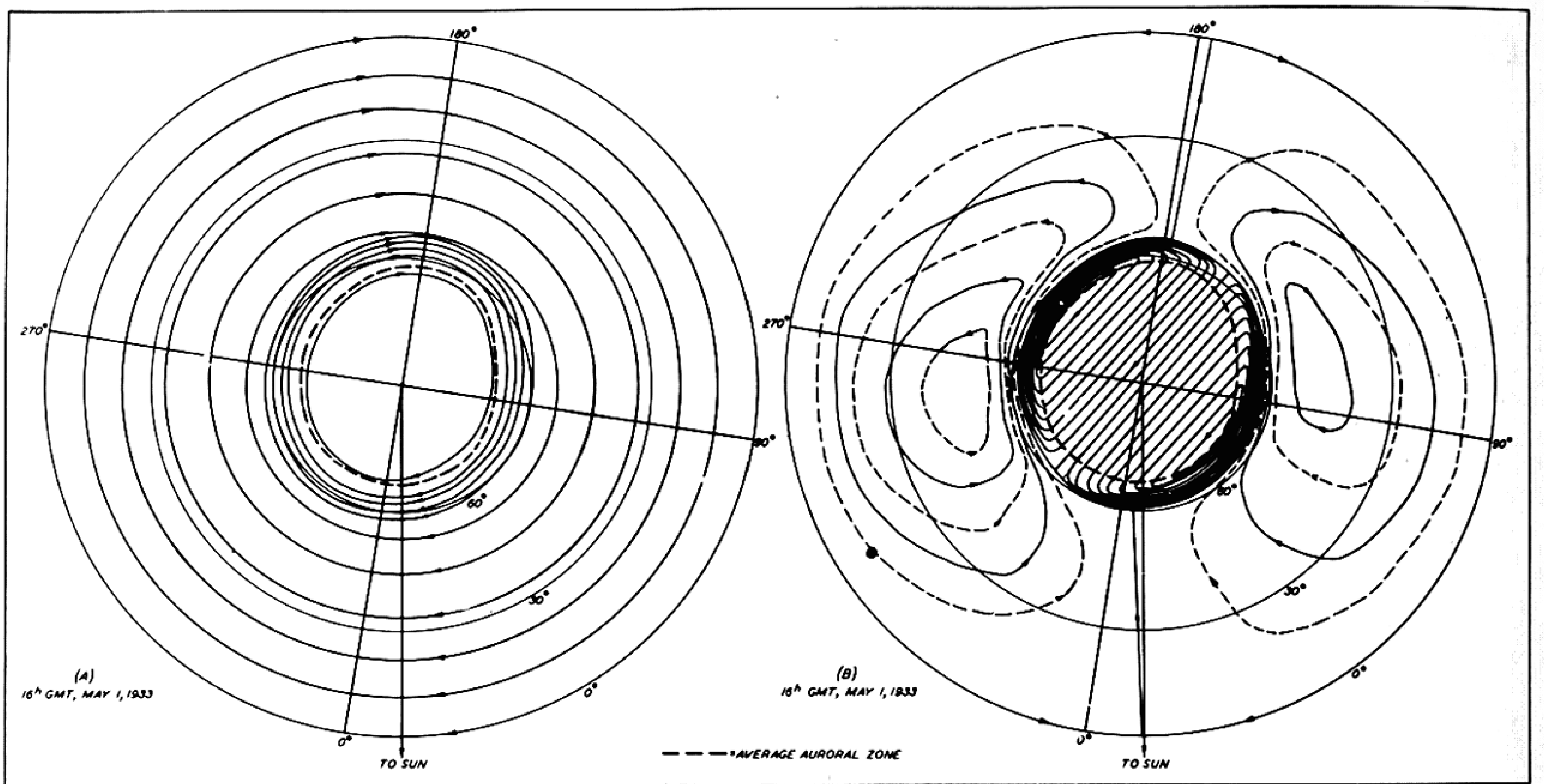

FIG. 238 – (A) AND (B), PARTIAL CURRENT-SYSTEMS, D_{St} AND S_D, RESPECTIVELY, MAIN PHASE OF STORM
(100,000 AMPERES FLOWS BETWEEN SUCCESSIVE FULL-DRAWN CURRENT-LINES)

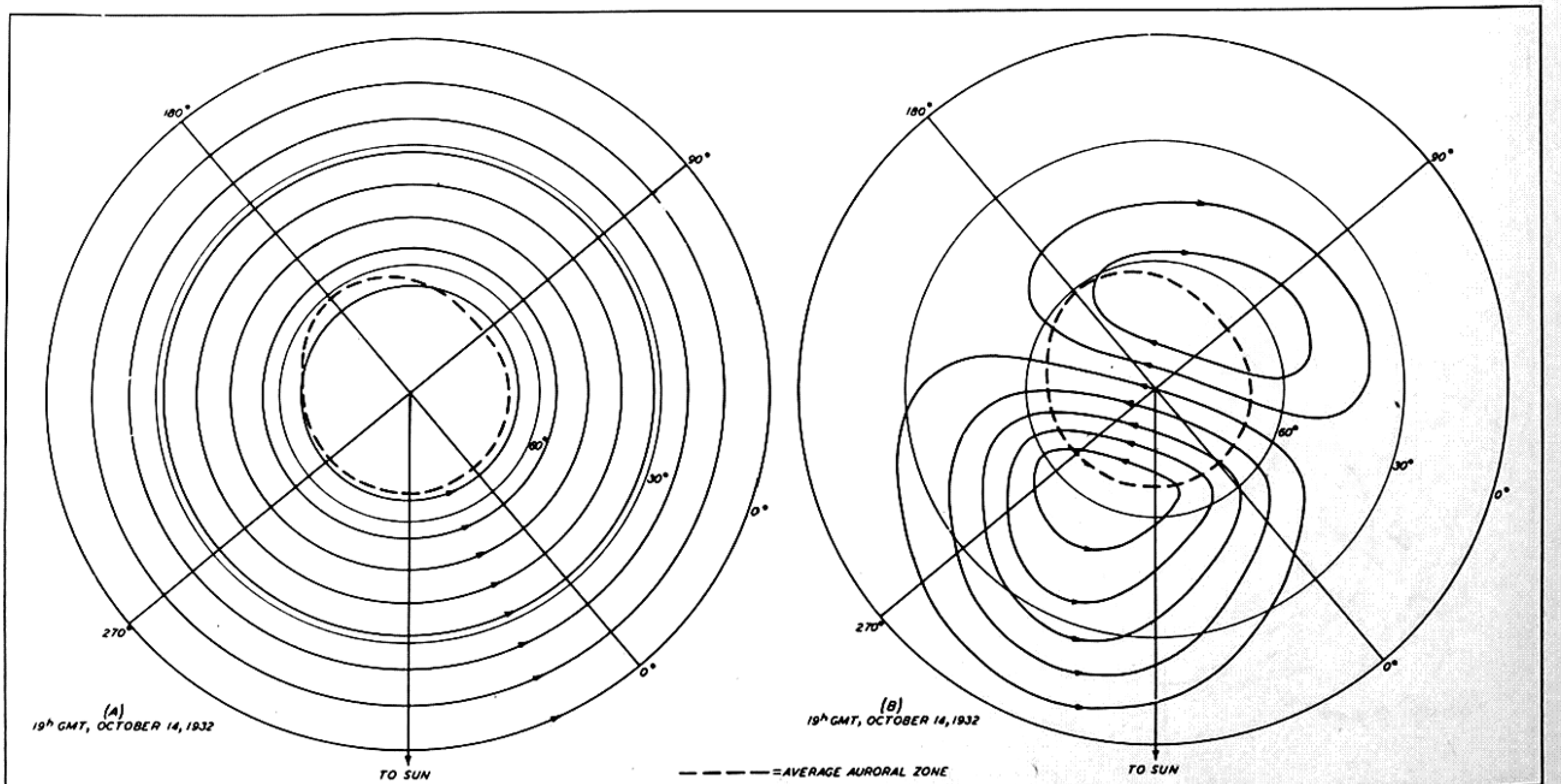

FIG. 237 – (A) AND (B), PARTIAL CURRENT-SYSTEMS, D_{St} AND S_D, RESPECTIVELY, INITIAL PHASE OF STORM
(10,000 AMPERES FLOWS BETWEEN SUCCESSIVE FULL-DRAWN CURRENT-LINES)

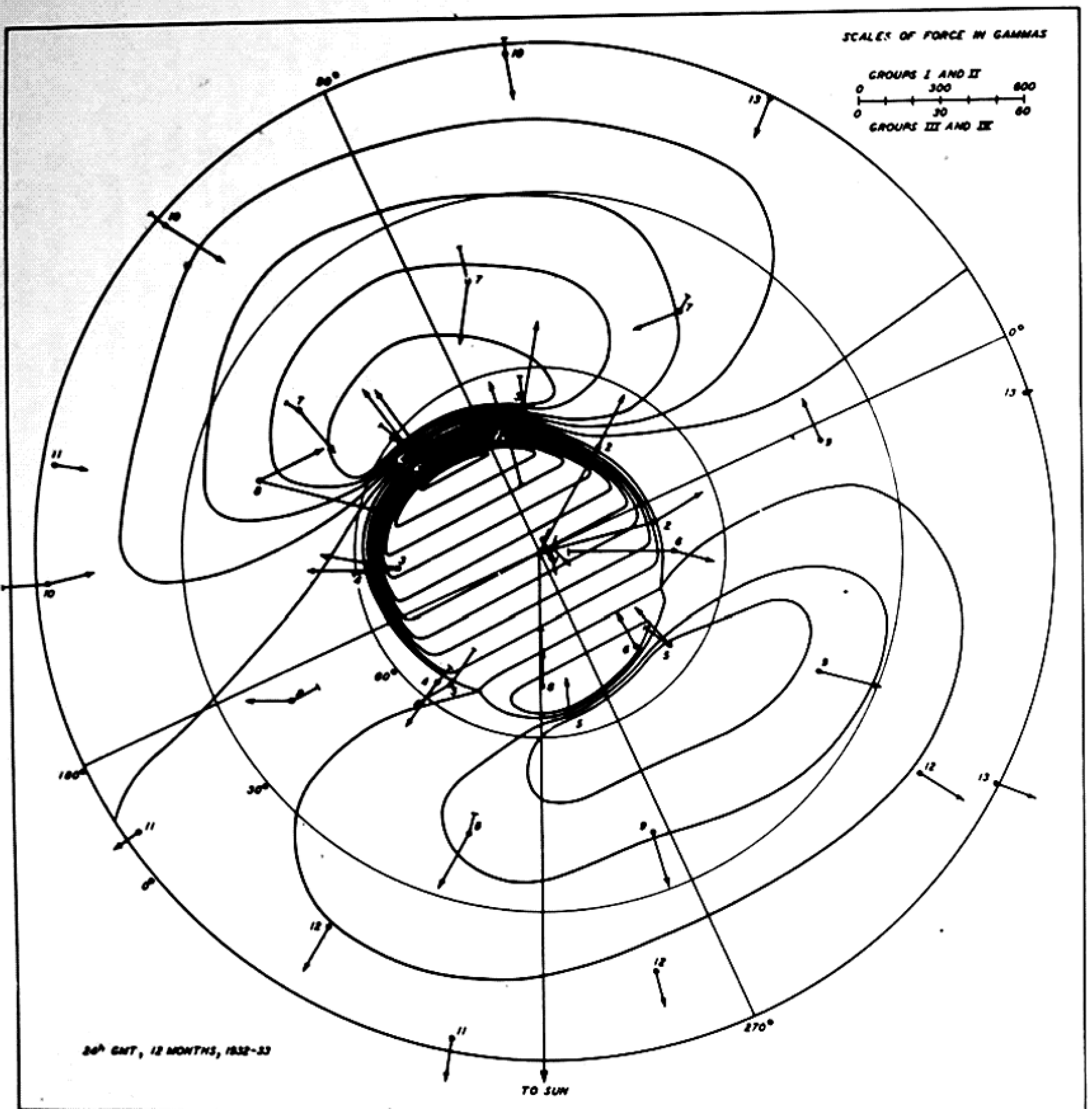

FIG. 238 —MEAN 3-HOUR DISTURBANCE-VECTORS OF MAGNETIC BAYS CENTERED AT 21h, 24h, AND 3h GMT (TENTATIVELY CORRECTED FOR INDUCED CURRENTS) AND CORRESPONDING AVERAGE ELECTRIC CURRENT-SYSTEM OF HEIGHT 150 KM VIEW FROM ABOVE GEOMAGNETIC NORTH POLE

LEGEND

HORIZONTAL FORCE ——→ VERTICAL FORCE —— (VERTICAL COMPONENT POSITIVE WHEN DRAWN OUTWARDS FROM GEOMAGNETIC NORTH POLE) (50,000 AMPERES FLOW BETWEEN SUCCESSIVE CURRENT-LINES)

STATIONS

GROUPS I AND II		GROUPS III AND IV	
1 THULE	4 DICKSON	7 EBRO	10 MOGADISCIO
2 JULIANEHAAB	5 COLLEGE-FAIRBANKS	8 WATHEROO	11 ANTIPOLO
3 TROMSÖ	6 FORT RAE	9 TUCSON	12 APIA
			13 HUANCAYO

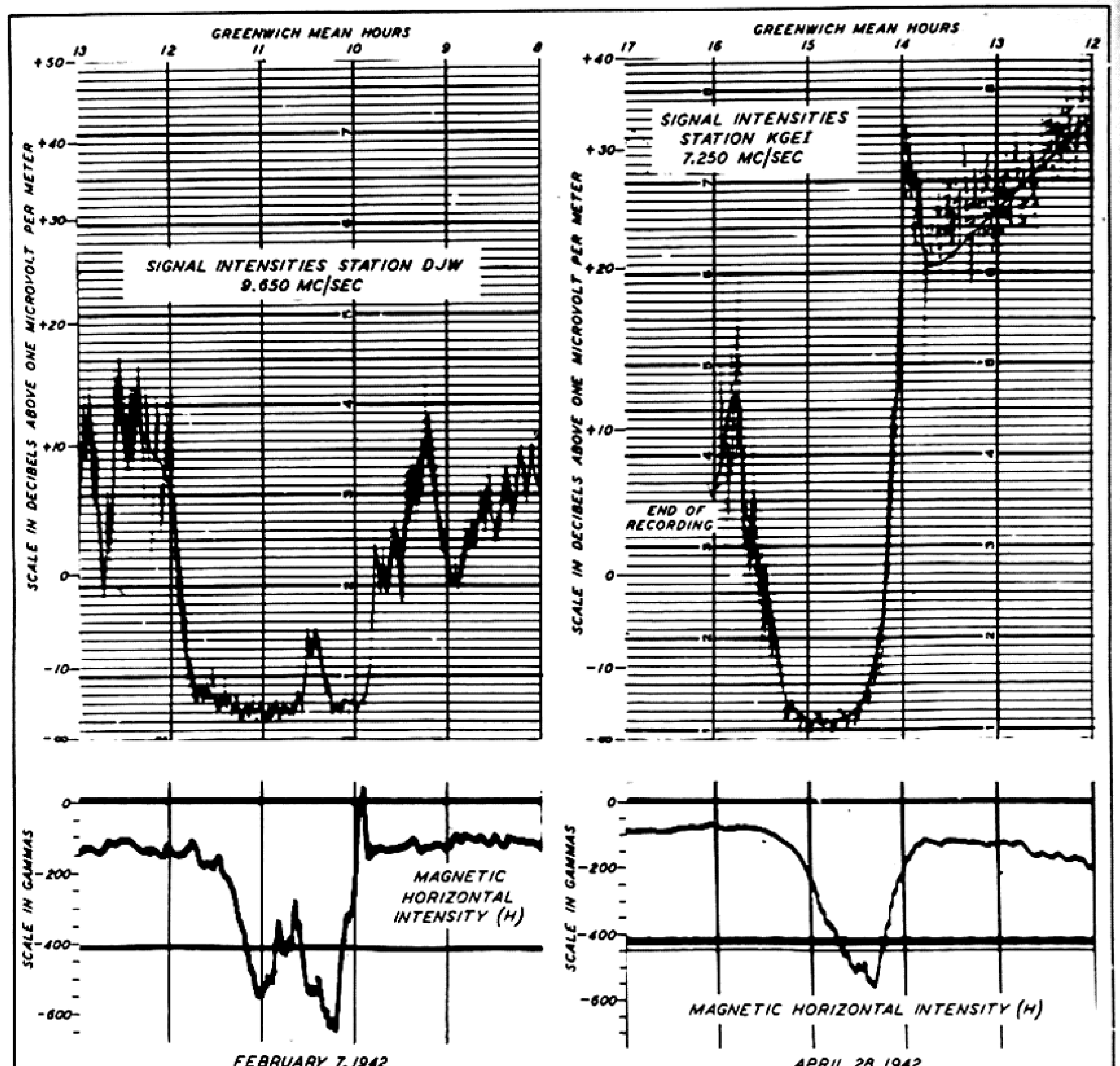

FIG. 239—HIGH ABSORPTION AT COLLEGE, ALASKA, DURING MAGNETIC BAYS

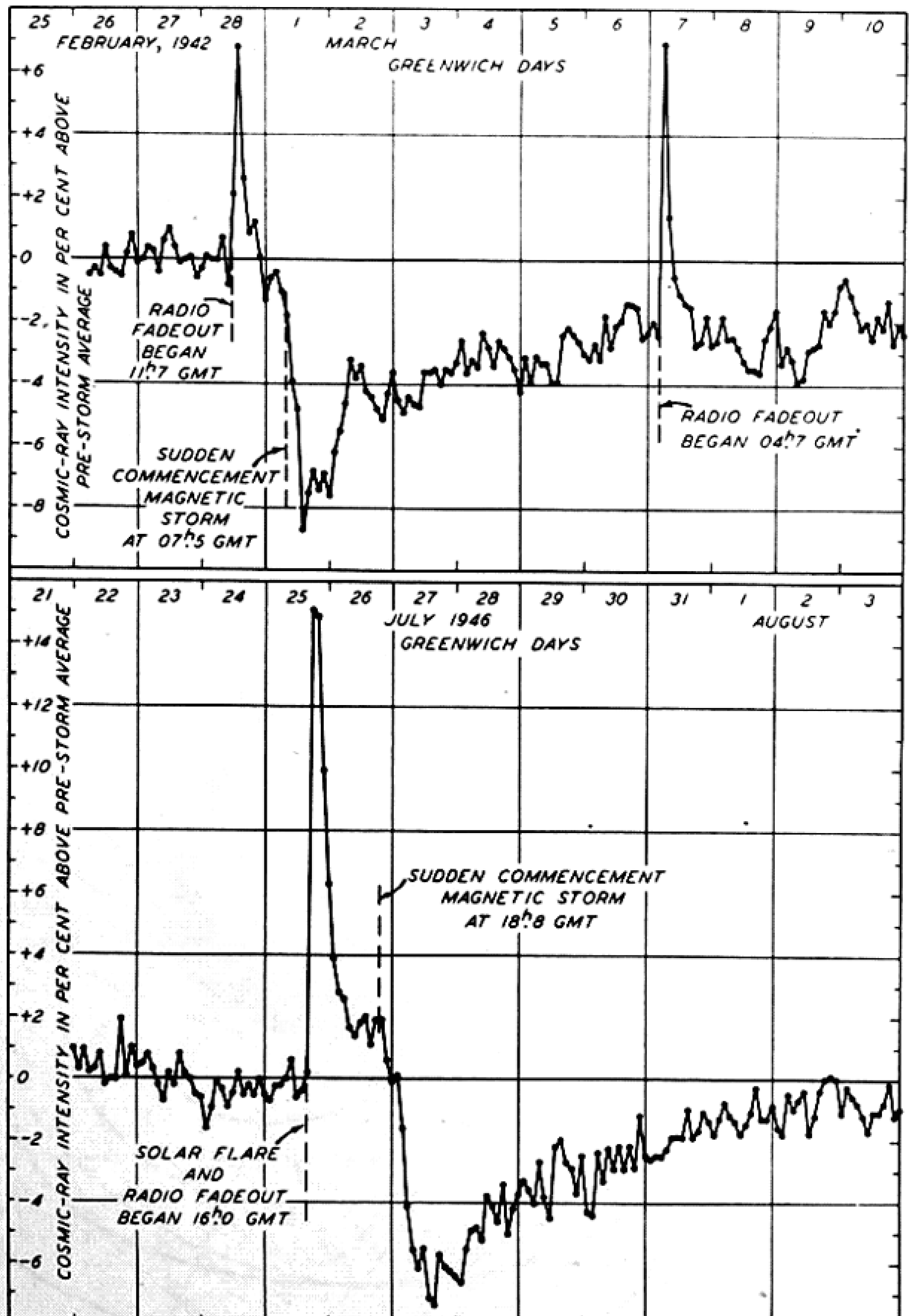

FIG. 240—THREE UNUSUAL INCREASES IN COSMIC-RAY INTENSITY AT CHELTENHAM, MARYLAND, DURING SOLAR FLARES AND RADIO FADEOUTS

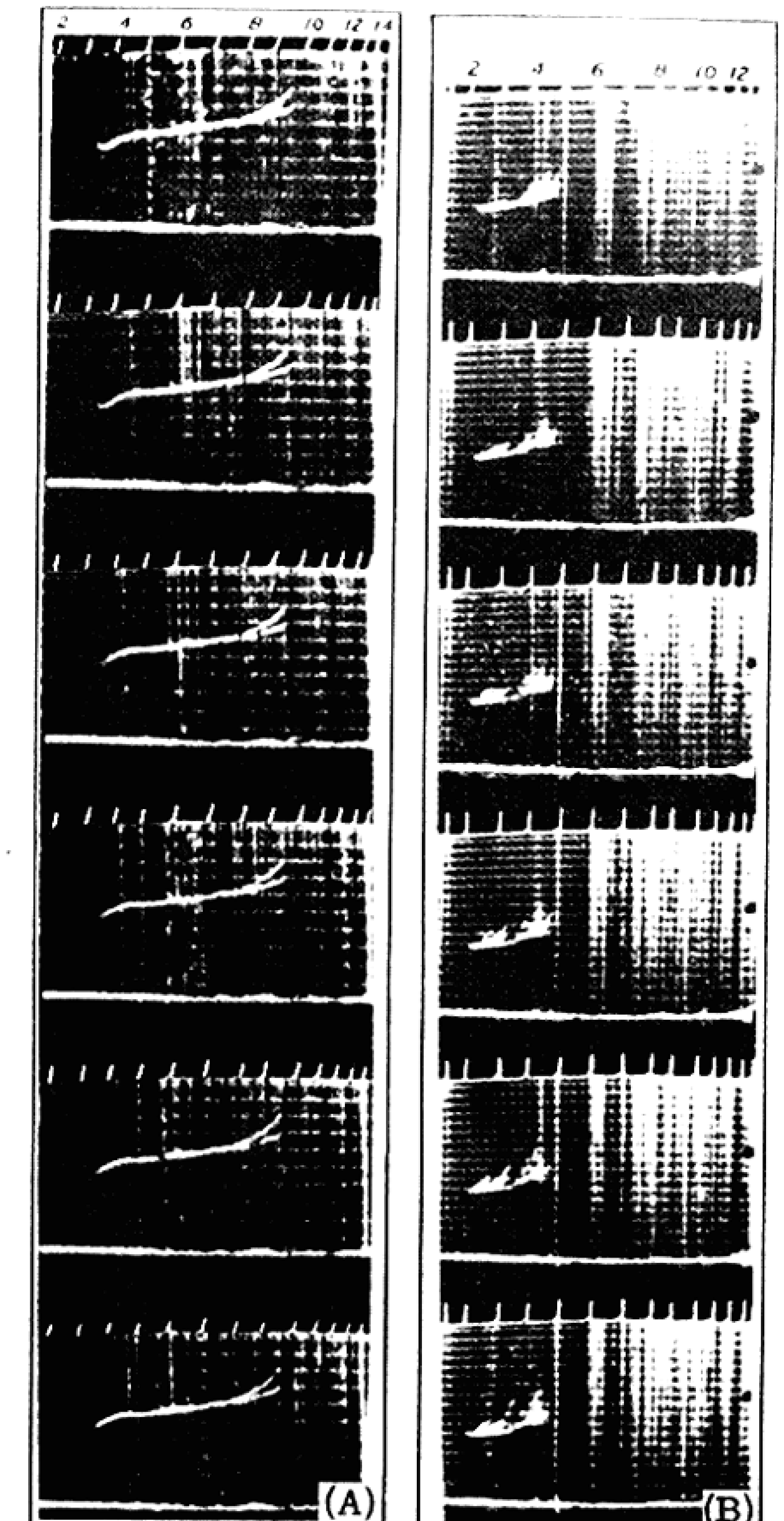

Fig. 241. (A) Six successive normal ionospheric 15-sec. records during three minutes afternoon March 19, 1946. (B) Six successive disturbed ionospheric 15-sec. records during three minutes of magnetic storm, March 25, 1946, showing rapid changes. (Records are reproduced from original 16-mm film; height-markers are at 50-km intervals, frequencies are indicated from 1.5 to 14 mc/sec.)

CHAPTER XI

PREDICTION OF GEOMAGNETIC FLUCTUATIONS

1. General remarks.--In practical applications of geomagnetism, as in closely related problems of radio communications, increasingly valuable use is being made of prediction. Accordingly, this short discussion of forecasting geomagnetic and allied geophysical conditions is included here.

Geomagnetic fluctuations have been closely linked with solar phenomena such as sunspots. Indices related to the magnitudes of geomagnetic fluctuations have been devised which have been successfully related in a statistical sense to solar indices, such as sunspot number, over a considerable number of years.

Since ionospheric and magnetic disturbances are associated, it has been found convenient to make use of geomagnetic indices in forecasting radio communications conditions, in much the same way as in weather forecasting, and with a similar degree of success. These forecasts from geomagnetic indices are facilitated by supplementary forecasts based on more or less continuous observations of solar phenomena, such as changes in size and activity of sunspots.

2. Bases for prediction.--For convenience, we may distinguish two major bases for prediction of geomagnetic fluctuations which in fact are apt to be found inherent in all successful schemes of prediction.

The first is that, given the past of a function (a geophysical time-series of fluctuations) arising from unspecified causes, it is assumed that these causes are also operative in the future. Each cause may make an independent contribution to the time-series, in which case the prediction may be described as linear (by analogy with electrical network theory). If this linear independence of causes does not exist, or does not exist to sufficiently good approximation, the problem of nonlinear prediction arises. In any event, since the causes are unspecified, the justification for choice of linear or nonlinear prediction can perhaps be made on the basis of experience with predictions of a given time series. In the linear case, a formal treatment is possible directly [74]; in the nonlinear case, it may be possible to arrive at a complete formal basis by trial and error.

The second basis for prediction involves knowledge of some or all of the actual causes or events with which the phenomena to be predicted are closely associated. Thus in geomagnetic predictions, appearance of large and active sunspots are usually followed by magnetic storms. It is known that solar and magnetic activity are on an average covariant, and plausible theories have been devised to explain the influence of the solar changes on geomagnetism. There occur active, regionally restricted areas on the Sun in the form of sunspots, prominences, and coronal-emission regions which have been studied in relation to geomagnetic disturbances [3]. It is found that the number and intensity of magnetic disturbances are covariant with the 11-year cycle of solar activity. Larger magnetic disturbances occur more frequently near sunspot maximum than near sunspot minimum.

Magnetic activity is usually measured in terms of ranges in geomagnetic elements, per three-hour interval, say. It is found that such ranges tend to be reproduced in magnitude at intervals of 26 to 28 days. This yields a valuable basis for prediction, especially successful during the few years immediately preceding a sunspot minimum, and moderately successful in other years. This recurrence tendency is of course useful in predicting magnetically quiet as well as disturbed conditions.

Large geomagnetic fluctuations are found associated with visible fluctuations in active solar areas, and especially with those in areas near the center of the solar disc. The activity in some solar regions may persist for several solar rotations of about 27 days, permitting forecasts of geomagnetic conditions 27 days in advance, with high probability of successfully forecasting moderate to strong disturbances. Such forecasts on a co-operative basis with staff members of the United States National Bureau of Standards and others were made by A. H. Shapley [75] of the Department of Terrestrial Magnetism during World War II, under sponsorship of the Wave Propagation Committee, Joint Communications Board, for utilization in systematic forecasts of magnetic disturbance and communications conditions issued by the Interservice Radio Propagation Laboratory, United States National Bureau of Standards. The over-all accuracy, as defined by the needs of this activity, was said to be about 65 per cent.

Large magnetic storms and large sunspots, however, are successfully associated in prediction about 80 per cent of the time. About 80 per cent of the storms commence during the three days the spot is near the central meridian of the Sun. However, as in weather forecasting, information of this type is applied somewhat subjectively in present forecasts of disturbance. With advance in our knowledge of solar phenomena and their effects near the Earth, there can be expected more accurate and useful forecasts in the future.

3. Formal methods of prediction.--Wiener [74] has recently made extensive analytical studies of the problem of prediction. These provide analyses for linear and nonlinear prediction, in the sense of analogy with electrical network theory. The techniques are therefore most conveniently applied by special predicting machines.

The writers have in fact made application of Wiener's linear prediction results to estimate future values of the geomagnetic variation with sunspot-cycle. These results, obtained on a trial basis, need not be given here, since our computing schemes seemed somewhat too complex for practical use.

4. Measures of magnetic activity.--In prediction of geomagnetic changes, much use is made of the ranges in the most disturbed elements D, H, or Z, per three-hour interval. These are known as K-indices. The ranges are selected to correspond to a nonlinear scale of zero to nine. A K-index of nine indicates a strong magnetic storm, whereas zero denotes very quiet magnetic conditions.

A and B of Figure 242 illustrate K-indices for a sunspot maximum year, 1938, and the sunspot minimum year, 1944. The data are arranged by solar rotations. It will be noted that there are at times pronounced

recurrence tendencies for quiet as well as disturbed days.

Since the semiquantitative predictions of K-indices are possible from solar phenomena and also, per three-hour interval, from the recurrence tendency of magnetic bays, it is of interest to translate this information in terms of the three-hour range at various geographical points.

Table 126 gives the K-scale at present in use at various magnetic observatories in different geographic locations. The average gamma-scale, referring to the most disturbed element of H, D, or Z per three-hour interval, depends mainly on geomagnetic latitude, except in auroral regions where it depends more closely upon the distance from the station to the average position of the auroral zone.

Table 127 presents the results of Table 126 in another way, and indicates in percentages the frequency of occurrence of various three-hourly ranges having magnitudes within certain assigned limits at the several stations for the year 1940.

Figure 243 illustrates roughly the magnitude of the three-hour range in the most disturbed of the elements H, D, or Z which was not exceeded 80 per cent of the time during the year 1940. This diagram has been prepared in much the same way as those of Chapter IX relating to amplitudes of geomagnetic fluctuations and can be improved advantageously by use of data from additional stations when such results become available in the future.

It will be noted that Figure 243 gives results for H, D, or Z, but provides no information as to which of the three elements yields the three-hour range at any given interval. Actually, the element chosen to provide the estimates of three-hour range varies with geomagnetic latitude, and in auroral regions depends especially on the distance to the auroral zone. The choice of element may also be different at different times of day, since the three-hour range in each element will have an amplitude corresponding more or less closely with the amplitude of the disturbance daily variation. Thus the average amplitude of the three-hour range in each geomagnetic element is in fairly close proportion to that of the average disturbance daily variation (S_D).

Figure 244 illustrates the average magnitude of S_D with geomagnetic latitude, referred to an auroral zone adjusted to a geomagnetic latitude 69° north and south, for four periods of day. These curves show that at the auroral zone, the largest three-hour ranges are expected in H, and just inside and just outside the auroral zone, large ranges are expected in Z during morning and evening hours. Near the center of the auroral zone, the three-hourly ranges are expected to be largest in H and D, and small in Z. In middle latitudes, the average ranges in H and D are largest, and obviously those in Z, I, or F will be considerably smaller. Near the equator, the fluctuations in H and F have the largest average range, whereas those in Z and I are relatively small. The currently available K-indices thus provide a rough indication of the probable upper limit in three-hour range in H, D, or Z, by use of diagrams such as Figure 243, which shows the amplitude of three-hour range in various geographical localities. Moreover, these K-indices, used in conjunction with the known average latitude distribution of S_D, permits tentative conclusions respecting the upper limits of average disturbance in other components not at present recorded, such as I and F. In practical applications where disturbance in I and F might become important, the average amplitudes of S_D, and their latitude distributions can of course be computed from the curves of Figure 244, by resolving the average disturbance in horizontal and vertical intensity along the directions I and F. These can be further improved by reference to basic data given for S_D earlier in this volume (only meager data exist for south polar regions and these have been summarized elsewhere [76]).

5. Relation of average auroral and geomagnetic characteristics.--It is well known that the manifestations of aurora and geomagnetic disturbances are more or less closely connected temporaly [3], near the auroral zones. Figures 245 and 246 give the results in percentages of a recent revision of data respecting the daily frequencies of aurora in various regions of the world [76,77]. These revisions were undertaken in conjunction with other studies of the present volume. Figures 247 to 250 provide similar results newly derived for hourly frequencies of aurora for the Northern Hemisphere, estimated on a like basis, taking into account corrections for effects of cloudiness, and other phenomena, on the observed frequencies of aurora.

6. The prediction of the systematic geomagnetic variations.--It has been noted that there is in current use a system of K-indices descriptive of intensity of disturbance and in particular of the maximum three-hour range in H, D, or Z. Obviously, the three-hour range is an indicator only of disturbance during the three-hour interval, and it often is derived from the maximum and minimum values of a short-period fluctuation that endures for a shorter interval of time. In other words, the K-indices are in part indicators of highly transient features of geomagnetic field which may be regarded as superposed on a number of other systematic variations. The variations in K-indices of course arise mainly from disturbances of type S_D or D_{st}.

In estimating K-indices from magnetograms, there is removed almost completely the three-hour range contributed by the solar daily variation, S_q, which is present daily throughout low and middle latitudes and is the most apparent and persistent feature of the daily records. On the other hand, S_D, which is often very small in these latitudes and at times varies greatly in intensity, is reflected in part in the K-indices. Thus, in practical applications requiring precise knowledge of the geomagnetic field, it may be desirable to predict amplitudes of the solar daily variation S_q and the post-perturbation P.

The prediction of the amplitude of S_q a day or two in advance, with an accuracy of about 20 per cent, for the great majority of days, is easily achieved by a simple graphing procedure of daily amplitude factors of S_q such as those listed in Table 1-Q of the preceding volume [1]. In the same way, the shifts in phase of S_q from day to day can be successfully predicted with fair success.

In the case of the post-perturbation P, the trend from day to day, as shown in Table 1-G in the earlier volume [1], is highly regular. Its prediction within 20 per cent, except possibly at times of onset of marked disturbance, seems relatively well assured.

It is therefore feasible in engineering applications of geomagnetism to take into account and reduce the limitations imposed by geomagnetic fluctuations through use of prediction schemes for various geomagnetic fluctuations.

TABLES 126-129

Table 126. Contributing observatories and lower limits of ranges (R) in D, H, or Z for three-hour-range indices (K)

Observatory (a) and abbreviation (b)		Geographical co-ordinates		For value of K									
(a)	(b)	ϕ	λ E	0	1	2	3	4	5	6	7	8	9
		°	°	γ	γ	γ	γ	γ	γ	γ	γ	γ	γ
Godhavn	Go	69.2	306.5	0	18	36	72	144	250	430	720	1200	1800
Sodankylä	So	67.4	26.6	0	10	20	40	80	140	240	400	660	1000
College	Co	64.9	212.2	0	25	50	100	200	350	600	1000	1650	2500
Dombaas	Do	62.1	9.1	0	8	15	30	60	105	180	300	500	750
Lerwick	Le	60.1	358.8	0	10	20	40	80	140	240	400	660	1000
Sloutzk	Sl	59.7	30.5	0	6	12	24	48	85	145	240	400	600
Sitka	Si	57.0	224.7	0	10	20	40	80	140	240	400	660	1000
Rude Skov	RS	55.8	12.5	0	6	12	24	48	85	145	240	400	600
Eskdalemuir	Es	55.3	356.8	0	8	15	30	60	105	180	300	500	750
Meanook	Me	54.6	246.7	0	15	30	60	120	210	360	600	1000	1500
Witteveen	Wi	52.8	6.7	0	5	10	20	40	70	120	200	330	500
Niemegk	Ni	52.1	12.7	0	5	10	20	40	70	120	200	330	500
Abinger	Ab	51.2	359.6	0	5	10	20	40	70	120	200	330	500
Chambon-la-Forêt	CF	48.0	2.3	0	5	10	20	40	70	120	200	330	500
Agincourt	Ag	43.8	280.7	0	6	12	24	48	85	145	240	400	600
Cheltenham	Ch	38.7	283.2	0	5	10	20	40	70	120	200	330	500
San Fernando	SF	36.5	353.8	0	4	8	16	30	50	85	140	230	350
Tucson	Tu	32.2	249.2	0	4	8	16	30	50	85	140	230	350
Zô-Sè	ZS	31.1	121.2	0	3	6	12	24	40	70	120	200	300
Honolulu	Ho	21.3	201.9	0	3	6	12	24	40	70	120	200	300
San Juan	SJ	18.4	293.9	0	3	6	12	24	40	70	120	200	300
Kuyper	Ku	- 6.0	106.7	0	3	6	12	24	40	70	120	200	300
Huancayo	Hu	-12.0	284.7	0	6	12	24	48	85	145	240	400	600
Apia	Ap	-13.8	188.2	0	3	6	12	24	40	70	120	200	300
Watheroo	Wa	-30.3	115.9	0	4	8	16	30	50	85	140	230	350
Pilar	Pi	-31.7	296.1	0	3	6	12	24	40	70	120	200	300
Cape Town	CT	-33.9	18.5	0	3	6	12	24	40	70	120	200	300
Amberley	Am	-43.2	172.7	0	5	10	20	40	70	120	200	330	500

Table 127. Per cent of time that three-hour-range of disturbance in D, H, or Z is less than the various ranges (R) derived from three-hour-range indices (K) for 1940 from 28 observatories

Observatory	Geo-magnetic latitude	Ranges (R) in gammas)								
		5	10	20	30	50	75	100	200	500
	°	%	%	%	%	%	%	%	%	%
Godhavn	79.8	0	0	1.3	6.6	19.0	38.9	55.9	83.8	98.3
College	64.5	0	6.6	19.3	29.2	48.8	61.1	69.4	82.1	93.6
Sodankylä	63.8	3.0	19.4	40.8	51.9	63.2	71.6	77.6	90.0	97.8
Lerwick	62.5	0	9.6	34.6	52.6	71.1	82.7	89.3	95.7	98.2
Dombaas	62.3	11.0	26.1	46.6	61.9	76.7	86.8	90.7	96.1	98.5
Meanook	61.8	0	7.0	32.7	43.1	57.3	68.1	74.9	87.2	96.7
Sitka	60.0	0	16.6	41.5	53.6	70.4	80.1	85.8	94.1	98.0
Eskdalemuir	58.5	0	11.0	40.6	61.3	80.4	91.3	94.8	98.2	99.5
Sloutzk	56.0	2.0	18.9	41.1	59.2	79.7	89.8	94.6	98.1	99.3
Rude Skov	55.8	13.8	34.0	55.5	69.1	84.5	92.0	95.3	98.3	99.5
Agincourt	55.0	7.0	28.0	51.0	65.9	83.1	90.1	93.7	98.1	99.7
Witteveen	54.2	12.4	31.5	58.2	72.1	87.3	94.3	96.7	99.1	99.9
Abinger	54.0	1.7	23.9	53.3	69.3	87.9	94.6	97.1	99.0	99.9
Niemegk	52.2	13.3	38.0	64.9	76.0	88.8	95.0	97.0	99.2	99.9
Chambon-la-Forêt	50.4	17.3	43.7	72.0	83.3	94.3	97.6	98.7	99.8	100.0
Cheltenham	50.1	13.9	35.0	60.7	73.1	88.7	94.8	97.4	99.0	99.9
San Fernando	41.0	13.8	32.3	60.2	75.8	91.1	96.7	98.2	99.6	100.0
Tucson	40.4	21.1	45.0	70.9	85.1	94.6	97.7	98.9	99.6	100.0
San Juan	29.9	37.5	65.6	86.7	93.7	98.0	98.7	99.0	99.9	100.0
Honolulu	21.1	43.2	66.9	87.0	94.6	97.9	99.0	99.2	99.9	100.0
Zô-Sè	19.8	10.7	34.3	70.6	86.6	96.1	98.3	98.9	99.9	100.0
Huancayo	- 0.6	9.0	30.0	54.6	70.6	86.8	93.0	95.5	98.8	99.9
Apia	-16.0	25.7	57.5	84.7	94.5	97.9	99.0	99.2	100.0	100.0
Kuyper	-17.5	33.0	59.2	82.3	92.5	97.0	98.6	99.0	100.0	100.0
Pilar	-20.2	24.3	48.9	77.6	88.9	97.1	98.5	99.0	99.9	100.0
Cape Town	-32.7	40.0	64.3	86.1	94.5	97.9	99.0	99.3	99.9	100.0
Watheroo	-41.8	23.0	48.0	78.6	89.8	96.5	98.3	98.7	99.6	100.0
Amberley	-47.7	9.8	33.8	67.2	80.3	92.7	96.7	98.1	99.5	99.9

Table 128. List of abbreviations for auroral stations, Northern Hemisphere

Station	Ab.	Station	Ab.	Station	Ab.
Abisko	Ab	Gordon Castle	GC	New York Harbor	NYH
Aberdeen	Abe	Gjöahavn	Gj	Oslo	Os
Albany	Al	Great Liakhovsky Is.	GLI	Ouellen	Ou
Angmagsalik	An	Godhavn	Go	Point Barrow	PB
Blue Hill	BH	Godthaab	Gt	Pentland Skerries	PeS
Bear Island	BI	Haroldswick	Ha	Polar Star	PS
Bossekop	Bo	Havre	Hav	Refuge Harbor	ReH
Balta Sound	BS	Houlton	Ho	Russian Harbor	RH
Bowdoin Harbor	BoH	Havnefjord	Hvn	Rudolph Island	RI
Burlington	Bu	Ithaca	It	Rice Strait	RS
Calm Bay	CB	Ivigtut	Iv	Saskatoon	Sa
Cape Desire	CD	Jacobshavn	Ja	Ssagastyr	Sag
College-Fairbanks	CF	Jan Mayen	JM	Sheridan	Sh
Chelyuskin	Ch	Juneau	Ju	Sitka	Si
Cape Hope's Advance	CHA	Kingua Fjord	KF	Sergei Kamenev Is.	SKI
Chesterfield Inlet	CI	Kirkwall	Ki	Sodankylä	So
Cleveland	Cl	Koutokaeino	Ko	Spokane	Sp
Coppermine	Co	King Point	KP	Scoresby Sund	SS
Contoocooksville	Con	Kultala	Ku	Sault Ste. Marie	SSM
Cape Otto Schmidt	COS	Lerwick	Le	Stornoway	St
Cape Thordsen	CT	Madison	Mad	Sukkertoppen	Su
Deerness	De	Maud I	Ma I	Tixi Bay	TB
Duntulm	Du	Maud II	Ma II	Tiree	Ti
Edmonton	Ed	Maud III	Ma III	Toronto T	To
Ellendale	El	Meanook	Me	Treurenberg	Tr
Eskdalemuir	Es	Malya Karmakuly	MK	Upsala	Up
Floeberg Beach	FB	Matochkin Shar	MS	Vega	Ve
Fort Conger	FC	Nain	Na	Wick	Wi
Fort Rae	FR	Nennortalik	Ne	Wrangel Island	WI
Gaasefjord I	Ga I	Northbrook Island	NI	Yerkes Y	Ye
Gaasefjord II	Ga II	Nome	No		

Table 129. List of abbreviations for auroral stations, Southern Hemisphere

Station	Ab.	Station	Ab.	Station	Ab.
Adelaide	Ad	Cape Schank	CS	Little America	LA
Ballarat	Ba	Endurance	End	Laurie Island	LI
Beechworth	Be	Deutschland	Deu	Macquarie Island	MI
Belgica	Bel	Framheim	Fr	New Zealand	NZ
Cape Adare	C Ad	Gauss-Station	GS	Port Charcot	PC
Cape Armitage	C Ar	Hobarton	Ho	Queen Mary Land	QML
Cape Denison	CD	Hut Point	HP	Santiago	Sa
Cape Evans	CE	Ile Petermann	IP	Scotia Bay	SB
Cape Royds	CR	Kerguelen	Ke	Victoria	Vi
Carnegie	Car	Kyneton	Ky	Wilson's Promontory	WP

FIGURES 242-250

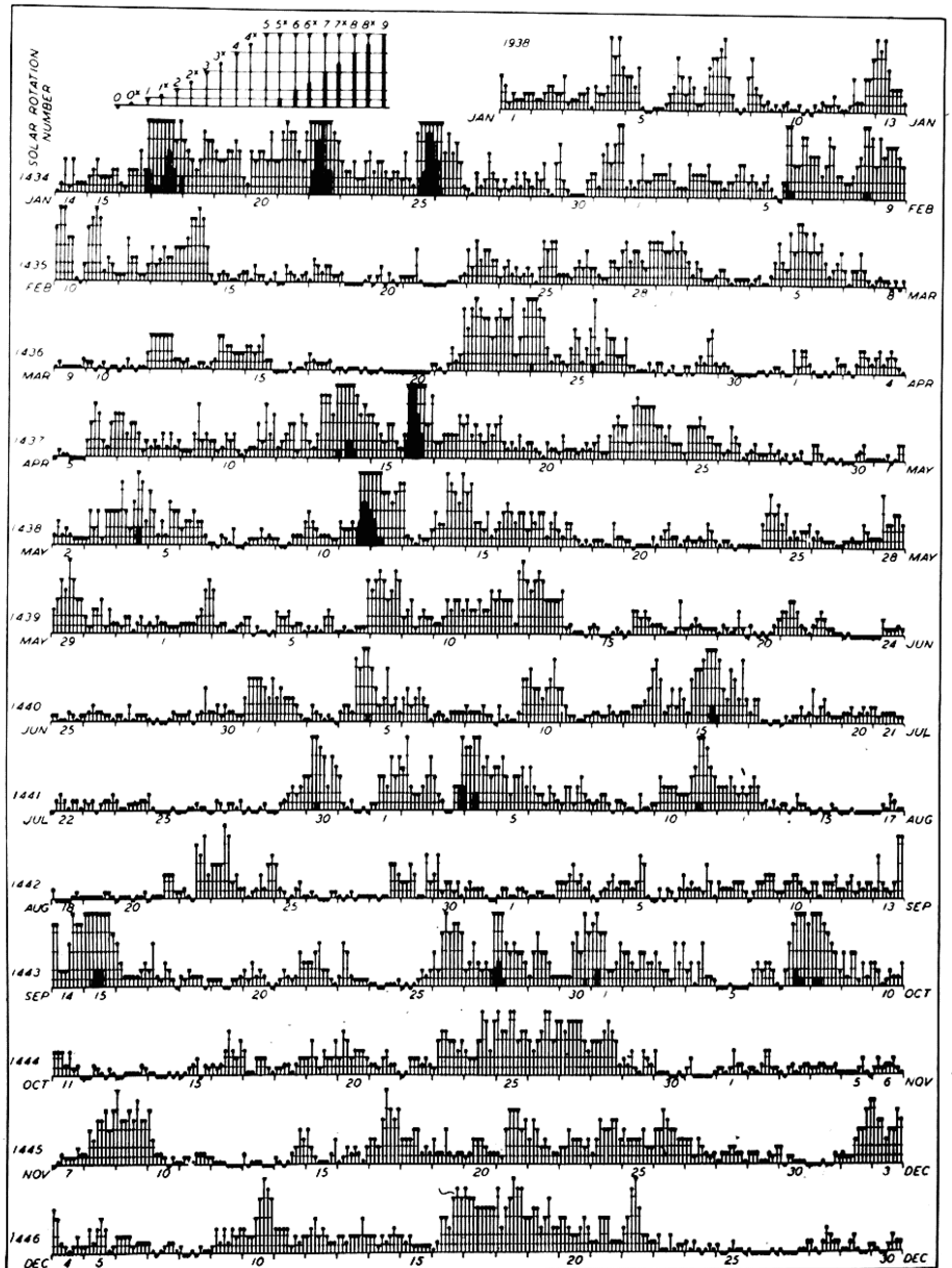

FIG. 242(A)—WORLD-WIDE MAGNETIC THREE-HOUR-RANGE INDICES K_W, JANUARY 1 TO DECEMBER 30, 1938

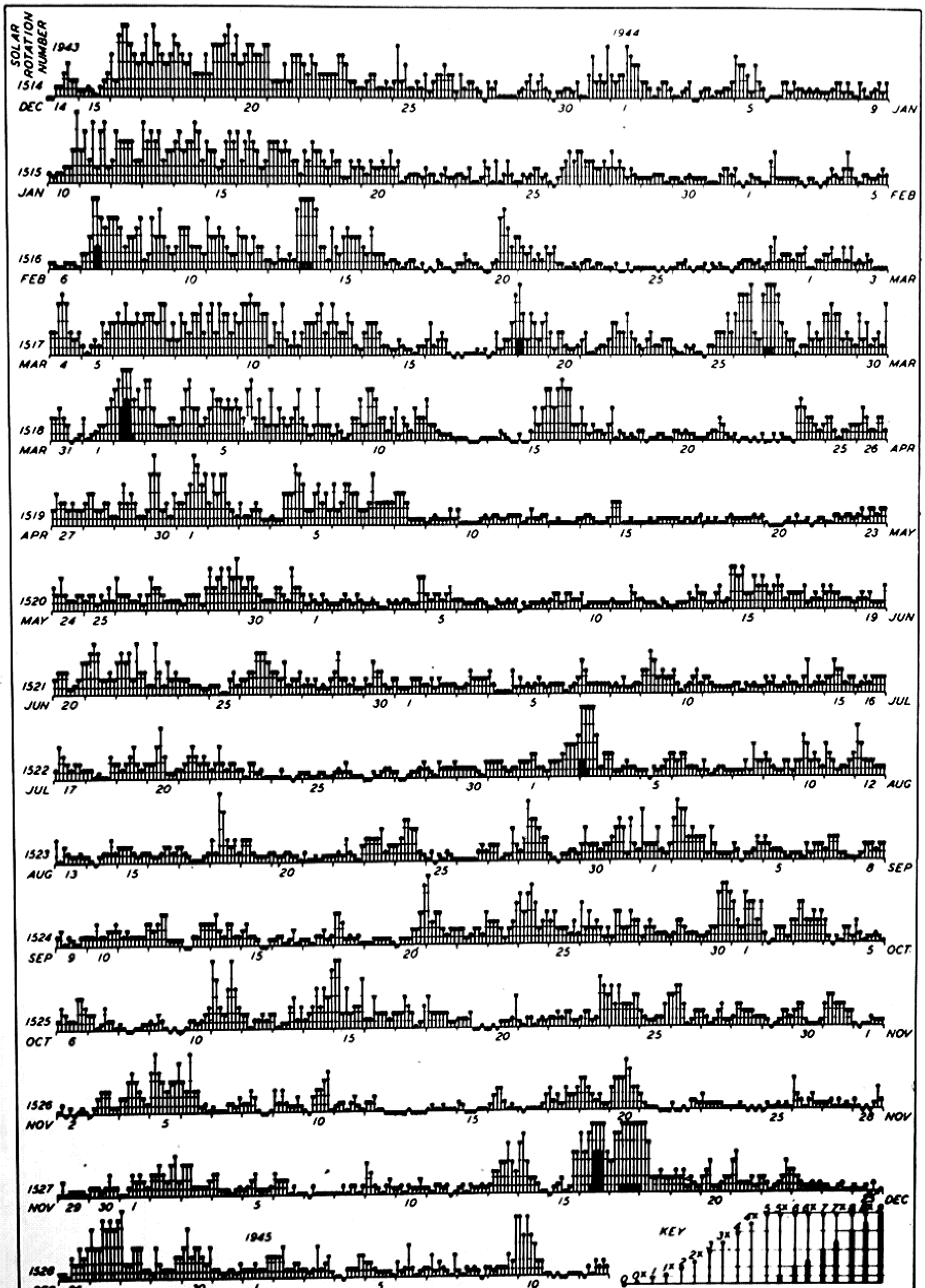

FIG. 242(B)—WEIGHTED AVERAGE, K_A, OF REDUCED INDICES, K_r, FROM SITKA, CHELTENHAM, TUCSON, SAN JUAN, HONOLULU, HUANCAYO, AND WATHEROO, DECEMBER 14, 1943 TO JANUARY 12, 1945

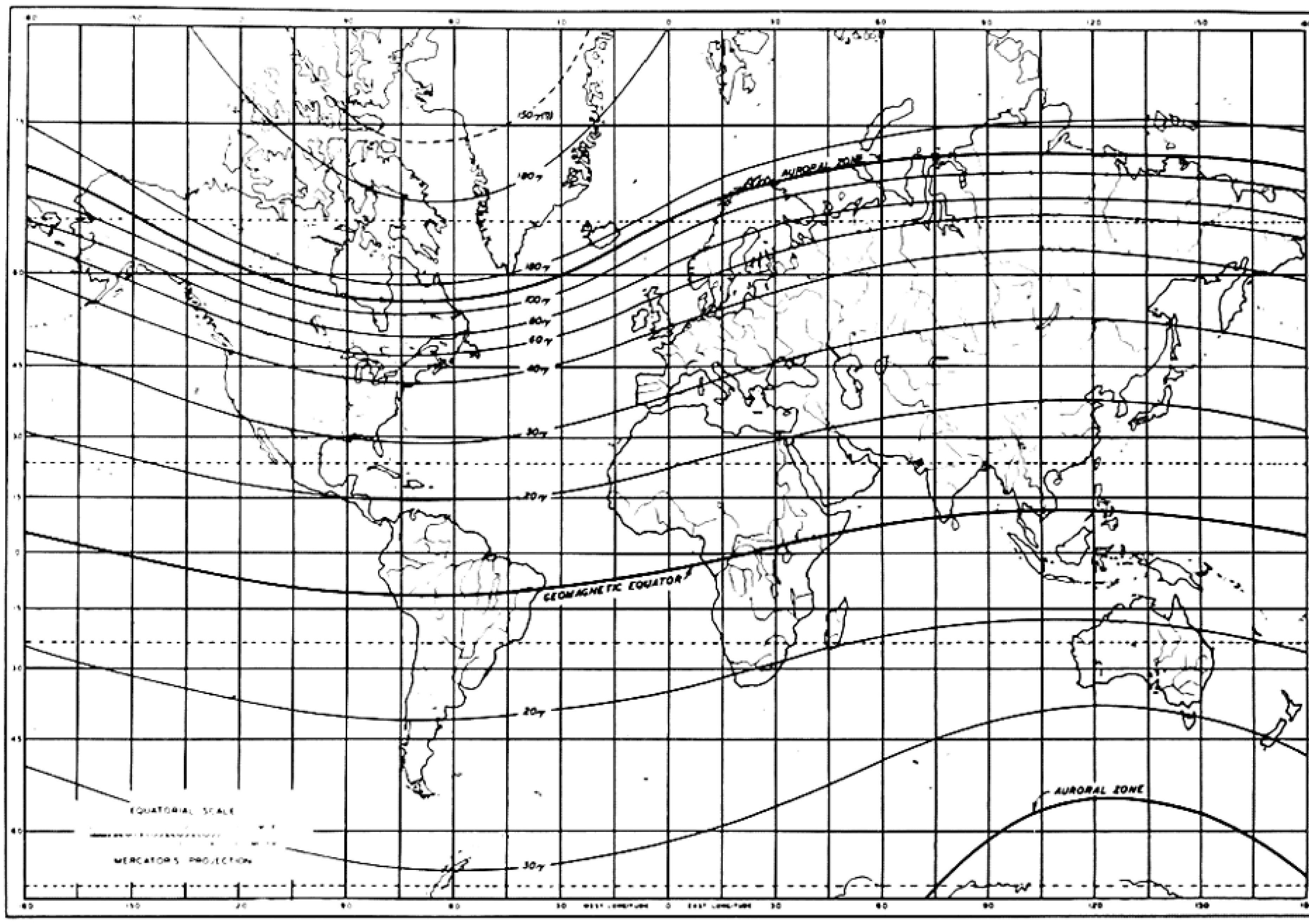

FIG. 243—MAGNITUDE OF THREE-HOUR RANGE IN THE MOST DISTURBED ELEMENTS D, H, Z, NOT EXCEEDING 80 PER CENT OF THE TIME DURING YEAR 1940

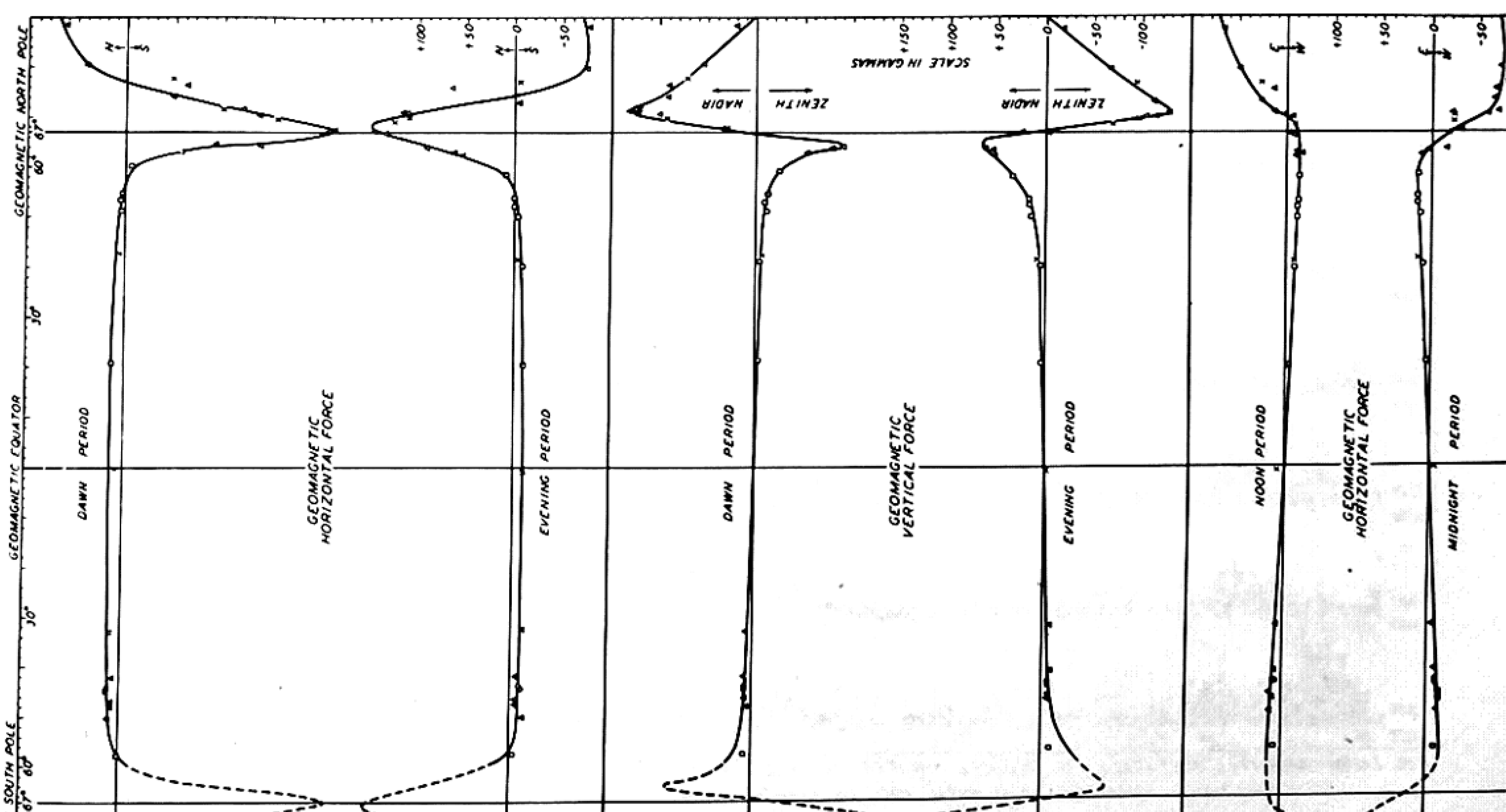

FIG. 244—VARIATIONS WITH LATITUDE OF MAXIMA AND MINIMA OF GEOMAGNETIC COMPONENTS OF DISTURBANCE DIURNAL-VARIATION FOR INTERNATIONAL DISTURBED MINUS QUIET DAYS (S_D) [DATA FOR MAGNETIC LATITUDES 62°N TO 72°N ARE ADJUSTED IN LATITUDE RELATIVE TO CIRCULAR AURORAL ZONE]

• = FIRST INTERNATIONAL POLAR YEAR, 1882-83; ▲ = SECOND INTERNATIONAL POLAR YEAR, 1932-33; ■ = YEAR 1933; □ = OBSERVATORIES VARIOUS EPOCHS, 1902-42

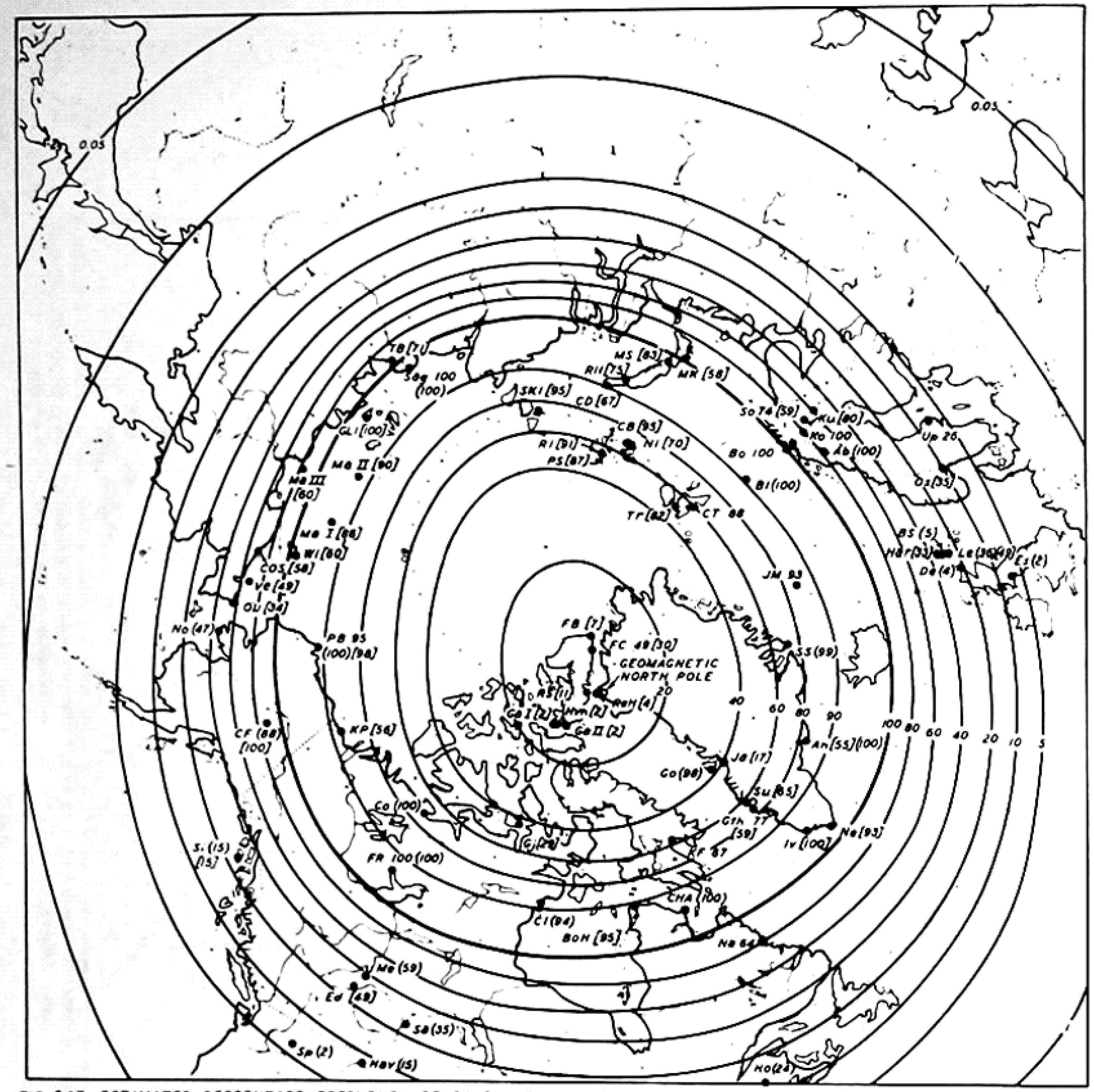

FIG. 245—ESTIMATED PERCENTAGE-FREQUENCY OF DAYS WITH OCCURRENCE OF AURORA, CLEAR, DARK NIGHTS, HIGH LATITUDES, NORTHERN HEMISPHERE (STATIONS SHOWN BY LETTERS AS INDICATED IN TABLE 128)

LEGEND

RESULTS FROM	YEARS	PERCENTAGE-FREQUENCY MARKED THUS
FIRST INTERNATIONAL POLAR YEAR	1882-83	90
SECOND INTERNATIONAL POLAR YEAR	1932-33	(90)
OTHER OBSERVATIONS	FROM 1871-1942	[90]

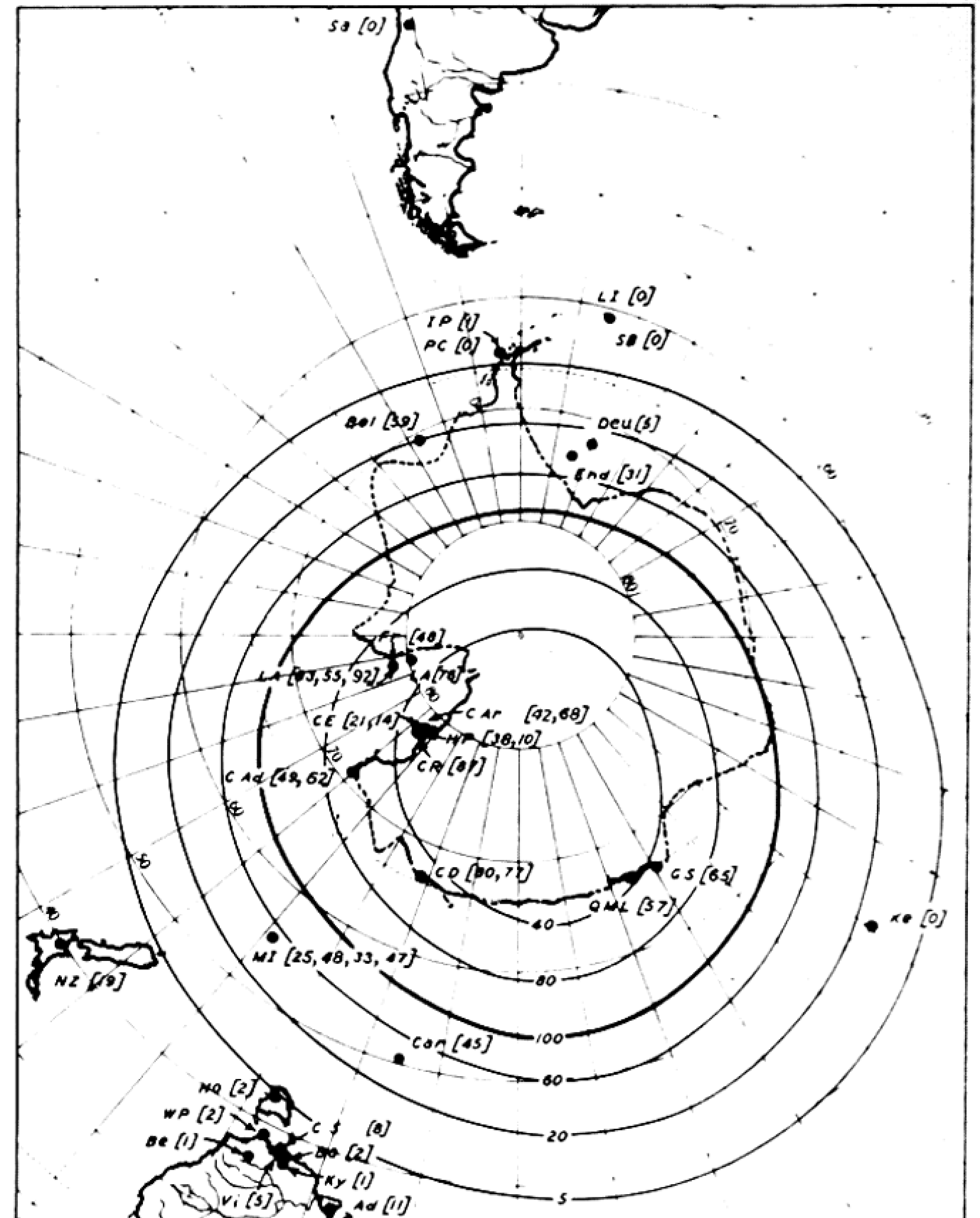

FIG. 246 - ESTIMATED PERCENTAGE-FREQUENCY OF DAYS WITH OCCURRENCE OF AURORA, CLEAR, DARK NIGHTS, HIGH LATITUDES, SOUTHERN HEMISPHERE (STATIONS SHOWN BY LETTERS AS INDICATED IN TABLE 129)

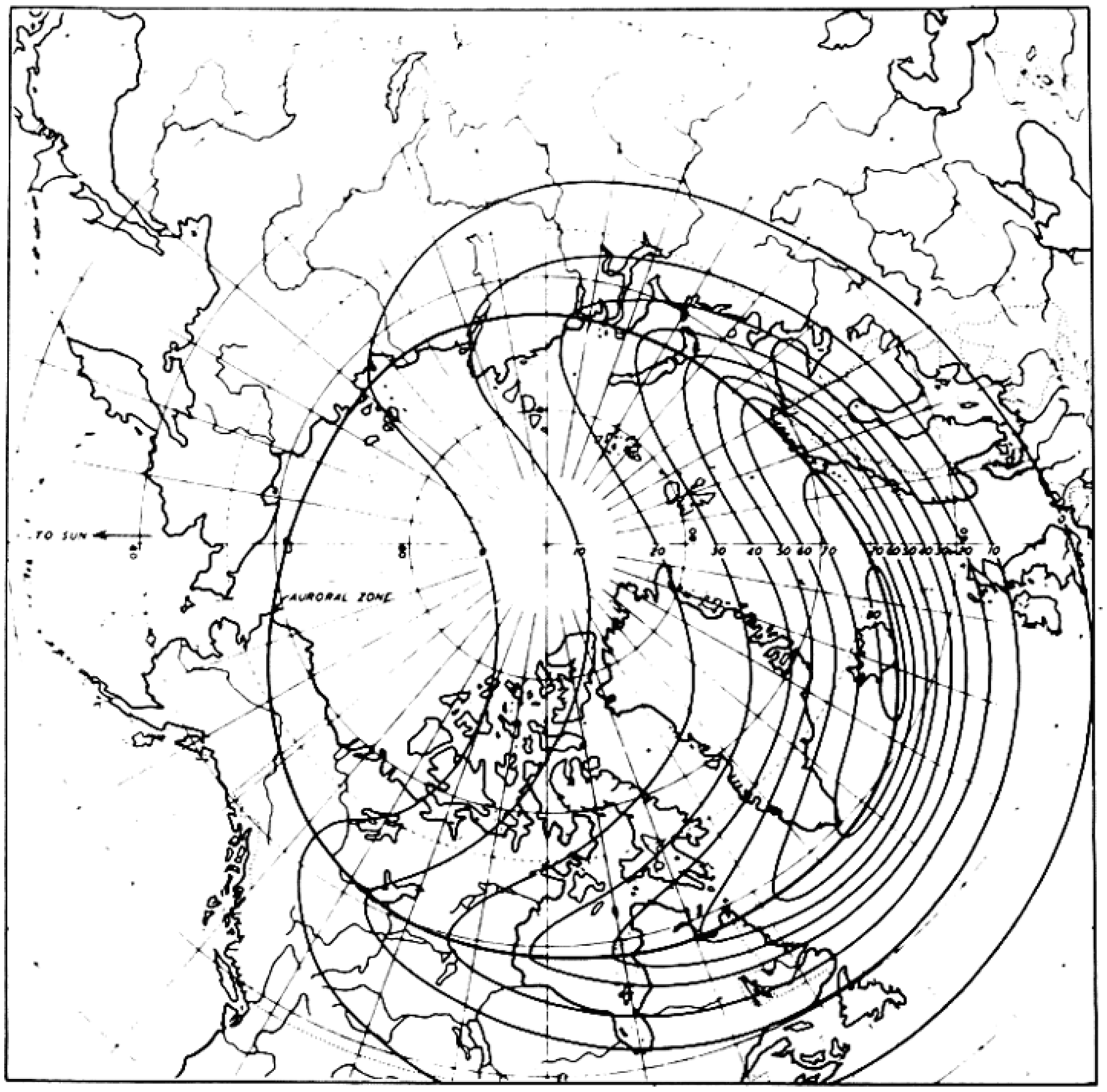

FIG. 247 — ESTIMATED PERCENTAGE-FREQUENCY OF HOURS WITH OCCURRENCE OF AURORA, CLEAR, DARK NIGHTS, HIGH LATITUDES, NORTHERN HEMISPHERE, FOR 0^h GMT

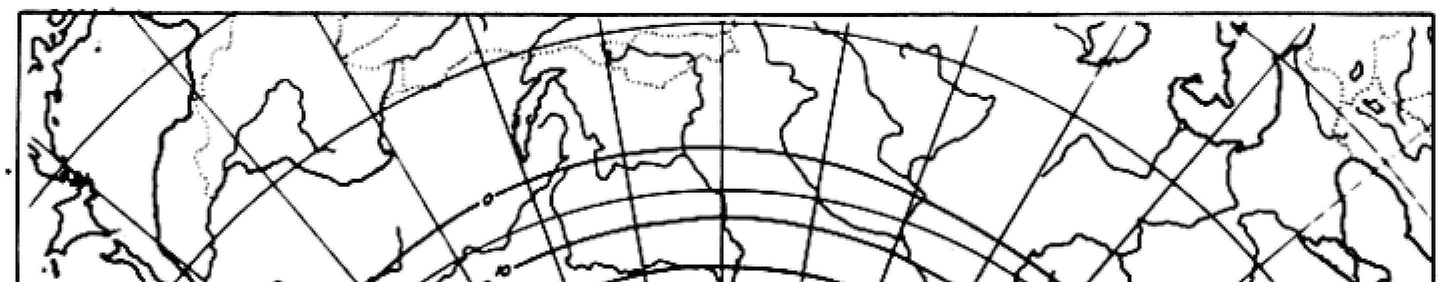

FIG. 248 — ESTIMATED PERCENTAGE-FREQUENCY OF HOURS WITH OCCURRENCE OF AURORA, CLEAR, DARK NIGHTS, HIGH LATITUDES, NORTHERN HEMISPHERE, FOR 6^h GMT

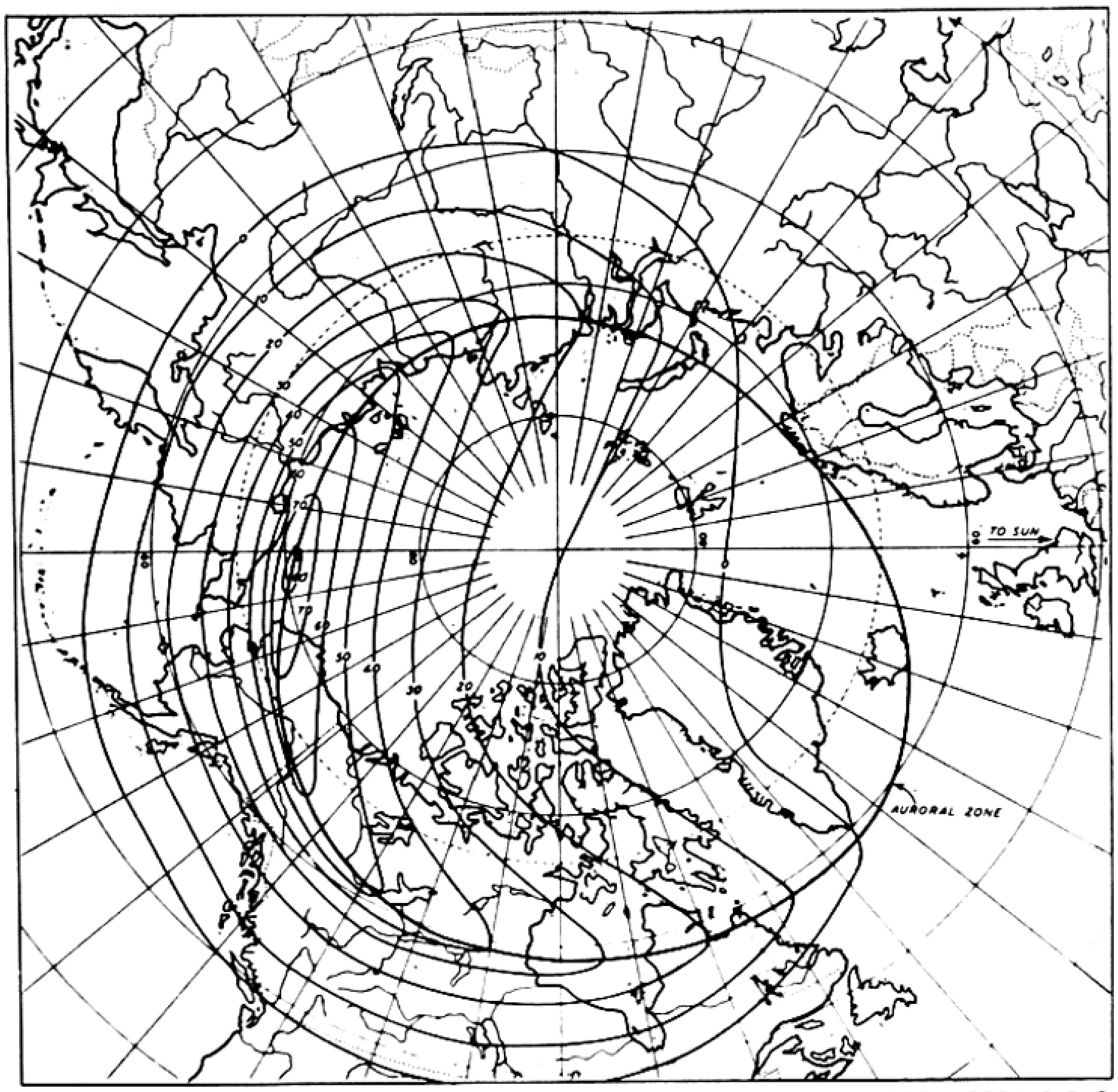

FIG. 249 — ESTIMATED PERCENTAGE-FREQUENCY OF HOURS WITH OCCURRENCE OF AURORA, CLEAR, DARK NIGHTS, HIGH LATITUDES, NORTHERN HEMISPHERE, FOR 12h GMT

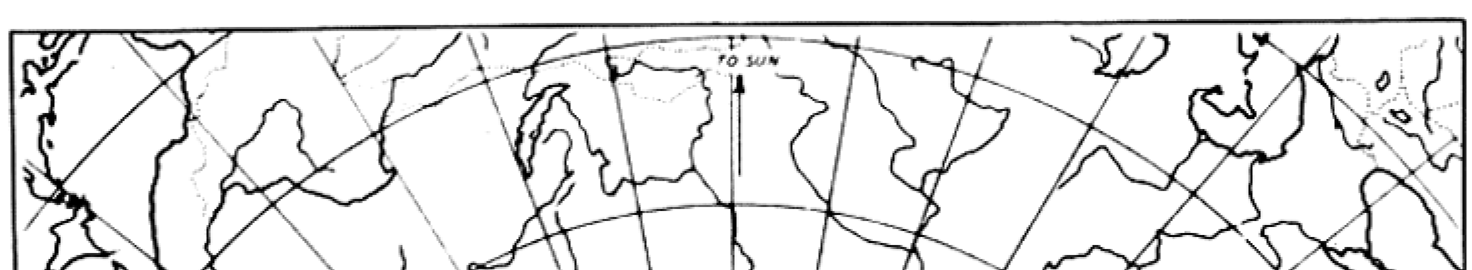

FIG. 250 — ESTIMATED PERCENTAGE-FREQUENCY OF HOURS WITH OCCURRENCE OF AURORA, CLEAR, DARK NIGHTS, HIGH LATITUDES, NORTHERN HEMISPHERE, FOR 18h GMT

LITERATURE CITED

1. Vestine, E. H., L. Laporte, I. Lange, C. Cooper, and W. C. Hendrix. 1947. Description of the Earth's main magnetic field and its secular change, 1905-1945. Carnegie Inst. Wash. Pub. No. 578.
2. Gauss, C. F. 1839. Allgemeine Theorie des Erdmagnetismus. Resultate aus den Beobachtungen des magnetischen Vereins im Jahre 1838, pp. 1-57. Leipzig. Also, 1877, Werke, vol. 5, pp. 119-180. Göttingen.
3. Chapman, S., and J. Bartels. 1940. Geomagnetism. Oxford Univ. Press. Vols. 1 and 2.
4. Dyson, F., and H. Furner. 1923. The Earth's magnetic potential. Mon. Not. R. Astr. Soc. Geophys. Sup., vol. 1, pp. 76-88.
5. Schmidt, A. 1935. Tafeln der normierten Kugelfunktionen und ihrer Ableitung nebst den Logarithmen dieser Zahlen sowie Formeln zur Entwicklung nach Kugelfunktionen. Gotha, Engelhard-Reyher Verlag.
6. Schrödinger, E. 1943. The Earth's and Sun's permanent magnetic fields in the unitary field theory. Proc. R. Irish Acad., A, vol. 49, pp. 135-148.
7. Vestine, E. H., M. A. Tuve, and E. A. Johnson. 1940. Various hypotheses regarding the origin and maintenance of the Earth's magnetic field. Trans. Washington Meeting, September, 1939. Internat. Union Geod. Geophys., Ass. Terr. Mag. Electr., Bull. No. 11, pp. 354-360.

   Schuster, A. 1912. A critical examination of the possible causes of terrestrial magnetism. Proc. Phys. Soc., vol. 24, pp. 121-137.
8. Vestine, E. H., L. Laporte, and C. Cooper. 1946. Geomagnetic secular change during past epochs. Trans. Amer. Geophys. Union, vol. 27, pp. 814-822.
9. Lahiri, B. N., and A. T. Price. 1939. Electromagnetic induction in nonuniform conductors, and the determination of the conductivity of the Earth from terrestrial magnetic variations. Phil. Trans. R. Soc., A, vol. 237, pp. 509-540.
10. Adams, L., and J. W. Green. 1931. The influence of hydrostatic pressure on the critical temperature of magnetization for iron and other materials. Phil. Mag., vol. 12, pp. 361-380; and Terr. Mag., vol. 36, pp. 161-169.
11. Elsasser, W. M. 1939. On the origin of the Earth's magnetic field. Phys. Rev., vol. 55, pp. 489-498. 1941. A statistical analysis of the Earth's internal magnetic field. Phys. Rev., vol. 60, pp. 876-883. 1946. Induction effects in terrestrial magnetism. Part I. Theory. Part II. The secular variation. Phys. Rev., vol. 69, pp. 106-116; vol. 70, pp. 202-212.
12. Balsley, Jr., J. R. 1946. The airborne magnetometer. U. S. Geol. Surv., Geophys. Invest., Prelim. Rept. No. 3, pp. 1-8.
13. Vening Meinesz, F. A. 1947. Shear patterns of the Earth's crust. Trans. Amer. Geophys. Union, vol. 28, pp. 1-61.
14. McNish, A. G. 1940. Physical representations of the geomagnetic field. Trans. Amer. Geophys. Union, 21st Annual Meeting, II, pp. 287-291.
15. McNish, A. G., and E. A. Johnson. 1938. Magnetization of unmetamorphosed varves and marine sediments. Terr. Mag., vol. 43, pp. 401-407. 1940. Determination of the secular variation in declination in New England from magnetic polarization of glacial varves. Trans. Washington Meeting, September, 1939; Internat. Union Geod. Geophys., Ass. Terr. Mag. Electr., Bull. No. 11, pp. 339-347.
16. Moos, N. A. F. 1910. Magnetic observations made at the Government Observatory, Bombay (Colaba magnetic data), for the period 1846 to 1905 and their discussion. Part II. The phenomenon and its discussion. Bombay, Government Central Press.
17. Schmidt, A. 1916. Ergebnisse der magnetischen Beobachtungen in Potsdam und Seddin in den Jahren 1900-1910. Abhandl. Kgl. Preuss. Meteorol. Inst., Band 5, No. 3, Berlin.
18. McNish, A. G. 1933. The apparent effect of magnetic activity upon the secular variation of the Earth's magnetic field. Trans. Amer. Geophys. Union, 14th Annual Meeting, pp. 139-144.
19. Scott, W. E. 1943. The mutual consistency of successive monthly means of declination, Huancayo Magnetic Observatory. Terr. Mag., vol. 48, pp. 45-48.
20. Wasserfall, K. F. 1941. Magnetic horizontal intensity at Oslo, 1843-1930. Terr. Mag., vol. 46, pp. 173-221.
21. Fisk, H. W. 1931. Magnetic secular variation and solar activity. Internat. Res. Council, Third Rept. Comm. on Solar and Terrestrial Relationships, pp. 52-59.
22. Fleming, J. A., and W. E. Scott. 1943. List of geomagnetic observatories and thesaurus of values. Terr. Mag., vol. 48, pp. 97-108; 171-182; 237-242. 1944. List of geomagnetic observatories and thesaurus of values. Terr. Mag., vol. 49, pp. 47-52; 109-118.
23. Cynk, B. 1939. Variations in the disturbance field of magnetic storms. Terr. Mag., vol. 44, pp. 51-57.
24. Schuster, A. 1889. The diurnal variation of terrestrial magnetism. Phil. Trans. R. Soc., A, vol. 180, pp. 467-512.
25. Chapman, S. 1919. The solar and lunar diurnal variations of terrestrial magnetism. Phil. Trans. R. Soc., A, vol. 218, pp. 1-118.
26. McNish, A. G. 1937. Progress of research in magnetic diurnal variations at the Department of Terrestrial Magnetism. Trans. Edinburgh Meeting, September, 1936: Internat. Union Geod. Geophys., Ass. Terr. Mag. Electr., Bull. No. 10, pp. 271-280. Terrestrial-magnetic and ionospheric effects associated with bright chromospheric eruptions. Terr. Mag., vol. 42, pp. 109-122.
27. Benkova, N. P. 1940. Spherical harmonic analysis of the Sq-variations, May-August, 1933. Terr. Mag., vol. 45, pp. 425-432.
28. Chapman, S., and J. M. Stagg. 1929. On the variability of the quiet-day diurnal magnetic variation. Proc. R. Soc., A, vol. 123, pp. 27-53; 1931, vol. 130, pp. 668-697.
29. Birkeland, Kr. 1908, 1913. Norwegian aurora polaris expedition, 1902-1903. vol. 1, part 1, pp. 39-315; part 2, pp. 319-551.
30. Broun, J. A. 1861. On the horizontal force of the Earth's magnetism. Trans. R. Soc., vol. 22, part 3, pp. 511-565.

31. Bemmelen, W. van. 1895. Die erdmagnetische Nachstörung. Met. Zeit., vol. 12, pp. 321-329.
32. Schmidt, A. 1925. Das erdmagnetische Aussenfeld. Zs. f. Geophysik, vol. 1, pp. 3-13.
33. Lüdeling, T. F. 1899. Über die tägliche periode des erdmagnetismus und der erdmagnetischen störungen an polarstationen. Terr. Mag., vol. 4, pp. 245-260.
34. Stagg, J. M. 1935. Aspects of the current system producing magnetic disturbance. Proc. R. Soc., A, vol. 152, pp. 277-298.
35. Slaucitajs, L., and A. G. McNish. 1937. The field of magnetic storms as deduced from the mean difference of magnetic intensity on quiet and disturbed days. Trans. Edinburgh Meeting 1936, Internat. Union Geod. Geophys., Ass. Terr. Mag. Electr., Bull. No. 10, pp. 289-301.
36. Forbush, S. E. 1938. On cosmic-ray effects associated with magnetic storms. Terr. Mag., vol. 43, pp. 203-218.
37. Vestine, E. H., and S. Chapman. 1938. The electric current system of geomagnetic disturbance. Terr. Mag., vol. 43, pp. 351-382. 1940. The disturbance field of magnetic storms. Trans. Washington Meeting, 1939, Internat. Union Geod. Geophys., Ass. Terr. Mag. Electr., Bull. No. 11, pp. 360-381.
38. Vestine, E. H. 1938. Asymmetrical characteristics of the Earth's magnetic disturbance field. Terr. Mag., vol. 43, pp. 261-282.
39. Silsbee, H. B., and E. H. Vestine. 1942. Geomagnetic bays, their frequency and current systems. Terr. Mag., vol. 47, pp. 195-208.
40. Hartnell, G. 1922. Horizontal-intensity variometers. Dept. of Commerce, U. S. Coast and Geod. Surv., Spec. Pub. No. 89, Serial No. 212.
41. Bateman, H. 1932. Partial differential equations of mathematical physics. Cambridge Univ. Press, p. 49.
42. La Cour, D., and V. Laursen. 1930. Le variomètre de Copenhague. Copenhagen, Met. Inst., Comm. Mag. No. 11, pp. 1-11. La balance de Godhavn. Balance magnétique à l'aimant monade dans d l'air raréfié. Comm. Mag. No. 8, pp. 1-27.
43. Standard handbook for electrical engineers. 1941. A. E. Knowlton, editor-in-chief. McGraw Hill Book Co., New York. Seventh edition, p. 235.
44. Stewart, B. 1861. On the great magnetic disturbance which extended from August 28 to September 7, 1859, as recorded by photography at the Kew Observatory. Phil. Trans. R. Soc., A, vol. 151, pp. 423-430.
45. Kohlrausch, F. 1896. Über sehr rasche Schwankungen des Erdmagnetismus. Wied. Ann., vol. 60, pp. 336-339.
46. Arendt, T. 1896. Des Wetter, vol. 13, pp. 241-253, 265-280.
47. Eschenhagen, M. 1897. On minute, rapid, periodic changes of the Earth's magnetism. Terr. Mag., vol. 2, pp. 105-114.
48. Birkeland, Kr. 1901. Résultats des recherches magnétiques faites par l'expédition Norwegienne de 1889-1900 pour l'étude des Aurores Boréales, Arch. Sci. Phys., Genève, vol. 12, pp. 565-586.
49. Bemmelen, W. van. 1899. Spasms in the terrestrial magnetic force at Batavia. Proc. K. Akad. Wet., pp. 202-211.
50. Terada, T. 1917. On rapid periodic variations of terrestrial magnetism. J. Coll. Sci. Imp. Univ., Tokyo, vol. 37, pp. 1-85.
51. Aschenbrenner, H., and G. Goubau. 1936. Eine Anordnung zur Registrierung rascher magnetischer Störungen. Hochfrequenztech, Leipzig, vol. 47, pp. 177-181.
52. Schindelhauer, F. 1928, 1929. Über elektromagnetische Störungen. Elektr. Nachr.-Technik. vol. 5, pp. 442-449; vol. 6, pp. 231-236.
53. Sucksdorff, E. 1936. Occurrences of rapid micropulsations at Sodankylä during 1932 to 1935. Terr. Mag., vol. 41, pp. 337-344.
54. Rolf, B. 1931. Giant micropulsations at Abisko. Terr. Mag., vol. 36, pp. 9-14.
55. Harang, L. 1939. Pulsations in an ionized region at height of 650-800 km during the appearance of giant pulsations in the geomagnetic records. Terr. Mag., vol. 44, pp. 17-19.
56. Fleming, J. A. 1939. Physics of the Earth, vol. 8, Terrestrial magnetism and electricity, pp. 370-376.
57. Wells, H. W., J. M. Watts, and D. E. George. 1946. Detection of rapidly moving ionosphere clouds. Phys. Rev., vol. 69, pp. 540-541.
58. General Electric Instructions 14903. 1941. Photoelectric recording fluxmeter. General Electric Co., Schenectady, N. Y.
59. Marburger, W. G. 1942. The design of a magnetic storm recorder. Navy Ord. Lab. Memo. No. 1430. Navy Yard, Washington, D. C.
60. Marburger, W. G. 1942. The adjustment and calibration of a magnetic storm recorder. Navy Ord. Lab. Memo. No. 1777. Navy Yard, Washington, D. C.
61. Campbell, E. A. 1942. Frequency response of magnetic storm recorder. Navy Ord. Lab. Memo. No. 2104. Navy Yard, Washington, D. C.
62. Chapman, S. 1918. An outline of a theory of magnetic storms. Proc. R. Soc., A, vol. 95, pp. 61-83.
63. Chapman, S. 1927. On certain average characteristics of world-wide magnetic disturbance. Proc. R. Soc., A, vol. 115, pp. 242-267.
64. Chapman, S. 1935. The electric current systems of magnetic storms. Terr. Mag., vol. 40, pp. 349-370.
65. McNish, A. G. 1938. Heights of electric currents near the auroral zone. Terr. Mag., vol. 43, pp. 67-75.
66. Hess, V. F., and A. Demmelmair. 1937. World-wide effect in cosmic-ray intensity, as observed during a recent magnetic storm. Nature, vol. 140, pp. 316-317.
Störmer, C. 1911. Sur les trajectoires des corpuscules électrisés dans l'espace sous l'action du magnétisme terrestre avec application aux aurores boréales. Arch. Sci. Phys., vol. 32, pp. 415-436.
Chapman, S. 1937. Cosmic rays and magnetic storms. Nature, vol. 140, pp. 423-324.
Angenheister, G. 1924. Die erdmagnetischen Störungen nach den Beobachtungen des Samoa-Observatoriums. Göttingen, Nachr. Ges. Wiss., pp. 1-42.
Birkeland [29]; Brown [30]; van Bemmelen [31]; Schmidt [32]; Forbush [36]; Vestine and Chapman [37]; Chapman [62].
67. Wells, H. W. 1942. Polar radio disturbances during magnetic bays. Unpublished report.
68. Appleton, E. V. 1933. Radio observations during the International Polar Year, 1932-33. Proc. R. Inst., vol. 28, pp. 1-17.
69. Berkner, L. V., and S. L. Seaton. 1940. Ionospheric changes associated with the magnetic storm of March 24, 1940. Terr. Mag., vol. 45, pp. 393-418.

70. Berkner, L. V., and H. W. Wells. 1938. Nonseasonal change of F2-region ion-density. Terr. Mag., vol. 43, pp. 15-36.
Harang, L. 1938. Annual variation of the critical frequencies of the ionized layer at Tromsö during 1937. Terr. Mag., vol. 43, pp. 41-43. 1939. Annual variation of the critical frequencies of the ionized layers at Tromsö during 1938. Terr. Mag., vol. 44, pp. 15-16.

71. Forbush, S. E. 1938. On world-wide changes in cosmic ray intensity. Phys. Rev., vol. 54, pp. 975-988.

72. Forbush, S. E. 1946. Three unusual cosmic ray increases possibly due to charged particles from the Sun. Phys. Rev., vol. 70, pp. 771-772.

73. Gartlein, C. W. 1945. Progress report on the National Geographic Society-Cornell University study of aurora. Trans. Amer. Geophys. Union, vol. 26, pp. 119-122.

74. Wiener, N. 1942. The extrapolation, interpolation, and smoothing of stationary time series with engineering applications. Mass. Inst. Tech., Cambridge, Mass., pp. 1-173.

75. Shapley, A. H. 1944. An estimate of the trend of solar activity, 1944-1950. Terr. Mag., vol. 49, pp. 43-45.

76. Vestine, E. H., and E. J. Snyder. 1945. The geographic incidence of aurora and magnetic disturbance, Southern Hemisphere. Terr. Mag., vol. 50, pp. 105-124.

77. Vestine, E. H. 1944. The geographic incidence of aurora and magnetic disturbance, Northern Hemisphere. Terr. Mag., vol. 49, pp. 77-102.